



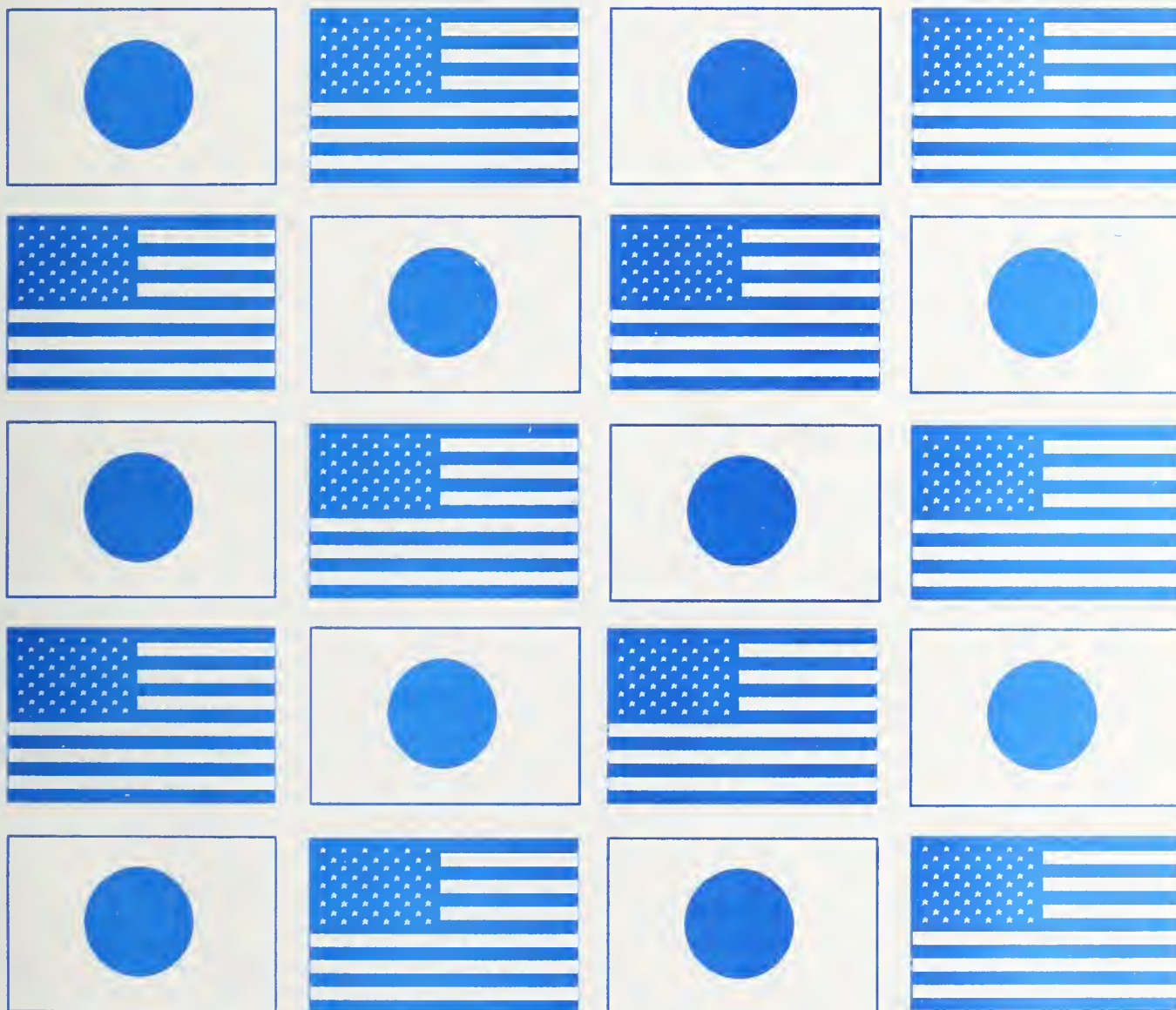
A11105 486845

NIST
PUBLICATIONS

Seismic Effects

Proceedings of the 30th Joint Meeting

NIST SP 931



QC

100

U57

NO. 931

1998

DEPARTMENT OF COMMERCE
Technology Administration
National Institute of Standards and Technology

The National Institute of Standards and Technology was established in 1988 by Congress to “assist industry in the development of technology . . . needed to improve product quality, to modernize manufacturing processes, to ensure product reliability . . . and to facilitate rapid commercialization . . . of products based on new scientific discoveries.”

NIST, originally founded as the National Bureau of Standards in 1901, works to strengthen U.S. industry’s competitiveness; advance science and engineering; and improve public health, safety, and the environment. One of the agency’s basic functions is to develop, maintain, and retain custody of the national standards of measurement, and provide the means and methods for comparing standards used in science, engineering, manufacturing, commerce, industry, and education with the standards adopted or recognized by the Federal Government.

As an agency of the U.S. Commerce Department’s Technology Administration, NIST conducts basic and applied research in the physical sciences and engineering, and develops measurement techniques, test methods, standards, and related services. The Institute does generic and precompetitive work on new and advanced technologies. NIST’s research facilities are located at Gaithersburg, MD 20899, and at Boulder, CO 80303. Major technical operating units and their principal activities are listed below. For more information contact the Publications and Program Inquiries Desk, 301-975-3058.

Office of the Director

- National Quality Program
- International and Academic Affairs

Technology Services

- Standards Services
- Technology Partnerships
- Measurement Services
- Technology Innovation
- Information Services

Advanced Technology Program

- Economic Assessment
- Information Technology and Applications
- Chemical and Biomedical Technology
- Materials and Manufacturing Technology
- Electronics and Photonics Technology

Manufacturing Extension Partnership Program

- Regional Programs
- National Programs
- Program Development

Electronics and Electrical Engineering Laboratory

- Microelectronics
- Law Enforcement Standards
- Electricity
- Semiconductor Electronics
- Electromagnetic Fields¹
- Electromagnetic Technology¹
- Optoelectronics¹

Chemical Science and Technology Laboratory

- Biotechnology
- Physical and Chemical Properties²
- Analytical Chemistry
- Process Measurements
- Surface and Microanalysis Science

Physics Laboratory

- Electron and Optical Physics
- Atomic Physics
- Optical Technology
- Ionizing Radiation
- Time and Frequency¹
- Quantum Physics¹

Materials Science and Engineering Laboratory

- Intelligent Processing of Materials
- Ceramics
- Materials Reliability¹
- Polymers
- Metallurgy
- NIST Center for Neutron Research

Manufacturing Engineering Laboratory

- Precision Engineering
- Automated Production Technology
- Intelligent Systems
- Fabrication Technology
- Manufacturing Systems Integration

Building and Fire Research Laboratory

- Structures
- Building Materials
- Building Environment
- Fire Safety Engineering
- Fire Science

Information Technology Laboratory

- Mathematical and Computational Sciences²
- Advanced Network Technologies
- Computer Security
- Information Access and User Interfaces
- High Performance Systems and Services
- Distributed Computing and Information Services
- Software Diagnostics and Conformance Testing

¹At Boulder, CO 80303.

²Some elements at Boulder, CO.

Wind and Seismic Effects

NIST SP 931

**PROCEEDINGS OF
THE 30TH JOINT
MEETING OF
THE U.S.-JAPAN
COOPERATIVE PROGRAM
IN NATURAL RESOURCES
PANEL ON WIND AND
SEISMIC EFFECTS**

Issued August 1998

**Noel J. Raufaste
EDITOR**

**Building and Fire Research Laboratory
National Institute of Standards and Technology
Gaithersburg, MD 20899**



**U.S. DEPARTMENT OF COMMERCE
William M. Daley, Secretary**

**TECHNOLOGY ADMINISTRATION
Gary R. Bachula, Acting Under Secretary for Technology**

**National Institute of Standards and Technology
Raymond G. Kammer, Director**

National Institute of Standards and Technology Special Publication 931
Natl. Inst. Stand. Technol. Spec. Publ. 931, 588 pages (Aug. 1998)
CODEN: NSPUE2

U.S. GOVERNMENT PRINTING OFFICE
WASHINGTON: 1998

For sale by the Superintendent of Documents, U.S. Government Printing Office, Washington, DC 20402-9325

PREFACE

This publication contains the Proceedings of the 30th Joint Meeting of the U.S.-Japan Panel on Wind and Seismic Effects. The meeting was held at the National Institute of Standards and Technology in Gaithersburg, Maryland during 12-15 May 1998. Forty-five papers were written, 22 by U.S. members and 23 by Japanese members. Thirty-eight papers were presented orally; 20 by the U.S.-side and 19 by the Japan-side. They were organized around seven themes: 1. Special Session in Celebration of the Panel's 30th Anniversary, 2. Storm Surge and Tsunamis, 3. Earthquake Engineering, 4. Joint Cooperative Research Programs, 5. Real Time Information Acquisition and Dissemination, 6. Wind Engineering, and 7. Reviews of the Panel's 11-Task Committee Activities and Highlights of Recent Task Committee Workshops. Eighteen Japan-side and 32-U.S.-side experts participated in these meetings

Two papers were presented at a mini-symposia conducted at USGS in Golden, CO during the technical site visit segment of the Joint Panel Meeting. The Japan-side paper is included in these proceedings in the section, Manuscripts Presented at Mini-Symposium.

BACKGROUND

Responding to the need for improved engineering and scientific practices through exchange of technical data and information, research personnel, and research equipment, the United States and Japan in 1961 created the U.S.-Japan Cooperative Science Program. Three collateral programs comprise the Cooperative Science Program. The U.S.-Japan Cooperative Program in Natural Resources (UJNR), one of the three, was created in January 1964. The objective of UJNR is to exchange information on research results and exchange scientists and engineers in the area of natural resources for the benefit of both countries. UJNR is composed of 18 Panels each responsible for specific technical subjects.

The Panel on Wind and Seismic Effects was established in 1969. Nineteen U.S. and seven Japanese agencies participate with representatives of private sector organizations to develop and exchange technologies aimed at reducing damages from high winds, earthquakes, storm surge, and tsunamis. This work is produced through collaboration between U.S. and Japanese member researchers working in 11 task committees. Each committee focuses on specific technical issues, e.g., earthquake strong motion data. The Panel provides the vehicle to exchange technical data and information on design and construction of civil engineering lifelines, buildings, and water front structures, and to exchange high wind and seismic measurement records. Annual meetings alternate between Japan and the United States (odd numbered years in Japan; even numbered years in the United States). These one-week technical meetings provide the forum to discuss ongoing research and research results; one-week technical study tours follow the meetings.

The National Institute of Standards and Technology (NIST) provides the U.S.-side chair and secretariat. The Public Works Research Institute (PWRI), Japan, provides the Japan Side chair and secretariat.

Cooperative research is done through formal Panel Programs. In 1981, cooperative research in Large-Scale Testing was started under the auspices of the Panel. Also, in 1981, joint research on Reinforced Concrete Structures was initiated. Full-scale testing was performed at the Building Research Institute (BRI), one of the six Japanese members' organizations, with supporting tests in Japan and in the United States. Two years later, a joint research program on Steel Structures was initiated. Full-scale testing again was led by BRI with supporting tests in the United States and Japan. The U.S.-Japan coordinated program

for Masonry Building Research was started in 1985. A U.S.-Japan coordinated program on Precast Seismic Structural Systems was initiated in 1991. A joint program on Seismic Performance of Composite and Hybrid Structures was initiated in 1993. In 1994, a joint program was started on Physical and Numerical Simulation of Structural Damages Due to Liquefaction and Development of Countermeasure Techniques.

Task Committee meetings, exchanges of data and information through technical presentations at annual Panel meetings, exchanges of guest researchers, visits to respective research laboratories and informal interactions between Panel meetings, joint workshops and seminars, and joint cooperative research programs all contribute to the development and effective delivery of knowledge that has influenced design and construction practices in both countries. Guest research exchanges have advanced the state of technology in areas of steel, concrete, and masonry structures under seismic forces; developed techniques to analyze risks from liquefaction; modeled water seepage in dam foundations; performed comparative analyses of seismic design of U.S. and Japanese bridges.

Direct communication between counterpart country organizations is the cornerstone of the Panel. Effective information exchanges and exchanges of personnel and equipment have strengthened domestic programs of both countries. There are opportunities for experts in various technical fields to get to know their foreign counterparts, conduct informal exchanges, bring their respective views to the frontiers of knowledge, and advance knowledge of their specialties.

The Panel's activities resulted in improved building and bridge standards and codes and design and construction practices in hydraulic structures in both countries, for example:

- created and exchanged digitized earthquake records used as the basis of design and research for Japan and the United States;
- transferred earthquake engineering information and strong-motion measurement techniques for use by seismically active countries, e.g., Australia, Canada, Italy, Mexico, Peru, Taiwan, Turkey, and North Africa;
- produced data that advanced retrofit techniques for bridge structures;
- developed field test data for use in aerodynamic retrofit of bridge structures;
- produced full-scale test data that advanced seismic design standards for buildings;
- advanced technology for repairing and strengthening reinforced concrete, steel, and masonry structures;
- improved *in-situ* measurement methods for soil liquefaction and stability under seismic loads;
- created a database comparing Japanese and U.S. standard penetration tests to improve prediction of soil liquefaction;
- created a database on storm surge and tsunamis and verified mathematical models of tsunami and storm surge warning systems;
- established a library resource of current research on wind and earthquake engineering and on storm surge and tsunamis;
- published proceedings of Panel meetings, Task Committee Workshops, and special publications such as List of Panel Publications and translated two-volume series on earthquake resistant construction using base isolation systems;
- gained better knowledge of both countries' research, design, and construction capabilities from in-depth visits to the host country's laboratories and building and public work projects. Results of such visits contribute to creation of new Task Committees, agendas for Joint Panel meetings and

task committee workshops, visits of U.S.-Japan researchers, and joint collaborative research.

HIGHLIGHTS OF THE JOINT TECHNICAL MEETING, 12-15 MAY 1998

The Panel celebrated its 30th joint meeting under the Theme, *Wind and Seismic Effects for the New Millennium*.

- ▶ Technical presentations highlighted important work by the U.S. and Japan Panel:
 - software emphasis for mitigation—beyond more resistant structures to emergency practices and national land management,
 - completing our Panel's work—more attention is needed for mitigation incentives and a focused 20-year effort to provide those technologies that will end disasters,
 - good correlations produced for real time component tests with systems simulation,
 - construction of a 20 m x 15 m, 1200 ton full-scale Japanese 3-D shake table test facility by 2005,
 - modeling long period surface waves at boundaries of deep sedimentary basins,
 - important surface wave effects for long period sea floor motions,
 - opportunities for systematic modeling of earthquake response of dams,
 - design and retrofit criteria for welded steel moment frames,
 - seismic isolation materials and systems for buried structures,
 - framework for performance-based design of buildings,
 - bases for major revisions of highway bridge design criteria,
 - physical and mental health of disaster survivors and disaster responders,
 - broad range of complementary work in developing disaster information systems; they should be distributed, open, and integrated with normal operating systems,
 - systematic use of Deer Island bridge to develop and improve models for wind response of bridges,
 - Japanese are developing new technologies and new design concepts for next generation of record long span bridges (2700 m) in earthquakes and typhoon areas,
 - practical, rational techniques for increasing wind and seismic resistance of housing,
 - new seismic design guidelines for concrete filled tubes, R/C column to steel beam systems, concrete core with exterior steel frame (hybrid wall system).
 - new technologies in GPS application and geospatial analysis to mitigate disasters.
- ▶ Panel Task Committee (T/C) activities grow in strength. The Panel created a new T/C on Seismic Information Systems to adapt information technology to reducing earthquake losses and two T/Cs were consolidated to better focus on intelligent structures. Interest was evident to pursue joint work in public health issues resulting from natural disasters. The T/C structure is an effective vehicle to explore in depth modern seismic and wind technologies being used by both countries. Four T/C workshops/conferences were held in the past year; ten workshops and joint meetings are planned for the coming year.
- ▶ The UJNR Panels on Wind and Seismic Effects, Fire Research and Safety, and Earthquake Research are contributing to the U.S./Japan Natural Disaster Reduction Effort of the Common Agenda.

- The Panel's newsletter is effective in disseminating its information. The Panel's Web Site is considered useful in deploying information to Japan and U.S. design and construction organizations. NIST will continue to maintain the Web Site during the next year. The site is available at <http://www.bfrl.nist.gov/info/ujnr>

HIGHLIGHTS OF THE TECHNICAL SITE VISITS 11 AND 16-21 MAY 1998

During the 30th Joint meeting of the Panel on Wind and Seismic Effects the delegation visited ten technical sites in the greater Washington, DC, Denver, and San Francisco metropolitan areas. Fourteen, eight, and nine Japan members participated in these site visits, respectively.

1. **U.S. Army Topographic Engineering Center** (www.tec.army.mil/tec_mission.html). Dr. William Roper, Director, Topographic Engineering Center (TEC), Panel co-chair of Task Committee "G" Seismic Information Systems, hosted the delegation. TEC supports the Army in developing terrain visualization models, computer image generation, 3-D graphics, distributed interactive simulation, precision surveying and mapping; global positioning system (GPS) development; image analysis; geographic information systems (GIS); data/image fusion and virtual reality modeling of the environment. TEC is developing capabilities to model human interactions with the environment and model environmental restoration and conservation.

Two TEC staff demonstrated enhanced environmental and terrain capabilities for distributed interactive simulations and discussed TEC's development of 3-D visualization capabilities to demonstrate virtual reality environments. In artificial intelligence for terrain analysis, TEC is developing R&D methods for automated terrain reasoning to support modeling and simulation of environmental impacts from burning, smoke flow, droughts, and hazardous wastes.

TEC staff have developed large data bases of geological, vegetation, and atmospheric spectral signatures (visible, thermal, fluorescence). Thermal infrared reflectance spectra reveal high spectral resolution information about the geological and vegetation components on the surface of the earth and the atmosphere. Radar images too are used to develop images of areas obscured by clouds to interpret the image beneath.

Of particular interest to the Panel is TEC's DrawLand. This software, developed by TEC, visualizes terrain data. It behaves like a flight simulator; what is seen on the monitor changes in response to how one manipulates the controls of a virtual vehicle. DrawLand reads from CD Roms; raster map data can be draped to create the appearance of a 3-D map. DrawLand has used imagery from sources such as Landsat, SPOT, and aerial photography. TEC developed this capability in 1994 with 10 m accuracy. Resolution capabilities of 2 m to 3 m accuracy exist to measure tides, map topography, and to determine elevation data surface water flow.

The Panel will benefit by having access to these capabilities in appropriate work such as its new Task Committee on Seismic Information Systems. Simulations of the built environment may be performed using data from topographic maps to model damages caused by fires and tsunamis following earthquakes or damages from earthquakes and high winds to the built environment.

TEC is one of four laboratories of the U.S. Army Corps of Engineers. It is located in Alexandria, VA and employs about 600 staff operating with a \$120 million budget.

2. **National Building Museum** (www.nbm.org/intro.htm). The delegation visited the 1887 Pension Building (now the National Building Museum) designed by Montgomery C. Meigs, who was Quartermaster General in charge of provisions during the Civil War. The building was constructed to serve as the government office for disbursing government checks to Civil War veterans and to their widows. Later, it was occupied by a variety of Government agencies. Created by an act of Congress in 1985, the building was designated the National Building Museum to serve as a focal point for permanent and temporary exhibitions; resource for collecting artifacts of design and construction; publisher of books and journals, and offers a variety of programs ranging from workshops on building crafts to tours of landmark buildings and construction sites, as well as films, lectures, concert series, and symposia.

The delegation visited one of the many exhibits, *Breaking Through the Creative Engineer*. This exhibit explores how creativity is expressed through the work of modern engineers. Its focus is on the creative impulse of the people who strive to give shape to the material world, built environment, and systems of information and power. Case studies in the exhibition are intended to stimulate reflection about the kind of thinking that allows an engineer to break through the ordinary and give birth to something novel. The displays are organized around eight themes that suggest some elements of engineering creativity and creativity in other areas of life: challenging, connecting, visualizing, collaborating, harmonizing, improvising, reorienting, and synthesizing.

Some interesting statistics about the Washington, DC National Building Museum reveals the original construction cost was \$887,000. It is 122 m by 111 m, 23 m to cornice level; constructed of 15,500,000 bricks with brick and terra cotta ornament; its terra cotta exterior frieze is 366 m long and 0.9 m high representing a continuous parade of Civil War military units. The Great Hall measures 96 m by 35 m and is 48 m at its highest point. Its Corinthian columns are among the tallest interior columns in the world measuring 23 m high; 2.4 m in diameter; 7.6 m in circumference each made of 70,000 bricks and painted to resemble Sienna marble. There are 72 ground floor Doric-style columns (terra cotta covered with cement) and 72 second floor Ionic-style columns (cast iron). Two hundred forty four busts reside in niches high above the center court that represent members of building occupations. A clever system of windows, vents, and open archways provided complete air circulation throughout the building; cooling in the summer and heating in the winter.

3. **Colorado State University, Fluid Dynamics and Diffusion Laboratory** (http://www.lance.colostate.edu/depts/ce/netscape/depts/fluid_mechanics/faculty.html). Professor Robert Meroney, Director, Fluid Dynamics and Diffusion Laboratory (FDDL) and staff hosted the delegation to discuss fluid mechanics and wind engineering research performed at FDDL. Professor Meroney reviewed work performed by the boundary-layer wind tunnels used in support of fundamental investigations of turbulence and turbulent diffusion. Research centers on wind engineering and wind effects on buildings and structures including low-speed turbulent flow, atmospheric flow near the earth's surface and around bluff bodies; computational fluid mechanics; physical modeling of the atmospheric boundary layer and flow phenomena within this layer; and wind tunnel testing of environmental design for urban centers and air-pollution control.

Dr. Jack Cermak, University Distinguished Professor and founder of FDDL, reviewed wind research developed during the last three decades. Professor Cermak noted a variety of laboratory investigations performed by FDDL. They include wind forces on proposed tall buildings and long-span bridges, wind forces on low-rise buildings, atmospheric diffusion near energy producing and storage facilities, and other

wind engineering projects. Wind research is performed for sponsors from consulting firms, research institutes and industrial firms throughout the United States. Often these studies identify new areas of needed research.

Professor Meroney reviewed the Colorado State/Texas Tech Universities (TTU) Cooperative Program in Wind Engineering supported by the National Science Foundation. The program is evaluating and mitigating the effects of severe wind storms on low-rise buildings. Experiments at the TTU field site and in FDDL's wind tunnels are examining external and internal pressures and wind loads under severe thunderstorm, tornado and hurricane wind conditions. This joint effort is examining the economic implications of code improvements, wind engineering, and insurance incentives through surveys and impact analysis programming.

Dr. Bogusz Bienkiewicz, FDDL Professor and member of the Panel's Task Committee "E" on Design for Wind and Wind Hazard Mitigation, reviewed his research in bridge aerodynamics and research being performed at FHWA under a guest researcher assignment. Some of his novel research addresses aerodynamics of racing boats, optimizing human ski positions, and helmet design that reduce drag.

A tour of the FDDL highlighted three wind tunnels. The 12.2 m long test section of the Meteorological Wind Tunnel is capable of independently heating and cooling air to generate thermally stratified flows. The tunnel is used to study flow characteristics of the atmospheric surface layer and to measure wind pressures on buildings and structures. The delegation observed meteorological wind tunnel research on correlated laser light visualization and pressure measurements. FDDL's Industrial Aerodynamic Wind Tunnel's test section is 1.8 m wide by 18.3 m long with adjustable ceiling height ranging from 1.5 m to 2.1 m. A 3 m section of the lower boundary can be heated to 93.3 °C. The Open Circuit Gust Wind Tunnel is equipped with a 3.7 m long test section that is 0.9 m wide and 0.9 m high. A 6-blade fan variable speed motor generates wind speeds ranging from 0.3 m/s to 9.14 m/s. Other FDDL tunnels include the Environmental Wind Tunnel, Thermal Stratification Wind Tunnel, Transpiration Wind Tunnel, and the Separation Wind Tunnel.

FDDL is in the Department of Civil Engineering, Colorado State University, Golden CO.

4. **U.S. Geological Survey** (geohazards.cr.usgs.gov). The delegation was welcomed by Dr. Randall Updike, Chief Scientist, Geohazards Team and Drs. E.V. Leyendecker and Erdal Saffak, and by staff of the Geologic Hazards and National Earthquake Information Center. The delegation was informed of mapping work performed by USGS in Golden, CO. They are developing ground motion maps and national seismic hazard maps for use in the development of U.S. seismic design maps. Also, these maps are used in the regulation of waste disposal sites, highway design, insurance, loss estimation, and damage mitigation. This data is available by CD Roms and maps are available on the Internet. This work forms the basis for the 1997 Recommended Provisions of the National Earthquake Hazards Reduction Program.

A mini-symposium was carried out with Dr. Arthur Tarr, USGS and Dr. Michio Okahara, Director, Bridge and Structures Department, PWRI. Dr. Tarr discussed his work in developing dynamic mapping of earthquake and landslide resources for distribution on the Internet. The soon to be published Internet map technology will permit rapid assessments of specific maps of specific locations. USGS used the January 1994 Northridge earthquake data to test their modeling in the development of the geologic hazards interactive maps for seismic intensity contours in real time. As new information is made available, the maps are automatically recontoured. The system facilitates assessments of damaged structures and buildings.

This work will be a valuable contribution to the Panel's new Task Committee "G" on Seismic Information Systems.

Dr. Michio Okahara discussed PWRI's research, following the January 1995 Kobe earthquake, on seismic retrofit of bridge substructures involving the redesign of reinforced concrete columns. The redesigned columns used base isolators in conjunction with a spiral reinforcements retrofit design. In areas of soil liquefaction, micro-piles were used. This paper is part of the Proceedings of the 30th Joint Meeting of the Panel on Wind and Seismic Effects.

During a review of USGS' National Earthquake Information Center (NEIC) the delegation learned of its mission to provide earthquake information to FEMA and other Federal Agencies, all 50-States, to worldwide scientists and engineers, and the public through the printed and electronic medium. Within 30 minutes following an earthquake, NEIC alerts FEMA and each of the affected States and the media about earthquake severity information, location and magnitude of the earthquake, and earthquake source parameters. This information aids disaster relief officials and scientists in evaluating earthquake hazards. NEIC works closely with the Japan Meteorological Agency and similar other country organizations.

USGS Central Region, Geologic Hazards, is in Golden, CO. The Geologic Hazards Team conducts global investigations of earthquake, geomagnetic, and landslide hazards. The Team consists of eight research groups and three information centers.

5. **Natural Hazards Information Center** (www.colorado.edu/hazards). The delegation was hosted by Dr. Dennis S. Mileti, Center Director and Dr. Mary Fran Myers, Center Co-Director. The delegation was informed of the Center's four key roles:

- o Publishes a bimonthly *Natural Hazards Observer* that reaches over 14,000 subscribers. The newsletter features information on disaster issues; hazards research; political and policy developments; world, national, and state program activities; upcoming conferences; and recent publications. Also, the Center produces a semimonthly E-mail newsletter *Disaster Research*.
- o Performs in-house research and a grant program enabling "quick response" study of disasters. Recently the Center completed a 6-year study and published its 1,200 page draft final report on *National Assessment of Natural Hazards*. This seminal work was performed through many groups. The latter program permits social scientists to go immediately to the site of a disaster to obtain information that might otherwise be lost. Their findings are subsequently published by the Center in brief Quick Response Reports.
- o Hosts an annual workshop, conducted each summer for the past 23 years in Colorado, the workshops bring the public and private sector together to share hazard-related problems and ideas for their solutions. The workshop involves participants ranging from researchers, hazard managers, government officials, professional and nongovernmental organization representatives.
- o Maintains a library research services with more than 14,000 books, articles, reports, journals, and other documents on the social, economic, and behavioral aspects of natural disasters. The holdings are cataloged in a computerized, bibliographic database. With this resource, the Center staff responds daily to requests for information from federal, state, and local officials, researchers, members of private and nonprofit organizations, and other concerned individuals around the world.

The Panel is encouraged to use relevant Center services during its planning of Task Committee activities and joint research.

The Center is at the University of Colorado, Boulder. Its goal is to increase communication between hazard/disaster researchers and those individuals, agencies, and organizations that are actively working to reduce disaster damage and suffering. The Natural Hazards Center has a variety of resources available from the Internet.

6. **Pacific Gas and Electric Corporation** (<http://www.pge.com/welcome.html>). Dr. Lloyd Cluff, Manager, Geosciences Department, reviewed his work assessing earthquake hazards and vulnerability of PG&E's facilities. Dr. Cluff stressed the importance of producing good design for nonstructural elements. Failures of nonstructural elements was the reason for closing PG&E's facilities which did not exhibit exterior structural damages. PG&E is performing a tsunami study to assess damages to PG&E's facilities following a major earthquake on the Juan de Fuca Plate near Eureka, CA. PG&E has appropriated \$2 billion for a 15 year to 20 year program to replace gas pipelines and to develop earthquake response planning and post earthquake inspection programs. The PG&E staff involved in earthquake engineering is small; PG&E collaborates with consultants.

The delegation centered their discussions on the restoration of PG&E's four-building headquarters complex following the 1989 Loma Prieta Earthquake and restoration of some powerplants and buildings damaged from the San Fernando and Loma Prieta earthquakes. Eric Elsesser of Forell/Elsesser Engineers, Inc. reviewed his work in seismic restoration/strengthening of PG&E's four-headquarters 1920s vintage buildings' design, restoration, and strengthening following the 1989 Loma Prieta earthquake. The site is on deep bay mud with immersed wooded pile foundations. The original buildings were steel-frame with non-load bearing unreinforced masonry tile infill. The buildings' exterior walls are terra cotta tiles. A variety of structural evaluations and options including demolishing the complex and construct anew were considered before choosing a massive structural shear-wall design as the best solution for rehabilitation. Base-isolation was considered and rejected as a solution. All wood piles were tied to a concrete foundation and into new reinforced walls. The terra cotta tile facade was articulated by cutting the tiles, fastening them to backing brick and setting it in concrete. The building's interiors were gutted, strengthened and repaired, and the infrastructure modernized. The total cost for this work was \$180 million. The design and construction costs were \$120 million; the remainder represents the costs of disrupting the staff and renting new facilities. A \$21 million tax incentive was provided by the State since PG&E maintained the architectural integrity of the building.

PG&E has a \$12 million 5-year applied research program with USGS in Menlo Park and with the Pacific Earthquake Engineering Research Center at UC Berkeley that centers on equipment vulnerability evaluation, building vulnerability, earthquake source characterization, ground deformation and ground motion. Also, PG&E and PEER are working on research to reduce damages following ignition of fires from earthquakes. PG&E's research activities and long-range planning to reduce damages from earthquakes is of much interest to the Panel and for possible collaborative efforts by some Panel's member laboratories.

PG&E headquarters is located in San Francisco. It provides electric service to over 4-million customers (households and businesses) using mixtures of energy resources such as natural gas, hydropower, geothermal and nuclear energy and wind and solar power. Its service area spans 182,000 km² within 48 of California's 58 counties, with a population of more than 13 million people. PG&E and other utilities in the state are regulated by the California Public Utilities Commission. PG&E has developed consumer

information on preparing for an earthquake (including design guidelines on bracing your water heater) and preparing for storms. This information is available on the Web at www.pge.com/customer_services/emergency/emquake.html and at http://www.pge.com/customer_services/emergency/storm.html respectively.

7. Pacific Earthquake Engineering Research (PEER) Center

(http://peer.berkeley.edu/html/about_peer.html). Professor Jack P. Moehle, PEER Director hosted the delegation. In Professor's Moehle's overview of PEER, he highlighted current research on performance-based earthquake engineering, response of unsafe concrete bridges, bridge response to ground motions, and safety and reliability of utility systems and lifelines. PEER developed an interactive Web site of research results from searches of experimental results and data. Professor Moehle told us he attended a San Francisco design review meeting, earlier in the morning, to review plans of a 41-story precast moment frame office building that proposes to use the NIST-Pankow developed precast concrete beam-column connection system able to withstand large inelastic deformations due to earthquakes and strong winds.

Three PEER papers were discussed. Dawn Lehman, graduate student, reviewed "Repair of Moderately and Severely Damaged Bridge Columns" an investigation of seismic performance of bridge columns and four methods of repair that included a mechanical coupler and varying amounts of epoxy injections with and without column jackets. Professor Raymond Seed reviewed his work, "Numerical Modeling and Simulation of Seismic Soil-Pile-Structure Interaction Experiments" on predicting seismic soil-pile-structure interactions under seismic loading from shaking table tests at U.C. Berkeley. Professor Gregory Fenves reviewed, "A Database of Experimental Results on Earthquake Protective Systems Hardware." This on-line database, PROSYS, accesses experimental results from passive protective systems such as seismic isolation and energy dissipation systems, elastomeric and sliding seismic isolators, damping devices, and other active and semi-active response control approaches. The three papers will be published in the Proceedings of the 30th Panel Meeting.

The delegation visited PEER's Earthquake Simulator Laboratory at the Richmond Field Station. The simulator is 6 m by 6 m in plan and configured to produce three cotranslational components of motion. The simulator can be used to subject structures weighing up to 580 kN to horizontal and vertical ground accelerations up to 1.5 g. The dynamic response, at 25 percent of the shake table capacity, of base isolators to three seismic records: Kobe; Newhall; and El Centro was being evaluated at the time of the visit.

During a visit to the Hayward fault (Berkeley Campus sits atop the Hayward fault), the delegation was informed of a recently developed uniform rating system to evaluate the seismic vulnerability of over 150 Berkeley campus buildings. This work was performed during a 6-month period at a cost of about \$200,000. The study identified 50 buildings that were rated poor to resisting seismic loads; they will require an estimated \$700,000 to \$1 million to retrofit. Berkeley has applied for funding from FEMA and other sources to perform the retrofit. A decision was made that it is more cost-effective to strengthen these buildings than demolish them.

PEER is a national earthquake engineering research center headquartered at UC Berkeley. It was established in 1998 by the National Science Foundation (NSF) and the participating universities and funded by NSF, the State of California, the University of California, the State of Washington, the University of Washington, and business and industry partners. It consists of a consortium of faculty researchers, core universities, and affiliated institutions that conduct programs in research, education and outreach, and information dissemination. PEER supports a business and industry partner program.

8. **California Department of Transportation CALTRANS** (www.dot.ca.gov/). Mr. Thomas Post, Chief, Earthquake Engineering Division, Caltrans and a Panel member hosted the delegation at the Caltrans Oakland facility and later, with the delegation and staff, visited the San Francisco-Oakland Bay Bridge. Mr. Post reviewed the repair and strengthening performed on the San Francisco-Oakland Bay Bridge following the Loma Prieta earthquake. Underway is a \$125 million retrofit program to reduce seismic risks to the west section and during the interim period before a new east section is constructed in 2003. The design is to withstand a magnitude 8.0 earthquake of a 1000 year to 2000-year return period. The bridge is retrofitted to remain operational following this design earthquake. As part of the work, Caltrans will be installing 96 dampers (500 K range) in the west section, clamping them from the cable to the main chord. The west section foundations and bents have been strengthened and bracing added to its legs. Friction pendulum isolators were installed at the top of the legs at the lower chord.

Feasibility studies were performed to estimate the costs of fully retrofitting the east section of the bridge versus construction of a new bridge. Cost of the retrofitting is in the \$900 million range and of a new east section, cost is estimated at \$1.2 billion. A decision was made to construct a new east section. In May 1998, the Metropolitan Transportation Commission (MTC) selected two bridge design options for the east section for further analysis. They are a single tower suspension bridge and a single tower cable-stayed bridge. T.Y. Lin International/Moffatt & Nichol Engineers, the joint-venture architectural and engineering team retained by Caltrans, is developing the designs to the stage of 30% completion so that a final evaluation can be made. When the new bridge is open for traffic in 2003, the old bridge will be dismantled and sold in sections for use by other countries.

The single tower suspension bridge concept will complement the other suspension bridges around the Bay: the Golden Gate, the Richmond-San Rafael bridges, and the western span of the Bay Bridge. The single steel tower will consist of four columns with horizontal link beams to add seismic strength to the tower. The decks are supported by suspending cables attached to a single main cable, which extends above the spine of the span. The suspending cables are attached to the inside of the decks, until near the tower, they traverse to the outside of the decks.

The single tower cable-stayed bridge concept consists of two concrete towers with an elliptical cross-section which gradually tapers toward the top. The two legs are joined by articulated link beams which strengthen the tower's seismic reliability. At the top of the tower, the link beams are protected and enclosed by a "lens." The cables are arranged in a semi-fan pattern and are splayed symmetrically from the central tower to the outside of the decks. This cable arrangement creates a spatial envelope and portal enclosure through which all vehicles and pedestrians pass. The deck is a closed steel box within the cable-supported span and a concrete box girder with ribs at the east viaduct portion of the bridge.

MTC is the transportation planning, coordinating, and financing agency for the nine-county San Francisco Bay Area. Created by the state Legislature in 1970, MTC functions as the regional transportation planning agency, a state designation, and for federal purposes, as the region's metropolitan planning organization. MTC is responsible for the Regional Transportation Plan, a comprehensive blueprint for the development of mass transit, highway, airport, seaport, railroad, bicycle and pedestrian facilities.

Caltrans' headquarters is in Sacramento, CA. They are responsible for the design, construction, maintenance, and operation of the California State Highway System, and that portion of the Interstate Highway System within the state's boundaries. Alone and in partnership with Amtrak, Caltrans also is

involved in the support of intercity passenger rail service in California, and is a leader in promoting the use of alternative modes of transportation. The current framework of Caltrans was set down by Assembly Bill 69 in 1972.

9. **San Francisco City Hall Seismic Retrofit** (www.dnai.com/~mbt/projdes/cityhall.html). Mr. Peter Borberg, project manager of Turner Construction and Mr. Paul Rodler, Principal and structural engineer of Forell/Elsesser Engineers, Inc. hosted the delegation to discuss retrofitting the 1915 Beaux Arts San Francisco City Hall. Turner Construction, the general manager of this seismic retrofit project awarded a \$103 million lump sum contract to Forell/Elsesser Engineers Inc. Forell/Elsesser is the prime architect/engineer firm performing the seismic retrofit of the 47,983 m² building; they are working with the San Francisco Bureau of Architecture who serves as the Executive Architect, and with the City and County of San Francisco. The total cost of seismic upgrade is \$181 million and includes \$38 million for employee relocation. A Change Order resulting from California's 1997 Proposition A, to upgrade the building's mechanical and electrical systems, extended the original 32-month construction schedule to 44 months. The building will be opened on New Year's Eve 1998.

The structural work is designed to withstand a 475-year magnitude 8 earthquake. The repair work involved: installing a new base isolation system for the entire City Hall building -- 530-1 m diameter rubber-lead core base isolators (designed to 0.5 m displacement) and 66 slider isolators under the ground floor. The building's columns were decoupled from the ground, supported and jacked to permit removal of the lower 1 m of column and set on temporary steel cruciform column supports. The new isolators were installed on a new slab-on-grade and a reinforced mat was built around each column footing. The isolators were tested for 635 mm deflection at 1500 K loading and to 216 mm for properties and quality control. A moat was constructed around the building to accommodate ground shaking. Shear walls, thicker than 1 m were installed in the basement and tied into the floor. A first floor wall system of about 0.7 m thick with a 10 mm thick steel plate extended along the light court up to the roof. Collector beams and new floor bracing were added. Structural strengthening was performed for the rotunda, dome, stairs and elevator shafts.

The architectural work includes new programming and space planning for the entire ground floor; replacing hollow clay tile walls; repairing the interior and exterior stone work; replacing the architectural finishes; and re-attaching stone arches and stone ornaments. The repair design maintained the soft first story to permit for long-vibration displacements. The exterior massive granite stairs were rebuilt with an underlayment stair slider bearing on the ground step. The slider bearing was fabricated of Teflon on stainless steel to allow movement in case of an earthquake. The architectural work emphasizes preservation of the building's historical fabric and significance, bringing the building back to its original architectural finishes, exposing ornamentation and ceilings, opening the two light wells for public use.

The 94 m by 124 m by 124 m height of dome City Hall is listed on the National Register of Historic Places. Its rotunda is a grand interior space and a landmark for the citizens of San Francisco. This City Hall replaced the first city hall which was destroyed in the 1906 San Francisco earthquake.

Following the renovation work, Dr. Hsi-Ping Liu, Structural Engineer from USGS presented USGS' work in instrumenting of selected San Francisco facilities near its four deep bore holes. Data records from these bore holes were used in developing ground shaking amplification mapping.

10. **National Weather Service** (<http://www.nws.mbay.net/>). The delegation was hosted by Mr.

Charles Morrill, Warning Coordination Meteorologist, National Weather Service (NWS) Forecast Office for the San Francisco Bay Area (located in Monterey). The office issues marine and land weather forecasts and warnings and provides semiweekly water temperature measurements, from Alaska to Mexico, of water skin temperatures from satellites. The information is available on the Web and from other sources. The NWS Climate Diagnostic Center is responsible for providing seasonal climate prediction and for year-to-year climate forecasts. NWS is in the process of upgrading its weather forecasting systems to advance its understanding of how sea temperature in the Pacific affect precipitation over the continental United States.

The delegation discussed research with three researchers offering papers on this topic. Dr. Wendell Nuss, Naval Post Graduate School (NPGS) briefed the delegation on a major 1998 west coast winter storm field experiments. Following the impact of El Nino, NOAA researchers, in collaborating with the U.S. Naval Research Laboratory, are working to improve numerical weather forecast models that will better simulate the present and future states of the atmosphere. These forecasts are in the 36 hour to 48 hour range and will be shared in another NOAA initiative that seeks to improve forecasts in the 0 to 12-hour range along the California coast. Improved observations and measurements are sought by measuring vertical profiles of wind, temperature, and moisture in the atmosphere. Measurements will be taken from deployed instrument packages over the Pacific and by aircraft and by satellites.

Dr. Elizabeth Ritchie of the NPGS reviewed her work in developing numerical model studies of typhoon flows over the Japan islands. Modeling is underway at the 1 km range producing finer resolution and understanding the effects of mountains on storms and rainfall. The model is approximating real time weather during the approach and landfall of typhoons.

Dr. Joseph Golden, OAR and co-chair of the Panel's Task Committee on Design for Wind and Wind Hazard Mitigation reviewed new NOAA technologies for forecasting weather. The United States has about 160 new Doppler weather radar stations and about 45 airports use Doppler radars for wind shear warnings. NOAA is working with industry to design instruments to measure wind speed at 100 m/s. They are experimenting with GPS dropsondes and through Doppler-on-wheels to better predict hurricanes before landfall and to model wind. NOAA is seeking new systems to collect wind measures such as: severe storm anemometers; unmanned aircraft to release recorders into storms; and use of appropriate DOD "Star Wars" advanced technologies. NOAA is featuring a global change program with several Federal Agencies and the National Academies of Science and Engineering. They are performing new work in measuring stratospheric ozone depletion and field investigations to characterize ozone losses. NOAA's coastal damage mitigation strategies for hurricanes and other coastal storms include: improve forecasting of 24 hour to 48 hours; reduce required excavation times; provide safe refuges of "last resort"; improve coastal and offshore observations; redirect development in high risk areas; and establish and enforce wind resistant building codes (the latter by working with NIST).

The mission of the National Weather Service is to provide weather and flood warnings, public forecasts and advisories for all of the United States, its territories, adjacent waters and ocean areas, primarily for the protection of life and property. NWS data and products are provided to private meteorologists for the provision of all specialized services. OAR is the principal weather and space weather research arm of NOAA and works synergistically with the NWS.

Noel J. Raufaste, Secretary-General
U.S.-side Panel on Wind and Seismic Effects

ABSTRACT

This publication is the Proceedings of the 30th Joint Meeting of the U.S.-Japan Panel on Wind and Seismic Effects. The meeting was held at the National Institute of Standards and Technology, Gaithersburg, Maryland, during 12-15 May 1998. The Proceedings include the agenda, list of Panel members, Panel Resolutions, the 45 technical papers written for this joint meeting, and the Panel's 11-Task Committee Reports.

Thirty-nine oral presentations centered on seven themes: 1. Special Session in Celebration of the Panel's 30th Anniversary, 2. Storm and Surge Tsunamis, 3. Earthquake Engineering, 4. Joint Cooperative Research Programs, 5. Real Time Information Acquisition and Dissemination, 6. Wind Engineering and 7. Reviews of the Panel's 11-Task Committee Activities and Highlights of Recent Task Committee Workshops. The Panel provides the vehicle to exchange technical data and information on design and construction of civil engineering lifelines, buildings, water front, and coastal structures. Panel findings continue to influence ongoing structural engineering research and contribute to the revision and creation of U.S. and Japanese building codes and standards.

KEYWORDS: Bridges; building technology; concrete; design criteria; disaster reduction; earthquakes; geotechnical engineering; GPS, ground failures; lifelines; liquefaction; risk assessment; seismic; shaking table; standards; storm surge; structural engineering; tsunamis; and wind loads.



TABLE OF CONTENTS

PREFACE.....	iii
ABSTRACT.....	xv
AGENDA: 30th JOINT MEETING PANEL on WIND AND SEISMIC EFFECTS	xxiii
PANEL MEMBERS:	
JAPAN-SIDE DELEGATION.....	xxxvii
JAPAN-SIDE MEMBERSHIP: PANEL on WIND AND SEISMIC EFFECTS	xxxix
U.S.-SIDE MEMBERSHIP: PANEL on WIND AND SEISMIC	li
PANEL TASK COMMITTEE MEMBERS.....	lxi
RESOLUTIONS.....	lxvii
SPECIAL SESSION in CELEBRATION of the PANEL'S 30th ANNIVERSARY	
<i>National Disasters and Protective Measures in Japan</i>	3
Yasutake Inoue	
<i>Completing Our Panel's Work</i>	13
Richard N. Wright	
THEME: STORM SURGE and TSUNAMIS	
<i>Tsunami and Storm Surge Characteristics Based on Long-Term Tide Observations</i>	23
Toshihiko Nagai, Kazuteru Sugahara, Hiroshi Watanabe, Koji Kawaguchi, Masahiro Mihara and Katsumi Takashima	
<i>International Responses to Pacific Tsunami Warnings and Watches</i>	33
Michael E. Blackford	

THEME: EARTHQUAKE ENGINEERING

<i>Real-time Hybrid Vibration Experiments with a 2-Degree-of-Freedom Model.....</i>	<i>41</i>
Keiichi Tamura and Hiroshi Kobayashi	
<i>A Vision for the Future of Strong-Motion Recording</i>	<i>50</i>
Roger D. Borchardt	
<i>Project on 3-D Full-Scale Earthquake Testing Facility--First Report</i>	<i>55</i>
Keiichi Ohtani, Tsuneo Katayama and Heki Shibata	
<i>Strong Motion from Surface Waves in Deep Sedimentary Basins.....</i>	<i>69</i>
William B. Joyner	
<i>Performance Based Design for Port Structures</i>	<i>84</i>
Susumu Iai and Koji Ichii	
<i>Analysis of Sea-Floor Earthquake Data</i>	<i>97</i>
Charles E. Smith and David M. Boore	
<i>Effect of Reservoir-Subbottom Energy Absorption on Hydrodynamic Forces on Dams</i>	<i>116</i>
Robert L. Hall, Luis de Bejar, Keith J. Sjostrom and Enrique E. Matheu	
<i>A Study on Stress in Concrete Gravity Dam using Seismic Data during Kobe Earthquake</i>	<i>130</i>
Takashi Sasaki, Tsuneo Uesaka and Isao Nagayama	
<i>Seismic Analysis of Hoover Dam</i>	<i>144</i>
Larry K. Nuss	
<i>Development and Operation of Large Centrifuge at PWRI.....</i>	<i>158</i>
Osamu Matsuo, Tatsuya Tsutsumi, Mitsu Okamura, Tetsuya Sasaki and Kunio Nishi	
<i>The Influence of Confining Stress on Liquefaction Resistance</i>	<i>167</i>
M. E. Hynes, R. S. Olsen and D. E. Yule	
<i>Evaluation of the Seismic Capacity of an Existing Thick Wall Reinforced Concrete Structure Using Probabilistic Criteria</i>	<i>185</i>
F. Locceff, G. Mertz and G. Rawls	

<i>Development of an Analysis of Structural Steel Fracture and Development of Technical Solutions.....</i>	<i>196</i>
Hiroyuki Yamanouchi, Akiyoshi Mukai and Takashi Hasegawa	

<i>Design Guidelines for the Seismic Modification of Welded Steel Moment Frame Buildings.....</i>	<i>201</i>
John L. Gross	

<i>Draft Manual for Seismic Isolation Design of Underground Structures.....</i>	<i>211</i>
Shigeki Unjoh, Jun-ichi Hoshikuma, Kazuhiro Nagaya and Kazuhiko Murai	

<i>Comparison between the Affected Population of Indirect Health Effects after the 1995 Great Hanshin-Awaji Earthquake.....</i>	<i>224</i>
Keiko Ogawa, Ichiro Tsuji, Shigeru Hisamichi and Keishi Shiono	

<i>New Framework for Performance Based Design of Building Structures - Design Flow and Social System</i>	<i>234</i>
Hisahiro Hiraishi, Masaomi Teshigawara, Hiroshi Fukuyama, Taiki Saito, Wataru Gojo, Hidoe Fujitani, Yuji Ohashi, Izuru Okawa and Hirashi Okada	

<i>Highway Bridge Seismic Design: How Current Research May Affect Future Design Practice</i>	<i>248</i>
Ian M. Friedland, W. Phillip Yen, Ronald L. Mayes and John O'Fallon	

<i>Development of Performance-Based Building Code in Japan -- Framework of Seismic and Structural Provisions</i>	<i>260</i>
Hisahiro Hiraishi, Mitsumasu Midorikawa, Masaomi Teshigawara and Wataru Gojo	

THEME: REAL-TIME INFORMATION ACQUISITION and DISSEMINATION

<i>American Red Cross -- Centers for Disease Control and Prevention Health Impact Surveillance System for Natural Disasters</i>	<i>275</i>
Enrique Paz-Argandona and Josephine Malilay	

<i>Development of the Disaster Information System (DIS/Earthquakes)</i>	<i>286</i>
Kazuo Okayama, Takaharu Kiriya and Seishi Yabuuchi	

<i>Recent FEMA Activities in Earthquake Risk Analysis and Mitigation</i>	<i>300</i>
Stuart Nishenko, Claire Drury and Jeff Milheizer	

<i>Seismic Information System for Civil Infrastructures</i>	306
Hideki Sugita and Tomofumi Nozaki	
<i>New Development in Seismic Risk Analysis for Highway Systems</i>	319
Stuart D. Werner, Craig E. Taylor, James E. Moore II, John B. Mander John B. Jernigan and Howard H. M. Hwang	
<i>Devastating Network in Miura Peninsula Japan</i>	344
Makoto Watabe and Satomi Hirokawa	
<i>Geospatial Analysis Support to Natural Disasters</i>	350
William E. Roper	

THEME: WIND ENGINEERING

<i>Analysis of Wind and Wind Effects Revisited -- A Case Study of Deer Isle-Sedgewick Bridge.....</i>	377
D. W. Marsh, B. Bienkiewicz and H. R. Bosch	
<i>New Generation Trans-Strait Road Projects and the State of Technology Development.....</i>	392
Michio Okahara and Masahiro Nishitani	
<i>New Hurricane Wind Structures and Wind Speed Measurements</i>	407
Peter G. Black and Fank D. Marks, Jr.	
<i>Consideration on Flutter Characteristics of super Long-Span Bridges ...</i>	415
Hiroshi Sato, Katsuya Ogihara and Ken-ichi Ogi	
<i>Structural Control for Wind and Earthquake Loads: NSF's Coordinated Research Program</i>	424
M. P. Singh and T. T. Soong	
<i>Wind and Seismic Research for Improved Engineering Consensus Standards and Housing Construction</i>	433
Jay H. Crandell and William Freeborne	

THEME: SUMMARY of JOINT COOPERATIVE RESEARCH PROGRAMS

<i>U.S.-Japan Cooperative Earthquake Engineering Research Program on Composite and Hybrid Structures -- Current Status of Japan-side Research</i>	443
Isao Nishiyama, Hiroyuki Yamamouchi and Hisahiro Hiraishi	

<i>U.S.-Japan Cooperative Earthquake Research Program on Composite and Hybrid Structures -- U.S.-side Progress</i>	452
Subhash C. Goel	

MANUSCRIPTS PRESENTED at MINI-SYMPOSIUM

<i>Development of New High Bridge Piers Containing Spiral Reinforcement</i>	459
Michio Okahara, Jiro Fukui, Takuya Adachi, Moriyuki Okoshi and Koga Yasuyuki	

U.S.-side Presentation addressed the U.S. Geological Survey development of ground motion maps and seismic intensity contours that will be available on the Internet. (No manuscript available).

MANUSCRIPTS AUTHORED for PANEL MEETING but NOT PRESENTED ORALLY

<i>Shaking Table on Base Isolated House Model</i>	477
Hiroyuki Yamanouchi, Mitsumasa Midorikawa and Masanori Iiba	
<i>Dense Strong Motion Instrument Array in Sendai</i>	484
Izuru Okawa, Toshihide Kashima and Shin Koyama	
<i>Deposition of Oil Spilled from a Russian Tanker on Coasts</i>	492
Fuminori Kato and Shinji Sato	
<i>GIS with Mobile Communication for Countermeasure Against Natural Disaster</i>	502
Naoki Takayama	
<i>Aerodynamic Databases and Electronic Standards for Wind Loads: A Pilot Application</i>	506
Timothy Whalen, Emil Simiu, Gilliam Harris, Jason Lin and David Surry	
<i>GPS Monitoring of Structures: Recent Advances</i>	515
Mehmet Celebi, Will Prescott, Ross Stein, Ken Hudnut, Jeff Behr and Steve Wilson	

APPENDIX: Summaries of Task Committee Reports	529
--	------------

AGENDA
30th JOINT MEETING
PANEL on WIND AND SEISMIC EFFECTS
12-15 May 1998

Sunday 10 May

Delegation Arrives

Monday 11 May

Technical Visits, Army Topographic Engineering Center and National Building Museum

Tuesday 12 May

0925 Meet in Lobby of Holiday Inn for NIST Shuttle to Administration Building

0930 Travel by bus to NIST

WIND AND SEISMIC EFFECTS FOR THE NEW MILLENNIUM

1000 OPENING CEREMONIES

(Employees Lounge, NIST Administration Building)

Call to order by Noel J. RAUFASTE, Secretary-General US-side Panel

Opening remarks by Raymond KAMMER, Director, National Institute of Standards and Technology

Remarks by Takao KURAMOCHI, Counsellor for Science and Technology, Embassy of Japan

Remarks by Richard N. WRIGHT, Chairman US-Side Panel on Wind and Seismic Effects, and Director, Building and Fire Research Laboratory

Remarks by Yasutake INOUE, Chairman Japan-Side Panel on Wind and Seismic Effects, and Director-General, Public Works Research Institute

Introduction of U.S. Members by U.S. Panel Chairman

Introduction of Japan Members by Japan Panel Chairman

Elect Joint Meeting Chairman

Adopt Agenda

1120 Break

SPECIAL SESSION TO CELEBRATE THE PANEL'S 30TH ANNIVERSARY

1140-1240 **THEME 1 -- SPECIAL SESSION IN CELEBRATION OF THE PANEL'S 30TH ANNIVERSARY**

Chairman: Mr. Yasutake INOUE

- 1140 Natural Disasters and Protective Measures in Japan, Yasutake INOUE* PWRI
- 1200 Completing our Panel's Work, Richard N. WRIGHT*, NIST
- 1220 Discussion
- 1240 **Adjourn**

1245 **Group Photograph**

- 1300 **Lunch:** Hosted by Raymond KAMMER, Director, National Institute of Standards and Technology, NIST Lunch Club

THEME 2 - STORM SURGE AND TSUNAMIS

1400-1500 **Technical Session - STORM SURGE AND TSUNAMIS**

Chairman: Mr. Yasutake INOUE

- 1400 Tsunami and Storm Surge Characteristics Based on Long-Term Tide Observations, Toshihiko NAGAI, Kazuteru SUGAHARA, Hiroshi WATANABE, Koji KAWAGUCHI, PHRI, Masahiro MIHARA, ECHO Corporation and Katsumi TAKASHIMA, Coastal Ocean Research Corporation. Presented by Shigetoshi KOBAYASHI* PWRC
- 1420 International Responses to Pacific Tsunami Warnings and Watches, Mike BLACKFORD*, NOAA
- 1440 Discussion
- 1500 **Break**

* denotes presenter

TASK COMMITTEE MEETINGS

1515-1700 Task Committee Meetings

T/C A **Strong-Motion Data and Applications**, BFRL Conf. Room B-317, Bldg. 226
Dr. Susumu IAI (Japan-side Chair) and Dr. Roger BORCHERDT (U.S.-side Chair)

T/C B **Testing and Evaluation Procedures for Building Systems**, BFRL Conf. Room B-221, Bldg 226
Mr. Keiichi OHTANI (Japan-side Chair) and Dr. H.S. LEW (U.S.-side Chair)

T/Cs C & G **Design Evaluation and Improvement of Structures and Structural Control and Intelligent Material Systems**, Admin. Bldg. NIST Employees Lounge
Dr. Hisahiro HIRAISHI (Japan-side Chair) and Dr. Ken CHONG (U.S.-side Chair)
Dr. Jun-ichi HOSHIKUMA (Japan-side Acting Chair) and Dr. Shi-Chi LIU (U.S.-side Chair)

T/C D **Earthquake Engineering for Dams**, BFRL Conf. Room A-368, Bldg. 226
Mr. Takashi SASAKI (Japan-side Acting Chair) and Dr. Robert HALL (U.S.-side Chair)

T/C E **Design for Wind and Wind Hazard Mitigation**, BFRL Conf. Room B-245 Bldg 224
Dr. Hiroshi SATO (Japan-side Chair) Dr. Joseph GOLDEN (U.S.-side Chair)

T/C F **Disaster Prevention Methods for Lifeline Systems**, ITL Conf. Room B-111 Bldg 225
Dr. Keiichi TAMURA (Japan-side Acting Chair) and Dr. Riley CHUNG (U.S.-side Chair)

1700 Conclusion of Day 1

1700 Depart NIST by bus to Holiday Inn

U.S.-side Panel Hosted Reception

1745 Bus depart Holiday Inn for residence of Dr. and Mrs. Charles SMITH for 30th Joint Panel Celebration

2200 Adjourn and, by bus, return to hotel

2245 Arrive at hotel

Wednesday 13 May

- 0740 Meet in lobby of Holiday Inn for NIST Shuttle Bus to Administration Building
- 0745 Travel by bus to NIST

THEME 3 - EARTHQUAKE ENGINEERING

0830-1230 Technical Session - Earthquake Engineering Part 1

Chairman: Dr. Richard WRIGHT

- 0830 Real-Time Hybrid Vibration Experiments with a 2-Degrees-of-Freedom Model, Keiichi TAMURA* and Hiroshi KOBAYASHI, PWRI
- 0850 A Vision for the Future of Strong-Motion Recordings, Roger BORCHERDT*, USGS
- 0910 Project on 3-D Full-Scale Earthquake Testing Facility -First Report, Keiichi OHTANI*, Tsuneo KATAYAMA and Heki SHIBATA, NIED
- 0930 Discussion
- 0950 Strong Motion from Surface Waves in Deep Sedimentary Basins, William JOYNER*, USGS
- 1010 Performance Based Design for Port Structures, Susumu IAI* and Koji ICHII, PHRI
- 1030 Analysis of Sea Floor Earthquake Data, Charles SMITH*, MMS and David BOORE, USGS
- 1050 Discussion
- 1110 **Break**
- 1130 Effect of Reservoir-Subbottom Energy Absorption on Hydrodynamic Forces on Dams, Robert HALL*, Louis de BEJAR, Keith SJOSTROM, and Enrique MATHEW, WES
- 1150 A Study on Stress in Concrete Gravity Dams Using Seismic Data During Kobe Earthquake, Takashi SASAKI*, Tsuneo UESAKA and Isao NAGAYAMA, PWRI
- 1210 Seismic Analysis of Hoover Dam, by Larry NUSS, BUREC
- 1230 Discussion
- 1250 **Adjourn for Lunch**
- 1300 **Lunch: Hosted by Dr. William ANDERSON, Hazard Reduction Program, Civil and Mechanical Infrastructure Systems Division, National Science Foundation, NIST Lunch Club**

1400-1500 Technical Session - Earthquake Engineering (Continued)

Chairman: Dr. Richard WRIGHT

- 1400 Development and Operation of Large Centrifuge at PWRI, Osamu MATSUO, Tatsuya TSUTSUMI, Mitsu OKAMURA*, Tetsuya SASAKI, PWRI and Kunio NISHI, Hazama Corporation
- 1420 The Influence of Continuing Stress on Liquefaction Resistance, Mary Ellen HYNES*, WES
- 1440 Evaluation of the Seismic Capacity of an Existing Thick Wall Reinforced Concrete Structure using Probabilistic Criteria by Frederick LOCEFF, George RAWLS, and Greg MERTZ*, DOE
- 1500 Discussion
- 1520 Break

TASK COMMITTEE MEETINGS

1535-1715 Task Committee Meetings

- T/C H Soil Behavior and Stability During Earthquakes, Admin. Bldg., NIST Employees Lounge
Dr. Mitsu OKAMURA (Japan-side Chair) and Dr. Mary Ellen HYNES, U.S.-side Chair)
- T/C I Storm Surge and Tsunamis, BFRL Conf. Room A-368, Bldg. 226
Dr. Shigetoshi KOBAYASHI (Japan-side Acting Chair) and Mr. Michael BLACKFORD (U.S.-side Chair)
- T/C J Wind and Earthquake Engineering for Transportation Systems, BFRL Conf. Room B-221 (Bldg. 226)
Dr. Michio OKAHARA (Japan-side Acting Chair) and Dr. Phillip YEN (U.S.-side Acting Chair)
- T/C K Wind and Earthquake Engineering for Offshore and Coastal Facilities, Admin. Bldg. BFRL Conf. Room B-245, Bldg. 224
Dr. Susumu IAI (Japan-side Acting Chair) and Dr. Charles SMITH (U.S.-side Chair)
- New T/C Seismic Information Systems, BFRL Conf. Room B-317, Bldg. 226
Mr. Takaharu KIRIYAMA and Dr. Hideki SUGITA (Japan-side Preliminary Co-Chairs) and Dr. William ROPER and Mr. Stuart NISHENKO (U.S.-side Preliminary Co-Chairs)
- 1715 Conclusion of Day 2
- 1720 Depart NIST by NIST van and Holiday Inn van to Holiday Inn

1745	Travel by NIST bus to the National Academy of Sciences
1830	U.S.-side hosted dinner at Members Room, NAS
2100	Return by bus to Holiday Inn by sightseeing portions of Washington, DC

Thursday 14 May

- 0740 Meet in Lobby of Holiday Inn
0745 Travel by bus to NIST

THEME 3 - EARTHQUAKE ENGINEERING - PART II

0820-1140 Technical Session - Earthquake Engineering-Part II

Chairman: Mr. Yasutake INOUE

- 0820 Development of an Analysis of Structural Steel Fracture and Development of Technical Solution, Hiroyuki YAMANOUCHI, Akiyoshi MUKAI* and Takashi HASEGAWA, BRI
- 0840 Design Guidelines for the Seismic Modification of WSME Buildings, John GROSS*, NIST
- 0900 Draft Manual for Seismic Isolation Design of Underground Structures, Shigeki UNJOH, Jun-ichi HOSHIKUMA*, Kazuhiro NAGAYA and Kazuhiko MURAI, PWRI
- 0920 Comparison Between Affected Populations of Indirect Health Effects after the 1995 Great Hanshin-Awaji Earthquake, Keiko OGAWA*, Ichirou TSUJI, Shigeru HISAMICHI, Tohoku University and Keishi SHIONO, Nagaoka Technology College
- 0940 Discussion
- 1000 **Break**
- 1020 New Framework for Performance-Based Design of Building Structures-Design Flow and Social System, Hisahiro HIRAISHI*, Masaomi TESHIGAWARA, Hiroshi FUKUYAMA, Taiki SAITOH, Wataru GOJO, Hideo FUJITANI, Yuji OHASHI, Izuru OKAWA and Hisashi OKADA, BRI
- 1040 Highway Bridge Seismic Design: How Current Research May Affect Future Design Practices, Ian FRIEDLAND, NCEER, W. Phillip YEN*, FHWA, Ronald L. MAYES, DIS, and John D. O'FALLON, FHWA
- 1100 Development of Performance-Based Design Building Code in Japan-Framework of Structural and Seismic Provisions, Hisahiro HIRAISHI*, Mitsumasa MIDORIKAWA, Masaomi TESHIGAWARA and Wataru GOJO, BRI
- 1120 Discussion
- 1140 **Break**

THEME 4 - SUMMARY RECENT PANEL WORKSHOPS

Chairman: Mr. Yasutake INOUE

1200-1255 Workshop Reports

- 1200 Task Committees B&C, 4th U. S.-Japan Technical Coordinating Committee Meeting on Composite and Hybrid Structural Systems, 12-14 October 1997, Monterey, CA, USA. (Presented by Hisahiro HIRASHI, BRI)
 - 1210 Task Committee E, 1st Workshop on Design for Wind and Wind Hazard Mitigation, 7-9 October 1997, East-West Center, University of Hawaii, HI, USA. (Presented by Joseph GOLDEN, NOAA)
 - 1220 Task Committee F, 7th Workshop on Earthquake Disaster Prevention for Lifeline Systems, 4-5 November 1997, Seattle, WA USA. (Presented by Keiichi TAMURA, PWRI)
 - 1230 Task Committee J, 13th Bridge Workshop, 2-3 October 1997, Tsukuba Japan. (Presented by Phillip YEN, FHWA)
 - 1240 Discussion
 - 1255 Adjourn for lunch
-
- 1300 Lunch: Hosted by Michael ARMSTRONG, Associate Director, Mitigation Directorate, Federal Emergency Management Agency

THEME 5 - REAL TIME INFORMATION ACQUISITION AND DISSEMINATION

Chairman: Mr. Yasutake INOUE

1400-1720 Technical Session - Real Time Information Acquisition and Dissemination

- 1400 American Red Cross/CDC Health Impact Surveillance System for Natural Disasters, Enrique PAZ-ARGANDONA* and Josephine MALILAY, CDC
- 1420 Development of the Disaster Information System (DIS/Earthquakes), Kazuo OKAYAMA, Takaharu KIRIYAMA*, and Seishi YABUUCHI, NLA
- 1440 Recent FEMA Activities in Earthquake Risk Analysis and Mitigation, Stuart NISHENKO* and Gil JAMIESON, FEMA (with a demonstration of HAZUS during the break)
- 1500 Seismic Information System for Civil Infrastructures, Hideki SUGITA*, Tomofumi NOZAKI and Tadashi HAMADA, PWRI
- 1520 Discussion
- 1540 Break

- 1600 New Developments in Seismic Risk Analysis for Highway Systems, Stuart D. WERNER Seismic Systems & Engineering Consultants, Craig E. TAYLOR, Natural Hazards Management Inc., James E. Moore II, University of Southern California, and John B. MANDER, State University of New York at Buffalo, John B. JERNIGAN, Ellers, Oakley, Chester & Rike & Howard H.M. HWANG, Univ. of Memphis
- 1620 Devastation Network in Miura Peninsula, Japan, Makoto WATABE*, Keio University and Satomi HIROKAWA, Yokosuka City
- 1640 Geospatial Analysis Support to Natural Disasters, William ROPER*, CORPS
- 1700 Discussion
- 1720 **Conclusion of Day 3**
- 1725 Return to hotel by van
- 1800 Individual hosted dinners

Friday 15 May

- 0735 Meet in Lobby of Holiday Inn
- 0740 Travel by bus to NIST

THEME 6 - WIND ENGINEERING

Chairman: Dr. Richard WRIGHT

0800-1040 Technical Session - Wind Engineering

- 0800 Analysis of Wind and Wind Effects Revisited - A Case Study of Deer Isle-Sedgwick Bridge, D.W. MARSH and B. BIENKIEWICZ, CSU and Harold BOSCH, FHWA
- 0820 Next Generation Trans-Strait Road Projects and the State of Technology Development, Michio OKAHARA* and Masahiro NISHITANI, PWRI
- 0840 New Hurricane Wind Structures and Wind Speed Measurements, Peter BLACK* and Frank MARKS, NOAA
- 0900 Discussion
- 0920 Consideration on Flutter Characteristics of Super Long-Span Bridges, Hiroshi SATO*, Katsuya OGIHARA and Ken-ichi OGI, PWRI
- 0940 Structural Control Research in the U.S. for Wind and Earthquake Loading, M. P. SINGH*, VPI and T.T. SOONG, State University of NY-Buffalo
- 1000 Wind and Seismic Research for Improved Engineering Consensus Standards and Housing Construction, Jay CRANDELL*, NAHBRC and William FREEBORNE, HUD
- 1020 Discussion
- 1040 Break

THEME 7 - SUMMARY JOINT COOPERATIVE RESEARCH PROGRAMS

Chairman: Dr. Richard WRIGHT

1100-1200 Technical Session - Joint Cooperative Research Programs

- 1100 U.S.-Japan Cooperative Earthquake Engineering Research Program on Composite and Hybrid Structures -Japan Side Plans and Accomplishments, Isao NISHIYAMA, Hiroyuki YAMANOUCHI and Hisahiro HIRAISHI (Building Research Institute) Presented by Akiyoshi MUKAI*, BRI
- 1120 U.S.-Japan Cooperative Earthquake Engineering Research Program on Composite and Hybrid Structures -- U.S.-side Progress, Subhash Goel, Subhash GOEL*, University of Michigan
- 1140 Discussion
- 1200 Break

TASK COMMITTEE REPORTS AND RESOLUTIONS

1215-1255 Report of Task Committees

Chairman: Dr. Richard WRIGHT

T/C A	Strong-Motion Data and Applications
T/C B	Testing and Evaluation Procedures for Building Systems
T/C C	Evaluation and Improvement of Structures
T/C D	Earthquake Engineering for Dams

1255 Adjourn for Lunch

1300 **Lunch:** Hosted by Dr. John FILSON, Acting Coordinator, Earthquake Hazard Program, US Geological Survey, NIST Lunch Club

1400-1520 Report of Task Committees (Continued)

T/C E	Design for Wind and Wind Hazard Mitigation
T/C F	Disaster Prevention Methods for Lifeline Systems
T/C G	Structural Control and Intelligent Materials Systems
T/C H	Soil Behavior and Stability During Earthquakes
T/C I	Storm Surge and Tsunami
T/C J	Wind and Earthquake Engineering for Transportation Systems
T/C K	Wind and Earthquake Engineering for Offshore and Coastal Facilities
New T/C	Seismic Information Systems

1520-1535 Break

1535-1620 Adoption of Final Resolutions

1620-1630 Break

CLOSING CEREMONIES

1630 Call to Order by Noel J. RAUFASTE, Secretary-General, U.S.-Side Panel

Closing Remarks by Yasutake INOUE, Chairman Japan-Side Panel

Closing Remarks by Richard N. WRIGHT, Chairman U.S.-Side Panel

1650 Conclusion of 30th Joint Panel Technical Sessions

1655 Depart NIST by bus to Holiday Inn

1800 Depart Holiday Inn by Bus

1900 Japan-side hosted dinner

2130 Return to hotel by bus

LIST OF PANEL MEMBERS



**30th JOINT PANEL MEETING
JAPAN-SIDE DELEGATION**

Mr. Yasutake Inoue
Director-General,
Public Works Research Institute
Ministry of Construction
1 Asahi, Tsukuba-shi, Ibaraki-ken
305 Japan

Dr. Michio Okahara
Director, Structure and Bridge Department
Public Works Research Institute
Ministry of Construction
1 Asahi, Tsukuba-shi, Ibaraki-ken
305 Japan

Dr. Hiroshi Sato
Head, Structure Division
Public Works Research Institute
Ministry of Construction
1 Asahi, Tsukuba-shi, Ibaraki-ken
305 Japan

Dr. Hideki Sugita
Head, Earthquake Disaster Prevention
Technology Division
Public Works Research Institute
Ministry of Construction
1 Asahi, Tsukuba-shi, Ibaraki-ken
305 Japan

Dr. Keiichi Tamura
Head, Ground Vibration Division
Public Works Research Institute
Ministry of Construction
1 Asahi, Tsukuba-shi, Ibaraki-ken
305 Japan

Dr. Hisahiro Hiraishi
Director, Structural Engineering Department
Building Research Institute
Ministry of Construction
1 Tatehara, Tsukuba-shi, Ibaraki-ken
305 Japan

Mr. Akiyoshi Mukai
Head, Aerodynamics Division
Building Research Institute
Ministry of Construction
1 Tatehara, Tsukuba-shi, Ibaraki-ken
305 Japan

Mr. Keiichi Ohtani
Director, Disaster Prevention Research
Division
National Research Institute for Earth Science
and Disaster Prevention
Science and Technology Agency
3-1 Tennodai, Tsukuba-shi, Ibaraki-ken
305 Japan

Dr. Susumu Iai
Chief, Geotechnical Earthquake Engineering
Laboratory
Port and Harbour Research Institute
Ministry of Transport
3-1-1 Nagase, Yokosuka-shi, Kanagawa-ken
239 Japan

Prof. Makoto Watabe
Environment and Information Department
Keio University
5322 Endo, Fujisawa-shi, Kanagawa-ken
252 Japan

TEMPORARY MEMBERS

Dr. Mitsu Okamura
Senior Research Engineer
Soil Dynamics Division
Public Works Research Institute
Ministry of Construction
1 Asahi, Tsukuba-shi, Ibaraki-ken
305 Japan

Mr. Takao Masui
Senior Planning Officer for Disaster
Prevention
Disaster Prevention Bureau
National Land Agency
1-2-2 Kasumigaseki, Chiyoda-ku, Tokyo
100 Japan

Mr. Takaharu Kiriya
Deputy Director, Earthquake Disaster
Countermeasure Division
Disaster Prevention Bureau
National Land Agency
1-2-2 Kasumigaseki, Chiyoda-ku, Tokyo
100 Japan

Dr. Keiko Ogawa
Division of Public Health
Postgraduate School of Medicine
Tohoku University
2-1 Seiryō, Aoba-ku, Sendai-shi, Miyagi-ken
980-77 Japan

Dr. Shigetoshi Kobayashi
Executive Director, Public Works Research
Center
1-6-4 Taitō, Taitō-ku, Tokyo
110 Japan

Mr. Takashi Sasaki
Senior Research Engineer
Dam Structure Division
Public Works Research Institute
Ministry of Construction
1 Asahi, Tsukuba-shi, Ibaraki-ken
305 Japan

Mr. Kazushige Endo
Senior Research Engineer
Earthquake Disaster Prevention Technology
Division
Public Works Research Institute
Ministry of Construction
1 Asahi, Tsukuba-shi, Ibaraki-ken
305 Japan

Dr. Jun-ichi Hoshikuma
Research Engineer
Earthquake Engineering Division
Public Works Research Institute
Ministry of Construction
1 Asahi, Tsukuba-shi, Ibaraki-ken
305 Japan

JAPAN-SIDE MEMBERSHIP: PANEL ON WIND AND SEISMIC EFFECTS

STEERING COMMITTEE MEMBERS

Mr. Yasukake Inoue
Chairman, Japan-side Panel on Wind and
Seismic Effects
Director-General, Public Works Research
Institute
Ministry of Construction
1, Asahi, Tsukuba-shi, Ibaraki-ken 305-0804
Tel: 0298-64-2821
Fax: 0298-64-2148

Dr. Michio Okahara
Secretary-General, Japan-side Panel on Wind
and Seismic Effects
Director, Structure and Bridge Department
Public Works Research Institute
Ministry of Construction
1, Asahi, Tsukuba-shi, Ibaraki-ken 305-0804
Tel: 0298-64-2211
Fax: 0298-64-0565
E-mail: okahara@pwri.go.jp

Dr. Hisahiro Hiraishi
Director, Department of Structural
Engineering
Building Research Institute
Ministry of Construction
1, Tatehara, Tsukuba-shi, Ibaraki-ken
305-0802
Tel: 0298-64-6633
Fax: 0298-64-6773
E-mail: hiraishi@kenken.go.jp

Dr. Susumu Iai
Chief, Geotechnical Earthquake Engineering
Laboratory
Port and Harbour Research Institute
Ministry of Transport
Nagase, 3-1-1, Yokosuka-shi, Kanagawa-ken
239-0826
Tel: 0468-44-5028
Fax: 0468-44-0839
E-mail: iai@cc.phri.go.jp

Dr. Keishi Ishimoto
Director, Road Department
Civil Engineering Research Institute
Hokkaido Development Agency
1-3, Hiragishi, Toyohira-ku, Sapporo-shi,
Hokkaido 062-0802
Tel: 011-841-5198
Fax: 011-841-9747
E-mail: ishimoto@ceri.go.jp

Dr. Toshio Iwasaki
President, Civil Engineering Research
Laboratory
1-18, Kanda Suda-cho, Chiyoda-ku, Tokyo
101
Tel: 03-3254-9481
Fax: 03-3254-9448

Mr. Takashi Kaminosono
Head, Construction Techniques Division
Department of Production Engineering
Building Research Institute
Ministry of Construction
1, Tatehara, Tsukuba-shi, Ibaraki-ken
305-0802
Tel: 0298-64-6665
Fax: 0298-64-6774
E-mail: kamino@kenken.go.jp

Prof. Kazuhiko Kawashima
Professor, Department of Civil Engineering
Tokyo Institute of Technology
2-12-1, O-okayama, Meguro-ku, Tokyo 152
Tel: 03-5734-2922
Fax: 03-3729-0728
E-mail: kawasima@cv.titech.ac.jp

Mr. Osamu Matsuo
Head, Soil Dynamics Division
Earthquake Disaster Prevention Research
Center
Public Works Research Institute
Ministry of Construction
1, Asahi, Tsukuba-shi, Ibaraki-ken 305-0804
Tel: 0298-64-2933
Fax: 0298-64-2576
E-mail: matsuo@pwri.go.jp

Mr. Chikahiro Minowa
Cooperative Research Officer
National Research Institute for Earth Science
and Disaster Prevention
3-1, Tennodai, Tsukuba-shi, Ibaraki-ken 305
Tel: 0298-51-1611
Fax: 0298-51-5658
E-mail: minowa@geo.bosai.gov.jp

Mr. Yasuyuki Miyamoto
Director, Road Disaster Prevention Section
Road Bureau
Ministry of Construction
2-1-3, Kasumigaseki, Chiyoda-ku, Tokyo 100
Tel: 03-5251-1896
Fax: 03-5251-1949

Mr. Toshitaka Miyata
Director, International Affairs Division
Economic Affairs Bureau
Ministry of Construction
2-1-3, Kasumigaseki, Chiyoda-ku, Tokyo 100
Tel: 03-3580-4311
Fax: 03-3502-3955

Mr. Eishi Mochizuki
Head, Seismology and Volcanology Research
Division
Meteorological Research Institute
Japan Meteorological Agency
1-1, Nagamine, Tsukuba-shi, Ibaraki-ken 305
Tel: 0298-53-8675
Fax: 0298-51-3730

Mr. Yoshinori Murakami
Director, Disaster Countermeasure Office
Coast Administration and Disaster Prevention
Division
Ports and Harbours Bureau
Ministry of Transport
2-1-3, Kasumigaseki, Chiyoda-ku, Tokyo
100-8989
Tel: 03-3580-7021
Fax: 03-5511-8280

Mr. Nobuo Nagai
Director, Geographic Department
Geographical Survey Institute
Ministry of Construction
1, Kitasato, Tsukuba-shi, Ibaraki-ken 305
Tel: 0298-64-2667
Fax: 0298-64-1804
E-mail: nagai@graph.gsi-mc.go.jp

Dr. Nobuyuki Narita
Member of Executive Board, Public Works
Research Center
17-15, Yawata-6, Ichikawa-shi, Chiba-ken
272-0021
Tel: 047-335-0324
Fax: 047-335-0324

Mr. Kazuhiro Nishikawa
Head, Bridge Division
Structure and Bridge Department
Public Works Research Institute
Ministry of Construction
1, Asahi, Tsukuba-shi, Ibaraki-ken 305-0804
Tel: 0298-64-2905
Fax: 0298-64-0565
E-mail: knishika@pwri.go.jp

Dr. Isao Nishiyama
Head, Housing Construction Division
Department of Production Engineering
Building Research Institute
Ministry of Construction
1, Tatehara, Tsukuba-shi, Ibaraki-ken
305-0802
Tel: 0298-64-2151
Fax: 0298-64-6774
E-mail: isao@kenken.go.jp

Mr. Fumiaki Nomura
Director, Office of Disaster Prevention
Research Planning Division
Research and Development Bureau
Science and Technology Agency
2-2-1, Kasumigaseki Chiyoda-ku, Tokyo
100-8966
Tel: 03-3503-8164
Fax: 03-3503-8169

Mr. Keiichi Ohtani
Director, Disaster Prevention Research
Division
National Research Institute for Earth Science
and Disaster Prevention
Science and Technology Agency
3-1, Tennodai, Tsukuba-shi, Ibaraki-ken 305
Tel: 0298-51-1611 ex.321
Fax: 0298-52-8512
E-mail: ohtani@knetgk.k-net.bosai.go.jp

Dr. Hisashi Okada
Associate Director for Composite Structures,
Department of Structural Engineering
Building Research Institute
Ministry of Construction
1, Tatehara, Tsukuba-shi, Ibaraki-ken
305-0802
Tel: 0298-64-6641
Fax: 0298-64-6773
E-mail: okada@kenken.go.jp

Prof. Tsuneo Okada
Professor, Department of Architecture and
Building Engineering
Shibaura Institute of Technology
3-9-14 Shibaura, Minato-ku, Tokyo 108-0023
Tel: 03-5476-2452
Fax: 03-5476-2446

Dr. Izuru Okawa
Head, Building Engineering Division
International Institute of Seismology and
Earthquake Engineering
Building Research Institute
Ministry of Construction
1, Tatehara, Tsukuba-shi, Ibaraki-ken
305-0802
Tel: 0298-64-6758
Fax: 0298-64-6777
E-mail: okawa@kenken.go.jp

Mr. Kazuo Okayama
Director, Earthquake Disaster
Countermeasure Division
Disaster Prevention Bureau
National Land Agency
1-2-2, Kasumigaseki, Chiyoda-ku, Tokyo
100-8972
Tel: 03-3501-5693
Fax: 03-3501-5199

Mr. Hiroshi Sasaki
Director, Building Disaster Prevention Section
Housing Bureau
Ministry of Construction
2-1-3, Kasumigaseki, Chiyoda-ku, Tokyo 100
Tel: 03-3580-4311
Fax: 03-3580-7050

Dr. Hiroshi Sato
Head, Structure Division
Structure and Bridge Department
Public Works Research Institute
Ministry of Construction
1, Asahi, Tsukuba-shi, Ibaraki-ken 305-0804
Tel: 0298-64-2874
Fax: 0298-64-0565
E-mail: hsato@pwri.go.jp

Dr. Shinji Sato
Head, Coast Division
River Department
Public Works Research Institute
Ministry of Construction
1, Asahi, Tsukuba-shi, Ibaraki-ken 305-0804
Tel: 0298-64-2327
Fax: 0298-64-1168
E-mail: sato@pwri.go.jp

Mr. Tatsuyuki Shimazu
International Cooperation Coordinator,
International Affairs Division
Science and Technology Agency
2-2-1, Kasumigaseki, Chiyoda-ku, Tokyo 100
Tel: 03-3593-0362
Fax: 03-3581-5909

Dr. Takahiro Sugano
Chief, Structural Dynamics Laboratory
Structural Engineering Division
Port and Harbour Research Institute
Ministry of Transport
3-1-1, Nagase, Yokosuka-shi, Kanagawa-ken
239-0826
Tel: 0468-44-5029
Fax: 0468-44-0839
E-mail: macsuga@ipc.phri.go.jp

Dr. Yasumasa Suzuki
Director, Hydraulic Engineering Division
Port and Harbour Research Institute
Ministry of Transport
3-1-1, Nagase, Yokosuka-shi, Kanagawa-ken
239-0826
Tel: 0468-44-5009
Fax: 0468-41-3888

Mr. Masaaki Takeuchi
Senior Assistant for Disaster Prevention,
Planning Division
Administration Department
Japan Meteorological Agency
1-3-4, Ohtemachi, Chiyoda-ku, Tokyo 100
Tel: 03-3212-8341 Ext. 2225
Fax: 03-3211-2453

Dr. Keiichi Tamura
Head, Ground Vibration Division
Earthquake Disaster Prevention Research
Center
Public Works Research Institute
Ministry of Construction
1, Asahi, Tsukuba-shi, Ibaraki-ken 305-0804
Tel: 0298-64-2926
Fax: 0298-64-0598
E-mail: tamura@pwri.go.jp

Dr. Masaomi Teshigawara
Head, Structure Division
Department of Structural Engineering
Building Research Institute
Ministry of Construction
1, Tatehara, Tsukuba-shi, Ibaraki-ken 305
Tel: 0298-64-6753
Fax: 0298-64-6773
E-mail: teshi@kenken.go.jp

Dr. Takaaki Uda
Director, River Department
Public Works Research Institute
Ministry of Construction
1, Asahi, Tsukuba-shi, Ibaraki-ken 305-0804
Tel: 0298-64-2211
E-mail: uda@pwri.go.jp

Mr. Tsuneo Uesaka
Director, Dam Department
Public Works Research Institute
Ministry of Construction
1, Asahi, Tsukuba-shi, Ibaraki-ken 305-0804
Tel: 0298-64-2211
Fax: 0298-64-2688

Dr. Shigeki Unjoh
Head, Earthquake Engineering Division
Earthquake Disaster Prevention Research
Center
Public Works Research Institute
Ministry of Construction
1, Asahi, Tsukuba-shi, Ibaraki-ken 305-0804
Tel: 0298-64-2932
Fax: 0298-64-0598
E-mail: unjoh@pwri.go.jp

Dr. Tatsuo Uwabe
Chief, Earthquake Disaster Prevention
Laboratory
Structural Engineering Division
Port and Harbour Research Institute
Ministry of Transport
3-1-1, Nagase, Yokosuka-shi, Kanagawa-ken
239-0826
Tel: 0468-44-5030
Fax: 0468-44-0839
E-mail: uwabe@cc.phri.go.jp

Prof. Makoto Watabe
Professor, Faculty of Environmental
Information
Keio University
5322, Endo, Fujisawa-shi Kanagawa-ken 252
Tel: 0466-47-5111
Fax: 0466-47-5041

Mr. Shoin Yagi
Director, Typhoon Research Department
Meteorological Research Institute
Japan Meteorological Agency
1-1, Nagamine, Tsukuba-shi, Ibaraki-ken 305
Tel: 0298-53-8663
Fax: 0298-53-8735

Dr. Hiroyuki Yamanouchi
Director, Code and Evaluation Research
Center
Building Research Institute
Ministry of Construction
1, Takehara, Tsukuba-shi, Ibaraki-ken
305-0802
Tel: 0298-64-6688
Fax: 0298-64-67701
E-mail: yamanoch@kenken.go.jp

Mr. Joji Yanagawa
Director, Disaster Management Division
River Bureau
Ministry of Construction
2-1-3, Kasumigaseki, Chiyoda-ku, Tokyo 100
Tel: 03-3580-4311 Ext. 3431
Fax: 03-5251-1946

Dr. Masahiko Yasuda
Director, Earthquake Disaster Prevention
Research Center
Public Works Research Institute
Ministry of Construction
1, Asahi, Tsukuba-shi, Ibaraki-ken 305-0804
Tel: 0298-64-2829
Fax: 0298-64-0598
E-mail: m-yasuda@pwri.go.jp

Mr. Hitoshi Yoshida
Head, Fill-type Dam Division
Dam Department
Public Works Research Institute
Ministry of Construction
1, Asahi, Tsukuba-shi, Ibaraki-ken 305-0804
Tel: 0298-64-2413
Fax: 0298-64-0164
E-mail: h-yshida@pwri.go.jp

SECRETARIES COMMITTEE
MEMBERS

Dr. Michio Okahara
Secretary-General, Japan-side Panel on Wind
and Seismic Effects
Director, Structure and Bridge Department
Public Works Research Institute
Ministry of Construction
1, Asahi, Tsukuba-shi, Ibaraki-ken 305-0804
Tel: 0298-64-2211
Fax: 0298-64-0565
E-mail: okahara@pwri.go.jp

Mr. Jiro Fukui
Head, Foundation Engineering Division
Structure and Bridge Department
Public Works Research Institute
Ministry of Construction
1, Asahi, Tsukuba-shi, Ibaraki-ken 305-0804
Tel: 0298-64-2211
Fax: 0298-64-0565
E-mail: fukui@pwri.go.jp

Dr. Hisahiro Hiraishi
Director, Department of Structural
Engineering
Building Research Institute
Ministry of Construction
1, Tatehara, Tsukuba-shi, Ibaraki-ken
305-0802
Tel: 0298-64-6633
Fax: 0298-64-6773
E-mail: hiraishi@kenken.go.jp

Mr. Masakatsu Horino
Head, Planning Division
Geographic Department
Geographical Survey Institute
Ministry of Construction
1, Kitasato, Tsukuba-shi, Ibaraki-ken 305
Tel: 0298-64-5917
Fax: 0298-64-1804
E-mail: horino@graph.gsi-mc.go.jp

Dr. Susumu Iai
Chief, Geotechnical Earthquake Engineering
Laboratory
Port and Harbour Research Institute
Ministry of Transport
3-1-1, Nagase, Yokosuka-shi, Kanagawa-ken
239-0826
Tel: 0468-44-5028
Fax: 0468-44-4095
E-mail: iai@cc.phri.go.jp

Prof. Kazuhiko Kawashima
Professor, Department of Civil Engineering
Tokyo Institute of Technology
2-12-1 O-okayama, Meguro-ku Tokyo 152
Tel: 03-5734-2922
Fax: 03-3729-0728
E-mail: kawasima@cv.titech.ac.jp

Mr. Osamu Matsuo
Head, Soil Dynamics Division
Earthquake Disaster Prevention Research
Center
Public Works Research Institute
Ministry of Construction
1, Asahi, Tsukuba-shi, Ibaraki-ken 305-0804
Tel: 0298-64-2211
Fax: 0298-64-0598
E-mail: matsuo@pwri.go.jp

Mr. Chikahiro Minowa
Cooperative Research Officer
National Research Institute for Earth Science
and Disaster Prevention
3-1, Tennodai, Tsukuba-shi, Ibaraki-ken 305
Tel: 0298-51-1611
Fax: 0298-51-5658
E-mail: minowa@geo.bosai.gov.jp

Mr. Akiyoshi Mukai
Head, Aerodynamics Division
Department of Structural Engineering
Building Research Institute
Ministry of Construction
1, Tatehara, Tsukuba-shi, Ibaraki-ken
305-0802
Tel: 0298-64-6643
Fax: 0298-64-6773
E-mail: mukai@kenken.go.jp

Mr. Kazuhiro Nishikawa
Head, Bridge Division
Structure and Bridge Department
Public Works Research Institute
Ministry of Construction
1, Asahi, Tsukuba-shi, Ibaraki-ken 305-0804
Tel: 0298-64-2905
Fax: 0298-64-0565
E-mail: knishika@pwri.go.jp

Dr. Nobuyuki Ogawa
Head, Earthquake Engineering Laboratory
National Research Institute for Earth Science
and Disaster Prevention
Science and Technology Agency
3-1, Tennodai, Tsukuba-shi, Ibaraki-ken 305
Tel: 0298-51-1611
Fax: 0298-51-5658
E-mail: ogawa@geo.bosai.go.jp

Mr. Keiichi Ohtani
Director, Disaster Prevention Research
Division
National Research Institute for Earth Science
and Disaster Prevention
Science and Technology Agency
3-1, Tennodai, Tsukuba-shi, Ibaraki-ken, 305
Tel: 0298-51-1611 Ext. 321
Fax: 0298-52-8512
E-mail: ohtani@knetgk,k-net,bosai.go.jp

Dr. Hisashi Okada
Associate Director for Composite Structures,
Department of Structural Engineering
Building Research Institute
Ministry of Construction
1, Tatehara, Tsukuba-shi, Ibaraki-ken
305-0802
Tel: 0298-64-6641
Fax: 0298-64-6773
E-mail: okada@kenken.go.jp

Mr. Masami Okada
Head, First Research Laboratory
Seismology and Volcanology Research
Department
Meteorological Research Institute
Japan Meteorological Agency
Ministry of Transport
1-1, Nagamine, Tsukuba-shi, Ibaraki-ken 305
Tel: 0298-53-8677
Fax: 0298-51-3730

Mr. Hidetsugu Onuma
Director, Research Planning and Coordination
Section
Administration Division
Civil Engineering Research Institute
Hokkaido Development Agency
1-3, Hiragisi, Toyohira-ku, Sapporo-shi,
Hokkaido 062
Tel: 011-841-1111
Fax: 011-824-1226
E-mail: h.onuma@ceri.go.jp

Dr. Hiroshi Sato
Head, Structure Division
Structure and Bridge Department
Public Works Research Institute
Ministry of Construction
1, Asahi, Tsukuba-shi, Ibaraki-ken 305-0804
Tel: 0298-64-2874
Fax: 0298-64-0565
E-mail: hsato@pwri.go.jp

Mr. Masashi Sato
Head, Structure Division
Civil Engineering Research Institute
Hokkaido Development Bureau
1-3, Hiragishi, Toyohira-ku, Sapporo-shi,
Hokkaido 062
Tel: 011-841-1111
Fax: 011-820-2714

Dr. Shinji Sato
Head, Coast Division
River Department
Public Works Research Institute
Ministry of Construction
1, Asahi, Tsukuba-shi, Ibaraki-ken 305-0804
Tel: 0298-64-2327
Fax: 0298-64-1168
E-mail: sato@pwri.go.jp

Dr. Hideki Sugita
Head, Earthquake Disaster Prevention
Technology Division
Earthquake Disaster Prevention Research
Center
Public Works Research Institute
Ministry of Construction
1, Asahi, Tsukuba-shi, Ibaraki-ken 305-0804
Tel: 0298-64-3244
Fax: 0298-64-0598
E-mail: sugita@pwri.go.jp

Dr. Keiichi Tamura
Head, Ground Vibration Division
Earthquake Disaster Prevention Research
Center
Public Works Research Institute
Ministry of Construction
1, Asahi, Tsukuba-shi, Ibaraki-ken 305-0804
Tel: 0298-64-2926
Fax: 0298-64-0598
E-mail: tamura@pwri.go.jp

Mr. Nobuyuki Tsuneoka
Head, International Cooperation Division
Planning and Research Administration
Department
Public Works Research Institute
Ministry of Construction
1, Asahi, Tsukuba-shi, Ibaraki-ken 305-0804
Tel: 0298-64-4412
Fax: 0298-64-4322
E-mail: tsuneoka@pwri.go.jp

Dr. Shigeki Unjoh
Head, Earthquake Engineering Division
Earthquake Disaster Prevention Research
Center
Public Works Research Institute
Ministry of Construction
1, Asahi, Tsukuba-shi, Ibaraki-ken 305-0804
Tel: 0298-64-2932
Fax: 0298-64-4424
E-mail: unjoh@pwri.go.jp

Dr. Tatsuo Uwabe
Chief, Disaster Prevention Laboratory
Structural Engineering Division
Port and Harbour Research Institute
Ministry of Transport
3-1-1, Nagase, Yokosuka-shi, Kanagawa-ken
239-0826
Tel: 0468-44-5030
Fax: 0468-44-0839
E-mail: uwabe@cc.phri.go.jp

Dr. Masahiko Yasuda
Director, Earthquake Disaster Prevention
Research Center
Public Works Research Institute
Ministry of Construction
1, Asahi, Tsukuba-shi, Ibaraki-ken 305-0804
Tel: 0298-64-2829
Fax: 0298-64-0598
E-mail: m-yasuda@pwri.go.jp

Mr. Hitoshi Yoshida
Head, Fill-type Dam Division
Dam Department
Public Works Research Institute
Ministry of Construction
1, Asahi, Tsukuba-shi, Ibaraki-ken 305-0804
Tel: 0298-64-2413
Fax: 0298-64-0164
E-mail: h-yshida@pwri.go.jp

ASSOCIATE MEMBERS

Dr. Minoru Fujiwara
Chief Engineer
Road Management Technology Center
9-9, Hisamatsu-cho, Nihonbashi, Chuo-ku,
Tokyo 103-0005
Tel: 03-5695-2711
Fax: 03-5695-2715

Dr. Masami Fukuoka
Honorable Chairman
Public Works Research Center
1-6-4, Taito, Taito-ku, Tokyo 110
Tel: 03-3835-3609

Dr. Masaya Hirose
Professor, Kogakuin University
1-24-2-91, Nishishinjuku, Shinjuku-ku, Tokyo
163
Tel: 03-3342-1211

Dr. Shiro Ibukiyama
President, Kogyokusha College of Technology
5-14-2, Nishigotanda, Shinagawa-ku, Tokyo
141
Tel: 03-3493-5671

Dr. Kaoru Ichihara
President, Public Works Research Center
1-6-4, Taito, Taito-ku, Tokyo 110
Tel: 03-3835-3609

Dr. Ryuichi Iida
President, Japan Dam Engineering Center
2-4-5, Azabudai, Minato-ku, Tokyo 110
Tel: 03-3433-7811

Dr. Takashi Iijima
President, Sekisui-jushi Co., Ltd.
1-11-1, Kaigan, Minato-ku, Tokyo 106
Tel: 03-5400-1850

Dr. Toshio Iwasaki
President, Civil Engineering Research
Laboratory
1-18, Kandasuda-cho, Chiyoda-ku, Tokyo 101
Tel: 03-3254-9481
Fax: 03-3254-9448

Mr. Shunichiro Kamijo
Mitsui Construction Co., Ltd.
3-10-1, Iwamoto-cho, Chiyoda-ku, Tokyo
106
Tel: 03-5223-3921

Mr. Kenji Kawakami
Adviser, Kubota Corporation
3-1-3, Nihonbashi-muromachi, Chuo-ku,
Tokyo 103
Tel: 03-3245-3660

Dr. Eiichi Kuribayashi
Professor, Toyohashi University of
Technology
1-1, Hibarigaoka, Tenpaku-cho,
Toyohashi-shi, Aichi-ken 440
Tel: 0532-44-6967

Mr. Mitsuru Nagao
President, Japan Construction Mechanization
Association
3-5-8, Shibakoen, Minato-ku, Tokyo 105
Tel: 03-3433-1501

Dr. Seiji Nakano
Formerly, Professor, Tokyo Denki University
2-2, Kandanishiki-cho, Chiyoda-ku, Tokyo
101
Tel: 03-5280-3501

Dr. Kazuto Nakazawa
President, Regional Development Consultants
Inc.
1-18, Kandasuda-cho, Chiyoda-ku, Tokyo 101
Tel: 03-3831-2916
Fax: 03-3836-4048

Dr. Nobuyuki Narita
Member of Executive Board, Public Works
Research Center
17-15, Yawata-6, Ichikawa-shi, Chiba-ken
272-0021
Tel: 047-335-0324
Fax: 047-335-0324

Dr. Setsuo Noda
President, Coastal Development Institute of
Technology
3-16, Hayabusa-cho, Chiyoda-ku, Tokyo
102-0092
Tel: 03-3234-5861
Fax: 03-3234-5877

Dr. Shin Okamoto
Director-General, Building Technology
Research Institute
The Building Center of Japan
3-2-2, Toranomom, Minato-ku, Tokyo 105
Tel: 03-3458-1011

Mr. Yoshijiro Sakagami
President, Rinkai Construction Co., Ltd.
2-3-8, Shiba, Minato-ku, Tokyo 105
Tel: 03-3453-4111

Mr. Tadahiko Sakamoto
President, Japan Dam Engineering Center
2-4-5, Azabudai, Minato-ku, Tokyo 110
Tel: 03-3433-7811

Prof. Yasushi Sasaki
Professor, Department of Civil and
Environmental Engineering
Hiroshima University
1-4-1, Kagamiyama, Higashihiroshima-shi,
Hiroshima-ken 739
Tel: 0824-24-7783
Fax: 0824-24-7783
E-mail: yasaki@ue.ipc.hiroshima-u.ac.jp

Dr. Yukihiro Sumiyoshi
Executive Counselor, Nippon Steel Co., Ltd.
2-6-3, Ohte-machi, Chiyoda-ku, Tokyo
100-71
Tel: 03-3275-5868

Mr. Jiro Taguchi
President, Construction Research Institute
11-8, Ohdenma-cho, Nihonbashi, Chuo-ku,
Tokyo 103-0011
Tel: 03-3663-2411
Fax: 03-3633-2417

Dr. Hiroshi Takahashi
Adviser, Engineering Department
Sato Kogyo Co., Ltd.
4-12-20, Nihonbashihon-cho, Cyuo-ku, Tokyo
103
Tel: 03-3661-2296

Dr. Masateru Tominaga
President, Public Works Research Center
1-6-4, Taito, Taito-ku, Tokyo 110
Tel: 03-3835-3609

Dr. Hajime Tsuchida
Executive Counselor, Nippon Steel Co., Ltd.
2-6-3, Ohte-machi, Chiyoda-ku, Tokyo
100-71
Tel: 03-3275-5894

Mr. Seizo Tsuji
Adviser, Road Management Technology
Center
9-9, Hisamatsu-cho, Nihonbashi, Chuo-ku,
Tokyo 103-0005
Tel: 03-5695-2711
Fax: 03-5695-2715

Prof. Makoto Watabe
Professor, Faculty of Environmental
Information
Keio University
5322, Endo, Fujisawa-shi, Kanagawa-ken 252
Tel: 0466-47-5111
Fax: 0466-47-5041

UNITED STATES-SIDE MEMBERSHIP: PANEL ON WIND AND SEISMIC EFFECTS

Dr. Richard N. Wright
Chairman, U.S.-side Panel
Director, Building and Fire Research
Laboratory
National Institute of Standards and
Technology
U.S. Department of Commerce
Gaithersburg, MD 20899
301-975-5900 FAX: 301-975-4032
E-mail: richard.wright@nist.gov

Mr. Noel J. Raufaste
Secretary-General, U.S.-side Panel
Head, Cooperative Research Programs
Building and Fire Research Laboratory
National Institute of Standards and
Technology
U.S. Department of Commerce
Gaithersburg, MD 20899
301-975-5905 FAX: 301-975-4032
E-mail: noel.raufaste@nist.gov

Dr. Daniel P. Abrams
Director, Mid-America Earthquake Center
Hanson Engineers Professor of Civil
Engineering
University of Illinois
1241 Newmark Laboratory
205 North Mathews Avenue
Urbana, IL 61801
244-6302 FAX: 217-333-3821
E-mail: d-abrams@uiuc.edu

Dr. Kharaiti L. Abrol
Principal Structural Engineering Consultant
Room 475
Department of Veterans Affairs
810 Vermont Avenue, NW
Washington, DC 20420
202-565-5579 FAX: 202-565-5478
E-mail: abrkha@hq.med.va.gov

Dr. John Ake
Geophysicist
Seismotectonics and Geophysics Section
Code D-8330
P.O. Box 25007
Bureau of Reclamation
U.S. Department of the Interior
Denver, CO 80225
303-236-4195 x276 FAX: 303-236-9127
E-mail: jake@seismo.usbr.gov

Mr. John Baals
Seismic Safety Coordinator
P.O. Box 25007 (D-8110)
Bureau of Reclamation
U.S. Department of the Interior
Denver, CO 80225
303-236-3999 x534 FAX: 303-236-9099
E-mail: jbaals@do.usbr.gov

Dr. Celso S. Barrientos
Supervisory Physical Scientist
National Environmental Satellite Data
Information Service - Code E/RA28
National Oceanic and Atmospheric
Administration
U.S. Department of Commerce
5200 Auth Road
Camp Springs, MD 20746
301-763-8102 FAX: 301-763-8020
E-mail: cbarrientos@nesdis.noaa.gov

Dr. Eddie N. Bernard
Director, Pacific Marine Environmental
Laboratory
National Oceanic and Atmospheric
Administration
U.S. Department of Commerce
7600 Sand Point Way, NE
BIN C15700/Building 3
Seattle, WA 98115-0070
206-526-6800 FAX: 206-526-6815
E-mail: bernard@pmel.noaa.gov

Mr. Mike Blackford
IOC-NWS/INTERNAL
Tsunami Information Center
737 Bishop Street, Suite 2200
Honolulu, HI 96813-3213
808-689-8207 x301 FAX: 808-689-4543
E-mail: michael.blackford@noaa.gov

Dr. David M. Boore
U.S. Geological Survey
345 Middlefield Road MS 977
Menlo Park, CA 94025
650-329-5616 FAX: 650-329-5163
E-mail: boore@samoa.wr.usgs.gov

Dr. Roger D. Borchardt
Branch of Seismology
U.S. Geological Survey
U.S. Department of the Interior
345 Middlefield Road, MS 977
Menlo Park, CA 94025
650-329-5619 FAX: 650-329-5163
E-mail: borchardt@samoa.wr.usgs.gov

Dr. Mehmet K. Celebi
Research Civil Engineer
Branch of Earthquake and Geomagnetic
Information
U.S. Geological Survey
U.S. Department of the Interior
345 Middlefield Road, MS 977
Menlo Park, CA 94025
650-329-5623 FAX: 650-329-5163
E-mail: celebi@samoa.wr.usgs.gov

Mr. Harish Chander
U.S. Dept. Of Energy (EH-31),
CXXI, Room 2016 (GTN)
19901 Germantown Road
Germantown, MD 20874-1290
301-903-6681 FAX: 301-903-8693
E-mail: harish.chander@hq.doe.gov

Dr. Ken P. Chong
Program Director, Mechanical & Structural
Systems
National Science Foundation
4201 Wilson Boulevard - Room 545
Arlington, VA 22230
703-306-1361 FAX: 703-306-0291
E-mail: kchong@nsf.gov

Dr. Riley Chung
Group Leader, Earthquake Engineering
Structures Division
Building and Fire Research Laboratory
National Institute of Standards and
Technology
U.S. Department of Commerce
Gaithersburg, MD 20899
301-975-6062 FAX: 301-869-6275
E-mail: riley.chung@nist.gov

Mr. James D. Cooper
Chief, Structures Division, HNR-10
Federal Highway Administration
U.S. Department of Transportation
6300 Georgetown Pike
McLean, VA 22101
703-285-2060 FAX: 703-285-2766
E-mail: jim.cooper@fhwa.dot.gov

Mr. William Freeborne
Housing and Urban Development
Room 8132
451 Seventh Street, SW
Washington, DC 20410
202-708-4370 x140 FAX: 202-708-5873
E-mail: william_e._freeborne@hud.gov

Mr. Joseph H. Golden
NOAA/OAR/USWRP
1315 East-West Highway
Room 11554
Silver Spring, MD 20910
301-713-0460, ext.123 FAX: 301-713-1459
202-482-1584
E-mail: joe.golden@noaa.gov

Mr. Peter E. Gurvin
Director, Building Design and Engineering
Division
Foreign Building Operations
Building SA-6, Room 335
U.S. Department of State
Washington, DC 20520
703-875-6117 FAX: 703-875-6204
E-mail: peter.e.gurvin@dos.us-state.gov

Dr. Robert L. Hall
Chief, Structural Analysis Group
U.S. Army Engineer Waterways Experiment
Station
3909 Halls Ferry Road
Vicksburg, MS 39180-6199
601-634-2567 FAX: 601-634-3412
E-mail: hallr3@mail.wes.army.mil

Dr. Walter W. Hays
Earthquake Hazards Reduction Program
U.S. Geological Survey
905 National Center
12201 Sunrise Valley Drive
Reston, VA 20192
703-648-6711 FAX: 703-648-6747
E-mail: whays@usgs.gov

Dr. Allen M. Hittelman
Chief, Solid Earth Geophysics Division
E/GC1, National Geophysical Data Center
NOAA, NESDIS
325 Broadway
Boulder, CO 80303-3328
303-497-6591 FAX: 303-497-6513
E-mail: allen.m.hittelman@noaa.gov

Mr. Larry C. Hultengren
Senior Structural Engineer
Office of Civil/Structural Engineering
Foreign Building Operations
Building SA-6, Room 346
U.S. Department of State
Washington, DC 20520
703-875-6194 FAX: 703-875-6204

Dr. Mary Ellen Hynes
Chief, Earthquake Engineering and
Geophysics Branch
Geotechnical Laboratory
USACE-CEWES-GG-H
3909 Halls Ferry Road
U.S. Army Waterways Experiment Station
Vicksburg, MS 39180
601-634-2280
E-mail: hynesm@ex1.wes.army.mil

Dr. William B. Joyner
Geophysicist
Branch of Seismology
U.S. Geological Survey
U.S. Department of the Interior
345 Middlefield Road, MS 977
Menlo Park, CA 94025
650-329-5640 FAX: 650-329-5163
E-mail: joyner@samoa.wr.usgs.gov

Mr. Roger M. Kenneally
Structural Engineer
Structural and Seismic Engineering Branch
Mail Stop T10-L1
U.S. Nuclear Regulatory Commission
Washington, DC 20555
301-415-6303 FAX: 301-415-5074
E-mail: rmk@nrc.gov

Dr. George Lee
Director, Center for Advanced Technologies
in Earthquake Loss Reduction
State University of New York at Buffalo
Red Jacket Quadrangle
Buffalo, NY 14261
716-645-3391 FAX: 716-645-3399
E-mail: gclee@acsu.buffalo.edu

Dr. H.S. Lew
Structures Division
Building and Fire Research Laboratory
National Institute of Standards and
Technology
U.S. Department of Commerce
Gaithersburg, MD 20899
301-975-6061 FAX: 301-869-6275
E-mail: hsl@nist.gov

Dr. Shih-Chi Liu
Program Director, Structural Systems
Division of Biological and Critical Systems
National Science Foundation
4201 Wilson Boulevard - Room 545
Arlington, VA 22230
703-306-1362 FAX: 703-306-0291
E-mail: slui@nsf.gov

Dr. Josephine Malilay
Disaster Assessment and Epidemiology
Section
National Center for Environmental Health
F-46 Center for Disease Control and
Prevention
4770 Buford Highway, NE
Atlanta, GA 30341
770-488-7295 FAX: 770-488-7335
E-mail: jym7@cehdehl.em.cdc.gov

Dr. Francis G. McLean
Value Engineering Program Manager
Code D-8170
P.O. Box 25007
Bureau of Reclamation
U.S. Department of the Interior
Denver, CO 80225
303-445-3091 FAX: 303-6475
E-mail: FMCLEAN@ibr8gw80.usbr.gov

Dr. Raymond E. Meyer
Department of State
SA14/Room 1705
USAID/Washington, DC 20523-1443
202-712-1078 FAX: 202-216-3707
E-mail: Rmeyer@usaid.gov

Dr. Jack Moehle
Director, Pacific Earthquake Engineering
Research Center
University of California Berkeley
721 Davis Hall
Berkeley, CA 94720-1710
510-231-9554
E-mail: moehle@eerc.berkeley.edu

Mr. Ugo Morelli
Policy Manager
Federal Emergency Management Agency
500 C Street, SW
Washington, DC 20472
202-646-2810 FAX: 202-646-2577
E-mail: ugo.morelli@fema.gov

Dr. Stuart Nishenko
Federal Emergency Management Agency
500 C Street, SW
Washington, D.C. 20472
202-646-3945 FAX: 202-646-4596
E-mail: stuart.nishenko@fema.gov

Mr. Howard D. Nickerson
Earthquake Engineering and Weapons
Specialist
Naval Facilities Engineering Command
Hoffman Building #2, Room 12S63, Code
04B2
200 Stovall Street
Alexandria, VA 22332
202-433-8599 FAX: 202-433-8777
E-mail: howard.d.nickerson@esc61@navfac
nfesc

Mr. Tom Post
Chief, Earthquake Engineering Division
California Department of Transportation
(CALTRANS)
P.O. Box 942873
Sacramento, CA 95814
916-227-8728 FAX: 916-227-8898
E-mail: tpost@trmx3.dot.ca.gov

Dr. Phillip Yen
Federal Highway Administration
6300 Georgetown Pike
McLean, VA 22101
703-285-2315 FAX: 703-285-2766
E-mail: wen-huei.yen@fhwa.dot.gov

Dr. William E. Roper
Director, U.S. Army Topographic Engineering
Center
7701 Telegraph Road
Alexandria, VA 22315-3864
703-428-6600 FAX: 703-428-8154
E-mail: wroper@tec.army.mil

Dr. Charles E. Smith
Research Program Manager
Offshore Minerals Management
Technology Assessment and Research Branch
Minerals Management Service
U.S. Department of the Interior
381 Elden Street, MS 4800
Herndon, VA 20170-4817
703-787-1561 FAX: 703-787-1555
E-mail: smithc@smtp.mms.gov

Dr. T. T. Soong
Deputy Director, Center for Advanced
Technologies in Earthquake Loss Reduction
State University of New York at Buffalo
Red Jacket Quadrangle
Buffalo, NY 14261

Mr. Stanley Strickland
Chief, Air Base Systems Branch
Stop 37, WL/FIVC/OL, Bldg. 1120
139 Barnes Drive, STE 2
Tyndall AFB, FL 32403-6001
904-283-3709 FAX: 904-283-3722
E-mail: stan@mail.interoz.com

ALTERNATE MEMBERS

Dr. Clifford J. Astill
Program Director
Division of Biological and Critical Systems
National Science Foundation
4201 Wilson Boulevard - Room 545
Arlington, VA 22230
703-306-1361 FAX: 703-306-0291
E-mail: castill@nsf.gov

Mr. Michael Changery
Chief, Global Analysis Branch
National Climatic Data Center
National Oceanic and Atmospheric
Administration
U. S. Department of Commerce
Federal Building
Ashville, NC 28801
704-271-4765 FAX: 704-271-4246
E-mail: mchangry@ncdc.noaa.gov

Dr. C.Y. Chen
Senior Civil/Geotechnical Engineer
Office of Foreign Buildings
Department of State
Code SA-6, Rm. 347
Washington, DC 20520
703-875-6207 FAX: 703-875-6204
E-mail: chency@state.gov

Mr. Vincent P. Chiarito
Research Structural Engineer
Structural Mechanics Division
Structures Laboratory
U.S. Army Engineer Waterways Experiment
Station
3909 Halls Ferry Road
Vicksburg, MS 39180-6199
601-634-2714 FAX: 601-634-3412

Dr. James F. Costello
Senior Structural Engineer
Structural and Geological Engineering Branch
Office of Nuclear Regulatory Research
U.S. Nuclear Regulatory Commission
Mail Stop T10-L1
Washington, DC 20555
301-415-6009 FAX: 301-415-5074
E-mail: jfc2@nrc.gov

Mr. Lucian G. Guthrie, P.E.
Structures Branch, Eng. Div.
U.S. Army Corps of Engrs.
UQUSACE (CECW-ED)
Washington, D.C. 20314-1000
202-761-8673 FAX: 202-761-4716
E-mail: civil_works.eng1_postguthrie(Lucian
Guthrie)

Dr. James R. Houston
Director, Coastal Engineering Research
Center
U.S. Army Engineer Waterways Experiment
Station/WESCV-Z
3909 Halls Ferry Road
Vicksburg, MS 39180-6199
601-634-2000 FAX: 601-634-2055
E-mail: houston@coafsl.wes.army.mil

Mr. James Lander
Geophysicist
Cooperative Institute for Research in
Environmental Sciences
University of Colorado
Campus Box 449, Room 152 RL3
3100 Marine Street
Boulder, CO 80309
303-497-6446 FAX: 303-497-6513
E-mail: jlander@ngdc.noaa.gov

Mr. Tingley K. Lew
Research Structural Engineer
Structures Division
Naval Facilities Engineering Service Center -
Code C62
1110 23rd Ave.
Port Hueneme, CA 93043-4370
805-982-1234 FAX: 805-982-1418
E-mail: tlew@nfesc.navy.mil

Mr. Michael Mahoney
Physical Scientist
Federal Emergency Management Agency
500 C Street, SW
Washington, DC 20472
202-646-2794 FAX: 202-646-4387
E-mail: michael.mahoney@fema.gov

Dr. Martin C. Miller
Chief, Coastal Oceanography Branch
USAE, Waterways Experiment Station
Coastal and Hydraulics Laboratory (CEWES-
CR-O)
3909 Halls Ferry Road
Vicksburg, MS 39180
601-634-3999 FAX: 601-634-4314
E-mail: m.miller@cerc.wes.army.mil

Dr. Erdal Safak
Research Structural Engineer
U.S. Geological Survey
Box 25046, MS 966
Denver Federal Center
Denver, CO 80225
303-273-8593 FAX: 303-273-8600
E-mail: safak@usgs.gov

Dr. John B. Scalzi
Program Director, Structures and Building
Systems
National Science Foundation
4201 Wilson Blvd. - Room 545
Arlington, VA 22230
703-306-1361 FAX: 703-306-0291
E-mail: jscalzi@nsf.gov



**PANEL TASK COMMITTEE
MEMBERS**

May 1998

LIST OF TASK COMMITTEE MEMBERS

<u>Task Committee</u>	<u>US Side</u>	<u>Japanese Side</u>
A. Strong-Motion Data and Applications	R.D. Borchardt* C.J. Astill M.K. Celebi W.B. Joyner F.G. McLean C.S. Barrientos T.K. Lew E. Safak +J. Kimball +J. Hunt W. Freeborne J. Ake	S. Iai* K. Tamura N. Nagai Y. Yamanouchi I. Okawa Y. Nakao K. Otani M. Miyata Y. Ichii E. Mochizuki M. Sato
B. Testing and Evaluation Procedures for Building Systems	H.S. Lew* V.P. Chiarito J.E. Sabadell C.E. Smith K. Abrol +S. Sweeney W. Freeborne	K. Ohtani* T. Fukuta T. Kaminosono T. Morino S. Nakata I. Nishiyama H. Noguchi A. Tanaka A. Wada
C. Evaluation and Improvement of Structures	K.P. Chong* +J.O. Jirsa H.S. Lew T.K. Lew H.D. Nickerson +D.H. Oh +M.A. Phipps J.B. Scalzi +S. Woodson +S.A. Asar M.K. Celebi K.L. Abrol R.L. Hall +K. Mutreja +P. Brady W. Freeborne	H. Hiraishi* H. Fukuyama T. Kaminosono A. Mukai M. Nakashima I. Nishiyama K. Nishikawa M. Okahara S. Otani H. Shiobara M. Teshigawara S. Unjoh A. Wada

D. Earthquake Engineering for
Dams

R. Hall*
W.E. Roper
F.G. McLean
L.G. Guthrie
+R. Davidson
+M.E. Hynes
A.G. Franklin
+R. Navidi
+L. Von Thun
+W. Allerton

T. Sasaki*
T. Fujino
Y. Iida
J. Inomata
T. Iwashita
J. Kashiwai
I. Nagayama
S. Nakamura
T. Ohmachi
Y. Ohne
T. Sasaki
S. Takasu
J. Tamura
M. Toyota
T. Uesaka
Y. Wakisaka
K. Watanabe
H. Watanabe
A. Yamagichi
Y. Yamaguchi

E. Design for Wind and Wind
Hazard Mitigation

J. Golden*
+B. Bienkiewicz
+H. Bosch
+G. Chiu
W. Freeborne
+A. Kareem
H.S. Lew
+K. Mehta
+D. Reed
+T. Reinhold
C. Smith
+P. Tertell
A. Chiu
M. Mahoney

T. Okada*
H. Sato*
N. Furuya
H. Kikitsu
K. Kimura
N. Kinoshita
T. Mabuchi
G. Naito
H. Shirato
T. Tamura
Y. Tamura
Y. Uematsu
S. Yagi
H. Yamada

F. Disaster Prevention Methods
for Lifeline Systems

R.M. Chung*
C.J. Astill
M.K. Celebi
J.D. Cooper
+G. Al-Chaar
T.K. Lew
J.B. Scalzi
+S. Wu

M. Yasuda*
M. Hamada
K. Honda
J. Hoshikuma
Y. Kajiya
M. Hamada
K. Honda
J. Hoshikuma

+S. Wu
+S. Sommér

Y. Kajiya
H. Kameda
M. Kaneko
T. Katayama
A. Kinoshita
O. Matsuo
K. Miyamoto
N. Ogawa
M. Ozaki
K. Sasabi
K. Shimamura
S. Takada
K. Tamura
J. Tohma
S. Unjoh
T. Uwabe

**G. Structural Control and
Intelligent Material
Systems**

S.C. Liu*
V.P. Chiarito
K.P. Chong
+J.R. Hayes
L.C. Hultengren
G. Lee

S. Unjoh*
Y. Adachi
K. Asano
Y. Fujino
H. Fukuyama
Y. Goto
H. Iemura
N. Inoue
Y. Inoue
T. Ishimaru
K. Kawashima
M. Kitazawa
H. Kosaka
Y. Makiguchi
C. Minowa
T. Moriya
A. Nishitani
H. Okada
S. Okamoto
A. Ogawa
M. Sato

**H. Soil Behavior and Stability
During Earthquakes**

M.E. Hynes*
C.J. Astill
R.D. Borchardt
C.Y. Chen
F.G. McLean
C.E. Smith

O. Matsuo*
J. Fukui
S. Iai
M. Iiba
H. Kobayashi
J. Koseki

R.M. Chung
+M.E. Hynes
+J.P. Koester
+R.H. Ledbetter

C. Minowa
J. Nishikawa
M. Okamura
T. Sugano
H. Suzuki
K. Tamura
I. Tohata
J. Tohma
Y. Yamaguchi
M. Yasuda
S. Yasuda
H. Yoshida
K. Zen

I. Storm Surge and Tsunami

M. Blackford*
C.J. Astill
C.S. Barrientos
E.N. Bernard
J. Lander
W.E. Roper
A.M. Hittelman

S. Sato*
S. Akeda
T. Goto
S. Iwasaki
K. Kawata
T. Konishi
K. Minami
T. Nagai
T. Nakayama
M. Okada
T. Sasajima
K. Satake
N. Shuto
T. Yamashita

J. Wind and Earthquake Engineering for Transportation Systems

J.D. Cooper*
J.B. Scalzi
H.S. Lew
J.B. Scalzi
P. Yen
+H.R. Bosch

K. Nishikawa*
Y. Fujino
N. Furuya
J. Fukui
T. Inatomi
M. Ishida
K. Kawashima
Y. Kimura
M. Kitazawa
Y. Nakao
H. Kosaka
T. Moritani
J. Murakoshi
A. Ogawa
K. Ogiwara
M. Okahara
H. Sato

M. Sato
Y. Tanaka
T. Terayama
K. Tamura
S. Unjoh
M. Yasuda

K. Wind and Earthquake Engineering C.E. Smith*
for Offshore and Coastal Facilities C.S. Barrientos
W.E. Roper
J.E. Sabadell
+M.C. Miller
M.K. Celebi

T. Uwabe*
J. Fukui
S. Iai
M. Kazama
S. Noda
A. Nozu
M. Okada
H. Shiojiri
T. Sugano
H. Tsuchida
Y. Yoshida

* Chairman
+ TC Members (not Panel Members)



RESOLUTIONS

RESOLUTIONS OF THE THIRTIETH JOINT MEETING U.S.-JAPAN PANEL ON WIND AND SEISMIC EFFECTS (UJNR)

National Institute of Standards and Technology, Gaithersburg, MD
12-15 May 1998

The following resolutions are hereby adopted:

1. The Thirtieth Joint Panel Meeting provided the forum to exchange valuable technical information that is beneficial to both countries. In view of the importance of cooperative programs on the subject of wind and seismic effects, the continuation of Joint Panel Meetings is considered essential.
2. The following activities have been conducted since the Twenty-Ninth Joint Meeting:
 - a. Technology Exchanges. Technical experts, technical documents, and applications of the electronic media have been exchanged. These exchanges have contributed to the development of new research programs and enhanced ongoing research in both countries.
 - b. Task Committee Workshops. The Panel held four workshops/committee meetings and technical site visits; more than 200 specialists from both countries participated in these activities:
 1. Task Committees (B&C), 4th U. S.-Japan Technical Coordinating Committee Meeting on Composite and Hybrid Structural Systems, 12-14 October 1997, Monterey, CA, USA.
 2. Task Committee (E), 1st Workshop on Design for Wind and Wind Hazard Mitigation, 7-9 October 1997, East-West Center, University of Hawaii, HI, USA.
 3. Task Committee (F), 7th Workshop on Earthquake Disaster Prevention for Lifeline Systems, 4-7 November 1997, Seattle, WA, USA.
 4. Task Committee (J), 13th Bridge Workshop, 2-3 October 1997, Tsukuba, Japan.
 - c. Common Agenda. The Panel recognizes the importance of providing earthquake science and technology expertise to the 17 April 1996 U.S.-Japan Natural Disaster Reduction Initiative of the U.S.-Japan Framework for New Economic Partnership (Common Agenda). Panel members organized and participated in the Second Earthquake Policy Symposium (EPS), 17-19 September 1997, Kobe, Japan and reviewed over 40-proposals for the Earthquake Disaster Mitigation Partnership (EDMP). The Panel will continue to provide in close cooperation with EDMP technical leadership and participation in the next EPS phase -- First High-Level Forum Meeting that will address three themes: 1. Development and Use of Real-Time Seismic Information Systems; 2. Development and Use of Loss Estimation Models; and 3. Post-Earthquake Response and Recovery Policies. Appropriate Task Committees will respond to the Common Agenda in planning their work.

3. The Panel approved the consolidation of Task Committees (C) and (G) into Task Committee (C). The Panel approved the establishment of a new Task Committee on Seismic Information Systems T/C (G).
4. The Panel will continue to seek methods to contribute to the International Decade for Natural Disaster Reduction (IDNDR) such as disseminating Proceedings of Joint Panel Meetings and of Task Committee Workshops to appropriate organizations of the IDNDR.
5. The Panel approved the Task Committee reports presented during the 30th Joint Panel Meeting. Each report included objectives, scope of work, accomplishments, future plans, and other information. The Panel will continue to review the Task Committees' progress toward meeting their objectives; consolidating, eliminating, and/or creating Task Committees as desirable.
6. The Panel endorses the following ten (10) proposed Task Committee Workshops/Committee Meetings during the coming year:
 - a. Task Committee (A), Workshop on Soil-Structure Interaction, September 1998 in USA.
 - b. Task Committee (B), 1st Workshop on Test Procedure, Documentation, Retrieval of Test Data, and Experimental Facilities, 1999, location to be determined.
 - c. Task Committee (B&C), 5th U.S.-Japan Technical Coordinating Committee Meeting on Composite and Hybrid Structural Systems, October 1998, Japan.
 - d. Task Committee (B&C), 20-year Commemoration Symposium on Cooperative Earthquake Engineering Research, October 1998, Tokyo.
 - e. Task Committee (C), Workshop on Smart Structural Systems, May 1998, Sonoma, CA, and Fall 1998, (to be determined), USA.
 - f. Task Committee (D), 2nd Workshop on Earthquake Engineering for Dams, in conjunction with the 31st Joint Panel Meeting, May 1999, Japan.
 - g. Task Committee (E), 2nd Workshop on Design for Wind and Wind Hazard Mitigation, Fall 1998, Japan.
 - h. Task Committee (H), Workshop on Soil Dynamics Studies by Centrifuge, 28-29 September 1998, Tsukuba, Japan.
 - i. Task Committee (I), 5th Tsunami Workshop, July 1998, Sapporo, Japan.
 - j. Task Committee (J), 14th Bridge Workshop, November 1998, Pittsburgh, PA .

Scheduling for the Workshops will be done by the U.S. and Japan Chairmen of the respective Task Committees with concurrence of the Joint Panel Chairmen. Both sides' Secretaries-General will be kept informed of the planning. Results of each activity conducted before the 31st Joint Meeting will be presented at the 31st Joint Panel Meeting.

7. The Panel recognizes the importance of continuing its joint research programs on Soil Liquefaction and Countermeasures and on Smart Structural Systems.
8. The Panel recognizes the importance of conducting research in the area of public health following natural disasters and recommends the subject be featured in the 31st Joint Panel Meeting.

9. The Panel will seek methods to contribute to the International Organization for Standardization (ISO) through participation of its members and related agencies in appropriate ISO Technical Committees.
10. The Panel published its fifth newsletter issue, *Wind and Seismic Effects*, Winter 1998. The newsletter featured articles on the 29th Joint Panel Meeting; the 2nd U.S.-Japan Earthquake Policy Symposium; the 1st U.S.-Japan Workshop on Design for Wind and Wind Hazard Mitigation; highlights of new Japanese laboratory facilities following the Kobe Earthquake; and a highlight of the National Research Institute for Earth Science and Disaster Prevention and the U.S. Geological Survey. The Panel endorses continuing the publication of the Panel's newsletter. The U.S.-side will publish the sixth newsletter during the winter of 1998-99.
11. The National Institute of Standards and Technology (NIST) will maintain the Panel's Web Site on an interim basis. The five Panel newsletters were added to the Web Site. The Panel encourages all members from both sides to use electronic media, as much as possible, in communicating Panel findings and summaries of its activities. The Web Site URL address is: <http://www.bfrl.nist.gov/info/ujnr/ujnr1.html>.
12. The Panel recognizes the importance of continued exchange of personnel, technical information, research results, and recorded data that lead to mitigating losses from strong winds and earthquakes. The Panel also recognizes the importance of using available large-scale testing facilities and other complementary capabilities in both countries. Thus, these activities should be continued, strengthened, and expanded. The Panel will provide official endorsement to facilitate these exchanges.
13. Thirty-First Joint Panel Meeting of the UJNR Panel on Wind and Seismic Effects will be held at the Public Works Research Institute, Tsukuba, Japan in May 1999. Specific dates, program, and itinerary will be proposed by the Japan-side with concurrence of the U.S.-side Panel.

**SPECIAL SESSION in CELEBRATION
of the PANEL'S 30th ANNIVERSARY**

Natural Disasters and Protective Measures in Japan

by

Yasutake Inoue*

ABSTRACT

As a country that suffers frequent natural disasters, Japan applies lessons learned from these experiences to the tasks of providing disaster protection facilities and improving the disaster resistance of infrastructures, but the Hanshin - Awaji Earthquake Disaster (January 1995) taught that because it is difficult to prevent all disasters from occurring, it is essential to accept that disasters will occur and to provide crisis management type disaster protection measures that minimize the damage that they cause. This report describes measures and technological research undertaken in order to supplement existing hardware measures involving the construction of disaster protection facilities with new software measures: those intended to provide crisis management capabilities.

Key words: Natural Disaster, Crisis Management, Disaster Protection Measure, Minimization of Damage, Seismic Safety Level, Seismic Information System.

1. INTRODUCTION

Hardly a year passes without a disaster occurring somewhere in Japan as a consequence of harsh natural conditions that make it one of the world's most disaster prone nations along with the high concentration of land use in a few small regions of the country. This report introduces examples of some recent disasters. It also discusses issues that construction administrators must address in response to the Hanshin - Awaji Earthquake Disaster (January 1995), and topics that will be the object of future technological research as an example of earthquake resistance measures.

2. NATURAL CONDITIONS, NATIONAL LAND USE PATTERNS AND NATURAL DISASTERS IN JAPAN

(1) Natural Conditions and National Land Use Patterns in Japan

Japan is a nation with many hills and mountains and generally precipitous topography, is drained by rivers that are shorter and steeper than those in other nations, and has an extremely long coastline in relation to its total land area. And geographically, it is part of the circum-pacific volcanic and earthquake zones and one of the most volcanic and earthquake activity prone nations in the world. Its geology features large faults and fracture zones and many places with weak geological structures. Climatic features of Japan include its position in the path of numerous typhoons and heavy winter snow accumulation in large areas of the country.

In addition to the harsh topographical, geographical, geological, and meteorological natural conditions found in Japan, about 50% of its population and 75% of its total productive activities are concentrated in inundation zones (regions lower than the river water level during the flood period) on alluvial planes covering no more than about 10% of the total national land. On top of this, advancing urbanization has been accompanied by the growing residential use of regions consisting of low swampy land, alluvial fans, precipitous slopes, and other ground with a high latent risk of natural disasters.

In addition to these natural conditions and this pattern of national land use, hardly a year passes without a natural disaster occurring somewhere in Japan as a result of typhoons,

* Director-General of Public Works Research Institute, Ministry of Construction, Asahi 1, Tsukuba-shi, Ibaraki-ken, 305-0804 Japan

extremely heavy rainfall, earthquakes, or volcanic eruptions.

(2) Natural Disasters

Figure 1 shows the numbers of fatalities and missing persons caused by natural disasters in recent years organized by the cause of the disasters. It reveals that frequent storm and flood damage caused by typhoons and heavy rainfalls are the cause of fatalities etc. almost every year, and that many people died or disappeared as a result of the Hokkaido Nansei-oki Earthquake (1993) and the Hanshin - Awaji Earthquake Disaster (Hyogo-ken Nanbu Earthquake: 1995).

Table 1 presents representative examples of each of the wide variety of disasters that occur in Japan.

3. LESSONS TAUGHT BY THE HANSHIN - AWAJI EARTHQUAKE DISASTER

To prepare for natural disasters that occur almost every year, we have systematically and continually carried out river improvement, dam construction, coastline preservation, landslide disaster prevention, road disaster prevention, and urban disaster protection projects in an effort to make Japan a safer place to live. To take changes to bridge technology standards as an example of earthquake resistance measures, as shown in Table 2, the Kanto Earthquake was followed by the introduction of design accounting for earthquakes so that it would be possible to design bridges able to withstand a similar earthquake. These standards were reassessed again following the later Niigata Earthquake and Miyagi-ken-oki Earthquake. In this way, we have continually taken advantage of our experiences with natural disasters to provide the capacity required to protect bridges from their effects.

But the Hanshin - Awaji Earthquake Disaster that struck the Kinki Region of Japan, a part of the country spared serious earthquakes for many decades and one believed to be relatively safe, resulted in damage on a scale that exceeded our expectations. By starting fires in districts with highly concentrated wooden housing and by cutting off lines supplying

essential services, it dealt a severe blow to the lives of the residents of the disaster region. It also cut traffic networks, with severe repercussions on productive activities both within and outside of Japan.

These events have taught us not only that present science can not necessarily be used to predict the exact time and location of a powerful earthquake, particularly a shallow intraplate earthquake under the land, but that the power of an earthquake can exceed any experienced in the past and that changes both in urban environments and in transportation and other features of the socioeconomic environments both within and outside of Japan mean there is a risk that a powerful earthquake can inflict terrible harm on human society.

4. ISSUES IN FUTURE CONSTRUCTION ADMINISTRATION

With the "creation of national land where people can be safe and secure" as one of the principal themes of construction administration in Japan, we have continually striven to reduce nature's ferocity by, for example, improving flood control and erosion prevention measures along with urban disaster protection measures, and strengthening the earthquake resistance of public works structures, homes, and buildings. But the Hanshin - Awaji Earthquake Disaster has taught us that in addition to improving disaster prevention facilities intended to keep such disasters from occurring, it is also important that we accept that it is impossible to prevent all disasters, and assuming that they will eventually occur, prepare for them by providing measures to minimize the damage they inflict. So as described below, it is essential that hardware measures be accompanied by efforts to create crisis management type disaster protection measures: software measures such as the provision of systems to provide information concerning disasters and strengthened coordination between concerned administrative bodies.

(1) Establishment of Regionally Managed Crisis Management Systems

To minimize the damage that disasters cause, the provision of disaster prevention facilities will be accompanied by risk management measures implemented at normal times in preparation for disasters: the clarification of the distribution of roles between concerned organizations, private companies, and residents (regional government bodies, fire fighting and flood response teams), and the complete distribution of hazard maps (Figure 2) etc. In addition, crisis management measures including the distribution of disaster information and the implementation by volunteers and others of various support activities will be carried out to reduce the damage after a disaster occurs.

(2) Switch-over to Facility Improvement for Damage Reduction

Taking levees as an example of this change in the basic concept guiding disaster protection facility provision, rather than being considered to be structures that must prevent flooding from ever occurring, it will be assumed that disasters are inevitable and levees will be treated as structures intended to minimize damage by, for example, emphasizing the prevention of extremely severe damage when a levee does break.

And past hardware measures to prevent landslides and debris flows that cause frequent fatal disasters, will be supplemented by software measures: providing belts of trees as buffer zones, strengthening regulations governing risk areas, and so on (Figure 3).

(3) Provision of Comprehensive Disaster Protection Measures for Urban Areas

With a large proportion of Japanese population and assets and most of its economic and social activities concentrated in its cities, in order to prevent the paralysis of the economic and public functions of the country, and to improve safety during large scale disasters, comprehensive large scale damage prevention measures will be undertaken by both the hardware and software sides: reinforcing the disaster resistance of housing and infrastructures and improving over-concentrated urban districts.

And to permit the rapid and smooth

restoration of the daily lives of the people along with economic and public life following a disaster, emergency roadways to replace wide area arterial roads, wide area disaster protection bases, emergency transport routes, etc. will be provided at the same time as multiutility tunnels are constructed to improve the disaster resistance of lifelines used to supply city dwellers with essential services (Figure 4).

5. TOPICS FOR FUTURE TECHNOLOGICAL RESEARCH

To minimize the damage caused by natural disasters, research on a number of technologies must be undertaken. This section of this report describes a number of technological research areas related to protection from earthquake disaster. The concepts on which this selection is based also apply to other types of disasters.

(1) Improving the Earthquake Resistance of Structures

The most basic category of technological research that is required is the search for ways to improve the earthquake resistance of civil infrastructures. Large scale centrifuge and large scale three-dimensional shaking table (Photograph 1) that have been recently installed will be used to conduct research into seismic design and retrofit technology.

(2) Earthquake Disaster Loss Estimation Methodology

In order to more efficiently conduct projects to increase the earthquake resistance of civil infrastructures, research will be conducted to find ways to quantitatively assess the loss caused by credible earthquakes and the effects of earthquake resistance improvement projects. These will enable to set the seismic safety level rationally, and to prioritize economical projects based on the cost - benefits analysis (Figure 5).

(3) Coordination of Seismic Safety Levels of Urban Infrastructures

Research to achieve coordination of seismic safety levels for the various kinds of infrastructures that constitute an urban area will

be carried out. The results will, by reflecting the role of infrastructures in each region and the effects of earthquake resistance improvement projects, enable to improve the seismic safety of overall cities (Photograph 2).

(4) Seismic Information Systems

In addition to providing structures with appropriate earthquake resistance, it is necessary to develop technology needed to implement efficient crisis management. Research to develop seismic information systems including early damage estimation technology, damage monitoring technology, and data communication technology will allow facility managers to take effective emergency action such as the temporary repair works on arterial roads immediately after the disaster (Figure 6).

6. SUMMARY

At the same time as the needs for infrastructures are diversifying, finding ways to skillfully utilize the nation's resources including its limited budget, housing stock, and infrastructures stock, has become a serious problem in the face of severe financial conditions, the aging of the population, the falling birth rate, the growing value attached to the natural environment and to the global environment, and other problems. In the future, the provision of hardware, new protective structures and the like, is sure to take longer than it does now, and it will be essential to adopt comprehensive measures that emphasize the software approach. This is a switch from "national land construction" to "national land management (improvement, use, preservation)." It will also be necessary to introduce more and better software measures to deal with the threat of natural disasters.

REFERENCES

- 1) Ministry of Construction : Construction White Paper , 1995
- 2) National Land Agency : Disaster Prevention White Paper , 1993,1994,1997

Table 1. Representative Disasters

Disaster Category	Location	Time	Description
Volcanic Disaster	Unzen Fugendake Mountsain in Nagasaki Prefecture	June 3, 1991	The eruption and increasing level of activity of Fugendake resulted in the repeated formation of lava domes that grew and collapsed, causing a series of pyroclastic flows followed by the formation of another lava dome and so on. A pyroclastic flow that occurred on June 3 killed 40 people and 3 more people went missing and have never been found.
Windblown tree disaster	In 30 prefectures, but mainly in those in Kyushu	September, 1991	Storm generated by typhoons 17, 18, and 19 knocked down and damaged trees. The damage to privately owned woodlots covered 60,000 hectares.
Earthquake disaster (Hanshin - Awaji Earthquake Disaster)	Centered in the Hanshin Region	January 17, 1995	A magnitude 7.2 earthquake (Hyogo-ken Nanbu Earthquake) occurred with its hypocenter 14 kilometers below the northern part of Awaji Island. A total of 6,425 people were killed, 2 went missing, and 43,772 people were injured. A total of 110,457 homes were totally destroyed and 147,433 more were partially damaged. Transportation routes, harbor facilities, and other infrastructure items were damaged along with lines carrying essential services such as water, communication lines, electricity, etc.
Rock Failure	The Toyohama Tunnel at Furubira in Hokkaido	March 20, 1996	A massive rock (about 11,000 m ³) collapsed on top of the portal of the Toyohama Tunnel. One bus and two passenger cars were destroyed. A total of 20 people were killed and 1 injured.
Debris Flow Disaster	The Harihara River at Izumi City in Kagoshima Prefecture	July 10, 1997	A stationary early summer rain front caused the a debris flow (about 200,000 m ³). A total of 21 people died, 13 were injured, and 16 buildings were damaged.

Note. These are representative examples of recent disasters of various kinds. Many other disasters have actually occurred, but they are not listed on this table.

Table 2. Reflection of Earthquake Disasters in Technical Standards for Bridges

Earthquake	Principal Damage	Reflection in Technical Standards for Bridges and Elevated Highways
1923 Kanto Earthquake Disaster (M 7.9)	Fatalities: 99,331 Injuries: 103,733 Buildings destroyed: 128,266	Details of Road Structure (draft) "Stipulated that design should account for earthquake" (1926)
"Based on surveys and research concerning design earthquake force"		Design Specifications of Steel Highway Bridges "Specifically stipulated design seismic coefficients" (1939)
1964 Niigata Earthquake (M 7.5)	Fatalities: 26 Injuries: 447 Buildings destroyed: 1,960	Specifications for Seismic Design of Highway Bridges "Stipulated the installation of falling-off prevention systems" "Stipulated the assessment of soil liquefaction" (1971)
1978 Miyagi-ken-oki Earthquake (M 7.4)	Fatalities: 28 Injuries: 11,208 Buildings destroyed: 1,383	"Part V: Seismic Design" in "Design Specifications of Highway Bridges" "Stipulated the design of the terminal point of longitudinal reinforcement (elongation of the anchor length of steel reinforcing rods)" "Expansion of the quantity of hoop tie reinforcement (minimum hoop tie steel diameter from 6 mm to 13 mm)" (1980)
"Based on surveys and research concerning the dynamic bearing strength and deformation performance of reinforced concrete bridge piers"		"Part V: Seismic Design" in "Design Specifications of Highway Bridges" "Stipulated an examination of the ultimate horizontal strength during an earthquake for reinforced concrete bridge piers" (1990)
1995 Hanshin - Awaji Earthquake Disaster (Hyogo-ken Nanbu Earthquake: M 7.2)	Fatalities: 6,425 Missing: 2 Injuries: 43,772 Buildings destroyed: 110,457	"Part V: Seismic Design" in "Design Specifications of Highway Bridges" "Stipulated design earthquake force accounting for earthquake motion caused by the Hyogo-ken Nanbu Earthquake" "Stipulated seismic design based on the ultimate horizontal strength during an earthquake method for structural members strongly effected by earthquakes" (1996)

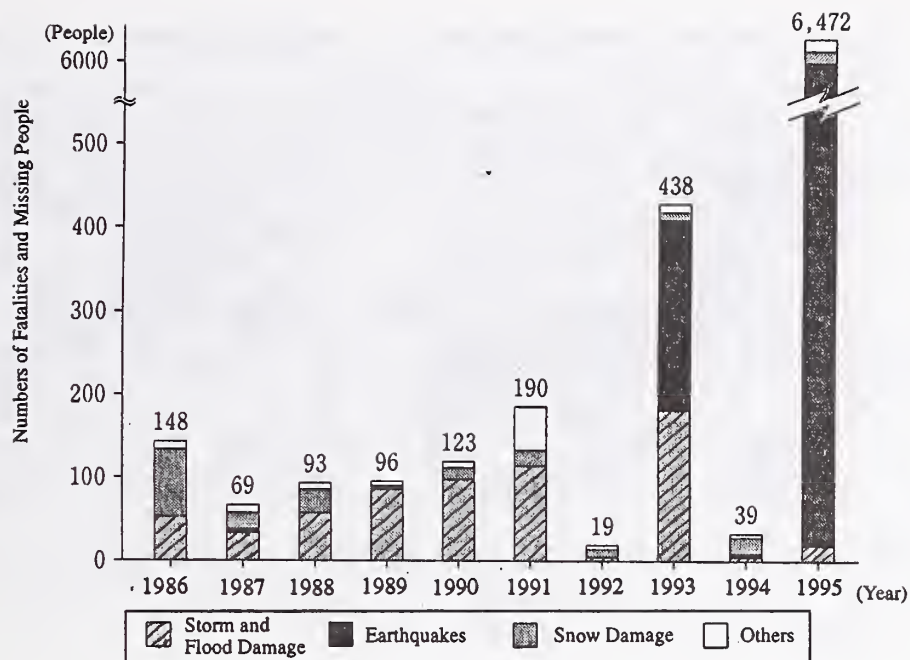


Figure 1. Fatalities and Missing People by Cause of Disaster

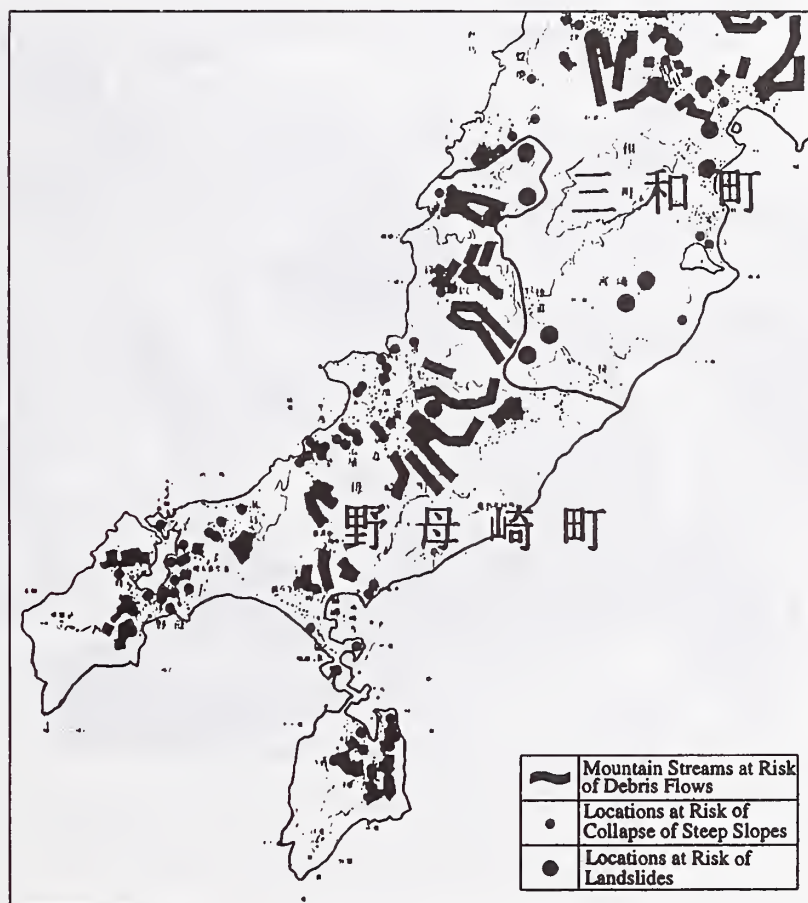
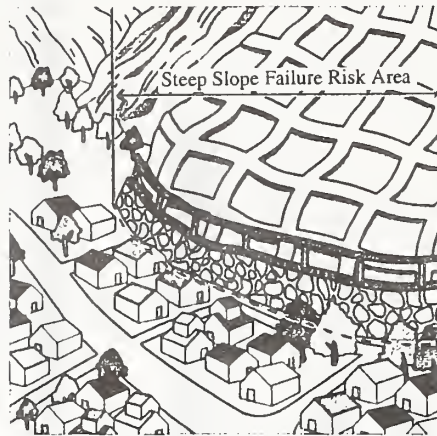


Figure 2. Hazard Map

Conventional Slope Protection Measure



New Slope Protection Measures

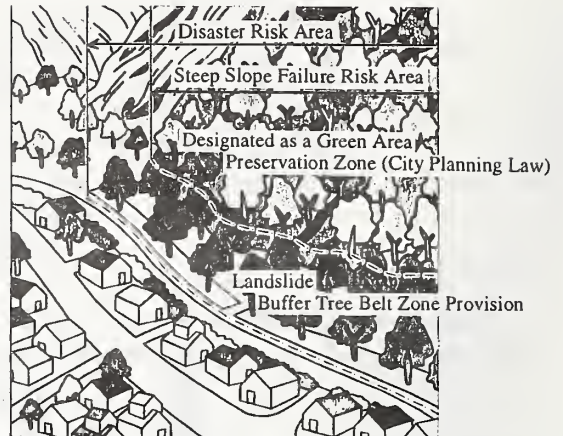


Figure 3. Provision of Buffer Tree Belts and Strengthening of Regulations for Risk Areas

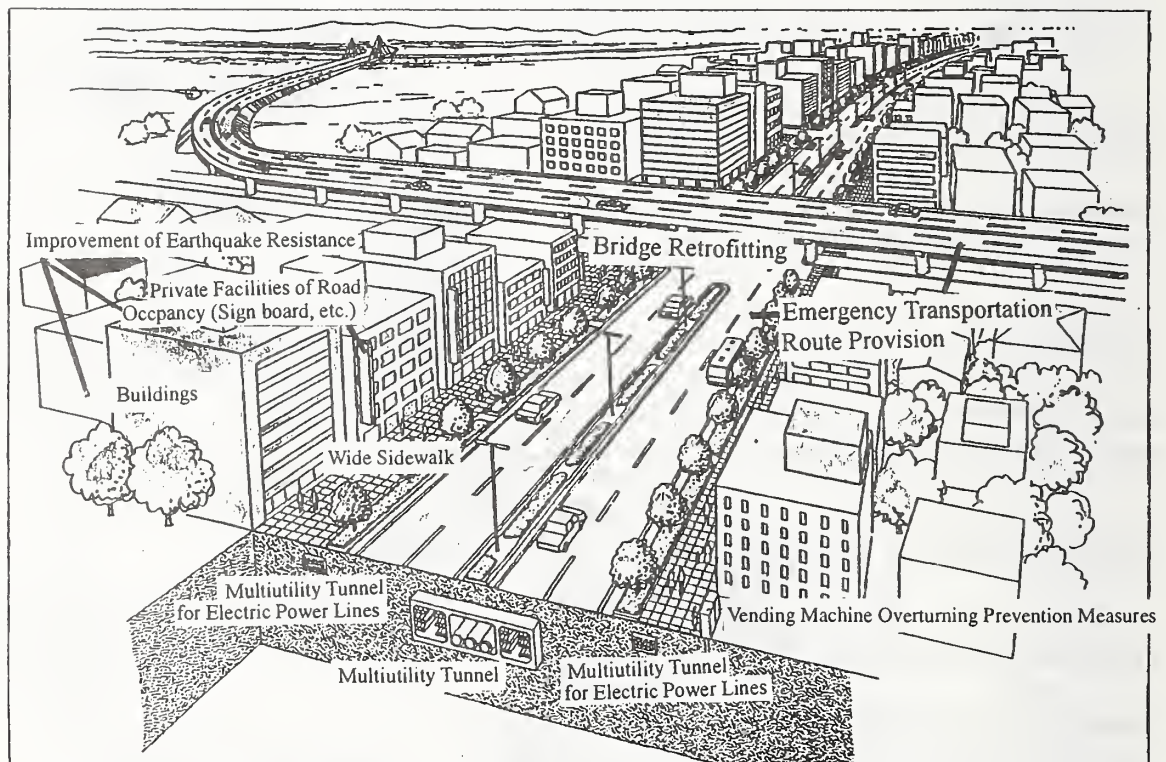


Figure 4. Improvement of Disaster Protection by Providing Emergency Transportation Routes

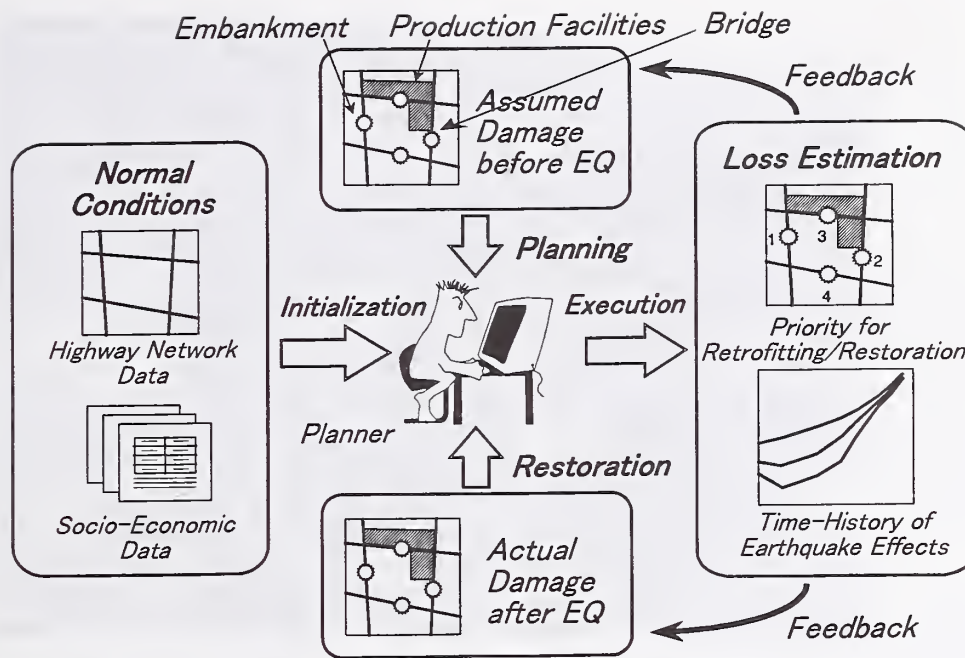


Figure 5. Loss Estimation for Pre-/Post Earthquake Risk Management

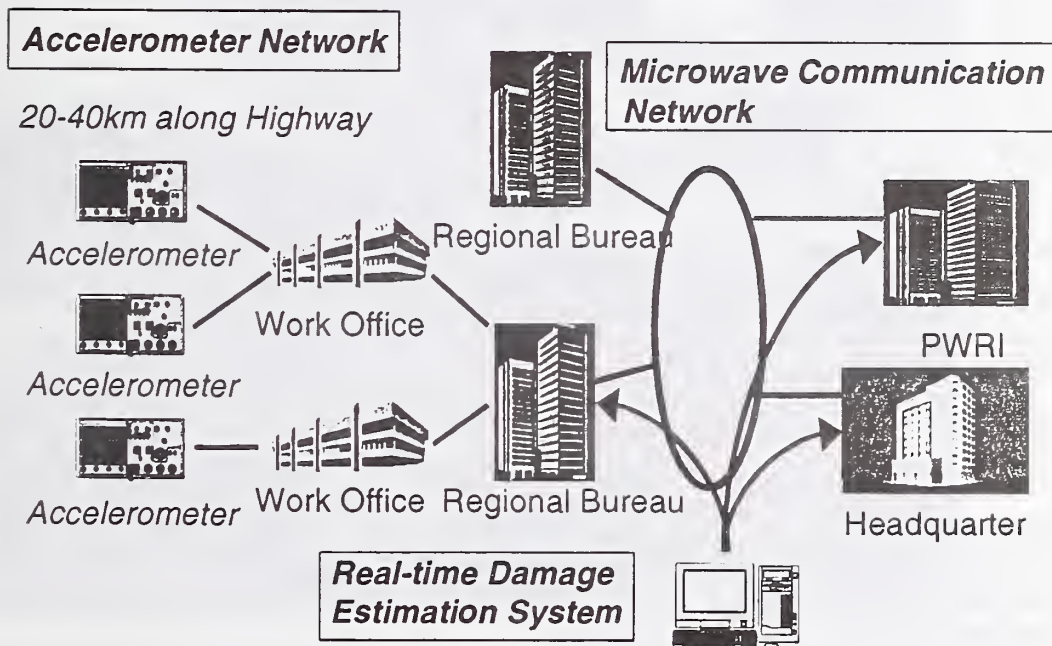
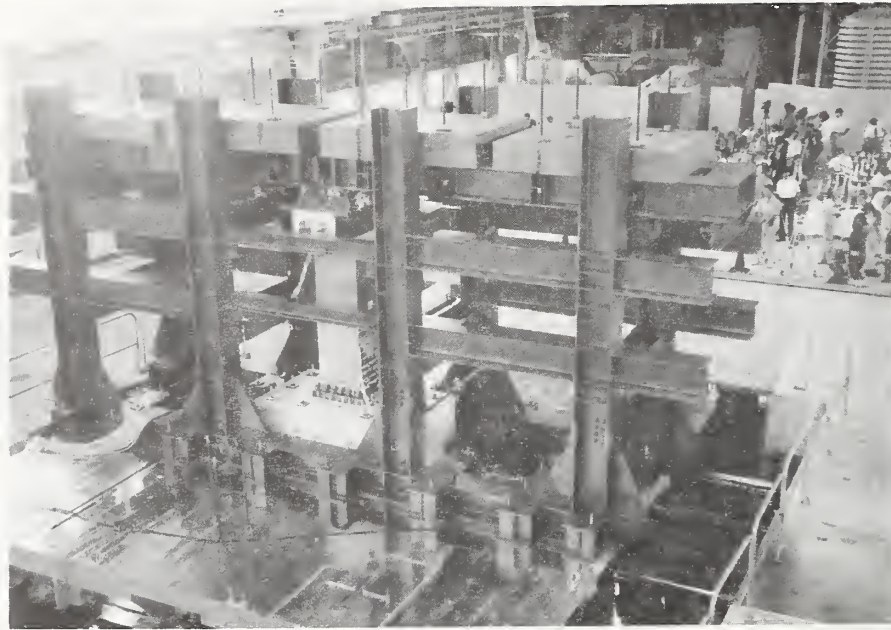
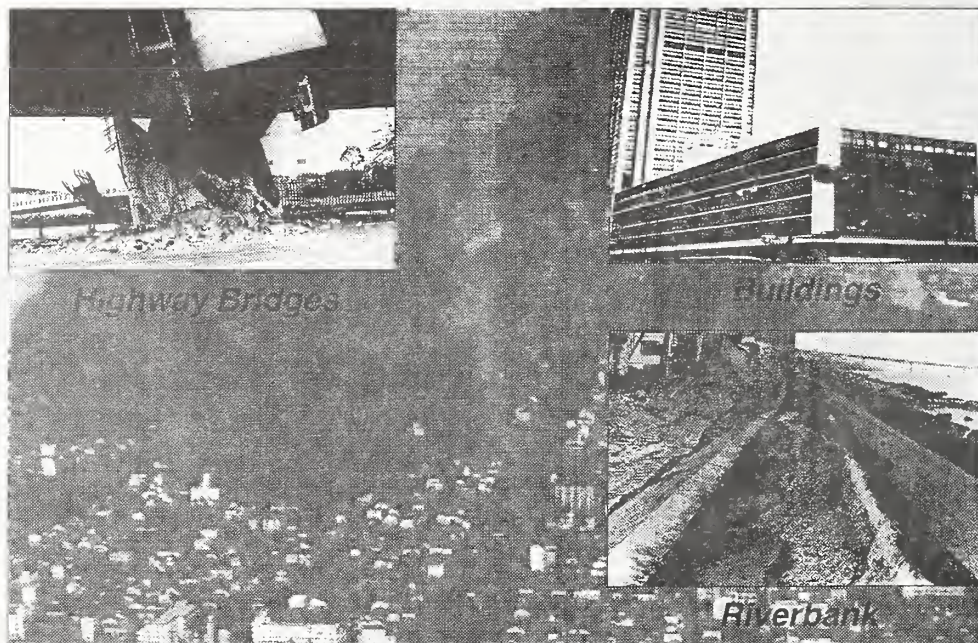


Figure 6. Earthquake Disaster Information System



Photograph 1. Large Scale Three-dimensional Shaking Table



Photograph 2. Upgrading Seismic Safety of Urban Area

Completing Our Panel's Work

by

Richard N. Wright¹

ABSTRACT

Our 30th Joint Meeting provides an opportunity to reflect on our work and accomplishments and establish our view for the future of our U.S./Japan Panel on Wind and Seismic Effects. The Panel has helped us, in the United States, in Japan, and in the world, to: (1) focus, coordinate and amplify efforts of government, academia and industry to better understand extreme wind and earthquake phenomena, and (2) increase the resistance of our built environment and society to their destructive effects. Is it not time to commit ourselves to the solution of the problem of destructive winds and earthquakes? Can we make it the objective for the next 20 years of the Panel to work together, with the international wind and earthquake communities, to provide: (1) the knowledge of extreme wind and earthquake phenomena; (2) the practices for planning, design, construction, operation, maintenance, and rehabilitation of our built environment; and (3) the incentives for societal actions to apply the practices that together will end the threat of wind and earthquake disasters?

KEY WORDS: Disaster Mitigation; Earthquakes; Earthquake Engineering; Earth Science; Japan; Meteorology; Seismology; Social Science; United States; Wind Engineering

1. INTRODUCTION

Our 30th Joint Meeting provides an opportunity to reflect on our work and

accomplishments and establish our view for the future of our U.S./Japan Panel on Wind and Seismic Effects. It is a wonderful opportunity, while the founders of the Panel can still be with us, to note how the Panel has helped us, in the United States, in Japan, and in the world, to: (1) focus, coordinate and amplify efforts of government, academia and industry to better understand extreme wind and earthquake phenomena, and (2) increase the resistance of our built environment and society to their destructive effects.

Moreover, we have the opportunity to define our objectives for future Panel collaborations. Therefore, I wish to build on the thoughts of Dr. Tsuneo Katayama, Director General of the National Research Institute for Earth Science and Disaster Prevention, at the 29th Joint Meeting and at the Second U.S./Japan Earthquake Policy Symposium: **Is it not time to commit ourselves to the solution of the problem of destructive winds and earthquakes?** Can we make it the objective for the next 20 years of the Panel to work together, with the international wind and earthquake communities, to provide: **(1) the knowledge of extreme wind and earthquake phenomena; (2) the practices for planning, design, construction, operation, maintenance, and rehabilitation of our built environment; and (3) the incentives for societal actions to apply the practices that together will end the threat of wind and earthquake disasters?**

¹ Director, Building and Fire Research Laboratory
National Institute of Standards and Technology

The appendix to this paper is an excellent summary of the activities and accomplishments of the Panel prepared by our U.S.-side Secretary General, Noel Raufaste. In the following paragraphs, I draw upon the facts from this summary to show that we have established a sound basis for committing ourselves to Completing Our Panel's Work and solving the problem of destructive winds and earthquakes.

Our Panel was established in 1969 to encourage, develop and implement the exchange of wind and seismic technologies; develop stronger links between the two countries; conduct joint research and cooperative programs; and exchange guest researchers and equipment. Now, we are holding our 30th joint meeting, and have established an active family of task committees that have held more than 60 workshops and conferences, have published more than 1700 papers, and exchanged over 200 guest researchers. These activities, our collaborative investigations of effects of U.S. and Japanese extreme winds and earthquakes and our 9 Cooperative Research Programs have resulted in knowledge and recommended practices used in the United States, Japan and other nations to reduce our vulnerability.

2. CHALLENGE TO THE PANEL

Our work is gaining new scope. We are beginning to address public health issues to understand how wind and seismic effects threaten illnesses and injuries and to define countermeasures. We are beginning to address emergency information services to adapt information and communication technologies to assist: (1) emergency managers in search and rescue and in avoidance of secondary damages such as post-earthquake fires; (2) scientists and engineers in understanding wind, earthquake and fire phenomena, and the performance of the built environment and political and economic systems; and (3) the

public and private sectors in recovery from the damages. We are increasingly involving leaders from industry and universities in the work of the Panel. This scope allows us to coordinate and focus public, private and academic R&D, in the U.S. and Japan, to provide the knowledge and recommended practices needed to reduce our vulnerability.

We have not yet developed cooperative activities aimed at defining and implementing the incentives needed by all levels of government, property owners, and the general public to apply the recommended practices systematically and economically to end the threat of wind and earthquake disasters. If this proposal for Completing Our Panel's Work is endorsed by the Panel, we will have to give substantial future attention to incentives for mitigation of wind and seismic effects. Our strategy for 20 years work would involve continued and strengthened collaborations to:

- Exploit the opportunities provided by wind and seismic disasters to gain knowledge and public and private policy support for mitigation.
- Improve knowledge of the destructive environments arising from extreme winds, earthquakes and post-event fires, the response of the built environment, and societal response during emergency and recovery periods.
- Develop cost effective recommended practices for planning, design, construction, and rehabilitation of the built environment.
- Develop cost effective recommended practices for emergency services and recovery.
- Develop incentives for public and private sector actions to implement recommended practices to end the threat of wind and earthquake disasters.

APPENDIX

Background On Panel On Wind And Seismic Effects

1. BACKGROUND - WHY ESTABLISHED

The U.S.-Japan Cooperative Program in Natural Resources (UJNR) was created in January 1964; one of three Programs comprising the U.S.-Japan Cooperative Science Program. The Panel on Wind and Seismic Effects was established in 1969. Its objectives are to: encourage, develop, and implement the exchange of wind and seismic technologies; develop stronger technical links between the two countries; and conduct joint research, cooperative programs, and exchange guest researchers and equipment.

Eighteen U.S. agencies participate in the Panel (see Attachment) to develop and exchange technologies aimed at reducing damages from high winds, earthquakes, storm surge, and tsunamis. This work is produced through collaboration between U.S. and Japanese member researchers working in 11 Task Committees¹ with

¹ Panel on Wind and Seismic Effects'
11 Task Committees (T/C):

1. T/C "A" Strong Motion Data and Applications
2. T/C "B" Testing and Evaluation Procedures for Building Systems
3. T/C "C" Evaluation and Improvement of Structures
4. T/C "D" Earthquake Engineering for Dams
5. T/C "E" Design for Wind and Wind Hazard Mitigation
6. T/C "F" Disaster Prevention Methods for Lifeline Systems
7. T/C "G" Structural Control and Intelligent Material Systems
8. T/C "H" Soil Behavior and Stability During Earthquakes
9. T/C "I" Storm Surge and Tsunamis
10. T/C "J" Wind and Earthquake Engineering for Transportation Systems
11. T/C "K" Wind and Earthquake Engineering for Offshore and Coastal Facilities

representatives of private sector organizations. Each committee focuses on specific technical issues. Task Committee activities include exchange of technical data and information on design and construction of civil engineering lifelines, buildings, and water front structures, promote and execute joint research projects, and exchange high wind and seismic measurement records. Annual meetings alternate between Japan and the U.S. (odd numbered years in Japan; even numbered years in the U.S.). One-week technical meetings provide the forum to discuss ongoing research and research results. They are followed by one-week technical site visits. The National Institute of Standards and Technology has been the U.S.-side Chair since the Panel's creation².

2. ACCOMPLISHMENTS

1. Held 29 annual joint Panel Meetings,
2. Conducted more than 50 Task Committee Workshops and 15 Task Committee Conferences,
3. Published more than 1700 papers in Joint Panel Proceedings, Workshop Proceedings, and in other technical journals,
4. Published 22 year listing of publications *List of Publications 1969-1991*,

² Chairman: Dr. Richard N. Wright, Director Building and Fire Research Laboratory National Institute of Standards and Technology, DoC

Secretary General: Noel J. Raufaste, Head, Cooperative Research Programs, Building and Fire Research Laboratory, National Institute of Standards and Technology, DoC

5. Exchanged over 200 guest researchers who performed short and long term joint cooperative research assignments that have enhanced host and supply laboratory's research mission and contributed to improved structural standards and building codes,
 6. Annually visit more than 10 major public works construction projects that are using innovative civil engineering techniques and research laboratories having unique test and measurement capabilities that enhance the joint Panel's understanding of research, design, and construction procedures used by both countries,
 7. Performed joint post disaster surveys and made entrees for counterpart panel members to participate in post disaster studies of the performance of constructed facilities exposed to wind, earthquake, and tsunamis; results are shared with the professional community which contribute to improved knowledge and practice for disaster resistant constructed facilities,
 8. Conducted specialty symposia, e.g.,
 - a two-day symposium on Hurricane Hugo, Charleston S.C., 1990 (22nd Joint Meeting);
 - a one-day international symposium on IDNDR in Gifu, Japan, 1991 (23rd Joint Meeting);
 - a mini-symposium during technical site visits at Lehigh University ATLSS Facility, at New Orleans Corps of Engineers Facility, and at LBL, 1992 (24th Joint Meeting);
 - 25th Panel Anniversary Symposium, IDNDR focus on lessons learned in post disaster investigations, Tokyo, 1993;
 - a mini-symposium during technical site visits at Waterways Experiment Station, Vicksburg, MI, 1994 (26th Joint Meeting);
 - a mini symposium during site visits at University of Minnesota's Wind Tunnel Facility and at the Department of Geology and Mineral Industries, Portland, Oregon, 1996 (28th Joint Meeting) .
- Each event has advanced technology transfer to participants and stimulated greater attention to promoting disaster mitigation programs.
9. Translated into English two Ministry of Construction reports, *Manual for Repair Methods of Civil Engineering Structures Damaged by Earthquakes* and 2-volume *Base Isolation Systems for Buildings*; publications distributed to U.S. civil engineering community as improved practices,
 10. Shared technical information during Joint Panel Meetings, Task Committee Workshops, and during routine correspondence between U.S. and counterpart Japanese researchers that improved researchers abilities to perform mission research.

3. COOPERATIVE RESEARCH PROGRAMS

Completed seven Cooperative Research Programs; two on-going Programs. Accomplishments have improved design and construction practices for both countries.

1. Reinforced Concrete Structures (1979-1987), accomplishments include testing six-story full scale

buildings which led to improve seismic design methods of reinforced concrete buildings.

2. Lifeline Facilities (1982-1989); accomplishments included development of improved seismic design methods of bridge columns.
3. *In-situ* Testing Methods for Soil Liquefaction (1983-1986); accomplishments include development of rationale for Standard Penetration Test (SPT) data based on energy ratio.
4. Masonry Structures (1984-1988); accomplishments include development of strength-based design guidelines for reinforced masonry buildings.
5. Steel Structures (1985-1987); accomplishments include testing of a full-scale five-story building to confirm prediction of performance based on components and subassemblages.
6. Hybrid Control (1990-1994); accomplishments include development of hybrid control algorithms that require less energy for controlling bridge response.
7. Precast Seismic Structural Systems (1991-1992); accomplishments include development of strength-based design guidelines.
8. Seismic Performance of Composite and Hybrid Structures (1993-).
9. Research on Countermeasures for Soil Liquefaction (1994-).

4. TYPES OF EXCHANGES

Guest research exchanges advanced state of technology in areas of steel, concrete, and masonry structures under seismic forces; developed techniques to analyze risks from liquefaction; modeled water seepage in dam foundations; performed comparative analyses of seismic design of U.S. and Japanese bridges.

5. BENEFITS

The Panel's activities resulted in improved building and bridge standards and codes and design and construction practices for constructed facilities in both countries, for example:

1. created and exchanged digitized earthquake records used as the basis of design and research for Japan and the United States.
2. transferred earthquake engineering information and strong-motion measurement techniques for use by seismically active countries, e.g., Australia, Canada, Italy, Mexico, Peru, Taiwan, Turkey, and North Africa;
3. produced data that advanced retrofit techniques for bridge structures;
4. developed field test data for use in aerodynamic retrofit of bridge structures;
5. produced full-scale test data that advanced seismic design standards for buildings;
6. advanced technology for repairing and strengthening reinforced concrete, steel, and masonry structures;
7. improved in-situ measurement methods for soil liquefaction and stability under seismic loads;
8. created a database comparing Japanese and U.S. standard penetration tests to improve prediction of soil liquefaction;
9. created database on storm surge and tsunamis and verified mathematical models of tsunami and storm surge warning systems;
10. established a library resource of current research on wind and earthquake engineering and on storm surge and tsunamis;
11. published proceedings of Panel meetings, Task Committee Workshops, and special publications such as List of Panel

- Publications and translated two-volume series on earthquake resistant construction using base isolation systems;
12. gained better knowledge of both countries research, design and construction capabilities from in-depth visits to host country's laboratories and building and public works projects. Results of such visits contribute to creation of new Task Committees, agendas for Joint Panel meetings and task committee workshops, special visits of U.S.-Japan researchers, and joint collaborative research.

6. FUTURE PLANS

The Panel is planning:

1. its 30th Joint Meeting to be conducted at NIST, Gaithersburg,

- MD in May 1998.
2. to conduct four Task Committee workshops before the 30th Joint Panel Meeting.
3. participation in appropriate research projects of the U.S.-Japan Earthquake Disaster Mitigation Partnership of the April 17, 1996 Agreement, U.S.-Japan Common Agenda. Appropriate Task Committees will respond to the Partnership in planning its work.
4. to publish its 5th newsletter for disseminating Panel's activities to peers and to decisionmakers at Government laboratories and agencies involved in construction.
5. a Panel Home Page to electronically disseminate Panel information worldwide. The effort will build on current Panel descriptions.

ATTACHMENT

U.S. Members -- Panel on Wind and Seismic Effects

Department of Commerce	National Institute of Standards and Technology National Oceanic and Atmospheric Administration
Department of Energy	
Department of Health and Human Services	Center for Disease Control and Prevention
Department of Housing and Urban Development	
Department of Interior	Bureau of Reclamation U.S. Geological Survey Minerals Management Service
Department of State	Office of Foreign Building Operations Agency for International Development
Department of Transportation	Federal Highway Administration
Department of Veterans Affairs	
Department of the Army	Corps of Engineers
Department of Navy	Naval Civil Engineering Laboratory
Department of Air Force	Civil Engineering Support Agency
Federal Emergency Management Agency	
National Science Foundation	
Nuclear Regulatory Commission	
California Department of Transportation	
NSF Earthquake Eng. Centers	Center for Advanced Technologies in Earthquake Loss Reduction, State University of New York, Buffalo Pacific Earthquake Engineering Research Center, University of California, Berkeley Mid-America Earthquake Center, University of Illinois, Urbana-Champaign

STORM SURGE and TSUNAMIS

TSUNAMI AND STORM SURGE CHARACTERISTICS BASED ON LONG-TERM TIDE OBSERVATIONS

by

Toshihiko NAGAI¹⁾, Kazuteru SUGAHARA¹⁾, Hiroshi WATANABE¹⁾,
Koji KAWAGUCHI¹⁾, Masahiro MIHARA²⁾, and Katsumi TAKASHIMA³⁾

ABSTRACT

Based on the 38-year tide observation records digitized every hour between 1958 and 1995, long waves-characteristics including Tsunamis and Storm surges were investigated. Long-waves with double amplitudes greater than 15cm were observed for 180 cases during the 38 years including 4 tsunamis.

Key Words: Tide Observation,
Long Waves,
Tsunami

1. INTRODUCTION

This paper presents the analysis of observed long-term tide data ; to clarify profiles of long-waves including tsunamis and storm surges. (Nagai.et.al.,1996)

2. TIDE OBSERVATIONS AND DATA ANALYSIS

38 years of tide data, between 1958 and 1995, obtained at the Kurihama-Tide-Station were analysed. The station is located at the entrance of the Tokyo-Bay (N35° 13' 28", E139° 43' 27"), and employs the Fuse type tide gauge with a well. Figure 1 and 2 shows location of the tide station. Photo 1 shows the Fuse type tide gauge. The tide well is connected to the sea with a tube as the Figure 3 shows. The tube of the diameter 131mm works as a low-pass-filter by omitting the high frequency sea level fluctuations caused by wind waves.

Observed data were recorded on an analog recorder for the entire observation term. All the data were digitized every hour in order to calculate the mean sea level and the harmonic components.

3. LONG-WAVE RECORDS

Figure 4 shows the observed long-waves with the heights (double amplitude) greater than 15cm. Among these 180 cases, 4 cases were tsunamis, and the others were caused by weather disturbances. Table 1 shows joint distribution between double amplitudes and periods of the observed long waves. Observed periods were either between 2-3 minutes or 15-20 minutes, which corresponds to the local topographical resonance periods of the two different modes, except the 1960-Chile-Tsunami event with periods of around 80 minutes.

-
- 1) Hydraulic Engineering Division,
Port and Harbour Research Institute,
Ministry of Transport
3-1-1, Nagase, Yokosuka 239-0026, Japan
TEL:+81-468-44-5017 FAX:+81-468-42-5246
 - 2) ECOH Co.
2-6-4, Kita-Ueno, Taito, Tokyo 110-0014,
Japan
TEL:+81-3-5828-2185 FAX:+81-3-5828-2176
 - 3) Coastal Ocean Research Co.
3-21-1, Shimo-Ochiai, Shinjuku-ku, Tokyo
161-0033, Japan
TEL:+81-3-3950-3740 FAX:+81-3-3951-9171

4. THE 1960-CHILE-TSUNAMI PROFILES

Figure 5 shows the observed 1960-Chile-Tsunami profiles by digitizing with a shorter interval, every 36s. The lower figure shows the observed water surface level with astronomical tides, while the upper figure shows the tsunami profiles by omitting lower frequency astronomical tide components. The marks ①, ②, ③, ④, and ①', ②', ③', ④', ⑤', ⑥', ⑦', ⑧' mean the data terms for frequency spectra analysis.

Frequency spectra analysis was conducted with different record lengths 1024, 2048, 4096, and 8192 data points, which corresponds to the sampling length of 10h, 20h, 40h, and 80h, respectively, as the Figure 6 shows. The results showed that the peak frequency of the tsunami was 0.0002Hz, and the second peak was at 0.001Hz. This second peak corresponded to the local topographic resonance frequency. The ratio of the second peak and the first peak increased with time. The results of this study provided more detailed tsunami spectra information than the previous study conducted in 1960's. (Hatori, 1969)

5. THE 1996-IRIANJAYA-TSUNAMI PROFILES

The frequency response of the well, connected with a tube to the sea water, was investigated at the occasion of the 1996 Irianjaya-Tsunami event by comparing the tide gauge data with the ultra-sonic direct sea surface elevation data. Photo 2 shows the Ultra-sonic direct sea surface measurement equipment.

Figure 7 is the tsunami profiles including the NOWPHAS offshore wave gauges continuous records (Nagai et.al. 1994), the low-pass-filtered Fuse type tide gauge records, and the ultra-sonic direct sea surface elevation records. The NOWPHAS offshore wave gauge is located 50km off the

tide station near the Izu-Ohshima Island.
(water depth 50 m ,
N 34° 40' 23", E 139° 27' 19")

Figure 8 shows the results of the spectra analysis of the three records of the Figure 7. The peak frequency of the tsunami was 0.001Hz, near to the local topographic resonance frequency. The response function indicates that the tsunami was amplified in the Kurihama Bay due to the topographic resonance. Figure 8 also proves that for longer period waves, greater than 5 minute periods, ratio is almost 1.0 between the two records of the low-pass-filtered Fuse type one and the direct sea surface elevation one.

5. STORM SURGE RECORDS

Harmonic analysis was conducted for every year from the hourly based observed data, and the 28 components' amplitudes and phases were obtained. Table 2 shows the results of the 4 principal components of M2 (period of 12.42h), S2(12h), K1(23.934h), and O1(25.819h). Z0 values defined as the sum of the amplitudes of the 4 components are also shown.

In addition to the each year's calculated 4 components and the Z0 value, maximum, minimum, and average amplitudes and the standard deviation (S.D.) are shown in Table 2. The 4 components' amplitudes fluctuations were small with the standard deviation less than 1%. Nevertheless, amplitudes of the longer period components such as Sa(1year) and SSa(0.5year), showed much larger fluctuations.

Astronomical tide was calculated from the 28 harmonic tide components' amplitudes and phases, and storm surge (meteorological tide) level was obtained as the difference between the observed tide and calculated one. Table 3 shows the records of the 40 highest storm surges during the 38 years with the

meteorological cause. Figure 9 shows an example of the storm surge records.

6. CONCLUDING REMARKS

Interesting facts related to the tsunami and long-wave profiles were found from the analysis of long-term tide records. It is desirable to apply these methods of analysis to additional tide stations, and to compare the results, in order to obtain more precise information. Efforts are now underway to establish a digital network system of tide data stations, with the cooperation of the concerned organizations. (Nagai, et. al., 1994)

REFERENCES

- Hatori, T. (1969) : Analysis of Oceanic Long-period Wave at Hachijo Island, Bull. Earthq. Res. Inst. Univ. Tokyo, Vol. 47, pp. 863-874
- Nagai, T., Sugahara, K., Hashimoto, N., Asai, T., Higashiyama, S. and Toda, K (1994) : Introduction of Japanese NOWPHAS System and its Recent Topics, Proc. of HYDRO-PORT'94, PHRI, pp. 67-82
- Nagai, T., Sugahara, K., Watanabe, H., and Kawaguchi, K. (1996) : Long Term Observations of the Mean Tide Level and Long Waves at the Kurihama-Bay, Rept. of PHRI, Vol. 35, No. 4, pp. 3-35

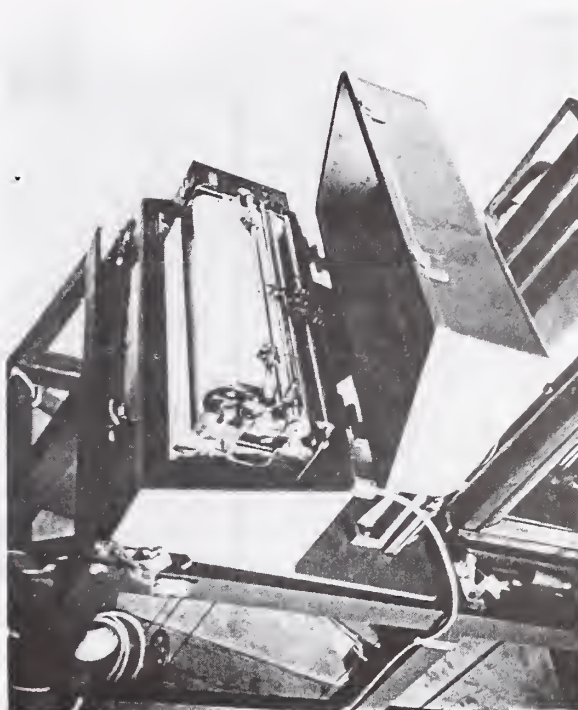


Photo 1 Fuse Type Tide Gauge

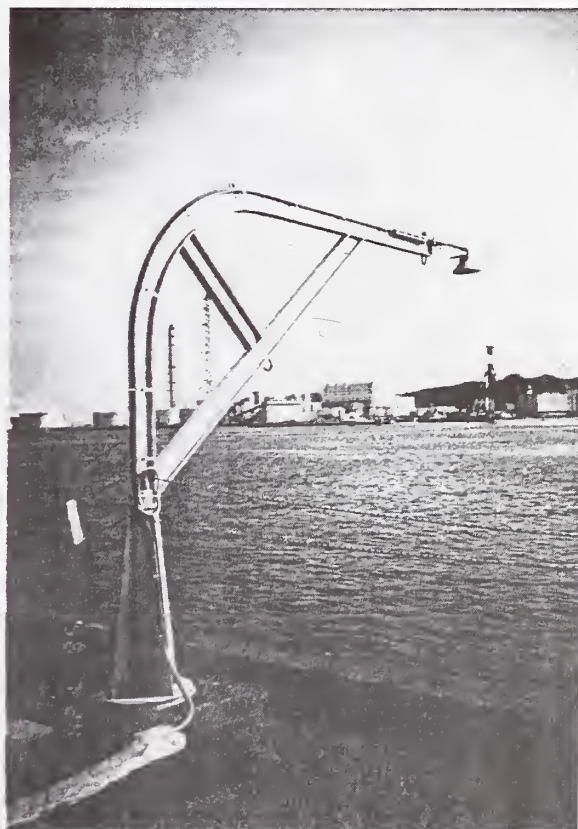


Photo 2 Ultra-Sonic Direct Sea Surface

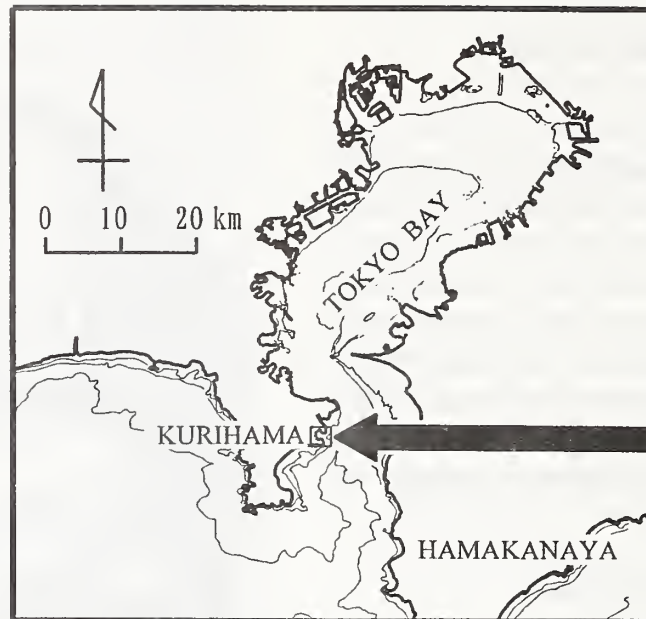


Figure 1 Location of the Tide Station (1)

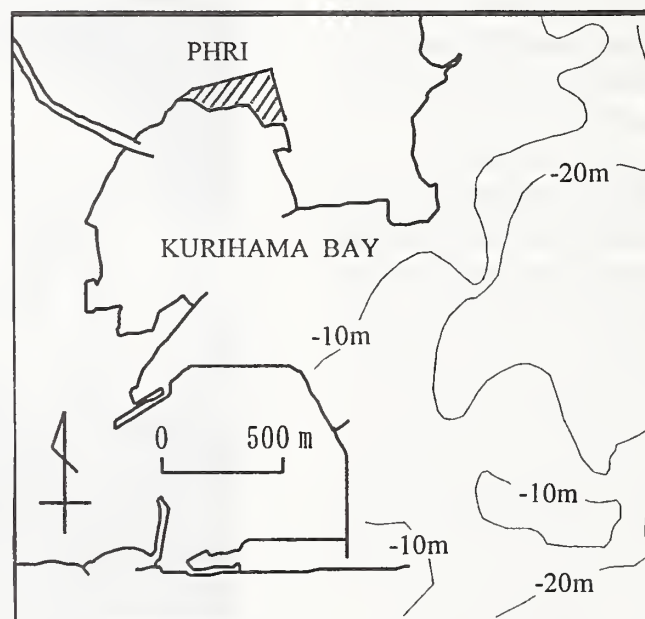


Figure 2 Location of the Tide Station (2)

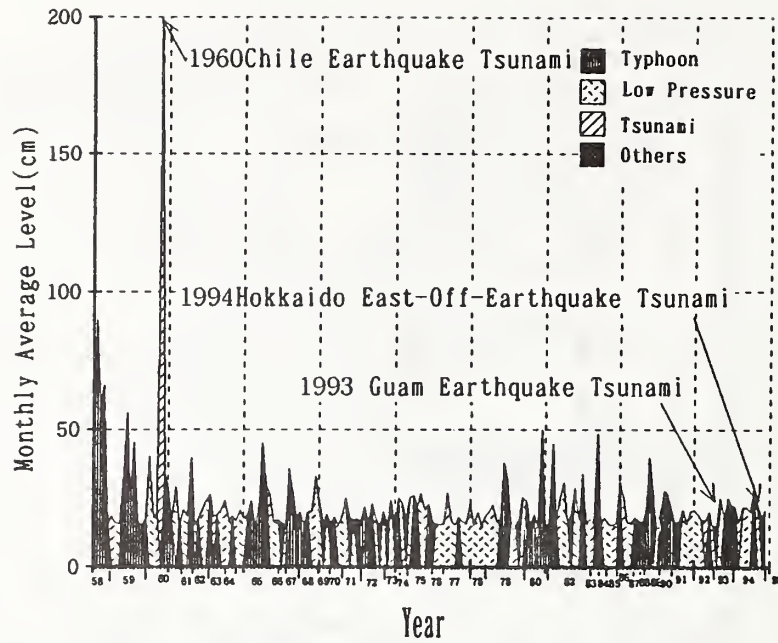


Figure 4 Observed Long-Waves

Table 1 Joint Distribution of the Observed Long Waves

Double Amplitude (cm)	Period (min)			Total
	-10	10-20	20-	
15 - 20	17	80	0	97
20 - 25	17	22	1	40
25 - 30	12	7	1	20
30 - 40	6	4	0	10
40 - 50	6	1	0	7
50 -100	5	0	0	5
100 -	0	0	1	1
Total	63	114	3	180

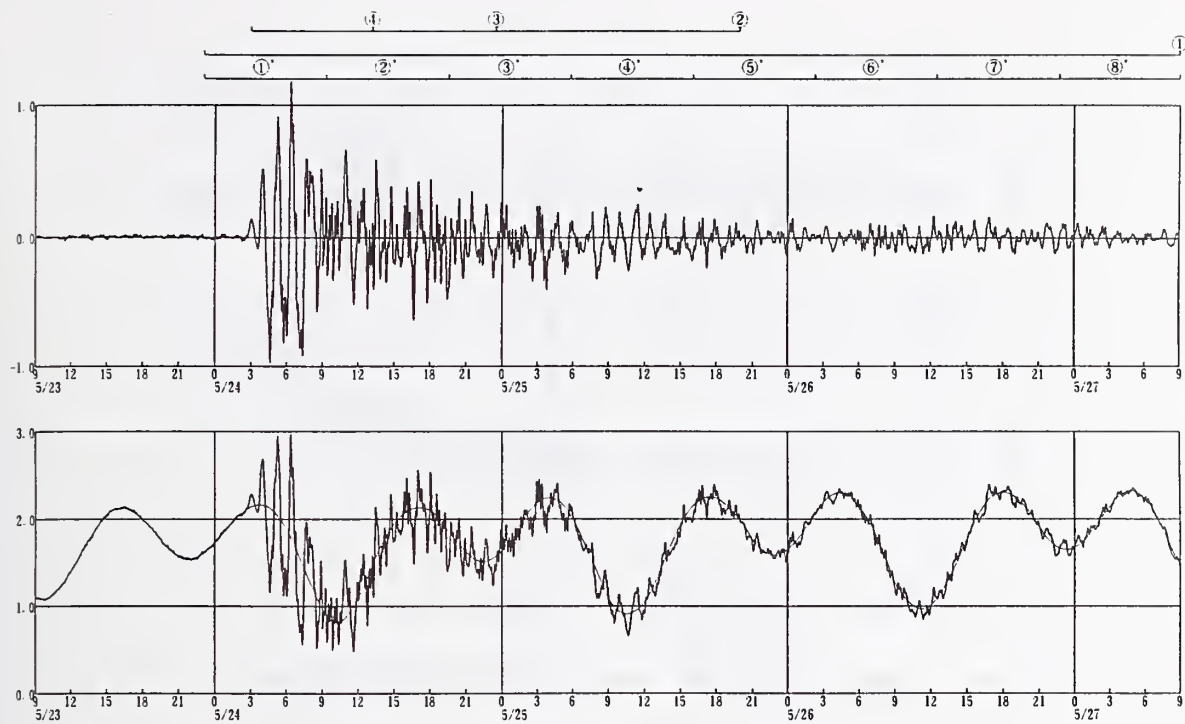


Figure 5 1960-Chile-Tsunami Profiles

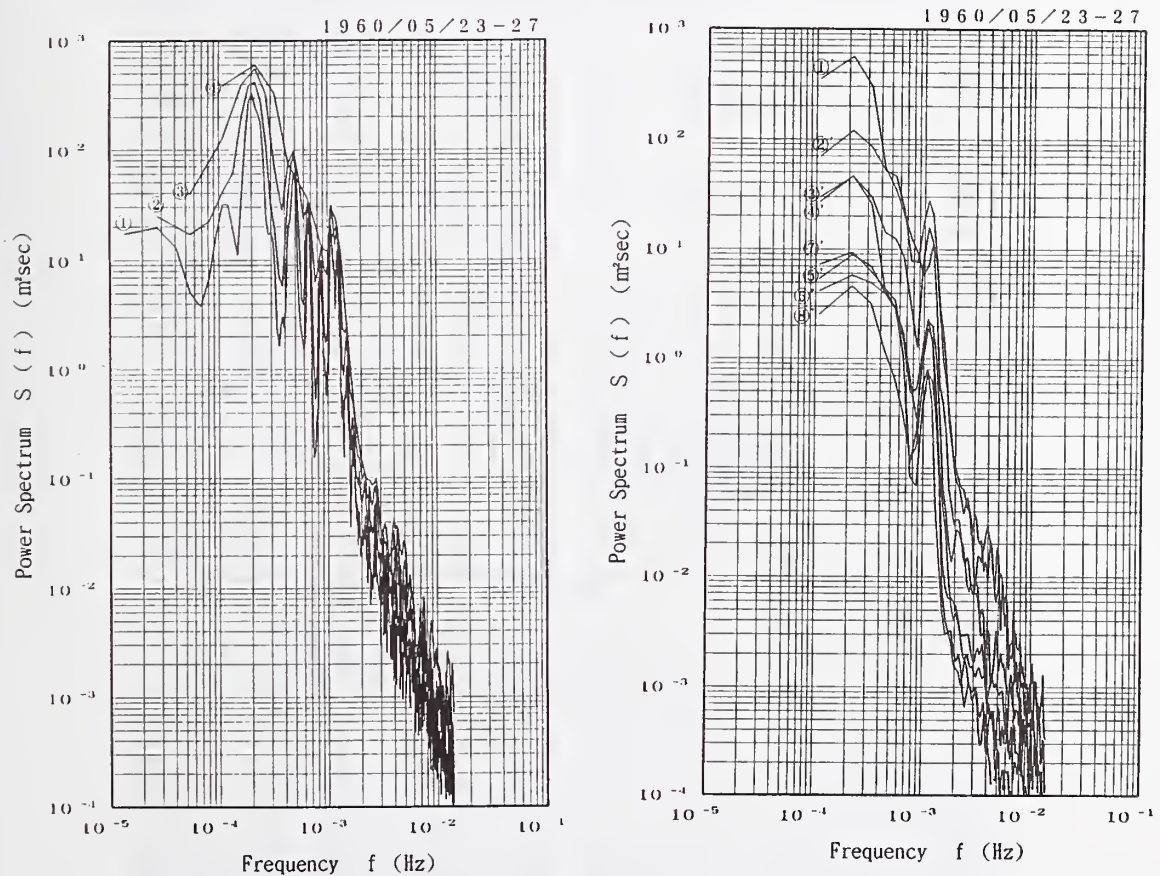


Figure 6 Spectra Analysis of the 1960-Chile-Tsunami

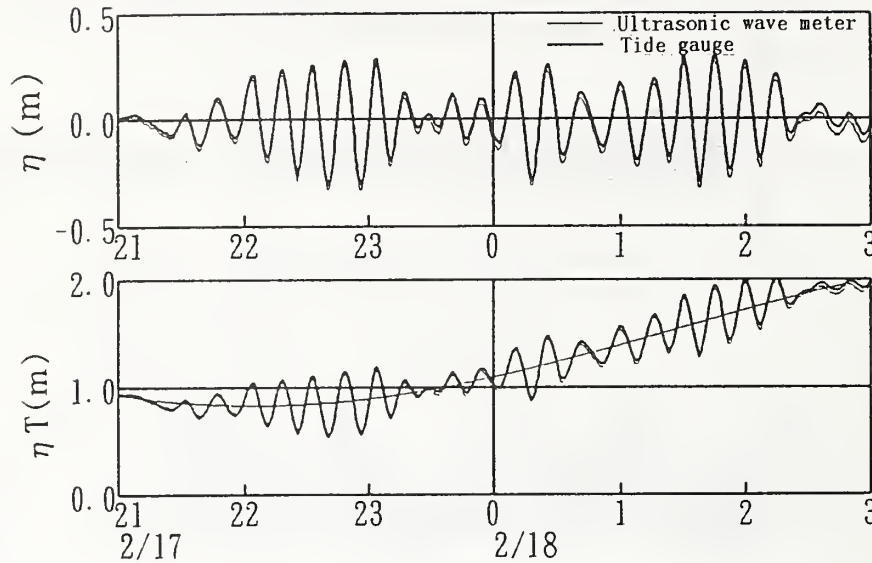


Figure 7 Comparison of the Observed 1996-Irianjaya-Tsunami Profile

Table 2 Results of the Harmonic Analysis

Year	M2		S2		K1		O1		Z0 (cm)
	amp. (cm)	pha. (°)	amp. (cm)	pha. (°)	amp. (cm)	pha. (°)	amp. (cm)	pha. (°)	
1958	35.851	147.174	17.103	175.561	23.259	176.155	18.653	157.503	94.866
1959	36.283	148.890	17.400	177.502	23.322	175.840	18.336	158.489	95.341
1960	36.359	149.025	17.492	177.282	22.985	175.924	18.453	157.851	95.289
1961	36.657	148.703	17.255	177.196	23.558	176.107	18.390	158.695	95.860
1962	36.409	148.588	17.283	176.549	23.367	176.397	18.461	158.798	95.520
1963	36.613	148.305	17.155	176.745	23.839	177.234	18.608	158.830	96.215
1964	36.322	147.703	17.273	176.151	23.758	177.406	18.832	158.756	96.185
1965	36.684	147.691	17.360	176.240	23.836	177.252	18.741	158.410	96.621
1966	36.111	147.768	17.089	176.167	23.330	176.683	18.553	158.464	95.083
1967	36.135	148.356	17.311	176.840	23.441	177.708	18.361	159.506	95.248
1968	36.022	148.286	17.300	177.755	23.665	177.742	18.737	159.494	95.724
1969	35.872	148.018	17.195	176.796	23.365	177.056	18.606	158.766	95.038
1970	36.106	148.227	17.241	176.343	23.527	177.685	18.519	159.058	95.393
1971	35.934	148.554	17.143	177.036	23.533	177.778	18.400	158.878	95.010
1972	35.717	148.323	17.202	177.354	23.216	176.795	18.342	159.066	94.477
1973	35.968	147.557	17.210	176.490	23.482	177.142	18.725	158.799	95.385
1974	35.932	148.005	17.329	177.023	23.483	177.646	18.638	158.196	95.382
1975	35.765	148.623	17.208	176.858	23.306	177.203	18.410	159.367	94.689
1976	35.881	148.163	17.170	177.034	23.118	176.123	18.247	158.766	94.416
1977	36.143	147.877	17.160	176.725	23.240	176.045	18.789	158.331	95.332
1978	36.215	148.242	17.118	176.825	23.452	175.720	18.473	157.551	95.258
1979	36.157	149.297	17.078	177.653	23.353	176.711	18.342	158.068	94.930
1980	36.073	148.018	17.009	176.002	23.552	177.001	18.533	158.661	95.167
1981	36.488	147.103	17.231	174.517	23.581	177.594	18.504	159.102	95.804
1982	35.873	148.513	17.115	176.502	23.398	176.664	18.517	159.451	94.903
1983	35.610	148.327	16.968	176.335	23.333	176.854	18.558	158.549	94.469
1984	35.982	147.877	17.340	176.165	23.688	177.357	18.532	158.382	95.542
1985	35.881	148.448	17.214	176.760	23.722	177.825	18.689	159.536	95.506
1986	36.246	148.788	17.301	176.891	23.944	178.198	19.006	159.474	96.497
1987	36.051	149.077	17.191	177.094	23.431	176.478	18.579	158.408	95.252
1988	36.169	148.087	17.409	176.662	23.436	177.100	18.516	158.727	95.530
1989	35.967	147.579	17.229	175.407	23.611	177.118	18.546	159.232	95.353
1990	35.739	147.573	17.240	176.442	23.178	176.204	18.633	158.962	94.790
1991	35.698	147.228	17.261	175.832	23.680	176.978	18.819	158.129	95.458
1992	35.848	147.281	17.380	175.770	23.464	176.785	18.598	158.040	95.290
1993	35.911	146.524	17.165	175.275	23.583	176.723	18.572	158.205	95.231
1994	35.761	147.616	17.147	175.612	23.519	176.296	18.759	158.445	95.186
1995	35.867	147.550	17.177	175.608	23.545	176.611	18.909	157.870	95.498
mean	36.061	148.078	17.222	176.500	23.476	176.898	18.576	158.653	95.335
S. D.	0.268	0.6	0.11	0.697	0.204	0.626	0.168	0.533	0.492

☆: maximum, ○: minimum, S.D.: Standard deviation

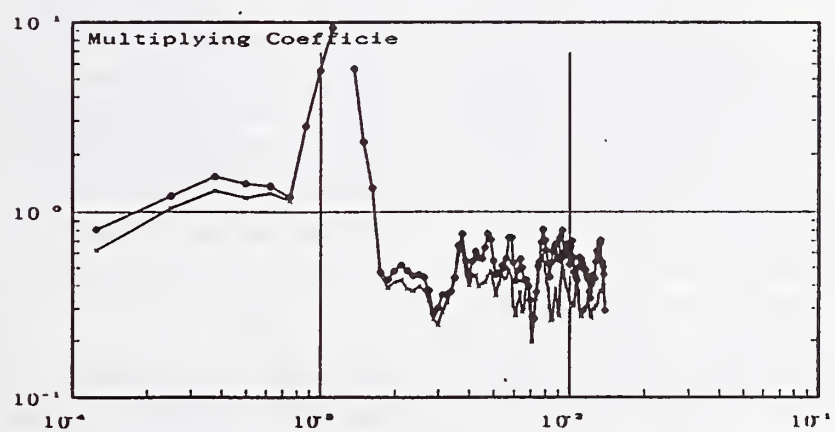
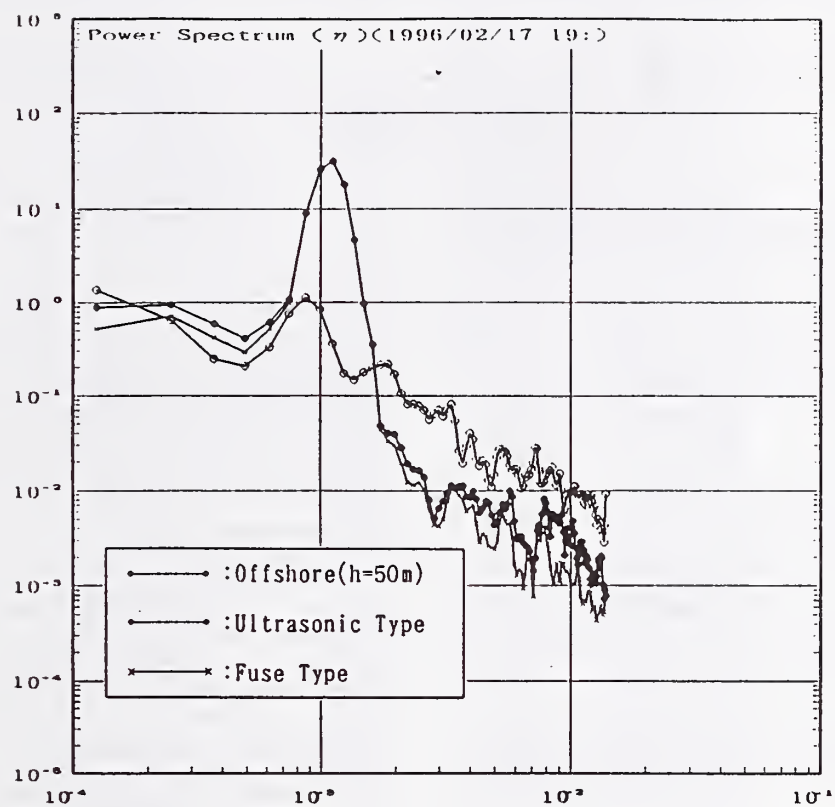


Figure 8 Observed Spectra of the 1996-Irianjaya-Tsunami

Table 3 Storm Surge Records

NO	Year/Mon/Day Time	Maximum Tide Deviation(cm)	Primary Factor
1	79/10/19 16:00	5 1	Typhoon7920
2	58/ 7/23 9:00	4 7	Typhoon5811
3	82/ 9/12 22:00	4 2	Typhoon8218
4	70/ 1/31 9:00	4 1	Low Pressuræ
5	85/ 7/ 1 3:00	4 1	Typhoon8506
6	67/ 9/15 2:00	4 0	Typhoon6722
7	58/ 9/18 8:00	3 8	Typhoon5821
8	59/ 9/26 23:00	3 7	*Typhoon5915
9	69/ 8/23 15:00	3 7	Typhoon6909
10	58/12/26 16:00	3 6	Low Pressuræ
11	66/ 4/16 14:00	3 6	Low Pressuræ
12	91/10/13 8:00	3 6	Typhoon9121
13	86/12/19 7:00	3 6	Low Pressuræ
14	91/ 2/16 6:00	3 6	Low Pressuræ
15	89/ 8/ 6 7:00	3 5	Typhoon8913
16	77/ 9/19 20:00	3 5	Typhoon7711
17	72/ 2/27 15:00	3 4	Low Pressuræ
18	83/ 3/13 16:00	3 4	Low Pressuræ
19	90/12/ 1 4:00	3 4	Typhoon9028
20	87/ 9/18 16:00	3 4	Typhoon8713
21	79/10/ 1 14:00	3 2	Typhoon7916
22	67/10/28 15:00	3 2	Typhoon6734
23	91/ 9/19 16:00	3 2	Typhoon9118
24	75/ 8/23 18:00	3 2	Typhoon7506
25	62/10/30 17:00	3 2	Typhoon6224
26	69/ 4/ 5 6:00	3 2	Low Pressuræ
27	75/10/ 8 7:00	3 2	Low Pressuræ
28	65/11/ 9 16:00	3 2	Low Pressuræ
29	88/10/ 7 3:00	3 1	Low Pressuræ
30	90/11/10 11:00	3 1	Low Pressuræ
31	65/ 6/ 4 7:00	3 1	Typhoon6508
32	68/10/26 9:00	3 1	Typhoon6819
33	82/10/20 7:00	3 1	Low Pressuræ
34	90/11/ 4 17:00	3 1	Low Pressuræ
35	58/ 3/18 16:00	3 0	Low Pressuræ
36	85/ 2/21 17:00	3 0	Low Pressuræ
37	64/ 5/25 17:00	3 0	Low Pressuræ
38	80/ 5/ 9 11:00	3 0	Low Pressuræ
39	80/12/26 19:00	3 0	Low Pressuræ
40	93/10/ 4 7:00	3 0	Low Pressuræ

* Isewan-Typhoon

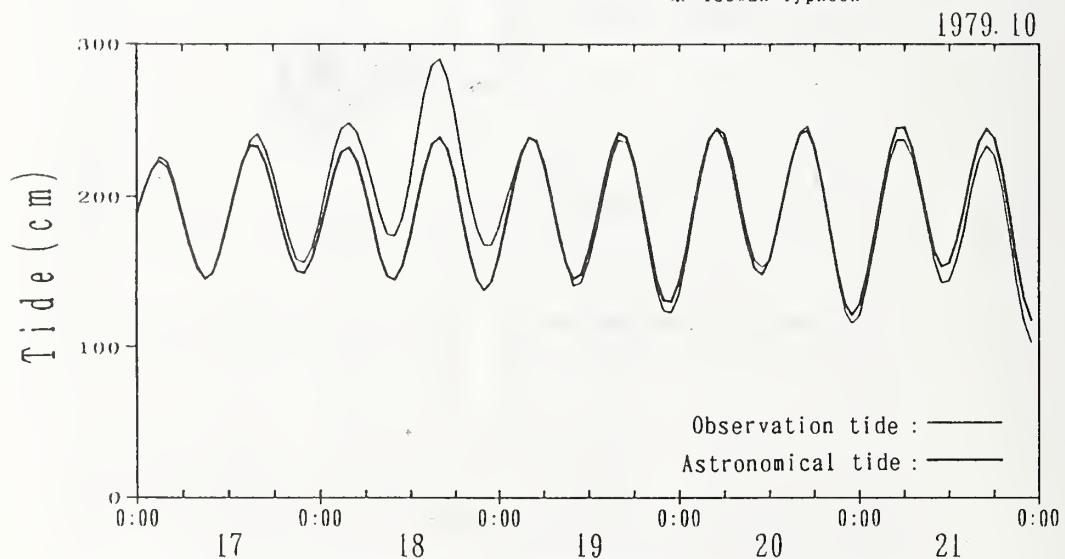


Figure 9 Astronomical and Observed Tide (Typhoon 7920)

International Responses to Pacific Tsunami Warnings and Watches

by

Michael E. Blackford

ABSTRACT

The Pacific Tsunami Warning Center has issued thirteen warnings to the participants in the Tsunami Warning System in the Pacific since the beginning of the International Decade for Natural Disaster Reduction. The average time for the dissemination of these warnings has been about 55 minutes. In most cases tsunami destruction has been confined to localities that are within one hour's tsunami travel time from the source. While the Warning Center's warnings may not reach those most affected by recent tsunamis, the information is nevertheless of great value to those emergency managers further down stream of the spreading tsunami. An examination of the warning process indicates the need for more feedback from the participants receiving the warnings regarding the applicability of the information to their needs and, if they are affected by the tsunami, a timely summary of these affects that can be used to ascertain the severity of the tsunami. The study also points up the critical need for independently functioning regional tsunami warning centers.

KEYWORDS: destructive tsunamis, emergency managers, feedback, response, tsunami warning, tsunami watch

1. INTRODUCTION:

Since the beginning of the International Decade for Natural Disaster Reduction

(IDNDR) the Pacific Tsunami Warning Center (PTWC), acting as the Operations Center for the Tsunami Warning System in the Pacific (TWSP), issued 13 warnings for earthquakes that were believed to have the potential to generate tsunamis. These events are summarized in Table 1. It was further believed that these tsunamis could be destructive in the Pacific beyond the earthquake macroseismic area. In nearly every case the tsunamis that were generated proved to be either non-destructive or non-existent in the far field. All 13 earthquakes for which warnings were issued resulted in at least a local tsunami. Some of these caused significant loss of life and property damage.

2. TSUNAMI WARNING ISSUANCE

The average time from earthquake origin time to the issuance of a warning for these events is fifty-five minutes. Information on the timing of warnings issued is found in Table 2. The issuance time ranges from 34 minutes to 92 minutes after the origin time. This range is affected by two factors: an organizational relationship with a regional warning center responsible for issuing tsunami warnings to the northeast Pacific region within 15 minutes and

International Tsunami Information Center,
IOC-US National Weather Service, Pacific
Region, National Oceanographic and
Atmospheric Administration (NOAA),
Honolulu, Hawaii 96813

the time necessary to acquire and interpret the seismic waves necessary to determine the size of the potentially tsunamigenic earthquake.

3. TSUNAMI SEVERITY

In most cases the destructiveness of a tsunami is confined to areas that are within one hour's tsunami travel time of the origin of the tsunami. A summary of some of the runup (R) and water level gauge (G) data for the warning events may be found in Table 3. In Table 3 runup values are in meters and gauge data are in centimeters, peak-to-trough. While the data do not necessarily reflect uniform fall off of tsunami heights with increasing distance from the source, it can be seen that in nearly every case tsunami heights are below 1.5 meters, a height that may be taken as the threshold of minimum tsunami destruction, for sites away from the source. A notable exception is the two meter runup observed at Hiva Oa where boats were swamped by the tsunami from the northern Chile earthquake of 30 July 1995.

4. CONCLUSIONS

Although, on the average, the warnings issued by the PTWC do not reach those most affected by the tsunami in time, the warnings are useful to those who are a few hours tsunami travel time from the source. This is because the warnings provide important input for emergency managers in this zone. They must make critical decisions on the appropriate action to take regarding the potential tsunami that is soon to arrive in their areas of responsibility.

With the exception of feedback received from emergency managers in the United States, the home country of the PTWC, little is known concerning the actions taken by those who were warned about the 14 events occurring thus far in the IDNDR. Japan, which has a

highly developed regional tsunami warning system, routinely informs the PTWC of warnings it issues to its citizens. Discussions with emergency managers from other areas indicate that there is a wide range of responses to the warnings. These range from doing nothing because historically only very great distant earthquakes have ever caused damage in a particular region to ordering coastal evacuation for all tsunamigenic events, without regard for the earthquake magnitude, upon receipt of the warning.

The results of this study indicate there is a critical need for more regional tsunami warning systems in those areas most susceptible to local tsunamis. This need was expressed earlier in the IDNDR by the Japan Meteorological Agency in their report on the mitigation of tsunami disasters (JMA, 1993). It also finds there is a need to formalize a process of feedback between those closest to the source of the expanding tsunami and the PTWC. In this way the TWSP operations center can better assess the severity of the tsunami and provide better information to those who are further away from the approaching tsunami. There is also a critical need for the operations center to acquire both seismic and water level data in at least near real time from sites close to the major tsunami source areas. These data will allow the PTWC to assess more quickly the size of the potentially tsunamigenic earthquake and the severity of the tsunami it generates.

5. REFERENCES

Japan Meteorological Agency, *The Study Report on the Mitigation of Tsunami Disasters in the Pacific Basin Countries*, March 1993, 58 pages.

No	YrMoDy	OT (UTC)	Lat.	Long.	Ms	Mw	Geographic Location
1	930712	1317	42.3N	139.4E	7.6	7.7	Japan, West of Hokkaido
2	930808	0834	13.0N	144.8E	8.0	7.8	Marianas Islands, South of Guam
3	941004	1323	43.7N	147.3E	8.1	8.3	Russia, Southern Kuril Islands
4	950407	2207	15.2S	173.6W	8.0	7.4	Northern Tonga Islands
5	950516	2013	22.9S	169.9E	7.7	7.7	New Caledonia, Loyalty Islands
6	950730	0511	23.4S	70.4W	7.3	8.0	Near Coast of Northern Chile
7	950816	1027	05.6S	153.9E	7.8	7.7	Papua New Guinea, Nr. Bougainville I.
8	951203	1801	44.6N	149.4E	7.9	7.9	Russia, Southern Kuril Islands
9	960217	0600	00.1S	137.0E	8.1	8.2	Indonesia, Irian Jaya Region
10	960610	0403	51.4N	177.8W	7.6	7.9	Alaska, Aleutian Islands, Andreanof Is.
11	960610	1526	52.4N	176.9W	7.1	7.3	Alaska, Aleutian Islands, Andreanof Is.
12	970421	1202	12.6S	166.7E	7.9	7.8	Vanuatu, Northwest of Torres Islands
13	971205	1127	55.9N	161.9E	7.6	7.9	Russia, Kamchatka Peninsula

Table 1. Earthquakes in the IDNDR through December 1997 for which the PTWC issued RWWs and a Pacific-wide Warning

No.	OT (UTC)	First Bull.	Mins. past OT	Supps.	Last Bull.	Total Warn Time
1	1317	1412	55	1	1457	0h45m
2	0834	0908	34	2	1145	2h37m
3	1323	1445	82	5	2150	7h05m
4	2207	2244	37	2	2322	0h38m
5	2013	2111	58	2	2300	2h49m
6	0511	0643	92	1	0750	1h07m
7	1027	1119	52	2	1354	2h35m
8	1801	1847	46	2	2101	2h14m
9	0600	0658	58	1	0081	1h13m
10	0403	0440	37	1	0541	1h01m
11	1526	1624	58	1	1643	0h19m
12	1202	1304	62	2	1444	1h40m
13	1127	1209	42	2	1351	1h42m

Table 2. Information on RWWs issued by the PTWC. Note: A Pacific-wide warning was issued for Event No. 3.

<u>930712</u>	<u>930808</u>	<u>941004</u>	<u>950407</u>	<u>950516</u>
R31 SW Okushiri I.	G98 Shikoku	G346-26 Hokkaido	G30 Pago Pago	G40 Port Vila, Vanuatu
R10 W Hokkaido	G68 Bonin Is.	G300 Yuzhno-Kurilsk	G05 Niue	G10 Pago Pago
R03 Russia	G56 Kyushu	G162 Bonin Islands		G06 Fiji
R02 NE South Korea	G19 Guam	G130-42 Honshu		G03 Apia, Samoa
R01 Aomori, Honshu	G19-5 Hawaii	G50 Midway		G03 Tonga
		G48 Hilo, Hawaii		G03 Raratonga, Cook I.
		G17 Wake		
		G17 Pago Pago		
		G15 Shemya, Alaska		
<u>950730</u>	<u>950816</u>	<u>951203</u>	<u>960217</u>	<u>960610</u>
G75 Hilo, Hawaii	G55 Rabaul, PNG	G41 Midway	R7 Biak I., Irian Jaya	G102 Adak, Alaska
G70 Kahului, Hawaii	G10 Kwajalein	G37-10 Hokkaido		G55 Kahalui, Hawaii
G55 Valparaiso, Chile		G31 Crescent City		G46 Midway
G30-9 Alaska		G20 Shemya		G38 Hilo, Hawaii
G29-26 Honshu		G13 Wake		G33 Nawiliwili, Hawaii
G27-10 California		G13-6 Honshu		G30 Crescent City
G25 Pago Pago		G10 Adak, Alaska		G15-10 Aleutians
G12 Nawiliwili, Hawaii				G10 Honolulu, Hawaii
G10 Easter Island				G10 Port Angeles
G09 Papeete, Fr. Poly.				
R2 Hiva Oe, Fr. Poly.				
<u>960610</u>	<u>970421</u>	<u>971205</u>		
In coda of main tsunami on several mareograms with about half the amplitude of the main tsunami.	R3 Santa Cruz Is.	G15 Aleutians, Alaska		

Table 3. Runup (R) in meters and Water Level Gauge (G) in centimeters tsunami measurements for warning events.

EARTHQUAKE ENGINEERING

THE UNIVERSITY OF CHICAGO PRESS
50 EAST LEXINGTON AVENUE, NEW YORK, N.Y. 10017-2473
1997

Real-time Hybrid Vibration Experiments with a 2-Degrees-of-Freedom Model

by

Keiichi TAMURA¹⁾ and Hiroshi KOBAYASHI²⁾

ABSTRACT

The real-time hybrid vibration experiment is a new concept experiment combining shaking table test and numerical response analysis in real-time. Real-time hybrid vibration experiments were conducted with a 2 degrees-of-freedom model. Results of experiments were compared with those of conventional shaking table tests, and the validity of real-time hybrid vibration experiment is demonstrated.

Key words: real-time hybrid vibration experiment, shaking table test, pseudo dynamic experiment, actuator delay compensation

1. INTRODUCTION

Most of the conventional hybrid experiments are pseudo dynamic experiments with an expanded time axis due to limitations of devices, e.g., capability of computation and compensation for actuator delay, and few precedents exist for hybrid vibration experiments using shaking tables. Differing from those conventional techniques, the real-time hybrid vibration experiment is a new concept experiment combining shaking table test and numerical response analysis in real-time.

We have developed a real-time hybrid experiment system at the Public Works Research Institute after the 1995 Kobe Earthquake. Presented are

the results of real-time hybrid vibration experiments with a 2 degrees-of-freedom model. Results are compared with those of shaking table tests and the validity of real-time hybrid vibration experiment is demonstrated.

2. OVERVIEW OF REAL-TIME HYBRID VIBRATION EXPERIMENT

As Figure-1 shows, in the real-time hybrid vibration experiment, an original structure is divided into two parts. One is an actual model specimen of original structure. This specimen is usually taken as a part of structure whose seismic behavior is unknown or complicated. The other is a numerical model for vibration response analysis. This model represents a part of structure whose seismic behavior can be evaluated by numerical analysis.

The numerical model consists of structural elements (mass, damping and stiffness matrices), external force, which is calculated from the acceleration of shaking table, and reaction force

1)Head, Ground Vibration Division, Earthquake Disaster Prevention Research Center, Public Works Research Institute, Ministry of Construction, Asahi 1, Tsukuba-shi, Ibaraki-ken, 305-0804, Japan.

2)Research Engineer, ditto.

generated at the boundary of the actual and numerical models. In the numerical analysis, the external and reaction forces are inputted, and the displacement of the actual model for the next time step is calculated. This displacement is realized by actuators. Then, the external and reaction forces are measured and taken into numerical analysis. Iterating these procedures, the seismic behavior of original structure can be accurately simulated.

3. FEATURES OF REAL-TIME HYBRID VIBRATION EXPERIMENT

Time Interval of Experiment

It takes short time from measuring reaction force to generating actuator signal for the next time step¹⁾. A central difference method is employed for numerical analysis. Time required for one cycle process is 2.08ms.

Actuator Delay Compensation

Since the response delay is inevitable with a hydraulic actuator, a compensation technique is adopted. This technique predicts the displacement of an actuator at the time after actuator delay $\delta t^{2)}$. A schematic illustration of compensation process is presented in Figure-2, in which the predicted displacement x'' is estimated from the calculated displacement x_j using an n th-order polynomial equation (1):

$$x'' = \sum_{j=0}^3 a_j x_j \quad (1)$$

where

$$a_0=4, a_1=-6, a_2=4, a_3=-1$$

The predicted displacement is modified so that the resulting displacement becomes equal to the calculated one.

4. HYBRID VIBRATION EXPERIMENTS WITH A 2-DEGREES-OF-FREEDOM MODEL

In order to demonstrate the validity of real-time hybrid vibration experiment, both real-time hybrid vibration experiments and conventional experiments with a whole structure model were conducted, and the results were compared.

The original structure for experiment is a 2 storied slab model supported by rubber bearings. Its conceptual view is presented in Figure-1. The slab part consists of H-shaped beams and infilled concrete. An advantage of rubber bearing is large bearing capacity and low rigidity. Using rubber bearings and heavy slabs makes it possible to prolong the natural period of test specimen, which is favorable for experiment. This test specimen basically represents a linear structure, however, nonlinear behavior of structure is also represented by installing a viscous damper between upper and lower slabs or between the shaking table and the lower slab.

Test cases of hybrid vibration experiments are listed in Table-1. In the hybrid vibration experiments, the mass, stiffness and damping of the upper level and the mass of the lower level were numerically modeled, as shown in Figure-1. Pseudo dynamic experiments with 50 times extended time axis were carried out to demonstrate the effects of experimental time axis on damping force estimation, which generally depends on velocity. Besides those hybrid vibration experiments, conventional experiments with the whole structure were also conducted, and the results of hybrid vibration experiments and conventional experiments were compared.

Input motions employed for experiments were five cycles of sinusoidal wave with the frequency

of 1.7Hz, which corresponds to the fundamental natural frequency of the whole structure, and the strong ground motion recorded at Kobe Maritime Observatory, Japan Meteorological Agency, during the 1995 Kobe Earthquake. The maximum peak acceleration was variously changed in experiments.

5. NUMERICAL MODELS FOR HYBRID VIBRATION EXPERIMENTS

5.1 Linear structure (Cases 1 and 2)

The equation of motion for numerical analysis is described by

$$M\ddot{x} + C\dot{x} + Kx = p + q \quad (2)$$

where

M : Mass matrix

C : Damping matrix

K : Stiffness matrix

x : Relative displacement vector

p : external force (seismic response) vector

q : reaction force vector

The mass, damping and stiffness were determined as follows:

Mass

Mass of slabs and rubber bearings were considered.

Damping

The damping matrix was estimated from the damping ratio to the critical $h=0.026$, which was obtained by free vibration tests, and the relationship $C = \beta K$ ($\beta = 2h/\omega$).

Stiffness

The relationship between load and displacement was obtained by forced vibration tests, where the frequency was set as 0.1Hz and

1.7Hz. The result is shown in Figure-3. Since the maximum peak displacement of the upper slab in experiments with the whole structure was 20-30mm, the stiffness coefficient was determined as $2.6 \times 10^6 \text{N/m}$.

5.2 Upper nonlinear structure (Cases 3 and 4)

Mass

Same as 5.1.

Damping and Stiffness

The damping and stiffness matrices can not be developed by usual matrix operation, when nonlinearity exists. In the present study, the reaction force vector q was divided into a linear part $q_1 (=Kx)$ and nonlinear part q_2 as shown in Figure-4. q_1 and q_2 can be estimated from measuring reaction force and nonlinear calculation, respectively. Since the damping force generally depends on velocity, the relationship between force and velocity was estimated from the forced vibration tests of dampers, which is shown in Figure-5. Figure-6 presents the relationship between the damping force and velocity. As seen from this figure, this damper generates force almost proportional to the velocity for the pull-side, and small and velocity independent force for the push-side.

5.3 Lower nonlinear structure (Cases 5 to 8)

Same as 5.1.

6. EXPERIMENT RESULTS

Figure-7 compares displacement time histories of the lower slab for hybrid vibration experiments and conventional shaking table tests with the whole structure, where the results of pseudo dynamic hybrid experiments are plotted with the actual time axis. The cross-correlation coefficients between hybrid vibration

experiments and conventional shaking table tests are calculated for displacements and shown in Table-2. The following points may be deduced from the experiment results.

(1) The real-time hybrid vibration experiment well reproduces the seismic behavior of the 2-degrees-of-freedom structure for both linear and nonlinear cases.

(2) The pseudo dynamic hybrid experiment yields excessive response and inappropriate response period. This may be attributed to the fact that pseudo dynamic experiment can not properly reproduce the damping force, which is generally proportional to velocity.

(3) The cross-correlation coefficients between the calculated and resulting displacements in hybrid vibration experiments show very high values, such as higher than 0.99, for all cases, which indicates that actuator delay compensation successfully works.

(4) Causes of slight error between real-time hybrid vibration experiments and conventional shaking table tests may exist in:

- a. Effects of noise associated with measuring instruments.
- b. Effects of high-frequency forced vibration of shaking table caused by actuators for hybrid vibration experiment.
- c. Slight difference of input motions for real-time hybrid vibration experiments and conventional shaking table tests.
- d. Error in establishing parameters for numerical analysis model.

7. CONCLUSIONS

The main conclusions of the present study may be summarized as follows:

- 1) The technique employed in this study to compensate actuator delay has sufficient accuracy.
- 2) The real-time hybrid vibration experiment well reproduces seismic behavior of the 2 degrees-of-freedom model and the validity of experiment is confirmed.

REFERENCES

- 1) Kazuhiro UMEKITA, et al., Development of C Language Library for Super Real-Time Controller (SRC) for Real-Time Hybrid Seismic Testing System with Three-dimensional-in-plane Excitation, 40th Japan Joint Automatic Control Conference, 1997 (in Japanese)
- 2) Toshihiko HORIUCHI, Masaki NAKAGAWA, Masaharu SUGANO and Takao KONNO, Development of a Real-Time Hybrid Experimental System with Actuator Delay Compensation, Eleventh World Conference on Earthquake Engineering, 1996

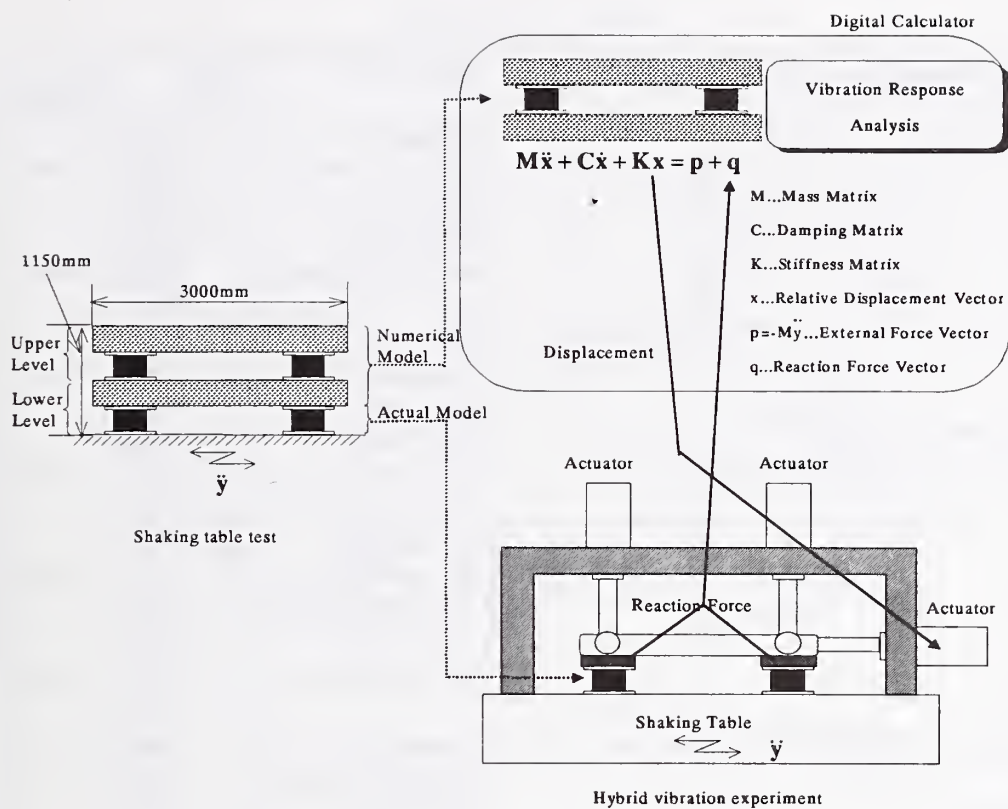


Figure-1 Conceptual view of hybrid vibration experiment

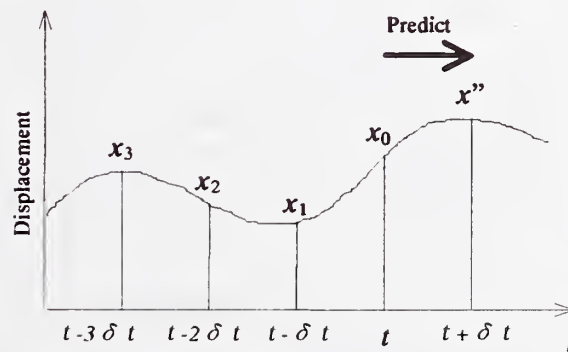


Figure-2 Calculation of predicted displacement x''

Table-1 Test cases

Experiment Method	Upper Level	Lower Level	Input Motion	Input Level	Case Number
Real-time	Linear Model	Linear Model	5 cycles of sinusoidal waves ($f=1.7\text{Hz}$)	50gal	Case 1
				70gal	
				100gal	
			JMA Kobe Record (NS comp)	100gal	Case 2
				300gal	
				500gal	
	Nonlinear Model	Linear Model	5 cycles of sinusoidal waves ($f=1.7\text{Hz}$)	50gal	Case 3
				70gal	
				100gal	
			JMA Kobe Record (NS comp)	100gal	Case 4
				300gal	
				500gal	
Pseudo Dynamic	Linear Model	Nonlinear Model	5 cycles of sinusoidal waves ($f=1.7\text{Hz}$)	50gal	Case 5
				70gal	
				100gal	
			JMA Kobe Record (NS comp)	100gal	Case 6
				300gal	
				500gal	
			5 cycles of sinusoidal waves ($f=1.7\text{Hz}$)	50gal	Case 7
				70gal	
				100gal	
			JMA Kobe Record (NS comp)	100gal	Case 8
				300gal	
				500gal	

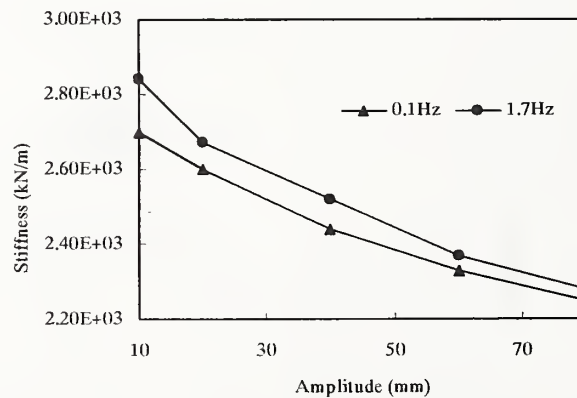


Figure-3 Relationship between amplitude and stiffness

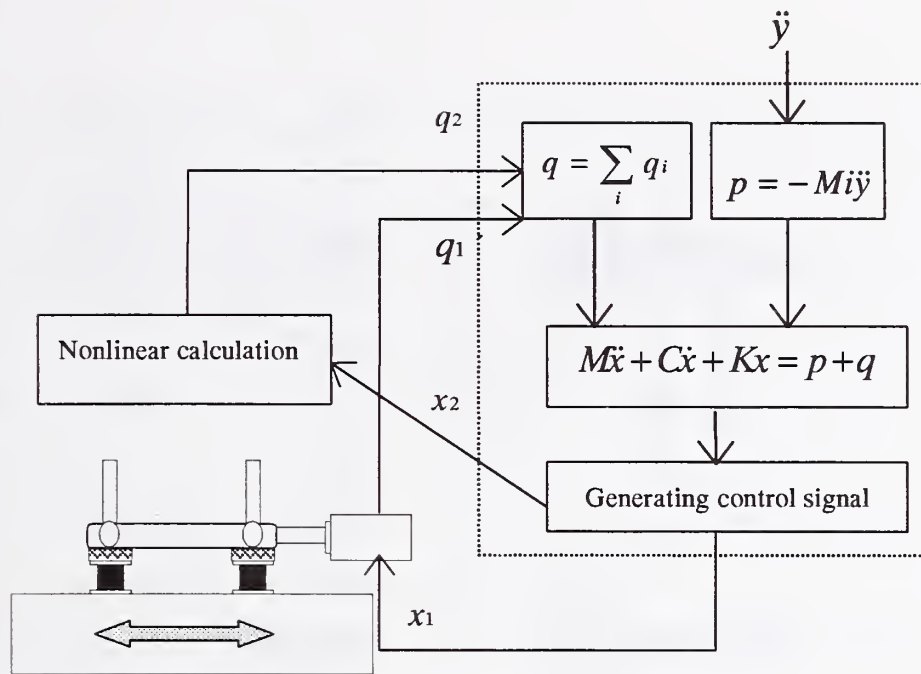


Figure-4 Hybrid experiment dealing with nonlinear factor in vibration response analysis

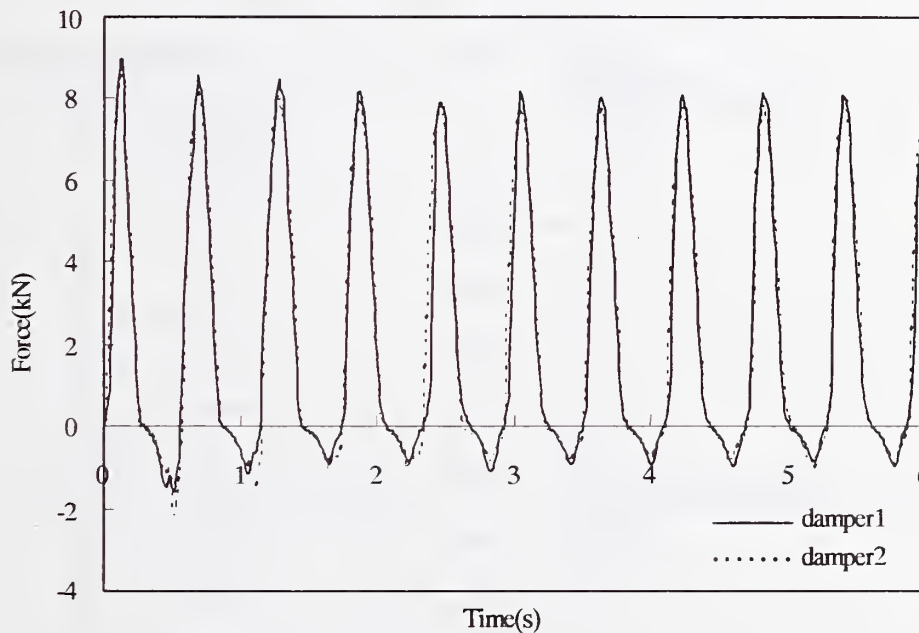


Figure-5 Forced vibration test of damper
(Sinusoidal wave, $f=1.7\text{Hz}$, Amplitude=80mm)

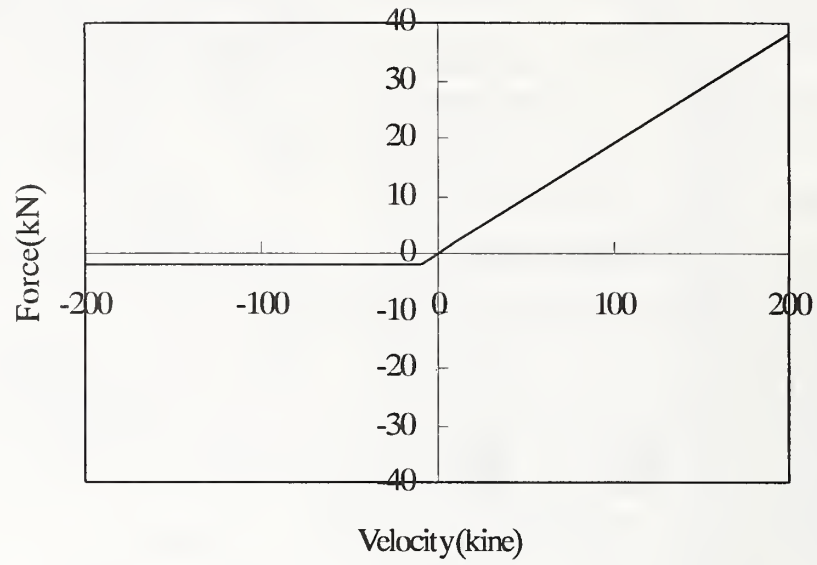


Figure-6 Relationship between damping force and velocity

Table-2 Correlation coefficients between
hybrid vibration experiments and shaking table tests

Case	Correlation coefficient
Case1 100gal	0.966
Case2 500gal	0.896
Case3 100gal	0.881
Case4 500gal	0.980
Case5 100gal	0.981
Case6 500gal	0.938
Case7 100gal	0.776
Case8 500gal	0.829

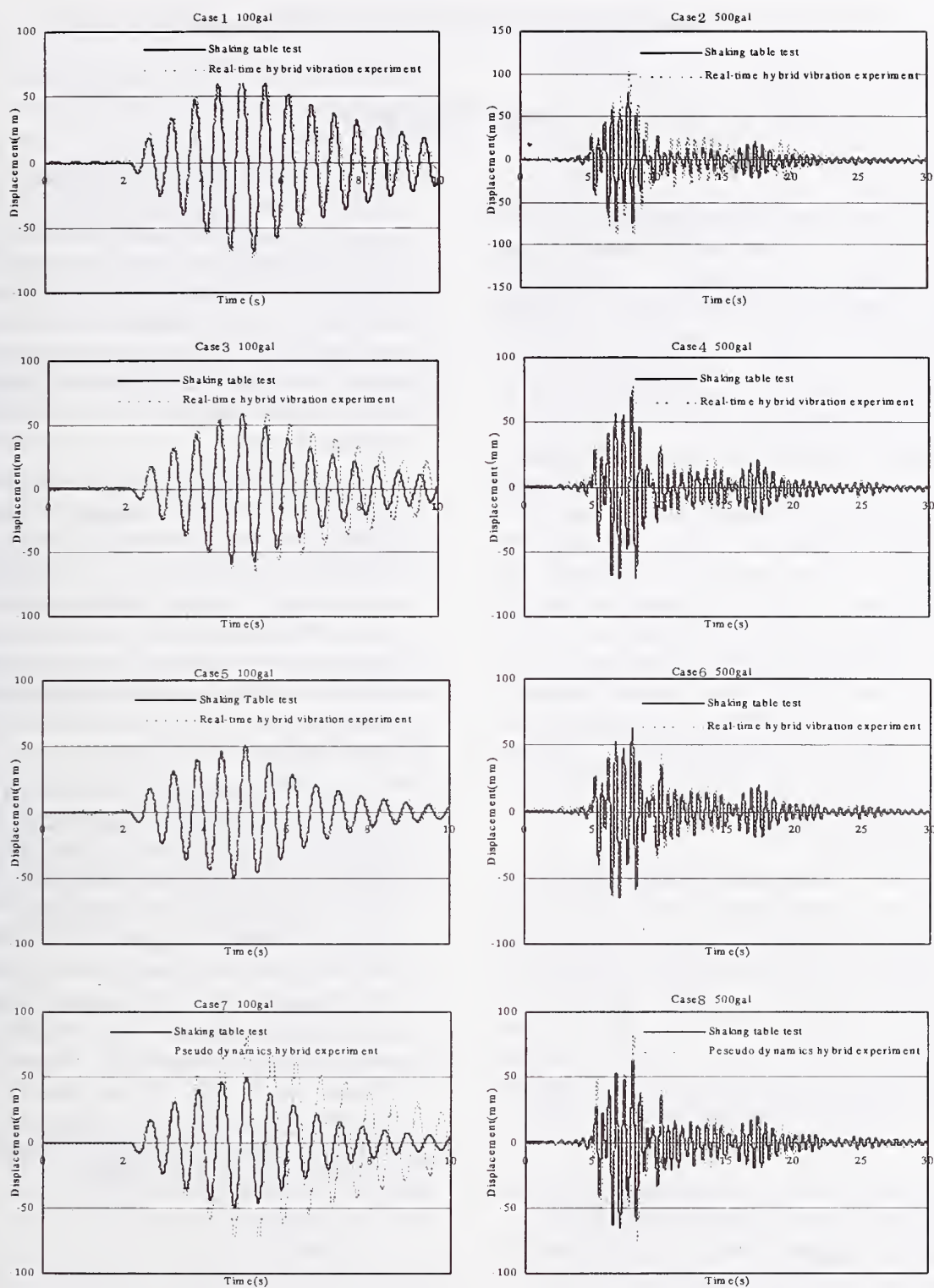


Figure-7 Displacement time histories of the lower slab

A Vision for the Future of Strong-Motion Recording

Roger D. Borcherdt*

ABSTRACT

Strong-motion recordings of shaking are the basis for earthquake resistant design, construction, and retrofit practices worldwide. They provide critical quantitative measurements of damaging earthquakes in urban environments needed for mitigation of future earthquake losses. The present critical lack of strong-motion information emphasizes that urgent action is required to significantly increase resources to adequately record future damaging earthquakes. Recent estimates for the US suggest that an urgent need to record the next major earthquake adequately throughout stricken urban areas requires that instrumentation and recording efforts be increased by nearly 20 times within the next five to ten years (Stepp, 1997; Borcherdt, et al., 1997). Justification for this dramatic increase as prepared by the "Committee for the Future of the US National Strong-Motion Program" (Borcherdt, ed., 1997) is summarized here.

1. INTRODUCTION

Staggering losses from recent earthquakes impacting Northridge, California (\$15 to \$25 billion, 64 lives) and Kobe, Japan (> \$100 billion and 5500 lives) clearly demonstrate the potential impact of moderate to large earthquakes on modern urbanized societies. If a major earthquake impacted some densely urbanized areas of the United States in the near future, life and economic losses are estimated to be at least

KEYWORDS: Strong-motion recording, Public Earthquake Safety, Earthquake hazards reduction, Emergency response, Strong motion.

twice as large. If these same earthquakes were to impact the areas in thirty to fifty years without any major changes in earthquake safety, losses could reach tens of trillions of dollars due to increased urbanization with inadequate safety standards. These tremendous potential losses with catastrophic and global consequences argue strongly for dramatically accelerated programs to improve public earthquake safety as quickly as resources permit.

Reduction of life and property losses to low and manageable levels requires significant improvements in both *Hazard Mitigation* and *Emergency Response*. Quantitative measurements of strong shaking referred to as "strong-motion recordings" are the critical and presently scarce element essential for significant progress in both areas. Modern technology offers important new opportunities to acquire these recordings.

This paper provides a brief summary of the justification for the need to significantly increase strong-motion observation for public safety. The application of the limited existing set of strong-motion information to earthquake hazard mitigation worldwide suggests that arguments for additional information need to be considered in international forums. This summary is presented here to further evaluate the need for strong-motion observation worldwide. The summary is presented as a series of answers to specific questions prepared by the "Committee for the Future of the US National Strong-Motion Program", (Borcherdt, ed., 1997).

* United States Geological Survey
Menlo Park, CA 94025

2. *How significant is the earthquake threat to public safety?*

- Staggering losses from recent earthquakes impacting Northridge, California (\$15 to \$25 billion, 64 lives) and Kobe, Japan (> \$100 billion and 5500 lives) clearly demonstrate the potential impact of moderate earthquakes on modern urbanized societies.
- Dramatic increases in urbanization based on inadequate safety standards imply that costs in lives and property from a future major earthquake in the United States could exceed \$200 billion dollars, cause several thousand deaths, and significantly impact the global economy.

3. *What are strong-motion recordings?*

- Strong-motion recordings are on-scale recordings of the main damaging earthquake at locations of most significance for public earthquake safety.
- Strong-motion recordings are recordings of the main shock, often on or near structures in densely urbanized environments, within 20 km of the earthquake-rupture zone for sites on rock and within about 100 km for sites on soft soils. Recordings of motions at levels sufficient to cause damage at sites at greater distances also are of interest for earthquake engineering in areas likely to be affected by large subduction zone earthquakes or in areas with exceptionally low attenuation rates.

4. *Why are strong-motion recordings critical for significant improvements in public safety?*

- Public safety requires that man-made structures resist strong, earthquake-induced shaking.
- Strong-motion recordings are the quantitative in-situ measurement of shaking and the resultant dynamic performance of structures needed to build and strengthen the built environment to resist future earthquakes.
- Strong-motion recordings are the basis for all current earthquake-resistant design, construction, and retrofit codes and practice.
- Strong-motion recordings are the basis for a significant proportion of the research products

produced for purposes of earthquake hazard reduction.

- Strong-motion recordings are necessary for real-time damage assessment and emergency response in densely urbanized areas as both efforts require dense sets of on-scale measurements of damaging levels of shaking on and near structures in earthquake stricken areas.
- The present scarcity of quantitative measurements of ground shaking and its damaging effects on the built environment is a major obstacle to reducing future losses of life and property to manageable levels.

5. *Why is the present set of US strong-motion recordings inadequate?*

- No recordings exist of any major ($M_w > 7.5$) US earthquake at locations experiencing damaging levels of shaking.
- No recordings of any high-rise, steel-moment-frame building within 20 km of a moderate to large ($M_w > 6.5$) US earthquake exist.
- No recordings exist in the US of any critical lifeline at damaging levels of motion, such as the six major bridges crossing the San Francisco Bay that are being presently retrofitted, based on as yet undocumented levels of ground shaking.
- Few (< 10) recordings of the dynamic response of soft soils exist, yet billions of dollars of bridges, buildings, pipelines, and highways are being built on such deposits each year.
- Few (< 10) recordings exist of large sudden coherent pulses of motion ("fault fling" or "killer pulses") that occur near the fault rupture and are expected to cause catastrophic losses for cities such as Hayward, Oakland and Berkeley, CA.
- Few recordings of most modern structures in their in-situ environment have been obtained of actual damaging levels of earthquake loading.

6. *Why is a thorough set of strong-motion recordings of the next damaging earthquake an urgent national need?*

- Billions of dollars are being expended each year to build and strengthen the built environment based in many cases on as yet undocumented strong ground shaking and structural performance levels.
- If thorough sets of strong-motion recordings of the next major earthquake are not obtained on and near structures in the stricken areas, then another important infrequent opportunity will be missed.
- Present expenditures based on a totally inadequate database will continue and the catastrophic costs of future earthquakes will increase exponentially with time as urbanization increases.
- The high likelihood for a major damaging earthquake to strike areas such as the San Francisco Bay region within the next five years, implies an urgent effort is required to acquire and install the necessary resources to prevent another major missed opportunity.

7. *What resources are required to provide an adequate set of strong-motion recordings of the next major earthquake in the coterminous United States?*

- Recent consensus of a national workshop (Stepp, 1997) implies a dramatic increase in resources (funding and people) is needed to ensure that critically needed instrumentation (20,000 stations) is operational by the year 2005.
- Estimates derived on the basis of recent National Seismic Hazard Maps (Frankel, et al., 1996) and estimates of population exposure imply that instrumentation at about 20,000 sites is needed with 7,000 for ground-motion, 7,000 for buildings, 3,000 for lifelines, such as bridges and pipelines, and 3,000 for critical facilities necessary for emergency response and near-real time disaster assessment (Borcherdt, 1997a, 1997b, Borcherdt, et al., 1997).

8. *What resources are required to record a specific earthquake in one of the areas with high population exposure to damaging ground motions?*

- Estimates of the density and location of strong-motion stations needed to record a specific earthquake can be developed for each urban area using modern GIS technology, regional estimates of ground shaking, inventories of the built environment, and modern methods to predict resultant earthquake losses.
- Application of the procedures to the San Francisco Bay Region for a repeat of the 1906 earthquake (Mw 7.7) provides significant insight for strong-motion planning purposes.
- Estimated losses for a repeat of the 1906 earthquake are expected to exceed \$200 billion with more than 5000 deaths (RMS, inc., 1995).
- 140 - 180 ground-motion stations are needed in the city of San Francisco with a spacing of no more than a few blocks in the heavily impacted financial district.
- Superposition of the built environment on predicted ground shaking maps shows that in the southern San Francisco Bay region 45% of the 1079 bridges, 69% of the 16 airports, 22% of the 233 hazardous material sites, 48% of the 99 medical facilities, and 48% of the 801 schools are located in areas expected to experience damaging levels of shaking that exceed 0.6 g in spectral response acceleration at 1.0 second.
- Superposition of the transportation facilities on a site class map based on the 1994 Recommend Building Code provisions shows that 69% of the bridges, 57% of the highways, and 100% of the railways are located on either stiff clays and sandy soils or on soft clays with a high to very high amplification capability and moderate-to-high liquefaction susceptibility.
- The large percentages of important structures (~ 990) and buildings (>3000) located in areas of potentially damaging ground shaking

suggest that more than 4000 sites in the SF Bay region need to be considered for instrumentation.

- If only 10 percent of especially vulnerable structures in the southern SF bay region are instrumented, then at least 400 instrumentation arrays on and near structures are needed.
- Instrumentation estimates show that the present level of strong-motion instrumentation in the densely urbanized areas of the San Francisco Bay Region is woefully inadequate to document the ground shaking and the resultant seismic performance of the built environment to a repeat of the 1906 earthquake.

9. *What proportion of strong-motion stations should be equipped with real time telecommunication for purposes of disaster assessment and emergency response?*

- Modern instrumentation with telecommunication capabilities permits areas of strongest shaking and the performance of structures to be quickly assessed (Nigbor, 1997). Instruments on structures such as major buildings, hospitals, schools, bridges, freeway overpasses, dams etc. permit rapid assessment of probable damage state, efficient dispatch and routing of emergency response resources, and efficient prevention of additional disaster. Several important examples illustrating the application of modern technology to Disaster Reduction now exist in Japan.
- Preliminary estimates on the basis of estimated shaking levels suggest that some 50-85% of the strong-motion instrumentation installed for ground-motion measurement purposes in cells of highest population exposure should be equipped with near-real time communication capabilities for at least some channels.
- Considerations based on the geographic distribution of the built environment for the southern San Francisco suggest some 25 to 50 percent of instrumented structures should also be equipped with telecommunication for a few

data channels to assess the damage state of the structures in near-real time.

10. CONCLUSION

Strong-motion recordings of shaking are the basis of earthquake resistant design, construction, and retrofit practice. For many issues important in earthquake safety, advances will not occur until a major earthquake provides new strong-motion data. It is vital that we plan wisely to obtain the greatest possible return from the next earthquake, so that societies will not be forced to wait for another disaster before acquiring the needed data to resolve important safety issues.

11. ACKNOWLEDGMENTS

The summary presented here was prepared by the "Committee for the Future of the US National Strong-Motion Program" comprised of B. Bolt, C. B. Crouse, G. Hart, K. Jacob, T. Shakal, C. Stepp and USGS Members H. Benz, R. Borchardt (Chair), M. Celebi, A. Frankel, W. Joyner, E.V. Leyendecker, D. Oppenheimer, R. Porcella, C. Stephens, and D. Wald.

12. REFERENCES CITED

- Borchardt, R. D., 1997a, US National Strong Motion Program, in Proceedings, Workshop, *Vision 2005: An Action Plan for Strong Motion Programs to Mitigate Earthquake Losses in Urbanized Areas*, C. Stepp, editor, Committee for the Advancement of Strong Motion Programs, Monterey, CA, April, 1997, 81-85.
- Borchardt, R. D., 1997b, Earthquake ground-motion measurement for public safety, Proceedings, 29th Joint Meeting UJNR Panel on Wind and Seismic Effects, Tsukuba, Japan, May 1997.
- Borchardt, R. D. ed., 1997, Vision for the future of the US National Strong-Motion Program, The committee for the future of the US National Strong Motion Program, US Geological Survey Open File Rept. 97 - 530 B, 47p.
- Borchardt, R. D., Frankel, A., Joyner, W.B, and Bouabid, J., 1997, Vision 2005 for

earthquake strong ground-motion measurement in the United States, in *Proceedings, Workshop, Vision 2005: An Action Plan for Strong Motion Programs to Mitigate Earthquake Losses in Urbanized Areas*, C. Stepp, editor, Committee for the Advancement of Strong Motion Programs, Monterey, CA, April, 1997, 112-130.

Frankel, A., Mueller, C., Barnhard, T., Perkins, D., Leyendecker, E.V., Dickman, N., Hanson, S., and Hopper, M., 1996, National Seismic Hazard Maps, June 1996, Documentation, <http://gldage.cr.usgs.gov/eq/hazmapsdoc/junecover.shtml>.

Nigbor, R.L., 1997, Present and future needs for strong-motion information, *Proceedings, Vision 2005: An Action Plan for Strong-motion Programs to Mitigate Earthquake Losses in Urbanized Areas*, C. Stepp, editor, Committee for the Advancement of Strong Motion Programs, National Science Foundation, Monterey, CA, April 1997.

Stepp, C. J., 1997, *Proceedings, Vision 2005: An Action Plan for Strong-motion Programs to Mitigate Earthquake Losses in Urbanized Areas*, Committee for the Advancement of Strong Motion Programs, National Science Foundation, Monterey, CA, April 1997.

Project on 3-D Full Scale Earthquake Testing Facility - First Report -

Keiichi OHTANI¹⁾, Tsuneo Katayama²⁾, Heki Shibata³⁾

ABSTRACT

The Hanshin-Awaji Earthquake (Hogoken-Nambu Earthquake, January 17, 1995) clearly demonstrated that the occurrence of very strong ground motion in the area near to the seismic fault is capable of causing severe structural damage beyond general estimation. It has emphasized the importance of earthquake engineering research into why and how structures collapse in real earthquake conditions and these processes are reproduced numerically. Considering the lessons learnt from recent earthquake disasters, NIED plan to construct a "3-D Full Scale Earthquake Testing Facility," which will be able to simulate the process of destruction of structures. This facility will be a central tool in a new concept of research bases for earthquake disaster prevention. NIED was conducted the research and development of core technology, such as the big and high performance hydraulic actuators, which have a long displacement and high velocity, and high performance three dimensional link joint since 1995 by the 4 year project. We constructed the prototype shaking table systems and confirmed the performance tests. NIED will begin the design and construction of this new facility in fiscal year

1998. This paper summarizes the fundamental concept of the facility and the result of R&D of core technology.

*Key Words: Earthquake Disaster,
High-performance actuator,
3-dimensional earthquake motion,
Shaking Table,
Structural damages.*

1. INTRODUCTION

The Hanshin-Awaji Earthquake gave a great impact to our society. More than 6,400 people lost their lives and a lot of structures, such as roads, railway bridges, buildings and other structures, suffered unexpectedly serious damages by this event. This earthquake event was made clear that our society, which is consisted the advanced, complexes facilities and concentrated population and city functions, has a over-expected weakness against natural disasters. The many major cities in Japan located a high potential area for earthquake hazard. Therefore, from this condition, it is pointed out that big hazard by a future earthquake at such big cities will affect the worldwide economic impact based on the border less, globalization, economic condition. And,

¹⁾ Director, Disaster Prevention Research Division, National Research Institute for Earth Science and Disaster Prevention (NIED), Science and Technology Agency (STA)

²⁾ Director-General, NIED, STA

³⁾ Guest Research Fellow, NIED, STA, Prof. Emeritus, Univ. of Tokyo

the high potential area of earthquake hazard are also located the many countries, such as United State and Asian region. The progress of research for earthquake disaster mitigation is very important them to prove world widely. It is the urgent subject to decrease the potential of earthquake hazard risk by the effective and economical technology and measures based on the appropriate engineering and scientific knowledge.

Based on these condition, National Research Institute for Earth Science and Disaster Prevention (NIED) has planned to construct a "3-D Full Scale Earthquake Testing Facility." NIED was conducting the research and development of core technology since 1995 and will start the design and construction works of this new facility in fiscal year 1998.

This paper summarizes the fundamental concepts of this facility and the current results of research and development of the core technology.

2. BACKGROUND

STA was enforced several actions relating with the promotion of research and development for earthquake disaster prevention since the occurrence of Hanshin-Awaji earthquake.

2.1. Basic plan for research and development on disaster prevention

The promotion of research and development of disaster prevention in Japan accelerated of the clutch based on the "Basic Plan for Research and Development on Disaster Prevention" reported by the Prime Minister's Council of Science and Technology, and finally

approved by the Prime Minister on December 1993.

2.2. Investigative committee for promoting earthquake disaster prevention

Given this Basic Plan, and in light of the lessons learnt from the recent earthquake devastation, an "Investigative Committee for Promoting Earthquake Disaster Prevention (Chairman: Prof. Shigeru Ito, Keio University)" was set up within the Research and Development Bureau, Science and Technology Agency (STA) in March 1995. This committee was investigated the research and development issues that need to be accelerated in disaster prevention related science and technology. The mandate of this committee was to quickly propose the research and development issues that need to be addressed, after which, on May 31, 1995, they published a report entitled "Policies for Accelerating Earthquake Disaster Prevention Based on the Experience of Great Hanshin-Awaji Earthquake and the Other Destructive Earthquakes."

This report produced the following four research and development issues for urgent attention:

- 1) Research and development into earthquake disaster prevention by appraisal methods that would act as a comprehensive basis for accelerating earthquake disaster prevention,
- 2) Research and development into information about earthquake disaster prevention and how to support the daily existence of the people,
- 3) Research and development into the strengthening of urban environment against earthquake,

- 4) Research and development into the maintenance of daily order and social activities during an earthquake.

2.3. Committee to examine the research bases for earthquake disaster prevention

Based on the lessons learnt from Hanshin-Awaji earthquake, the various research institutions, such as governmental, academic and private sectors, were conducting the research work for earthquake disaster prevention. Furthermore, the existing research institutions are encouraged the expansion, reinforcement and arrangement of organization for it's research potentials. But, we strongly recognized that the difficult problem, which is requested from the experience of Hanshin-Awaji earthquake to the science and technology of earthquake disaster prevention, was raised. For answer to this problem, we think to build up the new type research organization.

Based on this recognition, STA established a "Committee to examine Earthquake Disaster Research Bases (Chairman: Prof. Tuneo Okada, Shibaura Institute of Technology)" in November 1995. This committee published the report entitled "Promotion of Effective Improvement of Research Bases for Earthquake Disaster Prevention based on Consideration of Hanshin-Awaji Earthquake" in May 1996.

The following research needs were realized with the chain of comprehensive research to aim the mitigation of earthquake disasters in and around the urban areas;

- 1) The research and development required the arrangement of new large-scale experimental facilities,

- 2) The research and development by the fluid organization, such as participation of researchers from many research fields and different countries,

- 3) The comprehensive research and development for earthquake disaster prevention based on the non-physical aspects.

From these research needs, the committee recognized of new research bases for earthquake disaster prevention. The concepts for this research base were stated clearly the following five items;

- 1) By the basic consideration is sitting on the protection of human lives, this bases will be functioned the progress of cooperation, exchange and mutual comprehension with various fields of researchers, such as engineering, science, humanity-social science, information technology, medical science and other sciences,
- 2) The research subjects, which is difficult to conduct the fixed research organization, will promote by the fluid organization systems,
- 3) By the arrangement the common-use research facilities, the new research organization and personnel structures will arrange for the response the wide research needs from wide areas of research field and existing organizations,
- 4) To construct the bases of international research exchange for the focus to the Asia and Pacific region,
- 5) The bases will contribute the effective transmission of the experience of the Hanshin-Awaji earthquake to the future generation and the comprehension and support by the public for the research of disaster prevention.

Considering these concepts, the committee proposed the construction (arrangement) of new research bases for earthquake disaster prevention. The committee's report suggested the need in future comprehensive research to reduce earthquake damage mainly of urban area. As part of such research, the report indicated the need to establish a new research base with subjects of (1) comprehensive anti-seismic, base-isolation and response-control systems, (2) relation between active faults and earthquake disaster prevention, (3) comprehensive earthquake information. The report insisted upon the significance of further increasing the promotion of science and technology for earthquake disaster prevention.

2.4. Discussion at the Council for Aeronautics, Electronics and Other Advanced Technology

At the latest stage of discussion at the Committee to examine the Research Bases for Earthquake Disaster Prevention, STA recognized to need the wider discussion with the persons from various fields. The Minister of State for Science and Technology was refer to the Council for Aeronautics, Electronics and Other Advanced Technology, which is the one refer organization of the Minister, for the discussion of the effective arrangement of research bases for earthquake disaster prevention at March 29, 1996. The Council was requested the charge of discussion to the Sub-committee for Earth Science. The sub-committee was established the Sectional Committee for Research Bases of Earthquake Disaster Prevention (Chairman: Prof. Tuneo Okada, Shibaura Institute of Technology). And, following three working groups were

established under this sectional committee for the concrete discussion. (1) Working Group on Research Bases (Chairman: Prof. Hiroyuki Kameda, Kyoto University), (2) Working Group on the Objective Earthquake (Chairman: Prof. Syunsuke Otani, University of Tokyo), (3) Working Group on Large-Scale Three-Dimensional Earthquake Simulator Facility (Chairman: Prof. Emeritus Heki Shibata, University of Tokyo).

After the total 30 meeting at the council, subcommittee, sectional committee and working groups, the Council was reported to the Minister at September 3, 1997.

The report was clearly pointed out the arrangement of large-scale three-dimensional earthquake simulator facility as the core facility of the research bases for earthquake disaster prevention.

3. PROJECT ON 3-D FULL SCALE EARTHQUAKE TESTING FACILITY

NIED initiated the project on the large-scale 3-dimensional earthquake simulator facility just after the occurrence of Hanshin-Awaji earthquake. The research and development for core technology for this facility was conducting since 1995.

At the initiated stage, we named the "Large-Scale 3-Dimensional Earthquake Simulator Facility." But, at this moment, we renamed to the "3-D Full Scale Earthquake Testing Facility."

The fundamental concepts of this project based on the report by the Council for Aeronautics, Electronics and Other Advanced Technology.

3.1. Position to the project

This facility will construct as the core facility of the research bases for earthquake disaster prevention. Therefore, we need to clear the positions of this facility.

- 1) Position of earthquake simulator for the main element of development of the "Time-Space Domain Simulation System for Earthquake Disaster."

By the accumulation of the failure testing result for different type of structures, it will be possible to make a rapid progress the usefulness of numerical shaking table. This progress will connect the development of the "time-space domain simulation system for earthquake disaster prevention." This simulation system is imaged to the total simulation system of the sequence of earthquake disaster, such as where and how large earthquake occur, what kind of damage occur and propagate and other related events.

- 2) Position of the clearly understanding of failure mechanism of structures.

During the Hanshin-Awaji earthquake, the structures were suffered over-expected damage and failures. Therefore, it is necessary to arrange the high performance earthquake simulator for the understanding of failure process of structures during earthquake.

- 3) Position of the response mechanism for the request from major subject of earthquake engineering.

To apply the experience of structure damage and failures learnt from Hanshin-Awaji earthquake and other recent destructive earthquakes, and to create the safer city and society against earthquake, it is necessary to test the following items;

- [1] Development and verification of new design and construction technology for the building structures,
- [2] Development and verification of new design and construction technology for the civil work structures,
- [3] Development and verification of new design and construction technology for the structures sited on different soil conditions,
- [4] Verification of development, adaptability and safety of base-isolation system and response control technology
- [5] Verification of advancement of seismic performance and safety of the importance industrial facilities and equipment, such as to keep the social functions and to prevent disaster propagation.

3.2. Requested fundamental performance

This facility is requested the realization with fundamental performance as follows;

- 1) To be able to perform the failure test

It is necessary to have a performance of reproduce of failure phenomena by the long-period pulse waves (killer pulse), which was the one characteristics of Hanshin-Awaji earthquake motions.

- 2) To be able to produce the three-dimensional movements

It is necessary to perfectly reproduce the 3-dimensional strong motions of Hanshin-Awaji earthquake, including the displacement and velocity. This performance will set up to the minimum requirement.

- 3) To be able to test for the real-size structures

Many phenomena of structural failure were occurred at only the real size structures. For the detailed understanding of such phenomena, it is necessary to conduct the test for the real

size structural specimen. Therefore, it is necessary to have the sufficient specification of maximum model weight, allowable overturning moment capacity and others for the test of large-size specimen.

3.3. Major specification

Sufficient information needs to be gathered on how structures and foundations behave, and whether or not they are destroyed, during a major earthquake. The importance of promoting the strengthening and rationalization of earthquake-proof structural design is just one of the lessons learnt from the Hanshin-Awaji earthquake. Because earthquake vibrations involve three-dimensional movement, it is necessary to set up a three-dimensional earthquake simulator facility to accurately reproduce earthquake motions. More than 30 three-dimensional shaking table have already built throughout the world, but they are all only small- or medium-sized devices. To perform tests on real-size objects or large-scale models of test structures and foundations, it is desirable to have the large-scale 3-dimensional shaking table. If large-scale 3-dimensional shaking table was available, tests could be performed to shed new light on the mechanism of dynamic failure using real-size structures as test objects and on the mechanism that destroys submerged structures when soil liquefaction. If a stage reached whereby design based on such discovery can be performed, this will contribute immensely to reducing earthquake disaster.

1) The main specification is shown in Table 1.

The actuator performance for three axes, (X, Y (horizontal axis) and Z (vertical axis)), are shown in Fig. 1 to Fig. 3, respectively. The table size and maximum test model weight

are the largest specification of the world. These specification was determined for the conducting to the almost real-size 4 story, 2 X 3 span reinforced concrete buildings and the real-size reinforced concrete bridge columns.

- 2) The driving method is choose the accumulator charge and electro-hydraulic servo control system, which is very common method to make the earthquake simulator.
- 3) The maximum acceleration of shaking table is determined by the model weight. At the maximum test model weight, maximum accelerations for horizontal axis are limited to 0.9 G. This value was determined by the reproduce of ground surface earthquake motions, not reproduce the response movement of structures, which is the basic conception of this facility.
- 4) The maximum velocity and maximum displacement are set up to the maximum value of future imaged earthquake motions.
- 5) The maximum overturning moment is set to perform the real-size subjects.

We will construct several buildings, such as the control and measurement building, testing building, oil source building and others. The layout of the facility is shown in Fig. 4.

3.4. Construction site and time schedule

The government of Hyogo prefecture will develop the Miki Memorial Park of Hanshin-Awaji earthquake at the city of Miki. This park have been functioned three zones, such as athletic park zone, citizen recreation zone and disaster prevention zone. This facility will construct as the core facility of disaster prevention zone. For this zone, the disaster prevention center of Hyogo prefecture, school

for fire defense and helicopter spots will also construct in the near future.

The land for this park is located hilly area, and is not developed at this moment. Based on the result of soil condition survey, the foundation of shaking table will set the bottom of small valley. The current sectional design of foundation arrangement is shown in Fig. 5. The waved line illustrated the existing land profile in this figure. The bottom of foundation will construct on the Kobe layer, which is belonging with the tertiary layer.

The detailed design of mechanical system, such as shaking table, actuator, 3-dimensional link joint, oil supply system, control system and other equipment, and buildings will start in fiscal year 1998. The completion of this facility will be scheduled in fiscal year 2004 after 7 years plan.

3.5. Matter for management

The report by the Council was suggested that the management of this facility would be considered the following condition;

1) The international common use facility

This facility is the very large scale and high performance testing facility in the world. Therefore, many researchers, which are belong not only Japan but also worldwide organizations, can use this facility for their researches. This facility should be operated the international common use. It is important to arrange the utilizing structures, equipment and support section for the outside users.

2) Operation autonomous

The operation and maintenance of this facility should be done the professional experts, who have the professional knowledge and enough

experience. It is important that to secure those experts and to establish the operation organization.

3) Fundamental important matters

For the effective operation of this facility it is important to enough care the following items;

- [1] To operate the common use, such as users from government, academia, private sector and overseas organization,
- [2] To establish the appropriate administrative and operate mechanisms.
- [3] To secure the high carrier personnel and the continuous budget for the smoothly management of this facility.
- [4] To establish the encouragement, support and evaluation system for the testing research project by using this facility.
- [5] To arrange the good environment for the conducting research works.

4. RESEARCH AND DEVELOPMENT OF THE CORE TECHNOLOGY

4.1. Objectives of R & D of the core technology

The specification of the 3-D Full Scale Earthquake Testing Facility will be the largest and highest performance shaking table facility in the world. For the establishment of manufacturing technology of core technology for the new facility, we are conducting the research and development works since 1995.

The items of this research and development are as follows;

- 1) Development of the high performance actuator
- 2) Development of the three dimensional link joint
- 3) Conducting the performance test by the prototype facility

4.2. Development of the actuator

We set up that the maximum amplitude, maximum velocity and maximum load of the actuator are ± 100 cm, 200cm/s and 450 tonf, respectively. These values are the largest ones, which were never conducted.

For establishment of this high performance actuator, we mainly considered the following point. The drawing of horizontal actuator is shown in Fig. 6.

- 1) To prevent seizure between cylinder and piston rod,

After the several design-work, we developed the spherical hydro-static bearing. The structure of this bearing is shown in Fig. 7. By using this bearing system, the friction between cylinder and piston rod is established nearly zero.

- 2) To establish low friction capacity between cylinder and piston, as possible as we can,

We used the floating seal mechanism for the actuator. Then, we established very low friction capacity, which is 0.4 kgf/cm² of minimum moving pressure of piston rod. The relation between the hydraulic pressure and tolerance is shown in Fig. 8. The relation between hydraulic pressure and leakage is shown in Fig. 9. The measured value is shown good coincidence to calculated one at the using pressure region, which is greater than 100 kgf/cm².

- 3) To develop the large flow servo valve.

For the establishment of high velocity, 200 cm/s, we need to develop the 45,000 l/min servo valve for one horizontal actuator. We decided to use 3 servo valves for each actuator. Then we established 15,000 l/min servo valve, which is the largest flow rate servo valve in the world.

4.3. Development of 3-D link joint

To establish the three-dimensional movement of shaking table, we need to insert the link joint between the shaking table and actuator. For this shaking table system, the swing angle of link joint is reached to 12 degree. We used the spherical hydro-static bearing, which is same system as actuator, and the bearing clearance adjusting device for establishment of such large swing angle. The sectional drawing and bearing structure of link joint are shown in Fig. 10 and Fig. 11, respectively.

4.4. Conducting the performance test

We constructed the prototype facility by using the developed actuator and 3-D link joint. The specification and layout of prototype facility are shown in Table 2 and Fig. 12, respectively. The prototype facility are consisted 4 horizontal actuators and 4 vertical actuators. These actuators have same capacity as the 3-D Full Scale Earthquake Testing Facility. By the condition of construction site of this prototype facility, the capacity of maximum acceleration is limited to 0.4 G.

We conducted the following performance tests for the establishment of research and development result.

1) Maximum amplitude test

For the confirmation of maximum amplitude establishment, we conducted the maximum amplitude test by the sinusoidal wave. And, we confirmed the performance of cross-talk compensation at this test. Fig. 13 shows the test result of X-axis vibration of ± 100 cm. The movement of X-axis is shown the establishment of ± 100 cm vibration. The

movements of Y and Z axes are shown almost zero by the good accuracy of the cross-talk compensation.

2) Maximum velocity test

This test is the confirmation of maximum velocity establishment. By the limitation of the oil power supply, we conducted this test by the deformed sinusoidal wave. Fig. 14 shows the test result of maximum velocity establishment. The maximum velocity of 200 cm/s is established as planned.

3) Test by random vibration

We established the reproductive performance by the random vibration. Fig. 15 shows the of time history and frequency characteristics during random vibration. This result shows that the prototype shaking table system has good accuracy for the conducting of random vibration test.

5. CONCLUSION

We learnt many lessons from Hanshin-Awaji earthquake and other recent destructive earthquakes. Especially, we need more research to understand the failure mechanism of different types of structures during earthquake. For this research needs, NIED will begin the construction project of the "3-D Full Scale Earthquake Testing Facility" in fiscal year 1998 for the 7 years plan. After the completion, this facility will be perfectly opened to international use.

We consider that the researchers together from worldwide to this facility and the research projects will determine and evaluate by the international committee. We hope that this facility will be situated to one of the cooperative research organization for the earthquake disaster mitigation in the world.

TABLE 1 MAIN SPECIFICATION OF THE FACILITY

Item	Horizontal X	Horizontal Y	Vertical Z
Table Size	20 m x 15 m		
Driving Method	Accumulator Charge / Electro-Hydraulic Servo Control		
Maximum Test Weight	1200 tonf		
Maximum Acceleration (at Max. weight)	0.9 G	0.9 G	1.5 G
Maximum Velocity	130 cm/s	200 cm/s	70 cm/s
Maximum Displacement	± 50 cm	± 100 cm	± 50 cm
Maximum Overturning Moment	≥ 15,000 tonf · m (at Az=1G)	≥ 15,000 tonf · m (at Az=1G)	—

TABLE 2 SPECIFICATION OF PROTOTYPE FACILITY

	Horizontal X	Horizontal Y	Vertical Z
Table Size	6 m X 6 m		
Maximum Model Weight	50 tonf		
Maximum Acceleration	0.4 G	0.4 G	0.4 G
Maximum Velocity	200 cm/s	200 cm/s	70 cm/s
Maximum Displacement	+ - 100 cm	+ - 100 cm	+ - 50 cm
No. of Actuators	2	2	4

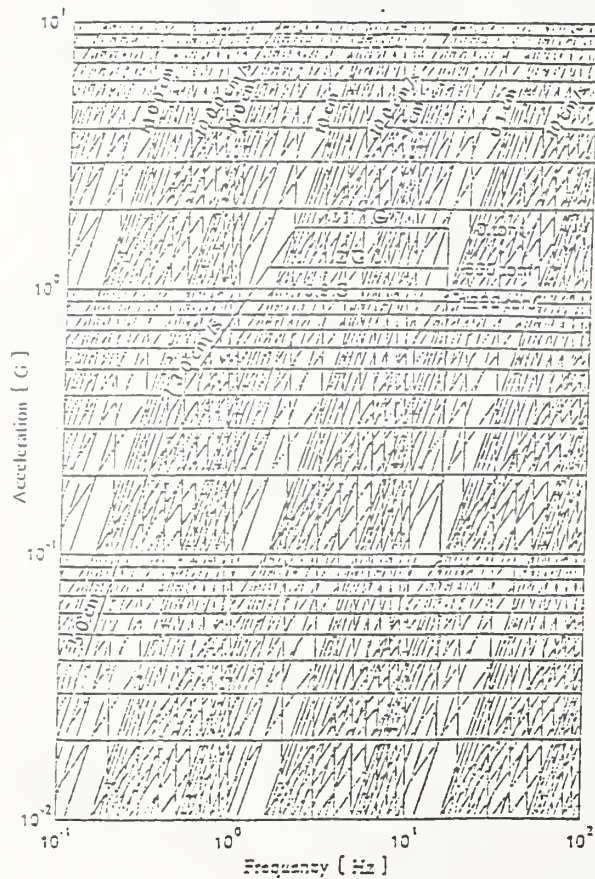


Fig. 1 Actuator Performance of X Axis

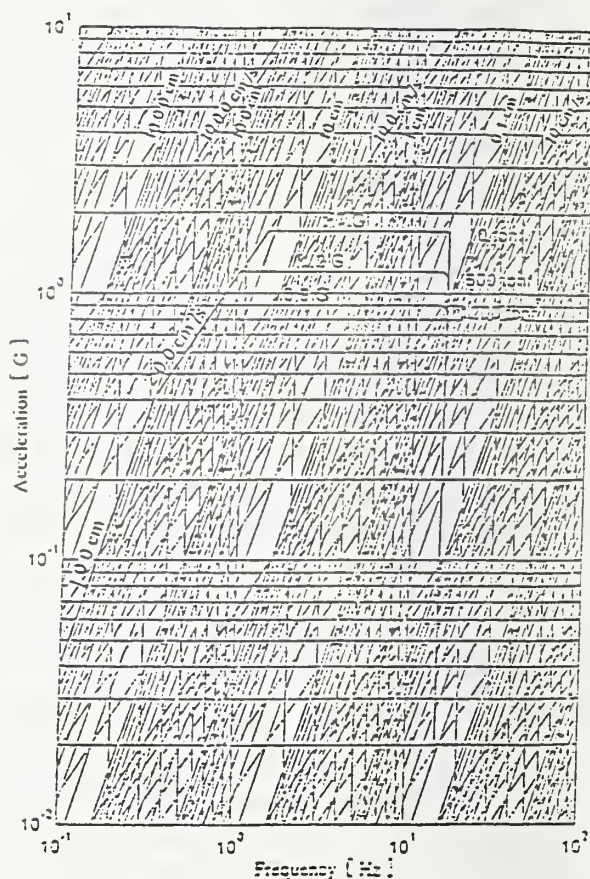


Fig. 2 Actuator Performance of Y Axis

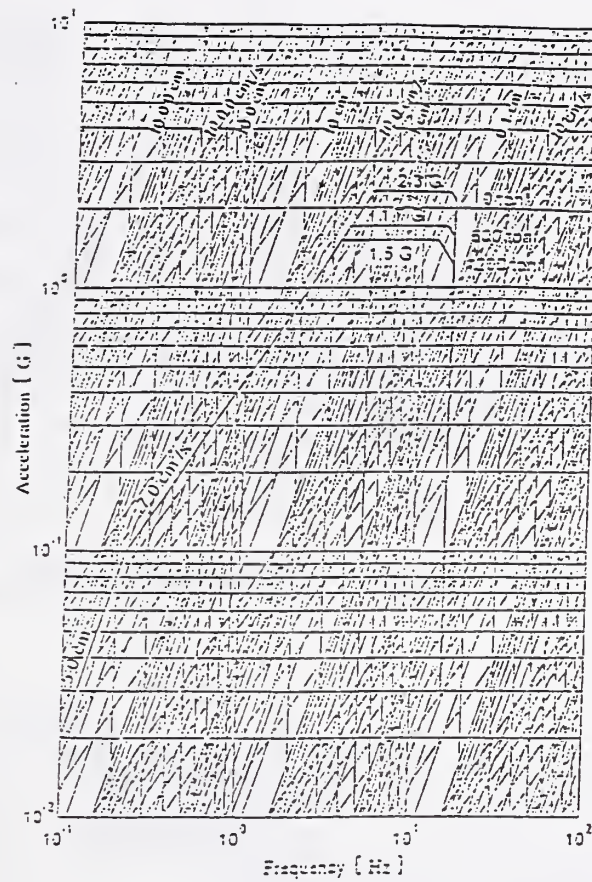


Fig. 3 Actuator Performance of Z Axis

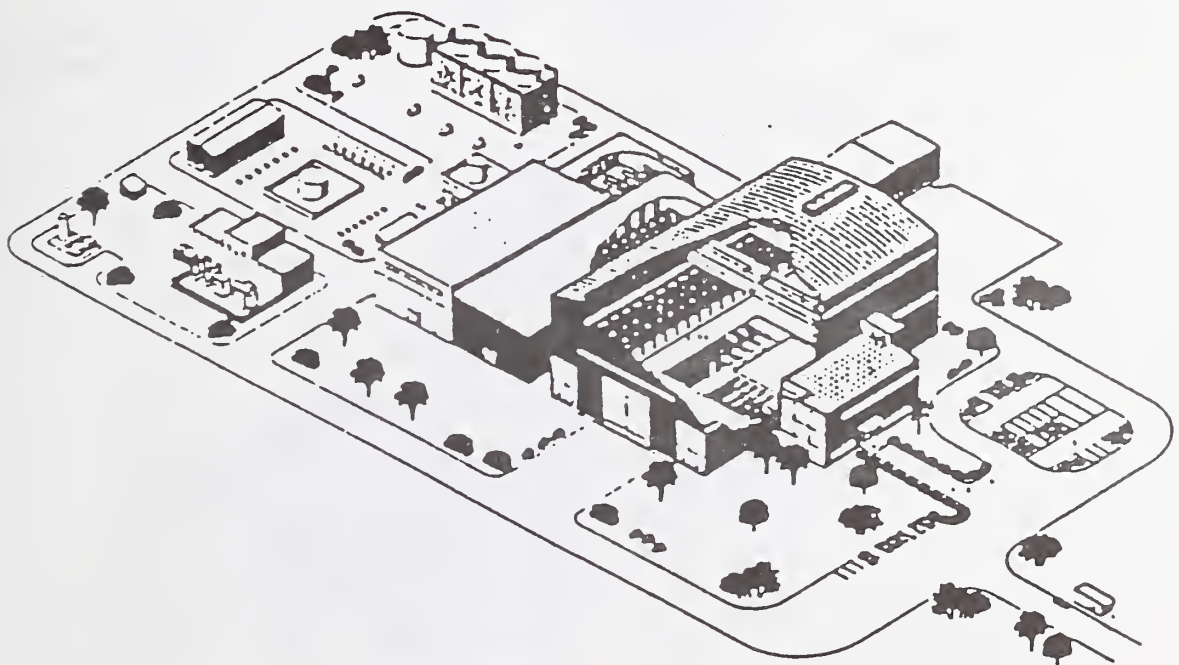


Fig. 4 Layout of the Facility

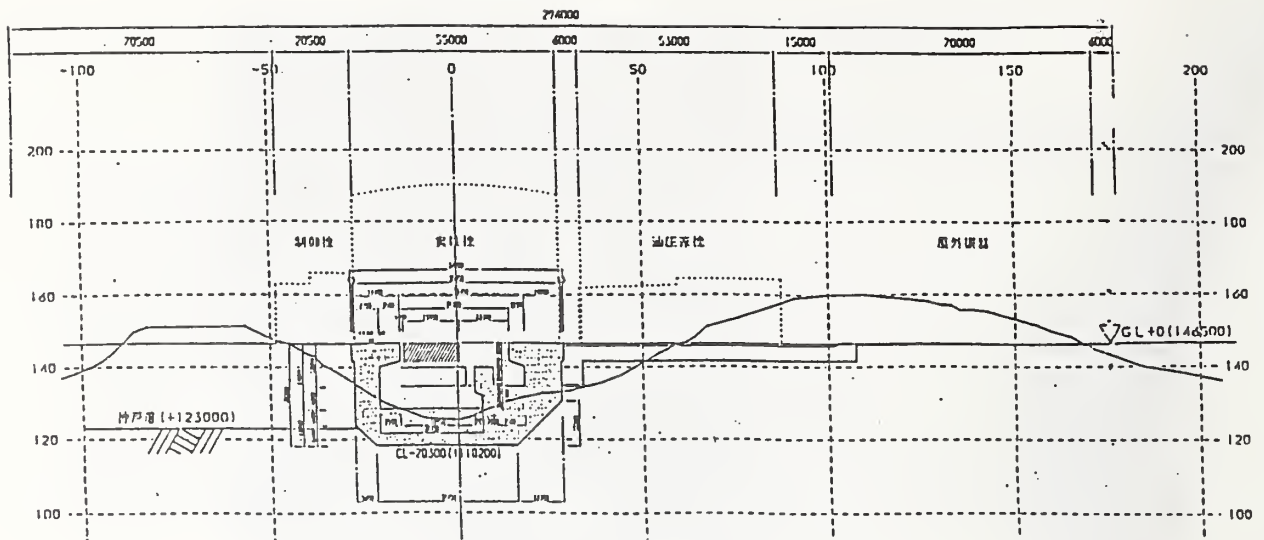


Fig. 5 Sectional Design of Shaking Table Foundation

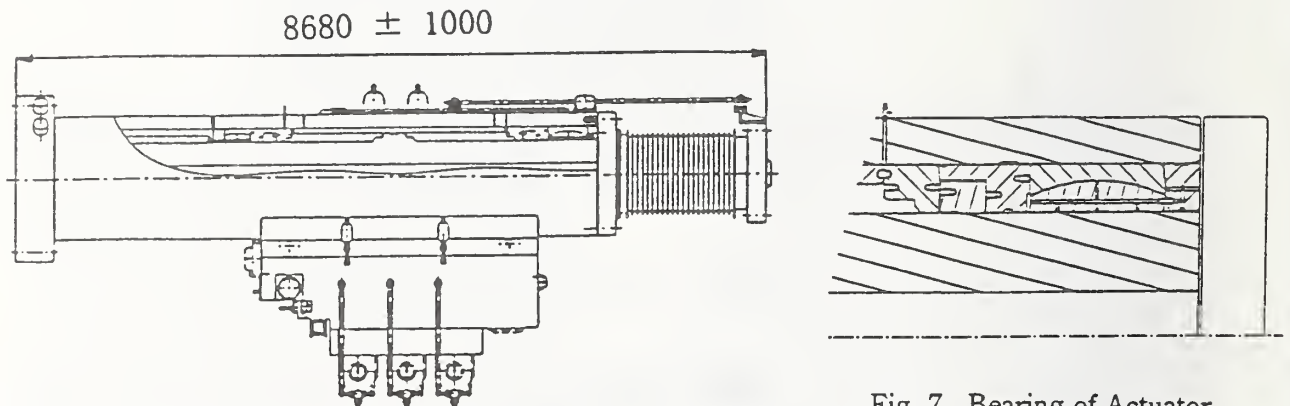


Fig. 6 Horizontal Actuator

Fig. 7 Bearing of Actuator

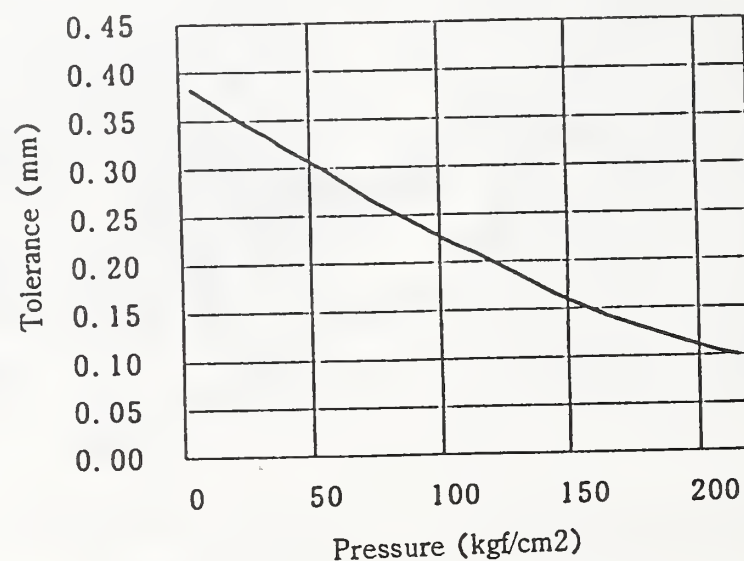


Fig. 8 Hydraulic Pressure vs. Tolerance

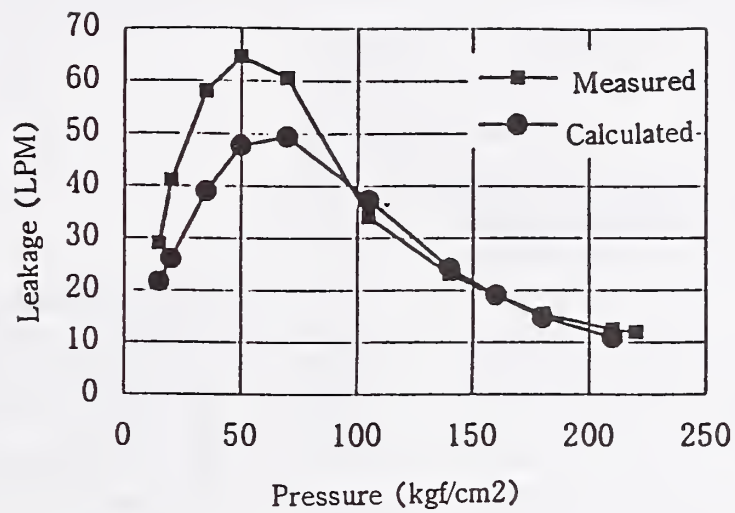


Fig. 9 Hydraulic Pressure vs. Leakage

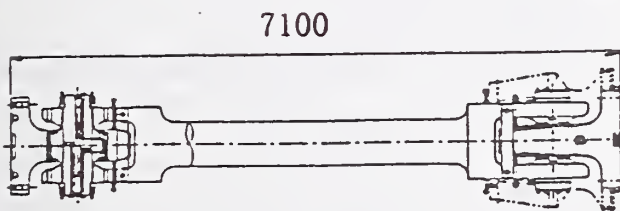


Fig. 10 Three Dimensional Link Joint

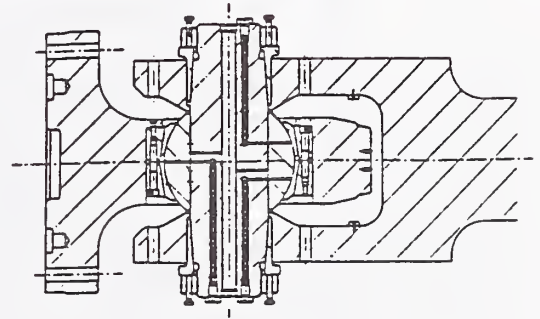


Fig. 11 Bearing of 3-D Link Joint

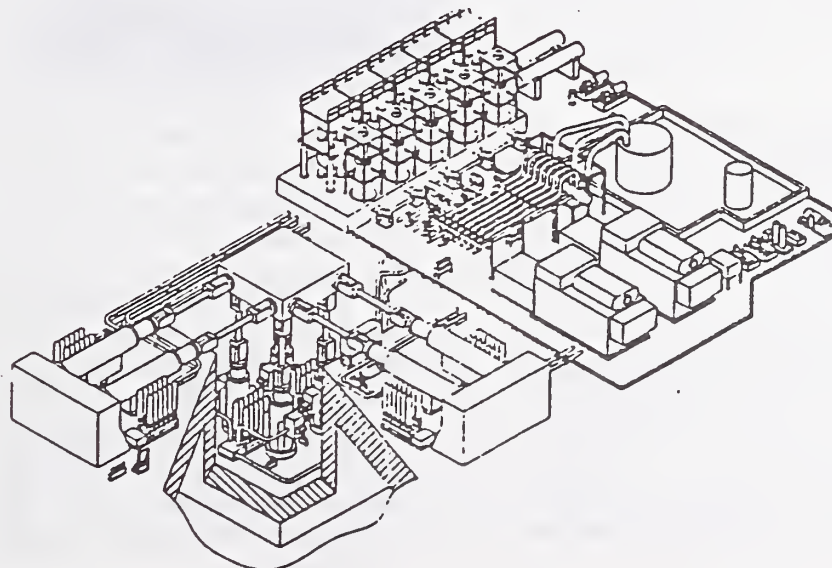


Fig. 12 Layout of Prototypy Facility

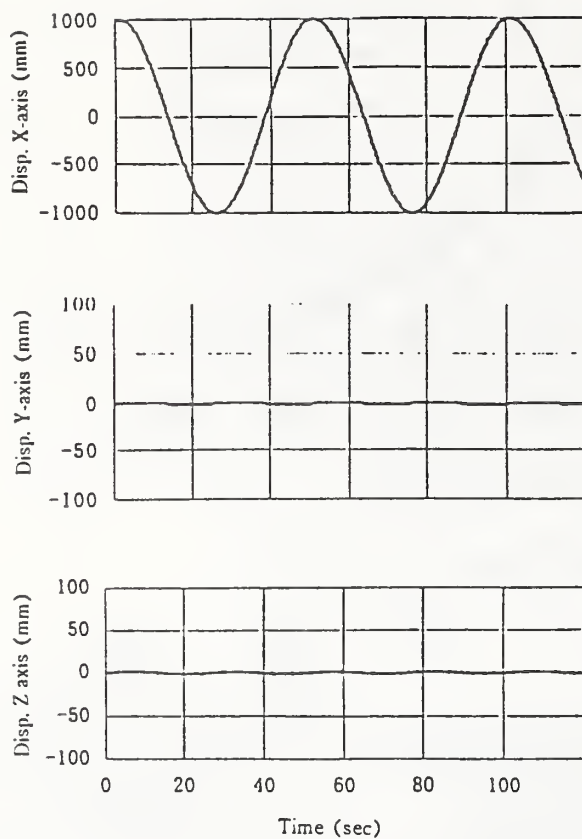


Fig. 13 Test Result of Max. Displacement

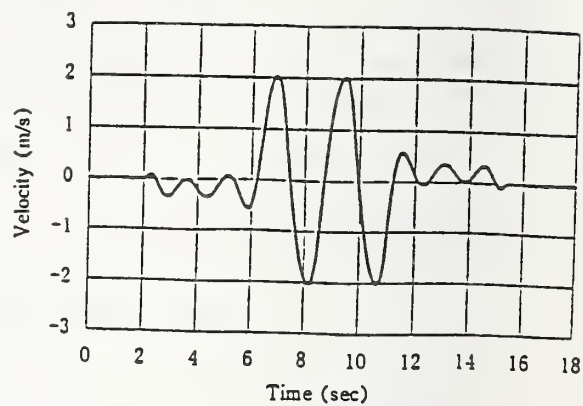


Fig. 14 Test Result of Max. Velocity

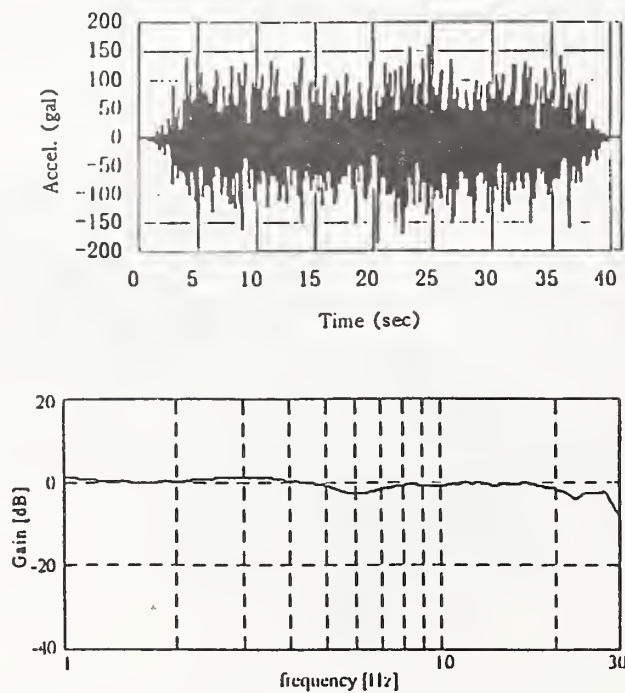


Fig. 15 Test Result of Random Vibration

Strong Motion from Surface Waves in Deep Sedimentary Basins

by

William B. Joyner¹

ABSTRACT

It is widely recognized that long-period surface waves generated by conversion of body waves at the boundaries of deep sedimentary basins make an important contribution to strong ground motion. The factors controlling the amplitude of such motion, however, are not widely understood. Compared to the body wave, the velocity of the surface wave is much less, and, as a result, the curvature of the wavefront and the geometric spreading are much less. The surface wave behaves approximately as if it were generated by a line source in a two-dimensional medium. On the other hand the low-Q basin sediments produce significant anelastic attenuation, even at relatively long periods. A study of pseudovelocity response spectra of records of the 1971 San Fernando and 1994 Northridge earthquakes at sites in the Los Angeles Basin shows that late-arriving surface waves with group velocities of about 1 km/sec dominate the ground motion for periods of 3 sec and longer. The rate of amplitude decay for these waves is less than for the body waves and depends significantly on period, with smaller decay for longer periods. The amplitude can be modeled by anelastic attenuation with decay proportional to the exponential of distance multiplied by an attenuation coefficient. Methods for estimating the response spectral amplitudes for these waves in future earthquakes are presented based on either the San Fernando or Northridge data. The response spectral amplitude of surface waves from the Northridge earthquake is less than from the San Fernando earthquake by factors as large as four. The surprisingly large difference between the San Fernando and Northridge earthquakes can be explained, at least in part, by directivity. Estimates of response values in future earthquakes based on the two different data sets give a sense of the range of

possibilities. These estimates are based on data from the Los Angeles Basin, but, in the absence of other data, they could be applied to sites in other deep Quaternary basins. The results presented in this paper indicate that inclusion of anelastic attenuation may be essential in modeling ground motion in deep sedimentary basins. Future progress in understanding strong motion from basin surface waves calls for attention to faithful recording of the long-period components of ground motion and to recording motion for times long enough to include the late-arriving surface waves.

1. INTRODUCTION

The importance of surface waves for long-period strong earthquake ground motion has long been recognized. Hanks (1975) examined displacement time series obtained by double integration of accelerometer records from the 1971 San Fernando, California, earthquake and showed that surface waves were a significant component of the long-period motion. Surface waves in the San Fernando earthquake were also studied by Lui and Heaton (1984) and by Vidale and Helmberger (1988) who showed that the surface waves were generated by conversion from body waves at the margins of deep sedimentary basins.

The factors controlling the amplitude of surface waves generated by conversion of body waves at basin margins are not widely understood. The amplitude of surface waves is commonly said to decay as the one-half power of distance. That statement is only true for laterally homogeneous media and then only in the frequency domain. The decay in the time domain is greater because of dispersion. With

¹ U.S. Geological Survey, 345 Middlefield Road MS 977, Menlo Park, CA 94025

lateral heterogeneity, as with a surface wave generated at the edge of a basin, the situation is very different. As shown in Figure 1, because the velocity of the surface wave is much less than the body wave, the curvature of the wavefront for the surface wave is much less and the geometric spreading of the surface wave is thereby much reduced. In Figure 1 the reduction would be greater if the boundary were concave inward. To a first approximation the wave behaves as if it were generated by a line source in a two-dimensional medium. On the other hand, the low- Q basin sediments produce significant anelastic attenuation. In this paper strong-motion data from the 1971 San Fernando, California, and the Northridge, California, earthquakes are examined to clarify the role of surface waves and the factors controlling their amplitude.

2. DATA

The focus of this study was surface waves in deep sedimentary basins generated by earthquakes outside the basin. The data used were strong-motion records of the San Fernando and Northridge earthquakes recorded at sites in the Los Angeles Basin (Figure 2). For the purposes of this paper, the boundary of the Los Angeles Basin were taken as the 300 m contour of depth to crystalline basement as determined by adjusting the subsea elevation contours on the map by Yerkes *et al.* (1965) for the effect of topography. With that definition of the Basin boundary, the San Fernando and Northridge earthquakes lie outside the Basin.

The San Fernando data were taken from the CD-ROM by Seekins *et al.* (1992). The horizontal components were rotated to north and east, approximately perpendicular and parallel, respectively, to the northern boundary of the basin. The records were then processed specifically for this study using as lowcut filter a second-order bidirectional Butterworth filter (Converse, 1992) with a cutoff at 0.125 Hz. The locut filter is similar to that recommended by Hanks (1975). Velocity time series were plotted in order of increasing distance from the source, and records with duration judged

insufficient to record the surface waves were eliminated, leaving 56 three-component records. The Northridge data were taken from the California Strong Motion Instrumentation Program and from the Los Angeles Strong Motion Accelerograph Network operated by the University of Southern California. Corrected data were obtained from processing by the network operators. Both operators employ a lowcut filter that is a ramp in the frequency domain. Records were excluded from this study if the frequency at the upper end of the ramp exceeded 0.16 Hz. Twelve three-component records remained after the exclusions. As with the San Fernando records the horizontal components were rotated to north and east.

3. PRELIMINARY ANALYSIS

In order to assess the contribution of surface waves to ground motion, pseudovelocity response spectra for 5 percent damping were computed for each record and the time of maximum response was determined for each oscillator period and each record. A regression analysis was performed between the time of maximum response and the closest horizontal distance from the recording station to the vertical projection on the surface of the earth of the fault rupture that generated the earthquake. The resulting regression coefficient is plotted against oscillator period for the San Fernando earthquake on Figure 3 and the Northridge earthquake on Figure 4. The regression coefficient represents the group slowness, that is, the reciprocal of the group velocity, of the seismic phase that carries the highest amplitude for each period. More precisely, the coefficient is the group slowness relative to the slowness of the triggering phase. An examination of the accelerograms shows that some of the records triggered on the P -wave and some on the S -wave, but it does not matter because the body-wave slownesses are negligible compared to the surface-wave slownesses. Group velocities and slownesses are usually measured by noting the time of the peak of the envelope of narrow-band-filtered seismograms. The approach used here should give similar results and has the advantage of employing quantities of

engineering significance. Figures 3 and 4 show that for periods up to about 0.75 sec body waves with relative slownesses near zero carry the maximum amplitude. At periods of 3.0 sec and greater the relative slowness is nearly 1 sec/km, representing surface waves whose absolute slowness may exceed 1 sec/km. Between periods of about 0.75 and 3.0 sec the regression coefficients take on intermediate values. These probably do not represent a seismic phase of intermediate slowness but rather a situation where the maximum amplitude is carried by the body waves on some records and by the surface waves on others. Using the distance dependence of the time of maximum amplitude to distinguish surface waves and body waves is a strategy employed by Hanks and McGuire (1981).

Regression analysis was also performed between the logarithm of the pseudovelocity response and the logarithm of distance. The regression coefficient is plotted against period on Figure 5 for the San Fernando earthquake and on Figure 6 for the Northridge earthquake. The surface waves at periods of 3.0 sec and greater have a decay rate generally less than the body waves at periods 0.75 sec and less. Note that the decay rate of the surface waves decreases sharply with period, suggesting that the decay represents anelastic attenuation, not geometric spreading.

4. EQUATIONS

The results of the last section suggest that the pseudovelocity amplitudes of the surface waves could be represented by an equation of the form

$$y = \frac{a}{R_E} \exp(-bR_B) \quad (1)$$

where y is the pseudovelocity response, R_E is the distance from the source to the edge of the basin, R_B is the distance from the edge of the basin to the recording site, and a and b are parameters chosen to fit the data. Values of R_E

and R_B are obtained by constructing the line between the recording site and the closest point on the vertical projection of the fault rupture on the earth's surface. The intersection point of the line with the basin boundary is noted, and the distance between the intersection point and the closest point on the vertical projection of the fault rupture is denoted by D_E . $R_E = \sqrt{(D_E^2 + 25)}$. R_B is the distance between the intersection point and the recording site. Values of a and b derived by fitting the San Fernando data and the Northridge data separately are given in Table 1. Values of Q implied by the values obtained for b are given in Table 2, along with one-standard-deviation ranges, for an assumed phase velocity of 1 km/sec. The ratios between observed values and values predicted by equation (1) are shown on Figure 7 for the perpendicular component of the San Fernando earthquake at periods of 3 to 6 sec. Data for the other components of the San Fernando earthquake and for the Northridge earthquake are similar. The standard deviation of the natural logarithm of the ratio between observed and predicted values ranges between 0.3 and 0.5. Figure 8 shows the values predicted by equation (1) with a and b fitted to data from the perpendicular component for the San Fernando (S) and Northridge (N) earthquakes. Also shown on Figure 8 for comparison are values predicted by two attenuation relationships derived from the general strong-motion data set. Figure 9 shows the corresponding results for the parallel component. The values predicted from fits to the San Fernando data are larger than predicted by the two attenuation relationships by as much as a factor of four. The values predicted from fits to the Northridge data are much less than those from fits to the San Fernando earthquake. This difference between the San Fernando and Northridge data is surprisingly large, but it can be explained, at least in part, by directivity.

Estimates of pseudovelocity response obtained from equation (1) fit to the San Fernando data can be extrapolated to other sites and other earthquakes by multiplying the result from equation (1) by the factor $f(M, R_E) / f(6.6, 23)$, where $f(M, R)$ is an appropriate attenuation relationship for pseudovelocity response in

terms of moment magnitude M and distance R in km, 6.6 being the moment magnitude of the San Fernando earthquake and 23 km the average distance between the source and the basin edge for the San Fernando records. The corresponding estimates for fits to the Northridge data can be obtained by multiplying the results from equation (1) by the factor $f(M, R_E) / f(6.7, 17)$. Estimates derived from the San Fernando and Northridge data would give some sense of the range of values that might occur in a future earthquake. Such estimates, though based on data from the Los Angeles Basin, could be applied to sites in other deep Quaternary basins where data is not available.

5. CONCLUSIONS AND RECOMMENDATIONS

The results presented here show that in a deep sedimentary basin such as the Los Angeles Basin the ground motion at periods of 3 to 6 sec is dominated by surface waves. Methods are described for estimating response spectral values for such motion. Estimates made using data from the San Fernando earthquake give values greater by as much as a factor of four than predicted by attenuation relationships derived from general strong-motion data sets. The engineering consequences of these large motions need to be considered for structures with periods of 3 sec and greater and perhaps also for structures of shorter elastic periods if those periods might be lengthened to 3 sec or beyond by deformation during an earthquake.

The results presented here also indicate the necessity of including anelastic attenuation in attempts to model ground motion in deep sedimentary basins.

Future progress in understanding basin surface waves and in predicting their amplitude will require additional data. Taking full advantage of moderate earthquakes to obtain additional data will require that operators of strong-motion networks take special care for the faithful recording of the long-period components of ground motion. Not only are instruments of sufficient dynamic range needed, but also

testing should be done to insure that sufficiently low noise levels are actually achieved. It is also necessary to insure that the recorder, once triggered, will continue to operate for a time sufficient for the surface waves to traverse the basin. With velocities of about 1 km/sec, that time may be as long as 100 sec.

6. ACKNOWLEDGMENTS

The author benefited from discussions with David Boore, John Tinsley, and Jerry Eaton. He is also grateful to Linda Seekins for her skilled efforts in making Figure 2 and to David Boore for his review of the manuscript and valuable suggestions for improvement.

7. REFERENCES

- Abrahamson, N. A. and W. J. Silva (1997). Empirical response spectral attenuation relations for shallow crustal earthquakes, *Seism. Res. Lett.*, **68**, 94-127.
- Converse, A. M. (1992). BAP: basic strong-motion accelerogram processing software; version 1.0, *U.S. Geol. Survey Open-File Rept.* 92-296A.
- Hanks, T. C. (1975). Strong ground motion of the San Fernando, California, earthquake: ground displacements, *Bull. Seism. Soc. Am.*, **65**, 193-225.
- Hanks, T. C. and R. K. McGuire (1981). The character of high-frequency strong ground motion, *Bull. Seism. Soc. Am.*, **71**, 2071-2095.
- Heaton, T. H. and D. V. Helmberger (1979). Generalized ray models of the San Fernando earthquake, *Bull. Seism. Soc. Am.*, **69**, 1311-1341.
- Joyner, W. B. and D. M. Boore (1982). Prediction of earthquake response spectra, *U.S. Geol. Survey Open-File Rept.* 82-977.
- Liu, H.-L. and T. H. Heaton (1984). Array analysis of the ground velocities and accelerations from the 1971 San Fernando,

California, earthquake, *Bull. Seism. Soc. Am.*, **74**, 1951-1968.

Seekins, L. C., A. G. Brady, C. Carpenter, and N. Brown (1992). Digitized strong-motion accelerograms of North and Central American earthquakes 1933-1986, *U.S. Geol. Survey Digital Data Series DDS-7*.

Vidale, J. E. and D. V. Helmberger (1988). Elastic finite-difference modeling of the 1971

San Fernando, California earthquake, *Bull. Seism. Soc. Am.*, **78**, 122-141.

Yerkes, R. F., T. H. McCulloh, J. E. Schoellhamer, and J. G. Vedder (1965). Geology of the Los Angeles Basin California – an introduction, *U.S. Geol. Survey Prof. Paper 420-A*, 57 p.

Table 1. Values of a and b obtained by fitting equation (1) to data from the San Fernando and Northridge earthquakes.

San Fernando earthquake

Period (sec)	a			b		
	Perpendicular	Parallel	Vertical	Perpendicular	Parallel	Vertical
3.0	741	581	341	0.0190	0.0205	0.0097
4.0	791	883	393	0.0139	0.0156	0.0064
5.0	690	887	265	0.0115	0.0075	-0.0001
6.0	514	644	167	0.0090	0.0045	0.0010

Northridge earthquake

Period (sec)	a			b		
	Perpendicular	Parallel	Vertical	Perpendicular	Parallel	Vertical
3.0	327	541	286	0.0116	0.0222	0.0241
4.0	254	488	238	0.0103	0.0166	0.0207
5.0	169	266	156	0.0001	0.0118	0.0167
6.0	132	195	112	0.0026	0.0109	0.0147

Table 2. Values of Q implied by the b values in Table 1, with one-standard-deviation ranges, for an assumed phase velocity of 1 km/sec.

San Fernando earthquake

Period (sec)	Perpendicular	Parallel	Vertical
3.0	55 (45-73)	51 (43-63)	110 (77-180)
4.0	56 (46-72)	50 (41-66)	120 (72-430)
5.0	55 (43-75)	84 (61-140)	∞ (180- ∞)
6.0	58 (41-99)	120 (70-360)	510 (120- ∞)

Northridge earthquake

Period (sec)	Perpendicular	Parallel	Vertical
3.0	90 (63-160)	47 (39-60)	44 (36-55)
4.0	76 (52-140)	47 (36-69)	38 (30-50)
5.0	5300 (140- ∞)	53 (37-91)	38 (29-53)
6.0	200 (78- ∞)	48 (34-84)	36 (28-49)

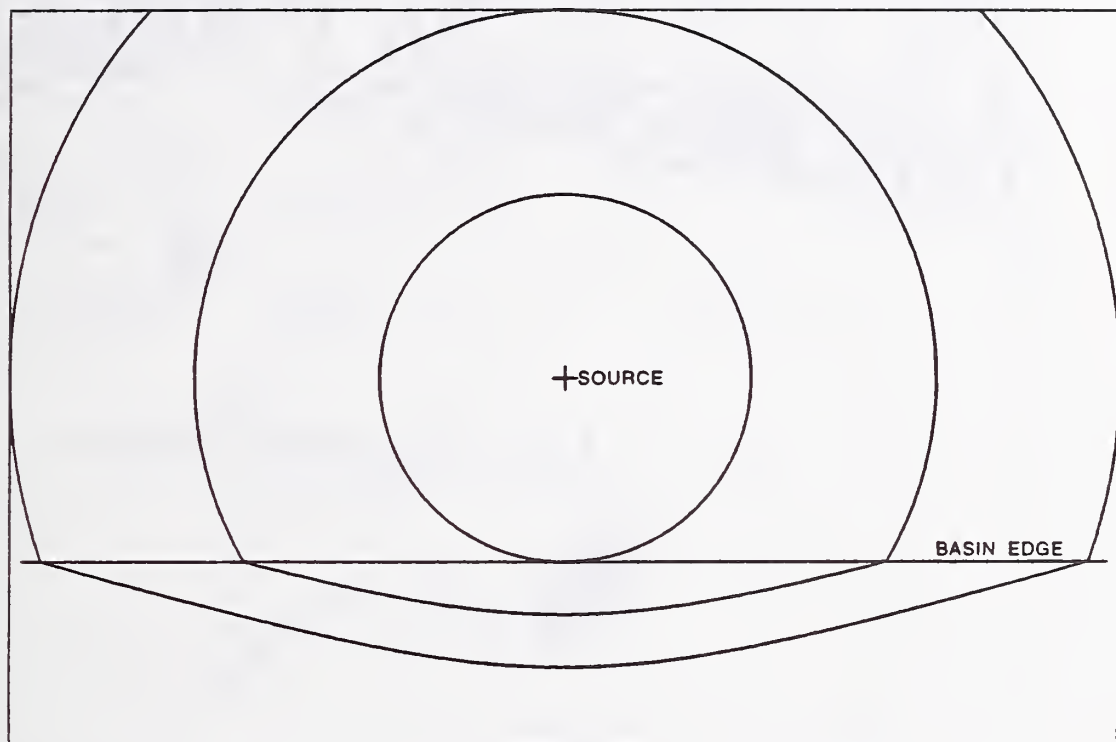


Figure 1. Schematic plan view of the wavefronts for an S wave from a point source converting to a surface wave at the edge of a basin. The phase velocity of the surface wave is one-third the S wave velocity.



Figure 2. Map showing the boundary of the Los Angeles Basin (double line) as defined in the text. Polygons outline the vertical projection of the rupture surface in the San Fernando earthquake (S) (Heaton and Helmberger, 1979) and the Northridge earthquake (N) (David Wald, written communication, 1995).

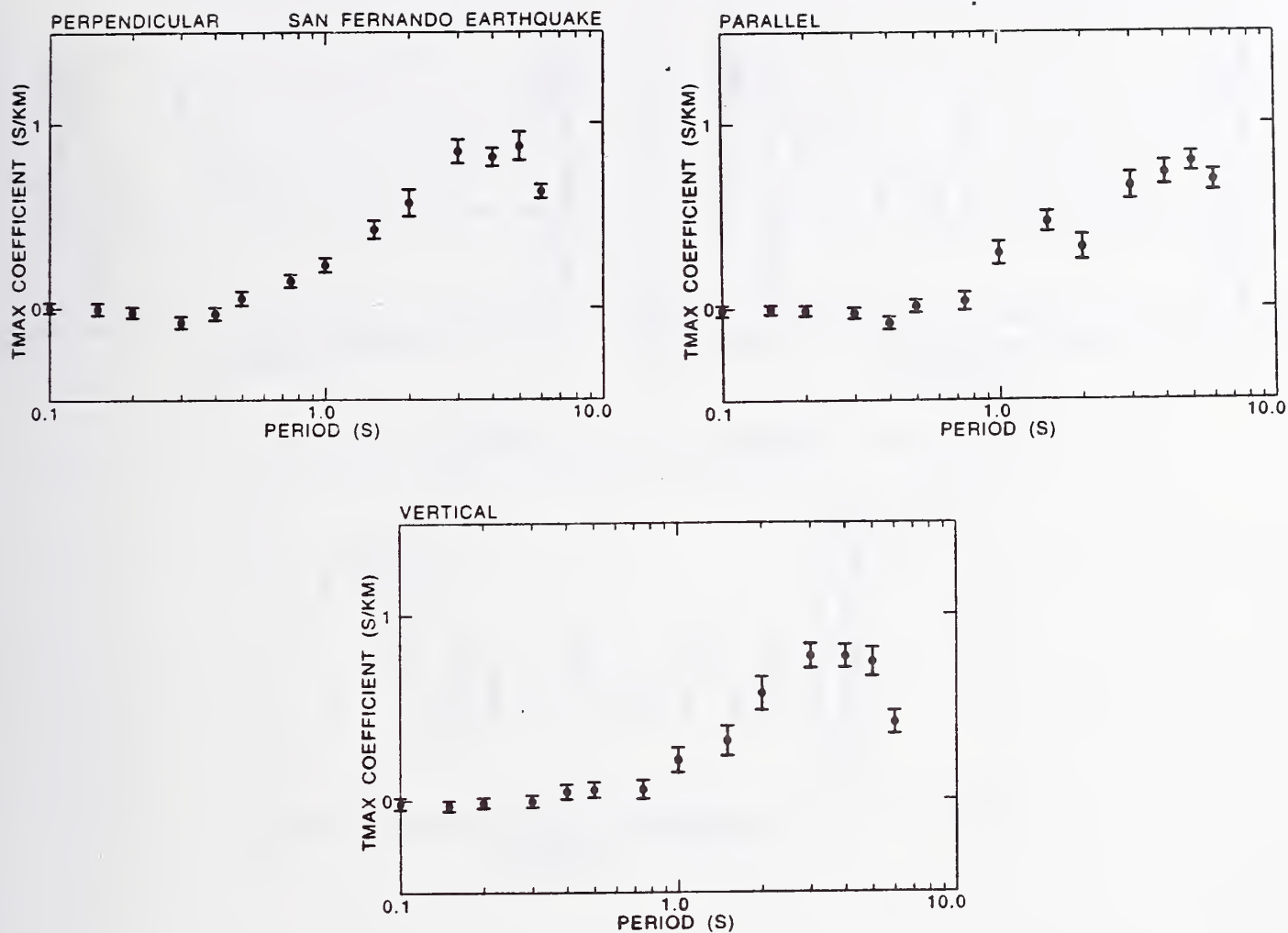


Figure 3. Regression coefficient between the time of maximum pseudovelocity response and closest horizontal distance to the vertical projection of the fault rupture for records from the San Fernando earthquake. The bars show the one-standard-error range for the coefficient.

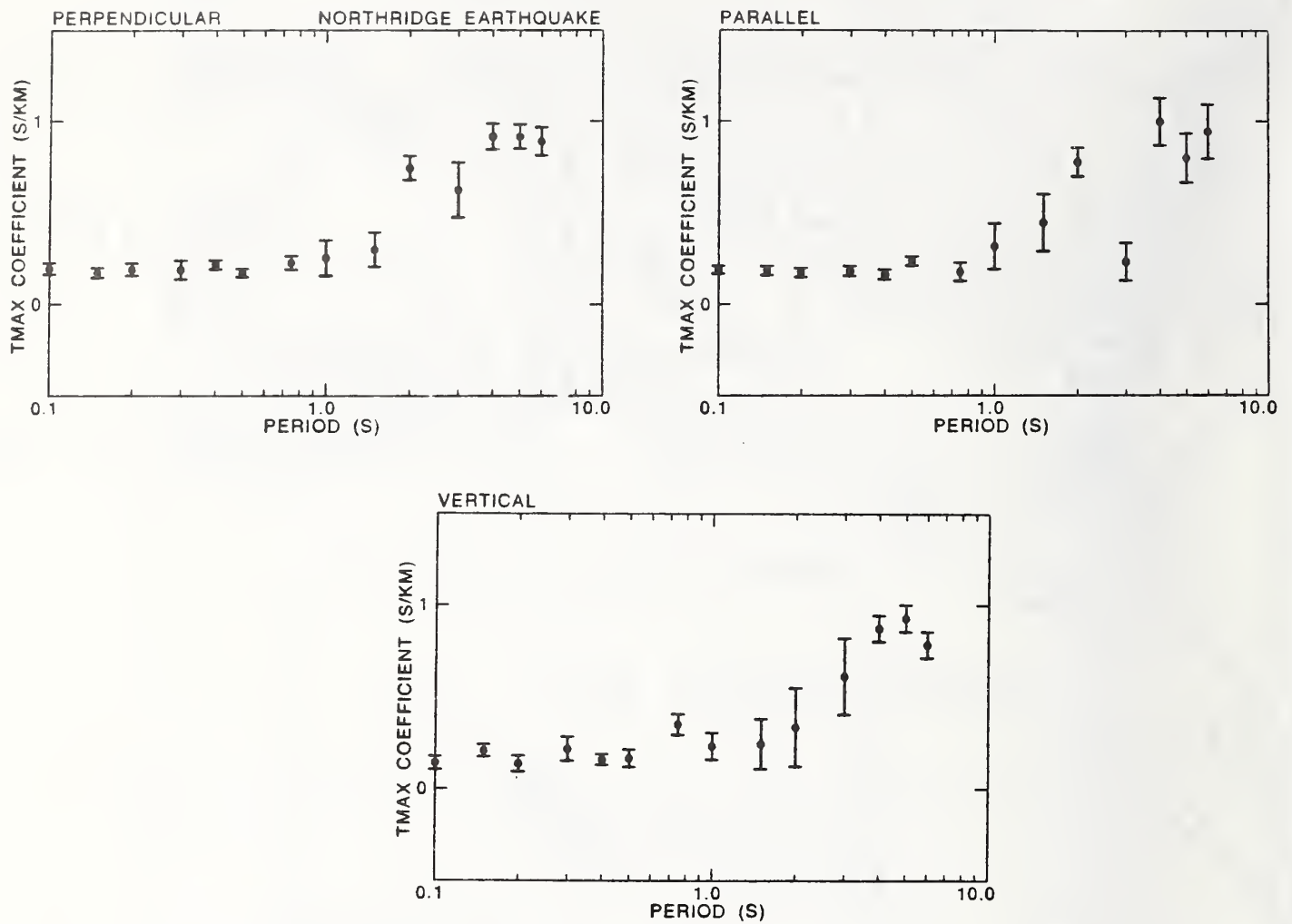


Figure 4. Regression coefficient between the time of maximum pseudovelocity response and closest horizontal distance to the vertical projection of the fault rupture for records from the Northridge earthquake. The bars show the one-standard-error range for the coefficient.

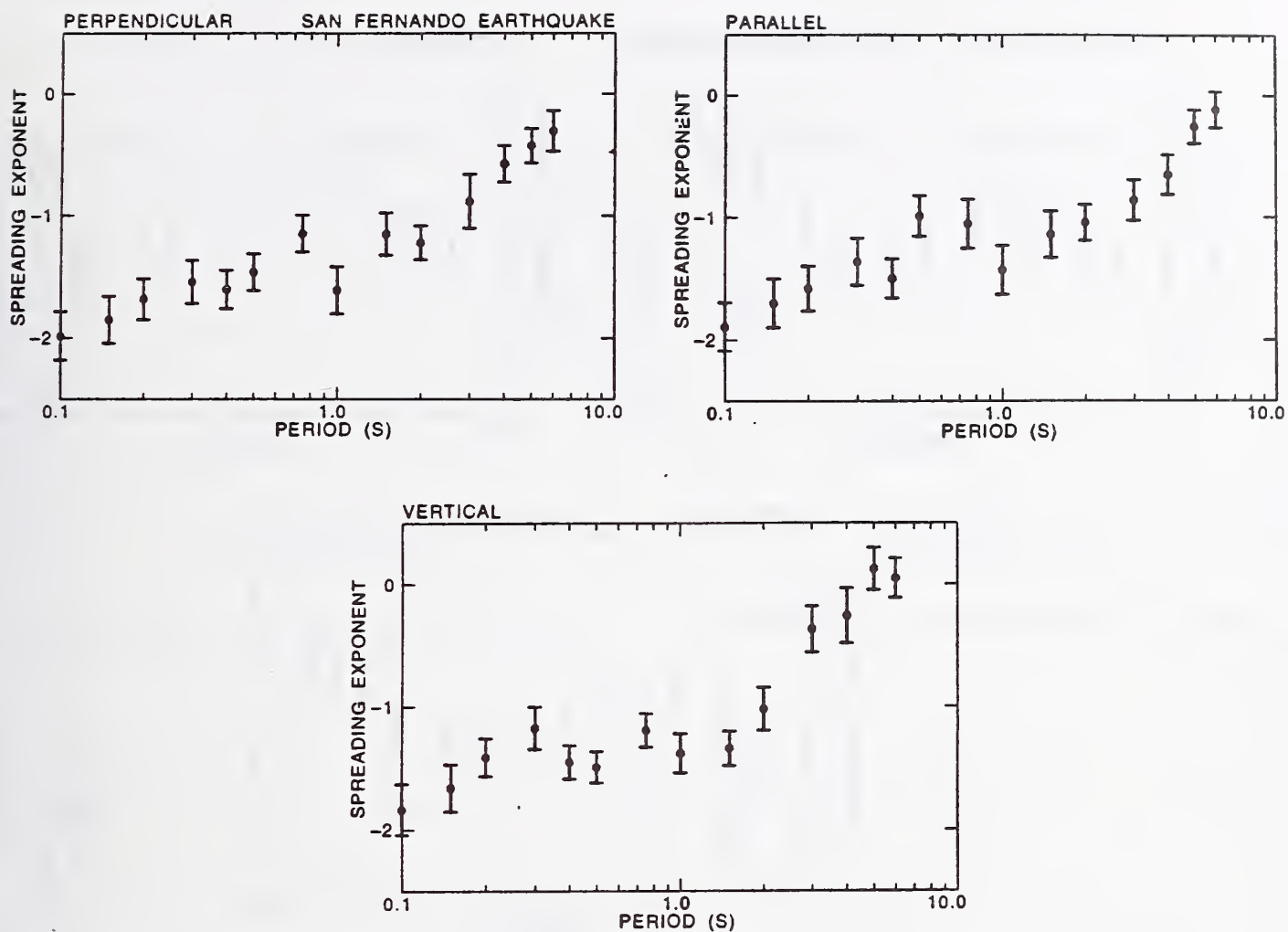


Figure 5. Regression coefficient between the logarithm of pseudovelocity response and the logarithm of closest horizontal distance to the vertical projection of the fault rupture for records from the San Fernando earthquake. The bars show the one-standard-error range for the coefficient.

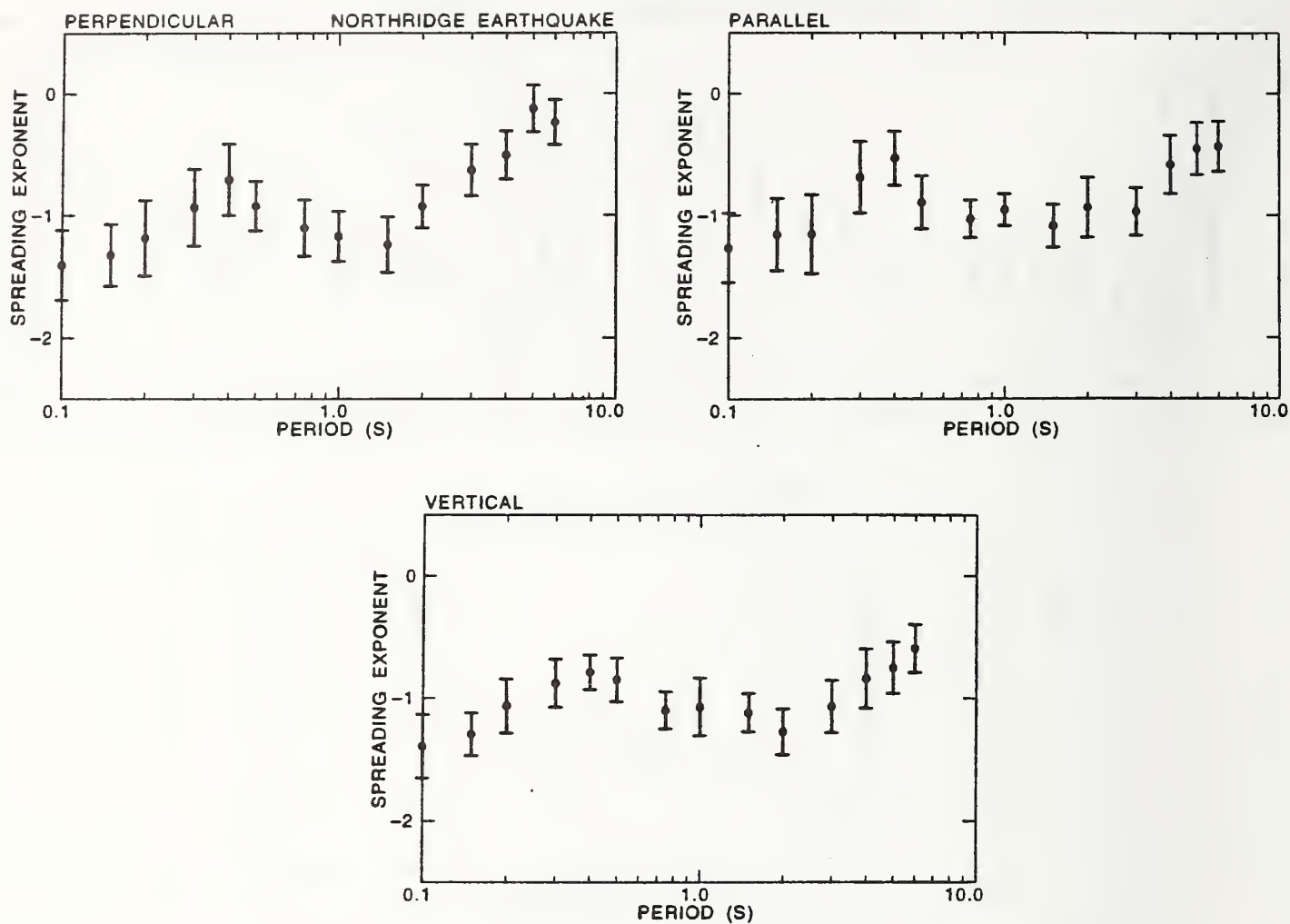


Figure 6. Regression coefficient between the logarithm of pseudovelocity response and the logarithm of closest horizontal distance to the vertical projection of the fault rupture for records from the Northridge earthquake. The bars show the one-standard-error range for the coefficient.

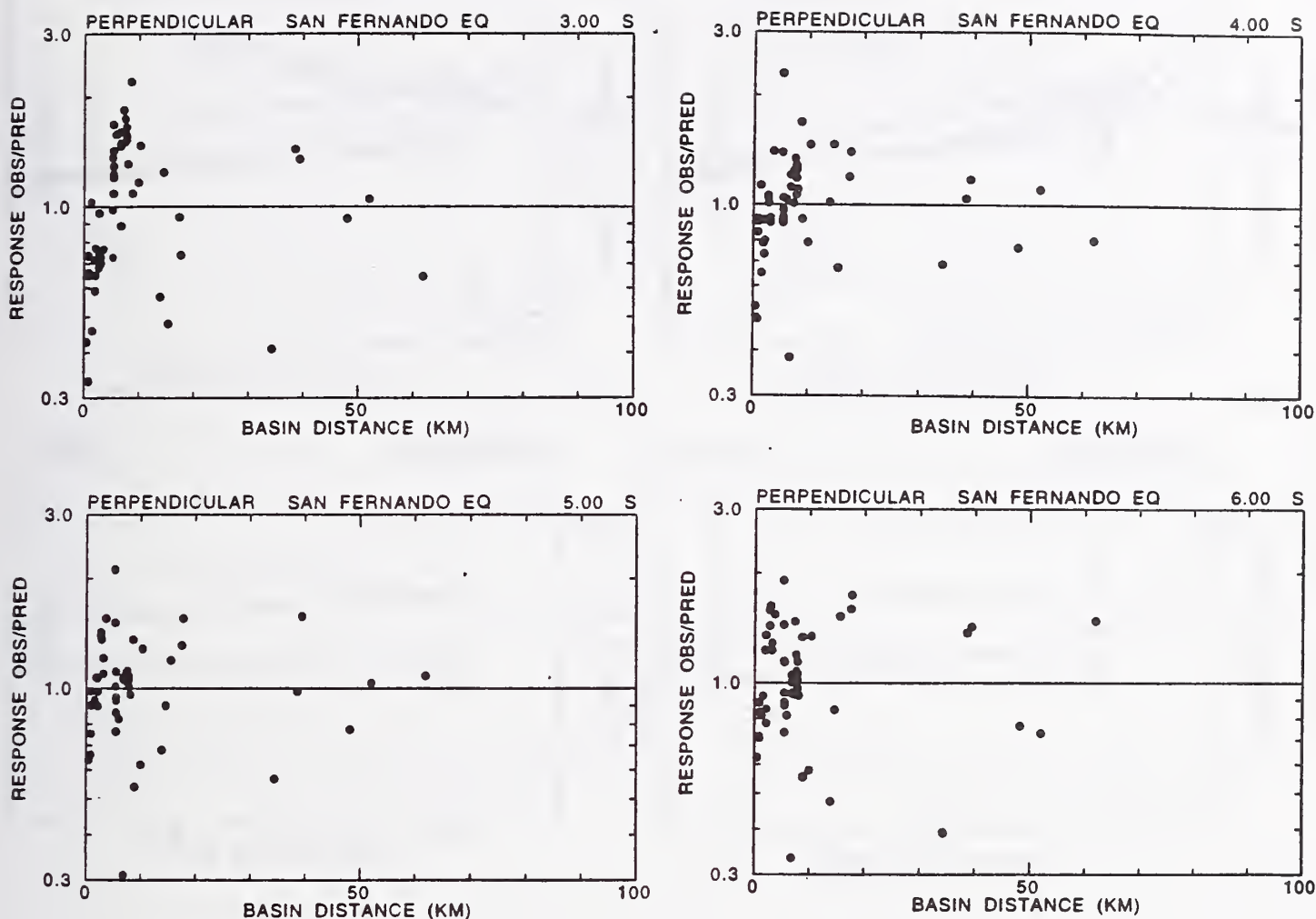


Figure 7. Ratios between observed values of pseudovelocity response and values predicted by equation (1) for the perpendicular component of the San Fernando earthquake.

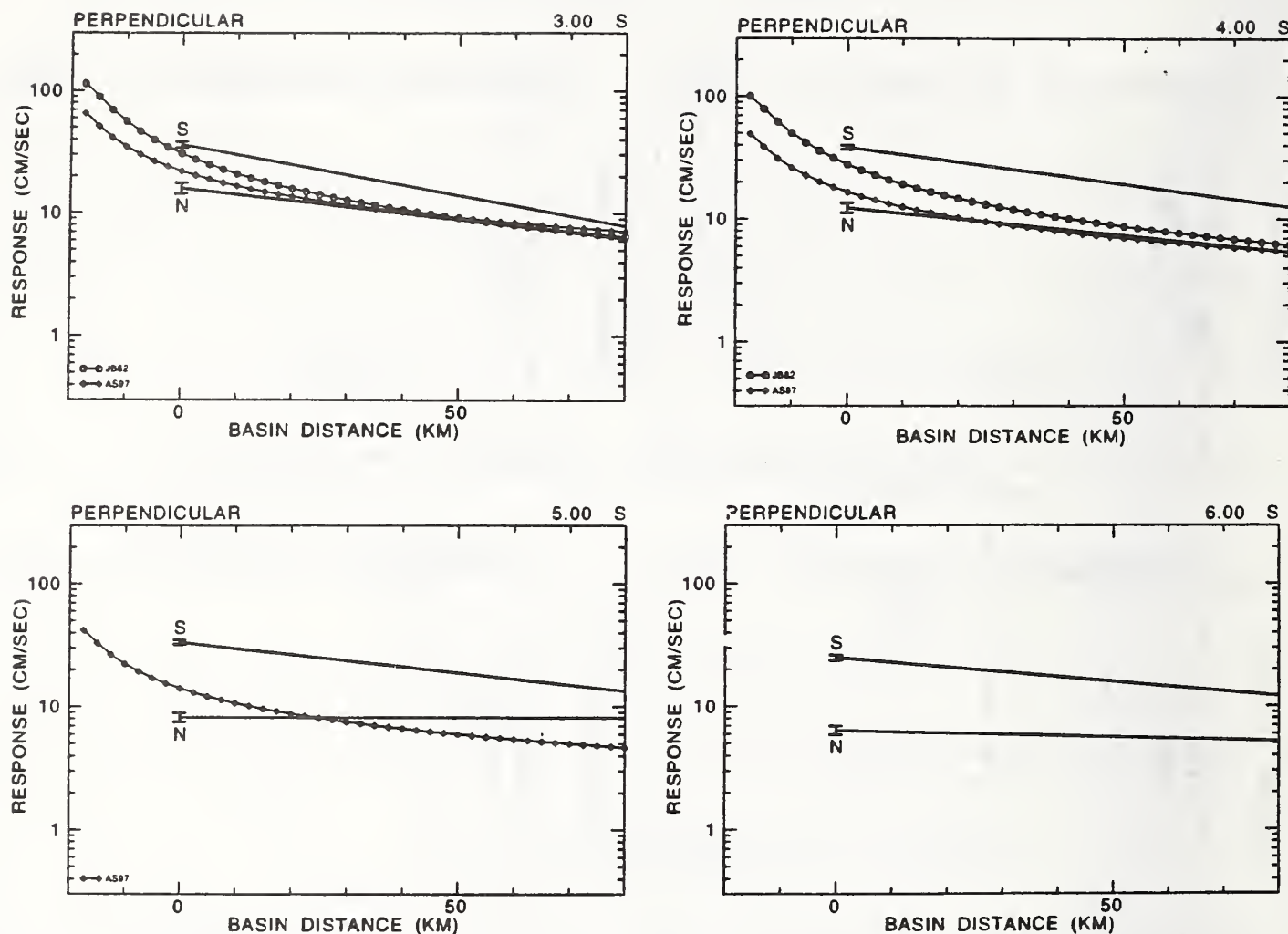


Figure 8. Values of pseudovelocity response for the perpendicular component predicted by equation (1) with coefficients fitted to data from the San Fernando earthquake (S) and the Northridge earthquake (N). The bars show the one-standard-error range for the coefficient a . Also shown are the values predicted by the equations of Joyner and Boore (1982) for soil sites (JB82) and the equations of Abrahamson and Silva (1997) for soil sites and reverse-fault earthquakes (AS97). A moment magnitude of 6.7 and a basin edge distance of 20 km were assumed for the JB82 and AS97 curves.

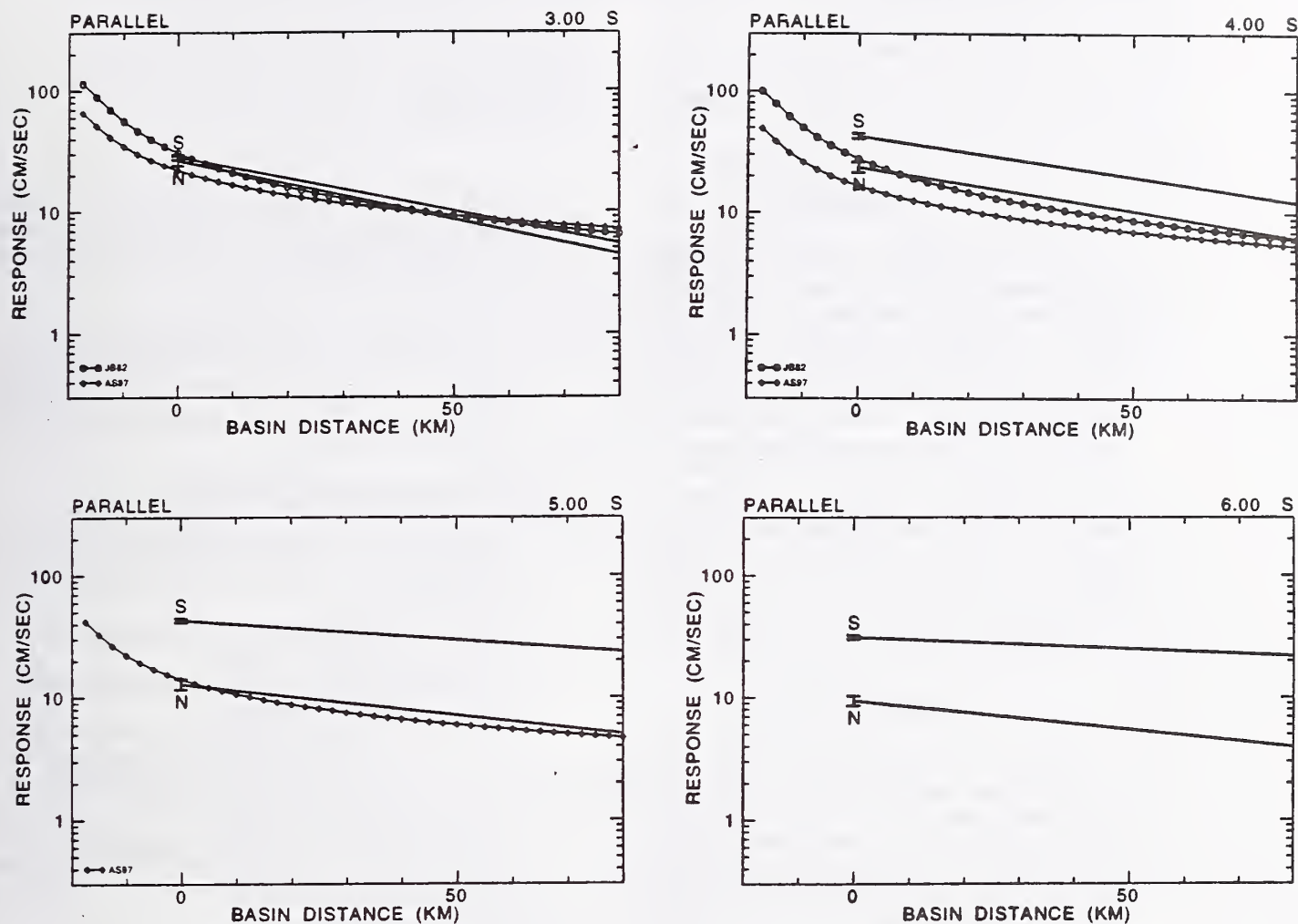


Figure 9. Values of pseudovelocity response for the parallel component predicted by equation (1) with coefficients fitted to data from the San Fernando earthquake (S) and the Northridge earthquake (N). The bars show the one-standard-error range for the coefficient a . Also shown are the values predicted by the equations of Joyner and Boore (1982) for soil sites (JB82) and the equations of Abrahamson and Silva (1997) for soil sites and reverse-fault earthquakes (AS97). A moment magnitude of 6.7 and a basin edge distance of 20 km were assumed for the JB82 and AS97 curves.

PERFORMANCE BASED DESIGN FOR PORT STRUCTURES

by

Susumu IAI¹⁾ and Koji ICHII¹⁾

ABSTRACT

This paper presents a performance based design approach for port structures. The performance based design is an emerging art, which was born from the lessons learned from the recent earthquakes in 1990's. This is to overcome the limitation in the conventional seismic design, which was based on the force balance against a design seismic force. The performance based design is a user friendly approach to take into account the requirements of the seismic performance of a structure against the probabilistic occurrence of earthquake motions. This paper is an initial proposal of the seismic performance based design for port structures.

Key Words : Performance, Design, Earthquake, Quaywall

1. INTRODUCTION

The performance based design is an emerging art, which was born from the lessons learned from the recent earthquakes in 1990's. This is to overcome the limitation in the conventional seismic design. In the conventional seismic design, the design is accomplished based on the force balance against a design seismic force but the design does not provide the information on the performance of a structure when exceeding the limit of the force balance. In the performance based design, design earthquake motions are defined in two levels and the required performance of a structure specified in terms of displacements and stress levels is defined for varying levels of the earthquake motions. The performance based design, thus, should be the key to accomplishing higher reliability of a structure against earthquake without appreciable increase in construction cost.

2. Definition of Performance Grades

In the seismic design considering structural performance, it is necessary to clearly define the required performance of a structure against design earthquake motions in terms of allowable displacements and stress levels. The defined performance is used as a criteria to evaluate an initial structural design. If the initial design does not

satisfy the required performance, then the design should be modified until it meets the requirements. The required performance thus defined is called seismic performance criteria.

The seismic design considering structural performance, called performance based seismic design, is accomplished according to the flowchart shown in Fig. 1. Relevant issues in this flowchart will be discussed below.

(1) Design Earthquake Motions

The levels of design earthquake motions for port structures are specified, in the two level approach, as follows.

Level 1 : Earthquake motion having a return period of 75 years

Level 2 : Earthquake motion having a return period of 475 years.

Level 2 earthquake motion includes a near field motion of a very rare event from an active seismic fault, if the fault is located nearby.

The earthquake motions having a return period of 75 and 475 years have a probability of 50 and 10% occurrence, respectively.

(2) Damage Criteria

The seismic performance criteria are defined by specifying acceptable extent of damage to a structure against the two levels of design earthquake motions. The performance criteria are specified as a function of earthquake motion levels as shown in Fig. 2.

The extent of damage, defining the longitudinal coordinate in Fig. 2, is determined by both serviceability and structural damage. The serviceability is defined in a broad sense. In addition to the original definition for sea transport, the definition of serviceability includes such effects of damage as threats to human lives and properties, loss of function as a emergency base for transportation, threats from hazardous materials, depend-

1) Port and Harbour Research Institute, Japan : Nagase 3-1-1, Yokosuka, 239 Japan

ing on the functions of port structures. The structural damage depends on a structural type; i.e. the extent of structural damage to a gravity quaywall is mainly specified by displacements and tilting while that to a sheet pile quaywall is mainly specified by stress states in the structure. The acceptable extent of damage thus depends on both function and type of a structure.

The extent of damage shown in Fig.2 is specified in the most general qualitative terms into three degrees. More specific descriptions for the extent of damage is defined in Table 1 with respect to the serviceability and the structural damage. The most specific and quantitative damage criteria will be described in 3 and 4 for each type of structures.

(3) Performance Grades

The damage criteria defined by three degrees described above permits to define the performance criteria as shown in Fig. 2. As shown in this figure, the performance grades are specified in four grades, XS, XA, XB and XC, as follows.

- Grade XS : The extent of damage remains degree I for Level 2 motion.
- Grade XA : The extent of damage remains degree I for Level 1 motion and degree II for Level 2 motion.
- Grade XB : The extent of damage remains degree I for Level 1 motion and degree III for Level 2 motion.
- Grade XC : The extent of damage remains degree II for Level 1 motion. Collapse of structure, if occurs at Level 2 motion, does not have threats to the surrounding.

(4) Importance of Structure and Performance Grades

The performance grades defined above closely relate to the importance of structures. A structure with higher importance requires a higher performance grade. The importance of port structures is generally measured by the seismic effects on serviceability (in a broad sense) and structural damage. For example, the importance of port structures specified in the current Japanese design code¹⁾ are categorized into four classes as shown in Table 2. These classes of importance approximately corresponds to the required performance grades as shown in Table 3.

3. Damage Criteria for Gravity Quaywall

In the performance based design, the ac-

ceptable extent of damage, i.e. the damage criteria, should be clearly specified based on the function and seismic response of a structure. The damage criteria should be generally established by a group of design engineers with assistance and advice from the user and owner of the structure/facility.

The guidelines for establishing the damage criteria for typical port structures will be shown in 3 and 4. These guidelines are for the most general case, considering a general purpose quay wall where the seismic damage poses no threats to human lives, no hazardous material is handled, without a movable crane, and the sea space in front of the quay wall is unlimited. Additional guidelines are offered in 5 for the quay walls having container and other movable cranes.

(1) Seismic response of gravity quaywall

A gravity quaywall is made of a caisson or other gravity wall put on seabed, and maintains its stability by the friction at the bottom of the wall against the earth pressures from the backfill soil behind the wall. Typical failure modes during earthquakes are seaward displacements and tilting as shown in Fig. 3(a) for a firm foundation. For a loosely deposited sandy foundation, the failure modes involve overall deformation of the foundation beneath the wall, resulting in large seaward displacement, tilting and settlements. A wall with a smaller width to height ratio exhibits tilting mode rather than horizontal displacements. A wall designed with a seismic coefficient of 0.15 in the pseudo static approach is on the border line for exhibiting tilting mode and horizontal displacements.

Large horizontal displacements and settlements of a gravity quaywall do not significantly reduce the residual state of stability, and are considered generally acceptable for structural damage. Tilting of the wall, however, significantly reduce the residual stability, thus providing restrictive conditions for structural damage criteria. The past case histories²⁾ show overturning/collapse of cellular block and cantilever types. These types of gravity walls need a careful consideration in specifying damage criteria regarding overturning/collapse.

(2) Items specifying damage criteria for gravity quaywall

Seismic performance of a gravity quaywall is specified based on the serviceability in safe mooring, safe operation of wheeled vehicles and cargo handling, flooding, and the structural dam-

age exhibiting displacements and tilting (including relative displacements between the blocks of a cellular block type quaywall.).

Items specifying damage criteria are the deformation of wall including displacements, settlements, tilting, and differential displacements (winding of a face line), and the deformation at apron including settlement, differential settlement at and behind apron, and tilting as shown in Fig. 4.

Damage criteria should be established by choosing and specifying appropriate items from the items mentioned above considering performance requirements mentioned above. More specifics are given in the next subsection.

(3) Damage criteria for gravity quaywall

The damage criteria are established, as mentioned earlier, considering both serviceability and structural damage. The criteria for a gravity quaywall regarding structural damage should be established by referring to Table 4 with additions and modification for the specific conditions of a structure designed. The criteria shown in Table 4 show minimum requirements. Thus, in evaluating seismic performance by referring to the damage criteria, if different damage degree results from different items evaluated, the highest damage degree should be the final results of the evaluation.

The criteria for a gravity quaywall regarding serviceability should be established by referring to Table 5 with additions and modification for the specific conditions of a structure designed. In particular, Table 5 is a reference for upper limit of damage degree I.

As mentioned earlier, the overall damage criteria should be established based on both serviceability and structural damage criteria established above.

4. Damage Criteria for Trestle Pier

(1) Seismic response of trestle pier

A trestle pier is composed of a pier and a retaining wall. The pier is a system composed of a deck supported by pile, embankment below the deck and a bridge between the pier and the retaining wall. Typical failure modes during earthquakes depends on the relative magnitude of inertia force and ground displacements as shown in Fig. 5.

Structural damage to a trestle pier is governed

by stress states rather than displacements. It is important to determine the sequence and degrees of ultimate states to occur in the composite system of a trestle pier. The 1995 Kobe earthquake caused various modes of damage, including displacements and tilting toward the sea or the land and collapse at the most serious case³⁾.

(2) Items specifying damage criteria for trestle pier

Seismic performance of a trestle pier is specified based on those of a retaining wall and a deck supported by piles. The seismic performance of the retaining wall is specified referring to those for a gravity or sheet pile wall. The effects of ground displacements, including the movement of the retaining wall and the embankment below the deck, should be carefully evaluated for the performance of the deck supported by piles. The seismic performance of the deck supported by piles is specified based on the serviceability and structural damage similar to those for a sheet pile quaywall.

Items specifying damage criteria are as follows (refer to Fig. 6).

■ Displacements

- deck and piles : settlement, tilting, differential displacements
- apron : differential settlement between deck and retaining wall, tilting, fall/fracture of bridge

■ Stresses

- piles (pile top and below mudline)
- deck (deck body, pile cap)
- bridge

Damage criteria should be established by choosing and specifying appropriate items from the items mentioned above considering performance requirements mentioned above.

The sequence to reach the ultimate states with increasing level of seismic load should be appropriately specified for a trestle pier as follows (refer to Fig. 7).

- 1) Pile cap
- 2) Pile top
- 3) Deck or Pile below mudline
(within allowable ductility factor)

Structural details for a bridge such as fail-safe device to prevent fall down or easily repairable structure should be also important, and, if applicable, a structure to absorb the displacements from the retaining wall should be introduced. This could lead to a further development of energy absorption device for a trestle pier.

(3) Damage criteria for sheet pile quaywall

The criteria for the retaining wall of a trestle pier should be established by referring to those for a gravity or sheet pile quaywall.

The criteria for a trestle pier regarding structural damage should be established by referring to Tables 4 and 6. The most restrictive conditions among displacements and stresses should be the damage criteria. The displacements in Table 4 is applied for residual displacements while the stresses in Table 6 is for peak stresses during an earthquake.

Structural damage to the embedded portion of a pile is generally difficult to restore and has a potential to trigger collapse of a trestle pier, and thus needs more restrictive ductility factor used for design. No case histories are reported on brittle fracture of steel piles during earthquakes. The case histories on brittle fracture of thick steel columns during the 1995 Kobe earthquake reminded, however, that it is still necessary to study this aspect of the steel piles.

The criteria for a trestle pier regarding serviceability should be similarly established as for the gravity quaywall by referring to Table 5.

As mentioned earlier, the overall damage criteria should be established based on both serviceability and structural damage criteria established above.

5. Damage Criteria for Quaywall having Wheeled Cranes

In order to be serviceable after an earthquake, the quaywalls equipped with such facilities as wheeled cranes or ferry facilities need to maintain the serviceability of these facilities in addition to the basic serviceability required for the general purpose quaywalls. Safety for human lives should also be secured. Consequently, the damage criteria for the quaywalls equipped with wheeled cranes, etc. should be specified based on additional consideration to those shown in 3. and 4. For example, the serviceability of the quaywalls having a conveyor belt is strongly affected by differential displacements and settlements. The effects of earthquakes on ferry wharves needs additional consideration on displacements of quaywalls, fail safe devices for passenger bridges, etc. to secure the safety of passengers and the passenger transport operation.

In this section, the additional criteria to those discussed in 3. And 4. are discussed, which are

needed for quaywalls having wheeled cranes such as container cranes.

(1) Seismic response of wheeled cranes

A wheeled crane consists of an upper structure, handling cargoes, and a foundation structure, supporting and transporting the upper structure as shown in Fig. 8. It is generally made of a steel framework. The foundation structure is either a rigid frame type (as shown in Fig. 8) or a hinged leg type, which have one hinge at the level A in Fig. 8). The foundation structure is supported by rails through the wheels. The rails are often directly supported by a portion of a retaining wall or the deck of a trestle pier for a gravity quaywall or a trestle pier. When the width of the gravity wall is small, or the quaywall is a sheet pile or cellular type, a separate set of foundations, often a pile foundation, is provided to support the rails.

A wheeled crane at rest is fixed to rails or a quaywall with clamps or anchors, whose strength provides the upper limit for the resistance of the crane against external forces. A wheeled crane in operation, however, is not supported with clamps or anchors, so that the resistance of the crane against external forces is only due to those from the friction and the flanges of the wheels.

Typical failure modes during earthquakes are derailment, detachment or pull-out of wheels, rupture of clamps and anchors, buckling, and overturning⁴⁾. As shown in Fig. 9(a), widening of a span between the legs due to the deformation of the quaywall results in derailment or buckling of legs. Conversely, as shown in Fig. 9(b), narrowing of a leg span can also occur due to rocking response of a crane. This is due to alternating action of horizontal component of resisting forces from the quaywall during rocking type response involving uplifting of one side of legs. Derailment and detachment of the wheel can also occur due to the rocking. As shown in Fig. 9(c), when a dent or differential settlement occur on a quaywall below the crane, the derailed leg can put into it, resulting in tilting and overturning of the crane. If the crane has one hinge type legs, the derailment can result in tilting and overturning of the crane as shown in Fig. 9(d).

Though the clamp or anchor provides more resistance for the motion against the external force, the internal stresses induced in the framework of a crane becomes larger with clamp or anchor than allowing rocking response.

The quaywall having wheeled cranes needs a

special consideration on the foundation of the crane such as for providing a monolithic upper structure to support the rails.

(2) Items specifying damage criteria for the quaywall having wheeled cranes

Seismic performance of the quaywall having wheeled cranes is specified based on the serviceability of and the structural damage to the crane. The serviceability of the crane is specified regarding the function of upper structure (i.e. cargo handling) and that of foundation structure (i.e. transportation and support for the upper structure). The structural damage regarding the crane is specified not only by displacements, derailment, tilting, and stress of the crane but also the displacements and stresses of the rails and the foundation. With regard to the serviceability of the crane, maintaining the power supply should also be considered.

Items specifying damage criteria are as follows (refer to Fig. 10). For rails and foundation, the items include rail span, rail winding (including discontinuity), differential settlement (differential levels between the rails, differential levels, inclination and vertical discontinuity along a rail), displacements and stresses of rail foundation. For a wheeled crane, the items include wheels (derailment), vehicles (detachment), clamps and anchors (rupture), and displacements of the crane (derailment, tilting, and overturning) and stresses in the framework (stress levels, location of buckling, possibility of collapse).

Damage criteria should be established by choosing and specifying appropriate items from the items mentioned above considering performance requirements mentioned above. More specifics are given in the next subsection.

(3) Damage criteria for the quaywall having wheeled cranes

The damage criteria are established, as mentioned earlier, considering both serviceability and structural damage to not only the quaywall but also the crane and its foundation. The damage criteria for the quaywall required with respect to the crane are discussed below. The criteria for the quaywall with respect to the crane foundation should be separately established by referring to the damage criteria for both the crane and the quaywall.

a) Damage criteria regarding structural damage

The criteria for a wheeled crane regarding structural damage should be established by refer-

ring to Table 7. The most restrictive conditions among displacements and stresses should be the damage criteria. The displacements in Table 7 is applied for residual value while the stresses is defined for peak stresses during an earthquake.

The damage criteria for the quaywall having wheeled cranes should be established by referring to the following discussions.

The damage degree I of the quaywall should be the displacements less than that to keep the foundation structure of the crane within a elastic limit. For example, this limit corresponds to the widening of the leg span of one meter for a rigid frame crane having a rail span of 30 m. There is no limit for the damage degree I for a one hinged leg type.

The damage degree II of the quaywall should be the level difference between the rails within overturning limit for the crane as well as the differential settlements and tilting of the apron within the same limit. In addition, a measure to increase the surface friction of the apron can increase the overturning limit of a derailed one hinged leg crane or a crane having a plastic hinge at a leg. The required friction coefficient is given by

$$\mu \geq \delta h / H \quad (1)$$

where μ : coefficient of friction

δh : expansion of leg span (m)

H : height of the hinge from the apron (m)
(refer to Fig. 11)

b) Damage criteria regarding serviceability

The damage criteria for serviceability of a wheeled crane should be specified by referring to Table 8.

The upper limit for assuring the original serviceability of a wheeled crane is given by Table 9, which is used as guidelines for daily maintenance⁵⁾. This limit can be used as the criteria for a very important quaywall or a quaywall having a monolithic upper structure to support the crane rails. In this case, this limit can be introduced as the damage degree 0. The performance grades should be newly classified in accordance with this new damage degree.

As mentioned earlier, the overall damage criteria should be established based on both serviceability and structural damage criteria established above.

6. Evaluation of Seismic Performance

As mentioned earlier, the seismic design considering structural performance is accomplished following the flowchart shown in Fig. 1. Thus, after establishing the performance criteria referring to the previous sections, the seismic performance of a designed cross section should be evaluated and compared with the performance criteria.

(1) Outline

Seismic performance is evaluated through seismic analyses and/or model tests of a designed structure for varying levels of earthquake motions. The analyses and/or tests results in an extent of damage defined as a function of an earthquake motion level. This curve will be called a seismic performance curve. Evaluation of seismic performance is accomplished by determining whether the seismic performance curve is included in the area of the performance grade required in Fig. 2.

For example, if a designed structure has the seismic performance curve "a" in Fig. 12, the curve is included in the area of performance grade XA through Levels 1 and 2 earthquake motions. Thus, this structural design assures the performance grade XA. If a designed structure has the seismic performance curve "b" in Fig. 12, however, the curve includes the portion to go through the area of performance grade XB. Thus this structural design assures only the performance grade XB.

(2) Initial design of a structure

The initial design of a structure to be evaluated for its seismic performance can be accomplished by any means, including the conventional pseudo static approach and other innovative design approaches. An efficient procedure to arrive at the final design to satisfy the required performance criteria need the initial design which closely approximates the final design. The candidate for this may be given by the conventional pseudo static approach with appropriate measures against soil liquefaction.

In the conventional pseudo static design, the importance factor of a structure is used to scale the design seismic force. In the performance based design, the importance of a structure is not reflected in the levels of design earthquake motions but is used in terms of a required performance grade of the structure. A fundamental difference seems to exist between the conventional and performance based approaches. The apparent differ-

ence in these approaches is resolved by referring to Fig. 13. In this figure, the levels of earthquake motions which corresponds to the same extent of damage correspond to the required performance grades, suggesting the two approaches are basically consistent with each other.

7. Introducing Performance Based Design

The performance based approach discussed in the preceding sections specifies a comprehensive seismic resistance against earthquakes. This approach will be very useful for establishing enough seismic resistance with a minimum cost. This approach, however, is an emerging art based on the recent earthquakes in 1990's. It is not practical to introduce this approach to the seismic design of all types of port structures. This approach should be introduced step by step by beginning from the structures of the highest importance such as those with the special class in Table 2. This approach is particularly useful for designing the structures with the following conditions.

- When a structure is located at the near field of an active seismic fault
- When a standard remediation measures against liquefaction is difficult to apply.
- When a structure is too complex to be designed by the conventional design approach.
- When a structure is a new (i.e. unconventional) type.

If the performance based approach can not be applied to, it is yet desirable to evaluate the seismic performance in an approximate way based on the past case histories and the existing results of the seismic response analysis. The following remarks can be useful.

- Structures with the importance factor higher than the Class B

By referring to the past case histories, it is desirable to avoid the types of structures which tended to collapse.

- Structures with the importance factor of the Class C

Effects on the surrounding of the structure should be evaluated in the event of the collapse of the structure.

In evaluating the seismic performance curve of a structure, appropriate methods or methodologies whose applicability were confirmed with respect to the past case histories and/or model test results. These methods and methodologies will be described in the next chapter. They include simplified and sophisticated methods. The structures with higher importance should be evaluated with sophisticated methods. For example, the structures

of the special class should be evaluated by effective stress analyses and/or model tests, and those of the class A can be evaluated simplified methods as well as effective stress analyses and model tests. If the simplified methods are used, however, the applicability of the methods should be confirmed by using a representative design of structures based on the results of the effective stress analyses and model tests.

References

- 1) Ministry of Transport (ed) : Technical Standards for Port and Harbour Facilities in Japan, Overseas Coastal Area Development Institute of Japan, 1991, pp.75
- 2) Uwabe, T. : Study on quantitative estimation of seismic damage to gravity quaywall, Technical Note of the Port and Harbour Research Institute, No.548, 1986, pp.33 (in Japanese)
- 3) Inatomi, T. : Damage to port structures by the 1995 Hyogoken-Nambu earthquake, Technical Note of the Port and Harbour Research Institute, No.857, 1997, pp.237 and pp.563 (in Japanese)
- 4) Tanaka, S. et al. : Seismic damage and response of container cranes during the Great Hanshin earthquake, Symposium on Great Hanshin earthquake, Japan Society of Civil Engineers, 1996, pp.413-420 (in Japanese)
- 5) Japan Cargo Handling Mechanization Association : Maintenance manual for container cranes, 1996, pp.158 (in Japanese)

Table 1 Damage Criteria for Performance Based Design

Extent of Damage	Serviceability (Amount of work needed for temporary restoration)	Structural Damage (Amount of work needed for full restoration)
Degree I	Full serviceability is maintained without temporary restoration, or with minor temporary restoration.	No damage, or minor damage
Degree II	Full or partial serviceability is recoverable with temporary restoration.	Intermediate damage
Degree III	Service is difficult to recover until full restoration.	Extensive damage without collapse

Table 2 Importance of structure defined in the current Japanese design code

Importance of Structure	Definition (Seismic effects on structures)
Special Class	Structures having more serious effects for ①~③ than Class A structures.
Class A	① Structures resulting in extensive loss of human lives and properties upon seismic damage ② Key structures designed serviceable for recovery from earthquake disaster ③ Structures handling hazardous materials ④ Structures, if disrupted, devastating the economic and social activities of the earthquake damage area ⑤ Structures, if damaged, being difficult to restore.
Class B	Structures other than those of Special Class and Classes A & C.
Class C	Small easily restorable structures other than those of Special Class and Class A.

Table 3 Importance of structures and Performance Grades

Importance of Structure defined in the current Japanese design code	Performance Grade for the PIANC seismic design guidelines
Special Class	XA(or XS)
Class A	XB
Class B	XC

Table 4 Damage Criteria for Gravity Quaywall regarding Structural Damage

Extent of Damage	Deformation Rate (δ/H) δ : Horizontal displacement H : Height of Gravity Wall	Tilting towards the sea
Degree I	less than 3 %	less than 3 deg
Degree II	3 ~ 10 %	3 ~ 5 deg
Degree III	larger than 10 %	5 ~ 8 deg (or less than 90 % of critical angle)

Table 5 Damage Criteria for Upper Limit of Degree I regarding Quaywall Serviceability

Main Body of Quaywall	Settlement	20 ~ 30 cm
	Tilting towards the sea	2 ~ 3 deg
	Differential Horizontal Displacements	20 ~ 30 cm
Apron	Differential Settlement on Apron	3 ~ 10 cm
	Differential Settlement behind Apron	30 ~ 70 cm
	Tilting towards the sea	2 ~ 3 deg

Table 6 Damage Criteria for Pile Supported Pier regarding Structural Damage
(Criteria with respect to Stresses)
(When pile cap should be the first to yield.)

Extent of Damage	Stresses in pile supported pier			
	Deck		Piles	
	pile cap	main body	pile top	below mudline
Degree I	elastic	elastic	elastic	elastic
Degree II	Plastic (less than allowable ductility factor)	elastic	elastic	elastic
Degree III	Plastic (less than allowable ductility factor)	Plastic (less than allowable ductility factor)	plastic (less than allowable ductility factor)	plastic (less than allowable ductility factor)

Table 7 Damage Criteria for Movable Crane regarding Structural Damage

Extent of Damage	Displacement	Stresses in Crane	
	gross displacement of crane	upper structure	supporting structure
Degree I	without derailment	elastic	elastic
Degree II	with derailment	elastic	Plastic (less than allowable ductility factor) for main framework. Damage to toe (including pull-out of vehicle, fracture of anchor/brakes)
Degree III	without overturning	plastic (less than allowable ductility factor)	without collapse

Table 8 Damage criteria for crane regarding serviceability

Extent of Damage	Serviceability Level
Degree I	Full serviceability is maintained with or without minor temporary restoration.
Degree II	Limited serviceability is restored with temporary restoration. (Limited serviceability does not include the ability to move.)

Table 9 Damage criteria for upper limit of degree 0 (no restoration needed) for crane serviceability
(Allowable limit for ordinary maintenance)

Items to be evaluated	Allowable Limit
Rail Span L (L < 25 m) (25 m ≤ L ≤ 40m)	± 10 mm ± 15 mm
Level difference between sea and land side rails	L/1000
Curving in vertical direction	5 mm per 10 m
Curving in horizontal direction	5 mm per 10 m
Inclination	1/500
Rail joint	1mm
Differential Displacements (vertical and horizontal) Gap	5mm

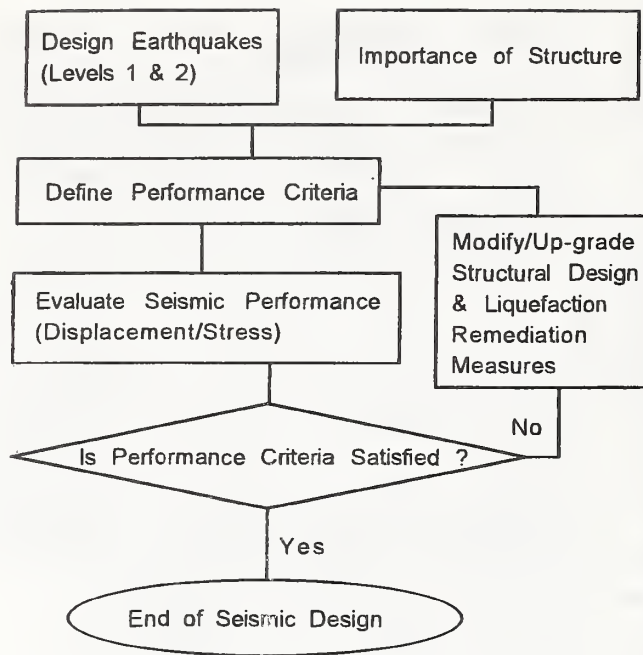


Fig. 1 Flowchart for Performance Based Seismic Design

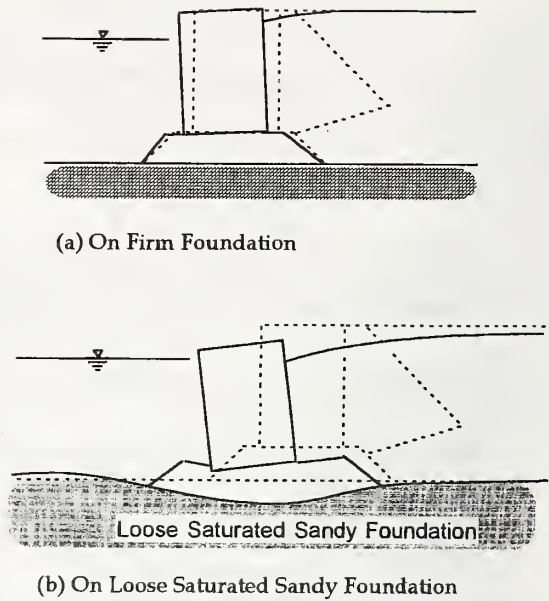
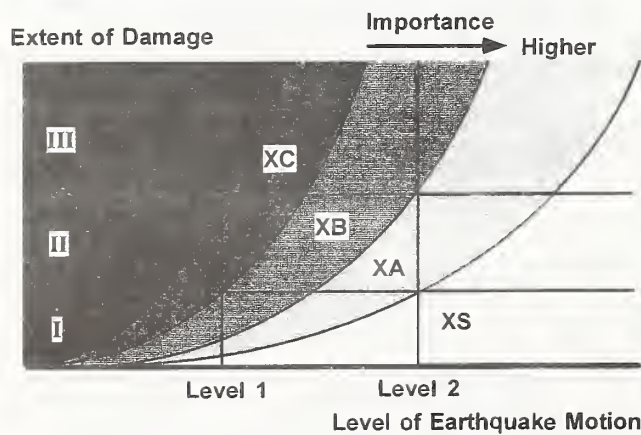


Fig. 3 Deformation/Failure Mode of Gravity Quaywall



Extent of Damage

I : No Damage or Minor Damage

II : Service Recoverable with Temporary Disruption

III : Extensive Damage without Collapse

Fig. 2 Schematic Figure of Performance Grades XS through XC

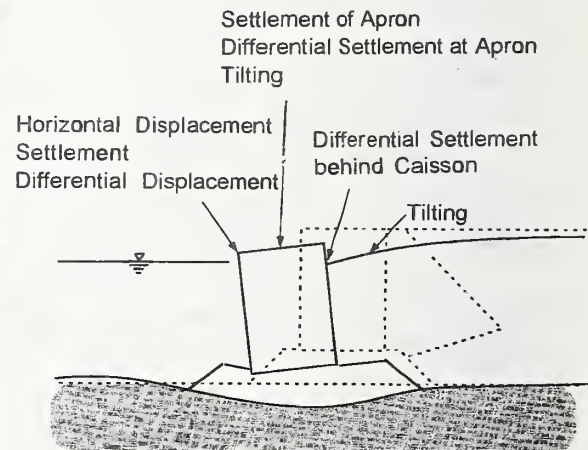
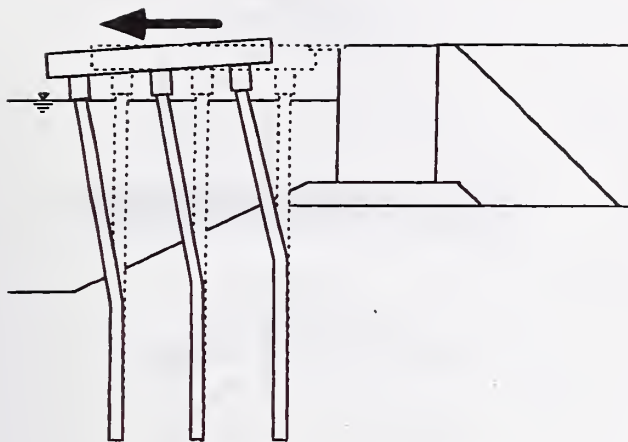
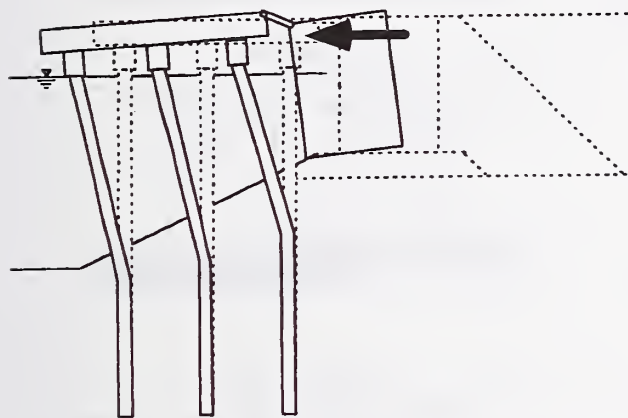


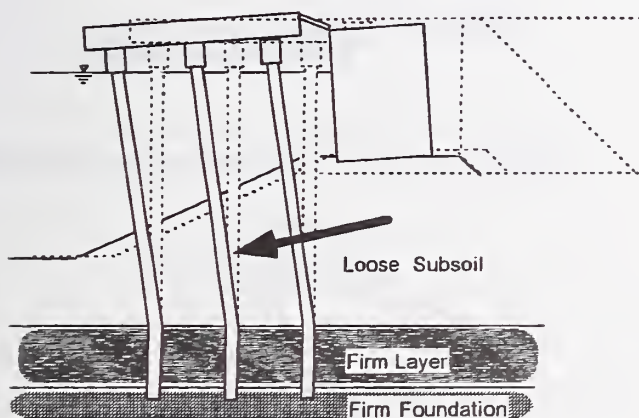
Fig. 4 Item to be evaluated for Gravity Quaywall



(a) Deformation due to Inertia force at Deck

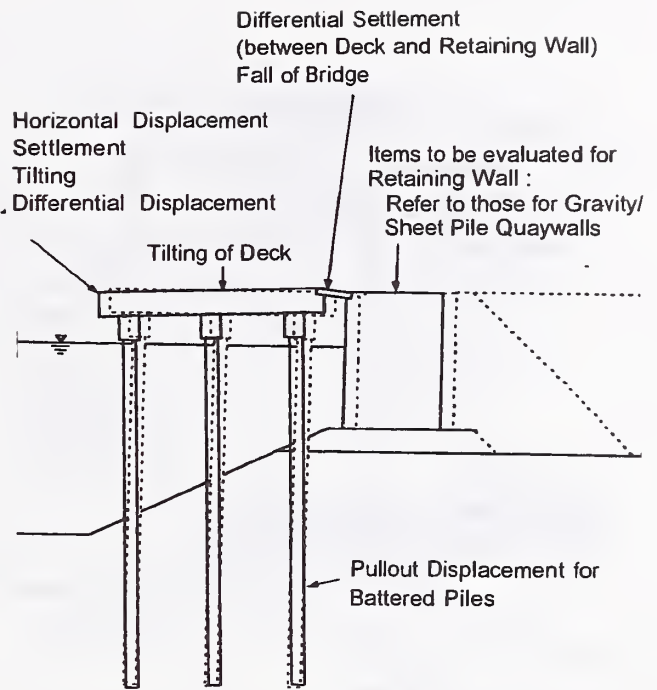


(b) Deformation due to Horizontal Force from Retaining Wall

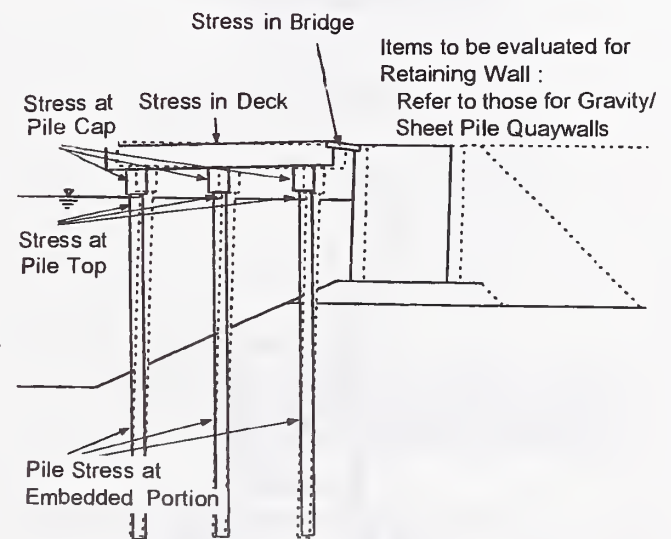


(c) Deformation due to displacement of loose subsoil

Fig. 5 Deformation/Failure Mode of Pile Supported Pier



(a) For displacement performance criteria



(b) For stress performance criteria

Fig. 6 Item to be evaluated for Pile Supported Pier

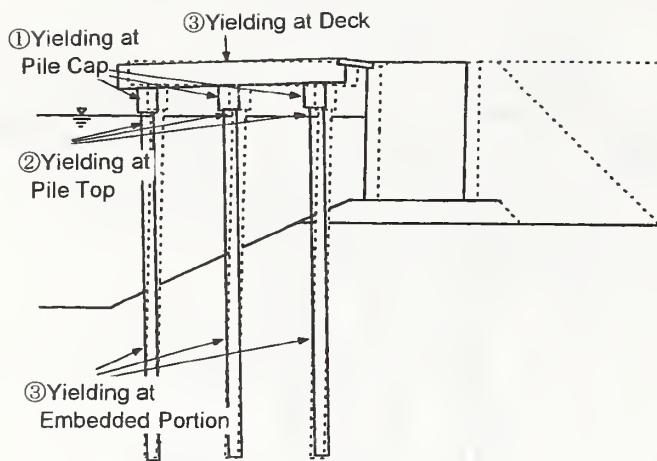


Fig. 7 Acceptable Order of Yielding for Pile Supported Pier

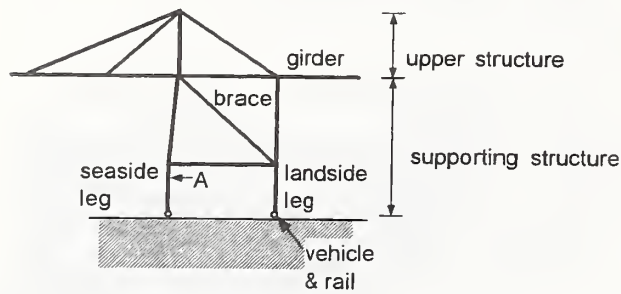
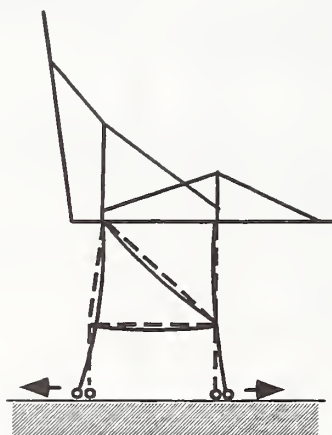
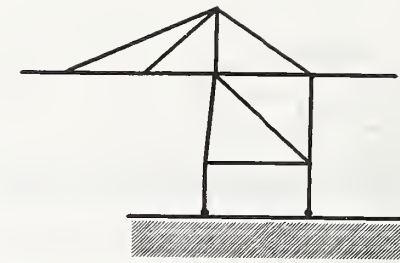


Fig. 8 Schematic figure of Movable Crane

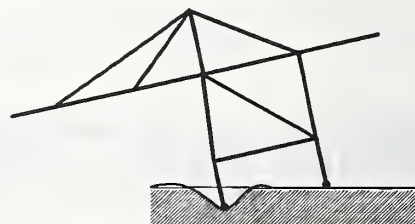


(a) Widening of Span between the Legs

Fig. 9 Deformation Mode of Movable Crane

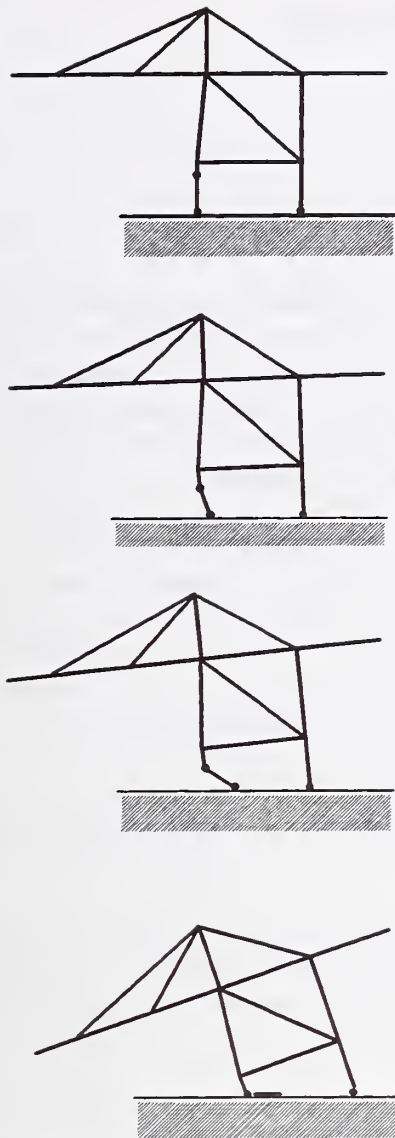


(b) Narrowing Span between the Legs due to Rocking Motion



(c) Tilting of Crane due to Differential Settlement of Foundation

Fig. 9 (Continued)



(d) Overturning of One Hinged Leg Crane due to Rocking/Sliding

Fig. 9 (Continued)

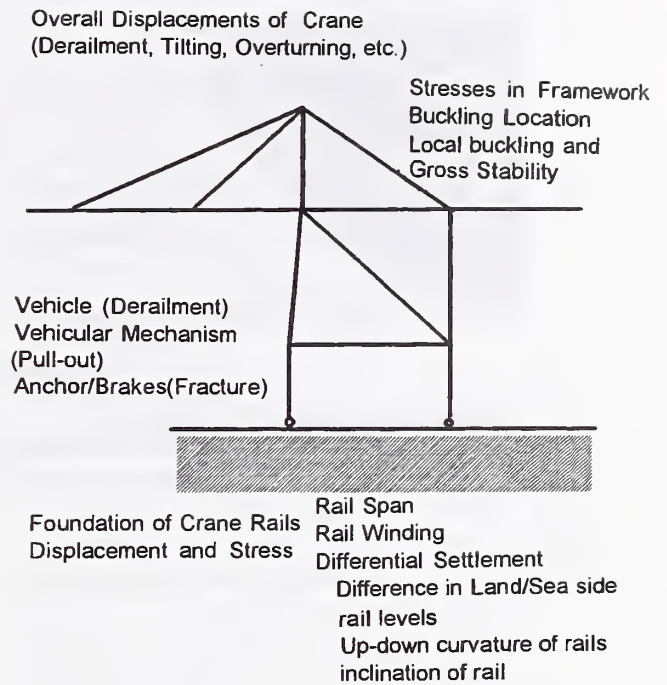


Fig. 10 Items to be evaluated for Crane

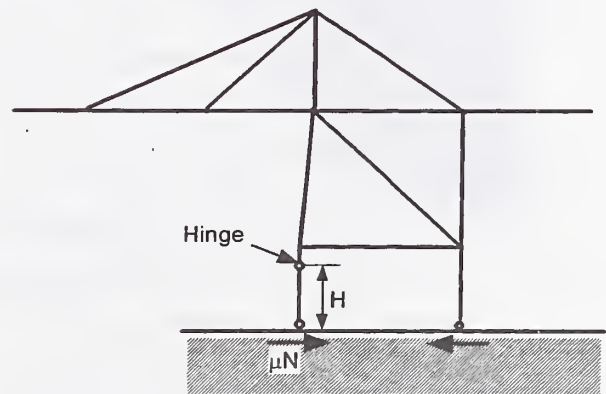
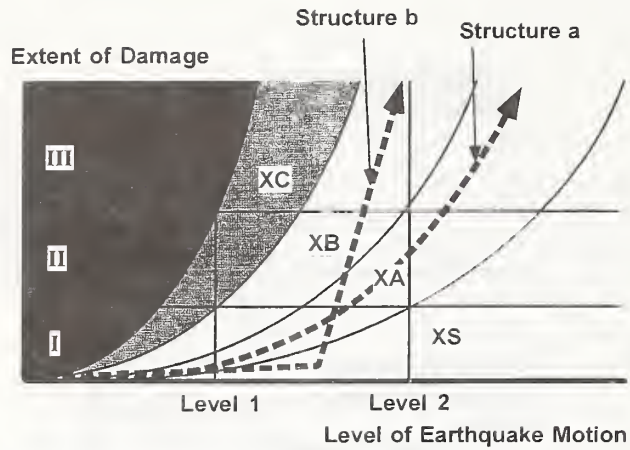


Fig. 11 Schematic figure for evaluating overturning of using Eq. (1)



Examples of Seismic Performance

Structure a : Satisfy Performance Grade XA

Structure b : Satisfy Performance Grade XB

Fig. 12 Examples of Seismic Performance

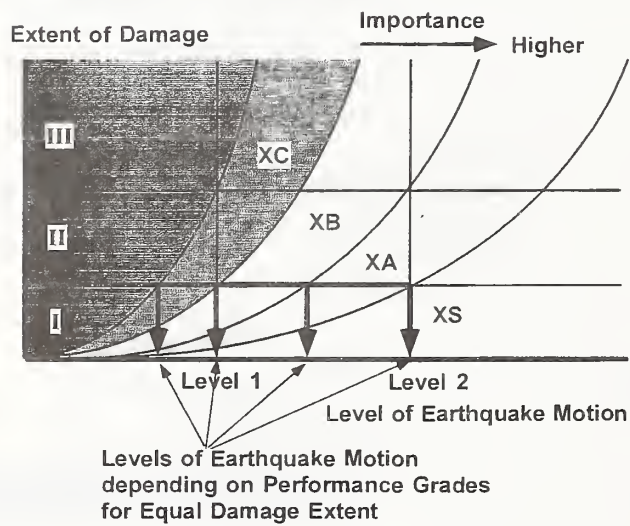


Fig. 13 Levels of Earthquake Motion depending on Performance Grades

Analysis of Sea-Floor Earthquake Data

by

Charles E. Smith¹ and David M. Boore²

ABSTRACT

The Minerals Management Service (MMS), in cooperation with several oil and gas companies, installed a seismometer network on the ocean floor in the Santa Barbara Channel off the coast of southern California. The program was called SEMS, for the Seafloor Earthquake Measurement System. The purpose of the program was to characterize the nature of the response of earthquake ground motions for use in the design and reassessment of offshore platforms used in petroleum drilling and production. The United States Geological Survey (USGS) was given a contract to provide seismological analysis of data obtained from the SEMS program and compared it to data from earthquakes measured onshore. This paper provides an overview of the work by the USGS on this initiative.

KEYWORDS: earthquake ground motions, offshore platforms, seafloor seismic measurements, seismological analyses, seismic-hazard uncertainties.

1. INTRODUCTION

A major effort was undertaken by both the Government and the oil and gas industry to obtain records of earthquake seafloor motions for the design of new platforms or in the reassessment of the integrity of existing offshore facilities. The prime goal of the program was to obtain data that might help answer the question of whether ground motions at offshore sites are significantly different than those at onshore sites; if this is true, then the decision of using onshore motions as the basis for the seismic design or reassessment of offshore platforms should be reevaluated. This paper provides an overview of the more detailed analysis presented in Boore

(1997), Boore and Smith (1998) and Boore (1998) of earthquake data obtained from seafloor seismic motions measured from the SEMS program.

2. SHORT HISTORY OF SEMS.

To obtain creatable data on the response of the seafloor to earthquake-induced ground shaking, the Sandia National Laboratory was commissioned, with funding by the MMS and several major oil companies, to develop, deploy, and recover data from instruments placed on the seafloor. A complete history of the SEMS program is contained in Reece, et. al (1991), Steefe and Engi (1987), Smith (1991), and Platzbecker (1997). A brief synopsis of the SEMS project is provided as background for this paper.

The SEMS program was developed in a number of stages beginning some 20 years ago. These are usually referred to as SEMS I, SEMS II, SEMS III, and SEMS IV (in this paper standard numbers are used rather than Roman numerals; thus SEMS 1, SEMS 2, SEMS 3, and SEMS 4 or more briefly, S1, S2, S3 and S4). The programs were very unique in that all stages of the SEMS project used digital reading of seafloor accelerations. Data were analyzed from S1, S2, and S4.

SEMS1: In 1978, a 3-axis accelerometer was embedded several meters below the seafloor, and the output from the accelerometer was fed to a self-contained instrument package resting on

¹ Research Program Manager, Minerals Management Service, Herndon, VA 20170

² Senior Geophysicist, U. S. Geological Survey, Menlo Park, CA 94025

the seafloor. This package digitized the input at a rate of 100 samples per sec and stored the data onboard. Data recovery was via an acoustic uplink to a ship deployed specifically for data recovery. The SEMS was installed at several offshore locations and at one onshore location. Data were analyzed from the onshore location (S1VC) and a nearby offshore location (S1HN) near platform Henry in the Santa Barbara channel (See table 1 for station information, and table 2 for earthquake information).

SEMS2: In 1985, the system was redesigned to have a longer system life, and was deployed near platforms Elly and Ellen, off Long Beach. In other respects, the system was similar to that of SEMS1 (a triggered system with data storage in a unit on the seafloor, using an acoustic uplink from data retrieval). The notation "S2LB" was used for this system. Data were analyzed for two earthquakes occurring in 1986, the North Palm Springs and the Oceanside earthquakes.

SEMS3: In 1989, the system was again redesigned, using better batteries, electronics, and triggering algorithm. The result was a longer-life, more sensitive system with fewer false triggers. A major improvement is in using data from horizontal as well as the vertical component in the triggering algorithm (the SEMS1 and SEMS2 units used only vertical component, which, generally has anomalously low amplitudes of motion). The system was deployed at two locations, one near the SEMS2 package off Long Beach (S2LB), and another off of Point Pedernales, near platform Irene (S2IR). This latter site used a datalogger onboard the platform, connected via a cable to the sensor, which was embedded in the seafloor. Apparently the hole did not slump in, and this, combined with cable drag due to strong currents, limited the usefulness of this installation. The only data from a SEMS3 unit used in this paper are that from the 1990 Upland earthquake recorded on S3LB (the recordings for this event, however, are very high quality and useful; they have a long enough duration and a good enough signal-to-

noise ratio to record late arriving long-period surface waves.) Unfortunately, recordings of the 1992 Landers earthquake and aftershocks were lost because the seafloor data acquisition system had been dragged away, apparently by a fisherman's net. This is very unfortunate because the earthquake was one of the largest to have struck southern California since 1952. The long-period motions of most concern to platform design were very strong for that earthquake and, as a result, they were well recorded on conventional strong-motion instruments onshore, thus providing an excellent set of onshore motions against which to check the offshore motions (this has been a problem with most of the SEMS recordings: the earthquakes were far enough away and of low enough magnitude that conventional onshore strong-motion recorders either did not trigger or did not record signals that could yield reliable long-period information; in contrast, the SEMS unit can faithfully record these weak motions).

SEMS4: To address the problem of data recovery from stand-alone sea-floor installations, it was decided to deploy a new system in 1995, SEMS4, using a commercial 24-bit datalogger on a platform, with a cable connecting the sensors to the datalogger. The dataloggers also have a dial-up capability, making it possible to interrogate the units remotely. The loggers are being run at 20 samples per sec. The sensors are force balance accelerometers, almost flat to acceleration between 0.4 and 1500 Hz (the response at 1 Hz is nominally down by 3 db relative to the 100 Hz response); the low frequency rolloffs starts at about 0.4 Hz. Three systems have been deployed, near platforms Eureks (S3EU), Grace (S4GR), and Irene (S4IR). Records of earthquakes in 1995 and 1997, recorded by S4GR and S4IR, are analyzed in this report. The SEMS4 instruments have been turned over to the California Strong-Motion Program of the California Division of Mines and Geology, who will operate the stations and collect and disseminate the data. See figure 1 for the layout of the SEMS4 instrument array.

3. ANALYSIS OF DATA

Because of the lack of onshore data for distances comparable to those from the source to the SEMS sites, the empirical interpretation of the data focused on the ratio of response spectra for the vertical and horizontal components (V/H) as a function of period. Comparisons to the few available ratios and to the ratios derived from regression analysis of strong motion data clearly show the offshore ground motions to have anomalously low ratios for short-period response. Some evidence is presented that the anomalous V/H at shore periods is due to very low values for the vertical component. The differences between the average onshore and offshore ratios become smaller as the period increases, but still persist at periods as long as 2 sec. A preliminary study suggests that the differences at the longer periods are more a function of the average shear-wave velocities under the site than to whether the site is offshore or onshore.

To augment the data, theoretical calculations were performed of wave propagation in earth models simulating the offshore environment. Comparisons of observed and theoretical V/H for Fourier spectral amplitudes are in reasonable agreement. The theoretical calculations show that the water layer makes almost no difference to the horizontal components of the motion, although it does influence the vertical components of the S-wave portion of the ground motion at frequencies related to the depth of water (around 6 Hz for depths of 60 to 70 M); the effect is negligible for periods near the resonant period of a platform (generally between 1.5 and 4.0 secs). This is not to say that the water is not an important factor, for it does allow relatively low shear-wave velocities to exist over wide regions. There are onshore locations with comparably low velocities, but they are sometimes fairly restricted in spatial extent.

Because of limited recording duration for some of the events, the study was restricted to ground motions less than a 2-sec. period. Recordings for

one event, however, were of long enough duration to capture clear long-period (near 6 sec), large amplitude waves, probably surface waves traveling through the Los Angeles basin. A choice of an upper limit of a 2 sec period effectively eliminates these surface waves from our analysis.

4. SUMMARY OF ACCELEROGRAMS USED

The data used in this report included the largest events recorded on the SEMS units. The stations from which data were obtained are listed in table 1, which contains a short summary of basic information for each station; geotechnical information, and estimates of shear-wave velocity for the sites are discussed in a later section. The earthquakes used are summarized in table 2, and table 3, containing event-to-station distances, and is a convenient summary of which station recorded which earthquakes. Tables containing more details about events and stations are contained in Boore (1997). A map showing the locations of the recording stations and earthquakes is given in -figure 2.

With one exception, each earthquake was recorded on only one of the offshore SEMS stations. The exception is the first Simi Valley, 1997 aftershock of the 1994 Northridge earthquake. This event was recorded on two SEMS4 stations: S4GR and S4IR. The lack of multiple offshore recordings for a given event limits, to an extent, the interpretation of the data.

A more important limitation than the lack of multiple offshore recordings is the relative scarcity of onshore data at sites near the offshore sites (by near, we mean along the same general azimuth from the earthquake to the SEMS site, and at distances as close to the SEMS site as the coastal configuration allows; for the earthquakes listed in table 3, there are generally numerous recordings of ground motions but at epicentral distances much smaller than the epicentral distances to the SEMS stations). As tables 2 and 3 show, most of the SEMS records were obtained

from moderate-size earthquakes at distances in excess of 70 km. The standard analog, onshore accelerographs do not have the sensitivity to provide digitizable data at these distances for the earthquakes recorded on the SEMS sites. The only earthquake for which we were able to obtain onshore and offshore data is the Santa Barbara Island 1981 earthquake, which was recorded on three onshore stations, one of which was a SEMS unit installed onshore near the Vic Trace Reservoir. The other two recordings, SC38 and SC51, were obtained on standard analog accelerometers maintained by the University of Southern California (USC).

Several sites recorded different earthquakes, thus allowing a check on the stability of the ratio of motions for the vertical and horizontal components. These sites include S2EE, with two recordings, S4GR, with three recordings, and S4IR, with two recordings. In addition, sites S2EE and S3EE were close to one another, so if counted as one site, three recordings are available for these sites.

5. V/H-OBSERVATIONS

Visually, the accelerograms recorded on the SEMS units look much like those from onshore sites. As an example, figure 3a shows the three components of motion for the 1990 Upland earthquake; because the units have pre-event buffers, the initial P-wave motion has been captured (unlike the records from analog accelerographs), and the P-wave is followed by a clear S arrival, which is followed by a slowly decaying coda or tail. The vertical component is small relative to horizontal components, but it is possible to find onshore records with comparable relations between the components.

The acceleration, velocity, and displacement time series for the 1990 Upland SEMS recording are also shown in figure 3. The acceleration traces are largest near the beginning of the record, and they decay to small motions at the time of arrival of the large amplitude long-period waves. The

outstanding features of these figures are the late arriving, long-period (≈ 6 sec) motions on all three components. These motions are not unexpected, for the travel path (Figure 2) traverses the Los Angeles basin, and the waves resemble the surface waves that have been observed to propagate in the basin. In seismological terms, the peak accelerations are probably carried by body waves, while the long-period arrivals are surface waves.

The main goal of the SEMS program was to study the similarities and differences of ground motions on the seafloor to those onshore. Because the earthquakes recorded at the SEMS sites were generally not recorded at nearby onshore sites, it is difficult to make a direct assessment of the agreement between onshore and offshore motions; ground motions depend on many variables, such as earthquake size and type of faulting, distance from the source, propagation path, and local site geology, and a comparison of only a few recordings is worthless unless adequate corrections can be made to remove these influences on the amplitudes of the motions. The ratio of vertical to horizontal motions (V/H), however, might be expected to remove all but the effect of local geology, at least to first order. By comparing ratios, it would then be possible to compare a few onshore and offshore recordings to see if they were comparable or not. This technique was performed in the study. The study also compared the ratios from offshore recordings with those predicted from regression analyses based on hundreds of onshore recordings from many earthquakes; this provides a measure of comparison that represents the average ratio for a typical site and earthquake of a specified magnitude and distance. In addition, the study compared the average V/H for offshore SEMS sites to the V/H from a few onshore recordings for which the shear-wave velocities beneath the recording sites are similar to the velocities we estimate to exist beneath the SEMS offshore sites.

Several events were recorded at the same station (table 3). It is interesting to compare V/H for the multiple earthquakes at a given site to assess the stability of the ratio. Similar ratios for different events might suggest that the ratio is strongly controlled by local site conditions, particularly if the events are different magnitude and have different travel paths to the site. Figures 4 and 5 show such comparisons for fourier amplitude spectra and response spectra. We have treated S2EE and S3EE as one site. In these figures, the geometric average of the two horizontal components has been used for the denominator. There is a general trend for the ratios to increase with period, and there is more scatter at short periods than at long periods. The first impression is that there is considerable scatter in the ratios, particularly at short periods. Careful inspection of the figures, however, shows that generally the ratios of V/H from different earthquakes recorded at individual sites are similar to one another; the large scatter is primarily due to site-to-site variations in the ratio (in particular, compare the S2EE and S3EE to S4IR).

The results are first presented from recordings of the 1981 Santa Barbara Island earthquake, which was recorded on an offshore station and several onshore stations. The ratios of 5 percent damped response spectra are shown in figure 6, in which it is clear that the offshore recording (S1HN) has a much different V/H than for the onshore recordings. The difference is largest at short periods and tends to decrease at long periods. The regression-based ratios are in much better agreement with the onshore ratios than with the offshore ratio. It was judged that with the possible exception of SC38, the onshore sites are underlain by materials with higher shear-wave velocities than the offshore site (SC38 is described to be on dune sand in Anderson et al. , 1981, whereas S1VC and SC51 are on marine terrace deposits), and, therefore, one would expect the spectral ratios for the onshore sites to be more similar to the ratios from regression-based results than for the

offshore site.

A comparison between the regression-based onshore results and the average of the SEMS offshore results is shown in figure 7. For the sake of clarity, the offshore ratios have been combined into a single average, in spite of the site-to-site differences demonstrated earlier; this will make no difference in the overall comparison of observed offshore and onshore V/H ratios. The distance at which the AS97 relations were evaluated was 120 km, which is close to the geometric mean distance of 113 km for the events used in forming the ratio. The regression-based results for C97 were evaluated at the greatest distance-60 km-for which two equations are valid. Also included in the comparison in figure 7 are results from analyses of specific earthquakes (Loma Prieta 1989 and Northridge 1994), as well as results from the SMART1 array in Taiwan. In general, the onshore results are above the SEMS offshore results, and the difference is largest at short periods.

The large difference between average onshore sites and the SEMS offshore recordings at short periods is consistent with the findings of Sleaf (1990), who made scatter plots of peak accelerations, with horizontal components on one axis and vertical components on the other. Using different symbols for offshore and onshore recordings, he clearly found two populations separated in the same sense as we found for response spectra. In addition, Smith (1990) found that V/H for peak acceleration and peak velocity from offshore sites was smaller than for onshore sites, again in qualitative agreement with the findings from the spectral ratios.

6. PEAK MOTIONS AS A FUNCTION OF DISTANCE

The previous figures show a clear difference in V/H at short periods between the offshore and onshore recordings. Is this due to onshore vs.

offshore differences in the vertical or the horizontal components, or both? To answer this question, figure 8 is plotted of the response spectral amplitudes for a few selected periods as a function of distance from the earthquake. Only the 1981 Santa Barbara Island data was considered since both onshore and offshore data are available. For comparison, the regression-based results of AS97 and C97 were included in the figure. From these plots, it is clear that the offshore vertical component is always smaller than the SEMS and USC onshore vertical components (after accounting for the attenuation with distance); the difference is greatest at shore periods. The same is not always true for the horizontal components. This comparison is strong evidence that the very low values of V/H at short periods are due to small values of V , rather than large values of H . A similar conclusion was drawn by Smith (1994), who plotted peak accelerations against distance for vertical and horizontal components (see figure 9).

7. RESULTS OF THEORETICAL ANALYSIS

The program HSPEC96 by R. Herrmann was used to do the theoretical modeling. This versatile program uses wave-number integration to compute the complete wavefield in an earth represented by a stack of laterally-uniform, constant-velocity layers. Our procedure was to generate synthetic seismograms for a specified type of faulting for the earth model of interest, and then to treat the synthetic seismogram as we would an observed seismogram. In most cases, the Fourier amplitude spectrum was computed of the S-wave portion of the seismogram, although in a few cases the P-wave portion was studied. The focal depth used in the model was 10km. The surface waves resulting from this depth will not be as energetic as the basin waves, which are probably generated by conversion of body waves at basin edges. For this reason, it is not claimed that the theoretical modeling includes basin waves. This is consistent with the possible lack of basin waves in the V/H ratios computed from

the data (because of the limited duration for some of the SEMS recordings or the presence of noise at long periods).

Comparison of observed and theoretical spectral ratios in figure 10 shows the observed and theoretical V/H ratios of Fourier amplitude spectra. The observed ratios are for the individual SEMS offshore sites, and the theoretical ratios are geometric averages for a range of focal mechanisms. Although they are somewhat model dependent, the theoretical ratios match the overall trend of V/H decreasing with frequency, although they do not predict the precise behavior of the observed ratio at frequencies above about 4 Hz. The ratios at these frequencies are apparently sensitive to details of the site that we are not including in the model. The overall reduction is probably due to refraction of the S-wave toward the vertical, with a resulting decrease in the V/H ratio.

8. CONCLUSIONS

The Seafloor Earthquake Measuring System (SEMS) is a multiphase instrumentation effort that has been in existence for almost 2 decades. The SEMS stations are excellent instruments and have produced high-quality data for a number of events. However, few data are available from which direct comparisons can be made of onshore and offshore motions from the same earthquake recorded at similar distances and for similar site conditions. For this reason, the analysis of the SEMS data has had to use a combination of somewhat indirect observational studies and theoretical calculations to answer the fundamental question: Are earthquake ground motions at the seafloor so different from onshore motions that the more numerous onshore recordings cannot be used for platform design?

The answer to the fundamental question is "It depends." It depends on the component of motion and the frequency of ground shaking. The ratio of vertical-to-horizontal motions (V/H) is clearly much smaller than for onshore

recordings at relatively high frequencies (above about 3 Hz). Studies of the vertical and horizontal motions separately suggest that the anomaly lies with the vertical motions.

Theoretical studies show that the reduction of vertical motions can be produced by interactions of S-waves in the solid materials below the seafloor and P-waves in the water layer. These interactions are most important at the resonant frequencies of vertically propagating acoustic waves in the water layer. A reduced vertical component can also be produced by refraction of an incoming wave toward the vertical, such as will occur for shear-wave velocities that decrease towards the Earth's surface. V/H computed from a few onshore sites with shear-wave velocity versus depth similar to that estimated to be beneath the SEMS offshore stations are much different at high frequencies than the ratios from the SEMS stations, suggesting that simple upward-refraction plays a small role in the difference between onshore and offshore motions at the higher frequencies.

The water layer indirectly influences motions by allowing low-velocity sediments to exist over a widespread area, and by increasing the pore pressure in the sediments, which will reduce the velocity in sands and silts.

As noted before, it is easy to get caught up in the complexities at high frequencies, which reflect the water layer as well as local shear-wave velocities. Although some parts of offshore platform systems are sensitive to high-frequency, vertical component waves (e.g., Smith, 1994, Brady, 1993), the motions are mudline motions and are far from the horizontal resonance frequencies of most offshore platforms. More importantly, for design and analysis of platforms, may be periods of motion longer than 1 second.

Particularly useful recordings for the study of long-period motions were made at a SEMS site offshore Long Beach. Comparisons of response spectra obtained from the SEMS instruments

with onshore empirical and theoretical calculations, as well as time-domain comparisons with onshore waves that have traveled through the Los Angeles basin, suggest that the seafloor motions at the SEMS site are significantly influenced by late arriving, large amplitude surface waves ("basin waves") at long periods. These waves may be more important for platform analysis and design than the higher frequency waves that are influenced by the water layer. In this sense, the travel path may be more important than the local site conditions.

9. REFERENCES

- Boore, D.M. (1997). *Analysis of Earthquake Recordings Obtained from the Seafloor Earthquake Measurement System (SEMS) Instruments Deployed off the Coast of Southern California*, U. S. Geol. Surv. Open-File Rept. 97-733, 242 p.
- Boore, D. M. (1998). *Basin Waves on A Sea-Floor Recording Near Long Beach, California from the 1990 Upland Earthquake: Implications for Ground Motions from a Larger Earthquake*: Bull. Seism. Soc. Am. (submitted for publication).
- Boore, D. M. and Smith, C. E. (1998). *Analysis of Earthquake Recordings Obtained from the Seafloor: Earthquake Measurement (SEMS) Instrument Deployed off the Coast of Southern California*, Bull. Seism. Soc. AM 89 (submitted for publications).
- Brady, A. G. (1993). *Offshore Strong Ground Motion and Onshore Surrogates*, Proceedings, International Workshop on Wind and Earthquake Engineering for Offshore and Coastal Facilities, Yokosuka, Japan, May 12-14.
- Reece, E. W., D. E. Ryerson, and R. L. McNeill (1981). *Long-Term Measurements of Ground Motions Offshore*, International Conference. On Recent Advances in Geotechnical Earthquake

Engineering and Soil Dynamics, St. Louis, Missouri, April 26-May 3, 1981, Vol I, 377-380.

Steeffe, G. E. (1990). *The long-Term Measurement of Strong-Motion Earthquakes Offshore Southern California*, Proceedings Offshore Technology Conference OTC 6336, 561-568.

Sleefe, G. E. and D. Engi (1987). *Seafloor Response for two Southern California Earthquakes*, Proceedings 1987 Spring Conf. On Exper. Mech., Houston, Texas, June 14-19, 1987, and Sandia report SAND86-2441C.

Smith, C. E. (1990). *Seismic Design Considerations for Offshore Oil and Gas Structures*, Proceedings 21st Joint Meeting of the U.S. - Japan Cooperative Program in Natural Resources: Panel on Wind and Seismic Effects, NIST SP 776.

Smith, C. E. (1991). *Seafloor Seismic Network Offshore Southern California*, Proceedings 23rd Joint Meeting of the U. S. - Japan Cooperative Program in Natural Resources: Panel on Wind and Seismic Effects.

Smith, C. E. (1994). *Dynamic Response of Offshore Steel-Jacket Platforms Subject to Measured Seafloor Seismic Ground Motions*, D. Sc. thesis, Graduate School of Engineering and Applied Science, George Washington University, 323 pp.

Ehasz, J. P., Franco, R. J., and Platzbecker, M. R. (1997). *Seafloor Earthquake Measurement System - SEMS4*, Sandia National Laboratories, SAND97 - 1630, Albuquerque, New Mexico, 70pp.

Table 1. Station Information (see Table 2 in Boore, 1997, for notes)

Code	Lat	Long	WaterDepth(m)	Nearest Platform
-----	-----	-----	-----	-----
S1HW	34.3367	-119.5600	50	Henry
S1VC	34.4033	-119.7150	onshore	located at Vic Trace Reservoir
SC38	33.8233	-118.3567	onshore	
SC51	34.0233	-118.7867	onshore	
S2EE	33.5867	-118.1233	73	Elly/Ellen
S3EE	33.5700	-118.1300	64	Elly/Ellen
S31R	34.6117	-120.7317	76	Irene
S4EU	33.5617	-118.1167	217	Eureka
S4GR	34.1800	-119.4700	99	Grace
S41R	34.6117	-120.7300	76	Irene
CM	33.6400	-117.9300	onshore	located in Costa Mesa
PV	33.8017	-118.3867	onshore	located in Palos Verdes

Table 2. Earthquake information (see Table 4 in Boore, 1997, for notes and references)

EqID	EqName	yy/mm/dd	hh:mm	EpcntrLat	EpcntrLong	M
-----	-----	-----	-----	-----	-----	-----
S881	Santa Barbara Island	81/09/04	15:50	33.66	-119.10	5.95
NP86	North Palm Springs	86/07/08	09:20	34.00	-116.61	6.10
OS86	Oceanside	86/07/13	13:47	32.97	-117.87	5.84
UP90	Upland	90/02/28	23:43	34.14	-117.70	5.63
RC95	Ridgecrest	95/09/20	23:27	35.76	-117.64	5.56
CL97	Calico	97/03/18	15:24	34.97	-116.82	4.85
S97A	Simi Valley	97/04/26	10:37	34.37	-118.67	4.81
S97B	Simi Valley	97/04/27	11:09	34.38	-118.64	4.72
SF71	San Fernando	71/02/09	14:01	34.40	-118.39	6.6

Table 3. Epicentral distances, in km, between earthquakes used in this report and stations recording the earthquakes. SF71 is the San Fernando earthquake; while not recorded on a SEMS unit, the onshore records are used in a comparison with offshore records from other earthquakes.

sta	S881	NP86	OS86	UP90	RC95	CL97	S97A	S97B	SF71
S1HW	86.0								
S1VC	99.9								
SC38	71.1								
SC51	49.4								
S2EE		147.5	72.5						
S3EE				74.4					
S31R									
S4EU									
S4GR						258.1	76.7	79.3	
S41R					309.1		191.2		
CM									94.6
PV									66.4

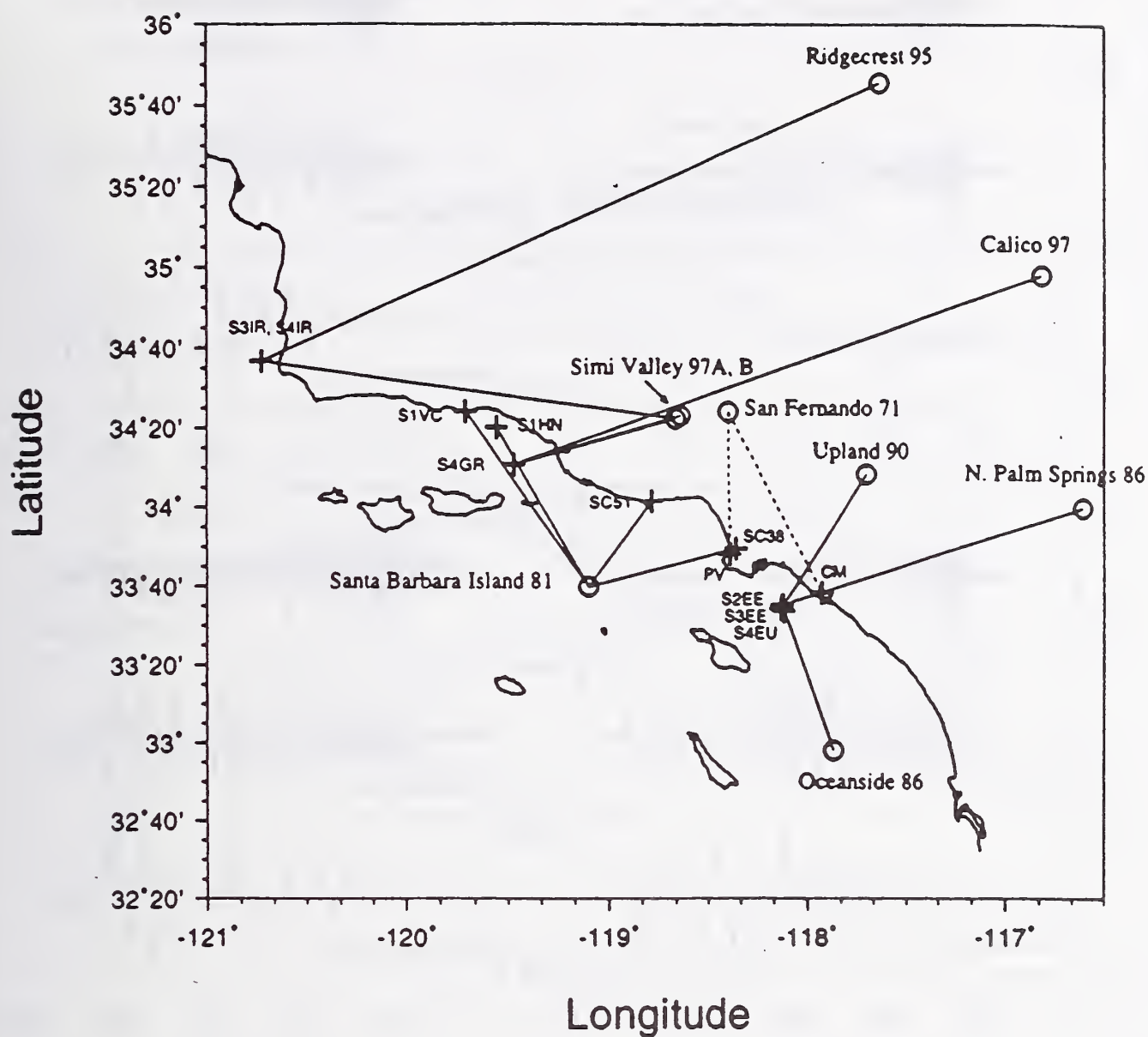


Figure 2. Map of southern California. Lines connect events (open circles) and stations (pluses) providing data for the corresponding event. The dashed lines show paths for two recordings of the 1971 San Fernando earthquake; these paths cross the Los Angeles basin, as does the path from the Upland 1990 earthquake to SEMS site S3EE. Waveforms of these two events are compared in this report. Although providing no data, station S4EU is shown for completeness.

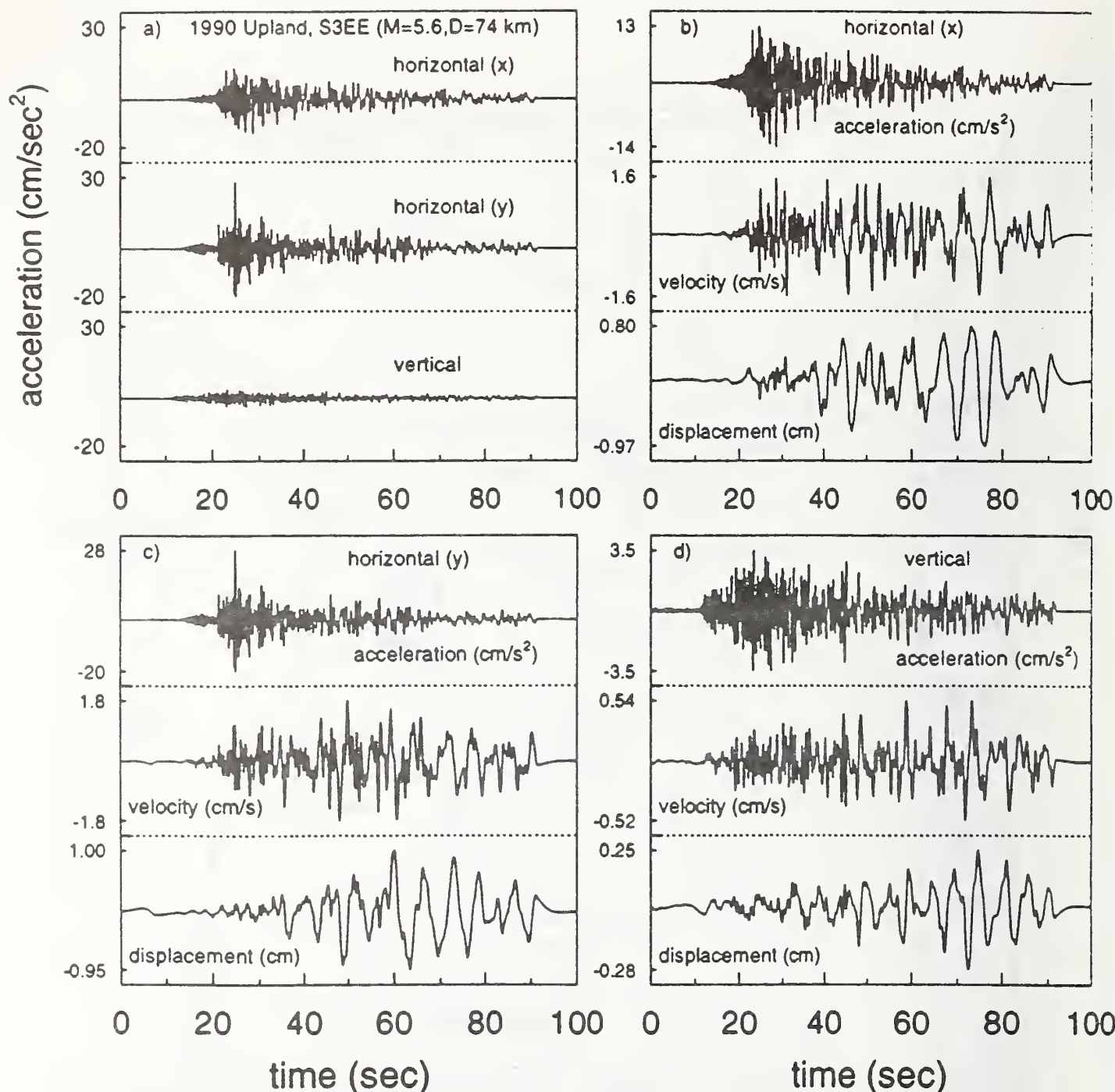


Figure 3. a): Three-component accelerograms, in cm/sec^2 , of the Upland 1990 earthquake recorded at SEMS station S3EE, plotted using the same vertical scale to emphasize the relative amplitude of the components. The time series are similar to those recorded onshore, with a clear portion of strong S-wave arrivals following the initial P-waves. Two interesting characteristics are the small amplitude of the vertical motion relative to the horizontal motions and the long-period energy arriving after the portion of strongest ground acceleration. b), c), and d): acceleration (cm/sec^2), velocity (cm/sec), and displacement (cm) time series for the three components of the S3EE recording of the 1990 Upland earthquake, plotted using different vertical scales, to emphasize the appearance of the waveforms. Note the dominance of late arriving 5 to 6 sec waves on the displacement trace, something not emphasized in the accelerogram.

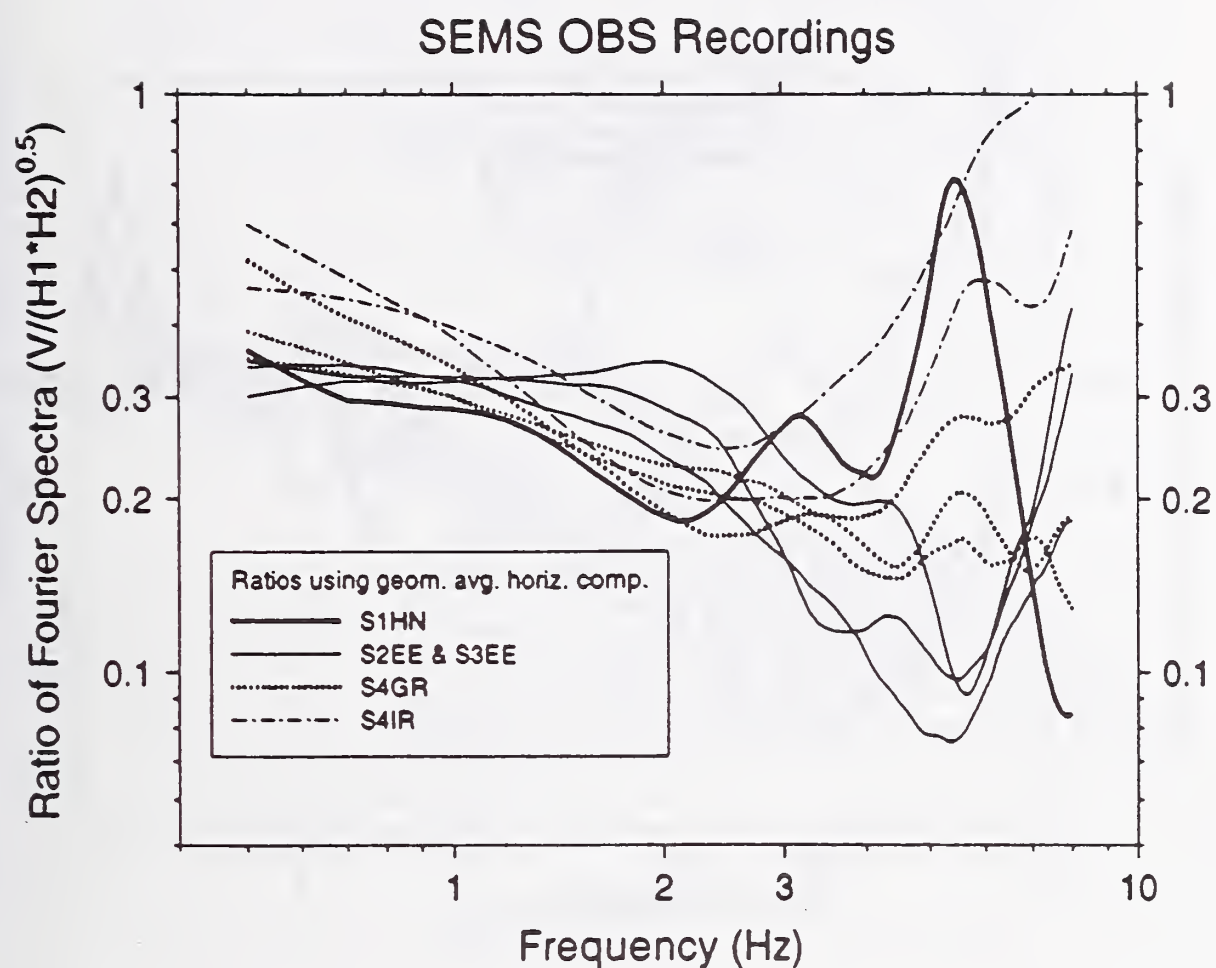


Figure 4. Comparison of V/H ratios of Fourier amplitude spectra for the offshore SEMS recordings through 1990. For clarity, the line type was used for all recordings at a given site, to emphasize the site-to-site variation of the ratios. The ratios for the various recordings at a given site are similar, and all of the ratios are very similar at low frequencies and show considerable divergence at high frequencies. Spectral ratios were computed after smoothing each component with a triangular operator spanning 2 Hz.

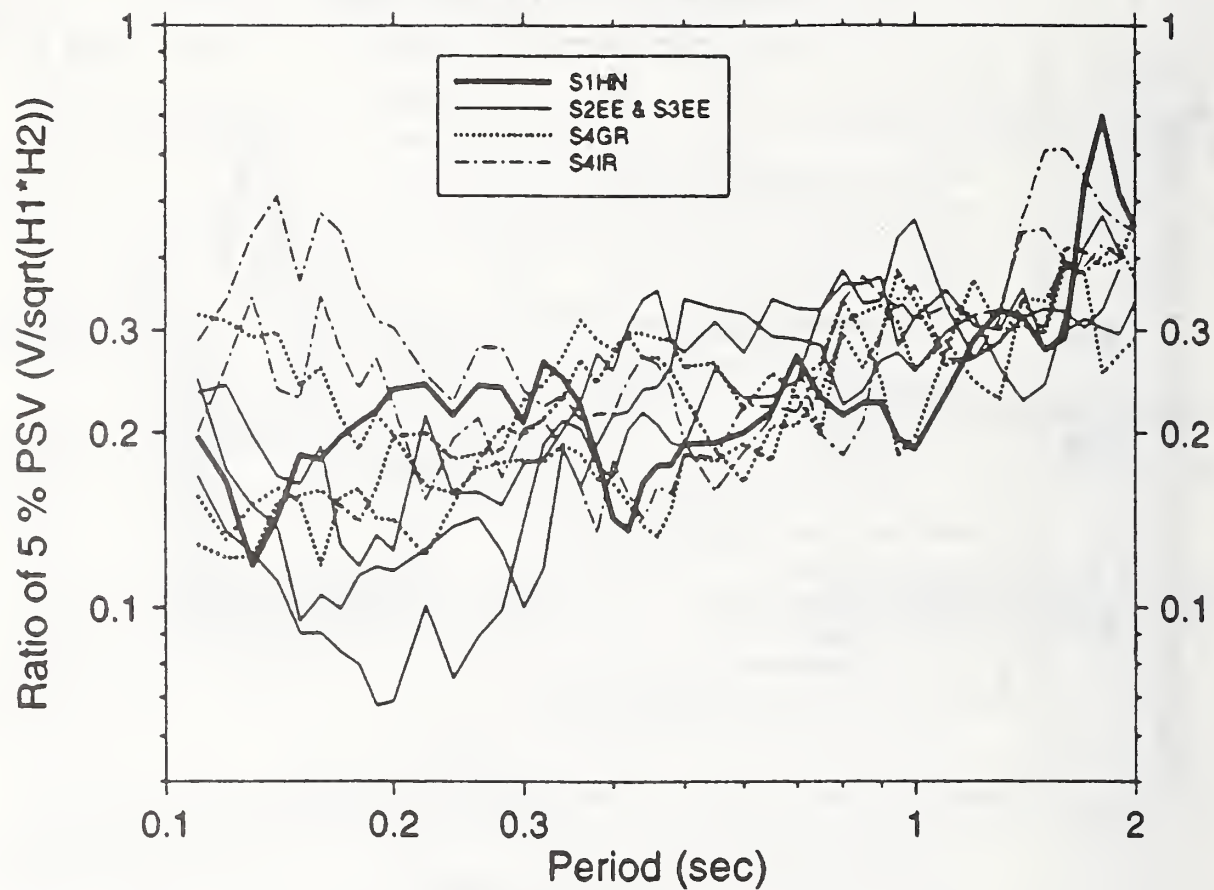


Figure 5. Comparison of V/H ratios of 5%-damped response spectra for recordings at all of the offshore SEMS sites considered in this report. In view of the widespread distribution of the stations, the ratios are remarkably similar, particularly for the longer periods. Theoretical calculations suggest that the spread in the ratios at short periods may be due to site-to-site variations in water depth and near-surface geological properties.

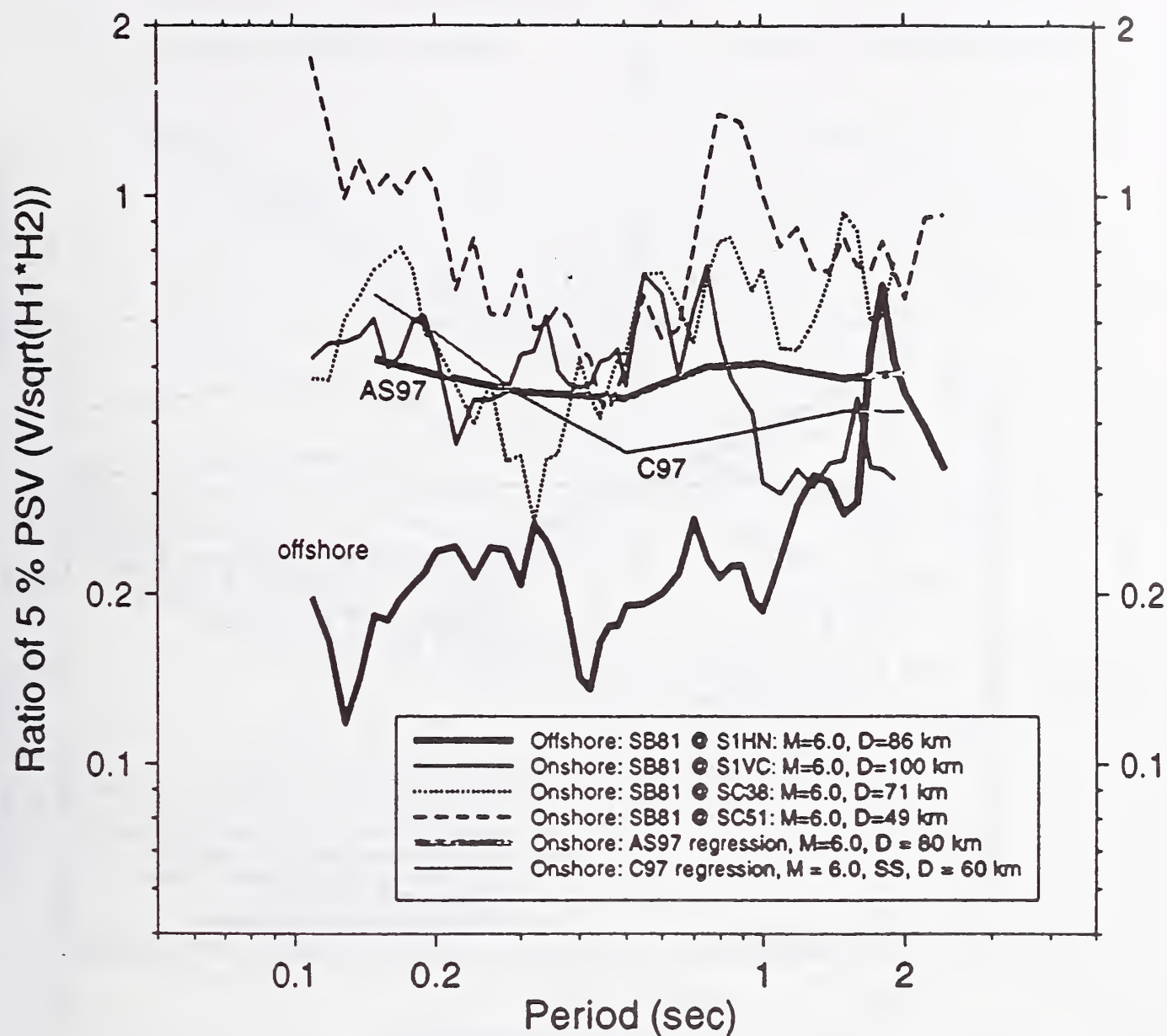


Figure 6. V/H ratios of 5%-damped response spectra for offshore and onshore recordings of the 1981 Santa Barbara Island earthquake, compared with the regression results of Abrahamson and Silva (1997) (AS97) and Campbell (1997) (C97). The ratio for the offshore site (S1HN) is much lower at short periods than are the ratios from the onshore sites.

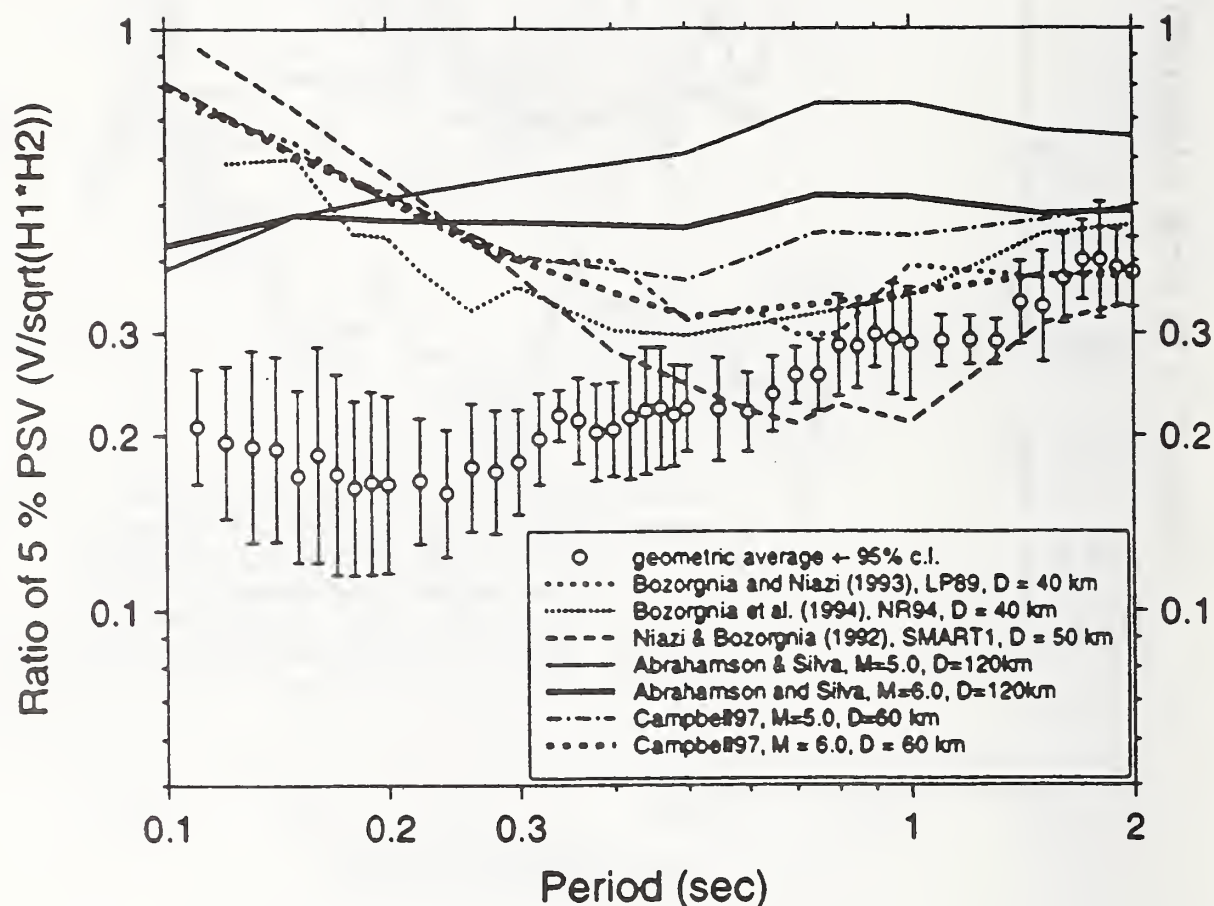


Figure 7. Observed offshore V/H ratios of 5%-damped response spectra (open circles) compared with onshore ratios from regression analyses. The results for the Loma Prieta and Northridge earthquakes are indicated in the legend by "LP89" and "NR94", respectively. The Bozorgnia *et al.* (1994) results for the Northridge earthquake differ slightly from those in the final published study (Bozorgnia *et al.*, 1995).

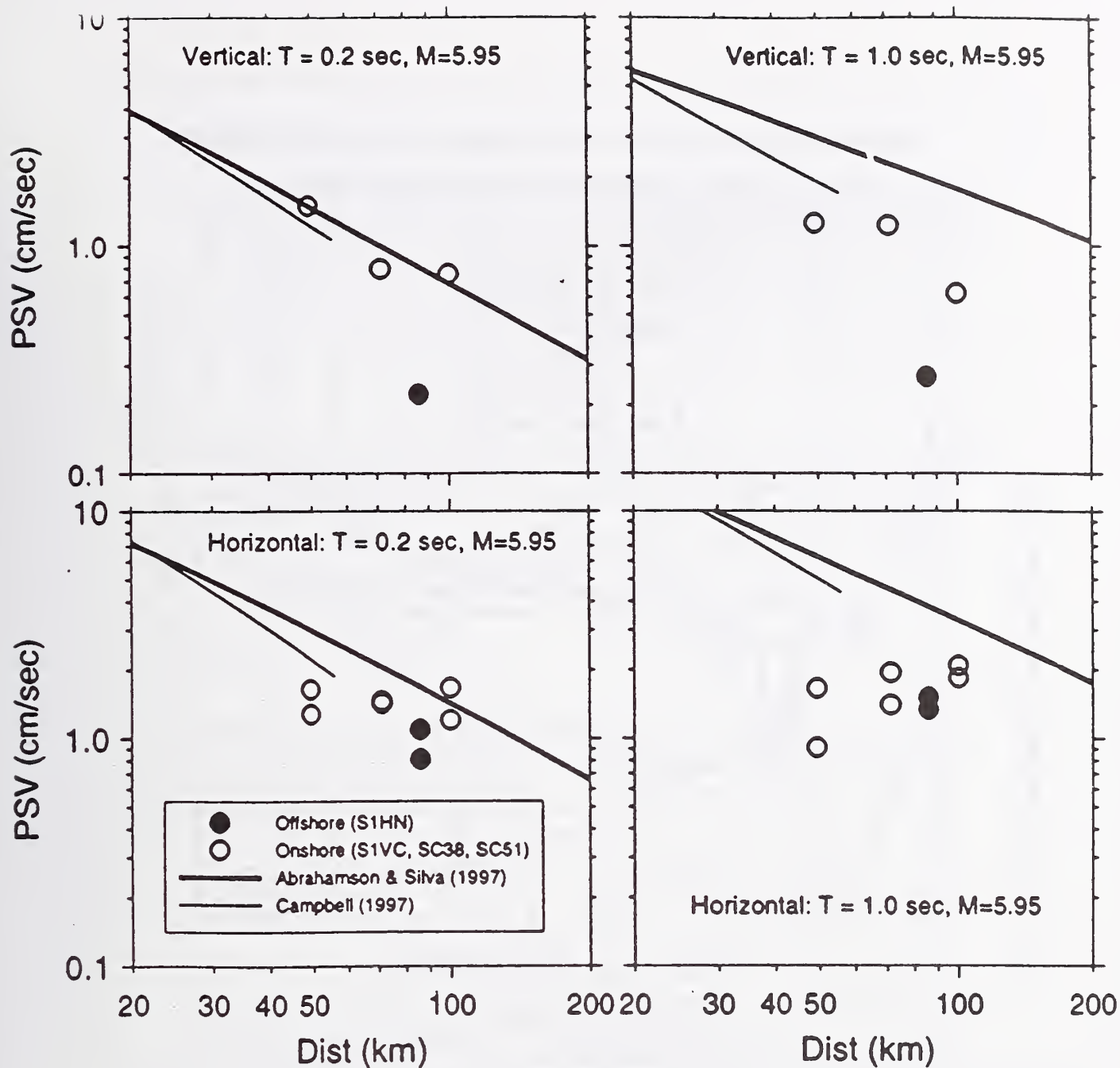


Figure 8. 5%-damped pseudo-velocity response spectra for 0.2 and 1.0 sec oscillator periods as a function of epicentral distance for the 1981 Santa Barbara Island earthquake, compared with predictions from regression analyses. The different symbols differentiate between the offshore and onshore recordings of the earthquake. Note that for the vertical component (top two panels), the spectra from the offshore recording is much lower than the onshore spectra, whereas for the horizontal components (bottom panels), the onshore and offshore spectra are comparable.

Epicentral Distance Versus Peak Vertical Ground Accelerations

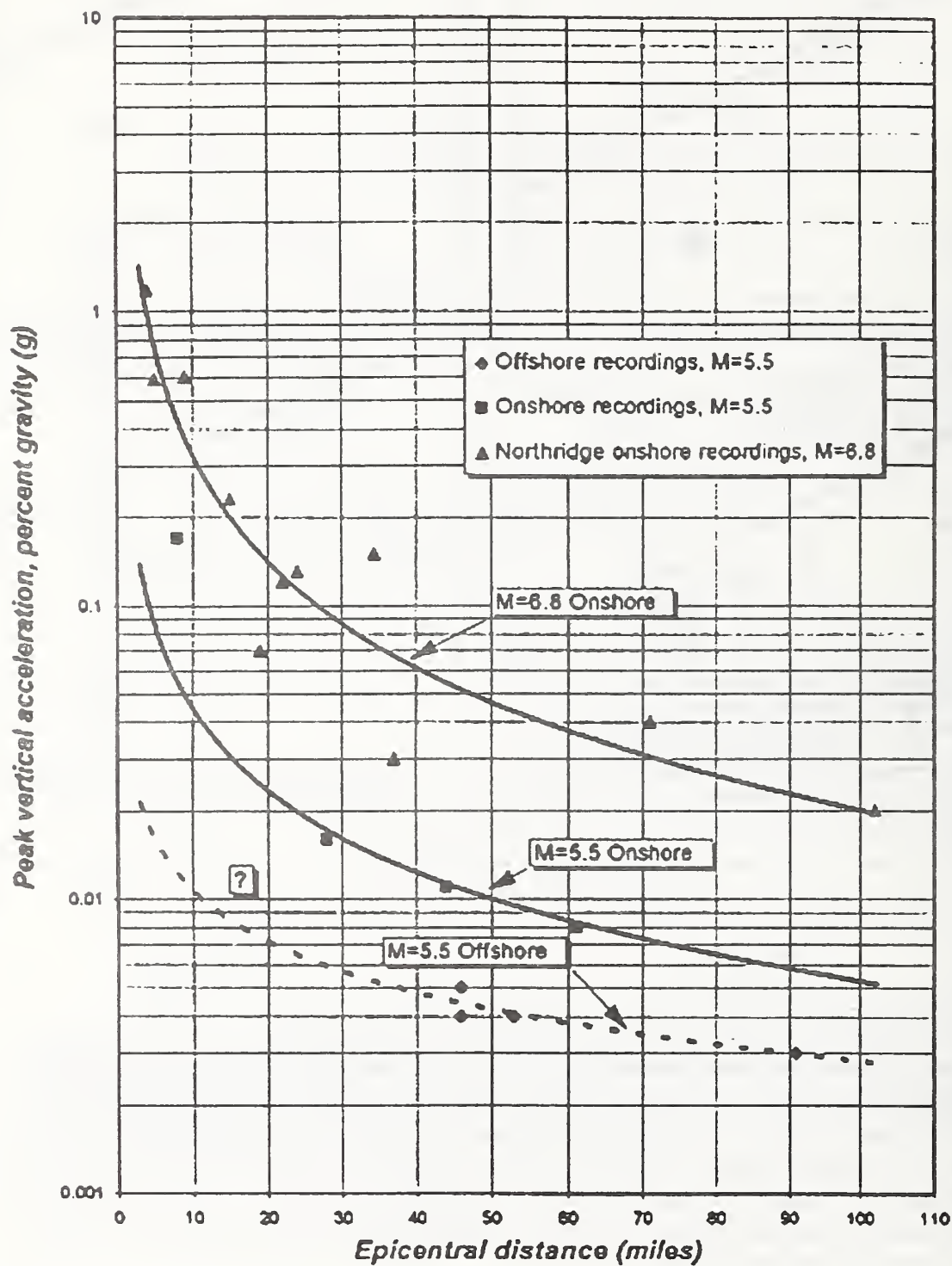


Figure 9. Epicentral distance versus peak ground accelerations

SEMS OBS Recordings and Theory

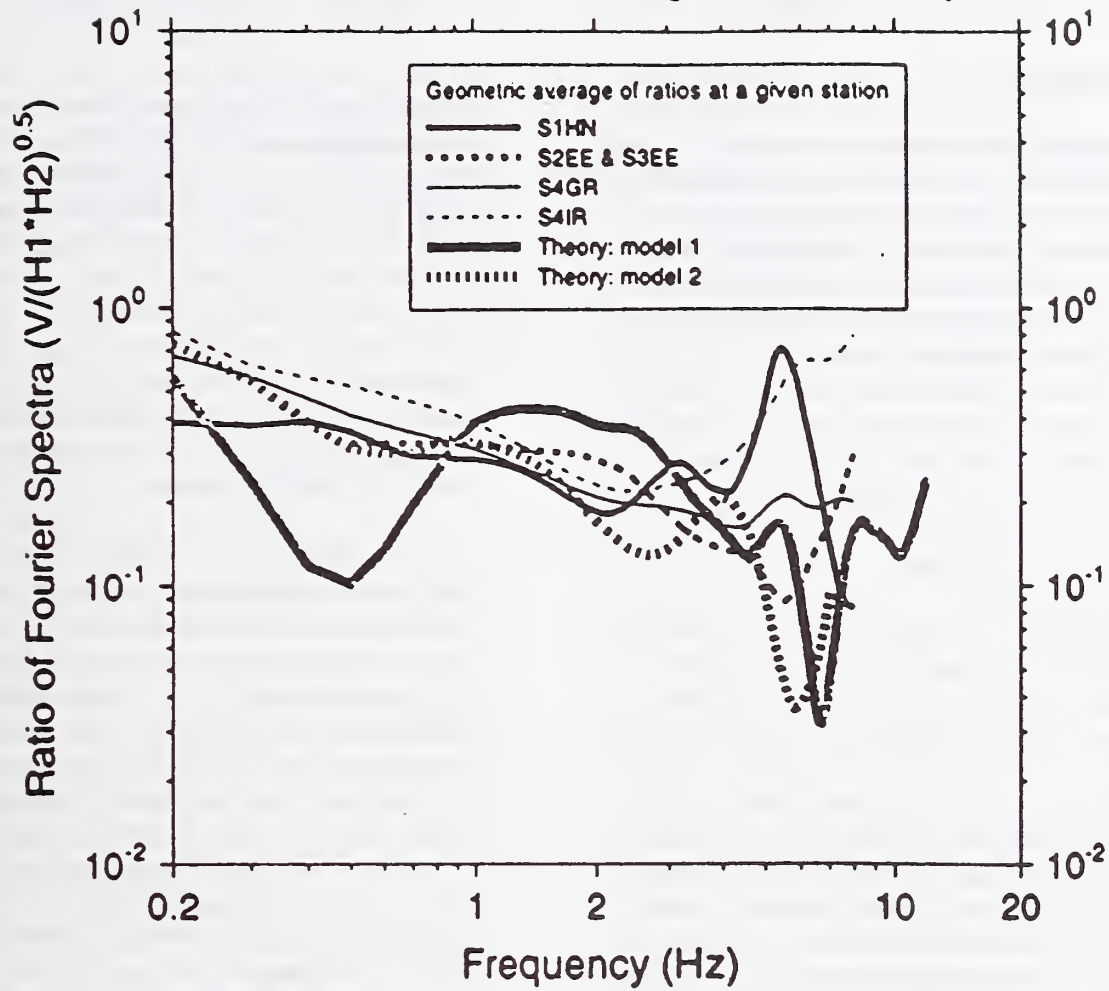


Figure 10. V/H ratios of Fourier amplitude spectra of the S-wave portion of offshore recordings, compared to theoretical predictions.

Effect of Reservoir-Subbottom Energy Absorption on Hydrodynamic Forces on Dams by

Robert L. Hall*, Luis de Béjar*, Keith J. Sjostrom* and Enrique E. Matheu*

ABSTRACT

This paper will summarize the recent experimental programs conducted in the U.S. and China to measure the reservoir-bottom reflection coefficient, α . Theoretical studies will also be presented demonstrating the impacts of the subbottom absorption on the hydrodynamic loads on the upstream face of a concrete dam. The seismic evaluation of the Folsom Dam will be used to demonstrate the impact of including the effect of reservoir bottom absorption on the stresses of a concrete gravity dam.

1. BACKGROUND

The interaction between the dam, the reservoir subbottom, and the reservoir significantly affects the structural stresses in concrete dams when subjected to strong earthquake ground motions. (Hall and Chopra 1980; Fenves and Chopra 1984; Lofti, Roesset, and Tassoulas 1987). The hydrodynamic pressure waves impinging on the reservoir subbottom are partially reflected back into the reservoir and partially absorbed by the reservoir-bottom materials. The absorption of the pressure wave reduces the hydrodynamic pressures on the upstream face of the dam. The absorption of the pressure wave into the materials on the bottom of the reservoir is modeled by a reflection coefficient known as " α ." Approximate analytical studies including the effects of this complex interaction demonstrate that the structural responses of concrete dams are strongly sensitive to the amount of energy absorbed by the reservoir bottom materials (Fenves and Chopra 1984; Fok, Hall, and Chopra 1986; Hall, Woodson and Nau 1987; Duron and Hall 1988).

Refraction and reflection procedures have been used to characterize material on the reservoir bottom (Ghanaat, et al. 1993; Ghanaat and Redpath 1995). These procedures were used at seven concrete dam sites in the United States and at the Dongjiang Dam, China. A seismic blasting cap was used to generate a hydrodynamic pressure wave for these experiments, and provided the first step toward determining average values to be used for current numerical procedures for modeling the reservoir-bottom absorption.

A more comprehensive waterborne seismic reflection investigation was performed at Pine Flat Lake, California. The objective of the geophysical investigation was to delineate the geologic stratigraphy and provide acoustic impedance versus depth plots to depths of 30 to 60 meters below the bottom surface upstream of the Pine Flat Dam. The results are intended to be used as input toward the development of seismic modeling algorithms of the Pine Flat Dam and reservoir. The study is also conducted, in part, to compare with the reflection coefficient value computed for the bottom sediments determined from a previous investigation (see Ghanaat and Redpath 1995) using a blasting cap for the generation of a pressure wave.

The current numerical procedures model the reservoir-bottom absorption as a boundary condition, approximating the reservoir-subbottom interaction by a one-dimensional (1-D) wave propagation model with a single parameter, the reflection coefficient, α (Hall and Fenves 1980). This procedure has been implemented into the two-dimensional (2-D)

* U.S. Army Engineer Waterways Experiment Station, Vicksburg, MS

code, EAGD (Fenves and Chopra 1984), for concrete gravity dams and into a three-dimensional (3-D) code, EACD, for arch dams (Fok, Hall, and Chopra 1986). Numerical procedures such as the Boundary Element Method (de Béjar 1996) can be used to model the reservoir-subbottom interaction, accounting for the spatial variation of material properties. Further, models will need to be developed to accurately reproduce the measured response of an actual concrete dam-reservoir-foundation system.

2. MEASUREMENTS

Acoustic subbottom reflections are produced when a source of acoustic energy is deployed just below the water surface and fired. In a homogeneous medium, the acoustic waves extend uniformly in all directions from the source in which the advancing wavefronts are spherical surfaces centered at the source and normal to the direction of propagation. When the acoustic energy arrives at a boundary between two materials of differing density and elastic velocity, part of the energy will be reflected back towards the surface and part transmitted downward into the medium below. Portions of the transmitted energy will also undergo absorption or attenuation in the material while the wavefront propagates through to the next stratigraphic boundary.

The amplitudes of the incident, reflected, and transmitted wave energies vary with respect to the density and velocity of the materials through which the wave energy is propagating. The ratio between the amplitudes of incident and reflected wave energy is called the reflection coefficient (α) and is defined as:

$$\alpha = \frac{A_R}{A_I}$$

where A_R and A_I are the amplitudes of the reflected and incident wave energy, respectively (Telford, et al. 1976). Reflected wave energies are detected using hydrophones or piezoelectric transducers which convert changes in water

pressure caused by the acoustic wavefronts into electrical impulses. The electrical signals are amplified, filtered, and recorded using a shallow seismic, digital data acquisition system.

Two independent geophysical techniques for determining α in-situ were used at seven concrete dam sites in the United States and at the Dongjiang Dam, China (Fig 1). The seismic reflection technique measures the incident and reflected shock waves generated by a blasting cap on the reservoir bottom. The seismic refraction technique measures the propagation velocity of the pressure wave in the subbottom materials by measuring the refracted waves and then computing the ratio of the acoustic impedances of the material. The refraction experiments were based on a technique developed by Hunter and Pullan (1990). Blasting caps serve as the source for the generation of a pressure wave for both types of experiments. The α value is computed from the ratio of the acoustic impedances of the reservoir-bottom material and the water in the reservoir (Ghanaat and Redpath 1995).

At the Dongjiang Dam, the reflection experiments were conducted above a submerged concrete cofferdam. The location of the cofferdam was determined during the processing of the experimental data when construction drawing became available. Analyses of the reflection experiments resulted in a completed α value of 0.63 for the reservoir-bottom sediments. This value was affected by the cofferdam. The results from the seismic refraction testing determined α to be 0.40 for the reservoir-bottom sediments and 0.80 for the granite rock (Ghanaat et al. 1993).

At the seven U.S. dam sites, the values of α for the reservoir-subbottom material varied over a range from -0.55 to 0.66. Pine Flat, Hoover, and Folsom had negative α values. The negative values are the result of the wave propagation velocity through the reservoir-bottom material being less than the propagation velocity through water. This can occur when the density of the material is less than that of water. This leads to

the conclusion that the reservoir-bottom material may contain decaying organic material which is producing gases in the material. Glen Canyon had a low α values of 0.15. Monticello, Morrow Point, and Crystal had α values greater than 0.66. This study concluded that conducting both refraction and reflection experiments is essential for determining α (Ghanaat and Redpath 1995).

A waterborne seismic reflection investigation was also performed in Pine Flat Lake. This study concentrated in the narrow neck of the reservoir upstream of the dam structure. The survey was conducted aboard the WES Research Vessel (R/V) *Waterways Explorer* with acoustic energy generated by two high-resolution subbottom profiling systems. The first system was operated at a frequency of 3.5 and 7.0 kHz and is typically called a 'pinger' because of the audible noise it makes during operation. The second system is a lower frequency 'boomer' system and hydrophone which has an output frequency range of 0.5 to 2.0 kHz to interrogate the subbottom sediment structure. The higher operating frequency of the 'pinger' system allows greater resolution of the bottom and subbottom stratigraphy than the 'boomer' or air gun systems but shallower depths of energy penetration depending on the characteristics of the subbottom material.

The pinger system consisted of a Datasonics SBP-5000 subbottom profiling system. The SBP-5000 transmitters were mounted within a towfish rigidly attached to a telescoping arm and deployed through the front deck of the *Waterways Explorer*. The system allows the transmission of variable-length acoustic pulses (0.2 - 3 msec) over frequency ranges of 3.5, 7.0, 10.0 kHz. The transducers of both the source and receiver were positioned 3 feet below the water surface during data collection. For the Pine Flat Lake study, the length of the pinger pulse width at frequencies of 3.5 and 7.0 kHz was set at 0.2 msec and is typically able to resolve stratigraphic layers having thicknesses greater than or equal to 0.6 meters. A total trace length of 700 samples were digitally acquired

every 42 μ sec which corresponds to a sampling rate of 16 samples/ μ sec. This sampling rate provides an effective depth of subsurface exploration of approximately 4.5 to 12.4 meters below the bottom surface, depending on the bottom and subbottom sediment characteristics.

The electro-mechanical source of the boomer system is mounted on a sled and, along with the hydrophone array, towed approximately 21.3 meters behind the R/V during the investigation. The EG&G Models 231 and 232 sources were operated in the frequency range of 0.5 to 2.0 kHz at an energy level of 300 joules. The length of the boomer pulse width at the central frequency of 1.2 kHz is typically able to resolve lithologic layers having thicknesses greater than 1.5 meters. Under typical surveying conditions, a total seismic trace length of 700 samples were collected every 88 μ sec (sampling rate = 8 samples/ μ sec), resulting in exploration depths in excess of 30 meters below the bottom surface.

These detailed studies confirmed the existence of negative values of α as reported by Ghanaat and Redpath in their studies. This study also provided the spacial variation of the reservoir-bottom materials, as well as the depth, of different subbottom material layers. As detailed numerical procedures are developed, this detailed description of the reservoir subbottom may be needed.

3. THEORETICAL SUBBOTTOM-RESERVOIR-DAM INTERACTION EFFECT

The effect of the interaction between the absorptive boundary and the dam via the pressure field transmitted by the fluid medium becomes apparent by considering the simple example in Figure 2. This 2-D model represents the longitudinal section of a reservoir with aspect ratio 3 (the ratio of the reservoir length to the dam height, at full capacity). The water is assumed impounded by a rigid boundary at the far end of the reservoir, and the bottom is characterized by a reflection coefficient typical of a solid continuum [$\alpha \in (0,1)$].

The system is subjected to a steady-state harmonic acceleration applied uniformly at the rock base, with amplitude 0.30g (where g is the acceleration of gravity), and frequency of 1.0 Hz. Figure 3 indicates the linear distribution of the hydrostatic pressure on the upstream face of the dam, normalized with respect to its value at the bottom. By comparison, the corresponding amplitude of the hydrodynamic pressure field on this front wall is computed at six nodes uniformly spaced along the wall height. These hydrodynamic pressures were estimated using Westergaard's approximation (Westergaard 1933) and appear in Figure 3 normalized with respect to the corresponding hydrostatic pressure at the point under consideration. Notice that the maximum value of the hydrostatic pressure on the wall takes place at node 13, located at a distance of 0.40 H from the bottom, where H is the dam height. At node 13, the hydrostatic pressure is increased by a hydrodynamic pressure with amplitude 33% of the hydrostatic pressure at this node.

The effect of the dynamic interaction between the flexible subbottom and the dam (H = 91.4 meters) is considered at nodes 13, 17, and 21, within the lower 40% of the wall height, where the hydrodynamic contribution to the total pressure field is significant. Figures 4, 5, and 6 show the normalized amplitudes of the hydrodynamic pressure at the nodes in question.

The corresponding abscissas in these figures are normalized with respect to the fundamental natural frequency of the impounded water, given by

$$\omega_1 = \frac{C}{4H} \text{ [Hz]}$$

where C is the velocity of propagation of the pressure waves in water. Multiple spectra appear in each figure according to the value of the parameter α . Physically, the two extremes of the domain of α mean as follows: (a) $\alpha = 0$ corresponds to an infinite water depth of the reservoir, and (b) $\alpha = 1.00$ corresponds to a rigid reservoir bottom. Intermediate values correspond to different degrees of foundation

rock acoustic impedance. Notice the resonant peaks at the natural frequencies of the impounded water, which grow without bound for $\alpha = 1.00$ (as in the case of a resonant elastic system without damping). The elasticity of the rock subbottom (assumed to extend to infinity) effectively acts within the dam-reservoir-subbottom system as an energy-dissipating mechanism.

Even a small amount of α -decrease from the vicinity of $\alpha \approx (0.95, 1.00)$ serves as a powerful moderator of maximum hydrodynamic responses. For frequency components of the excitation such that the ratio (ω/ω_1) smaller than about 0.50, the effect of α is negligible, and the system response remains relatively unaffected with respect to that for a rigid bottom. For frequency components of the excitation such that the ratio (ω/ω_1) lies between 0.50 and 0.80, the reduction in the system response is of intermediate magnitude, reaching up to 30% reduction at $(\omega/\omega_1) = 0.80$, for $\alpha = 0.20$, as compared to the corresponding dynamic magnification for $\alpha = 1.00$. The most dramatic attenuation of the system response occurs for frequency contents in the range for the ratio (ω/ω_1) from 0.80 to about 1.00, where the reduction reaches about 75% for $\alpha = 0.35$, for example, as compared to the dynamic magnification corresponding to α in the vicinity of 0.95. For $(\omega/\omega_1) > 1.00$, the effect of α on the system response is inconclusive due to oscillation according to the specific frequency content of the excitation.

4. EVALUATION

A seismic evaluation of the Folsom Dam and reservoir project has been performed (Hall, Woodson, and Nau 1989). The structure is located on the American River, 32 airline kilometers northeast of the city of Sacramento. The Folsom Project was designed and built by the Corps of Engineers during the period from 1948 to 1956 under the authority of the Flood Control Act of 1944 and the American River Basin Development Act of 1949. In May 1956, ownership was transferred to the U.S. Bureau of

Reclamation for operation and maintenance. The concrete gravity section (Fig 7) of the dam was designed with pseudo-static acceleration of 0.05 g acting upstream. Based on their studies of the horizontal ground acceleration recorded on an array of accelerometers normal to the Imperial Valley fault during the Imperial Valley earthquake of 1979, Bolt and Seed (1983) recommend the following ground motions:

Peak horizontal ground acceleration = 0.35 g

Peak horizontal ground velocity = 0.20 m/sec

Bracketed duration (0.05 g) = 16 sec

The seismic analyses of the critical nonoverflow monolith of the dam were conducted using the 2-D program, EACD-84 (Fenves and Chopra 1984). In this approach, the time history response of the dam subjected to the specified earthquake motions is determined with the simultaneous effects of dam-water interaction, dam-foundation rock interaction, and reservoir-bottom absorption included. Water compressibility is included in the analysis since the earthquake response of the concrete dam can be significantly affected by this factor. The foundation rock supporting the dam is idealized as a homogenous, isotropic, visco-elastic half plane. The dam monolith is idealized with an assemblage of four-node nonconforming planar finite elements. Dissipation of strain energy in the concrete is modeled with a constant hysteretic damping factor. A viscous damping ratio for all the natural vibration modes of the concrete dam on a rigid foundation with no reservoir corresponds to a constant hysteretic damping factor of twice the viscous damping ratio (Fenves and Chopra 1984).

The absorption nature of the reservoir subbottom is characterized by the wave reflection coefficient, α . The coefficient represents the dissipation of hydrodynamic pressure waves in the reservoir bottom and is modeled approximately by a boundary condition of the reservoir bottom which partially absorbs incident hydrodynamic pressure waves (Fenves

and Chopra 1984). The wave reflection coefficient is defined as the ratio of the amplitude of the reflected hydrodynamic pressure wave to the amplitude of the vertically propagating pressure wave incident on the reservoir bottom. The material at the bottom of the reservoir determines the wave coefficient α , in the following equation:

$$\alpha = \frac{1 - K}{1 + K}$$

where

$$K = \rho c / \rho_r c_r$$

c = Velocity of pressure waves in water

ρ = Density of water

$$c_r = \sqrt{E_r / \rho_r}$$

E_r = Young's modulus of reservoir bottom material

ρ_r = Density of reservoir bottom material

For foundation rock module values of 40, 54.5, and $76 \times 10^9 \text{ N/m}^2$, the above equation leads to α values of 0.75, 0.79, and 0.82, respectively.

The pertinent stress analysis results are shown in Table 1. The greatest principal stresses occur for the case in which the foundation modulus and the reservoir-bottom coefficient are the largest. For this set of parameters, a maximum principal stress of $6 \times 10^3 \text{ N/m}^2$ occurs on the downstream face at an allocation of 22.5 meters from the crest. This region corresponds to that at which the vertical downstream face begins its transition to an inclined surface. The stress of $6 \times 10^3 \text{ N/m}^2$ is greater than the recommended tensile strength of $5.8 \times 10^3 \text{ N/m}^2$ for rich concrete. To investigate the depth to which possible cracking might penetrate, contours of envelope values of maximum principal stresses are shown in Fig 8. For the worse case, an area approximately 0.6 meters in depth on the downstream face is subjected to tensile stresses exceeding $4.8 \times 10^3 \text{ N/m}^2$, the least tensile strength of the dam concrete. By including the effects of the reservoir-bottom absorption, it is reasonable to conclude that cracking will be quite limited in extent and depth of penetration into the monolith.

5. CONCLUSIONS

The effect of reservoir-subbottom energy absorption of the hydrodynamic loads on concrete dams subjected to large seismic ground motions may be substantial, particularly for excitation frequency contents in the range of $0.50 < (\omega/\omega_1) < 1.00$, where ω_1 is the fundamental frequency of the impounded reservoir. The measurement of the absorptive nature of the reservoir subbottom can be measured with different geophysical techniques. These techniques range from simple blasting cap techniques to very sophisticated waterborne measuring equipment. Analytical procedures are available from the simple 1-D wave propagation models to nonlinear constitutive models of partially saturated materials. What has not been determined is the needed degree of sophistication of the measurements or the analytical models. Further research needs to be performed to quantify the effect the spatial variation of the subbottom materials, as well as the geometry of the reservoir bottom, has on the hydrodynamic loads. These results will determine the needed parameters of an engineering model for the reservoir subbottom and the corresponding geophysical techniques.

6. ACKNOWLEDGEMENTS

The research presented in this paper was sponsored by the Civil Works Direct-Allotted EQEN Program. We appreciate the cooperation of the authorities at the U. S. Army Engineer Waterways Experiment Station and the Office, Chief of Engineers, U. S. Army Corps of Engineers, that permitted us to prepare and present this paper for publication. Permission to publish this paper was granted by the Chief of Engineers.

7. REFERENCES

- Hall, J. F., and Chopra, A. K. (1980). "Dynamic response of embankment, concrete-gravity, and arch dams including hydrodynamic interaction," Report No. UCB/EERC-80/39, Earthquake Engineering Research Center, University of California, Berkeley, CA.
- Fenves, G., and Chopra, A. K. (1984). "EAGD-84: A computer program for earthquake analysis of concrete gravity dams," Report No. UCB/EERC-84-11, Earthquake Engineering Research Center, University of California, Berkeley, CA.
- Fok, K. L., Hall, J. F., and Chopra, A. K. (1986). "EACD-3D: A computer program for three-dimensional earthquake analysis of concrete dams," Report No. UCB/EERC-86/09, Earthquake Engineering Research Center, University of California, Berkeley, CA.
- Lotfi, V., Roesset, J. M., and Tassoulas, J. L. (1986). "A technique for the analysis of the response of dams to earthquakes," *Earthquake Engineering and Structural Dynamics*, Vol 15, pp 463-490.
- Hall, R. L., Woodson, S. C., and Nau, J. M., (1987). "Seismic stability evaluation of Folsom Dam and reservoir project," Technical Report GL-87-14. U.S. Army Engineer Waterways Experiment Station, Vicksburg, MS.
- Duron, Z. H., and Hall, J. F. (1988). "Experimental and finite element studies of the forced vibration response of the Morrow Point Dam," *Journal of Earthquake Engineering and Structural Dynamics*, Vol 16, pp1021-1039
- Ghanatt, Y., Chen, H., Redpath, B. B., and Clough, R. W. (1993). "Experimental study of the Dongjiang Dam dam-water-foundation interaction," Technical Report QS93-03. Report to the National Science Foundation on Research conducted under the U. S. - China Protocol for Scientific and Technical Cooperation in Earthquake Studies, Quest Structures, Emeryville, CA.
- Ghanaat, Y., and Redpath, B. B. (1995). "Measurements of reservoir-bottom reflection coefficient at seven concrete dam sites," Technical Report QS95-01, Report to the U.S.

Army Engineer Waterways Experiment Station
and the Bureau of Reclamation, Quest
Structures, Emeryville, CA.

Hunter, J.A., and Pullan, S.E. (1990). "A
vertical array method for shallow seismic
refraction survey of the Sea Floor," *Geophysics*,
Vol 55, No 1, pp 92-96.

de Béjar, L. A. (1996). "Subbottom absorption
coefficients for seismic analysis of concrete
dams," *Proceedings from the First U.S. - Japan
Workshop on Earthquake Engineering for
Dams*, Vicksburg, MS.

Caulfield, D. C., Caulfield, D. D., and Yim, Y.
(1985). "Shallow subbottom impedance
structures using an iterative algorithm and
empirical constraints," *Journal of the Canadian
Society of Exploration Geophysicists*, 21(1),
pp7-14.

Caulfield, D. D., and Yim, Y. (1983).
"Prediction of shallow subbottom sediment
acoustic impedance while estimating absorption
and other losses," *Journal of the Canadian
Society of Exploration Geophysicists*, 19(1),
pp44-50.

Hamilton, E. L. (1980). "Geoacoustic modeling
of the Sea Floor," *Journal of the Acoustical
Society of America*, 68(5), pp1313-1340.

McGee, R.G., Ballard, R.F. Jr., and Caulfield,
D.D. (1995). "A technique to assess the
characteristics of bottom and subbottom marine
sediments," Technical Report DRP-95-3, U.S.
Army Engineer Waterways Experiment Station,
Vicksburg, MS.

Telford, W.M., Geldart, L.P., Sheriff, R.E., and
Keys, D.A. (1976). *Applied Geophysics*.
Cambridge University Press, New York.

Westergaard, H.M. (1933). "Water pressures on
dams during earthquakes," *Trans. ASCE* (98),
pp 418-433.

Table 1. Effect of Reservoir Bottom Absorption

CASE	FOUND, MODULUS (10^9 N/m ²)	RESERVOIR BOTTOM REFLECTIVITY	MAXIMUM PRINCIPAL TENSILE STRESS (10^3 N/m ²)	
			UPSTREAM FACE	DOWNSTREAM FACE
18	40.0	0.99	3433.71	3164.81
19		0.90	3013.12	2633.89
20		0.75	2585.63	2420.15
21	54.5	0.99	3833.62	4081.84
22		0.90	3213.07	3433.71
23		0.75	2744.21	3171.70
25	76.0	0.99	5619.43	6426.14
26		0.90	4716.18	5260.89
27		0.75	3819.83	4336.96

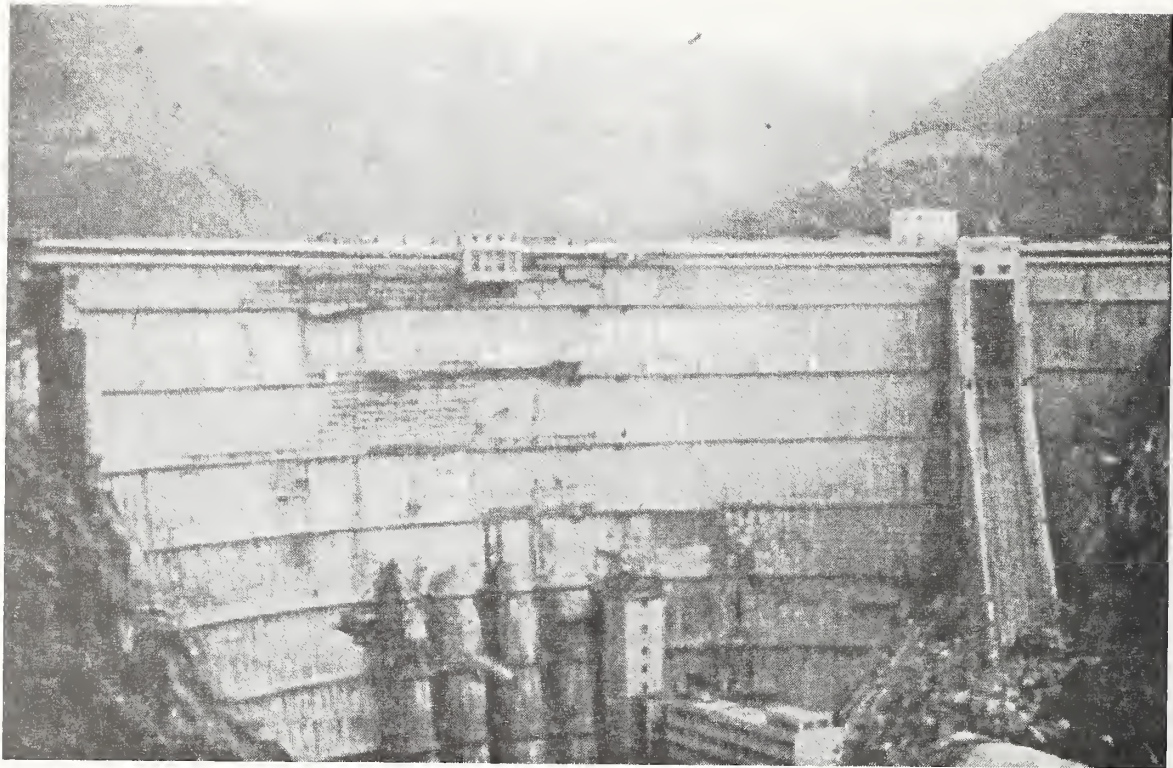
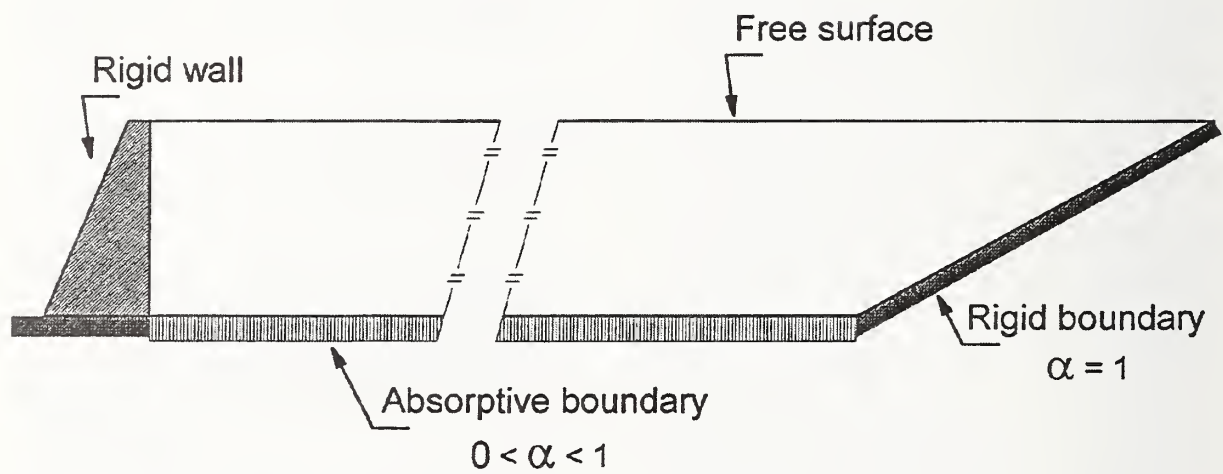


Figure 1. Dongjiang Dam



α : Wave reflection coefficient

Figure 2. Trapezoidal Reservoir Incorporation of Bottom Absorption Characteristics

Maximum Ground Acceleration = 0.30g
Excitation Frequency = 1 Hz

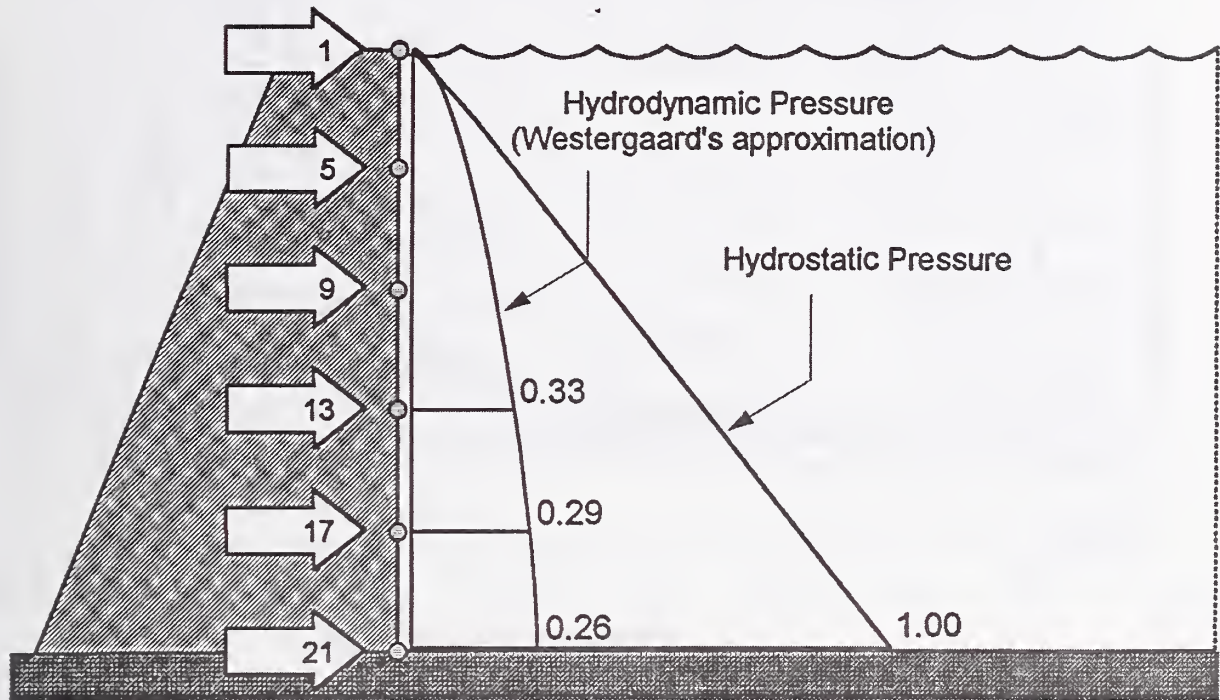


Figure 3. Trapezoidal Reservoir – Front Wall

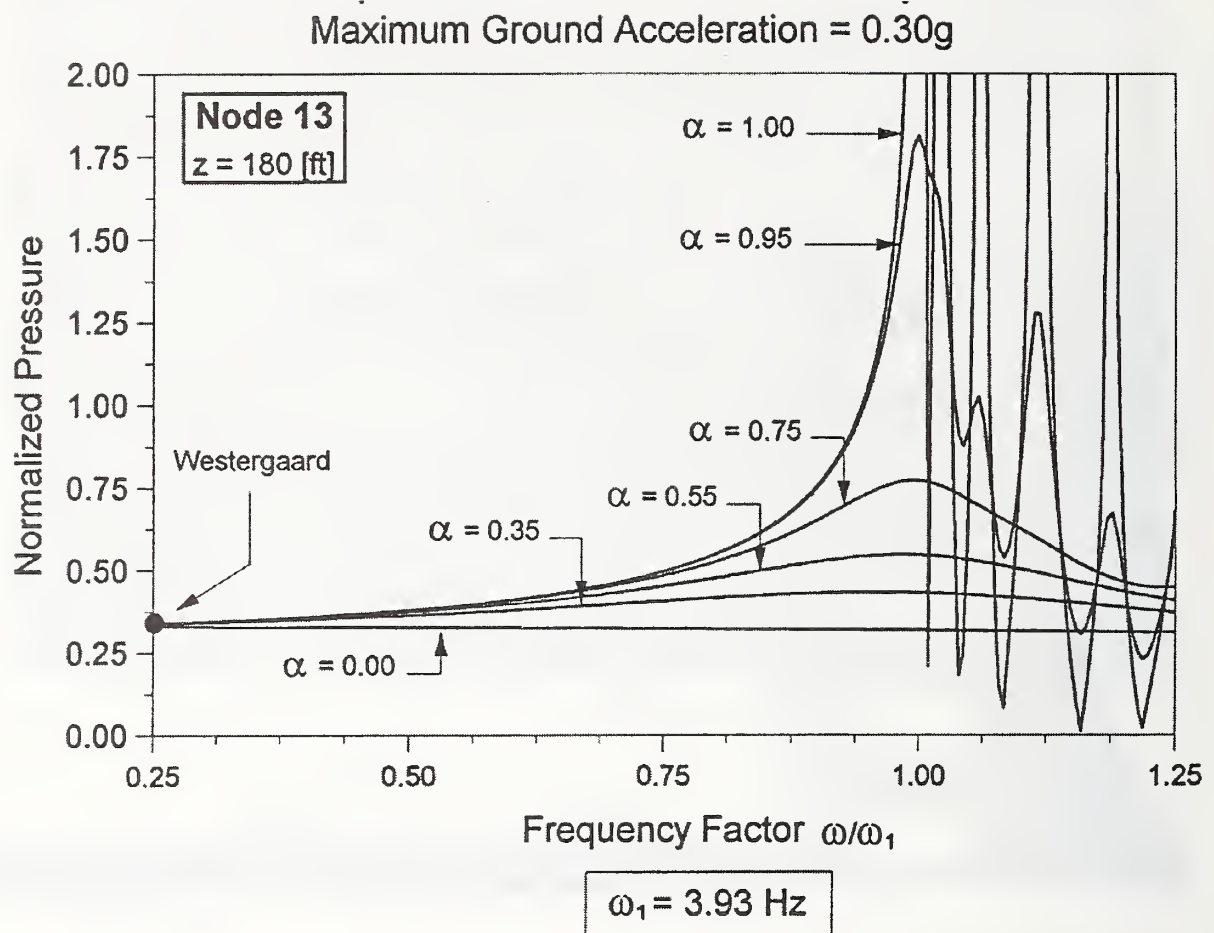


Figure 4. Trapezoidal Reservoir – 2D Analysis

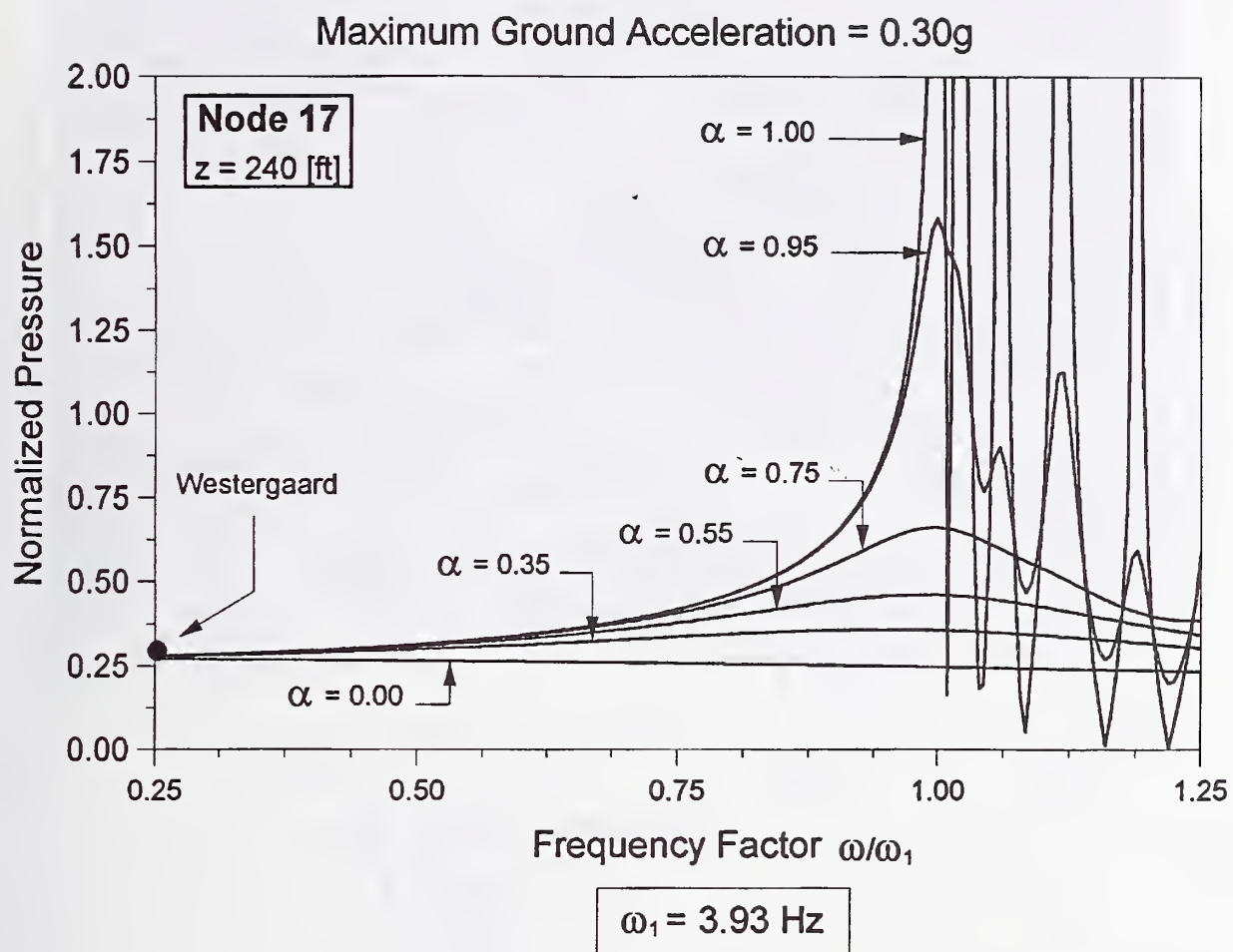


Figure 5. Trapezoidal Reservoir – 2D Analysis

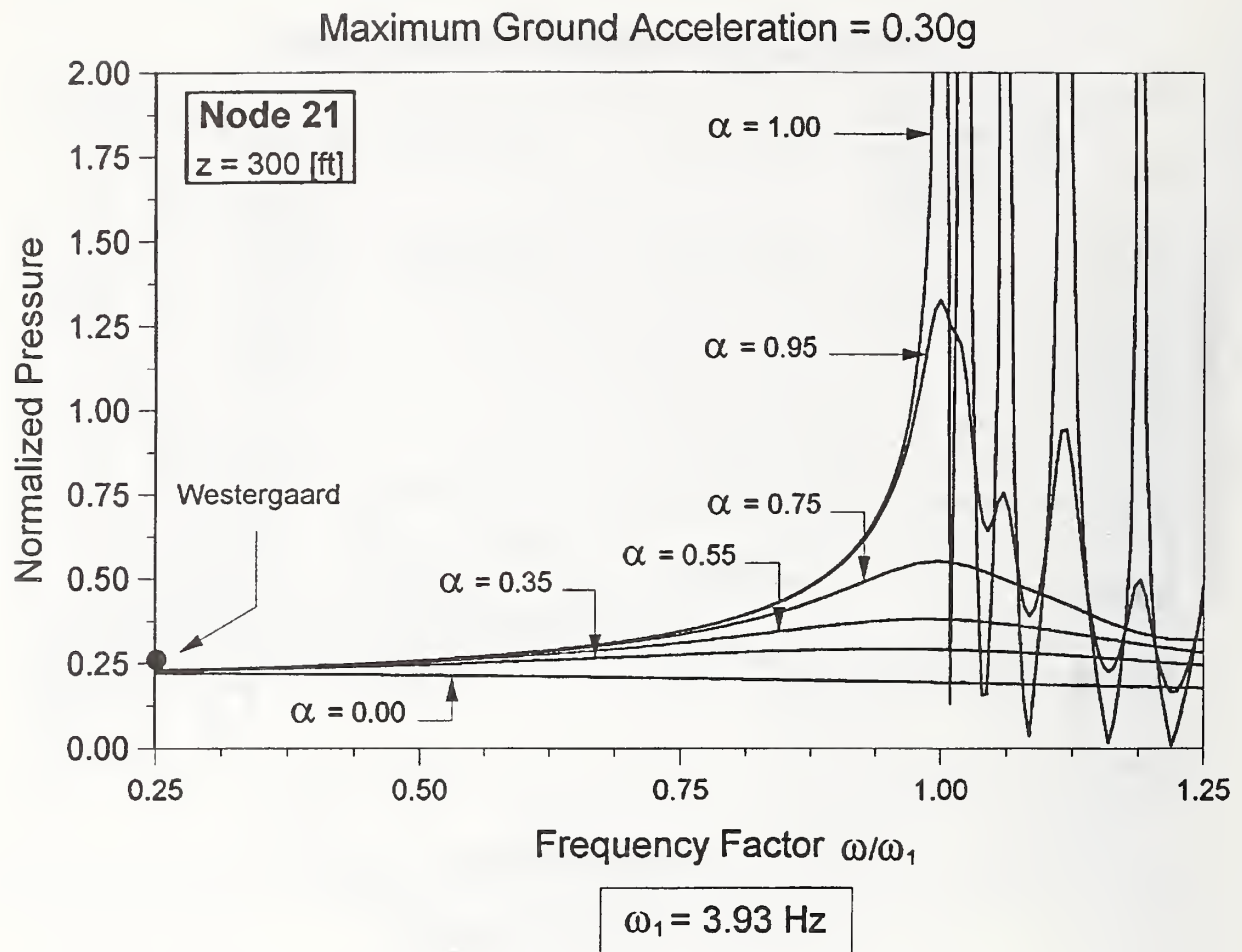


Figure 6. Trapezoidal Reservoir – 2D Analysis



Figure 7. Folsom Dam

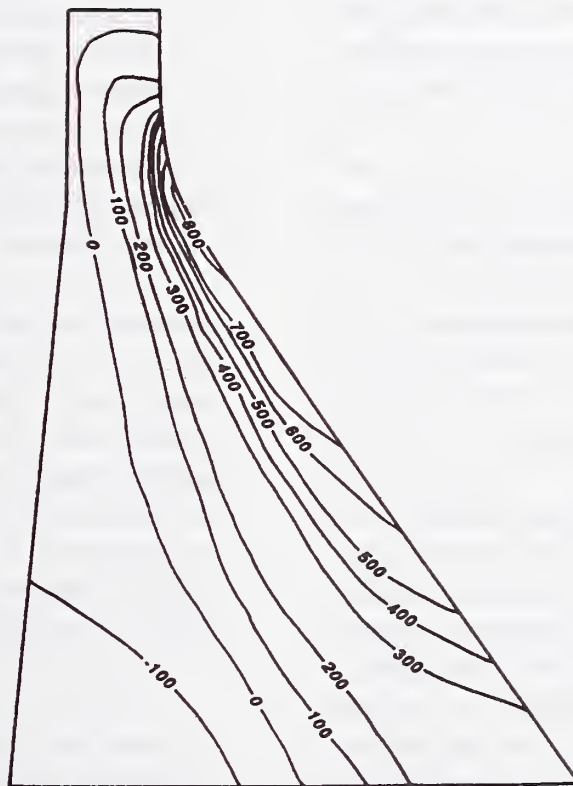


Figure 8. Maximum Principal Stress

A Study on Stress in Concrete Gravity Dam using Seismic Data during Kobe Earthquake

by

Takashi Sasaki, Tsuneo Uesaka and Isao Nagayama

ABSTRACT

The Kobe Earthquake (the Hyogoken-Nambu Earthquake of January 17, 1995) inflicted severe damage on many structures in the Hanshin and Awaji areas such as had not been experienced in Japan in recent decades. However, there was no damage on dams which affected their safety.

This paper introduces the characteristics of ground acceleration observed at dam sites during the Kobe Earthquake and discusses the effect of vertical seismic motion and the safety of concrete gravity dams in such big earthquakes. The result of the dynamic analysis shows that concrete gravity dams have the high safety against such big earthquakes.

*Key Words: concrete gravity dam,
dynamic analysis,
Kobe Earthquake,
seismic resistance,
vertical ground motion*

1. PREFACE

In the early morning of January 17, 1995, the Kobe Earthquake (Hyogoken-Nambu Earthquake) inflicted severe damage in the Hanshin and Awaji areas.

About 250 dams received the shock of the earthquake within 300 km of its epicenter. The Tokiwa Dam was located in a distance only 800 m from the Nojima earthquake fault. There were also a number of old dams in Kobe City where the earthquake damage was most severe. The dam safety inspection immediately

after earthquake showed that there were no damage on the dams which affected their safety.

This paper introduces the characteristics of ground acceleration observed at dam sites during the Kobe Earthquake and discusses the effect of vertical seismic motion and the safety of concrete gravity dams in such big earthquakes.

2. CHARACTERISTICS OF EARTHQUAKE MOTION AT DAM SITES

2.1. Maximum Acceleration at Foundation of Dams

(1) Attenuation of Peak Acceleration

About 50 ground acceleration records were obtained at dam sites during the Kobe Earthquake. All the dams were constructed on the rock foundation. Table 1 shows the peak acceleration recorded at the foundation of dams during the earthquake (including the acceleration obtained at the lowest gallery in the concrete dams or at the gallery beneath the embankment dams). The maximum ground acceleration is 183 gal which was recorded at the lowest gallery of the Hitokura Dam (concrete gravity dam, height = 75 m). The dam

-
- 1) Senior Research Engineer, Dam Structure Division, Dam Department, Public Works Research Institute, Ministry of Construction, Tsukuba, Science City, 305 Japan
 - 2) Director, Dam Department, ditto
 - 3) Head, Dam Structure Division, Dam Department, ditto

was located in a distance of 47 km from the epicenter or only 10 km from the estimated earthquake source fault in the ground. The location of the earthquake source fault in the Kobe area was estimated from the distribution of aftershocks on January 17, while it coincides with the Nojima fault in the Awaji area.

The attenuation of the horizontal peak acceleration of the foundation of dams is shown in Figure 1, and the attenuation of the vertical peak acceleration in Figure 2. The envelopes of the peak acceleration can be expressed by a straight line in the semi-logarithm plot. They are expressed as follow:

$$\ln Ah = \ln 217 - 0.0170 L$$

$$\ln Av = \ln 93 - 0.0114 L$$

where

Ah : horizontal peak acceleration (gal)

Av : vertical peak acceleration (gal)

L : distance from the earthquake source fault (km)

From the figure and the above equation, it can be estimated that the maximum of horizontal peak acceleration induced at the rock sites near the earthquake source fault was about 220 gal.

(2) Horizontal Peak Acceleration versus Vertical Peak Acceleration

Figure 3 shows the relationship between the horizontal peak acceleration and the vertical peak acceleration observed at dam sites during the Kobe Earthquake. The ratio of the vertical peak acceleration to the horizontal peak acceleration ranges from 1/3 to 1/1. This ratio tends to decrease as the horizontal peak acceleration increases.

2.2. Acceleration Response Spectrum

The response spectra of the acceleration in the stream direction (damping ratio of 10%) at 21 dam sites in the Kobe Earthquake are shown in Figure 4. Each spectrum is normalized so

that the maximum ground acceleration is equal to 1. The average value of the normalized response spectra is about 2 for the natural period ranging from 0.1 to 0.6 seconds. The response spectra decrease rapidly when the natural period exceeds about 0.6 seconds.

3. EFFECT OF VERTICAL SEISMIC MOTION

3.1. Model Concrete Gravity Dams

The concrete gravity dams used in the analysis have the typical cross section whose downstream slope is 0.8:1, and whose upstream slope is vertical (0.0:1). The height of the dams ranges from 25 m to 150 m. Figure 5 shows the finite element model of the dam, and Table 2 shows the physical properties of the material.

3.2. Methodology

The response spectrum method with the modal analysis was used in the analysis of dynamic stresses in dam body. The first 6 modes of vibration were considered. The damping ratio was assumed 10 %. This value is based on the results of behavior analysis of the Hitokura Dam (height = 75 m), where the acceleration of the foundation was 183 gal and the acceleration of the top gallery (8 m lower than the crest of the dam) was 482 gal in the Kobe Earthquake. Figure 6 shows the result of the analysis of the Hitokura Dam.

The effect of reservoir water was accounted for as the added mass matrix in the modal analysis. The added mass matrix is calculated assuming that reservoir water is incompressible.

3.3. Acceleration Records Used in Analysis

Acceleration records (sets of horizontal and vertical acceleration) obtained at the foundations of 21 dam

sites. These records include data measured in the bottom gallery in the dam. Two types of acceleration were used in this section. One is the acceleration record which adjusted so that the maximum value was 100 gal for both horizontal and vertical acceleration. And the second is original acceleration record.

3.4. Results of Analysis

(1) Tensile Stress for Ground Acceleration of 100gal

Figure 7 shows the results of the tensile stress at the heel of the dam for the horizontal seismic motion and the vertical seismic motion. The horizontal motion and vertical motion are separately applied to the dam. Figure 7 (a) is the results for the full reservoir, and (b) is the results for the empty reservoir. The symbols are the individual result and the solid line indicate the average value for each dam height. These figures show the tensile stresses at the heel of the dam for the horizontal motion and the vertical motion are in proportion to the dam height, and the stresses for horizontal motions vary more widely than the stresses for vertical motions.

Figure 8 compares the results of the tensile stress when the horizontal seismic motion and the vertical seismic motion are separately applied. Figure 8 (a) is the results for the full reservoir and (b) is the results for the empty reservoir. The figures show that the tensile stress at the heel of the dam generated by the vertical seismic motion is about 20% - 40% of the tensile stress generated by the horizontal seismic motion in the case of the full reservoir, and about 30 - 60% in the case of the empty reservoir. And the greater the tensile stress for the horizontal seismic motion is, the smaller the effect of the vertical seismic motion becomes.

(2) Tensile Stress for Original Ground Acceleration

Figure 9 compares the results of the tensile stress at the heel of the dam when the horizontal seismic motion and the vertical seismic motion are separately applied. Figure 9 (a) is the results for the full reservoir and (b) is the results for the empty reservoir.

When the tensile stress at the heel of the dam generated by the horizontal seismic motion become large, the tensile stress generated by the vertical seismic motion decrease to less than 10% of the tensile stress generated by the horizontal seismic motion in the case of the full reservoir, and to less than 20% in the case of the empty reservoir. In general speaking, the time when the stress by horizontal motion gets maximum value and the time when the stress by vertical motion gets maximum value do not coincide. So, the above-mentioned estimations are the upper limits of effects of vertical ground motions. The vertical ground motions, therefore, have less effects in the actual situation.

4. EVALUATION OF SEISMIC RESISTANCE OF CONCRETE DAMS

4.1. Conditions for Analysis

The model concrete gravity dam and the methodology used in this chapter is the same in Chapter 3.

4.2. Acceleration Records Used in Analysis

In Chapter 3, the effects of vertical ground motions are very small especially in the case of the full reservoir. So, only horizontal ground motions are considered in this chapter.

Two types of acceleration were used in the analysis. At first, 21 original acceleration records were used and the

results of the analysis were examined with regard to the distance from the earthquake source fault. Then, the typical 4 acceleration records (ACC-1 to ACC-4) which were observed at the dam sites near the earthquake source fault were used. In this case, the horizontal peak acceleration was enlarged as much as 220 gal. It is the estimated maximum acceleration in the Kobe Earthquake. Figure 10 shows the response spectrum of acceleration records ACC-1 to ACC-4 (damping ratio = 10 %).

4.3. Results of Analysis

(1) Maximum Tensile Stress versus Distance from Earthquake Source Fault

The maximum tensile stress was induced at the bottom portion of the upstream face of the dams in all cases. Figure 11 shows the maximum tensile stress in the dams excluding static stress with regard to the distance from the earthquake source fault. The envelope is almost in a straight line, although the maximum tensile stress has wide range depending on the characteristics of the acceleration records. Figure 12 shows the maximum tensile stress in the dams including static stress with regard to the distance from the earthquake source fault. It can be estimated from the figures that the maximum tensile stress induced in the dams near the earthquake source fault is about 3.1 N/mm^2 in 150m high dams, 2.2 N/mm^2 in 100 m high dams and 0.4 N/mm^2 in 50 m high dams.

(2) Maximum Tensile Stress for Ground Acceleration of 220 gal

Figure 13 shows the maximum tensile stress in the dams of the different height induced by the ground acceleration of ACC-1 to ACC-4. The stress includes the static stress in all cases. The acceleration ACC-1 produces

the largest stress in higher dams, since the dominant period of the acceleration is close to the natural period of those dams. On the contrary, the acceleration ACC-4 produces the lowest stress in higher dams, since the dominant period of the acceleration is far from the natural period of those dams.

The figure shows that the maximum tensile stress increases in proportion to the height of the dam. The envelope is expressed as:

$$\sigma = 0.0226 H \quad (\text{at } 220 \text{ gal})$$

or

$$\sigma = (0.0129 \alpha - 0.568) H/100$$

where

σ : maximum tensile stress (N/mm^2)

α : maximum ground acceleration (gal)

H : height of dam (m)

It can be estimated from the figure or the above equations that the maximum tensile stress by the ground acceleration of 220 gal is about 3.4 N/mm^2 even in 150 m dams. Since the dynamical stress occurs instantaneously, it is considered that dams can withstand such a level of tensile stress.

5. CONCLUSION

The Kobe Earthquake inflicted severe damage in the Hanshin and Awaji areas such as had never been experienced in Japan in recent decades. However, there was no damage on the dams affecting their safety.

This paper introduces the characteristics of ground acceleration observed at dam sites during the Kobe Earthquake and discusses the effects of vertical seismic motions on dam and the safety of concrete gravity dams in such big earthquakes. The results of the analysis are as follows:

(1) It is estimated that the maximum peak acceleration at rock sites induced

by the Kobe Earthquake was about 220 gal.

(2) The effect of the vertical seismic motion on the stress of dam body is very small as compared with the effect of the horizontal seismic motion. The tendency can be obvious when the stress by horizontal seismic motion is large, and the reservoir is full.

(3) It is estimated that the maximum tensile stress in the concrete gravity dams induced by the earthquakes is:

$$\sigma = 0.0226 H \quad (\text{at } 220 \text{ gal})$$

or

$$\sigma = (0.0129 \alpha - 0.568) H/100$$

where

σ : maximum tensile stress (N/mm^2)

α : maximum ground acceleration (gal)

H : height of dam (m)

Therefore, the maximum tensile stress in 150 m high concrete gravity dams induced by the ground acceleration of 220 gal is about 3.4 N/mm^2 . Since the

dynamical stress occurs instantaneously, it is considered that dams can withstand such a level of tensile stress. So, the concrete gravity dams are safe in such big earthquake as Kobe Earthquake.

REFERENCES

- (1) Committee on Evaluation of Earthquake Resistance of Dams: Report of Committee on Evaluation of Earthquake Resistance of Dams, November, 1995
- (2) A. Nakamura, I. Nagayama, T. Sasaki and T. Iwashita: Safety of Dams during Hyogoken-Nambu Earthquake on January 17, 1995 in Japan, 11WCEE, Acapulco, 1996
- (3) I. Nagayama, S. Jikan: Study on Dynamic Behavior of Concrete Dams During Earthquake with Hydrodynamic Interaction, Int. Symp. on Earthquake & Dams, China, 1987

Table 1 Peak Acceleration Recorded at Foundation of Major Dams

Dam Site	Acceleration (gal)	
	Horizontal Direction	Vertical Direction
Hitokura	183	64
Minoo	128	75
Donto	111	-
Gongen	103	67
Kisenyama	90	44
Kurokawa	85	53
Tataragi	65	20
Shirakawa	50	48
Zao	49	25
Yasumuro	38	31
Nishidaira	38	25
Seto	35	12
Masaki	33	33
Senzoku	32	16
Fukui	32	15
Hase	30	22

Table 2 Physical Properties of Materials

Item	Value
Concrete	
Density	2300 kg/m ³
Elastic Modulus	30 kN/mm ²
Poisson's Ratio	0.2
System	
Damping Ratio	10%

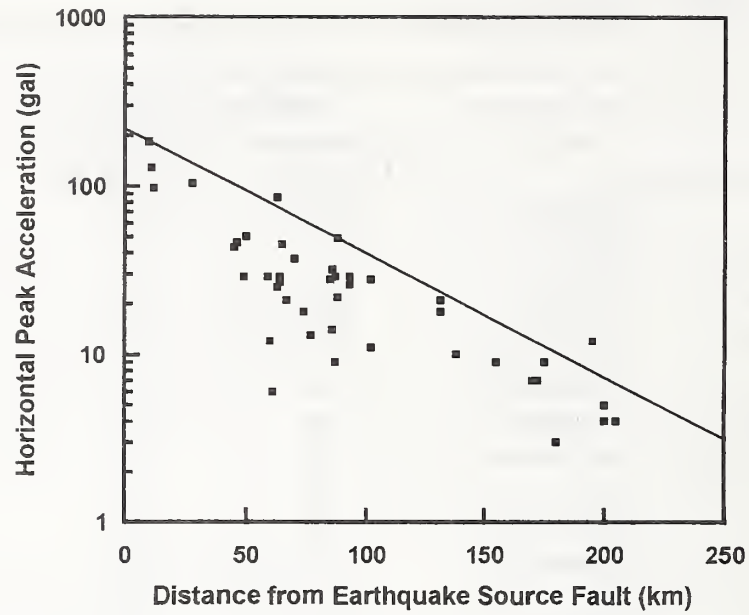


Figure 1 Attenuation of Horizontal Peak Acceleration

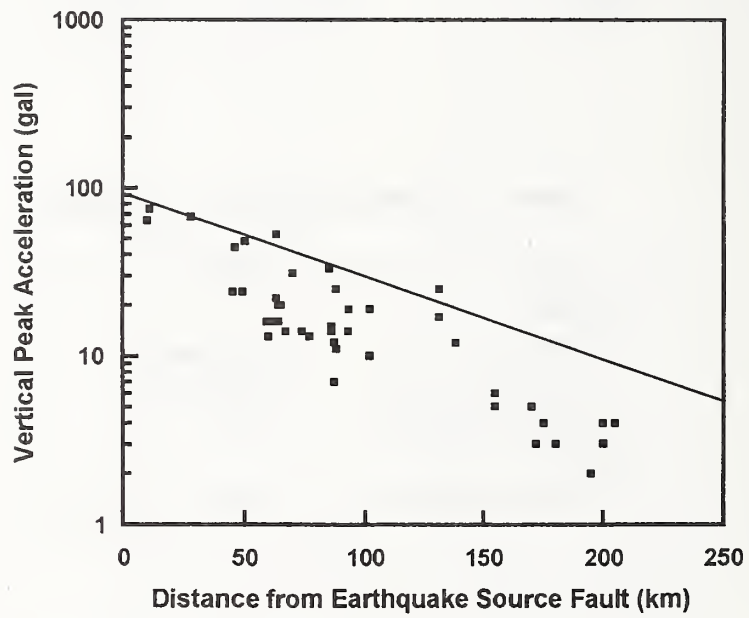


Figure 2 Attenuation of Vertical Peak Acceleration

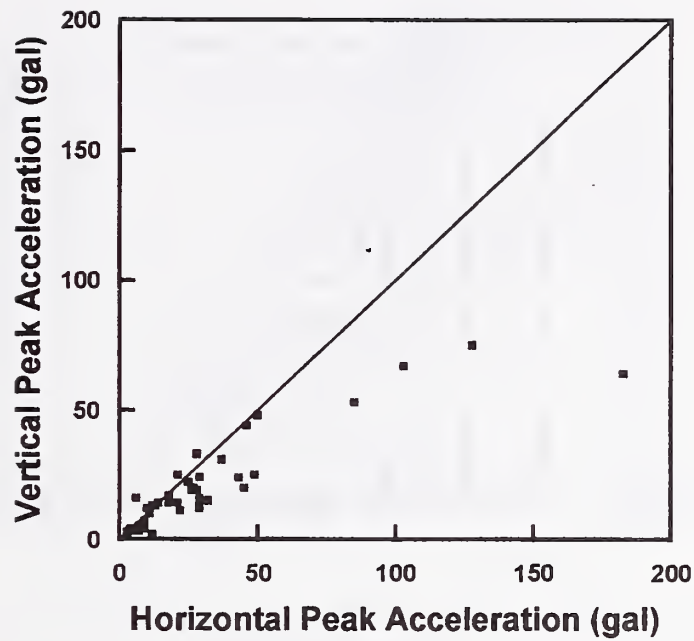


Figure 3 Horizontal Peak Acceleration versus Vertical Peak Acceleration

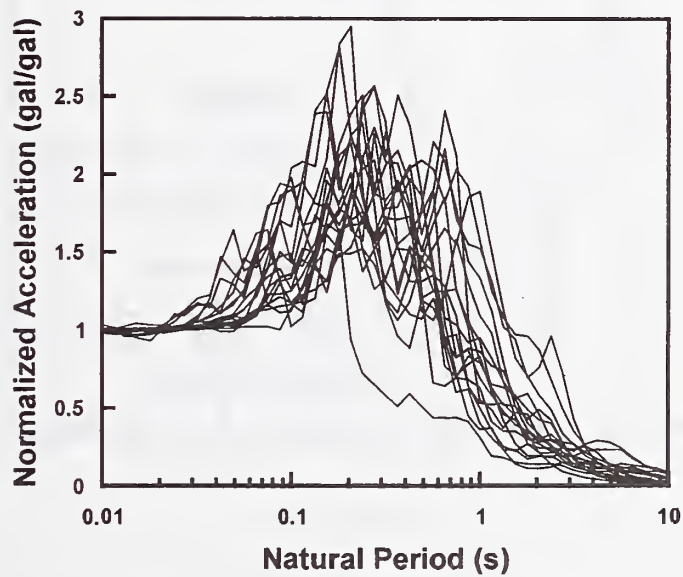


Figure 4 Normalized Response Spectrum of Acceleration (Horizontal Direction)

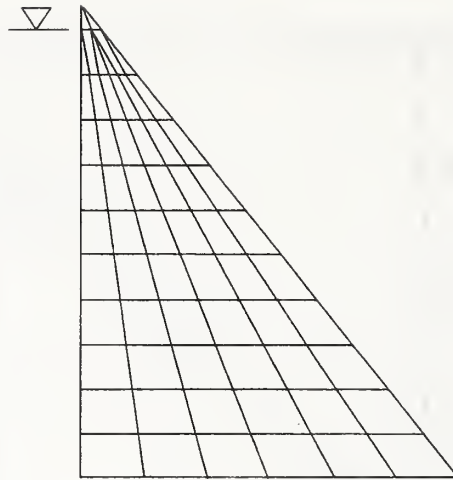


Figure 5 Finite Element Model of Concrete Gravity Dam

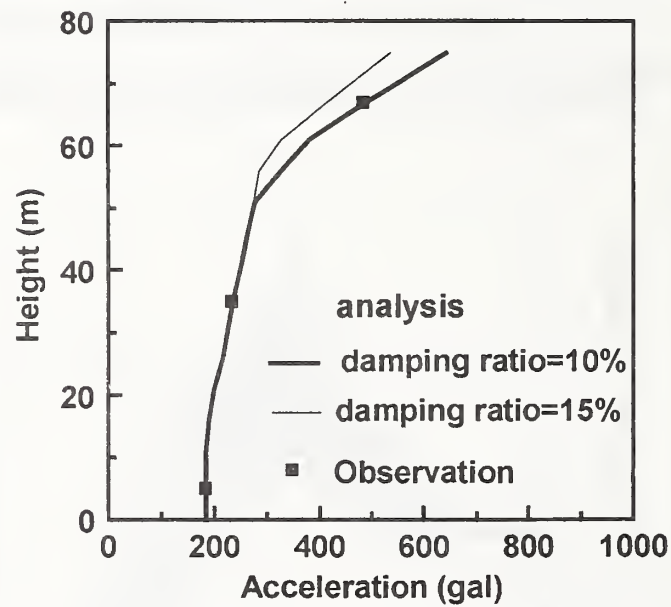
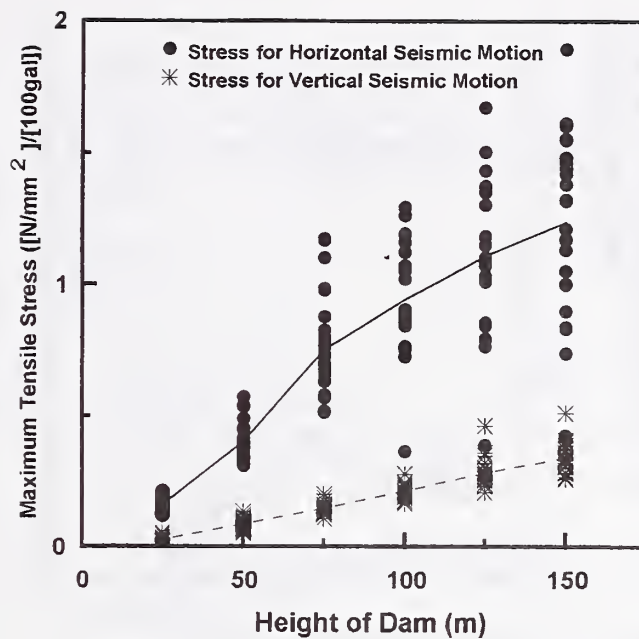
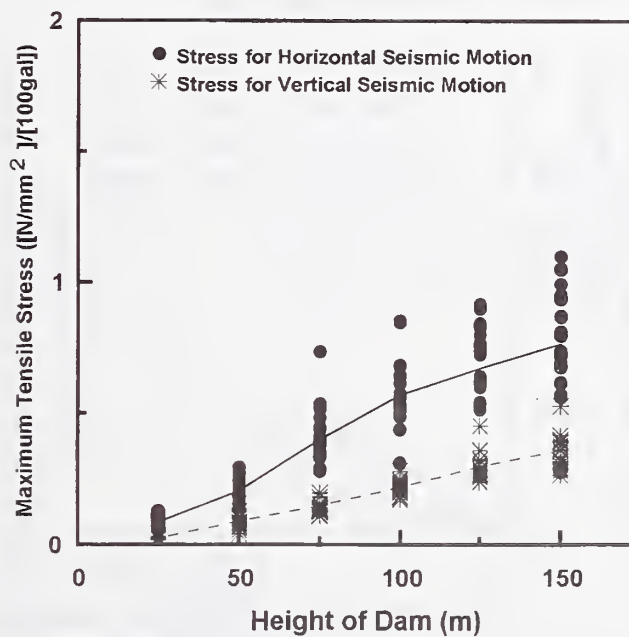


Figure 6 Distribution of Acceleration at the Hitokura Dam

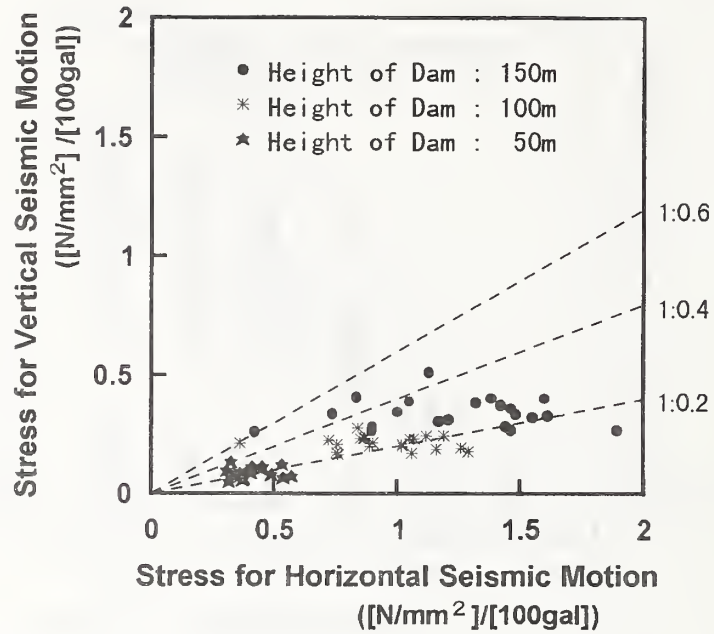


(a) Full Reservoir

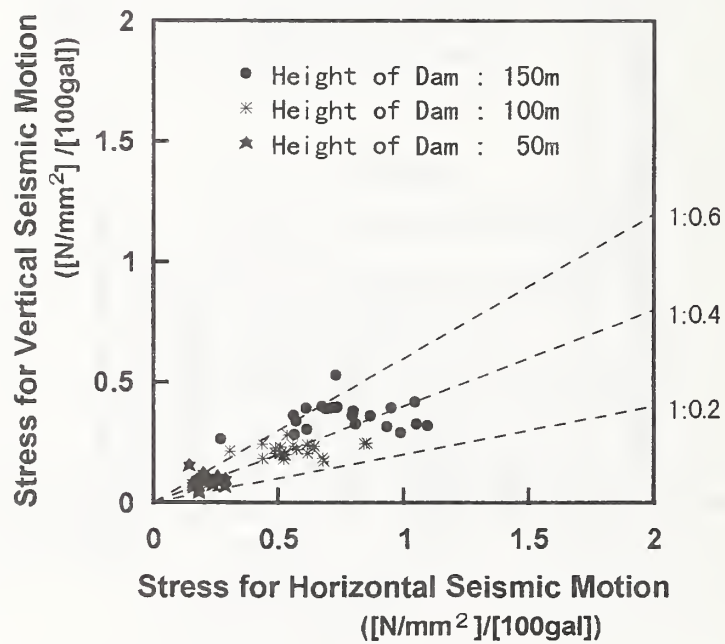


(b) Empty Reservoir

Figure 7 Height of Dam versus Maximum Tensile Stresses for Horizontal Seismic Motion and Vertical Seismic Motion

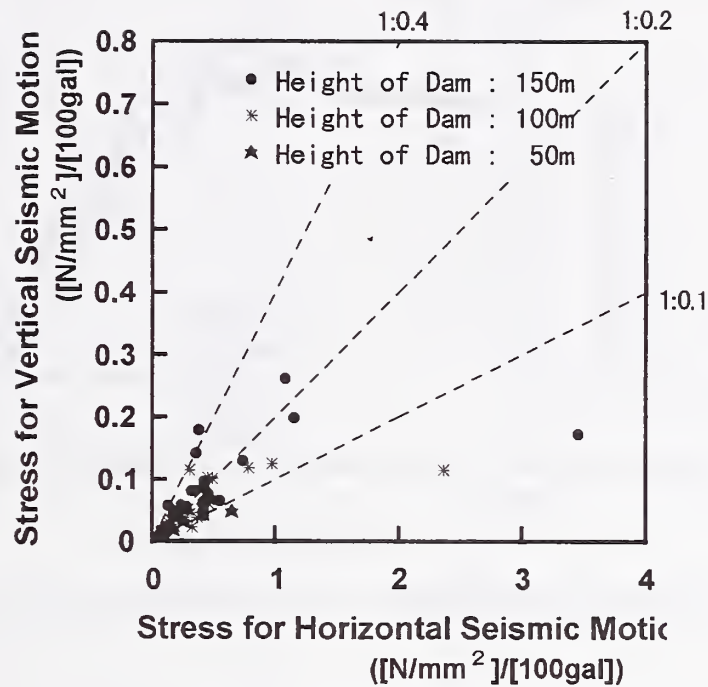


(a) Full Reservoir

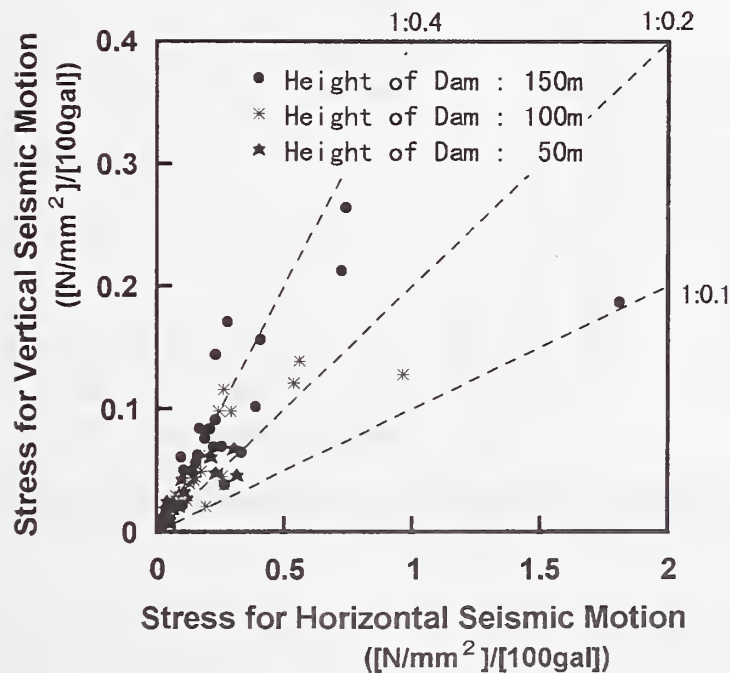


(b) Empty Reservoir

Figure 8 Comparison of Maximum Tensile Stresses for Horizontal Seismic Motion and Vertical Seismic Motion (Maximum Acceleration : 100gal)



(a) Full Reservoir



(b) Empty Reservoir

Figure 9 Comparison of Maximum Tensile Stresses for Horizontal Seismic Motion and Vertical Seismic Motion (Maximum Acceleration : Measured Value)

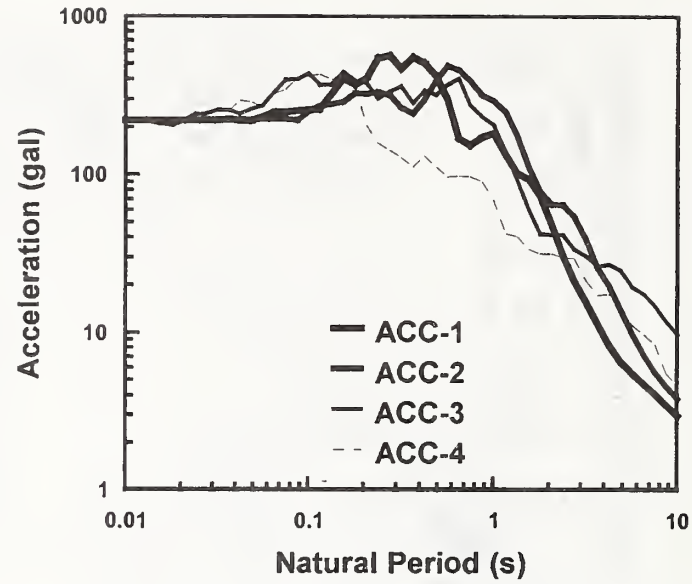


Figure 10 Modified Response Spectra of Four Acceleration Records (Horizontal Direction)

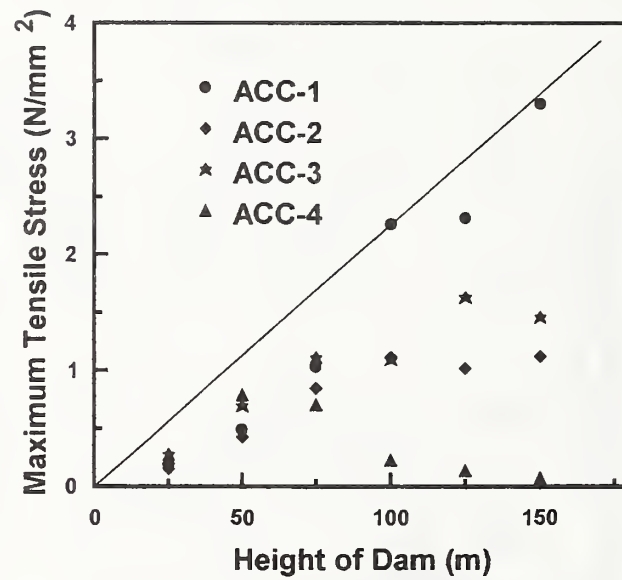
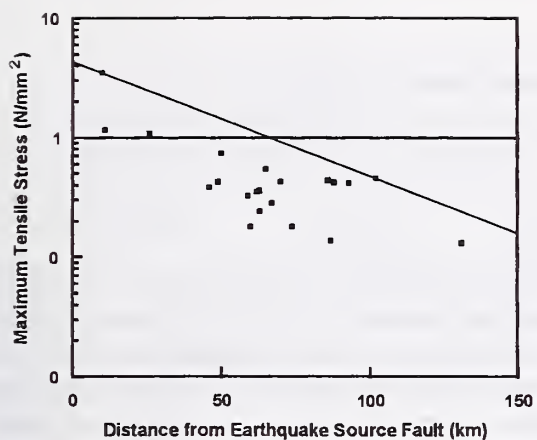
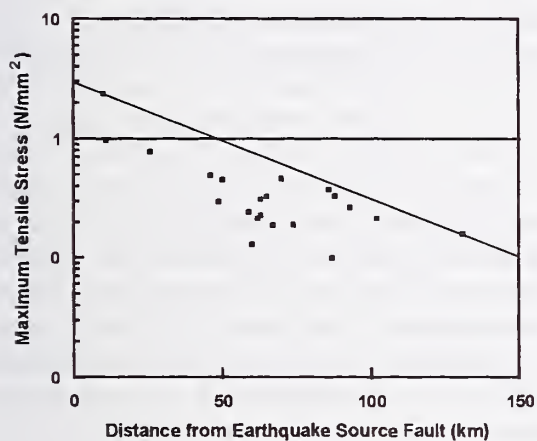


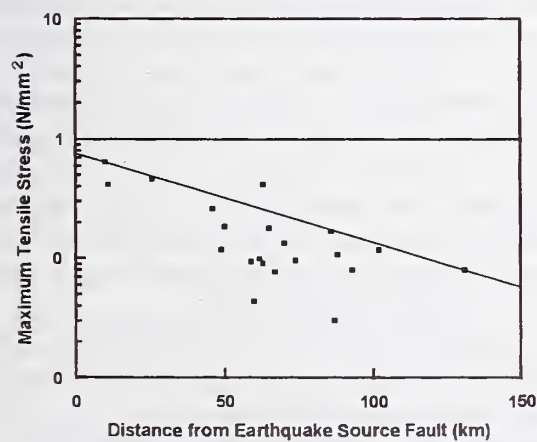
Figure 13 Maximum Tensile Stress versus Height of Dams



(a) Dam Height = 150m

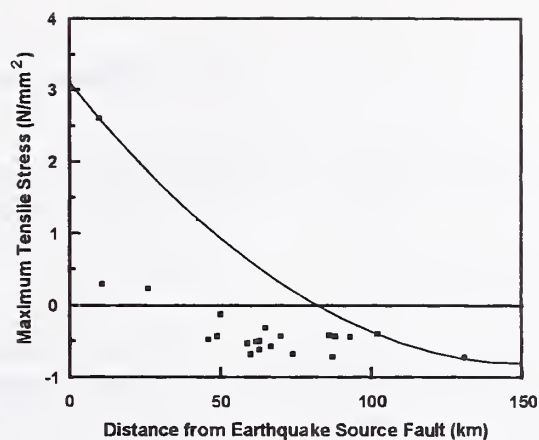


(b) Dam Height = 100m

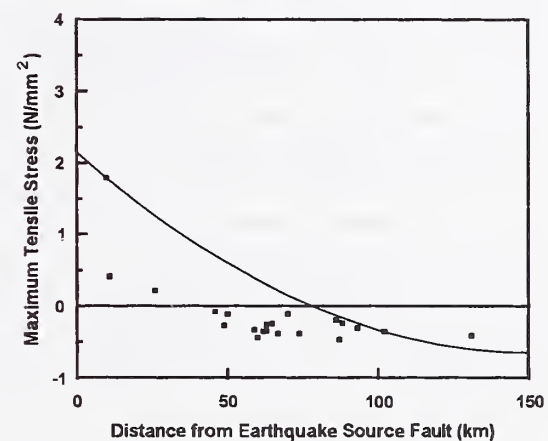


(c) Dam Height = 50m

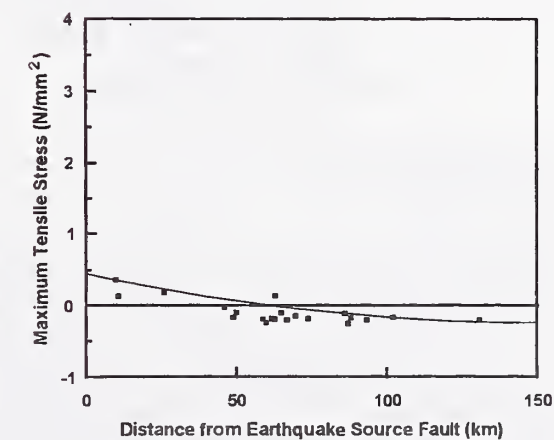
Figure 11 Maximum Tensile Stress versus Distance from Earthquake Source Fault (Excluding Static Stress)



(a) Dam Height = 150m



(b) Dam Height = 100m



(c) Dam Height = 50m

Figure 12 Maximum Tensile Stress versus Distance from Earthquake Source Fault (Including Static Stress)

Seismic Analysis of Hoover Dam ¹⁾

by

By Larry K. Nuss ²⁾

ABSTRACT

Hoover Dam is a 221-m (727-foot) high concrete thick-arch dam located on the border between Arizona and Nevada about 58 km (36 miles) from Las Vegas, Nevada. The postulated maximum credible earthquake (MCE) for Hoover Dam is a magnitude Ms 6.75 on the Mead Slope Fault. Initial structural finite element analysis calculated stresses larger than the tensile strength on the upper portions of the dam. More sophisticated analysis followed when additional data was obtained for material properties and seismic loading. The first approach was a linear-elastic analysis incorporating foundation-structure interaction with mass in the foundation. The second approach was a non-linear analysis incorporating concrete cracking and contraction joint interaction using smeared crack techniques and kinematic stability analysis of the top of the dam.

KEYWORDS: Hoover Dam; concrete arch dam; nonlinear and linear dynamic structural analysis; foundation impedance; hydrodynamic interaction, reservoir bottom reflection coefficient; EACD3D96; ANACAP.

1. INTRODUCTION

Hoover Dam is a 221-m (727-foot) high concrete thick-arch dam located on the border between Arizona and Nevada about 58 km (36 miles) from Las Vegas, Nevada. The dam was completed in 1935, has a crest length of 380 m (1244 feet), a crest thickness of 14 m (45 feet), and a maximum base width of 201 m (660 feet) (see figure 1). It is the highest concrete dam in the United States, the eighteenth highest dam in the world, and forms the largest manmade reservoir in the United States

[USCOLD, 1995]. The postulated maximum credible earthquake (MCE) for Hoover Dam is a magnitude Ms 6.75 on the Mead Slope Fault, with primarily normal fault rupture mechanism involving rupture from 15 km (9.3 miles) depth to the surface and 3 km (1.8 miles) closest surface approach to the dam [O'Connell, 1996]. The probability of the MCE is postulated to be as frequent as 1:10,000 years or as infrequent as 1:100,000 years. Initial structural analysis using conventional linear-elastic three-dimensional dynamic finite element methods, assuming material properties and a massless foundation, calculated stresses larger than the tensile strength on the upper portions of the dam. These results indicate concrete cracking occurs in the upper 61 m (200 feet) of the dam. If the top 61 m (200 feet) of the dam failed during a seismic event, the downstream consequences would be massive. An estimated loss-of-life of 400 people and damages not including losses from project benefits totaling \$17 billion (US) could occur.

More sophisticated analysis followed when additional data was obtained for material properties and seismic loading. Currently, there is no software code available that incorporates all the important aspects (hydrodynamic interaction, impedance of dam-foundation interaction, contraction joint action, or rigid block kinematic movements) associated with a concrete dam for a complete structural analysis. For this reason, various software programs were run using the Hoover finite element model and knowledge of the influence of each aspect

1) Submitted for presentation at the 30th joint meeting of the U.S-Japan Panel on Wind and Seismic Effects, May 12-15, 1998, Gaithersburg, Maryland.

2) Larry K. Nuss, Senior Structural Engineer, Bureau of Reclamation, Structural Analysis Group (D-8110), P.O. Box 25007, Denver, Colorado 80123, (303) 445-3231, lnuss@do.usbr.gov.

affecting the dam was gleaned. This way the relative impact of each aspect on the stability of Hoover Dam was determined. These analyses took two different approaches. The first approach was a three-dimensional linear-elastic analyses (EACD3D96) incorporating foundation-structure interaction with mass in the foundation, impedance contrast between the dam and foundation, and hydrodynamic interaction using compressible fluid [Chopra 1996; Payne 1998]. The second approach was a non-linear three-dimensional dynamic finite element analysis incorporating concrete cracking and contraction joint interaction using smeared crack techniques [ANATECH 1997, Koltuniuk 1997] and kinematic stability analysis of the top of the dam [Scott 1982; Mills 1997].

2. GROUND MOTIONS

In 1993, a regional seismotectonic study was conducted for the Hoover Dam area [O'Connell 1993]. In 1994, estimates for strong ground motions that seismogenic sources, identified in the regional seismotectonic report, could be produced at Hoover Dam. Recommended ground motions representing the Mead Slope Fault are the Convict Creek record of the May 27, 1980 Mammoth Lakes, California earthquake and the Corralitos recording from the Loma Prieta 1989 earthquake (see figures 2 and 3). These ground motions were modified and accepted based on recommendations by the consultant review board [Bolt 1995, O'Connell 1995].

3. CONCRETE CORE AND LABORATORY TESTING

Laboratory tests [Reclamation 1995] on extracted 15-cm (6-inch) diameter concrete core from the dam showed the concrete was very strong and had average properties as shown in the table.

The 29,854 MPa (4,330,000-lb/in²) dynamic modulus of elasticity was suspect. A literature search of published dynamic concrete properties showed that the dynamic modulus is typically equal to or greater than the static modulus [Harris 1997]. Therefore, the measured static modulus was used for

the dynamic modulus.

Tested Material Properties		
Description	MPa (lb/in ²)	Static Dynamic
Compressive	50 (7230)	55 (8040)
Splitting tensile	4 (600)	7 (970)
Concrete Modulus	45,436 (6,590,000)	29,854 (4,330,000)
Foundation Modulus		
Lower elevations	26,200 (3,800,000)	26,200 (3,800,000)
Upper elevations	16,547 (2,400,000)	16,547 (2,400,000)
Apparent cohesion (see figure 4)	0.63 (91)	0.63 (91)
Friction angle	48°	48°

4. RESERVOIR BOTTOM REFLECTION COEFFICIENT

Dr. Yusof Ghanaat measured the reservoir-bottom reflection coefficient (alpha coefficient) at Hoover Dam in 1995 [Ghanaat 1995]. The silt elevation at the dam heel is at elevation 216 m (708.8 ft) (depth of 54 m (176.8 ft)). Reflection surveys measured alpha coefficients of -0.09 for the bottom surficial material, 0.68 for the dam concrete, and 0.77 for the canyon rock walls. Refraction surveys measured alpha coefficients of -0.02 and -0.05 for the bottom surficial material.

5. HYDRODYNAMIC INTERACTION

The effect of hydrodynamic interaction on Hoover Dam was studied and included in all the various dynamic studies [Payne 1997, 1995]. Sensitivity studies included the affects of incompressible fluid, compressible fluid, and various reservoir bottom reflection coefficients. The findings were that hydrodynamic interaction had a relatively small affect on the stress of state in the dam during an earthquake because of the massive size and inertia of the dam body compared to the inertia force of the water. There was no single correction factor to convert stress values when incompressible fluid or compressible fluid is used. Stress magnitudes and

areas of high stresses and the time they occur vary with each earthquake. Use of compressible fluid instead of incompressible fluid did not always produce smaller stresses.

6. STRUCTURAL ANALYSIS

Currently, there is no software codes available that incorporate all the important aspects (hydrodynamic interaction, impedance of dam-foundation interaction, contraction joint action, or rigid block kinematic movements) associated with a concrete dam for a complete structural analysis. For this reason, various software programs were run using the Hoover finite element model and knowledge of the influence of each aspect affecting the dam was gleaned. This way the relative impact of each aspect on the stability of Hoover Dam was determined. The same finite element model was used in all the studies (see figure 5).

6.1 TRADITIONAL STRUCTURAL ANALYSIS

Traditional structural analyses were made using the SAPIV linear-elastic three-dimensional dynamic finite element code with a massless foundation, 10 percent viscous damping, and hydrodynamic interaction using incompressible fluid added masses [Nuss 1996, Dollar 1994]. Maximum calculated arch tensile stresses, with superimposed static stresses, were 12.2 MPa (1772 lb/in²) on the upstream face and 12.7 MPa (1840 lb/in²) in the downstream face. Maximum calculated cantilever tensile stresses were 10.0 MPa (1445 lb/in²) on the upstream face and 11.6 MPa (1684 lb/in²) on the downstream face. This is well over the dynamic tensile strength of the concrete and would indicate cracking of the structure.

6.2 INCORPORATING STRUCTURE - FOUNDATION INTERACTION

The influence of including mass in the foundation during a structural finite element analysis is investigated using a relatively new program EACD3D96 [Chopra 1996]. This program was tested and evaluated for consistency with the

previous EACD3D version and for reasonability of the results when foundation and dam moduli were varied [Payne 1998]. The impedance between the dam and foundation and radiation damping is included in the analysis. This is believed to be the most realistic linear-elastic structural analysis to date.

Analysis, incorporating mass in foundation, shows great reduction of stress in the dam to the point that cracking of the dam is not expected from the MCE (thus, lack of nonlinear capability in this program is no longer a concern). For example, calculated stress levels are reduced from 11.6 MPa (1684 lb/in²) not including the foundation mass to 4.1 MPa (600 lb/in²) by including foundation mass and interaction (see figure 6). Lower stresses are attributed to the following: First, the stiffness of the concrete compared to the stiffness of the foundation material inhibits seismic energy from entering the structure and thus reduces the seismic affect. Second, the infinite boundary of the foundation provides a radiation damping affect that allows earthquake energy to dissipate from the structure.

6.3 NONLINEAR DYNAMIC ANALYSIS

Despite the above finding, a non-linear analysis with a "traditional" massless studies were continued as a back up and also because of the paucity of testing and experience with the new program incorporating foundation mass.

The influence of including contraction joints and concrete cracking in structural finite element analyses is investigated using smeared crack techniques in program ANACAP [Anatech 1997]. However, this analysis does not include the dam-foundation and produces higher dynamic inertia forces, which shake the dam enough to open and close contraction joints and crack the concrete in the finite element analysis. Since these analyses were nonlinear, various verification studies are performed to determine the appropriate solution time step, damping, convergence tests, and modeling. Four finite element models evolved during these studies: a 5-joint element model, a 24-pre-directed joint

model, a 16-pre-directed joint model, and an 8-pre-directed joint model [Koltuniuk 1997].

Using the Convict Creek ground motion, the ANACAP analysis predicted horizontal cracking 46 m (150 feet) below the dam crest on the upstream face, continuing through the dam in the downstream direction, sloping upward toward the downstream face (see figure 7). ANACAP indicated stability and 3-cm (1.1-inch) movement of the dam upstream. This cracking pattern forms concrete blocks capable of sliding independently from the dam body along the cracked basal plane and bounded on the sides by vertical contraction joints.

Using the Corralitos ground motion, the calculated cracking, which is significantly less, is located 82 m (270 feet) below the dam crest on the downstream face, and does not progress through to the upstream face. Therefore, further stability analysis using this earthquake record is not needed.

The capability of extracting an XYZ time history of hydrodynamic pressures at nodes on the upstream face from EACD3D was developed which made it possible to apply hydrodynamic forces to other finite element codes. This allowed for the ability to apply full compressible hydrodynamic forces including reservoir bottom reflection effects to the nonlinear ANACAP model of Hoover Dam. Incorporating full hydrodynamic compressible fluid effects in the nonlinear ANACAP model of Hoover Dam showed cracking developed sooner, cracking advanced at a slower rate, but the final cracking pattern was very similar compared to the incompressible fluid effect. Thus, use of full hydrodynamic would not have changed results in terms of preventing formation of a potential sliding mass in the upper part of the dam.

6.4 KINEMATIC STABILITY OF THE TOP OF DAM

Kinematic studies were performed to investigate the sliding stability of an independent concrete block formed separate from the dam body bounded by horizontal cracking and vertical contraction joints.

The computer program RIGID uses a Newmark procedure to determine movements of a rigid body [Scott 1982]. Loads applied to the block were the accelerations calculated in the concrete dam at 46 m (150 feet) from the crest, static reservoir loads, and forces representing full hydrodynamic and reservoir boundary effects [Mills 1997] (see figure 8). The maximum "expected" displacement if a "cracked block" were to form in upper part of dam during the earthquake is about 9 cm (3.5 inches) in the upstream direction. Such small displacement would not impair stability of the dam or result in reservoir release because the dam is 30 m (100 feet) thick at this depth arch action and the wedging provides side restraint.

7. CONCLUSIONS

Based on structural analysis incorporating foundation mass, Hoover Dam is predicted to withstand shaking from the maximum credible earthquake without significant cracking. This improved performance over previous traditional analyses is attributed to the impedance contrast between the dam and foundation, which inhibits earthquake energy from entering the structure. Calculated stress levels during the maximum credible earthquake are below the tensile strength of the concrete when incorporating the impedance between the dam and foundation.

Based on nonlinear structural analysis with a massless foundation (performed in the event that the impedance between the dam and foundation proves to be inaccurate) concrete cracking at 46 m (150 feet) below the dam crest is indicated. However, even if this cracking extends through the upstream to downstream thickness of the dam, forming independent blocks separate from the dam body, the calculated block movements are on the order of a few inches, which would not cause instabilities nor an uncontrolled release of the reservoir.

The top of dam is considered stable for the post-earthquake condition because of many positive factors. The dam has 20-cm (8-inch) diameter formed drains at 3-m (10-foot) centers cross-canyon

in the dam body to reduce uplift pressures from infiltration of water along any upstream cracking. Arch action is maintained during and after an earthquake, which inhibits any downstream movements. The top 46 m (150 feet) of the dam resembles a gravity dam section with a downstream slope of 0.7:1. This size gravity section is stable for static loads without arch action. Calculated earthquake induced cracking is radial so arch action is maintained. The horizontal basal plane formed by cracking during an earthquake slope upward toward the downstream face, which produces a stable slide plane.

8. ACKNOWLEDGEMENTS

The author would like to thank the Consultant Review Board: Ray Clough, Bruce Bolt, and Alfred Hendron; peer review members: Larry Von Thun and Gregg Scott, team members: Terry Payne, Barbara Mills-Bria, Roman Koltuniuk, Dan O'Connell, Mike Romansky, Chuck Sullivan, Dave Harris, and Jack Touseull; and other contributors Dave Dollar, Yusof Ghanaat, Randy James, Anil Chopra, Hanchen Tan, John Hall, Greg Fenves, and Ka-Lun Fok.

9. REFERENCES

- Nuss, L.K., HVD-8110-MDA-97-1, "*Executive Summary of the Static and Dynamic Stability Studies for Hoover Dam for the Modification Decision Analysis*", Bureau of Reclamation, May 1998.
- Payne, T.L., HVD-8110-MDA-97-2, "*Linear-Elastic Dynamic Structural Analysis Including Mass in the Foundation for Hoover Dam*", Bureau of Reclamation, April 1998.
- Payne, T.L., HVD-8110-MDA-97-3, "*Effects of Water Compressibility on Dynamic Structural Analysis for Hoover Dam*", Bureau of Reclamation, November 1997.
- Koltuniuk, R.M., HVD-8110-MDA-97-4, "*Non-linear Dynamic Structural Analysis of Hoover Dam Including Modeling of Contraction Joint Opening and Concrete Cracking*", Bureau of Reclamation, September 1997.
- Mills, B.L., HVD-8110-MDA-97-5, "*Kinematic Studies to Determine the Stability of Postulated Independent Concrete Blocks Indicated by the Non-linear Analysis of Hoover Dam During Seismic Loading*", Bureau of Reclamation, December 1997.
- Nuss, L.K., HVD-8110-MDA-97-6, "*Orientations for the Modified Convict Creek and Corralitos Ground Motions for use in the Structural Analysis of Hoover Dam*", Bureau of Reclamation, June 1996.
- Payne, T.L., HVD-8110-MDA-97-7, "*EACDFOK - A Modified Version of EACD-3D to Obtain Hydrodynamic Pressure Time Histories at Nodes on the Upstream Face of Dams*", Bureau of Reclamation, September 1997.
- Payne, T.L., HVD-8110-MDA-97-8, "*EACDFOK - Procedure and Verification for Incorporating Full Hydrodynamic Interaction Other Finite Element Codes*", Bureau of Reclamation, October 1997.
- Payne, T.L., HVD-8110-MDA-02-95 - "*Influence of Water Compressibility - Dynamic Linear Elastic Structural Analyses - Hoover Dam*", Bureau of Reclamation, September 10, 1995.
- Anatech Corporation, "*ANACAP - Concrete Analysis Program*", Version 2.1e, 1997.
- Scott, G., "*RIGID - Dynamic Response of Jointed Rock Masses*", University of Colorado, 1982.
- Chopra A. and Hanchen, T., "*EACD-3D-96: A Computer Program for Three-Dimensional Analysis of Concrete Dams*", University of California, Berkeley, California, Report No. UCB/SEMM-96/06, October 1996.
- Chopra, A., Hall, J., and Fok, K., "*EACD-3D - A*

Computer Program for Three-Dimensional Earthquake Analysis of Concrete Dams", University of California, Berkeley, California, Report No. UCB/EERC-86/09, July 1986.

O'Connell, R.H., "*Modified Convict Creek and Corralitos Ground Motions for Hoover Dam - Boulder Canyon Project, Arizona and Nevada*", Bureau of Reclamation, Technical Memorandum No. D8330-96-004, February 22, 1996.

O'Connell, D. and Ake, J., "*Ground Motion Analysis for Hoover Dam*", Bureau of Reclamation, Seismotectonic Report 94-1, January 1995.

O'Connell, D. and Anderson, L., "*Seismotectonic Study of the Northern Lower Colorado River - Arizona, California, and Nevada for Hoover, Davis, and Parker Dams*", Bureau of Reclamation, Seismotectonic Report 93-4, April, 1993.

Harris, D., "*Review of Hoover Dynamic Tests Relative to Other Published Literature*", Bureau of Reclamation, Materials Engineering and Research Laboratory, March 20, 1997.

Bolt, B., Clough, R., and Hendron, A., "*Report of Board of Consultants on Hoover Dam Modification Decision Analysis, Boulder Canyon Project, Nevada*", August 1994, November, 1995, and September 1997.

Bureau of Reclamation, "*Results of Direct Shear Tests on Concrete Core Specimens, Hoover Dam, Boulder Canyon Project*", Earth Sciences and Research Laboratory Referral Number 8340-96-03, February 5, 1996.

Bureau of Reclamation, "*Report of Mass Concrete Core Testing - Hoover Dam - Boulder Canyon Project*", Materials Engineering Branch Referral Memorandum No. 8180-95-003, November 27, 1995.

Bureau of Reclamation, "*Arizona Abutment-Geologic Field Data Report-Modification Decision Analysis Study-Hoover Dam-Boulder Canyon*

Project", Lower Colorado Regional Office, May 27, 1993.

Dollar, Dave, "*Preliminary Analysis of Structural Engineering Issues Including Effects of the MCE - Hoover Dam*", Bureau of Reclamation, May 13, 1994.

Ghanaat, Y. and Redpath, B., "*Measurements of Reservoir-Bottom Reflection Coefficient at Seven Concrete Dams*", Quest Structures, Orinda, California, October 1995.

United States Committee On Large Dams, "*U.S. and World Dam, Hydropower, and Reservoir Statistics*", USCOLD Committee on Register of Dams, 1995.

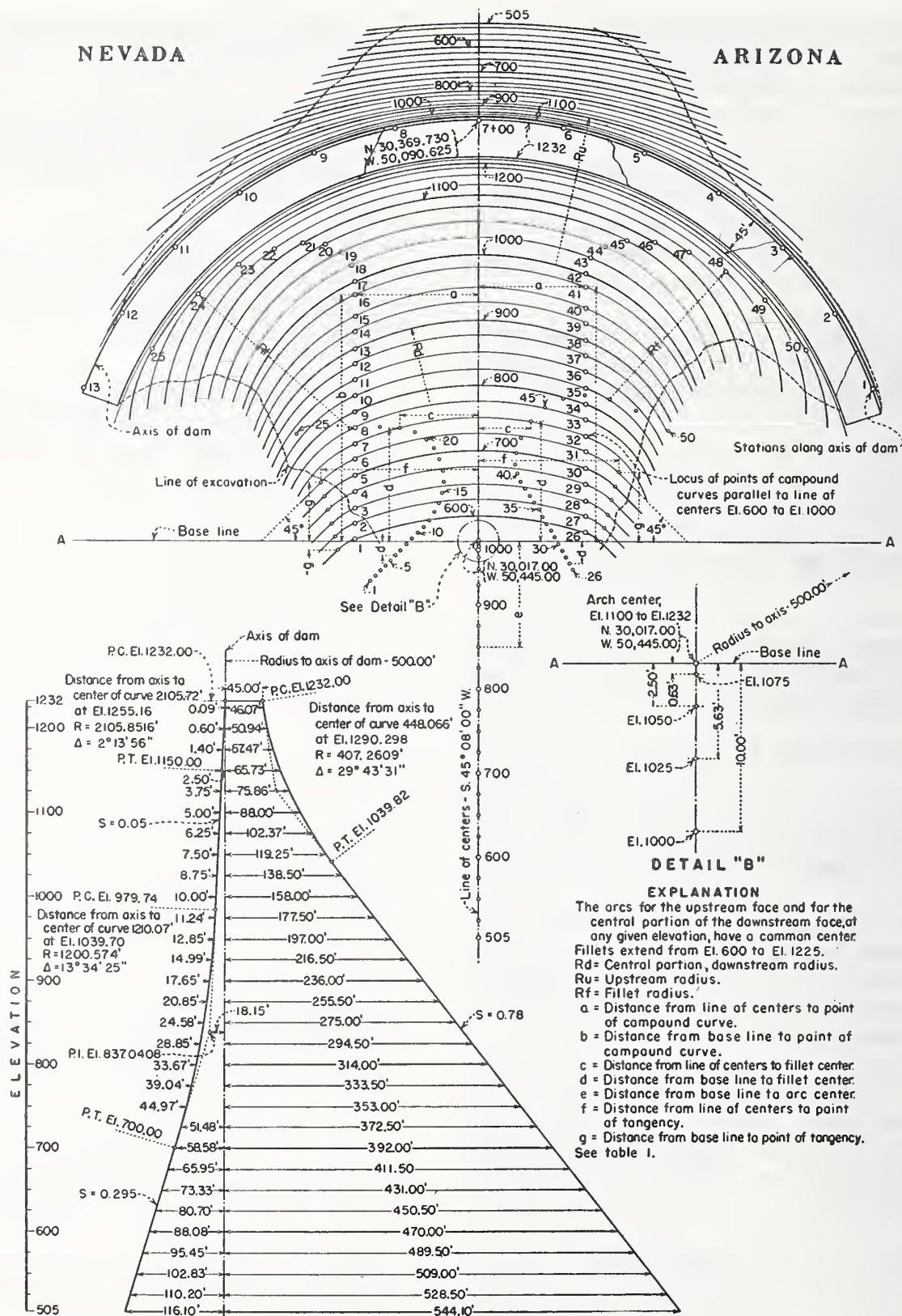


Figure 1 - Plan and Section of Hoover Dam
(reprint from Boulder Canyon Project - Final Reports - 1941)

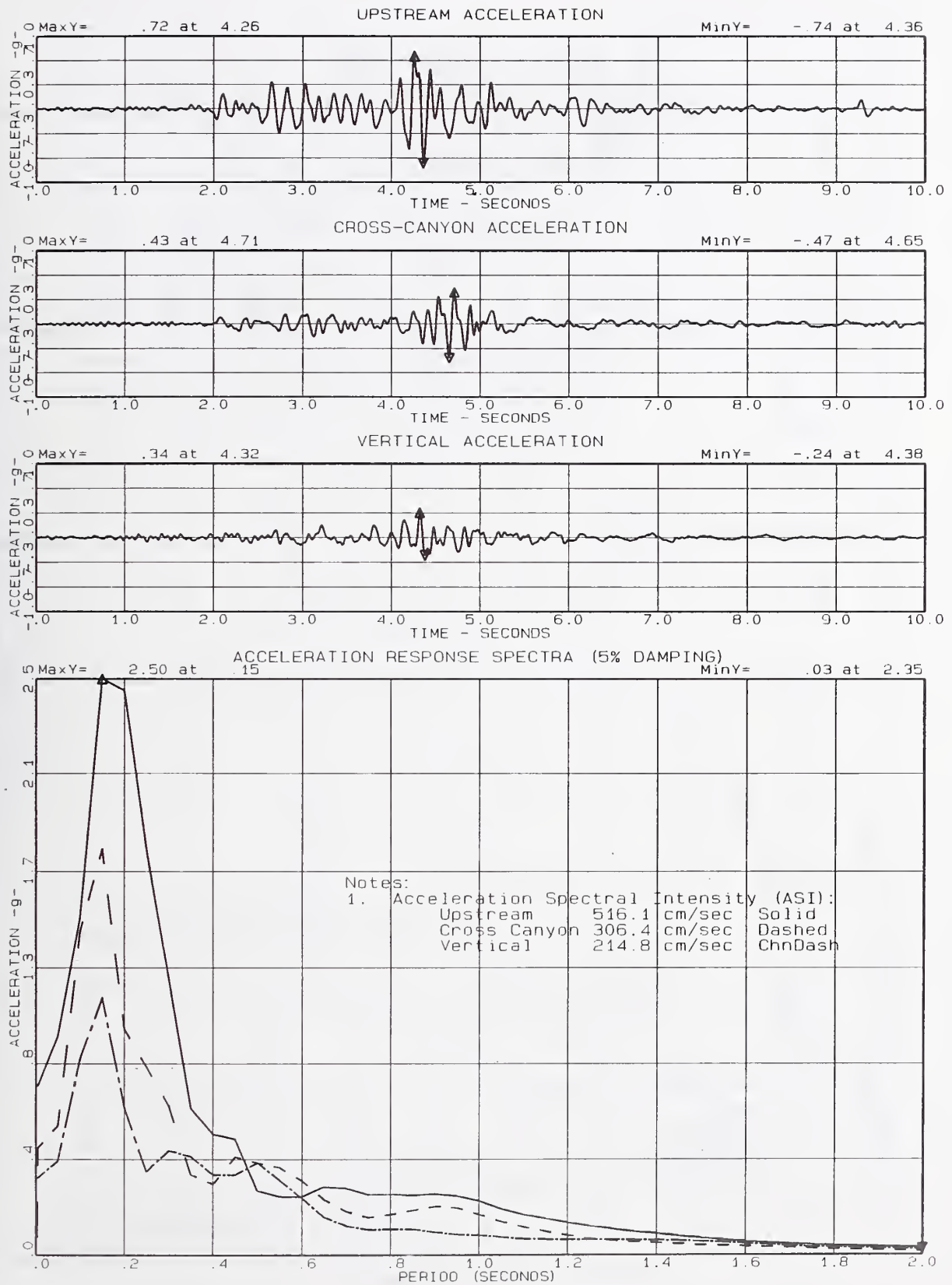


Figure 2 - Convict Creek Accelerograms And Acceleration Response Spectra

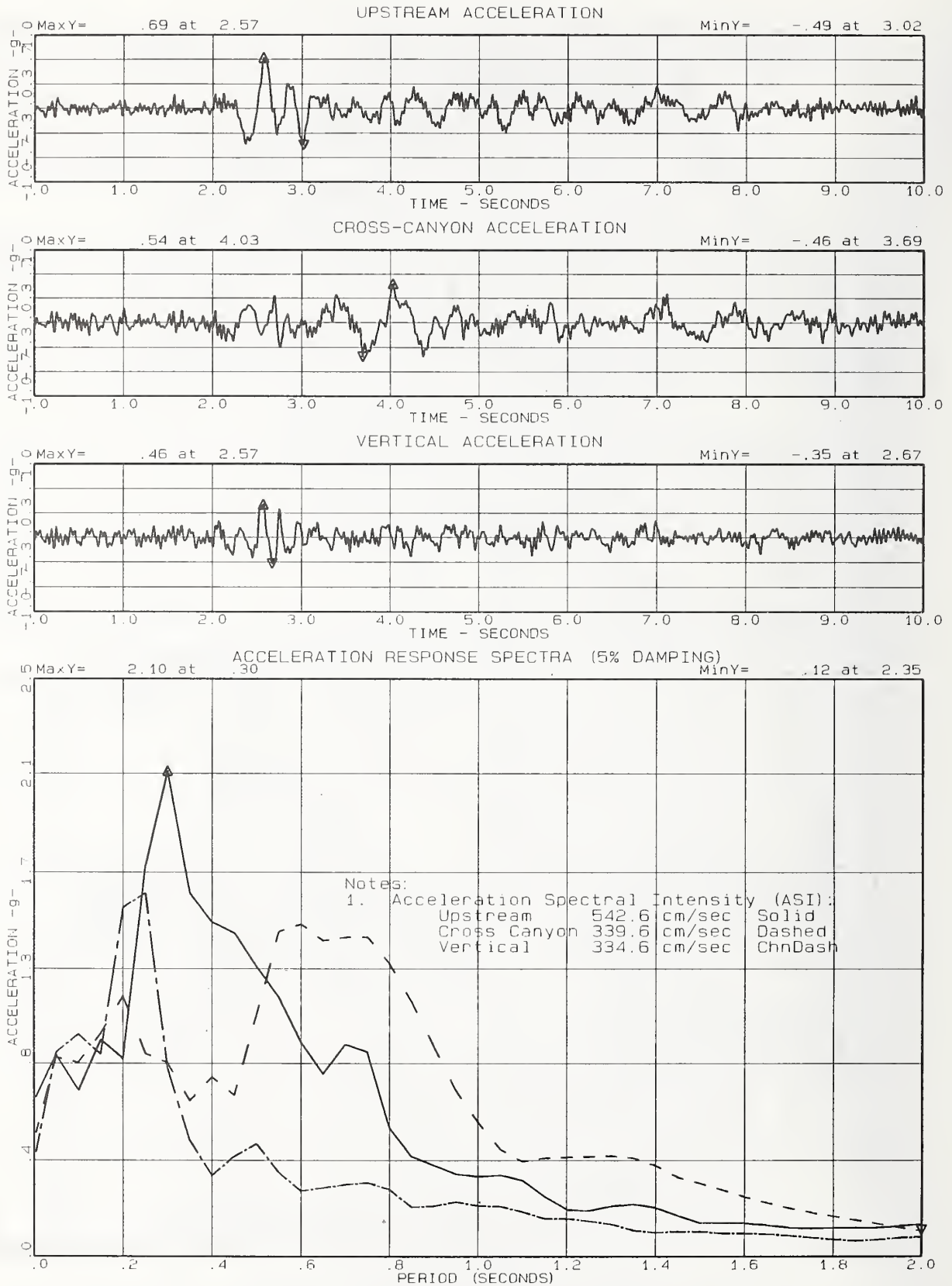


Figure 3 - Corralitos Accelerograms And Acceleration Response Spectra

DIRECT SHEAR TEST ALL LIFT LINE SPECIMENS

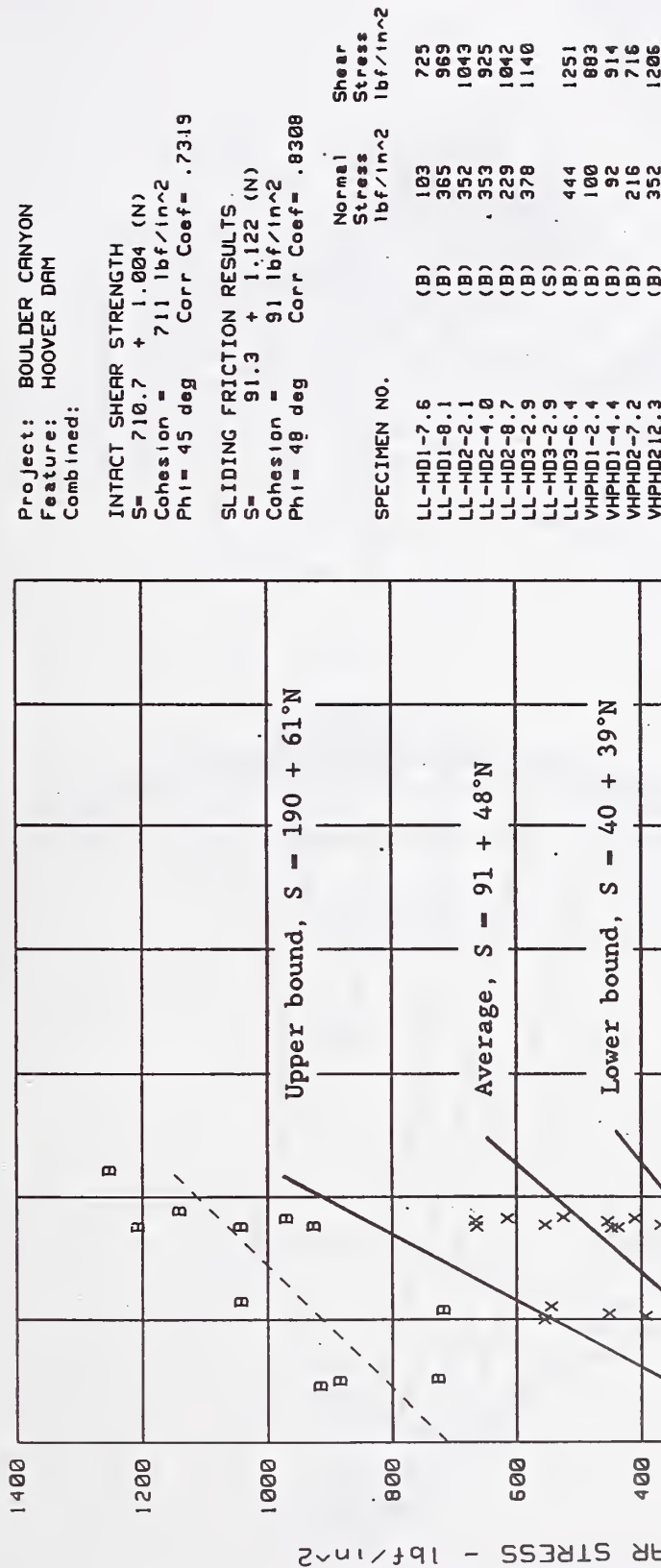


Figure 4 - Tested Shear Properties On Extracted Concrete Core

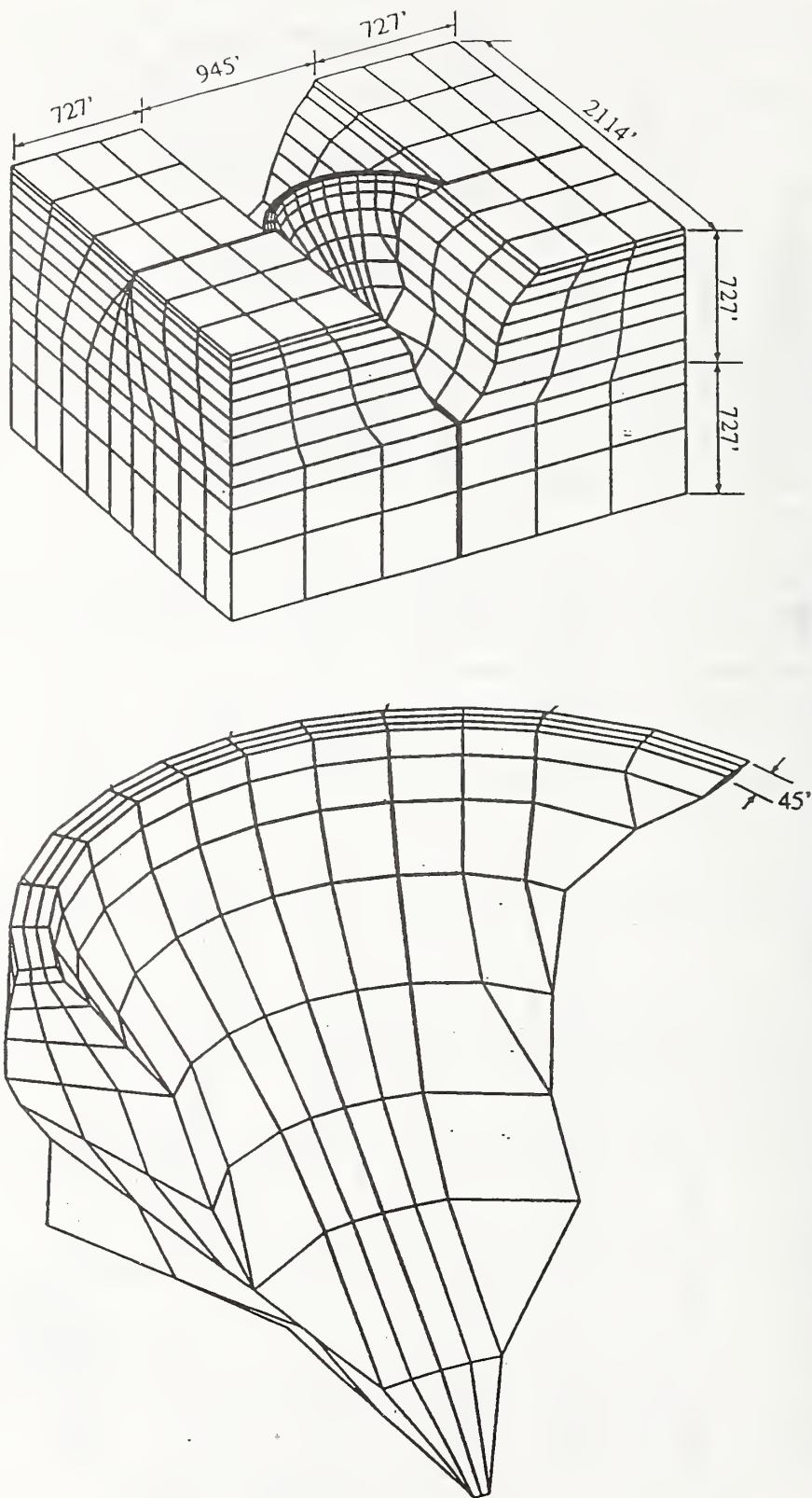
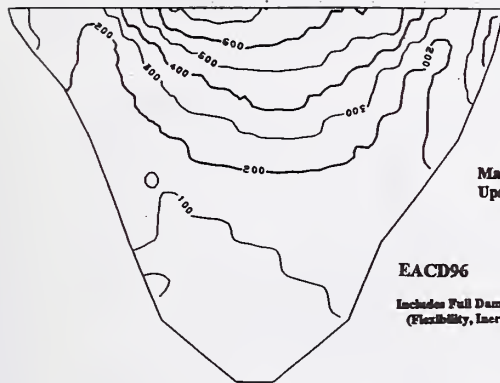


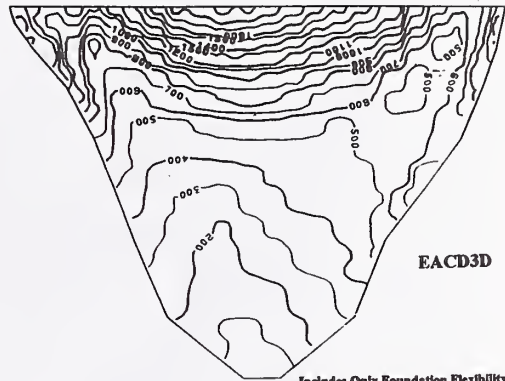
Figure 5 – Finite Element Model Of Hoover Dam And Foundation



Max. ARCH Stresses
Upstream Face

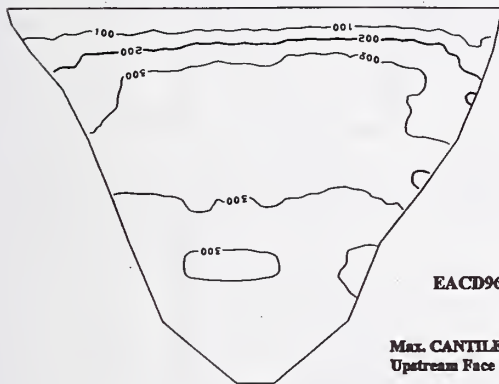
EACD96

Includes Full Dam-Foundation Interaction
(Flexibility, Inertia, and Damping)



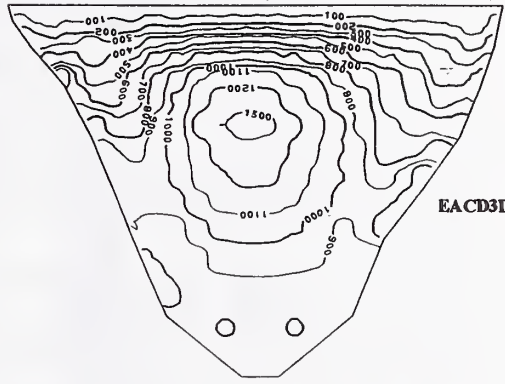
EACD3D

Includes Only Foundation Flexibility Effects

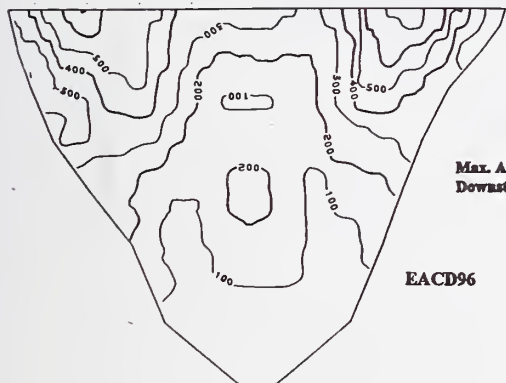


EACD96

Max. CANTILEVER Stresses
Upstream Face

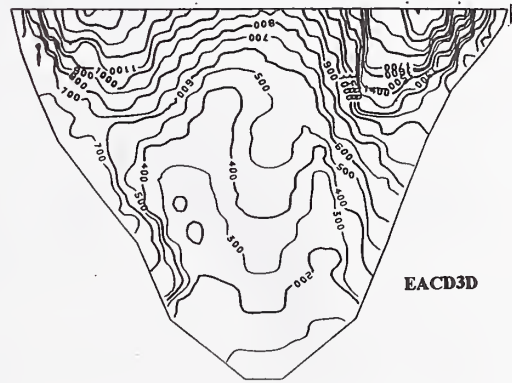


EACD3D

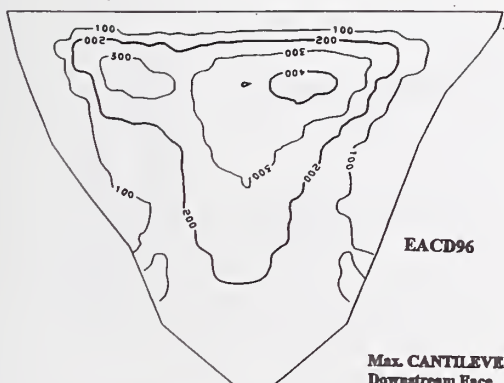


Max. ARCH Stresses
Downstream Face

EACD96

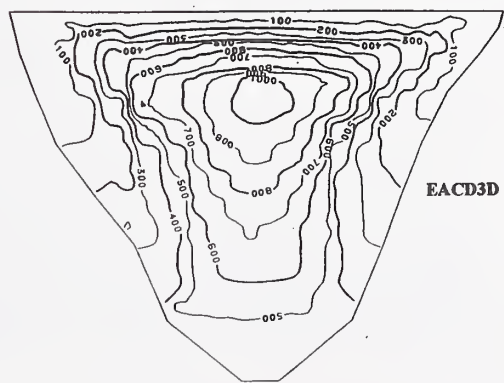


EACD3D



EACD96

Max. CANTILEVER Stresses
Downstream Face



EACD3D

Figure 6 – Comparison of Maximum Arch And Cantilever Stresses
With Foundation Mass And Without Foundation Mass

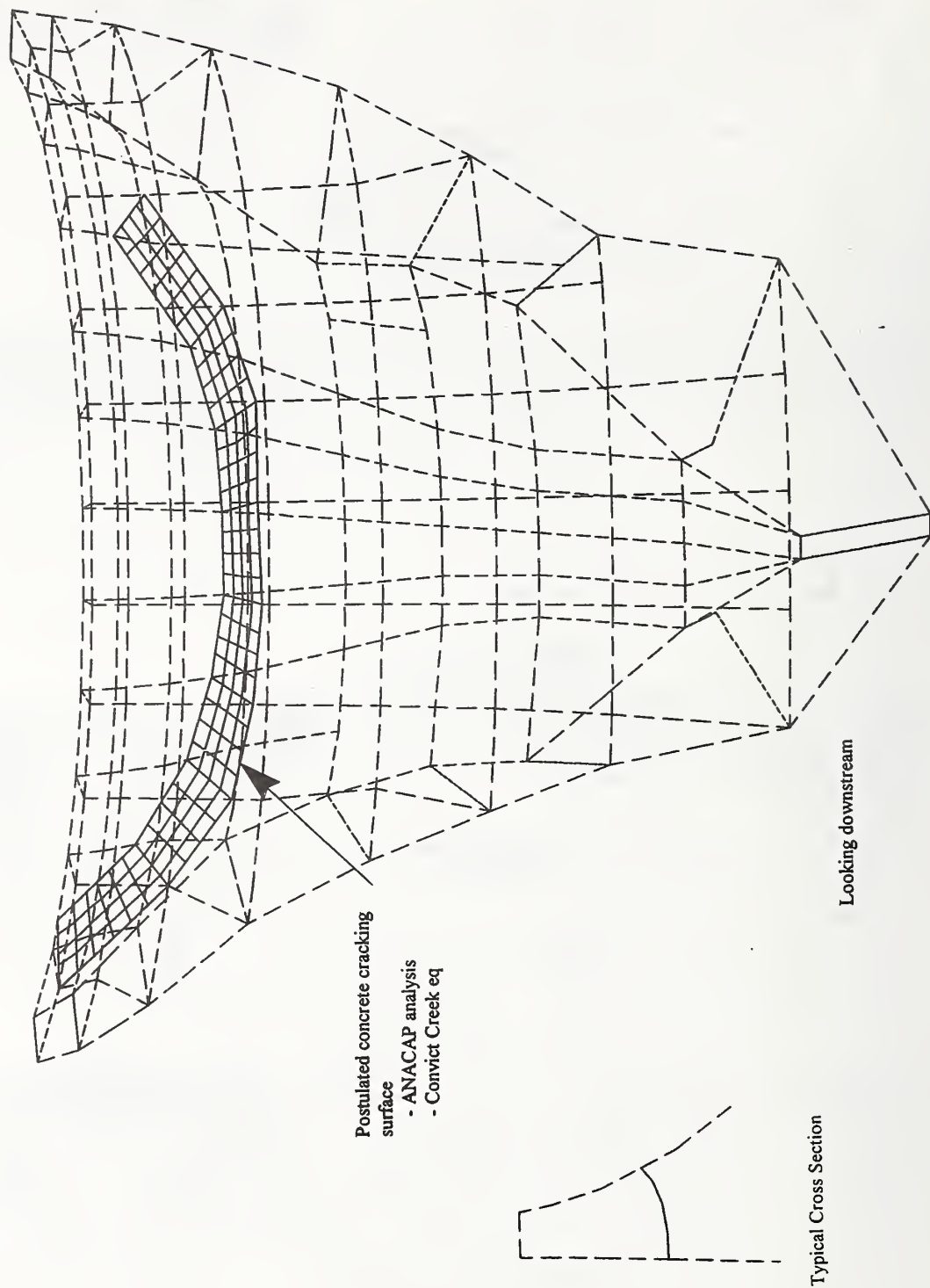


Figure 7 – Postulated Cracking Of Hoover Dam From A Non-linear Dynamic Analysis With A Massless Foundation

Inertial, Hydrodynamic & Static Reservoir Forces Values at top of dam

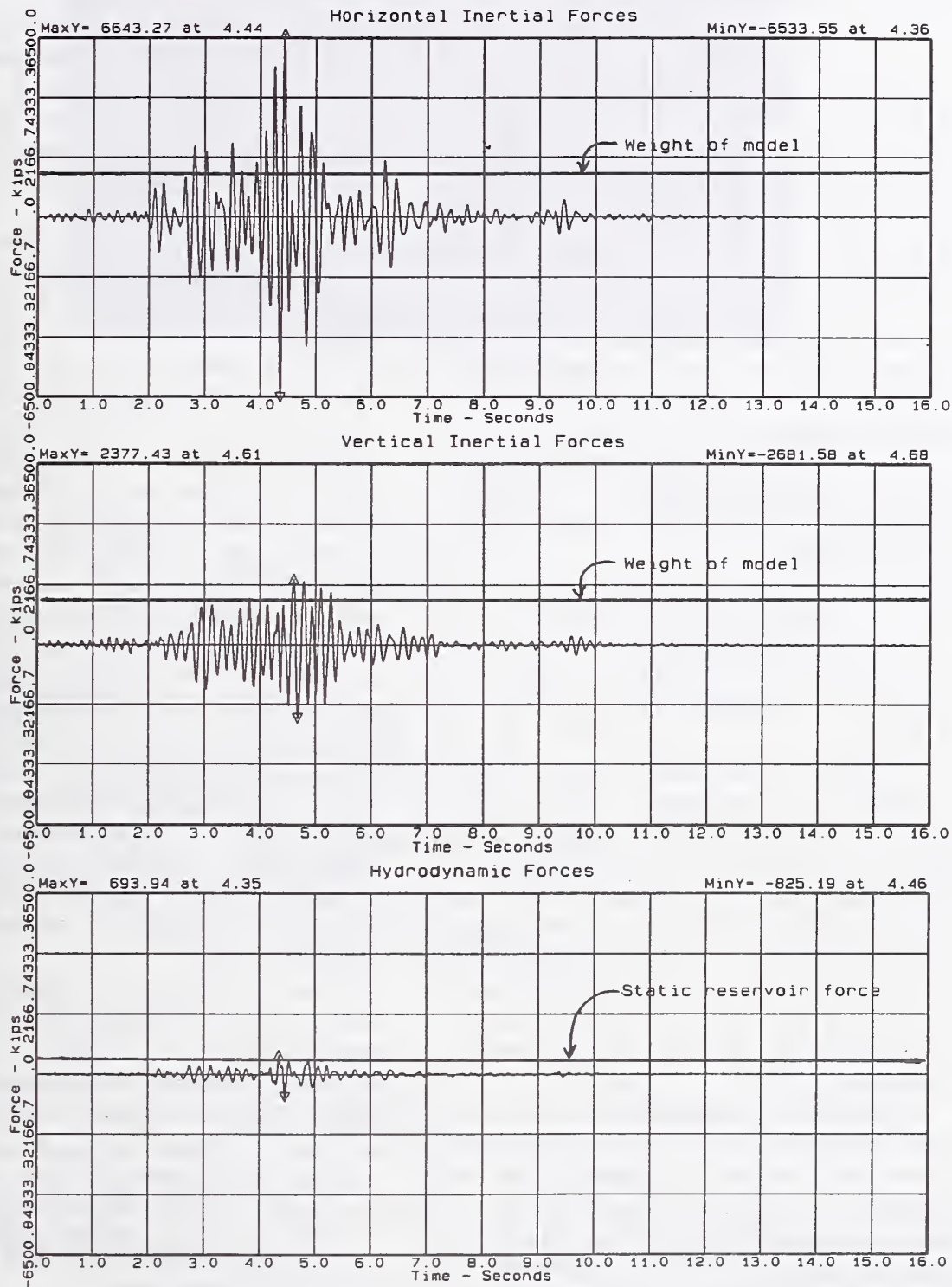


Figure 8 – Hydrodynamic And Inertia Forces At The Top Of Hoover Dam

Development and Operation of Large Centrifuge at PWRI

by

Osamu Matsuo¹⁾, Tatsuya Tsutsumi²⁾, Mitsu Okamura³⁾, Tetsuya Sasaki²⁾ and Kunio Nishi⁴⁾

ABSTRACT

A large geotechnical centrifuge with a radius of 6.6 m has been developed at Public Works Research Institute in 1997. For the purpose of the geotechnical earthquake studies, a powerful electro-hydraulic shaking table designed to work in the centrifuge has also been developed. This shaking table provides 40G shaking acceleration to a model of 1 ton, which acceleration is equivalent to the maximum ground acceleration observed during the 1995 Hyogoken Nanbu earthquake for a model at 50G centrifugal acceleration field.

The centrifuge has been under extensive use to investigate various geotechnical problem. Results of centrifuge tests carried out so far are briefly described.

*Key Words: Geotechnical Centrifuge,
Shaking Table, Model test
Retaining Wall*

1. INTRODUCTION

Public Works Research Institute (PWRI) constructed first geotechnical centrifuge with a radius of 1.25 m in 1961. With increasing needs of geotechnical earthquake studies, the second centrifuge with a radius of 2.0 m was introduced in 1987 with a shaking table having a capacity of 4G·ton. This centrifuge has been used to study various boundary value problems including soil liquefaction, seismic slope stability, soil improvement techniques, tunnel excavation, and so on.

The Hyogoken Nanbu earthquake, January 17, 1995, that hit the densely populated area caused devastating damages to human lives and properties. It also demonstrated various earthquake geotechnical problems. Immediately after the quake, PWRI, the Ministry of Construction headquarters and the Government

decided to construct a new centrifuge with a shaker which can simulate strong ground motion observed in the past earthquake. PWRI initiated basic and detailed design works in May, 1995. Construction of the centrifuge and the enclosure started in March, 1996 and completed in March, 1997.

In this paper, notable features of the centrifuge are described in detail and results of dynamic centrifuge tests on retaining walls are also discussed.

2. CENTRIFUGE SPECIFICATIONS

The centrifuge that has been newly installed at PWRI is the largest centrifuge in Japan, with a effective radius of 6.6m and maximum payload of 2.7 tons at up to 150G (400G · ton). A photograph and a schematic illustration of the centrifuge are shown in Fig.1 and 2, respectively. Notable specifications are summarized in Table 1. The main parts of the centrifuge are housed in an underground reinforced concrete pit, 17.0 m in diameter and 4.6 m deep. A pair of hydraulic jacks is installed at one side of rotation arm. When the platform swing up, these jacks push the swing platform to sit on the end plate of the arm so that strong earthquake motions can be simulated by fixing the swing platform to the rigid rotating arm. This is called "Touch-down System" (Nagura et al. 1994).

In order to eliminate the imbalance moment produced during spinning, a in-flight automatic balancing system is equipped. In-flight balancing is achieved by moving two balancing weights on the rotation arm. When the balance

-
- 1) Head, Soil dynamics division, Earthquake Disaster Prevention Research Center, Public Work Research Institute, Ministry of Construction, Tsukuba city 3050804, Japan
 - 2) Research Engineer, ditto
 - 3) Senior Research Engineer, ditto
 - 4) Research Engineer, Technical Institute, Hazama Corporation, Tsukuba city, Japan



Fig.1 Photograph of the centrifuge

Table 1 Specification of centrifuge

Effective Rotor Radius	6.6 m
Maximum Acceleration	static test : 150 g dynamic test : 100 g
Payload Weight	5 ton
Payload Capacity	400 g-ton
Swing Platform	static test : 2 dynamic test : 1
Platform Space	length : 2.4 m width : 1.3 m height : 1.0 m
Data Acquisition	static test : 100 ch dynamic test : 80 ch

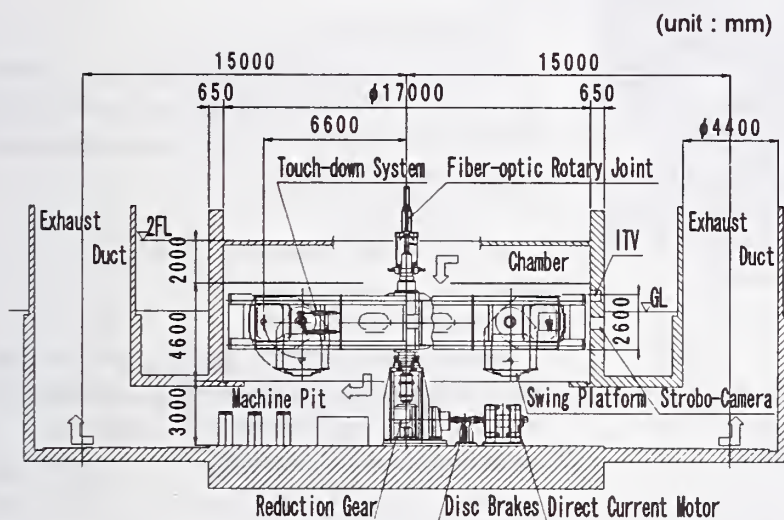


Fig.2 Schematic view of centrifuge

of the arm is lost and the horizontal displacement of the rotating axis measured with a gap sensor becomes large, the imbalance error signals are delivered and the weights are moved. The auto-balance capacity is 5 % of the maximum payload, that is 20G·ton.

3. DETA ACQUISITION AND MONITORING SYSTEM

(1) Rotary Joints

The centrifuge is equipped with rotary joints through which fluids can be sent to the platform. There are a total of 8 passages, with 6 rotary joints for oil and 2 rotary joints for either water or air.

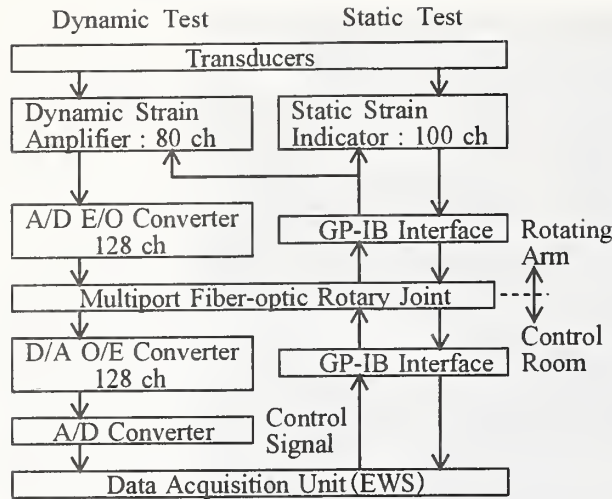


Fig.3 Flow of data acquisition

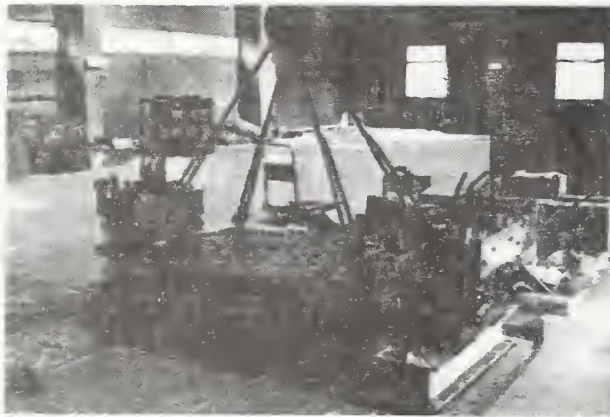


Fig.4 Photograph of Shaking table

Table 2 Specification of shaking table

Table Size	length : 1.7 m width : 1.0 m
Shaking Direction	horizontal : 1
Type of Shaking Wave	sinusoidal wave irregular wave
Maximum Centrifugal Acceleration	100 g
Maximum Shaking Acceleration	40 g
Maximum Velocity	90 cm/s
Maximum Displacement	±5 mm
Capacity	40 g-ton
Frequency Range	10 - 400 Hz

The capacity of working pressure is 10 MPa for oil and 0.7 MPa for water or air, respectively.

(2) Data Acquisition System

A diagram of the data acquisition system is shown in Fig.3. For dynamic tests, the analogue signals from transducers are amplified, digitized and converted into optical signals through the electro-optic converting unit mounted on the arm. Through the multiport fiber-optic rotary joint, the data are sent to the optic-electric converting unit in the control room and recorded on the internal disk of a workstation. For static tests, the signal outputs of transducers are recorded on the static strain indicator on the rotating arm. The data are sent to the workstation through the GP-IB interfaces. The dynamic strain amplifier and the static strain indicator are controlled from the workstation through the GP-IB interfaces.

(3) Monitoring System

Photographs and video images of a model on the swing platform in-flight can be taken with the strobo-camera and the CCD camera mounted on the arm, respectively.

4. SHAKING TABLE

(1) Specifications

An electro-hydraulic shaking table shown in Fig.4 has been developed. Specifications of the shaking table are shown in Table 2. The capacity of the shaking table is as large as that of the shaker at UC Davis (Kutter et al. 1994) which is the largest in the world. The shaking table provides horizontal acceleration of 40G to a model of 1 ton. For the tests conducted at 50G, horizontal acceleration of 40G is equivalent to the maximum ground acceleration observed during the 1995 Hyogoken Nanbu earthquake.

(2) Earthquake Simulation System

The earthquake simulation system is composed of the excitation device, the hydraulic supply system, and the control system as shown in Fig.5.

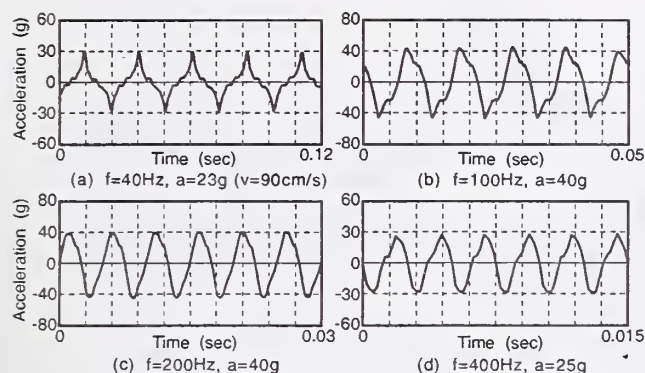


Fig.9 Recorded response acceleration-time history

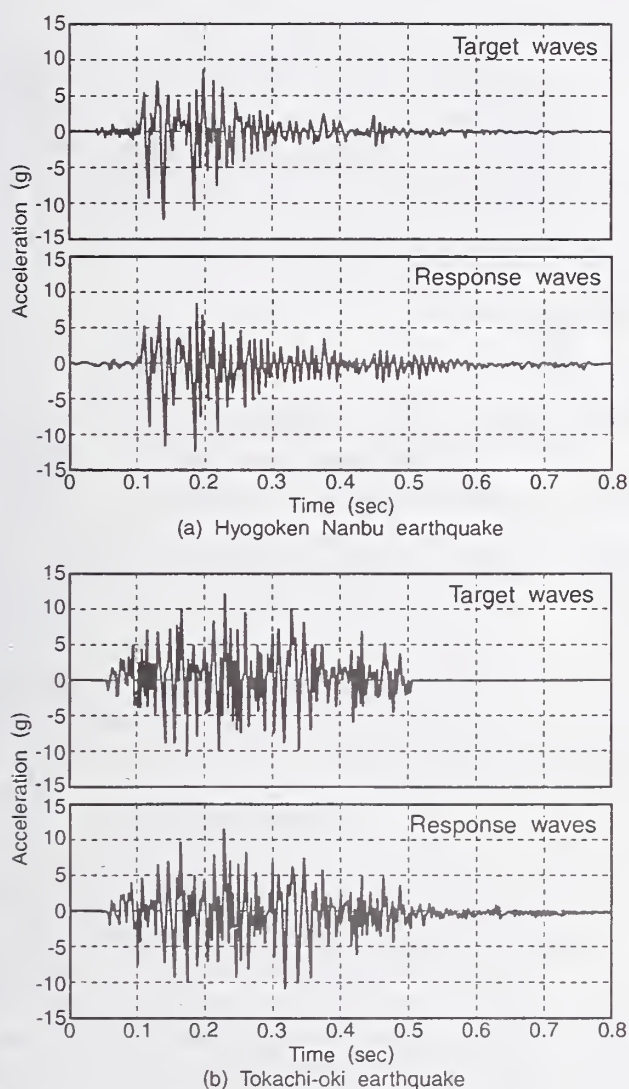


Fig.10 Comparison between target waves and response waves

extremely high frequency.

Next, two earthquake waves were used under 30G: the NS component of the Kobe Marine Observatory acceleration record in the 1995 Hyogoken Nanbu earthquake (Kobe wave), and the EW component of the Aomori Harbor acceleration record in the 1968 Tokachi-oki earthquake (Aomori wave). Each of the target waves was scaled so that the maximum acceleration was 12 g and the predominant frequency became 60 Hz. In Fig.10 the response acceleration waves of the shaking table with a weight of about 1.4 ton are compared with the target earthquake waves. These input waves were corrected with the excitation control system. Figure 11 shows that the response waves almost coincides with the target waves.

6. DYNAMIC CENTRIFUGE TEST

Several series of tests, aiming at investigating seismic behavior of huge bridge foundations on weak rock, retaining walls and embankment, and lateral spreading of liquefiable sand behind quay walls, were conducted in the centrifuge so far. Among them, results of tests on the retaining wall are briefly described in this section.

(1) Test procedures and conditions

In a rigid container with an internal dimensions of 150cm long \times 50cm deep \times 30cm wide, dry Toyoura sand was rained to form dense foundation soil of 10cm deep with relative density of approximately 80%. A model gravity retaining wall with a height of 30cm was placed on the foundation soil and the sand was rained again to build backfill behind the wall. The sand was rained intermittently so that accelerometers were set at the predetermined positions in the model. Configurations of various sensors in the model are shown in Fig.11. On the bottom and side of the model, a total of ten load cells which could measure normal and shear forces were built in.

Test conditions are summarized in Table 3. Relative density of the backfill was approximately

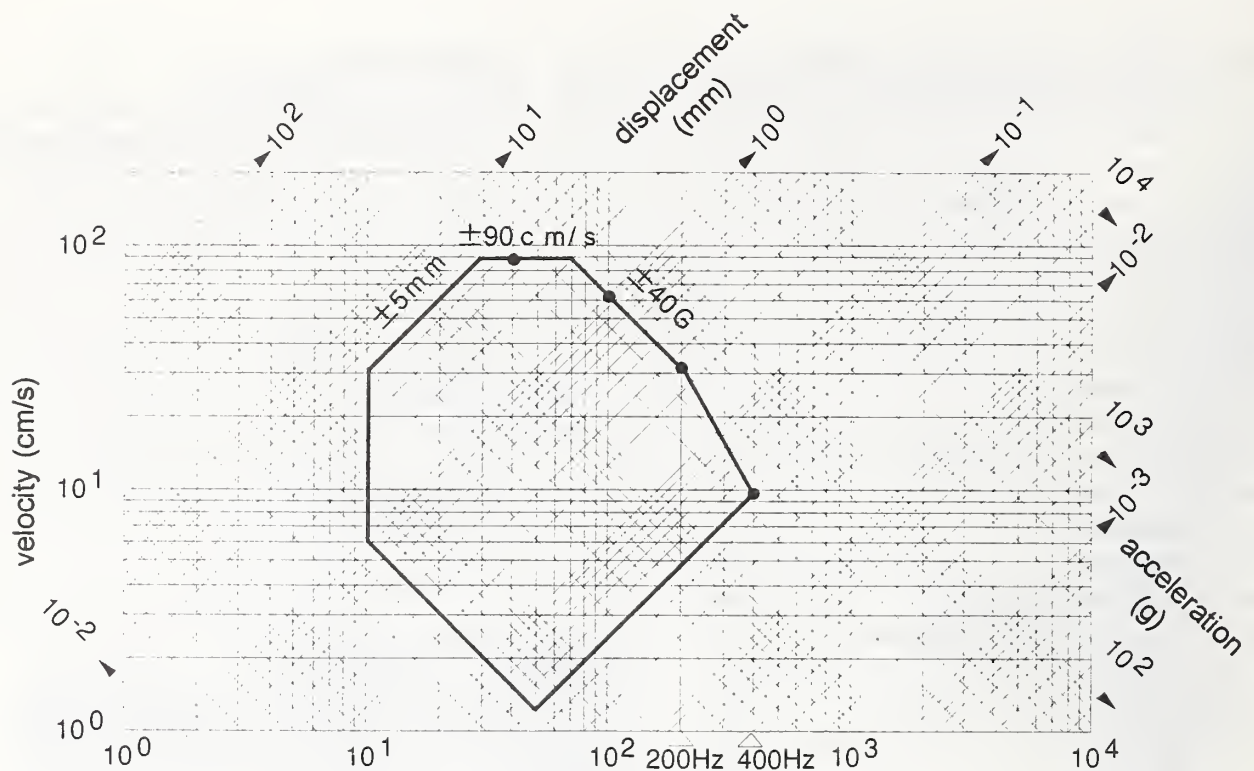


Fig.8 Shaking limit diagram

- The torque motor swings the armature according to the current.
- The pilot spool is driven up and down by the swing of armature.
- The quantity and the direction of oil supplied to a main spool are controlled by the movement of the pilot spool, and the main spool is driven right and left.
- The quantity and the direction of oil supplied to the actuator are controlled by the movement of the main spool, and the actuator is moved right and left.
- The excitation power is transmitted to the shaking table.

b) Hydraulic supply system

When dynamic tests are performed, it is necessary to supply a large amount of pressurized oil to the excitation device. Therefore, the oil is supplied continuously from the hydraulic pump in the machine pit to the accumulator on the rotation arm through the rotary joints.

c) Excitation control system

The excitation control system consists of the signal generation unit and the servo control unit. The control signal is transferred to the excitation device through the optical rotary joint. The signal generation device has the functions to generate input signal and to correct the input signal so as to adjust response waves to target waves according to the feedback signal from the excitation device.

5. PERFORMANCE

In order to check the performance of the shaking table, proof tests were carried out. At first, sinusoidal input acceleration was tested at 100G. Several points on the shaking limit line shown in Fig.8 were selected. Figure 9 shows the response acceleration time-histories of the shaking table with a model of some 400 kg fixed on it at frequencies of 40, 100, 200, 400 Hz. The figure indicates that response waves were distorted in the case of large displacement or

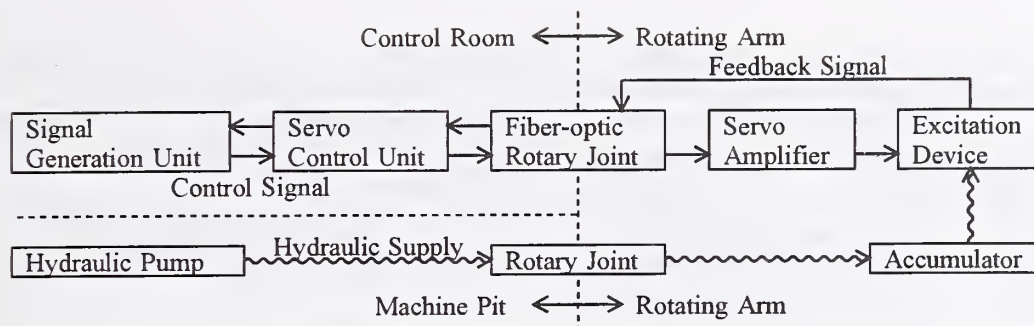


Fig.5 Earthquake simulation system

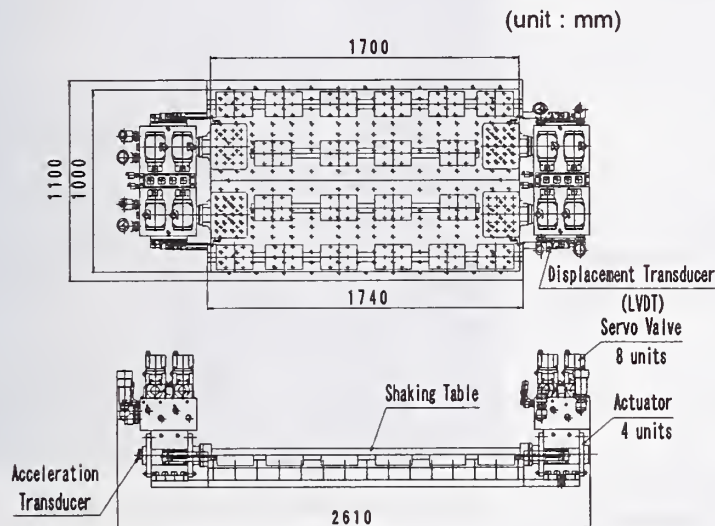


Fig.6 Plan and side view of shaking table

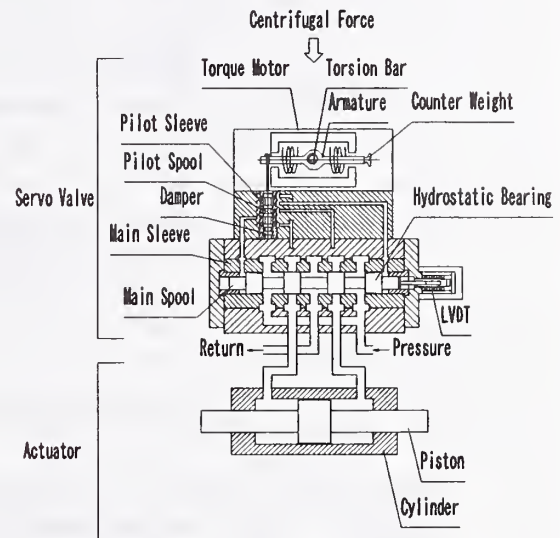


Fig.7 Schematic view of Actuator and servo valve

a) Excitation device

As shown in Fig.6, the excitation device is designed symmetrically. Two actuators which have two servo valves in each are arranged on both sides of the shaking table. In order to measure the displacement of actuators and the acceleration of shaking table for the control, LVDTs and accelerometers are put on the shaking table.

Figure 7 shows the structure of the actuator and the servo valve. The servo valve is composed of a large-scale torque motor, a pilot spool and a main spool, and controls the quantity and the direction of flowing oil to the actuator according to the movement of a main spool. In order to make the excitation capacity larger, it is necessary to

supply a large quantity of flowing oil to the actuator. Therefore the diameter of the main spool become large, and the pilot spool is installed in order to drive the main spool hydraulically. The pilot spool hangs on the one end of armature in the direction of a centrifugal acceleration, and the counter weight is put on the opposite end. As a result, an unbalanced torque caused by the self-weight of the pilot spool and a friction torque by the vertical motion is deduced. The movement of the servo valve and the actuator is controlled along the following operation.

- The signal from the servo control unit is converted to the electric current by the servo amplifier, and the current is input to the torque motor.

Table 3 Test conditions

Test code	Relative density of backfill	Input motion	Max. acceleration tested (gals in prototype scale)	Centrifugal acceleration
Case1	82%	Sinusoidal	60, 95, 176, 288, 309, 353, 418	30G
Case2	61%	Sinusoidal	77, 198, 305, 450	
Case3	82%	Kobe wave	207, 262, 382, 481, 571, 600, 747, 823	
Case4	83%	Aomori wave	150, 173, 288, 358, 437, 498, 590	
Case5	83%	Sinusoidal	341, 424	

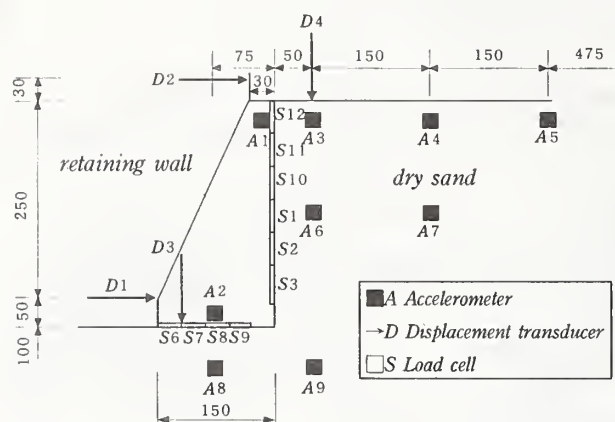
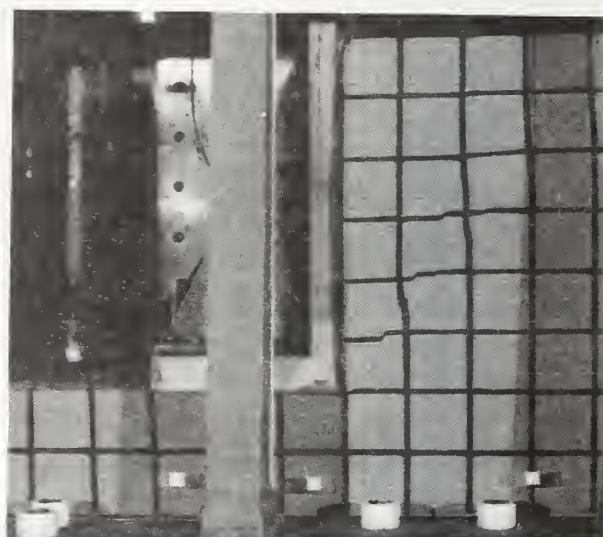


Fig.11 Model retaining wall

80% with an exception for Case2 where sand was prepared in the medium dense condition(61% relative density). All the tests being carried out at 30G centrifugal acceleration field, the models are equivalent to prototype walls of 9m high. The models were excited horizontally with approximate sinusoidal wave with 30 uniform cycles of predominantly 60Hz acceleration for Case1, 2 and 5, Kobe wave for Case 3 and Aomori wave for Case 4. The time axis of the acceleration time histories of the two earthquake records were scaled so that predominant frequency becomes 60Hz. Shaking test was repeated several times for each model, with increased maximum acceleration α_m ; for Case 1, for instance, 30 cycles of sine wave was applied for every step, with $\alpha_m = 1.99G$ (65 gals in prototype) for the first step, $\alpha_m = 2.76G$ (90 gals) for second step, and so on.

(2) Results and discussions

In the following discussion, test results are



(a) after first shaking (341 gals)



(b)after second shaking (424 gals)

Fig.12 Deformation of wall and backfill with clear slip surfaces (Case5)

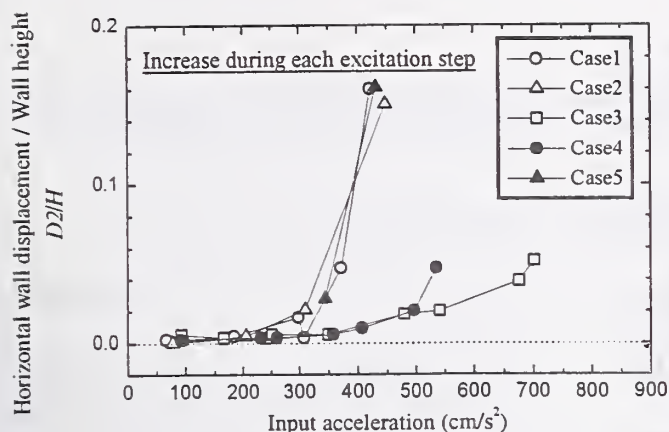


Fig.13 Variation of horizontal displacement increment versus input base acceleration

shown in the prototype sense otherwise mentioned; measured acceleration and frequency in the models are divided by a factor of 30. Figure 12 shows photographs taken after shaking tests with $\alpha_m = 341$ gals and 424 gals in Case 5. It can be clearly seen in Fig.12(a) that the wall slid outwards and rotated counterclockwise and an active wedge with apparent slip surface developed in the back fill after shaking event of $\alpha_m = 341$ gals. The angle of the slip surface to the vertical agrees well with that predicted from well-known Mononobe-Okabe approach (Mononobe and Matsuo, 1929; Okabe, 1924) in conjunction with peak input acceleration and an angle of shearing resistance of the sand of 45 degree. After the shaking test with $\alpha_m = 424$ gals another slip surface with gentle slope was formed as shown in Fig.12(b), as was predicted by Mononobe-Okabe approach.

Horizontal displacement increment of the top of the wall during each step divided by the wall height is plotted against α_m in Fig.13. For cases with sinusoidal wave, that is Case 1, 2 and 5, it was observed that there is a threshold acceleration of approximately 300gal below which displacement of the wall was less than 1% of the wall height and no slip surfaces developed during shaking. In the step with α_m higher than the threshold acceleration the model wall displaced largely and apparent slip surfaces were observed. This fact is consistent with results of a

detail study by Bolton (1991) that active conditions are reached by outward movement of the order of 0.1% of the wall height in dense sand.

For Case 3 and 4, in which Kobe wave and Aomori wave were used, slip surfaces were observed after shaking step with $\alpha_m = 571$ gals and 498 gals respectively, and deformation of the walls did not largely increase in the subsequent step. This may be due to the fact that earthquake waves used in this study, in particular Kobe wave, had only several cycles of large acceleration, while 30 cycles of the maximum acceleration for the sinusoidal wave. It should be noted in Fig.13 that displacement of the test with Aomori wave (Case 4) was larger than that with Kobe wave (Case 3). These observation confirms that many cycles with smaller peak acceleration contained in the real earthquake waves had little contribution to accumulate the deformation of the retaining walls.

The exact level of earthquake design of the retaining wall is uncertain, however, it is apparent that the threshold acceleration observed for Case 3 and 4, that is 571 gals and 498 gals respectively, was considerably in excess of any code requirement. This may indicate that displacement-based design approaches are needed.

The results presented in this section are part of ongoing project. Authors have been validating the Newmark's sliding block approach as a displacement based design method of retaining walls (Steedman, 1998) by comparing with test results.

REFERENCES

- Kutter, B. L., Idriss, I.M., Khonke, T., Lakeland, J., Li, X.S., Sluis, W., Zeng, X., Tauscher, R.C., Goto, Y. and Kubodera, I. 1994. Design of a large earthquake simulator at UC Davis. Proc. Int. Conf. Centrifuge 94, Singapore. Balkema: 169-175.
- Nagura, K., M. Tanaka, K. Kawasaki & Y. Higuchi 1994. Development of an earthquake simulator for the TAISEI centrifuge. Proc. Int. Conf. Centrifuge 94, Singapore. Balkema: 151-

- Mononobe N. and Matsuo H. 1929. On the determination of earth pressure during earthquakes, Proc World Engng. Congress, Vol.9, pp.177-185
- Okabe S. 1924. General theory of earth pressure, Journal of Japan Civil Engng Society, Vol.12, No.1
- Bolton M.D. 1991. Geotechnical stress analysis for bridge abutment design, Contractor report 270, Transport and Road Research Laboratory, Crowthorne, Berks.
- Steedman R.S. 1998. Seismic design of retaining walls. Proc. Institution of Civil Engineers, Geotechnical Engineering, Vol.131, pp.12-22

The Influence of Confining Stress on Liquefaction Resistance

by

M. E. Hynes, R. S. Olsen and D. E. Yule*

Abstract

Laboratory measurements typically indicate that for a given soil, consistency (relative density for sands and gravels) and stress history there is a non-linear relationship between liquefaction resistance and confining stress (Seed and Idriss 1981; Seed 1983; Seed 1984; Vaid, Chern & Tumi 1985; Seed 1987; Hynes 1988; Harder 1988; Seed & Harder 1990; Pillai & Byrne 1994; Youd & Idriss 1998). Consequently, if cyclic strengths, either from laboratory measurements performed at a confining stress of 1 atm or estimated from correlations to in situ measurements such as Standard Penetration Tests (SPT), are linearly extrapolated to higher effective confining stress levels, the calculated liquefaction resistances may be too high. The effect of confining stress on liquefaction resistance is further complicated by soil compressibility and stress history.

The state-of-the-practice approach to account for the non-linear relationship between liquefaction resistance and vertical effective stress is to use published charts derived from existing laboratory data on similar materials or to determine a site specific relationship with a comprehensive laboratory testing program. Whichever approach is used, liquefaction resistance is conventionally represented as the Cyclic Resistance Ratio (CRR, the ratio of cyclic shear strength divided by the vertical effective stress, σ_v'). For a given soil at a given consistency and stress history, the CRR generally decreases with increasing vertical effective stress. This decrease is

described by the factor K_o which is defined as the ratio of CRR for a given σ_v' to the CRR at a vertical effective stress of 1 atm, CRR_1 (compared at the same relative density).

1. Introduction

The use of laboratory tests to establish CRR_1 for a material has decreased over the last decade in favor of in situ test correlations because of the cost-effectiveness of in situ measurements, the robustness of the Seed SPT-liquefaction chart (Seed et al. 1985, Youd and Idriss 1998), and concerns over sample disturbance and other issues associated with laboratory test results. The CRR_1 can be determined from in situ measurements such as the SPT, Cone Penetration Test (CPT), or shear wave velocity (V_s), or from laboratory measurements. The state-of-the-art for estimating CRR_1 using the SPT is given by Seed et al. (1985); using the CPT is given by Stark et al. (1995) or Olsen, Koester and Hynes (1996); and using V_s is given by Andrus and Stokoe (in Youd and Idriss 1998). The data base for these CRR_1 correlations consists of information from water-laid deposits of sands and silty sands, level to slightly sloping ground, under vertical effective stresses of less than 3 atm. Consequently, laboratory tests have been used to provide a relative scale to adjust the

*Earthquake Engineering and Geosciences Division, Geotechnical Laboratory
USAE Waterways Experiment Station
Vicksburg MS 39180-6199

CRR₁ values from in situ tests to higher confining stress levels and non-level ground stress conditions. The purpose of this study was to review and report the current state of knowledge with respect to the influence of overburden stress on liquefaction resistance.

2. Historical K_o Data and Charts

Seed and Idriss (1981) to Seed and Harder (1990)

Early tests on sands and silty sands indicated considerable scatter in the values of K_o . These data, summarized in Figure 1 and taken in part from Harder (1988), include Sacramento River sand (Lee 1965), Monterey No. 0 and Reid-Bedford sands (Townsend and Mullulis 1976), Upper and Lower San Fernando Dams (Seed et al. 1973) and Fort Peck Dam (Marcuson and Krinitzsky 1976). Superimposed on Figure 1 is an early K_o relationship suggested by Seed and Idriss (1981). As more data became available, the K_o chart was updated by Seed (1984 and 1987), Harder (1988), and Seed and Harder (1990), shown in Figure 3.

Upper and Lower San Fernando Dams, Seed et al. (1973) and Seed et al. (1989)

Seed et al. (1973) and Seed et al. (1989) report the results of cyclic triaxial tests on undisturbed samples of silty sand and sandy silt from the Upper and Lower San Fernando Dams (USFD and LSFD). LSFD came within inches of being overtopped after an upstream slide developed in the dam as a result of the 1971 San Fernando earthquake. USFD settled 3 ft and moved about 5 ft downstream, but did not fail; if it had failed,

the downstream dam would also have been breached. This event resulted in the evacuation of 80,000 people immediately downstream of the two reservoirs.

Construction of LSFD began in 1912, and construction of USFD began in 1925. The method of construction was hydraulic fill, resulting in an in situ relative density of about 55 percent. Seed et al. (1973) and Seed et al. (1989) observed that the cyclic strength was about the same for the silty sands and sandy silts; the method of deposition resulted in a consistency that now had a uniform cyclic strength, although the material type changed. Comparison of the cyclic strength interpreted from SPT correlations was very similar but slightly greater than the strength determined from the undisturbed specimens of the hydraulic fill (Figure 4).

Fort Peck Dam, Marcuson and Krinitzsky (1976)

Marcuson and Krinitzsky (1976) report the results of cyclic triaxial tests on undisturbed and reconstituted (wet pluviation) samples of hydraulic fill and foundation soils from Fort Peck Dam. Construction of Fort Peck Dam began in 1934. Relative densities determined in the laboratory resulted in values of about 40 to 50 percent, rather than the 70 percent average value indicated from the Gibbs and Holtz relationships for corresponding blowcounts. Marcuson and Krinitzsky (1976) made a comparison of the cyclic strength of undisturbed and reconstituted specimens at a confining stress of 8.3 psi (0.57 atm). These data indicate that the cyclic strength of the undisturbed specimens was about 80 (foundation material) to 150 (shell material) percent greater than for reconstituted specimens.

Sardis Dam, U.S. Army Engineer District, Vicksburg (1985, 1988)

Sardis Dam is one of the three hydraulic fill dams owned by the Corps of Engineers. Reevaluation of the seismic stability of Sardis Dam began shortly after the near catastrophic failure of LSFD, in part because of its proximity to the New Madrid fault zone in Central U.S. Sardis Dam was constructed in the late 1930's. Material mixtures in the fill and foundation range from sands to silts to high-water-content, low-plasticity clays. The results of cyclic laboratory tests, conducted over the course of the reevaluation, were provided by U.S. Army Engineer District, Vicksburg, for inclusion in this study.

Olsen (1984)

Olsen (1984) generalized the data trends from the preliminary K_o relationship by Seed (1984), together with project data at WES into the following expression: $K_o = (\sigma'_v)^{f-1}$. Olsen (1984) reported that the stress exponent, f , ranged from 0.6 to 0.95 with 0.7 recommended for sands. This recommendation is similar to the updated Seed curves shown in Figure 2, and also bounds the data from Vaid and his colleagues described next.

Vaid et al. (1985), Vaid and Thomas (1994)

Cyclic strength, K_o for pluviated clean sands

Vaid et al. (1985) conducted cyclic triaxial tests on two fine, clean sands, well rounded Ottawa sand and an angular tailings material, to investigate the effects of relative density, compressibility, confining stress, and particle angularity on cyclic strength. CRR for confining stresses of 200, 800, 1600 and

2500 kPa were determined as a function of consolidated relative density. The samples were constructed by dry pluviation, and vibrated to increase density.

Vaid et al. (1985) observed that there are competing effects of increased confining stress; one is densification due to the compressibility of the material with increasing confining stress which has the effect of increasing CRR and the other is the curvature in the cyclic strength envelope which tends to decrease CRR as confining stress increases. If CRR values are compared at the same consolidated relative density, the data indicate a trend toward convergence of the cyclic strength curves, developed for different confining stresses, at lower relative densities. These data imply that K_o is approximately one for very loose materials, and increases as relative density increases. These data indicate that K_o for clean sands and silty sands have a limiting value of about 0.6 at a confining stress of about 8 atm. The cyclic triaxial test data from Vaid and Thomas (1994) on Fraser River sand (dry pluviated and vibrated specimens) follow a similar trend.

Stress focus plots of cyclic strength and CRR for pluviated clean sands

Trends and deviations in geotechnical data with confining stress are sometimes easier to see when the data are plotted in log-log plots. These log-log plots are termed stress focus plots from Olsen (1994). If data fit as a straight line on a log-log stress focus plot, then that data is well fitted by a simple exponential curve. Stress focus plots were used in this study as a framework for investigating confining stress effects on cyclic strength and CRR. The Vaid et al. (1985) and Vaid and Thomas (1994) data are plotted on stress focus charts (\log_{10} cyclic

strength plotted versus \log_{10} effective confining stress, atm) in Figure 5. This figure shows that at confining stresses of 400 kPa and greater, the cyclic strength envelope is well fitted with an exponential curve (plots as a straight line on a log-log plot).

These data follow the stress focus concept, namely that the cyclic strength curves for different relative densities tend to converge as confining stress increases. This point (or zone) of convergence is termed the stress focus. As shown by Olsen (1994), the location of the stress focus is a function of soil type and mineralogy. The slope of a line in a stress focus plot corresponds to the inverse of the exponent used by Olsen (1984) to describe K_o : $K_o = (\sigma'_v)^{f-1}$. Consider generalized stress focus cyclic strength lines for a very loose, medium dense and dense sand. As density increases, the cyclic strength at a confining stress of 1 atm, CRR_1 , increases. As density increases, the slope, $1/f$, of the stress focus cyclic strength line increases. The corresponding K_o curves are determined as: $K_o = (\sigma'_v)^{f-1}$. As density increases, the exponent f decreases and K_o decreases, resulting in a more severe reduction to CRR.

Gravelly Soils, Hynes (1988 and 1996)

Hynes (1988) conducted 15-in. diameter cyclic triaxial tests on moist tamped gravel specimens from Mormon Island Auxiliary Dam, constructed to relative densities of about 40 and 64 percent. Similar tests were conducted at WES on Ririe Dam gravels (Sykora et al. 1991) compacted to a relative density of about 45 percent, and Success Dam gravels compacted to a relative density of about 50 percent (U.S. Army Engineer District, Sacramento 1996). Banerjee et al. (1979) conducted tests on well-compacted Oroville Dam gravels (relative density of

about 84 percent, 12-in. diameter, specimens constructed in 6 layers with surface vibrator applied for compaction). Cyclic strengths for this study were compared at $N = 10$ load cycles.

Hynes (1996) observed that the cyclic strength envelopes for these gravels have an upward turn at low confining stress, less than 3 atm. Hynes (1996) proposed that this behavior is caused by a stress history that the sample construction process builds into the specimen, causing it to behave as an overconsolidated (oc) soil; oc material has greater axial and horizontal stiffness, is more resistant to volume change, and thus is more resistant to development of residual excess pore pressures when subjected to cyclic loading. In a stress focus chart, over-consolidation is indicated by a steepening of the cyclic strength line as confining stress decreases. Over-consolidation results in reduced values of K_o .

The K_o values interpreted from the gravel data depend upon how the CRR_1 is estimated (also the failure criterion used such as maximum pore pressure response and cyclic strain level, and membrane compliance corrections applied). The most conservative K_o values are obtained by straight-line projection of the cyclic strength-effective confining stress Mohr-Coulomb envelope to estimate CRR_1 . The resulting K_o values for Oroville gravels are: $K_o = 0.54$ at 2 atm and 0.2 at 8 atm confining stress. The most optimistic K_o values are obtained by ignoring the apparent "overconsolidated" data at 2 atm, and then projecting the cyclic strength envelope to the origin. This results in K_o values of 0.50 at 8 atm and 0.44 at 14 atm for Oroville gravels. The range of K_o interpretations for the gravel data collected in this study are plotted in Figure 6, with the Seed and Harder (1990) curve for reference.

Except for the most optimistic interpretations, these gravel data generally plot below the data for clean and silty sands (resulting in a more severe K_o reduction to CRR_1).

Byrne & Harder (1991), Pillai & Byrne (1994) and Pillai & Stewart (1994)

Byrne and Harder (1991) selected K_o values for clean sands from previous work to develop a recommendation for the clean sands and gravels present at Terzahgi Dam, Canada. Their data set included the work by Vaid and his colleagues at the University of British Columbia at Vancouver (UBC), as well as clean sand data from Seed and Harder (1990). This clean sand curve is plotted in Figure 7. Pillai and Byrne (1994) estimated K_o values for Duncan Dam foundation materials. At Duncan Dam, the foundation contains a water-laid unit of very fine sand ($D_{50} = 0.2$ mm) with 5 to 8 % fines (typical gradations shown in Figure 11a). Foundation soils were frozen in situ to extract high quality samples for laboratory testing. Pillai and Byrne (1994) and Pillai and Stewart (1994) report constant values of CRR for confining stresses of 2 to 12 atm from cyclic triaxial laboratory results, and also constant values of CRR for confining stresses of 2 to 6 atm from cyclic simple shear laboratory results. If CRR is constant regardless of confining stress (for a fixed relative density), then K_o is equal to one.

The in situ freezing procedure resulted in undisturbed samples with a wider range of void ratios and slightly lower average than the values measured in situ by other means (including gamma-gamma logging). When these samples were reconsolidated to effective confining stress levels of 2, 4 and 6 atm, they densified. The CRR values at 10 cycles correspond to a relative density of

about 55 percent, and indicate K_o values of about one.

For the liquefaction analysis of the fine sand unit in the Duncan Dam foundation, CRR was estimated to be constant with confining stress in the fine sand, with $CRR = 0.12$ (earthquake magnitude = 6.5). Pillai and Byrne (1994) and Pillai and Stewart (1994) state that the N -values measured in the unit at various effective confining stress levels (various overburden depths) were converted to $N_{1,60}$ values using an energy correction measured for the SPT equipment and Gibbs and Holtz (1957) relative density relationships to determine N_1 for a given relative density (known from the gamma-gamma logging and undisturbed samples). CRR_1 values from Seed's liquefaction chart (Seed et al. 1985) were inferred from the $N_{1,60}$ values. K_o values were estimated as the ratios of CRR (equal to 0.12) to CRR_1 values. This procedure combines changes in CRR due to confining stress with changes due to densification, and requires considerable confidence in the relationships used to determine $N_{1,60}$ for a given relative density. However, in this case, the resulting CRR is about the same as would be obtained if densification effects are treated separately and C_N and K_o corrections are determined for fixed values of relative density.

Gibbs and Holtz (1957) performed chamber tests on a coarse sand ($D_{50} = 1.5$ mm) with zero fines and a fine sand ($D_{50} = 0.3$ mm) with 14 percent fines. Gibbs and Holtz (1957) performed chamber tests on dry, moist and saturated coarse sand specimens and dry and saturated fine sand specimens. They used confining stresses of 0 (self-weight), 10, 20 and 40 psi (0, 0.68, 1.36 and 2.72 atm). For the Duncan Dam analysis, it appears that $N_{1,60}$ values were linearly interpolated from the measured value of $N_{1,60} = 10$ for the fine sand at 1 atm and $D_r = 30$

% , to the estimated value of $N_{1,60} = 19$ at $D_r = 65\%$, using Gibbs and Holtz (1957) relationships as a guide.

Marcuson and Bieganousky (1976) performed SPT chamber tests to determine C_N corrections and relative density relationships for fine to coarse sands with low fines contents. They used two fine sands, Reid-Bedford Model sand and Ottawa sand, with gradations similar to Duncan Dam. Marcuson and Bieganousky (1976) used effective confining pressures of 10, 40 and 80 psi (0.68, 2.72 and 5.44 atm). Their relationship between $N_{1,60}$ and D_r for fine, submerged sand is similar to the Gibbs and Holtz (1957) relationship for dry coarse sand. The Marcuson and Bieganousky (1976) data indicate that C_N values decrease (a more severe reduction from N to N_1) as grain size and relative density decrease (Hynes-Griffin and Franklin 1989). Skempton (1986), Olsen (1994) and Olsen and Mitchell (1995) provide summaries of data and estimated C_N corrections. The potential range in C_N values is large.

It is difficult to compare the K_o values from the Duncan Dam study with other sources since: a) the data reduction process couples densification due to increased confining stress with confining stress effects on cyclic strength and penetration resistance; and b) the resulting confining stress corrections are highly site specific. In this case, the confining stress and densification effects appear to cancel each other, so CRR would be found to be constant with depth using procedures that treat densification and confining stress

separately.

Consensus K_o Curve (Harder 1996, Youd and Idriss 1998)

The K_o correction was an issue discussed at the Salt Lake City Workshop (Youd and Idriss, editors, 1998). Published K_o trends indicate a wide range of possible K_o relationships. After a presentation by Harder (1996) and considerable discussion by the participants, a consensus K_o relationship was selected as the clean sand curve from Byrne and Harder (1991, Figure 7). It roughly corresponds to the average for all tested soil types and relative density levels, and serves as a lower bound for medium dense to loose sands and silty sands. The data that support the consensus K_o curve correspond generally to medium dense clean sands. The consensus K_o curve may be unconservative for gravelly soils or very dense soils, and may be very conservative for loose sands and silts.

Summary K_o Curves for Different Soil Types

Clean Sands. The K_o data for clean sands are grouped in Figure 8. The data from Vaid show a consistent trend that K_o decreases as relative density increases for loose to medium dense clean sands. However, the CRR_1 values determined from the laboratory tests are significantly less than would be estimated for a clean sand at that relative density based on blowcount correlations.

Gravels. The limited data for gravels

indicate lower values of K_o than for sands and silty sands. (A lower value of K_o means a more severe reduction in cyclic strength.) However, the range of possible values of K_o is large, depending on the procedure used to estimate CRR_1 . The K_o boundary for the clean sand data is the upper bound for interpretation of the gravel data. The K_o values are minimum when CRR_1 is estimated from straight-line extrapolation in a shear strength vs. confining stress plot, with samples at lower confining stresses behaving as overconsolidated material. The K_o values are maximum when CRR_1 is estimated from straight-line extrapolation in a shear strength vs. confining stress plot, ignoring "overconsolidated" data.

Hydraulic Fill and Foundation Soils. The K_o and cyclic strength data for hydraulic fills are shown in Figures 9 and 10. Data from loose samples of silty sand formed by wet pluviation (Fort Peck Dam shell and foundation material) have K_o values of about 0.9 to 0.95 at confining stresses of 6 to 8 atm. Values of K_o from tests on undisturbed samples of hydraulic fill from Sardis, USFD and LSFD generally plot below the earlier Seed curves. The USFD data form a lower bound to the K_o data set for hydraulic fill material. Figure 9 also shows K_o data for silty, sandy foundation soils (primarily alluvial) from Sardis, Fort Peck, Arcadia and Enid Dams.

Soil Mixtures (Silty, Sandy Foundation Soils). Figures 11 and 12 show K_o and cyclic strength values from cyclic triaxial tests on undisturbed samples of silt, carved

from block samples of the foundation materials at Enid Dam. Also shown in these figures are K_o values for foundation soils at Arcadia Dam. The Arcadia samples were undisturbed, thin-wall Shelby tube samples. For Enid silt, the maximum value of K_o results from including densification of the sample during consolidation. The minimum value comes from comparing cyclic strengths at a constant void ratio. The Enid and Arcadia points plot close to the hydraulic fill data from USFD, LSFD and Sardis Dam. Consequently, the USFD data also form a lower bound K_o curve for silty, sandy mixtures.

Stress History, Undisturbed samples, Reconstructed Specimens and CRR_1

Stress History Effects The database of cyclic strength and K_o values assembled for this study indicate that K_o is very sensitive to the stress history of the soil. The effect of the in situ stress history on cyclic strength can be obscured due to sample disturbance unless special measures, such as freezing (Singh et al. 1982, Tani and Yasunaka 1988), are taken to minimize disturbance. Reconstruction of specimens in the laboratory may introduce an artificial stress history, as is caused by moist tamping, or result in a near virgin state, as is the case with wet or dry pluviation.

Undisturbed and Moist-Tamped Specimens Increased cyclic strength caused by stress history effects introduced during laboratory construction of a specimen may not simulate in situ conditions unless a similar stress

history exists in the field. Samples constructed by moist tamping may approximately simulate a stress history for rolled-fill materials (which are known to perform very well under cyclic loading, Seed et al. 1977). However, for cohesionless soils, high quality undisturbed samples obtained by in situ freezing are needed to quantify past stress history effects on cyclic strength and determine the appropriate K_o correction (Singh et al. 1982).

Undisturbed and Pluviated Specimens

Sample construction by wet or dry pluviation may simulate deposition of hydraulic fill or foundation deposits beneath a dam, typically recent alluvium, colluvium or lacustrine deposits. However, the in situ deposit may have some stress history and aging effects that are not simulated by freshly constructed laboratory samples. These in situ stress history and aging effects would be most apparent at low levels of confining stress. An elevated cyclic strength at low confining stress leads to a more severe K_o correction. If high quality undisturbed samples are used to determine cyclic strength as a function of confining stress, as was the case for LSFD and USFD, then the cyclic strength may be somewhat elevated at low confining stress and the K_o correction less than one. If recently constructed (pluviated) laboratory tests are used for relative scaling of strength to extend field correlations, then the K_o correction may be close to one, and cyclic strength at high confining stresses may be overestimated. This can be observed by comparing the K_o correction for LSFD and USFD with that for Fort Peck Dam.

CRR₁ from Laboratory Tests Compared with CRR₁ from Penetration Tests Cyclic strengths of undisturbed samples correspond fairly well with cyclic strengths inferred from penetration tests (examples: USFD and LSFD data; data from Japan on samples excavated using in situ freezing reported in Prakash and Dakoulas 1994). Cyclic strengths of samples prepared by wet or dry pluviation are generally much lower than expected for a soil at that relative density (examples: data from Vaid and others for clean sands; comparison of cyclic strength of reconstructed specimens and undisturbed specimens from Fort Peck Dam). The cyclic strength data for gravels (Folsom, Ririe and Oroville Dams) were compared with an estimated CRR₁ for soils at that relative density. Estimation of CRR₁ from the laboratory gravel data in stress focus plots leads to values that are significantly less than expected for a given relative density. This underestimation of CRR₁ can also be observed in the Fraser River sand data; the CRR₁ values from the laboratory tests on freshly constructed pluviated specimens are much less than would be expected for a material at that relative density.

The data for freshly deposited materials (Fort Peck Dam, Vaid) indicate a straight line relationship on the stress focus plot but the CRR₁ values are well below (80 to 150 percent too low for Fort Peck) those expected for a material at that relative density. Consequently, if specimens are constructed by wet or dry pluviation, the results should be similar to the observations from Fort Peck and Vaid's work, and are not

necessarily representative of field conditions; these results may also greatly overestimate K_o . The Duncan Dam laboratory data contradict this trend; these data were obtained from cyclic tests on undisturbed samples of fine, clean sand that had been frozen prior to sampling. The freezing process has been shown to preserve stress history effects on cyclic strength (Singh et al. 1982). The Duncan Dam laboratory data indicate K_o equal to one for confining stresses ranging from 2 to 12 atm.

The stress focus theory described shows that the cyclic strength envelopes for a given gradation and mineralogy merge at very high confining stress, regardless of stress history and relative density. In the stress range of interest for dams, however, cyclic strength envelopes can be very sensitive to these factors. The cyclic strength chart from Seed et al. (1983) shows blowcount values at sites that have and have not liquefied. For the sites that did liquefy, the process of liquefaction in the field may have the effect of redepositing the affected soils, thus erasing past stress history, and resulting in a near virgin deposit. For the sites that did not liquefy, the past stress history may be preserved and possibly added to by the earthquake shaking.

3. Conclusions

1. Laboratory cyclic strength tests on relatively loose soil samples reconstituted by dry or wet pluviation result in high K_o values (nearly linear strength envelope with

intercept near zero, little reduction in CRR as confining stress increases).

2. The CRR_1 values for reconstituted, pluviated specimens are too low by about a factor of two when compared to CRR_1 values from tests on high quality undisturbed specimens.

3. The CRR_1 values for reconstituted, pluviated specimens are too low by about a factor of two when compared to CRR_1 values estimated from penetration tests for soils at about the same relative density as the reconstituted specimens.

4. The K_o data base developed in this study from laboratory tests on undisturbed samples of fine sands, silts and silty sands, including hydraulic fill and water-laid foundation deposits, indicates K_o values ranging from a minimum of 0.55 to 0.45 (LSFD and USFD), and a maximum of 1 to 0.9 (Duncan Dam) for confining stresses of 4 to 6 atm.

5. Experience at USFD and LSFD indicates that although material type is variable in hydraulic fills, the method of deposition results (for practical purposes) in a uniform relative density and a uniform cyclic strength.

6. It is hypothesized that stress history (including aging effects) is an important factor in determining appropriate values for K_o . Pluviation in the laboratory results in near-virgin specimens, but the cyclic strengths of these specimens does not correspond to values from undisturbed

samples and inferred from penetration tests. Moist-tamping results in specimens with considerable stress history that may or may not correspond well to field conditions.

7. Direct measurement of K_o in the laboratory will require testing high quality undisturbed specimens. Pluviated, reconstituted specimens may overestimate K_o . Moist-tamped, reconstituted specimens may underestimate K_o .

8. Stress Focus theory, originally developed for interpreting CPT cone resistance, was investigated as a framework for interpreting the non-linear relationship between cyclic strength and confining stress. The data indicate a locus for a stress focus boundary for liquefaction resistance which varies with soil type. The stress focus format simplifies the mechanics of relating CPT measurements to soil properties.

4. Recommendations

1. Before conducting a costly, complex laboratory testing program for site-specific values of K_o , parametric dynamic analyses and liquefaction evaluations should be conducted to determine whether a detailed laboratory testing program is warranted.

2. Initially, the analyses should consider the most optimistic K_o values. If the dam or site is judged unsafe with these values, remedial construction is indicated.

3. If the dam is found to be safe, with factors of safety against liquefaction greater than 2, the analyses should then be performed with the lower bound K_o values.

4. If the dam is still judged to be safe with these values, for example with factors of safety against liquefaction greater than 1.5, then further laboratory testing or analysis may be unnecessary to demonstrate adequate seismic performance.

5. However, if the analyses (with the lower bound K_o values) indicate factors of safety less than 1.5, then a laboratory testing program is recommended to quantify the appropriate K_o relationships for this site.

5. References

- Andrus, R. D. and Stokoe, K. H. 1996. "Guidelines for Evaluation of Liquefaction Resistance Using Shear Wave Velocity," Salt Lake City Workshop, NCEER.
- Bieganousky, W.A. and Marcuson, W. F. III, 1976. "Liquefaction Potential of Dams and Foundations, Report 1: Laboratory Standard Penetration Tests on Reid-Bedford Model and Ottawa Sands," Research Report S-76-2, USAEWES, Vicksburg, MS.
- Bieganousky, W.A. and Marcuson, W. F. III, 1977. "Liquefaction Potential of Dams and Foundations, Report 2: Laboratory Standard Penetration Tests on Platte River Sand and Standard Concrete Sand," Research Report S-76-2, USAEWES Station, Vicksburg, MS.

FUGRO Inc 1980. "Cone Penetration Testing of Arcadia Dam Site," Tulsa District of the Corps of Engineers, Long Beach, CA.

Harder, L.F. 1988. "Use of Penetration Tests to determine the Cyclic loading Resistance of Gravelly Soils during Earthquake Shaking", PhD Dissertation, UC Berkeley.

Hynes, M.E. 1988. "Pore pressure characterization of gravels under undrained cyclic loading," PhD Dissertation, UC Berkeley.

Hynes, M.E. 1996. "Liquefaction Potential of Gravels," Salt Lake City, NCEER

Hynes-Griffin, M. E. and Franklin, A. G. 1989. "Overburden Correction in Gravels," Proceedings of the 20th Joint Meeting of the UJNR Panel on Wind and Seismic Effects, NIST SP 760, NIST, Gaithersburg, MD.

Gibbs, H. J. and Holtz, W. G., 1957. "Research on determining the density of sand by spoon penetration testing," Proceedings, 4th ISSMFE Conference, Vol. I.

Marcuson, W. F. III and Krinitzsky, E. L. 1976. "Dynamic Analysis of Fort Peck Dam," Technical Report S-76-1, USAEWES, Vicksburg, MS.

Olsen, R.S. 1984. "Liquefaction analysis using the Cone Penetrometer Test (CPT)," Proceedings of 8th World Conference on Earthquake Engineering, San Francisco.

Olsen, R.S. 1994. "Normalization and Prediction of Geotechnical Properties using

the Cone Penetrometer Test (CPT)," PhD Dissertation, UC Berkeley.

Olsen R.S. and Mitchell J.K. 1995. "CPT stress normalization and prediction of soil classification" Proceedings of International Symposium on Cone Penetrometer Testing - CPT'95, October, Linkoping, Sweden.

Pillai, V.S, and Byrne, P.M. 1994. "Effect of overburden pressure on liquefaction resistance of sands," Canadian Geotechnical Journal, Vol. 31, pg 951-966.

Pillai, V.S, and Stewart, R. A. 1994. "Evaluation of liquefaction potential of foundation soils at Duncan Dam," Canadian Geotechnical Journal, Vol. 31, pg 53-60.

Seed, H. B. and De Alba, P. 1986. "Use of SPT and CPT tests for evaluating the liquefaction resistance of soils," Proceedings of the Specialty Conference on the Use of In Situ Tests in Geotechnical Engineering, Blacksburg, VA, ASCE Geotechnical Special Publication No. 6, pp. 120-134.

Seed, H. B. and Idriss, I. M. 1981. "Evaluation of Liquefaction Potential of Sand Deposits Based on Observations of Performance in Previous Earthquakes," Proceedings of the ASCE National Fall Convention, St. Louis, Session No. 24.

Seed, H.B. 1983. "Earthquake-Resistant Design of Earth Dams," Proceedings of Symposium on Seismic Design of Embankments and Caverns, May, ASCE pg 41-64.

Seed, H.B. 1984, 1987. Pers. communication

Seed, H. B., Idriss, I. M. and Arango, T. 1983. "Evaluation of Liquefaction Potential Using Field Performance Data," Journal of Geotechnical Engineering Division, ASCE, Vol. 109, No. 3, March 1983, pp. 458-492.

Seed, R.B. and Harder, L.F. 1990. "SPT-based analysis of cyclic pore pressure generation and undrained strength" Proceedings, H. B. Seed Memorial Symposium, Bitech Publishers, Vol. 2, pg 351-376.

Singh, S., Seed, H.B. And Chan, C.K. 1982. "Undisturbed sampling of saturated sands by freezing," Journal of Geotechnical Engineering, ASCE, New York, Vol. 108, No. 2.

Skempton, A. W. 1986. "Standard Penetration Test Procedures and the Effects in Sands of Overburden Pressure, Relative Density, Particle Size, Aging and Overconsolidation," Geotechnique, Vol. 36, No. 3.

Stark, T. D., and Olson, S. M. 1995. "Liquefaction Resistance using SPT and Field Case Histories," Journal of Geotechnical Engineering, ASCE, New York, Vol. 121, No. 12, pp 856-868.

Tani, S. And Yasunaka, M. 1988. "Effect of sampling methods on liquefaction resistance of loose sand," Proceedings, 9th World

Conference on Earthquake Engineering, Tokyo-Kyoto, Japan, Vol. III, pp 219-224.

Thomas, J. 1992. "Static, cyclic and post liquefaction undrained behavior of Fraser River Sand," MS Thesis, UBC, Canada.

U.S. Army Engineer District, Tulsa. 1982. "Arcadia Lake, Deep Fork River," Supplement No. 1 to Design Memorandum No. 9, "Embankment and Spillway."

U.S. Army Engineer District, Vicksburg. 1988. "The Sardis Earthquake Study," Supplement No. 1 to Design Memorandum No. 5 (1985).

Vaid, Y.P., Chern, J.C. and Tumi, H. 1985. "Confining pressure, grain angularity, and liquefaction," Journal of Geotechnical Engineering, ASCE, October, Vol. 111, No. 10.

Vaid, Y. P. and Thomas, J. 1994. "Post liquefaction behavior of sand," Proceedings of the 13th ISSMFE Conference, New Delhi.

Vaid, Y. P. and Thomas, J. 1995. "Liquefaction and post liquefaction behavior of sand," Journal of Geotechnical Engineering, ASCE, Vol. 121, No. 2.

Youd, L. and Idriss, I. M. editors. 1998. "Workshop on Evaluation of Liquefaction Resistance," Proceedings, Salt Lake City, sponsored by FHWA, NSF and WES, in publication, NCEER, Buffalo, NY.

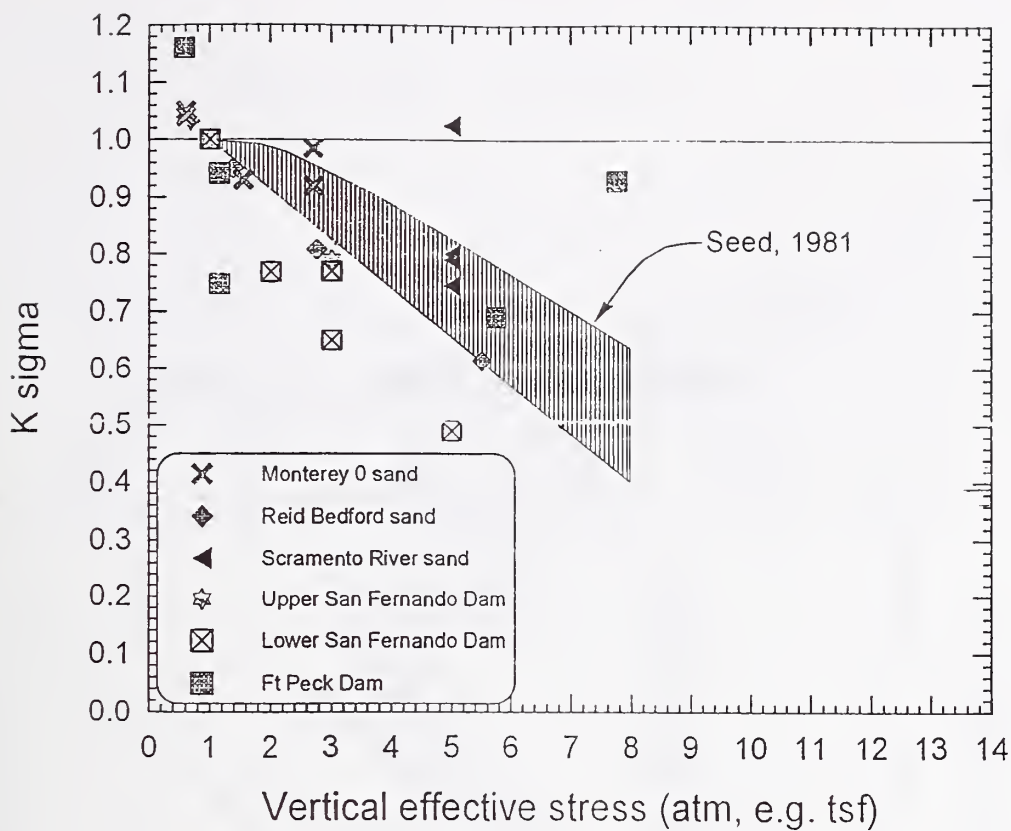


Figure 1 Relative reduction in cyclic stress ratio causing liquefaction with increase in confining stress, K_σ (Seed and Idriss 1981)

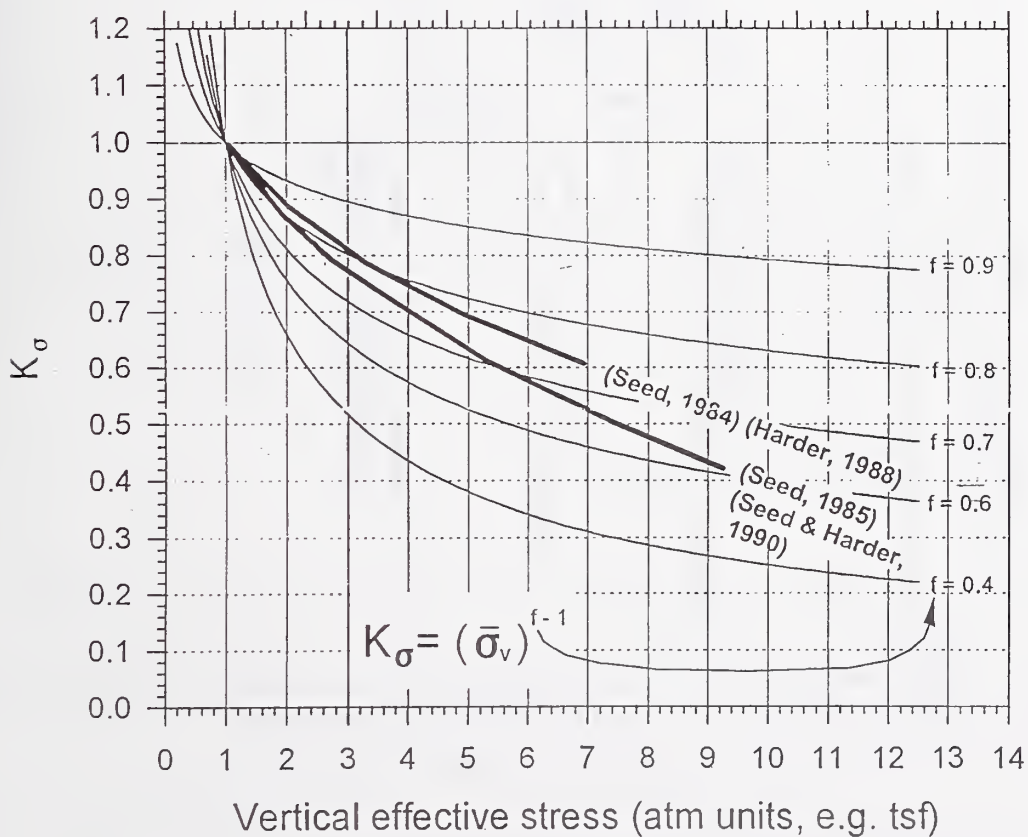


Figure 2 Contours of liquefaction stress exponents on the K_σ chart

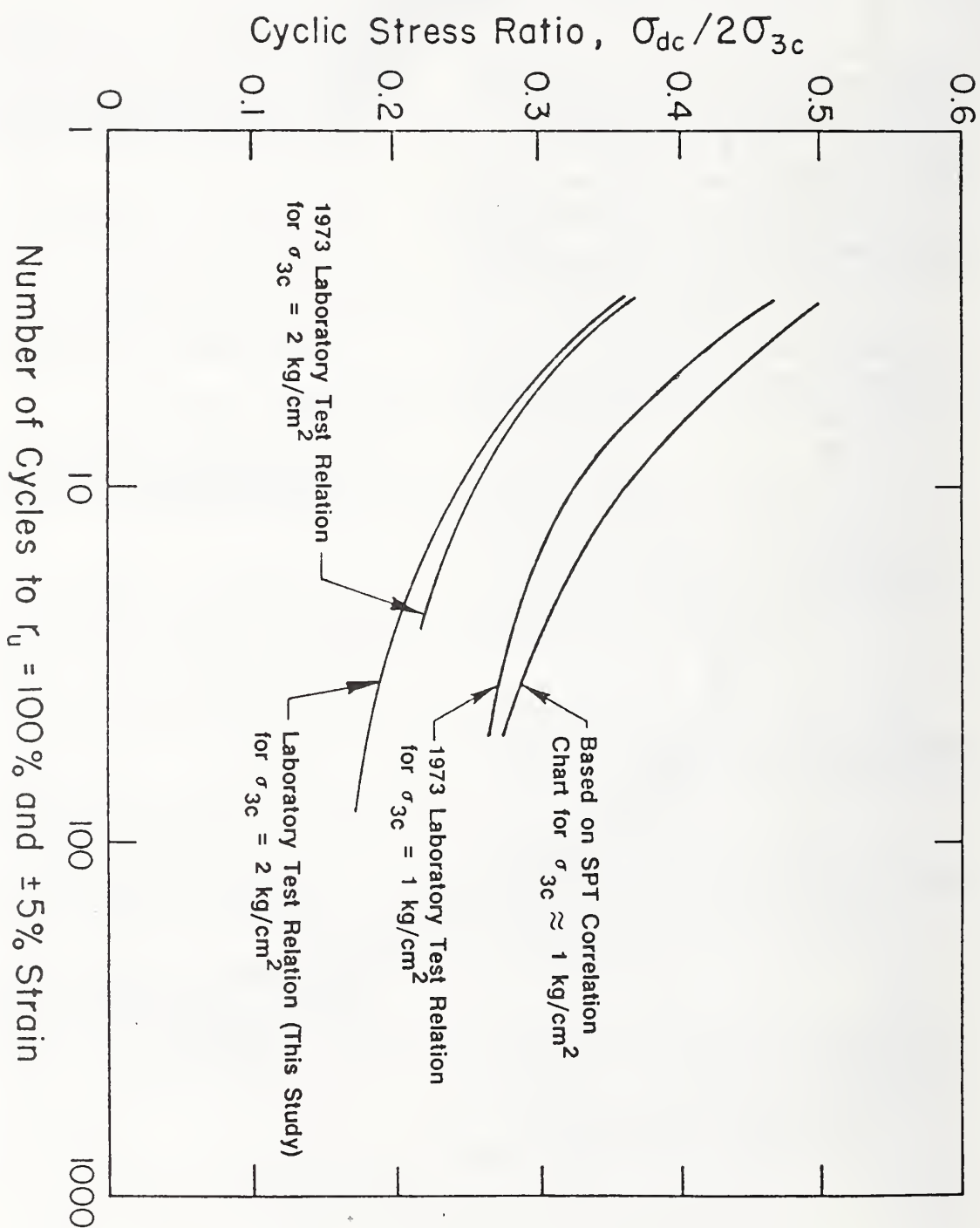


Figure 3 Comparison of results of laboratory cyclic load tests with data determined from field case studies (Seed et al. 1989)

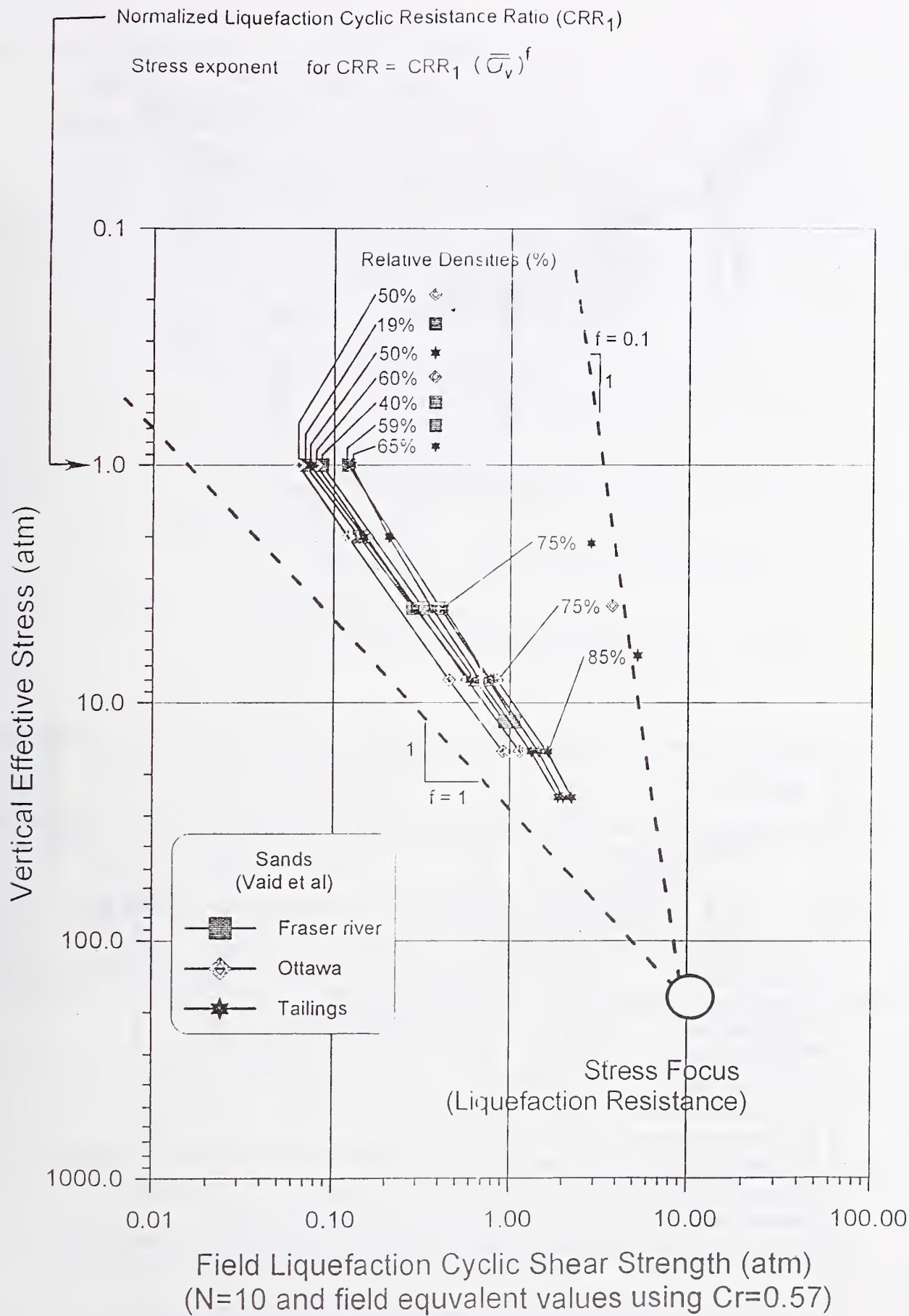


Figure 4 Stress focus plot of cyclic strength for tailings, Ottawa and Fraser River sands (after Vaid et al. 1985 and Vaid and Thomas 1994)

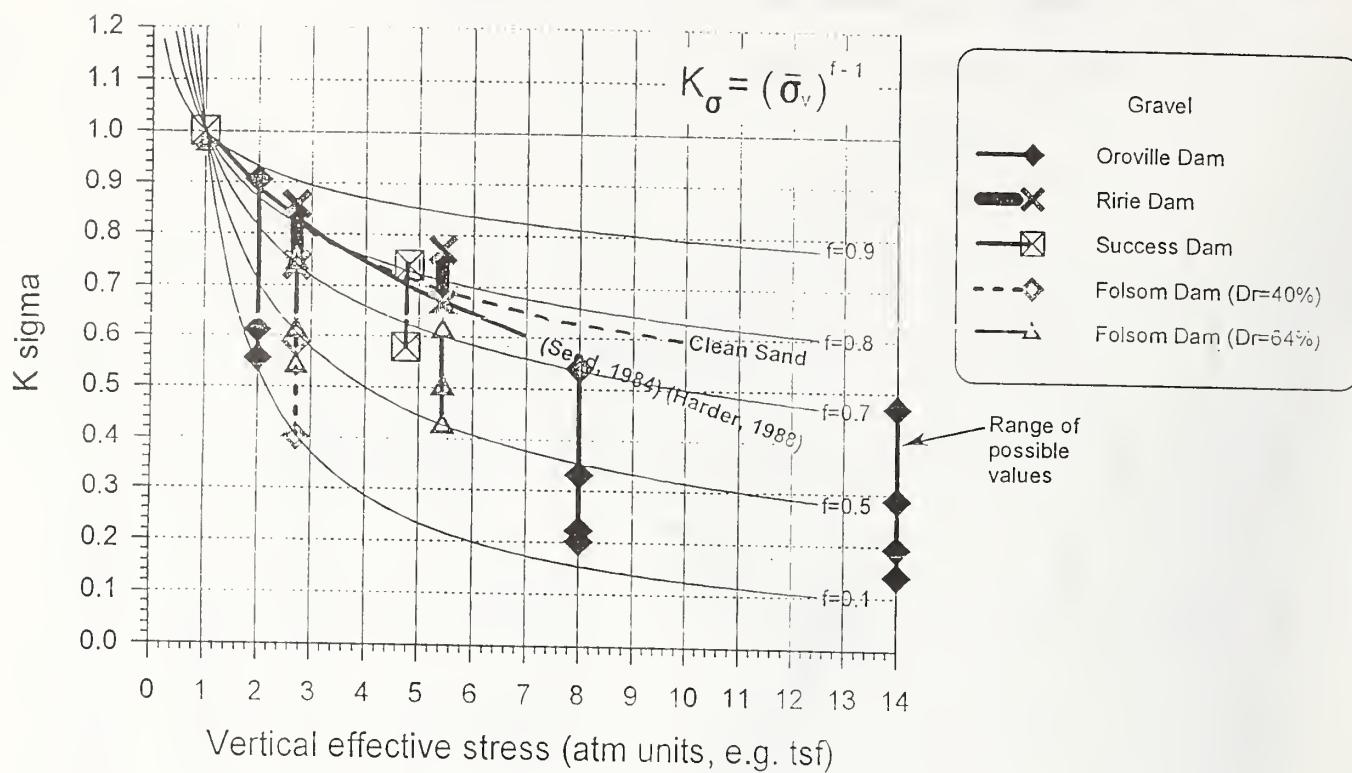


Figure 5 K_{σ} and CRR stress focus data for gravels

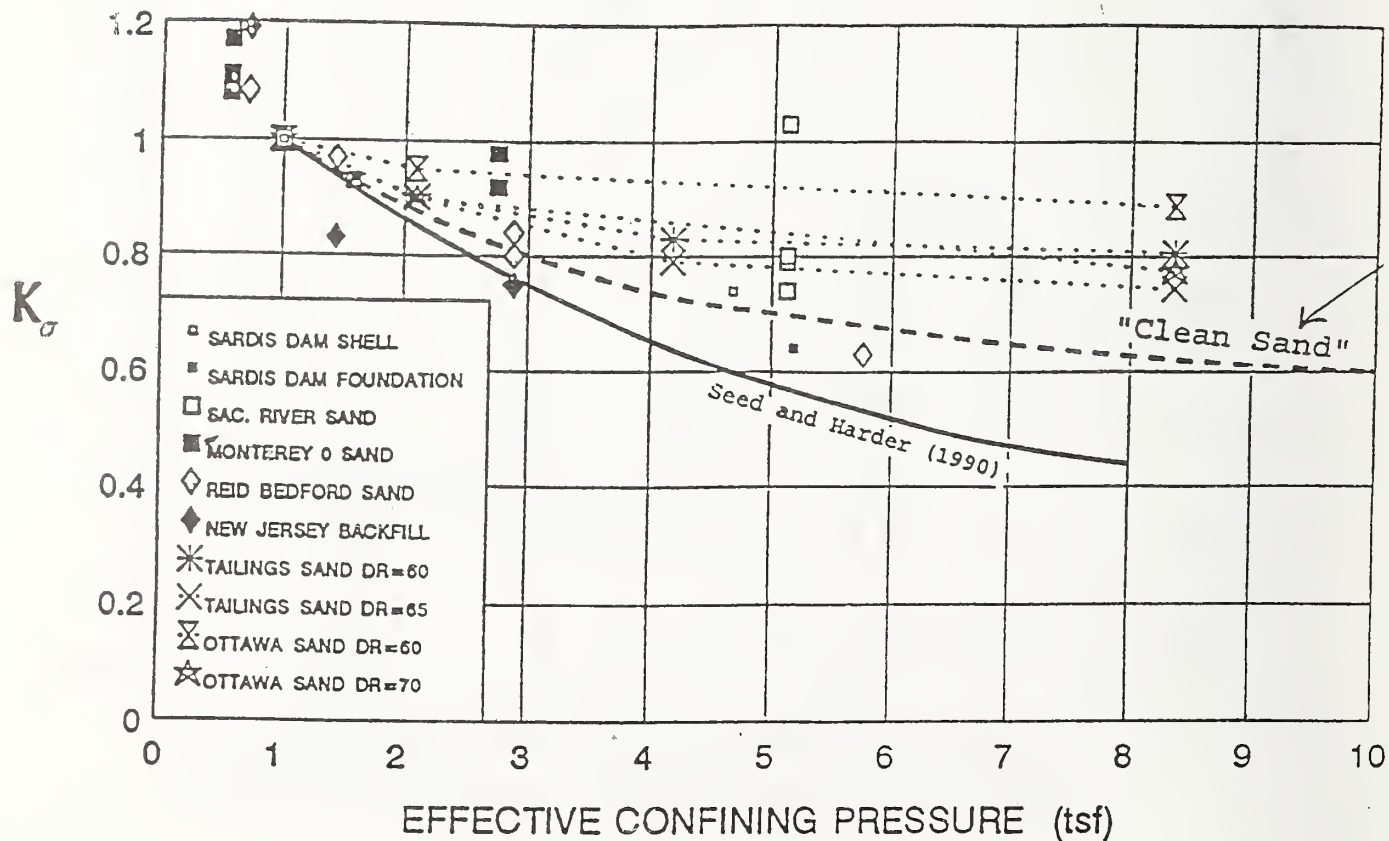


Figure 6 Recommended K_{σ} values (Harder 1996)

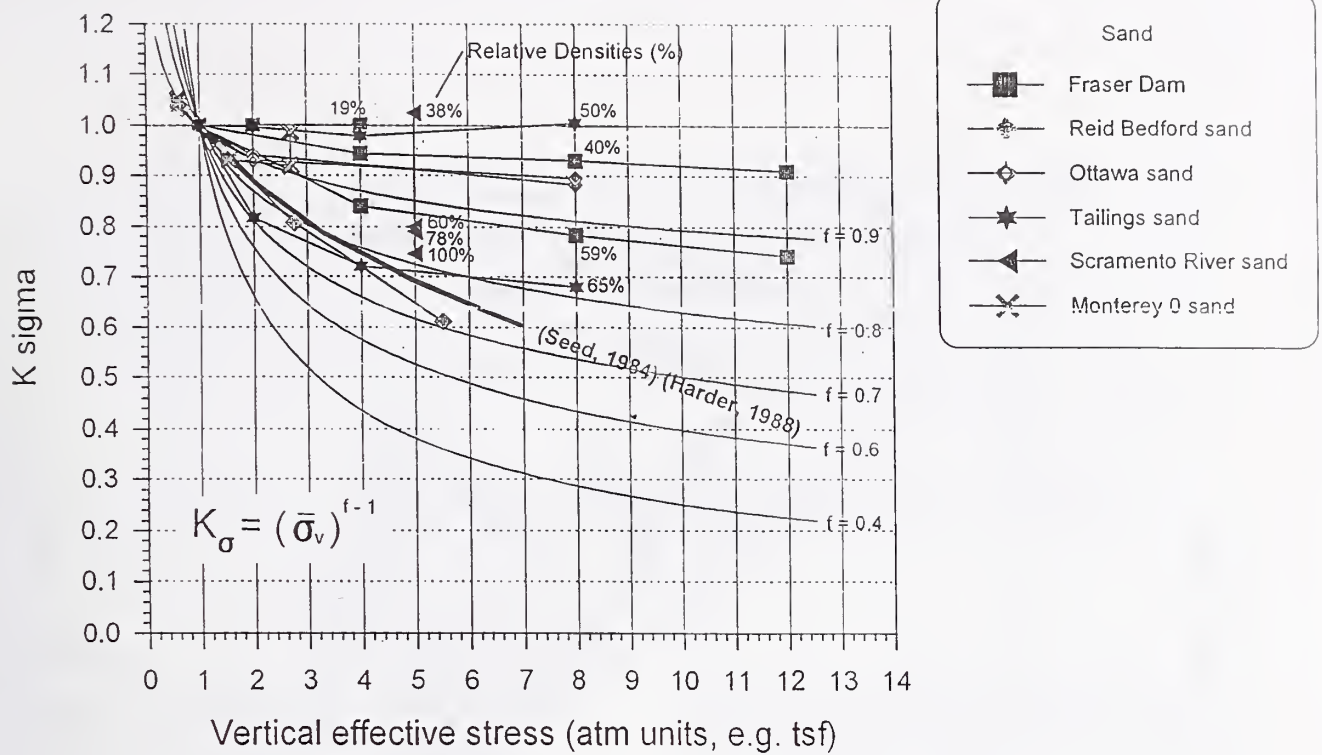


Figure 7 K_σ and CRR stress focus data for clean sands

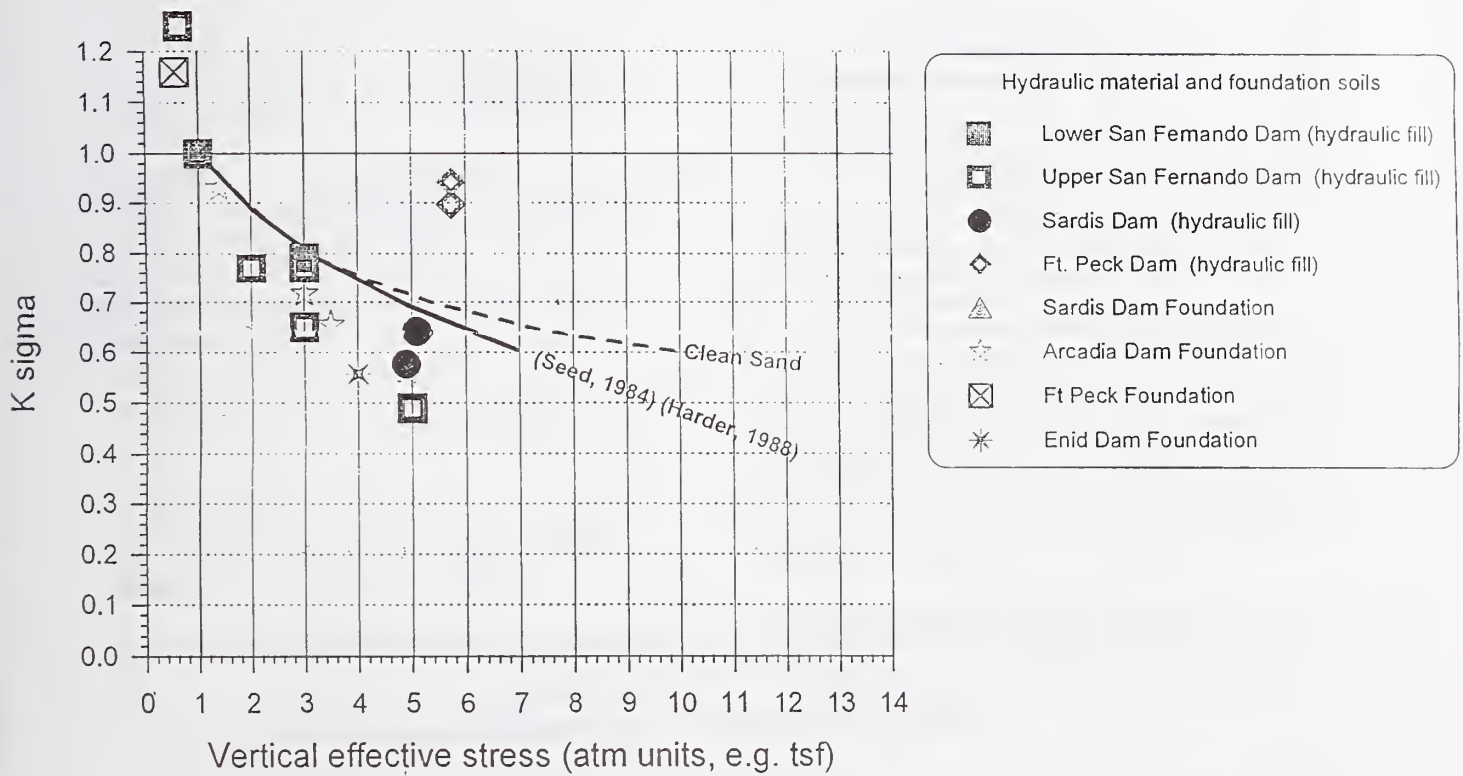


Figure 8 K_σ and CRR stress focus data for silty sands and hydraulic fills

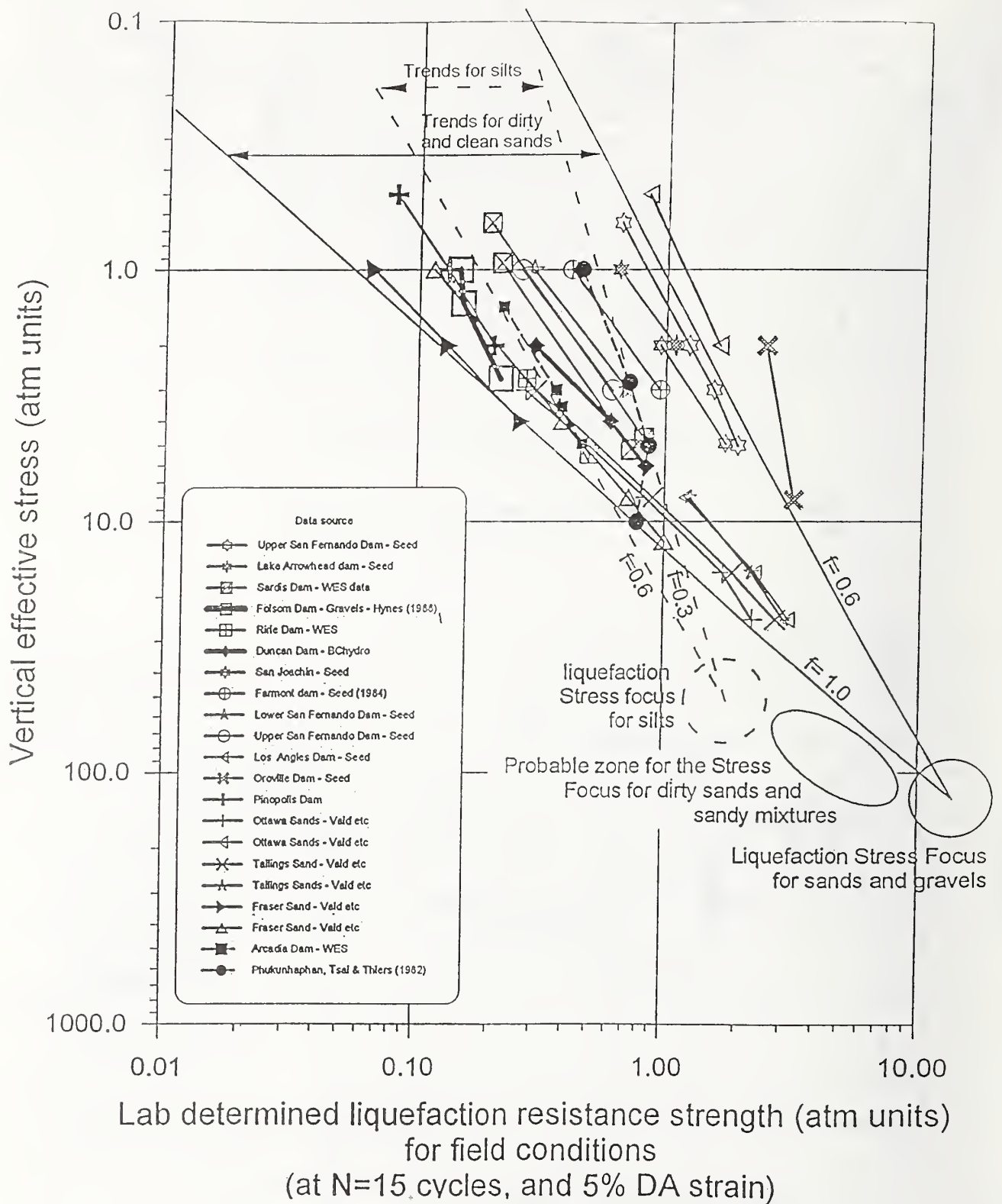


Figure 9 Trends of liquefaction resistance in stress focus format

Evaluation of the Seismic Capacity Of An Existing Thick Wall Reinforced Concrete Structure Using Probabilistic Criteria

by

F. Loceff¹, G. Mertz¹ and G. Rawls¹

ABSTRACT

A seismic qualification of a reinforced concrete nuclear materials processing facility using performance based acceptance criteria is presented. Performance goals are defined in terms of a minimum annual seismic failure frequency. Pushover analyses are used to determine the building's ultimate capacity and relate the capacity to roof drift and joint rotation. Nonlinear dynamic analyses are used to quantify the building's drift versus earthquake magnitude using a suite of time histories representing varying soil conditions and levels of seismic hazard.

A probabilistic correlation between joint rotation and damage state is developed from experimental data. The results of the deterministic pushover and nonlinear time history analyses are evaluated statistically to develop a probability of seismic failure or fragility. The building fragility level is convolved with the seismic hazard curve to determine annual seismic failure frequency.

KEYWORDS

**BUILDING; FRAGILITY, NONLINEAR;
SEISMIC**

1. INTRODUCTION

This paper discusses the seismic qualification of an existing nuclear material processing facility. This work was part of an effort to update the facility safety analysis

The material processing facility is a heavy concrete structure that was built in the early 1950's. Radiation shielding was the primary design consideration. Lateral load resistance was given scant attention in 1950's vintage design codes. This combination of factors resulted in large, lightly reinforced concrete sections which do not meet today's seismic detailing requirements.

The safety analysis is updated to include our current understanding of the seismic hazard at the building site and the building's seismic response. The current seismic design loading is several times larger than the lateral loads considered in the original design. When the current seismic loads are combined with the lack of current code detailing, the structure will not meet a design-code seismic qualification.

An probabilistic evaluation methodology that addresses the lightly reinforced concrete buildings with 1950's detailing, typically found in older facilities, is discussed in this paper. Using this methodology, the authors have shown that a nuclear material processing facility is capable of surviving the postulated design basis earthquake (DBE).

This paper emphasizes the probabilistic aspects of this evaluation while a companion paper (Mertz et al, 1998) emphasizes the analysis methodology.

¹ Westinghouse Savannah River Company, Aiken SC 29808.

1.1 ACCEPTANCE CRITERIA

DOE Standard 1020 sets acceptance criteria for DOE facilities based on performance goals. For the structure discussed in this paper the performance goal is an annual failure frequency of 2×10^{-4} . The standard allows considerable latitude in evaluation methodology as long as the specified performance goal for a given category of structures, systems and components (SSCs) are met. This latitude consists essentially of three approaches to meet the performance goals for the SSC.

- For a hazard probability specified for the facility use, apply conservative deterministic evaluation techniques based on national consensus standards as supplemented by DOE Standard 1020 requirements for the facility performance goal.
- Achieve less than a 10% probability of unacceptable performance of an SSC subjected to a scaled design basis earthquake (SDBE) that is 50% larger than the DBE.
- Demonstrate acceptable structural behavior by showing that the building annual probability of seismic failure is less than the facility performance goal.

A key factor in the probabilistic approach is the specification of an acceptance criteria, stated in probabilistic terms, that conforms to the performance goals in DOE Standard 1020.

The structure discussed in this paper consists of a reinforced concrete frame with partially developed joints. Failure for a specific joint is defined, in this paper, as the reduction of capacity below a nominal value. Frame failure is conservatively assumed to occur when the first joint fails. Thus, this probabilistic assessment has a definite conservative bias. Identifying a joint failure, as such, does not imply the failure of the building frame. In fact, substantial conservatism exists since a failure of the frame cannot occur until a sufficient number of joints sustain sufficient damage to cause a collapse mechanism.

Using this definition of unacceptable structural behavior, the evaluation methodology leads to the calculation of the conditional probability of seismic failure. This conditional failure probability is measured against the acceptance criteria in DOE Standard 1020.

1.2 ANALYSIS METHODOLOGY

There are several options available to evaluate older existing facilities for seismic loads. The choice should consider the in-situ building condition, the level of seismic load, the effects of foundation embedment, the functional requirements, the level of acceptable damage, the confinement requirements, and the performance category of the facility. This paper concentrates on the more rigorous approach to demonstrate the capability of a facility to withstand a postulated seismic event.

1.3 FACILITY DESCRIPTION

The material processing facility, designed and constructed in the early 1950s, are reinforced-concrete buildings. They are 66 ft high, 122 ft wide (Figure 1) and consist of eighteen segments, typically 43 ft long. One-inch expansion joints separate the segments from each other. The exterior walls range from 2.5 to 4.8 ft thick and support a haunched roof slab. A frame structure is contained within the building. The lower portion consists of continuous walls and discrete columns while the upper portions contain continuous walls. The specified design strength of the concrete is 2,500 psi and Grade-40 reinforcing steel was used. The structure is supported on a 5-foot-thick reinforced-concrete foundation mat. The total weight of a typical segment is 24,800 kips.

Primary longitudinal (N-S) stiffness against seismic loading comes from the 4 ft thick shear walls while the transverse (E-W) stiffness is provided by frame action of the reinforced-concrete walls.

The original design was based on the Uniform Building Code (UBC, 1946) with a 1951 Addenda and on the American Concrete Institute (ACI) Code ACI 318-47. The design focused on gravity loading with only a nominal seismic lateral load applied statically to the building structure. The exterior walls were

designed to resist a uniform external over-pressure. This design condition resulted in heavier reinforcement on the inside face of the walls than on the outside face. Many of the embedment and splice lengths of the reinforcing steel do not satisfy current ACI specifications with some embedment lengths only 25 percent of that required by the current code.

A typical joint that connects the roof to the exterior wall is shown in Figure 2. This joint was designed for gravity loads and the bottom slab reinforcing is not fully anchored in the wall. Seismic loads will cause load reversal, putting the bottom bars in tension and the capacity of this underdeveloped bar is reduced due to bond slip. This joint is 43 feet long and the geometry of the joint constrains the concrete around the reinforcing bar.

2. DEVELOPMENT OF SEISMIC INPUT

The probabilistic structural analysis requires that the median responses of the building be determined. The building sits on a deep layered site consisting of sands and clays over bedrock. Bedrock is approximately 950 ft below free field. Seismic motions were developed for: 1) an evaluation basis earthquake (EBE) with 2000 year return period, and 2) a seismic margin earthquake (SME) with a 10,000 year return period. Both the EBE and SME ground motions are defined in the form of 5% damped rock-outcrop response spectra. Eight acceleration time histories were prepared; four compatible with the EBE spectrum and four compatible with the SME spectrum.

To consider the variabilities in the soil between the free field and the bedrock each time history was convolved through several soil columns, as shown schematically in Figure 3. At the site, there were four deep borings (≈ 950 ft) to bedrock, and five shallow borings, (≈ 150 ft). Each EBE and SME time history was convolved through 20 soil columns that were formed by combining each deep boring with all five shallow borings, resulting in 80 time histories at the base of the building.

The response spectra of the convolved time histories are plotted at the elevation of the basement of the building and a mean spectrum

was calculated for both the EBE and the SME motions. To reduce the computational effort in developing the building response, a subset of 11 out of 80 time histories were chosen for both the EBE and SME events. These 11 time histories were selected such that the mean of their response spectra closely matches the mean of the full suite of 80 time histories. Furthermore, the 11 spectra are evenly spaced between the maximum and minimum envelopes of the 80 spectra from the convolved time histories, and have an equal probability of occurrence.

The median response spectra of these time histories are shown in Figure 4 for the 2,000-year and the 10,000-year events.

3. DETERMINISTIC BUILDING RESPONSE

The building behavior was determined by performing a static pushover analysis to determine the structure's overall lateral load resistance. Nonlinear dynamic analyses, using a simplified dynamic model, were performed to determine the seismic response.

3.1 STATIC PUSHOVER ANALYSIS

In the east-west direction, the structure consists of a moment resisting lateral frame with a rigid penthouse structure. A static pushover analysis of the lateral load resisting frame is performed to determine the building's lateral load capacity and the relationship between displacement and joint rotation.

Lumped nonlinear springs are located at critical joints to represent, cracking of the gross section, yielding of the longitudinal reinforcing and bond slip due to inadequate development. In partially developed joints, the members' capacity is reduced by the ratio of the actual development length to the code development length.

A typical monotonic load-deformation curve or backbone curve for the structure is shown in Figure 5. The structure remains elastic below a base shear of about 5% of the building weight. Above this load, individual joints crack and yield at different load levels, which gradually soften the overall structural response. A plastic collapse mechanism is nearly formed after six

inches of displacement. For displacements beyond this point, the slight increase in capacity due to strain hardening of the reinforcement is nearly offset by the increasing $P-\Delta$ forces. The ultimate capacity corresponds to about 11% of the structure's weight.

3.2 NONLINEAR DYNAMIC ANALYSIS

A fragility analysis for a reinforced-concrete structure subjected to strong earthquake motions requires realistic conceptual structural models that consider changes in stiffness and material properties, the variability of seismic source and in-situ soil conditions. To adequately address these parameters, numerous non-linear time history analyses were performed. Since non-linear time history analyses are numerically intensive, reduced dynamic models are used to perform the analyses.

The elastic response of the frame in Figure 1 is dominated by the response of the first mode, with roof drifts in-phase with joint rotations. Thus, the structure is represented with a single-degree-of-freedom (SDOF) model having an equivalent elastic response as the full structural model. The elastic natural frequency of the structure is on the order of 1 to 1.3 Hz.

The nonlinear response of the SDOF model is represented by the Takeda hysteresis model (Takeda, 1970) that represents the experimentally observed behavior of reinforced concrete beams subject to cyclic loads. The 11 EBE and 11 SME ground motions are evaluated using a SDOF model which represent the nominal capacity of the building based on 'design' material properties. The range of roof displacements, for the 11 representative 2,000 and 11 representative 10,000 year ground motions is summarized in Table 1.

The initial structural stiffness of the SDOF model was also perturbed to address the uncertainty in natural frequency on response. The range of roof displacements for the 11 representative ground motions with lower bound (-30%), best estimate, and upper bound (+30%) stiffness is summarized in Table 2. This structure is more sensitive to variations in soil column than to variations of initial stiffness.

Table 1 Range Of Roof Displacements For Different Earthquake Magnitudes and Soil Columns

Ground Motion	#	Minimum (in)	Maximum (in)
EBE	33	1.30	2.78
SME	33	6.52	10.2

Table 2 Range Of Roof Displacements For Different Earthquake Magnitudes, Soil Columns, And Natural Frequencies

Ground Motion	#	Minimum (in)	Maximum (in)
EBE	33	1.30	2.78
SME	33	6.52	10.2

The 11 EBE ground motions were also evaluated using a SDOF model that represented the median building capacity to investigate the change in response with capacity. The lateral load capacity of the frame, calculated using median material properties, is about 27% larger than the lateral load capacity calculated using material properties that are exceeded by 95% of the test data. The influence of material strengths on the range of seismic displacement, shown in Table 3, is small because the structure is responding in the displacement controlled region of the spectra.

Table 3 Range Of SME Roof Displacements For Different Material Strengths

Material Properties	#	Minimum (in)	Maximum (in)
95% Exceedance	33	6.52	10.2
Median	33	7.21	10.1

Representative nonlinear MDOF were also performed to validate the SDOF analyses. These comparisons indicate that the SDOF mass

participation was overestimated and consequently, the SDOF models tend to over-predict the roof displacements.

4. PROBABILISTIC ANALYSIS

Ground motions and the resulting structural drifts were developed in the proceeding sections. These values are combined in this section with the probability of joint failure to determine the mean annual probability of seismic failure which is compared to the structures performance goal specified by DOE Standard 1020.

4.1 PROBABILITY OF PARTIALLY DEVELOPED JOINT FAILURE

Rotations are imposed on the joints when a frame drifts under seismic lateral loads. Joints that do not meet the ACI 318-95, development length requirements may not develop their full yield moment. In this evaluation, the ACI bond stress is used to limit the bending capacity (ϕM_n), of a partially developed joint, by the ratio of actual development length, to the ACI development length. The amount of bar slip at the reduced moment is determined by the rotation imposed on the joint and ultimately by the lateral drift of the frame as shown in Figure 6. Failure is defined as the inability of a joint to resist the reduced moment, at a given drift.

Typical confined bar pullout test results (Eligehausen, 1983), are shown in Figure 7. Monotonic tests indicate that for low magnitudes of bond slip the bars have a much larger capacity than the ACI 318-95 code allows and that the code bond capacity corresponds to the capacity at large deformations. Cyclic tests indicate that the capacity degrades with an increasing number of cycles and the degradation is more pronounced when cycled with larger ranges of slip. After 10 cycles, the code capacity is obtained when loading beyond the maximum post-bond slip. This test data was reviewed and judged that 13% and 75% of the specimen would fail to maintain the ACI bond capacity at peak slip ranges of 0.2 in and 0.36 in respectively. A lognormal probability distribution is fit to these two failure estimates as shown in Figure 8.

Test of full scale joints with partially developed bars, shown in Figure 9 (Beres, 1992, Aycardi, 1992), demonstrate that the joint is capable of resisting considerable rotation at the reduced bending moment $\phi M_n l/d$. Joint rotations for this data are converted to bar slip, ranked, and used to validate the bar slip probability of failure in Figure 8. Note that the bar slip in Figure 6 is the product of joint rotation and the distance between the neutral axis to the reinforcing, d . A joint rotation of 0.02 radians of the 24 inch deep test specimen, in Figure 9, causes the same bond slip as a 0.01 radian rotation on a section that is 48 inches thick. Thus, allowable joint rotation limits should be viewed with caution when evaluating thick sections.

Individual joint rotations corresponding to each increment of roof drift in the pushover analysis, Figure 5, are converted into components of bending rotation and bond slip. Bond slip failure probabilities from Figure 8 are assigned to each joint based on the computed bar slip. Bending failure probabilities are also assigned using a similar relationship and combined with the bond slip failure probability. Bond slip dominated the failure probabilities of this structure.

It was assumed that the loss of any critical member in the load path could result in building failure. Therefore, an envelope of the individual critical member joint failure probabilities represents the probability of structural failure, and is shown in Figure 10. Parametric studies indicate that this indeterminate structure can survive the loss of a single critical joint with a reduced lateral load capacity. As shown above the seismic drift is insensitive to lateral load capacity because the building responds in the displacement controlled region of the spectra. Thus, the probability of structural failure, shown in Figure 10, has a conservative bias.

For roof displacements less than 4 inches (0.5% drift) the probability of failure is negligible while a roof displacement of 5.8 inches (0.8% drift) corresponds to a 50% probability of failure. The probability of failure for the structure is dominated by a joint on the exterior frame that fails by bond slip.

4.2 SEISMIC FRAGILITY

To evaluate the results of the structural analysis described above, to probabilistic acceptance criteria, an estimate of the conditional probability of seismic failure or fragility is calculated. The fragility analysis provides an estimate of the median seismic capacity (50 percent conditional probability of failure) and the associated uncertainty. The capacity for this analysis is defined in terms of the building drift. The drift is then correlated to a seismic ground motion parameter.

The fragility estimate for this evaluation is formulated as a log-normal distribution, which is mathematically expressed as:

$$P_f(\Delta) = \Phi \left[\frac{\ln \frac{\Delta}{\Delta_m}}{\beta} \right] \quad (1)$$

where $P_f(\Delta)$ = Conditional Probability of Failure

Δ_m = Median Drift

β = Logarithmic Standard Deviation

Φ = Standard Normal (Gaussian) Distribution

A fragility curve for the structure is provided in Figure 11. The variability or uncertainty in the analysis is expressed through the logarithmic standard deviation or beta (β) value. The variability is the slope of the fragility curve with larger β resulting in a flatter slope. In this analysis both the randomness in the earthquake motion and the lack of knowledge or uncertainty is treated as a combined variability.

The sources of variability in the analysis include the input time history motion, the structural stiffness, the strength of R/C sections, and the ground motion correlation equation. The variability for each of the above sources was combined using the square root of the sum of the squares method to obtain the combined variability.

The response variability due to input time history, structural stiffness and strength was calculated by performing a statistical analysis of the nonlinear SDOF drift data. In developing the drift data, 99 nonlinear time history calculations were performed. Three different combinations of concrete strength and earthquake annual probability were evaluated. These cases are identified in Table 4.

Table 4 Nonlinear SDOF Analyses

Case	Concrete Strength	EQ Return Period
1	95%	2,000 year
2	95%	10,000 year
3	50%	10,000 year

For each of the three cases and the 11 time histories described above, three different building stiffness (natural frequency) values were evaluated. The stiffness values correspond to the best estimate, the +30 percent and the -30 percent estimates. Therefore, for each case, 33 (11 time histories x 3 stiffness values) drift values were calculated. Each of the 33 drift values was considered to have an equal probability of occurrence.

The variation in the drift values, β_R , accounts for both the earthquake time history randomness and the structural stiffness uncertainty and was calculated by fitting the 33 data points from each of the three cases for nonlinear SDOF analysis to a log-normal distribution. The slope of the distribution provides the β value. The highest β_R value from the three cases is used in the fragility analysis. The larger β value will produce a flatter fragility curve that will result in a larger change in failure probability over a specified range of ground motion. In this analysis the β_R value was calculated to be 0.23.

The variability in strength (β_S) is determined by performing two seismic analyses. The first analysis was performed using nominal material properties (95% exceedance) to calculate the ultimate strength, and the second analysis was based on median material properties. For a constant earthquake level, represented by Cases

2 and 3 in Table 4, the variability in a fragility analysis is measured by the change in building response due to the change in ultimate strength. The median drift values in cases 2 and 3 are the same because the building is responding in the displacement control region of the spectra. Thus, the variability for this structure with respect to strength is zero ($\beta_s = 0$).

The fragility level for a structure is correlated to a ground motion parameter. Studies provided by Sozen, (Gulkan, 1974), Iwan, (Iwan, 1980), and Kennedy, (Kennedy, 1984), show that the drift of nonlinear SDOF systems can be reasonably correlated to the spectral displacement by the equation

$$\delta \approx S_D(f_e, \Delta_e) \quad (2)$$

Where $S_D(f_e, \Delta_e)$ is the input ground motion spectral displacement at an effective frequency f_e and an effective damping Δ_e .

The data in this analysis provided a good correlation between the average spectral displacement (\bar{S}_D) taken over a frequency range from 0.35-0.65 Hz at an effective damping level of 10%. Therefore, the following equation was used to represent the drift response (δ_R) in terms of spectral displacement

$$\delta_R \cong \bar{S}_D \quad (3)$$

A small level of variability in the ground motion equation is addressed by assigning a beta value (β_{EQ}) to the equation. Based on engineering judgement $\beta_{EQ} = 0.05$ was assigned to the equation.

The median capacity of the structure is defined as the lateral drift that results in a 50% probability of structural failure. To develop the median capacity and the associated variability the drift verses probability of failure data in Figure 10 is fit to a log-normal distribution. The log-normal fit of the data provides a median drift capacity of 5.8 inches with an associated

variability on capacity $\beta_C = 0.17$. The median capacity of 5.8 inches represents a 50 percent probability of failure.

The variability for each individual source is summarized in Table 5. These variabilities were combined using square root of the sum of the squares as the statistical method to determine a composite variability. A composite variability of 0.29 is calculated for this structure.

Table 5 Seismic Fragility

Variability	Value
Response - β_R	0.23
Strength - β_S	0.00
Equation - β_{EQ}	0.05
Capacity - β_C	0.17
Composite - β^*	0.29

$$*\beta = \text{Composite Variability} = \sqrt{\beta_R^2 + \beta_S^2 + \beta_{EQ}^2 + \beta_C^2}$$

Comparing Figure 10 with Figure 11, the building median drift capacity of 5.8 inches and its associated variability β_C of 0.17, as shown in Figure 10, can be considered a lower bound fragility curve because it does not contain all of the sources of variability. The other sources of variability including response, strength, and ground motion correlation provide adjustments that flatten the distribution, as shown in Figure 11. The flattening of the fragility curve using the composite beta value of 0.29 results in a wider range on probability of failure verses seismic input motion. Correlating the drift response to the ground motion parameter spectral displacement completes the final seismic fragility for the structure. The seismic fragility for this structure is expressed in term of the spectral displacement by the equation:

$$S_D = \hat{S}_D e^{\beta x} \quad (4)$$

Where S_D = Spectral displacement at a given probability of failure

\hat{S}_D = Median spectral displacement (5.8 inches)

β = Composite variability (.29)

X = The number of normal standard deviations the given probability is from the median.

4.3. ANNUAL PROBABILITY OF SEISMIC FAILURE

The fragility curves were convolved (integrated) with the site mean hazard curve to obtain an estimate of the mean annual probability of seismic failure. Equation 5, from DOE Standard 1020, is a good approximation for more formal numerical integration, was used.

$$P_r = \frac{H_D e^{\frac{1}{2}(K_H \beta)^2}}{\left(\frac{C_{50}}{SME} \right)^{K_H}} \quad (5)$$

Where P_r = Mean annual probability of seismic failure

C_{50} = Median spectral displacement capacity

β = Composite logarithmic standard deviation

SME = Median SME response

H_D = Annual probability of exceeding the median SME

K_H = Slope parameter of the spectral displacement hazard curve

This equation assumes that the fragility curve is log-normal and that the hazard curve of average spectral displacement can be approximated by a straight line on a log-log plot. Values summarized in Table 5 were used to calculate the mean annual probability of failure. For the structure evaluated in this analysis the mean annual probability of seismic failure was

determined to be 1.8×10^{-4} , which is less than the acceptance criteria performance goal of 2×10^{-4} . Thus, this structure meets the probabilistic acceptance criteria specified in DOE Standard 1020.

5. CONCLUSIONS

A methodology to predict structural behavior in older DOE reinforced concrete facilities was implemented. This methodology can be used to demonstrate seismic capability consistent with the performance goals stated in DOE Standard 1020 when traditional deterministic methods indicate deficient seismic designs. Adaptations of the methodology can be used to meet performance goals developed for other nuclear and non-nuclear buildings.

Key to the development of realistic estimates of the ultimate lateral load resisting capacities for existing structures is the understanding of the behavior of reinforced concrete joints with partially developed bars. These joints do not necessarily demonstrate brittle behavior and the limited rotation capability of partially developed joints can contribute significantly to the overall ductility of the reinforced concrete frame. Notwithstanding the ductility available when estimating the limit state, significant damage in the structure is expected to occur, thus new construction should fully develop bars.

This structure has an elastic frequency on the order of 1 to 1.3 Hz, which increases further as the lateral load increases. This high period structure is displacement controlled thus computed drifts are relatively insensitive to the initial structural stiffness and capacity. The drifts are a function of the low frequency displacements in the ground motions.

6. ACKNOWLEDGMENTS

The information contained in this article was developed during the course of work done under Contract No. DE-AC09-89SR18035 with the U.S. Department of Energy.

The analyses presented in this paper were performed by the engineers in the Structural Mechanics Section and the Site Geotechnical Services Department of the Westinghouse Savannah River Company. The generous

guidance provided by Dr. Robert P. Kennedy, Prof. Charles E. Miller, and Prof. Mehta Sozen are gratefully acknowledged.

7. REFERENCES

- American Concrete Institute, ACI-318-51, *Building Code Requirements for Reinforced Concrete*, 1951.
- American Concrete Institute, ACI-318-95, *Building Code Requirements for Structural Concrete and Commentary*, 1995.
- APPLIED TECHNOLOGY COUNCIL, ATC-19, "Structural Response Modification Factors", 1995.
- APPLIED TECHNOLOGY COUNCIL, FEMA 273, "NEHRP Guidelines for the Seismic Rehabilitation of Buildings", 1996.
- APPLIED TECHNOLOGY COUNCIL, FEMA 274, "NEHRP Commentary on the Guidelines for the Seismic Rehabilitation of Buildings", 1996.
- Aycardi, A. E., Mander, J. B., and Reinhorn, A. M., "Seismic Resistance of Reinforced Concrete Frame Structures Designed Only for Gravity Loads: Part II - Experimental Performance of Subassemblages, NCEER-92-0028, National Center for Earthquake Engineering Research, December 1992.
- Beres, A., White, R., Gergely, P., "Seismic Performance of Interior and Exterior Beam-to-Column Joints Related to Lightly Reinforced Concrete Frame Buildings: Detailed Experimental Results", NCEER-92-0024, National Center for Earthquake Engineering Research, September 1992
- DOE-STD-1020-94, "Natural Phenomena Hazards Design and Evaluation Criteria for Department of Energy Facilities", April 1994.
- Eligehausen, R., Popov, E. P., Bectero, V. V., "Local Bond Stress-Slip Relationships of Deformed Bars Under Generalized Excitations," Report UCB/EERC-83/23, October 1983.
- Gulkan, P. and Sozen, M.A., "Inelastic Responses of Reinforced Concrete Structures to Earthquake Motions," ACI Journal, Vol. 71, No. 12, December, 1974.
- International Conference of Building Officials, *Uniform Building Code*, 1994.
- Iwan, W. D., "Estimating Inelastic Response Spectra from Elastic Spectra", Earthquake Engineering & Structural Dynamics, Vol. 8, 1980.
- Kennedy, R.P., et.al. "Engineering Characterization of Ground Motion - Task I: Effects of Characteristics of Free-Field Motion on Structural Response," NUREG/CR-3805, Vol. 1, U.S. Nuclear Regulatory Commission, 1984.
- Mertz, G., Loceff, F., Houston, T., Rawls, G., and Mulliken, J., "Performance Based Seismic Qualification of Reinforced Concrete Nuclear Materials Processing Facilities", 6th National Conference on Earthquake Engineering, Seattle, May, 1998.
- Takeda, T., Sozen, M. A., and Nielson, N. N., "Reinforced Concrete Response to Simulated Earthquakes", ASCE *Journal of the Structural Division*, Vol. 96, No. ST 12., 1970

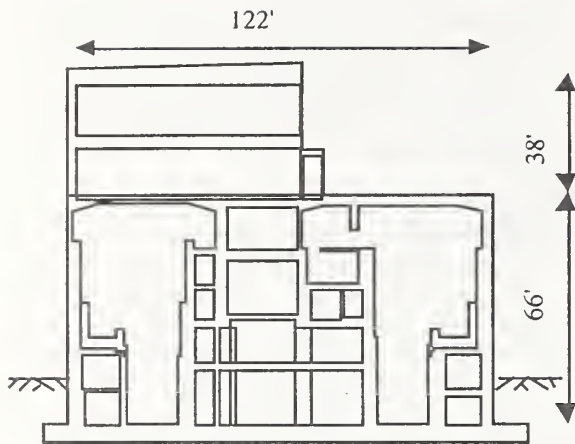


Figure 1. Frame cross section and vertical mass distribution

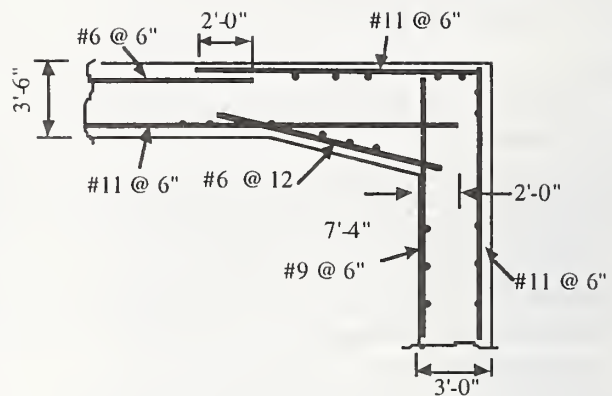


Figure 2. Typical joint detail

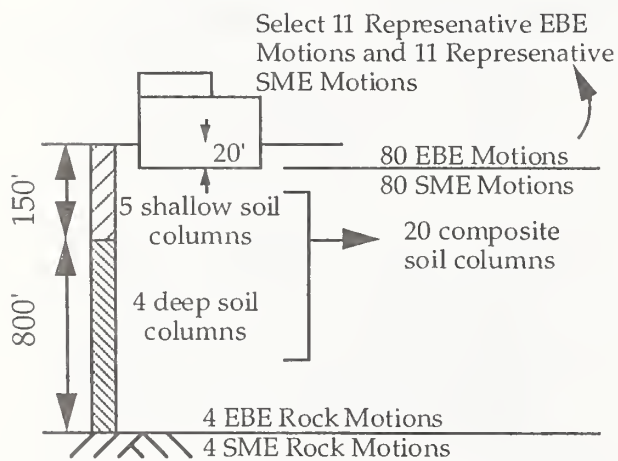


Figure 3. Development of Seismic Input

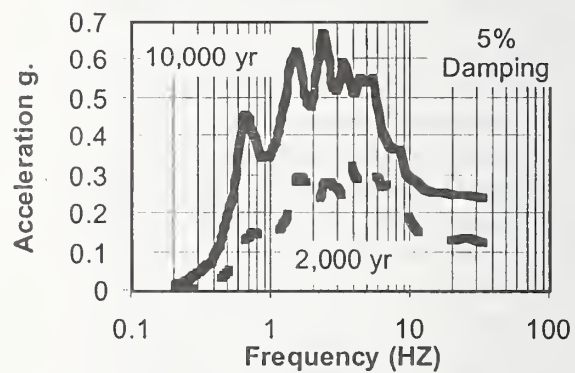


Figure 4. Mean site specific spectra

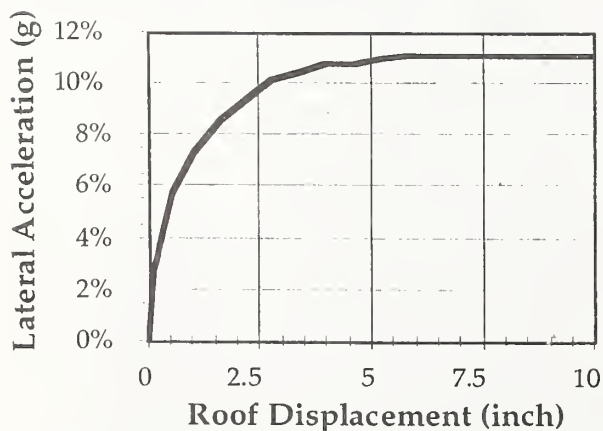


Figure 5. Monotonic load-deformation curve

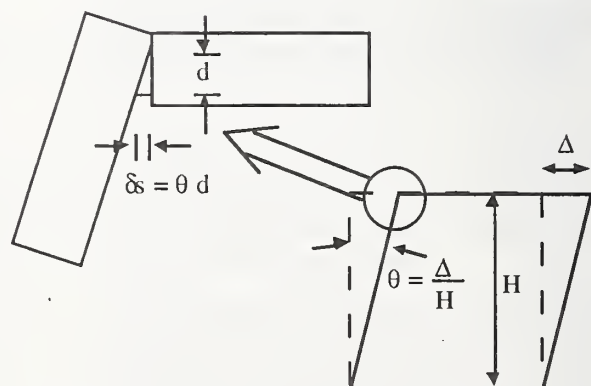


Figure 6. Relationship between bar slip and drift

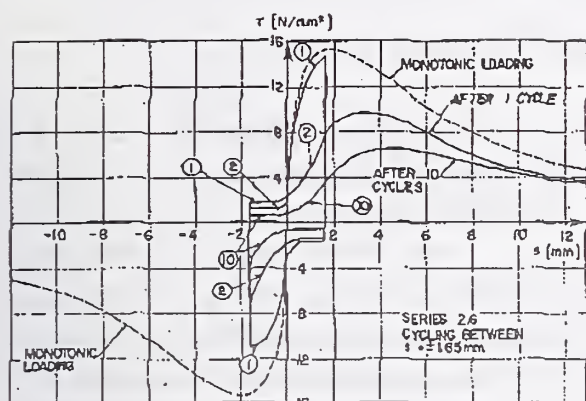


Figure 7. Bar pullout test (Eligehausen, 1983)

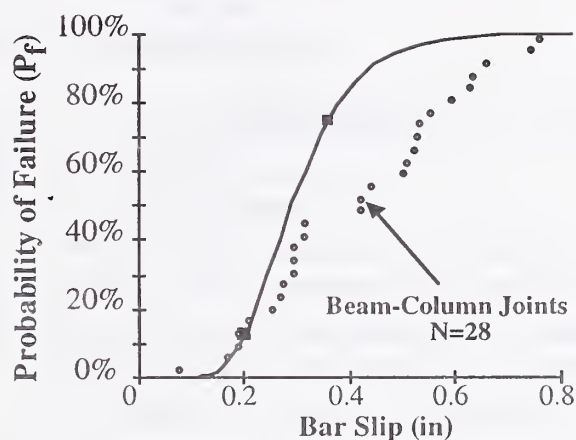


Figure 8. Probability of failure versus bar slip for confined joints

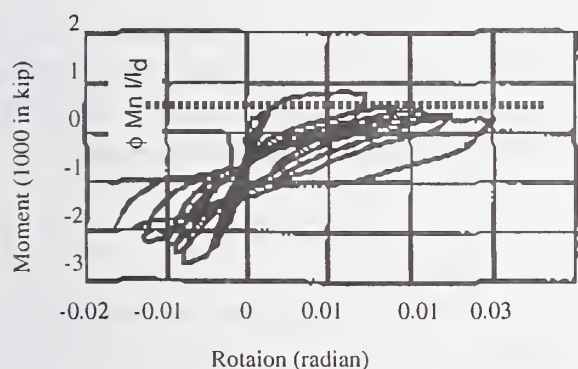


Figure 9. Full scale joint test (Beres, 1992)

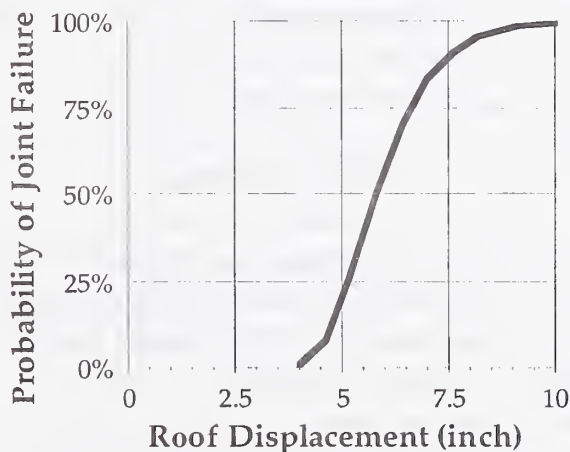


Figure 10. Envelope of joint failure probability versus roof displacement

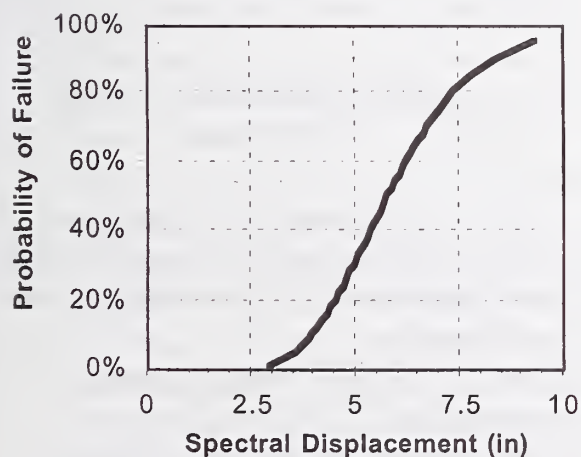


Figure 11. Building fragility curve

Development of an Analysis of Structural Steel Fracture and Development of Technical Solutions

by

Hiroyuki Yamanouchi ¹⁾, Akiyoshi Mukai ²⁾ and Takashi Hasegawa ³⁾

ABSTRACT

This paper presents the outline of a comprehensive technology development project by the Ministry of Construction, Japan, in which an analysis of structural steel fracture and technical solutions should be developed. Material properties and welding effects on steel fracture, fabricating and fracture of connections and collapse mechanism and fracture of steel structures are now being investigated.

Key Words: Steel Fracture

Material properties

Welding

Collapse mechanism

1. INTRODUCTION

In the extremely strong earthquake that struck Kobe and other parts of southern Hyogo Prefecture on January 17, 1995, structural steel in high-rise buildings and elsewhere was found to have snapped like sticks of chalk.

Presently, the approach to construction of buildings and other structures using steel materials has two facets: elastic design to resist ordinary loads and small or medium-strength earthquakes by ensuring that no residual deformation will result from small-to-medium stresses to structural steel; and plastic design to ensure that in the event of a major earthquake, inelastic deformation of structural steel will dissipate enough energy to prevent the entire structure's collapse.

In the Kobe earthquake, however, structural steel materials broke before they could dissipate energy through inelastic deformation, suggesting that a force smaller than the design force was able to destroy them.

This is why studies will analyze these phenomena and devise ways to analyze, investigate, and develop effective remedies.

This project initiated in April, 1996 and will be finished in March, 1999. In this project, Building Research Institute (BRI) is responsible for organizing and implementing the development of the analysis and solutions of steel members, welding and building structures.

2. FINAL GOAL

Our final goals are to clarify the demand for structural steel, to develop the guideline on welding procedures and to propose the design method for avoiding the brittle fracture of steel structures.

3. ORGANIZATION

BRI is carrying out the project as a cooperative research with The Kozai Club (KC). We have three sub-committees as shown in Fig.1. In addition, we are carrying out Research for Innovation(RFI) and US-Japan Cooperative Research as part of this project. In the following chapters, the outline of these activities will be introduced.

4. WELDING AND FRACTURE OF MATERIALS

In this sub-committee, five subjects are

- 1) Director, Codes and Evaluation Research Center, Building Research Institute, Ministry of Construction, Tachihara 1, Tsukuba, Ibaraki, 305-0802 Japan
- 2) Head of Aerodynamics Division, Department of Structural Engineering, ditto
- 3) Research Engineer of Structural Dynamics Division, ditto

being investigated to clarify the material properties and welding effects on steel fracture. Those subjects are as follows:

(1) Effect of Size

Experimental variables are plate thickness (25mm, 40mm, 100mm) and toughness of steel plates (low toughness, high toughness).

(2) Effect of welding

Experimental variables are heat input (CO_2 : 40 kJ/cm, ES: 800 kJ/cm) and toughness of steel plates (low toughness, high toughness).

(3) Effect of Impact

Experimental variable is loading rates (Static, 1 m/sec, 3 m/sec, 10 m/sec).

(4) Effect of Amplitude

Experimental variable is displacement amplitudes (monotonic, $\pm 2 \delta_p$, $\pm 4 \delta_p$, $\pm 8 \delta_p$).

(5) Effect of Time

Experimental variable is the time of load duration (10 seconds, 5 minutes, 2.5 hours).

These subjects have been examined by beam bending tests; experiments with low toughness steel are almost completed.

5. FABRICATING AND FRACTURE OF CONNECTIONS

The objectives of this sub-committee are to analyze the factors of brittle fracture observed in the welded connection and to verify reliable measures for the new-generation steel, the fabrication procedures, in-process inspection of the construction of new buildings. The final goals of this sub-committee are to clarify the phenomenon of beam-to-column connections, truss connections, etc., to develop guidelines on the fabrication procedures for improving the seismic performance, to assess the economic, social and political costs of implementing the recommendations in details of connections for more reliable inelastic action and to revise AIJ's Standard

for the Ultrasonic Inspection of Weld Defects in Steel Structures. There are four working groups in this sub-committee.

(1) Data Analysis

In this working group, to investigate the steel properties for building structures, fracture data base is under construction.

(2) Fundamental Study

In order to evaluate the material properties of steels prepared for full scale tests and to study the welding effects on material properties, material tests were conducted. Those were tensile tests, hardness tests, Charpy impact tests, fracture toughness tests, etc.

(3) Full Scale Connection Test

To investigate the relationship between the plastic deformation capacity of beam-to-column connection and the toughness of materials/connection details/fabrication level, cyclic loading tests of beam-to-column connection have been conducted. The parameters are toughness of steel materials (low toughness/high toughness), connection details (conventional type/revised type), welding condition (normal heat input/high heat input), loading speed (static/dynamic) and slab contribution.

(4) Strain Rate/ Weld Defects Test

Butt welded joints and T weld joints with low toughness steel have been tested, to investigate the strain rate and weld defects on the strength/fracture of beam-to-column connection.

6. COLLAPSE MECHANISM AND FRACTURE OF STEEL FRAMES

The main objective of this sub-committee is to determine the required plastic deformation capacity of members in steel rigid frames subjected to earthquakes. It is presumed that the required plastic deformation capacity of steel members depends on the ultimate resistance of the frames, the formation of mechanism, the intensity of the input earthquake ground motions, and so on. In order to accomplish this objective, the following studies are now well

underway in this subcommittee.

(1) Earthquake response analysis of the frames having brittle fracture at beam-ends

The earthquake response analyses of the 9-story 3-bay planar frame with brittle fracture were performed in order to investigate the effect of brittle fractures at beam-ends on seismic response of steel rigid frames.

Fig 2 shows the hysteresis model of plastic hinges at beam-ends assumed in the analysis model. The most important parameter of this analysis is the plastic rotation capacity (θ_F) of the hinges. In this model frame, the plastic rotation capacity (θ_F) of the hinges at beam-ends was assumed to be 0, 0.005, 0.01, 0.02rad.. Fig 3 demonstrates an example of the analysis results in terms of maximum interstory drift angles in each story. In case of $\theta_F = 0.01$, the maximum interstory drift angle of the frame against the Kobe earthquake ground motion is larger than that against the other earthquake ground motions.

(2) Simplified Response Prediction Models

In this sub-committee, the simplified fish bone model were developed to predict the seismic behavior of the frames. The predictions by using the fish bone model were compared to the results by using the frame model for verifying the predictability of the fish bone model.

(3) Column Overdesign Factor (COF) for Ensuring Beam-Collapse Mechanism in Earthquake Response

The objectives of this analysis is as follows;

- 1) To determine the COF needed for ensuring beam-collapse mechanism
- 2) To investigate plastic rotation expected to columns if the COF smaller than 1

From the results of the earthquake response analysis using the fish bone model, following the results were obtained.

- 1) Even if column yielding is permitted, overall behavior (including max. overall drift angle, max.

story drift angle, max. beam rotation) remains relatively unchanged as long as the $\text{COF} \geq 1.1$.

- 2) For the case where the max. velocity of input EQ is 0.5 m/sec, max. column plastic rotation was smaller than 0.01rad. (3-story model) and 0.005rad. (6 and 9 story models) when the $\text{COF} \geq 1.1$.

(4) Experimental Study on Inelastic Behavior of Joint Panel Zone

This study was conducted to investigate the elastic-plastic behavior of joint panel zone and to propose the adequate guide on strength and rigidity. The following three series of tests were carried out in this study.

Series 1: Test on the beam to SHS (square hollow section) column connections subjected to diagonal bending moment (see Fig. 4)

Series 2: Test on the effect of manufacturing process of SHS column

Series 3: Test on the H-shaped column connections

(5) Model Building Studies

The objectives of this study is to investigate the seismic performance of U.S. steel perimeter frames and Japanese spatial moment resisting frames. For this purpose, the SAC theme structures have been redesigned by Japanese seismic code under similar soil and hazard conditions as spatial moment resisting frames using box columns.

A comparison between nonlinear responses of U.S. perimeter(SAC3-LA) and of redesigned Japanese spatial moment resisting frames(BRI3A, BRI3B) is performed. From the results of the earthquake response analysis, a clear difference in seismic performance of U.S. frames and Japanese frames in terms of interstory drift angles, cumulative plastic rotations(η_{\pm}) was found. (see Table1, Fig. 5, Fig.6 and Fig.7)

7. RESEARCH FOR INNOVATION

We have just started the research on the

new generation steel, new connection, new inspection and new structural system to create the new steel structural system.

8. US-JAPAN WORKSHOP

US-Japan workshops on steel fracture issues were held three times. The first workshop was held in June, 1996 in San Francisco and UC Berkeley. The second one was in February, 1997 in San Francisco. And the third one was in April, 1998 in Tokyo. In those workshops, the information on the research results was exchanged between both countries and future cooperative research items were discussed. The proceedings of the first two workshops have been available, (Ref.1) (Ref.2).

9. CONCLUSION

The outline of the project on the steel fracture issues was presented. It is hoped to complete our project with practical recommendations in the next year.

REFERENCES

1. "Report of First US-Japan Workshop on Steel Fracture Issues" Building Research Institute, The Kozai Club, September, 1996
2. "Report of US-Japan Workshop on Brittle Fracture of Steel Building subject to Earthquakes" Science and Technology Agency, Building Research Institute, March, 1997

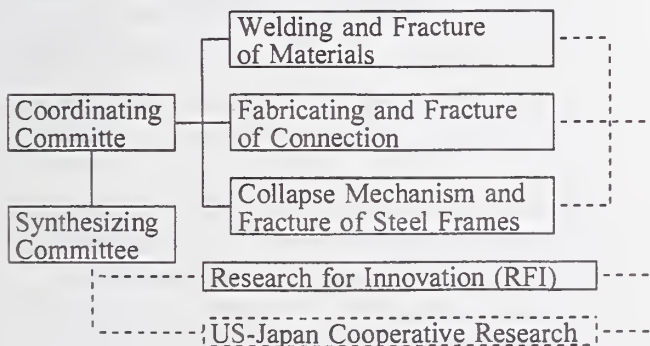


Fig.1 Organization

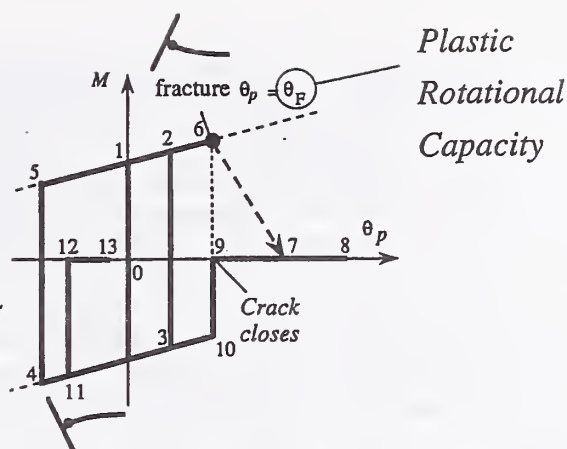


Fig.2 Hysteresis Model of Plastic Hinges at Beam-ends

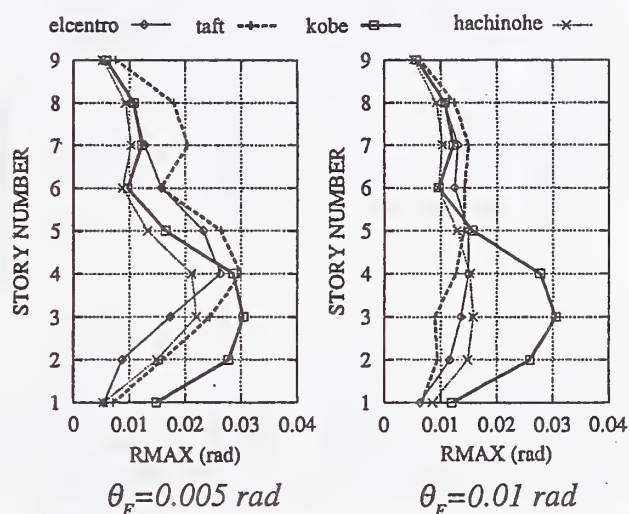


Fig.3 Maximum Interstory Drift Angles

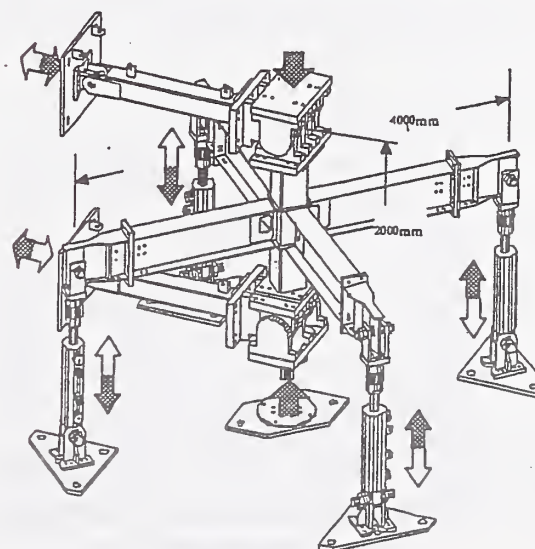


Fig.4 Diagonal Loading Test

Table 1 Beam and Column Sections of 3-Story Frames

Story/Floor	BRI3-A		BRI3-B		SAC3-LA		
	Column (BCR295)		Column (BCR295)		Column (50ksi)		Girder (36ksi)
	Ext.	Int.	Ext.	Int.	Ext.	Int.	
3/4	□-450×16	H-550×200×9×19	□-400×16	H-550×200×9×16	W14×257 (H-419×407×31×49)	W14×311 (H-437×412×36×58)	W24×68 (H-602×228×11×15)
2/3	□-450×19		□-400×19	H-550×200×9×19			W30×116 (H-762×267×14×22)
1/2	□-450×22		□-400×22	H-550×200×9×22			W33×118 (H-835×292×14×19)

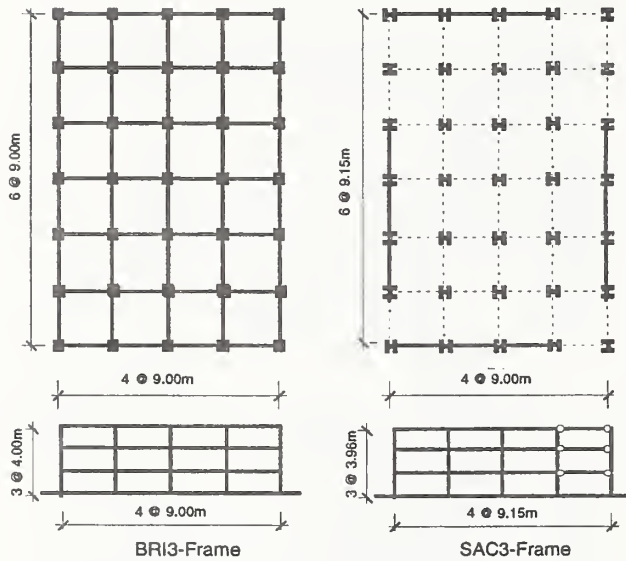


Fig.5 Plan Views and Elevations of 3-Story Frames

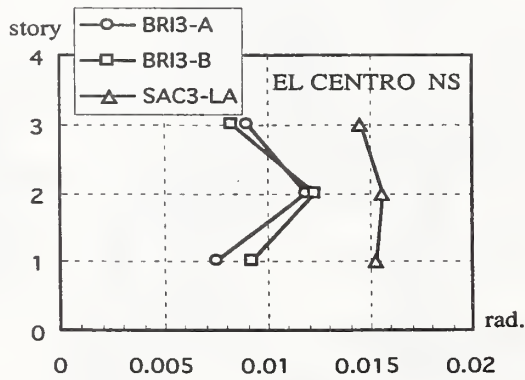


Fig.6 Maximum Interstory Drift Angles (Vt=150kine)

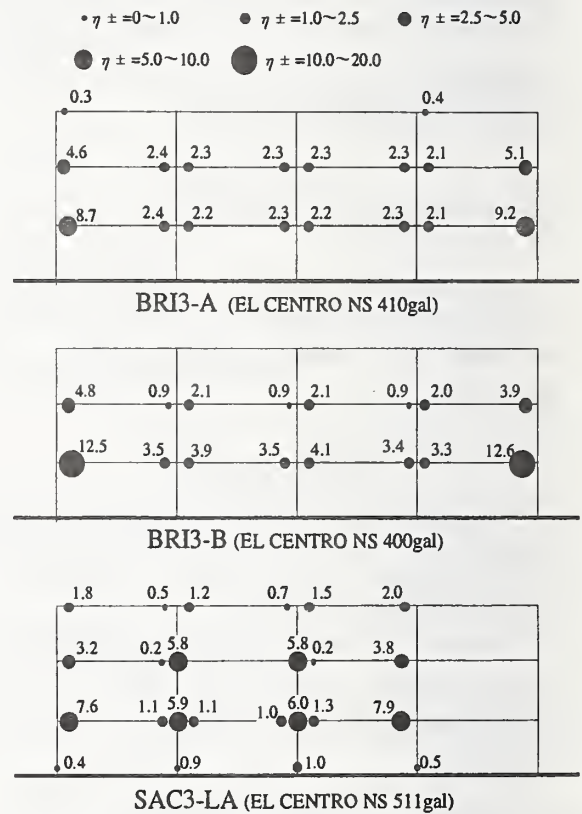


Fig.7 Damage Distribution (Vt=150kine)

Design Guidelines for the Seismic Modification of Welded Steel Moment Frame Buildings

by

John L. Gross, Ph.D., P.E.¹

ABSTRACT

Prompted by the widespread damage to welded beam-to-column connections as a result of the 1994 Northridge earthquake, the National Institute of Standards and Technology (NIST) initiated a study to determine the efficacy of various techniques for the modification of existing welded steel moment frame connections to improve their seismic performance. Problems associated with retrofitting of existing WSMF buildings are discussed and the alternative strategies selected for study are described. Results of 18 full-scale tests of two-sided (interior) connections, some having a lightweight concrete slab on metal deck, are presented. Design guidelines, based on the experimental results, have been written in cooperation with the American Institute of Steel Construction (AISC) and are described.

KEYWORDS: buildings; connections; design; earthquake engineering; frames; rehabilitation; steel

1. INTRODUCTION

The January 17, 1994 Northridge earthquake caused significant unexpected damage to welded steel moment frame (WSMF) construction. In particular brittle fractures in the beam-to-column moment connections were found in over 100 buildings (Youssef et al. 1995). In some instances the beam flange-to-column flange welds fractured completely resulting in greatly reduced moment resistance at the connection. Fortunately, no members or buildings collapsed as a result of the connection failures and no lives were lost. Nevertheless, the widespread occurrence of these connection failures is indicative of basic deficiencies in welded steel moment frame design and

construction practice prior to the 1994 Northridge earthquake. Indeed, the beam-to-column connection detail in common use at the time of the Northridge earthquake was deleted in an emergency code change ("ICBO Board" 1994). There is concern that existing structures incorporating these pre-Northridge welded moment connections may not provide the desired level of seismic performance in a major earthquake. The work described in this paper addresses the design of modifications to the WSMF connections to provide improved seismic performance.

1.1 Background

In the United States, seismic design of WSMF construction is based on the assumption that, in a severe earthquake, frame members will yield in a ductile fashion thereby dissipating energy. The welds and bolts that connect the frame members, being considerably less ductile, must be designed so as not to fracture (SEAOC 1990). The beam-to-column moment connections should be designed, therefore, for either the strength of the beam in flexure or the moment corresponding to the joint panel zone shear strength.

The Uniform Building Code, or UBC (ICBO 1994), is adopted by nearly all California jurisdictions as the standard for seismic design. From 1988 to 1994 the UBC prescribed a beam-to-column connection that was deemed to satisfy the above strength requirements. This "prescribed" detail required that the beam flanges be welded to the column using complete joint penetration (CJP) groove welds.

¹ Building and Fire Research Laboratory
National Institute of Standards and Technology
Gaithersburg, Maryland 20899 USA

The beam web connection was made by either welding directly to the column or by bolting to a shear tab which in turn was welded to the column. A version of this prescribed detail is shown in Figure 1. Although this connection detail was first prescribed by the UBC in 1988, it has been widely used since the early 1970's.

In general, fractures of these "prescribed" moment connections were found to initiate at the root of the beam flange CJP weld and propagate through either the beam flange, the column flange, or the weld itself. In some instances, fracture extended through the column flange and into the column web. The steel backing, which was generally left in place, produced a mechanical notch at the weld root. Fractures often initiated from weld defects in the root pass which were contiguous with the notch introduced by the weld backing. A schematic of a typical fracture path is shown in Figure 2. A fracture analysis, based upon measured material properties and measured weld defect sizes (Kaufmann et al. 1997), revealed that cleavage fracture would occur at stress levels roughly equal to the nominal yield strength of the beam.

1.2 Connection Failures

Brittle fracture will occur when the applied stress intensity, which can be computed from the applied stress and the size and character of the initiating defect, exceeds the critical stress intensity for the material. The critical stress intensity is in turn a function of the fracture toughness of the material. In the fractures that occurred in WSMF construction as a result of the Northridge earthquake, several contributing factors were observed which relate to the fracture toughness of the materials, size and location of defects, and magnitude of applied stress. These factors are discussed here.

The self-shielded flux cored arc welding (FCAW-SS) process is widely used for the CJP flange welds in WSMF construction. The E70T-4 electrode in common use prior to the Northridge earthquake, is not rated for notch

toughness and has been found to have very low Charpy V-notch (CVN) toughness, frequently on the order of 7 J at 20° C (Kaufmann et al. 1997).

The practice of leaving the steel backing in place introduces a mechanical notch at the root of the flange weld joint as shown in Figure 2. Also, weld defects in the root pass, being difficult to detect using ultrasonic inspection, may not have been rejected by the inspectors and therefore were not repaired. Further, the use of "end dams" in lieu of weld tabs was widespread.

The weld joining the beam flange to the face of the relatively thick column flanges is highly restrained. This restraint inhibits yielding and results in somewhat more brittle behavior. Further, the stress across a beam flange connected to a wide flange column section is not uniform but rather is higher at the center of the flange and lower at the flange tips. Also, when the beam web connection is bolted rather than welded, the moment is carried principally by the beam flanges. Finally, the actual yield strength of a steel member may exceed the nominal yield strength by a considerable amount. Since seismic design of moment frames relies on beam members reaching their plastic moment capacity, an increase in the yield strength translates to increased demands on the CJP flange weld.

Modifications to pre-Northridge WSMF connections to achieve improved seismic performance seek to reduce or eliminate some of the factors which contribute to brittle fracture mentioned above. Methods of achieving improved seismic performance are addressed next.

2. IMPROVING SEISMIC PERFORMANCE

There are several approaches to minimizing the potential for fracture including, 1) strengthening the connection thereby reducing the beam flange stress at the column face, 2) limiting the beam moment at the column face, or 3)

increasing the fracture resistance of welds. Any of these basic approaches, or a combination of them, may be used. This paper presents three connection modification methods: welded haunch, bolted bracket, and reduced beam section. The first two of these modification methods employ the approach of strengthening the connection and thereby forcing inelastic action to take place in the beam section away from the face of the column and the CJP flange welds. The third method seeks to limit the moment at the column face by reducing the beam section at some distance from the column thereby introducing a structural "fuse."

2.1 Reduced Beam Section

The reduced beam section (or RBS) technique is illustrated in Figure 3. As shown, the beam flange is reduced in cross section thereby weakening the beam in flexure. Various profiles have been tried for the reduced beam section but only the circular cut is considered here. The intent is to force a plastic hinge to form in the reduced section. By introducing a structural "fuse" in the reduced section, the force demand that can be transmitted to the CJP flange welds is also reduced. The reduction in beam strength is acceptable in most cases since drift requirements frequently govern moment frame design and the members are larger than needed to satisfy strength requirements. The RBS technique applied to the bottom flange only tends to reduce the overall frame stiffness on the order of 5%. This technique has been shown to be promising in tests intended for new construction.

The RBS plays a role quite similar to that of connection reinforcement schemes such as cover plates. Both the RBS and connection reinforcement move the plastic hinge away from the face of the column and reduce stress levels in the vicinity of the CJP flange welds. Connection reinforcement often requires welds that are difficult and costly to make and inspect. These problems are lessened with the RBS, which is somewhat easier to construct.

On the other hand, a greater degree of stress reduction can be achieved with connection reinforcement. With the RBS, there is a practical limit to the amount of flange material that can be removed and consequently, there is a limit to the degree of stress reduction that can be achieved with the RBS.

The reduced beam section appears attractive for the modification of existing connections because of its relative simplicity, and because it does not increase demands on the column and panel zone. For new construction, RBS cuts are typically provided in both the top and bottom beam flanges. However, when modifying existing connections, making an RBS cut in the top flange may prove difficult due to the presence of a concrete floor slab. Consequently, in this study addressing the modification of existing connections, the RBS cut is provided in the bottom flange only.

2.2 Welded Haunch

Welding a tapered haunch to the beam bottom flange (see Figure 4) has been shown to be very effective for enhancing the cyclic performance of damaged moment connections (SAC 1996) or connections for new construction (Noel and Uang 1996). The cyclic performance can be further improved when haunches are welded to both top and bottom flanges of the beam (SAC 1996) although such a scheme requires the removal of the concrete floor slab in existing buildings. Reinforcing the beam with a welded haunch can be viewed as a means of increasing the section modulus of the beam at the face of column. However, a more appropriate approach is to treat the flange of the welded haunch as a diagonal strut. This strut action drastically changes the force transfer mechanism of this type of connection and can be shown to greatly reduce the stress in the beam flange welds.

The tapered haunch is usually cut from a structural tee or wide flange section although it could be fabricated from plate. The haunch

web is fillet welded to the beam and column flanges. The haunch flange is then groove welded to the beam and column flanges (see Figure 4).

2.3 Bolted Bracket

The bolted bracket is an alternative to the welded haunch and has the added advantage that no field welding is required. Rather, high strength bolts are used to attach a welded steel bracket, fabricated from plate, to both the beam and column as shown in Figure 5. Installation of the bolted bracket eliminates the problem associated with welding such as venting of welding fumes, supply of fresh air, and the need for fire protection.

As with the welded haunch, the bolted bracket forces inelastic action in the beam outside the reinforced region. Tests have shown this to be an effective repair and modification technique producing a rigid connection with stable hysteresis loops and high ductility (Kasai et al. 1997).

Various types of bolted bracket have been developed. The haunch bracket (Figure 5) consists of a shop-welded horizontal leg, vertical leg and vertical stiffener. The two legs are bolted to the beam and column flanges. An angle bracket (not shown), cut from a relatively heavy wide flange section, has been used for the top flange where it is desirable to conceal the modification within the concrete slab.

3. EXPERIMENTAL PROGRAM

The modification of pre-Northridge moment connections differs from new construction in two significant ways:

- 1) Existing welds are generally of low toughness E70T-4 weld metal with steel backing left in place and their removal and replacement using improved welding practices and tougher filler metal is both difficult and expensive, and

- 2) Access to the connection may be limited, especially by the presence of a concrete floor

slab which may limit or preclude any modifications to the top flange.

With these limitations in mind, the National Institute of Standards and Technology (NIST) initiated an experimental program for the express purpose of determining the connection performance for various levels of connection modification. As such, initial tests were conducted on specimens that typically involved modifications only to the bottom flange. Based on successes and failures, additional remedial measures were applied until acceptable performance levels were obtained.

The NIST experimental program was designed to complement other test programs that had been completed or were in progress. In the majority of the tests conducted prior to NIST involvement, the test specimens consisted of bare steel frame subassemblages representing one-sided (exterior) connections. The NIST program sought to obtain data on interior, or two-sided, connections to determine if such connections perform as well as one-sided connections. Additionally, the presence of a concrete slab, whether designed to act compositely or not, tends to shift the elastic neutral axis of the beam upward thereby increasing tensile flexural strains at the bottom beam flange weld as compared to those in a bare steel frame. To address this issue, some NIST tests included a steel deck-supported lightweight concrete slab. The concrete slab was not designed for composite action, however, shear studs designed to transfer lateral forces into the moment frame force the slab to act compositely with the steel beam.

Beam sections used in the NIST experimental program were selected to conform to those used in the SAC Phase 1 test program (SAC 1996). Two-sided connections, however, required larger columns than those used in the SAC tests to accommodate the unbalanced beam moments. Columns were selected so as to not require the addition of column web stiffening, commonly referred to as "doubler plates." The columns selected also did not

require continuity plates as would be consistent with practice in the early 1980's. The two test specimen sizes consisted of the following beam and column sections, respectively: W30x99, W12x279 and W36x150, W14x426.

The NIST experimental program involved the testing of 18 full-size beam-to-column connections which had been modified using the techniques described herein. One specimen was repaired and re-tested. A diagram of the test specimens and representative test apparatus is shown in Figure 6. The tests were conducted at the University of Texas at Austin, the University of California, San Diego and Lehigh University's ATLSS Research Center.

4. EXPERIMENTAL RESULTS

The objective of modifying moment connections in existing buildings is to improve their performance in future earthquakes. Experimental results indicate that the modified connections are generally capable of developing at least 0.02 radian of plastic rotation. A plot of the moment at the face of the column versus total plastic rotation for a representative haunch modification with concrete slab is shown in Fig. 7. While not meeting new construction standards, these modified connections will provide a significant improvement in performance compared to existing pre-Northridge connections. The use of these modified connections should reduce potential economic losses and mitigate safety concerns for existing WSMFs in future earthquakes. A minimum plastic rotation of 0.02 radian provides a reasonable and realistic basis for the seismic rehabilitation of a wide variety of ordinary buildings constructed with WSMFs.

4.1 RBS Results

The experimental data indicate that the addition of the beam flange cutout, by itself, is not sufficient to significantly improve connection performance. In all cases in which the low toughness beam flange groove welds were not replaced, the welds fractured at low levels of

plastic rotation indicating that additional measures would be required to significantly improve performance. Better performance was achieved by not only providing a flange cutout, but also by replacing the existing top and bottom beam flange groove welds with a higher toughness weld metal. Tests indicated that this level of modification permits the development of plastic rotations on the order of 0.02 radian to 0.025 radian.

4.2 Welded Haunch Results

For both sets of member sizes tested, the test data show that, when the beam top flange groove welded joint was left in its pre-Northridge condition, the welded haunch modification outperformed the RBS modification. Of the three sets of bare steel specimens tested, five beams experienced welded fracture at the top flange. Two-thirds of the beams, however, were able to develop plastic rotations of at least 0.025 radian. When the concrete slab was present, none of the beams experienced weld fracture and the plastic rotation achieved for the six beams tested varied from 0.028 radian to 0.031 radian, more than adequate for modification purposes.

4.3 Bolted Bracket Results

For the bolted bracket tests, four specimens showed early fracture of the top flange weld when the top flange connection was not modified. When a stiff double angle was bolted to the top flange and column face, the top flange did not fracture and the connections were able to develop 0.05 radian plastic rotation. The addition of a top angle, however, necessitates the removal of a portion of the concrete slab.

5. DESIGN GUIDELINES

Based on the results of 18 tests conducted under the program described herein, design guidelines have been developed which allow the proportioning and detailing of the three modification techniques described above. The

guidelines have been written in cooperation with the American Institute of Steel Construction (AISC) and will be available as part on their Design Guide series.

The design procedures account for the expected material yield strength and the design plastic moment for each modification has been calibrated to experimental results through a factor which accounts for strain hardening. A plot of this strain hardening factor versus story drift ratio for the RBS modification (W36x150 beams) is shown in Fig. 8. Because the seismic modification of existing welded steel moment connections is not fully investigated and there are many options to consider, the guideline contains a significant amount of commentary. Additionally, the guideline reports, in a common format, the results of 47 tests conducted by others.

6. CONCLUSIONS

This paper has provided a brief overview of the issues surrounding the modification of existing welded steel moment connections to improve their seismic performance. Three modification schemes were described; the welded haunch, bolted bracket and reduced beam section. An experimental program involving 18 tests of full-scale beam-to-column subassemblages was described. Results indicated that the modified connections are capable of developing a minimum of 0.02 radian of plastic rotation. Recommendations for the proportioning and detailing of the various connection modifications are contained in a design guide.

7. REFERENCES

- ICBO (1994). Uniform Building Code. International Conference of Building Officials (ICBO), Whittier, CA, 1994.
- "ICBO Board Approves Emergency Structural Design Provisions" (1994). Building Standards. September-October, 1994, p26.
- Kasai, K., Hodgon, I. And Mao, C. (1997). "Bolted Repair Methods for Fractured Welded Moment Connections," *Proceedings, Behavior of Steel Structures in Seismic Areas (Stessa '97)*, Kyoto, Japan, August 3-4, PP 939-946.
- Kaufmann, E.J., Fisher, J.W., DiJulio, R.M. and Gross, J.L. (1997). "Failure Analysis of Welded Steel Moment Frames Damaged in the Northridge Earthquake," NISTIR 5944, National Institute of Standards and Technology, Gaithersburg, MD.
- Noel, S. and Uang, C.-M. (1996). "Cyclic Testing of Steel Moment Connections for the San Francisco Civic Center Complex," Report No. TR-96/03, University of California, San Diego, La Jolla, CA.
- SAC (1996). "Experimental Investigations of Beam-Column Subassemblages," Technical Report SAC-96-01, Parts 1 and 2, SAC Joint Venture, Sacramento, CA.
- SEAOC (1990). Recommended Lateral Force Requirements and Commentary, Structural Engineers Association of California (SEAOC), Sacramento, 1990.

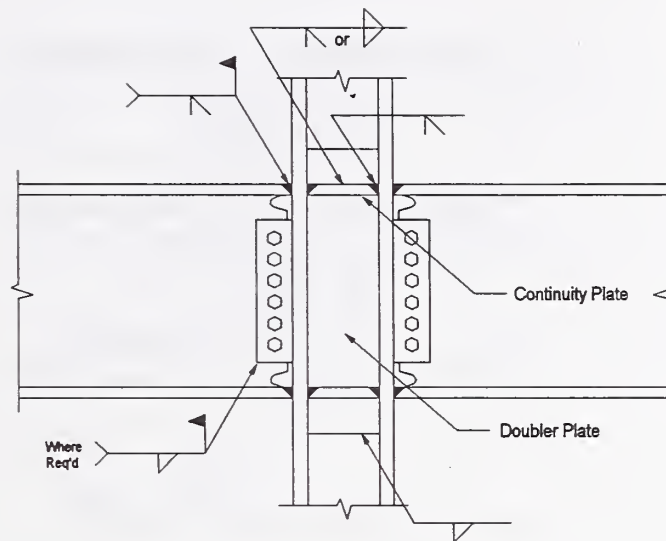


Figure 1 - "Prescribed" Moment Connection Detail

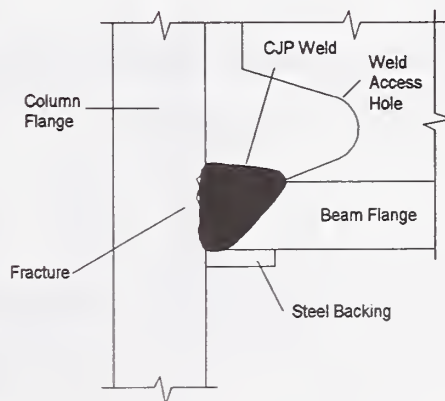


Figure 2 - Fracture of Complete Joint Penetration Flange Weld

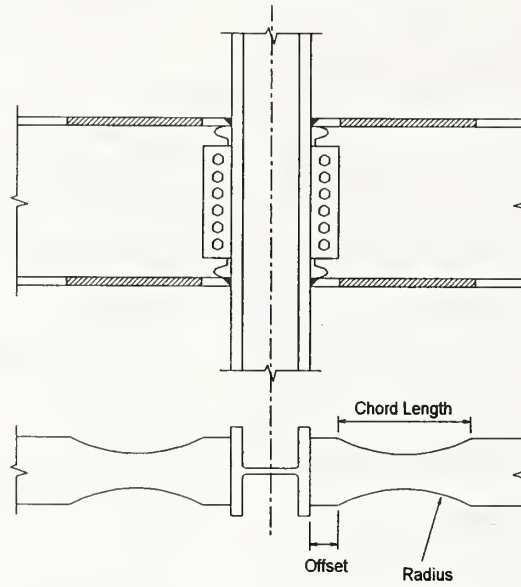


Figure 3 - Reduce Beam Section (RBS) Modification

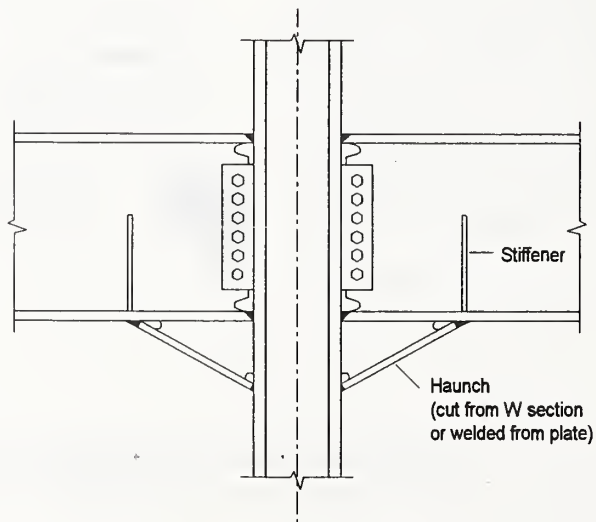


Figure 4 - Welded Haunch Modification

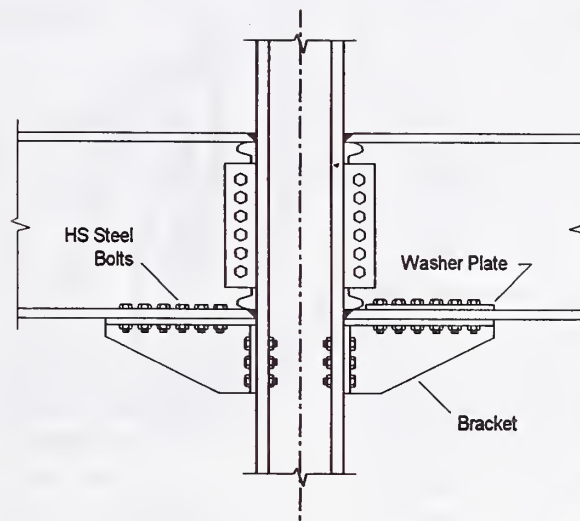


Figure 5 - Bolted Bracket Modification

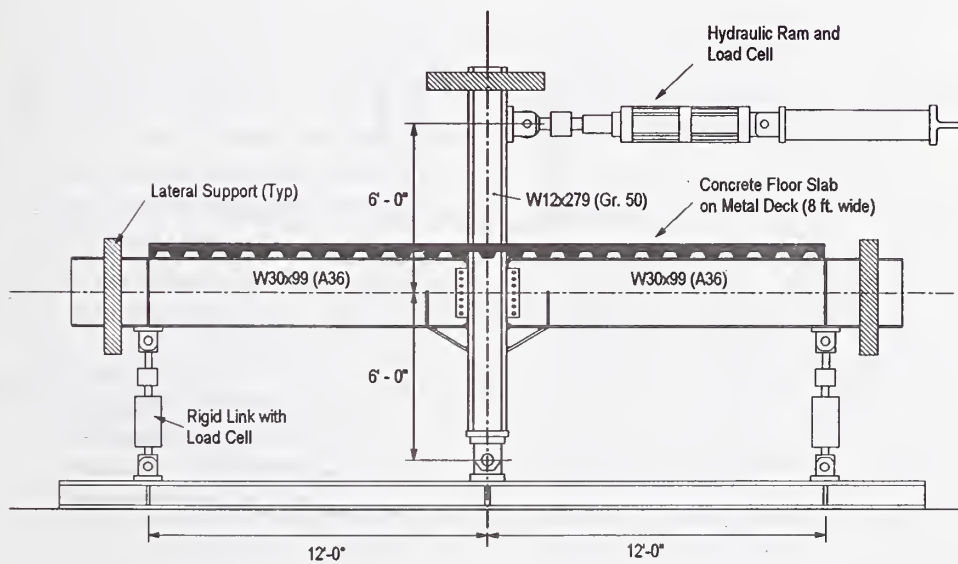


Figure 6 - NIST/AISC Test Set-Up

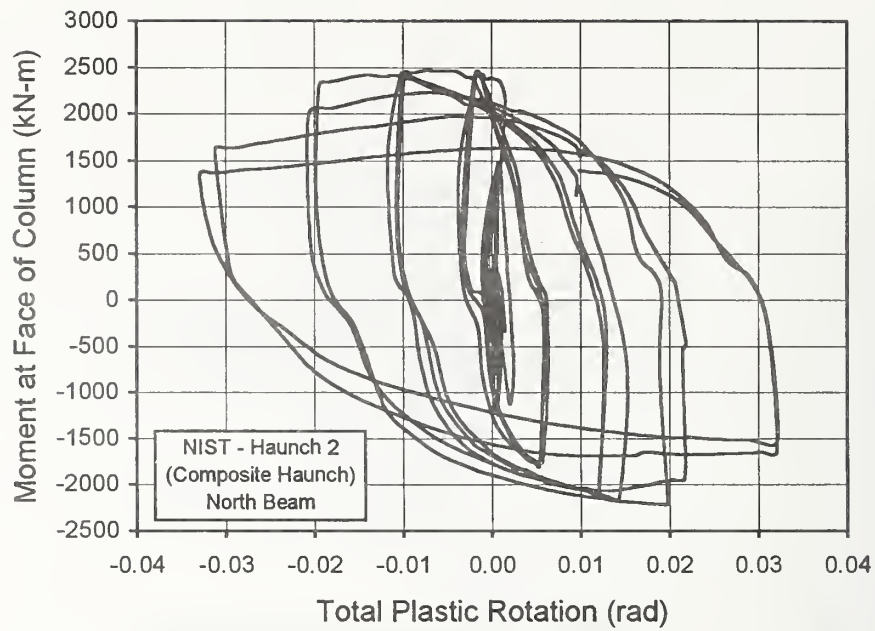


Figure 7 - Moment vs. Plastic Rotation for Haunch Modification

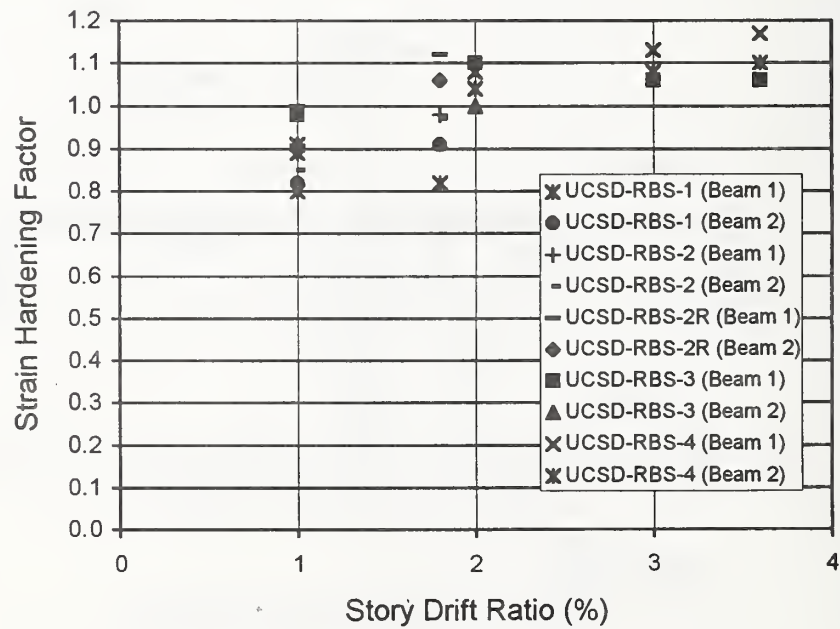


Figure 8 - Strain Hardening Factor vs. Story Drift Ratio for RBS Modification of W36x150 Beams

DRAFT MANUAL FOR SEISMIC ISOLATION DESIGN OF UNDERGROUND STRUCTURES

by

Shigeki UNJOH¹⁾, Jun-ichi HOSHIKUMA²⁾, Kazuhiro NAGAYA³⁾ and Kazuhiko MURAI³⁾

ABSTRACT

Public Works Research Institute has conducted 3-year joint research program on seismic isolation systems for underground structures to improve the structural performance and the safety during earthquakes. This project has been made through the joint research program between Public Works Research Institute, Public Works Research Center and 17 private companies. Developed seismic isolation systems for the underground structures are made by constructing the isolation materials with low-shear modulus around the underground structures to absorb the effect of ground deformation. Five kinds of seismic isolation materials have been developed and the analysis and design methods for the underground structures with the seismic isolation systems have been also studied and developed. The final accomplishment is complied as a "Draft Manual for Seismic Isolation Design of Underground Structures" in March 1998.

KEY WORDS : *Seismic Design*
Underground Structure
Seismic Isolation
Seismic Isolation Material
Seismic Isolation Design
Design Manual

1. INTRODUCTION

Underground structures such as tunnels and pipelines are generally affected by the

displacement and deformation of the surrounding ground during earthquakes. In general, therefore, the underground structures are less influenced by the effect of earthquakes than the structures on the ground in which the earthquake response is amplified through the structures.

On the other hand, the underground has recently been starting to be developed and to be densely used especially in urban areas. The underground structures are often required to be constructed at the sites where the effect of earthquake becomes critical in the design, such as the sites with soft soil conditions, the sites where the ground condition is drastically changing, and the sites where structures with different vibrational characteristics are constructed closely or jointly.

During the 1995 Hyogo-ken-nanbu Earthquake, the damage to the underground structures were relatively slight comparing the structures on the ground such as buildings and bridges. However, some of the underground structures such as subway station were damaged destructively. At the Daikai-Station of the Kobe High Speed Train, the RC columns were failed in shear and the upper slab was settled.

1) Head, Earthquake Engineering Division, Earthquake Disaster Prevention Research Center, Public Works Research Institute, Ministry of Construction, Tsukuba-shi, Ibaraki-ken, 305, Japan

2) Research Engineer, ditto

3) Visiting Research Engineer, ditto

The damage to sewage systems such as cracks and dislodgement of pipes were also found. The Public Works Research Institute has been studied and developed the seismic isolation systems for the underground structures to improve the seismic performance and the safety by constructing the isolation materials with low-shear modulus surrounding the underground structures. The isolation materials absorb the deformation of the ground during the earthquakes. This study was made through the joint research program between Public Works Research Institute, Public Works Research Center, and 17 private companies including material makers, general contractors, design consulting firms.

In the Joint research program, major objectives of the research and development are as follows:

- 1) Development of Isolation Materials Applicable for the Seismic Isolation Systems
- 2) Construction Methods of Seismic Isolation Materials
- 3) Design Methods for Underground Structures with Seismic Isolation Systems

The final accomplishments of the research and development is compiled as the "Draft Manual of Seismic isolation design for Underground Structures" in March 1998.

This paper presents the concept of the seismic isolation systems for the underground structures and the outline of the draft design manual.

2. SEISMIC ISOLATION SYSTEMS FOR UNDERGROUND STRUCTURES

2.1 Concept of Seismic Isolation Systems

In general, underground structures are subjected to the deformation through the interaction between the ground and the structures. Therefore, when the stiffness of the

structures are increased, the flexibility of the structures is decreased then the section force developed against the same deformation is increased. Hence, the design to increase the section or number of reinforcing bars to ensure the earthquake force developed like usual structures is not effective in general. In this case, it is effective to isolate the structures from the deformation of the ground.

There are several ways to decrease the effect of ground deformation to be transmit to the underground structures. Major ways are the followings :

- 1) To make the underground structures flexible by decreasing the stiffness
- 2) To decrease the effect of ground deformation to be transmitted to the underground structures

The usual way, which has been employed for actual submerged tunnels and shield tunnels and common utility ducts, is the above 1) using flexible joints. When the stiffness of the joints are decreased, the ground deformation is absorbed at the joints and the section force of the structures is decreased. However, when the displacement developed at the joints becomes excessive, there are cases in which such excessive displacement is not acceptable or the special water-proof joints are required depending on the performance level required to the structures during large earthquakes.

On the other hand, the above 2) includes the methods in which the seismic isolation layer consisted of the materials with low shear modulus comparing the surrounding soils are constructed around the structures as shown in Fig.1. Since the shear deformation of the ground is absorbed by the seismic isolation layer, the excessive displacement, which may be developed at the specific joints, is prevented by this methods. Furthermore, since the ground deformation is absorbed, the isolation layer is

effective to earthquake ground deformation both in the longitudinal and transverse directions.

Here, the method to decrease the effect of earthquakes by constructing the seismic isolation layer around the underground structures is defined as "Seismic Isolation Systems for Underground Structures".

2.2 Application of Seismic Isolation Systems

The effect of earthquake is generally large for the underground structures under the following conditions based on the past earthquake damage experiences.

- 1) Boundary section where the ground conditions are critically changed

The effect of earthquakes on the underground structures becomes large at the sites where the ground condition is changing from stiff ground to soft ground, or from cut ground to embanked ground. The deformation and the strain is concentrated at the boundary of the such sections with the change of ground conditions.

- 2) Connection section of two different structures

The deformation is concentrated at the connection section between shaft and tunnels, or junction sections, by the difference of the vibrational characteristics of two adjacent structures.

Therefore, the application of the seismic isolation systems is effective such boundary sections with different ground conditions or different structural conditions as shown in Fig.2. The concentration of the deformation and the strain is absorbed by the seismic isolation layer and the seismic performance of the underground structures can be improved.

Also, the transmission of shear deformation can be decreased by the seismic isolation layer, the effect of earthquakes is decreased for the

transverse direction of the structures with wide section in which the surrounding shear stress is critical in the seismic design.

Furthermore, when it is required to prevent water from coming in the structure depending on the required performance of the structures, the application of the seismic isolation layer with a water-proof function is effective both for the increase of the earthquake resistant performance and the water-proof performance.

2.3 Seismic Isolation Materials

Seismic isolation materials applicable to the underground structures are required to have the performances of seismic isolation functions and the function as the backfill materials. The development of the seismic isolation materials have been made for the shield-driving tunnels and the open-cut type tunnels. The required performances are as follows:

- 1) Low shear modulus and high shear deformability
- 2) High durability, long-term stability, and small volumetric changes
- 3) High constructionability (for example for shield-driving tunnels : transportability by pumping in a liquid state and high filling-up performance
- 4) Watertightness
- 5) No dilution by ground water
- 6) No contaminants

Based on the above required performances, in the joint research program, 5 kinds of the seismic isolation materials were developed as shown in Table 1. The material characteristics including mechanical one, such as shear modulus, durability, watertightness, creep, and constructionability were tested using developed materials.

Fig.3 shows examples of the mechanical properties of the developed materials obtained through the hollow cylindrical cyclic shear

tests. The all materials were tested by the same testing methods.

To simulate the actual condition in the tests, the surface soil layer with about 3m are assumed for the open-cut type tunnels. And for the shield driving tunnels, the surface layer with about 20 m was assumed. Then the confined pressures were selected as 0.5, 1.5 and 3.5 kgf/cm². The cyclic loading rate is assumed as 1 Hz considering the natural period of the surface layer. The strain range tested was assumed up to 10% considering the large deformation during the large earthquakes based on the analytical results.

Fig.3 shows that the shear modulus and damping ratio for Urethan-based material, Silicon-based material and Liquid Rubber material are almost constant in the range of the strain tested. And the confinement dependency was not found.

On the other hand, Asphalt-based material has the strain dependency in which when the strain increases the shear modulus decreases and the damping increases. The confinement dependency is found at the small strain range but is not remarkable.

For Precast Rubber Panel, the strain dependency and confinement dependency are found. Since the precast rubber panel is made by binding the rubber tips by resin, the precast rubber panel has the void inside the panel. The strain dependency is developed by the resin characteristics is changed in the high strain range then the shear modulus decreases.

Seismic isolation design of the underground structures has to be made based on the material characteristics as above mentioned. Some materials have other dynamic characteristics such as velocity dependency. They are also obtained through the necessary tests.

2.4 Construction Methods

Fig.4 shows the outline of the construction methods of seismic isolation materials. For the shield-driving tunnels, the same construction methods of the backfill to the tale void is applicable. The materials are injected to the tale void from the inside of the tunnels and the seismic isolation layer has constructed around the structures. To prevent the inflow of the isolation materials toward the shield machine and to construct seismic isolation layer certainly in the tale void, the shield machine requires the inflow prevention devices but not important remodeling. For the open-cut type tunnels, the seismic isolation layer can be constructed with the construction of the tunnels. In the joint research project, both construction methods are verified through the construction tests of the seismic isolation layer.

3. VERIFICATION TESTS OF THE EFFECTIVENESS OF SEISMIC ISOLATION SYSTEMS

3.1 Test Models

To verify the effectiveness of the seismic isolation systems, the model tests were made using large shake table at the Public Works research Institute.

Fig. 5 shows the scale of the model. Tunnel is assumed to be constructed at the change section of ground conditions. The tunnel was the almost 1/70 size of actual structures with a diameter of 70mm and the thickness of 2mm. The ground was made of Silicon where the soft soil was assumed to have the shear modulus of 1kgf/cm², and the stiff soil was assumed to have the 20kgf/cm². Seismic isolation layer was assumed to have the thickness 10mm and the shear modulus of 0.05kgf/cm².

The model was subjected to the sinusoidal ground motion and the random earthquake

ground motion. Since the natural frequency of the model was 6.5Hz, the sinusoidal wave with the natural frequency of the ground was input to the shake table.

3.2 Test Results

Fig. 6 shows the typical test results. In the right side section where the ground condition is changed, the seismic isolation layer is constructed. The strain in the tunnels in the longitudinal direction developed at the change section of the ground conditions was decreased by 30% by employing the isolation layers. This was the almost expected effectiveness through the analysis.

4. DRAFT MANUAL FOR SEISMIC ISOLATION DESIGN OF UNDERGROUND STRUCTURES

4.1 Table of Contents

The draft manual consists of 9 chapters, 4 design examples and the 12 reference materials. The table of contents is as follows.

1. General
 - 1.1 Scope
 - 1.2 Definition of Terms
 - 1.3 Symbols
2. Basic Principle of Seismic Isolation Design for Underground Structures
3. Design Earthquake Ground Motion and Design Ground Displacement
 - 3.1 General
 - 3.2 Design Ground Displacement during Earthquakes
 - 3.3 Dynamic Soil Properties
 - 3.4 Design Earthquake Response Spectrum
 - 3.5 Input Ground Motion for Dynamic Analysis
4. Seismic Design of Underground Structures in Transverse Direction
 - 4.1 General
 - 4.2 Horizontal Ground Displacement during Earthquakes
 - 4.3 Static Analysis Methods of Underground Structures in Transverse Direction
 - 4.3.1 General
 - 4.3.2 Response Inertia Force Methods
 - 4.3.3 Other Static Analysis Methods
 - 4.4 Model of Underground Structures in Transverse Direction
 - 4.4.1 Model of Shield Driving Tunnel
 - 4.4.2 Model of Open-Cut Type Tunnel
 - 4.5 Evaluation of Safety
 - 4.6 Check of Safety by Dynamic analysis Methods
 - 4.6.1 General
 - 4.6.2 Analytical Model
 - 4.6.3 Evaluation of Safety
5. Seismic Design of Underground Structures in Longitudinal Direction
 - 5.1 General
 - 5.2 Horizontal Ground Displacement during Earthquake
 - 5.3 Static Analysis Methods of Underground Structures in Longitudinal Direction
 - 5.3.1 General
 - 5.3.2 Analysis Methods using Beam-Mass Model
 - 5.3.3 Analysis Methods using Axisymmetric Model
 - 5.3.4 Analysis Methods using Simplified 3-Dimensional FEM Model
 - 5.3.5 Analysis Methods using 3-Dimensional FEM Model
 - 5.4 Model of Underground Structures in Transverse Direction
 - 5.4.1 Model of Shield Driven Tunnel
 - 5.4.2 Model of Open-Cut Type Tunnel
 - 5.5 Evaluation of Safety
 - 5.6 Check of Safety by Dynamic analysis Methods
 - 5.6.1 General
 - 5.6.2 Analytical Model
 - 5.6.3 Evaluation of Safety
6. Seismic Design of Connection Section between Shaft and Tunnel

- 6.1 General
- 6.2 Horizontal Ground Displacement during Earthquake
- 6.3 Static Analysis Methods of Connection Section between Underground Structures
- 6.4 Model of Shaft and Underground Structures
- 6.5 Evaluation of Safety
- 7. Design of Isolation Material and the Material Properties
 - 7.1 General
 - 7.2 Asphalt-based Material
 - 7.2.1 General
 - 7.2.2 Material Properties
 - 7.3 Urethan-based Material
 - 7.3.1 General
 - 7.3.2 Material Properties
 - 7.4 Silicon-based Material
 - 7.4.1 General
 - 7.4.2 Material Properties
 - 7.5 Liquid Rubber Material
 - 7.5.1 General
 - 7.5.2 Material Properties
 - 7.6 Precast Rubber Panel Material
 - 7.6.1 General
 - 7.6.2 Material Properties
- 8. Design of Seismically Isolated Tunnels against Usual Loads

Design Examples

- 1. Design Example of Open-Cut Type Tunnel in Transverse Direction
- 2. Design Example of Shield-driving Tunnel which is constructed at Changing Site of Ground Condition
- 3. Design Example of Shield-driving Tunnel which is constructed under the Retaining Caisson
- 4. Design Example of Connecting Section between Shaft and Tunnel

Reference Materials

- 1. Mechanical Properties of Isolation Materials
- 2. Construction Methods of Shield Tunnels

- with Isolation Design
- 3. Construction Methods of Open-Cut Type Tunnels with Isolation Design
- 4. Applicability of Seismic Isolation Design for Longitudinal Direction of Underground Structures
- 5. Applicability of Seismic Isolation Design for Transverse Direction of Open-Cut Type Tunnels
- 6. Applicability of Seismic Isolation Design for Transverse Direction of Shield driving Tunnels
- 7. Applicability of Seismic Isolation Design for Connection section between Shaft and Tunnels
- 8. Applicability of Analysis Methods in Longitudinal Direction of Underground Structures with Isolation Design
- 9. Applicability of Analysis Methods in Transverse Direction of Underground Structures with Isolation Design
- 10. Analysis Examples of Settlement of Surrounding Soils around Underground Structures with Isolation design
- 11. Verification Tests Results of Effectiveness of Seismic Isolation Design of Underground Structures
- 12. Verification Tests Results of Effectiveness of Seismic Isolation design of Underground Structures

4.2 Basic Principle of Seismic Isolation Design

In the draft design manual, the basic principle of the seismic isolation design is specified as follows:

- (1) The objective of the seismic isolation design for the underground structures is to decrease the section forces developed during earthquakes
- (2) The thickness and the length of the isolation layer shall be designed so as to get the effective isolation function.
- (3) When the seismic isolation systems are employed, the stability during the construction

and the stability against the usual loads shall be verified.

(4) In the seismic isolation design, the two type of earthquake ground motion shall be taken into account. They are the earthquake ground motion with high probability to occur during the lifetime of the structures and the earthquakes ground motion with strong intensity and the low probability to occur during the lifetime of the structures. Against these two types of earthquake ground motions, the underground structures shall be designed to insure the seismic performance level depending on the structural characteristics, purposes of use, importance, etc.

(5) Seismic isolation systems are applied both for the transverse and longitudinal directions of the underground structures. In the transverse direction, the earthquake response is analyzed by using Finite Element Method (FEM) model where the inertia force of ground is applied to the model. In the longitudinal direction, the earthquake response is analyzed using beam-spring model where the deformation of the ground applied is analyzed through the dynamic analysis of the ground. In the analysis of the connection of the shaft and the tunnels, the beam-spring model or axisymmetric FEM model. The properties of soils and structures shall be given appropriately depending on the response level.

(6) In the design of the underground structures with complicated vibrational characteristics during earthquakes, the safety shall be check by using detailed model and analysis methods.

(7) Isolation materials shall be selected considering the constructionability, watertightness, durability, material properties, etc., and shall be used in the reliable range of the material properties.

5. CONCLUDING REMARKS

The preceding pages presented an outline of 3-year joint research program on seismic

isolation systems for underground structures to improve the structural performance and the safety during earthquakes. There is an idea of the seismic isolation system for the underground structures long time ago, but the isolation materials and the construction methods applicable for the systems had not yet been developed. Through the joint research program, 5 kinds of seismic isolation materials have been developed and the analysis and design methods for the underground structures with the seismic isolation systems have been also studied and developed. The final accomplishment is complied as a "Draft Manual for Seismic Isolation Design of Underground Structures". Since the draft manual is now under printing, it will be available in around June.

This research is one of the first steps to realize a new earthquake resistant structure. We are planning to study furthermore about the practical application of the isolation systems and the verification tests using full-scale structures should be studied.

ACKNOWLEDGMENTS

This study was made the joint research program between Public Works Research Institute, Public Works Research Center and 17 private firms. The authors thank all members of the joint research program who have conducted research and development eagerly. In particular, Mr. Isao TAKATORI, Director of the Public Works Research Center and Dr. Takeyasu SUZUKI, Kumagai-gumi Cooperation for their faithful contribution to the joint research program.

REFERENCES

- 1) Public Works Research Institute : Report of The Disaster Caused by the 1995 Hyogo-ken Nanbu Earthquake, Journal of

- Research, Public Works Research Institute, Vol.33, March 1997 (in English)
- 2) Public Works Research Institute, Public Works Research Center, 17 Private Firms : Report of The Joint Research on Seismic Isolation Design of Underground Structures Vol.1 and Vol.2, Joint Research Report, No.154 and 192, November 1996 and December 1997, (In Japanese)
 - 3) Public Works Research Institute, Public Works Research Center, 17 Private Firms : Report of The Joint Research on Seismic Isolation Design of Underground Structures, - Draft Manual for Seismic Isolation design of Underground Structures -, Joint Research Report, March 1998 (Under Printing)
 - 4) Unjoh, S., Hoshikuma, J., Nagaya, K, and Murai, K: Development of Seismic Isolation Systems for Underground Structures and the Mechanisms of Seismic Isolation, 7th US-Japan Workshop on Earthquake Disaster Prevention for Lifeline Systems, November 4-7, 1997, Seattle, Washington
 - 5) Suzuki, T, and Tanaka, T : Research and : Development on the Seismic Isolation Systems applied to Urban Tunnels (Part-1: Development of Seismic Isolation Materials and Construction Methods), 7th US-Japan Workshop on Earthquake Disaster Prevention for Lifeline Systems, November 4-7, 1997, Seattle, Washington
 - 6) Tanaka, T, and Suzuki, T : Research and : Development on the Seismic Isolation Systems applied to Urban Tunnels (Part-1: Effects of Seismic Isolation and Seismic design), 7th US-Japan Workshop on Earthquake Disaster Prevention for Lifeline Systems, November 4-7, 1997, Seattle, Washington

Table 1 Seismic Isolation Materials Developed

Construction Methods	Isolation Material	Material Contents
Shield Driving Tunnel	Asphalt-based Material	Asphalt and portland cement with high-water absorbing polymer
	Urethan-based Material	Urethan with fly ash and polyor
	Silicon-based Material	Silicon oil and fly ash with polyether
Open-Cut Type Tunnel	Liquid Rubber Material	Polybutadiene-type liquid rubber with polyisocyanate
	Precast Rubber Panel	Rubber tips made of shredded tires with urethan polymer resin

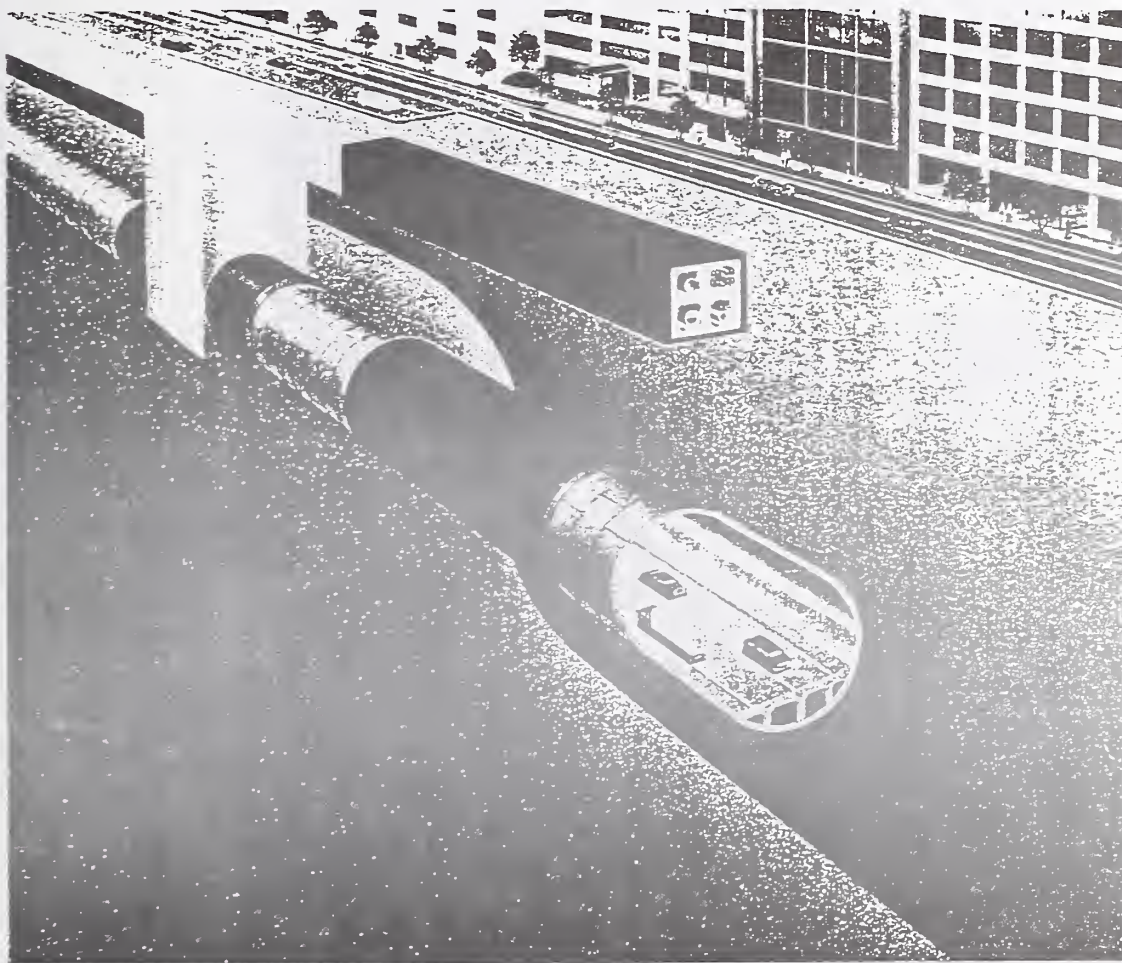
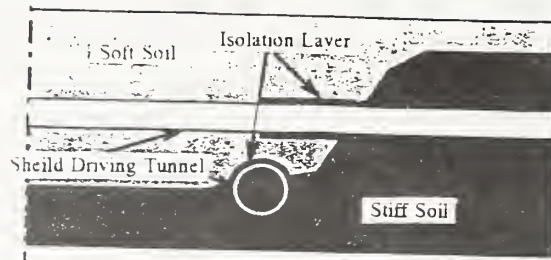
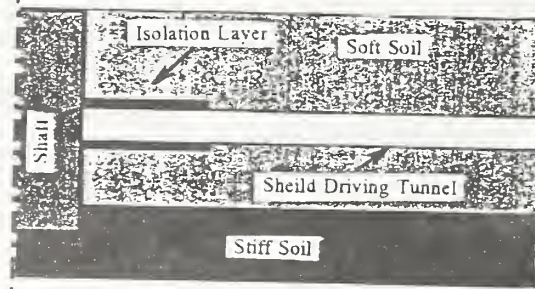


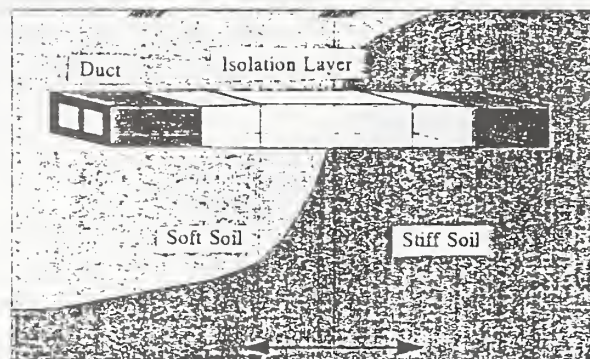
Fig.1 Concept of Seismic Isolation Systems for Underground Structures



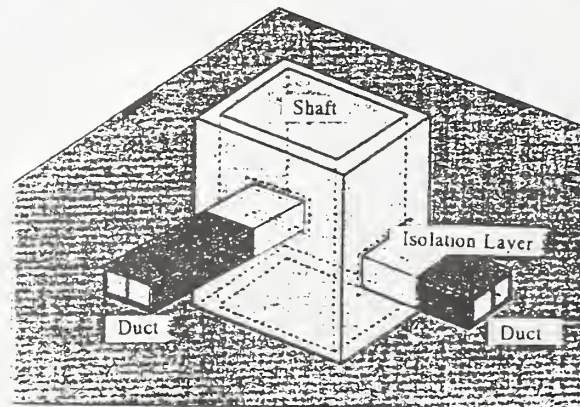
(1) Boundary of the Change of Ground Condition



(2) Connection between Shaft and Tunnel
(a) Shield Driving Tunnels



(1) Boundary of the Change of Ground Condition



(2) Connection between Shaft and Tunnel
(b) Open-Cut Type Tunnels

Fig.2 Application of Seismic Isolation Systems

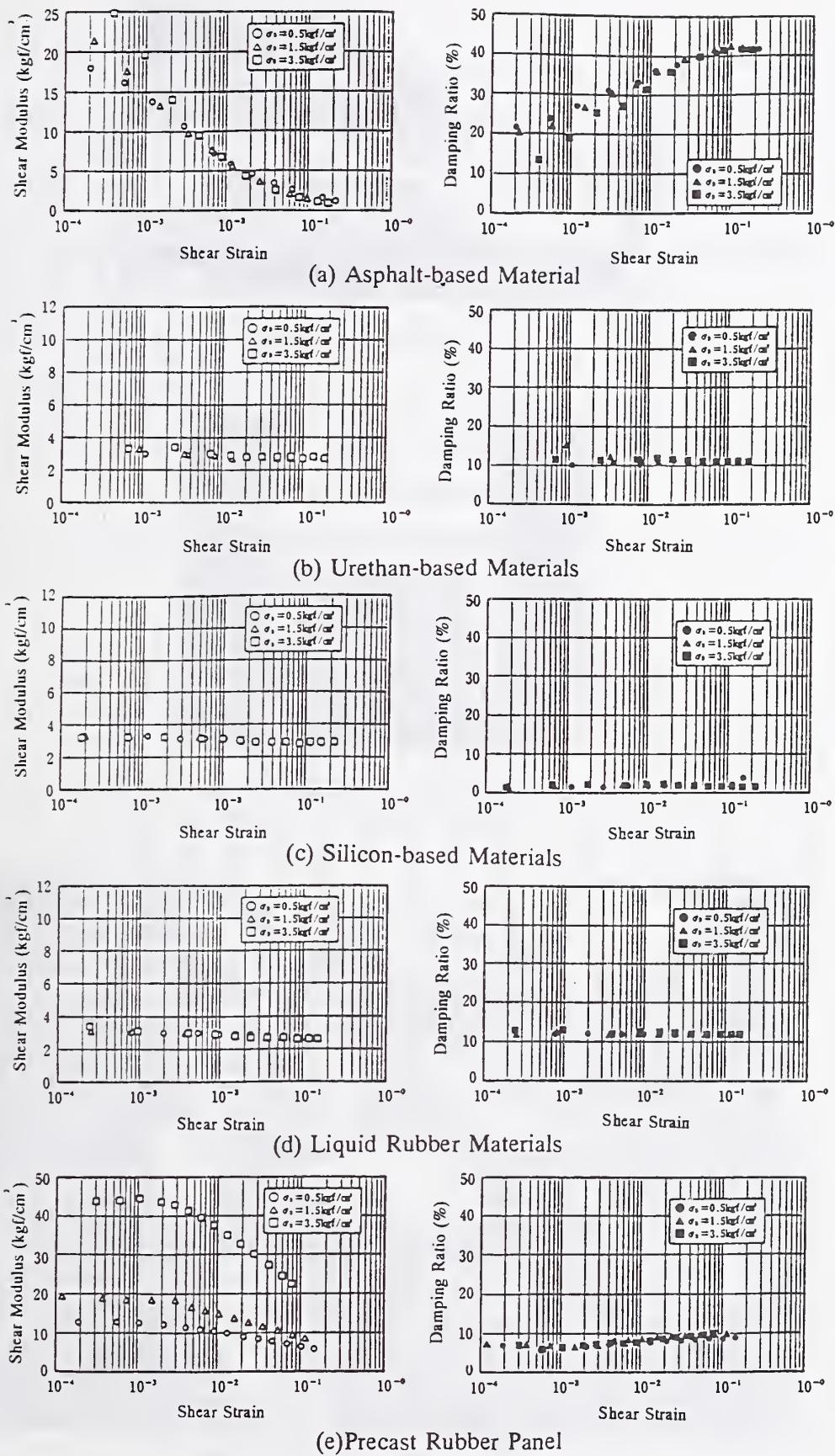
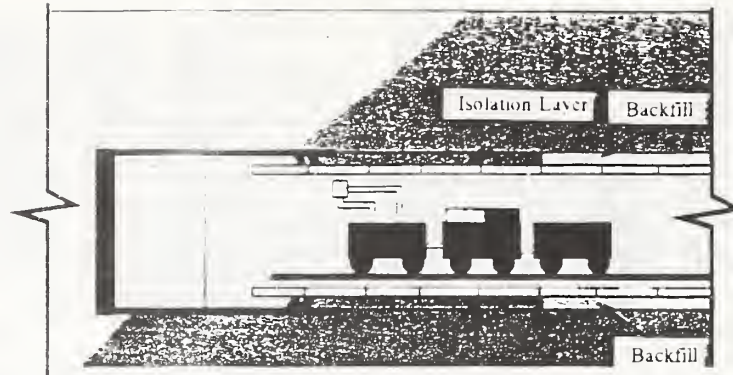
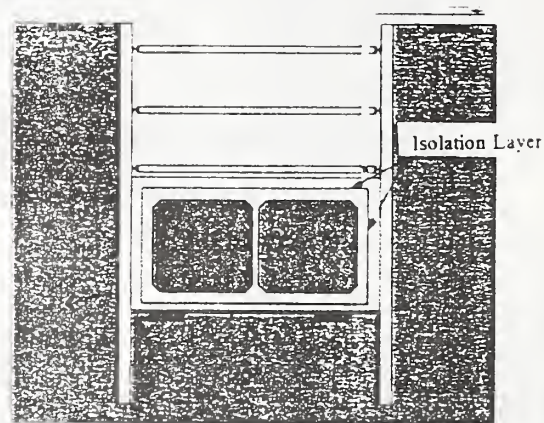


Fig.3 Dynamic Mechanical Properties of Seismic Isolation Materials Developed



(a) Shield Driving Tunnels



(b) Open-Cut Type Tunnels

Fig.4 Outline of Construction Methods

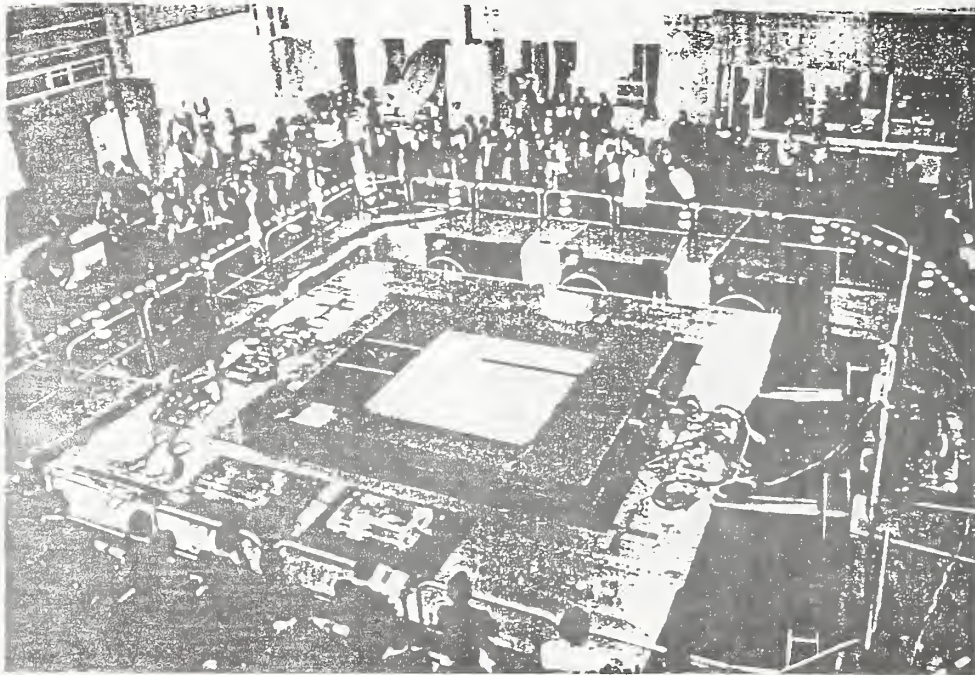
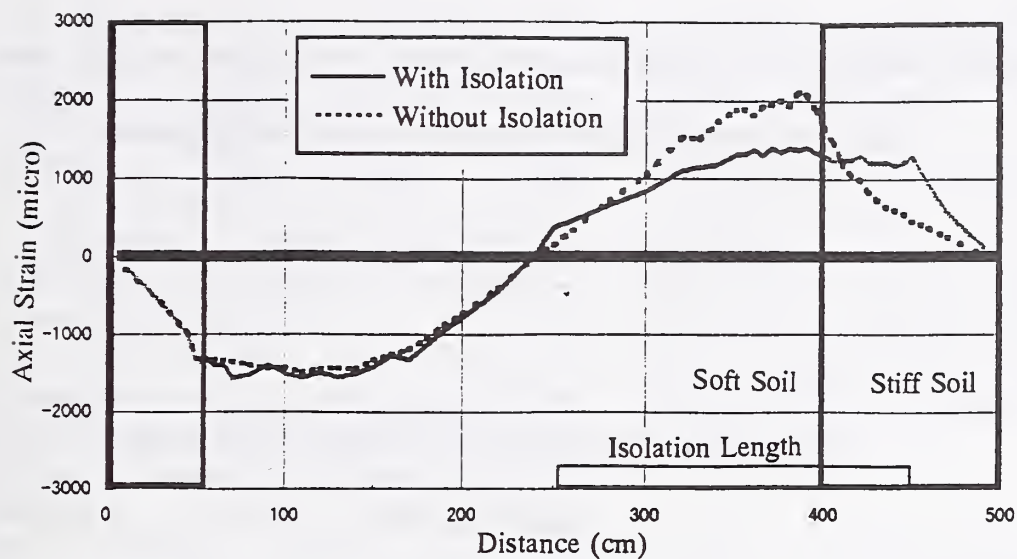
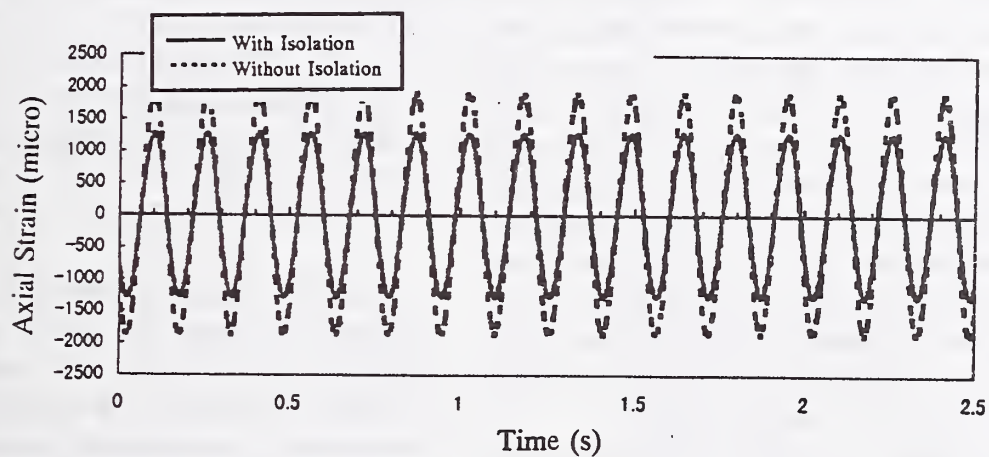


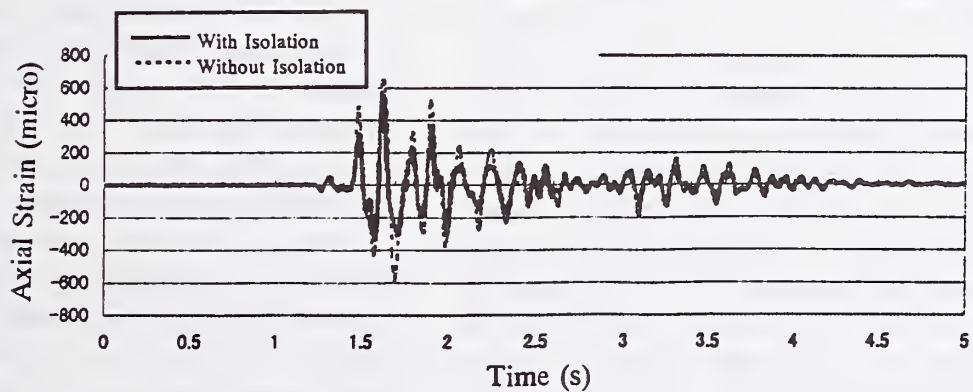
Fig.5 Model for Shake Table Tests



(a) Strain Distribution in Tunnel Model in The Longitudinal Direction
(Sinusoidal Input : 6.5Hz, 150gal)



(b) Strain Response
(Sinusoidal Input : 6.5Hz, 150gal)



(c) Strain Response (Earthquake Wave)
Fig.6 Test Results of Shake Table Tests

Comparison between the affected populations of indirect health effects
after the 1995 Great Hanshin-Awaji earthquake

by

Keiko Ogawa¹⁾, Ichiro Tsuji¹⁾, Shigeru Hisamichi¹⁾

Keishi Shiono²⁾

ABSTRACT

Indirect health effects (any kinds of health outcomes, not directly caused by the structural damages) after the earthquake have come to be the issue after the fatal earthquakes such as the 1995 Great Hanshin-Awaji earthquake. The investigations about the mortality and morbidity due to both direct and indirect health effects at the community level are required to identify the most effective countermeasures in the pre-impact and post impact phase.

As an example of indirect health effects, age-adjusted death rates of acute myocardial infarction were compared among several affected regions. In Nada, Higashi-Nada, Hyogo, Nagata districts in Kobe City we observed the sharp increase in the average death rates between January and March, 1995 in comparison with 1994 and 1996. Outside of Kobe City, the similar increase was observed in Amagasaki and Tsuna. The different patterns in the increase of rates between January and March, 1995 are suggestive of the multiple risk factors. The further investigation is required to

identify the environmental factors (structural and non-structural) to reduce the total health outcomes.

KEYWORDS:

indirect health effects
age-adjusted death rate
acute myocardial infarction

1. INTRODUCTION

The first step in preventing adverse health outcomes would be to identify the risk factors and to establish the effective measures in adverse. There have been numerous reports regarding the human casualties directly caused by structural damage after the earthquake (Glass, 1977; de Bruycker, 1985; Coburn, 1987; Jones, 1990; Noji, 1990; Shiono, 1991b). Not only the death and injuries caused by the structural damages but also indirect health effects have also been reported

1)Department of Public Health, Tohoku University School of Medicine, Miyagi, Japan

2) Nagaoka Technology College, Niigata, Japan

(Logue, 1978; 1979; 1980; 1981a; 1981b).

For instance, it has been reported that the incidence of coronary heart disease increased after the disasters (Trichopoulos, 1983; Katsouyanni, 1986; Suzuki, 1995; Leor, 1996). Nevertheless, there are very few studies to describe the indirect health effects after the earthquake at the population level (Kloner, 1997).

Indirect health effects after the earthquake in this paper refers to as all the medical health consequences not directly caused by the structural damages. Description of the magnitude of indirect health effects and identification of their risk factors would lead us to better implementation of preventive measures after the disasters. For this purpose, we compared age-adjusted death rate of acute myocardial infarction (AMI) in Kobe and seven other cities in Hyogo Prefecture before and after the Great Hanshin-Awaji Earthquake.

2. SUBJECTS AND METHOD

The Great Hanshin-Awaji Earthquake hit the southern part of Hyogo Prefecture on 17 January, 1995. The epicenter was reported to be located on the northern tip of Awaji island. The magnitude was given at 7.2 on the Japan Meteorological Agency. We obtained all death certification data ($n=127,474$) at Hyogo Prefecture between 1994 and 1996 from the Vital Statistics Recording Office, Ministry of Health and Welfare, Japan. The data included data of death, age of death, sex, area code, date of death for each decedent, but did not include personal name or other identifier. We classified cause of death according to

International Classification of Diseases, 9th Revision (ICD-9) for 1994 and 10th Revision (ICD-10) for 1995 and 1996. Age-adjusted death rates of AMI, as standardized to the model population of Japan in 1985, by month were calculated in all nine districts within Kobe City and seven cities in southern part at Hyogo Prefecture (Amagasaki, Nishinomiya, Sumoto, Ashiya, Itami, Takarazuka and Tsuna).

3. RESULT

Fig. 1 shows the age-adjusted death rate of AMI by month. Monthly trends of the age-adjusted death rate of AMI could be classified into two different patterns. One example was presented in Fig. 1A. It was the result in Nada district, Kobe City. Notable increase in the age-adjusted death rate was observed only in January, February and March, 1995. The other pattern was presented in Fig. 1B; Kita district, Kobe City. The death rates did not increase in January, February and March, 1995.

Fig. 2 summarizes the age-adjusted death rates of AMI at each region between January and March in 1994, 1995 and 1996, respectively. We compared the average rates between January and March in each year. The notable increase in the average death rate was observed in some regions such as East Nada, Nada, Hyogo and Nagata districts among Kobe City and Amagasaki and Tsuna. We could not observe uniform trend between men and female in each region.

Fig. 3 showed different patterns of the monthly trend of age-adjusted death rates of AMI from January to March, 1995. The peak in the death rates in

Nagata district in men and women was observed in January. On the other hand, the peak in the death rates in Nada district was observed on February, one month later. In case of Ashiya in men, the peak was observed in March. The death rates in men in Tsuna showed two peaks in January and March. The trend in the death rates in Ashiya and Tsuna was different between men and women.

Table 1 showed the actual number of death of AMI according to the 17 regions. We compared the total number of death between January and March in each year. The number of death of AMI in 1995 was more than twice as that of 1994.

4. DISCUSSION

Our population based study showed excess mortality of AMI in some regions after Great Hanshin-Awaji earthquake. The pattern of the increase in death rates were different among the affected regions. Fig. 2 suggests us the need to measure the risk factors at the regional level for the causing inference. The different trend in death rates for the early recovery stage as shown in Fig. 3 are suggestive of the multiple risk factors to AMI.

Several cases reports about the increase in the incidence of ischemic heart diseases after the disasters have been reported (Faich, 1979; Trevisan, 1992). Although the mechanisms to increase the mortality and morbidity of cardiovascular diseases have still to be clarified, the stresses in the post-disaster period could be considered as a possible explanation (Bertazzi, 1989; Willich, 1993).

The following three points are possible explanation of the increase in death rates between January and March, 1995.

One possibility is due to the change of the classification of cause of death, namely from ICD-9 to ICD-10. It was recommended that we should put the exact cause of death on "heart failure" cases. This recommendation could possibly increase the death rate of AMI. The increase of death rates in our study, however, was limited between January and March, 1995. Therefore the monthly trend observed in our study could not be explained by the change of the classification.

The second possibility is due to the deterioration of hospital services by the structural and non-structural elements in the damage by the seismic activities with the same of the incidence of death rates. The increase of death rates could be explained by the increase of fatal rate. We are analyzing the relationship between the function loss in the hospital and prognosis of AMI patients.

The third possibility is the increase of the incidence of AMI. Actually the number of death of AMI from January to March, 1995 became the double of that of the same term, 1994. Considering the magnitude, the possibility cannot be denied.

Identification of the risk factors is mostly required. For this purpose, we are measuring "the inconvenience of daily life due to lifeline disruption" to analyze the relationships between them (Shiono, 1989; 1991a).

The further research will be required to identify the additional possible environmental factors to influence the

overall health outcomes on the affected populations.

5. CONCLUSION

The epidemiological research at the population level is essential to identify the risk factors for the health consequences after the catastrophic disasters which need the external assistance. The public health approach should be defined on the investigation about the magnitude of health outcomes on the affected population.

6. ACKNOWLEDGMENT

This study was supported in part by Grants-in-Aid for Scientific Research on Priority Areas from the Ministry of Education, Science and Culture of Japan (Grant No. 09234102).

REFERENCES

Bertazzi P.A. et al.(1989) .Ten-year mortality study of the population involved in the Seveso incident in 1976. *Am J Epidemiol* 129, 1187-1200

Coburn A.W. et al (1987) .Factors affecting fatalities and injury in earthquakes. Internal report, Engineering seismology and earthquake disaster prevention planning. Hokkaido, Japan, Hokkaido University, 1-80

de Bruycker, M. et al (1985) .The 1980 Earthquake in Southern Italy: Morbidity and Mortality. *Int J Epidemiol* 14, 113-117

Faich G. and Rose R.(1979). *Blizzard Morbidity and Mortality: Rhode Island,1978.*
Am J Public Health 69, 1050-1052

Glass R.I. et al (1977). Earthquake injuries related to housing in a Guatemala village. *Science* 197, 638-664

Jones N.P. et al (1990). Considerations in the epidemiology of earthquake injuries. *Earthquake Spectra*. Vol 6, No.3, 507-528

Jones N.P. et al (1994) .Risk factors for casualty in earthquake: The application of epidemiologic principles to structural engineering. *Structural Safety* 13, 177-200

Katsouyanni K. et al (1986). Earthquake-related stress and cardiac mortality: *Int J Epidemiol* 15, 326-330

Kloner R.A. et al (1997). Population-based analysis of the effect of the Northridge Earthquake on cardiac death in Los Angeles County, California. *Am J Coll Cardiol* 30 (5), 1174-80

Leor J. et al (1996). Sudden cardiac death triggered by an earthquake. *N. Engl. J. Med.* 34, 413-9

Logue J.N. (1978) .Long-term effects of a major natural disaster: The Hurricane Agnes flood in the Wyoming Valley of Pennsylvania, June,1972. Doctoral Dissertation, Columbia University Faculty of Medicine, School of Public Health, Division of Epidemiology, New York

- Logue J.N. et al (1979). Emotional and physical distress following Hurricane Agnes in Wyoming Valley of Pennsylvania. *Public Health Reports* 94, 495-502
- Logue J.N. , Hansen H. (1980). A case-control study of hypertensive women in a post-disaster community. *Journal of Human Stress* 6 (2), 28-34
- Logue J.N. et al (1981a). Some indications of long term health effects of a natural disaster in American Society. *Public Health Reports* 96 (1), 67-79
- Logue J.N., et al (1981b). Research issues and directions in the Epidemiology of health effects of disasters. *Epidemiologic Reviews* 3, 140-162
- Meisel S.R. et al (1991). Effects of Iraqi missile war on incidence of acute myocardial infarction and sudden death in Israeli civilians. *Lancet* 338, 660-61
- Noji E.K. et al (1990). The 1988 earthquake in Soviet Armenia: a case study. *Annals of Emergency Medicine* 19, 891-897
- Shiono K. (1989). Inconvenience in resident's daily living activities from post-earthquake suspension of utility services. *Comprehensive Urban Studies* No. 38, 149-167
- Shiono K. , Shumuta Y. (1991a). Inconvenience in resident's daily living activities from post-earthquake suspension of utility services, part 2. Procedure for estimation. *Comprehensive Urban Studies* No. 41, 37-46
- Shiono K. et al (1991b). Post-event rapid estimation of earthquake fatalities for the management of rescue activity. *Comprehensive Urban Studies* No. 44, 61-106
- Suzuki S. et al (1995). Hanshin-Awaji earthquake and acute myocardial infarction. *Lancet* , 345, 981
- Trevisan M. et al (1992). Earthquake and Coronary Heart Disease Risk Factors: A Longitudinal Study. *Am J Epidemiol* 135, 632-7
- Trichopoulos D. et al (1983). Psychological stress and fatal heart attack; the Athens (1981) earthquake natural experiment. *Lancet* 1, 441-3
- Willich S.N. et al (1993). Sudden cardiac death:support for a role of triggering in causation. *Circulation* 87, 1442-50

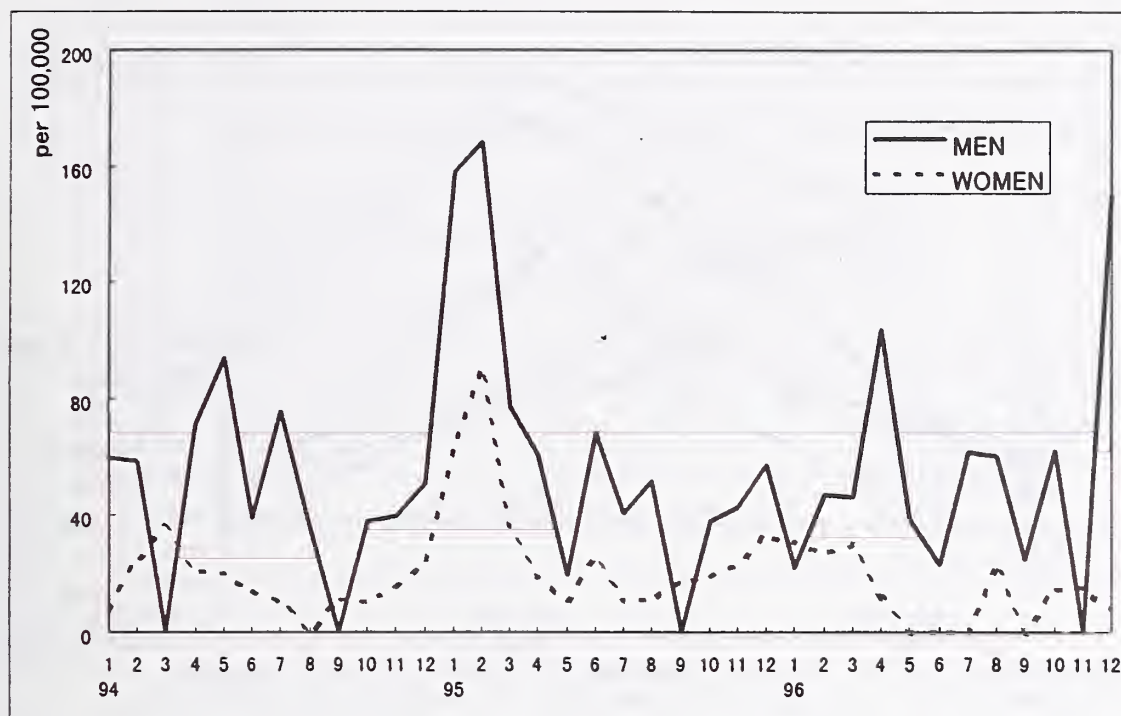


Fig. 1A Age-adjusted death rate of acute myocardial infarction by month in Nada district, Kobe City

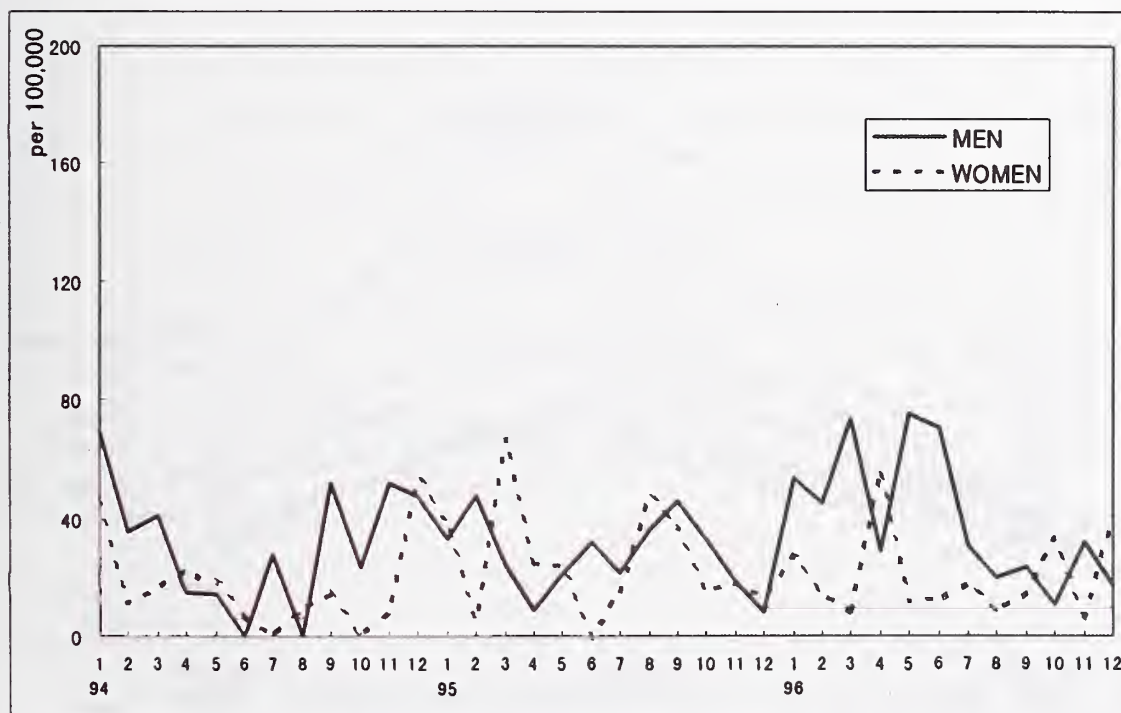


Fig. 1B Age-adjusted death rate of acute myocardial infarction by month in Kita district, Kobe City

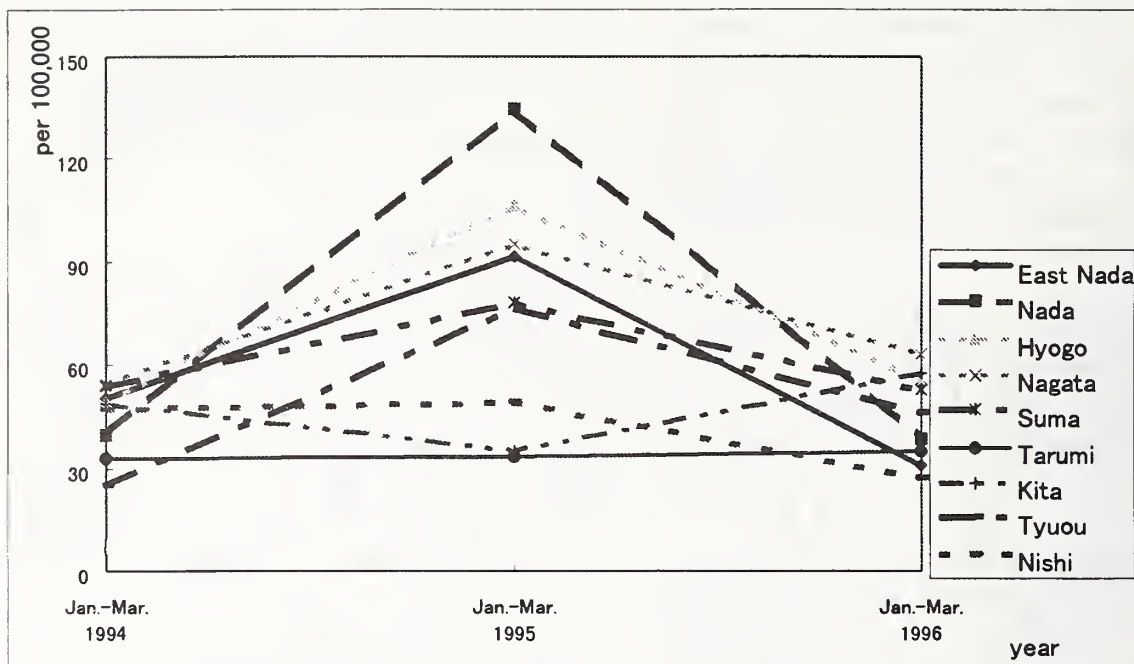


Fig. 2A Age-adjusted death rate of acute myocardial infarction according to the district of Kobe City in men #

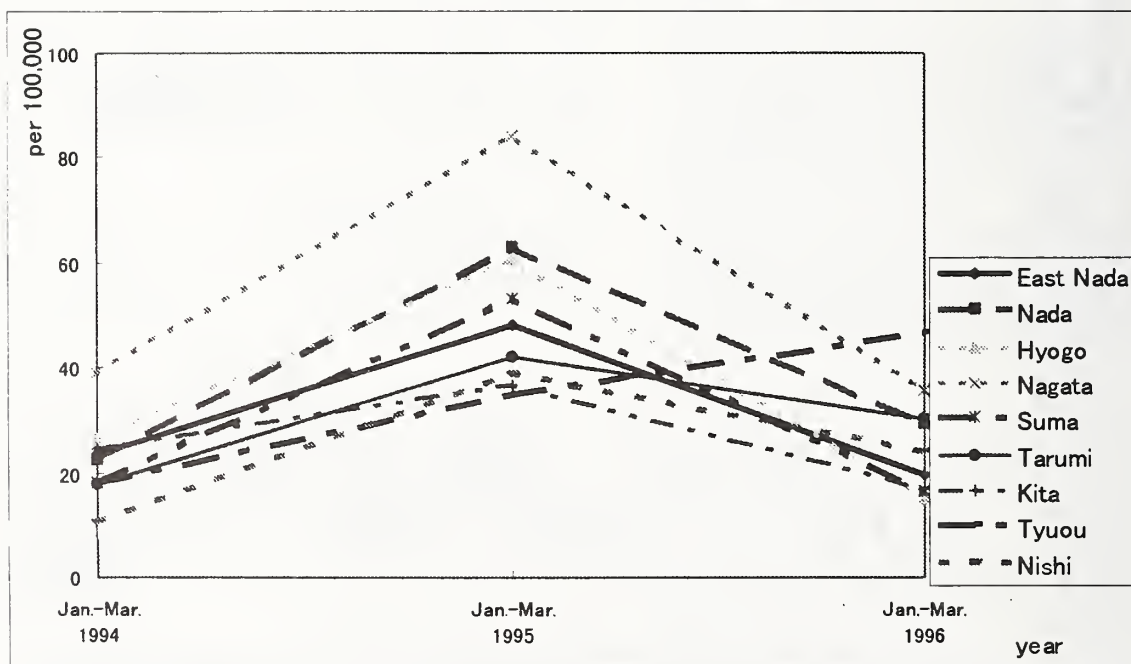


Fig. 2B Age-adjusted death rate of acute myocardial infarction according to the district of Kobe City in women #

The values are the average rates between January and March in each year

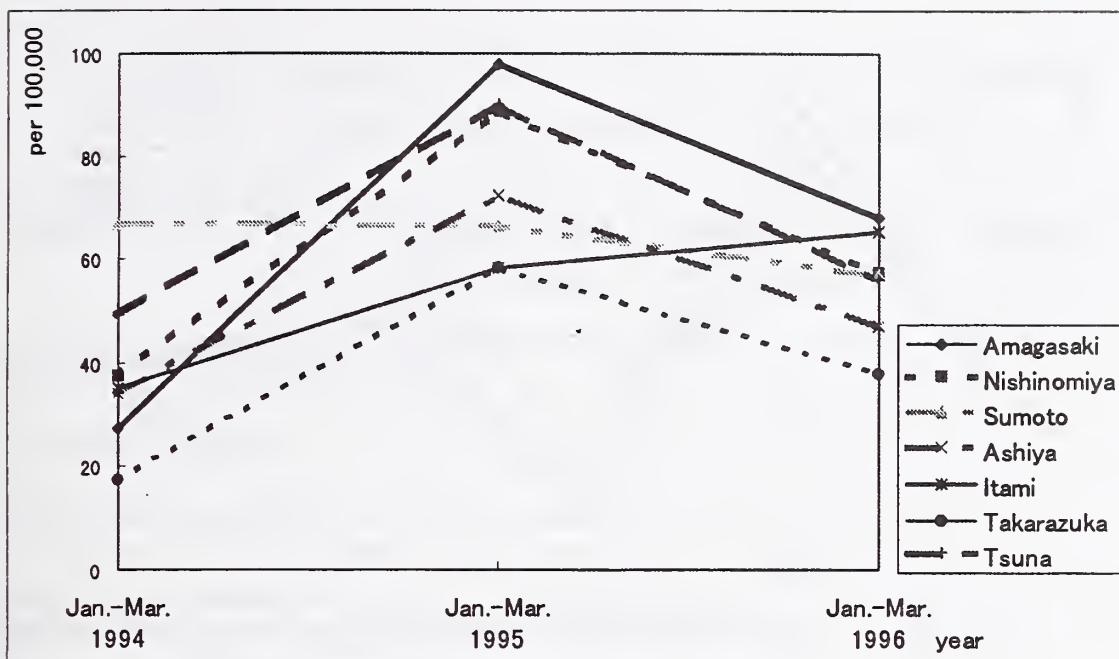


Fig. 2C Age-adjusted death rate of acute myocardial infarction according to the city of Hyogo Prefecture in men #

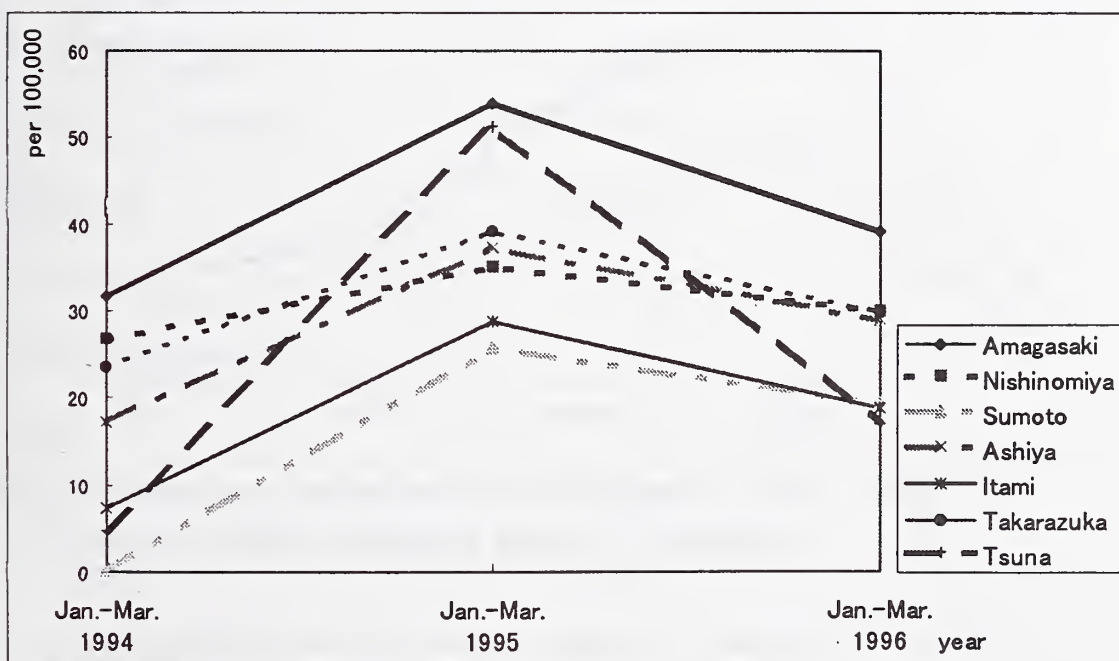


Fig. 2D Age-adjusted death rate of acute myocardial infarction according to the city of Hyogo Prefecture in women #

The values are the average rates between January and March in each year

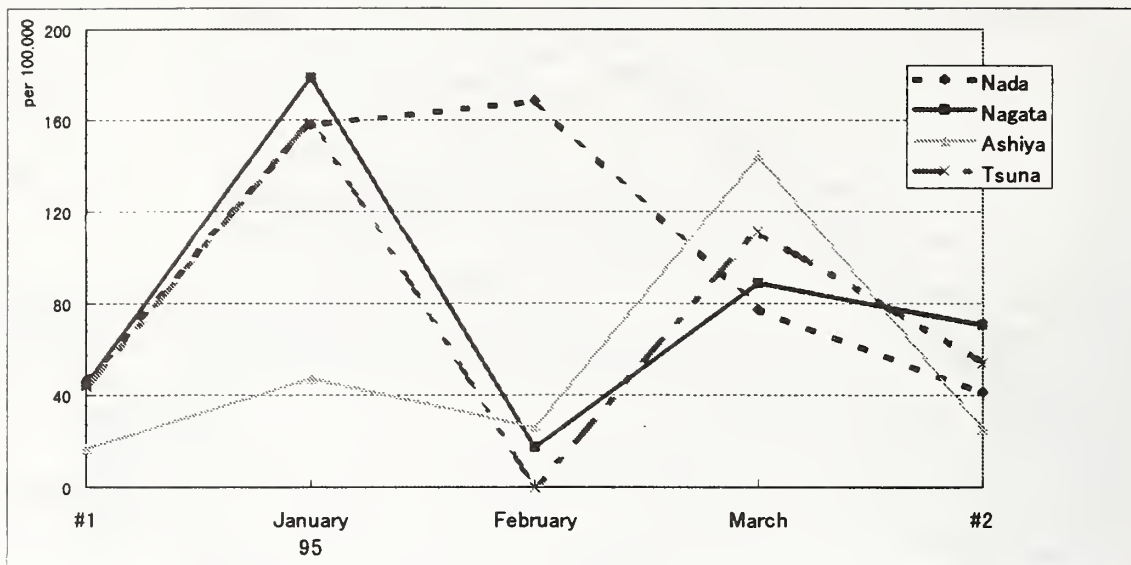


Fig. 3A Age-adjusted death rate of acute myocardial infarction in January, February, and March, 1995 in men

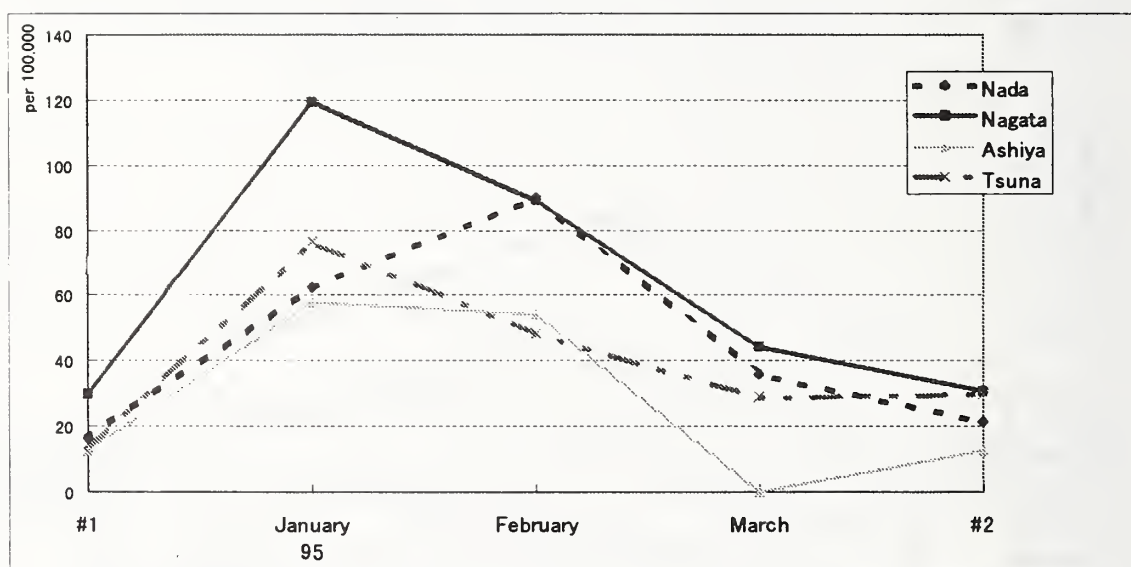


Fig. 3B Age-adjusted death rate of acute myocardial infarction in January, February, and March, 1995 in women

#1 The values are the average rates between January, 1994 and December, 1994.

#2 The values are the average rates between April, 1995 and March, 1996

Table1 Number of death of acute myocardial infarction
between January and March in each year

REGION	NUMBER OF DEATH FOR THREE MONTH IN 1994	NUMBER OF DEATH FOR THREE MONTH IN 1995	NUMBER OF DEATH FOR THREE MONTH IN 1996
East Nada District, Kobe City	19	34	12
Nada District, Kobe City	11	35	11
Hyogo District, Kobe City	17	38	14
Nagata District, Kobe City	20	38	18
Suma District, Kobe City	16	33	17
Tarumi District, Kobe City	16	28	25
Kita District, Kobe City	23	24	24
Cyuou District, Kobe City	9	20	17
Nishi District, Kobe City	13	25	16
Amagasaki	44	105	80
Nishinomiya	39	69	51
Sumoto(Awaji island)	5	9	6
Ashiya	7	15	10
Itami	8	20	19
Takarazuka	12	28	20
Tsuna(Awaji island)	7	25	14
TOTAL	266	546	354

New Framework for Performance Based Design of Building Structures -Design Flow and Social System-

by

Hisahiro HIRAISHI¹⁾, Masaomi TESHIGAWARA¹⁾, Hiroshi FUKUYAMA¹⁾, Taiki SAITO¹⁾,
Wataru GOJO¹⁾, Hideo FUJITANI¹⁾, Yuji OHASHI¹⁾, Izuru OKAWA¹⁾, Hisashi OKADA¹⁾

ABSTRACT

This paper introduces the outline of the new structural engineering framework and social system for the performance-based design of building structures proposed under the 3-year Comprehensive Research and Development Project on "Development of a New Engineering Framework for Building Structures" was launched in fiscal 1995. In the project, the clarification of target performance, the evaluation of performance and the indication of performance, are emphasized as the main three elements of this framework. The implementation of the proposed framework is also expected to promote engineering innovation, the progress in building engineering, and globalization.

*Key Words :Performance-based Design,
Performance Evaluation,
Target Performance Level,
Social System*

1. INTRODUCTION

The present structural design framework prescribes the design load and external force, as well as the allowable stress and deformation, but does not specify the performance requirements explicitly. Only detailed calculation methods are specified without clear indication of target performance and building performances (Figure 1).

As a result of that, the present framework cannot explain explicitly the real building performance and is becoming increasingly inappropriate for new technologies and

performance indication. Then it has been needed to establish a new "performance-based structural design framework". This framework would also encourage the communication between consumers and engineers in order to make a consensus on building structural performance, and the application of new materials and new technologies, by its rational performance requirements and its flexibility in evaluation of performance.

To establish such a performance-based framework, a 3-year Comprehensive Research and Development project on "Development of a New Engineering Framework for Building Structures (referred to below as Comprehensive R&D Project)" was launched in fiscal 1995. The concept of the performance-based structural design has been discussed in the technical coordinating committee of the project (Chairman: Prof. Dr. Tsuneo OKADA). Three sub-committees are organized under the technical coordinating committee.

This paper introduces the outline of the concept and the framework of Performance Based Design (P.B.D.) with the structural performance evaluation system discussed in the "Performance Evaluation" sub-committee (Chairman: Prof. Dr. Hiroshi AKIYAMA), the target performance of buildings structures and their levels from various point of view in "Target Performance Level" sub-committee (Chairman: Prof. Dr. Yoshitsugu AOKI), and the social background and supporting systems should be to conduct P.B.D. practice

- 1) Building Research Institute, Ministry of Construction, 1 Tatehara, Tsukuba, Ibaraki, 305-0802, Japan

smoothly in the market in the "Social System sub-committee (Chairman: Dr. Katsumi YANO)".

This paper introduces the outline of the performance based structural framework in a stage of research. So, this framework should be reconsidered in adopting into the regulation or code, for example Building Standard Law.

2. OBJECTIVES

The primary objective of the new framework is to create an system in which the performance of buildings is clearly indicated and "consumers" (owners and users) are well informed of how their buildings perform and how much it costs to attain the performance (design, supervision and construction costs). The new framework would also bring about other benefits, such as progress in building engineering and design techniques, greater flexibility in design, and closer international cooperation. It is important to clarify target performance and verify by the rational performance evaluation method, so that the building performance satisfies the target performance initially clarified.

Such an approach allows more flexibility in choosing design techniques and calculation methods, because it aims to understand performance requirements, and to clarify the target performance and evaluate the building performance rationally.

Next, it is important for engineers to explain the building structural performance to owners, users, and the public. In the process of decision of target performance, engineers are expected to communicate with owners, in order to understand the requirements of owners, and to make advices to them from the engineering and public point of view. Then, users and the public are able to understand the building performance.

Moreover, it is also important that the building structural performance will be one of the most important measures for consumers to define the building value. As a result of that, the concept of cost-performance is treated in structural

engineering by the new framework with a performance-based approach.

3. CONCEPT OF THE NEW PERFORMANCE-BASED DESIGN FRAMEWORK

Figure 2 shows a flow of the new performance-based structural framework proposed by the Project (referred to below as the "new framework"). The new framework consists of three key procedures: "clarification of target performance", "evaluation of performance" and "indication of performance".

At the first stage of (frame-1), "Basic Structural Performances" which are primarily required for the building structures are established. Safety, Reparability and Serviceability are itemized as the Basic Structural Performance.

In the second stage, "Basic Structural Performances" which are described as the "Limit States" for each "Performance Evaluation Item" in general expression in the frame-3. The types of loads or external forces and their magnitude in the frame-2 are set along with setting of the frame-3. Performance levels of each performance evaluation item should be defined by the relationships between the magnitude of loads and external forces which affects to the structure, and the limit states that the structure should be in.

The performances evaluated in the frame-4 of each evaluation items should be indicated clearly in the frame-5.

4. CLARIFICATION OF TARGET PERFORMANCE

In principle, the target performance of a building is clarified how the building should perform according to each performance evaluation items, i.e. the state of the structural frame and each building elements under assumed loads and external forces. To do so, it is necessary to study the performance requirements for the building (items and levels of the performance required).

First of all, a building is required to have public functions. Buildings have certain meanings in the society and have to be suitable for the general public, or society. The minimum requirements of building performance are defined in the code. Building is required to have functions specific to its usage. In other words, a building should fulfill essential functions that can be understood with its context in the public.

Next, there are needs or requirements of building owners and users. Any owner or user has some ideas of the building performance they require, however vague they might be, based on the information available to them. These requirements might be classified into those required generally by owners and users and those specifics to each case.

On the other hand, the engineering performance of a building has been based on the judgements of the experts in structural engineering, based on empirical records of damages caused by loads and external forces of past earthquakes and other events. In recent years, however, explicit methods of making such expert judgement have been developed.

By using available methods, structural engineers will specify the target performance of each building that would reflect the requirements of lay "consumers".

4.1 Basic Structural Performance

Three basic structural performances, Safety, Reparability and Serviceability are itemized. Each of them corresponds to security of human lives, security of property from the viewpoint of easiness to repair, and security of serviceability, respectively. Table 1 describes the objectives and the contents to evaluate these basic structural performances.

4.2 Performance Evaluation Items and Limit States

The combination of basic structural performances and the objects to be evaluated are defined as Performance Evaluation Items.

Limit state for each performance evaluation item is listed in general expression in Table 2. In the left column of Table 2, the objects to be evaluate are enumerated. These are structural frame, structural member, non-structural member, equipment/machine, fixture, furniture and soil. Structural member and non-structural member might be arrange into one term as building members.

For example, safety limit state of structural frame is defined as that the destruction directly affects human life should be avoided. And in the safety limit of the building member, it is defined that falling out or scattering of building members that directly affects human life should be avoided. Safety limit state for safety performance, reparability limit state for reparability performance, and serviceability limit state for serviceability performance are set.

4.3 Types and Magnitude of Loads and External Forces

Usual loads (such as dead or live loads, buoyancy, negative friction, soil pressure, water pressure etc.), unusual loads of snow, wind, earthquake, other forces such as temperature stress, special soil or water pressure etc. should be considered. The magnitude of loads and external forces and their combination might be set corresponding to the three basic performances level; considering social situation, and frequency of occurrence.

The idea of design earthquake load in that scheme is introduced in Appendix I.

4.4 Performance Level

Performance levels of each performance evaluation item will be indicated by the relationships between the magnitude of loads and external forces which affects to the structure, and the limit states which the structure should be in.

Performance levels themselves can be determined by designer and owner as the distance from empirical reference level such as code requirement, or a reliability method, etc.

Some issues which need to be considered in determining the performance level of buildings are discussed in Appendix II.

5. DESIGN AS A SOLUTION TO FULFILL THE TARGET PERFORMANCE

Structural design is carried out to attain the target performance. Note that a structure means the structural system as a whole here, which involves not only the structural frame but also every building element including interior and exterior members, equipment, devices, furnishings and grounds.

The structural engineers practice their philosophy in developing a structural system that realizes the target performance. For example, several solutions may be possible when trying to attain the target performance of a structural frame to resist earthquakes; the engineers can either design the structural frame to bear the seismic forces and energies on its own, or use some devices to control the responses. In either way, detailed measures are developed through studies. The new framework will thus encourage technological innovation, such as the development of new structural frames or new devices. This will eventually motivate the structural engineers to embrace technological development.

After determining the details, the structural engineers prepare drawings and specifications, on which construction works are to be based.

6. EVALUATION OF PERFORMANCE

"Evaluation of Performance" is conducted in the third stage according to the "Principle of Performance Evaluation"; the response value should not exceed the limit value to satisfy the performance level. The performance level is represented by engineering expression in this stage.

Some definite evaluation methods will be developed in accordance with this flow to realize

"The Principle of Performance Evaluation."

The performance level is represented by engineering expression in this stage. "Evaluation of Performance" is conducted according to the following steps.

1) Quantitative determination of the magnitude of loads and external forces

Magnitude of loads and external forces are determined in accordance with reliable materials relating to the background and the setting method.

2) Set the type of engineering value used for the response value and limit value

Suitable types of engineering value for response value and limit value should be determined for performance evaluation. Not only force, but displacement, velocity, and acceleration, energy, etc. can be selected for evaluating the structural performance. It means that the structural performances are defined by engineering terminologies.

3) Establishment or calculation of the limit value

The limit value which satisfies the limit state should be established (calculated or judged) according to the items describing the quantitative determination method of limit states values.

4) Calculation of the response value

The response value should be calculated by the suitable analytical method.

5) Comparison of the response value with the limit value

The response value should be compared with the limit value and confirm the performance level.

Practical methods for evaluating the structural performance and designing are necessary to be developed in accordance with this "Principle of Performance Evaluation" flow. The principle of performance evaluation should promote the renewal of the conventional evaluation method, following to the development of social fulfillment and the advancement of evaluation technology. Accordingly, detailed performance evaluation or design methods established by current knowledge are only exemplified in order to renew easily or select

practically.

7. INDICATION OF PERFORMANCE

The evaluated performance should be indicated for each performance evaluation items. For example, destruction of structural frame which affects human lives directly by ○○ (loads or external forces) will almost be avoided. Probability for satisfying the basic performances may also be indicated.

This ultimately serves as a bridge between the engineers and society, i.e. consumers (owners, users and the public) of buildings. Easily, indication of building performance will become one of the key roles of structural engineer. This new responsibility will eventually give a recognized social status to the profession that society can rely on. The recognized structural engineers would be those who can clearly explain to the public how the buildings' performance was achieved at reasonable cost.

By the new framework, the performance required by the public for building structures is translated into the target performance by the structural designer in the technological domain. The engineers work to achieve this target performance and then announces the actual performance to the public.

8. SOCIAL SYSTEM

In order to make buildings actually performance-based-designed and the objective of this Project fulfilled, new "Social System" has to be developed, which is composed of various supporting devices for P.B.D. practice like social codes/rules, institutions, technical tools, information systems, etc. The outline of the new Social System and its necessary elements are as follows:

(1) Process of P.B.D.

P.B.D. can be assumed to be conversion between three phases of information related to structural performance: "Design Brief, identifying clients'

needs and other requirements for the project", "Design Criteria, specifying target performance for the project" and "Design Solutions, verified to comply with the Design Criteria". P.B.D. is carried out through the following process:

- a) Identifying needs about expected performance through appropriate communication between the structural engineer and the client (consequently supporting the clients to develop the Design Brief)
- b) Developing the Design Criteria including the structural design policy, target performance and verification methods
- c) Obtaining the approval for the Design Criteria from the client
- d) Developing the Design Solutions (i.e. repeating cycles of preparative design and its verification of conformity to the target performance)
- e) Presenting verified performance of the Design Solutions to the client
- f) Delivering Design Solutions and other necessary information (e.g. construction methods, quality control conditions, supervision methods, etc.) to the production/construction stage

(2) Need for functions of the new Social System

The following four functions are to be attained by the new Social System:

--- Functions mainly beneficial to clients ---

- a) To support clients to concretize their needs based on correct understanding of structural performance
- b) To ensure sufficient reliability of conversion of clients' needs into target performance
- c) To ensure sufficient reliability of conversion of target performance into performance of Design Solutions

--- Function mainly beneficial to engineers ---

- d) To prepare appropriate environment for those who intend to implement the P.B.D. practice

(3) Framework for the elements of the new Social System

To fulfill the four expected functions, the framework of the Social System should be as

shown in Table 3. They need to be developed to cover any of the following three types of P.B.D. practice.

a) "Individualized objective-oriented type" -- To set target performance fittest for the needs and design and verify the solutions by unique, individualized manner

b) "Standardized verification method type" -- To set or choose target performance within given range or menu, design freehand and verify the solutions utilizing ready-made methods

c) "Dependent on deemed-to-satisfy solutions type" -- To set or choose target performance within given range or menu and design and verify the solutions depending on ready-made prescriptive (deemed-to-satisfy) design guide

(4) Key Elements of the new Social System

Various elements need to be developed within the above mentioned framework.

The followings are examples of key elements.

- Performance certification service
- Structural design information managing system
- Quality assurance scheme for structural design practice
- Information system on abilities and qualifications of engineers and organizations
- Data base of reference technical information
- Evaluation system for technical tools
- Standard guide of design practice and model contract documents
- Independent bodies to provide technical services for engineers
- Insurance system suitable for P.B.D. practice
- System to support engineers to acquire knowledge and ability

9. CONCLUSIONS

In this paper, The Performance-Based Design Framework was outlined. This framework would encourage the making consensus between consumers and engineers on building structural performance, and the

application of new materials and new technologies, by its rational performance requirements and its flexibility in performance evaluation. The new framework explained here would result in proper recognition of high-quality technologies, and would ultimately improve the performance and quality of building structures. And the building structural performance would be one of measures for consumers to define the building value.

The following items are considered as R&D subjects and the guideline give the directions.

- 1) Background study to determine the magnitude of loads and external forces.
- 2) Determination methods for limit value which can be represent the limit state appropriately.
- 3) Calculating / analytical methods for response value which can be represent the response appropriately.
- 4) Monitoring the performance of building, especially after earthquake.
- 5) Indication methods of evaluated performance
- 6) To make sure the structural designer (including inspectors) can carry out their jobs smoothly in the new framework, it is essential to set up the suitable social system including technological tools, customs and institutional arrangements which affect the structural designer's practice.

ACKNOWLEDGMENTS

Support from the R&D committee members on the Development of a New Engineering Framework for Building Structures are gratefully appreciated.

REFERENCES

- 1) The Building Center of Japan, and Japan Institute of Construction Engineering: Fiscal 1995 Report of Development of a New Engineering Framework for Building Structures, March 1996.
- 2) Building Research Institute, Ministry of Construction, The Building Center of Japan, and Japan Institute of Construction Engineering:

Table 1 Basic Structural Performance (required performance)

1) Safety	
Purpose :	To avoid hazard which directly affects human lives inside and outside of the buildings. (Security of human lives)
Contents to evaluate the performance :	To prevent the loss of supporting capacity of structural elements and soils which supports vertical forces from the viewpoint of safety. To prevent the falling out or scattering of building elements (structural members, nonstructural members), equipment/machines, fixtures and urniture from the viewpoint of safety.
2) Reparability	
Purpose :	To maintain the function against the damage caused by the outer stimuli (actions) to the buildings. (Security of property)
Contents to evaluate performance :	To control the deterioration and/or damage degrees on structural frames, building elements. (structural members, non-structural elements), equipment/machines, fixtures, furniture and soil from the viewpoint of easiness for repair.
3) Serviceability	
Purpose :	To secure the serviceability (function and habitability) of the buildings. (Security of serviceability)
Contents to evaluate the performance :	To eliminate harmful deformation or vibration on structural frames, building elements (structural members, non-structural members) and members, equipment/machines, fixtures, furniture and soil from the viewpoint of human sense and building function.

※ Deterioration of material properties and affected damage during the lifecycle of building should be considered as a factor in the evaluation of every basic structural performances.

Table 2 Evaluated Objects and Fundamental Performance

Perform. Limit state	Safety (keep of Human Life)	Reparability (keep of Properties)	Serviceability (keep of Function and Habitability)
Objects	Safety Limit	Reparability Limit	Serviceability Limit
Structural Frame	Non-destruction* ¹ to human life	within Assigned Damage	Non-Harmful* ² Def. or Vib. for normal use
Building Members (Structural/ Non-Structural Members)	Non-drop, Scatter to human life	within Assigned Damage	Non-Harmful* ² Def. or Vib. for normal use
Equipment/ Machines/ Fixture	Non-Overturn, Drop, Movement by deformation or vibration of structural frames or members	within Assigned Damage by deformation or vibration of structural frames or members	Non-Harmful* ² Def. or Vib. of structural frames or members for normal use of equipments / machines
Furniture	Non-Overturn, Drop, Movement by deformation or vibration of structural frames or members	within Assigned Damage by deformation or vibration of structural frames or members	Non-Harmful* ² Def. or Vib. for normal use
Soil	Non-destruction* ¹ (decrease of support ability or change* ³ of soil)	within Assigned Damage (decrease of support ability or change* ³ of soil)	Non-Harmful* ² Change* ³ for normal use of buildings or traffic

<Supplement>

(*1) destruction: loss of supprting capacity of structure elements and soil which supports vertical forces

(*2) harmful: available without interference in the usual usage

(*3) change: landslide, movement, deformation, decrease of stiffness (ex. by liquefaction), gap, crack of soil

Table 3 Framework of the new Social System

Expected functions Type of sub-systems	Mainly beneficial for clients			Mainly beneficial for engineers
	(a) To support clients to concretize their needs	(b) To ensure sufficient reliability of conversion of clients' needs into target performance	(c) To ensure sufficient reliability of conversion of target performance into performance of Design Solutions	(d) To prepare appropriate environment for P.B.D. practice
(I) Basic systems	I-a-1) Performance evaluation and certification system I-a-2) Environment to provide technical service to support concretization of needs	I-b-1) System to ensure reliability of conversion process	I-c-1) System to ensure reliability of design and performance verification process	I-d-1) System to define liability and responsibility of each body involved I-d-2) System to support engineers to acquire necessary knowledge/abilities I-d-3) Environment in which P.B.D. practice can be economically feasible
(II) Evaluation system of engineers/ organizations	II-a-1) Qualification/ information system of engineers' consultation abilities	II-b-1) Qualification/ information system of engineers' abilities for conversion process	II-c-1) Qualification/ information system of engineers' abilities for design and performance verification process	II-d-1) Liability insurance system taking the level of qualification of engineers into account
(III) Technical information /tools	III-a-1) General information on relation between performance and its benefit III-a-2) Information on social /community needs including minimum requirements stipulated in building regulations	III-b-1) Technical information on conversion process III-b-2) Service by independent bodies to evaluate the result of conversion, etc.	III-c-1) Technical information on design and performance verification process III-c-2) Service by independent bodies to evaluate Design Solutions, verification and technical tools, etc.	III-d-1) Technical information for acquirement of knowledge/ abilities III-d-2) Technical information, technical evaluation system of independent bodies, etc. provided by bodies who have liabilities for them

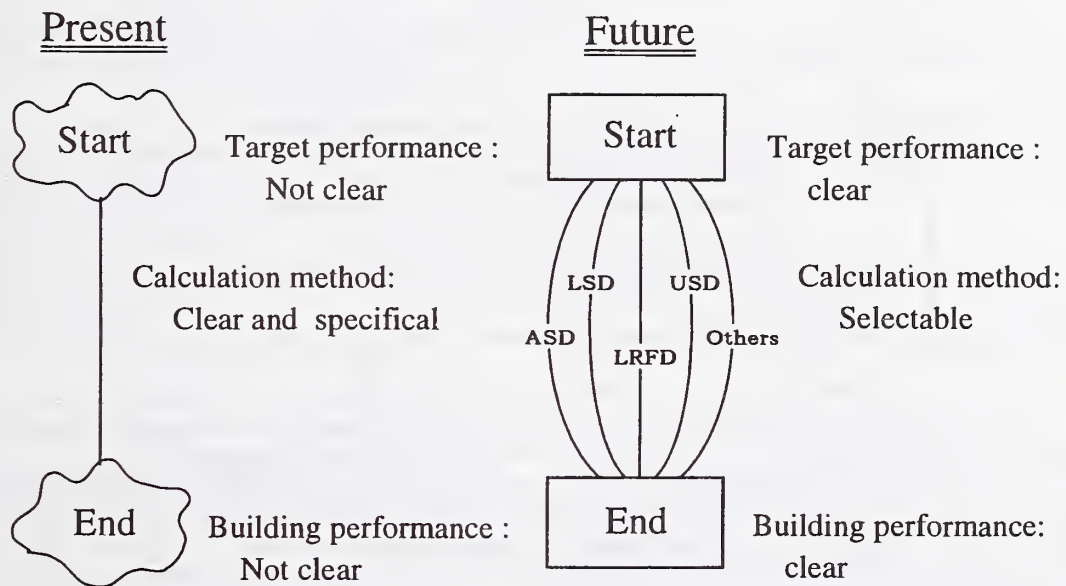


Figure 1 Present and Future Structural Framework

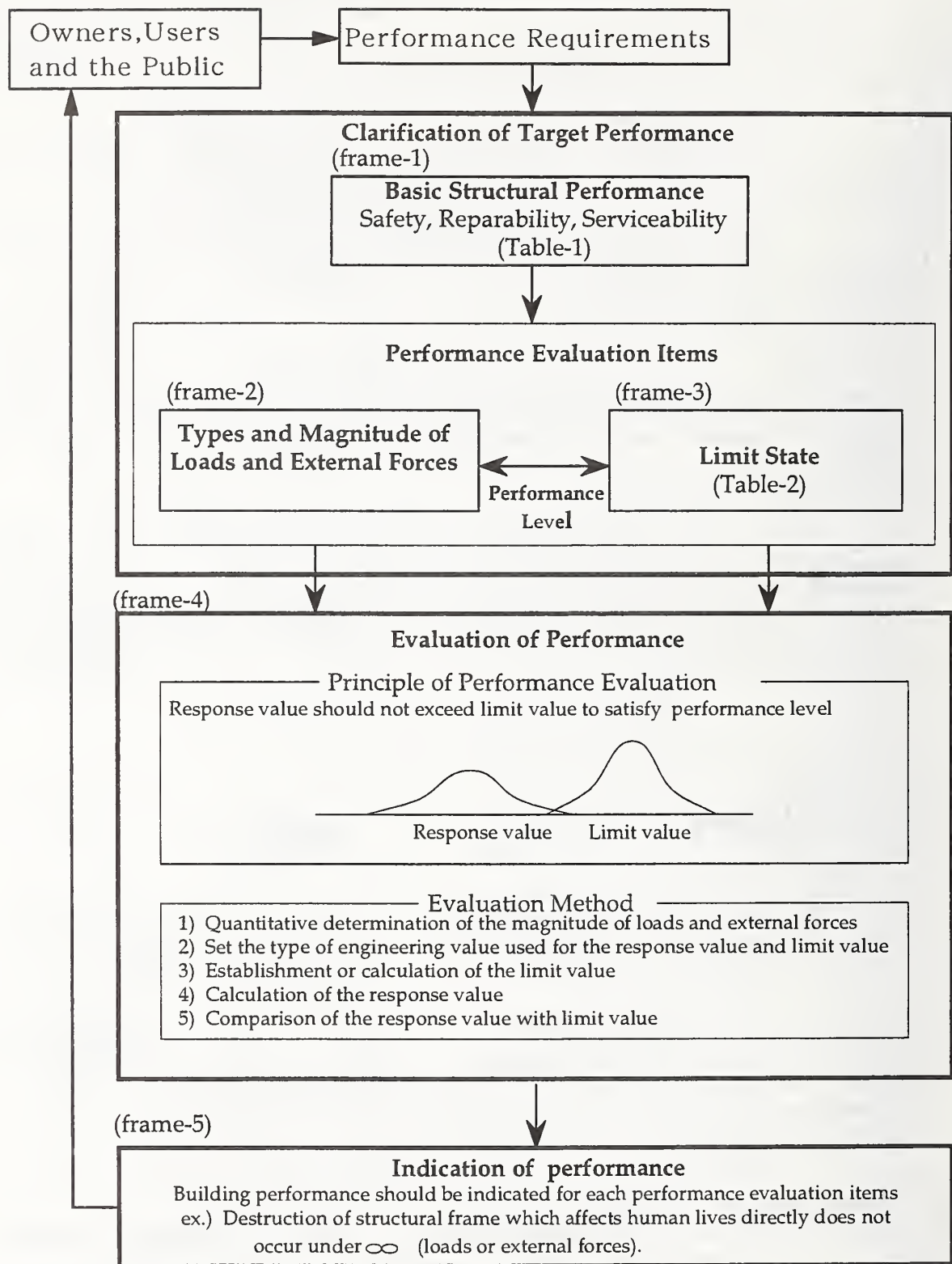


Figure 2 Evaluation system of Structural Performance

APPENDIX I. New Design Earthquake Motion

A.I.1 Design Earthquake Motion

The followings are the basic concept of our proposal for prospective design seismic force in performance-based design scheme (BRI proposal).

In our new proposal, the design earthquake load is specified with earthquake ground motion not with seismic force. The earthquake Ground Motion is basically given at the engineering bedrock which is defined as larger with more than 400 m/s in shear wave velocity.

The basic concept in evaluating the design earthquake motions is expressed in the followings.

- (1) Based on the historical earthquakes, active faults, seismotectonics, earthquakes shall be selected considering the intensity indices such as peak acceleration with its occurrence rate at the construction site.
- (2) A site specific earthquake ground motion or its characteristics of the selected earthquakes shall be determined.
- (3) The earthquake ground motion thus determined shall be modified with the effect of dynamic soil structure interaction.
- (4) The ground motion will be converted into seismic force with evaluation of response of the structure

A.I.2 Evaluation of Earthquake Load Evaluation of Seismic Activity

The seismic activity shall be estimated using the following equation.

where, E denotes earthquake, PGA represents peak ground acceleration or its alternative intensity index, T_e denotes the return period of the earthquake, and $PGA(T_e)$ is the expected value during the return period T_e .

The seismic activity, source mechanism, and source locations vary with site. The types of earthquake sources to be considered in design are

at least in the following three conditions.

- (1) Damaging earthquake in historical data
 - (2) Earthquake due to active faults
 - (3) Earthquake for which occurrence is appropriate from seismotectonics but source locations is not identified.
- (3) is assumed recognizing that (1) and (2) are not completely compiled and similar earthquake can occur in any place within a seismotectonic region.

Evaluation Earthquake Ground Motion

Earthquake ground motion or its characteristics shall be evaluated by selecting the earthquakes considered at the site and with the property of source, path and site effect

- (1) Case in which source mechanism should be considered.

The hypocentral distance is comparable with or less than the fault dimension, the effect of source mechanism and rupture process to the earthquake ground motion property can not be ignored. Therefore, the estimation of design earthquake ground motion should be done using model capable of taking those effects into account. For example,

$$A_{ij}(f) = G(f, E_i) * P_{ij}(f) * S_j(f)$$

$i=1, \dots, n$; n : number of earthquakes to be considered

where, $A_{ij}(f)$: Design earthquake ground motion characteristics at ground surface or standard position

f : frequency

$G(f, E_i)$: Source property of i -th earthquake E_i

$P_{ij}(f)$: Property of propagating path from i -th source to j -th site (e.g., attenuation due to distance)

$S_j(f)$: Soil amplification property of j -th site

In estimating the earthquake ground motion, uncertainty and variation of the data and method applied should be considered, since the source mechanism and rupture process of an earthquake cannot be predicted deterministically and the underground structure above bedrock cannot be

investigated thoroughly.

(2) Case in which source mechanism need not be considered

The effect of minute variation in source mechanism on ground motion in case that the hypocentral distance is larger than the source dimension, is generally small. Therefore, the following equation can be used.

$$A_{ij}(f) = G_{Pij}(M, D, f) * S_j(f)$$

where,

$G_{Pij}(M, D, f)$: spectrum at bedrock

D: distance from source to site

$G_{Pij}(M, D, f)$ can be estimated by the M-A regressive equation. The long-period property ascribed to deep underground structure above seismic bedrock shall be considered when it is appropriate to incorporate.

A.I.2.1 Estimation of Site Amplification Property

Site amplification property for i-th site $S_j(f)$ shall be estimated with the amplification due to the surface soil above bedrock, the correction coefficient for topographical irregularity. However, earthquake response analysis is preferable for excessive irregular topography or in case soil amplification changes due to nonlinear response of soils.

$$S_j(f) = S_{1j}(f) * S_{2j}(f)$$

where, $S_{1j}(f)$: Amplification coefficient for surface soil

$S_{2j}(f)$: Correction coefficient for topographical irregularity

(1) Amplification coefficient for surface soil

When the surface soil is almost horizontally layered and the influence of excess pore water pressure is ignored, the amplification coefficient can be estimated with the predominant frequency of shear wave propagating vertically in the horizontally layered structure.

(2) Correction coefficient due to topographical irregularity

The correction coefficient due to topographical irregularity is use for considering the influence of irregular surface land form or non-horizontal layers. Therefore, in case that the surface soil is almost horizontally layered and then the influence can be ignored, the coefficient shall be one.

A.I.2.2 Evaluation of Dynamic Soil Structure Interaction Effect

The effect of dynamic soil structure interaction shall be considered since the soils supporting the foundation is not rigid. The inclusion of he effect in input earthquake motion means that the

$$C_{ijk}(f) = A_{ij}(f) * I_k(f)$$

where, $C_{ijk}(f)$: design earthquake ground motion at building foundation

$I_k(f)$: Correction coefficient of the effect of dynamic soil structure interaction

However, when the excessive nonlinearity in soil and foundation is expected, a more realistic model should be used.

A.I.2.3 Evaluation of Earthquake Load

Earthquake load equivalent to effective input motion in fixed base condition or equivalent design earthquake load index can be obtained by the following formula

$$D_{ijkl}(f) = C_{ijk}(f) * B_l(f)$$

where, $D_{ijkl}(f)$: Design earthquake load index

$B_l(f)$: Coefficient to translate to earthquake load such as story shear force coefficient considering the structural property.

However, since the design earthquake load index is an average or overall intensity index, it may not be able to grasp the destructiveness of the design motion. In such case, a specific method such as dynamic analysis procedure using earthquake motion time history shall be used.

APPENDIX II. Performance Level

There are many issues which need to be considered in determining the performance levels of buildings. Some of these issues are listed below and discussed in the sections to follow.

- (1) Performance Level of Existing Buildings
- (2) Acceptable Risk Level
- (3) Minimum Cost Level

(1) Performance Level of Existing Buildings

The current building code in Japan provides design and analysis procedures to achieve the primary design objectives such as the life safety under a large (severe) earthquake. Even the current code doesn't describe the level of safety explicitly, it has been accepted in the society by revising its context reflecting the building damage by past earthquakes. Therefore, it is quite reasonable to determine the target performance level of buildings in a new design procedure by referring to the performance level of existing buildings which were designed in accordance with the current code.

The performance level should be examined under consideration of the possibility of future earthquake damage. Since there is large uncertainty in estimating future earthquake loads, the seismic safety of existing buildings should be examined in terms of probabilistic measures such as the reliability index β in a building life time.

- Model of buildings

Two typical buildings designed in accordance with the current design code are selected as the representatives of existing buildings; one is an 8-story reinforced concrete building and the other is a 6-story steel building. Construction sites are assumed to be in Tokyo and Osaka, Japan. Since the design seismic zone factor is the same for both sites ($Z = 1.0$), the design shear forces are identical for both buildings. The uncertainties associated with structural properties are assumed to be negligible comparing the uncertainties of earthquake loads, and not considered in this study.

- Model of earthquake ground motions

Input earthquake ground motions are

simulated referring to the guideline, "Recommendations for Loads on Buildings," published by the AIJ (Architectural Institute of Japan) in 1993. This study assumes that the maximum earthquake acceleration and the ground amplification factor are random variables. - Seismic reliability estimate

Sample input ground motions are generated and the nonlinear response analyses of the designed buildings are carried out. From the relation between the input scale and the maximum story drift ratio, the reliability index β is evaluated as a function of the design criterion.

Figure A.II.1 shows the relation between the maximum drift ratio Y and the safety index β for the reinforced concrete building and the steel building, respectively. As shown in the figures, the reliability index β of Tokyo site is generally smaller than those of Osaka site. The difference of the safety indices between RC building and Steel buildings in the same site is not so large.

From the calculated results, the performance of the buildings and its reliability index could be approximately summarized in Table A.II.1.

Table A.II.1

Example of Reliability Index for RC Buildings

Performance items	β *
Concrete crack	$\beta = 0$
Failure of secondary elements	$\beta = 1.0$
Failure of structural elements	$\beta = 2.0$
Collapse of building	$\beta = 3.0$

* reference period is 50 years

(2) Acceptable Risk Level

In daily life, we usually neglect the very small risk such as the risk of being hit by a comet, however, the risk of being hit by a car may not be considered negligible. If we reduce the strength of a building, the risk associated with earthquake-induced building damage may increase. So, the question is how large risk people may think acceptable, and what level of safety should be assigned to building structures.

We call the potential risk in daily life, such as

the risk by disease, traffic accident, etc., as "background risk," and gathered statistical data of such risks from various sources. Obtained data are summarized into a risk database where the data of death of people are categorized by the type of causes, years, etc. The annual death ratios (=risks) in Japan by different causes are summarized in Table A.II.2.

Table A.II.2

Examples of Annual Risk in Japan	
Risk items	Annual risk
Fire	10^{-5} to 10^{-6}
Earthquake	10^{-4} to 10^{-7}
Suicide	10^{-5}
Traffic accident	10^{-4}
Disease	10^{-3} to 10^{-2}

In case of earthquakes, the death ratio was evaluated by taking moving average with twenty year intervals, and it shows some fluctuation between the range of 10^{-4} and 10^{-7} . Some people reports that people will neglect the event which annual occurrence ratio is below 10^{-6} , however, when we think about the huge disaster at the Great Hanshin-Awaji earthquakes, it is clear that the frequency of event is not only a measure to judge its acceptability. The impact of the event to the society should be discussed together. Figure A.II.2 is a schematic figure showing the relation between the frequency of the risk events and their social impact, and the boundary of acceptable region may be drawn in this figure.

(3) Minimum Cost Level

Total cost of a building in its lifetime is generally modeled by the following equation:

$$C_{\text{total}} = C_{\text{ini}}(R) + C_f(R)P_f(R)$$

where, R is the design parameter of the building to represent its resistance, C_{total} is the total cost, C_{ini} is the initial cost for construction, C_f is the damage cost, and P_f is the probability of the occurrence of such damage. In this study, the damage cost C_f is assumed to consist of three different components,

$$C_f = C_{\text{rep}} + C_{\text{los}} + C_{\text{spd}}$$

where, C_{rep} is the cost for repairing the building damage, C_{los} is the cost associated with the loss of contents, and C_{spd} is the cost considering the secondary damage such as the loss of business. The initial cost, C_{ini} , is assumed to be a simple function of the parameter R , and the damage costs, C_{rep} , C_{los} and C_{spd} , are modeled as functions of the maximum story drift ratio. Figure A.II.3 shows the analytical flow to obtain the total cost by the Monte-Carlo simulations.

The optimum design parameter to minimize total cost are evaluated for various types of buildings. Table A.II.3 shows the results of for the buildings in Tokyo. In case of the private house and the office building, the minimum cost levels are found to be less than the level of current code requirement, however, in case of the school building and the hospital building, the minimum cost levels are much larger than the current design level because of the large cost of damage to their functions. These results suggest the necessity of higher performance levels of such public buildings more than the code requirement levels of general buildings.

Table A.II.3

Examples of Minimum Cost Design Levels	
Building type	Minimum cost level*
Private house	92
Office	98
School	120
Hospital	200

* current design level =100

It is very sensitive issue to include the loss of human life into the calculation of damage costs. Of course, it may be possible to consider the loss of human life as the price of life insurance or cost for compensation, etc., however, it doesn't mean that the human life is equal to such costs. Therefore, we didn't include the loss of human life into the above cost calculations. Multiple design criteria including costs and human life in different axes should be discussed.

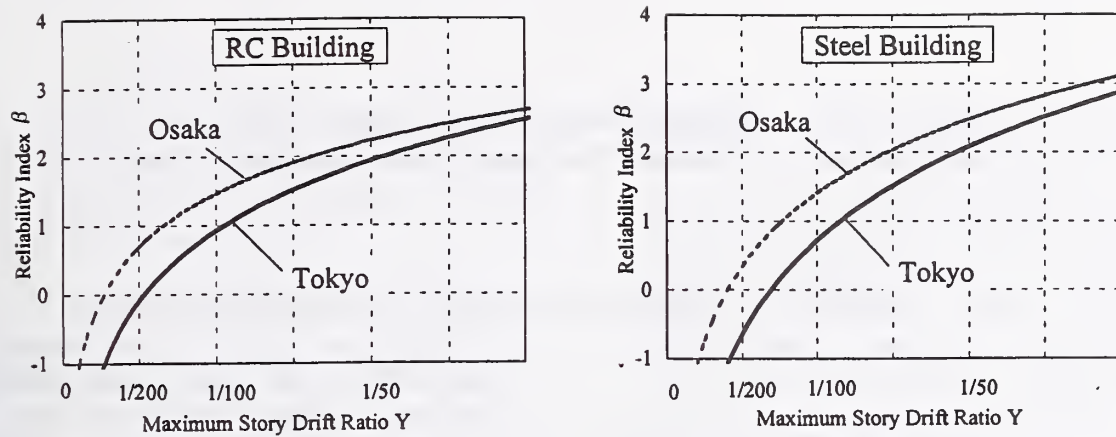


Figure A. II.1 Relation between the maximum story drift Y and the reliability index β in 50 years

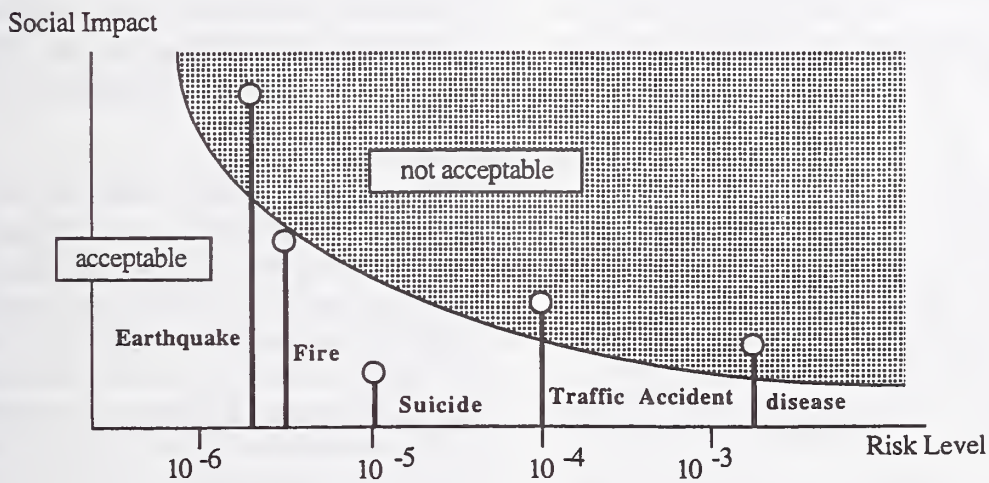


Figure A. II.2 Concept of Acceptable Risk

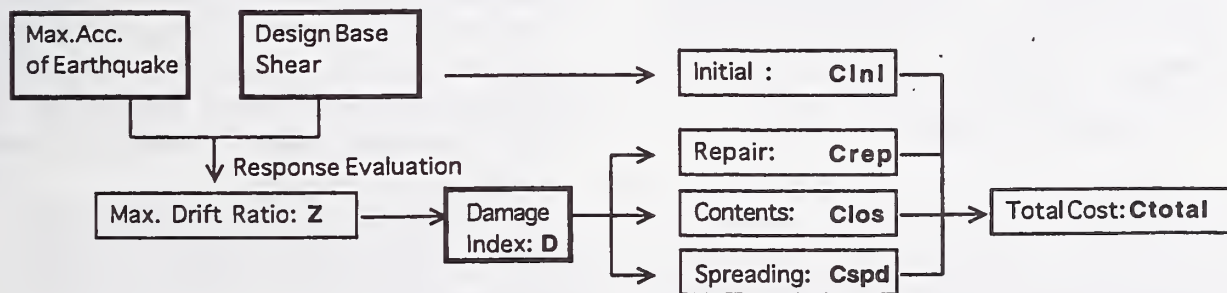


Figure A. II.3 The Analytical Flow to Obtain the Total Cost by the Monte-Carlo Simulations

Highway Bridge Seismic Design: How Current Research May Affect Future Design Practice

by

Ian M. Friedland¹, W. Phillip Yen², Ronald L. Mayes³ and John O'Fallon²

ABSTRACT

Under a program sponsored by the Federal Highway Administration, the National Center for Earthquake Engineering Research is conducting a research program on new highway structure design and construction which has among its objectives studies on the seismic vulnerability of tunnels, retaining structures and bridges and the development of technical information on which, in the case of bridges, revisions can be made to current national design specifications. As a wrap-up to the program, research results are being reviewed and assessed in order to determine the impact that their results may have on the future development of a consistent seismic design specification for highway structures. This paper summarizes some of the important results of the research conducted under the program and discusses issues resulting from this impact assessment task with respect to expected effects on future design practice.

KEYWORDS: bridges, codes, criteria, design, earthquake, highways, retaining structures, specifications, structures, tunnels

1. INTRODUCTION

1.1 Background

The loss of life and extensive property damage suffered during the 1989 Loma Prieta, 1994 Northridge and 1995 Kobe earthquakes emphasized the need for research to provide new procedures and

specifications for constructing earthquake-resistant bridges and highways. In recognition of this need, the Federal Highway Administration (FHWA) initiated a comprehensive Seismic Research Program for bridges and highways in the fall of 1992. This program is being conducted by the National Center for Earthquake Engineering Research (NCEER) in cooperation with agencies participating in the Federally-sponsored National Earthquake Hazards Reduction Program.

The research being conducted by NCEER consists of two separate FHWA-sponsored projects. Both projects involve research studies on the seismic vulnerability of highway construction in the U.S. including bridges, tunnels, retaining structures, slopes and embankments, culverts and pavements. One project focuses on existing transportation infrastructure while the other is concerned with new highway construction.

The motivation for these studies comes from the fact that the present guidelines for seismic design and retrofit of highway bridges are 10–15 years old, and that there are no national seismic design or retrofit standards for the other components of typical highway systems. In addition, recent

¹ National Center for Earthquake Engineering Research, State University of New York at Buffalo, 102 Red Jacket Quadrangle, Buffalo, NY 14261-0025

² Federal Highway Administration HNR-10, Turner-Fairbank Highway Research Center, 6300 Georgetown Pike, McLean, VA 22101

³ Dynamic Isolation Systems, 3470 Mt. Diablo Boulevard, Suite A200, Lafayette, CA 94549

experience in California, Costa Rica, the Philippines, and Japan has provided new insight into bridge and highway response during earthquakes.

Significant progress has also been made in understanding the seismic risk of the U.S., in geotechnical engineering terms and in seismic resistant design, such that a comprehensive review of design and retrofit philosophies and procedures can now be undertaken. However, although much has been learned, there are still many gaps in basic knowledge. Furthermore, not all existing knowledge can be immediately applied to the highway arena and further studies are required to facilitate the transfer of this technology.

As a result, the FHWA initiated the two major studies comprising the NCEER Highway Project; one on existing transportation infrastructure and the second on new design and construction. Research on these projects was initiated by NCEER in mid-1993 and has a national focus. It is intended to address differences in seismicity, bridge types, and typical design details between eastern and central U.S. bridges and those which have been studied in California. Furthermore, unlike the western U.S., design and retrofit strategies for the eastern and central U.S. need to reflect the probability that an earthquake significantly larger than the design earthquake can occur.

1.2 FHWA Research for New Highway Structure Design and Construction

The FHWA program on new highway structure design and construction (officially known as the FHWA Seismic Research Program) has among its objectives studies on the seismic vulnerability of tunnels, retaining structures and bridges and the development of technical information on

which, in the case of bridges, revisions can be made to the current national design specifications. This research has national applicability, but in view of the relatively advanced state-of-practice on the West Coast, is focussing on low-to-moderate seismic zones. The program includes both analytical and experimental studies, with a focus on the following technical areas:

- seismic hazard exposure and ground motion input for the U.S. highway system;
- foundation design and soil behavior
- structural issues of importance, response and analysis;
- design issues and details; and
- design criteria review.

As a wrap-up to the program, a final task is being conducted which is providing a review of the results obtained from each of the studies conducted under the program, in order to assess the impact that their results may have on the future development of a consistent seismic design specification for highway structures.

The purpose of this paper is to summarize some of the important results of the research conducted under the program and to discuss issues resulting from the wrap-up impact assessment task, with respect to their expected effects on future design practice.

2. SEISMIC HAZARD EXPOSURE AND GROUND MOTION INPUT

The research in the area of seismic hazard exposure has focused on the evaluation of alternative approaches for portraying and representing the national seismic hazard exposure in the U.S., quantifying and developing an understanding of the effects of spatial variation of ground motion on highway structure performance, and the

development of inelastic design spectra for assessing inelastic deformation demands.

2.1 Representation of Seismic Hazard Exposure

Research in the area of seismic hazard exposure representation was conducted in order to:

- explore a number of important issues involved in national representations of seismic ground motions for design of highway facilities;
- recommend future directions for national seismic ground motion representation, especially for use in nationally applicable guidelines and specifications such as the AASHTO seismic design provisions for bridges; and
- identify areas where further development and/or research are needed to define ground motion representation for guidelines and specifications.

The ground motion issues that have emerged in recent years as potentially important to highway facilities design and that were considered in this work included consideration of:

- (a) Should new (1996) USGS maps provide a basis for the national seismic hazard portrayal of highway facilities? If so, how should they be implemented in terms of design values?
- (b) Should energy or duration be used in a design procedure?
- (c) How should site effects be characterized for design?
- (d) Should vertical ground motions be specified for design?
- (e) Should near-source ground motions be specified for design?

The following summarize the key elements of each issue and conclusions of the research.

(a) New USGS maps – In 1996, the U.S. Geological Survey (USGS) developed new seismic ground shaking maps for the contiguous U.S. These maps depict contours of peak ground acceleration (PGA) and spectral accelerations (SA) at 0.2, 0.3, and 1.0 second (for 5% damping) of ground motions on rock for probabilities of exceedance (PE) of 10%, 5%, and 2% in 50 years, corresponding to return periods of approximately 500, 1000, and 2500 years, respectively.

The research considered whether the new USGS maps should replace or update the maps currently in AASHTO, which were developed by the USGS in 1990. The key issue regarding whether the new USGS maps should provide a basis for the national seismic hazard portrayal for highway facilities is the degree to which they provide a scientifically improved representation of seismic ground motion. Based on an analysis of the process of developing the maps, the inputs to the mapping, and the resulting map values, it was concluded that these new maps represent a major step forward in the characterization of national seismic ground motion. The maps are in substantially better agreement with current scientific understanding of seismic sources and ground motion attenuation throughout the U.S. than the current AASHTO maps. It was therefore concluded that the new USGS maps should provide the basis for a new national seismic hazard portrayal for highway facilities.

The issue of an appropriate probability level or return period for design ground motions based on the new USGS maps was also examined. Analyses were presented

showing the effect of probability level or return period on ground motions and comparisons of ground motions from the new USGS maps and the current AASHTO maps. It was recommended that for design of highway facilities against collapse, consideration should be given to adopting probability levels for design ground motions that are lower than the 10% probability of exceedance in 50 years that is currently in AASHTO. This is consistent with proposed revisions to the 1997 NEHRP provisions for buildings, in which the new USGS maps for a probability of exceedance of 2% in 50 years have been adopted as a collapse-prevention design basis.

(b) Consideration of energy or duration – At the present time, the energy or duration of ground motions is not explicitly recognized in the design process for bridges or buildings, yet many engineers are of the opinion that the performance of a structure may be importantly affected by these parameters, in addition to the response spectral characteristics of the ground motion. As a result, it was concluded that some measure of the energy of ground motions is important to the response of a bridge, but, at present, there is no accepted design procedure to account for energy. Research in this area should be continued to develop energy-based design methods that can supplement current elastic-response-spectrum-based design methods. It was also concluded that energy rather than duration is the fundamental parameter affecting structural behavior.

(c) Characterization of site effects – At a Site Effects Workshop held in 1992 at the University of Southern California (USC), a revised quantification of site effects on response spectra and revised definitions of site categories were proposed. Subsequently, these revised site factors and

site categories were adopted into the 1994 NEHRP provisions and the 1997 Uniform Building Code (UBC). Since the development of these revised site factors, two significant earthquakes occurred (the 1994 Northridge and 1995 Kobe earthquakes) which provided substantial additional data for evaluating site effects on ground motions, and research using these data has been conducted.

The site factors and site categories in the current AASHTO specifications are those that were superseded by the USC Workshop recommendations in the NEHRP Provisions and the UBC. Under this research, the question was whether the USC Workshop recommendations should be utilized in characterizing ground motions for highway facilities design and whether they should be modified to reflect new data and new knowledge since the 1992 Workshop. The most significant differences in the USC Workshop recommendations and the previous site factors (those currently in AASHTO) are: (1) the revised site factors include separate sets of factors for the short-period and long-period parts of the response spectrum, whereas the previous site factors were only for the long-period part; (2) the revised site factors are dependent on rather than independent of intensity of ground shaking, reflecting soil nonlinear response; and (3) the revised site factors are larger (i.e., show a greater soil response amplification) than the previous factors at low levels of shaking, as appropriate to the lower-seismicity regions in the U.S.

It was found that the post-Northridge and post-Kobe earthquake research conducted to date generally was supportive of the site factors derived in the 1992 USC Workshop, although revisions to these factors might be considered as further research on site effects is completed. It was therefore recom-

mended that the factors developed at the USC Workshop and adopted by the NEHRP Provisions and the UBC be proposed as part of a new national representation of seismic ground motion for highway facilities design.

(d) Vertical ground motions – At present, the AASHTO specifications do not contain explicit requirements to design for vertical accelerations. Ground motion data from many earthquakes in the past 20 years have shown that, in the near-source region, very high short-period vertical spectral accelerations can occur. For near-source moderate-to-large magnitude earthquakes, the rule-of-thumb ratio of 2/3 between vertical and horizontal spectra is a poor descriptor of vertical ground motions. At short periods, the vertical-to-horizontal spectral ratios can substantially exceed unity, whereas at long periods, a ratio of two-thirds may be conservative. It was demonstrated that our current understanding and ability to characterize near-source vertical ground motions is good, especially in the western U.S. where the near-source region is better defined (i.e., near mapped active faults). It was also demonstrated that high vertical accelerations as may be experienced in the near-source region can significantly impact bridge response and design requirements in some cases. On the basis of these findings, it was concluded that vertical ground motions should be considered in bridge design in higher seismic zones for certain types of bridge construction. It was recommended that specific design criteria and procedures be developed for certain bridge types.

(e) Near-source ground motions – The characteristics of near-source horizontal ground motions and the effects of near-source ground motions on bridge response were examined. As the distance to an earthquake source decreases, the intensity of

ground motions increases, and this increase in ground motion intensity is incorporated in new USGS maps. However, in addition to their higher intensity, near-source ground motions have certain unique characteristics that are not found at greater distances. The most significant characteristic appears to be a large pulse of long-period ground motions when an earthquake rupture propagates toward a site. Furthermore, this pulse is larger in the direction perpendicular to the strike of the fault than in the direction parallel to the strike. This characteristic of near-source ground motions has been observed in many earthquakes, including most recently in the Northridge and Kobe earthquakes. Preliminary analyses of bridge response indicate that near-source ground motions may impose unusually large displacement demands on bridge structures. It was therefore concluded that traditional ground motion characterizations (i.e., response spectra) may not be adequate in describing near-source ground motions, because the pulsive character of these motions may be more damaging than indicated by the response spectra of the motions. Recommendations include the need for additional research to evaluate more fully the effects of near-source ground motions on bridge response and to incorporate these effects in code design procedures. Until adequate procedures are developed, consideration should be given to evaluating bridge response using site-specific analyses with representative near-source acceleration time histories.

2.2 Spatial Variation of Ground Motion

The objective of the research in this area was to develop procedures for determining spectrum compatible time histories that adequately represent spatial variations in ground motion including the effects of different soil conditions. The procedures

were then used to examine the effects of spatial variability on critical response quantities for typical structures.

The methodology used a spectral representation to simulate stochastic vector processes having components corresponding to different locations on the ground surface. An iterative scheme was used to generate time histories compatible with prescribed response spectra, coherency, and duration of motion. Analysis results for eight example bridges were tabulated, showing the relative ductility demand ratio for column flexure due to seismic wave propagation spatial effects. In general, there was about a 10% maximum increase when using linear analysis, and a 25% maximum increase when using non-linear analysis for bridges up to 1000 feet in length. Results were also tabulated for relative opening and closing at expansion joints for bridges with superstructure hinges. In general, the relative joint opening movement was up to two times when using either linear or non-linear analysis for bridges up to 1000 feet in length.

Potential future code impacts resulting from this work are as follows:

- For right bridges under 1000 feet in length with at least two spans and uniform soil conditions, the use of synchronous support ground motions may be recommended. If a conservative approach is desired, the seismic response coefficient could be increased by 10% or the R-factor could be decreased by 20%.
- For bridges over 1000 feet in length, with supports on different local soil conditions or with high skews, the use of time history analyses involving asynchronous support ground motions may be advisable. In so doing, a number of scenario earthquakes and several

different values of wave velocity should be investigated. It is important to note, however, that these results are preliminary and have not been independently validated as yet.

The implementation of time history analyses may significantly increase overall design cost for complicated bridges. However, it is expected that overall structural performance would also be significantly improved by the ability to account for differing soil conditions.

2.3 Inelastic Design Spectrum

The research in this area had the objective of developing inelastic response spectrum which would allow designers to assess the inelastic deformation demands, ultimately leading to improved seismic performance for new bridge construction. The spectrum are being derived for nationwide use, accommodating different seismic environments and site soil conditions. They are also being developed for design applications, by accounting for scattering and variabilities that exist in real earthquake ground motions and for non-linear structural response.

Under the current program, the research has not progressed to the point where its results are ready for implementation. When complete, it is likely to have a major impact on seismic design code requirements for bridges, as inelastic spectra will be one of the key elements in a displacement-based or energy-based design procedure. Future work in this area should include procedures for determining inelastic spectra at a specific site. The current state of research provides an approximate method that starts with an elastic spectrum rather than time history; as time histories for the eastern U.S. are currently lacking, this approach will have an obvious appeal.

3. FOUNDATION DESIGN AND SOIL BEHAVIOR

Research tasks in this area investigated and improved criteria for the design and analysis of major foundation elements including abutments, retaining walls, pile and spread footings, and drilled shafts. In addition, work was performed on soil liquefaction and lateral spread identification and mitigation.

3.1 Abutments and Retaining Walls

Research on bridge abutments and retaining walls focused on modeling alternatives, clarifying the process of design for service loads versus seismic loading, and providing simplified approaches for design that incorporate key issues affecting seismic response. The research also attempted to provide a new procedure for determining the seismic displacements of abutments and retaining walls founded on spread footings, which differ from current procedures by addressing mixed-mode behavior (i.e., including rotation due to bearing capacity movement and sliding response). Both experimental and analytical studies were conducted; the experimental studies included sand-box experiments on a shaking table and centrifuge models. Results of this research included:

- Development of a simplified procedure for estimating abutment stiffness. A key element of this approach is determining the portion of the wall that can be relied on to mobilize backfill resistance.
- Extending current AASHTO design procedures to the more general case of translation and rotation of walls and abutments. The results are presented in a manner that will allow the methods to be easily introduced into a future code revision. The new procedures will be of greatest use for free-standing gravity

walls and for active mode abutment and wall movements.

- Consideration of passive loading conditions for walls and abutments. Current AASHTO provisions only address active loading conditions. Since passive loading can result in forces that are up to 30 times those for active conditions, there is a strong possibility that many bridges will not develop passive resistance without abutment damage.

3.2 Pile and Spread Footings and Pile Groups

Studies on pile footings, spread footings and pile groups included experimental and analytical research tasks which were intended to: provide improved understanding of the lateral response of pile-cap foundations; evaluate the influence of modeling parameters on estimated displacement and force demands; recommend methods for characterizing the stiffness of pile footings; quantify the importance of radiation damping and kinematic interaction on response; and evaluate conditions under which uplift becomes significant and how best to model uplift in a design procedure. Results from these studies included the following:

- For pile-cap systems, the research demonstrated that design procedures should use simple additions for the contribution from the base, side and active/passive ends when estimating the lateral capacity of embedded spread footings in dense sand, along with elastic solutions with an equivalent linear soil shear modulus at shallow depths to estimate the secant stiffness of the footing. This effectively confirms that existing procedures can be used to obtain reasonable approximations of pile-cap

foundation response, as long as consideration is given to the levels of deformation and embedment for the system.

- Axial and lateral loading response and stiffness characteristics are important parameters for the design of single piles and pile groups, although such information is not currently addressed in the AASHTO provisions. Axial response often controls rocking response of a pile group. New procedures and simplified stiffness charts are provided for determining the lateral load-deflection characteristics of single piles and groups.
- Nonlinear load-deflection analyses illustrate the sensitivity of results to uncertainties in p-y stiffness, gapping, pile-head fixity, bending stiffness parameters, and embedment effects. The analyses have demonstrated that load-deformation response is more affected by input variations than by the moment within the pile.
- For spread footings without uplift, the research demonstrated that (a) ignoring soil-structure interaction reduces the fundamental period of the system, resulting in higher accelerations; (b) increasing the effectiveness of embedment increases radiation damping and reduces the fundamental period of the system; and (c) neglecting radiation damping has only a minor effect on the system. Uplift of the spread footing results in a softer mode of vibration for the system, with increasing fundamental period as the amount of uplift increases.

3.3 Drilled Shafts

Research on drilled shafts was conducted in order to provide information on the influence of modeling procedures on the response of the structure, evaluate the

effects of modeling on estimated displacement and force demands on the foundation, and to summarize methods for characterizing the response of drilled shaft foundations, including their limitations. Results of this work included the following:

- Foundation stiffness has been shown as a key parameter and contributor to the dynamic response of the structure, necessitating realistic estimates and appropriate integration into a detailed structural analysis. The response of a soil-foundation system to load is nonlinear; however, for practical purposes, an equivalent linear representation is normally used.
- Guidance is provided on the development of equivalent linear and nonlinear stiffness values, and the importance and sensitivity of foundation geometry and boundary conditions at the shaft head are identified. A key conclusion is that realistic representation of pile-head fixity can lead to a much more economical design.
- The p-y approach is recognized as the most common method of analyzing the nonlinear response of the shaft to lateral load. Parameters that must be considered include the effects of soil property variation, degradation effects, embedment, gapping, and scour effects.

3.4 Liquefaction Processes and Liquefaction Mitigation Methodologies

A significant amount of research has been conducted under the NCEER Highway Project on liquefaction processes, screening for liquefaction potential, and the development and/or improvement of liquefaction mitigation methodologies. Much of this work was conducted under the companion FHWA project on seismic vulnerability of existing transportation

infrastructure, but all of it is appropriate for either new design or existing construction evaluation. Among the major studies conducted under this project was a review, synthesis, and improvement to recent developments in simplified procedures for evaluating the liquefaction resistance of soils, and the compilation and evaluation of case studies and procedures for ground liquefaction mitigation. Results of this research included:

- Identification of a consensus simplified procedure for evaluating liquefaction resistance. Minor modifications for the determination of the stress reduction factor used in the calculation of the cyclic stress ratio were recommended, which allow the stress reduction factor to be calculated to depths greater than 30 meters.
- Identification of the latest procedures for determining cyclic resistance ratios (CRR) using cone penetration test (CPT) procedures. One of the primary advantages of CPT is the consistency and repeatability of the method. Plots for determining the liquefaction resistance directly from CPT data, rather than converting to an equivalent standard penetration test (SPT) N-value, are presented. Procedures are also provided for correcting CPT data based on overburden pressures, fines contents, and for thin layers.
- Plots for determining CRR from shear wave velocity data have been prepared, and procedures for correcting shear wave velocity data due to overburden stress and fines content are explicitly given.
- Methods which have been employed successfully for liquefaction mitigation include deep dynamic compaction, deep vibratory densification, gravel drains, permeation grouting, replacement

grouting, soil mixing, and micro blasting. Parameters and limitations for each of these approaches are summarized, including typical treatment depths and applicable soil types.

- Flow charts for assessing ground deformations for pre- and post-treatment conditions were developed. These are accompanied by recommendations for preferred ground improvements methods based on differing site conditions.

4. STRUCTURAL IMPORTANCE, ANALYSIS, AND RESPONSE

Several studies were conducted in order to provide a definition of structural importance, which is necessary in the development of design and performance criteria, and to evaluate methods of analysis and structural response. These studies also provided a synthesis of current systems and details commonly used to provide acceptable seismic performance in various states and regions. Among the findings of these studies were the following:

- Provisions employed by the California Department of Transportation (Caltrans) were generally more rigorous than those used by the majority of states (who primarily used current AASHTO provisions). However, adoption of Caltrans' design provisions nationwide would likely complicate designs and add to construction cost; this may be unjustified for many low-to-moderate seismic hazard states. In addition, if Caltrans' experience is to be adapted nationally, some adjustments are required in order to accommodate bridge types and details commonly used elsewhere.
- Studies that were conducted on the application of advanced modeling methods for concrete bridge components

provided a computer program which determines moment-curvature and force-deflection characteristics for reinforced concrete columns; excellent correlation was obtained between analytical and experimental test results for these components.

- A refined model to simulate the hysteretic behavior of confined and unconfined concrete in both cyclic compression and tension was developed. The model includes consideration of the nature of degradation within partial hysteresis looping and the transition between opening and closing cracks.
- A study on energy and fatigue demands on bridge columns resulted in design recommendations for the assessment of fatigue failure in reinforcing steel, based on the results of nonlinear dynamic analyses. This methodology incorporates traditional strength and ductility considerations with the fatigue demands. Based on parametric studies, it was concluded that low cycle fatigue demand is both earthquake and hysteretic model dependent.
- Based on an examination of existing and proposed methods for quantifying bridge importance, a specific method was selected and tested against a database of bridge information commonly available within the FHWA's National Bridge Inventory. One limitation of the study is that it deliberately avoided addressing political and economic issues related to bridge seismic design criteria and highway network considerations.
- Following the Northridge earthquake, concerns were raised as to the role vertical accelerations may have played in causing damage to one or more bridges. In a study conducted to investigate the effects of vertical acceleration on bridge response, preliminary results indicate that vertical

components of ground motion could have a significant effect on bridge response for structures within 10 km of the fault, and even within 20 – 30 km for certain conditions. The results of this study will be controversial when publicized; however, a far too limited study was conducted (only six example bridges were analyzed) in order to provide definitive guidance at this time.

- In a study which investigated the applicability of simplified analysis methods to various types and configurations of bridges, a number of design and analysis limitations were identified. Parameters evaluated included curvature, span length ratio, pier height, skew and span connectivity. Based on the analyses, a definition for "regular" bridges and for which simplified methods are appropriate was developed. In general, regular bridges must have three or fewer spans, variation of mass distribution between adjacent spans varying by less than 50%, a maximum ratio between adjacent pier stiffnesses in the longitudinal and transverse directions not greater than 4.0, and a subtended angle in plan not greater than 90°.

5. STRUCTURAL DESIGN ISSUES AND DETAILS

A number of studies were conducted in order to improve design procedures and structural detailing for highway structures, but the focus was primarily on bridges; one study also examined movement detailing for tunnels. These studies looked at issues of capacity detailing for ductility, elastic behavior, and movements. Among the results of this research were the following:

- A design concept termed Damage Avoidance Design (DAD) was

developed which attempts to avoid plastic hinging in columns, thereby avoiding loss of service for important bridges following a major earthquake. The concept evaluated details which provide for rocking of columns and piers, which rotate about their ends but are restrained from collapse through gravity and the optional use of central unbonded post tensioning in the column core.

- A second design concept termed Control and Repairability of Damage (CARD) was also developed, which provided structural and construction details for reinforced concrete columns that provide replaceable or renewable sacrificial plastic hinge zone components. In this concept, the hinge zones are deliberately weakened and regions outside the hinge zones are detailed to be stronger than the sacrificial (fuse) zone; the remaining elements of the structure then remain elastic during strong earthquakes.
- In a study on transverse reinforcing requirements for concrete bridge columns and pier walls, it was found that the current AASHTO requirements could be lowered by up to 50% while still achieving displacement ductilities of 4 to 7 for bridges in low to moderate seismic zones. An important aspect of this work though was that the end anchorages for transverse steel hoops must be maintained for the reinforcing to be effective; 90° bends on J-hooks were found to be inadequate.
- Research was conducted on moment overstrength capacity in reinforced concrete bridge columns, and a simplified method for determining column overstrength was developed. The upper-bound overstrength factors developed in this task validate prescriptive overstrength factors recommended in ATC-32, but also

indicate that some factors in current Caltrans and AASHTO provisions may be too low.

- A synthesis was conducted on details commonly used to accommodate expected movements on bridges and retaining walls in the eastern and western U.S. Based on the synthesis, design and detailing recommendations were made in order to provide the basis for improved bridge design standards. The specific elements considered in this effort included restraining devices, sacrificial elements, passive energy dissipation devices, and isolation bearings. A similar effort was conducted on movement criteria and detailing for tunnels.
- For steel superstructures, a number of issues were considered, including ductility based on cross-section configuration, applicability of eccentrically-braced frames, details which allow for easy repair of steel sections following a moderate to large earthquake, anchor bolt performance under lateral uplift loads, and economical moment connection details between steel superstructures and concrete substructures.

6. CONCLUSIONS

As a result of a research program sponsored by the Federal Highway Administration, researchers working for the National Center for Earthquake Engineering Research have developed a number of analytical tools, methods of analysis, structural design details, and specification recommendations appropriate for seismic design of highway system structures. The primary focus of this work has been on highway bridges, but some research on tunnels and retaining structures was also performed. The program has also resulted in recommendations

regarding the representation of seismic hazard in future design codes, the performance and improvement of soils under seismic shaking, and an improved understanding of the behavior of structural systems and components under seismically-induced forces and displacements. In addition, it is likely that additional recommendations regarding the use of a performance-based design philosophy and dual-level design and performance criteria will be made to AASHTO as a result of this work.

The results of this program will likely be considered and incorporated into an effort soon to be initiated under the AASHTO-sponsored National Cooperative Highway Research Program (NCHRP). NCHRP Project 12-49 will start in the summer of 1998 and has as its objective the development of the next generation of seismic design specifications for the

AASHTO *Load and Resistance Factor Design Specifications*. Analysis tools and design details will be disseminated to the practicing engineering community and are also expected to impact future highway structure design practice.

7. ACKNOWLEDGMENTS

Dr. George C. Lee is the principal investigator on the NCEER Highway Project. The authors would like to acknowledge Dr. Lee's guidance and direction on this project. In addition, the Impact Assessment task conducted under the project is managed by the Applied Technology Council, with Mr. Christopher Rojahn as task principal investigator. Task participants include Donald Anderson, John Clark, C. Stewart Gloyd, Richard V. Nutt, and Maurice Power; much of the summary information reported in this paper was extracted from their task reports.

DEVELOPMENT OF PERFORMANCE-BASED BUILDING CODE IN JAPAN

- FRAMEWORK OF SEISMIC AND STRUCTURAL PROVISIONS -

By

HIRAISHI Hisahiro¹⁾, MIDORIKAWA Mitsumasa²⁾,
TESHIGAWARA Masaomi³⁾, and GOJO Wataru⁴⁾

ABSTRACT

On February of 1996, it was officially announced by the Ministry of Construction that the Building Standard Law of Japan should be revised into that based on performance. The building code in Japan will be changed from current prescriptive type into performance-based type in a few years. In responding this announcement, the performance-based building code is now under development at the Building Research Institute (BRI).

In this paper, presented is the framework and concepts of the performance-based seismic and structural provisions in Japan proposed by BRI. In the principles of structural safety, the required performance and loads/forces levels are clearly defined. There are four routes in verification procedures and associated structural specifications following the principles of structural safety; proposed route, conventional route, small building route requiring no calculation, and other route including alternative verification procedures, deemed-to-satisfy provisions, and expert judgments. Seismic effects to buildings are considered on the basis of basic seismic design spectrum defined at the engineering bedrock under surface soil layers.

There are three levels in the objectives and requirements to building structures and loads/forces levels. The objectives are life safety, damage prevention,

and continuous normal operation of a building. The principle of verification procedures is that the predicted response values should not exceed the estimated limit values.

The newly proposed verification procedure for major earthquakes is illustrated, as all others remain basically the same as those actually in use. There are indeed various analytical methods for predicting the response of structures subjected to earthquake excitations. The one which is shown here is based on the equivalent single-degree-of-freedom system and response spectrum method.

KEY WORDS: performance-based building code, seismic and structural provisions, required performance level, verification procedures.

1. INTRODUCTION

The need for the development of performance-based standards is a logical consequence of the rapid economic growth of Japan, which is strongly affected by the

1) Director, Structural Engineering Dept., Building Research Institute, Ministry of Construction, 1 Tachihara, Tsukuba, Ibaraki, 305-0802 Japan.

2) Research Director for International Codes and Standards, BRI, MOC.

3) Head, Structure Div., BRI, MOC.

4) Head, Building Economy Div., BRI, MOC.

international economic progress.

In 1995, World Trade Organization (WTO) initiated first the idea of performance-based standards, which was concluded in the form of the Agreement on Technical Barriers to Trade (TBT). This agreement calls for an obedience will towards the guidelines and recommendations issued by the International Standards and International Standardization Institutions. Furthermore, International Organization for Standardization (ISO) is strongly promoting the revision of the current international standards on the basis of performance principles.

According to U.S.-Japan Framework Talks on Bilateral Trade, the American side has requested that the deregulation policy for restructuring the Japanese administration should be extended to the building industry as well, where the review of Building Standard Regulations and reduction of construction cost for housing are required.

Reflecting this developments, on February in 1996 it was officially announced by the Ministry of Construction authorities that the Building Standard Law of Japan should be revised on the basis of performance principles. Very recently, in the Building Council report of March 24, 1997, entitled "For a New Building Administration Framework, which could cope with the economic & social changes and their prospects in the 21st century", it was clearly stated that in order to compile a highly flexible New Building Standard Law, the current provisions must be revised into those based on performance. That served as a basis for the compilation of "Guidelines for the Performance-based Building Code".

2. PERFORMANCE-BASED BUILDING CODE

Unlike the in-current-use conventional Building Code, the Performance-Based Building Code prescribes clearly the type and the level of the required performance for a given building structure. In other words, for the precisely determined

response of the structure subjected to assumed loads and forces, it prescribes the verification procedures to be used for the estimation of structure's conformity with the required structural safety.

However, even in the case of the performance-based provisions, the prescription of a minimum required level is necessary, being this the same as in the current Building Code Provisions. In this sense, the performance-based code is different from the performance-based design, which has been a current topic among structural engineers. The latter deals with a design procedure which is based on a clearly defined target performance for the structure considered, normally being prescribed higher than the minimum required performance level. Basically, the performance-based design is the structural design on the basis of consultation between the structural engineer and the owner of the building.

In this paper are presented the framework and the conception of the Performance-Based Structural Code, which is now under development at Building Research Institute (BRI) in Japan. The main aspects considered here are the conceptual framework of the Structural Code; the level and conception of the earthquake, wind, snow and live forces/loads; required structural performance against each forces/loads and the verification procedures to be used for the estimation of structure's conformity with the required performance level.

It should be noticed here that presented in this paper is just the state-of-the-art and up-to-now level of development of the Performance-Based Structural Provisions at BRI in Japan. It should not be considered as a fully completed version, ready to be presented for the final official approval.

3. CONCEPTUAL FRAMEWORK OF PERFORMANCE-BASED STRUCTURAL CODE

The conceptual framework of Performance-Based Structural Code proposed

by BRI is shown in Fig. 1. Following the principles of structural safety, the verification procedures to be used for the estimation of structure's conformity with the required performance level are roughly classified as (see Fig. 1):

- a. Proposed route
- b. Conventional route
- c. Small building route, and
- d. Others

The proposed route represents a new verification procedure to be used instead of the current one, which is based on the calculation of allowable stress and estimation of ultimate capacity for lateral load. It considers the effects of major earthquakes as well as other forces and loads. The other effects which are not considered in the structural calculations, such as construction quality, durability, quality of construction materials, and nonstructural elements, are covered by structural specifications. In essence, by using this procedure it is possible to evaluate and verify the structural performance possessed by a designed structure, regardless of the design method used. It is just a verification procedure which verifies whether or not the prescribed performance objectives are met. Accordingly, for structural specifications as well the minimum required supplementary specifications are prescribed.

The second route represents the conventional verification procedure now in use, adopted as the standard structural calculation method. It can be supplemented with additional provisions in addition to those of the first route described above. However, if the principles of performance-based provisions are to be followed, it should be noticed that the obviously unnecessary parts to be considered by structural calculations are eliminated. To this extent, the second route can be considered as a kind of deemed-to-satisfy verification procedure.

The third route applies to small buildings. This route does not require structural calculations and is considered to be deemed-to-satisfy provisions. It prescribes

only conventional-based structural specifications. Through this route, is attempted to make as clear as possible the details of each structural specification. In case of a possible structural calculation alternative, special clauses which allow for the implementation of newly developed materials, design methods and construction methods are provided.

In the fourth route are included all other alternative verification procedures and deemed-to-satisfy provisions, such as those developed and certified by private institutions as well as those requiring expert judgments.

The types of loads and forces considered in the newly proposed verification procedure remain almost the same with those currently in use. However, for the case of earthquake effects only, new earthquake motion provisions are prepared to replace the current earthquake force provisions.

In a definite proposal, the earthquake motion response spectra at the engineering bedrock, assumed to be the stratum having shear wave velocity in the range of several hundreds m/s, is considered as the basic design spectra. On the basis of this conception for the earthquake input motion, it is possible that earthquake effects be not only accounted rationally through the incorporation of influence of local soil conditions on ground motion characteristics at the free surface but also conveniently incorporated in the newly developed design procedures of seismically isolated and response controlled structures. Furthermore, it is anticipated that the future proposals expected for the verification and design procedures be suitably implemented.

4. REQUIRED PERFORMANCE LEVEL FOR BUILDING STRUCTURES

An outline of requirements for building structures and loads/forces levels is shown in Table 1. In the vertical column on the left hand side of the table are shown the requirements for building structures, while in the rest of the table are shown the main types

of loads/forces to be considered and their corresponding levels for each of the requirements assigned for building structures. Undoubtedly, the loads/forces shown in Table 1 are to be combined according to specified rules.

As it is shown in Table 1, requirements for building structures are classified in three categories, which are explained below.

4.1 Life Safety

The essential purpose of this requirement is the safety of life. It should be expected that under the action of loads/forces taken into consideration, the building should not experience any story collapse. In other words, it is required that the situation of not providing sufficient space for possible survival of building occupants should not be experienced.

4.2 Damage Prevention

The aim of this requirement is damage prevention. Under this provision, it is required first that after the action of the loads/forces taken into consideration, no structural damage which could threaten the structural safety of the building will take place. Furthermore, it is required that no other kind of damage which causes in the building structure a situation which does not comply with other requirements of the Building Standard Law should be experienced. The above mentioned requirement for no structural damage which could threaten the safety of the structure means that the structural safety performance required by Section 4.1 should be preserved. The second requirement related to other kind of damage means that the provisions of Building Standard Law concerning fire safety should be satisfied. It should be mentioned here that, the requirements for Damage Prevention described in this section are included in the Life Safety requirements as well.

4.3 Continuous Normal Operation

The purpose of this requirement is the assurance of continuous normal operation of the building structure. It aims at avoiding the harmful deformations and vibrations in structural frames, members, interior and exterior finishing materials of the building structure while subjected to loads/forces taken into account. The above mentioned harmful deformations and vibrations are assumed to be those related to dead, live and snow loads acting for a relatively long time on the structure causing thus excessive deformations in slabs and beams, and consequently discomfort to the occupants or difficulties in the operation of the building. The details for the requirements concerning the discomfort to the occupants or difficulties in the operation are not yet clearly formulated. Therefore a further investigation is necessary. It should be mentioned here again that, the requirements for Continuous Normal Operation described in this section are included in the Life Safety requirements and Damage Prevention requirements as well.

For each of the three categories of requirements for building structures described above are assumed the following levels of loads/forces:

4.4 Maximum Probable Event Level

This level of loads/forces corresponds to the category of requirements in Section 4.1 for building structures and is assumed to produce the maximum possible effects on the structural safety of a building to be constructed at a given site. The maximum possible earthquake motion level is determined on the basis of historical earthquake data, recorded strong ground motions in the past, seismic and geologic tectonic structures, active faults, and others. This earthquake motion level corresponds nearly to that of highest earthquake forces used in the current seismic design practice, representing the horizontal earthquake forces induced in the building structures in case of major seismic events. Wind forces and snow loads are determined on the basis of a

100-500 year return period. This level is somewhat higher than the current one used in the actual design practice.

4.5 Once-in-a-Lifetime Event Level

This level of loads/forces corresponds to the category of requirements in Section 4.2 for building structures and is assumed to be experienced more than once during the lifetime of the building. Strictly speaking, earthquake, wind and snow are natural phenomena with different probability of occurrence and normally for each of them should be assumed different return period. Therefore a return period interval of 30-50 years is supposed to cover all these three natural events. This level of earthquake motion corresponds nearly to the middle level earthquake forces used in the current seismic design practice, representing the horizontal earthquake forces induced in the building structures in case of moderate earthquakes. The levels of wind forces and snow loads are nearly the same with those being actually used in the current design practice.

4.6 Ordinary Event Level

This level of loads/forces corresponds to the category of requirements in Section 4.3 for building structures and is normally assumed to be experienced several times during the lifetime of the building. For the case of snow loads it is roughly assumed a return period of 3-5 years. This level is not clearly prescribed even in the current provisions. Therefore a further careful investigation is needed for it.

Finally, the way the live loads will be treated in accordance with building structures requirements is still under investigation. Because of its totally different character compared to earthquake, wind and snow loads/forces, known as natural phenomena of temporary effects, it is considered that the live loads could be better prescribed through two separate options: extraordinary and ordinary options.

5. VERIFICATION PROCEDURES FOR A REQUIRED PERFORMANCE LEVEL

Various response and limit values are considered for use in proposed verification procedures, in accordance with each of the requirements prescribed for building structures. A representative example of this arrangement is shown in Table 2. The principle of verification procedures is that the predicted response values due to the action of forces/loads on building structures should not exceed the estimated limit values. Fundamentals of proposed verification procedures corresponding to each level of earthquake, wind and snow loads/forces are described below.

5.1 Verification Procedures Corresponding to Maximum Probable Event Level

In case of earthquakes, the maximum displacement response of the building structure subjected to strong ground motions should be smaller than the displacement limit. While in case of wind and snow, it is required that the maximum stresses developed in the structure should be smaller than the stress limits. In defining displacement and stress limits for earthquake motion and wind forces respectively, it may be necessary to consider the effects of repeating cycles in the plastic region of the response as well. However, fixing some stress limit values for the case of wind forces is very difficult at the moment, because the actual design of building structures against wind forces in general do not account yet for the inelastic behavior. Concerning the analytical methods to be used for predicting structural response, it is noted that they should not be necessarily the same as the current ones. Accordingly, in the newly proposed verification procedures, it is expected that analytical methods to be used for the case of earthquake excitations and that of wind/snow forces/loads be different. In the former case it is expected to apply Equivalent Single Degree of Freedom System

and Response Spectrum Method, while in the latter one Static Elasto-Plastic Analysis.

5.2 Verification Procedures Corresponding to Once-in-a-Lifetime Event Level

For this level of earthquake, wind and snow loads/forces it is required to be confirmed whether the stresses taking place at each structural element satisfy the condition of being smaller than the limit stress. The limit stress mentioned here implies that the whole structure behaves generally within the elastic range. In case of snow loads, it is additionally required that the creep effect be taken into account in defining limit stress values. In any case, the fundamental conceptions of the current and newly proposed verification procedures are not much different. Therefore, it is expected that the actual static elastic analysis be of further use.

5.3 Verification Procedures Corresponding to Ordinary Event Level

Actually, the verification for this level of loads/forces is not definitely required. Only in case of special need or situation, the necessary performance is examined in the current design process. Displacement, stress and acceleration limit values are used in the verification procedures of this level. Defining these limit values seems to be a rather difficult issue which indispensably needs a careful investigation.

The verification procedures for live loads are expected to be almost the same as those being used in the current practice. Moreover, from Table 2 it can be noticed that no description on foundations and soils are given. This subject is also under investigation.

Besides the limit values defined on the basis of the requirements for building structures as it is shown in Table 2, other displacement-, stress- or acceleration-related limit values, defined on the basis of the requirements for architectural, mechanical and electrical elements permanently attached to buildings, are considered in certain cases if

necessary. On this point, a special investigation is needed.

As it was mentioned above, excluding the newly proposed verification procedure for maximum probable earthquake events, all others remain basically the same as those actually in use. Therefore, hereafter the focus is put on the proposed verification procedure for the case of earthquake excitations. A flow chart of this procedure is illustrated in Fig. 2. There are indeed various analytical methods for predicting the response of structures subjected to earthquake excitations. The one which is shown here is based on the equivalent single-degree-of-freedom system and response spectrum method.

5.4 Proposed Verification Procedure for the Case of Major Earthquakes

According to this procedure the steps to be followed are:

- I. Determine the limit displacement of the structure.
- II. Determine the hysteretic characteristic, equivalent stiffness and equivalent damping ratio of the structure.
 - i) Model the structure as a simplified equivalent single-degree-of-freedom system (ESDOFS) and establish its force-displacement curve (see Fig. 2a).
 - ii) Assume now that the limit displacement determined in step I corresponds to the above mentioned ESDOFS.
 - iii) Determine the equivalent stiffness in accordance with the limit displacement.
 - iv) Determine the equivalent damping ratio on the basis of viscous damping ratio, hysteretic dissipation energy and elastic strain energy of the structure (see Fig. 2b).
- III. Determine the response spectra to be used in the verification procedure.
 - i) For a given basic design spectrum at the engineering bedrock level, draw up the free-field site-dependent acceleration (S_a) and displacement response spectra (S_d), for different damping levels.

- ii) In the estimation of free-field site-dependent acceleration and displacement response (step i) above), consider the strain-dependent soil deposit characteristics.
- iii) In case of need, present graphically the relation of S_a - S_d , for different damping levels.

IV. Examine the safety of the structure.

In this final step, it is verified whether the response values predicted on the basis of the response spectra determined according to the step III satisfy the condition of being smaller than the limit values estimated on the basis of step II (see Fig. 2c).

The verification procedure presented above is in essence a blend of equivalent single-degree-of-freedom modeling of structures with the site-dependent response spectrum concept, which makes possible the prediction of maximum structural response in case of major earthquakes as well as the confirmation whether the predicted response values are smaller than the limit ones. Moreover, it is also noted that the soil-structure interaction effects should basically be considered. The factor of structural characteristics D_s , used in the current practice for verifying the ultimate capacity of the structure to resist lateral loads, is determined on the basis of the concept that the structural strength necessary to keep the displacement response during earthquakes smaller than the limit displacement, estimated on the basis of plastic deformation capacity of the structural members, should be guaranteed.

From the above discussion, it can be concluded that the newly proposed verification procedure is just the process to estimate the D_s values. The difference lies on the fact that the proposed procedure does not go up to the calculation of the D_s values. It ends just before this step.

In order to determine the limit displacement of the structure, a specific displaced mode is necessary to be assumed in advance for its inelastic response (see Fig. 2a).

Basically, any predominant or possible to be experienced displaced mode of the structure subjected to earthquake forces can be applied. The predominant or possible to be experienced displaced mode implies any of the failure modes observed during the major earthquakes such as beam failure mode, story failure mode or any other definite failure mode. Furthermore, precisely determined characteristics of structural materials should also be provided.

In the illustration presented above for the proposed verification procedure the limit value referred to is the maximum displacement. Nevertheless, besides displacement any other measures can be used, for example energy. In this case, both the response and limit values should be expressed in terms of energy.

The application of the proposed verification procedure for building structures where torsional vibration effects are predominant requires a further detailed investigation.

Finally, a more appropriate consideration of the loading duration time and material properties in the current verification procedure based on the allowable stress concept is under investigation.

6. FUTURE SCOPE

Having established the fundamental principles for the revision of the current Building Standard Law of Japan does not mean that everything is done. The framework and concepts of performance-based building provisions presented in this paper constitute just the beginning of an enormous task to be done in the future. In order to realize the intentions of performance-based standards, directed towards the expansion of free initiative, the promotion of new technologies, and the activation of market competition, as well as the verification of the designed performance level in constructed building structures, the establishment of building related institutions is needed. For this purpose, The Building

Council is appealing for the openness of private institutions towards building verification procedures and inspection. Expanding the role of private institutions in the verification/inspection system is also a very important condition for the implementation of performance-based provisions. Consequently, for a successful operation of this verification/inspection system, high level of competence, organizing ability and responsibility are required.

Furthermore, the emphasis should not be given only to the performance-based provisions. In order to widen the use of recently emerged performance-based design, it is necessary to further intensify the efforts towards a marketable performance. In this sense, the popularization of performance indication system proposals is desired.

7. CONCLUDING REMARKS

In this paper, presented is the state of the art of the Performance-Based Building Code of Japan, currently under development at the Building Research Institute. In essence, performance-based provisions intend to provide as clearly as possible answers to the frequently raised questions: for what purpose, towards what objective, and for what conditions. The greatest advantage of this new approach lies on the fact that it focuses primarily on the achievement of the prescribed objectives, regardless of the methodology used. As a result, while promoting technical development, it may become possible some time in the future that the owner himself to select the desired performance of the building. On the other hand, due to the long time and high cost required for its implementation, it may happen that the performance-based approach results in a complicated verification procedure, pointing out thus the need for a much more careful judgment in selecting between specification-based or performance-based provisions. There are still many issues to be considered in the future and in dealing with them it should be kept always in mind the

purpose that the performance-based concept is to be applied.

ACKNOWLEDGMENT

This manuscript was stimulated by the authors' participation as members of the "Task Committee to Draft Performance-Based Building Provisions", where they have shared their opinions with other members. They would like to express their gratitude towards all of them.

REFERENCES

- 1) BRI: *Towards performance-based standards*, BRI-H9 Autumn Seminar Notes, Building Research Institute, Ministry of Construction, November, 1997 (in Japanese).
- 2) BCR: *For a New Building Administration Framework, which could cope with the economic & social changes and their prospects in the 21st century*, Building Council Report, March, 1997 (in Japanese).
- 3) ISO/IEC Directives - Part 2: *Methodology for the development of international standards*, 1992.
- 4) BCJ: *Structural provisions for buildings, Commentary on Building Standard Law*, The Building Center of Japan, 1997 (in Japanese).
- 5) AIJ: *Recommendations for loads on buildings*, Architectural Institute of Japan, 1996.
- 6) ISO 6240: *Performance standards in building - Contents and presentation*, 1980.
- 7) ISO 6241: *Performance standards in building - Principles for their presentation and factors to be considered*, 1984.
- 8) ISO 7162: *Performance standards in building - Contents and format of standards for evaluation of presentation*, 1992.

Table 1 Requirements for Building Structures and Loads/Forces Levels

Load & Force Requirement	Earthquake	Wind	Snow	Live	
				Extraor- dinary	Ordinary
(a) Life Safety (to prevent failure of stories in structural frames)	Probable Maximum Earthquake (earthq. records, seismic and geologic tectonic structures, active faults, etc.)	Probable Maximum Event (return period: 100-500 years)	Once-in-a-Lifetime Event (return period: 30-50 years)		
(b) Damage Prevention (to prevent damage to structural frames, members, interior and exterior finishing materials in order to avoid the conditions not satisfying the requirement (a) and others)					
(c) Continuous Normal Operation (to eliminate harmful deformation or vibration on structural frames, members, interior and exterior finishing materials, equipment and foundation deteriorating functions)					
			Ordinary Event (return period: 3-5 years)		

Note: The deterioration of materials during the life time of a structure should be considered.

Table 2 A Representative Illustration of Proposed Verification Procedures

Load/Force Requirement		Earthquake	Wind	Snow	Live	
a) Life Safety	Level	Maximum Probable Earthquake	Maximum Probable Event (Return Period 100 - 500 years)		Extraordinary	Ordinary
	Response Value	Maximum Displacement	Maximum Stress	Maximum Stress	Maximum Stress	
	Limit Value	Limit Displacement ^{*1}	Limit Stress ^{*1}	Limit Stress ^{*2}	Limit Stress ^{*2}	
b) Damage Prevention	Level	Once-in-a-life-time-Event (Return period 30 - 50 years)			Extraordinary	Ordinary
	Response Value	Stresses taking place at each structural element			Stresses taking place at each structural element	
	Limit Value	Limit Stress ^{*3}		Limit Stress ^{*4}	Limit Stress ^{*4}	
c) Continuous Normal Operation	Level			Ordinary Event Level (Return Period 3 - 5 yrs)	Ordinary	
	Response Value				Stress and Displacement at required elements only	
	Limit Value				Limit Stress and Displacement ^{*5}	

*1 - Repeating cycles effect at plastic region of response to be taken into account.

*2 - Creep effect to be taken into account.

*3 - The whole building structure behaves roughly within elastic range.

*4 - The whole building structure behaves roughly within elastic range and creep effect to be taken into account.

*5 - Stresses should be less than the elastic limit and creep effect to be taken into account.

Notes :

- 1) The limit values corresponding to Maximum Probable Event Level are determined based on the condition that equilibrium of forces and displacement compatibility in the structural system are guaranteed.
- 2) Displacement and acceleration related limit values, determined on the basis of the requirements for architectural, mechanical and electrical elements permanently attached to building structures, are thought to be considered in certain cases.

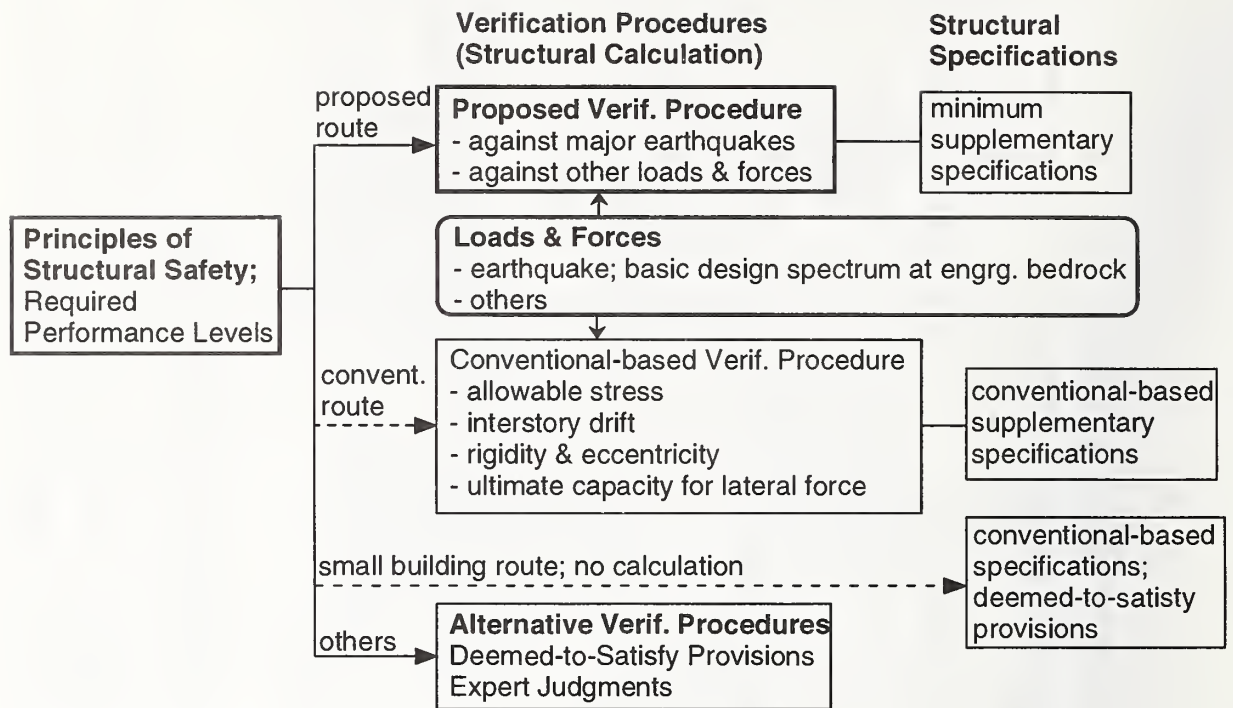
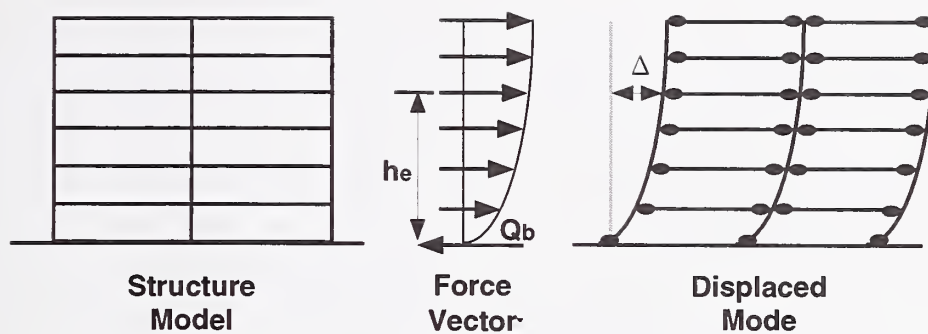


Fig. 1 Conceptual Framework of Proposed Performance-Based Structural Provisions



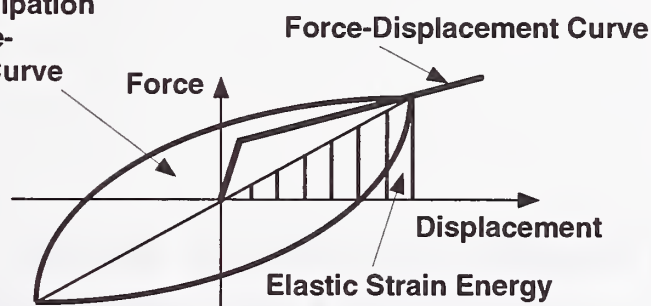
h_e : equivalent height

Δ : horizontal displacement at equivalent height

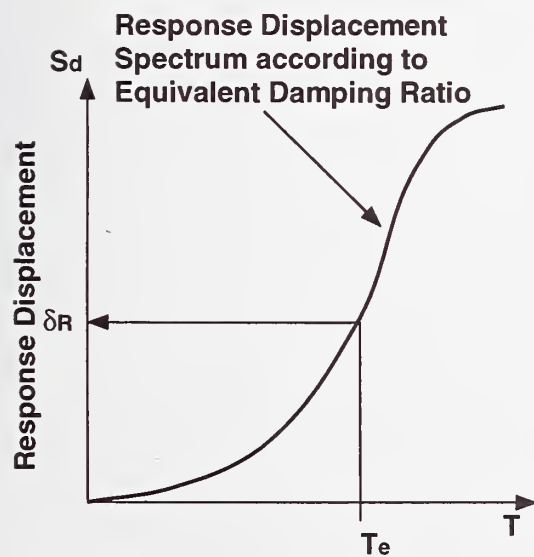
Q_b : base shear force

(a) Structure Model and Inelastic Response

**Hysteresis Dissipation
Energy in Force-
Displacement Curve**

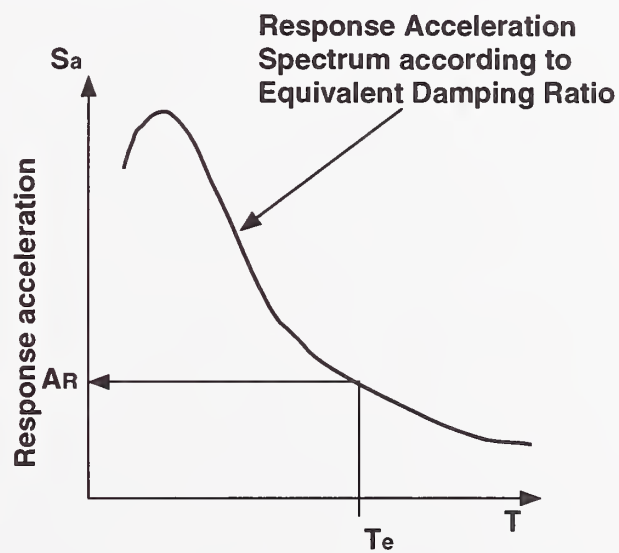


(b) Energy for Equivalent Damping Ratio



Equivalent Natural Period

$\delta_R < \text{limit displacement}$



Equivalent Natural Period

$A_R < \text{limit acceleration}$

(c) Comparison of Expected Response Values and Estimated Limit Values

Fig. 2 An Illustration of Proposed Verification Procedure for Major Seismic Events

**REAL TIME INFORMATION
ACQUISITION and DISSEMINATION**

The American Red Cross - Centers for Disease Control and Prevention Health Impact Surveillance System for Natural Disasters

by

Enrique Paz-Argandoña¹ and Josephine Malilay²

ABSTRACT

Since 1987, the American Red Cross and the Centers for Disease Control and Prevention have collaborated on the Health Impact Surveillance System for Disasters, which collects data on morbidity and mortality related to disasters in the United States and its territories. We describe the surveillance system and present an analysis related to 104 disasters occurring from 1994 to 1996. Associated with these disasters were 426 fatalities, 9,846 cases of morbidity in the disaster-affected populations, and 2,752 cases of morbidity among 45,066 American Red Cross personnel. Injuries were the most frequent cause of death in 1994 and 1995, whereas drowning were the most common in 1996. The percentage of disaster-related deaths that were due to drowning increased from 32.9% in 1994 to 52% in 1995; however, the distribution of disaster types also changed. The use of motor vehicles was heavily implicated in drowning deaths. Injuries and illnesses in the disaster-affected population occurred with greater frequency during the impact phase of acute-onset disasters such as tornadoes and hailstorms and during the post-impact phase of floods and tropical cyclones. The estimated risk for morbidity among ARC staff members was greatest for tropical cyclones. Illnesses exceeded injuries among ARC staff members for every disaster type except wildfires across the 3 study years. We recommend that prevention efforts focus on preventing deaths by drowning and those caused by motor vehicle-related injuries.

KEYWORDS: earthquakes; epidemiology; floods; hurricanes; natural disasters; public health surveillance; tornadoes

1. INTRODUCTION

The public health importance of natural disasters -- defined as ecological disruptions causing human, material, or environmental losses that exceed the ability of the affected community to cope using its own resources and that often require outside assistance -- have been documented worldwide (1). During 1971 to 1995, approximately 141.5 million people worldwide were killed, injured, made homeless, or otherwise affected by an estimated 5,240 natural disaster events; economic damages were estimated at \$439.3 million (2). In the United States, economic losses of \$70 billion were incurred from 15 major weather-related disasters between August 1992 and January 1995. Human vulnerability to natural disasters has increased with population growth, increased urbanization, and increased population concentration in hazard-prone areas (3). The post-disaster setting is often characterized by deteriorating environmental conditions that can compromise sanitation and hygiene. The risks for increased mortality and morbidity are potentiated by: 1) changes in pre-existing levels of disease, 2) ecological changes as a result of the disaster, 3) population displacement, 4) changes in population density, 5) disruption of public utilities, and 6) interruption of basic public health services. In addition, disasters may also lead to an exacerbation of psychological problems in the community, as the

-
1. Epidemiology Intelligence Service, Epidemiology Program Office, Centers for Disease Control and Prevention, Atlanta, Georgia 30333 USA
 2. National Center for Environmental Health, Centers for Disease Control and Prevention, Atlanta, Georgia 30345 USA

normal routines of people are disrupted. Common health hazards after disasters have been 1) exacerbation of chronic illness; 2) psychological effects; 3) a lack of food, water, and shelter resulting from population displacement; and 4) climatic exposure (4).

Responding to natural disasters in a timely and appropriate manner requires epidemiologic tools that can rapidly provide information upon which public health decisions may be made. These tools may be used to control epidemics; monitor rates of preventable deaths, illness, and injuries; monitor health care needs among the affected population; and identify appropriate interventions.

A commonly used epidemiologic tool following a disaster is surveillance. Surveillance is the ongoing and systematic collection, analysis, and interpretation of outcome-specific data for use in planning, implementing and evaluating public health practice (5). Data from surveillance systems are used both to determine the need for public health action and to assess the effectiveness of programs.

In the post-disaster setting, surveillance provides information that can serve as the basis for action during the immediate disaster and also for planning of future activities. Such information is used to answer the following questions (6):

- What problems are occurring? Why are they occurring?
 - Where are problems occurring?
 - Who is affected?
 - What problems are causing the greatest morbidity and mortality?
 - What problems are increasing or decreasing?
 - What problems will subside on their own? When?
 - What problems will increase if unattended?
 - What relief resources are available?
 - What relief activities are in progress?
 - Are relief activities meeting relief needs?
- What additional information is needed for decision-making?

Such systems for collecting the above information must be flexible to changes in the definitions of health outcomes; acceptable to users of the data; sensitive and specific for capturing valid and reliable information; timely in collection, analysis, and response; accurate, representative, and ethical (7).

2. BACKGROUND

To improve the reporting of health events related to disasters -- defined as any death, injury, or illness occurring during the pre-impact, impact, or post-impact phase of a disaster -- the American Red Cross (ARC) and the Centers for Disease Control and Prevention (CDC) developed the Health Impact Surveillance System for Natural Disasters (HISSD) under a memorandum of agreement in 1986. The objectives of HISSD were:

- To estimate the magnitude of morbidity and mortality associated with major disasters in the United States and its territories.
- To characterize the impact of each disaster type.
- To identify risk factors for disaster-related injury, illness, or death among disaster-affected populations.
- To monitor health and identify risk factors for injury and illness among ARC personnel involved in relief operations.
- To stimulate epidemiological research aimed at preventing or mitigating morbidity and mortality associated with disasters.

The role of the ARC in this surveillance system is to determine the need for emergency and preventive health services by documenting the number of deaths, illnesses, and missing persons related to a disaster event (defined as disasters costing \$50,000 or more for ARC operations). The role of CDC is to analyze the data collected

by the ARC, to assess the adverse health effect of the disaster event, and to advise the ARC on response and prevention.

From 1988 to 1993, the ARC summarized and forwarded disaster-related morbidity and mortality statistics to CDC for compilation (8, 9). In 1996, CDC conducted a survey to assess the usefulness of the system, improved collection instruments, field-tested new forms, and evaluated the flow of information from ARC service centers and shelters, to its headquarters, and finally to CDC (10, 11).

3. COMPONENTS AND OPERATION OF THE SYSTEM

The population under surveillance is the entire population in the disaster area, who seek assistance in ARC shelters or service centers, including the ARC staff members who are paid employees or volunteers for relief operations.

Information about deaths is population-based and is collected by ARC volunteers and nurses who query their clientele, local hospitals, doctors' offices, medical examiners or coroners, and local authorities, such as sheriffs' offices. Information about injuries and illnesses is provided by the ARC health services based on visits for these services. The flow of health information is generated and processed in ARC field disaster-relief facilities. From these field facilities, the flow of the mortality and morbidity data is traced through the field operations headquarters to the ARC national office, and finally to CDC (see Figure 1.)

Such information is organized by year to include:

- The number of fatalities, injuries, and illnesses per individual event.
- The number of fatalities, injuries, and illnesses by type of disaster.
- The geographic location at which these health conditions occurred.
- Demographic information on individual clients, including decedents.
- Causes of injuries, illnesses, and

deaths.

- Descriptions of circumstances in which individual cases of injuries, illnesses, and deaths occurred.
- The number of ARC volunteers and staff who are injured, ill, or die during relief operations.

The results of the analysis are presented in a preliminary report to the ARC and CDC. A final report is subsequently produced and disseminated to the disaster community (12). The reports serve the following objectives:

- To recommend ways of preventing deaths in future natural disasters based on the systematic description of past events.
- To describe disaster-related morbidity in the disaster-affected population and among ARC staff members.
- To provide the descriptive epidemiology needed to generate hypotheses for further analytic studies.
- To evaluate the surveillance system's performance for the years under study and to recommend ways of improving the system.

4. ANALYSES FROM THE SURVEILLANCE SYSTEM

In this section, we present surveillance data from the years 1994, 1995 and 1996. The number of disaster events by natural hazard, state, and year when the event occurred are shown in Figures 2-4.

4.1 Mortality Results

4.1.1 Causes of death

A larger number and greater variety of disasters occurred in 1995 and 1996 than in 1994, but fewer fatalities were associated with these disasters. The Northridge earthquake was perhaps the most severe disaster of 1994 and accounted for the largest number of fatalities. Injuries and drowning remained the leading

causes of death across the 3 study years. Injuries were the leading cause of death in 1994 and 1995 and accounted for most of the deaths associated with earthquakes and tornadoes. Crushing injuries and unspecified multiple injuries were the leading causes of death in all 3 years. Motor vehicle-related injuries may have been under represented.

The proportion of deaths by drowning increased across the study years, accounting for 32.9%, 43.4%, and 52.3% of all deaths in 1994, 1995, and 1996, respectively. The use of a motor vehicle was heavily implicated in disasters associated with drowning, such as floods, flash floods, and Tropical Storm Alberto. The results are consistent with the use of a motor vehicle being a risk factor for death by drowning. Whether these motor vehicle deaths were entirely preventable is unknown, but at least eight of the deaths were known to have occurred during floods when drivers ignored "road closed" signs or when "road closed" signs were not used properly. Other deaths by tree fall injuries and structural collapse of roadways could have been prevented if drivers stayed off roads during tropical cyclones and floods. These deaths point to the need for better communication of prevention messages.

Heart attacks were the third most frequent cause of death in the earthquake year, 1994, but were not as frequent in other disaster years except during the clean-up phase of tropical cyclones and floods in 1996. These findings point to the need for hospitals to be ready to treat patients who have heart attacks precipitated by earthquakes, tropical cyclones, or floods. The proper operation of backup electrical power in hospitals during and after an earthquake is important in critical care facilities; three fatalities were associated with failure of mechanical ventilators. Fires resulting from candles and stoves being lit during power outages were a preventable cause of death.

4.1.2 Demographic characteristics

During studied years, more men than women

have died from disaster-related causes. The number of deaths among men consistently exceeded the number among women in every phase of tropical cyclones, and male sex is a risk factor for death during these events. It may be that men are more likely than women to be engaged in high-risk clean-up activities, such as cutting tree limbs, or that men are more likely to engage in risk-taking behaviors that involve motor vehicles. Men may also be more likely to be exposed to risks as a result of employment on power crews and other occupationally related activities.

The consistent finding across 3 years that more than half of deaths occurred in persons 60 years or older during disasters indicated the greater physical vulnerability of this population. The results may demonstrate the need for preventive messages, improved evacuation efforts, and an identification of risk factors among older people.

4.1.3 Place of death and place of injury

For the 3 years studied, most deaths occurred outdoors, in single-family homes, or in motor vehicles. The distribution of place of injury was not consistent over the 3 years, mainly because the data were skewed by the 1994 Northridge earthquake, in which fatal injuries occurred mainly in multi-family dwellings, and by a church roof collapse in the same year, in which a number of fatal injuries also occurred.

The two fatalities among ARC staff members were due to cardiovascular events. Further circumstances are unknown; the deaths may have been brought on by the physical activity associated with disaster relief.

4.2 Morbidity Results

Morbidity occurred more frequently during the post-impact phase of floods and tropical cyclones than during the impact phase, a pattern also noted in previous years (8, 9). In contrast, in disasters with sudden acute onset, such as tornadoes, morbidity was more likely to occur during the impact phase. Our finding that

illnesses were more common than injuries among field personnel may be somewhat useful in planning health assistance to staff members, but further study of disaster-related morbidity is necessary.

5. DISCUSSION

The ARC-CDC Health Impact Surveillance System is the only known surveillance system in the U.S. that systematically collects morbidity and mortality data related specifically to natural and technological disasters. As the nation's designated relief agency, the ARC is in a unique position to collect data as disaster-relief operations are conducted. The surveillance information helps the ARC to target resources for future disaster assistance, and it helps CDC, as the nation's prevention agency, to better focus prevention efforts. The system also collects valuable information on the circumstances of each case of illness, injury, or death among personnel specifically trained in disaster relief.

Like most surveillance systems, the ARC-CDC Health Impact Surveillance System has limitations that analysts should keep in mind when interpreting the data. For example, as with most surveillance systems, a number of limitations arose with interpretation of the data. Whereas the difference between disaster categories such as "earthquake" and "tornado" is straightforward, the difference between others, such as floods vs flash flood, may be more difficult to distinguish. There also may be additional floods with tornadoes that were not characterized as such. Because of this lack of standard definitions for disaster types, the analysis of mortality and morbidity within disaster types is most useful for those categories that are clearly distinct from one another, such as earthquakes and hurricanes.

Another limitation is that the accuracy of whether a fatality was truly disaster-related was a function of how well the circumstances of the fatality were described. Responses varied widely from a few words (e.g., "died by

drowning") to detailed descriptions providing all circumstances, including the date, time, and location of death, and details regarding events leading up to the death. Some deaths recorded by the system and included in the analysis were probably not actually disaster-related, and other deaths may have been indirectly related to disasters even though they are not classified as such because of a lack of detail provided. Particularly suspect are deaths by chronic disease processes or because of pre-existing medical conditions, which may or may not have occurred in the absence of the disaster.

As with disaster-relatedness, the determination of whether a death occurred before or after impact or whether it was related to a secondary disaster was largely a function of the level of detail provided in the form. As a result, there may be significant under reporting of deaths related to a secondary disaster and of deaths occurring during the pre- and post-impact periods, as well as an over estimate of the number of deaths that occurred during the impact phase.

A fourth limitation is that even though the system asks that the cause of death be ascertained from the death certificates of the victims, many fatality forms list the information source as nonmedical, such as the police or a family member. Furthermore, many deaths are listed with a circumstantial rather than a medical cause, such as "car accident." Conversely, injuries sustained in car accidents may not be noted as such, and there is likely to be some overlap between the injury and the motor vehicle categories. The causes of death presented in this report should therefore be interpreted as broad categories describing a general circumstance of death rather than specific physiological events.

The consistent difficulties with morbidity reports described above, have led to the development of a new form on which to report morbidity. This form provides information individually rather than as an aggregate tally. The new form will improve the quality of data by providing pre-existing categories of injuries and illnesses, as

well as by prompting for the location, time, and circumstances of the injuries. After 1997, the year in which this form was first implemented, an improved analysis of the morbidity associated with disasters will be possible.

6. RECOMMENDATIONS FOR THE PREVENTION OF DISASTER-RELATED MORTALITY AND MORBIDITY

In addition to pointing to the need for improved weather forecasting and for dissemination of weather information to at-risk populations, the above analysis indicates that the following could help reduce disaster-related mortality and morbidity in disaster-affected communities.

- Make the avoidance of deaths in motor vehicles during flooding or heavy rains a major focus of prevention efforts. The National Weather Service, meteorologists, and local emergency management authorities should coordinate their announcement of warnings and establish safe detour routes in communities affected by severe flooding. During a flood watch, for example, public advisories should be broadcast to caution people to observe existing barricades and avoid routes that authorities have declared unsafe. Moreover, people in cars should be advised not to attempt to outrun the flood, but to seek shelter in a nearby public building.
- Make the prevention of deaths and injuries following the impact of a tropical cyclone a major focus of disaster-related health education. Health education should emphasize tree-cutting safety, power-line safety, the avoidance of candles as a light supply following power outages, and the proper use and ventilation of generators.
- Make the avoidance of deaths and injuries among people 60 and over a

major focus of prevention efforts. In educational campaigns, people in the community should be encouraged to keep in touch as much as possible with elderly neighbors and family members over the course of a disaster so that they can provide assistance when necessary.

- Focus disaster-response plans for acute-onset disasters on mass-casualty preparedness and the immediate care of victims under disaster conditions (e.g., search and rescue, triage, and transportation). Large numbers of casualties may be expected during the impact phase of tornadoes and earthquakes. The hospital deaths associated with power loss following the Northridge earthquake demonstrate the need for constant vigilance.

7. CONCLUSIONS

The Health Impact Surveillance System for Disasters provides a basis for case definitions of injuries and illnesses associated with disasters; documents disaster-related mortality and morbidity; and provides data with which to perform cost analyses. Further improvements include a revision of the ARC's data collection training manual and in procedures used by with ARC staff, implementation of standardized case definitions for injuries and illnesses under International Classification of Diseases-9 coding, computerization of the ARC field collection, and the Centers for Disease Control collaboration with the ARC to gather information from emergency rooms and other health providers in disaster sites.

8. REFERENCES

1. Gunn SWA. Multilingual dictionary of disaster medicine and international relief. Dordrecht, The Netherlands: Kluwer Academic Publishers, 1990.
2. International Federation of Red Cross

- and Red Crescent Societies. World disasters report 1997. Oxford, UK: Oxford University Press, 1997.
3. U.S. Federal Subcommittee on Natural Disaster Reduction (SNDR). Natural disaster reduction: a plan for the nation. Washington, DC: SNDR 1996.
4. Western KA. Epidemiologic surveillance after natural disaster. Scientific Publication No. 420. Washington, DC: Pan American Health Organization, 1982.
5. Thacker SB, Berkelman RL. Public health surveillance in the United States. *Epidemiol Rev* 1988;10:164-90.
6. Sidel VW, Onel E, Geiger HJ, Leaning J, Foege WH. Public health responses to natural and human-made disasters. In: Maxcy, Rosenau, Last, eds. *Public Health & Preventive Medicine*, 13th ed. CT: Appleton & Lange, 1992: 1173-86.
7. Centers for Disease Control and Prevention. Guidelines for evaluating surveillance systems. *MMWR Morb Mortal Wkly Rep* 1988;37, No. S-5.
8. Duclos P. American Red Cross disaster database collaborative project: surveillance system for natural disasters using American Red Cross records. Atlanta, GA: Centers for Disease Control and Prevention, 1988.
9. Quenemoen L. Evaluation of the health impact surveillance system for disasters. Atlanta, GA: Centers for Disease Control and Prevention, 1993.
10. Fiedler L, Malilay J. A formative evaluation of the health impact surveillance for natural disasters. A report to the American Red Cross. Atlanta, GA: National Center for Environmental Health, Centers for Disease Control and Prevention, 1996.
11. Paz E, Gorjanc M, Gunderson E. A field evaluation of the health impact surveillance for disasters. A report to the American Red Cross. Atlanta GA: National Center for Environmental Health, Centers for Disease Control and Prevention, 1996.
12. Paz E, Hall SA, Malilay J. American Red Cross--Centers for Disease Control and Prevention health impact surveillance system for disasters. A report to the American Red Cross for years 1994, 1995, 1996. Atlanta, GA: National Center for Environmental Health, Centers for Disease Control and Prevention, 1997.

Figure 2. Frequency of disasters and related fatalities by state, 1994

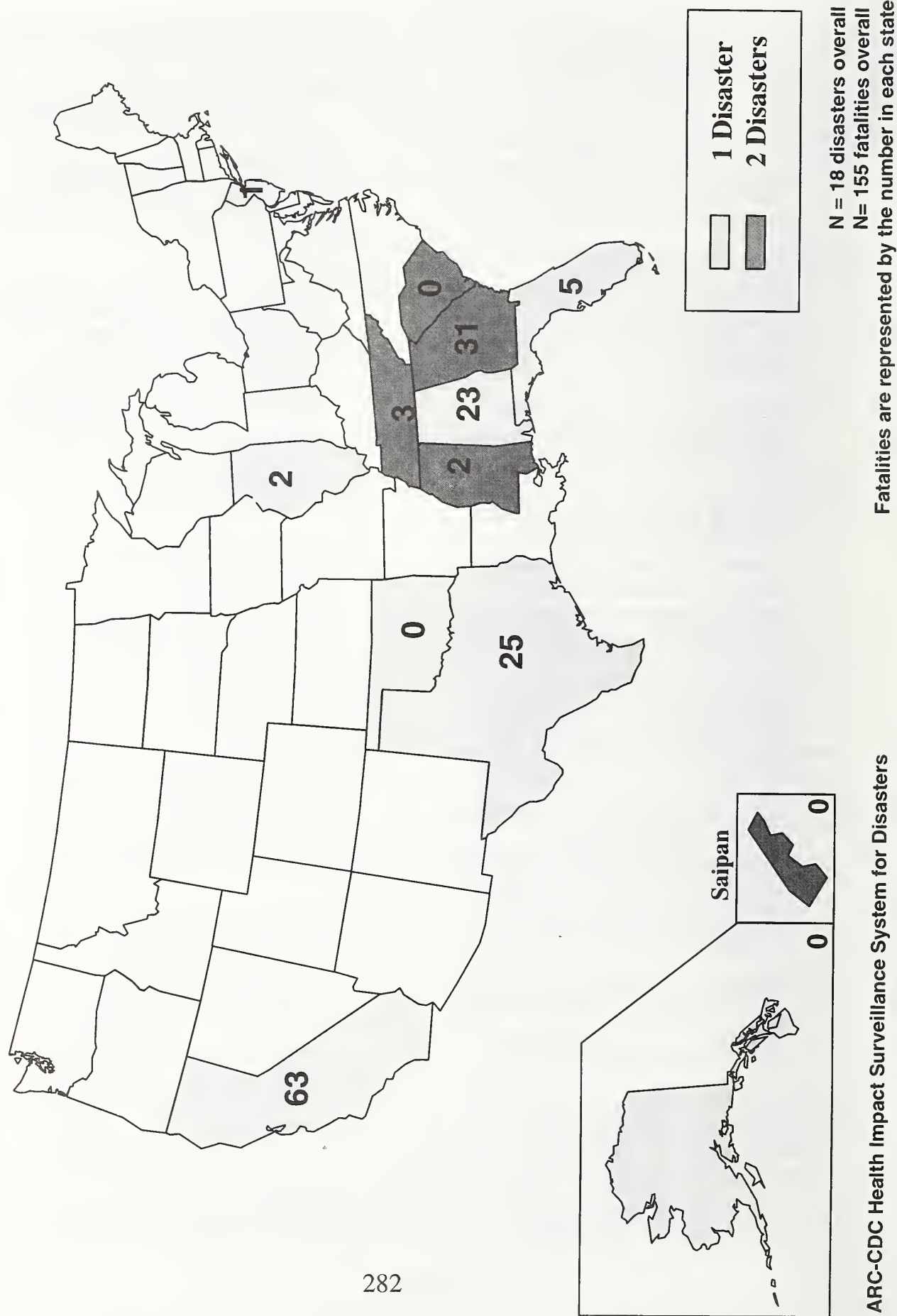


Figure 3. Frequency of disasters and related fatalities by state, 1995

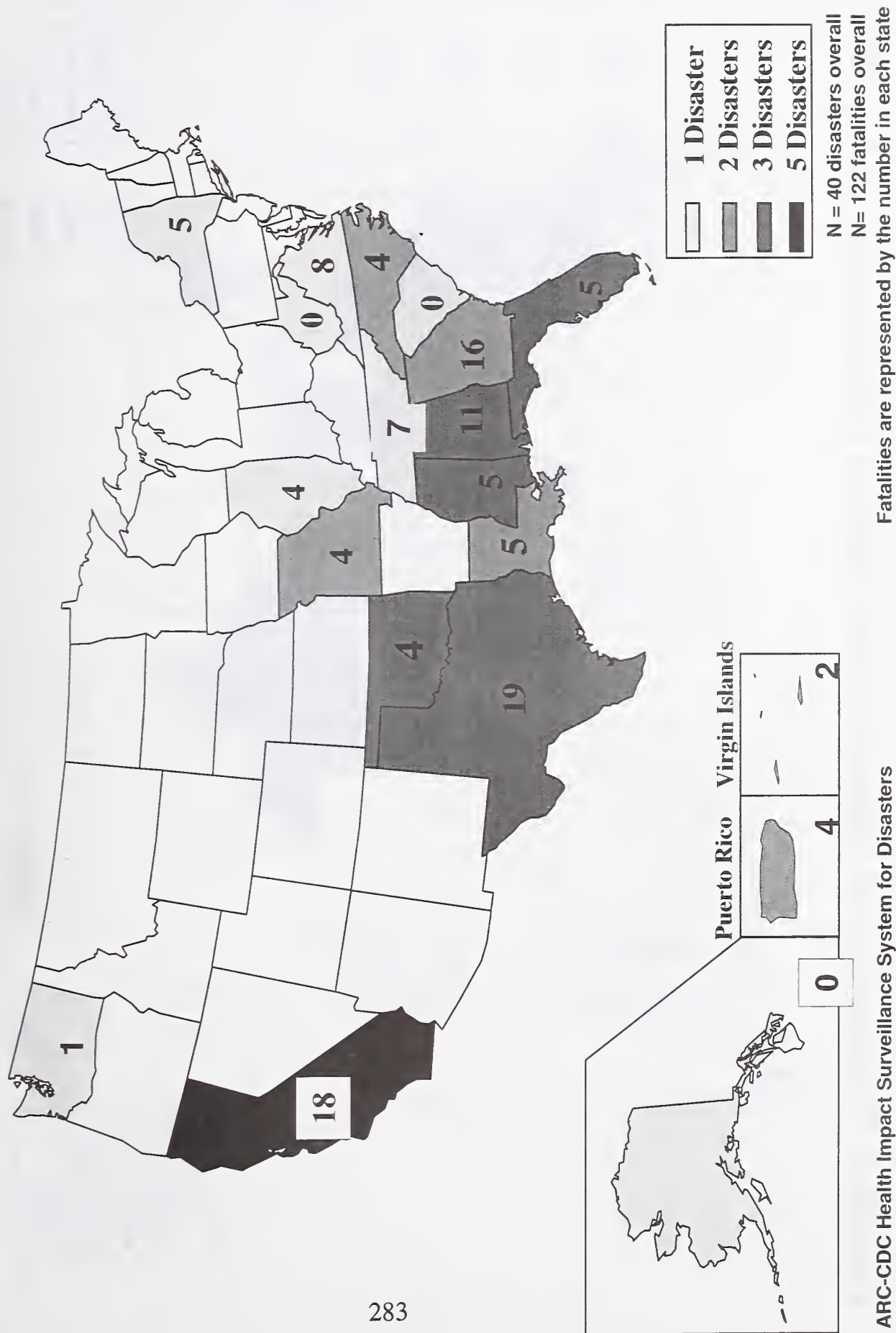


Figure 4. Frequency of disasters and related fatalities by state, 1996

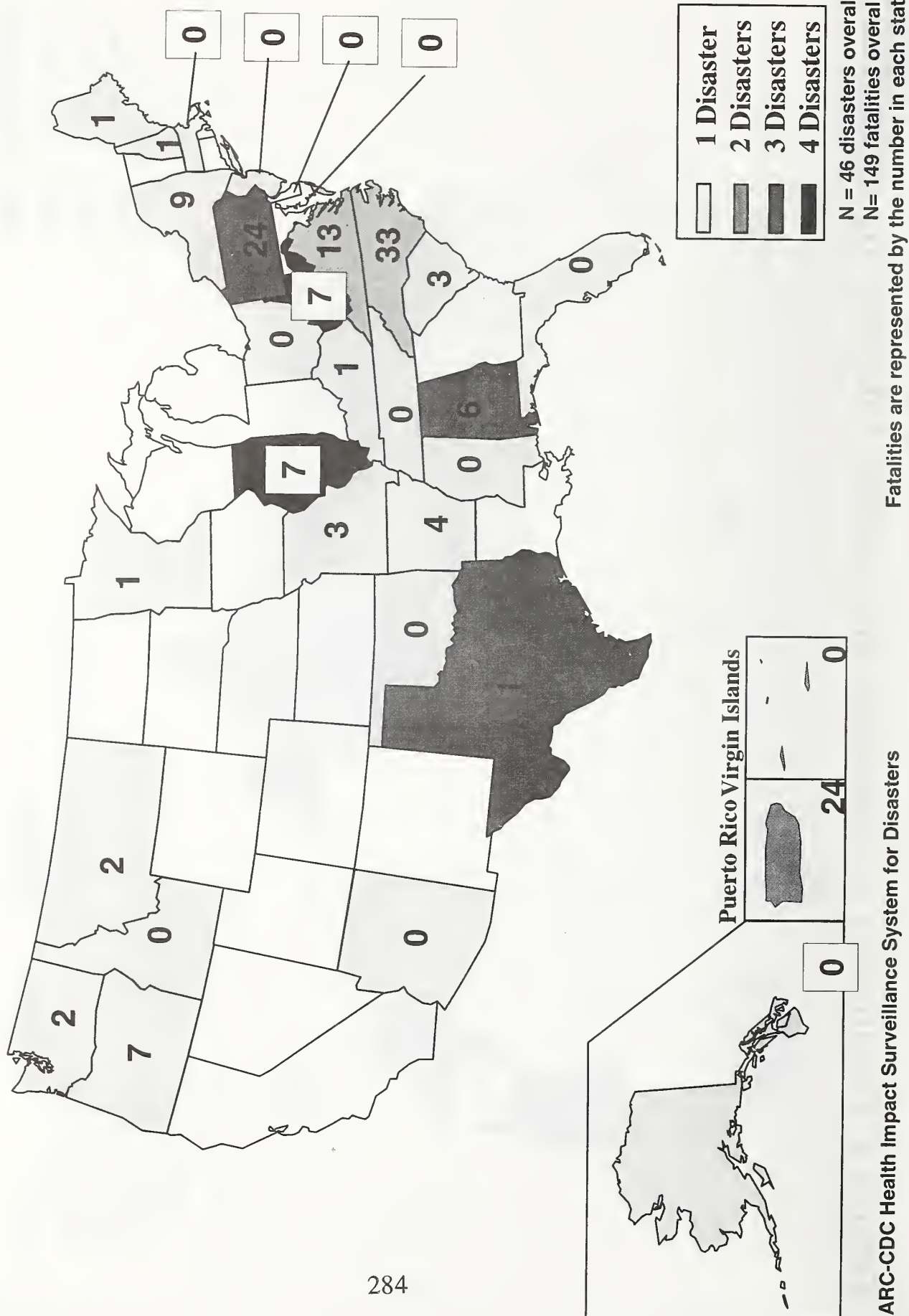
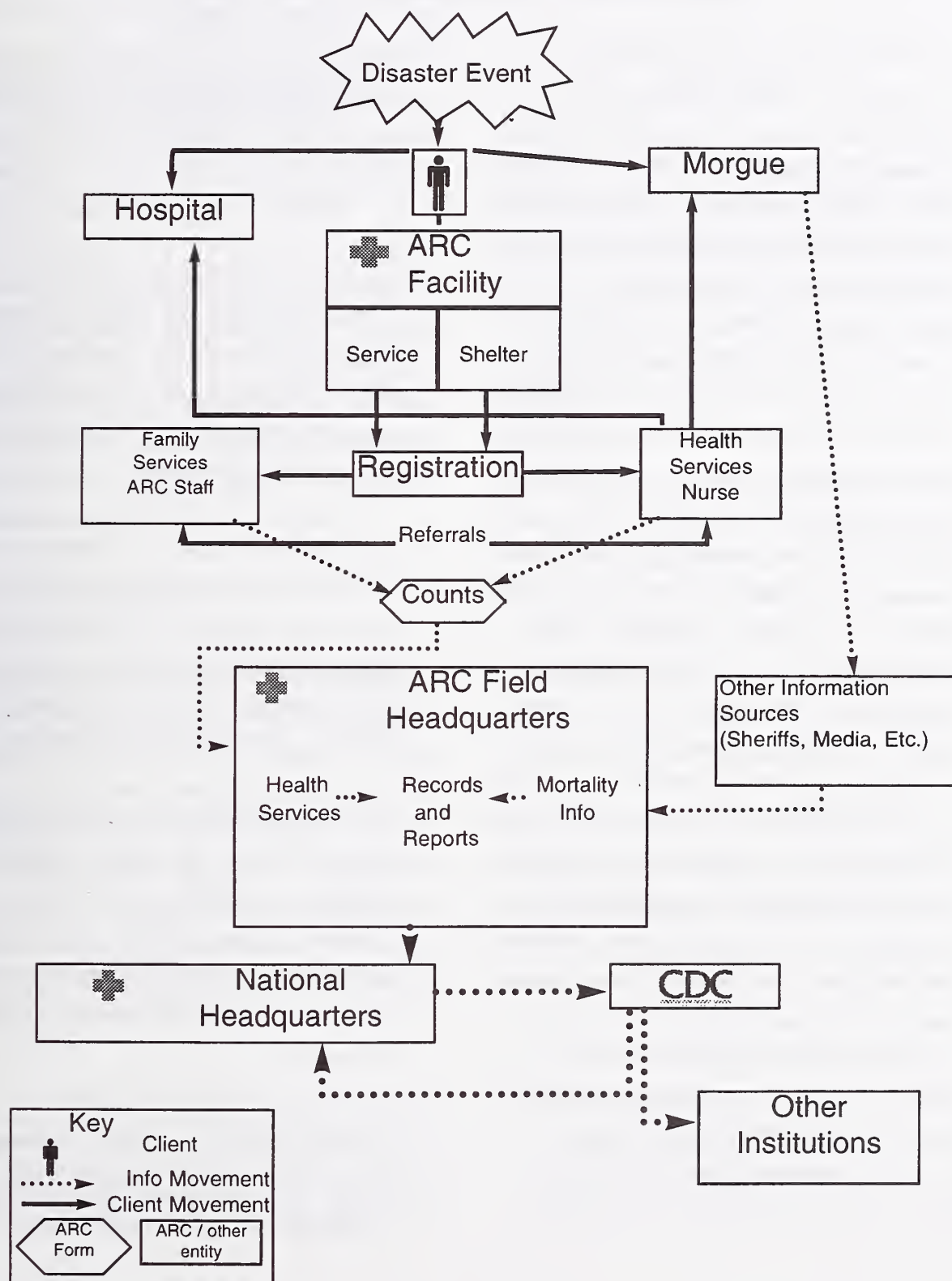


Figure 1. Flow Chart of Client and Health Information in Disaster Relief Operations, American Red Cross - CDC Health Impact Surveillance Systems for Natural Disasters



Development of the Disaster Information System(DIS/Earthquakes)

by

Kazuo Okayama¹⁾, Takaharu Kiriama²⁾, Seishi Yabuuchi³⁾

ABSTRACT

Utilizing the experiences of the Great Hanshin-Awaji Earthquake, the National Land Agency has been promoting the development of the Disaster Information System (DIS/Earthquakes) which uses the Geographic Information System (GIS). This system is expected to provide quick and appropriate decision making in all three phases, "preparation", "emergency measures" and "recovery/rehabilitation". Since April 1996, the National Land Agency has been operating the Early Estimation System (EES) which automatically estimates the scale of damage caused by an earthquake using the very limited information available immediately after an earthquake occurs. Currently, the agency is pursuing the development of an Emergency Measures Support System (EMS), which will consolidate and share information through the construction of an on-line network linked with other disaster-prevention organizations, and utilize such information in support of emergency measures such as rescue and medical care, emergency transportation, evacuation, lifelines, and volunteers..

Key Words : Disaster Prevention Information

Geographic Information System(GIS),

Early Estimation of Damage

Support of Emergency Measure

1 OVERALL CONCEPT AND STATUS OF DEVELOPMENT OF THE DIS

1.1 Background

The Great Hanshin-Awaji Earthquake, which occurred right under the city of Kobe on January 17, 1995, again showed the importance of rapid response activities by the national government, particularly the importance of estimating damage immediately after an earthquake.

If organizations concerned with disaster prevention have numerical map and geographical location data and a system that combines this data for quick and efficient application, they should be able to quickly determine the state of damage, and support rescue and recovery activities quickly and effectively.

The difficulty encountered in collecting appropriate information after the Great Hanshin-Awaji Earthquake reemphasized the importance of information. How to collect, put in order and analyze information efficiently have become major factors in recognizing the necessity of building a new system.

1)Director, Earthquake Disaster Countermeasures Division, Disaster Prevention Bureau, National Land Agency, 1-2-2 Kasumigaseki Chiyoda-ward, 100 Japan,

2)Deputy Director, 3)Former Deputy Director

The new basic plan of disaster prevention which was amended in July 1995 considers the importance of information in the following three stages: prevention, emergency measures and recovery/rehabilitation. It shall promote the construction of geographic information systems to support the realization of disaster-preventive measures.. It also states that the on-line database network shall be construct.

Based on this experience, the National Land Agency has been promoting preparation of a Disaster Information System by utilizing Geographic Information System (GIS) that manages information on topography, ground conditions, population, building stock, disaster response facilities, etc., connected to digital maps on a computer.

1.2 Overall concept

In order to develop the DIS, the National Land Agency is examining ways in which the Geographic Information System (GIS) is being used/utilized domestically and abroad in relation to disaster prevention. It has established committees and coordinating groups composed of academic experts on disaster prevention and systems development, and of persons from related agencies, incorporating the views of such groups into its development of the system.

As shown in Figure 1, the DIS focuses on three stages of an earthquake disaster. They are emergency period, recovery/rehabilitation period, and preparation period for the next disaster. This

system is expected to effectively support quick and appropriate decision making by the organizations concerned.

The DIS includes plans for the preparation of a "Map and Disaster Prevention Information Data Base" containing map data and other information relating to government agencies, public facilities, roads, disaster prevention facilities, etc. Through a network, the system will tie in such information as post-earthquake damage, the status of emergency measures, and the state of reconstruction of public facilities, lifelines, etc. to digitalized maps on the computer.

As part of its effort to support post-disaster responses, the agency is also developing an Early Estimation System (EES), which aims to provide approximate estimates of the scale of damage in the immediate aftermath of a disaster, under conditions of limited information; and an Emergency Measures Support System (EMS), which aims to support a variety of emergency measures (details to follow).

As time passes, recovery/rehabilitation measures become more important, and here comes the Recovery/Rehabilitation Measures Support System, which provides information to support the establishment of recovery and rehabilitation plans at various levels, and to help manage their progress.

While the above deals with responses after a disaster, the agency is also considering utilizing its resources at the stage of "preparations for disaster." Such resources include its Map and Disaster Prevention

Information Data Base, which has accumulated over the course of developing the systems, and the know-how that the agency has developed in the past, including its methods of estimating earthquake damage.

By utilizing data bases that have been developed beforehand, the Earthquake Damage Estimation System estimates damage caused by hypothetical earthquakes, and, on the basis of such estimates, supports efforts to propose disaster-prevention and emergency-response measures. The Support System for the Improvement and Planning of Earthquake-related Disaster Prevention Facilities estimates the number of disaster prevention facilities needed, assists in the selection of possible sites, and forecasts the impact that such facilities would have, thus supporting the planning of appropriate earthquake-related disaster prevention facilities.

1.3 Status of development

The National Land Agency has been working on the development of such systems since fiscal 1995. For its Map and Disaster Prevention Information Data Base, it has developed digital maps on a scale of 1/25,000 and 1/2,500, and, as shown in Table 1, has prepared data linked to these maps on natural conditions, such as topography and geology, social conditions such as population, public works facilities, lifelines and disaster prevention facilities.

With regard to its comprehensive systems, the agency has been operating the EES since April 1996, and is currently pursuing the development of the

EMS, which will create a network linking various disaster prevention-related agencies, and will consolidate, organize and analyze the information provided by such agencies in support of emergency measures.

2. THE EARLY ESTIMATION SYSTEM (EES)

2.1 The aims of EES development

The EES provides quick estimates of the approximate scale of damage caused by an earthquake under conditions of limited information immediately after the disaster. The system has been designed to provide information that will contribute to prompt and appropriate judgments relating to emergency measures.

In Japan, past records on earthquakes and earthquake damage are available, making it possible, to a certain extent, to organize a coherent picture of the relationship between earthquakes and the damage caused by them in different areas. By applying to such records analytical methods newly obtained in recent years, it has become possible to estimate injury and loss of human life resulting from buildings that are destroyed by earthquakes.

The EES is equipped with forecasting tools that utilize such know-how, as well as with a data base containing information on topography, ground conditions, buildings, population, etc. for the entire country. The system is also characterized by its ability to receive in real time data from

seismographs installed in approximately 1200 locations around the country by both the Meteorological Agency and local governments, and to use such data on seismic intensity in its estimates. The EES is also connected to the Meteorological Agency's Comprehensive Observation System for Seismological Activity, which enables it to immediately use seismic data that has been collected by the Meteorological Agency. Based on this data, the system estimates the distribution of seismic intensity for each mesh (approximately 1 square km) in the country, and the damage to buildings and the casualties due to building damage (Figure 2).

2.2 Verification of estimates and results of system operation

In a simulated response to the Great Hanshin-Awaji Earthquake, the system produced estimates within roughly five minutes of its receipt of data from the Meteorological Agency. The system's estimate was that the earthquake destroyed approximately 100,000 buildings, and that damage resulted in casualties (deaths) to about 4,000 people. Thus, it was generally capable of assessing the scale of earthquake damage immediately after the disaster struck.

From the time the system went into operation in April 1996 through the end of March 1998, it has recorded 69 earthquakes with seismic intensities above 4, of which five have registered readings higher than 5. In the largest of these earthquakes, which occurred on May 13, 1997 in the Satsuma region of Kagoshima Prefecture, the system

recorded a maximum seismic intensity of "weak 6," and estimated destruction to 832 buildings and resultant human casualties (deaths) of 15 (Figure 3). Although this exceeded the actually reported damage of 77 buildings totally or partially destroyed and one person seriously injured, it roughly expressed the scale of the largest earthquake disaster of the past two years. Because the system tends to estimate on the high side for earthquakes of this size, there is a need to consider making further improvements hereafter. However, when assessments of damage based on reports from the scene require time, the system permits a quick, albeit rough, grasp of the scale of damage caused by an earthquake, and in this way has contributed substantially to the material available for the government to make judgements on initial response activities.

Since September 1997, as a result of having added new forecasting categories, including the number of persons seriously injured, the number in critical condition, and the number evacuated, the system's information is being used by related agencies in preparing emergency response activities. Hereafter, the agency plans to encourage the use of the system for speedier launches of response activity, and as preliminary information for the EMS, which is now under development.

3. THE EMERGENCY MEASURES SUPPORT SYSTEM (EMS)

3.1 The aims of the EMS development

The EMS establishes a mechanism for organizing and sharing information through the GIS on damage sustained in a disaster and on the status of preparations and actions relating to various emergency measures. This is information that must be shared, and which the system provides by organizing information that is available from related agencies, and other information required for the adoption of emergency measures. The system constructs a data network that links related agencies through use of data processing and telecommunications methods.

Under the EMS, the agency will develop a system that takes such shared information and generates from it useful, value-added information that can be utilized in the formulation of emergency measures, ranging from rescue and medical care to emergency transportation, evacuation, lifelines, and volunteer-related activities.

3.2 The construction of networks linked with related agencies

By constructing an on-line network that ties the DIS to the various disaster-prevention information systems owned by related agencies, it will become possible to share data bases and to exchange information among related agencies. With ample consideration given to needs for safety during disasters, the agency will utilize the Central Disaster Prevention Radio Network as its means of telecommunications, a system being developed to link related agencies.

By overlapping onto digitalized maps information gathered from related agencies and previously established data bases of disaster prevention-related information, and, moreover, by organizing such information onto reports and providing it to related agencies as effective, added-value information aiding various emergency measures, the EMS fosters the following kinds of objectives and makes it possible for the government to execute prompt and appropriate emergency measures, together.(Figure 4):

- the sharing of various kinds of information;
- coordination with related agencies;
- greater efficiency in analyzing and organizing data.

3.3 Applications of the EMS

The EMS will be systematically developed with a focus on the following kinds of applications, which consolidate onto the GIS the information and knowledge that has been gathered regarding the emergency measures that will be required immediately after earthquakes.

* Support system for rescue and medical care

To support the dispatching of rescue and emergency medical teams, the transporting of injured or sick persons outside the disaster area, and the transporting of medical supplies, etc.

* Support system for emergency transportation

To support emergency transportation activity

for food, water and other material.

* Support system for evacuation

To support evacuation measures, such as the appropriate accommodation of large numbers of evacuees during extensive disasters.

* Support system for lifelines

To support the utility industry and others in their efforts, so as to foster the effective and concentrated restoration of lifeline functions.

* Support system for volunteers

To support an efficient and appropriate deployment of volunteers.

These systems are being methodically developed, beginning with those for which mechanisms of information distribution etc. have been established.

4. FUTURE OUTLOOK

In this way, the DIS is being built through the methodical development of systems appropriate for each stage. To utilize the DIS even more effectively, however, there is a need to reinforce its ability to distribute information--to coordinate with related agencies and the media, to release public information to businesses, residents, etc.--and to dynamically introduce new technologies.

First, in terms of strengthening coordination with related agencies, there is the need to go beyond the establishment of mechanisms for the sharing of disaster prevention information during disasters, and

to work toward increased coordination aimed at enhancing the sharing and maintenance of information during ordinary times as well. There is also the need to foster use of data bases in everyday operations and to use the system in training activity and in programs aimed at developing disaster-prevention specialists. Moreover, as a step toward closer coordination with local governments, the further sharing of data bases should be encouraged between such governments and the departments and bureaus possessing map information and data bases on houses etc.

By appropriately providing businesses, residents and others with information organized according to objectives of utilization, the effectiveness of disaster prevention measures is strengthened. Conversely, it would also be possible to consider a system of information gathering that utilizes the Internet and other means to collect such information from businesses and residents.

Among the new technologies that will be considered as a part of fostering more sophisticated uses of the DIS are those aimed at securing methods of data transmission, including the Central Disaster Prevention Radio Network, the telecommunications systems of other agencies, satellite telecommunications, the Internet, and so on.

Among the possible methods of gathering information from disaster areas is the utilization of remote sensing technology which would allow the assessment of scale of damage over wide areas and mobile terminals. Mobile terminals can also be

utilized as a mechanism for providing appropriate information from the DIS to disaster sites.

To supplement the development of the GIS data base, efforts should be made to utilize the digital maps and disaster-prevention information that are being developed by the private sector, as well as satellite photography. In addition, to foster more sophisticated uses of the GIS, efforts to promote the utilization of car navigation technology should be considered.

Making the DIS easier to use is also an issue that needs to be dealt with hereafter, and in this regard efforts should be made to improve display methods through such means as adopting three-dimensional display technology, utilizing more versatile visualization technology, and so on. Also, it will be necessary to provide better methods of checking the system and the disaster prevention structure and of providing better ways of enhancing their utilization.

While always considering systematic and technological improvements, the agency will develop the DIS in stages, coordinating its efforts more and more closely with other agencies. The aim will be to develop a system that supports disaster prevention measures that utilize information in the most effective way possible.

Table 1 Map and disaster prevention facilities data base (1/2)

Data Item		Major Attribute
Basic Map	* Map of Prefecture Boundaries	#
	* Map of Administrative Districts and Coastlines	#
	* 1/2,500 vector map	
	* Town name and numbers	* Total population, households
Natural conditions	* Surface layer features (Mesh data)	* Soil classification
Social conditions	* Population/Households	* Name, family, etc.
	* Business Places	* Office, employees
Earthquake	* Epicenter, scale in the past	* date, scale, seismic intensity, etc.
Basement, etc.	* Active fault	* Direction of displacement, activity, etc.
	* Dangerous sediment disaster area	* Classification, degree of risk
	* Dangerous liquefaction area (Mesh data)	* Degree of risk
Buildings	* Multistoried buildings	* Name, address, number of floors, height, etc.
	* Underground markets, underground passageways	* Name, address, floor area, etc.
	* Special disaster prevention districts (petrochemical complex, etc.)	* Name, supervisor, floor area, etc.
	* Facilities that stock hazardous items	* Number of stocked places
	* Roads	* Road No., traffic lanes, width, etc.
Public civil engineering facilities	* Railways and stations	* Type, name, Line No., etc.
	* Harbors	* Supervisor, name, etc.
	* Quays	* Supervisor, available boat capacity alongside pier, etc.
	* Airports	* Type, manager, runway length, etc.
	* Heliports	* Type, name, area, etc.
	* Coastal maintenance facilities	* Type, length, height, etc.
Lifelines	* Electric power	* Supplying district, number of households, etc.
	* City gas	* Supplying district, number of households, etc.
	* Water supply	* Supplying district, number of users, etc.
	* Sewage water	* Processing district, population, etc.
	* Telephone	* Operating district, number of subscribers, etc.
	* Broadcasting station	* Name of broadcast station, address, etc.

Table 1 Map and disaster prevention facilities data base (2/2)

Data Item		Major Attribute
Disaster prevention facilities	* Police station	* Name, address, number of cars, etc.
	* Fire station	* Name, address, number of cars, etc.
	* Self-Defense Force facilities	* Name, address, number of cars, etc.
	* Maritime Safety Agency facilities	* Name, address, number of vessels, etc.
	* Hospitals	* Supervisor, name, number of beds, etc.
	* Hygienic facilities	* Name, address, manager, etc.
	* Office buildings for administrative organs	* Type, name, address, etc.
	* Designated institutions	* Name, address, telephone no., etc.
	* Schools	* Type, name, address, number of classes, etc.
	* Education facilities, etc.	* Type, name, address, supervisor, etc.
	* Public areas	* Name, address, area, manager, etc.
	* Wide-area shelters	* Name, total area, number of refugees, etc.
	* Refuge facilities	* District name, structure, number of persons to be admitted, etc.
	* Social welfare facilities	* Type, name, address, etc.
	* Roads for emergency transportation	* Name of route
	* Transportation base points for large regions	* Name, supervisor, space, etc.
	* Distribution facilities	* Type, name, space, etc.
	* Places reserved for emergency use	* Items stored, quantity, etc.
	* Temporary Heliports	* Name, address, size of take-off/landing space, etc.
	* Emergency water supply	* Number of places, name, capacity, etc.

Items indicated with a # have been developed as national numerical information and cover all of Japan.

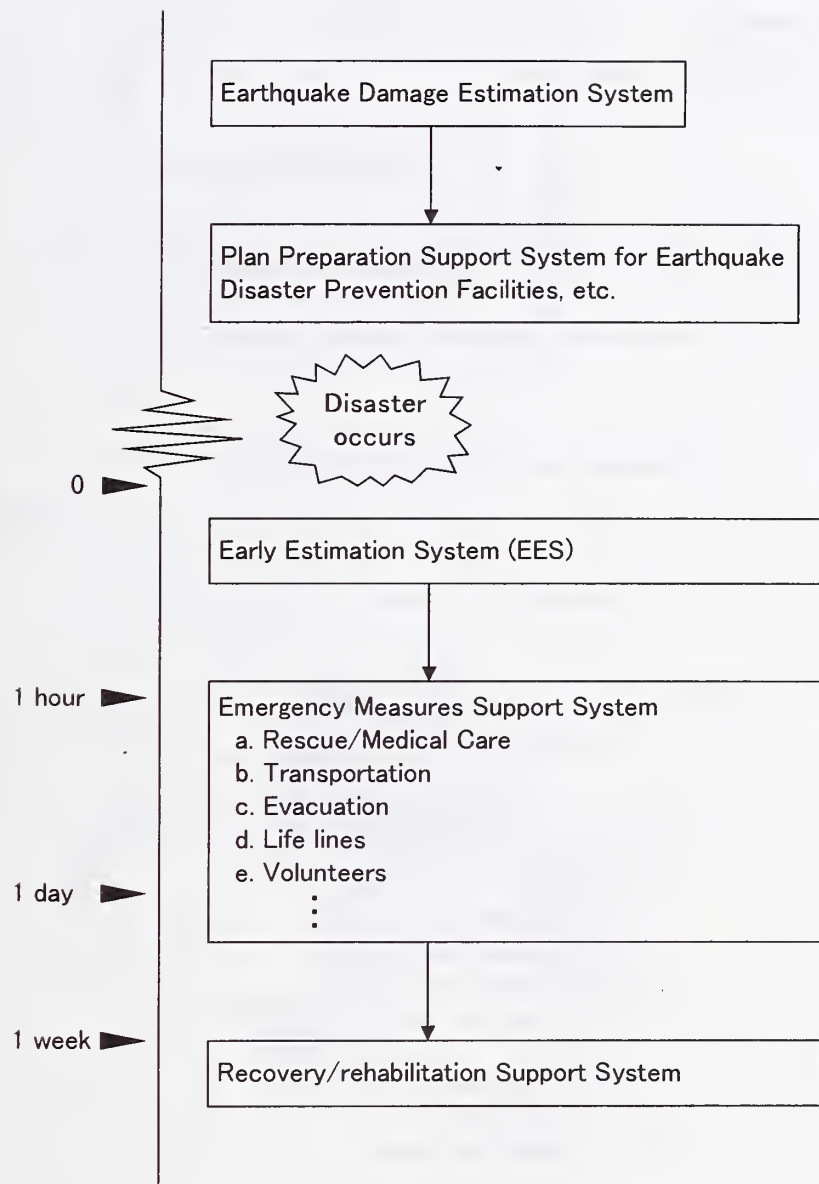


Figure 1 Composition of Disaster Information System (DIS /Earthquakes)

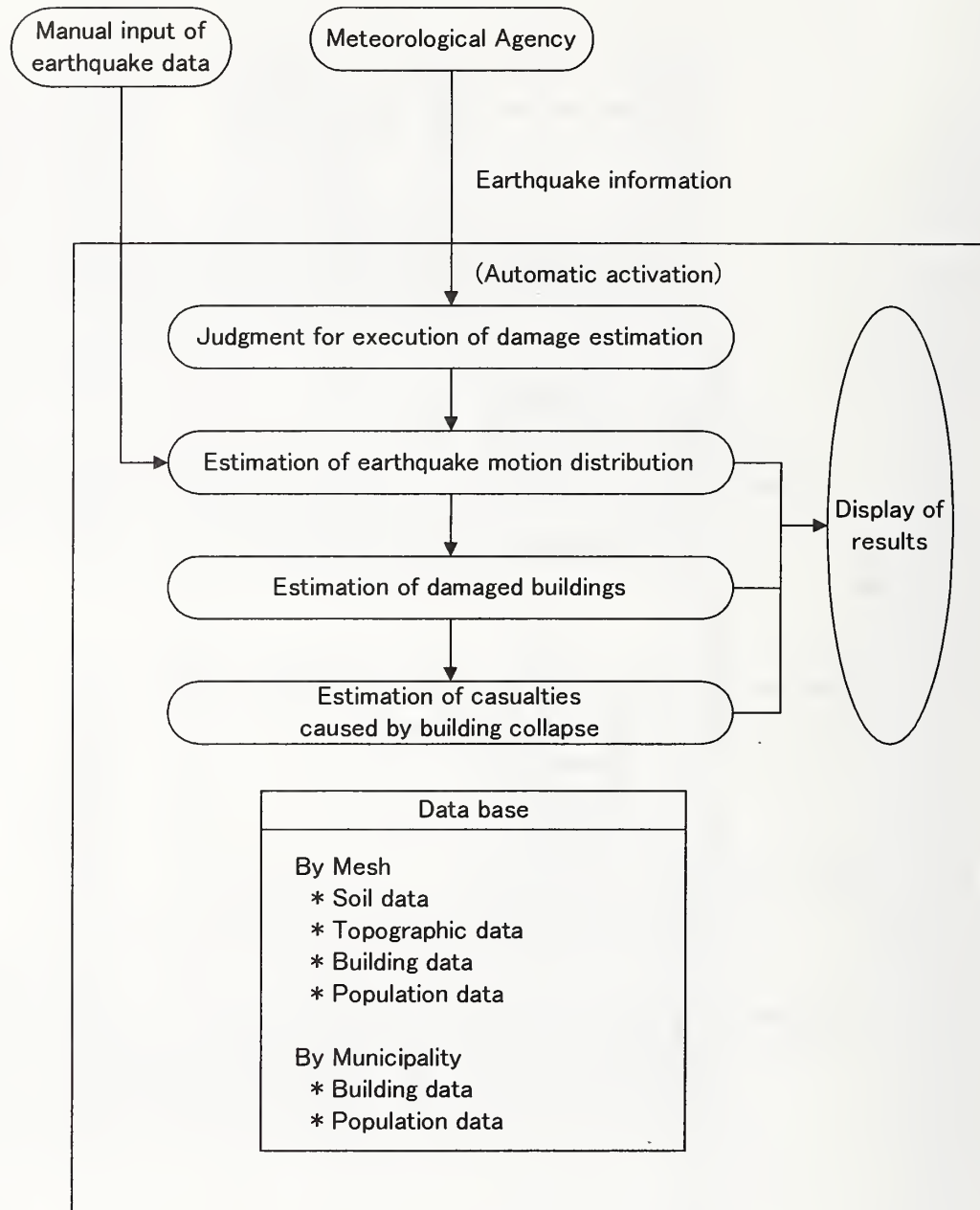


Figure 2 Flow of Earthquake Damage Estimation

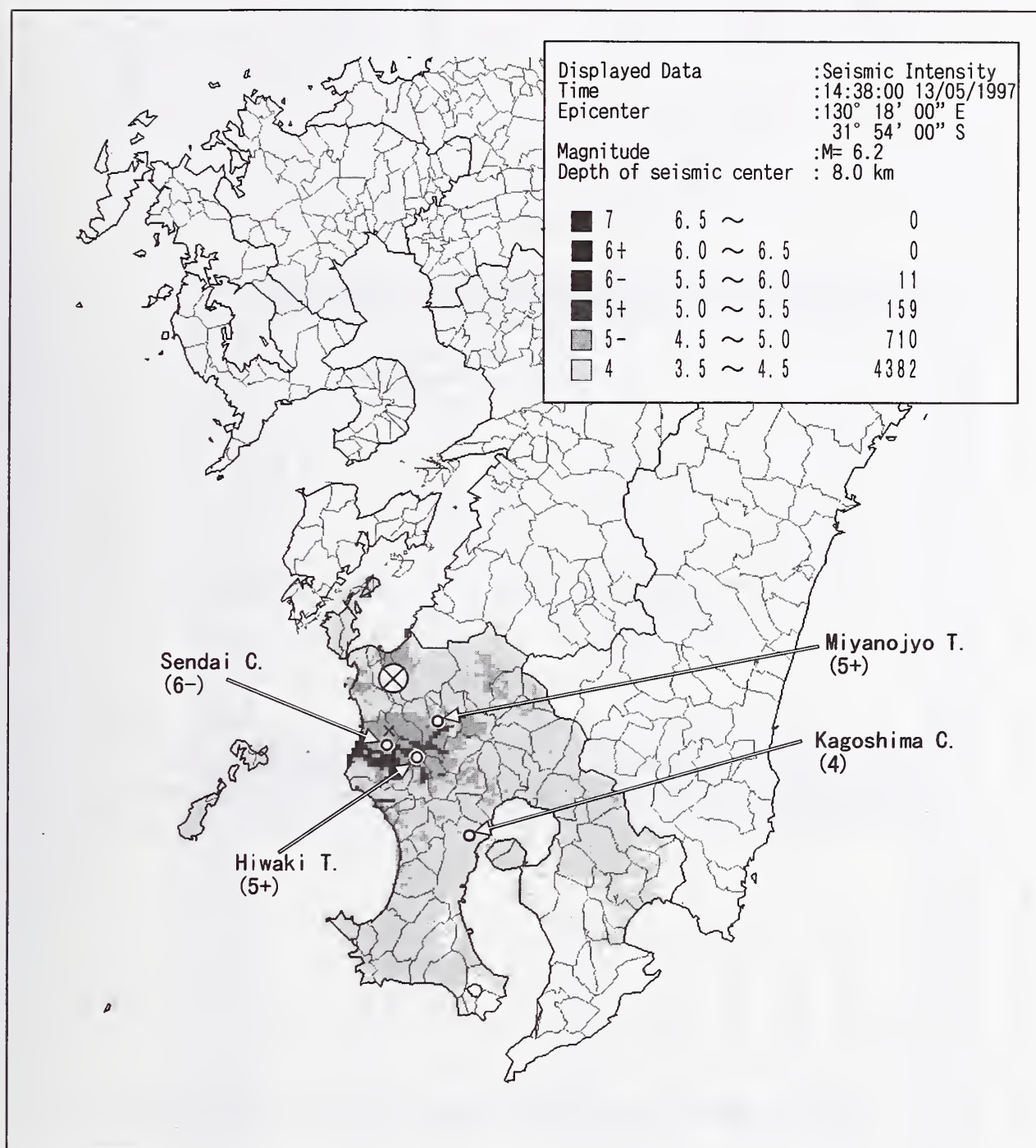


Figure 3 The estimated result of distribution of seismic intensities in the case of the earthquake in the Satsuma Region of Kagoshima Prefecture on May 13th, 1997

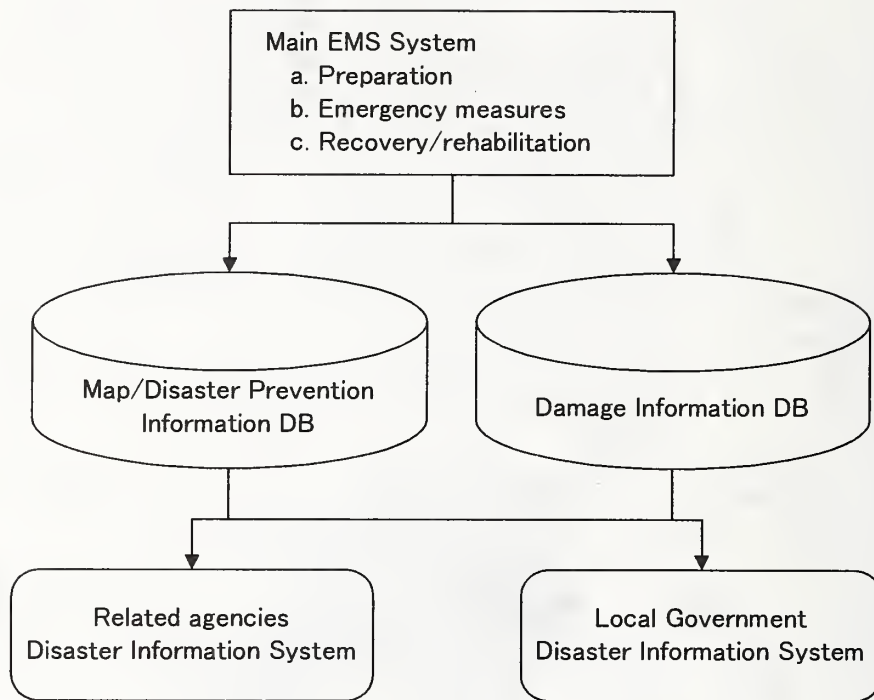


Figure 4 System Image of EMS (Emergency Measures Support System)

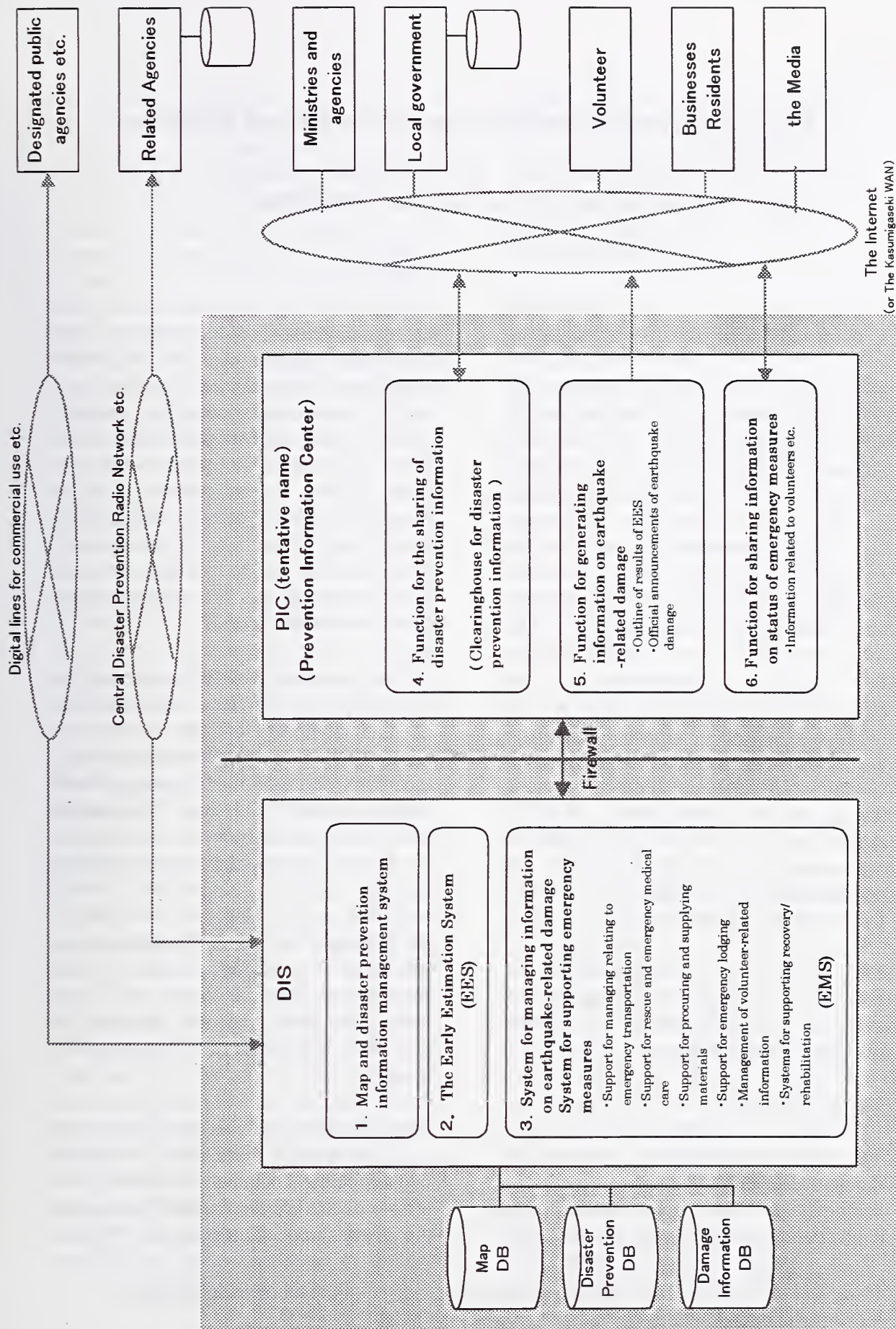


Figure.5 Future Image of the Disaster Information System (DIS/Earthquakes)

Recent FEMA Activities in Earthquake Risk Analysis and Mitigation

by

Stuart Nishenko, Claire Drury and Jeff Milheizler¹

ABSTRACT

The Federal Emergency Management Agency (FEMA), in collaboration with the National Institute of Building Sciences (NIBS), released the HAZUS earthquake loss estimation methodology in 1997. This methodology assists state and local emergency managers in estimating seismic risk to their jurisdictions in order to focus planning and mitigation strategies. The methodology also provides the capability to conduct post-earthquake loss estimation for emergency response, and provides a nationally consistent exposure and inventory database to compare seismic risk across multiple regions throughout the United States. HAZUS-related research and outreach activities are summarized, as well as plans for the development and release of wind and flood loss estimation modules.

KEYWORDS: earthquake modeling; geographic information systems; HAZUS; loss estimation; mitigation; Project Impact.

1. INTRODUCTION

The recent Northridge, California and Kobe, Japan earthquakes were wake up calls for the earthquake community. These events raised awareness about the

damage potential of a moderate-sized earthquake striking close to an urban center, and demonstrated that high risk could be present in areas of low seismic hazard. Many questions were raised about the earthquake problem in the United States – were seismic policies focused on regions of high risk or high hazard? Did cities like Boston or New York have a high enough risk to experience a disaster like Kobe, despite their low seismic hazard?

In the past, much of the perception of the 'earthquake problem' was based on an understanding of the *earthquake hazard* – the location of faults, geology, and the distribution of strong ground motion in space and time - instead of *earthquake risk*, which is a product of the hazard, the population and building exposure, and the vulnerability. Policy, land use, and development decisions at the Federal, state, and local level are risk-based decisions and need appropriate inputs. Areas of high earthquake risk may not always be coincident with areas of high earthquake hazard.

Detailed information is available about the earthquake hazard in different regions of the United States through the efforts of the US Geological Survey and the National Earthquake Hazards

¹ Program Policy and Assessment Branch, Program Assessment and Outreach Division, Mitigation Directorate, Federal Emergency Management Agency, Washington DC 20472

Reduction Program. There are few corresponding risk maps, however, that could be used for risk-based earthquake planning and mitigation. Most of the general understanding about risk is restricted to property damage, insured losses, and casualties related to specific scenario events or regional probabilistic loss studies (NRC, 1989; NIBS, 1994). Until recently, there was no nationally consistent earthquake loss estimation methodology for the United States. Without such a standardized technology, it was infeasible to compare levels of damage or losses between regions.

In support of the National Mitigation Strategy, FEMA has developed a standardized earthquake loss estimation methodology, HAZUS (Hazards United States) that uses a nationally consistent hazard, exposure, and inventory database to estimate earthquake losses throughout the United States. HAZUS provides local, state, and regional emergency management officials with the tools necessary to plan and stimulate efforts to reduce risk from earthquakes and to prepare for emergency response and recovery following an earthquake.

HAZUS is built on an integrated geographic information system (GIS) platform that rapidly produces regional profiles and estimates of earthquake loss. HAZUS is currently available in both MapInfo and ArcView versions. The methodology has been tested against the experience from several past earthquakes and against the judgment of experts, and has been judged capable of producing results that are credible for the intended purpose. Additionally, a series of pilot studies were conducted in Portland, OR and Boston, MA. Detailed descriptions of the HAZUS methodology can be

found in the HAZUS Users Manual and Technical Manuals (NIBS, 1997a,b). A series of articles in the special issue of *Earthquake Spectra* on Loss Estimation (Brookshire et al., 1997; Kircher et al., 1997a,b; Whitman et al., 1997) provide additional information.

Jamieson and Milheizler (1997) reviewed the development of the HAZUS methodology and provided a description of the individual modules (Potential Earth Science Hazards, Inventory, Direct Damage, Induced Damage, Direct Loss, and Indirect Loss) that comprise the HAZUS methodology.

This article summarizes research and outreach activities in the United States since the release of HAZUS in 1997 and discusses plans for the development of wind and flood loss modules.

2. CURRENT HAZUS ACTIVITIES

2.1 National Activities

2.1.1 Project Impact

FEMA's Disaster Resistant Community initiative, Project Impact, utilizes a 4-step approach to creating safer communities – forming partnerships, assessing risk, prioritizing mitigation needs, and communication with the community. Examination of the community's risk for natural disasters and identification of its vulnerabilities to those risks are essential to successful mitigation. HAZUS inventory data is being used for the analysis of several different hazards, including earthquake, flood, wind, and wildfire, to produce a Community Profile for Project Impact communities. The HAZUS loss

estimation methodology is being used to estimate earthquake losses in areas with an earthquake risk. Two Project Impact communities with significant exposure to earthquakes are Oakland, CA and Seattle, WA. The other hazards are being examined by overlaying the HAZUS inventory with hazard layers and using GIS capabilities to approximate exposure and potential losses. These multi-hazard data layers are available with HAZUS on supplemental CD-ROM's. In addition, FEMA plans to provide each Project Impact community with HAZUS software and assistance as needed to use HAZUS to conduct baseline earthquake risk analyses to facilitate mitigation planning.

2.1.2 Annualized Earthquake Loss

Since HAZUS is a standardized methodology with a nationally consistent inventory, it provides the perfect platform to assess and compare seismic risk across multiple regions throughout the continental United States. This analysis compares earthquake risk in terms of average annualized losses (AAL), which is the average loss over different return periods, normalized annually. These loss estimates help to compare the average level of risk between regions. Risk management decisions also need to account for the exposure of the region in addition to the absolute level of loss. A new index has been developed, the annualized loss ratio (ALR), which is the ratio of average annual loss to exposure. This index provides a measure of relative risk and can be used to compare risk across different geopolitical units such as census tracts, metropolitan areas, counties, or states.

2.1.3 Training

Regularly scheduled training classes have been held at contractor facilities in Menlo Park, CA and FEMA's National Emergency Training Center in Emmitsburg, MD. These classes provide 3 1/2 days of in-depth training on HAZUS and GIS. In 1997 and 1998, over 100 users have been trained in HAZUS. These users include emergency managers, planners, geologists, GIS analysts and others from 45 states, three territories, local governments, the Red Cross, the three regional earthquake consortia, and FEMA personnel.

2.1.4 Technical Support

Technical support is being provided to HAZUS users via phone, fax, and e-mail. FEMA is also developing a HAZUS homepage, which will describe current HAZUS developments and applications nationwide, and provide a network for HAZUS users. The HAZUS home page is located in the Mitigation section of the FEMA Internet site (<http://www.fema.gov>).

2.2 Regional Activities

In addition to national scale studies, HAZUS is being used by state and local officials for earthquake response and recovery planning, and to investigate mitigation alternatives. Results of an initial survey (Anagnos et al., 1998) conducted after the first release of HAZUS to state emergency managers indicated at that time that users had conducted analyses using the default inventory data included with the methodology. The survey also showed

that users are now beginning to undertake the task of refining existing inventories and collecting more detailed local data for incorporation into HAZUS to improve loss estimates.

2.2.1 Western United States

Throughout California, the HAZUS methodology is being used to estimate levels of ground motion for specific fault systems (e.g., the San Andreas Fault near Parkfield; the northern Hayward Fault near Berkley, as well as the Rodgers Creek and San Jacinto Faults). These estimates have been used to develop emergency response plans and to conduct response exercises in both northern and southern California.

FEMA Region 9 is engaged in developing a San Francisco Bay Area HAZUS users group that would enable widespread public and private sector participation. The goal of this group is to improve preparedness for the next major earthquake in the Bay area.

In the state of Washington, initial HAZUS projects in Seattle are focusing on transportation systems. Additionally, a volcano hazards database for Mt. Rainier and other Cascades volcanoes is being developed for use with the HAZUS inventory information to identify the exposure of communities to mudflows and other volcanic hazards.

Shortly after the release of HAZUS in the spring of 1997, the Portland METRO Emergency Planning Program used HAZUS analysis and maps generated by HAZUS to facilitate discussions of earthquake hazard mitigation measures at a workshop attended by

representatives of the business, utilities, and public sectors of the community.

2.2.2 Central United States

In Kentucky, Alabama, Tennessee, and Indiana efforts are underway, typically in cooperation with state university systems, to refine the existing default data and to incorporate inventory data from state and local sources.

Largely due to the efforts of the Central United States Earthquake Consortium (CUSEC), HAZUS has played a significant role in the Southwestern Indiana Disaster Recovery Business Alliance and the Southwestern Indiana Disaster Resistant Community Initiative. Both groups are working to coordinate and guide long-term planning and implementation of regional efforts to reduce vulnerability to earthquakes, floods, and other natural disasters. They are developing a HAZUS demonstration project that will emphasize training, team building, data inventory, strategy development, and program review at the community level. The Central US Earthquake Consortium is documenting this demonstration project for the benefit of other Central US communities.

2.2.3 Eastern United States

A compilation of detailed geologic information is currently underway in the New York City metropolitan area to better define seismic site response. Additionally, inventory collection programs are underway to upgrade the default HAZUS inventory data and prepare for the multi-hazard version of HAZUS. The formation of the New York City Metropolitan Area Loss Reduction Consortium in 1998 will

provide technical assistance for the development and implementation of mitigation and loss reduction strategies.

The Northeast States Emergency Consortium (NESEC) has developed an automated default Report Format to assist in developing HAZUS reports at the state, county, and community level.

Vermont has been active in mapping earthquake hazards in 'soft' soils and will use this information to develop appropriate mitigation activities in vulnerable areas.

Additional inventory collection efforts are underway in New Hampshire, where an innovative program is using Americorps volunteers to collect site-specific, all-hazards inventory data for incorporation into HAZUS.

North and South Carolina are working with HAZUS to refine the default inventory databases and are learning to use HAZUS products.

3. FUTURE HAZUS ACTIVITIES

3.1 Multi-Hazard Loss Estimation

FEMA and NIBS are currently in the process of expanding the capabilities of HAZUS to make it a multi-hazard loss estimation methodology. Flood and wind loss modules are under development and will be integrated into HAZUS in approximately two years. Flood and Wind committees were created to oversee the development of these two modules. Each is comprised of members with experience and expertise in the flood and wind fields. Dr. Joseph Minor, University of Missouri-Rolla, chairs the nine-member Wind

committee; and Mr. Douglas Plasencia, Kimley-Horn and Associates, chairs the eleven-member Flood committee.

A key element in the development of these modules is to have users provide input throughout the process. Users' Workshops are scheduled for both the Flood and Wind Modules. These will be attended by a wide variety of potential users, including emergency managers, floodplain managers, state and local representatives, and others. The outcome of these workshops will be a Users' Requirements Report that will be furnished to the development contractor to ensure that the end product meets the needs of potential users.

2.3 International Loss Estimation

The United States-Japan Common Agenda for Cooperation in the Global Perspective has identified real-time seismic information systems and earthquake loss estimation methodologies as topics for discussion at the 1st High-Level US - Japan Earthquake Policy Cooperation Forum. The creation of the Seismic Information Systems Task Committee, as part of the US-Japan Panel on Wind and Seismic Effects, is an opportunity to foster cooperation between US and Japanese researchers and policy makers. The Task Committee will provide technical support to the Common Agenda, and will act as a forum for identifying, developing, and reviewing data systems and methodologies involved with seismic information systems, earthquake loss estimation, geospatial and topographic information systems, and early seismic warning systems.

4. CONCLUSIONS

The introduction of HAZUS in the United States has sparked interest and activity in earthquake loss estimation at the Federal, state, and local level. Loss estimation also provides a unique opportunity for international collaboration and partnership. Inquiries about HAZUS and earthquake loss estimation in general from China, Japan, Latin America and Russia demonstrates the common challenges that we all face with respect to natural disasters and the willingness to work together to create safer communities for the future.

5. REFERENCES

- Anagnos, T., Lawson, R. S., Schneider, P., and Drury, C., 1998, Initial Problems and Successes in Implementing the HAZUS Loss Estimation Methodology Throughout the United States, in *Proc. 6th National Conference Earthquake Engineering*, Seattle, WA.
- Brookshire, D., Chang, S. E., Cochrane, H., Olson, R., Rose, A., and Steenson, J., 1997, Direct and Indirect Economic Losses from Earthquake Damage, *Earthquake Spectra*, **13**, 683-701.
- Jamieson, G., and Milheizler, J., 1997, The Use of GIS in Loss Estimation and Risk Assessment, *Proc. 29th Joint Meeting of the US-Japan Panel on Wind and Seismic Effects*, UJNR, May 13-16, 1997 Tsukuba, Japan.
- Kircher, C., Nassar, A. A., Kustu, O., and Holmes, W., 1997a, Development of Building Damage Functions for Earthquake Loss Estimation, *Earthquake Spectra*, **13**, 663-682.
- Kircher, C., Reitherman, R. K., Whitman, R. V., and Arnold, C., 1997b, Estimation of Earthquake Losses to Buildings, *Earthquake Spectra*, **13**, 703-720.
- National Institute of Building Sciences, 1997a, HAZUS Technical Manual, 3 vol., Washington DC
- National Institute of Building Sciences, 1997b, HAZUS97 Users Manual, Washington DC
- National Institute of Building Sciences, 1994, Assessment of State-of-the Art Earthquake Loss Estimation Methodologies, FEMA 249, Washington DC 300 pp.
- National Research Council, 1989, Estimating Losses from Future Earthquakes, FEMA-177, Washington DC 231 pp.
- Whitman, R. V., Anagnos, T., Kircher, C. A., Lagorio, H. J., Lawson, R. S., and Schneider, P., 1997, Development of a National Earthquake Loss Estimation Methodology, *Earthquake Spectra*, **13**, 643-661.

SEISMIC INFORMATION SYSTEM FOR CIVIL INFRASTRUCTURES

by

SUGITA Hideki¹⁾, NOZAKI Tomofumi²⁾

ABSTRACT

This paper describes comprehensive image of the seismic information system (SIS). Two points are included in the paper: i.g., a new system architecture to realize SIS with systematic control, possibility of extension and the independence of the subsystems, and several element technologies applicable to the subsystems of SIS. The proposed concept does not only concentrate on the technologies of the supply-side, but also the philosophy and the technologies that is "objective oriented." As the counter-earthquake activity system is responsible many complex jobs at a time, and as the information technologies is becoming highly technical, the concept introduced here is very much help for the personnel of the counter-earthquake activity system.

Key Words: Counter-earthquake activity system, Information system, New technology and philosophy

1. INTRODUCTION

Since the Hyogo-ken Nanbu Earthquake, which revealed the necessity for quickly monitoring damage, communicating information, and making decisions, many organizations have constructed various systems to deal with earthquake information, which are listed in

Table 1-1. Their principal functions are to:

- 1) monitor, collect, and adequately display accelerograph measurements and data from other organizations and systems (*observation and collection*),
- 2) estimate the damage to facilities and injury to people by the earthquake and consequent fires, from the data collected (*damage estimation*),
- 3) take emergency measures based on the data collected, and the estimated damage, such as immediate suspension of facility functions and warnings to users (*emergency response support*), and
- 4) support the decision making processes by presenting instructions given in emergency manuals and proposing optimum strategies (*counter-earthquake system support*).

So far, most of these systems are developed for use within the organization. Although each system remotely accelerographs, collects and communicates information through the network, and exchanges data between its submodules constructed for each function, it has its own independent database. When users encounter the occasion to exchange data between systems, they must conduct a series of complicated operations and must know the

1) Head, Earthquake Disaster Prevention Technology Division, Earthquake Disaster Prevention Research Center, Public Works Research Institute, Ministry of Construction, Tsukuba, Ibaraki, 305-0804 Japan

2) Senior Research Engineer, ditto

methods for operating the systems, which may differ by system. As such information systems usually use common earthquake motion measurements, ground condition and facility data, we should investigate methods for sharing such data without losing the possibilities for extension and independence of each system.

2. CONVENTIONAL APPROACHES FOR CONSTRUCTING SEISMIC INFORMATION SYSTEMS AND BREAKTHROUGH

2.1 Top-Down Approach

Most seismic information systems have been constructed with a top-down approach. For example, a system that 1) collects ground motion data, 2) estimates human casualties and fire occurrence from the data, and c) suggests the actions necessary for preventing damage is designed to include all these functions in one host machine as shown in Figure 2.1. Although it is possible to supplement functions to the system later, the top-down approach fundamentally creates the image of an entire system first. Hence, the top-down approach has disadvantages such as

- 1) a system does not operate until the whole system is completed,
- 2) it is difficult to renew the system, since a slight change may largely affect the entire system (thus such systems easily become obsolete), and
- 3) all users within an organization must fully know the provided

operation method.

2.2 Bottom-up Approach

A new movement is occurring in the

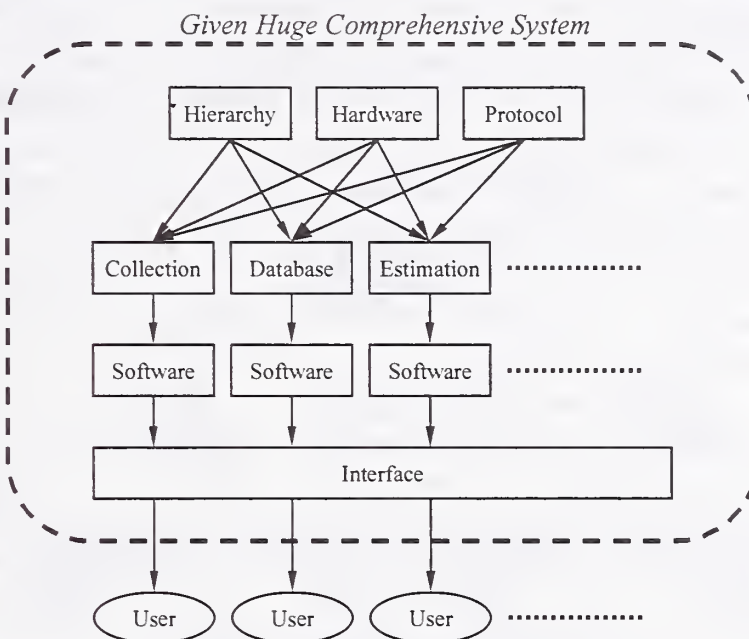


Figure 2.1 Top-down Approach

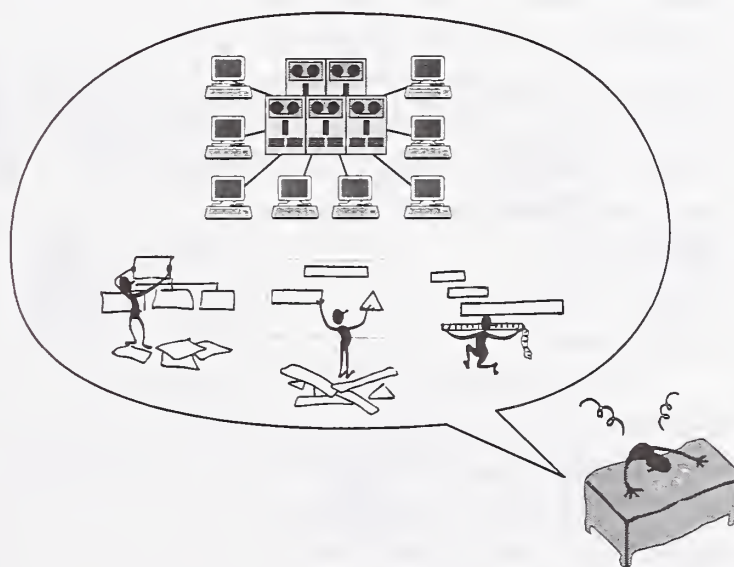


Figure 2.2 Disadvantage of Top-down

construction of information systems along with the recent development and diffusion of information network technologies, such as the internet. In the WWW, for example, each terminal freely constructs a server according to a minimum set of integrated rules including the TCP/IP protocol, and communicates information to many and unspecified clients. Such a state forms a contrast to the above top-down approach in terms of flexibility and possibilities of extension of each function of servers. This construction method is called the bottom-up approach.

With the bottom-up approach, it is possible to construct a database and run an application on one server as its administrator hopes. Other persons can use the same system by using a browser or other similar software. When the administrator needs a new function, he/she only either adds the desired function to the server or supplements a new server. In this situation, there is no need for considering other users. However, systems constructed with the bottom-up approach are inappropriate for systematic activities since servers usually use different functions and data independently.

2.3 Breakthrough

The top-down approach constructs systems that share data and functions but are not flexible or free. On the other hand, the bottom-up approach constructs systems that are easy to add new functions and to access but may not be using common data.

These two approaches are both extremes of system construction (or system formation). By integrating the advantages and characteristics of both, a new and more efficient method for constructing seismic information systems (SIS) may be developed. The ideas are summarized as follows:

- 1) It clarifies the minimum set of information

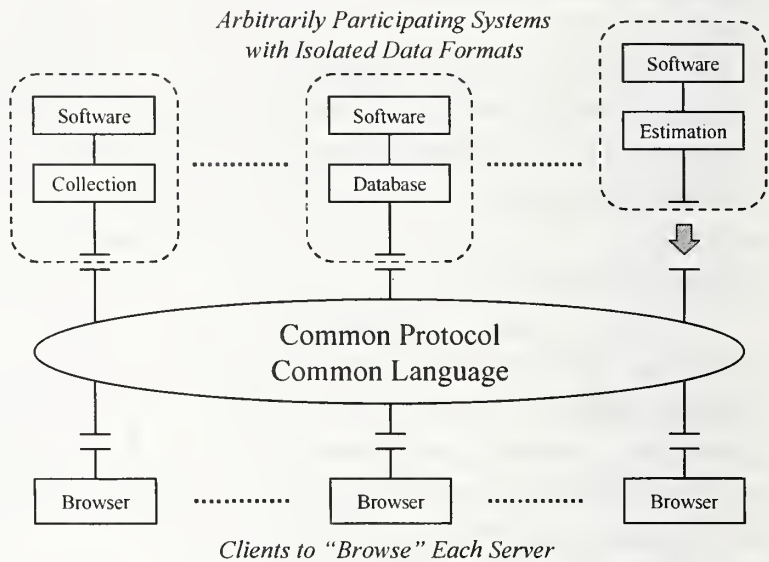


Figure 2.3 Bottom-up Approach

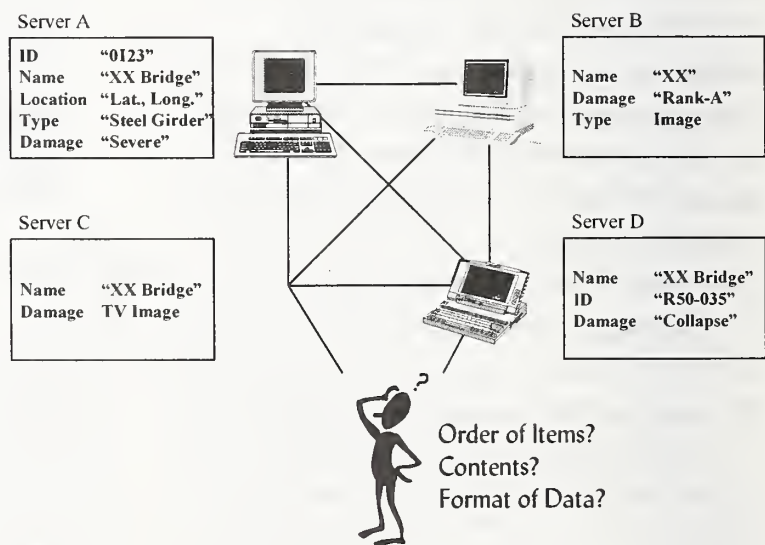


Figure 2.4 Disadvantage of Bottom-up

that is needed for each level of an organization. The information that is open to a level is also open to lower levels (*data sharing*).

- 2) All divisions that have acquired permission can operate or refer to outputs of SIS with shared data (*function sharing*).
- 3) A certain level of an organization can supplement its own data and function to the SIS (*system flexibility*).

To actualize these ideas, integrated methods should be developed and organized for sharing data and functions in different levels of an organization. The recent diffusion of network technologies has spread common protocols and software such as http and java applets. However, more precise data items and format definitions must be defined for using a large amount of data and functions needed for systematic counter-earthquake activities. The following alternatives may be adopted for sharing data and functions:

- 1) An entire organization uses one database and the same application software.
- 2) All databases are constructed with a single format (schema).
- 3) All databases contain at least a minimum set of data items, which make users possible to use the data by converting them with simple application software.

To make data accessible to all users, all organizations that use the SIS must clearly understand their duties concerning counter-earthquake

measures and make lists of necessary information. Although such operations are labor consuming for the organizations, the initial cost in terms of money, time, and labor is sure to be well spent in constructing a more comprehensive, flexible, and organized system. Incidentally, Geographical Information Systems (GIS), which display collected data and

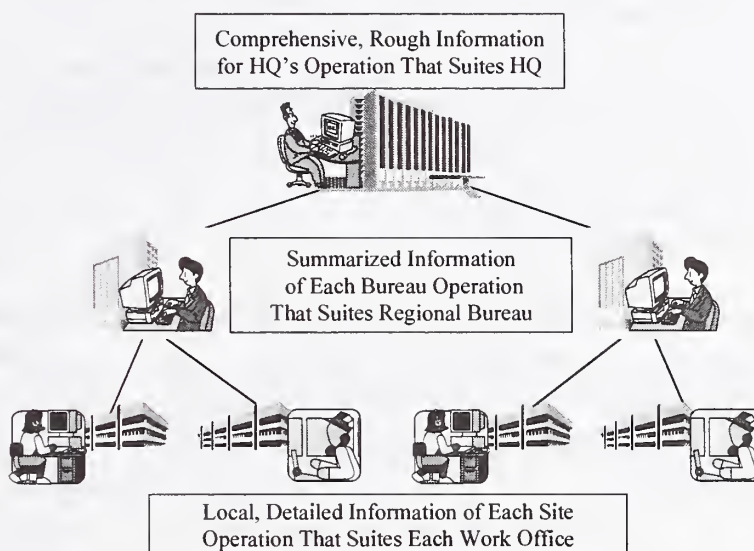


Figure 2.5 Data/Function Sharing

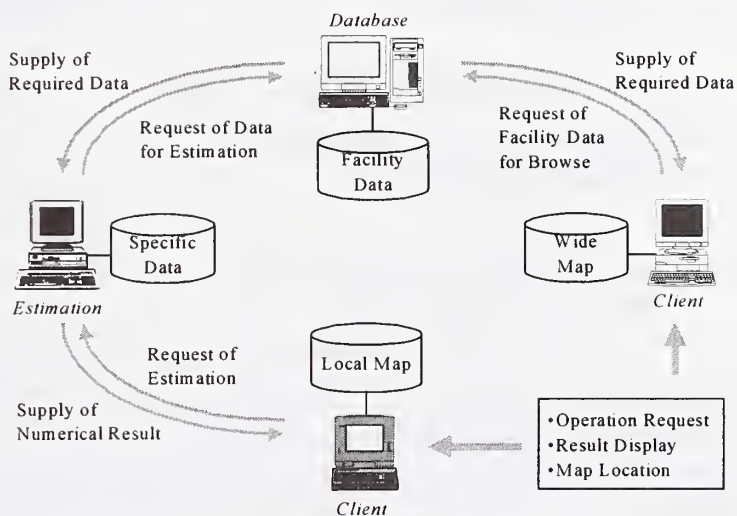


Figure 2.6 Breakthrough Technology

Table 2.1 A&D of Respective Approach

	Top-down	Bottom-up	Breakthrough
Development/Improvement Speed	slow	rapid	comparatively rapid
Possibility of Extension	small	large	comparatively large
Independence of Subsystems	Almost none	Almost independent	Independent under some control
Physical Cost in Development	Quite much	Small	Not much
Labor Cost	Large when studying manipulation	Responsibility of each server administrator	Initial coordination is required
Uniformity of Data	Secured	Difficult to establish	Secured when necessary
Systematic Development and use	Strict	Chaotic	Practical

estimations on maps, will be independent from the collecting and estimating procedures. In the approach introduced here, data interfaces can be jointly used even when GIS applications/data are different.

The advantages and the disadvantages are summarized on Table 2.1. According to this, strict coherence of the top-down approach, the incoherence of the bottom-up approach and the advantages of the proposed approach against others are clearly depicted.

3. FUNCTIONS, TECHNOLOGIES, AND APPLICATIONS OF SEISMIC INFORMATION SYSTEMS

3.1 Functions to be Included in Seismic Information Systems

This section summarizes functions to be included in SIS of organizations that administer civil infrastructures, such as the Ministry of Construction. The following functions are proposed to be included in SIS.

(a) Evaluation of counter-earthquake

projects

SIS should help determine the priority of reinforcing projects, based on their influence over emergency activities and economic damage.

(b) Evaluation of counter-earthquake activity systems

SIS should help evaluate the speed and accuracy for collecting and communicating information of counter-earthquake activity systems.

(c) Monitoring, collection and estimation of earthquake data

SIS should collect characteristic values and wave data that are monitored and

calculated by accelerographs and should estimate epicenters, etc.

(d) Support of anti-seismic activities

SIS should spontaneously inform of earthquakes, display manuals for emergency activities.

(e) Detection of facility damage

SIS should directly detect and communicate damage to public facilities by sensors and so on.

(f) Real-time estimation of damage

SIS should quickly estimate the damage to facilities based on earthquake information and ground and structure data.

(g) Collection of inspection data

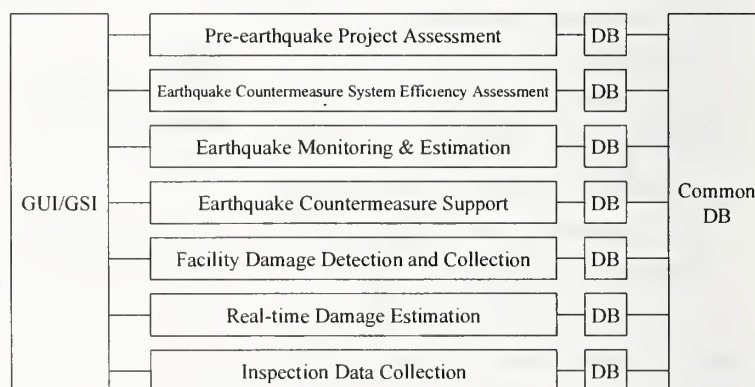


Figure 3.1 Functions of SIS

SIS should record and communicate actual inspection data collected at the sites.

(h) Display of maps, images, and animated pictures

SIS should have the interfaces to refer and input information appropriately.

(i) Communication of information (sound, images, animated pictures, and data)

SIS should transmit data through public and private telephone lines, facsimiles, internets, intranets, extranets, etc.

The following sections outline several technologies and systems that the Public Works Research Institute (PWRI) is developing. These functions, which are now independently studied, may be integrated into subsystems by coordinating data and by refining each function.

3.2 Accelerograph Network and Urgent Damage Estimation System

The Ministry of Construction has installed approximately 800 online accelerographs throughout Japan (accelerograph network) to help urgent inspection of its facilities, such as highways and river facilities, after earthquakes. This accelerograph network falls in the category (c) 'monitoring and collection of earthquake data' of Section 3.1. PWRI collects seismic information experimentally from approximately 100 accelerographs in the Kanto Area, and is developing a system for estimating liquefaction risks and bridge damage in this area. This system corresponds to

the category (f) 'real-time estimation of damage.' Example displays of the system for maximum acceleration, estimated liquefaction risk, and estimated damage to facilities are shown in Figures 3.2 to 3.4. The system is also installed with a multiple-address device, which

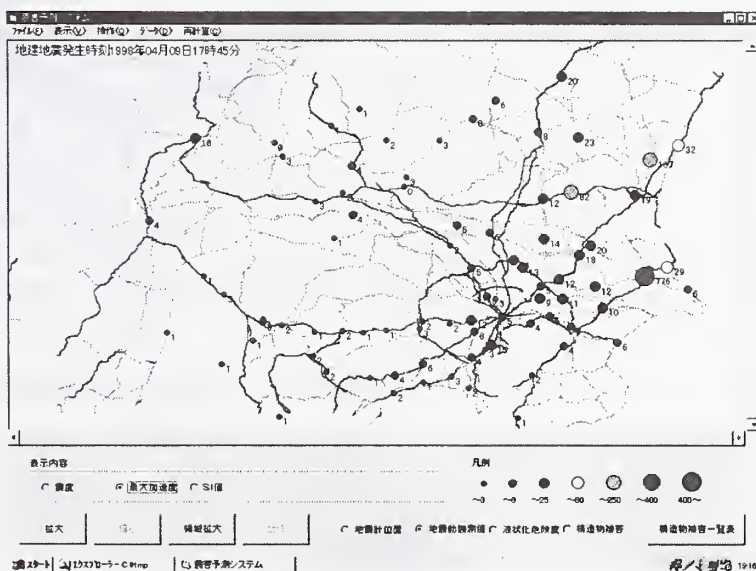


Figure 3.2 Estimation of Max. Acc.

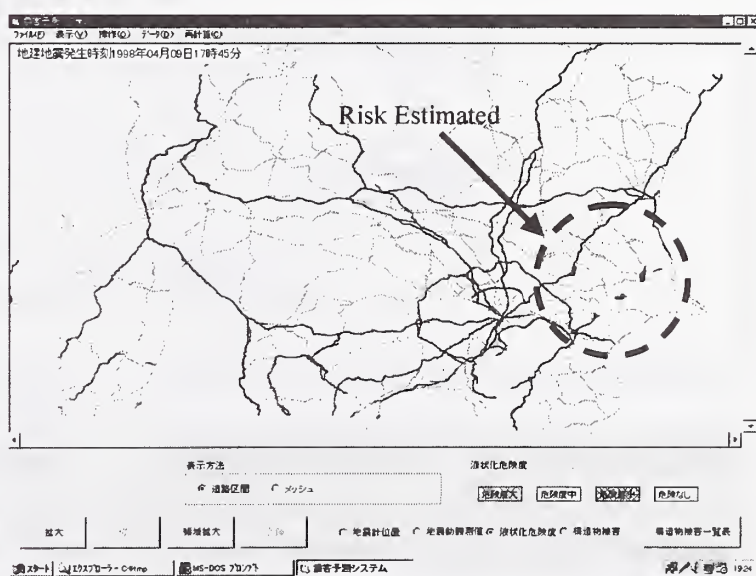


Figure 3.3 Estimation of Liquefaction Risk

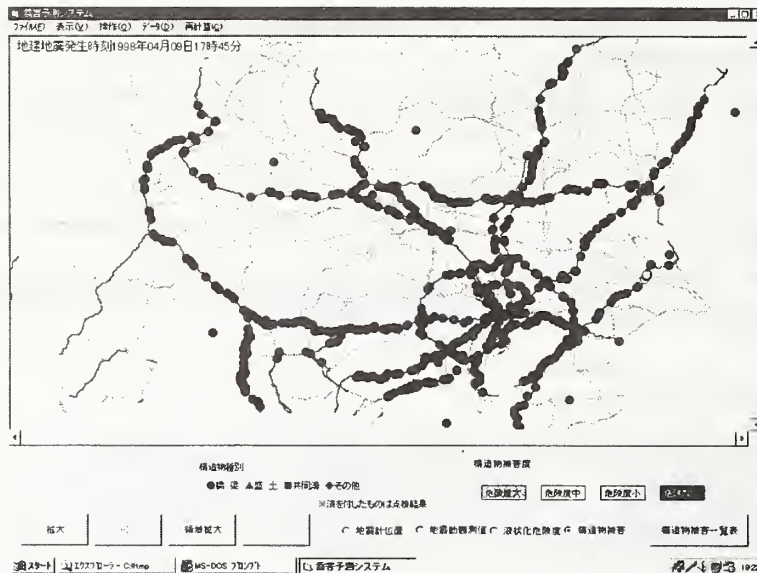


Figure 3.4 Estimation of Facility Damage

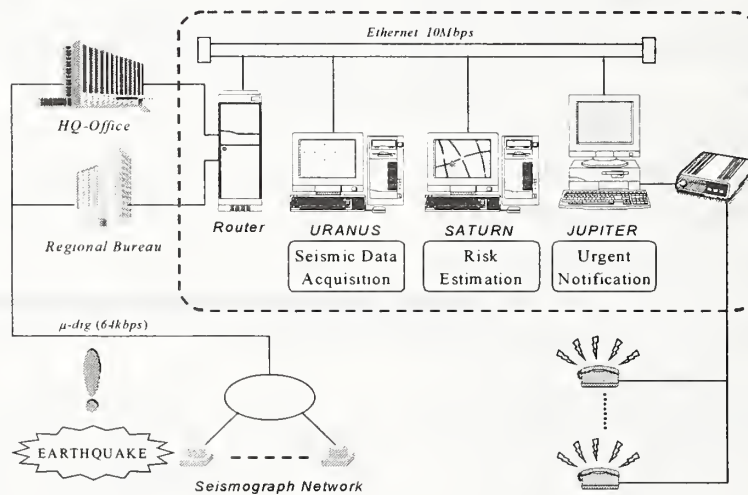


Figure 3.5 System Architecture

immediately and automatically dials all numbers registered when an earthquake occurs. This device corresponds to the category (d) 'support of anti-seismic activities.' A connection and operation diagram of the system is shown in Figure 3.5.

The characteristic values of earthquake

motion (e.x., maximum acceleration and SI values) are transmitted from accelerographs immediately after the earthquake occurs and are recorded in files within a communication server. The urgent damage estimation system calculates liquefaction risks and facility damage levels based on these numerical files as well as ground

and facility information collected in advance. The system also contains map data and can display the collected seismic data and the results of calculation on maps.

3.3 Earthquake Assessment System for

Socioeconomic Effect (EASSE)

The earthquake assessment system for socioeconomic effect (EASSE) calculates quantitatively the mid-term and long-term economic losses by damage to transportation facilities, such as highways and railways. The

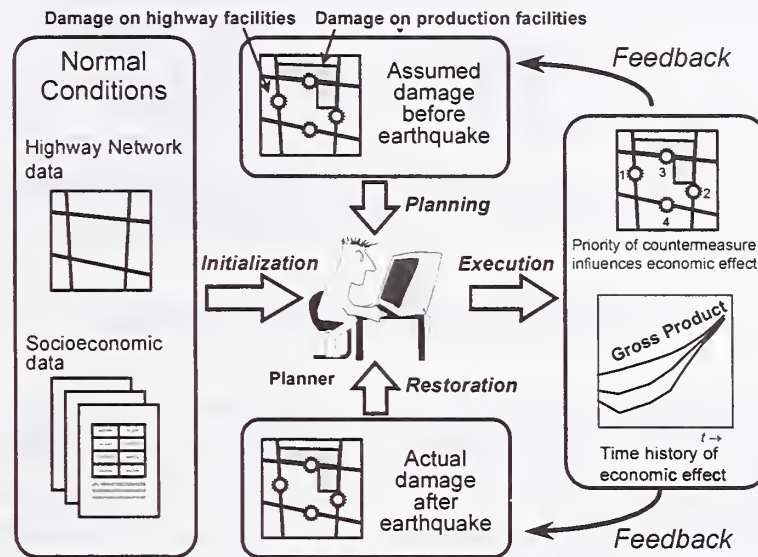


Figure 3.6 Idea of EASSE

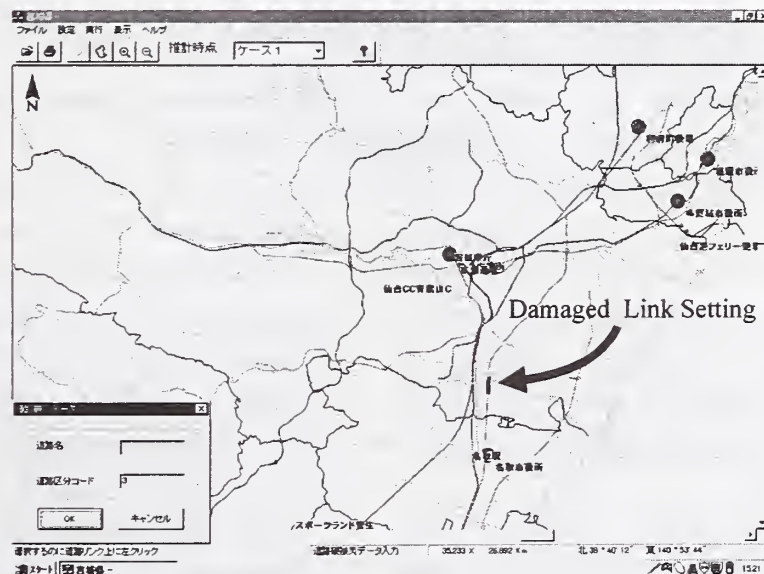


Figure 3.7 EASSE Display

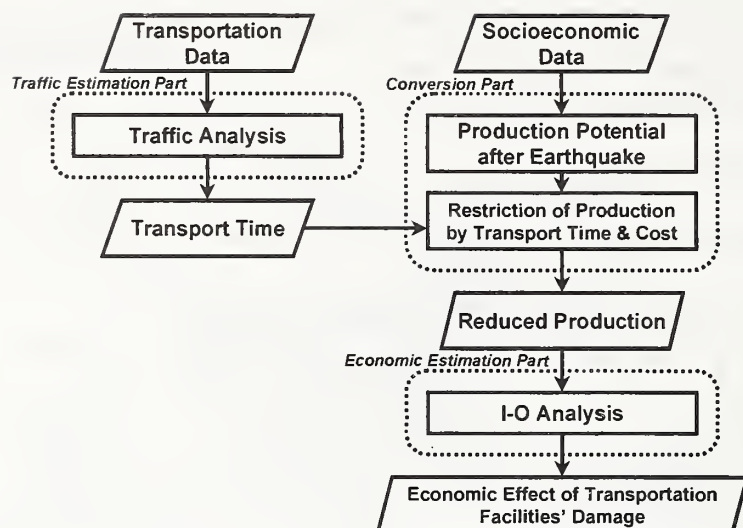


Figure 3.8 Module Structure of EASSE

PWRI has been developing a prototype for 3 years, from 1995 to 1997. As shown in Figure 3.6, this prototype system, which runs on a standalone PC, computes the drop in production due to damage to highway or railway sections input on a map display. Data for investigating reinforcement projects of transportation facilities in an area, such as the economic loss for each reinforcement pattern, are obtained simply by inputting damaged sections based on a hypothesized earthquake and reinforcement pattern. An example display for inputting damaged road sections and an output image are shown in Figure 3.7. EASSE, which falls in the category (a) 'evaluation of counter-earthquake projects,' may also be used for creating post-earthquake restoration projects. Since this system is now operating independently, it contains map data and also falls in the category (h) 'display of maps.'

For developing EASSE, the procedures necessary for estimation were converted into independent modules as shown Figure 3.8. The traffic estimation module

calculates the increase in trip time by the earthquake based on highway-network data and socioeconomic data that are necessary for computing traffic demand. The conversion module calculates the drop in productivity in a target district from the results of the traffic estimation. The economic estimation module computes the effect of the drop in productivity in and out of the damaged district.

3.4 Seismic Performance of Highway Network

We should investigate if transportation facilities are able to serve satisfactorily even immediately after an earthquake. The seismic performance of the entire highway network should be studied to assure that no district is isolated by damage to highway sections and that disaster prevention activities are taken within a required period of time. PWRI is developing a system which calculates the degree of performance with which satisfactory prevention activities can be taken. The institute is also investigating a method for expressing the



Seismic Performance of Total Network?
Priority of Links in Terms of Seismic Performance?

Figure 3.9 Network Seismic Performance

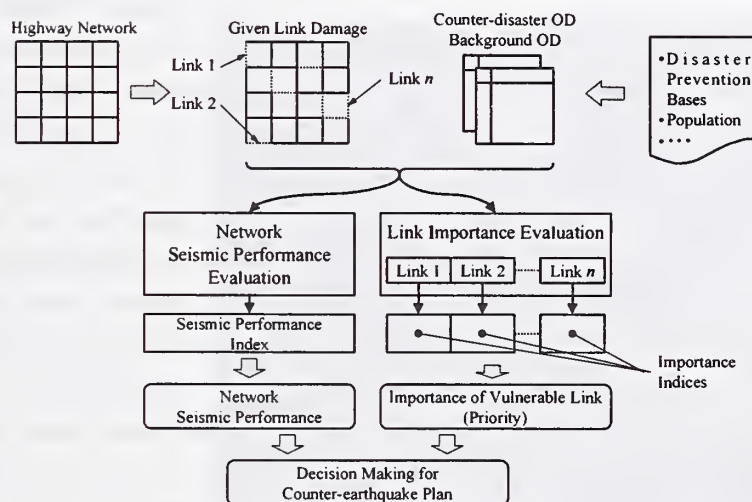


Figure 3.10 Flow of Calculation

importance of a damaged section quantitatively. Like EASSE, this system corresponds to the category (a) 'evaluation of anti-seismic projects.'

This system evaluates the seismic performance of the entire network and the importance of damaged sections when an earthquake disconnects the link of the network. The seismic performance of the network is

calculated by computing the sum of disaster prevention activities' effects, which are determined based on the trip times of traffics in the network after the earthquake. A method is also investigated for calculating importance indices of network sections using the network seismic performance indices above.

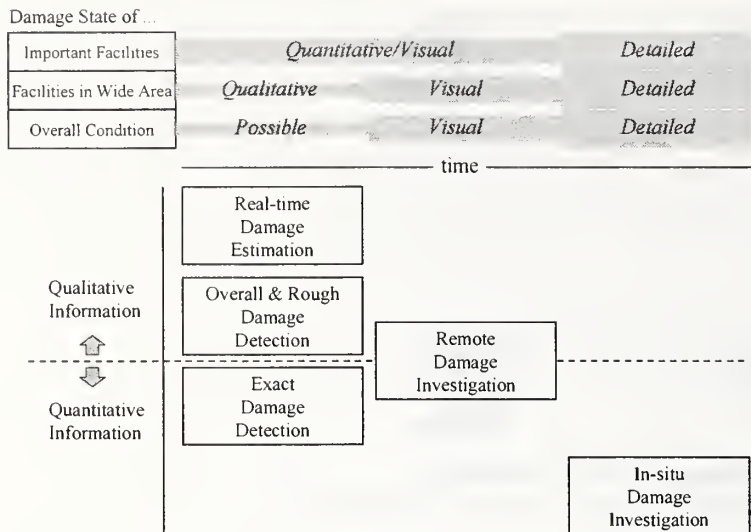


Figure 3.11 Combination of Damage Detecting Method



Figure 3.12 Example Image From Helicopter

3.5 Other Subsystems for SIS

Besides the subsystems' technologies and methods above, several other issues are studied which can be parts of SIS. Those include (1) earthquake damage detection technologies and (2) counter-earthquake activity system performance evaluation method.

The first one includes various technologies to detect the damage to infrastructures by utilizing sensors attached to them and remote sensing technologies. Some sensors such as laser distance meter can detect phenomena precisely, but they are expensive, while other sensors as wire cutting sensor are inexpensive and give only rough information of possible damage. Important facilities such as large bridges need to be watched carefully by sophisticated sensors. On the other hand, most of the facilities that stretch over wide area are enough to be observed roughly to detect possible damage. As for the remote sensing technologies, animated images taken from a helicopter and pictures sent from the investigation team directly are useful and important information to examine the restoration/rehabilitation strategies. Images from satellites are useful if they can be obtained immediately after the earthquake. Taking the these ideas into account, a menu for utilizing the damage detection sensors from the point of view of the cost, exactness and speed is studied as a guideline by PWRI.

Another useful method is that to evaluate the performance of a counter-earthquake activity system in terms of the rapidity and the preciseness to cumulate the damage information. In this method, all the personnel and equipment are expressed as abstract "gates" which transform the data from input and send to output. In the method, the information is defined as a combination of the

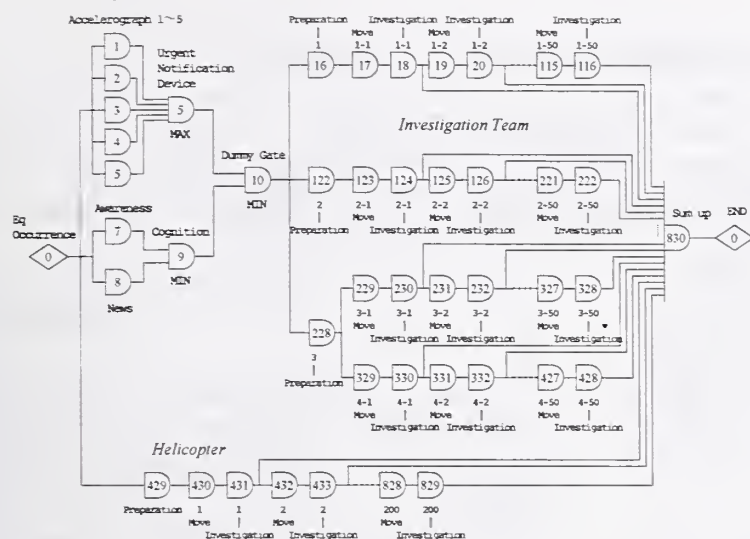


Figure 3.13 Network Expression of Counter-earthquake Activity System

time and the information quantity: i.g., (t, I) . By defining the gates for all the entities in the system, and by connecting them with each other, the counter-earthquake activity system is expressed as an abstract network system. Analyzer can obtain the cumulating pattern of the information quantity and examine the performance of the system quantitatively. This also helps him/her to determine the bottle neck and the weak point part in the system.

4. CONCLUSION

The conventional SISs of the Ministry of Construction and most of other seismic systems under development are independent and do not share databases or map data. As described in Section 3.3, data should be shared and functions should be separated according to a minimum set of defined rules to create efficient and flexible systems. The methods for operating SIS must be familiar to the system staff since they must quickly treat an enormous

amount of information after an earthquake. Using SIS in the normal conditions can improve the familiarity of the stuff. Rules concerning seismic information systems, common databases, and the development of independent functions are also helpful for the systems and functions used in the normal condition. By applying these concepts, we can construct a comprehensive system that is easy to use during both normal and earthquake times and to enlarge when necessary.

Because the idea introduced here includes comprehensive systematic regulation, it cannot be applied only by parts of organization, say, two or three work offices or regional bureaus. To realize the concepts here some adequate promotion system to coordinate all the organization must be established.

REFERENCES

- 1) Kazuhiko KAWASHIMA, Kenichi TOKIDA Hideki SUGITA, Tomofu NAKAJIMA, Hideo MATSUMOTO, "Guidelines for Disaster Information Systems for Important Infra-structures", Proceedings of the 25th Joint Meeting of U.S.-Japan Panel on Wind and Seismic Effects, May 1993
- 2) SUGITA Hideki, HAMADA Tadashi, "Development of Real-time Earthquake Damage Estimation System for Road Facilities", Seventh U.S.-Japan Workshop on Earthquake Disaster Prevention for Lifeline Systems, Nov. 1997
- 3) NOZAKI Tomofumi, SUGITA Hideki, "System to Assess Socio-economic Effect of Earthquake Disaster", Seventh U.S.-Japan Workshop on Earthquake Disaster Prevention for Lifeline Systems, Nov. 1997
- 4) "Real-time Earthquake Damage Estimation System for Road Facilities", PWRI Newsletter No. 71, Jan. 1998
- 5) "Earthquake Assessment System for Socioeconomic Effects (EASSE)", PWRI Newsletter No. 67, Jan. 1997
- 6) Shun-etsu ODAGIRI, Hideki SUGITA et al, "Development of Real-time Seismic Information System for MOC", Proceedings of the 29th Joint Meeting of U.S.-Japan Panel on Wind and Seismic Effects, UJNR, May 1997

Table 1.1 Example of SISs developed in Japan

Sytem Name	Organization	Monitoring	Damage Estimation	Emergency Response	Activity Support	Inputs	Notes
Disaster Information System	National Land Agency		○		○	JMA Seismographs	DIS
Rial-time Earthquake Damage Estimation System	Ministry of Construction	○	○			Seismograph	SATURN
Strong Motion Observation Network	Natl. Research Inst. for Earth Science and Disaster Prevention, Science and Technology Agency	○				Seismograph	K-net (Kyoshin-net)
Strong Motion Observation Network	Japan Meteorology Agency	○				Seismograph	
Seismic Intensity Observation Network	Fire-Defense Agency	○				Seismograph for Seismic Intensity	
Simple Earthquake Disaster Estimation System	Fire-Defense Agency		○			Seismic Conditions	
Seismograph Information System	Hokkaido Dev. Bureau	○				Seismograph	WISE
Earthquake Disaster Estimation System	Tokyo Fire Department	○	○			Seismograph	
Earthquake Disaster Countermeasure Support System	Kawasaki City	○	○		○	Seismograph	
Dense Array Strong Motion Monitoring Network	Yokohama City	○				Seismograph	
Seismograph Network	Tokyo Metro. Government	○				Seismograph	
Phonics Disaster Prevention System	Hyogo Prefecture	○	○		○	Seismograph	
Yokohama-city Disaster Prevention Information System	Yokohama City	○				Other Systems	
Disaster Image Transmitting System	Yokohama City	○				TV Camera	
UrEDAS/HERAS	Japan Railway	○	○	○		Seismograph	
Seismograph Network	Japan Highway Public Corporation	○				Seismograph	
Seismic Information Gathering and Network Alert System	Tokyo Gas	○	○	○		Seismograph, SI sensor, Liquefaction sensor	SIGNAL

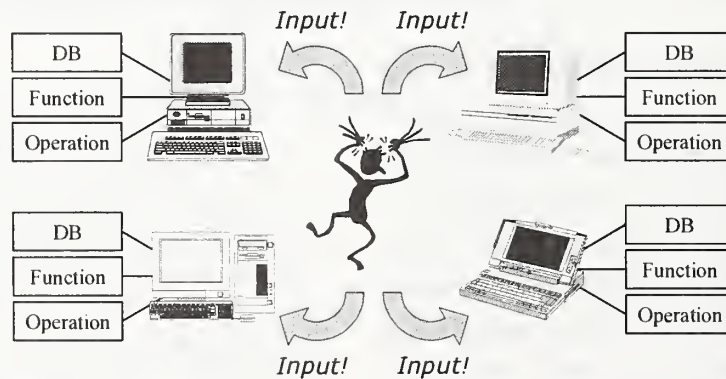


Figure 1.1 Isolated SISs

New Developments in Seismic Risk Analysis for Highway Systems

by

Stuart D. Werner¹, Craig E. Taylor², James E. Moore II³,
John B. Mander⁴, John B. Jernigan⁵, and Howard H. M. Hwang⁶

ABSTRACT

This paper summarizes current research to develop a new seismic risk analysis (SRA) procedure for highway and roadway systems. The procedure synthesizes geoseismic, engineering, network, and economic models to assess earthquake effects on system-wide traffic flows and travel times. The SRA results provide an improved basis for prioritizing highway components for seismic retrofit, and for defining seismic performance requirements for these components.

KEY WORDS: earthquake, seismic, risk, highways, roadways, bridges, hazards, system, network

1. INTRODUCTION

Past experience has shown that earthquake damage to highway components (e.g., bridges, roadways, tunnels, retaining walls, etc.) can severely disrupt traffic flows and this, in turn, can impact the economy of the region as well as post-earthquake emergency response and recovery. Furthermore, the extent of these impacts will depend not only on the seismic response characteristics of the individual components, but also on the characteristics of the highway system that contains these components. System characteristics that will affect post-earthquake traffic flows include: (a) the highway system network configuration; (b)

- locations, redundancies, and traffic capacities and volumes of the system's links between key origins and destinations; and (c) component locations within these links (e.g., Moore et al, 1997).

From this, it is evident that earthquake damage to certain components (e.g., those along important and non-redundant links within the system) will have a greater impact on the system performance (e.g., traffic flows) than will other components. Unfortunately, such system issues are typically ignored when specifying seismic performance requirements and design criteria for new and existing components; i.e., each component is usually treated as an individual entity only, without regard to how its damage may impact highway system performance. Furthermore, current criteria for prioritizing bridges for seismic retrofit represent the importance of the bridge as a traffic-carrying entity only by using average daily traffic count, detour length, and route type as parameters in the prioritization process. These criteria do not account for the systemic effects associated with the loss of a given bridge, or for combinatorial effects associated with the loss of other bridges in the highway system. However, consideration of these systemic and combinatorial effects can provide a much more rational basis for establishing seismic retrofit priorities and performance requirements for highway components.

¹Seismic Systems & Engineering Consultants, 8601 Skyline Blvd., Oakland CA 94611

²Natural Hazards Management Inc., 5402 Via del Valle, Torrance CA 90505

³University of Southern California, 3518 Trousdale Parkway, Los Angeles CA 90089

⁴State University of New York at Buffalo, 230 Ketter Hall, Buffalo NY 14260

⁵Ellers, Oakley, Chester, & Rike, 5100 Poplar Avenue, Suite 1600, Memphis TN 38137

⁶University of Memphis, 3890 Central Avenue, Memphis TN 38152

In recognition of these issues, the National Center for Earthquake Engineering Research (NCEER) has included system seismic risk analysis (SRA) in its current six-year seismic research project entitled "Seismic Vulnerability of Existing Highway Construction." This paper describes the SRA research being conducted under the NCEER project including: (a) a new SRA procedure that has been developed under the project; (b) an initial demonstration application of the procedure to the Memphis Tennessee highway system; (c) current research to further develop the procedure; and (d) the applicability of the procedure for real-time post-earthquake loss estimation.

2. SEISMIC RISK ANALYSIS PROCEDURE

2.1 General Description

The highway system SRA procedure is shown in Figure 1. It can be carried out for any number of scenario earthquakes and simulations, in which a "simulation" is defined as a complete set of system SRA results for one particular set of input parameters and model uncertainty parameters. The model and input parameters for one simulation may differ from those for other simulations because of random and systematic uncertainties (Werner et al., 1996).

For each earthquake and simulation, this multi-disciplinary procedure uses geoseismic, geotechnical and structural engineering, transportation network analysis, and economic evaluation models to estimate: (a) earthquake effects on system-wide traffic flows (e.g., travel times, paths, and distances); (b) economic impacts of highway system damage (e.g., repair costs and costs of travel time delays); and (c) post-earthquake traffic flows along vital roadways (to facilitate emergency response planning). Key to this procedure is a modular GIS data base that contains the data and models needed to implement the system SRA.

This SRA procedure has several desirable features. First, it has a GIS framework, to enhance data management, analysis efficiency,

and display of analysis results. Second, the GIS data base is modular, to facilitate the incorporation of improved data and models from future research efforts. Third, the procedure can develop aggregate SRA results that are either deterministic (consisting of a single simulation for one or a few scenario earthquakes) or probabilistic (consisting of many simulations and scenario earthquakes). This range of results facilitates the usefulness of SRA for a variety of applications (e.g., seismic retrofit prioritization and criteria, emergency response planning, planning of system expansions or enhancements, etc.). Finally, the procedure uses rapid engineering and network analysis procedures, to enhance its future use as a real-time predictor of system states and traffic impacts shortly after an actual earthquake.

2.2 GIS Data Base

The GIS data base consists of four modules with data and models that characterize the system, seismic hazards, component vulnerabilities, and economic impacts of highway system damage. To facilitate analysis efficiency, these modules are pre-processors to the four-step SRA procedure shown in Figure 1.

2.2.1 System Module

The system module contains the following information to characterize the highway system, as provided by transportation and urban planning specialists:

System Data – including: (a) system network configuration linkages, and component types and locations; (b) numbers of lanes, traffic flows, capacities, and congestion functions for each roadway link; (c) origin-destination zone locations and trip tables; and (d) any special system characteristics, such as certain roadways being critical for emergency response or national defense.

Traffic Management – including measures by transportation authorities for modifying the system to ease post-earthquake traffic flows

(e.g., detour routes, modifications of roadways from two-way to one-way traffic, etc.)

Transportation Network Analysis Procedures – to estimate post-earthquake traffic flows for each simulation and scenario earthquake.

2.2.2 Hazards Module.

The hazards module contains input data and models provided by geologists and geotechnical engineers for characterizing system-wide ground motion, liquefaction, landslide, and surface fault rupture hazards. Input data include: (a) the ensemble of scenario earthquake events developed during the initialization phase of the SRA (Sec. 3.1); (b) locations and topographic data for slopes within the system that could be prone to landslide; and (c) local soil conditions throughout the system, as needed to estimate local geologic effects on ground shaking and the potential for liquefaction and landslide. Models contained in the hazards module will estimate: (d) the attenuation of rock motions with increasing distance from the earthquake source, for a range of earthquake magnitudes; (e) the effects of local soil conditions on the motions at the ground surface; and (f) permanent ground displacements due to earthquake-induced landslide, liquefaction, and surface fault rupture. A deterministic representation of hazards models will use mean values of these quantities. A probabilistic representation will use probability distributions to account for uncertainties in the seismologic, geologic, and soil input parameters and in the hazard evaluation models.

2.2.3 Component Module

The component module contains input data and models provided by structural and construction engineers to characterize each component in terms of a “loss model” and a “functionality model”. The loss model represents the component’s direct losses (i.e., repair costs), and the functionality model represents its “traffic states” (i.e., whether the component will be partially or completely closed to traffic

during the repair of the earthquake damage, the durations of these closures, and speed limits for traffic along the component during repair). Both models are a function of the level of ground shaking at the component’s site, as well as the level of permanent ground displacement due to liquefaction, landslide, or surface fault rupture. The models for each component are developed by evaluating: (a) its seismic response to each designated level of ground shaking and permanent ground displacement; (b) its “damage state”, (i.e., the degree, type, and locations of any earthquake damage to the component); (c) its damage repair procedures; and, from this (d) its traffic states at various times after the earthquake (to reflect the rate of traffic restoration as repairs proceed).

After each component’s traffic states are obtained, they are incorporated into the highway system network model to obtain the overall “system state”, i.e., the ability of each link in the system to carry traffic at various times after the earthquake (in terms of number of open lanes, speed limits, etc.). These system states will reflect the effect of each component’s damage state on adjacent and underlying roadways. This, of course, will also depend on the location of the component within the overall system, as well as system network characteristics.

A deterministic representation of loss and functionality models will use mean values of the component repair costs and traffic states. A probabilistic representation will use probability distributions to account for uncertainties in the evaluation of the component seismic response, and in the estimation of the resulting repair costs and traffic states.

2.2.4 Socio-Economic Module

The socio-economic module contains models and data for evaluating broader social and economic impacts of earthquake-induced traffic flow disruptions. These impacts can include indirect dollar losses (e.g., to commuters and businesses), effects on emergency response (e.g., reduced access to medical, police, fire-

fighting, airport, government centers, etc.), and societal effects (e.g., reduced access to residential areas, shopping areas, etc.). This module is developed by transportation specialists, urban planners, and economists.

3. ANALYSIS PROCEDURE

3.1 Step 1: Initialization of Analysis

The initialization of the SRA (Step 1) contains two parts. First, regional earthquake source models are used to define an ensemble of scenario earthquakes, in which each earthquake is most commonly defined in terms of its magnitude, location, and frequency of occurrence. Uncertainties in defining the values of the various earthquake input parameters may also be modeled at this stage. The second part of Step 1 establishes the total number of simulations for each scenario earthquake, as further described in Werner et al. (1996).

3.2 Step 2: Development of Each Simulation for Each Scenario Earthquake

Under Step 2, the following evaluations are carried out to develop each of the simulations for each scenario earthquake:

Hazard Evaluation. First, the data and models contained in the hazards module are used to estimate the earthquake ground motions and geologic hazards throughout the system.

Direct Loss and System State Evaluation. Once the hazards are estimated, the data and models from the component module are used to evaluate direct losses and system states (defined at various times after the earthquake).

Traffic Flow Evaluation. The system data and transportation network analysis procedure from the system module are applied to the pre-earthquake system and post-earthquake system states, to assess earthquake effects on system-wide travel times, travel distances, and travel paths, as well as traffic flows along roadways vital to emergency response.

Socio-Economic Impact Evaluation. Once the earthquake effects on traffic flows within the system are evaluated, the data and models from the socio-economic module are used to evaluate impacts of the impeded traffic flows in terms of: (a) indirect dollar losses; and (b) reduced access to and from emergency response centers.

3.3 Step 3: Incrementation of Simulations and Scenario Earthquakes

Under Step 3, the evaluations from Step 2 are repeated, in order to develop multiple simulations for multiple scenario earthquakes (if the SRA is to be probabilistic).

3.4 Step 4: Aggregate System Analysis Results

This final step in the SRA process is carried out after the system analyses for all simulations and scenario earthquakes have been completed. In this step, the results from all simulations and earthquakes are aggregated and displayed. Depending on user needs, these aggregations could focus on the seismic risks associated with the total system or with individual components. Furthermore, the system or component results could be provided: (a) for individual simulations, which is termed a seismic vulnerability analysis, and/or (b) for the broader (probabilistic) range of simulations, leading either to loss statistics (e.g., average annualized loss) or to loss distributions that show the severity of earthquake-induced system losses for different probability levels⁷. For research purposes, the impacts of incorporating uncertainties into the SRA will be of considerable interest. For other purposes, such as the planning of seismic strengthening programs for existing highway systems, outputs can be adapted and/or simplified to meet the particular requirements of each user audience.

⁷The "loss" can be defined in several ways, such as direct repair cost, travel time delays due to earthquake damage (between certain key origin-destination zones or aggregated over all zones), indirect losses due to travel time delays, or other adverse consequences.

4. DEMONSTRATION ANALYSIS

4.1 Objective and Scope

Early in the NCEER Highway Project, the SRA procedure was used with then-available data and models to carry out a demonstration SRA of the Memphis, Tennessee highway-roadway system (Fig. 2). The objective of the analysis was to: (a) illustrate the application of the SRA procedure, and the types of results that can be obtained; and (b) provide a basis for identifying and prioritizing research needs to improve the procedure. Because of limitations in many of the then-available data and models, the results from this SRA are preliminary. Nevertheless, it is of interest to briefly summarize this SRA, in order to illustrate the applicability of the procedure. This SRA application is described in more detail by Werner and Taylor (1995).

4.2 Assumptions

The Memphis highway-roadway system is shown in Figure 2. This demonstration SRA consisted of deterministic analysis of the response of this system to four different earthquake events (Fig. 3a). This paper presents results from one of these earthquakes, termed Earthquake D, which has a moment magnitude of 5.5 and is centered about 35 km to the north of the northern segment of the beltway that surrounds the city of Memphis. Assumptions for this SRA are summarized below.

4.2.1 System Input Data

The system's network configuration was obtained from the University of Memphis. Traffic data, roadway traffic capacities, and O-D zones within the system were provided by the Memphis and Shelby County Office of Planning and Development (OPD). The traffic flow data were from their 1988 traffic forecasting model.

4.2.2 Network Analysis Procedure

The MINUTP traffic forecasting software (Comsis, 1994) was used to analyze pre- and

post-earthquake traffic flows. This software was chosen because it is used at the Memphis-Shelby County OPD, and all regional traffic data were available in the input format for this software. MINUTP is based on the Urban Transportation Planning System (UTPS), which was developed over two decades ago by the U.S. Dept. of Transportation (see Sec. 5.5.1). Also, the then-available version of MINUTP was not GIS-compatible, which increased the effort needed for our system analysis.

4.2.2 Seismic Hazards

The system-wide ground shaking due to Earthquake D was represented in terms of peak ground acceleration (PGA), and was based on soil conditions obtained from prior local geologic mapping by the University of Memphis (Fig. 3b). The PGA at each bridge site was estimated by: (a) computing site-specific bedrock accelerations by using an early version of the Hwang and Huo (1997) attenuation equation; and (b) applying the Martin and Dobry (1994) soil amplification factors to these rock accelerations, to obtain corresponding ground surface PGAs that include effects of local soil conditions (Fig. 4).

4.2.3 Bridge Loss Models

Loss models previously developed under the ATC-25 project for conventional highway bridges were used to estimate direct losses for each bridge in the system due to each earthquake (ATC, 1991). In these models, the direct losses depend only on whether the bridge has simple spans or is continuous/monolithic; i.e., other bridge structural attributes that could impact seismic performance are not considered.

4.2.4 Bridge Functionality Models

Functionality models for this demonstration SRA represented bridge traffic states as the number of lanes open at discrete times after an earthquake, as a function of PGA and the original number of lanes along the bridge. They were developed by modifying ATC-25 bridge

restoration models based on prior observations of the seismic performance and repair and reconstruction processes for California bridges during the Loma Prieta and Northridge Earthquakes (Werner and Taylor, 1995). Two different models were developed in accordance with the ATC-25 conventional highway bridge designations -- one for simple-span bridges and one for continuous bridges. In addition, to illustrate effects of bridge damage repair rates on post-earthquake system performance, functionality models were developed for two discrete times -- three days and six months after the earthquake.

4.2.5 Economic Model

Studies of economic impacts of earthquake-induced highway system damage have shown that indirect dollar losses due to such damage can far exceed the direct losses for repair of the damage (e.g., Gordon and Richardson, 1996). However, methods for estimating such impacts for future earthquakes are not yet well developed. Therefore, for this demonstration SRA, a simplified procedure from BAA (1994) was used to estimate costs due to deterioration in commute time only. These cost estimates are based on vehicle-hours of delay (as obtained from the MINUTP system analyses), corresponding person-hours of delay (based on an assumed average vehicle occupancy rate of 1.4 persons/vehicle), truck-hours of delay (assuming 30 percent of the vehicles are trucks), and excess fuel costs due to travel time delays.

4.3 RESULTS

4.3.1 Direct Losses

In accordance with the ATC-25 model used in this demonstration SRA, direct losses due to damage to the system's bridges are represented as a damage ratio, DMG (%), which is defined as the ratio of the repair cost for each bridge to its total replacement cost. For Earthquake D, the average damage ratio (averaged over all of the 286 bridges in the system) was 37.4%.

4.3.2 Travel Times and Distances

System State Results. Figure 5 shows the pre-earthquake system state and post-earthquake system states at times of three days and six months after Earthquake D. This figure indicates that, although Earthquake D has only a moderate magnitude ($M_W = 5.5$), its proximity to the northern segment of the Memphis highway system causes extensive roadway closures in that segment, with lesser impacts on other segments of the system.

Total System-Wide Travel Times. Table 1 contains the total pre- and post-earthquake travel times and distances for the Memphis highway system. This table shows that the modified system states due to Earthquake D result in a total system-wide travel time three days after the earthquake that is nearly 34 percent longer than the pre-earthquake values. At six months after the earthquake, the bridge repairs within that time have reduced the total travel time; however it is still nearly 20 percent longer than the pre-earthquake value.

Total System-Wide Travel Distances. Table 1 shows that the total system-wide travel distances at times of three days and six months after the occurrence of Earthquake D are not sensitive to the modified system states. This trend may be due to the significant loss of service along the faster but less direct highway segments at the north and northeastern portions of the beltway, because of the many damaged bridges along those segments. As a result, drivers would be forced to use ground surface routes with fewer damaged bridges that are shorter but slower than the beltway routes.

O-D Zone Travel Times. Table 2 shows that, at a time of three days after the earthquake, the travel times between the O-D zones listed in the table are, on the average, nearly 16 percent larger than those for the pre-earthquake system. The travel time increases are largest for northernmost of the highlighted zones, which are at Shelby Farms (Zones 249 and 252), Bartlett (Zone 264), and the Covington Pike

(Zone 274). This is because, as previously noted, it is this section of the Memphis area highway and roadway system that is most severely damaged. At a time of 6 months after the earthquake, Table 2 shows that the travel times to and from these zones have been reduced substantially, and are now only 5.3 percent larger than the pre-earthquake values.

O-D Zone Travel Distances. The travel distances to and from the O-D zones listed in Table 2 are insensitive to system damage from Earthquake D (Werner and Taylor, 1995).

Economic Impacts. Estimates of economic impacts for times of both three days and six months after the earthquake are shown in Table 3. They are based on total system-wide travel time delays per 24-hour day of 126,000 vehicle-hours and 73,000 vehicle-hours at times of three days and six months after the earthquake respectively (as previously shown in Table 1). From this, the BAA (1994) cost estimation procedure leads to a total cost per day of the earthquake-induced time delays of \$1.6 million at three days after the earthquake, and \$930 thousand at six months after the earthquake. We then estimated the total time delay costs over a one-year time period after Earthquake D, by assuming an average daily time-delay cost for the year of \$930 thousand (which corresponds to the above daily cost at a time of six months after the earthquake). From this, the total cost of the system-wide time delays over this one-year time period was computed to be $365 \text{ days} \times \$930,000 = \$340 \times 10^6$.

5.0 NEW DEVELOPMENTS

Since the above demonstration SRA was carried out, there have been significant further developments and improvements to the procedure. The improved procedure will be used in a re-analysis of the seismic risks to the Memphis highway-roadway system that is planned later during this year (1998). This analysis will be probabilistic, using multiple scenario earthquakes and simulations.

The new developments to the SRA procedure have focused on the establishment of improved models for: (a) multiple scenario earthquakes; (b) ground shaking and liquefaction hazards; (c) bridge vulnerability modeling; and (d) transportation network analysis. These new developments are summarized in the remainder of this section.

5.1 Scenario Earthquakes

In a SRA of a system with spatially dispersed components, individual scenarios are required to evaluate correlation effects of earthquakes, i.e., the simultaneous effects (including systemic consequences of damages) of individual earthquakes on components located at diverse sites. Scenario earthquake models for our SRA procedure for highway systems are based on an adaptation of work by Frankel et al. (1996) for the Central and Eastern United States (CEUS), as part of the United States Geological Survey (USGS) National Hazard Mapping Program.

The Frankel et al. work for the CEUS uses four different spatially smoothed models based on historical seismicity data, plus a special model for the New Madrid Seismic Zone (NMSZ). Our adaptation of these models is summarized in Sections 5.1.1 and 5.1.2.

5.1.1 Historical Seismicity Models

For developing scenario earthquakes for our SRA of the Memphis highway-roadway system, we have defined a large seismicity zone around Memphis that extends from 88.0 to 92.0 degrees longitude and from 34.0 to 38.0 degrees latitude. This zone has been divided into small microzones, with dimensions of about 11.1 km in both length and width.

Three different models are weighted to establish the earthquake activity within each microzone, based on historical seismicity data from a USGS catalogue that is an updated and improved version of the Seeber-Armbruster (1991) earthquake catalogue. These models are developed from earthquakes with the following

magnitude cutoffs and completeness times: (1) magnitude 3+ earthquakes since 1924; (2) magnitude 4+ earthquakes since 1860; and (3) magnitude 5+ earthquakes since 1700. In addition, Frankel et al. include a fourth model (Model 4) that is a large background seismicity model that applies to the entire seismicity zone, and is weighted with the above three models to establish earthquake activities.

The number of earthquakes shown in the USGS catalog to exceed the respective minimum magnitude of Models 1 through 3 respectively is counted and, based on the starting and end date of the model (e.g., 71 years for Model 1), is converted to a frequency of occurrence. Then, to account for uncertainties in the locations of these earthquakes, a relatively flat gaussian model is applied that redistributes and smooths the earthquake locations among the microzones. Given this redistribution of earthquake occurrences for each of Models 1-3, and assuming a threshold magnitude of 5.0 for the onset of earthquake damage, a "b" value of 0.95 in the Richter magnitude-frequency relationship is assumed (derived elsewhere) to estimate the frequency of occurrence of earthquakes with magnitude ≥ 5.0 in each microzone (for each of these models). For Model 4, a uniform distribution is used to allocate potential earthquakes with magnitudes ≥ 5.0 among all of the microzones.

Based on a method of adaptive weighting, we followed Frankel et al. in combining the four above-mentioned models in order to derive frequencies of occurrence of earthquakes of magnitude ≥ 5.0 in each microzone. Next, we summed these frequencies to determine the corresponding frequency of occurrence within the overall seismicity zone. Using this frequency and the frequencies in each microzone, we then developed a conditional cumulative probability matrix for the overall seismicity zone. This two-column matrix contains microzones (numbered) in one column, and cumulative conditional probabilities (from 0 to 1) in the other column. In addition, we used a

Poisson model to convert the frequency of occurrence of earthquakes with magnitudes ≥ 5.0 in the overall seismicity zone to a corresponding probability of occurrence.

At this stage, a natural way to develop these scenarios for purposes of analyzing system performance and for eventually compiling information on loss distributions and their variability over a time dimension is to employ a "walk-through" analysis. (Daykin et al., 1994). The first step in such an analysis is to select an appropriate time frame over which the analysis would be carried out (e.g., one or more time frames of 10 years, 50 years, 100 years, etc.). Then, for each year in each time frame (starting with Year 1 and then repeating the process for each successive year), successive uniform random number generators are applied with the appropriate cumulative conditional probability distribution to evaluate: (a) whether or not at least one earthquake of magnitude ≥ 5.0 has occurred somewhere in the large seismicity zone during the year; (b) if so, whether or not a second earthquake has occurred in the zone during the year; and (c) for each earthquake that has occurred in the zone during the year, the microzone where the earthquake is located. We also use a random generation technique to estimate the earthquake magnitude, with the likelihood of diverse magnitude levels assumed to be represented by a Richter (lognormal) magnitude-recurrence relationship.

5.1.2 New Madrid Fault Zone

For modeling the New Madrid fault zone while the Frankel et al. approach was undergoing modifications, we have initially followed earlier USGS procedures described by Leyendecker et al. (1995). In this, we have: (a) modified the Der Kiureghian et al. (1977) approach to distribute earthquake occurrences within the fault zone; (b) applied estimates of the frequency of occurrence for earthquakes in the zone based on the Frankel et al. approach and other relevant studies, and converted these to probabilities of occurrence using a Poisson

model; and (c) postulated that the fault zone is comprised of four parallel linear faults.

Following this, a walk-through analysis is used to develop a random sequence of earthquakes occurring within the zone during the time period of interest. To illustrate, let us assume that the probability of occurrence of an earthquake with a given magnitude (say magnitude 8.0) within the New Madrid fault zone is 0.002. From this, the walk-through process for each year involves the use of successive random number generators to indicate: (a) whether an earthquake of this magnitude has occurred within the fault zone; and (b) if so, which of the four fault traces is the source of the earthquake. Then, subsequent steps involve: (c) estimation of the rupture length along the fault trace, using the Wells-Coppersmith (1994) relationship between rupture length and earthquake magnitude and including a normally distributed uncertainty factor (in log space) with a standard deviation of 0.22; and (d) estimation of the location of the rupture length within the overall fault trace, by using a polar method to generate a normally distributed uncertainty factor in log space (Law and Kelton, 1991)⁸.

The results of this walk-through analysis of earthquakes occurring within the New Madrid fault zone are combined with the results of the walk-through analysis of potential earthquakes from the historical seismicity models (Sec. 5.1.1) to estimate the total earthquake activity during each year of the time frame of interest.

5.1.3 Current Status

The above approach has been used to develop an initial set of scenario earthquakes for the Memphis area. The modeling assumptions leading to these earthquakes are now being

reviewed, prior to our developing a final set of scenario earthquakes for our forthcoming SRA of the Memphis highway-roadway system.

5.2 Ground Motion Hazards

The ground motion hazards for our updated SRA of the Memphis highway-roadway system will be represented as five-percent damped ground response spectra at the ground surface. The estimation of these spectra for a particular site will involve: (a) use of a rock motion attenuation relationship to estimate spectral amplitudes of rock motions; and (b) application of soil amplification factors to these rock motion spectra, to develop corresponding spectra of motions at the ground surface that incorporate effects of local soil conditions.

For our SRA of the Memphis highway-roadway system, we will be using: (a) the Hwang and Huo (1997) rock motion attenuation relationships for peak acceleration and for spectral accelerations over a wide range of natural periods; and (b) the Hwang et al. (1997) soil amplification factors for NEHRP site classifications A through E. These procedures have the following benefits: (a) they are internally consistent, i.e., they are intended for use together to compute ground surface peak accelerations and spectral accelerations (as the product of the Hwang and Huo rock motions and the Hwang et al. soil amplification factors); (b) they specifically focus on anticipated CEUS ground shaking characteristics; (c) the Hwang and Huo rock motion attenuation relationships compare well with other well-established relationships for the CEUS; (d) the Hwang et al. soil amplification factors are developed from state-of-the-practice analytical procedures; and (e) effects of uncertainties in various input parameters are considered.

5.3 Liquefaction Hazards

The treatment of liquefaction hazards within the multi-scenario framework of the SRA procedure involves the following steps: (a) compilation of soils data for the region; (b) for a given scenario

⁸In this, the difference between the rupture length and the total length of the fault is computed, and a uniform random number generator is used to indicate where the fault rupture is initiated relative to one end of the fault trace.

earthquake and simulation, evaluation of the potential for liquefaction throughout the highway-roadway system, including estimation of permanent ground displacements; and (c) estimation of traffic states at bridges and along roadways within the system due to these ground displacements. Our plans for carrying out these steps in our SRA of the Memphis highway-roadway system are summarized below.

5.3.1 Soils Data

Under a prior project carried out at the Center for Earthquake Research and Information (CERI) of the University of Memphis, data from 8,500 boring logs throughout Shelby County were compiled by Ng et al. (1989). Ng et al. then divided the county into a series of cells with dimensions of about 2,500 ft. by 3,000 ft., and used the data from the boring logs to develop the following information for those cells where boring logs were available: (a) estimated average values SPT blowcounts, natural soil density, and unconfined compressive strength for each soil layer, as well as ground surface elevation, and groundwater level; and (b) development of a representative soil log for the cell. A GIS data base containing these data has been made available by CERI for use in our SRA of the Memphis highway-roadway system. For those cells, where no data were available, soil properties have recently been estimated using data from the nearest cells with soils of the same geologic unit (Hwang and Lin, 1997). It is noted that CERI is currently updating this data base; however this updated data base will not be completed and available for use until early 1999.

5.3.2 Hazard Evaluation Procedure

Evaluation of the potential for liquefaction hazards to the Memphis highway-roadway system for a given scenario earthquake event will be carried out only for those cells that contain bridges and/or roadways within the system. This evaluation will consist of the following steps, which generally follow the approach by Youd and Gummow (1995):

Initial Screening. An initial screening of soils and geologic will be carried out to initially establish which cells in the system have a low potential for liquefaction and therefore can be eliminated from further analysis. Our initial screening efforts will be guided by prior liquefaction evaluations of the Memphis area by Hwang and Lin (1997) for earthquakes of magnitudes 6.5, 7.0, and 7.5 centered in Marked Tree, Arkansas.

Further Screening. For those cells shown by the initial screening to have a potential for liquefaction, further screening will be carried out through very simplified and conservative assessment of the range of possible ground shaking hazards in the cell due to the various scenario earthquakes for the SRA, in order to eliminate additional cells shown by this further screening to have a low liquefaction potential.

Seed-Idriss Procedure. For those cells that are still shown to have a potential for liquefaction, the Seed-Idriss (1982) procedure will be used for a final evaluation of liquefaction potential.

Permanent Ground Displacement. For the cells shown from the above steps to have potentially liquefiable soils, permanent ground displacements will be estimated as follows: (a) for bridge or roadway sites with gently sloping ground or a free face condition, the Bartlett-Youd (1995) procedure will be used to estimate lateral spread displacements; and (b) the Tokimatsu-Seed (1987) procedure will be used to estimate vertical settlements.

5.3.3 Liquefaction Effects on Traffic States

Estimation of the effects of liquefaction on traffic states along the bridges and roadways within the Memphis highway-roadway system will be based on analysis of: (a) empirical data compiled by Youd (1997) that describes bridge damage modes due to liquefaction-induced ground displacement for 116 bridges during earthquakes in the United States, Costa Rica, and Japan; and (b) liquefaction maps for the San Francisco Bay Area due to the 1989 Loma Prieta Earthquake that are now being completed at the USGS; and (c) a data base of liquefaction-induced road closures in the Bay Area following the Loma Prieta Earthquake (ABAG, 1997).

5.4 Bridge Modeling

5.4.1 Background

Essential to the SRA process is the incorporation of models for estimating bridge damage states and traffic states. This section describes candidate bridge models now under development.

Damage-state modeling of individual bridges can be carried out using conventional structural analysis tools that employ either the Capacity/Demand or Lateral Strength (pushover) methods of analysis, as described in the FHWA (1995) Retrofit Manual. However, application of these methods would lead to an intractable task if applied to each of the large number of bridges that will comprise a highway-roadway system. Therefore, any analysis tools that are used for bridge damage-state modeling for highway system SRA must be rapid and efficient to implement. In addition, to increase efficiency of the damage-state modeling process, we are exploring the feasibility of developing damage-state models for bridge groups rather than individual bridges (where each group would consist of bridges with certain similar attributes important to seismic response). To enhance analysis efficiency, the damage-state models (for individual bridges or groups) will be developed in a pre-processor to the main SRA procedure

As an option to the use of analytical models, an alternative damage-state modeling approach is the use of empirical models developed from experiential observations. However, the principal problems with such models are: (a) they use vague damage descriptors such as "slight", "moderate" or "extensive" that neither account for the post-earthquake serviceability of bridges nor provide a clear basis for estimating post-earthquake repair costs and traffic states; and (b) they are mostly based on California bridges, whose structural characteristics are often very different from those for the stock of bridges found elsewhere in the United States. These two reasons negate the use of empirical modeling techniques by themselves. However, empirical observations of the actual performance of bridges

during past earthquakes will, of course, provide a valuable basis for validating analytical bridge damage state models that are developed.

For these reasons, it is our view that analytical procedures are the methods of choice for developing bridge damage-state models for highway system SRA. In this, alternative models with differing degrees of refinement will be incorporated into the component module, in which the selection of one of these models for a particular SRA application would depend on such factors as available bridge data, bridge characteristics, etc. Results from these models will then be used with expert-opinion and empirical information in order to estimate bridge traffic states due to each damage state.

With this as background, the remainder of this section is organized into three main parts. Section 5.4.2 describe one damage-state modeling approach that is being developed specifically for use with highway-roadway system SRA -- the "rapid-pushover" method by Mander and Dutta (1997). Following this, Section 5.4.3 summarizes other candidate damage-state modeling methods that are being developed under the NCEER Highway Project or other research programs. Finally, Section 5.4.4 summarizes our plans for developing bridge and roadway traffic states, once the damage states are established.

5.4.2 Rapid-Pushover Method

The rapid-pushover method (Mander and Dutta, 1997) is a new non-linear static (pushover) procedure for rapid estimation of bridge damage states. It accounts for the contributions of the piers and the arching (3D) action of the deck to the total base-shear capacity of the bridge system.

Deck Contribution. The contribution of the deck to the bridge system's total base shear capacity has been systematically overlooked in most capacity analyses. This contribution is due to the resistance of the deck resulting from plastic moments that are mobilized by the bearings working as a group. This action occurs because, as the deck rotates, there also occurs some lateral

displacement which is resisted by frictional forces arising in each bearing. Mander and Dutta (1997) have evaluated this effect for bridges with multiple simply-supported spans and with continuous spans. For these cases, a plastic mechanism analysis is used to establish the deck capacity as the lowest capacity of all possible postulated failure mechanisms. These failure mechanisms incorporate the geometry of the deck spans, the relative flexibility of the pier bents, and resistance and the capacities of the bearings.

Pier Contribution. Under longitudinal or transverse excitation, a bridge pier is presumed to display a marked degradation of strength capacity as the earthquake shaking proceeds. The magnitude and rate of the strength decay will depend upon the design details at or near the potential plastic hinge zones -- particularly connection details such as lap splices and anchorage zones -- and the shear capacity of the columns and the column-to-cap connections. Although sophisticated energy-based evaluation techniques are available for evaluating these sources of strength decay, a more simplified displacement-based method of analysis is instead proposed, in order to increase the speed and efficiency of the evaluation process. This method uses a simplified strength decay model for the bridge pier, in which the total pier capacity is assumed to consist of: (a) diagonal strut (or arch) action which constitutes the concrete resistance; and (b) resistance contributions arising from the longitudinal and transverse reinforcing steel. Mander and Dutta (1997) suggest that these contributions to the pier capacity can be simply expressed in terms of geometric factors alone, many of which may be obtained (or inferred) from existing Bridge Management System data bases.

Discussion of Rapid-Pushover Method. This method is a rapid yet technically rational approach for developing bridge capacity spectra. Furthermore, the capacity spectra include various displacement thresholds that each represent the onset of a new damage state. Each of these damage states are physically defined so as to facilitate their interpretation during subsequent estimation of bridge traffic states. For example,

depending on a bridge's geometry and detailing, various damage states may be defined in terms of: (a) first yield; (b) the onset of cracking and spalling; (c) loss of anchorage; (d) concrete failure; (e) pier damage or collapse, due to such causes as splices in plastic hinge zones or inadequate transverse or longitudinal reinforcement; (f) deck unseating; (g) bearing failure; and (h) abutment backwall failure. In addition, although the rapid pushover method has been formulated as a deterministic approach, procedures are being studied that would extend it to be probabilistic as well, in which model and material property uncertainties are represented.

Capacity-Demand Resolution. Once the capacity spectrum is developed, a capacity-demand analysis is carried out to determine each bridge's damage state for a given scenario earthquake and simulation. The first step in this process is to establish the demand spectrum at the bridge site by adjusting the five-percent damped site-specific ground-response spectrum at each bridge site to account for increased effective damping due to increased yielding and damage to the bridge as the level of displacement increases. Then, the damage state for the given scenario earthquake and simulation is taken to correspond to that damage state within which the demand and capacity spectra intersect. This is determined analytically by computing the difference between demand vs. capacity base shear coefficients at displacement levels that represent the onset of each successive damage state, and then identifying the damage state where the sign of the difference first changes.

Current Status. Although the basic framework of the rapid-pushover method is established, it is still under development to incorporate such phenomena as effects of bridge skew, foundation damage modes, etc. In addition, the method is currently being validated through its application to actual bridges that have been subjected to earthquake shaking and have well-established seismic response characteristics. It is noted that a simplified version of the rapid-pushover method is currently under development for enhancing the transportation lifeline module in HAZUS (Basoz and Mander, 1998).

5.4.3 Other Damage State Models

This section briefly summarizes other candidate bridge damage state models. One model is being developed specifically for application to the large Mississippi River crossings in Memphis (Liu, 1997). The other models are presented as possible options or supplements to the rapid pushover method. These include modeling procedures currently being developed by Jernigan and Hwang (1997) and by Shinozuka (1998).

Major Bridges. The rapid-pushover method and the other bridge modeling methods described below would be applied to all bridges in the Memphis highway-roadway system, except the two large steel bridges that cross the Mississippi River along Interstate Highways 40 and 55. For these major bridges, capacity spectra will be developed from results of a prior detailed seismic vulnerability analysis of the Interstate 40 river crossing, and from an approximate assessment of the Interstate 55 river crossing, which has not yet been subjected to a detailed seismic vulnerability evaluation (Liu, 1997).

Jernigan and Hwang (1997). In an ongoing study to develop damage state fragility curves for the 452 bridges within the highway-roadway system in Memphis and Shelby County, Tennessee, Jernigan and Hwang (1997) are applying the capacity-demand method described in the FHWA (1995) seismic retrofit manual. This study has consisted of the development of a GIS data base of structural attributes for these bridges, a grouping of bridges according to superstructure and substructure characteristics, and the development of fragility curves for each grouping that establish the probability of achieving none/minor, repairable, or significant damage as a function of peak ground acceleration (ATC, 1996). Dynamic analysis is used to develop the demands for bridges within each group, whose attributes are selected from random sampling of the range of attributes for that group. To date (April 1998), fragility curves have been developed for most of the bridge groups defined for the Memphis and Shelby County bridges.

Shinozuka (1997). Another damage state modeling approach is being developed under the NCEER Highway Project by Shinozuka (1997). This approach will establish bridge damage state fragility curves through the use of numerical simulation based on rigorous dynamic analysis, in conjunction with professional judgment and quasi-static and design-code type analysis. The approach will be validated through comparisons of analytical predictions against observed performance of bridges during past earthquakes.

5.4.4 Traffic States

The final step in this bridge modeling process is the establishment of traffic states along the roadways at each end of the bridge, and also along roadways that pass beneath, above, or adjacent to the bridge. These traffic states represent the ability of the various roadways to carry traffic, in terms of the number of lanes that remain open to traffic and possibly any reduction in speed limit as well. Once they are established for a given scenario earthquake and simulation, they are incorporated into a system network model to establish overall post-earthquake system states (to which transportation network analysis procedures are applied to estimate earthquake effects on system-wide traffic flows). Therefore, the estimation of traffic states from the bridge damage states is a key step in the overall system SRA process.

These traffic states will vary with time after the earthquake, to reflect the estimated rate and type of post-earthquake repair of the bridge. This rate of repair will, in turn, depend not only on the type and extent of damage to the bridge, but also on construction practices within the region of the country that contains the highway system being analyzed. To account for these variables when establishing improved bridge models for the planned re-analysis of the Memphis highway system, an expert opinion approach is being developed that will involve: (a) establishing each possible damage state for the various bridges in the system; (b) having experienced bridge engineers from the Memphis area and the Tennessee Department of Transportation review these damage states and provide their opinion as

to the costs, types, durations, and traffic impacts associated with the repair process for each damage state; (c) interpreting these estimates using bridge repair cost and functionality data from past earthquakes (in California and elsewhere); (d) from this, establishing models that provide repair costs and traffic states (at various times after the earthquake) for each bridge damage state; and (e) incorporating these models into the component module for the SRA procedure, for use during our subsequent SRA for the Memphis highway-roadway system.

5.5 Transportation Network Analysis Procedure

5.5.1 Background

As previously noted, the network analysis portion of our prior demonstration SRA of the Memphis highway system relied on MINUTP -- a standard program that implements Urban Transportation Planning System (UTPS) algorithms (Werner et al., 1996). Experience from that analysis showed that data preparation and implementation of MINUTP was unacceptably time consuming -- partially due to the fact that MINUTP was not GIS-compatible. Also, although UTPS models and their derivatives are standard planning tools in cities receiving Federal support for local transportation projects, such models have the following deficiencies for SRA applications: (a) consideration of an adequate level of detail for representing the region served by the system (i.e., region boundaries, O-D zones, and the system network structure) is costly; (b) loss-of-service measures developed from UTPS network assignment models are inconsistent with loss-of-service measures from other UTPS models; (c) behavioral shifts due to major disasters such as large earthquakes are difficult to represent; and (d) the UTPS procedure has little capacity for considering time dependence of system performance characteristics.

In view of this, it became clear that an alternative transportation network analysis procedure was needed that: (a) provides a capacity for more rapid estimation of network

flows; (b) represents the latest well-developed technology and circumvents technical limitations of the UTPS algorithms; (c) is compatible with the GIS-based framework of our current SRA procedure; and (d) provides a capability for using transportation system input data typically available from Metropolitan Planning Organizations (MPOs).

We have found that a new Associative Memory (AM) procedure for rapid estimation of traffic flows that was developed at the University of Southern California (USC) best meets the above objectives (e.g., Moore et al., 1997). The objective of this AM work has been to provide rapid and dependable estimates of flows in congested networks, given changes in link configuration due to earthquake damage, and to attach these changes to the decision-making procedures used to prioritize bridges for seismic retrofit. Such a procedure articulates well with existing efforts in the field, because these flow estimates are input to both total transportation system cost and accessibility measures.

5.5.2 Overview of AM Procedure

The AM procedure is derived from the artificial intelligence field to predict changes in highway system flows. These predictions are based on good approximate solutions to constrained optimization problems that represent the economic determinants of network flows. As such, the AM procedure has the capability to determine changes in the system's total commuting time due to changes in the highway system network. To illustrate, if one link of a freeway is being considered for retrofit, the change in the total system commuting time due to removal of this link is calculated by the following steps: (a) identification of equilibrium flows and commuting times for each link in the intact (pre-earthquake) network; (b) calculation of total system commuting times by summing the commuting times for all links; (c) removal of the link from the highway system, simulating closure due to earthquake damage; and (d) determination of the change in total system commuting time due to the link's removal.

5.5.3 Development of AM Matrix

The AM procedure focuses on the development of an AM matrix that is used to map given sets of system network configurations (stimulus) to lead to corresponding traffic flows (response). The AM matrix is developed from the following steps:

Step 1. Training and Test Cases. Standard numerical analysis is used to develop an ensemble of user equilibrium traffic flows for various network configurations, all of which represent the same general type of network and traffic flow characteristics. Most of these solutions are designated as training cases, with the remainder designated as test cases. These flows are computed for each link in the system in terms of equivalent passenger-car-units per hour.

Step 2, AM Training. The training cases from Step 1 are used to train the AM; i.e., to determine the elements of the AM matrix that minimize the mean-square difference between the true user equilibrium traffic flows for all training cases and the estimated flows using the AM matrix.

Step 3. AM Testing. The basic premise of this approach is that the AM matrix will provide a good estimate of traffic flows from other network configurations that represent similar conditions to those of the training cases, but have not been included in these cases. To check this, the AM matrix is used to predict traffic flows for each test case from Step 1, and these predicted flows are compared to the actual flows for the test cases as obtained during that step.

Step 4. AM Refinement. From past experience, Step 3 will usually lead to excellent comparisons between predicted and actual traffic flows if an adequate number of training cases has been selected. However, if needed, additional training and test cases can be developed in Step 1 and used to further refine the AM matrix and the accuracy of its traffic flow predictions.

5.5.4 Current Status

We are programming the AM procedure for rapid estimation of traffic flows developed at the University of Southern for incorporation into the SRA methodology. In addition, we have compiled network data for the Memphis highway-roadway system for an updated SRA of this system.

Our programming of the AM procedure considers that the procedure has two sub-modules -- the training and stimulus-response sub-modules. The training sub-module solves conventional user-equilibrium flow problems given different configurations for the Memphis network. The stimulus-response sub-module constructs an AM matrix that best fits these user equilibrium inputs (network configurations) and outputs (traffic flows). In this way, the exact user-equilibrium solutions "train" the AM, which then can be used to obtain very rapid estimates of traffic flows for other network configurations not included in the training sub-module. These AMs have been shown to provide good approximations of user-equilibrium flows associated with new network configurations, including networks in which capacity has been lost.

Creation of training data is a pre-processing step, but users of the SRA methodology will also have the opportunity use the training sub-module to solve for exact user-equilibrium flows for various post-earthquake network configurations. Regardless of why users might elect to solve these flow problems exactly, the results of the analysis can usually be added to the training data provided to the stimulus-response sub-module.

We have programmed user-equilibrium traffic-assignment and the generalized inverse-matrix modules in the C programming language, specifically Watcom C/C++ V11.0. These sub-modules must be integrated into one model to be tested and applied. We are now programming an integrated analysis environment that contains a transportation data-

base management system, training module, stimulus-response module, and output generation module.

We have also been working with the Memphis and Shelby County Office of Planning and Development (OPD), who is the MPO for the Memphis region, to compile network input data for use in our forthcoming SRA of the Memphis highway-roadway system. The data for this system is based on OPD's most recent (1995) MINUTP model. These network data includes 665 origin-destination zones and associated trip tables, 3,853 nodes and their attributes, and 9,716 directional links and their attributes. These data have now been incorporated into the GIS data base for our Memphis system SRA.

6.0 REAL-TIME APPLICATIONS

Research is being carried out by earthquake scientists and engineers to develop procedures for estimation of seismic effects in real time. Such procedures facilitate rapid emergency-response decision making by using scientific and engineering monitoring systems and models for seismic data collection, analysis, initial real time prediction of seismic effects, and updating of real-time predictions as new earthquake data becomes available (e.g., Eguchi et al., 1997; Taylor et al., 1998).

The highway system SRA procedure described in this paper features is well suited for real-time prediction of highway system seismic performance. Particular benefits of the procedure for such applications include its use of GIS-based modules with rapid procedures for: (a) predicting seismic hazards, component performance, and system-wide traffic flows; and (b) display of prediction results.

We envision that the use of the SRA procedure for real-time predictions of highway system seismic performance would require the following pre-earthquake steps, as a unified effort of regional government officials, emergency response planners, earthquake engineers, and transportation specialists.

System Inventory. Engineers and planners should: (a) identify the extent of the highway-roadway system to be analyzed; (b) compile relevant data for the system, including network, traffic, component, and origin-destination zone data as described earlier in this paper; and (c) identify locations and access routes for key emergency response/recovery facilities.

Real Time Information Needs. Government and emergency response planning officials should identify their particular post-earthquake information needs from the results of the real-time application of the SRA procedure. This could include information on: (a) locations of earthquake damage to the highway-roadway system; (b) impacts of this system on traffic flows, including alternative routes that would be taken by users immediately after the earthquake; (c) accessibility to and from hospitals, police and fire departments, airports, and other key emergency response centers; and (d) the effectiveness of alternative short-term traffic management procedures in reducing post-earthquake traffic congestion and improving access to emergency response facilities.

SRA Module Development. After the above steps have been carried out, systems and engineering information needed to rapidly carry out highway-roadway system SRAs in real time can be developed within the GIS-based SRA preprocessor modules. This would include development and incorporation of: (a) models for estimating seismic hazards throughout the system that are based on regional seismologic and geologic characteristics; (b) vulnerability and fragility models for characterizing damage states and traffic states of the bridges and other components that comprise the system; and (c) an AM matrix for estimating traffic flows for the highway-roadway system and its range of potential post-earthquake system states.

Integration into Real-Time Earthquake Damage Assessment System. We envision that this highway-roadway system performance predictions would be part of a larger real-time earthquake damage assessment system that

would be in place for the region. Accordingly, the predictions developed in the previous step, together with the SRA procedure itself, should be integrated into this real-time system, so that information on future earthquake magnitudes and locations can be readily accessed for rapid estimation of post-earthquake system performance and losses.

6.0 CONCLUDING COMMENTS

This paper has described a new SRA procedure for highway systems. A demonstration application of the procedure to the Memphis highway system has provided preliminary results that show the type of information that can be obtained using SRA. Significant research has been carried out that will dramatically improve the reliability of the system performance results obtained using the SRA procedure.

SRA can enhance the prioritization, planning, and implementation of seismic risk reduction for highway systems. Its principal benefit is its ability to directly represent seismic performance of highway systems – in terms of post-earthquake traffic flow – and to represent systemic effects associated with the damage to various highway components. This information will provide a much improved basis for decision-making pertaining to such issues as prioritizing various components for seismic strengthening, establishing component seismic performance and design criteria, and justifying funding for seismic retrofit or other seismic risk reduction measures. In addition, because the SRA procedure uses rapid GIS-based methods for estimating seismic performance of highway-roadway systems, it can be readily adapted to real-time prediction applications.

ACKNOWLEDGEMENTS

This research is being funded by the National Center for Earthquake Engineering Research (NCEER) under their Highway Project. This financial support is gratefully acknowledged. The authors also wish to acknowledge: (a) Dr.

Ian Buckle and Mr. Ian Friedland of NCEER and Prof. Masanobu Shinozuka of the University of Southern California, for their encouragement and helpful suggestions; (b) Mr. Jon Walton, for his programming and GIS support; (c) Messrs. Clark Odor and Esther Anderson of the Memphis and Shelby County OPD, for providing system, traffic, and trip-table data for the Memphis area highway-roadway system; and (d) Mr. Edward Wasserman and his staff at the Tennessee Department of Transportation in Nashville, Tennessee, for providing valuable bridge data, drawings, and reports from their files.

7.0 REFERENCES

- Applied Technology Council (ATC) (1991). *ATC-25 -- Seismic Vulnerability and Impact of Disruption of Lifelines in the Conterminous United States*, Redwood City CA.
- Applied Technology Council (ATC) (1996). *ATC-32 -- Improved Seismic Design Criteria for California Bridges: Provisional Recommendations*, Redwood City CA.
- Association of Bay Area Governments (ABAG) (1997). *Riding Out Future Quakes: Pre-Earthquake Planning for Post-Earthquake Transportation System Recovery in the San Francisco Bay Region*, Oakland CA, October.
- Bartlett, S.F. and Youd, T.L. (1995). "Empirical Prediction of Liquefaction-Induced Lateral Spread" *Journal of Geotechnical Engineering ASCE*, 121(4), April, pp 316-329.
- Barton-Aschman Associates (BAA) (1994). *Interstate 10 Recovery Report -- Northridge Earthquake Recovery* California Department of Transportation, District 7, Office of Operations, Los Angeles CA. September 15.
- Basoz, N. and Mander, J. (1998). *Enhancement of the Highway Transportation Lifeline Module in HAZUS*, Draft Report to National Institute of Building Sciences, Washington D.C., April 3.

Comsis Corporation (1994). *MINUTP Technical Users Manual* Silver Springs MD, July.

Daykin, C. D., Pentikainen, T., and Pesonen, M. (1994). *Practical Risk Theory for Actuaries*, London: Chapman & Hall.

Der Kiureghian, A. and A. H-S. Ang, 1977, "A Fault Rupture Model for Seismic Risk Analysis," *Bulletin of the Seismological Society of America*, 64(4), pp 1173-1194, August.

Eguchi, R.T., Goltz, J.D., Seligson, H.A., Flores, P.J., Blais, N.C., Heaton, T.H., and Bortugno, E. (1997). "Real-Time Loss Estimation as Emergency Response Decision Support System: The Early Post-Earthquake Damage Assessment Tool", *Earthquake Spectra*, 13(4), November, pp 815-832.

Federal Highway Administration (FHWA) (1995). *Seismic Retrofitting Manual for Highway Bridges*, Publication No. FHWA-RD-94-052, Turner-Fairbank Highway Research Center, McLean VA, May.

Frankel, A., Mueller, C., Barnhard, T., Perkins, D., Leyendecker, E.V., Dickman, N., Hanson, S., and Hopper, M. (1996). *National Seismic Hazard Maps, June 1996 Documentation*, Preliminary Report prepared at U.S. Geological Survey, Denver CO, July 19.

Gordon, P., Richardson, H.W., and Davis, B. (1996). *Transport-Related Business Interruption Impacts of the Northridge Earthquake* Lusk Center Research Institute, University of Southern California, Los Angeles CA, March.

Hwang, H.H.M. and Huo, J-R. (1997). "Attenuation Relations of Ground Motion for Rock and Soil Sites in Eastern United States", *Soil Dynamics and Earthquake Engineering*, Vol. 16, pp 363-372.

Hwang, H.H.M. and Lin, H. (1997). *GIS-Based Evaluation of Seismic Performance of Water Delivery Systems*, University of Memphis, Memphis TN, February 10.

Hwang, H.H.M., Lin, H., and Huo, J-R. (1997). "Site Coefficients for Design of Buildings in Eastern United States", *Soil Dynamics and Earthquake Engineering*, Vol. 16, pp 29-40.

Jernigan, J.B. and Hwang, H.H. (1997). *Inventory and Fragility Analysis of Memphis Bridges*, Center for Earthquake Research and Information, University of Memphis, Memphis TN, September 15.

Law, A.M. and Kelton, W.D. (1991). *Simulation Modeling & Analysis*, New York: McGraw-Hill, Inc., New York NY.

Leyendecker, E. V., D. M. Perkins, S. T. Algermissen, P. C. Thenhaus, and S. L. Hanson, (1995). *USGS Spectral Response Maps and their Relationship with Seismic Design Forces in Building Codes*, Open-File Report 95-596, U.S. Geological Survey, Denver CO.

Liu, W.D. (1997). "Major Bridge Damage State Modeling", *Year 5 Research Plan, NCEER Highway Project*, National Center for Earthquake Engineering Research, Buffalo NY, October 3.

Mander, J.B. and Dutta, A. (1997). "A Simple Pushover Method for Rapid Evaluation of Bridge Capacity", *NCEER Bridge Damage-State Modeling Workshop*, San Francisco CA, August 6-7.

Martin, G.R. and Dobry, R. (1994). "Earthquake Site Response and Seismic Code Provisions" *NCEER Bulletin*, 8(4), pp 1-6.

Moore, J.E. II, Kim, G., Xu, R., Cho, S., Hu, H-H, and Xu, R. (1997). *Evaluating System ATMIS Technologies via Rapid Estimation of Network Flows: Final Report*, California PATH Report UCB-ITS-PRR-97-54, December.

Ng, K.W., Chang, T.S., and Hwang, H.H.M. (1989). *Subsurface Conditions of Memphis and Shelby County*, Report NCEER-89-0021, National Center for Earthquake Engineering Research, Buffalo NY, July 26.

Seeber, A. and J. G. Armbruster, 1991, *The NCEER-91 Earthquake Catalog: Improved Intensity-Based Magnitudes and Recurrence Relations for U. S. Earthquakes East of New Madrid*, Report NCEER-91-0021, National Center for Earthquake Engineering, Buffalo NY.

Seed, H.B. and Idriss, I.M. (1982). *Ground Motions and Soil Liquefaction during Earthquakes* Earthquake Engineering Research Institute, Berkeley CA, December.

Shinozuka, M. (1997). "Development and Validation of Bridge Fragility Curves", *Year 5 Research Plan, NCEER Highway Project: Seismic Vulnerability of Existing Highway Construction* October 3.

Taylor, C.E., Chang, S.E., and Eguchi, R.T. (1998). "Updating Real-Time Earthquake Loss Estimates: Methods, Problems, and Insights", *Proceedings of Sixth U.S. National Conference on Earthquake Engineering*, Seattle WA, May 31-June 4.

Tokimatsu, K. and Seed, H.B. (1987). "Evaluation of Settlements in Sands due to Earthquake Shaking" *Journal of Geotechnical Engineering Division, ASCE*, 113(8), August, pp 861-878.

Wells, D.L. and Coppersmith, K.J. (1994). "New Empirical Relationships among Magnitude, Rupture Length, Rupture Width, Rupture Area, and Surface Displacement" *Bulletin of the Seismological Society of America* Vol. 84, No. 4, pp 974-1002.

Werner, S.D. and Taylor, C.E. (1995). *Interim Year 2 Report for Task 106 E-7.3.1: Demonstration Seismic Risk Analysis of Highway/Roadway System in Memphis, Tennessee*, Report prepared for National Center for Earthquake Engineering Research, Buffalo NY, at Dames & Moore, San Francisco CA, September.

Werner, S.D., Taylor, C.E., and Moore, J.E. II (1996). *Volume 1 Strawman Report: Seismic Risk Analysis of Highway Systems*, Report prepared for National Center for Earthquake Engineering Research, Buffalo NY, at Dames & Moore, San Francisco CA, October.

Youd, T.L. and Gummow, G.A. (1995). *Screening Guide for Rapid Assessment of Liquefaction Hazard to Highway Bridges*, Draft Report to National Center for Earthquake Engineering Research, Buffalo NY, August 8.

Youd, T.L. (1997). Empirical Data: Performance of Bridges Subjected to Permanent Ground Displacement, Personal Communication to S.D. Werner and C.E. Taylor, July.

Table 1
Effects of Earthquake D on Total System Travel Times and Distances

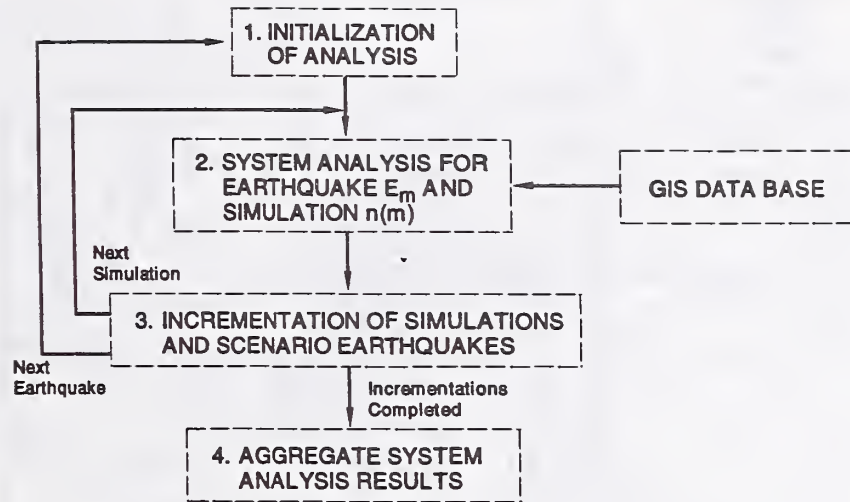
PARAMETER	PRE-EARTHQUAKE VALUE	TIME AFTER EARTHQUAKE = 3 DAYS		TIME AFTER EARTHQUAKE = 6 MONTHS	
		Value	Percent Increase over Pre-EQ	Value	Percent Increase over Pre-EQ
Total vehicle hours traveled over 24-hour period (incl. congestion)	3.73×10^5	4.99×10^5	33.8	4.46×10^5	19.6
Total travel distance (mi) over 24-hour period	15.5×10^6	15.6×10^6	small	15.6×10^6	small

Table 2
Effects of Earthquake D on Travel Times to/from Origin-Destination Zones (24-Hour Time Period)

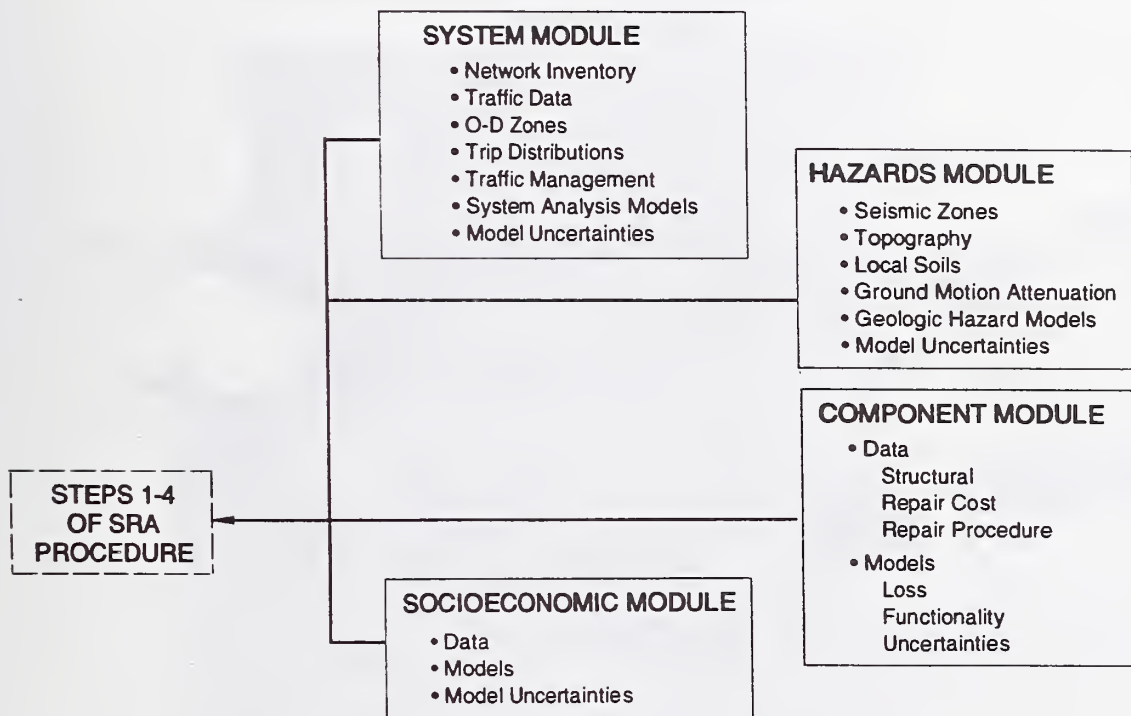
Origin-Destination Zone		Pre-Earthquake Travel Time (Hours)	3 Days After Earthquake		6 Months After Earthquake	
Description	Number		Travel Time (hrs)	Percent Increase over Pre- Earthquake Time	Travel Time (hrs)	Percent Increase over Pre-Earthquake Time
Government Center (downtown Memphis)	7	128	143	11.7	133	3.9
	8	122	141	15.6	130	6.6
Medical Center	28	122	136	11.5	127	4.1
	28	114	129	13.2	129	6.1
	27	114	129	13.2	121	6.1
	28	115	129	12.2	121	6.2
	28	119	133	11.5	129	4.2
University of Memphis	111	119	141	10.1	122	2.5
President's Island (Port)	151	138	153	10.9	141	4.3
Memphis Airport	188	130	150	10.3	142	4.3
Federal Express	188	130	145	11.5	130	4.6
Mall of Memphis	201	127	145	14.2	133	4.7
Hickory Hill	213	171	145	8.2	177	6.6
Poplar-Ridgeway	230	130	141	13.2	130	4.6
	231	130	147	10.1	136	4.6
Germantown	230	130	157	10.3	141	4.3
	241	176	141	6.3	141	2.8
Shelby Farms	249	169	141	4.1	141	3.0
	252	127	211	66.1	152	19.7
Bartlett	264	148	199	34.5	155	4.7
Covington Pike	274	137	181	32.1	151	10.2
TOTALS		2813	3255	15.7	2963	5.3

Table 3
Economic Impacts of Travel Time Delays due to Earthquake D

Time After Earthquake	Time Delay (Vehicle-Hours/24-Hour Day)			Cost/Day
	Total	Non-Trucks	Trucks	
3 Days	126,000	88,200	37,800	\$1.6 x 10 ⁶
6 Months	73,000	51,100	21,900	\$9.3 x 10 ⁵

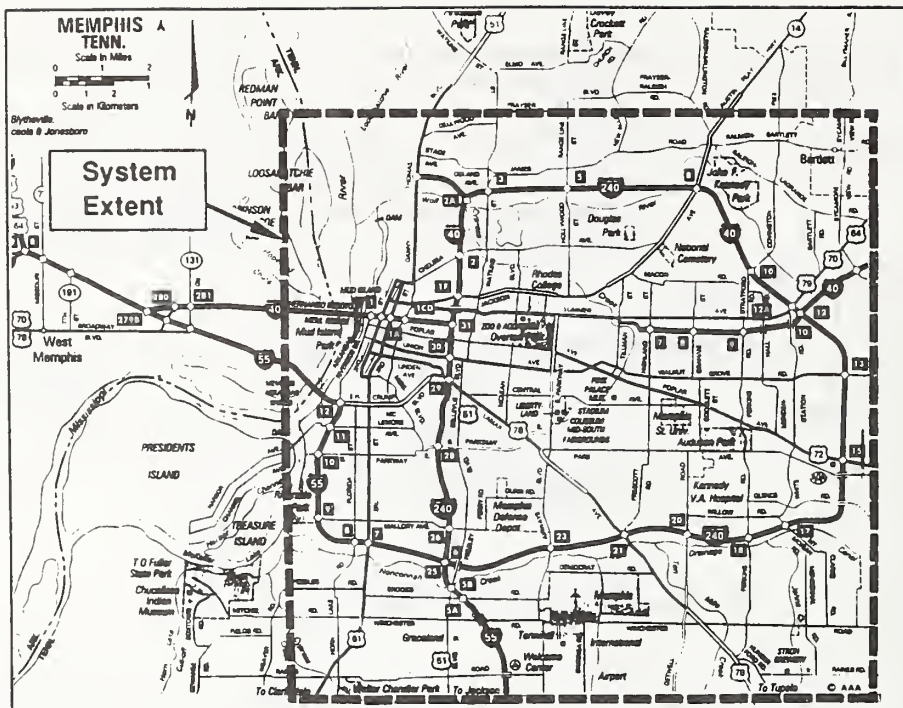


a) Overall Four-Step Procedure

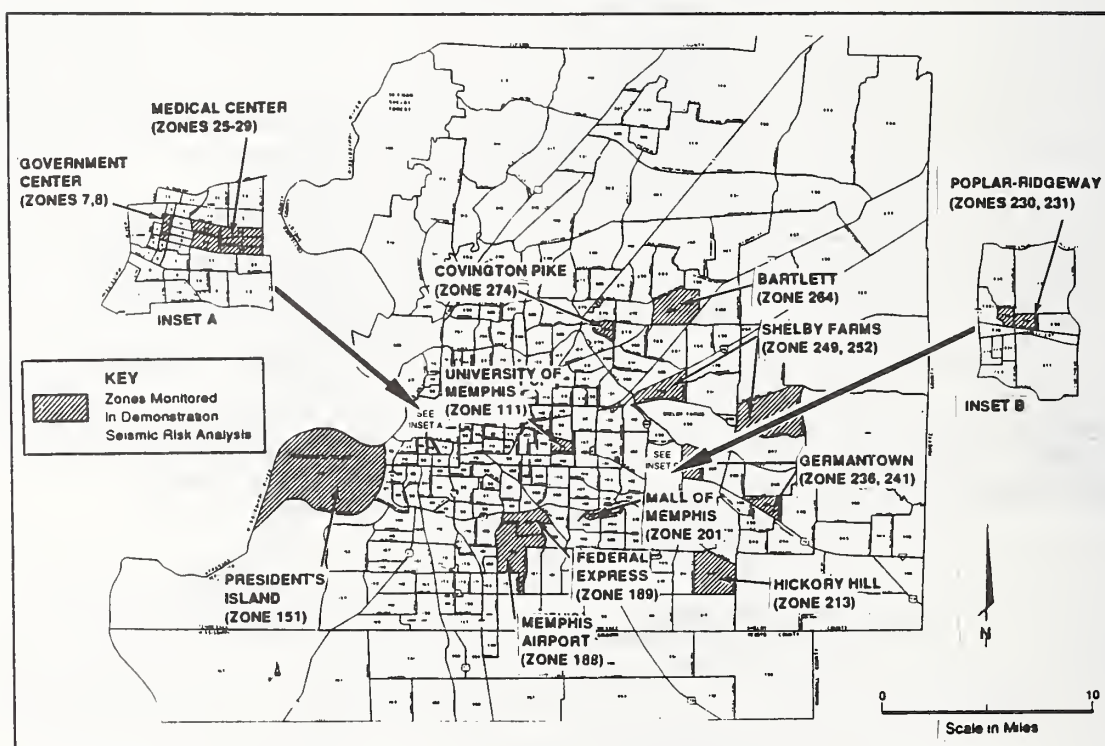


b) GIS Data Base

Figure 1. SRA procedure for highway transportation systems

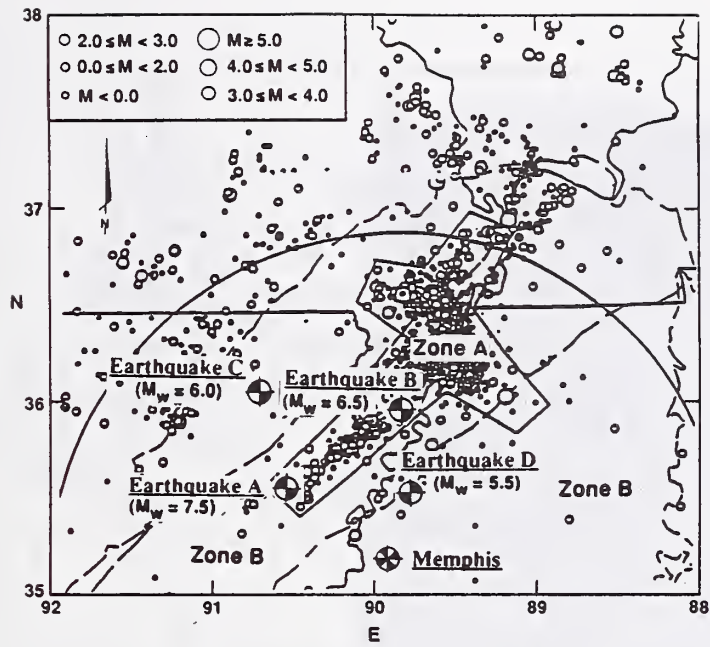


a) System Extent



b) Origin - Destination Zones

Figure 2. Memphis area highway system



a) Scenario Earthquakes



b) Local Geology (Hwang and Lin, 1993)

Figure 3. Scenario earthquakes and local geology

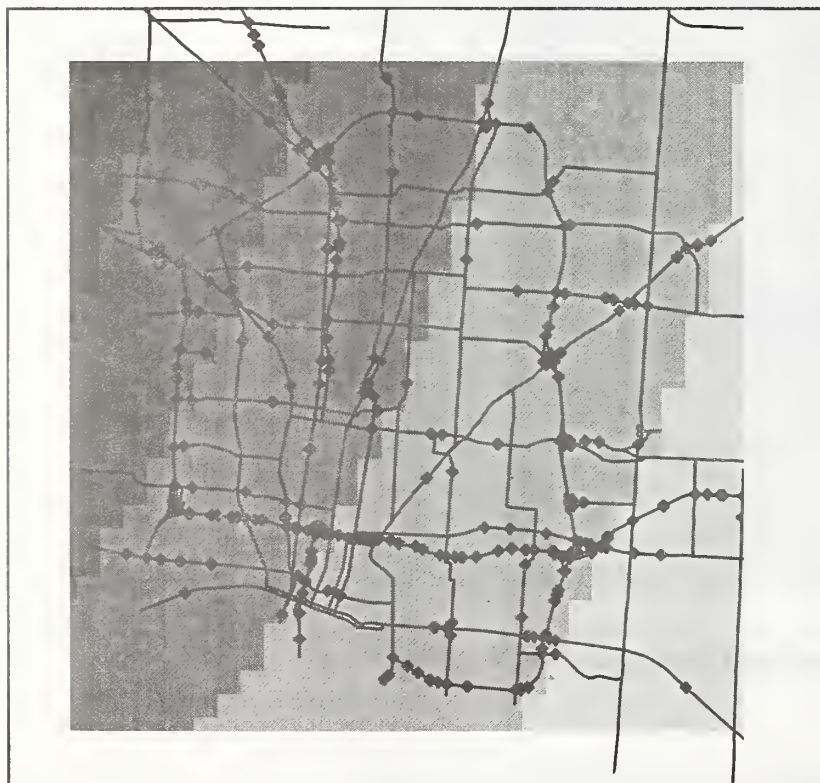
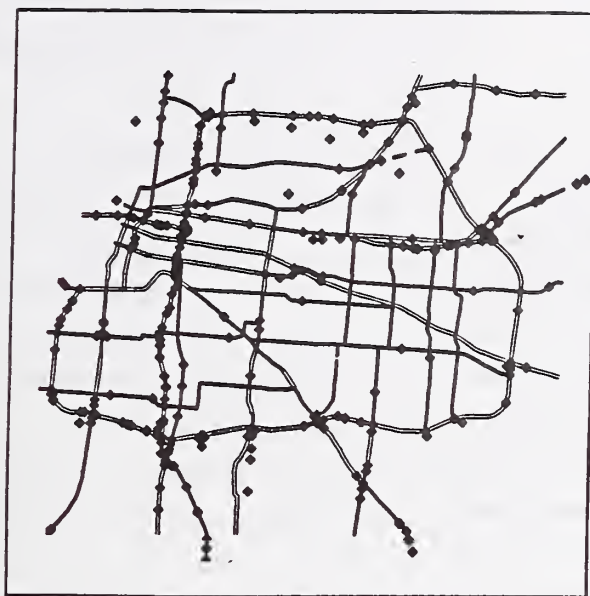


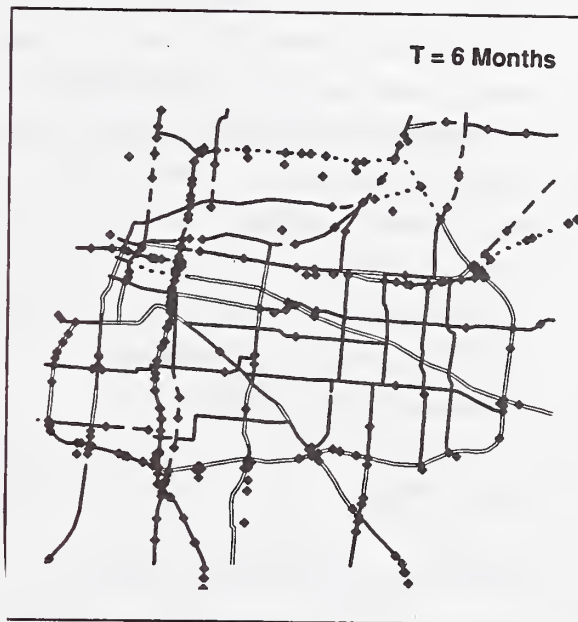
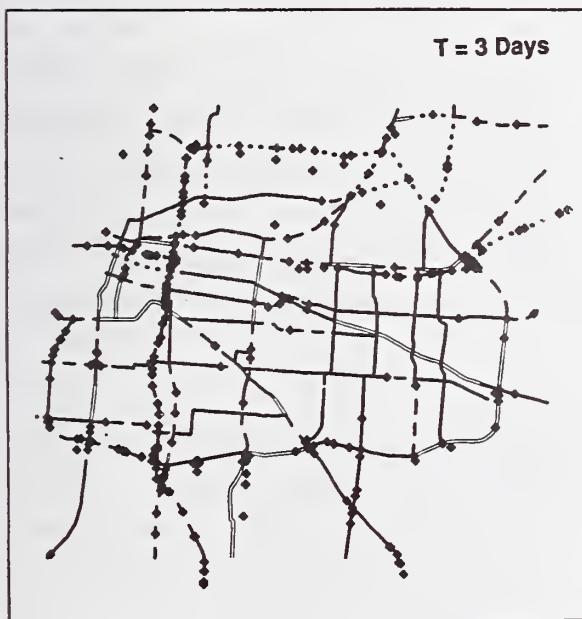
Figure 4. Peak acceleration (g) due to Earthquake "D."



Legend

- ◆ Bridge Location
- ⋯ Road Closed
- One Lane
- ≡ Two Lanes
- ≡≡ Three Lanes
- ≡≡≡ Four Lanes

a) Pre-Earthquake



b) Post-Earthquake

Figure 5. System states

"Devastating Network In Miura Peninsula Japan"

Professor of Keio University (Chairman of the Above Committee)

Makoto WATABE

Director of The Devastating Preventive Network of Yokosuka City

Satomi HIROKAWA

ABSTRACT

This paper presents about the report of devastating network in Miura peninsula near Tokyo. 1995, January. 17, early in the morning, Kobe Earthquake damaged many people in Japan. At this earthquake, informations were very poor. Since then various cities had committees to modify these situations. Yokosuka City and NTT (Nipon Telephone and Telegram) (Chairman was myself) started the committee in the same year of March 1. They were using the ordinary multimedia because of difficulties of using extra methods (like the battery not working) when devastating earthquake comes. By 2 years, we could finish basic ideas and the now were realizing.

Key Words: Yokosuka City

Multimedia

Information network

Application software

Devastating network

1 INTRODUCTION

1995 January 17 early in the morning, we had Kobe-Awaji devastating earthquake, and Japanese people had the big damages. The cities of Japanese at that time, should consider the informat

ion systems, important to inform the damages of, for instance, people in the damaged areas from the cities or firefighting offices of the cities. Fortunately, Yokosuka City was quite eager for information systems of natural disaster. Especially the reservation of drinking water, they must carry it from Sagami River, far from Yokosuka, so they form the tanks of water before Kobe Earthquake.

2 DEVASTATING NETWORK

Devastating network was useful, of course, at natural disaster events, but even ordinarily times using multimedia information and correspondent networks, and information between related organizations are very important. These are the basic ideas of "devastating network". Safeties of the people in the districts and better services of administrations will be also important. The above network systems are used for ordinarily time, for the information ser

vices, education information's common use and for information between administration offices. At devastating time, to change application software, using the same tools of ordinary time, information of damages degrees, of accumulation, of good timing about the loss of the people, the common knowledge about the devastating information for each information offices are necessary. Uses of devastating network, on ordinary times, were not only the effective uses of devastating network in ordinary times but devastating network systems must be used ordinary daily because use on devastating times, the ordinary people, sometimes, could not use special devastating network or devastating network was broken and the people could not realize it until they start to use or the batteries of devastating network were run out.

The reason of multimedia for devastating network were the following; combinations of various information of pictures, of places, of voices and letters to understand easily the damaged degrees by coming devastation will be especially necessary at devastating times.

3 MIURA PENINSULA City (Yokosuka City)
MADE A COMMITTEE FOR DEVASTATING NETWORK

Not only peninsula's closed situations but also this peninsula area are called "Tanito" (valley and door), mixed with valleys and hills, and when devastating earthquake comes, in the above

areas are quite difficult to inform their damages to their area or near areas. Actually, some places of firefighting radios and portable telephones could not communicate each other (PHS: portable telephone became better communications recently). Yokosuka City was as eager about devastating network since long time ago, and drinking water were stored in the water tanks, for instance under the parks because drinking water were brought from Sagami River by the steel pipes as already written before. Beside the above, they are promoted to prepare machine materials, food and medicines. However the method of information, between firefighting offices or cities devastating network radios and general telephones could only use. Correspondent method between self defense armies, police and medical offices are known to be only by telephones. These the above reasons became to start the committee of devastating network. Beside the above items, NTT's roles could not be missed. In Yokosuka City, NTT may have research office soon, and so many people of NTT live in Miura peninsula area. So NTT plans the similar devastating network with Yokosuka City.

And this was the one of the reasons why Yokosuka City made the committee of devastating network.

4 CONSIDERATION AND PROCESS

Almost all cities of Miura peninsula have similar conditions, so other than Yokosuka City, 3 cities, 1 town, NTT and Kanagawa prefecture office joined together for this committee. And self defense army offices, marine security offices, polices, medical offices and lifeline business groups (all together 33 offices) joined together. 2 years long, committee started from March 1 the same year of Kobe-Awaji devastating earthquake. In year of 1995, 11 times of meetings (considerations: 3 times organizer meetings: 4 times top committee: 4 times) and 45 times of person's hearings were held to find out the real problems. And basic concepts were determined.

Through these meetings, each related offices discussed and considered the real necessary information, styles of these information and what the real useful information will be. Finally, October 26 of the same year, 『ARCS』 (Aid For District Devastating Network) were made as the result for the local devastating network.

The second year of devastating network committee, depending upon basic concepts, realized devastating network, discussed the specifications of devastating network. 11 times of meetings and all together 41 times of hearings were done. The specifications of necessary

functions and practical uses of this function were settled, and concluded the 2 years project. By this devastating network project, the trust each others of the related offices were much more increased. After this committee of devastating network, at Miura peninsula area, many offices got together to do the training of devastating network. In that sense, the new connections of each others will be made.

The second years of this project, 1996 April, 4 cities and 1 town, collected together the policies of the common purpose and once again get together to fix the satellite telephones, that were established in prefecture's office and polices offices so that at anytimes they can contact with each other. Upon the above ideas, communications network by the real multimedia will be prepared. The later of the second years, depending upon the final results, started the real devastating network.

The research people of NTT's developed application software and Miura peninsula area became the fields and by many people of the related joined together for the experiences of application software

s. Points of this development were the use of the standard communication system, at the same time, to many address, the communication traffic were flown about and treated them with composure. Hardware to load the software were made by Yokosuka City with some assistance from the administration of trades and industries. Using LAN and servers of Yokosuka City and of their education study offices, the communication circuits and for the edge PC will be maintained after 1997.

At August 31 1997, using the studied facilities, the exercise was performed by Yokosuka City. The information of devastating network was to the main measure office and we stayed there to estimate the results. The main measure office necessarily changed some system and brought the new portable terminations with staffs of firefighting, to exercise to send multimedia information to that main measure office through pictures, GPS data, voices and letters.

5 FUTURE

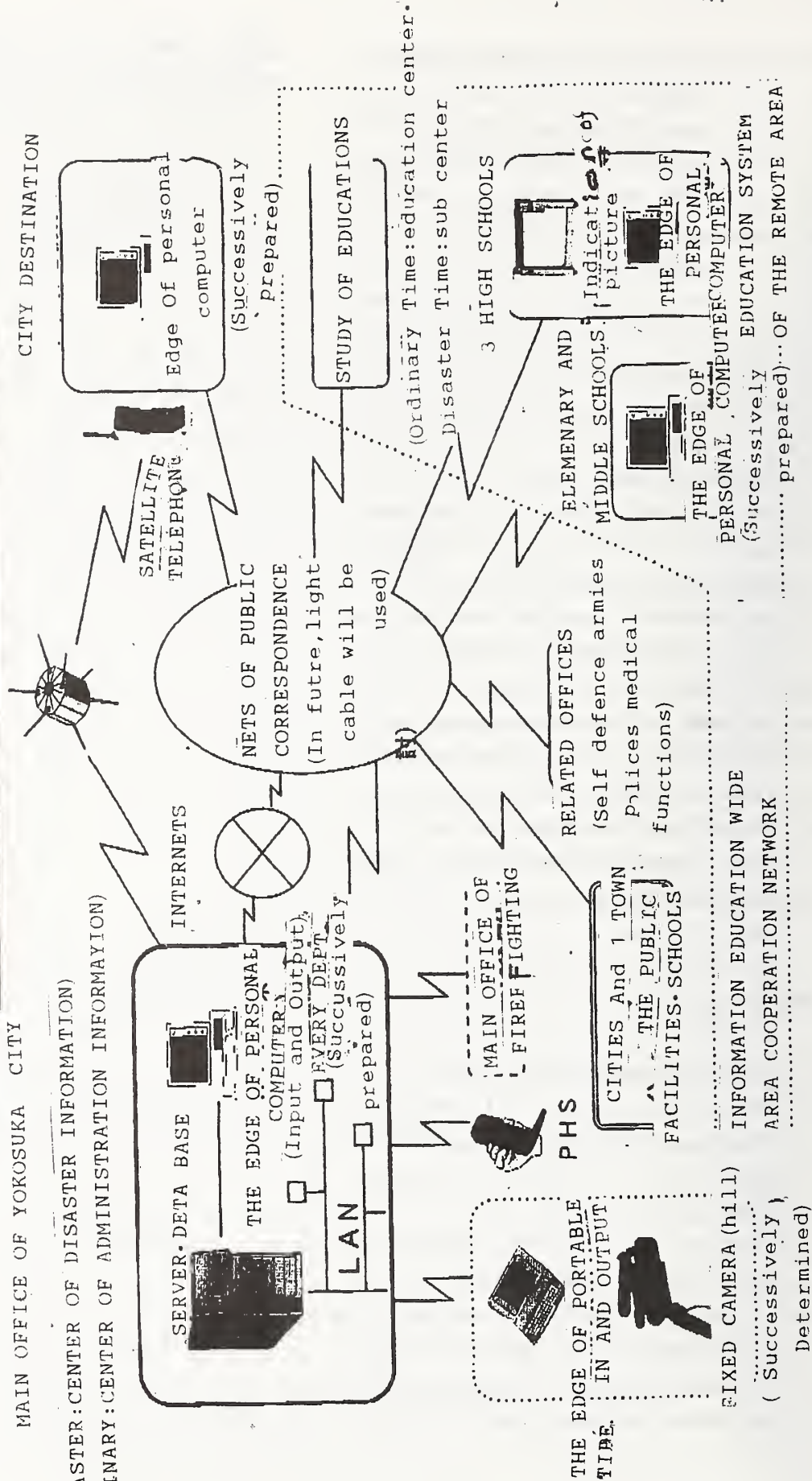
The brushup of examined systems and prepare the real system will be necessary to improve these systems. Through these improvement, finally the wonderful systems will be made.

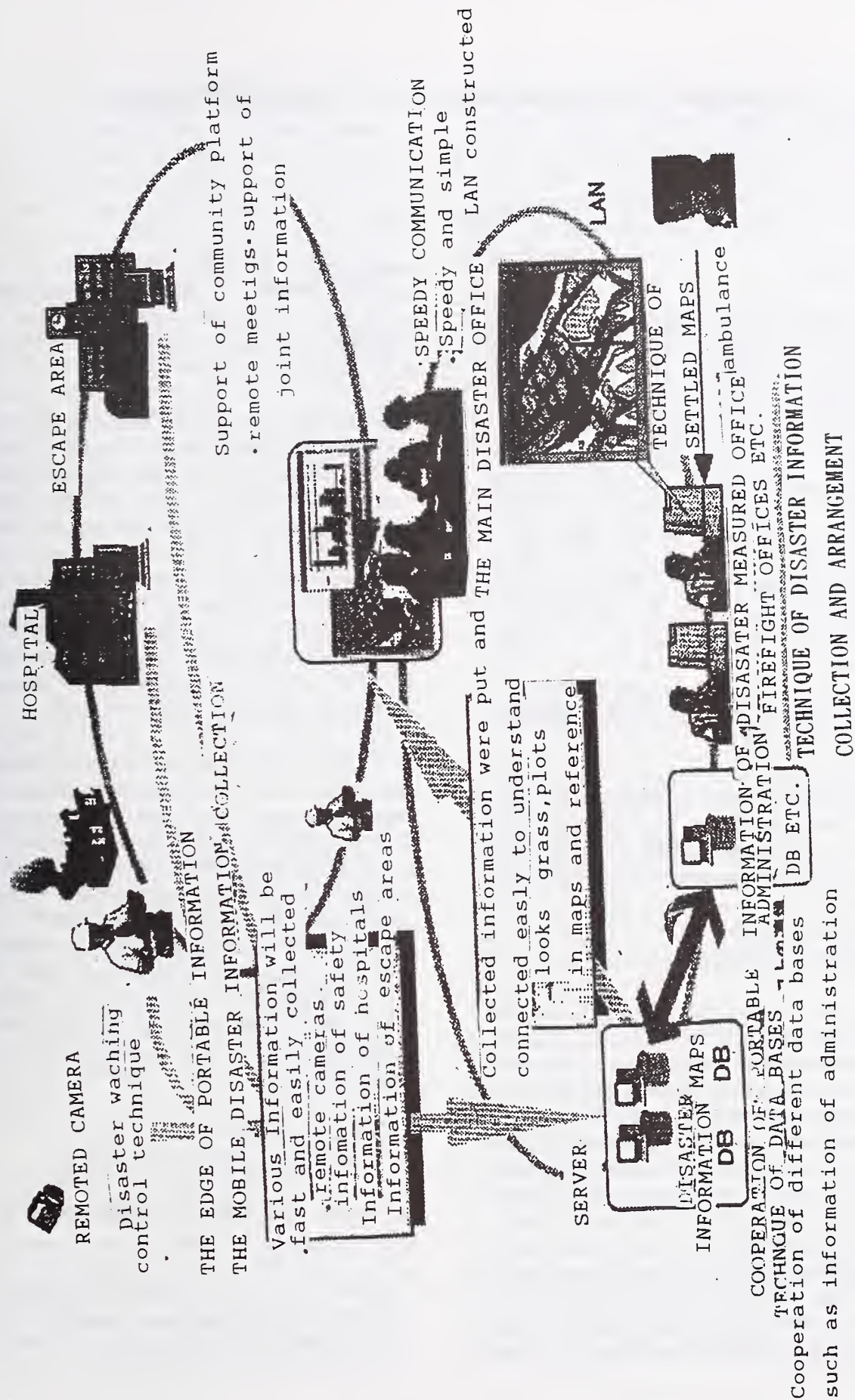
The practical use of the regulations will be sometimes quite difficult, so the through experiment system, hearings will be expected and the practical rules and systems will be obtained through the forms of [rules].

The costs of correspondent maintenances were not cheap, so ordinal correspondent information systems were used. We would like to use the exclusive correspondent safe systems in the future.

MAIN OFFICE OF YOKOSUKA CITY

(AT DIDASTER: CENTER OF DISASTER INFORMATION)
(AT ORDINARY: CENTER OF ADMINISTRATION INFORMATION)





Geospatial Analysis Support to Natural Disasters

By

William E. Roper¹

ABSTRACT

Natural disasters have a major impact, globally and within the United States (U.S.) causing injury and loss of life, as well as economic losses. To better address disaster response needs, a task force has been established to leverage technological capabilities to improve disaster management. Geospatial analysis is one of these important capabilities. A cross section of geospatial technologies applicable to disaster management are presented. These include: 3-D visualization, hyperspectral imagery, use of spectral libraries, digital multispectral video, fluorescence, radar imaging systems, photogeologic analysis, shaded relief imagery, differential global positioning system, and geographic information systems. A sample of satellite and sensor systems currently available is presented.

KEYWORDS: disaster management; mapping; hyperspectral; geospatial; spectral library; radar imaging; fluorescence; GIS; photogeologic analysis; GPS; satellite sensors; shaded relief; 3-D fly through.

1. INTRODUCTION

Natural disasters are a constant threat to mankind on a global scale. Global disaster costs are continuing to rise. Annual global economic costs related to disaster events average \$440 billion per year (World Disaster Report, 1996) with floods being the major cause (Figure 1). In the U.S., the number of lives lost due to natural disasters has been decreasing over the last several decades, largely because of advances in disaster indication and warning capabilities. In terms of damage to property, however, the trend is reversed. For the period 1992-1996, the average cost of natural disasters in the U.S. has been \$54.3 billion, with hurricanes and earthquakes tied as the leading

cause (Figure 2). These rising costs are the combined result of increased urbanization, particularly in high-risk coastal areas, and the increased complexity and size of our infrastructure.

The loss of life and property continues to rise in many regions of the world because of these events. One example is the Bangladesh weather event of 1970, when a tropical cyclone slammed into its delta region killing 300,000 people (Tobin and Montz, 1997). The crop losses were estimated at \$63 million, and more than 280,000 cattle were drown (Burton, Kates, and White, 1993). The rich delta soil is an agricultural resource that still draws people to settle there, therefore a recurrence of this type of weather event could likely pose a similar disaster.

This paper will focus on geospatial analysis and some of the specific developments in this rapidly changing area that can assist the disaster manager. There has been significant capability growth in the geospatial areas of remote sensing, spectral analysis, global positioning systems (GPS), geographic information systems (GIS), and modeling and simulation techniques (Roper, 1997). Each adds important value in characterizing infrastructure, risk areas, disaster zones, and control points that are essential to rapid deployment of scarce resources in the most effective manner.

2. GLOBAL DISASTER INFORMATION NETWORK

In February 1997, Vice President Albert Gore sent a letter to key Federal departments and agencies

¹ Director, U.S. Army Topographic Engineering Center, 7701 Telegraph Road, Alexandria, VA 22315-3864, www.tec.army.mil

requesting that senior officials discuss the feasibility of establishing a global disaster information network. In response to this request, a Disaster Information Task Force was established to evaluate the needs and issues, examine the feasibility, and outline a phased, integrated approach to address this important global need (Disaster Information Task Force Report, 1997).

There has been considerable effort expended in developing and coordinating activities in the U.S. Federal government over the last 1 1/2 years relating to the Global Disaster Information Network (GDIN). Some of the initial Geospatial-related efforts focused on the integration of archival and real-time data sets, and the adaptation of new and emerging technologies. Ongoing activities of the Disaster Information Task Force related to geospatial technology include directed technology support, information integration, and modeling technologies for disaster effects. The specific recommendation for the directed technology area includes development of approaches to integrate new and emerging tools and technologies for modeling, simulation, data fusion, etc., for use by disaster managers and planners.

It is important to consider the application of geospatial data and analysis across the comprehensive Disaster Management Cycle. This basic four-phased framework of mitigation, preparedness, response, and recovery, when integrated with GDIN capabilities, can be a strong supplement to current disaster support functions (Figure 3). Geospatial information can make a critical contribution to the disaster management community through enhancing the definition, identification, accuracy, and availability of essential information for community resilience.

3. GEOSPATIAL RESEARCH COMMUNITY INVOLVEMENT

The flow of disaster related information can be conceptually shown as a seven step process as shown in Figure 4. The geospatial research community may have a role in each of these steps, depending on the particular disaster situation.

This could include assistance in defining the problem through current image analysis. Assistance in determining collection and analysis methodologies assists in defining the requirement.

A key area of support is providing supporting data in the form of maps, imagery, and spectral information.

An even more important support area is data exploitation. This includes the processing of digital data, image integration, feature classification and attribution, classification output, accuracy assessments, and post-processing operations. It is the most technically challenging step in the process. The decision support phase includes geospatial visualization, merged data analysis, and specialized decision support products. This involves the synthesis of data types in order to generate data layers (such as, soils, vegetation, terrain) along with models and simulation techniques that use the various data layers.

It is during this phase that the concept of virtual forums could take place. These forums would allow expert input from multiple locations to be jointly focused on problem solving for the disaster situation. Within the geospatial community this could include virtual fly-through support showing the impacts of possible decisions on the natural environment, the built environment, and on the population, including those with special needs. It also could include analysis of changing situational information, and image-based change detection and analysis.

In the final two phases, tailored map products and GIS overlay information can be used as integral parts of directives and guidance to disaster managers in the field. These specific products could be maps delineating evacuation routes, area identification for damage assessments, or point locations for water distribution.

The geospatial research community has typically been interdisciplinary, including the natural sciences, engineering, architecture, land use planning, photogrammetry, etc. However, in the disaster management arena, broader

interdisciplinary teaming will be required. This could include public policy and health specialists at the Federal, state, and local level. It may include other medical specialists, police, national guard, and communications experts.

The greatest potential for loss reduction is during the mitigation phase (Disaster Information Task Force Report, 1997), when communities can be made more disaster resistant. The largest share of costs, however, are directed toward the recovery phase, where good mitigation principles also need to be put into practice rather than just rebuilding to be impacted by a similar disaster in the future. geospatial products and location specific tools developed during the response phase of the disaster may be excellent vehicles for planning and implementing effective mitigation.

4. GEOSPATIAL TECHNOLOGY OPPORTUNITIES

There are a number of new and evolving technologies and capabilities in the geospatial area that have application to disaster management. Some of these techniques assess and present data in new and innovative ways. Others are possible today because of new sensor and data processing capabilities.

4.1 DrawLand Visualization

DrawLand is one of the software programs used to support terrain visualization research. It was developed by the U.S. Army Topographic Engineering Center (TEC) and continues to be refined and used in research and operational applications. TEC has recently entered into a cooperative research and development agreement with ERDAS Corporation to make DrawLand available commercially as part of the ERDAS Imagine software program. Its release is planned for late in 1998.

DrawLand's main input is digital terrain elevation data (DTED), which can load the program into memory directly from CD-ROM. The user can specify the geographic area to be loaded. Given the southwest corner and the size of the cell,

DrawLand searches for the appropriate files and can combine data from several files to produce a 3-D terrain scene. A sample scene over a mountainous valley terrain is shown in Figure 5. A 1 minute digital fly-through of this geospatial database will be presented during the oral presentation.

DrawLand has been used to visualize imagery from a variety of sources to include: Landsat, SPOT, high-altitude aerial photography, and Interferometric Synthetic Aperture Radar (IFSAR). It also can use data from commonly used commercial software for disaster management support, such as ArcInfo, ArcView, and ERDAS Imagine. DrawLand can drape raster data over digital terrain elevation data within minutes to create the appearance of a 3-D map.

In the interactive or flight mode, the terrain is displayed as a reduced resolution polygon surface. Users can adjust the resolution and vary the rendering mode to suit their purpose (e.g., wire frame for speed, photo texture for realism). Coordinates, altitude above Mean Sea Level, distance above ground, yaw, pitch, and roll, are displayed for the viewpoint or for a model. The software also provides mission planning tools, such as masked area depiction, line-of-sight calculations, and flight path design, and can include unit symbols or polygon models of objects based on ground locations. All of these tools could be tailored to the particular disaster management situation and requirements.

During flight mode, the movement of the user's viewpoint can be recorded, as can the movement of any selected model that is being controlled. The animation can be recorded one frame at a time to a VCR tape or various digital movie formats. Model movements also can be played back in real time.

4.2 Hyperspectral Imagery

Hyperspectral remote sensing combines imaging and spectroscopy in a single system that includes data sets and processing methods. Hyperspectral data sets are generally composed of about 100 to

200, or more, spectral bands of relatively narrow bandwidths (5-10nm). The spectral range of interest of these data sets usually encompasses the portion of the spectrum dealing with reflected energy from the visible to the short-wave infrared (0.4 to 2.5 μ m). Hyperspectral airborne sensors can image ground materials in many bands of relatively high spectral resolution in a digital mode (Samuel Barr, 1997). Figure 6 illustrates this as applied to the Jet Propulsion Laboratory's Airborne Visible Infrared Imaging Spectrometer (AVIRIS) sensor. If a stack of picture elements (pixels) of a single target were extracted from the data set and plotted out as a function of wavelength (Figures 6 and 7), an average spectrum of all of the materials in the pixel would result. Because of the 3-D nature of these data sets, they are generally referred to as image cubes as depicted in Figure 8.

The large amount of data in the hyperspectral image cube may provide an important new tool in disaster management. However, there is still much to learn about the practical application of this technology. An example application, the mosaic image of Landsat Thematic Mapper data and AVIRIS data of a portion of the Bighorn Basin, northeast of Worland, WY, U.S., is shown in Figure 9. This image illustrates the synergy between large area coverage by satellite sensors and targeted airborne imaging hyperspectral data. The background image is a roughly 20 by 30 km portion of a Landsat Thematic Mapper color composite of bands 3,2,1 (true color), saturation-enhanced to contrast with the AVIRIS overlay. North is shown toward the bottom of the page. The 3-D hyperspectral image cube demonstrates the high spectral resolution nature of the AVIRIS data, which has 224 bands covering the spectral range of 0.4 - 2.5 μ m at 10 nm resolution. The AVIRIS cube face is a true color composite using bands 31, 19, and 10 (0.66 μ m, 0.55 μ m, and 0.45 μ m). The cube sides represent color-coded reflectance spectra for the pixels along the edges of the image. The color scheme of black, blue, green, yellow, red, and white indicates increasing reflectance (ENVI internet home page, 1998). These data are used together in a hierarchical strategy in this application for geologic mapping

and exploration using Landsat to provide an overview and to locate targets for more detailed study. The hyperspectral data are used for mineral species identification and abundance mapping, and field mapping and field spectroscopy for verification. Similar analysis of this kind of geospatial data might be used to identify earthquake, landslide, or soil liquefaction potential in the mitigation phase of disaster management. It is important to note that the commercialization of hyperspectral systems will soon make these data widely available. Commercial aircraft systems are in use today, and several satellite systems are planned for deployment by the year 2000.

4.3 Socet Set 3-D Visualization

Socet Set is a geospatial analysis software system jointly developed by the TEC and the private sector. Some of the main features of the Socet Set System are to triangulate images from a variety of sensors, automatically generate elevation data at almost any resolution, generate 3-D features, and generate orthophotos. Near real-time fly-through is achieved using Rapid Scene software in conjunction with Socet Set. Both will run on the Sun computers in near-real time, and an NT version is expected to be available this fall.

The next generation will be Rapid Scene Open Graphics Library (OGL), which will operate real time on a Pentium PC running the NT operating system. The advantages of this NT version are that the hardware and software required are much less expensive. A top-of-the-line graphics card, costing approximately \$2,500, and a 200 MHz Pentium will perform impressively. Another advantage is that the software uses the native Socet Set database, therefore no conversion process is needed.

This software gives the user the capability to properly register (triangulate) the following sensors: standard aerial digitized frame imagery, SPOT, LANDSAT, RADARSAT, Japanese Earth Remote Sensing Satellite, Omni, generic panoramic, and generic close range. The Socet Set Development Toolkit enables a programmer to

insert additional math models into the software to perform registration in conjunction with other sensors.

Whenever stereo imagery is available for the above sensors, one can generate high-resolution elevation data using the Automatic Terrain Extraction (ATE) module of the Socet Set software. Thus, it is possible to generate data that has a post spacing of 1m, if so desired. The horizontal and vertical accuracy of this data depends on a number of factors, such as the resolution of the imagery, the type of control points used, and the convergence angle of the stereo images. Further applications, such as terrain shaded relief images, and line of sight analysis, can be done within Socet Set. The line of sight capability provided within Socet Set also integrates buildings and trees into the analysis (if constructed in the feature extraction module described below).

Where the elevation data generated using automatic terrain extraction does not meet quality control criteria, a full suite of interactive editing tools is available to manually update the data. Typically this may be required over features such as lakes where there is little contrast in the imagery for the automatic correlation process to perform efficiently.

Another key capability is the ability to create digital orthophotos where the displacement is accounted for because of terrain relief. This in turn can be made into a map substitute with grid lines and feature annotation overlain for quick updates of maps in emergency situations.

The Feature Extraction module enables the user to collect arial, line, and point features while in a 3-D stereo environment. Thus, a true coordinate exists for every point digitized. The feature extraction tool also allows the construction of 3-D wire frame models that high resolution simulator fly-through packages depend on to make the generated scenes appear realistic. The wire frames can be exported into several other software packages for further exploitation.

A module called Image Perspective Transformation (IPT) is available, which renders high resolution fly-throughs in non-real time. Although this is not a real-time interactive fly-through capability, several features are still unique on this module. The software allows the user to texture the rendered scenes from multiple images that are registered in an automated fashion. Thus, a building can have texture on four sides and the roof from five different images, and the user does not have to manually register each image. Since the images have already been tied to the ground, and with each other photogrammetrically, all of the image texture from all of the images will correctly cover the appropriate building face as shown in Figure 10 (a 1 minute dynamic fly-through was shown in the oral presentation).

As mentioned previously, Socet Set is one of the premier database development tools for constructing high resolution fly-throughs. All of the above tools give the user the ability to put together, from two or more images, a complete, accurate database. The interface with the Evans and Sutherland, Inc., simulator databases is a final important step in allowing the database to maintain its integrity. Typically, in the translation of data from one software package to the next, important attributes are lost or altered, decreasing the accuracy and usefulness of the database.

The applications of these tools are numerous. TEC has done work to help locate where World War I-era munitions were buried in the Spring Valley neighborhood of Washington, D.C., by triangulating images taken in the 1920s with modern imagery. This gave analysts the ability to precisely locate where potential burial locations existed in a modern coordinate system.

For disaster assistance Socet Set can create high resolution data sets from a wide variety of image sources. Using Rapid Scene with Socet Set, 3-D depictions of the terrain and building features can be created. The disaster manager could virtually walk into the situation to conduct assessments and planning activities.

In summary, this software provides the ability to provide rapid, high resolution databases that can support a multitude of applications in today's dynamic environment.

4.4 Spectral Library Database Program

The ever increasing amount of data and spectral information that is in current databases, and the future flood of data from hyperspectral sensors, will require a more usable spectral database library for more effective interpretation and development of products. The possibility of an open cross platform web-based spectral library is a very powerful concept. It could provide an invaluable tool for future spectral related research, and greatly reduce the time and resources necessary to produce useful products from spectral data. The design of such a library would require careful assessment of user needs, minimum data characterization requirements, and easy input and access controls.

TEC currently has more than 5000 spectral signatures, as well as signatures from other organizations in its existing database catalogue. These include visible-near infrared, fluorescence and thermal spectra obtained from field, laboratory and imagery. These data are being organized and characterized into an interactive library structure. The initial design concept is shown in Figure 11a. Upon completion, the library is intended to have multiple scientific tools for viewing spectral data and performing numerical and statistical tools for viewing data and performing numerical and statistical analysis. The distributed system will house the database and scientific tools on different servers and possibly different platforms. The system structure will be transparent to the user who will access the data over the Internet via a web browser or similar interface. A prototype of the computer metadata display and spectral signature is shown in Figures 11b and 11c. This is an activity where we will be seeking broad collaborative partnerships to build a comprehensive and useful spectral data library.

4.5 Digital Multispectral Video

Digital Multispectral Video (DMSV) is an emerging technology that has strong potential application to disaster response and mitigation activities, as well as many other site characterization applications. The DMSV is an airborne instrument that acquires high spatial and temporal resolution multispectral (visible to near infrared) imagery. This technology is very useful for accurately characterizing complex tidal, atmospheric, geologic, anthropogenic induced change, and geometric events that would be difficult to measure with other systems.

The surface characterization application of DMSV, shown in figures 12 and 13, illustrates the system's tuning ability for detection of whether shoreline or aquatic vegetation are predominate in an environmental monitoring application. In Figure 12 the location and density of shoreline vegetation is very evident, but only the presence or absence of aquatic vegetation is observable using the 0.75, 0.66, and 0.55 micrometer bands. If a band combination of 0.77, 0.75, and 0.55 micrometers is used, the density of aquatic vegetation can be observed (Figure 13).

The DMSV system is comprised of four charged coupled device (CCD) cameras with 12-mm focal length lenses, a ruggedized 486 PC, 32 Mb of RAM, a 500 Mb hard disk, and a 4-Mb AT frame-grabber board. Each of the four cameras were fitted with a 25-nm band pass interference filter. These filters were centered at 450-nm, 550-nm, 650-nm, and 750-nm, respectively. The four bands are captured simultaneously and stored on internal RAM. Each 8-bit, 740 by 578 pixel four-band frame is a little over 1.7 Mb in size, which allows for the collection of 17 frames before the data must be transferred to the PC hard drive.

4.6 Fluorescence

Fluorescence is the emission of light or other electromagnetic radiation of longer wavelengths by a substance as a result of the absorption of some other radiation of shorter wavelengths. Fluorescence spectroscopy is a common technique used in many scientific fields including geology, biology, and medicine, and more

recently, remote sensing. Fluoresced energy is considered to contain more information about a features structure than reflected energy. There are two primary techniques to obtain fluorescence information, active fluorescence and passive fluorescence. Active fluorescence is the more common method in which the excitation energy is supplied by some source other than the sun. Normally, this is a laser or some other monochromatic light source. Passive fluorescence uses solar radiation as the excitation source and emission can only be measured in solar absorption regions, also called Fraunhofer lines (J. N. Rinker, 1997).

TEC is active in many areas of fluorescence research. Currently, there are two operating bench-top spectral fluorimeters being used in this research. One is a portable passive spectrofluorometer. The second is a new Laser-Induced Fluorescence Imaging System (LIFI), which will begin operation this summer. The LIFI instrumentation is used to derive basic relationships between an objects physical state and fluorescence response. Fluorescence sensors have been used very successfully to study petroleum spills, plant stress, and aquatic chlorophyll.

The significance of fluorescence signatures for petrochemicals, such as oil, is shown in Figures 14a and 14b. Figure 14a represents the fluorescence frequency distribution of an organic garden soil. When only one drop of oil is mixed into the soil, the frequency distribution is dramatically changed. This same characteristic could be used to remotely detect, and precisely locate, small underground gas and oil leaks following earthquakes and other natural disasters.

There are a number of ongoing collaborative research projects in the fluorescence area between TEC and other groups and agencies, including U.S. Department of Energy, Disney's Epcot Center, and the Virginia Institute of Marine Science. Much of the work in this area will be incorporated into the spectral library program.

4.7 Radar Systems

The state-of-the-art in exploiting interferometric synthetic aperture radar (IFSAR) for terrain information is advancing rapidly, and provides significant potential for use in crisis support operations. Unlike conventional SAR imagery, IFSAR data permits the generation of rectified SAR images co-registered with an accurate terrain elevation file. In addition, this imagery can have an absolute geographic accuracy of 3m RMS or less. The rapidity with which IFSAR data can be collected and processed over wide areas, and the all-weather, day-night capability, offers significant potential for providing direct support to crisis situations, as well as enhancing the performance of spectrally-based assistance. In addition, IFSAR terrain elevations can be employed to rectify hyperspectral imagery, allowing for the registration of radar and hyperspectral imagery in the ground plane, thus providing an improved database for the extraction of topographic information (Figure 15).

The contractor for this program, titled Interferometric Synthetic Aperture Radar for Elevations (IFSARE), was the Environmental Research Institute of Michigan (ERIM). Their efforts resulted in the fabrication of an interferometric radar system integrated with a GPS internal navigation system which was mounted on a Learjet 36A. The National Aeronautic and Space Administration jointed with the Jet Propulsion Laboratory in California to develop the processing software and the ground-processing environment. This software and ground processing capability has now been transitioned to the Intermap Technologies Company, and is available for commercial applications.

This effort represents a convergence of technology developed by a large number of investigators, only a few of whom are referenced above, and a pressing need for low cost, fine resolution, highly accurate terrain elevations for a wide variety of applications. It is critically dependent on recently devised GPS capabilities and the advent of high-speed data processing capabilities.

In summary, the IFSARE system for collecting digital elevation map information, at low cost, is just now becoming available for application to problems such as disaster responses. It is anticipated that significant IFSAR data collections will occur in the next few years. Ongoing activities within TEC are focused quantifying the performance of IFSAR techniques. Additional work will be done for demonstrating the capability to merge radar and hyperspectral data. There is significant potential for application of IFSAR data in all four phases of disaster management.

4.8 Photogeologic Analysis

Historical Photogeologic Analysis using Aerial Photography allows mapping of terrain features, such as fractures or the surface expression of these fractures, which are called lineaments. Fractures in the bedrock are important to identify because they often serve as contaminate conduits. They are the "doorways" that allow surface contamination to enter the ground water system (Figures 16, 17, and 18). Changes in land use and land cover often obscure the surface expression of these fractures in the underlying bedrock.

Additionally, knowledge of the location, direction, and length of fractures significantly improves the speed and results of costly Geophysical Studies by correct alignment of their survey track planning. Also, surveys that, for lack of good planning input, do run parallel to fractures, often produce erroneous data.

In an area of Karst terrain, photogeologic analysis identification of historical sinkhole depressions can be used. These features also frequently "disappear" with changes in Land Use and Land Cover. Like fractures, sinkholes serve as a direct contaminate conduit for connecting the surface with the ground water system.

Photogeologic analysis can be applied to the identification of historic seismic shear zones, and to the geo-positioning of these features onto current maps and GIS products. Such products could be used in all phases of disaster

management.

4.9 Shaded Relief Products

Shaded relief image and vector products are intended to give the user a better perspective of the ground terrain of interest. Figure 19 shows the registration of a 20-degree angle hyperspectral image with a 90-degree vertical hyperspectral image of the same area.

The co-registered image gives the perspective of higher resolution and near 3-D presentation. In this application, the same land-use color coding was used for each image. The classification was done using automatic delineation of roads, grasses, trees, water, etc., using only the spectral response of those materials.

4.10 Differential Global Positioning System

Techniques developed to process signals from two GPS receivers operating simultaneously can be used to determine the 3-D vector between the two receivers. These techniques are known as Differential GPS (DGPS), and can be used to produce results ranging from millimeters to a few meters, depending on the method used. DGPS can easily achieve centimeter-level accuracy using the carrier phase information broadcast by the GPS satellites. The On-The-Fly (OTF) system has been under development at the TEC since the late 1980s. This system provides real-time 3-D positions with horizontal and vertical accuracy of 3 cm over ranges up to 20 km from a single reference station without static initialization.

This high accuracy DGPS technology, developed at TEC, is being used aboard various platforms (i.e., airboats, helicopters, and wheeled vehicles) to support the U.S. Geological Survey's efforts to accurately map the Everglades National Park and surrounding suburban areas. This mapping project is in direct support of the South Florida Ecosystem Restoration Initiative, which involves various federal, state, and local agencies. Data collected for this effort will be used to produce water flow models to accuracies that were previously impossible, and, thus, will enable the

assessment of the effect of flood control structures and urbanization on this fragile natural ecosystem.

The DGPS technology also is being used to very accurately measure tides at the boat or inlet location without the need to construct a physical tide measurement station. The first application of this system is underway at Kings Bay inlet in South Georgia (Figure 20). This could dramatically change the way tides are measured. It also has application to all disaster management situations where rapid accurate knowledge of tide levels is needed to better plan or respond to the emergency.

4.11 Geographic Information Systems

Geographic Information Systems (GIS) collect, manage, analyze, and display geographic data. While GIS has much in common with other information systems technologies, it is unique in its ability to process information about the location of geographic features (Board of Earth Sciences and Resources, 1997). Because of this emphasis on location, GIS technology has found application in a wide variety of fields, including banking, precision farming, real estate, forestry, military operations, and emergency management.

A key feature of GIS is its ability to integrate data from different sources. GIS data comes from maps, satellite imagery, aerial photography, survey data, pictures, and text (Berry, 1995). GIS software takes this disparate information and puts it in a common framework.

The power of GIS lies in its sophisticated tool set for analyzing geographic information. Distance, direction, and area measurements can be calculated. Map layers can be overlaid and combined in different ways as shown (Figure 21). Buffers inside or outside of features can be generated. Shortest paths through a network, or across a surface, can be calculated. Relationships among features, like connectivity, adjacency, or nearness, can be determined.

The analysis functions of a GIS can be combined in powerful ways. A GIS can answer complex

queries, such as "Find the closest support vehicle near point A, and route it along the shortest path between its current location, point A and point B. Choose the path that avoids roads within 200 yards of the floodplain, and roads that are currently under construction."

GIS technology is particularly relevant to emergency management and can be used in all four phases: mitigation, preparedness, response, and recovery. For mitigation, a GIS can show the locations of hazards and analyze the vulnerability of people and property under different potential disaster scenarios. For preparedness, a GIS can map the locations and characteristics of resources available to respond to a disaster. Evacuation routes can be predetermined for different disaster scenarios. When disaster strikes and the response phase starts, GIS can support the identification, location and deployment of resources. Adjustments can be made in real time to reflect the changing hazard, infrastructure, or availability of resources. For short-term recovery, GIS is a valuable tool used during damage assessment, and for the creation of documentation required for relief support. Finally, GIS can be used for redevelopment or relocation planning as part of a longer-term recovery effort.

An example application of GIS in the project management area is the Civil Works Digital Project Notebook (DPN). The objective of the DPN was to develop a Windows-based software package capable of replacing the 38 3-in binders of Civil Works project maps and information, and enabling geographically referenced queries of project information. The DPN is composed of a series of functions to display information about the Civil Works projects referenced to district, division, congressional district, state, and national boundaries. Each project, defined as a point on a map of the U.S., has associated tabular data, such as name, type, status, funding amount, etc., that can be displayed on command. In addition, there is a linked description, large-scale map, and picture associated with each project as shown in Figure 22. The project information used in the DPN was compiled from the hard copy project notebooks and/or district input.

ArcView, a commercial-off-the-shelf GIS package from ESRI, Inc., was used as the fundamental building block of the DPN. The ArcView-based DPN displays various themes of importance to HQ personnel, district and division personnel, and congressional staffs, who are accustomed to using the traditional bound document. These themes are displayed on a map of the U.S., which includes projects (represented by dots), major waterways, major roads, district boundaries, division boundaries, congressional boundaries and state boundaries. The user can query projects based on geographical area, type, category class subclass, status, funding and/or name. The menu was designed to be simple and usable by those with no ArcView experience, and minimal computer experience.

5. SATELLITE SENSOR INFORMATION

There are a number of satellite based sensors currently available for image-based product production. A sampling of current satellites and some near-term projected systems scheduled for deployment is shown in Figure 23. Landsat and SPOT were the sources of space-based imagery during the 1970s and 1980s. Spatial resolution for these systems ranged from 120 to 10 meters, with most applications using 30-m spatial resolution data during that time frame. Revisit times for these systems were 16 to 18 days for Landsat, and 26 days for SPOT (Remote Sensing Users' Guide, 1997).

More recent systems have added all-weather capabilities with RADARSAT and IFSAR in 1995, and spatial resolutions down to 5 m. Revisit times also decreased to every 2 to 9 days. The EarlyBird sensor, launched in late 1997, had a spatial resolution of 3 m and a 2 to 3 day revisit time. Unfortunately, communication with the sensor was lost and no images were ever received from the system. The follow-on sensor system, by EarthWatch, Inc., is QuickBird, which is scheduled for launch in late 1999.

Space Imaging, Inc, plans to launch a new satellite, in June of this year, that could add significant imagery resources. It will have a 1-m

spatial resolution in the panchromatic mode and a 2- to 4-day revisit capability. In the multispectral mode, its spatial resolution will be 4 m using 4 bands in the 0.45- to 0.90-um range.

6. CONCLUSION

The opportunity to leverage technology in the geospatial area to assist in disaster management has never been greater. There are many tools and processes currently in use that have not been applied to assist in disaster management. Examples include the application of hyperspectral sensor data, use of digital multispectral video, and geospatial 3-D fly-through analysis. All of these capabilities could support and enhance the information available to the disaster management decision maker.

There are exciting changes expected to occur during the next few years in the geospatial data community. New aircraft and space-based sensor systems are planned that will revolutionize the spectral and spatial resolution of data available for commercial applications. There will be challenges, particularly in the data processing and management area, because of the extremely large spectral databases these new sensors will generate.

The spectral library project also provides an opportunity to expand cooperatively our global understanding of the vegetative and geologic spectral makeup of the earth. The baseline data from this effort would be invaluable in conducting change analysis assessments following a natural disaster, such as an earthquake or hurricane. Using some of the analysis tools described earlier, the analysts and decision makers could virtually walk into the disaster situation. Other spectral technologies, such as fluorescence, could be used to precisely locate very small underground gas and oil leaks remotely.

Within the next decade, there may be the ability to better harness geospatial analysis capabilities to help reach the vision for the cooperative exchange of timely, relevant information useful during all phases of disaster management--to save lives and reduce economic loss.

7. REFERENCES

Barr, Samuel, Hyperspectral Imagery Exploitation Tutorial, International Symposium on Spectral Sensing Research, San Diego, CA, 1997.

Berry, Joseph K., Spatial Reasoning for Effective GIS, Fort Collins, CO, GIS World Books, 1995.

Board on Earth Sciences and Resources, Rediscovering Geography, National Research Council, National Academy Press, Washington, D.C., 1997.

Burton, Ian, Robert W. Kates, and Gilbert F. White, The Environment as Hazard, 2d Edition, New York, NY: The Guilford Press, 1993.

Disaster Information Task Force Report, Harnessing Information and Technology for Disaster Management, Global Disaster Information Network, 1997.

ENVI Inc., AVIRIS Image of Big Horn Basin, Wyoming, <http://www.envi-sw.com/images/asprs>, 1998.

Remote Sensing Users' Guide, U.S. Army Topographic Engineering Center, 1997.

Rinker, J.N., Spectral Remote Sensing Tutorial, International Symposium on Spectral Sensing Research, San Diego, CA, 1994.

Roper, William E., Challenges in Spectral Sensing Research; Observations to Information, International Symposium on Spectral Sensing Research, San Diego, CA, 1997.

Tobin, Graham A., and Burrell E. Montz, Natural Hazards: Explanation and Integration, New York, NY: The Guilford Press, 1997.

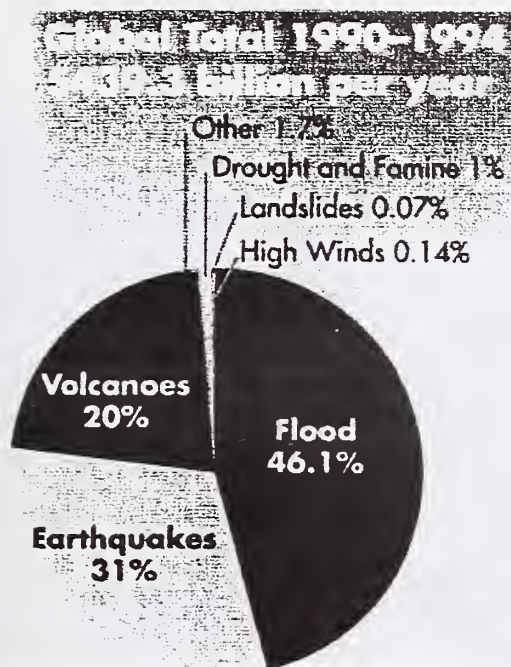


Figure 1: Global Natural Disaster Costs and Distribution by Event Categories (GDIN Task Force Report, 1997)..

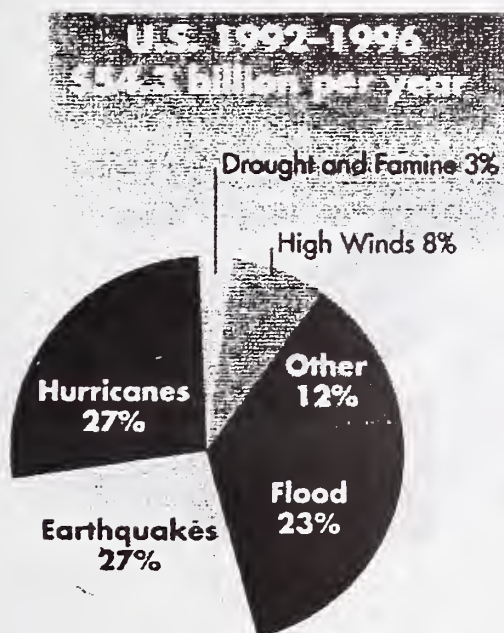


Figure 2: United States Natural Disaster Costs and Distribution by Event Category (GDIN Task Force Report, 1997).

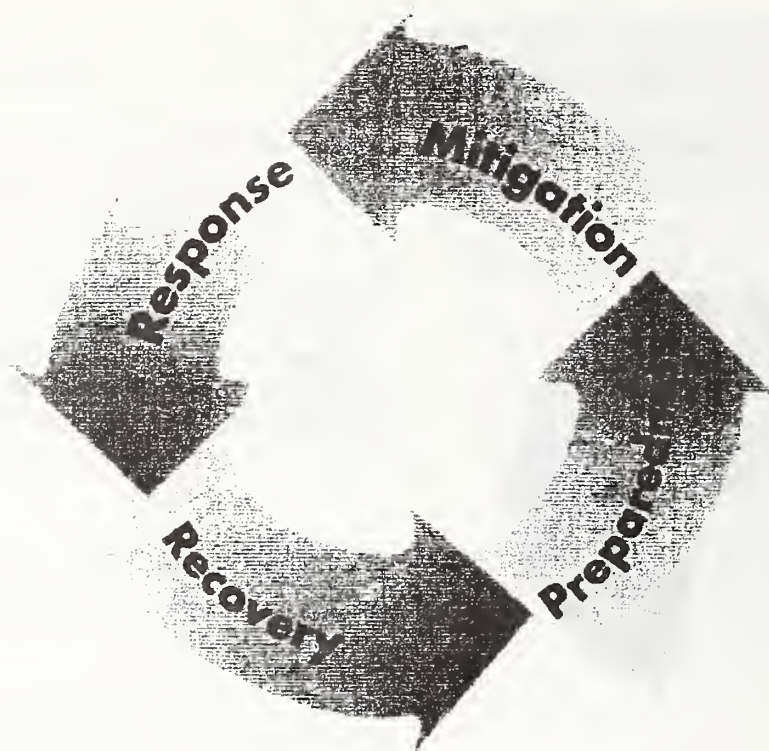


Figure 3: The Four Fundamental Elements of Disaster Management.

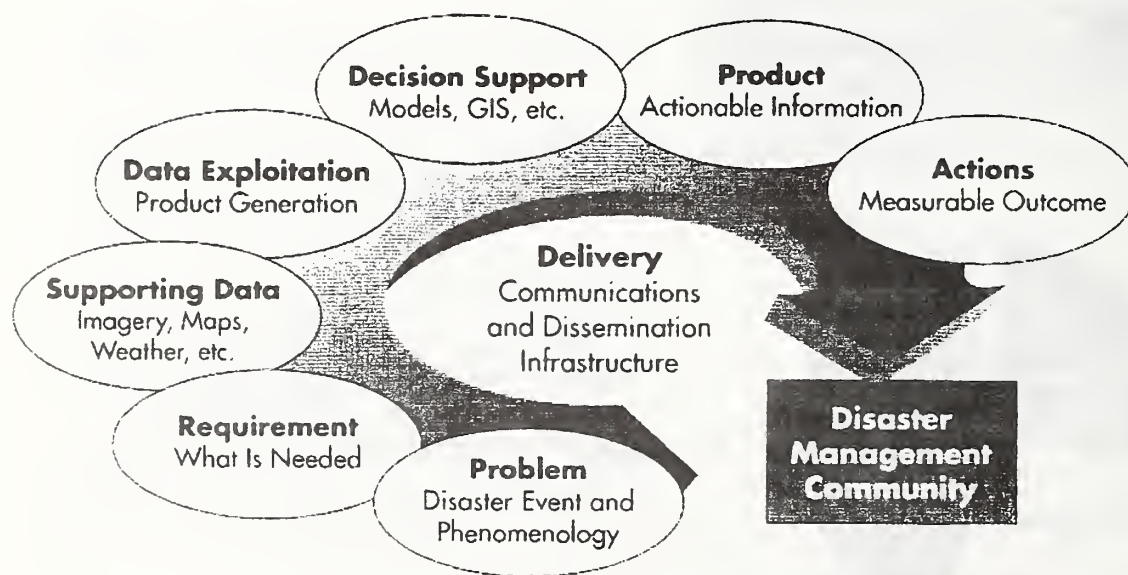


Figure 4: Elements of the Disaster Management Process (GDIN Task Force Report, 1997).



Figure 5: Image of River Valley used in DrawLand Fly-Through.

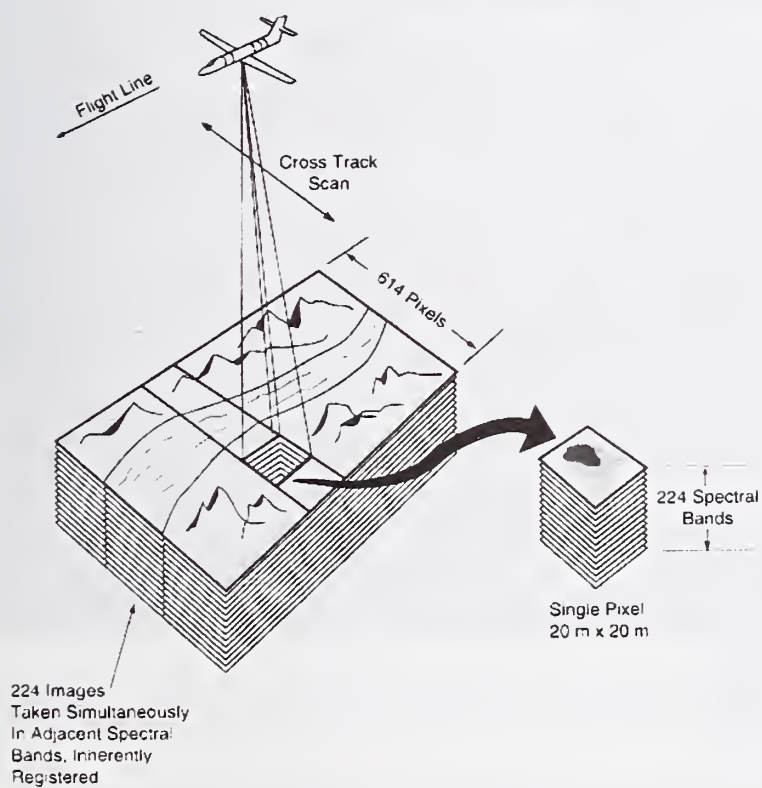


Figure 6: Data Collection Illustration of the AVIRIS Hyperspectral System.

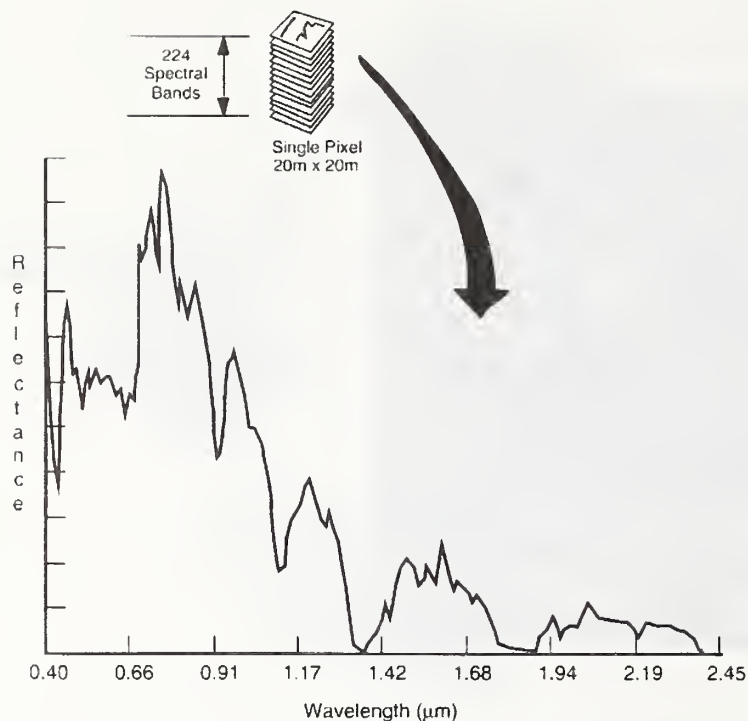


Figure 7: Spectral Distribution from a Single AVIRIS Image Cube.

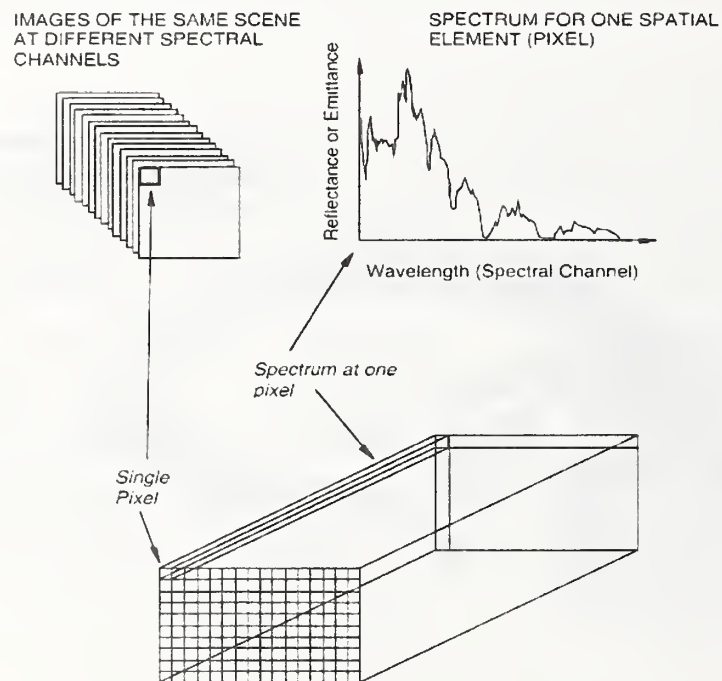


Figure 8: Pixel, Spectral Distribution, and Image Cube, Relationships in a Hyperspectral Analysis.



Figure 9: Mosaic of Landsat Thematic Mapper and AVIRIS Images of a Portion of Big Horn Basin near Worland, WY, U.S.

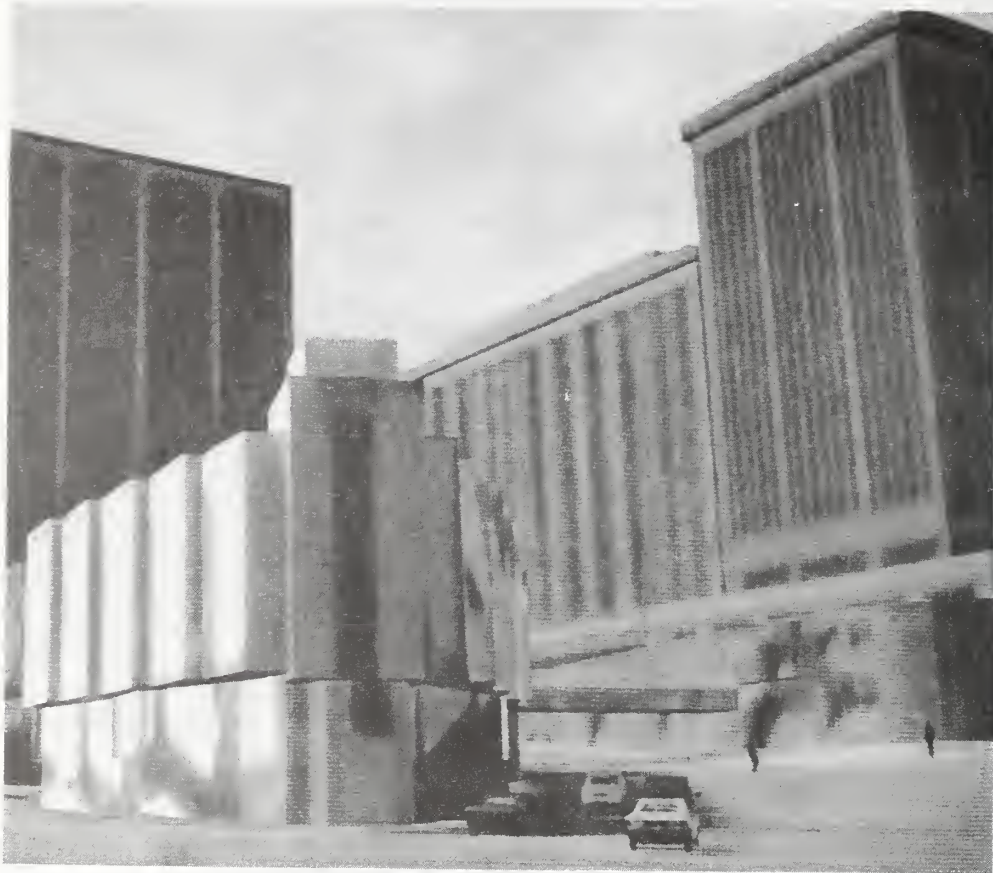


Figure 10: Scene for Geospatial Fly-Through of Rosslyn, VA, using Socet Set Image Exploitation.

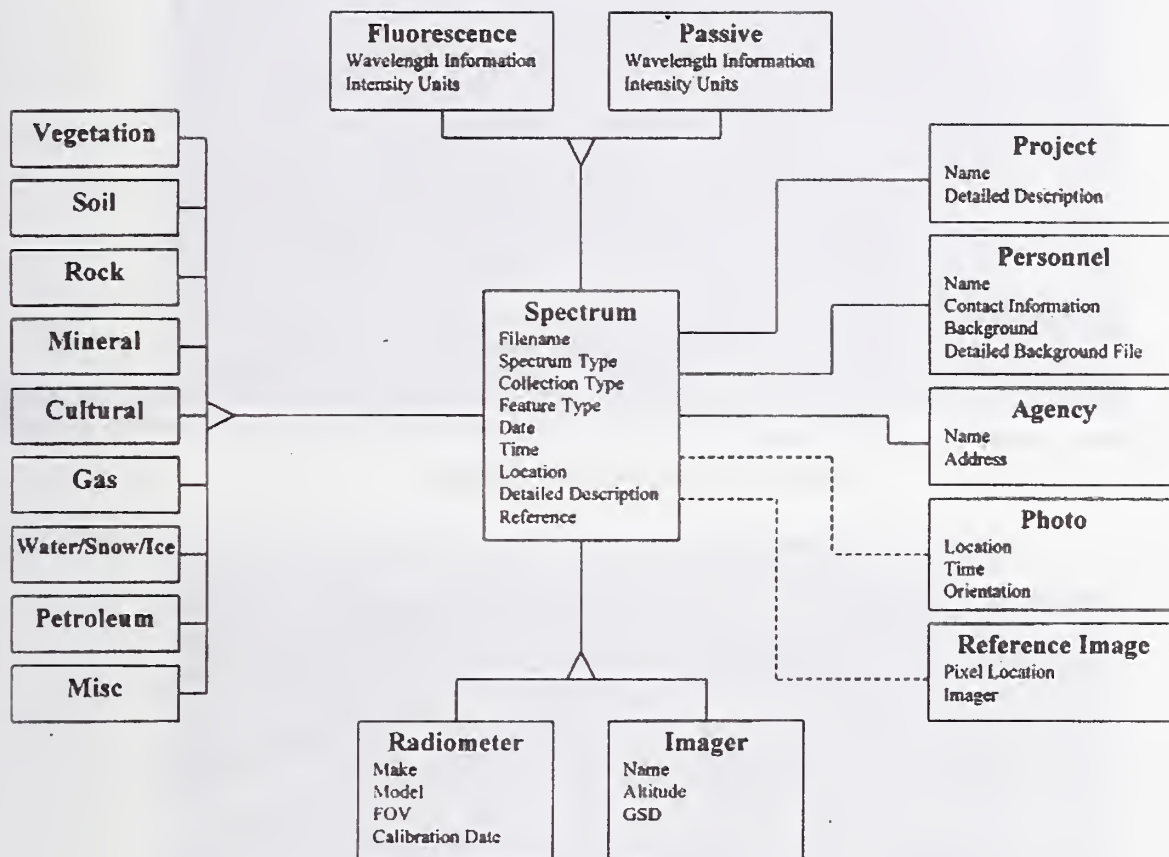


Figure 11a: Framework for the Spectral Library Database Structure.

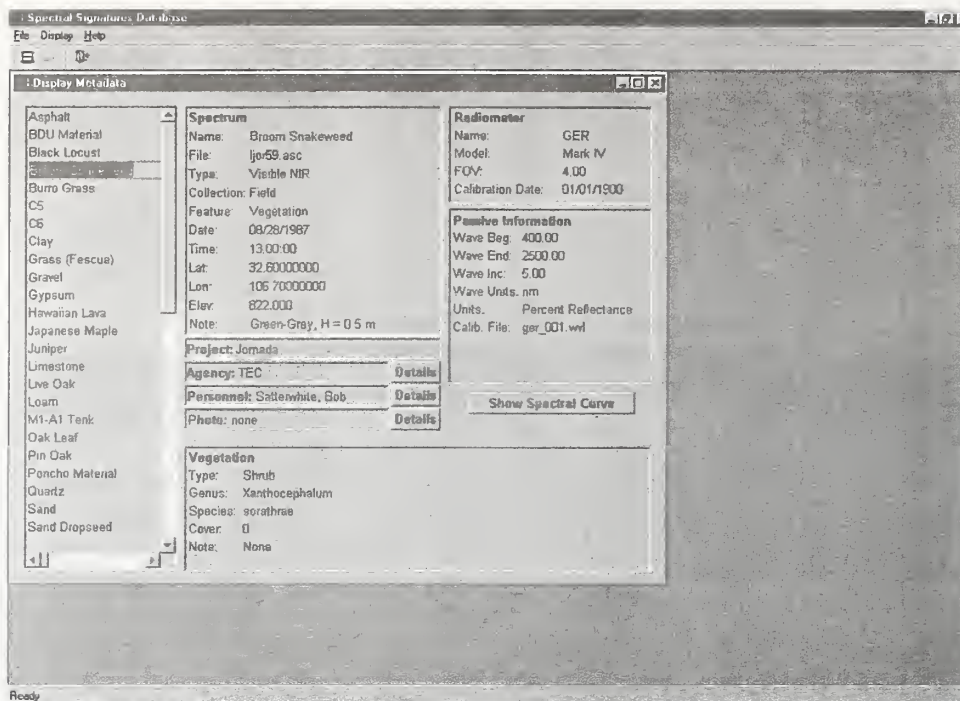


Figure 11b: Prototype Metadata Display.

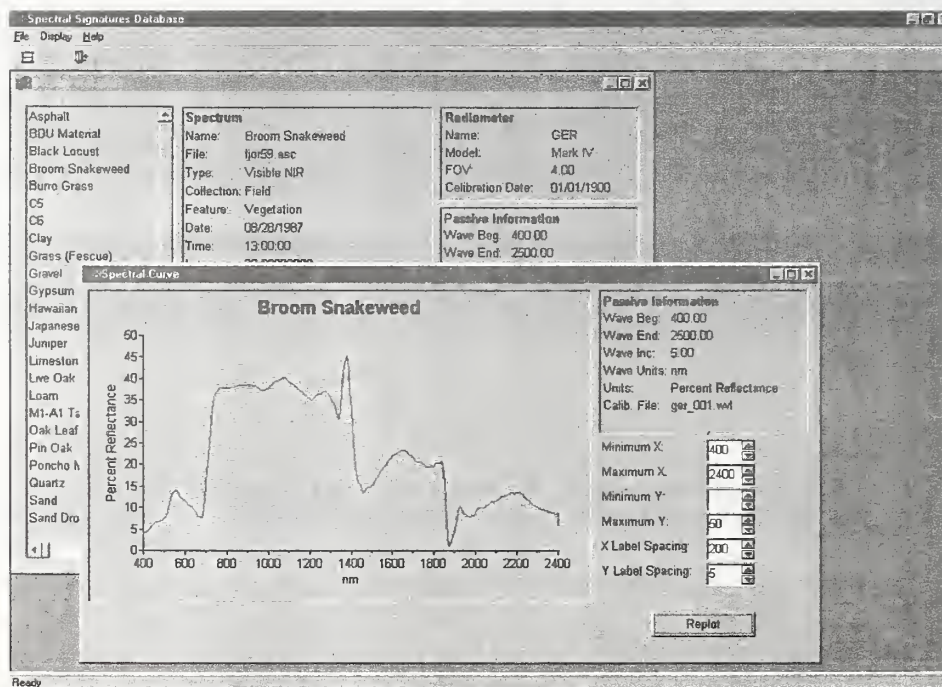


Figure 11c: Prototype Spectral Signature Display.



Figure 12: Digital Multispectral Video (DMSV) image compiled using bands 0.75, 0.65 and 0.55 micrometers. This combination shows the shoreline vegetation as well as the presence or absence of aquatic vegetation.



Figure 13: Digital Multispectral Video (DMSV) image using a different combination of bands. Changing the band combinations to 0.77, 0.75 and 0.55 micrometers shows density of aquatic vegetation.

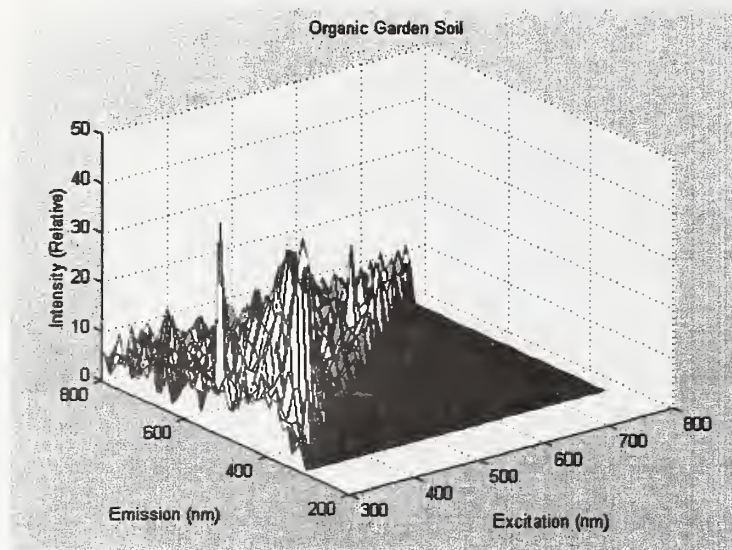


Figure 14a: Fluorescence frequency distribution for organic garden soil.

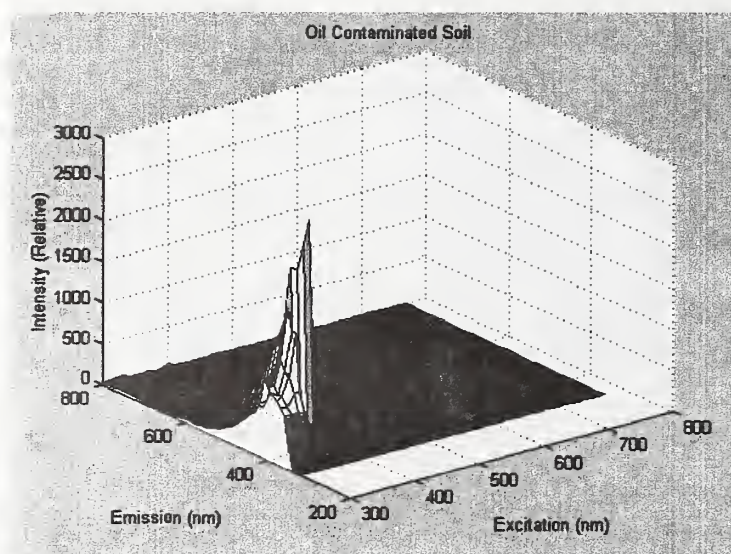


Figure 14b: Fluorescence frequency distribution for the same organic soil mixed with one drop of oil.



Figure 15: Interferometric Synthetic Aperture Radar (IFSAR) image.

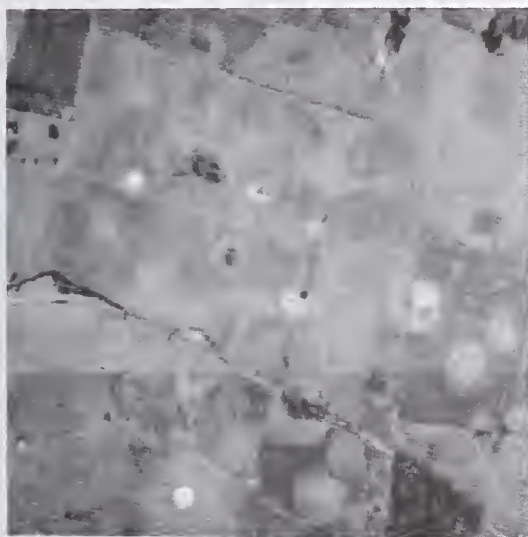


Figure 16: Photogeologic Analysis using 1937 and 1992 Aerial Photo Images.

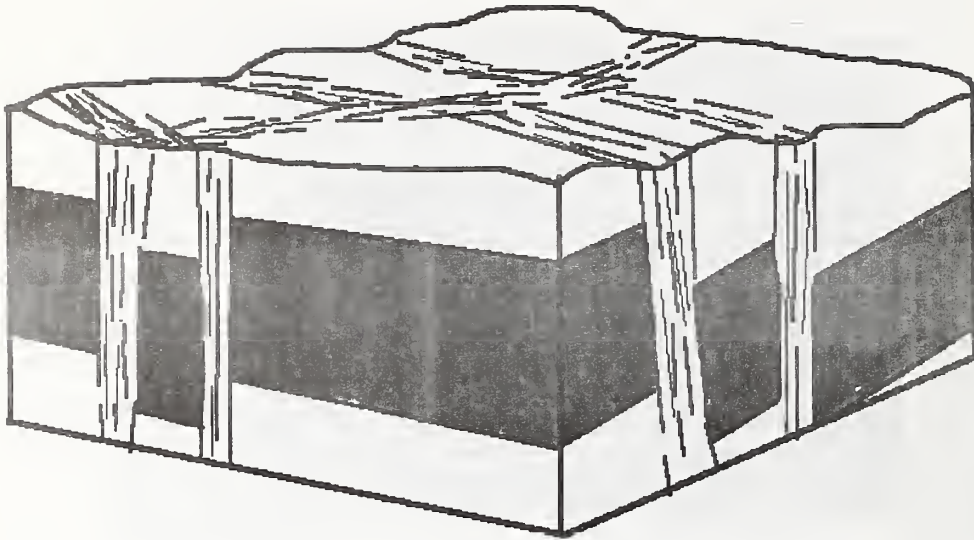


Figure 17: Schematic of Fracture Traces and Lineaments.

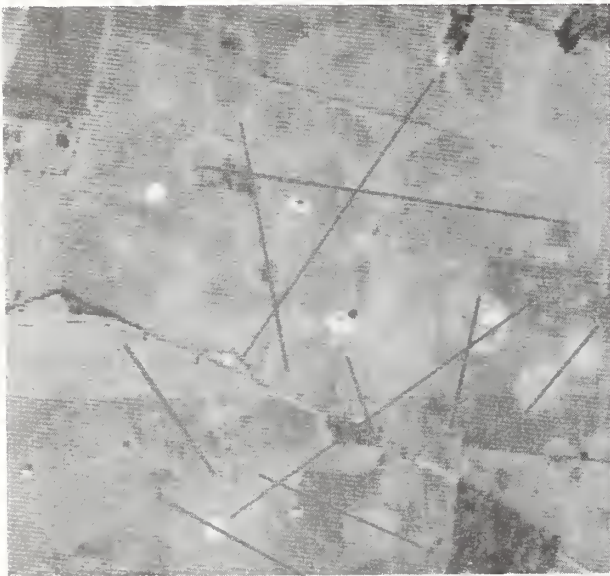


Figure 18: Fracture Trace Analysis and Image Overlays.

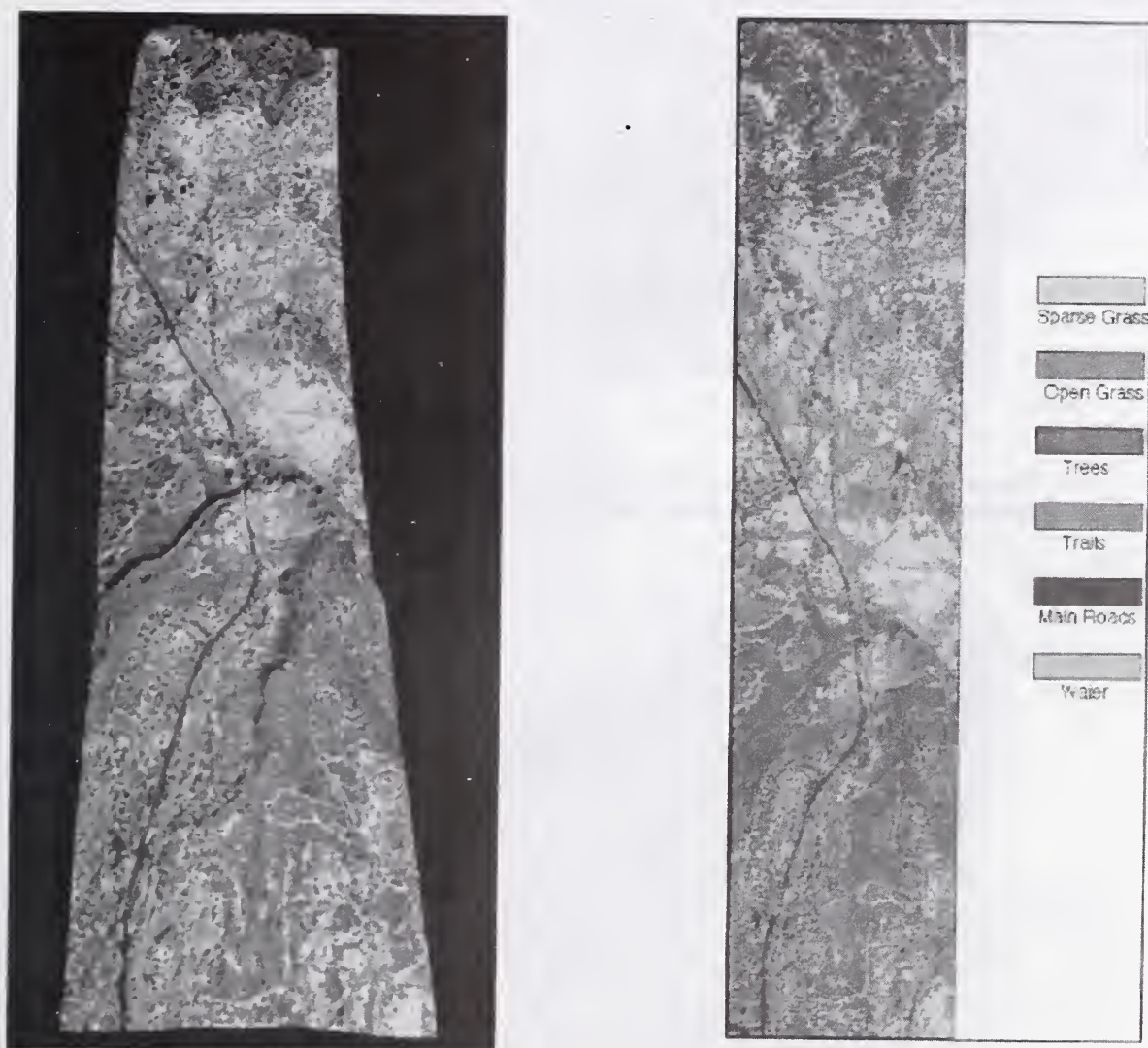


Figure 19: Comparison of a shaded relief image and a 2D land use image.

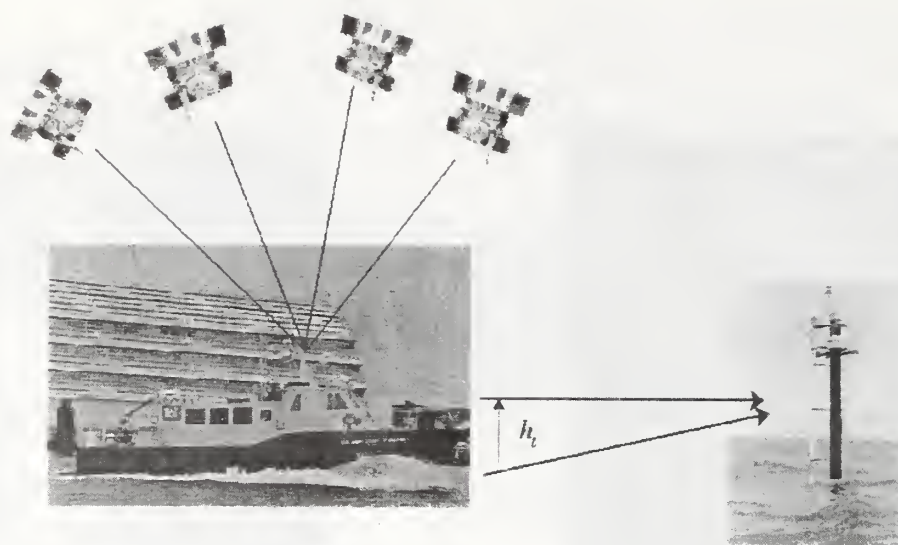


Figure 20: Differential Global Positioning System (GPS) application for precise tide level measurement using the Nav-Star Satellite Constellation.

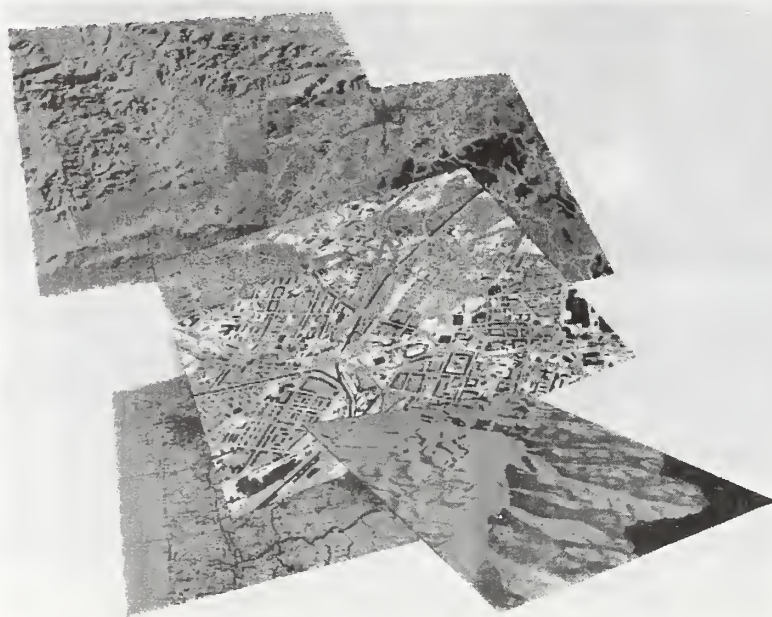


Figure 21: Geographic Information System (GIS) Data Layers.

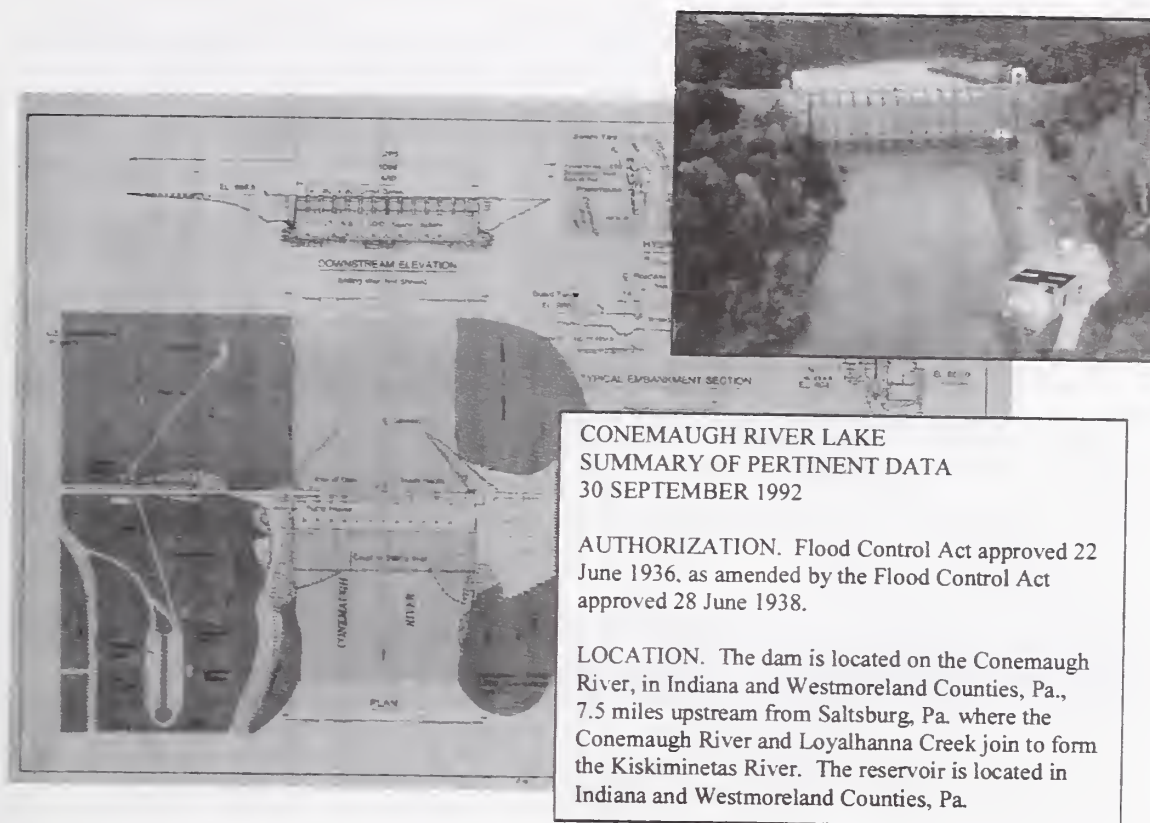


Figure 22: GIS-Based Digital Project Notebook.

Sensor	Spatial Resolution	Revisit Time	Operational Dates	Wavelength Regions	# of Bands
Landsat MSS	80 meter	16-18 days	since 1972	0.50-1.1 μ m	4
Landsat TM	30 meter	16 days	since 3/84	0.45-2.35 μ m	6
	120 meter	16 days	since 3/84	10.4-12.4 μ m	1
SPOT PAN	10 meter	26 days	since 2/86	0.51-0.73 μ m	1
SPOT XS	30 meter	26 days	since 2/86	0.50-0.89 μ m	3
Std. Aerial Photo	variable	user-defined	since 1980	B&W, Color IR, Color	
RADARSAT	10-30 meter	2-9 days	since 10/95	C-Band SAR	
IFSAR	5-10 meter	user-defined	since 1995		
Digital Orthophoto	variable	user-defined	since 1980s	user-defined	
Digital MSI Video	0.25 meter potential	user-defined	since 1994	0.35-0.95 μ m	4
EarthWatch, Inc.		2-3 time/day			
EarlyBird-Pan	3 meter		lost communication	0.45-0.80 μ m	1
EarlyBird-MSI			lost communication	0.50-0.89 μ m	3
QuickBird-Pan			launch late 1999	0.45-0.90 μ m	1
QuickBird-MSI			launch late 1999	0.45-0.90 μ m	4
Space Imaging, Inc.					
Panchromatic	1 meter	2-4 days	Spring 1998	0.45-0.90 μ m	1
Multispectral	4 meters			0.45-0.90 μ m	4

Figure 23: Table of Current Satellite System Availability and Capability.

WIND ENGINEERING

Analysis of Wind and Wind Effects Revisited - A Case Study of Deer Isle-Sedgwick Bridge

by

D. W. Marsh¹, B. Bienkiewicz², and H. R. Bosch³

ABSTRACT

In 1980 the Federal Highway Administration began a detailed study of the wind-induced oscillations of the Deer Isle-Sedgwick Bridge. The bridge is instrumented with an array of anemometers and accelerometers which measure wind velocity and bridge response. The present study analyzes the wind-induced motion of the bridge to determine fundamental frequencies and mode shapes. It introduces Proper Orthogonal Decomposition (POD) as a technique for determining primary frequencies and mode shapes and compares the results to those obtained using spectral analysis exclusively. It utilizes wavelet transform (WT) analysis to investigate energy content of temporal flow events and peaks of the bridge deck response. Both the POD and WT techniques are found to be useful in analysis of wind flow and wind-induced response of the bridge deck.

KEYWORDS: wind, proper orthogonal decomposition, wavelet analysis, bridge response, field measurements, aerodynamic response.

1. INTRODUCTION

The Deer Isle-Sedgwick Bridge (DISB) is a long-span suspension bridge similar in cross-section to the old Tacoma Narrows Bridge, which failed catastrophically in 1940 due to wind-induced structural vibration. The failure of the Tacoma Narrows Bridge made evident the need for detailed analysis of the dynamic behavior of long-span bridges subjected to wind loading. The DISB's design was augmented with many structural modifications to minimize wind-induced oscillations, but significant response is still observed. In 1980, the Federal Highway Administration (FHWA) began a detailed study of the wind-induced motion of the DISB. The present paper describes analysis

of the FHWA data to establish wind characteristics at the bridge site and to determine mode shapes and natural frequencies of bridge oscillation. It introduces new tools for wind and bridge response data analysis: the Proper Orthogonal Decomposition (POD) and Wavelet Transform (WT) analysis. The POD is shown to be effective in determining vibrational characteristics of the bridge. The WT is employed in analysis of the bridge peak response.

2. BACKGROUND

2.1 Conventional Analysis

Conventional analysis of wind and wind induced effects on bridges, buildings and other structures is frequently carried out in frequency domain, using spectral approach.

2.1.1 Wind Field

Wind flow in the atmospheric boundary layer is usually described for wind components in three orthogonal directions: along-wind, lateral, and vertical. The characteristics of fluctuations of these components are typically specified by power spectra, which are compared with empirical

¹ Dept. of Civil Engineering, Colorado State University, Fort Collins, Co 80523-1372.

² Turner-Fairbank Highway Research Center, Federal Highway Administration, McLean, VA 22101-2296 (on leave from Dept. of Civil Engineering, Colorado State University, Fort Collins, CO 80523-1372).

³ Turner-Fairbank Highway Research Center, Federal Highway Administration, McLean, VA 22101-2296.

spectral formulas based on field measurements. A number of such formulas have been proposed. The spectral models recommended by Kaimal, Harris, and Lumley and Panofsky, Simiu and Scanlan (1996), are considered in this paper.

2.1.2 Bridge Response

Fundamental frequencies of oscillation of lightly damped structures can be determined from spectral analysis of response measurements. The peaks in the autospectra of the response are either due to peaks in the excitation spectra or normal mode oscillations. The cause of such peaks can be determined by analyzing the phase information of the cross-spectra between measurements at different points on the structure. In case of a bridge deck, vertical (bending) and torsional modes can be distinguished by analyzing the cross-spectrum between measurements at two laterally spaced points on the structure. The measurements in phase indicate a vertical mode, while measurements that are 180 degrees out of phase indicate a torsional mode.

The fundamental modes of oscillation of a lightly damped structure can be defined using the autospectra of response measurements taken at different points on the structure. For a given natural frequency, the square root of the autospectral value at this frequency gives the magnitude of the ordinate of the mode shape at a considered location. The sign of this modal value is determined with respect to a reference point using the phase information from the cross-spectrum between the measurements at the reference point and the selected location.

The coherence function provides important information for determining fundamental frequencies and modal shapes. It can be used to estimate the random errors in the phase values and thereby establish the statistical significance of the phase information. In general, the autospectral values should be used to determine the fundamental mode shapes only if the cross-spectra between the considered locations produce near unity coherence and near 0 or 180 degrees phase, Bendat and Piersol (1993).

2.2 Proper Orthogonal Decomposition

Proper Orthogonal Decomposition, also called the Karhunen-Loeve expansion, is a mathematical technique to establish deterministic spatial function that is best correlated with a given random field. This is accomplished by finding the function of the largest projection (in the mean-square sense) on the field. The procedure leads to an eigenvalue problem involving spatial covariance.

The simplest implementation of the POD is for variables measured at uniformly spaced locations. In this case the POD for a variable r reduces to the following (discrete) eigenvalue problem

$$[R_r] = \lambda \{\Phi\}$$

where $[R_r]$ is the space covariance of the random variable r , λ is the eigenvalue, and $\{\Phi\}$ is the eigenvector (eigenmode). The eigenvectors are used in a series expansion of the variable r ,

$$r(x, y, t) = \sum_n q_n(t) \Phi_n(x, y)$$

where the principal coordinates $q_n(t)$ can be computed (in a discrete form) as follows

$$q_n(t) = \frac{\sum_i \sum_j r(x_i, y_j, t) \Phi_n(x_i, y_j) \Delta x_i \Delta y_j}{\sum_i \sum_j \Phi_n^2(x_i, y_j)}$$

Each principal coordinate $q_n(t)$ corresponds to a specific eigenvector Φ_n , which in turn represents n -th modal shape of the variable r .

It is shown that the spatial distribution of the variance of r can be written in terms of the eigenvalues and eigenvectors

$$\overline{r^2(x, y)} = \sum_n \lambda_n \Phi_n^2(x, y).$$

It follows that the relative magnitude of the

eigenvalue indicates contribution of a particular mode to the random field r .

In this study, the POD is employed to determine the eigenmodes and principal coordinates of approach wind flow and the natural frequencies as well as normal modes of the bridge deck oscillation. These quantities are then compared with the results obtained using spectral analysis.

2.3 Wavelet Transform Analysis

Conventional spectral analysis is based on Fourier Transform (FT), which is of a global nature. In the process, time localization of occurrence of extreme values of a given signal, such as peaks of wind speed and/or wind-induced bridge response, is lost. In addition, the standard FT is only applicable for stationary data. This limitation is to some extent overcome by a modified FT, the Short Time Fourier Transform (STFT). In this approach, short fractions of the original data record, resulting from application of fixed-duration filtering window, are used in the FT and a time-frequency decomposition of the original signal is obtained. However, the STFT has a number of shortcomings. The most critical is a limited frequency resolution.

Limitations of the FT and STFT are overcome by the Wavelet Transform (WT). Instead of using a window of a fixed time duration, the base functions of span dependent on time-scale (or frequency) of interest, are employed. Typically, these functions have a wavy nature and their duration is finite. These "small waves" are labeled wavelets. This is in contrast to harmonic (sine and cosine) waves of infinite span, employed in the FT. The WT base functions are obtained by dilatation (stretching or compressing) of a reference function, called the mother wavelet. A number of the mother wavelet functions have been developed. One of the functions - the Mexican hat wavelet- is employed in analysis presented in this paper.

The WT unfolds the signal as a time-frequency (or time-scale) function represented by wavelet coefficients. It leads to a good time-frequency resolution for both short and long-duration components of the signal. The parameter similar to

the autospectrum (calculated for example using the STFT), the wavelet modulus or its square, can be computed. It is typically plotted as a function of time and frequency (or scale) and such representation of the WT results is called a scalogram. The volume enclosed by the surface of the scalogram is directly related to the energy of the signal, just as the volume under the STFT autospectrum and the area enclosed by the conventional FT autospectrum, correspond to the variance of the analyzed signal.

The real, continuous WT is defined by the following transform pair

$$X(a, t) = \int_{-\infty}^{\infty} x(u) \psi_a(u) du$$

$$x(t) = \frac{1}{C} \int_{-\infty}^{\infty} \int_0^{\infty} X(a, u) \psi_a(u) \frac{1}{a^2} da du$$

where

$$\psi_a(u) = \frac{1}{\sqrt{a}} \psi\left(\frac{u-t}{a}\right)$$

and

- $\psi(u)$ = mother wavelet function,
- a = scale parameter,
- t = time instant,
- $x(t)$ = original signal,
- $X(a, t)$ = wavelet transform, and
- C = normalization constant.

The choice of the mother wavelet depends on the intended use. The 'Mexican Hat' wavelet function

$$\psi(u) = (1 - u^2) e^{(-u^2/2)}$$

was used in the analysis presented herein.

3. FIELD CONFIGURATION

3.1 Deer Isle-Sedgwick Bridge

The Deer Isle-Sedgwick Bridge (DISB) is a long-span, girder-stiffened suspension bridge, on the Atlantic coast of Maine, which connects the

mainland at Sedgwick with Deer Isle, in the NE-SW direction. It was constructed in 1938 and opened to traffic in 1939. Its main span is 1080 feet long, while the two side spans are 484 feet in length. In addition, there is a 100-foot long approach span on each end giving a total bridge length of 2248 feet. The 20-foot wide deck carries two traffic lanes and it has an H-type cross-section, similar to that of the old Tacoma Narrows Bridge. Originally, the deck was supported only with vertical hangers from the main cables. Later, cable stays, traverse bracing, and cable ties were added to increase the bridge resistance to wind. Although these modifications were effective in attenuating wind-induced bridge oscillations, instances of excessive response attributed to wind are still observed. As a result, the bridge continues to be the subject of an ongoing field measurement program carried out by FHWA, in collaboration with the State of Maine.

3.2 Instrumentation

The bridge is instrumented with an array of anemometers and accelerometers to monitor the wind speed and bridge accelerations, see Figure 1. There are six tri-axis Gill anemometers mounted on outriggers which extend 12 feet from the side and 3 feet above the deck. In addition, two skyvane anemometers are mounted on the east tower. One is located 18 feet above the tower top, while the remaining anemometer is at the tower base, approximately 33 feet above the water surface. The anemometers provide information on three components of the wind velocity: horizontal normal to the deck, horizontal along the deck, and vertical, see Figure 1.

Six pairs of single-axis servoaccelerometers are distributed along the span of the bridge, with four pairs of accelerometers on the main span and two pairs of accelerometers on the North side span, see Figure 1. Three additional accelerometers are used to measure the motion of one of the bridge towers.

Signals from pairs of the accelerometers on the deck are combined to monitor the torsional and vertical (heaving) motion of the deck, while the response in torsion, bending, and sway is extracted for the tower. Readings from the anemometers and accelerometers are acquired nearly simultaneously,

with a sampling rate of approximately 20 samples per second and a typical record length of 10 minutes.

4. DATA ANALYSIS

4.1 Conventional Data Analysis

4.1.1 Wind Field

The wind data were broken into 4096-data point records, of approximately 205-second length. Typically three such records were employed in spectral and cross-spectral analysis, which included ensemble averaging. The spectra were corrected for the frequency response of the anemometers, using approach proposed by McMichael and Cleveland (1978). Representative normal to the deck horizontal and vertical velocity spectra (uncorrected and corrected for the frequency response of the anemometers) are shown in Figure 2. They are compared with empirical wind spectra models proposed by Harris, Kaimal, and Lumley and Panofsky, Simiu and Scanlan (1996).

4.1.2 Bridge Deck Response

Since the analyzed data was dominated by the response in vertical (heave) direction, the results presented herein are limited to this direction. Representative autospectra of the deck vertical motion are depicted in Figure 3, while the natural frequencies and modal shapes, determined from the spectral/cross-spectral analysis are shown in Figure 4. A comparison of the natural frequencies for the three vertical modes is presented in Table 1. A very good agreement with the results reported by Kumarasena et al. (1991) can be observed.

4.2 Proper Orthogonal Decomposition

4.2.1 Wind Field

As mentioned earlier, the POD analysis is significantly simplified when the data is specified at (spatially) uniformly distributed locations. From the data set defined by anemometer locations in Figure 1, approximately equally spaced

anemometers 2, 5, and 6 were selected for the POD calculations. Representative results are shown in Figures 5 and 6, where the convergence of the reconstructions of the horizontal (normal to the deck) and vertical velocity components near the deck mid-span (anemometer location 5) are presented. It can be seen that the reconstruction involving only one POD mode was sufficient to fully recover the original time series of the vertical velocity component. Similar conclusions were found for the remaining anemometer locations.

4.2.2 Bridge Deck Response

The POD analysis of the bridge response was carried out for accelerometer data at locations 7 through 12. The signals from three pairs of the accelerometers (7-8, 9-10, and 11-12) were combined to obtain vertical and torsional accelerations at three, equally spaced bridge deck locations (quarter-span, half-span, and three-quarter-span), respectively. These six quantities (vertical and torsional accelerations at three locations) were used to calculate the space covariance matrix $[R_r]$, of the dimension six-by-six. Next, six eigenvalues, eigenmodes and principal components of the bridge accelerations were computed. Each eigenmode was arranged into two parts: (1) associated with the vertical degree of freedom and (2) associated the torsional motion. In this format the six vertical-torsional pairs of the modes are depicted in Figure 7, together with the corresponding six eigenvalues. The modes are arranged in a descending order of the eigenvalues. It can be seen that the first three modes are essentially vertical, while the remaining three modes are torsional. Included also in Figure 7 are power autospectra of the six principal coordinates q_n . The frequency of the dominant spectral peak is marked for the first four modes. It can be seen that the (three) POD vertical modes in Figure 7 closely resemble the natural modes obtained from spectral analysis. Also a comparison of the natural frequencies in Table 1 and spectra in Figure 7, shows that the spectral peak frequencies in Figure 7 are equal to the natural frequencies in Table 1. When the POD modes are ordered according to a descending magnitude of the spectral peak frequencies in Figure 7, then there exists one-to-one

equivalency between the POD results and the natural modes and frequencies resulting from conventional spectral analysis.

The last three modes in Figure 7 are torsional. As is indicated by the spectra of the principal coordinates associated with these modes, their participation in the bridge deck response is significantly smaller than that for the vertical modes. Mainly due to this fact, extraction of torsional modes was difficult using spectral analysis. It follows that this limitation is overcome when POD approach is employed.

Further analysis, not presented herein, shows that regardless of nature of the acceleration signals and the level of participation of natural modes in the structural response, the POD always leads to a set of the natural frequencies and structural modes. However, this approach has also a drawback. The number of modal contributions possible to be detected using the POD can not exceed the number of input signals used in analysis. If the number of the data channels is higher than the number of expected significant modes, this may not be a problem. Effort to apply the POD results to aid determination of the modal structural damping is currently underway.

4.3 Wavelet Transform Analysis

Wavelet transform (WT) analysis was used in this study to investigate frequency content of (temporal) peaks of the wind field and bridge deck response. Scalograms involving WT modulus were employed in the study. Also the wavelet coefficients were used in (wavelet) filtering and reconstruction of the analyzed signals.

4.3.1 Wind Field

Representative results of WT analysis of wind field are shown in Figure 8, for the anemometer near the deck mid-span, anemometer 5 in Figure 1. A fraction of the record of the horizontal (normal to the deck) velocity component and plot of the corresponding WT modulus are depicted. The time series in the figure is centered at the time instant of occurrence of the peak vertical

acceleration at the center of the deck. This scalogram highlights discontinuities in the wind velocity signal and reveals the spectral content of the wind velocity peaks. Significant contributions reaching down to 0.18 Hz, at several time instants, are exhibited.

4.3.2 Bridge Deck Response

Figures 9 and 10 show representative results of WT analysis of the bridge deck response. A fraction of the time series of the deck response at the mid-span location (accelerometers 9-10, Figure 1) is shown in Figure 9, together with its WT scalogram. The scalogram indicates a slightly modulated harmonic signal, with maxima at approximately 0.7 Hz. A closer examination of the numerical values of the WT modulus shows that the peaks actually occur at the frequency of 0.698 Hz. This is in a close agreement with the POD results in Figure 7, where a dominant participation (in the vertical motion) by the mode with the natural frequency of 0.698 Hz is apparent. Compare also spectral results in Figure 3.

Application of the WT results in decomposition and reconstruction of the bridge response time series is illustrated in Figure 10. The original signal (upper plot), the signal contribution at the frequency of 0.698 Hz (middle graph), and the signal reconstructed using the WT results (lower plot) are shown. It can be seen that indeed the 0.698 Hz-component of the signal is dominant (middle graph) and that the original signal can be reconstructed from the WT results.

It has been shown elsewhere, Bienkiewicz and Ham (1997), that the cross-wavelet analysis of the approach wind and wind-induced loading may provide useful physical insight, not available using traditional (e.g. FT based) techniques.

5. CONCLUDING REMARKS

The Deer Isle-Sedgwick Bridge data displays motion dominated by vertical modes of oscillation. Bridge response in the first three vertical modes was identified using traditional spectral approach. Compatible results were obtained using the POD analysis. In addition, by application of the POD it

was possible to identify modes of vibration not clearly apparent from FT spectral analysis. Wavelet transform was found useful in time-frequency analysis of extreme wind speed and bridge response. It made possible determining energy content of both the peak wind speed and bridge deck acceleration.

Further investigation is needed to fully evaluate the potential of application of the proper orthogonal decomposition and wavelet transform, as well as other novel techniques, in study of wind effects on long-span bridges and other wind-prone structures.

6. REFERENCES

- Bendat, J. S., and Piersol, A. G. (1993) Engineering Applications of Correlation and Spectral Analysis, John Wiley and Sons, Inc.
- Bienkiewicz, B. and Ham, H. J. (1997), "Wavelet Study of Approach-Wind Velocity and Building Pressure," *Journal of Wind Engineering and Industrial Aerodynamics*, Vol. 69-71, pp. 671-683.
- Bienkiewicz, B., Ham, H. J., and Sun, Y. (1993) "Proper Orthogonal Decomposition of Roof Pressure," *Journal of Wind Engineering and Industrial Aerodynamics*, Vol. 50, pp. 193-202.
- Bosch, H. R., and Miklofsky, H. A. (1993) "Monitoring the Aerodynamic Performance of a Suspension Bridge," *Proceedings of the 7th U.S. National Conference on Wind Engineering*, Los Angeles, CA, Vol. I, pp.125-134.
- Kumarasena, T., Scanlan, R. H., and Morris, G. R. (1989) "Deer Isle Bridge: Field and Computed Results," *Journal of Structural Engineering*, Proc. ASCE, Vol. 115, No. 9, pp. 2323-2328.
- Kumarasena, T., Scanlan, R. H., and Ehsan, F. (1991) "Wind-Induced Motions of Deer Isle Bridge," *Journal of Structural Engineering*, Proc. ASCE, Vol. 117, No. 11, pp. 3356-3374.
- McMichael, J. M. and Cleveland, W. G. (1978) "Characteristics of Helicoid Anemometers," NBSIR 78-1505, National Bureau of Standards,

Washington, D.C., 1978.

Simiu, E. and Scanlan, R. H. (1996), Wind Effects on Structures, 3rd Edition, John Wiley and Sons, Inc.

Table .1 Natural Frequencies of Deer Isle-Sedgwick Bridge

Vertical Mode	Spectral Analysis [Kumarasena et al.]	POD Analysis [Present Study]
1 st Symmetric	0.28 Hz	0.308 Hz
1 st Anti-symmetric	0.49 Hz	0.508 Hz
2 nd Symmetric	0.68 Hz	0.698 Hz

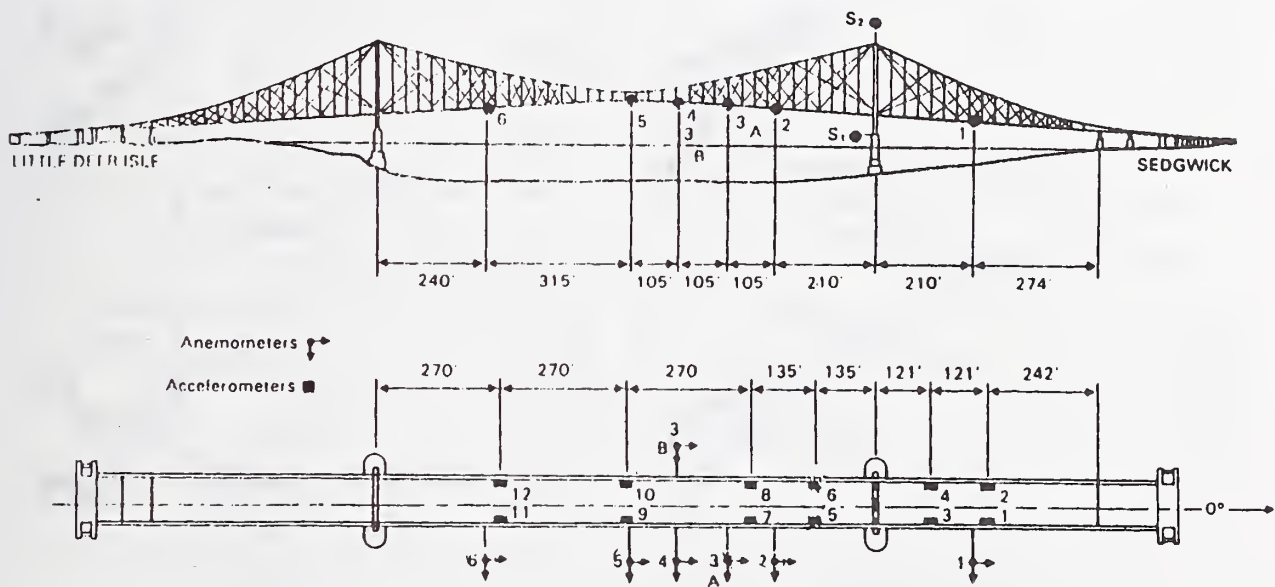


Figure 1. Deer Isle - Sedgwick Bridge -- Instrumentation Layout

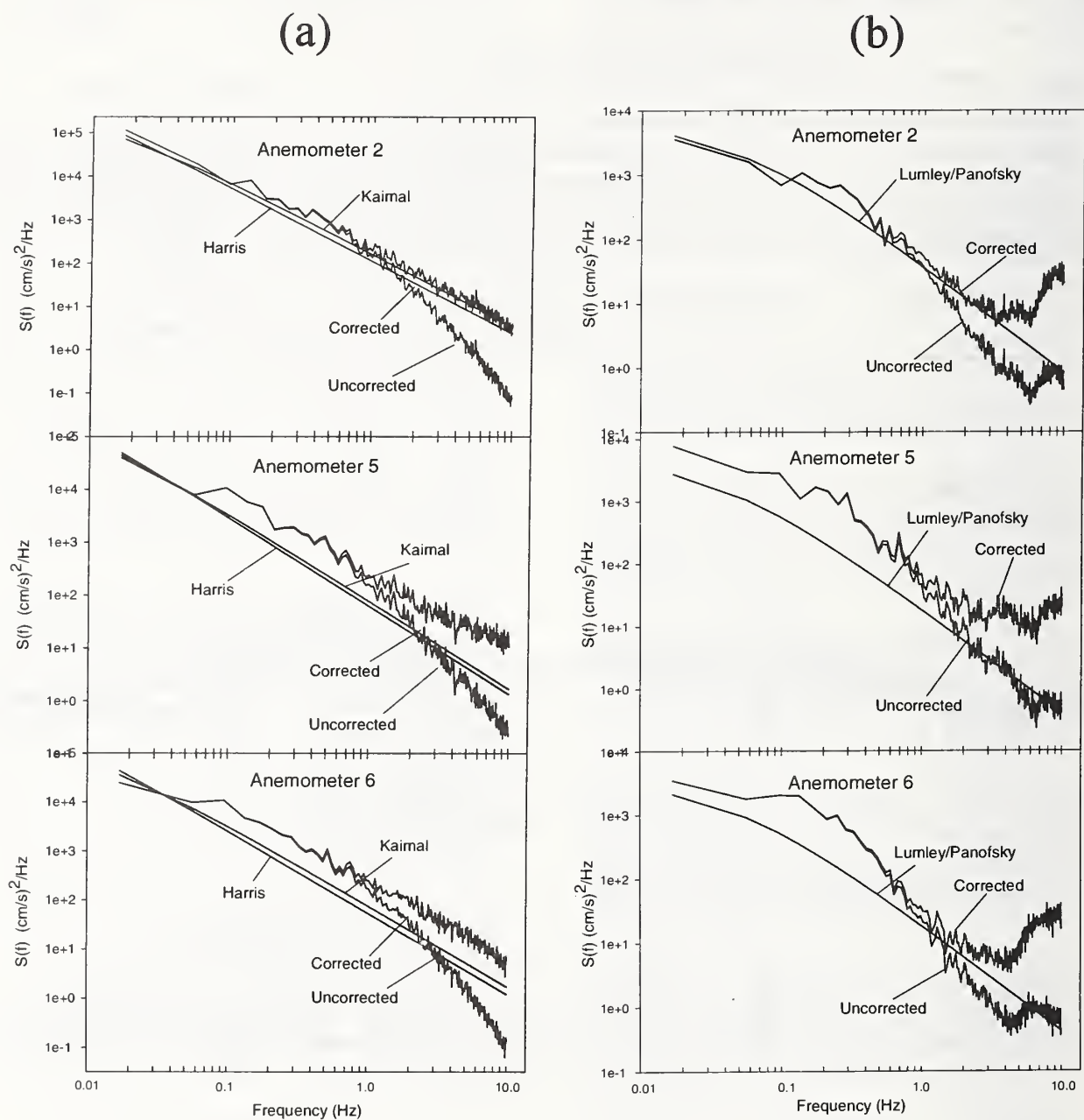


Figure 2. Autospectra of Horizontal (a) and Vertical (b) Velocity Components

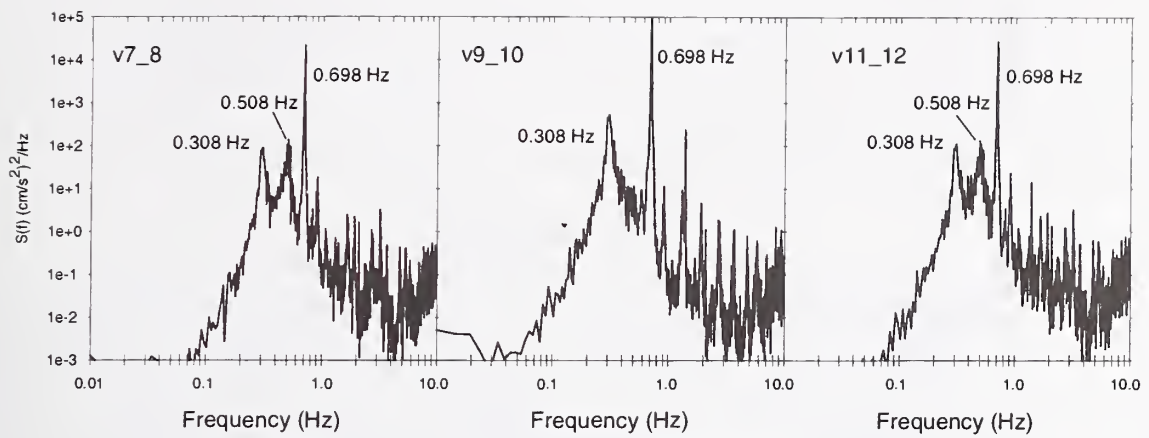


Figure 3. Autospectra of Vertical Accelerations of Bridge Deck

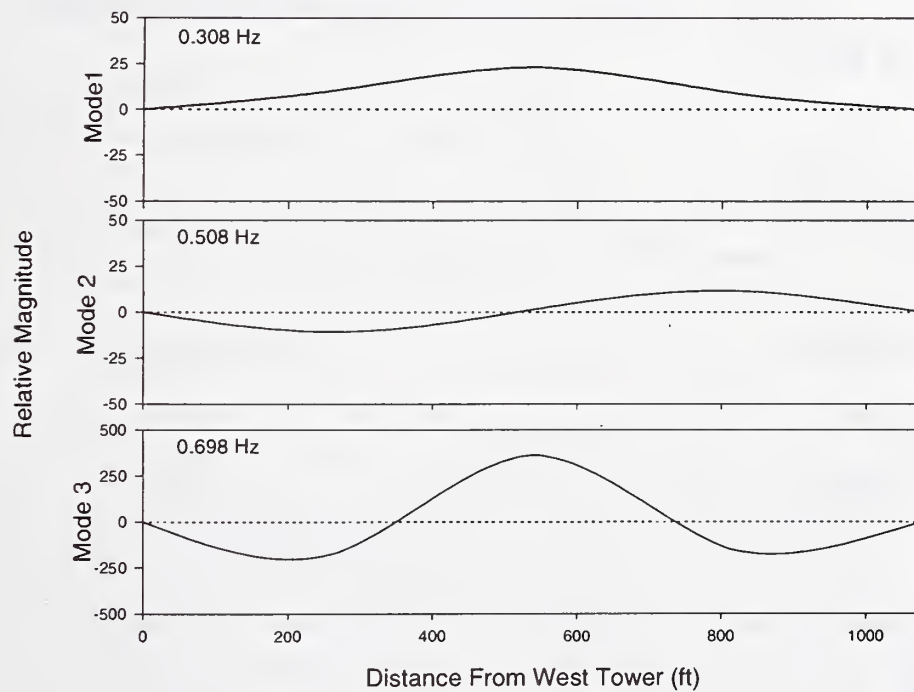


Figure 4. Natural Modes and Frequencies Determined from Spectral Analysis

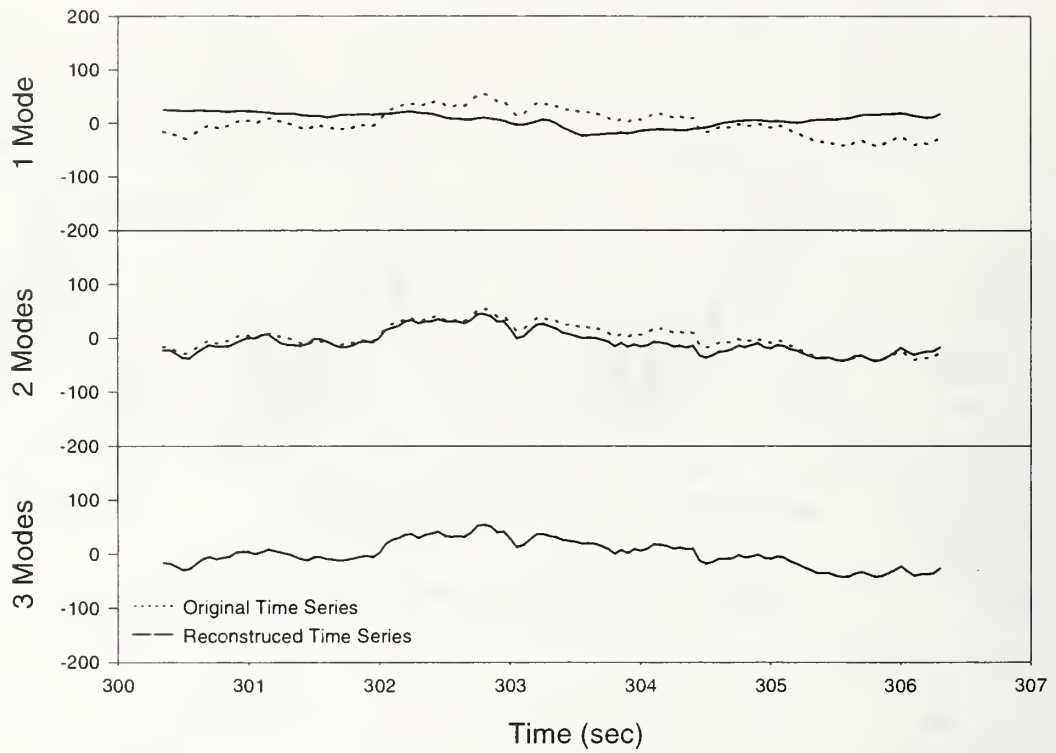


Figure 5. POD Reconstruction of Horizontal Velocity Component

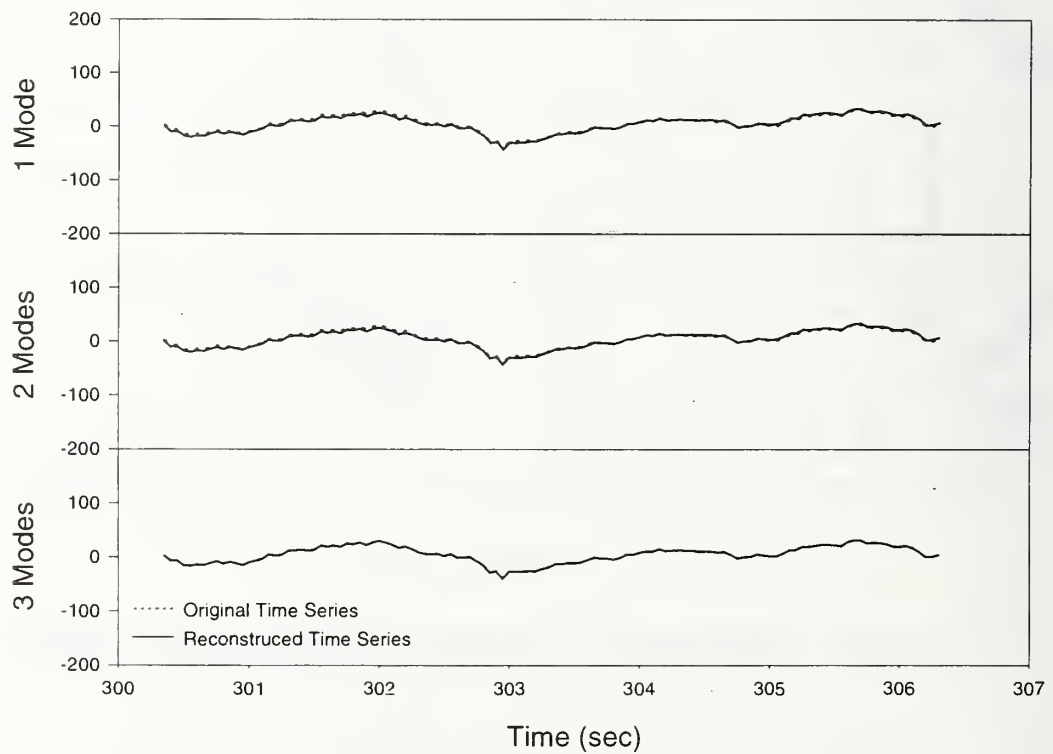


Figure 6. POD Reconstruction of Vertical Velocity Component

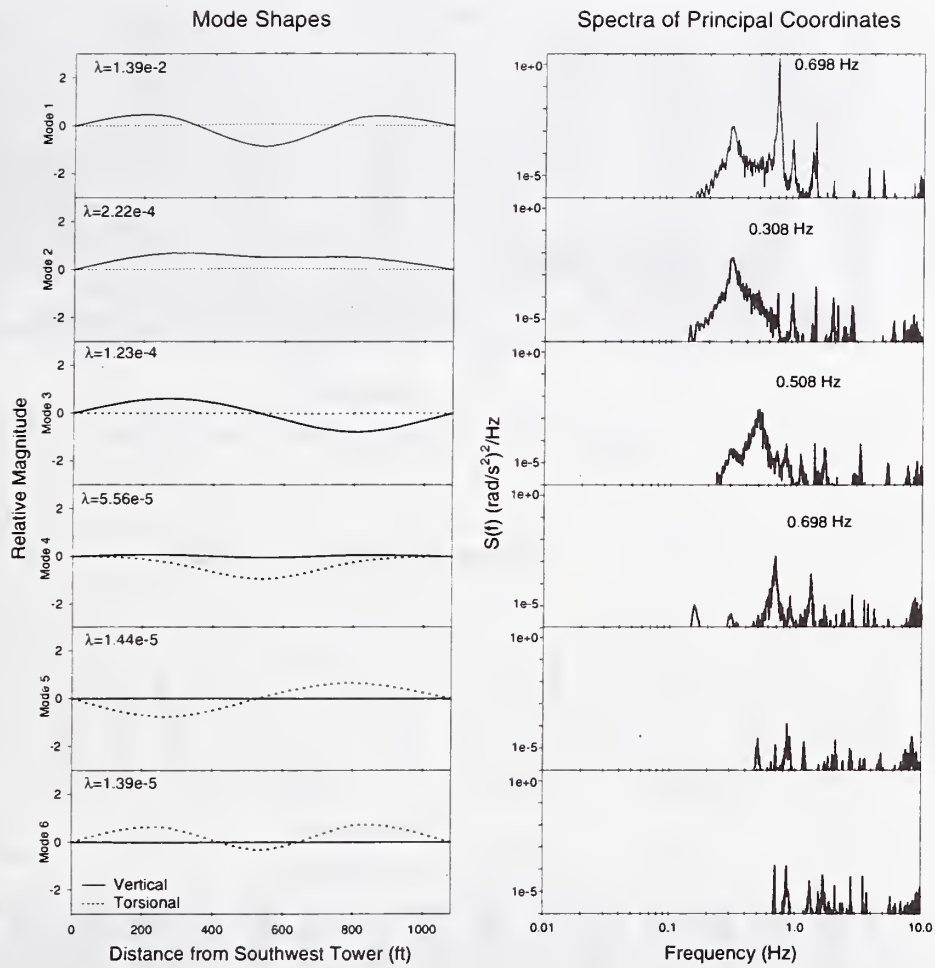


Figure 7. POD Mode Shapes and Autospectra of Principal Components

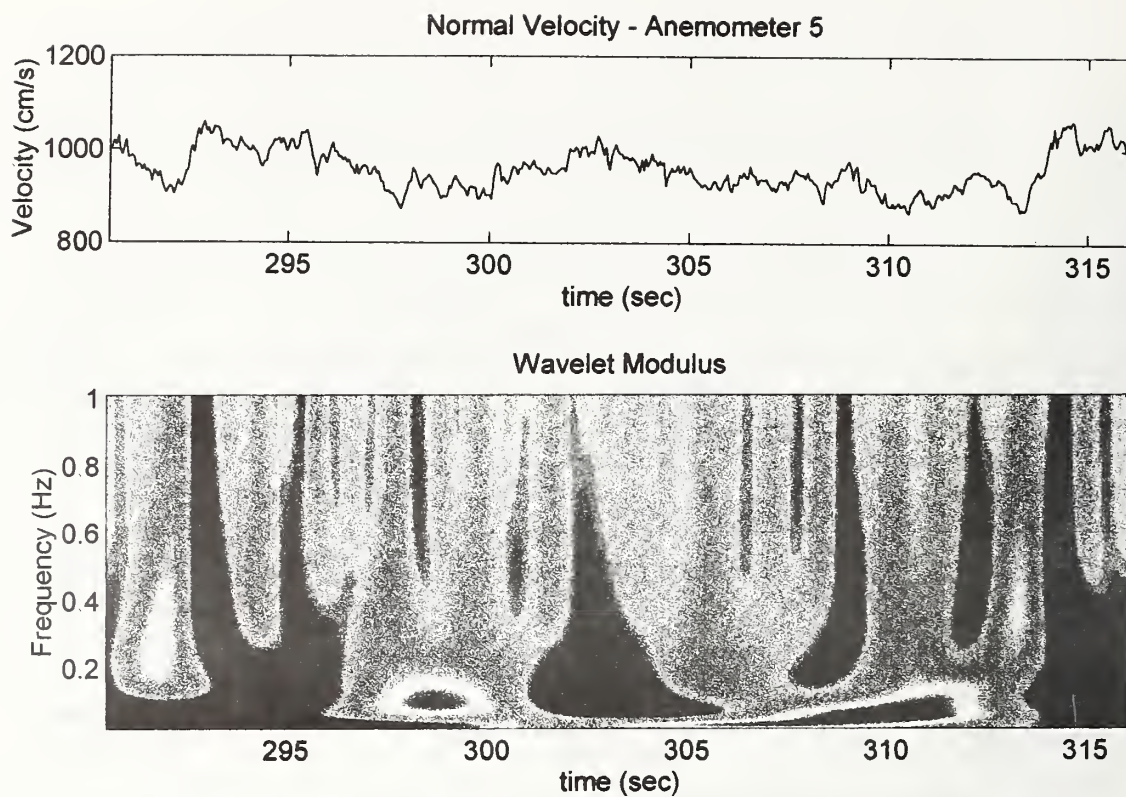


Figure 8. WT Spectrogram of Normal Velocity

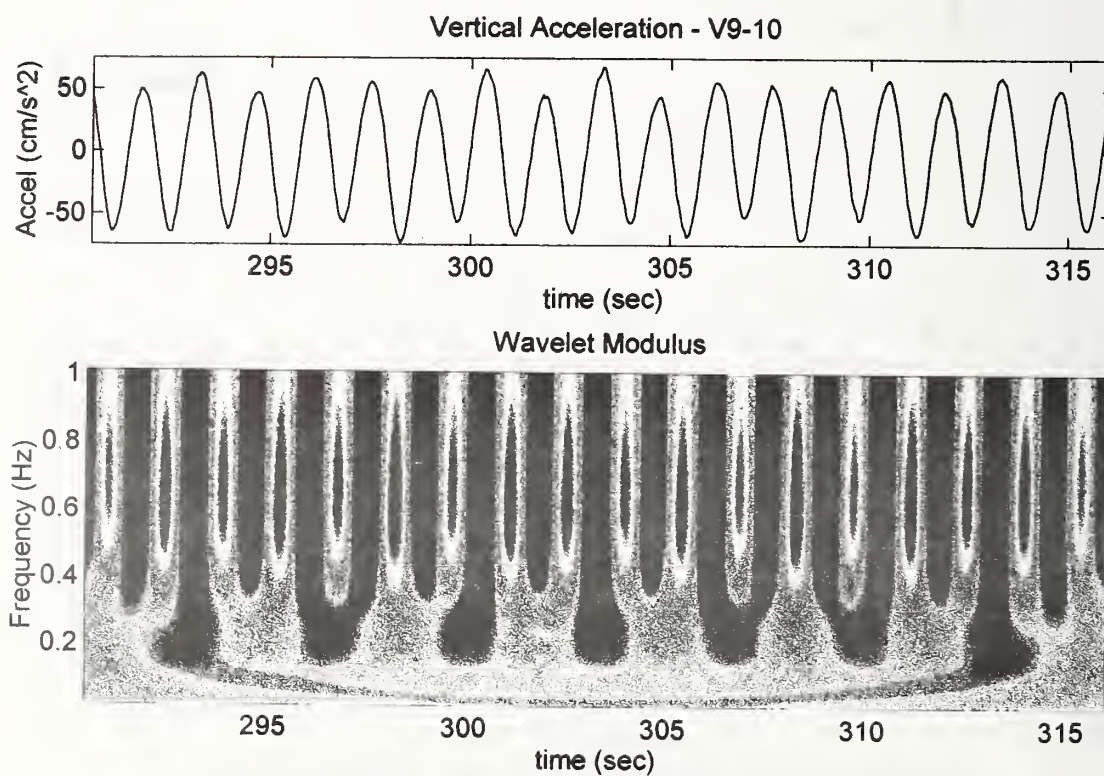


Figure 9. WT Spectrogram of Vertical Acceleration at Deck Mid-Span

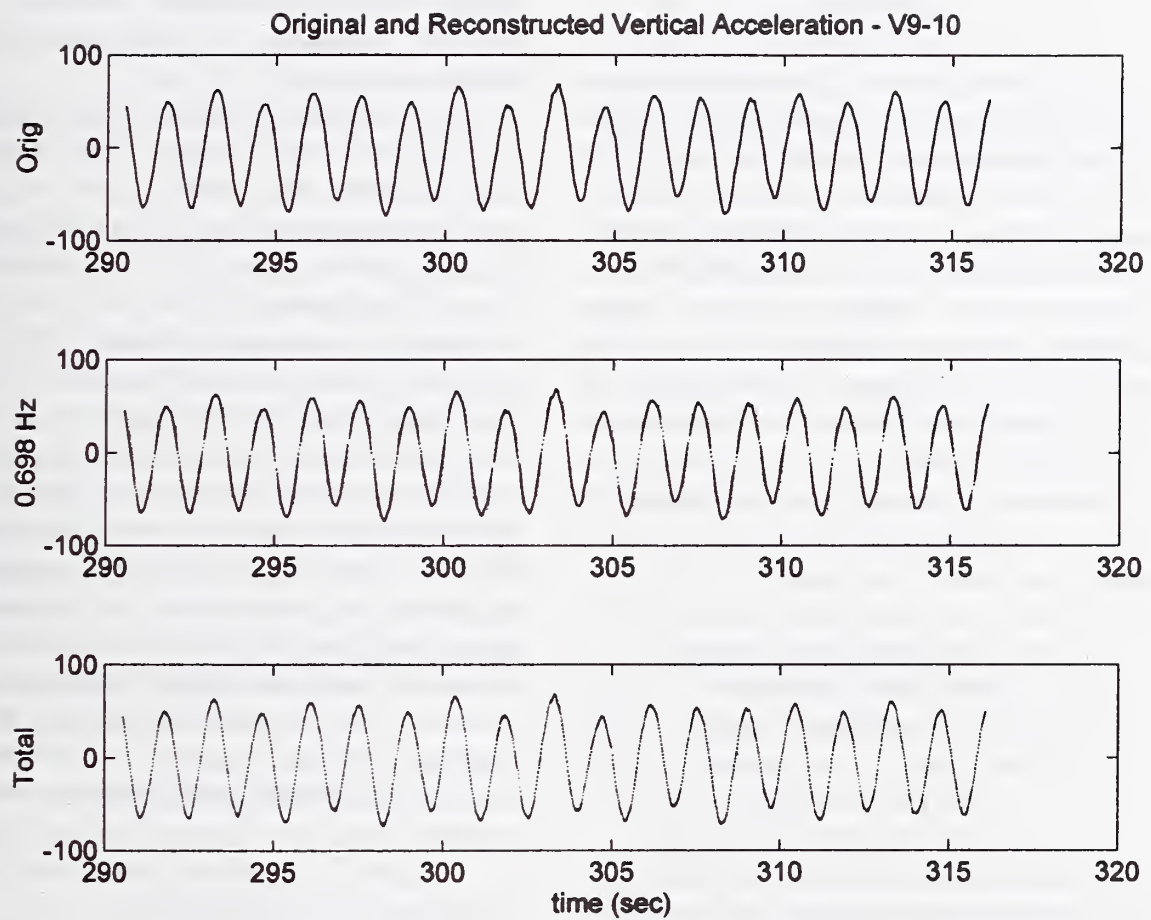


Figure 10. Wavelet Transform Reconstruction of Vertical Acceleration at Deck Mid-Span

Next Generation Trans-Strait Road Projects and the State of Technology Development

by
Michio Okahara ¹⁾, Masahiro Nishitani ²⁾

ABSTRACT

Super long-span bridges between 20 and 30% greater than the Akashi Kaikyo Bridge need to be constructed in order to create new traffic axes to enliven and stimulate outlying regions of Japan for the 21st century. Studies have been undertaken to develop ways to construct super long-span bridges more economically and rationally. As the results, new types of structures, new concepts of designs, and innovative execution technologies have been introduced, permitting the construction of super long-span bridges at much lower cost than by simply extending and applying existing technologies.

*Key Words : Trans-Strait Road Projects
Super Long-Span Bridges
New Types of Structures
New Concepts of Designs*

1. INTRODUCTION

The Akashi Kaikyo Bridge, the longest one among not only bridges between Honshu and Shikoku but also all bridges in the world, opened on April 5, 1998. When the Kurushima Bridges and Tatara Bridge will open as scheduled in the spring of 1999, Honshu and Shikoku will be linked completely by the three routes as envisioned in the original plans.

New traffic axes are being advocated as the key to making effective use of the limited land area of Japan to provide this country with a more balanced national land structure for the

21st century. And the lessons learned by the Hyogo-ken Nanbu Earthquake have shown us that the redundancy in infrastructures is extremely important.

For such backgrounds, new traffic axes to play a key role in creating newly defined multi national land axes to enliven and stimulate outlying regions of Japan occupy the following position in the "New Comprehensive National Development Plans" authorized by the Japanese Government in March, 1998. The Tokyo Bay Mouth Road, Ise Bay Mouth Road, Kitan Strait Road, Kanmon Strait Road, Hoyo Strait Road and Shimabara-Amakusa-Nagashima Bridges projects, that should be implemented with close attention paid to cost-benefits effects and other related conditions, are planned to promote the development of new technologies including those that reduce the cost of long-span bridges construction, to protect their surrounding environments, and to stimulate outlying regions by promoting increased cooperation and interaction among regions.

Figure 1.1 presents trans-strait road projects now at the concept stage.

To complete the Akashi Kaikyo Bridge and other Honshu-Shikoku Bridges, new technologies of various kinds were developed, permitting the construction of safe and

-
- 1) Director, Structure and Bridge Department, Public Works Research Institute, Ministry of Construction, Tsukuba, JAPAN
 - 2) Advisory Engineer for Bridge, Planning and Research Administration Department, ditto

reliable long-span suspension bridges in the 2,000m class. It will be necessary to apply even more advanced versions of these technologies in order to construct the next generation projects.

But the meteorological and oceanographic conditions in terms of topography, geology, water depth, wind speed and so on at the planned sites of future projects are expected to be severer than those at the Seto Inland Sea area where the Honshu-Shikoku bridges were constructed. Since the straits to be crossed will be wider and deeper, planned bridges will require superstructures with longer spans and substructures appropriate for deeper water. Faced to the Pacific Ocean, they will be vulnerable to the effects of typhoons and ocean waves. They must also be constructed in earthquake prone area. Considering these conditions, it has been concluded that super long-span bridges constructed as the part of future projects will be between 20 and 30% longer than the Akashi Kaikyo Bridge. It is believed that it would be technically possible to use the same technology applied to the construction of the Honshu-Shikoku bridges to build bridges greater than ever before, but to build them more economically and rationally, newer technologies must be developed.

2. OUTLINES OF TRANS-STRAIT ROAD PROJECTS

Three trans-strait road projects, namely the Tokyo Bay Mouth Road, Ise Bay Mouth Road, and Kitan Strait Road, are introduced below.

2.1 Tokyo Bay Mouth Road

The Tokyo Bay Mouth Road is about 20km long trans-strait road (marine section : about 10 to 15km) crossing the Uraga Strait to link the Yokosuka-shi in Kanagawa-ken with the Futtsu-shi in Chiba-ken.

The Uraga Strait is an international navigation channel (channel width : 1,750m) where ships converge. The Tokyo Bay Mouth Road will be constructed close to the location of the epicenter of the Great Kanto Earthquake of 1923.

The bridge now under consideration is a long-span suspension bridge with a center span length of 2,250m.

2.2 Ise Bay Mouth Road

The Ise Bay Mouth Road is about 90km long trans-strait road (marine section : about 20km) crossing the Ise Bay Mouth from Irigo Cape at the tip of the Atsumi Peninsula in Aichi-ken to the Shima Peninsula in Mie-ken.

The Ise Bay Mouth is a strait designated as an international navigation channel (channel width : 1,200m). Plate boundary-type earthquakes of Magnitude 8 class occurred near the planned site around 1945, and there is a fear of the Tokai earthquake near the route.

The plan now under consideration hypothesizes a long-span suspension bridge with a center span length of 2,000m.

2.3 Kitan Strait Road

The Kitan Strait Road is a trans-strait road with a length of about 40km (marine section : about 11km) linking the Wakayama-shi in Wakayama-ken with the Sumoto-shi in Hyogo-ken.

The Kitan Strait Road locates parallel to the Median Tectonic Line where the high level of activity is forecast and close to the epicenters of the Nankai Earthquake and other plate boundary-type earthquakes.

The study underway in preparation for the construction of the bridge over the Kitan Strait hypothesizes a long-span suspension bridge with a center span length of 2,700m. Figure 2.1 shows the planned route and Figure 2.2 shows the Kitan Strait Bridge.

3. INTRODUCTION TO NEW TECHNOLOGICAL DEVELOPMENTS

3.1 Introduction to New Technological Developments

Priority and preferential studies of technologies believed to have the potential to contribute to the shortening of construction period and reduction of construction cost are now in progress.

The major technological developments that have been promoted are broadly categorized into three groups : 1) new types of structures, 2) new concepts of designs, and 3) innovative execution methods. An outline of these technological developments is presented in Table 3.1.

3.2 New Types of Structures

(1) Girder Sections with Lower Cost and Better Aerodynamic Stability

It is vital to guarantee that super long-span suspension bridges remain stable during strong wind conditions. Methods of guaranteeing aerodynamic stability include increasing the stiffness of stiffening girders and devising innovative new girder sections.

For the Akashi Kaikyo Bridge, a truss type stiffening girder already used in earlier bridges has been adopted. And because of their small center span lengths of about 1,000m, single box type stiffening girders have been used for the Kurushima Bridges.

Problems that must be overcome to construct super long-span suspension bridges with a center span length greater than 2,000m include 1) the steel weight increase caused by measures to increase the stiffness of the stiffening girders and 2) the truss girders are vulnerable to the effects of wind by the high drag force. To overcome these problems, studies now in progress are focused on the use of slotted box girders and single box girders on two premises: 1) the use of box girders will improve the wind resistance, improving the

vibration properties and aerodynamic properties and 2) it is possible to construct a superstructure using the hoisting erection method that raises the box girder blocks directly from the sea surface at the erecting location.

(2) Underwater Foundations with Lower Cost and Better Earthquake Resistance

Comparisons of the planned sites of future projects with those of the Honshu-Shikoku Bridges reveal that 1) the former tend to be closer to the epicenters of large scale earthquakes, 2) their foundations must be constructed in deeper water, 3) and the properties of the bearing ground supporting their foundations are worse than in the case of earlier bridges. It will, therefore, be necessary to develop underwater main tower foundation types that are of more highly earthquake resistance and more economical and rational to construct than existing cylindrical solid foundations (the main tower foundations of the Akashi Kaikyo Bridge for example).

Studies to meet these needs are based on the twin-shaft type foundation shown in Figure 3.1. The benefits of this type include 1) lower concrete volume that reduces construction cost and shortens construction period, 2) the light weight that allows its use on relatively softer ground, and 3) the light weight and lower center of the gravity for superior earthquake resistance. It is essential that future projects be preceded by studies to determine the shape most appropriate for each project considering design and construction conditions such as the water depth, geology and so on at the planned sites.

3.3 New Concepts of Designs

(1) Wind Resistant Design

While the Honshu-Shikoku Bridges were being designed, a number of wind resistant design methods for long-span bridges were studied and tested experimentally to improve

design precision. The knowledges obtained from the results of the full model wind tunnel studies conducted to study the aerodynamic stability of the Akashi Kaikyo Bridge in particular has been applied to propose a number of new concepts that may be incorporated into wind resistant design of future super long-span bridges.

[1] Review of Wind Fluctuation Characteristics

As the span length of bridges increases, the cross section of girders will be determined in accordance with wind load. It is, therefore, possible to create more economical and rational designs by improving the precision of wind load calculations.

Wind load is calculated by increasing the static load calculated from mean wind speed accounting for the effect of wind fluctuation. The results of the full model wind tunnel tests of the Akashi Kaikyo Bridge and observations of natural winds have confirmed that it is possible to achieve a relative reduction of the effect of wind fluctuation acting on the girder of a long-span suspension bridge. In other words, the wind load used to design super long-span suspension bridges can be lower than that calculated based on conventional standards.

[2] Development of Flutter Analysis

Aerodynamic stability of long-span suspension bridges has been studied based on wind tunnel tests in use of a section model supported by spring, but it is now known that since the span of bridges has increased, it is impossible to fully reproduce their behavior using a section model. For this reason, the wind resistant design for the Akashi Kaikyo Bridge involved the clarification of aerodynamic stability by conducting the wind tunnel tests using the 40m long full model to reproduce the complex vibration properties of the real bridge. The findings of this studies have permitted the development of a flutter analysis to be used to precisely clarify the aerodynamic stability of a long-span bridge.

(2) Seismic Design

It has been pointed out that future projects sites are close to the epicenters of large scale plate boundary-type earthquakes and the existence of active faults in the vicinity. It is, therefore, necessary to adopt appropriate design earthquake ground motions and corresponding analytical methods so that it will be possible to practice economical and rational design and will guarantee the aseismicity of the structures.

[1] Basic Concepts of Seismic Design

As a basis of seismic design, the design earthquake ground motions and the corresponding safety levels of structures will be considered at two stages. At Level-1 (L1), "damages which destroy transportation functions shall be prevented for moderate ground motions induced in the earthquakes with high probability to occur within the life time of structures". At Level-2 (L2), "recoverable functional damages shall be allowed, but collapses shall be prevented for extreme ground motions induced in the earthquakes with low probability to occur at future projects sites."

[2] Input Design Earthquake Ground Motions

The input design earthquake ground motion used for L1 design is evaluated by statistically analyzing past earthquakes within 300km of the center of future projects sites to hypothesize ground motion with return period of 150 years.

The input design earthquake ground motion used for L2 design is evaluated on the hypothesis that either large scale plate boundary-type earthquakes or inland intra-plate earthquakes caused by active faults will occur relatively close to future projects sites. This ground motion is evaluated in some ways : 1) attenuation equations, 2) fault rupture process models, 3) recorded strong ground motion at near field of large scale earthquakes.

[3] Seismic Design Methods of Foundations

The seismic design of foundations is

conventionally done based on the response spectrum method : the use of a rigid body using a two-degree-of-freedom model that represents soil stiffness as a linear spring. But because it is clear that during a large scale earthquake, the stiffness and damping properties of surrounding soils produce nonlinear behaviors, the L1 seismic design method that accounts for these properties has been developed. It is, therefore, now possible to perform high precision rational seismic design of foundations.

The check of the stability of foundations against L2 ground motion is made by elasto-plastic FEM time history response analyses. In the analyses, the nonlinear stress-strain relation of surrounding soils is modeled as the modified Ramberg-Osgood model, and a model that can represent the characteristics of the separation between a foundation and ground is used. The properties of ground are analyzed in detail by this method.

(3) Design of Superstructures

In superstructure design standards of the Honshu-Shikoku Bridges, provisions contributing substantially to lower construction cost and shorter construction period have been reviewed.

[1] Allowable Stress of Main Cables

Because the weight of main cables in a super long-span suspension bridge with a span length exceeding 2,000m will account for between 20 and 30% of the steel weight of the bridge, and lowering the weight of main cables will make a large contribution to lowering construction cost and shortening construction period.

The design of main cables in the Honshu-Shikoku Bridges were adopted as the allowable stress of 56kgf/mm^2 for the Innoshima Bridge (completed in 1983) and 64kgf/mm^2 for the Seto-Ohashi Bridge (completed in 1988). In the design of the Akashi Kaikyo Bridge, because the cable

strands material was improved to increase the tensile strength from 160kgf/mm^2 to 180kgf/mm^2 , the allowable stress was raised to 82kgf/mm^2 .

In the design of super long-span suspension bridges, it was found that the allowable stress of main cables could be set at 100kgf/cm^2 on such grounds as, 1) the quality of high strength strands material will stabilize, 2) bridge erection will have high precision, 3) corrosion prevention technologies will be sure to have improved, and 4) there will be leeway considering the safety balance of an entire suspension bridge system.

A comparison of the allowable stress of main cables with a case where it would be identical to that of the main cables of the Akashi Kaikyo Bridge (82kgf/mm^2) reveals that the weight of main cables can be lowered by about 40%.

[2] Methods of Live Loading

The design live load of super long-span suspension bridges is based on a calculation method that reduces live load according to the span in the same way as the design of the Honshu-Shikoku Bridges. And the method of loading only a traffic lane width instead of loading a carriage way width is adopted to account for the real situation of motor vehicle traffic.

Main towers have conventionally been designed by performing influence line loading : loading live load in a loading range that represents the severest possible conditions on the design section. But because it is highly unlikely for such loading conditions to actually occur, it is clearly possible to increase the allowable stress.

(4) Design of Substructures

Because the selection of the bearing layer to support a foundation is governed to a great degree by the dimensions of a foundation, the quantity of soils to be excavated to reach the bearing layer, etc., this is an important

matter in determining the construction cost and period. To practice an economical and rational design, the bearing capacity of ground and deformation of a foundation must be precisely calculated and reflected in the design.

Accordingly, the method involving the clarification of the on-site ground properties through geological explorations and laboratory tests, the precise modeling of the results, and FEM analyses accounting for these ground properties have been developed. Specifically, 1) the geological properties of ground are clarified by acoustic explorations, boring explorations, or borehole loggings at the site, 2) the undisturbed specimens obtained by boring are used to clarify the deformation properties of ground from a minute strain level to a failure range, and 3) the nonlinear properties of ground are modeled and analyzed based on the results of the first two steps.

3.4 Innovative Execution Methods

(1) Execution Methods of Superstructures

Execution methods of superstructures have been introduced existing execution methods from other countries. Examples include 1) the use of tension bolts to assembly tower shaft joints, 2) the use of the hoisting erection method to install girder blocks, and 3) finishing tower bases with grouting. Other methods under consideration are the systematic overlapping of work steps by, for example, simultaneously erecting hanger ropes and girders, a main cable erection method that does not require catwalks, and more economical use of tower erection cranes.

(2) Execution Methods of Substructures

Maritime conditions will be particularly severe at the sites of future projects : ones to be constructed facing the Ocean where they will be exposed to the effects of typhoons and ocean waves. Execution methods that minimize the effects of the maritime conditions at the sites in order to improve working days ratio

under these severe conditions now being studied include the use of semi-submersible pontoons immune to the effects of waves, the prefabrication of caissons and other steel members, and so on.

3.5 Effect of New Technological Developments

A comparison of the results of the trial design performed using newly developed technologies with that based on existing technologies has confirmed that new technological developments have been effective.

Table 3.2 presents the comparison of the results for the Tokyo Bay Mouth Bridge. It indicates that it is possible to reduce construction cost roughly by 30 to 50% in case developing new technologies are utilized. The factors for this reduction are presented below. But assuming that the factors overlap, the percentages representing the contributions of each new technology to the reduction of construction cost are just rough yardsticks.

1) Developments of new types structures (about 25%)

- Adoption of a slotted box girder (with an open grating)
- Adoption of a twin-shaft type foundation
- 2) Introduction of new concepts designs (about 10%)

- Reduction of wind load
- Classification of design earthquake ground motions at two stages
- Review of safety factors
- Appropriate evaluations of bearing capacity of ground

3) Innovative execution methods (about 5%)

- Review of fabrication precision and introduction of overlapping execution works
- Improvement of submarine drilling and working days ratio

The developments of new types structures contribute greatly to the construction cost reduction.

4. SPECIFIC EXAMPLES OF NEW TYPES STRUCTURES

4.1 New Types of Superstructures

(1) Slotted Box Girders

[1] Development of girders with better aerodynamic stability

A slotted box girder has an opening at the center of girder. Section models premised on a center span length of 3,000m with two side spans of 1,500m have been used for wind tunnel tests to study the relationship of the flutter onset wind speed with the opening pattern, opening width and aerodynamic appendages.

The results have revealed the following facts.

- 1) Aerodynamic stability is improved by providing an opening at the center of girder, and the larger the width, the better aerodynamic stability.
- 2) It is possible to improve aerodynamic stability by installing center barriers in the center of the opening.
- 3) It is possible to improve aerodynamic stability by installing guide vanes at the end of girder.
- 4) Guard rails contribute to improved aerodynamic stability and it is possible to improve aerodynamic stability during negative angle of attack by installing under barriers at the bottom of girder to create vertically symmetrical cross sections.

Figure 4.1 shows a cross section proposed based on the results of the wind tunnel tests.

[2] Developments of girders with lower cost

The central part of a slotted box girder must be provided with an opening as a wind resistance measure (the solidity factor of the opening is about 50%). But it is more economical and rational to provide the necessary opening width by installing an open grating to permit motor vehicles to drive on the

top of the open grating than to provide the width of traffic lanes on the top of box girder. The girder with an open grating sharply cuts construction cost and shortens construction period. Specifically, 1) a main tower interval need not be expanded, 2) a foundation width need not be increased, and 3) the steel weight of a super long girder can be reduced.

The number of traffic lanes of future projects is assumed to be four lanes. In this case the central two lanes will have to be located on the open grating. The adoption of a slotted box girder will also permit stage construction, as the first two lanes are opened on the top of box girder and two more lanes are added later after an open grating has been installed.

In Japan, open gratings have been installed on some long-span bridges, such as the Seto-ohashi Bridge and the Akashi Kaikyo Bridge. But because they were introduced to guarantee aerodynamic stability, they were installed on parts of these bridges that normally load no traffic such as the central strip and road shoulder. They have never been used to form a roadway. Table 4.1 presents some examples of their use as a roadway in foreign countries. Photograph 4.1 shows the open grating of the Mackinac Bridge in the United States. It has not been replaced during the forty years since it was constructed.

At the PWRI, driving tests are planned to confirm the running safety of motor vehicles to travel at high speed on open gratings. The tests will be carried out to study 1) skid resistance on open gratings, 2) running safety when road surface conditions differ between the left and right wheels of motor vehicles (when changing lanes for example), 3) human engineering verification during driving on them (riding comfort, uneasiness experienced by drivers and so on), and 4) traffic management measures (speed limits and so on), etc.

Skid resistant tests are now underway (Photographs 4.2 and 4.3). The tests are being

done with two kinds of open gratings : the open grating used at the Akashi Kaikyo Bridge and the open grating with notches formed on its lattice members surface to increase skid resistance.

The tests were done with the Test Vehicle running to the direction of the principal members of the open gratings and with the Test Vehicle running at right angles to the direction of these members. And sprinklers were used to reproduce rainy weather conditions in order to test their skid resistant properties during rainfall.

Figure 4.2 shows the results of the tests. The results reveal the following facts, 1) the sliding friction coefficients of gratings are smaller at slow speeds than at high speeds, 2) the notches on the gratings surface can slightly improve their sliding friction coefficients, 3) a lane changing can be performed surely for a motor vehicle running in the same direction as that of the principal members, but braking is more unsurely, 4) it is necessary to develop an open grating that provides far greater safety when braking and changing lanes.

It has also been confirmed that the adoption of a slotted box girder with an open grating will reduce the steel weight of girder by about 30% from the weight of a truss girder. This weight reduction will encourage the rationalization of main cables, main towers and substructures, permitting an entire suspension bridge to be constructed more economically and rationally.

It is now assumed that only the center of girder will be open gratings, but girders with the entire roadway width formed by open gratings (that is, all-grating girders) are also under consideration. The adoption of these types would permit both sharp reduction in the steel weight and large cost saving.

(2) Single Box Girders

It is considered that it would be difficult to guarantee a flutter onset wind speed

(hypothetically 80m/s) on a center span length longer than 2,000m by adopting single box girders without improvements.

So studies are now being conducted in an effort to improve vibration properties of super long-span suspension bridges by connecting the main cables to the stiffening girder with cross-hangers (Figure 4.3) crossing over the deck to restrict the structural torsion.

The cross-hangers under consideration are a steel box type and cable type. A steel cross-hanger is also effective against compressive force.

Flutter analyses have been carried out, confirming their effectiveness. The cross-hangers would be installed at the locations shown in Figure 4.4 in the case of a super long-span suspension bridge with a center span length of 2,500m with two side spans of 1,250m. The flutter analyses results have demonstrated that the flutter onset wind speed is improved by about 10m/s by the single box girder with cable cross-hangers from that of the bridge without the system about 60m/s and by about 20m/s by the single box girder with steel cross-hangers.

But to design the single box girders with steel cross-hangers, it is necessary to overcome problems related to the connection between cross-hangers and girder and the structural details of cross-hangers intersection part.

4.2 New Types of Substructures

(1) Main Tower Foundations for Super Long-Span Suspension Bridges

To propose a main tower foundation for super long-span suspension bridges, research has been focused on the following items that are assumed to contribute significantly to saving cost to study a structure created by improving the twin-shaft type foundation shown in Figure 3.1.

[1] Rationalizing the large foundation design methods

The use of the seismic design methods

and substructural design methods described in 3.3 permits more rational foundation design.

[2] Improving the shape of foundations

The adoption, premised on design method rationalization, of a drastic structural shape that achieves a sharp reduction in the body quantities will sharply lower cost.

[3] reducing the quantity of submarine drillings

To cut the cost of submarine drillings, studies must be carried out to develop substructural design and construction methods that eliminate the need for submarine drillings.

[4] Adoption of reinforced concrete main towers

The adoption of reinforced concrete main towers will lower cost by rationalizing the reinforced concrete tower's construction method. And the construction of reinforced concrete towers will result in large reduction in the size of tower foundations made possible by the smaller dimensions of main tower's bottoms.

[5] Rationalization of concrete works

The concrete works that accounts for the principal share of the cost of substructure works must be rationalized by, for example, devising new execution methods or structures that do not require the use of a concrete plant barge.

Figure 4.5 shows a hybrid caisson foundation that has been proposed as a new structure that will permit these improvements.

A hybrid caisson foundation is a structure that transmits tower reaction forces from the top slab made of reinforced concrete to ground through the caisson wall that is a combined steel and concrete structure. The wall, a type called a full sandwich structure, is formed by casting highly flowable concrete between steel plates with stiffeners. The adoption of the full sandwich structure can save labor by eliminating the need to assemble reinforcements and to compact fresh concrete. The main towers are made of reinforced concrete for lower cost and continuity with a

foundation. To minimize the quantity of expensive underwater concrete used, the interiors of the caissons are filled with sea water instead of underwater concrete. This type also can reduce ground reaction forces and permits a shallower bearing layer.

Another innovation being studied is a measure to reduce foundation size and eliminate the need for submarine drillings by spreading crushed rocks and grouting in their mound, forming a skirt on the bottom surface of a foundation, and inserting the skirt into the mound.

Figure 4.6 shows the work procedure.

(2) Anchorages for Super Long-Span Suspension Bridges

Figure 4.7 shows an anchorage with the splay saddle mount and anchor block separated. A splay saddle mount and anchor block is separated to reduce the quantity of concrete used. The bottom surfaces of both are inclined to minimize sliding forces.

Downward inclined compressive force produced by the bending in main cables acts on the splay saddle mount. So it is designed with the axis of the member oriented in this direction to transmit this force directly to ground. The adoption of this shape can reduce the size of the body and the maximum ground reaction force to install it vertically on ground in the direction of the force.

The anchor block is the part that resists the huge horizontal force of main cables. Inclining its bottom surface can reduce the quantity of concrete used while satisfying the required sliding safety factor.

Figure 4.8 presents the execution procedure.

The anchor block and splay saddle mount are prefabricated separately as reinforced concrete caissons, and after they are towed to the site by tug boats and installed at the fixed location, concrete is casted inside them respectively. In anticipation of cases that

the reinforced concrete caisson of the anchor block will be too heavy to be executed while floating and setting, a method of dividing the anchor block in some parts then joining them on the water is under study.

Technical issues that must be resolved for this anchorage type include preliminary submarine drillings, inclining of the bottom surface related to concrete works, and others.

5. CONCLUSIONS

The studies have shown that new technologies such as developments of new types structures, introduction of new concepts designs and innovative execution methods will permit the construction of super long-span bridges at much lower cost than if existing technologies were applied.

Further studies of new structures, design methods, and execution methods are necessary in order to achieve even lower construction cost and shorter construction period.

And for each project, the investigations of natural conditions at the planned sites will be continued and reinforced. Then based on their results, the studies will be made to make the design and construction plans more economical and rational in the view of the

unique local situations.

ACKNOWLEDGEMENTS

The Ministry of Construction has established the Investigation Committee on Trans-Strait Road Projects to efficiently conduct surveys of super long-span bridges in conception with the trans-strait road projects. Some of the newly developed technologies introduced in this report have argued in the Committee.

We sincerely thank Dr.Yoshida (Chairman : President of Honshu-Shikoku Bridges Engineering Co. Ltd.) and all of the Committee members for their encouraging guidance.

REFERENCES

Public Works Research Institute, "Report of the Investigation Committee on Trans-Strait Road Projects in Japan", August 1993 (in Japanese)

Public Works Research Institute, "Report of the Investigation Committee on Trans-Strait Road Projects in Japan", March 1996 (in Japanese)

Table 4.1 Suspension Bridges with Open Grating Used as Roadway

Bridge	Country	Center Span Length(m)	Year Completed	Location of Open Grating	Purpose
New Tacoma Br.	US	853	1948	Lane boundaries	Aerodynamic stabilization
Mackinac Br.	US	1,158	1957	Sidewalks, inside lanes	Aerodynamic stabilization
Salazar Br.	Portugal	1,013	1966	Inside lanes	Aerodynamic stabilization
Angostura Br.	Venezuela	712	1967	Inside lanes	Weight reduction Aerodynamic stabilization

Table 3.1 Outline of Technological Developments

Item		Outline of technological developments
Developments of new types structures	Girder sections with lower cost and better aerodynamic stability	Studies of slotted box girders with an open grating at the center of girder and single box girders with cross-hangers for lower cost and better aerodynamic stability.
	Underwater foundations with lower cost and better earthquake resistance	Studies of underwater main tower foundations and anchorages for lower cost and better earthquake resistance.
Developments of new concepts designs	Wind resistant design	Study of the possibility of reducing wind load by reviewing natural wind fluctuation characteristics. Development of flutter analysis.
	Seismic design	Setting two stages of design earthquake ground motions and studies of seismic design methods for each stage.
	Design of superstructures	Review of the safety balance of entire suspension bridge systems in order to achieve lower construction cost. Studies of live load loading method that accounts for real conditions of motor vehicle traffic.
	Design of substructures	Studies of appropriate methods of evaluating ground bearing capacity and deformation.
Innovative execution methods	Reduction of construction cost	Studies of construction cost reductions by reviewing material standards and fabrication precision.
	Shortening of construction period	Studies of construction period reduction based on systematic overlapping of work steps. Studies of work methods that increase the working days ratio under severe marine conditions.

Table 3.2 Effect of New Technological Developments (Case of Tokyo Bay Mouth Bridge)

Item			Trial design based on existing technologies	Trial design based on new technologies
Basic specifications		Span lengths (m)	720 + 2,250 + 720	860 + 2,250 + 860
		Cable interval (m)	30.5	25.5
		Dead load (tf/m/Br)	42.33	25.12
Superstructures	Girder	Shape Width × Height (m)	Truss 30.5 × 14.0	Slotted box girder with open grating 32.0 × 4.0
	Tower	Shape Tower height (m) Tower shaft interval (m)	Truss-type/reverse Y-type tower shaft +324 30.5 ~ 52.0	Rahmen-type / single tower shaft +295 25.5 ~ 36.0
	Cable	Allowable stress (kgf/mm2) Diameter (cm)	82 115	100 86
Substructures	1A	Dimensions (m)	90 × 68	90 × 55
	2P	Dimensions (m)	58 × 80	35 × 75
	3P	Dimensions (m)	58 × 80	35 × 75
	4A	Dimensions (m)	90 × 68	90 × 55
Volume	Super-structures	Tower (tf)	60,000 (1.00)	37,000 (0.62)
		Cable (tf)	64,000 (1.00)	35,000 (0.55)
		Girder (tf)	78,000 (1.00)	58,000 (0.74)
		Totals (tf)	202,000 (1.00)	130,000 (0.64)
	Concrete of substructures (m3)		1,448,000 (1.00)	756,000 (0.52)
Approximate construction period (years)			11 (1.00)	6.5 (0.59)
Approximate construction cost	Superstructures	(100 million yen)	2,420 (1.00)	1,250 (0.52)
	Substructures	(100 million yen)	1,730 (1.00)	1,060 (0.61)
	Total	(100 million yen)	4,150 (1.00)	2,310 (0.56)
Remarks				



Straits	Strait width (km)	Maximum water depth (m)	Maximum tidal current speed (m/s)	Maximum wave height (m)
Tokyo Bay Mouth	12	80	1.0	8
Ise Bay Mouth	20	100	1.5	21
Kitan Strait	11	150	3.5	18
Kanmon Strait	2	20	1.5	almost 0
Hoyo Strait	14	200	3.0	12
Hayasaki Strait	5	110	3.5	12
Nagashima Strait	2	70	4.0	18
Akashi Strait	4	100	4.5	10

Figure 1.1 Major Trans-Strait Road Projects

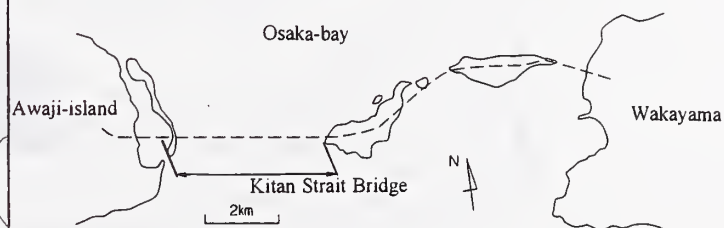


Figure 2.1 Kitan Strait Road Route

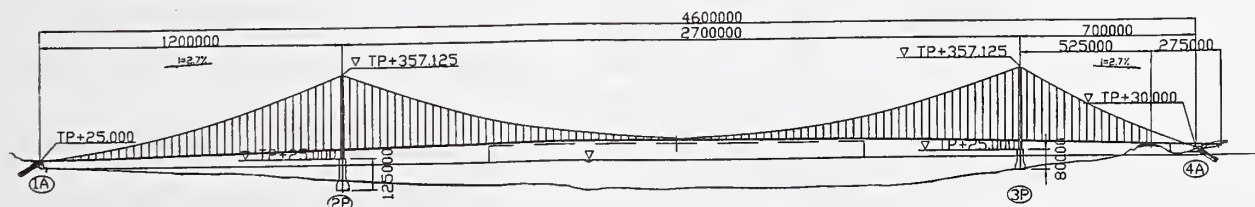


Figure 2.2 Kitan Strait Bridge

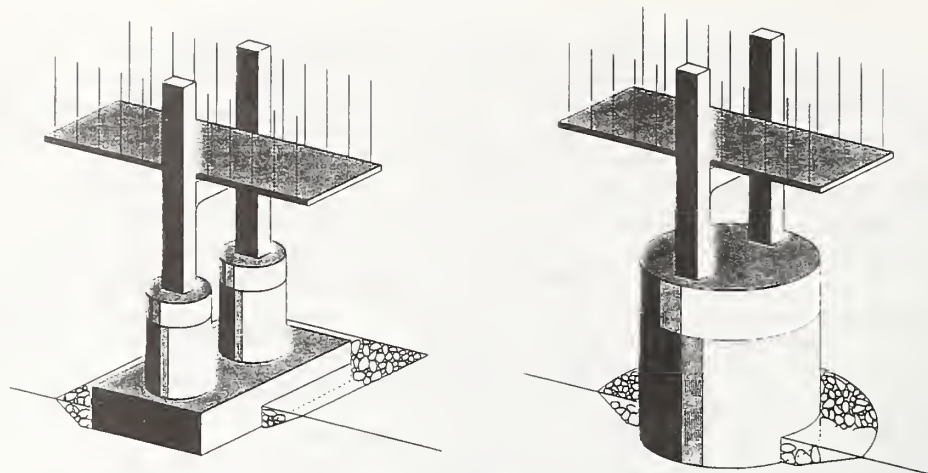


Figure 3.1 Twin-Shaft Type Foundation (left) and Cylindrical Solid Foundation (right)

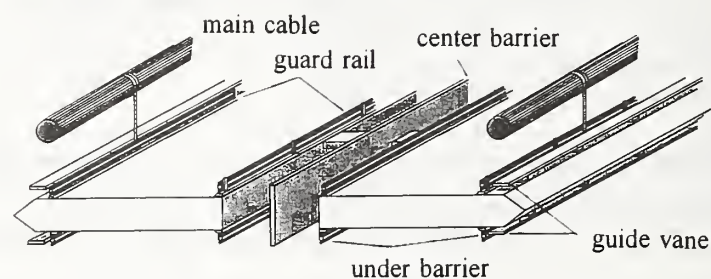


Figure 4.1 Slotted Box Girder with Aerodynamic Appendages

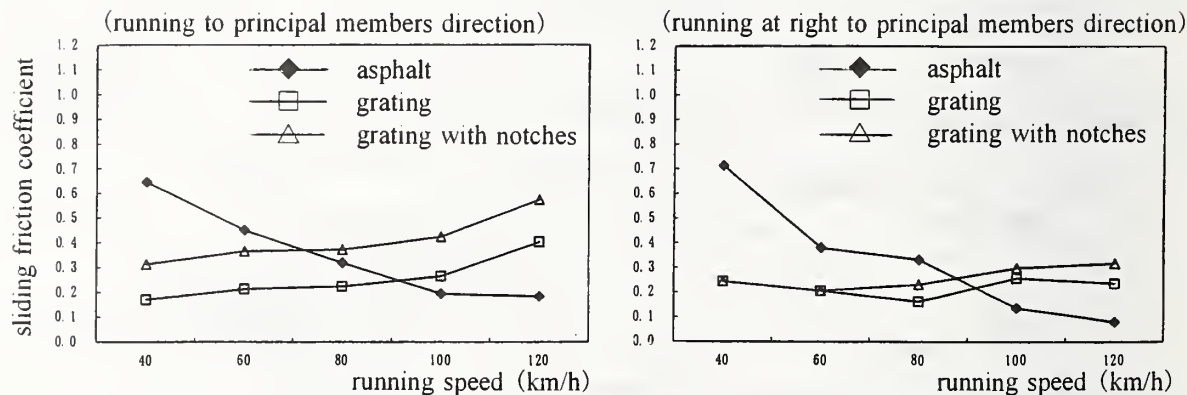


Figure 4.2 Results of Skid Resistant Tests

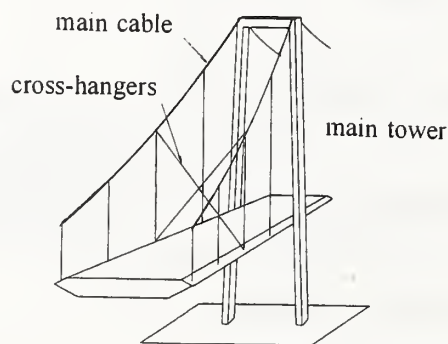


Figure 4.3 Single Box Girder with Cross-Hangers

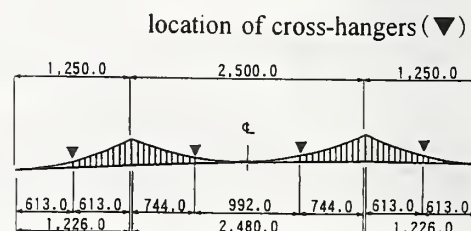


Figure 4.4 Location of Cross-Hangers

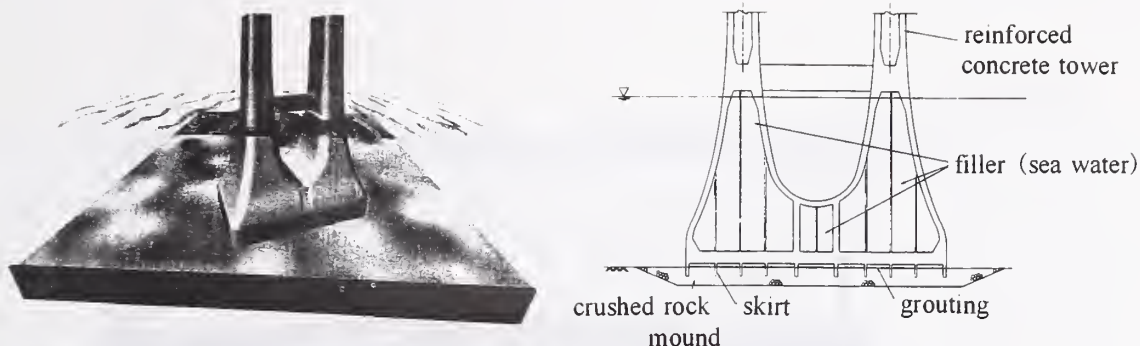


Figure 4.5 Hybrid Caisson Foundation

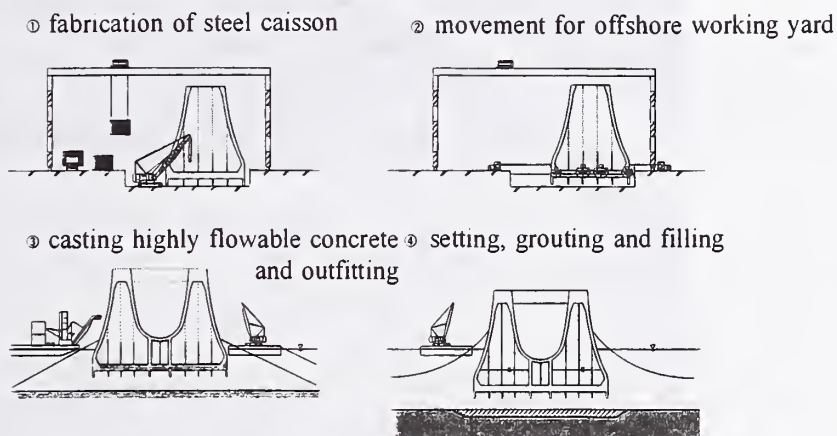


Figure 4.6 Execution Procedure of Hybrid Caisson Foundation

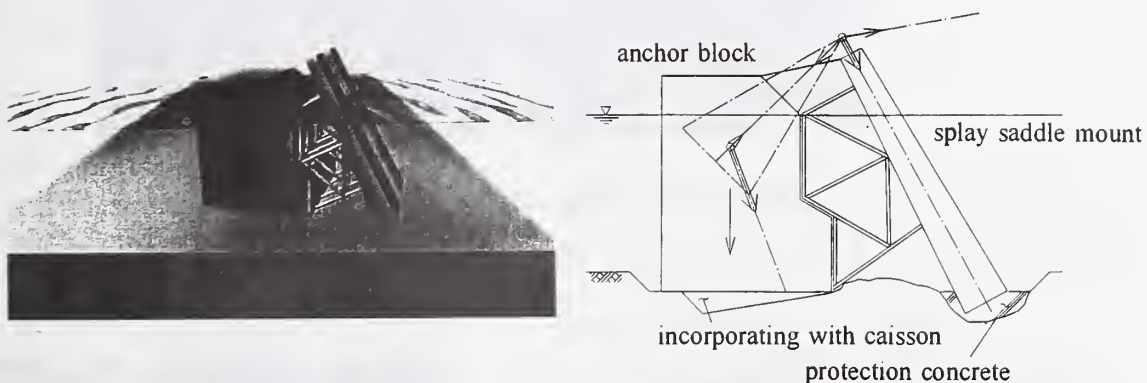


Figure 4.7 Anchorage Separated of Splay Saddle Mount - Anchor Block

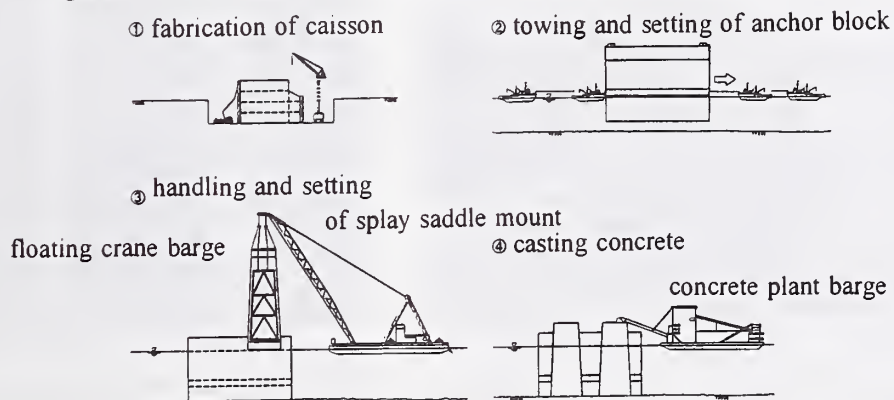
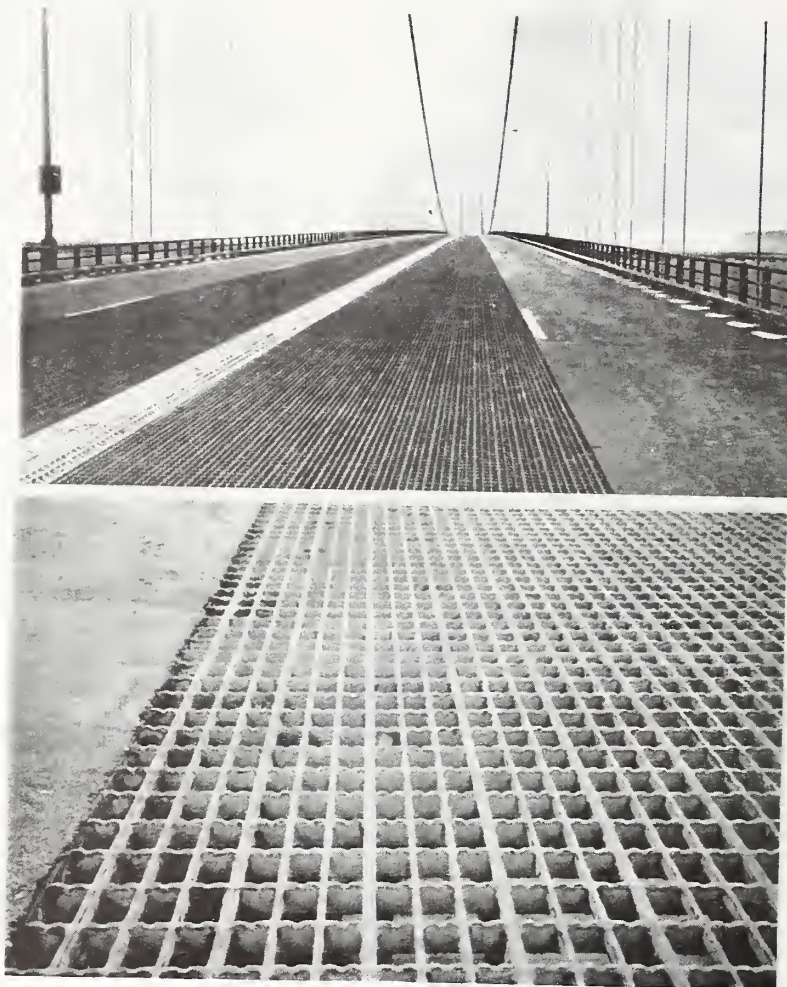


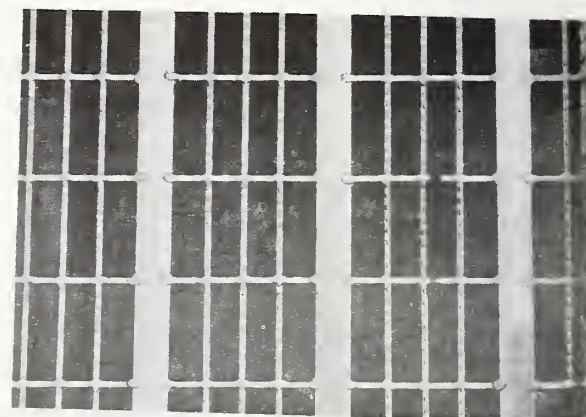
Figure 4.8 Execution Procedure of Anchorage Separated of Splay Saddle Mount - Anchor Block



Photograph 4.1 Open Grating of the Mackinac Bridge



Photograph 4.2 Situation of Skid Resistant Tests



*Photograph 4.3 Open Grating used Tests
(with Notches)*

New Hurricane Wind Structures and Wind Speed Measurements

by

Peter G. Black¹
and

Frank D. Marks, Jr.¹

ABSTRACT

A major source of difficulty in past efforts to predict TC intensity, wind fields, and storm surge at landfall has been the inability to measure the surface wind field directly and the inability to predict how it changes in response to external and internal forcing. A synthesis of past observations of gust factors in hurricanes, in addition to new GPS dropsonde observations, have made it possible to estimate peak gust, 1-min and 10-min sustained mean windfields at the 10-M level. Significant departures from the traditional log law have been found. Recently, multiple low-level wind maxima were observed in eyewall observations from GPS dropsondes.

Recent Observations of eyewall mesovortices have made it possible to observe the structure and characteristics of these features as they make landfall. They have been found to be associated with strong convection in the eyewall at a time when rapid strengthening is occurring. This can produce short periods of intense winds at considerably larger distances inland than is normally expected for landfalling hurricanes.

KEYWORDS:

boundary layer; eyewall; gust factor; hurricane; mesocyclone; mesovortex; satellite; radar; tropical cyclone; typhoon.

1. INTRODUCTION

It is an important international priority to improve the forecasts of surface wind field,

intensity, structure and storm surge in landfalling tropical cyclones (TC) in order to successfully mitigate the detrimental physical impacts associated with these storms. Coastal population growth in the U.S. of 4-5% yr⁻¹, is outpacing the historic 1-2% yr⁻¹ rate of improvement in official hurricane track predictions. While specific track prediction models have indicated a 15-20% improvement over the past 2-3 years, very little skill has been shown in the prediction of intensity change or wind field distribution (Neumann et al 1997). For this reason, the average length of coastline warned per storm, about 570 km, has not changed much over the past decade, nor has the average overwarning percentage, about 75%. However, the average preparation costs have increased eight-fold in the past 7 years from \$50M storm⁻¹ in 1989 (Sheets 1990) to an estimated \$300M storm⁻¹ in 1996, or about \$1M nm⁻¹ of coastline warned (Jarrell et al 1992; Neumann et al 1997). The increasing potential for severe loss of life as coastal populations soar, and potential monetary losses of tens of billions of dollars requires that greater effort be directed to understanding all physical processes which play an important role in modulating TC wind fields and storm surge at landfall.

A major source of difficulty in past predictions of TC intensity, wind fields, and storm surge at landfall has been the inability to measure the surface wind field directly and the inability to predict how it changes in response to external and internal forcing. The surface wind field must presently be estimated from a synthesis of scattered surface ship and/or buoy observations and aircraft measurements at 1.5 km to 3.0 km altitude (Powell 1980; Powell et al 1996; Powell and Houston 1996). This task is complicated by variations with height of the storm's structure, such as the change with height of storm-relative flow due to environmental wind shear and to the variable outward tilt of the wind maximum with height.

¹ NOAA/AOML, Hurricane Research Division,
4301 Rickenbacker Causeway, Miami, FL 33149

Numerous studies of TC structure have been made previously using various combinations of remote sensing and *in situ* data. Numerous studies of TCs have been made concentrating on NOAA aircraft data, ground based radar and surface damage reports, e.g., Willoughby and Black (1996) and Black and Marks (1991).

Based on NOAA aircraft observations, eyewall mesovortices and attendant supercell convection were associated with intense turbulence, vertical air motions in excess of 20 m s^{-1} at cloud base and momentary loss of aircraft control during low-level penetrations in rapidly developing Hurricanes Gladys (1975) and Hugo (1989). Vorticity perturbations were deduced with magnitudes on the order of Midwest thunderstorm mesocyclones. Land based radar observations and damage surveys after Hurricane Andrew (1992) suggested that enhanced swirling motion associated with convectively initiated eyewall mesovortices may have been responsible for the intense inland wind damage associated with landfall in South Florida (Wakimoto and Black 1994; Willoughby and Black 1996). Convective perturbations along the inner edge of the outer eyewall of Typhoon Paka (1997) led to three distinct destructive wind surges over the northern half of Guam.

An in-depth examination of 3-5 s gust factors at 10-m level derived from a number of sources suggest that separate populations of gust factors are associated with mid-latitude storms, over-water and over-land TC conditions. The mean over-water gust factors for 1-min, 10-min and 30-min measurement duration in TC's were found to be 1.23, 1.40 and 1.48, respectively.

The ratio of average maximum wind estimates in West Pacific TCs from the post-1970 data set over those from the pre-1970 data set, is found to be about the same as the ratio between flight-level (cloud base) winds and surface winds, an average of 0.8 (Powell, 1980). Recent Global Positioning System (GPS) dropsonde (GPS sonde) data in the eyewalls of Hurricanes Guillermo (1997) and Erika (1997) in 1997 suggest that different ratios may apply in the TC outer region beyond the eyewall than in the eyewall itself. The difference in wind estimates between the two time periods in the western Pacific may be due to the failure to take into account the decrease of the wind with height in the boundary layer of the TC for the pre-1970 era observations.

Black (1993) suggested that the TC gust factor increased with height at the same rate that the mean wind decreases with height in the TC atmospheric boundary layer (ABL), implying that convection conserves momentum in the ABL, maintaining a nearly constant peak gust wind speed with height. The recent Guillermo and Erika GPS sonde data have shown that the vertical structure in the ABL is much more complex than previously thought containing multiple wind maxima. Multiple wind maxima in the ABL was first observed by Wilson (1979) with instrumented tower observations.

2. EYEWALL MESOVORTEX STRUCTURE

In Hurricane Andrew (1992), an eyewall replacement cycle developed as the storm moved across the Gulf Stream. The Miami WSR-57 radar was able to observe the dissipation of the old eyewall over the Bahamas simultaneously with its replacement by a larger eyewall. A slow contraction of the new eyewall followed and two centers of convective activity formed in the eyewall and rotated around the eye. As the storm approached Miami, two distinct cyclonic mesovortices could be seen adjacent to the convective centers of action on opposite sides of the eyewall, which rotated about a common center in the middle of the eye. The presence of two meso-vortices indicated a predominance of wave number-2 asymmetric structure. However, as the eyewall approached the coast and came into view of the Tampa WSR-57 radar, as well as the Melbourne WSR-88D radar, a transition was observed from a rotating wave number-2 asymmetric flow to a fixed wave number-1 asymmetric flow relative to the translating center, even as the intense winds destroyed the Miami WSR-57 radar.

The Tampa WSR-57 radar, which was being recorded digitally by a team from the Hurricane Research Division, scanned the eyewall at 30-s intervals, covering an altitude band of 3-8 km. The WSR-57 revealed that a series of 7 intense raincells developed in the north portion of the eyewall as it made contact with the coast, moved across south Dade County and dissipated in the south portion of the eyewall, south of Homestead, FL, during the 45 min required for the eyewall to move ashore. Development of the intense raincells, which began as the eyewall made contact with the coast, continued at intervals of 3- to 7-min, and ended once the eyewall was completely over land. Each had a

life cycle of 8-15 min growing in intensity from 30 dBZ ($\sim 10 \text{ mm h}^{-1}$) to 50 dBZ (150 mm h^{-1}). The rapid growth in cell intensity implied intense updrafts within the cells. These updrafts, imbedded within the background TC-scale vorticity, enhances the vorticity locally on the scale of the updraft by means of vortex tube stretching and tilting of horizontal vorticity into the vertical. Thus, meso-vortices, similar to that associated with the tornado cyclone in rotating severe thunderstorm cells, were probably produced in Andrew's eyewall in association with each intense raincell.

Through the process of geostrophic adjustment, the pressure field adjusts rapidly to perturbations in the wind field on the mesoscale which are larger than the Rossby radius of deformation (on the order of 10 km for TC eyewalls). Hence, as the perturbation vortex grows with the raincell, an accompanying pressure perturbation develops near the inner edge of the eyewall, where the updraft is located. Anecdotal evidence for the existence of this pressure perturbation was obtained from two sources. First, by pure serendipity, the NOAA-11 polar-orbiting spacecraft passed over South Florida at a time exactly midway through the raincell production process as the eyewall was moving onshore. The 1-km resolution infrared image (not shown) revealed a "hot spot" in the image, not in the center of the eye, as normally expected, but offset from the center immediately adjacent to the eyewall convection. The second serendipitous observation was made by a private citizen, who observed their minimum pressure reading for the storm from a home barometer, later calibrated, which was situated exactly within the warmest pixel of the image and within 3 min of the satellite image time. Four additional private pressure observations in the nearby area confirmed the existence of a pressure perturbation along the edge of the eyewall that was 9 hPa lower than the minimum pressure in the center of the eye observed by Air Force reconnaissance aircraft at nearly the same time.

Such a mesovortex was actually penetrated by research aircraft at low altitude (300 m) in Hurricane Hugo (1989), obtaining detailed flight-level measurements. The Hugo aircraft flight revealed a classic meso-vortex signature with a wind speed perturbation of 30 m s^{-1} and a pressure perturbation of 13 hPa and was tracked for 5 revolutions about the eye center during a 1.5 h period as 5 separate cells developed and decayed, an almost identical scenario to Andrew.

An eyewall mesovortex was first photographed from above by a U-2 aircraft in Typhoon Ida (1958) (Fletcher et al 1961). The eyewall actually folds into the eye as it attempts to partially wrap around the meso vortex in Ida. Both Ida and Hugo shared a common characteristic with Andrew in that they were both very intense and deepening rapidly. One might conclude that meso-vortices and their attendant enhanced and streaky surface winds are a characteristic of intense, deepening storms, and that, should this occur as landfall approaches, then intense inland wind damage is to be expected.

2.1 Hurricane Hugo

On 15 September 1989, a NOAA WP-3D made the first aircraft penetration into Hurricane Hugo at an altitude of 450 m when it was $\sim 500 \text{ km}$ northeast of Barbados. The aircraft encountered intense turbulence and suffered the loss of an engine. Data from this aircraft showed that it penetrated a mesoscale vortex imbedded in the inner edge of the eyewall adjacent to intense convection.

The mesovortex had a diameter of 1 km at 500 m altitude which is a factor of 10 smaller than the eye diameter. This is about the same ratio as suction vortex size to its parent tornado (Fujita, 1971). The 1 km is also 10 times smaller than a tornado's parent mesocyclone and about 5 times larger than a tornado. The wind and pressure perturbations about a linear pressure and wind speed profile are 30 m s^{-1} and 12 hPa, respectively. The former is about a factor of 3 smaller than the eyewall maximum winds. In contrast, suction vortex winds are about a factor of 2 greater than tornado rotational winds (Fujita 1971). The perturbation vorticity is $\sim 10^{-1} \text{ s}^{-1}$, an order of magnitude greater than eyewall or mesocyclone vorticity and about the same as tornado vorticity.

During 14 subsequent orbits of the eye the aircraft penetrated the vortex on nine different occasions with diameters of 1-2 km. The vortex penetrations, at gradually increasing altitude, showed that the vortex's maximum strength and smallest diameter appeared to be at cloud base and broadened with height. The vortex rotated around the center of circulation with a period of 19 min, implying a translation speed of 30 m s^{-1} . This was the first time that an aircraft had penetrated such a phenomena in a TC, although vortices of this type have been observed, and are probably more common than previously

believed (e.g., Fletcher et al 1961; Marks and Houze 1984; Muramatsu 1986; Bluestein and Marks 1987).

2.2 Hurricane Luis

During the daylight hours of 6 September 1995, 1-km resolution GOES-9 1-min interval images and GOES-8/9 15-min stereo images were obtained over Hurricane Luis. These data were concurrent with NOAA WP-3D one-min horizontal and vertical airborne radar scans. These observations revealed a series of 8 cycloidal loops. The low-level center is indicated by the primary low-cloud swirl, while the upper-level center is indicated by the center of the cirrus cloud rim and the infrared maximum temperature. Secondary low-cloud swirls appeared to rotate around the primary swirl. The cycloidal loops had an average period of 90 min and an average diameter of 20 km. The upper eye diameter averaged 60 km, while the low-level diameter averaged 40 km. The upper-level center was displaced to the east-southeast of the primary low-cloud swirl by an average of 25 km. Overshooting convective turret clusters were observed in the eyewall with similar 90-min periods and duration averaging 20 min.

One event, corresponding to the first WP-3D eye penetration, was analyzed in detail using the radar and one-min GOES-9 data. Several minutes after rapid increase in radar reflectivity occurred in the northeast eyewall sector, a cluster of overshooting turrets was observed emerging above the cirrus shield in the north eyewall sector. The cluster continued to bubble as the turret and reflectivity maximum rotated around to the west eyewall sector. Strong evidence of cyclonic rotation of the turret elements was observed during the peak overshoot period. Simultaneously, the GOES-8/9 stereo imagery revealed that thin cirrus elements at the upper edge of the eyewall were being entrained into the eye as they descended toward the primary low-level center adjacent to the overshooting turret cluster. During this period, the low-level center was migrating toward the eyewall sector where the turret cluster was observed.

2.3 Synopsis

Features observed here are very similar to those encountered during a NOAA WP-3D flight into Hurricane Hugo (1989) (Black and Marks 1991). The storm structure was somewhat different in that case with a smaller eye than Luis, but the intense convection was clearly

associated with a mesovortex which was separable from the intense background vortex circulation. The mesovortex had perturbation pressure on order of 15 hPa and wind perturbation on order 30 m s^{-1} . Vertical reflectivity structure was similar to that in Luis with intense cores sloping outward and upstream.

The mesovortex in Luis never penetrated to low levels, and did not appear to be as strong. However, the 6 revolutions about the eyewall in Hugo were very similar to the 8 loops observed for Luis. Only the revolution period was longer for Luis (90 min) compared to Hugo's (20 min) due to the larger eye diameter (60 km vs. 14 km respectively). A schematic composite of the flow fields, depicted in Fig. 1, illustrates how the mesovortex flow is superimposed upon the TC-scale flow.

3. RECENT ABL OBSERVATIONS IN HURRICANES GUILLERMO AND ERIKA (1997)

The successful deployment of the new GPS sondes with reliable wind, temperature, humidity and pressure measurements every 0.5 s to within less than 10 m of the surface were made for the first time from the NOAA WP-3D and Gulfstream IV (G-IV) aircraft in the inner core of eastern Pacific Hurricane Guillermo (1997). Additional drops were made on three days in Atlantic Hurricane Erika (1997).

Preliminary analysis of a few of the eyewall soundings have revealed several new and unusual ABL structures. Figure 2 shows three normalized eyewall ABL soundings of potential temperature (θ), specific humidity (q) and wind speed (WS) from Hurricanes Guillermo and Erika. The vertical coordinate is normalized by the depth of the ABL, defined as the depth of the constant θ layer ($\sim 300 \text{ m}$). These eyewall soundings indicate three consistent low-level wind maxima at approximately 0.7 normalized height units ($\sim 200 \text{ m}$), at 1.4 units ($\sim 400 \text{ m}$), and at 2.5 units ($\sim 750 \text{ m}$). The lowest wind maximum appears just above the top of a constant- q layer, whose depth is shallower than the constant- θ layer. The other two wind maxima occur at and just above the constant- θ layer. These soundings are typical of other eyewall soundings that show multiple wind maxima in the ABL and exhibit a shallow constant- q layer. The latter corresponds with a layer of nearly

constant wind direction (not shown), and may be representative of the surface layer. These wind observations are consistent with Australian tower observations in the inner, high-wind core of TC first reported by Wilson (1979) and recently discussed by Kepert and Holland (1997). These data showed a low level wind maximum consistently at the 60-m level, as well as a wind maximum near the top of the 400-m tower.

The observation of a thin layer of elevated specific humidity in the high wind region beneath the eyewall is very suggestive of a spray layer which may enhance evaporation in the >90% relative humidity air. The existence of a wind maximum above this layer indicates that upward vapor fluxes in the ABL may be controlled more by shear-induced turbulence at the top of the high specific humidity layer than by direct flux from the sea. Sea spray processes such as discussed by Fairall et al (1994) may become important. Additional analysis of this revolutionary new data source should lead to profound new insights into the workings of the TC eyewall ABL.

4. CONCLUSIONS

A unique combination of 1-min interval super-rapid-scan GOES-9 images and NOAA aircraft data provides unprecedented insights into the dynamics of eyewall convective outbreaks, eye motion, and low-level cloud motion in the eye. The mesovortices observed in concurrent GOES/Aircraft 1-min animations appear to be similar to features of eyewall mesovortices observed by the flights into Gladys (1975) and Hugo (1989) and to observations in Andrew (1992). It is hypothesized that the mesoscale vortices are advected by the TC-scale vortex causing significantly higher winds in regions where the wind velocities of the two vortices are near their maxima and in the same direction. The insights gained from this work have potentially far reaching implications as to an improved understanding of the track and intensity fluctuations associated with these features and to strategies for mitigating attendant damages at landfall.

5. REFERENCES

Black, P.G., 1993: Evolution of maximum wind estimates in typhoons. *Tropical Cyclone*

Disasters, J. Lighthill and Z. Zhemmin, eds., Peking University Press, Beijing, PRC, 104-115

Black, P. G. and F. D. Marks, Jr., 1991: The structure of an eyewall meso-vortex in Hurricane Hugo (1989). *Proc. 19th Conference on Hurricanes and Tropical Meteorology*, AMS, Miami, FL, 579-582.

Black, P. G. and L.K. Shay, 1998: Observations of tropical cyclone intensity change due to air-sea interactions. *Proc. Symposium on Tropical Cyclone Intensity Change*, Phoenix, AZ, AMS, 161-168.

Bluestein, H.B., and F.D. Marks, 1987; On the structure of the eyewall of Hurricane Diana (1984): Comparison of radar and visual characteristics. *Mon. Wea. Rev.*, **115**, 2542-2552.

Fairall, C. W., J. D. Kepert and G. J. Holland, 1994: The effect of sea spray on surface energy transports over the ocean. *The Global Atmosphere and Ocean System*, **2**, 121-142.

Fletcher, R.D., J.R. Smith, and R.C. Bundgaard, 1961: Superior photographic reconnaissance of tropical cyclones. *Weatherwise*, **14**, 102-109.

Fujita, T. T., 1971: Proposed mechanism of suction spots accompanied by tornadoes. *Proc. 7th Conference on Severe Local Storms*, AMS, Kansas City, MO, 208-213.

Hasler, A.F., P.G. Black, V.M. Karyampudi, M. Jentoft-Nilsen, K. Palaniappan, D. Chesters, 1997: Synthesis of eyewall mesovortex and supercell convective structure in Hurricane Luis with GOES 8/9 stereo, concurrent 1-min GOES-9 and NOAA airborne radar observations. *Proc. 22nd Conference on Hurricanes and Tropical Meteorology*, AMS, Ft. Collins, CO, 201-202.

Jarrell, J. D., P. J. Hebert and M. Mayfield, 1992: Hurricane experience levels of coastal county populations from Texas to Maine. *NOAA Tech. Memo. NWS NHC-46*, 152 pp.

Kepert, J. D. and G. J. Holland, 1997: The Northwest Cape tropical cyclone boundary layer monitoring station. *Proc. 22nd Conference on Hurricanes and Tropical Meteorology*, AMS, Ft. Collins, CO, 82-83.

Marks, F.D., and R.A. Houze, 1984: Airborne Doppler radar observations in Hurricane Debby. *Bull. Amer. Meteor. Soc.*, **65**, 569-582.

- Muramatsu, T., 1986: The structure of polygonal eye of a typhoon. *J. Met. Soc. of Japan*, **64**, 913-921.
- Neumann, C., H. Nicholson, C. Guard, 1997: National Plan for Tropical Cyclone Research and Reconnaissance (1997-2002), FCM-P25-1997, Office of the Federal Coordinator for Meteorological Services and Supporting Research.
- Powell, M. D., 1980: Evaluations of diagnostic marine boundary layer models applied to hurricanes. *Mon. Wea. Rev.*, **108**, 757-766.
- Powell, M. D., S. H. Houston and T. A. Reinhold, 1996: Hurricane Andrew's landfall in South Florida. Part I: Standardizing measurements for documentation of surface wind fields. *Wea. and Forecasting*, **11**, 304-327.
- Powell, M. D. and S. H. Houston, 1996: Hurricane Andrew's landfall in South Florida. Part II: Surface wind fields and potential real-time applications. *Wea. and Forecasting*, **11**, 329-349.
- Sheets, R. H., 1990: The National Hurricane Center, past, present and future. *Wea. and Forecasting*, **5**, 185-232.
- Wakimoto, R., and P.G. Black, 1994: Damage Survey of Hurricane Andrew and Its Relationship to the Eyewall. *Bull. Amer. Meteor. Soc.*, **75**, 2, 189-200.
- Willoughby, H.E., and P.G. Black, 1996: Hurricane Andrew in Florida: Dynamics of a Disaster. *Bull. Amer. Meteor. Soc.*, **77**, 543-549.
- Wilson, K. J., 1979: Characteristics of the subcloud layer wind structure in tropical cyclones. *International Conference on Tropical Cyclones*, Perth, Australia.

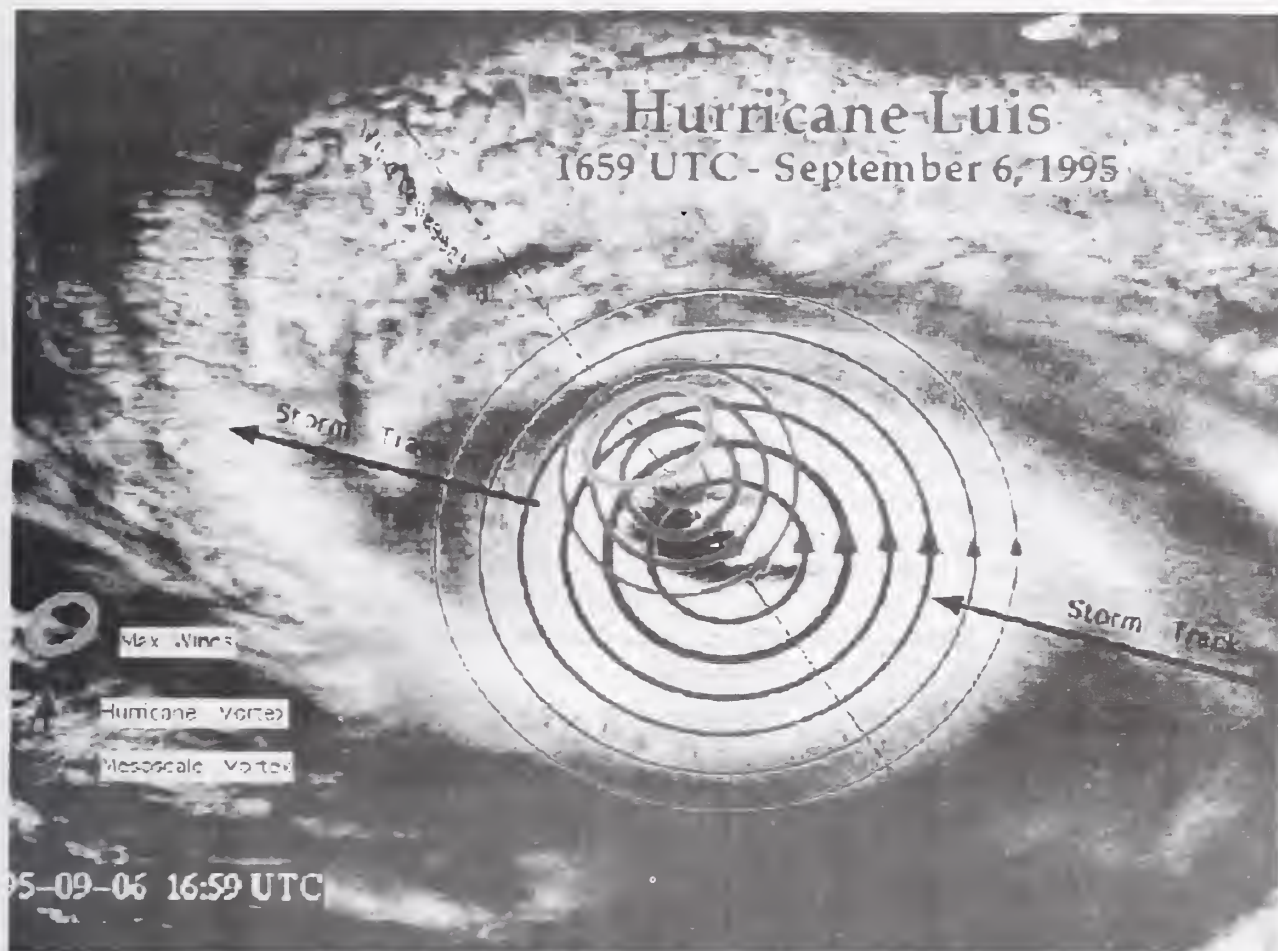


Fig. 1 Schematic representation of the flow field in a eyewall mesovortex superimposed upon the hurricane scale circulation. Both circulations are superimposed on a visible image of Hurricane Luis, September 6, 1995.

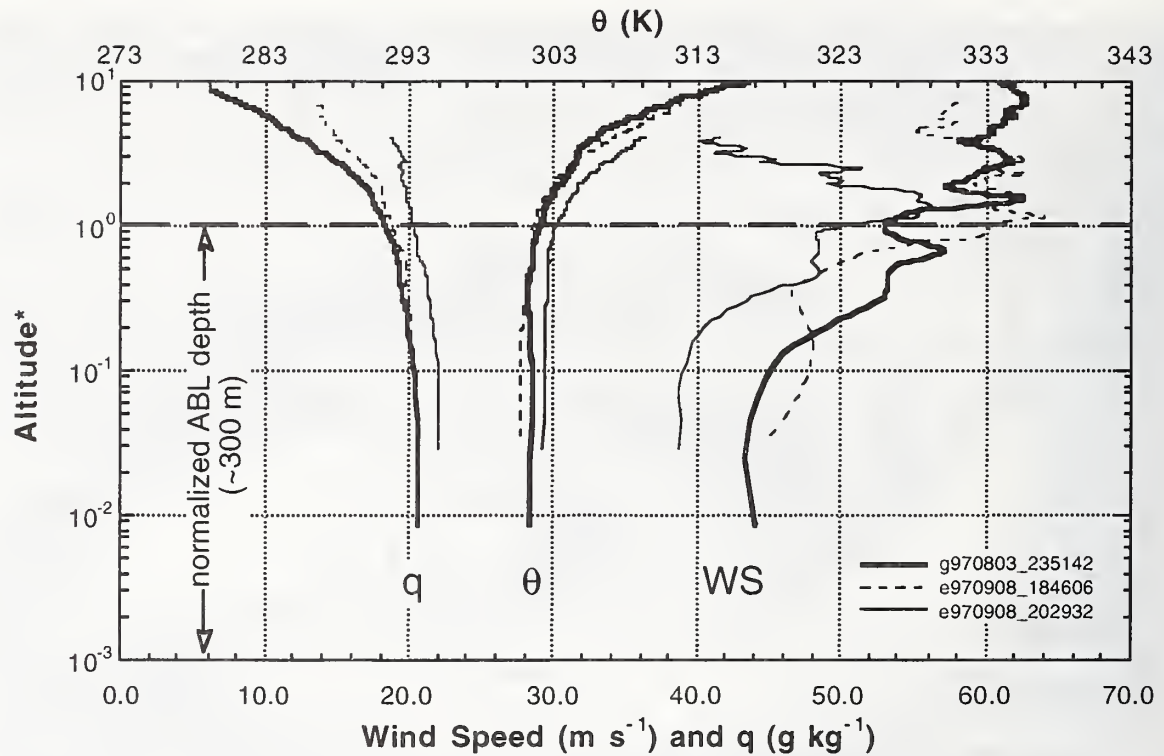


Fig. 2. GPS dropsonde profiles of specific humidity ($q \text{ g kg}^{-1}$), potential temperature ($\theta \text{ }^{\circ}\text{C}$) and wind speed ($WS \text{ m s}^{-1}$) for three typical profiles in the eyewall of Hurricanes Guillermo (thick solid lines) and Erika (thin dashed lines). Vertical coordinate is normalized by the depth of the ABL defined as the depth of the constant q layer ($\sim 300 \text{ m}$).

Consideration on Flutter Characteristics of Super Long-Span Bridges

by

Hiroshi SATO¹⁾, Katsuya OGIHARA²⁾ and Ken-ichi OGI³⁾

ABSTRACT

Aerodynamic stability is one of the most important themes in the design of a super long-span bridge. To improve the aerodynamic stability of a super long-span bridge, a series of wind tunnel studies and analytical studies were conducted, and it was found that slot at the center of girder was effective to improve the aerodynamic stability. The relationship between flutter characteristics and unsteady aerodynamic forces was discussed, and it was found that flutter characteristics were closely correlated with unsteady aerodynamic force coefficients $M_{Z1} L_{\theta R}/M_{\theta 1}$ and $M_{\theta R}$.

KEYWORD: flutter, super long-span bridge, slotted box girder, unsteady aerodynamic force

1. INTRODUCTION

The Akashi Kaikyo Bridge has the world-longest span length of 1990m. In Japan and in the world, there are several plans or ideas to construct bridges longer than the Akashi Kaikyo Bridge. In the design of such super long-span bridges, aerodynamic stability is one of the most important themes. The approaches to improve aerodynamic stability can be classified into structural one and aerodynamic one. This paper deals with the latter approach.

It was proposed by the authors that slotted box girders were effective to increase flutter speeds of super long-span bridges [1]. In this paper discussed is the relationship between flutter characteristics and unsteady aerodynamic forces of slotted box girders.

2. FLUTTER CHARACTERISTICS OF SLOTTED BOX GIRDERS [1]

The effect of location and size of slot on aerodynamic characteristics was examined through section model wind tunnel tests. Considering a

super long-span bridge which has center span length of 3,000m with two side spans of 1,500m, the structural conditions were assumed. Reduced mass $\mu (=m/(\rho B^2))$, m : mass per unit length, ρ : air density, B : girder width), reduced polar moment of inertia $\nu (=I/(\rho B^4))$, I : polar moment of inertia per unit length), and natural frequency ratio $\varepsilon (=f_{\theta}/f_z)$, f_{θ} : torsional natural frequency, f_z : vertical bending natural frequency) were 16, 2.1, and 2.1, respectively. The cross section of the model is shown in Fig.1. From the test results, it was found that the slot at the center increased the flutter onset wind speed. It was also found that the flutter onset wind speed was increased with the width of slot at the center of the girder (Fig.2).

In order to understand the effect of slot at the center of girder, preliminary analysis was conducted for slotted plate. For the analysis, aerodynamic forces acting on each plate was calculated using the Theodorsen's function. The aerodynamic interference between the 2 boxes was neglected. Using these aerodynamic forces, two degree-of-freedom flutter analysis was conducted by U-g method [2]. The result of the flutter analysis (Fig.2) indicated that the flutter onset wind speed increased with size of slot. The differences between the analysis and the experiment seemed to be caused by aerodynamic interference between the 2 boxes.

Although wide slot at the center of the girder improves flutter characteristics, narrower slot

-
- 1) Head, Structure Division, Structure and Bridge Dept., Public Works Research Institute, Ministry of Construction
 - 2) Deputy Manager, Second Design Division, Design Department, Honshu-Shikoku Bridge Authority, (Former Senior Research Engineer, Structure Division)
 - 3) Research Engineer, Structure Division, Structure and Bridge Dept., Public Works Research Institute, Ministry of Construction

would be preferable from the viewpoint of construction cost of towers and foundations. To improve aerodynamic characteristics, the effect of some devices was studied by section model tests. The tested devices are illustrated in Fig.3. The results showed that the center barrier and guide vanes improved flutter characteristics very well (Fig.4). However, the flutter speed was not so high when angle of attack was -3 deg. It was found that the guard rails at the bottom deck increased the flutter speed considerably at this angle of attack (Fig.5).

3. UNSTEADY AERODYNAMIC FORCES OF SLOTTED BOX GIRDERS

From the above studies, it was found that slotted plates and slotted box girders have better flutter characteristics than single plates and single box girders. It was also found that the devices such as center barrier and guide vanes are effective to improve flutter characteristics of slotted box girders.

In order to understand causes of flutter characteristics of slotted plates and box girders more precisely, unsteady aerodynamic forces were measured for three models: model A (single box girder, $b=0$ in Fig.1), model B (slotted box girder, $b=0.22B$ in Fig.1) and model C (slotted box girder with devices, Fig.3). The measurement was made by forced oscillation method [3] with angle of attack 0 degree. Coefficients of the unsteady aerodynamic forces were defined as follows:

$$L = \pi \rho \{ B^2 [L_{ZR} \omega^2 z + L_{ZI} \omega z'] + B^3 [L_{\theta R} \omega^2 \theta + L_{\theta I} \omega \theta'] \} \quad (1.1)$$

$$M = \pi \rho \{ B^3 [M_{ZR} \omega^2 z + M_{ZI} \omega z'] + B^4 [M_{\theta R} \omega^2 \theta + M_{\theta I} \omega \theta'] \} \quad (1.2)$$

where, L: lift (upward positive), M: aerodynamic moment (head up positive), z: vertical displacement (upward positive), θ : torsional displacement (head up positive), ω : circular frequency, ()': d()/dt, L_{xx} or M_{xx} : coefficients of unsteady aerodynamic forces (z: caused by vertical vibration, θ : caused by torsional vibration, R: in phase with displacement, I: in phase with velocity).

Among measured unsteady aerodynamic force coefficients, the most effective coefficients for flutter, which will be explained next, are shown in Fig. 6. For comparison, theoretical coefficients for single plate and slotted plate, which were calculated from the Theodorsen's function, are shown in the same figures. The slot ratio of the slotted plate was the same as the Model B and C.

In general, it is difficult to predict coupled flutter characteristics directly from these coefficients. For 2-degrees of freedom system, Nakamura [4] showed approximate relationship between unsteady aerodynamic coefficients M_{ZI} , $M_{\theta I}$, $L_{\theta R}$ and $M_{\theta R}$ and some flutter properties as follows:

$$\delta a \doteq -\pi^2 M_{ZI} X / \nu - \pi^2 M_{\theta I} / \nu \quad (2.1)$$

$$X \equiv z_0 / \theta_0 / B \\ \doteq \pi L_{\theta R} / (-1 + (f_z / f_\theta)^2 \sigma^2) / \mu \quad (2.2)$$

$$\sigma^2 \equiv (f_\theta / f)^2 \\ \doteq 1 + \pi M_{\theta R} / \nu \quad (2.3)$$

where, δa : aerodynamic damping in logarithmic decrement.

These equations were derived by assuming that absolute value of aerodynamic damping and phase angle are small, and that absolute value of the amplitude ratio X is small. As is shown here, $M_{\theta R}$ affects the frequency ratio σ . $L_{\theta R}$ and σ affect the amplitude ratio X. M_{ZI} , $M_{\theta I}$ and X affect the aerodynamic damping.

Assuming ε , μ and ν as 2.0, 15 and 2.0, respectively, frequency ratio, amplitude ratio and aerodynamic damping were calculated for three Models, single plate and slotted plate. The results are shown in Fig. 7. The critical reduced frequency of slotted plate and slotted box girder, where aerodynamic damping turns negative, is smaller than that of single plate and single box girder. It means that slotted plate and slotted box girder have better flutter characteristics than single plate and single box girder. It is also found that flutter speed of single plate is higher than single box girder (Model A), and that flutter speed of slotted plate is higher than slotted box girder (Model B).

Comparing unsteady aerodynamic force coefficients of single plate and single box girder (Model A), it is found that they are almost identical except for $M_{\theta 1}$. Since $M_{\theta 1}$ produces positive aerodynamic damping as can be seen in eq.(2.1) and Fig. 6, it is found that the difference of $M_{\theta 1}$ explains the different flutter speeds of single plate and single box girder (Model A). In a similar way, it is found that the difference of M_{Z1} explains the different flutter speeds of slotted plate and slotted box girder (Model B), because M_{Z1} produces negative aerodynamic damping. Therefore, Nakamura's equations are effective to explain flutter characteristics. However, flutter characteristics such that slotted plate and slotted box girder have better flutter characteristics than single plate and single box girder, can not be explained directly from these equations.

4. INEQUALITY FOR FLUTTER ONSET

If onset of flutter is defined as $\delta a \leq 0$, simpler inequality for onset of flutter can be derived from (2.1)-(2.3) as follows:

$$\alpha M_{Z1} L_{\theta R}/M_{\theta 1} + \beta M_{\theta R} \geq 1 \quad (3.1)$$

$$\alpha \equiv (\varepsilon^2/(\varepsilon^2-1))(\pi/\mu) \quad (3.2)$$

$$\beta \equiv (1/(\varepsilon^2-1))(\pi/\nu) \quad (3.3)$$

The left hand side of inequality (3.1) was calculated for the Models A, B and C using measured unsteady aerodynamic forces, as well as for single plate and slotted plate using the Theodorsen's function. ε , μ and ν were assumed as 2.0, 15 and 2.0, respectively. The results are shown in Fig.8. The slotted box girders and slotted plate show higher flutter speed than the single box girder or single plate. Since the first term of the left hand side of inequality (3.1) is much larger than the second term, it can be said that this higher flutter speed was caused mainly by the property of $M_{Z1} L_{\theta R}/M_{\theta 1}$.

In Fig.8, reduced flutter speed $U/(fB)$ of slotted box girder with devices is almost identical with that of slotted box girder. In Fig.9, the results are plotted with $f_{\theta}B/U$. Flutter speed of slotted box girder with devices is higher than that without

devices. It means that the effect of devices came from small value of $M_{\theta R}$, which affected apparent frequency in wind.

5. CONCLUSION

Slotted box girders have good flutter characteristics, and they can be improved by some devices like center barrier and guide vane. In this paper, the relationship between flutter characteristics and unsteady aerodynamic forces of the slotted box girders was discussed. The main findings are as follows:

(1) Flutter characteristics of single plate, slotted plate, single box girder and slotted box girder can be explained by their unsteady aerodynamic forces through Nakamura's equations and the following inequality for flutter onset:

$$\alpha M_{Z1} L_{\theta R}/M_{\theta 1} + \beta M_{\theta R} \geq 1$$

(2) The higher flutter speed of slotted box girders and slotted plate than the single box girder or single plate was caused mainly by property of $M_{Z1} L_{\theta R}/M_{\theta 1}$.

(3) The effect of the devices like center barrier and guide vane came from small value of $M_{\theta R}$, which affected apparent frequency in wind.

REFERENCES

- [1] Sato H. and Ogihara K., Aerodynamic characteristics of slotted box girders, Proceedings of the 28th Joint Meeting of the Panel on Wind and Seismic Effects, UJNR, 1996
- [2] Washizu K., "Aeroelasticity", Kyouritsu Shuppan, Tokyo, 1957 (in Japanese).
- [3] Okubo, T., Narita N. and Yokoyama K., Some approaches for improving wind stability of cable-stayed girder bridges, Proc. of the 4th International Conference on Wind Effects on Buildings and Structures, 1975
- [4] Nakamura, Y., An analysis of binary flutter of bridge deck sections, J. of Sound and Vibration, 57(4), 1978

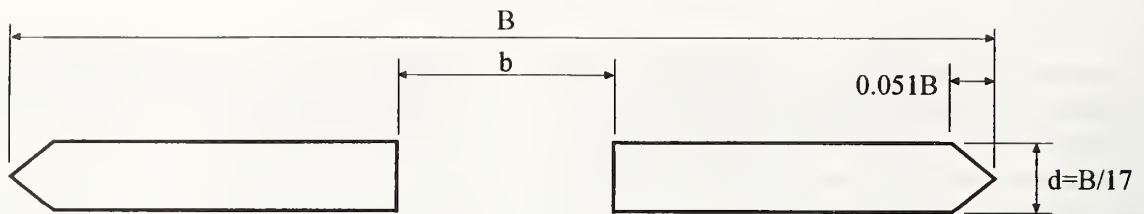


Fig.1 Cross Section of Slotted Girder

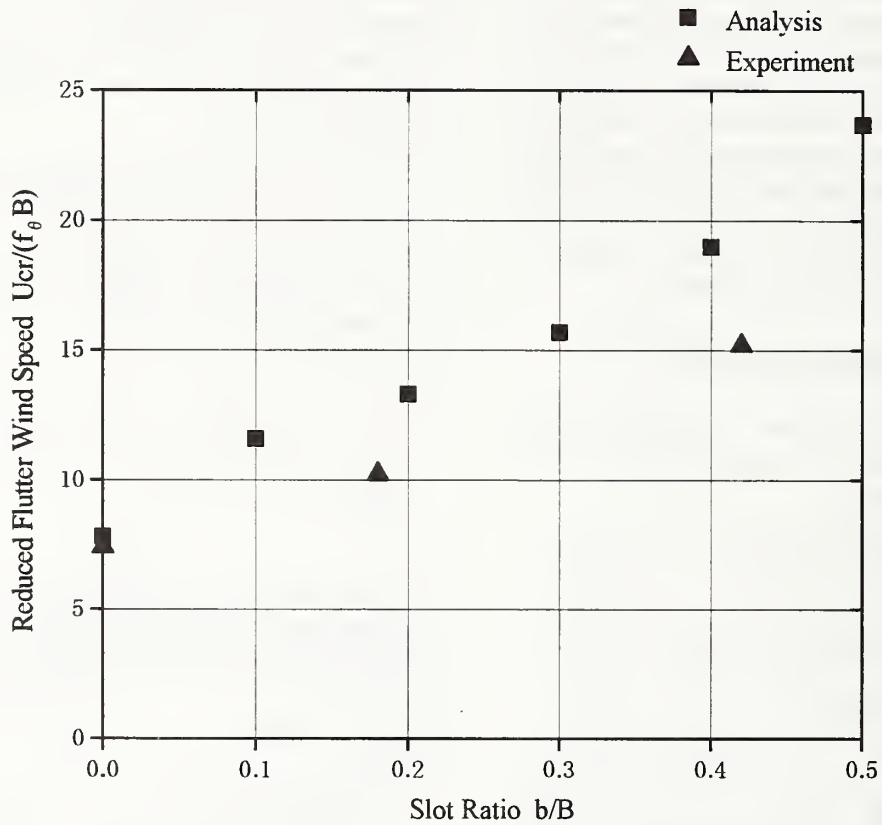


Fig.2 Flutter Onset Speed and Slot Ratio

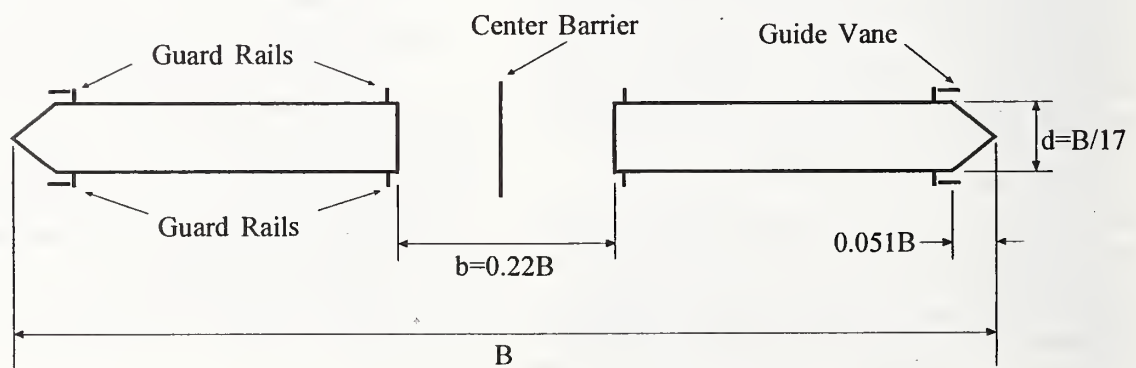


Fig.3 Slotted Box Girder with Devices

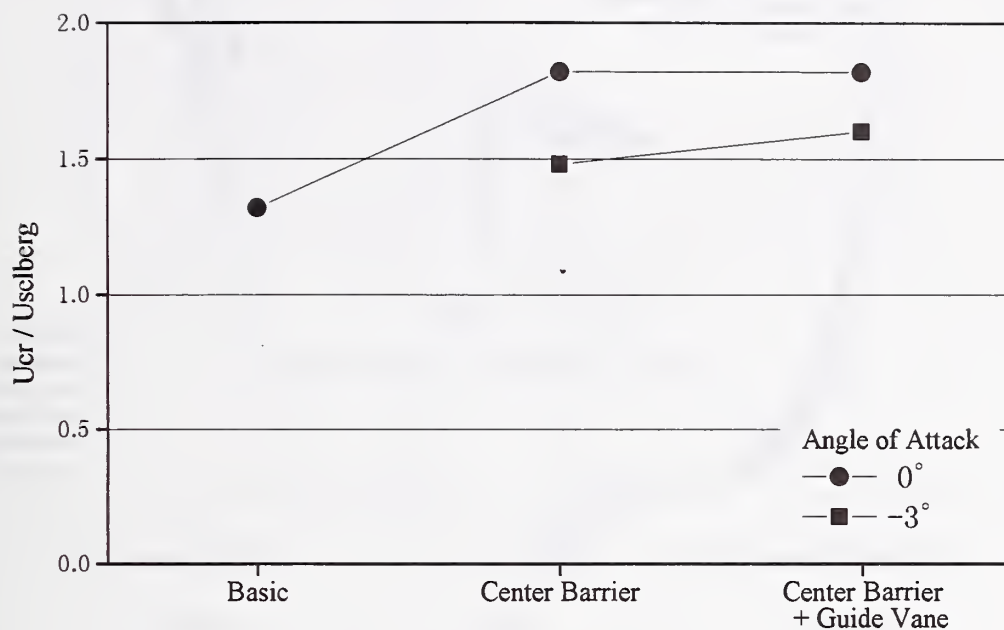


Fig.4 Effect of Tested Devices

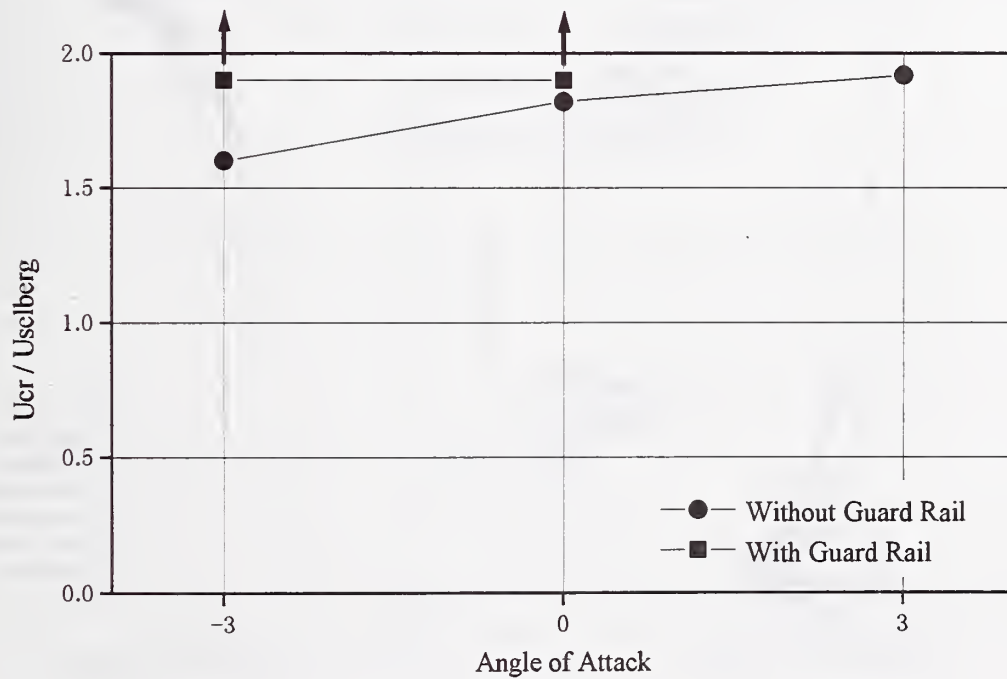
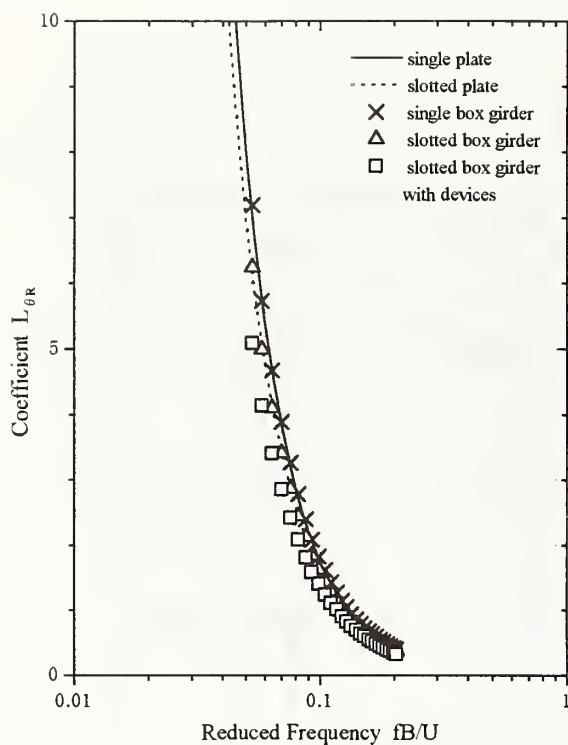
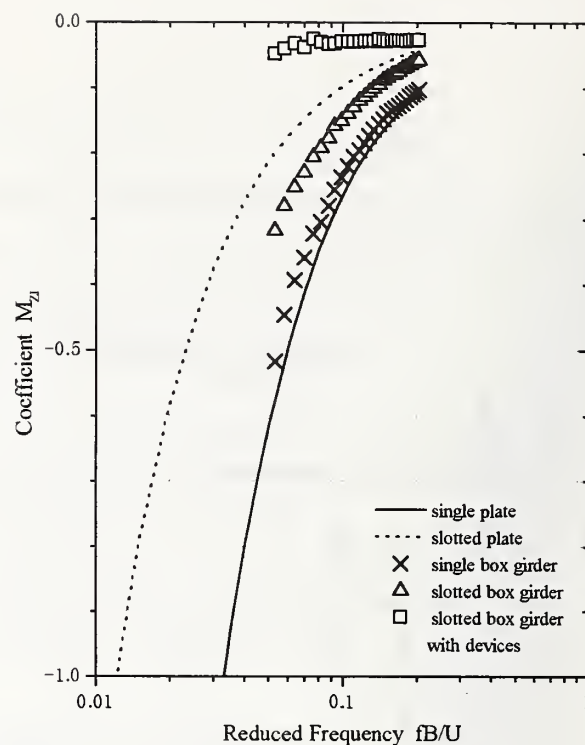


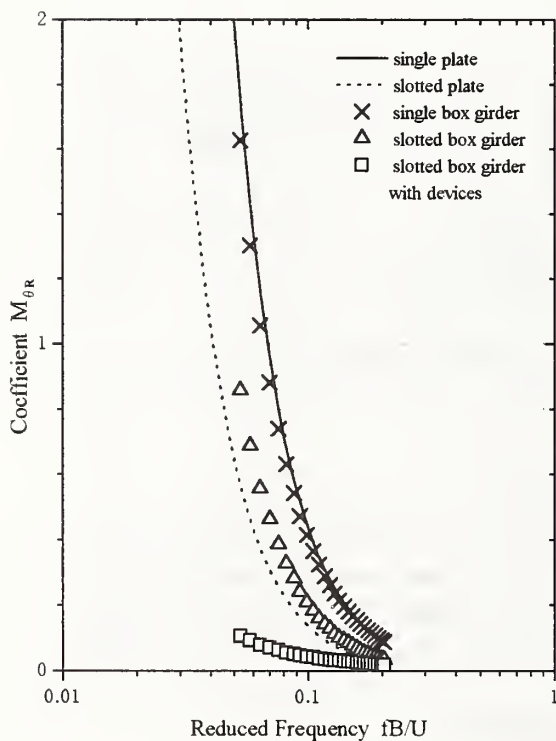
Fig.5 Effect of Guard Rails at the Bottom Deck



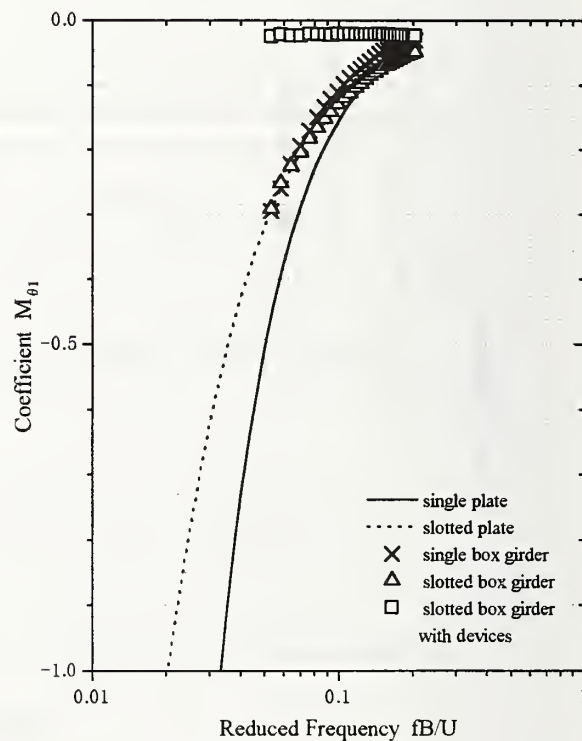
(a) $L_{\theta R}$



(b) $M_{\theta I}$

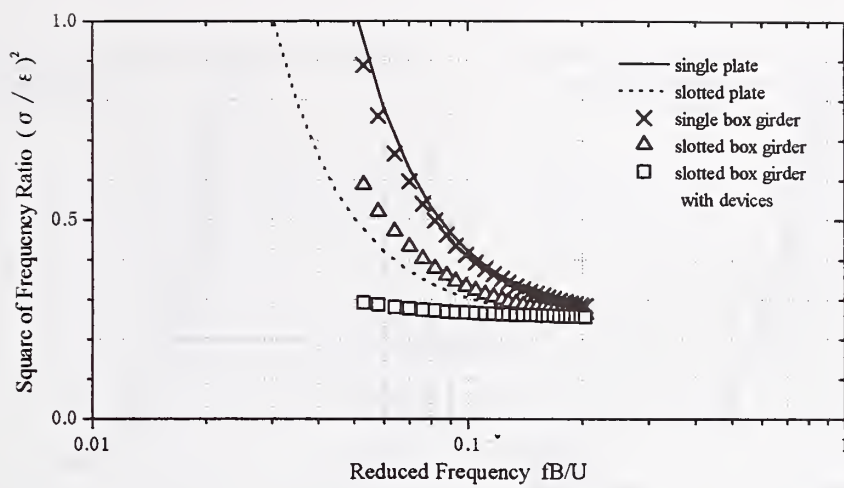


(c) $M_{\theta R}$

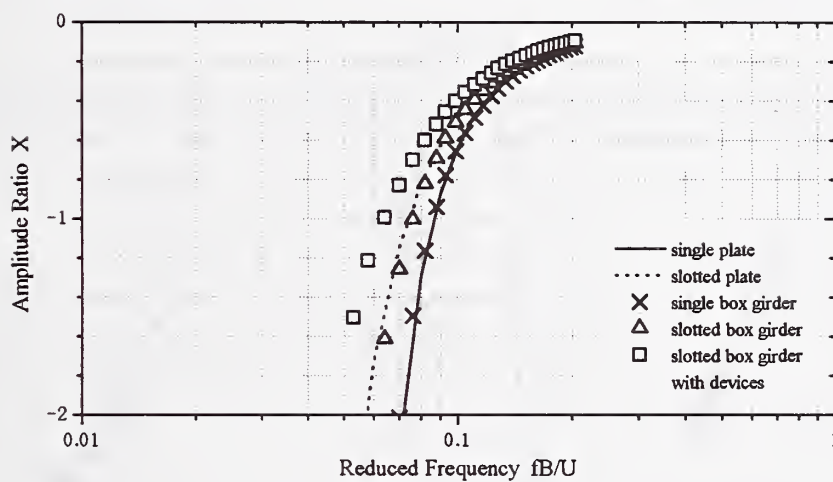


(d) $M_{\theta I}$

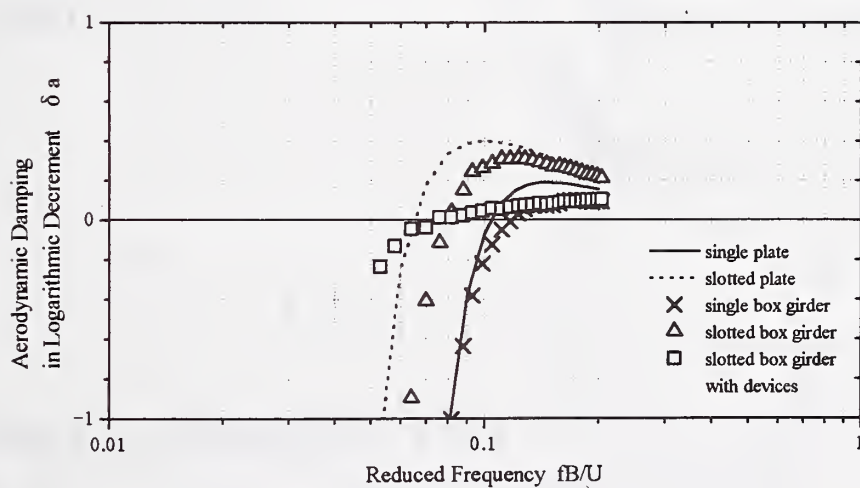
Fig.6 Coefficients of Unsteady Aerodynamic Forces



(a) Square of Frequency Ratio $(\sigma / \epsilon)^2$

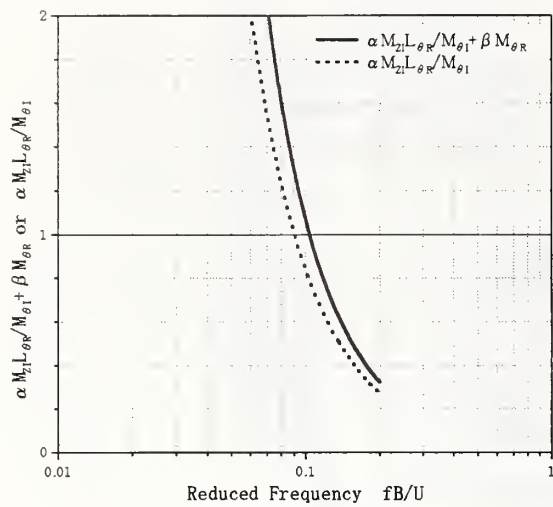


(b) Amplitude Ratio X

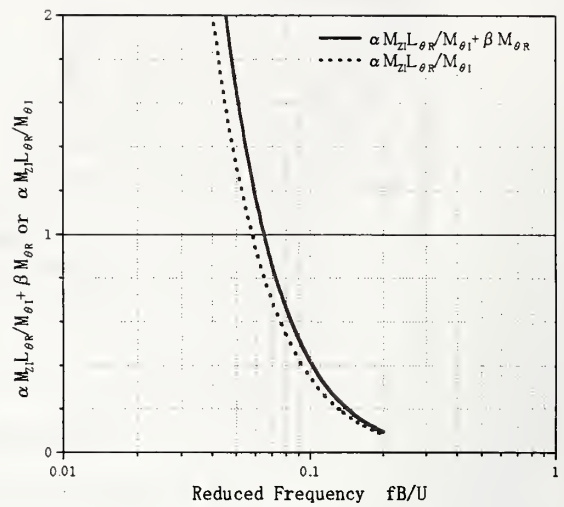


(c) Aerodynamic Damping in Logarithmic Decrement δa

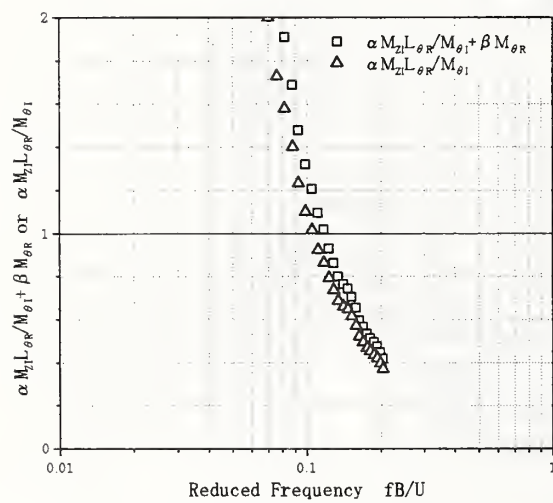
Fig7. Parameters Related to Flutter Characteristics



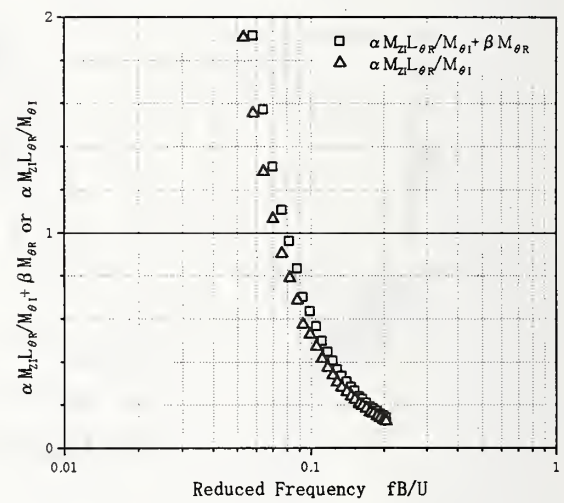
(a) Single Plate



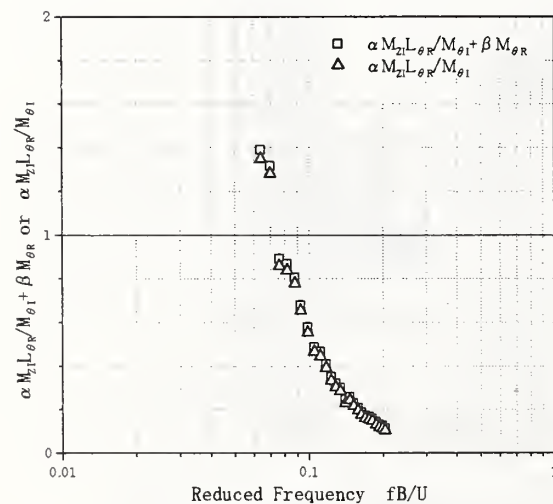
(b) Slotted Plate



(c) Single Box Girder



(d) Slotted Box Girder



(e) Slotted Box Girder with Devices

Fig8. Judgement of Flutter Onset
(plotted with fB/U)

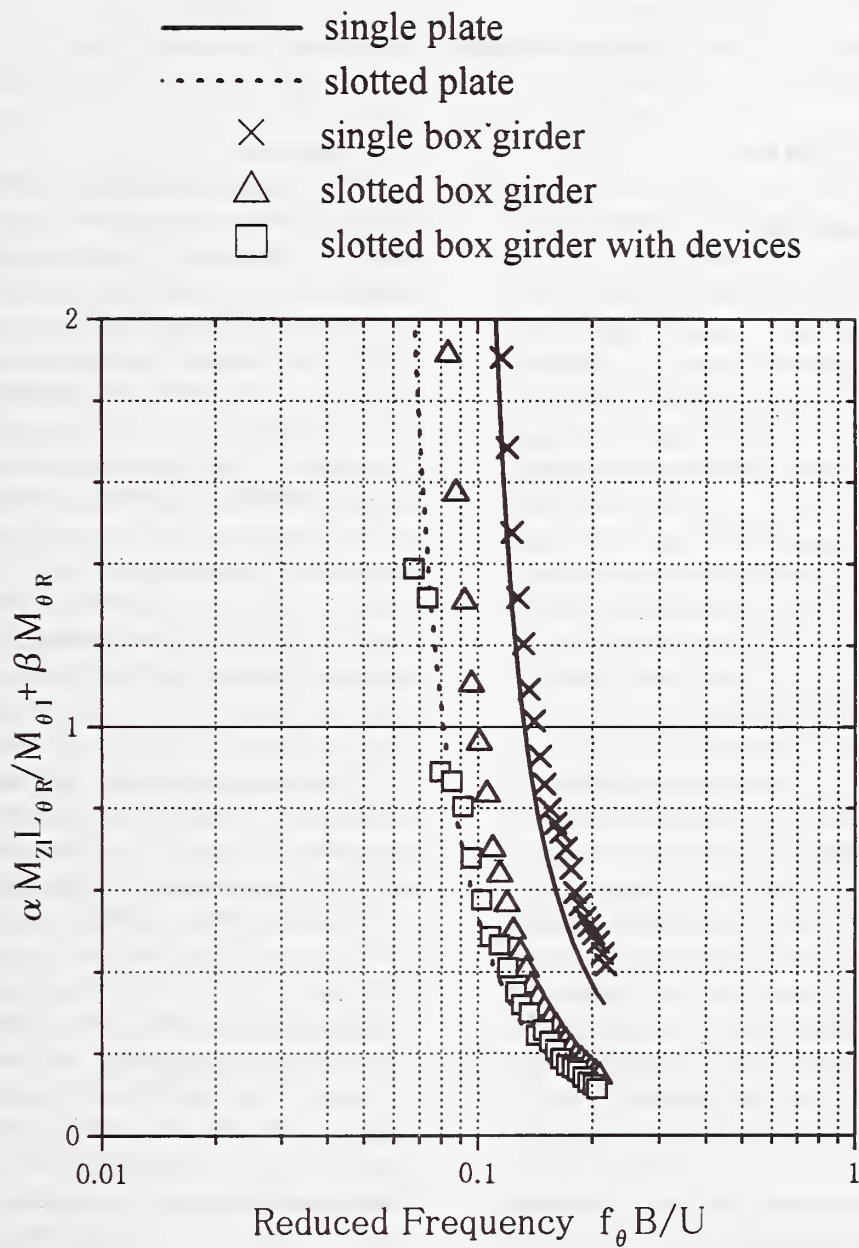


Fig.9 Judgement of Flutter Onset
(plotted with $f_{\theta} B/U$)

Structural Control for Wind and Earthquake Loads: NSF'S Coordinated Research Program

by

M. P. Singh¹ and T. T. Soong²

1. INTRODUCTION

Civil engineering structures are commonly designed for their strength and stability. The structural systems are analyzed to calculate forces in various load-carrying elements such as beams, columns, etc. These elements are then proportioned such that they can withstand the calculated forces without overstressing or instability failures. Since elastically designed structures could be bulky and costly, they are allowed to yield, at least for extreme loads such as earthquakes. Such designs, therefore, admit the possibility of structural damage of the load carrying elements in an extreme event.

In the last two decades, there has been a growing interest to find ways to reduce or control the effect of the extreme events. The earthquake-induced effects on structures can be reduced either by filtering or absorbing the damaging energy transmitted to a structure. A significant amount of research has been done to develop base isolation methods that primarily filter out the damaging energy from reaching the superstructure. The base isolators increase the fundamental period of the system such that combined structure isolator systems shift into the lower response spectrum range.

The energy dissipaters or energy sinks, placed at suitable locations in structures, have also been used for reducing dynamic response. The energy dissipater that have been recently considered for earthquake applications are the viscous, viscoelastic, and friction dampers, and yielding devices that add damping and stiffness (ADAS) to the system. These devices absorb vibration energy that otherwise would have gone to deform and possibly damage the structural elements. These devices can be designed such that they are disposable. That is, an overly deformed or damaged energy dissipater can be replaced with new ones after a strong event, if considered necessary.

The aforementioned approaches are commonly referred to as passive control approaches, as the devices come into action only after the structure has responded to the external disturbance. The reliability and usefulness of these methods is now quite well established in structural engineering community. As such, these methods are being increasingly used in practice in buildings in seismically active regions. The National Science Foundation (NSF) has played a major role in the development of these passive control approaches; it has made it possible to bring these useful concepts to fruition and to implementation.

¹ Professor, Dept. of Eng. Science and Mechanics, Virginia Tech, Blacksburg, VA 24060

² Samuel Capen Professor, Dept. of Civil Engineering, State Univ. of New York at Buffalo, Buffalo, NY 14260

stage by providing continuous funding to research projects dealing with this topic over the past twenty five years.

Along with the development of passive devices, the research community has also been exploring the development of the active control methods. In the active methods, the external forces are applied to control the response. The application of forces through tendons or other forms of actuators have been examined. When, where, and how much the forces should be applied is decided according to a suitable algorithm based on the measurements made on the response of the structure, and sometimes also on the external excitation. Each control system consists of three basic components: (a) a sensing system, (b) a decision making unit, which determines the necessary control actions required to achieve the desired control objectives, and (c) an actuation system that apply control forces determined by the algorithm.

Although the active control methods have been used in electrical, mechanical and aerospace engineering, these methods are not directly usable with civil engineering structures as these structures have their unique set of challenges and different design issues. The reasons for this are:

- (1) Civil structures are massive systems, and therefore the required control force and power can be several orders of magnitude higher than those required for mechanical systems.
- (2) The civil structures also have large degrees of freedom.
- (3) Civil structures and loading on them have larger uncertainties levels. Thus control robustness is an important issue.
- (4) The control system must be extremely reliable, as life safety is one of the primary design criteria for civil structures.
- (5) The functionality control of distributed civil infrastructure system has no

parallel in the mechanical systems, and these will require different innovative control concepts.

- (6) The problem of control of existing structures pose a different set of problems with various constraints, requiring significantly different control solutions

2. STRUCTURAL CONTROL RESEARCH PROGRAM OF NSF

Realizing the potential of the new technology, the National Science Foundation actively sought community opinion through following national and international workshops and panel to start a new research program.

- (1) U.S. Panel on Structural Control Research, established in 1989 under the direction of Professor George Housner.
- (2) International Workshop on Intelligent Structures, Taipeh, Taiwan, July 1990.
- (3) Joint NSF-EPRI Workshop on Research Needs in Intelligent Control Systems, Oct. 1990.
- (4) U.S. National Workshop on Structural Control Research, University of Southern California, Los Angeles, Oct. 1990.
- (5) Workshop on Sensors and Signal Processing for Structural Control, Washington, DC, Feb. 1991.

These forums provided the intellectual framework to start a new research initiative entitled Program on Structural Control for Safety, Performance, and Hazard Mitigation by the NSF in 1992 (Ref. 4). The program was initiated for five years. The broad objectives of the program were to foster, on a coordinated basis, multi-disciplinary research and development of passive, active and hybrid control technology for application to buildings and civil infrastructure systems subjected to dynamic

loads. The emphasis of research program was to extend the control concepts so that they can be implemented on civil infrastructure systems, by providing sustained support for the:

- (1) Development of passive, active, semi-active, and hybrid control systems suitable for civil structures.
- (2) Investigations of the robustness and reliability of control systems.
- (3) Development of advance sensors and actuator technology suitable for civil structures
- (4) Development of advance signal processing techniques and their applications in structural control.
- (5) Development of innovative integrated structural and control systems, smart structures, smart materials and sensing devices.
- (6) Sensing and control systems for distributed civil infrastructure systems.

A total of 51 research projects, examining various aspects of structural control have been funded to develop new control methodologies applicable to civil structures. This involves a research expenditure of about \$ 9.6 million over a period of 5 years. NSF has also provided additional support for research in this area through National Center for Earthquake Engineering Research (NCEER) at the State University of New York at Buffalo. The projects have been awarded to academic institutions and private consultant, and are dispersed all over the country. The control concepts that appeared to be futuristic only a few years ago, now seem feasible, primarily due to quantum developments that have occurred in the sensors and information-processing field in the recent past.

The funded projects are focused on research in the following areas:

- Active, passive, and hybrid control technologies for civil structures
- Innovative systems for energy dissipation
- Variable damping and stiffness devices to reduce dynamic response
- New control algorithms applicable to civil structural systems
- Robustness and reliability of control systems
- Actuator dynamics and time delays
- Emerging technologies for structural systems, smart and self healing materials, sensors, remote sensing, monitoring, and diagnostics systems
- Optimal placement of sensors and actuator

The research projects have developed innovative algorithms for application to civil structures. The algorithms that have been used, improved or developed are: feedback control, optimal feedback/ feed-forward control; Lyapunov-based control; bang-bang control; nonlinear optimal control; acceleration feedback control; sliding mode control with linear and nonlinear controllers; fuzzy control; neural-net based control; H_2 and H_∞ controls; adaptive controls; frequency weighted controls; peak response control. The classical control approaches are now being taken to new levels so that they can be applied to massive civil structures.

To apply large forces required by civil structures, several dampers and actuation devices are being considered. Active mass dampers and mass drivers, active tendons, and active bracing systems operated by hydraulic actuators have been used in scaled experiments. The regeneration concept used for stopping and braking of suburban electric trains is being considered to develop the so-called regenerative actuators. The use of potential energy to apply large forces is being considered to develop the so-called gravity actuators. Passive and active liquid

dampers are also being considered for wind response control applications.

Since the reliability of active control schemes is still not established, hybrid control methods utilizing a proper combination of passive and active control approaches are being considered by several investigators to provide desired levels of control over a spectrum of external load effects. Base isolation in combination with active control is one popular hybrid scheme. Controllable sliding isolators, that regulate the friction at the sliding interface, have been examined. This scheme can be effective in achieving a balance between the conflicting requirements of being able to provide only limited sliding displacement one hand and reducing the superstructure accelerations on the other hand. Passive energy dissipating cladding systems in buildings can be supplemented by active devices to enhance the overall system performance. Another concept of mega-substructure control, which utilizes a part of the building mass to act as an active mass damper, has also been explored in analytical studies.

Since the traditional active control of civil structures may require a large power source, semi-active schemes that do not require large power source are being examined. The semi-active devices primarily regulate the structural parameters, such as stiffness and damping, in a timely fashion. In civil engineering community, these schemes have been called semi-active primarily because they do not require a large infusion of outside energy to the structure. In the semi-active systems, structural parameters can be controlled by either of the following dampers: orifice-controlled dampers, friction controllable dampers, electro-rheological dampers, or magneto-rheological dampers. Some of these devices can regulate both the damping and stiffness, and that it can be done without a large power source. The development of

an efficient control algorithm for a semi-active device is, however, more challenging because the problem is highly nonlinear.

The applications of the control systems are being considered for earthquake, wind, wave forces, vehicle loading, and human loading. The structural systems that are being examined are buildings, bridges, distributed systems, and nonstructural subsystems.

To evaluate the performance of different control algorithms, devices, and strategies on a common standardized analytical platform, two benchmark problems have been recently developed. To evaluate the control of earthquake effects, a twenty-story building designed for the FEMA's SAC project has been adopted, whereas for the control of wind induced vibrations, a 76-story building model is used as a benchmark structure. The details of these building are available through Internet on the University of Notre Dame web page at: www.nd.edu/~quake. The investigators are invited to use these models to evaluate their control schemes. There will be 17 technical papers, using these benchmark models, presented at the upcoming 2nd World Conference on Earthquake Engineering to be held in Kyoto, Japan in June28 – July 1, 1998.

There is also a need to develop benchmark problems for other structures such as bridges. However, since the bridge control procedure are in their very early stage of development, it will be sometime before such a standardized benchmark problem will be available for control scheme evaluations.

One immediate positive outcome of the structural program has been in the area of education. One of the NSF's important missions is to support research that will lead to scientifically educated and well-trained workforce. A direct measure of this

outcome is number of students with masters and Ph.D. dissertation and theses produced in this area of research. Figure 1 shows the

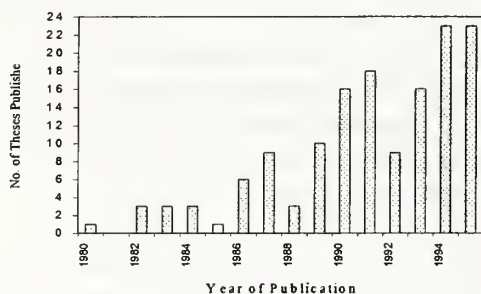


Figure 1: Total Control Theses

total number of theses produced in the area of control. Since the fields of system identification, damage detection, and health monitoring are integral part of the control research, Figure 2 shows the number of

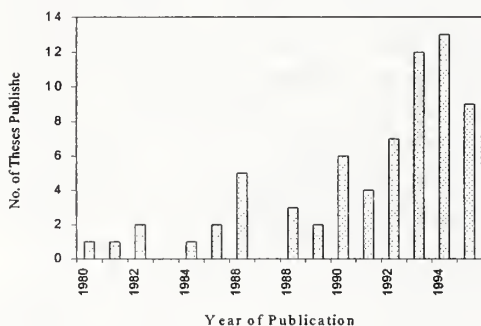


Figure 2: Total System Identification, Health Monitoring, and Damage Detection Theses

theses produced in these particular areas. A clear trend of increasing activity, especially since the beginning of the nineties is quite evident from this data. Since the NSF's research program is primarily focused on the control of civil engineering structures, Figures 3 and 4, respectively, show the number of civil engineering theses produced

in various years in the control area and the system identification, damage detection, and

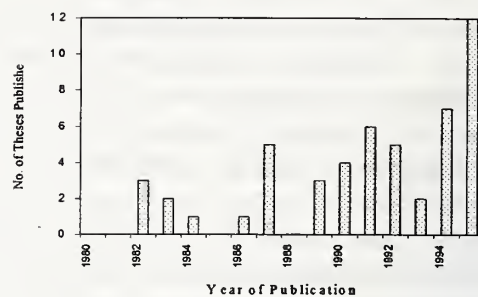


Figure 3: Civil Engineering Control Theses

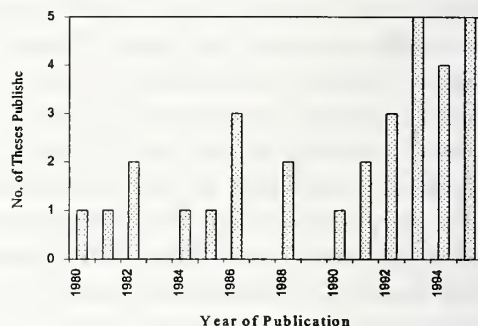


Figure 4: Civil Engineering System Identification, Damage Detection, and Health Monitoring Theses

health monitoring areas. Here again the increasing trend, especially since the beginning of the nineties is quite evident. Figures 5 and 6, respectively, compare the relative level of activity in different engineering disciplines in the two areas. The discipline of civil engineering has clearly taken a lead in research activity in this area. It is quite relevant to mention here that it is this educated workforce that will change the way the civil engineering structures will be designed in the future. This data in Figures 1 through 6 has been

extracted from the report submitted by the US Panel on Structural Control

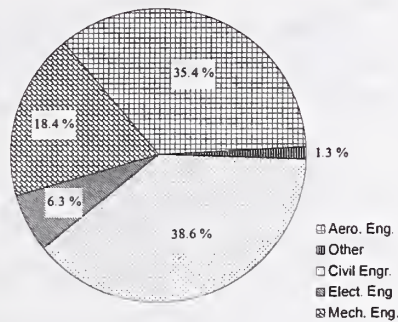


Figure 5: Control Theses Surveyed by Discipline

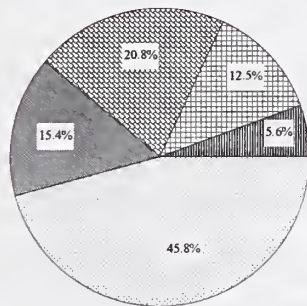


Figure 6: System Identification, Health Monitoring, and Damage Detection Theses Surveyed by Discipline

Research to the National Science Foundation (Ref. 2).

3. PRACTICAL APPLICATIONS STRUCTURAL CONTROL RESEARCH

The final objective of the research program is to utilize the research in full-scale implementations. The passive control schemes are being increasingly used in structural engineering practice. The active, semi-active and hybrid schemes, however, are still in the experimental stage. Japan has taken the lead in using active devices in existing buildings, but only for the low-level wind and earthquake response control. There have been many laboratory experiments on scaled models, attesting to the success of active schemes. These model tests, however, do not address the actual

power and force requirements problem realistically. Similarly semi-active methods with on-off control have been implemented on one or two degrees of freedom simple laboratory models subjected to earthquake type motions. The semi-active devices such as controllable sliding bearings, electro-rheological dampers and magneto-rheological dampers, are getting ready for scaled model demonstration. The experiments have been undertaken to characterize the mechanical characteristics of these dampers. The next step is to develop efficient algorithms and actual demonstration on scaled models. It is expected that full-scale implementation of semi-active devices is likely to occur soon, as the risk involved in their utilization in real buildings are not as much as those with active devices. It is primarily because these devices do not infuse external energy into a structure whereas the active devices do. As for the hybrid schemes, no significant experimental work even on a scaled building model, demonstrating their application in the laboratory, has been reported yet.

Once a concept has been developed, its utilization in practice lies in the industrial domain. That is, the industry must take the bold step of implementing a new technology. In the US, it can be a slow process. Such was the case in the implementation of base isolation and other passive control methods in practice. International collaboration in terms of exchange of ideas and technical data, utilization of complementary resources and strengths of different countries, taking advantage of the differences in construction practices in different countries, can help accelerate implementation of a useful technology. Thus NSF has always encouraged the participation of the US scientists and engineers in international joint research program, exchange programs, international symposium, workshops and conferences. There are many other advantages of international collaboration

such as the (1) elimination of duplication, (2) better identification of research needs, (3) creation and effective utilization of international test beds, (4) improvement of research skills, (5) better educational and exchange opportunities, (6) increased visibility and awareness of earthquake engineering in the general public, and (7) strengthening of research and educational infrastructure for the future.

4. FUTURE RESEARCH NEEDS IN STRUCTURAL CONTROL

Based on a careful assessment of the current research activities in the US and other countries, and the input received from the researchers involved in the structural control program through various workshops and meetings, the following six broad areas have been identified for future research endeavors:

1. Research in passive, active, semi-active and hybrid control with emphasis on nonlinear systems, nonlinear control, nonlinear identification, predictive and adaptive control, actuator saturation, actuator and sensor and malfunction, application to strong seismic inputs, especially vertical components.
2. Research on control of large dispersed and distributed parameter systems (lifelines) with special emphasis on intelligent sensors and fore-warning systems, information processing and decision making systems.
3. Research on high performance, innovative, and intelligent materials
4. Research on system integration with emphasis on hardware/software integration, integrated design of structure-control system, optimal sensor and actuator locations, reliability cost-

benefit considerations, and integration of health monitoring systems.

5. Control system evaluation through analytical and experimental benchmark studies.
6. Education and technology transfer involving training of graduate students, practitioners, and development of design guidelines and code provisions

More details of these broad research areas and the genesis of their development are provided in the reports of the following workshops/meetings.

1. Joint US-Japan Workshop on Mitigation of Urban Disasters: Cooperative Research on Structural Control, Kyoto, Japan, March 14-15, 1996
2. "Fourth Coordination Meeting for NSF Research Program on Structural Control," University of Notre Dame, South Bend, Indiana, October, 4-5, 1996
3. Second International Workshop on Structural Control, Hong Kong, December, 18-21, 1996
4. Fifth Coordination Meeting for NSF Research Program on Structural Control," University of Nevada, Reno, Nevada, August, 18-19, 1997 (Ref. 5)

5. FUTURE PROGRAMS IN HAZARD MITIGATION

The NSF is developing a new Major Research Equipment Program that is intimately related to the area of structural control in hazard mitigation. The program is still in the planning stage. It has also been referred to as the National Network for High Performance Seismic Simulation (NHPS) program. The program is proposed to respond to the need for an integrated

network of experimental research facilities and a new research environment. It is expected to advance the scientific understanding of the impacts of earthquakes. It will help mitigate the effect of disasters attributable to a lack of knowledge about the behavior of engineering materials, soils, and construction during earthquakes. The network will include advanced-design earthquake simulation facilities, large scale testing systems, and field facilities. It will provide a means for the rapid exchange of ideas and information, and offer immediate access to research data generated anywhere in the network. It will also serve as a forum for bringing researchers and practitioners together to share their expertise with students and professionals engaged in earthquake engineering. It will create an environment where students are learning through research that is supported by the latest experimental and communication technologies. It is expected to enhance the synergy and vitality in earthquake engineering.

The objective of NHPS is to advance scientific knowledge, avoid future catastrophes, and protect the populace, built environment and economy in future earthquakes. NHPS will consist of three special purpose (new and enhanced) laboratories to simulate earthquake generated actions on structures and to monitor the motions and response of the built environment during such motions or during actual earthquakes. NHPS will include the following new or enhanced equipment and facilities.

- *Advanced-design earthquake simulation facilities.* To meet the challenge of high-intensity ground motion parameters stipulated by the 1994 Los Angeles and 1995 Kobe events, this NHPS component will include new advanced-design earthquake simulation systems for structural testing and

development of "on-board" shaking units in centrifuges for soil testing. Similarly, the complexities of Tsunami waves and their effects on shorelines and coastal facilities will be studied using an advanced wave generator mounted in a large wave tank.

- *Large-scale testing system.* Failures of structural steel elements in the Los Angeles and Kobe earthquakes have created an exigency for testing structural elements, assemblies of elements, and response modification devices in full scale. These elements exhibit complex nonlinear behavior and require the development of large-scale actuators and improvement of existing capabilities for combined vertical and lateral loading of test specimens.
- *Field simulation and laboratories.* This component of NHPS will comprise field testing installations and mobile laboratory units to monitor the behavior of constructed facilities before, during and after an earthquake. It is needed in order to accumulate behavioral data that cannot be obtained in the laboratory because of difficulties in replicating the structure replete with complications introduced by site, construction, and architectural effects.

This program when implemented will have far reaching effect in the development and implementation of the structural and systems control methods.

6. CONCLUDING REMARKS

The paper describes the development of the NSF's Program on Structural Control. NSF views the research on structural control as an important means for natural hazard reduction. NSF has invested significant resources to initiate this program by funding 51 research projects with a research expenditure of \$9.6 millions. Some of these

projects are still continuing. The researchers are involved in solving several issues related to the control of civil engineering structures. They are developing new algorithms, actuation devices, materials, and new control concepts. Although the five-year program is formally over, the NSF's support of the research activities in this promising area has continued.

The active and semi-active control technologies, however, are not quite ready for implementation in practice. The requirements of large control forces and large external power source are serious impediments in the application of active control. In this respect, the semi-active schemes seem to be more promising for their application to civil structures, as they do not need a large power source. However, these schemes are still in the laboratory-testing phase.

The NSF and the structural control research community consider the coordinated international collaboration and active industrial participation very important component of the program for a successful utilization of this technology.

7. ACKNOWLEDGEMENTS

The writers have had the opportunity of coordinating the research activities of the NSF's program of research on structural control. Their views on the program, gained through this coordination, are reflected in this paper. The writers acknowledge the help and information they have received from different sources, including the NSF Program Directors S. C. Liu and E. J. Sabadell, and Prof. Sami Masri of the University of Southern California. However, the opinions, interpretations, and views presented in the paper are entirely those of the writers, and not of the NSF Program Directors or the National Science Foundation.

8. REFERENCES

1. Chong, K. P., Liu, S. C., and Li, J. C., Editors, "Intelligent Structures", (1990), Elsevier Applied Science, London and New York, 460 pp.
2. Housner, G. W., Masri, S. F., Singh, M. P., and Soong, T. T., "Structural Control Research: Future Horizons of the General Field of Structural Control", Report by U.S. Panel on Structural Control submitted to National Science Foundation, August 1997.
3. Liu, S.C., Chong, K. P., and Singh, M. P., "Civil Infrastructure Systems Research: Hazard Mitigation and Intelligent Material Systems", *J. of Smart Materials and Str*, 3 (1994), A169-174
4. National Science Foundation, "Structural Control Initiative", NSF 91-62, Arlington, VA, 1991
5. Soong, T. T. and Singh, M. P., "Fifth Coordination Meeting Report for NSF Research Program on Structural Control", University at Buffalo, School of Engineering and Applied Sciences, State University of New York at Buffalo, NY, October 15, 1997

Wind and Seismic Research for Improved Engineering Consensus Standards and Housing Construction

by

Jay H. Crandell¹ and William Freeborne²

ABSTRACT

This paper provides an overview of recent engineering research that has resulted in improved engineering standards, design methods, and building codes for the construction of housing and other types of buildings in the United States. The engineering advancements include the development of a new hurricane wind map, new load and directionality factors for wind, and a new method of analyzing wood-frame shear walls.

KEYWORDS:

Houses, Engineering, Research, Wind, Seismic, Consensus Standards, Building Codes

1. INTRODUCTION

Housing construction in the United States has become subject to increased scrutiny with respect to its performance in high wind and earthquake risk regions. As a result of this scrutiny the need for affordable and simple construction methods has been challenge by the need to improve the safety of these buildings. The focus of this summary paper is to give a broad overview of recent efforts to improve the safety of residential buildings while maintaining affordability and simplicity of construction methods or regulations.

Over the past two years, the National Association of Home Builders and the U.S. Department of Housing and Urban Development have joined in a multi-year cooperative program to address the safety and affordability of future housing in the United States. The title of the program is *Housing Affordability Through Design Efficiency* (HATDE). The program is under the management of the NAHB Research Center, Inc.

Other partners have included State Farm Insurance Companies, Applied Research Associates, Virginia Polytechnic Institute and State University, Johns Hopkins University, Clemson University, and Andersen Corporation. The program has extended recent research funded by other institutions such as the National Science Foundation and the U.S. Department of Agriculture to applications related to efficient design of residential buildings and other types of structures.

2. OVERVIEW OF THE HATDE PROGRAM

The objective of the HATDE program is simply stated as follows:

"To conduct practical research activities which support the development and implementation of innovative and efficient engineering principles and construction practices in support of reasonably affordable and safe housing in all hazard conditions in the United States."

To meet this objective a comprehensive research agenda was developed and continues to be subject to review and input from a broad-based research coordination group. The research program and agenda encompasses the following major elements:

¹NAHB Research Center, Inc., 400 Prince George's Boulevard, Upper Marlboro, MD 20774-8731.

²U.S. Department of Housing and Urban Development, 451 Seventh Street, SW, Washington, D.C. 20410.

- Coordination

Research Coordination Group (90 representatives)

Peer Review Group (6 experts in engineering, architecture, and housing)

- Research Areas

Loads

Resistance (Strength)

Performance Assessment

Quality/Defects Analysis

- Dissemination

Building Codes

Engineering Standards

Education & Demonstration

Publication/Reports/Articles

The research coordination effort serves several purposes including identification and prioritization of research needs, dissemination of research findings, coordination with similar research programs and initiatives, and development of partnerships. Research activities are selected from the research agenda based on priority and funding availability among the collaborators. A smaller peer review group assists in the direction of program funding and critical review of research activities, plans, results, and proposed applications. The program is specifically designed to address research needs in a manner that will have the most immediate and effective impacts on improving residential construction and design practices. The underlying principle is that more efficient engineering approaches will result in improved performance of homes (relative to current day practices) without adversely impacting the cost of construction or housing affordability.

The remainder of this paper will present the key research and dissemination activities accomplished to date in the HATDE program.

3. STRUCTURAL LOADS (WIND)

A major emphasis in the formation of the HATDE program was related to wind loads, particularly in hurricane prone regions. This emphasis was associated with the construction cost impacts realized when homes were subject to engineered design using existing engineering load standards such as the American Society of Civil Engineer's standard Minimum Design Loads for Buildings and Other Structures (ASCE 7)[1]. Because of this concern two projects were directed toward research needs which would improve the accuracy of this wind load standard when applied to homes and other structures.

The first project focused on the development of a hurricane coast wind map that utilized the latest advancements in hurricane wind field and risk modeling [2][3]. Using these models which were validated by data from numerous actual hurricane events, Applied Research Associates (Raleigh, NC) produced a new generation design wind map for the hurricane coast regions of the United States. The map shown in Figure 1 is essentially the same map that is now being considered for approval in the ASCE 7 consensus standard. It is important to note that the new map results in a faster degradation of hurricane wind contours over land. This shift of the wind contours toward the coast is a result of the more accurate hurricane wind field modeling.

The second project related to wind loads re-evaluated the wind load factor for probability-based design formats such as Load and Resistance Factor Design (LRFD). LRFD load combinations are supported in the ASCE 7 standard and they are advancing in application to residential construction with the advent of LRFD provisions for wood construction [4]. The load factor study included a delphi process of wind engineering experts in the United States to help identify the latest knowledge regarding the stochastic parameters related to wind loads. Also included in this work was the investigation of a wind directionality factor that adjusts wind loads to account for the probability that wind will not always come from a direction that produces the

worst-case wind effect on any particular structure or its components.

As a result of this work a new wind load factor and a separate directionality factor is being proposed for inclusion in the next version of the ASCE 7 consensus standard. The previous wind load factor of 1.3 included a 0.85 factor adjustment for directionality. By removing the 0.85 directionality factor, the wind load factor would numerically change to 1.5 ($1.3/0.85 = 1.5$). This change was also supported by the re-analysis of the wind load factor using the delphi results and principles of uncertainty [5]. The directionality factor is then treated as an adjustment parameter (depending on shape of the structure) when calculating the nominal (50-year return period) wind load. Based on this work, a possible representation of a wind load combination and the wind velocity pressure equation might be as follows:

$$0.9D + 1.5W$$

$$q = 0.613K_zK_{zt}K_dV^2I$$

where,

D = dead load

W = wind load

q = wind velocity pressure (N/m²)

K_z = exposure coefficient

K_{zt} = topographic factor

K_d = directionality factor of 0.85

V = nominal design wind speed (m/s)

I = building importance factor

Other research has shown that the load factor should be higher for hurricane prone regions. The final outcome of these changes will be forthcoming through the ASCE 7 consensus standard balloting process.

4. STRUCTURAL RESISTANCE

A major focus in the area of seismic design and wind resistance of wood-frame homes has been in the area of wall bracing or the lateral force resisting system (LFRS). The major components

of the LFRS of a home are light-frame shear walls with wood structural panels. Of course, the performance of these walls is dependent on the manner of restraining the walls against rotation. Common practice is to include hold-down brackets and special metal connectors to transfer overturning loads to the building foundation. Other fasteners, including nails, anchor bolts, and shear plates, transfer shear loads collected by horizontal diaphragms (floors and roofs) to the shear walls. Similarly, the base of the shear wall is connected to the walls or foundations below. While this scheme provides a reasonably simple method of engineering analysis, it is not the most efficient practice for relatively light residential buildings such as single-family detached homes.

To improve the efficiency of designing the LFRS of homes, a shear wall research project was initiated in the HATDE program. The project was designed to build on previous research on the perforated shear wall method [6]. By this method, an engineer may readily and accurately determine the strength of a fully-sheathed wall with openings, and hold-downs are only required at the ends of the walls. While resulting in a moderate reduction in capacity compared to a wall with hold-downs restraining each full-height segment, it provides sufficient strength for many light-frame residential construction applications, even in high wind and seismic conditions. The perforated shear wall method was first developed by researchers in Japan over 20 years ago [7].

The HATDE program expanded the work to include investigation of perforated walls with full restraint of each segment and with no restraint other than conventional anchor bolts through the sill plates. These tests included numerous opening configurations in walls that were 12.2 m (40 ft) long. Both cyclic and monotonic loading conditions were investigated [8][9]. Finally, four walls of a 3.7m (12 ft) length with corner framing and no hold-down restraints were subjected to the cyclic loading test protocol [10]. The unit shear strength obtained in these tests was more than 85 percent of that achieved with the fully restrained walls previously tested. This

finding is a strong indication that corners may be considered as providing adequate shear wall restraint when properly designed and detailed. This phenomenon is known as the "corner effect". The testing information has been used to assist in the development of improved wall bracing provisions of the proposed *International Residential Code*.

Additional tests have been recently completed that investigate the inclusion of narrow wall segments within a fully-sheathed perforated shear wall (NAHB Research Center, Inc., unpublished report). The tests also investigated walls with garage door openings having narrow shear wall segments and varying degrees of framing enhancements relative to conventional framing practices. One pilot test was conducted to investigate the effect of reduced base restraint of the perforated shear wall (i.e. anchor bolt spacing increased from 0.6 m (2 ft.) to 1.8 m (6 ft.)). An additional pilot test looked at enhancement of shear wall performance using strategically placed metal truss plates at the wall and window corners. The walls tested in these recently completed tests are shown in Table 1.

The preliminary results of these later tests indicate that the perforated shear wall design method is applicable to walls with narrow aspect ratio wall segments (i.e. a 4:1 ratio of height to width of segments between openings). However, the opening heights adjacent to the 4:1 aspect ratio wall segments were limited to 50 percent of the total wall height in these tests. Also, some very economical and simple enhancements to garage opening framing can provide useful design solutions in relatively high lateral loading conditions. Increasing the anchor bolt spacing on the sill plates had a negligible effect on the perforated shear wall capacity and stiffness for the pilot test. Additional testing will be conducted to better quantify the effects of further reductions to the base restraint of perforated shear walls. Finally, the use of metal truss plates to reinforce key joints in the wall framing enhanced the shear wall performance by as much as 40 percent

5. SUMMARY AND CONCLUSIONS

In the first two years of the HATDE program, several research activities related to structural loads and resistance has been conducted to improve the efficiency of engineering residential buildings. The findings have been implemented in engineering consensus standards and in the development of new residential building code provisions in the United States. The following conclusions can be drawn from these efforts:

1. The resistance (strength) of residential construction, particularly the lateral force resisting system, is significantly underestimated (or not optimized) with current engineering methods of design. Future efforts should continue to develop and apply innovative engineering approaches that better quantify the lateral strength of light-frame residential buildings. From this work the design of residential buildings for high wind and seismic conditions will be addressed in an optimal fashion.
2. Wind loads in hurricane coastal regions have been improved by implementing improved models for hurricane winds as they degrade over land.
3. A new study on a wind load factor and wind directionality will result in a more tractable and risk-consistent design method for determining wind loads on various types of structures.

6. REFERENCES

- [1] *American Society of Civil Engineers Minimum Design Loads for Building and Other Structures*, American Society of Civil Engineers, New York, NY (1995).
- [2] Vickery, P.J., P.F. Skerlj, A.C. Steckley, and L.A. Twisdale, *Hurricane Wind Field and Gust Factor Models for Use in Hurricane Wind Speed Simulations*, Applied Research

Associates, Raleigh, NC (1997) pending publication.

[3] Vickery, P.J., P.F. Skerlj, and L.A. Twisdale, *Simulation of Hurricane Risk in the United States Using an Empirical Storm Track Modeling Technique*, Applied Research Associates, Raleigh, NC (1997) pending publication.

[4] *Load and Resistance Factor Design Manual for Engineered Wood Construction*, American Forest & Paper Association, American Wood Council, Washington, DC, (1996).

[5] Ellingwood, B. and P. Beraki, *Wind Load Statistics for Probability-Based Design*, prepared for the U.S. Department of Housing and Urban Development, the National Association of Home Builders, and the NAHB Research Center, Inc. by Johns Hopkins University, Baltimore, MD, October 1997 (pending journal publication; available through NTIS).

[6] Dolan, J. and Johnson, A., *Monotonic Tests of Long Shear Walls with Openings*, prepared for the American Forest and Paper Association by Virginia Polytechnic Institute and State University, 1996.

[7] Sugiyama, H. and Matsumoto, T., *Empirical Equations for the Estimation of Racking Strength of a Plywood Sheathed Shear Wall with Openings*, Summary of Technical Papers Annual Meetings, Trans. of A.I.J., 1994.

[8] Dolan, J. and Heine, C., *Monotonic Tests of Wood Frame Shear Walls with Various Openings and Base Restraint Configurations*, Prepared for the NAHB Research Center, Inc. by Virginia Polytechnic Institute and State University, 1997.

[9] Dolan, J. and Heine, C., *Sequential Phased Displacement Cyclic Tests of Wood Frame Shear Walls with Various Openings and Base Restraint Configurations*, Prepared for the NAHB Research Center Inc. by Virginia Polytechnic Institute and State University, 1997.

[10] Dolan, J. and Heine, C., *Sequential Phased Displacement Tests of Wood Framed Shear Walls with Corners*, Prepared for the NAHB Research Center Inc. by Virginia Polytechnic Institute and State University, 1997.

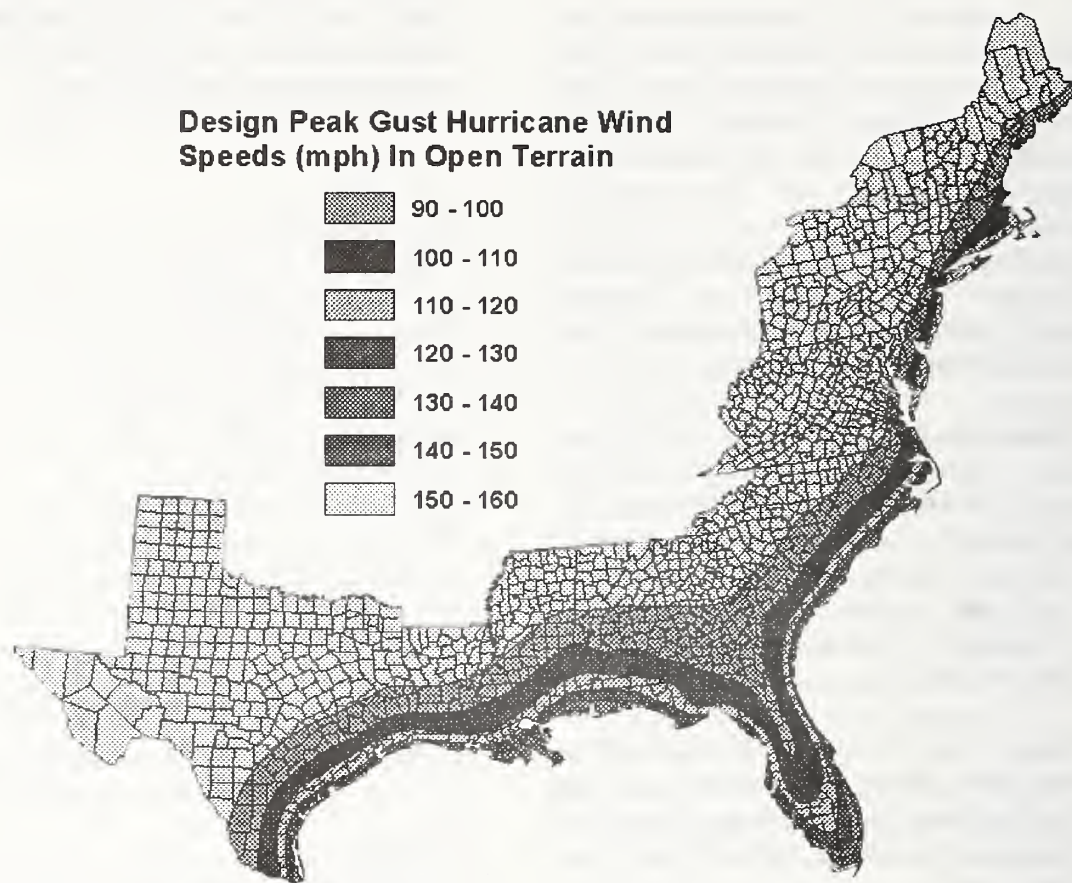
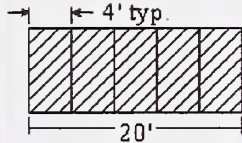
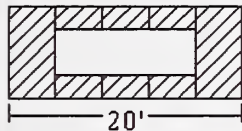
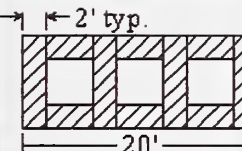
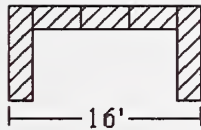
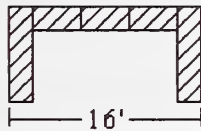
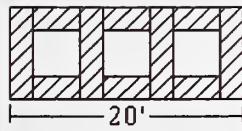
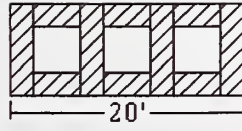


Figure 1: New Hurricane Design Wind Contours for the ASCE 7 Consensus Standard (courtesy Peter Vickery, Applied Research Associates).

Table 1: Shear Wall Configurations

Specimen	Wall Configuration	Openings	Sheathing Area Ratio, r	Anchor Bolt Spacing	Hold-downs
Wall 1		None	1.0	2' o.c.	Ends
Wall 2		(1) - 12' x 4'	0.57	2' o.c.	Ends
Wall 3		(3) - 4' x 4'	0.57	2' o.c.	Ends
Wall 4		(1) - 12' x 6'-8"	0.29	2' o.c.	Ends
Wall 5 ¹		(1) - 12' x 6'-8"	0.29	2' o.c.	Ends
Wall 6 ¹		(3) - 4' x 4'	0.57	2' o.c.	None
Wall 7		(3) - 4' x 4'	0.57	6' o.c.	Ends

For SI: 1 ft.(') = 0.3048 m, 1 in.(") = 25.4 mm.

¹ Alternative framing methods used.

TABLE I	
Summary of the results of the experiments	
Experiment	Results
1. Effect of temperature on the rate of reaction	The rate of reaction increases with increasing temperature.
2. Effect of concentration on the rate of reaction	The rate of reaction increases with increasing concentration.
3. Effect of catalyst on the rate of reaction	The rate of reaction increases with the addition of a catalyst.
4. Effect of surface area on the rate of reaction	The rate of reaction increases with increasing surface area.
5. Effect of pressure on the rate of reaction	The rate of reaction increases with increasing pressure.
6. Effect of solvent on the rate of reaction	The rate of reaction increases with the use of a polar solvent.
7. Effect of pH on the rate of reaction	The rate of reaction increases with increasing pH.
8. Effect of ionic strength on the rate of reaction	The rate of reaction increases with increasing ionic strength.
9. Effect of dielectric constant on the rate of reaction	The rate of reaction increases with increasing dielectric constant.
10. Effect of viscosity on the rate of reaction	The rate of reaction increases with decreasing viscosity.

**SUMMARY of JOINT COOPERATIVE
RESEARCH PROGRAMS**



**U.S.-Japan Cooperative Earthquake Engineering Research Program
on Composite and Hybrid Structures
- Current Status of Japan Side Research -**

by

Isao Nishiyama *1, Hiroyuki Yamanouchi *2 and Hisahiro Hiraishi *3

ABSTRACT

The U.S.-Japan Cooperative Earthquake Engineering Research Program started in 1979 following the recommendations as outlined in the final report of the U.S.-Japan Planning Group for the program (Ref.1). The overall objective of the total program is to improve seismic safety practices in both countries through cooperative studies to determine the relationship among full-scale tests, small-scale tests, component tests, and related analytical and design implication studies. A five-year research program on Composite and Hybrid Structures was recommended to start in 1993 fiscal as the Phase 5 based on a number of technical meetings between the U.S. and Japan (Ref.2).

Because of diverse and broad scope of the subject area, the research program was organized into the following four groups: Concrete Filled Tube Column Systems; Reinforced Concrete (RC) and Steel Reinforced Concrete (SRC) Column Systems; RC / SRC Wall Systems; and New Materials, Elements and Systems. In addition to the objectives of the total program, Phase 5 aimed at (1) developing design guidelines (for a unified code development) for typical composite and hybrid structures, and (2) developing new and innovative composite structural elements and hybrid systems using advanced new materials and / or devices.

Japan side has just completed his assignment of the cooperative research work in the fiscal year of 1997. This report presents the outlines of the research conducted during five years and the general contents of the proposed draft guidelines.

KEYWORDS:

composite and hybrid structures; concrete filled tube column systems; reinforced concrete and steel reinforced concrete column systems; RC/SRC wall systems; new materials, elements and systems; outline of research results; proposed draft guidelines.

1. RESEARCH RESULTS ON CFT

1.1 Basic Research Plan

There are many experimental and analytical studies on concrete filled tube column (CFT) systems which are reported in technical journals. First, the strength and ductility of the CFT systems are predicted by processing these existing data. Secondly, the effectiveness of these predictions is verified by supplementary experimental studies. As the materials' strengths in use are quickly increasing, wide range of structural steel strength and concrete strength are considered to verify the applicability of the predictions. Finally, draft design guidelines are developed.

1.2 Research Items and Results

(1) Database

Test data of CFT columns and beam-columns were collected from the Japanese literature published in 1971 through 1995, and a database was developed. A total of 786 test data (test specimens) were found: 501 square CFT and 285 circular CFT. A database for the tests of connections between CFT column and steel beam was also prepared. Column bases and connections between CFT frame and brace are also important structural elements of CFT system, but however very few test data were available so far in Japan.

-
- *1 Head, Housing Construction Division, Production Engineering Department, Building Research Institute (BRI), Ministry of Construction (MOC), Tachihara-1, Tsukuba, Ibaraki, 305-0802, Japan.
 - *2 Director, Codes and Evaluation Research Center, BRI, MOC.
 - *3 Director, Structural Engineering Department, BRI, MOC.

(2) Trial Design of Theme Structure

Structural designs of 10, 24 and 40 storied CFT moment frame buildings and CFT dual system buildings were carried out on the theme structure shown in Fig.1. In these structural design, CFT member strengths were calculated based on the simple (generalized) superposing method proposed in the AIJ-SRC standards (Ref.3). The buildings with the same floor plan were also designed as pure steel frames.

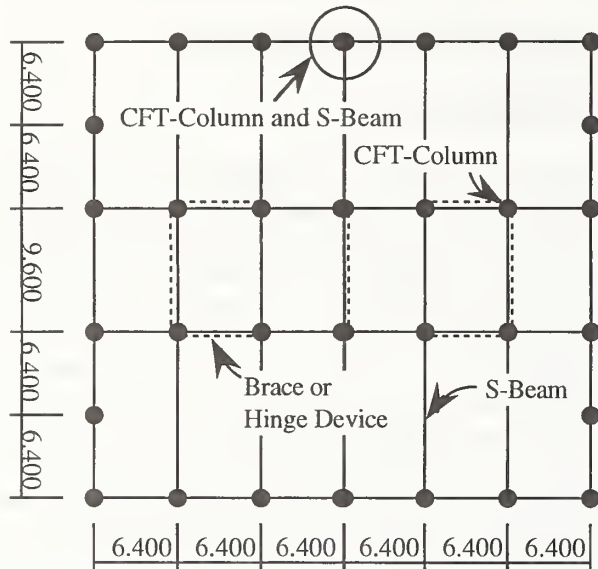


Figure 1 Floor Plan of Theme Structure on CFT

The total amount of structural steel, which is the index for estimating the economy of buildings, used for CFT buildings was compared with that used for pure steel buildings. In this comparison, CFT showed advantages over pure steel especially for higher buildings. The economical difference in CFT buildings with / without bracings was not large. It was because that the weight of bracings and the weight increase in the braced bay frame members compensated with the weight reduction of other frames which carried less horizontal force.

The modified plans which have 16 or 24 columns in each story, which were expected to show more advantages by CFT columns, were also investigated.

(3) Experimental and Analytical Study

The objectives of the experimental study are to evaluate the synergistic effects of structural steel tube and filled concrete and to evaluate stress transfer mechanisms in beam-to-column connections. So as to clarify these problems, four test programs were planned with several study parameters.

a) Experiments

- 1) stub-column tests
- 2) stub-column eccentric loading tests
- 3) beam-column tests
- 4) beam-to-column connection tests

b) Study Parameters

- 1) tube shapes (rectangular, circular)
- 2) tube strengths (400, 600, 800 MPa)
- 3) width-to-thickness ratio
(FA, FC, FD-rank* 1)
- 4) concrete strengths (20, 40, 80-103 MPa)
- 5) connection details (diaphragm, etc.)

*1 FA-rank of width-to-thickness ratio means that large member ductility is expected thanks to its compact section. FC-rank means that it can at least assure the yield strength of the member without deterioration. The width-to-thickness ratio of FD-rank is chosen as 1.5 times of that of FC-rank.

133 stub-column tests on rectangular ($B=100-324\text{mm}$) or circular ($D=108-450\text{mm}$) sections were completed. As the dimensions of the selected specimens were relatively large, and material strengths of structural steel tube ($\sigma_y=400-780\text{N/mm}^2$) and concrete infill ($F_c=20-103\text{N/mm}^2$) were also large, the maximum test strength reached 1,400tonf (13.72MN). As for the stub-column eccentric loading tests, 80 specimens were completed. From these test results, flexural moment (M) versus axial force (N) interaction of CFT section was obtained. The analytical $M-N$ interaction estimated on the basis of the proposed stress versus strain models for concrete infill and steel tube considering synergetic effects well agreed with the test results.

As for the beam-column tests, 20 rectangular and 13 circular specimens were tested. Most of the specimens (16 for rectangular and 9 for circular sections) were tested under the constant axial thrust of 40% of compressive yield strength and others (4 specimens each for rectangular and circular sections) were tested under varying axial thrust of 70% of compressive yield strength and 30% of tensile yield strength. The structural steel strengths (400, 600, 800MPa), concrete strengths (40, 90MPa) and width-to-thickness ratios (FA, FC-rank) were selected as test parameters. As for rectangular sections, 4 specimens (constant axial thrust) were loaded in the direction of the plane which inclined 22.5 or 45 degrees from the axes of side plates. Fairly good agreements both in restoring force and axial shortening characteristics were obtained between test results and analytical ones, in which the proposed models for concrete infill and steel tube from

stub-column concentric and eccentric tests were adopted with arbitrary selected hinge length. Inelastic 3D-FEM analyses were also carried out to see the stress flow (distribution) in the CFT beam-columns.

11 beam-to-column connection specimens were tested. Ten of them were one-way frame specimens (eight of them were tested with constant column axial force of 20% of compressive yield strength and two were tested with varying axial force between 70% of compressive yield strength and 30% of tensile yield strength) and the rest was the two-way frame specimen. Test results showed quite stable restoring force characteristics. The maximum shear strengths of the beam-to-column connections were well above the maximum panel shear strength proposed by AIJ-SRC (Ref.3). The recommended maximum panel shear strength proposed by AIJ-Steel Tube (Ref.4) coincided with the lower bound of the test results.

A slightly detailed test results and analytical studies on stub-columns, beam-columns and beam-to-column connections were summarized in Ref.5 and Ref.6.

(4) Empirical Study on Ductility

As for the strength of beam-columns, the analytical evaluation was quite satisfactory. However, the analytical evaluation on the ductility of beam-columns looked not promising, as the selection of the hinge length was arbitrary. Therefore, the empirical formulation for the ductility of beam-columns was tried both for rectangular and circular sections using existing test results. Empirical formulas taking into account the factors of axial force, the width-to-thickness ratio of steel tube and the strength of concrete infill were proposed for rectangular and circular sections, respectively.

As shown in Fig.2, the envelop of the shear force versus deflection relationship of the beam-column shown by OABC, where O is the origin, A is the yield strength, B is the maximum strength and C is the deteriorating curve, is simply characterized by OAB'B'', where B' is the 95% pre-maximum strength point and B'' is the 95% post-maximum one. From the empirical study, B' was given as the stiffness reduction factor in comparison with equivalent elastic stiffness and B'' was estimated as the deformation capacity.

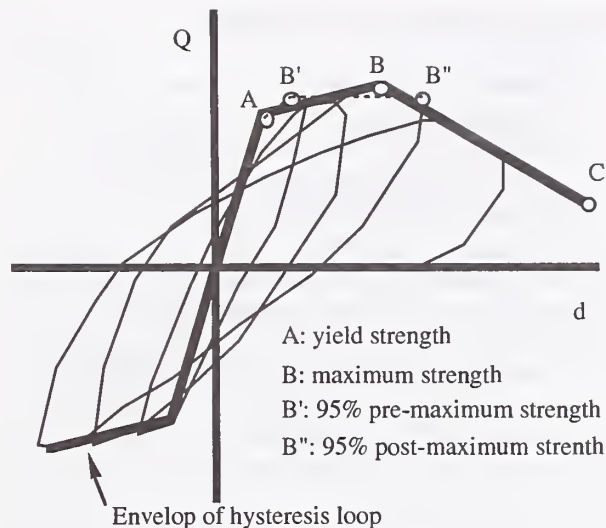


Figure 2 Envelop of Hysteresis Loop of CFT Beam-Columns

(5) Design Guidelines

Any of the structural design standards used in Japan do not contain provisions concerning the structural characteristic factor D_s (R_w in the U.S.) of CFT structures, which is necessary to calculate the required value of the lateral load resisting capacity of the story. Under this circumstance, Japanese working group for CFT systems tried to develop guidelines to the structural design of CFT systems, which contain the following items: i) formulas to evaluate strength, deformation capacity and D_s of CFT column considering the effects of confined concrete, local buckling, axial force and biaxial bending, ii) design formulas for diaphragm and shear panel of the beam-to-column connection, iii) modeling of restoring-force characteristics of column, connection and overall CFT system, and iv) method of concreting, concrete mixture and material tests at site.

Table 1 shows the tentative contents of the draft guidelines for the design of CFT column system.

Table 1 Draft CFT Design Guidelines

1. Introduction
1.1 Structural characteristics of CFT column system
1.2 State-of-the-art of research on CFT
1.3 Research carried under U.S.-Japan Program
1.4 Contents
2. Basic seismic design concept of CFT column system
2.1 Basic seismic design concept and scope of application
2.2 Seismic design method based on current method
2.3 Seismic design method based on performance criteria

3. Behavior and design of CFT member
 - 3.1 General
 - 3.2 Behavior of CFT short column under concentric compression force
 - 3.3 Behavior of CFT short column under combined compression force and bending moment
 - 3.4 Behavior of CFT beam-column
 - 3.5 Design of CFT column
 4. Behavior and design of CFT joints
 - 4.1 Behavior of CFT column to steel beam connection panel
 - 4.2 Design of CFT column to steel beam connection
 - 4.3 Design of brace connection
 - 4.4 Design of CFT column bases
 5. Construction of CFT column system
 - 5.1 Steel tube
 - 5.2 Concrete infill
 6. Example of trial design
 - Appendix 1. Trial design of CFT column system
 - Appendix 2. Test specimens carried under U.S.-Japan Program
-

2. RESEARCH RESULTS ON RCS

2.1 General

In Japan, a great number of beam-to-column sub-assembly tests on RCS (reinforced concrete column and structural steel beam) systems have been conducted. However, the variations of the joint details are quite wide and so the test results have not been thoroughly investigated yet. Therefore, these existing test results are first compiled in a common format as a database. Then, the joint panel shear strength and ductility are investigated. In this consideration, the joint details are classified into through column type and through beam type.

As the existing test data are partial to interior through beam type joints, necessary exterior joint tests and through column type joint tests are planned. A basic study to investigate the stress transfer in the joint is also planned. In Japan, two-way frame system is more common, so 3D joint tests are planned. Frame test is also planned so as to increase the accuracy of the evaluation of the strength and ductility. Inelastic 3D finite element analyses are also planned to more precisely understand the behavior of the joints. Finally, draft design guidelines is developed.

2.2 Research Items And Results

(1) Review and Database

A total of 436 experimental data was included into a database, in which the information of about

160 items such as generals, the details of columns, beams and joints, experimental results and so on is written for each test. The collected test data are sort into 17 typical details for through beam type joints and 13 for through column type joints based on the types of reinforcing details. The data are also classified into 1) panel shear yielded data and 2) others.

Panel shear yielded data were used to verify the accuracy of the existing design formulas (maximum strength) for each typical details of the RCS connections. Adding the test data produced by the U.S.-Japan program, a better panel shear strength design formula was proposed by Eq.1.

$$Q_p = Q_w + Q_f + Q_h + Q_c \quad (1)$$

where,

$$Q_w = C_1 * A_w * \sigma_{wy}$$

$$Q_f = 0.5 * A_f * \sigma_{fy}$$

$$Q_h = 0.25 * P_w * \sigma_{wy} * B_c * mcd$$

$$Q_c = 0.4 * C_2 * C_3 * B_c * D_c * 0.1 * c\sigma_b * j\delta$$

A_w : sectional area of web plate

σ_{wy} : shear yield stress of web plate

A_f : sectional area of web of cover plate

σ_{fy} : shear yield stress of cover plate

P_w : shear reinforcement ratio

σ_{wy} : yield stress of shear reinforcement

B_c : width of column

mcd : central distance between external reinforcements

B_c : column width

D_c : column depth

$c\sigma_b$: concrete compressive strength

$j\delta$: joint panel shape factor (=3 for +, 2 for T, and 1 for L joints)

C_1 : 0.8 for without FBP (face bearing plate) and 0.9 for with FBP

C_2 : 0.8 for without FBP and cover plate; 1.0 for with FBP or cover plate (prototype); 1.1 for prototype with extended FBP, or with outer side small column, or with inner side band plate; 1.5 for prototype with outer side band plate or with FBP + vertical rebar, or for diagonal stiffener; 1.6 for diagonal stiffener + wide FBP, or diaphragm.

C_3 : 0.9 for without transverse beam and 1.0 for with transverse beam.

The displacement information was used to estimate the shear force versus shear deformation relation of the joint panel.

(2) Trial Design of Theme Structure

6 and 12 story building frames were designed by the current Japanese design standards (Ref.3 &

Ref.7), whose floor plan is identical to Fig.1. The allowable stress design method was used with the static lateral forces corresponding to the base shear force coefficients of 0.918 and 0.133 for the 6 and 12 story buildings, respectively. Time history analyses using the equivalent multi-mass shear system for four recorded ground motions with 50 cm/sec of velocity amplitude were also conducted in which the hysteresis model was assumed by normal tri-linear with the monotonic envelop obtained by static pushover analysis. The maximum story drift and the maximum ductility ratio of the designed building frames were studied.

The designed buildings are also utilized to further investigate the realization of the proposed design guidelines from the practical view points.

(3) Beam-To-Column Connection

a) Stress Transfer Mechanism Study

The shear strength of the joint panel is thought to be estimated as the sum of the shear strengths of inner concrete, outer concrete, web of the structural steel and hoops. However, the contribution of outer concrete on the shear strength is quite doubtful as it is not known how the shear stress is transferred between inner and outer parts. So as to make clear the stress transfer mechanism, several sophisticated experiments were carried out.

b) Through Column Type Joint Tests

Ten specimens for interior beam-to-column connections were tested. In these tests, the effects of vertical stiffeners and the cover plates were investigated. These test results were useful for developing design formula for panel shear strength. The detailed test results are shown in Ref.8.

c) T- and L-Shaped Joint Tests

Fifteen beam-to-column connection specimens were tested to make clear the effects of the geometry (cruciform, T and L) of the joints. Here, the joint details of the through beam type with FBP, extended FBP, cover plate and band plate are all included. The through column type is also considered. Through these experiments and 3D-FEM analyses, the shape factors for cruciform shaped joint, T-shaped one and L-shaped one are evaluated as 3.0, 2.4 and 1.4, respectively. However, in the proposed design guidelines, the traditional shape factors as 3.0, 2.0 and 1.0 are adopted for practical simplification with safer side

decision. The detailed test results are shown in Ref.8.

d) 3D Joint Tests

So as to see the inelastic behavior of beam-to-column connections under two directional loading, four 3D joint test specimens were constructed. Three of them are through column type with the identical shape and one is through beam type. One of the three identical through column joints was loaded in the direction of the frame (beam) in an ordinary manner. Second one was loaded in the direction of 45 degrees with respect to the axis of the frame. The third one was loaded following a circle shaped orbit. The strength and restoring force characteristics of the first and second specimens were quite resemble each other and the effect of loading direction can be considered negligible. However, the circle orbit loading largely reduced the strength. This effect was not included in the proposed design guidelines, which will be the future problem. The detailed test results are presented in Ref.9.

(4) Frame Test

So as to understand the overall inelastic behavior and required ductility in each structural elements of RCS frame, a two story (1.35m in story height) and two bay (2.1m in beam span) frame specimen was tested. The frame was designed as weak joint panel. The test results showed fairly good ductility, but the hysteresis loop showed pinched.

(5) 3D-FEM Analyses

Elastic and inelastic behavioral characteristics of bond and friction between concrete and steel were investigated by fundamental experiments. The test results were reflected to modify the constitutive models for the inelastic 3D-FEM program. Analytically obtained monotonic load versus deflection relationships were compared with the envelopes of the cyclic behaviors of beam-to-column connections with excellent agreements, which verified the effectiveness of 3D-FEM analyses. The 3D-FEM analyses also gave us better understanding of the stress distribution in the beam-to-column connection. This analytical method was also applied to 3D-joint test and frame test and fairly good results were obtained. The detailed analytical results are shown in Ref.8.

3D-FEM analyses will be continued to complement data on the structural performance of RCS connections out of the extent of test data

and to further improve the shear design formulas of RCS connections.

(6) Equivalent Damping of Joints and Frames

Equivalent viscous damping of 15 beam-to-column connections and 4 frames was calculated at each displacement amplitudes. The estimated damping was summarized as follows; i) Beam hinging specimens showed the largest damping and it reached 40% at the large displacement amplitude. ii) Column failure or bearing failure specimens showed the least damping and it was about 10% even at the large displacement amplitude. iii) Joint panel shear yielding specimens showed intermediate damping between 10-20% and the cover plate improved the energy dissipation capacity.

(7) Draft RCS Design Guidelines

In recent years, a large number of RCS connection details have been developed and applied to the real construction practices. However, many of the new connection details and systems developed are not covered by the existing standards, and thus the establishment of original design procedures for RCS connections and systems are urgently needed in Japan.

Japanese working group for RCS systems developed draft design guidelines for RCS systems, which contained the following items: i) formula to evaluate panel shear strength, ii) yield mechanisms to be recommended and how to realize the intended mechanism, iii) modeling of restoring force characteristics of beam-to-column connections, and iv) fabrication and construction method.

Table 2 shows the tentative contents of the draft guidelines for the design of RCS system.

Table 2 RCS Draft Guidelines

Preface

Part 1: Draft design guidelines

1. General

1.1 Scope of application

1.2 Terminology

1.3 Notations

1.4 Related codes and standards

2. Materials

2.1 Kind and quality of materials

2.2 Material constant

2.3 Allowable stress and material strength

3. Structural design

3.1 Fundamentals for structural planning

3.2 Fundamentals for panel design and details

3.3 Design methods

3.4 Method based on current practice

3.5 Method based on performance criteria

3.6 Design example

4. Fabrication and Construction

5. Example of Construction

Part 2: Technical Information

1. Database

1.1 Introduction

1.2 Profile of database

1.3 Investigation of existing shear strength design formulas

1.4 Proposed design formula

1.5 Proposed skeleton model

2. Experimental and Analytical Results done by U.S.-Japan Program

2.1 Stress transfer in the joint panel

2.2 Behavior of through beam type joint

2.3 Behavior of interior through column type joint

2.4 Behavior of exterior joint

2.5 Behavior of 3D joint

2.6 Behavior of frame

2.7 Inelastic 3D-FEM analysis

2.8 Equivalent damping of RCS joints and frame

3. RESEARCH ON HWS

3.1 General

The structural system of core wall with exterior steel frame is not common in Japan and its design method is not established yet. So, six, twelve and twenty-four storied theme structures were preliminary designed. According to the preliminary design, six storied model was considered to be designed just depending on the large shear strength of walls. Twenty-four storied model needed hat truss (and belt truss) to reduce large overturning moment induced at the foot of the coupled shear walls, which made the development of general design procedure rather difficult. Therefore, twelve storied theme structure was first selected and the design problem was picked up. Then, the design implication is expanded into much higher or lower systems. The rationality of the designed system is verified through the analytical and experimental studies.

3.2 Research Items And Results

(1) Trial Design of Theme Structure

First, twelve story model building (see Fig.3) was designed on the basis of the general design concept (Ref.7). The strength of the designed building was too large to be investigated as the target structure to be developed. Then, the building was revised considering the design

concept for the coupled-shear wall in New Zealand (Ref.10). In New Zealand practice, earthquake load is distributed to each wall according to the overturning moment ratio carried by boundary beams. As the building still had large overstrength, the reinforcements in the core walls were intentionally reduced to reach reasonable strength level, 35 percent as the base shear coefficient. The final designed building was investigated whether it performed well or not under the seismic effects through the dynamic inelastic analyses using fish-bone model or frame model.

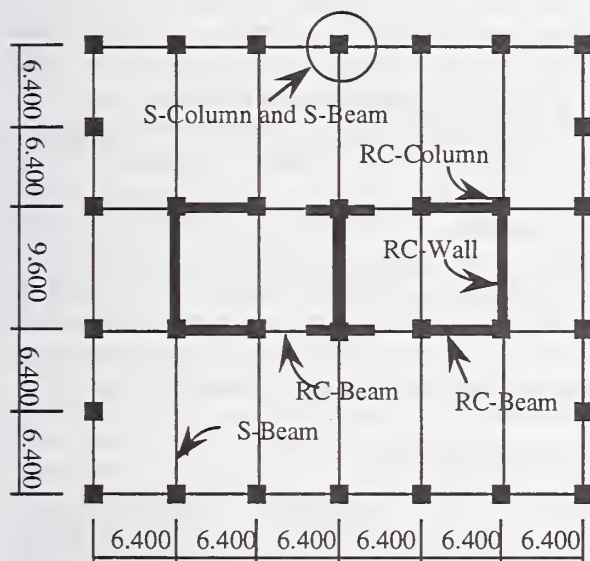


Figure 3 Floor Plan of Theme Structure on HWS

(2) Coupled-Shear Wall Test

One-third scale model of 12 storied coupled-shear wall test was carried out. During the test, the forces acting in each member was measured so as to understand the force re-distribution in the coupled-shear walls and boundary beams for design purpose. For this purpose, load cells were installed into all boundary beams. The coupled-shear walls showed very stable hysteresis loops until $1/67$ radian in drift index. From the readings of the load cells, it was observed that the boundary beams act like wedges inserted between walls after they cracked and expanded in length. These test results were investigated by FEM and MS (multi spring) model analyses. The detailed test results and some analytical studies were discussed in Ref.11 and Ref.12.

(3) T- and L-Shape Shear Wall Test

To understand the stiffness, strength and deformability of 3D-wall is essential for the

design implication to HWS systems. Three one-third scale T-shaped shear wall specimens without boundary columns, which represented the walls of the lowest story of the 12 storied prototype HWS system, were conducted. In these tests, the shear force and flexural moment with different moment-to-shear ratios were applied with varying axial forces.

Large axial force was expected at the corner of the 3D-wall of lowest story when two directional seismic force affected on the HWS system. Then, the ductility of the corner part of the wall depended much on its confinement. Therefore, four L-shaped shear walls varying their confinement level were tested with large axial force. These test data were utilized to develop hysteresis model of 3D-walls.

The detailed test results were discussed in Ref.13.

(4) Theoretical Study

Theoretical investigation was carried on the dynamic behavior of 3D HWS under the bi-directional earthquake motion, in order to establish a rational mathematical model in view of the experimental results, and the fluctuation of shear forces acting on dynamically-behaving rigid walls and flexible steel frames, to determine the design shear force for HWS.

(5) Literature Survey

About eighty papers on boundary beams and thirty papers on RC wall to steel beam connections were surveyed. As for the inelastic behavior of the boundary beams, the past analytical and experimental information was considered to be enough for design purpose. On the other hand as for the RC wall to steel beam connections, the isolated joint strength tests were found in the reports and no sub-assembly tests were found. From this viewpoint, some verification test might be necessary for RC wall to steel beam connection. However, as the flexural stiffness of the steel beam with long span was very small and the rotational deformability of the joint itself was not so large, the experiment was not carried out.

(6) Design Guidelines

Seismic performance of each member in HWS differs significantly. Coupled walls and link beams may be damaged within a relatively small drift, while exterior steel frames will remain elastic at the limit drift of the walls. Design guidelines for HWS system should consider these different performance of each structural element. It is also indicated that the following items are important in

the design of HWS, in addition to the design methodology of the coupled shear walls and link beams: design for diagonal loading, soil spring effect, seismic use of perimeter steel frame, confinement of compression wall, and method of energy dissipation.

Table 3 shows the tentative contents of the draft guidelines for the design of HWS system. The detailed explanation of the design concept is presented in Ref.13.

Table 3 HWS Draft Guidelines

Introduction

1. Scope of Application

- 1.1 Structural components
- 1.2 Scale and geometry of building
- 1.3 Materials

2. Target Performance in Seismic Design

- 2.1 Establishment of target performance
- 2.2 Confirmation of target performance

3. Check of Target Performance

- 3.1 Input ground motion
- 3.2 Analytical methods
- 3.3 Check of design criteria

4. Check of member performance

- 4.1 Fundamentals for member performance
- 4.2 Walls
- 4.3 Boundary beams
- 4.4 Exterior frames
- 4.5 Steel beam to core wall connections
- 4.6 Foundations

Appendix 1. Design examples

Appendix 2. References, Test report and Other

Appendix 3. Examples of Dynamic Analyses

4. RESEARCH RESULTS ON RFI

4.1 Feasibility Study

Following items were discussed as possible research topics: Fiber reinforced plastics (FRP), high-performance concrete (HPC), intelligent material, prestressed steel member, hinge device, mega-structure system, recycle element, fire-proofing material for CFT, and high-performance steel. Some hearing-type meetings with material manufacturers and general contractors were conducted with a view to study a possibility of above items as research topics of RFI, and FRP and HPC were selected for feasibility studies on effective use.

4.2 Research on FRP

The research program on effective utilization of FRP materials for composite and hybrid

structures contained three research items as follows. These items were selected through the feasibility study on effective utilization of FRP.

- a) Development of the evaluation method for high-performance FRP-RC panels.
- b) Development of the effective repair and / or strengthening method by using FRP for existing RC members.
- c) Feasibility study on the effective utilization of FRP to the electrical facilities.

The behaviors of FRP-RC panels of flat- and tube-types reinforced by 2-dimensional FRP reinforcements, under axial tension and compression, in-place flexure and shear and out-of-plane flexure were experimentally investigated. The flexural and shear behaviors and confinement of concrete of RC columns which were wrapped by FRP strand or FRP sheet / tape with resin for repairing and / or strengthening were also investigated. The application of FRP to the electrical facilities such as a power station, and structures that had to be sheltered from electrical noise was studied from the literature survey.

4.3 Research on HPC

There are few cooperative research between concrete makers and structural designers in Japan. The makers have many technologies but they don't know how to use it. On the other hands, designers have a few information about new technologies of concrete. But they have many hints about the idea of future concrete.

The main objective is to exchange the information of makers and structural designers to discuss about how to use effectively the concrete materials to the structural members and how will be the future concrete. Through the discussions, the following two topics were depicted.

- a) Light weight concrete with high strength of which the specific gravity is imaged to be about 1.2 and 1.6, and the compressive strength of 30 and 60 MPa, respectively
- b) Advanced concrete with high tensile strength and ductility of which the tensile strength is imaged from 30 to 200 MPa, and the tensile ductility from 1 to 10 %.

As for the light weight concrete, two kinds of imaged concrete were realized and several fundamental tests on bond strength and compressive strength were carried out.

As for the high tensile strength concrete, various types of fibers with mortar were tested and some of them showed high tensile strength and good compressive ductility. However, it was made clear that such performance was quite sensitive to the kind of fibers.

4.4 Technical Information

The research results can not be summarized as design guidelines but they can be used as technical information. Design guidelines will contain the items concerning the design, fabrication, construction and application of the advanced materials mentioned above, that is, FRP-RC panel element, FRP strand and sheet / tape for repairing and strengthening of existing RC members, FRP for electrical facilities, light weight concrete with high strength and concrete with high tensile strength and ductility.

5. SUMMARY

U.S.-Japan Cooperative Earthquake Engineering Research on Composite and Hybrid Structures initiated in 1993 fiscal as a five year program came to the final stage. This paper presents the outlines of the research results conducted during this five years and the general contents of the proposed draft guidelines by Japan side. Research results by the U.S. side which will come out in other two or three years shall be reflected to improve the design guidelines presented in this paper.

ACKNOWLEDGMENTS

The authors wish to express their great thanks to the Members of Japan Technical Coordinating Committee for their useful comments and suggestions to the development of design guidelines and /or technical information on CFT, RCS, HWS and RFI.

REFERENCES

1. "Recommendations for a U.S.-Japan Cooperative Research Program utilizing Large-Scale Testing Facilities", Report No. UCB/EERC 79-26, 1979.9.
2. "Recommendation for U.S.-Japan Cooperative Research Program -Phase 5 Composite and Hybrid Structures", Report No. UMCEE 92-29, 1992.11.
3. "Standards for Structural Calculation of Steel Reinforced Concrete Structures," Architectural Institute of Japan, 1987 revision.
4. "Recommendations for the Design and Fabrication of Tubular Structures in Steel," Architectural Institute of Japan, 1990 revision.
5. S. Morino, "An overview of U.S.-Japan Cooperative Earthquake Research Program on

- CFT column systems," SEWC'98, July 19-23, 1998.
6. K. Sakino et al., "Experimental studies and design recommendations on concrete filled steel tubular columns -U.S.-Japan Cooperative Earthquake Research Program-," SEWC'98, July 19-23, 1998.
7. "Structural Provisions for Buildings," Building Center of Japan, 1994.9. (in Japanese)
8. H. Noguchi et al., "Shear strength of beam-to-column connections in RCS system," SEWC'98, July 19-23, 1998.
9. I. Nishiyama et al., "Bi-directional seismic response of reinforced concrete column and structural steel beam subassemblages," SEWC'98, July 19-23, 1998.
10. T. Paulay and M. J. N. Priestley, "Seismic Design of Reinforced Concrete and Masonry Buildings," John Wiley & Sons, Inc.
11. M. Teshigawara et al., "Seismic test on 12-story coupled shear wall with flange walls," SEWC'98, July 19-23, 1998.
12. M. Teshigawara et al., "Energy absorption mechanism and the fluctuation of shear force in the coupled shear walls," SEWC'98, July 19-23, 1998.
13. T. Kabeyasawa et al., "Displacement-Based Design of Hybrid Core Wall System," SEWC'98, July 19-23, 1998.

U.S.-Japan Cooperative Earthquake Research Program on Composite and Hybrid Structures - U.S.-side Progress

by

Subhash C. Goel¹

ABSTRACT

A five-year research program on Composite and Hybrid Structures as Phase 5 of the U.S.-Japan Cooperative Earthquake Research Program was recommended to be initiated in 1993 in both countries. The research work in Japan started in fiscal year 1993. However, fuller participation of researchers on both sides started in early summer 1995. The sponsorship of the program is by the National Science Foundation in the U.S. and by the Ministry of Construction along with a number of industry groups in Japan. This paper presents a brief status report of the program and research progress made to date on the U.S. side. Because of diverse and broad scope of the subject area, the research program is organized into the following four groups: Concrete Filled Tube Column Systems (CFT); Reinforced Concrete (RC) and Steel Reinforced Concrete (SRC) Column Systems (RCS); and RC/SRC Wall Systems (HWS); New Materials, Elements and Systems (RFI). A theme structure with well selected layout, geometry and design loads for the research is also presented, which provides a common focus for various systems to be studied, and also a common prototype structure from which the components and sub-assemblages are drawn.

Key Words:

Concrete Filled Steel Tube;
RC Column with Steel Girder;
RCS Core Wall with Exterior Steel Frame;
New Materials Elements and Systems.

1. INTRODUCTION

The U.S.-Japan Cooperative Earthquake Research Program began in 1979 under the auspices of the UJNR Panel on Wind and Seismic Effects. The overall objective of the total program is to improve seismic safety practices in both countries through cooperative studies to determine the relationship among full-scale tests, small-scale tests, component tests, and related analytical

and design implication studies. First four phases of the program have been Reinforced Concrete (RC) Structures, Steel Structures, Masonry Structures, and Precast Concrete Structures. Research on Mixed Steel/RC Structures was identified as an important phase of the program as recommended in the planning group report.

It is widely recognized that innovative uses of two or more different materials in a structure leads to more efficient system for resisting seismic forces. During the past ten years the use of composite and hybrid structures has increased in the U.S. and Japan. In spite of some research and development work by Japanese construction companies, not enough is known at present regarding their seismic behavior or performance. Design procedures and codes for use in typical design offices are not well developed at present.

Considering the importance of developing design guidelines (a unified code development) for typical composite and hybrid structures that are used in current practice, and of developing new and innovative composite structural elements and hybrid systems using advanced new materials and/or devices, a five-year research program on Composite and Hybrid Structures was recommended as the fifth phase of the ongoing U.S.-Japan Cooperative Earthquake Research Program. The recommendations were based on a number of technical meetings of the U.S. and Japan Planning Groups and finally a Joint Planning Group Workshop held in Berkeley on September 10-12, 1992 (Ref. 1).

Because of diverse and broad scope of the subject area, the research program is organized into the following four groups: Concrete Filled Tube Column Systems (CFT); RC/Steel Reinforced Concrete Column Systems (RCS);

¹ Professor, Dept. of Civil and Environmental Engrg., University of Michigan, Ann Arbor, MI 48109-2125, USA

and RC/SRC Wall Systems (HWS); New Materials, Elements and Systems (RFI). A theme structure provides a common focus of the program to facilitate cross comparison between various system types identified and to derive structural elements and sub-assemblages for detailed studies.

2. PROGRAM MANAGEMENT, COORDINATION AND CURRENT STATUS

The research program is planned for a period of five years in both countries, and funding has been provided accordingly. Research work on the Japanese side started in the spring of 1993. However, fuller participation and coordination of research work on both sides started in early summer 1995 when the first group of U.S. research projects were awarded. Cooperation and coordination of work by all participants are most essential to successful completion of this program. Various committees have been formed for this purpose. A Joint Technical Sub-Committee (JTSC) in each of the four components of the research program provides technical advice and coordination. Each JTSC has a co-chairman from each side with membership including all researchers in that area. These groups meet as often as needed. All participants and institutions are also part of the bigger Joint Technical Coordinating Committee (JTCC) to review progress and discuss scientific and technical issues on a common basis. This committee meets once a year. The last (fourth) JTCC meeting was held in Monterey, California, in October 1997. The fifth JTCC meeting is scheduled to be held in fall 1998 soon after the award of fourth year U.S. research projects which is expected in April-May 1998. A smaller group called Joint Steering Committee (JSC), which consists of key representatives from the JTCC, oversees the entire program and provides guidance on issues that are common to the four components of the program. The overall program has a technical coordinator and a co-chairman from each side.

In addition to sharing of technical information and ideas among researchers, exchange of personnel involved is strongly encouraged. This is happening more now as the research program has gotten into its advance stage. Active participation of practitioners and various industry representatives in planning, coordination and execution of the research

work is also a strong feature of this program.

3. PROGRAM OBJECTIVES

Since the subject area of the Composite and Hybrid Structures is diverse and broad, the research program was organized into the following four groups: CFT Column Systems; RC/SRC Column Systems; and RC/SRC Wall Systems; New Materials, Elements and Systems. The first three groups aim at developing practical design guidelines (a unified code development) for typical composite and hybrid structures currently used. The last group aims at developing new and innovative composite structural elements and hybrid systems using advanced new materials and/or devices.

4. THEME STRUCTURE

The theme structure provides a common focus and a strong link between various components of the research program, facilitate cross comparisons between various systems to be studied, and also provides a common prototype structure from which the structural elements and sub-assemblages for detailed studies are drawn. The following criteria were used for selection of the theme structure:

- The building plan was selected so as to reflect the benefits that the hybrid structures provide over non-hybrid structures.
- The basic plan is common to various types of hybrid structures. The number of stories and the make-up and combination of structural components and details can be varied.
- Rules to determine dead load, live load and seismic forces to be used in design simulation are common in the U.S. and Japan Groups.

5. RESEARCH ON CFT SYSTEMS

A number of research projects were funded during the first two years. These projects focused on the behavior of CFT column-to-WF beam moment connections. The specimens are nearly full size and include circular and square tube sections for columns. The connection details include the use of diaphragms, shear studs, welds, and bolts. The main variables are the connection details to transfer beam forces into the column. The objectives are:

1) To determine the force transfer mechanism, examine the effects of various connection details on this mechanism, and on the connection strength, stiffness and ductility under cyclic loading.

2) Develop and evaluate practical and economical connection details for seismic resistance.

3) Formulate practical design guidelines.

Some testing work also includes study of beam-columns under combined axial force and bending. Analytical studies accompany the experimental work. The analytical models include complex finite element formulations in an effort to develop simpler empirical or mechanics based models for practical design work. Analytical work is also aiming at studying the bond and shrinkage effects, and confinement effects in CFT members subjected to different load conditions.

6. RESEARCH ON RCS SYSTEMS

RCS structures in the U.S. generally consist of columns made of light steel shapes encased in RC. The light steel shape provides ease of erection and connection to the steel beam. Currently, there are seven active projects in the U.S., that are related to RCS structures. The projects include preparation of database on connections, testing of exterior and interior beam-to-column connections with and without floor slab, composite frames with partially restrained connections, and use of high strength steel and concrete. The joint detail variables include: lateral ties, beam bearing plates, use of FRC in place of stirrups. Analytical studies focus on modeling the connection and frame behavior to address practical analysis and design issues.

7. RESEARCH ON HWS SYSTEMS

In one research project on seismic behavior of steel/composite coupling beams and their connections to the RC shear wall has been studied experimentally and analytically. Four one-third scale specimens were tested which represented a portion of the wall and one half length of the coupling beam from a 20 story theme structure. The effect of concrete encasement of the steel beam and details of the connection in the embedded portion have been studied. Two more research projects were started in the second year which deal with

studies of composite SRC shear walls with steel boundary elements, and steel frames with RC cast-in-place in-fill walls.

8. RESEARCH ON NEW MATERIALS, ELEMENTS AND SYSTEMS (RFI)

The research work in this group aims at developing and application of new and advanced materials in innovative composite structural elements and systems (Research For Innovation - RFI). Thus, the studies in this group are more of feasibility type than those in the previous three groups where the objectives are to develop detailed guidelines for practical design work.

Significant amount of research work has been devoted to advanced cementitious and plastic composite materials. Albeit, the available information needs to be expanded to application in seismic load conditions. In two projects under this program, work is in progress on developing innovative composite systems consisting of steel and fiber reinforced concrete (FRC). The structural elements are made of selective combinations of FRC and steel members. The combinations under study include: FRC-encased open web steel joists, and high performance FRC core encased in slurry infiltrated mat concrete (SIMCON) shells for reinforcement as well as stay-in-place form work. In another project application of fiber reinforced concrete in the joint regions of RCS systems is being studied. Work is also in progress on further development of Engineered Cementitious Composite (ECC) materials and their selective use in structural elements, such as columns with large ductility demands.

9. CONCLUDING REMARKS

A brief overview of the progress of U.S.-Japan Cooperative Earthquake Research Program on Composite and Hybrid Structures has been presented in this paper. This five-year program started in 1993 in Japan and in 1995 in the U.S. The two year time lag is being taken as an opportunity to plan the future research work in a more careful and useful manner in order to derive the most benefit from the work that has already been completed on both sides. The overall coordination efforts, cooperation and exchange of information have been excellent. More active exchange of research personnel is currently occurring in this program. At least

four or five researchers from each side have participated for short and long term durations.

More details on the current status and technical progress made in this program can be found in the minutes of the last (fourth) JTCC meeting (Ref. 2). A listing of the general recommendations from that meeting is given in the Appendix of this paper. A www site has also been established which contains updated information on the overall status of this program as well as summary of results and findings from individual research projects (www.eerc.berkeley.edu/usjhcs).

10. REFERENCES

1. "Recommendation for U.S.-Japan Cooperative Research Program - Phase 5 Composite and Hybrid Structures," Report No. UMCEE 92-29, Department of Civil and Environmental Engineering, The University of Michigan, Ann Arbor, MI, 48109-2125, November 1992.
2. "Summary, Resolutions and Recommendations of the Fourth Joint Technical Coordinating Committee Meeting," Report No. UMCEE 98-03, Department of Civil and Environmental Engineering, The University of Michigan, Ann Arbor, MI, 48109-2125, January 1998.

11. APPENDIX

General Recommendations from the 4th JTCC meeting:

1. Exchange of researchers, and research data (e.g., via www) on both sides should be continued at an increased level.
2. Close cooperation and collaborative research effort on both sides should be continued till the end of the five year program of both countries.
3. Scope of this program may be expanded to include more thorough examination of promising innovative technologies and materials (such as those explored in the RFI Program) applied to repair and upgrading of existing structures, application to infrastructure systems, and so on.
4. Efforts to synthesize and interpret knowledge gained in the program, and to disseminate this knowledge and design/analysis methodologies to the design profession and industry should be accelerated.
5. Consideration should be given to perform testing work on carefully selected full frames in possible cooperation with other research programs.
6. Material manufacturers, construction and other industrial organizations should continue to actively support the research program.
7. Each JTSC should meet as needed to achieve good coherence in the cooperative research work.
8. Each JTSC should study development of performance criteria as related to design guidelines to be developed in each country.
9. Use of common set of ground motions is encouraged to permit more direct comparison of dynamic analysis results.
10. The funding agencies in both countries should maintain proper balance of research effort among the four areas of the program consistent with the research needs.
11. Funding should be provided for joint coordinated publication of research work with practical implications.
12. The 5th JTCC meeting should be held in early fall of 1998 at a place to be hosted by the Japan side.



**MANUSCRIPT PRESENTED
at MINI-SYMPOSIUM**

Development of New High Bridge Piers Containing Spiral Reinforcement

by

Okahara Michio ¹⁾, Fukui Jiro ²⁾, Adachi Takuya ³⁾, Okoshi Moriyuki ³⁾, Koga Yasuyuki ⁴⁾

ABSTRACT

The construction of expressway and other arterial roads in Japan is shifting from those running the length of the Japanese Archipelago to roads across its islands, a change in emphasis that has increased the number of roads constructed through mountainous regions of the country. Recent years, a strong demand for the preservation of natural environments has been accompanied by the need for bridge construction methods that have minimal effects on nature. To meet this new requirement, high bridge piers must be constructed.

In response to these circumstances, rationalize execution and to develop the 3H (Hybrid Hollow High Pier) Method: a new high bridge pier structure that is both economical and provides earthquake resistance.

Key Words: High Pier

Spiral Reinforcement

Development of Construction

Performance Confirmation Tests

1. INTRODUCTION

The construction of expressway and other arterial roads in Japan is shifting from those running the length of the Japanese Archipelago to roads across its islands, a change in emphasis that has increased the number of roads constructed through mountainous regions of the country. Past roads through mountainous areas included many sections constructed by means of large scale cutting and embankment work. But in recent years, a strong demand for

the preservation of natural environments has been accompanied by the need for bridge construction methods that have minimal effects on nature. To meet this new requirement, high bridge piers must be constructed. And the work performed to construct bridge piers must include environmental measures such as cutting less soil and reducing the size of execution yards. It is also necessary to reduce labor requirements and the quantity of work performed to deal with both a shortage of and an increase in the average age of skilled construction workers.

During the Hyogo-ken Nanbu Earthquake of 1995, road bridges that play important roles as evacuation routes and emergency transportation arteries, were destroyed with serious effects on the life of local society. It is now essential to develop new kinds of bridge piers that provide earthquake resistance superior to that of conventional reinforced concrete bridge piers.

In response to these circumstances, the Public Works Research Institute of the

1) Director, Structure and Bridge Department, Public Works Research Institute, Ministry of Construction

Tsukuba Science City, 305-0804, Japan

2) Head, Foundation Engineering Division, Structure and Bridge Department, Public Works Research Institute, Ministry of Construction

ditto

3) Researcher, Foundation Engineering Division, Structure and Bridge Department, Public Works Research Institute, Ministry of Construction

ditto

4) Director, Research Section 3, Advanced Construction Technology Center, Tokyo-to, 112-0012, Japan

Ministry of Construction has worked in cooperation with the Advanced Technical Center, and private companies to rationalize execution and to develop the 3H (Hybrid Hollow High Pier) Method: a new high bridge pier structure that is both economical and provides earthquake resistance.

2. OUTLINE OF THE 3H METHOD

2.1 Present Problems and Development Goals

Most high bridge piers now designed and constructed are reinforced concrete bridge piers. Extremely large quantities of steel reinforcing material is used in order to minimize their cross section dimensions. The revision to the Road Bridge Guidelines completed in 1996 stipulates that bridge piers shall be provided with sufficient stiffness by installing highly concentrated hoop ties and intermediate hoop ties. This has made execution of bridge piers extremely difficult, resulting in many problems related to construction periods and costs. It is also necessary to guarantee safe execution at high work locations.

In response, technical development has been undertaken in an effort to improve high bridge piers by

- (1) increasing execution efficiency,
- (2) improving bridge pier earthquake resistance,
- (3) preserving the environment,
- (4) cutting costs, and
- (5) improving the quality and appearance of the work.

2.2 Structure of a 3H Method Bridge Pier

Figure 1 through Figure 4 present an outline of the structure of 3H Method bridge piers.

The most important distinguishing feature of the structure of a 3H Method bridge pier is the fact that part of the axial direction reinforcing

rods installed with the conventional method are replaced with steel (H-steel or steel pipes). As Figure 3 and Figure 4 show, the intermediate hoop ties are replaced with spiral reinforcement. This spiral reinforcement forms a spiral column consisting of the steel and axial direction reinforcement surrounding it. Figures 5 and 6 show spiral columns. These are installed around the full circumference of the bridge pier section to form the bridge pier column. Because this is a steel - reinforced concrete structure that includes steel material, its buckling load carrying capacity is greater than that of a reinforced concrete structure. This permits a reduction in the decline in its bearing strength after maximum load during bending behavior. And by closing the axial direction reinforcement, the spiral reinforcement confines the buckling of the steel reinforcement generated during large deformation of the bridge pier. This provides the same function as intermediate hoop ties. These features improve the toughness of bridge piers. It is also possible to construct bridge piers with far greater earthquake resistance than that of conventional bridge piers.

2.3 3H Method Execution Procedure

The 3H method execution has been developed basically by effectively combining existing technologies. It is also more rational than past methods of constructing bridge piers. It is extremely important, however, to make sure that the initial assembly of the spiral columns is performed precisely. And to reduce labor, the spiral columns must be as long as possible. Depending on the bridge pier height and other construction conditions, appropriate measures must be taken to prevent vibration, oscillation, etc. of the spiral columns during execution.

Execution methods can be broadly categorized into the following two methods

depending upon the type of forms used.

2.3.1 Execution Method Using Precast Forms

This execution method is used mainly to build high bridge piers with a height ranging from 30 to 60 meters. Because precast forms are used on the inside and outside surfaces of the bridge pier, it is the best method from the viewpoint of execution properties, quality, and appearance.

The execution is performed by first installing the spiral columns, assembling the precast forms into appropriate units on land, using a crane to lower the units into place, then anchoring them. Finally, the spaces between the precast forms are filled with secondary concrete.

2.3.2 Execution Method Using Movable Forms

This execution method is used mainly to construct bridge piers higher than 50 meters in height. The use of large movable forms permits improved execution properties and shorter work periods.

With this method, the spiral columns and hoop ties are installed, then jacks are used to simultaneously or alternately raise the forms and the scaffolding in order to construct the bridge piers.

2.4 Special Features of the 3H Method

The following are the special features of the structure and the execution method described above.

(1) More Efficient Execution

- Replacing part of the axial direction reinforcement with H-shaped steel, steel pipes, or other steel material sharply reduces the quantity of complex reinforcing work that is necessary. This can bring substantial improvements in execution efficiency and speed up the execution.
- The use of spiral columns can eliminate the work required to install intermediate hoop ties.
- The use of precast forms or large movable

forms also contributes to more efficient execution.

(2) Improving Earthquake Resistance

It is a steel - reinforced concrete structure built by replacing part of the axial direction reinforcement with H-shaped steel or steel pipes to provide buckling load carrying capacity and toughness superior to that possible with a reinforced concrete structure.

(3) Environmental Protection

- The use of precast forms or large movable forms can reduce the quantity of natural resources consumed.
- The method can reduce the size of execution yards, mitigating the effects of the work on the surrounding environment.

(4) Cost Reductions

- More efficient execution shortens construction periods, lowering costs.

(5) Improved Quality and Appearance

- The use of factory made or processed structural members contributes to more dependable quality and more attractive bridges.

3. PERFORMANCE CONFIRMATION TESTS CONDUCTED TO DEVELOP NEW TECHNOLOGY

In order to develop the 3H Method, it was necessary to accurately clarify previously unknown dynamic properties and their behavior. The authors have performed element tests of several kinds. These tests have confirmed that the 3H Method has properties equal or superior to those of the conventional method.

And loading tests of conventional reinforced concrete structures and structures made using the 3H method were performed with models 1/4 the size of real bridge piers.

The remainder of Section 3. describes the tests and their results.

3.1 Column Specimens

3.1.1 Outline of the Test

The specimens modeled part of the hollow cross section of bridge piers. With dimensions of $1,600 \times 450 \times 1,700$, they were about 1/2 the size of those of an actual bridge. The test cases are shown in Table 1 and outlines of the specimens are shown in Figure 7. Case 1 (standard specimen) represented a conventional reinforced concrete structure; Cases 2 through 7 represented steel - reinforced concrete structures made using H-shaped steel; Cases 8 and 9 represented steel - reinforced concrete piers made using steel pipes; and Case 10 represented a reinforced concrete bridge pier made using spiral reinforcement. Cases 2 through 9 were tested by varying factors such as the pitch of the spiral reinforcement, the intervals between the columns, and the axial direction reinforcement ratio (percentage of the total steel cross section area accounted for by the axial direction reinforcing steel area), the hoop tie pitch, etc. The total steel material section areas in the steel - reinforced concrete structures and the reinforced concrete structures were almost identical and the axial direction reinforcement ratio in the steel - reinforced concrete structure was about 10%.

The tests were performed by monotonically increasing the vertical load and measuring the displacement of the specimens in the height direction and the strain etc. of the steel reinforcement.

3.1.2 Test Results

Fracturing of the specimens in every case occurred in the form of cracking of the concrete surface in the loading direction at the ends and in the middle of the specimens. As the load increased, the centers of the specimens bulged out at right angles to the loading direction. Afterwards, the protective concrete

covering peeled off, and the testing ended when the axial direction reinforcement buckled. Photographs 1 and 2 show the way that the H-shaped steel and steel pipes fractured.

Table 2 summarizes the test results. The strength ratio (P / σ) that clarifies the bearing strength in each case compared the maximum stress found from the maximum load and the concrete strength of the test pieces. The following information is revealed by this strength ratio.

(1) In Case 2 through Case 4, the confining effects of the spiral reinforcement provided maximum stress almost equal to that in Case 1 where intermediate hoop ties were used. And only slight differences were observed in the maximum stress and strength ratio as a result of the pitch of the spiral reinforcement.

(2) Case 3 and Case 5 reveal that the intervals between columns has almost no effect on the maximum stress.

(3) Case 3 and Case 7 reveal that as the interval between the hoop ties is increased, the maximum stress declines by about 30%.

Figure 8 shows the strain of the spiral reinforcement at about the center of the Case 2 specimen. Up to maximum load, the strain in the middle (S12, S12) was highest. But the strain of the spiral reinforcement at that time ranged from 1,000 to 1,500 μ , which was less than the yield strain (between 1/7 and 1/5 of approximately 7,300 μ). At the stage where the continued loading had reduced the load to about 80% of the maximum load, the strain of the spiral material in a part corresponding to the intermediate hoop ties (S2, S7, S15) abruptly increased. This spiral reinforcement displays behavior typical of intermediate hoop ties.

Figures 9 and 10 show the displacement at right angles to the load direction in the center of the specimens. In Case 2 and Case 3,

displacement did not increase immediately after the maximum load, then after the load fell to about 80%, displacement began.

In Case 7 where the hoop tie pitch was 150 mm, displacement began immediately after maximum load. And even in Case 5 where the column interval was large, displacement occurred immediately after maximum load just as it did in Case 7. These results reveal that the pitch of the spiral reinforcement, column interval, and pitch of the hoop ties provide deformation confinement in the lateral direction that can be counted on to provide effects that substitute for those of intermediate hoop ties.

Figure 11 presents the relationship between the stress and the strain when the pitch of the spiral reinforcement is varied. Little change was observed in either the maximum stress or the behavior after maximum stress as the pitch of the spiral reinforcement was varied. From a specimen strain near $3,000 \mu$, the greater the pitch of the spiral reinforcement, the higher the percentage that the stress declined. And in these cases, even at the stage where the specimen strain reached $10,000 \mu$, the specimen's stress remained at 150 kgf/cm^2 or more. This confirmed its superior deformation properties.

Figure 12 presents the relationship between the stress and the strain when the pitch of the spiral reinforcement is held constant while other conditions are varied. When the pitch of the hoop ties was large at 150 mm, the maximum stress of the specimens declines sharply. But if the strain of a specimen surpasses approximately $3,000 \mu$, the percentage decline of the stress is almost identical in every case.

Figure 13 presents the relationship between the stress and strain in three cases: principal steel is H-shaped steel + axial direction reinforcement (Case 4), steel pipe + axial

direction reinforcement (Case 9), and only axial direction reinforcement (Case 10). This figure reveals that differences in the kind of principal steel used have little effect on the maximum stress of the specimens nor on the strain of the specimens at maximum stress. But when the maximum stress is exceeded, the stress declines more when only axial direction reinforcement is used than it does in other cases.

3.1.3 Summary

The study was performed to confirm the performance of "steel reinforced concrete plus spiral reinforcement": the basic structure of a 3H bridge pier. The results have confirmed that the basic structure of a bridge pier made using the 3H Method provides axial compressive strength equal to that of conventional bridge piers and superior deformation properties.

3.2 Alternating Loading Tests

3.2.1 Outline of the Tests

Figure 14 presents cross sections and dimensions of specimens that are scaled down replicas of real bridges and outlines of the tests. The modeling was done by arranging the axial direction steel to obtain the same bending bearing strength as models of conventional bridge piers. The testing was done by applying axial force corresponding to the dead load from the superstructure. Afterwards, the horizontal displacement at the loading point when the axial direction reinforcement and the steel at the outside edge of the cross section of the bridge pier foundation reached the yield value was set at $1 \delta_y$. The displacement of this integral multiple was loaded alternately negatively and positively under displacement control. And the number of repetitions at each loading step was set at 3.

3.2.2 Test Results

Figures 15 through 17 show the hysteresis curves of the horizontal load - horizontal

displacement of the conventional method and the 3H Method (models with H-shaped steel and steel pipes), while photograph 3 presents a view of the test. The displacements at about $1 \delta y$ where the tensile side steel reached the yield value were almost identical at about 15 mm for both the conventional method model and 3H Method model. The maximum bearing strength was a little higher in the case of the 3H Method model. Both methods provide sufficient deformation performance. But the percentage decline in the bearing strength during large deformation seems to have been smaller in the 3H Method model case. And a comparison of the shapes of the hysteresis curves reveals spindle-shapes with superior energy absorption in both cases. The area of the hysteresis loop of the 3H Method model is clearly larger than that of the conventional method model. And because a reversed S-shaped slip is not observed, it is concluded that its earthquake resistance is greater than that of the conventional method.

Detailed analysis is now in progress.

4. CONCLUSIONS

The 3H Method can substantially reduce labor requirements from the level necessary to implement the conventional method.

Various element tests and negative - positive alternating horizontal loading tests using specimens that are scaled down models of real bridges that have already been performed have clarified the structural properties of piers constructed using the 3H Method. But because it is a new type of structure, some aspects of its execution are still not clearly understood. The next task is to incorporate knowledge of these points obtained from future executions in design, execution, and estimation manuals as it is obtained.

Table 1. Test Cases

No.	Structure	Steel Material (Number)	Axial Direction Reinforcement (Number)	Axial direction Reinforcement Ratio (%)	Hoop Ties Diameter, Pitch (mm)	Spiral Reinforcement	
1	RC	—	D25 × 42	100	D10 × 75	—	—
2	H-shaped Steel	H-200 × 3	D16 × 16	14.3		φ 5.1 × 75	100
3						φ 5.1 × 100	
4						φ 5.1 × 150	
5						φ 5.1 × 100	200
6	Steel Pipe	H-150 × 3	D25 × 16	40.2	D10 × 150	φ 5.1 × 100	100
7		H-200 × 3	D16 × 16	14.3			
8		φ 216 × 3		16.5	D10 × 75		
9			φ 5.1 × 150				
10	RC	—	D25 × 40	100		φ 5.1 × 100	

Table 2. Test Results

No.	Structure	Maximum Load F (tf)	Equivalent Cross Section Area A (cm ²)	Maximum Stress P F/A (kgf/cm ²)	Concrete Strength σ (kgf/cm ²)	Strength Ratio P/σ
1	RC	1797	9619	187	164	1.14
2	H-shaped Steel	2157	8995	240	218	1.10
3		2129	9041	235	214	1.10
4		2093	8887	236	223	1.06
5		2176	9052	240	214	1.12
6		2156	8816	245	242	1.01
7		1919	9092	211	257	0.82
8	Steel Pipe	1854	8613	215	231	0.93
9		1934	8620	224	231	0.97
10	RC	2027	8646	234	245	0.96

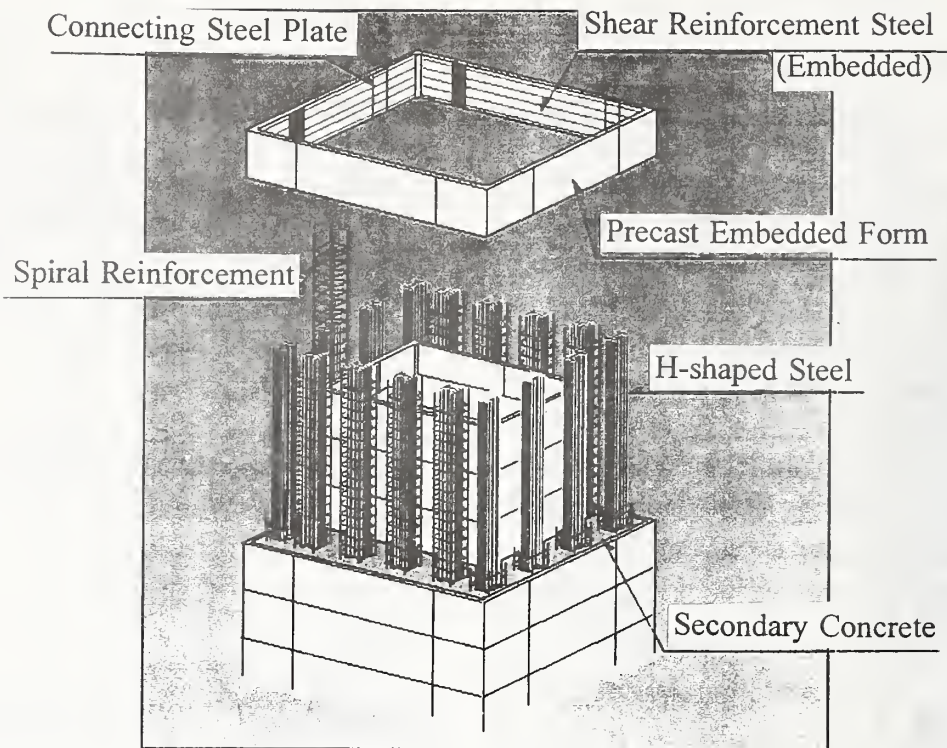


Figure 1. Precast Form Structure

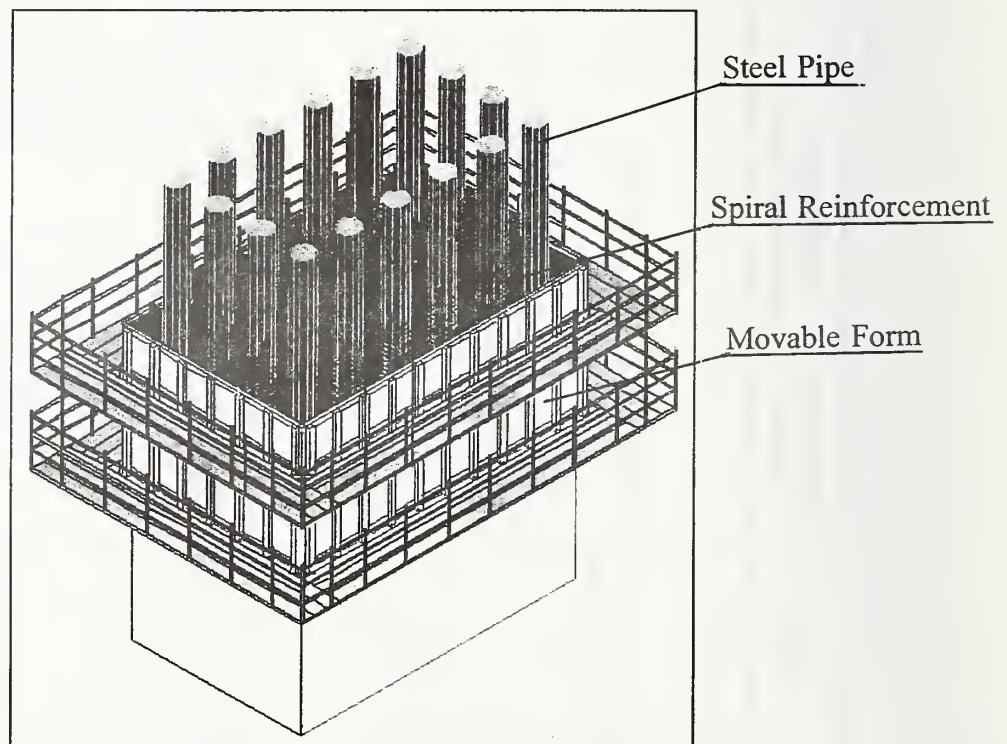


Figure 2. Movable Form Structure

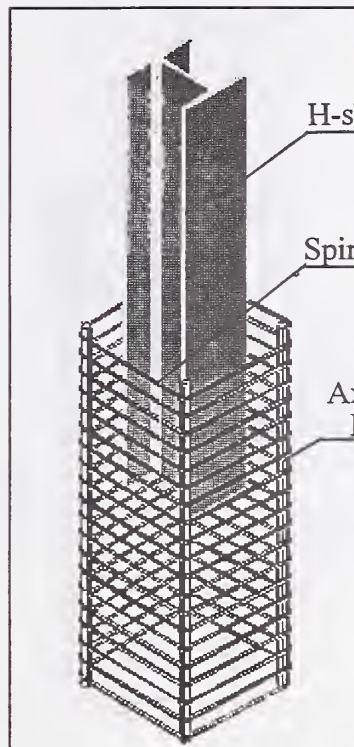


Figure 3. H-shaped Steel Type

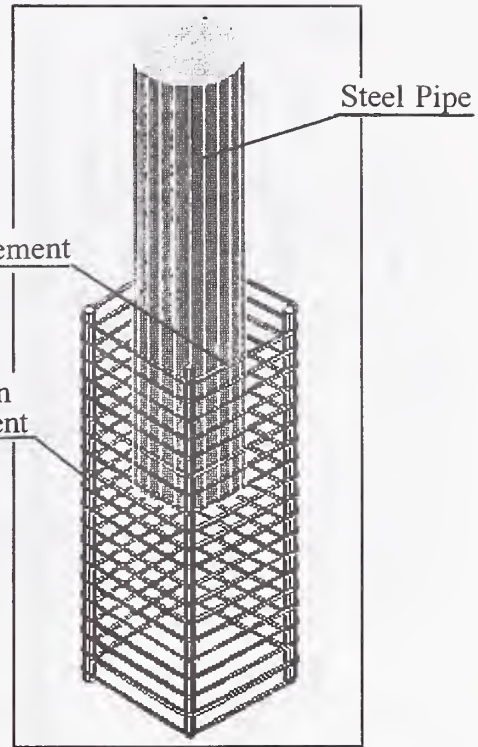


Figure 4. Steel Tube Type

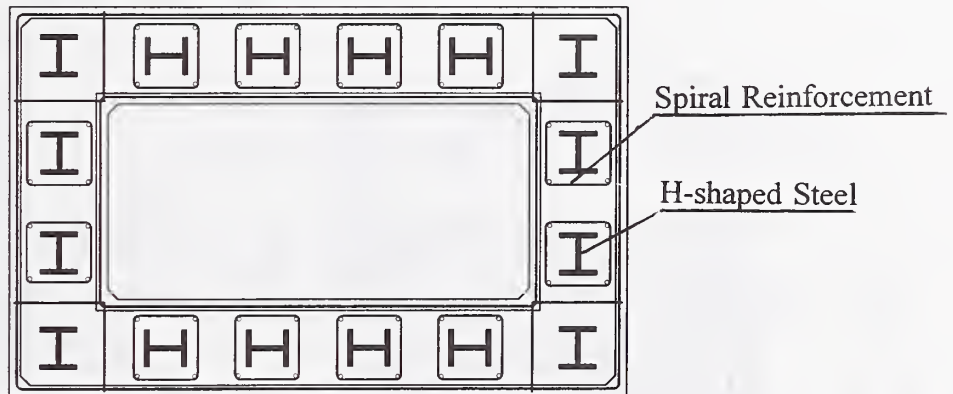


Figure 5. H-shaped Steel Type Arrangement Diagram

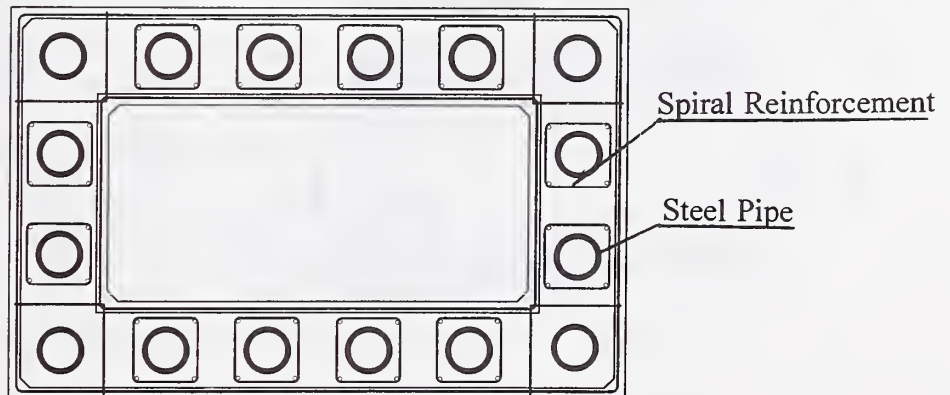
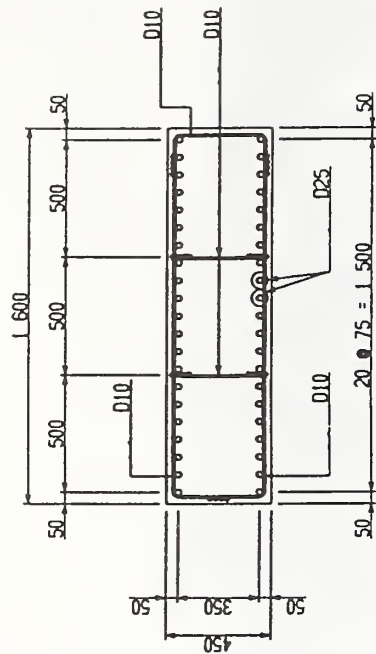
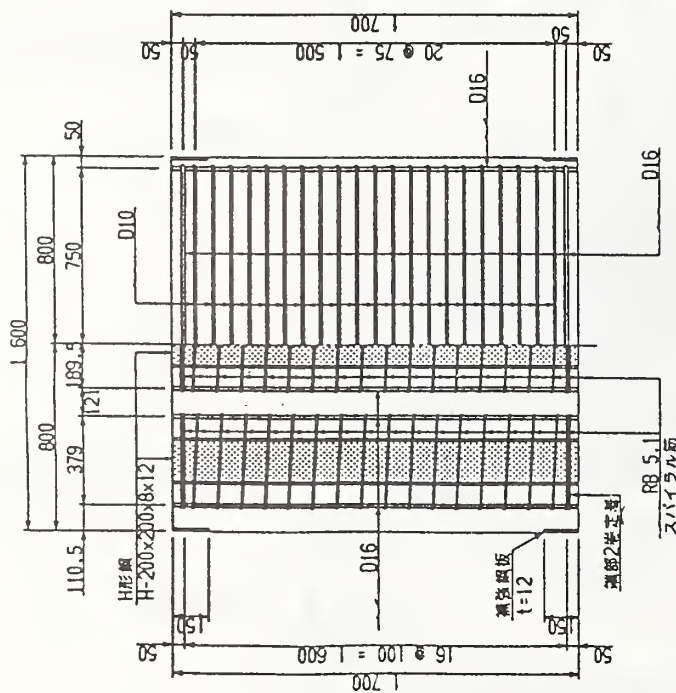
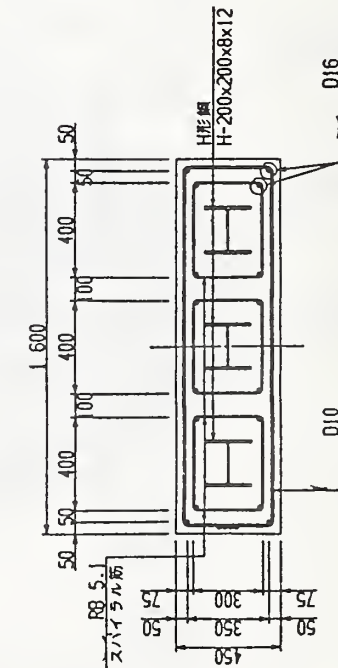


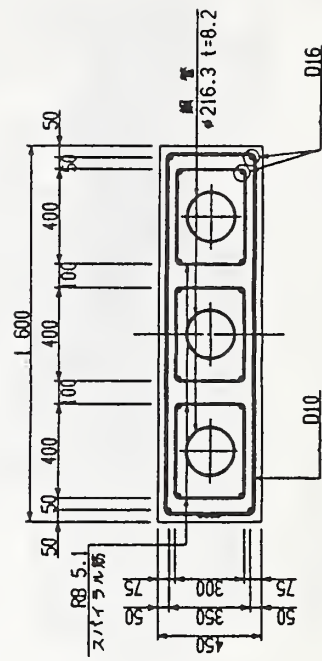
Figure 6. Steel Tube Type Arrangement Diagram



Specimen Cross Section (Case 1: Standard Specimen)



Specimen Reinforcement Diagram (Case 3)



Specimen Cross Section (Case 9)

Figure 7. Outline of Specimens

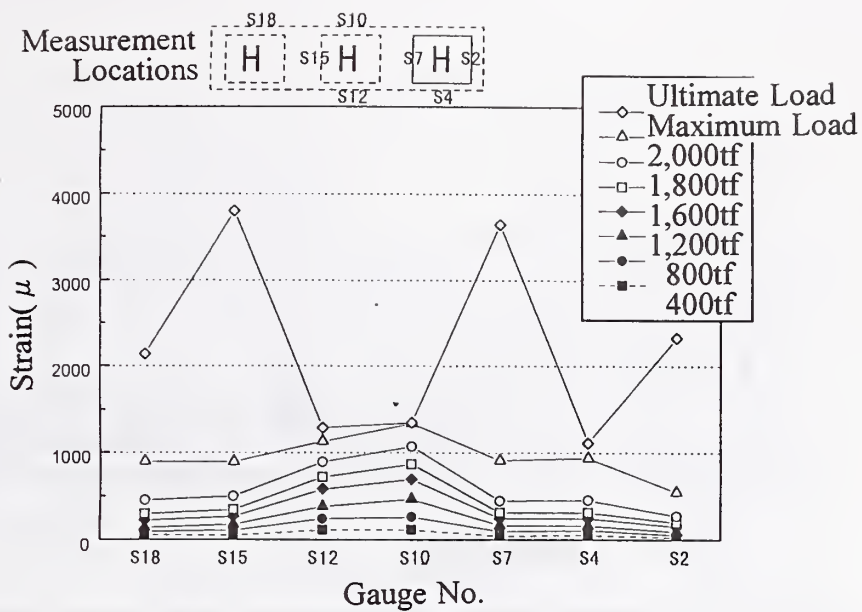


Figure 8. Strain Distribution of Spiral Reinforcement

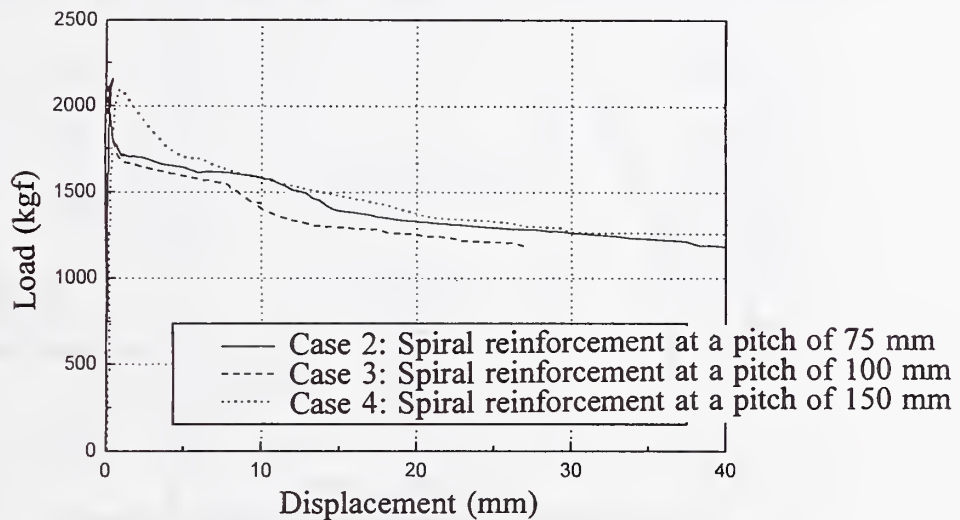


Figure 9. Load - Displacement Under Varying Spiral Reinforcement Pitch

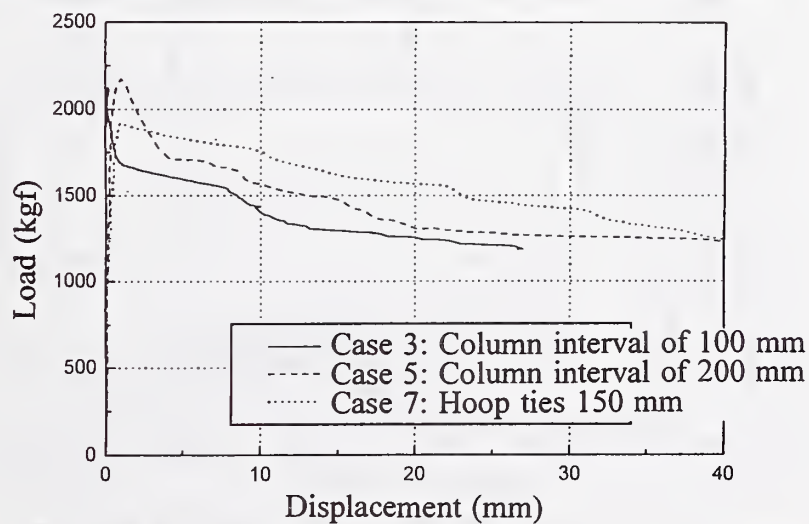


Figure 10. Load - Displacement Under Varying Conditions

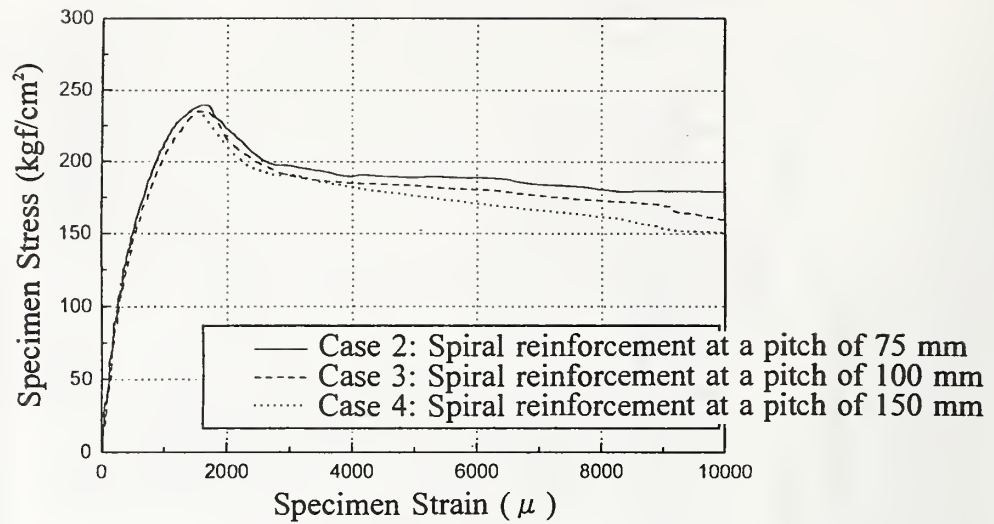


Figure 11. Stress - Strain Caused Under Varying Spiral Reinforcement Pitch

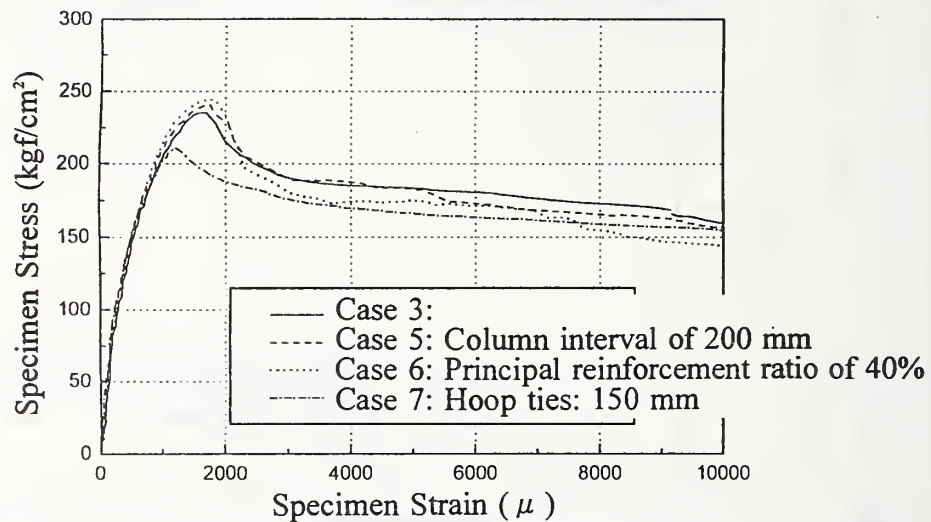


Figure 12. Stress - Strain Under Varying Conditions

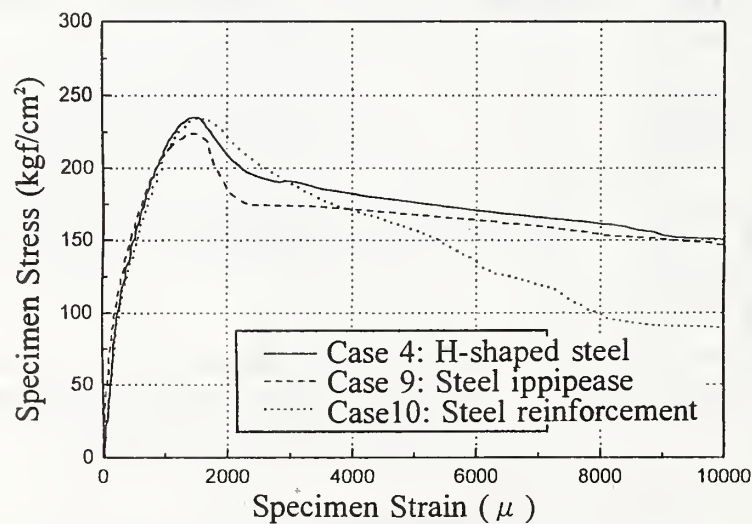


Figure 13. Stress - Strain Under Varying Principal Steel

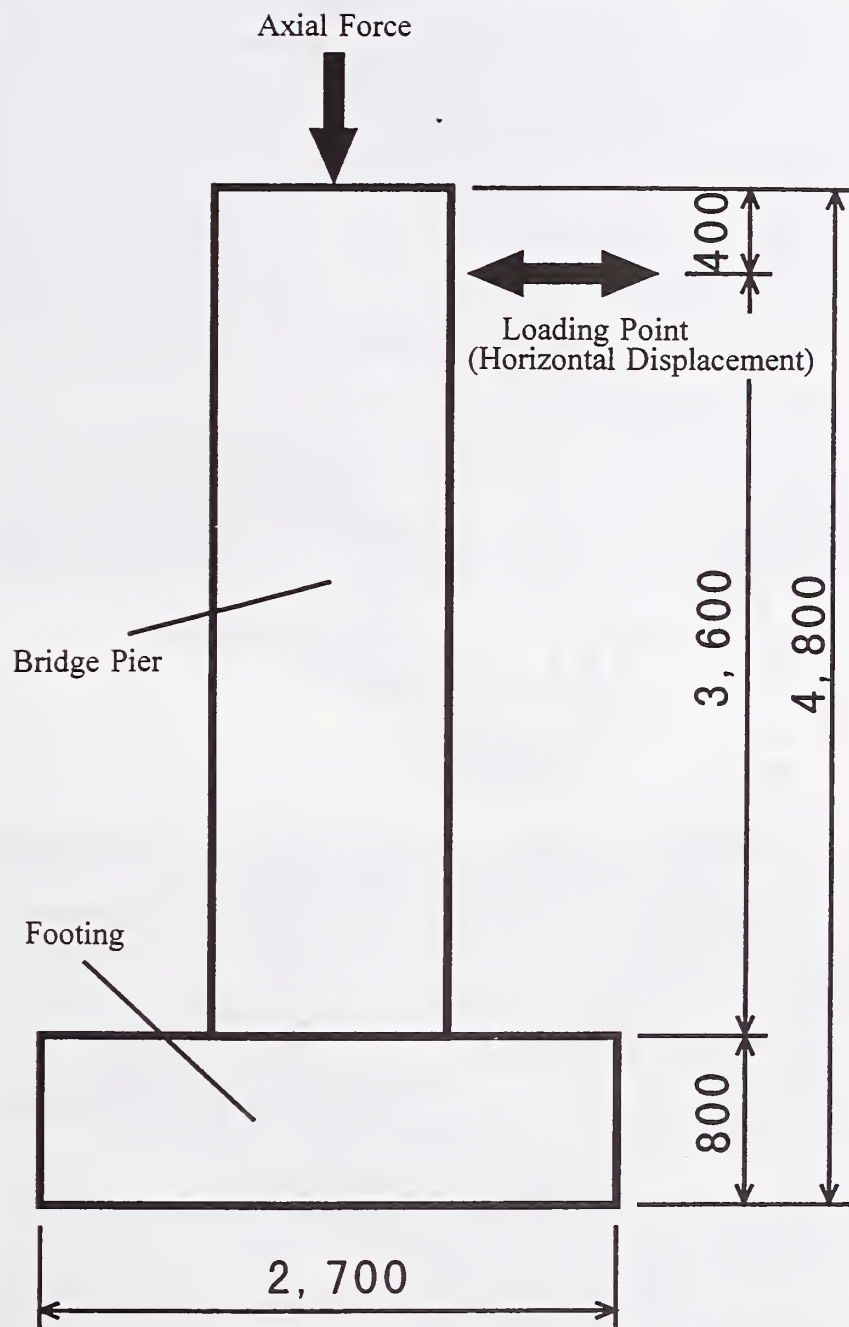


Figure 14. Alternate Loading Testing: Outlines of the Specimens

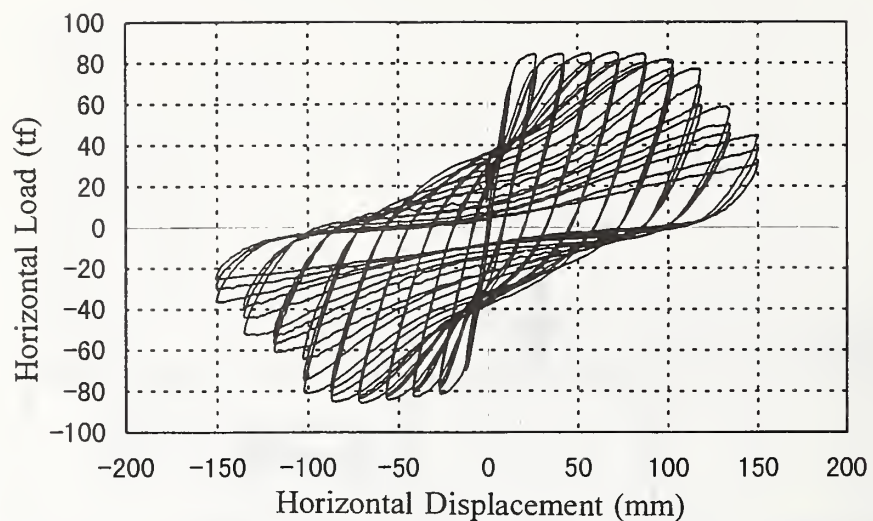


Figure 15. Alternate Loading Testing: Conventional Method

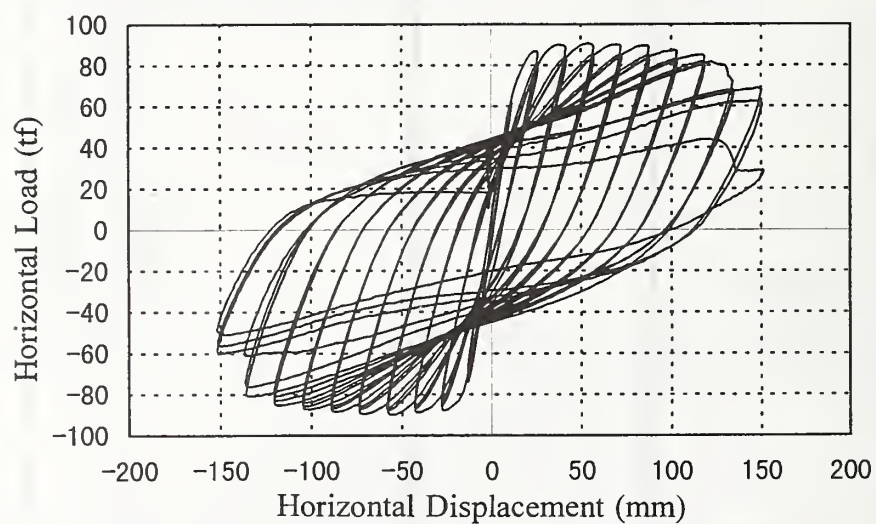


Figure 16. Alternate Loading Testing: H-shaped Steel Model

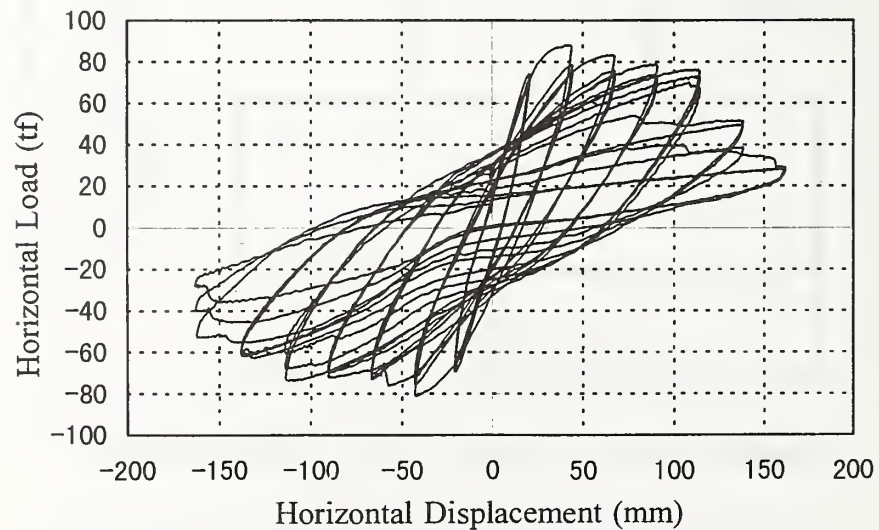
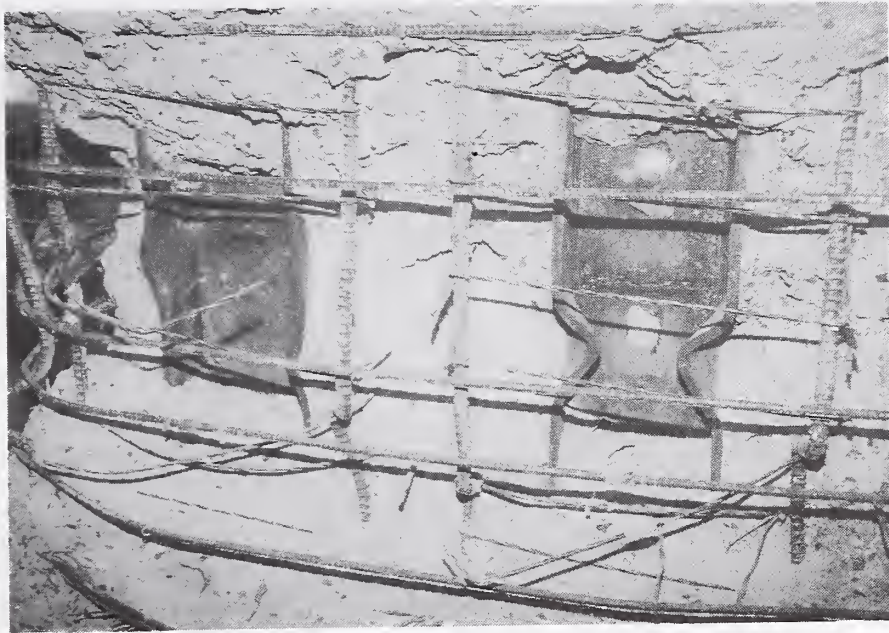


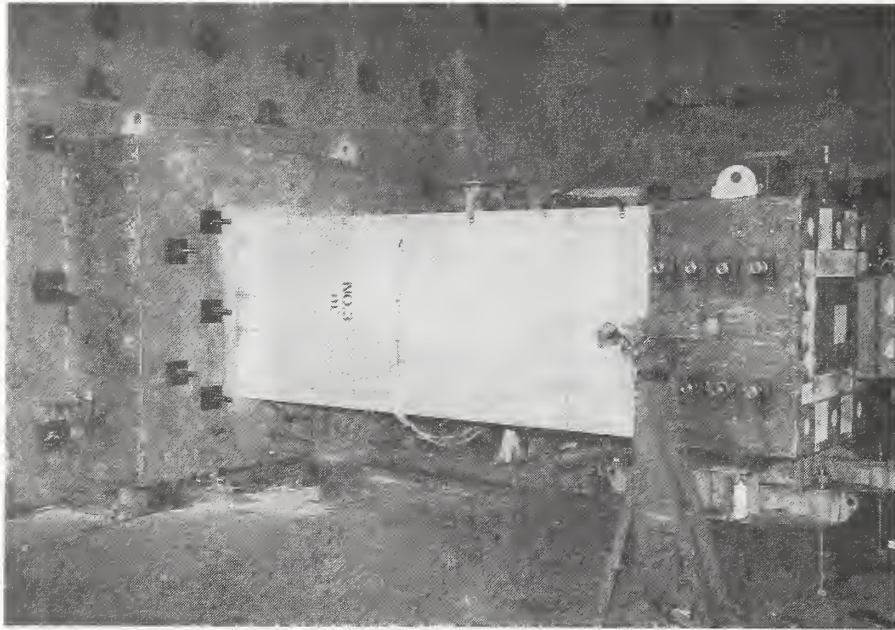
Figure 17. Alternate Loading Testing: Steel Tube Model



Photograph 1. Fracturing of H-shaped Steel



Photograph 2. Fracturing of Steel Pipe

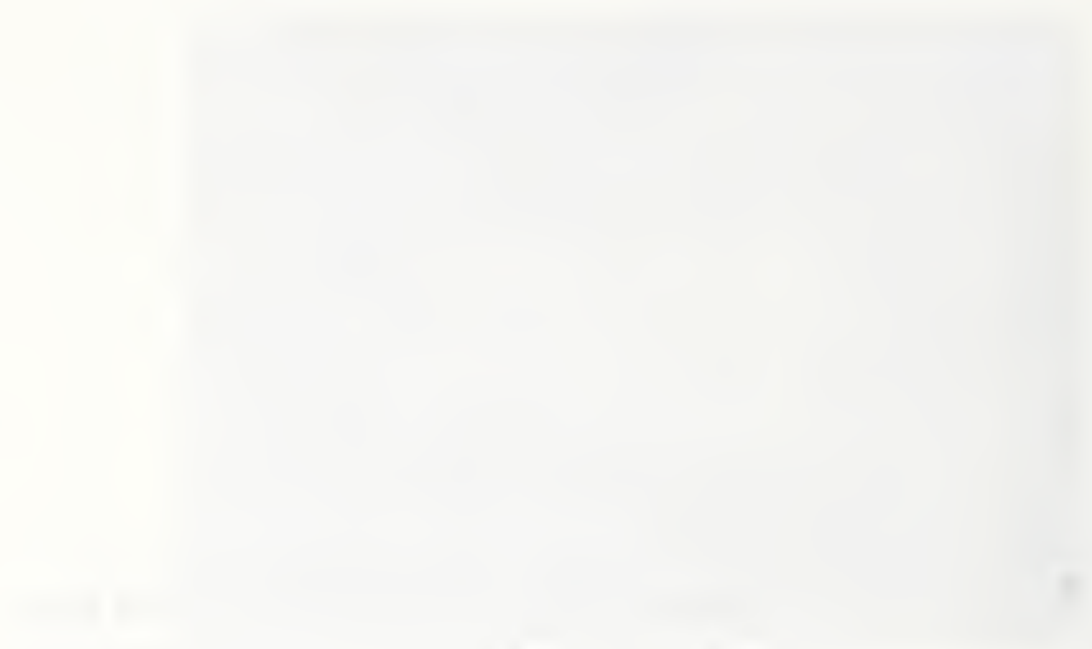


Photograph 3. Alternate Loading Testing

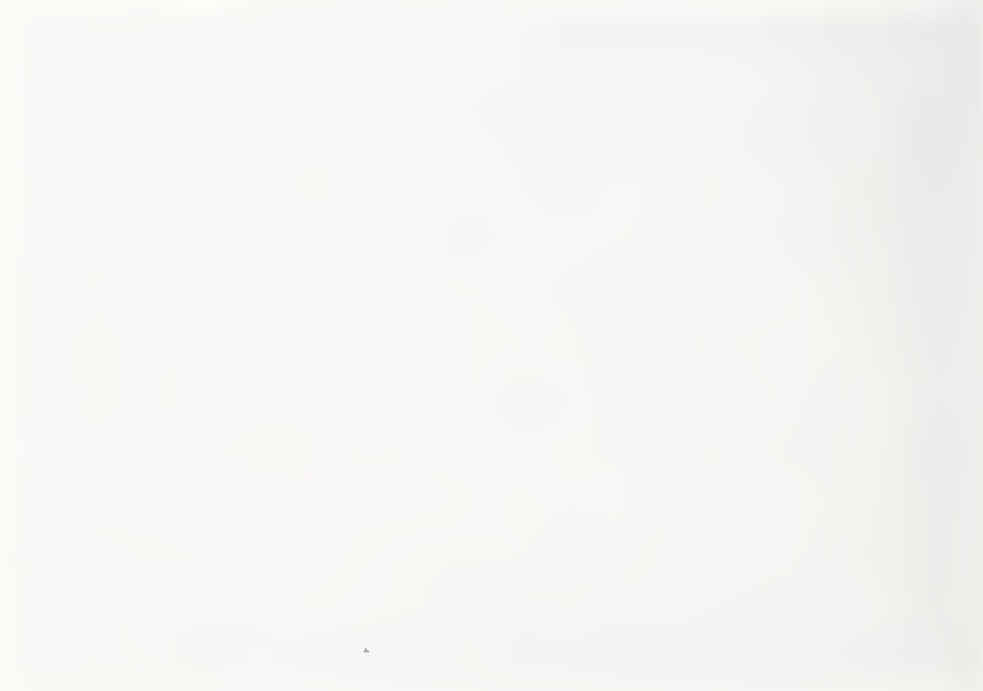


Photograph 4. Case2 H-shaped Steel 10 δ y

**MANUSCRIPTS AUTHORED for
PANEL MEETING but NOT
PRESENTED ORALLY**



11



SHAKING TABLE TEST ON BASE ISOLATED HOUSE MODEL

by

Hiroyuki Yamanouchi¹⁾, Mitsumasa Midorikawa²⁾ and Masanori Iiba³⁾

ABSTRACT

Base isolation is very effective on keeping safety during earthquakes(reduction of acceleration response at floors and inter-story drifts of structure, etc.). In case of houses, it is difficult to elongate a period of building by laminated rubber bearing isolators because of the light weight of building. In addition to rubber bearing devices, sliding and rolling type devices are needed to be developed or applied. In this paper, the effects of base isolation on response of houses and mechanical characteristics of various kinds of seismic isolators will be discussed. Shaking table tests of base isolated house models were carried out. Various kinds of isolators, such as rubber, sliding, and rolling bearings were tested. The effect of these isolators on the response of a superstructure during earthquakes has been demonstrated, through the comparison with response for a non-isolated house. It is shown that the response of houses is remarkably dependent on characteristics of isolators.

Key words : Base Isolation,

House,

Shaking Table Test,

Earthquake Response,

Effect of Isolation

1. INTRODUCTION

Many structures suffered from the 1995 Hyogoken-Nanbu Earthquake. Some buildings have collapse of 1st or intermediate stories¹⁾. Engineers and researchers recognized the necessity for countermeasures against earthquakes. Since the earthquake occurred in the gray dawn (5:45am), there were many persons which were dead and injured at their houses.

Two buildings with base isolation were

constructed in Kobe City. The observed earthquake motion in the buildings showed the effect of base isolation on reduction of acceleration response²⁾. After the earthquake, many low- and medium-rise buildings with isolators have been designed and constructed. But base isolation of individual houses has not become popular.

Base isolation is very effective on keeping safety during earthquake(reduction of acceleration response, at floors and inter-story drift response, and protection from overturning of furniture, etc.). In order to promote construction of base isolated houses and development of isolator devices for houses, required performance for base isolated houses has to be clarified. Building Research Institute has a project on this theme in collaboration with house builders and isolator device companies³⁾.

Base isolated buildings in Japan and current issues for spreading base isolated houses are summarized, and shaking table test results of base isolated house models are discussed. Various kinds of isolators, such as rubber, sliding, and rolling bearings were tested.

2. RECENT TENDENCY OF BASE ISOLATED BUILDINGS IN JAPAN

Figure 1 illustrates the number of base isolated

1) Director, Codes and Evaluation Research Center, Building Research Institute, Ministry of Construction, 1, Tatchara, Tsukuba-shi, Ibaraki-Ken, 305-0802, Japan

2) Associate Director for International Codes and Standards, Codes and Evaluation Research Center, ditto

3) Head, Geotechnical Division, Department of Structural Engineering, ditto

buildings in Japan by fiscal year. The number of buildings is classified by building use. The number from 1985 to 1994 (before 1995 Jan.17 Hyogoken-Nanbu Earthquake, JMA M7.2) is summed up. Table 1 shows kinds of isolators by year. As isolators, lead rubber, high damping rubber, and natural rubber bearings with lead and steel dampers have been much used.

Table 1 Kind and Number of Isolators Utilized for Buildings in Japan

Type of Device	year				total
	1985-1994	1995	1996	1997	
HDB	13	26	79	36	154
LRB	18	20	49	27	114
NRB+LD+SHD	2	14	37	24	77
LRB+NRB	4	2	21	10	37
NRB+SHD	17	0	2	0	19
LRB+SL	9	0	1	2	12
NRB+LD	4	1	2	5	12
NRB+SL	3	3	0	2	8
NRB+VD	5	1	0	0	6
Others	7	19	34	27	87
total	82	86	225	133	526

LRB: Lead Rubber Bearing SL: Sliding Bearing LD: Lead Damper
 HDB: High Damping Rubber Bearing SHD: Steel Hysteresis Damper
 NRB: Natural Rubber Bearing VD: Viscous Damper

The number of base isolated buildings in 1995 is almost equal to the sum of that in the past. The number increased in 1996. Before the Hyogoken-Nanbu Earthquake there are offices and research centers for building use. On the other hand, residential buildings, offices and hospitals have been designed after the earthquake.

The reason why base isolated buildings have been constructed after the earthquake seems that the effects of base isolation were demonstrated through the 1994 Northridge Earthquake in USA and the 1995 Hyogoken-Nanbu Earthquake. The earthquake motions of base isolated building (6-story, steel-reinforced concrete structure) constructed in the mountainous area were observed as shown in Fig. 2. The ratio of the maximum response acceleration of 1st and 6th floors to that of foundation in the east-west direction are 0.35, 0.34, respectively ²⁾. As the building is constructed on very stiff soil ground, the ground motion contains much high frequency component. Unfortunately there was no base isolated building in the area of much damaged on buildings, road and rail ways, and the

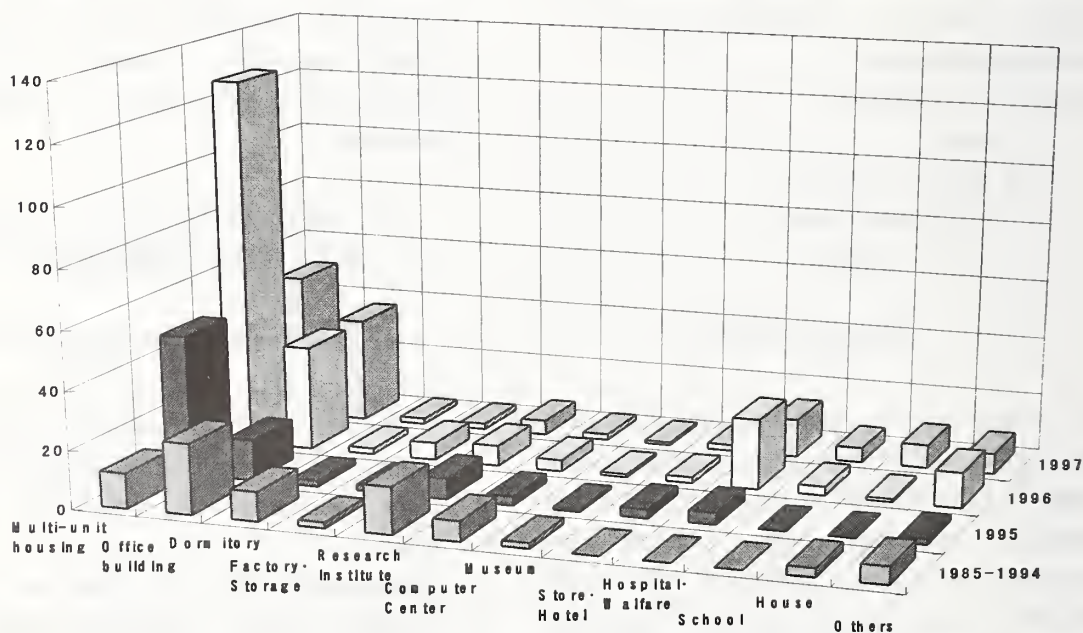


Fig.1 Number of Base-isolated Building and Building Use

reclaimed ground along the sea coast.

3. ISSUES OF SAFETY AND SPREAD OF BASE ISOLATED HOUSE

In order to promote the development of isolator devices and spread base isolated houses, the required performance for base isolated houses shall be made clear. Many issues shall be necessary to be discussed. Following items are taken into consideration for the performance of base isolated houses.

1) Weight of building is relatively small.

In addition to laminated rubber bearing devices, sliding and rolling type devices are needed to be developed.

2) Countermeasures against wind is important.

Even if the behavior of building during earthquakes is sufficient, it is not acceptable that the habitability in daily life and during strong wind will be insufficient.

3) Reinforcement of 1st floor and foundation is added.

In case of houses without base isolation, weight of buildings is transferred to foundations through sills. As the sills are put on the foundation, the sills are not necessary to support the weight of floors. In case of base isolated houses, girders are necessary to support the weight of 1st floor. The dimensions of

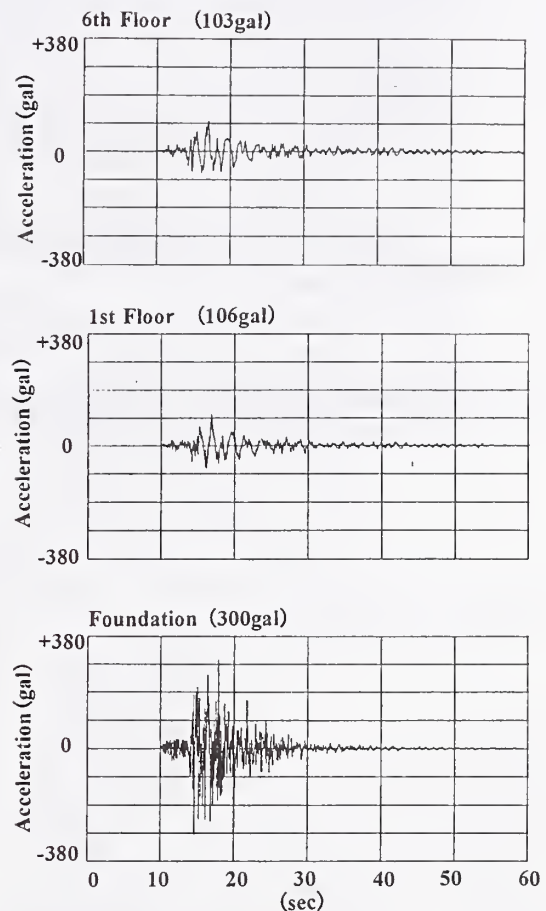


Fig.2 Earthquake Motion Records(EW-direction)in Base-isolated Building in 1995 Hyogoken-Nanbu Earthquake(Ref.2)

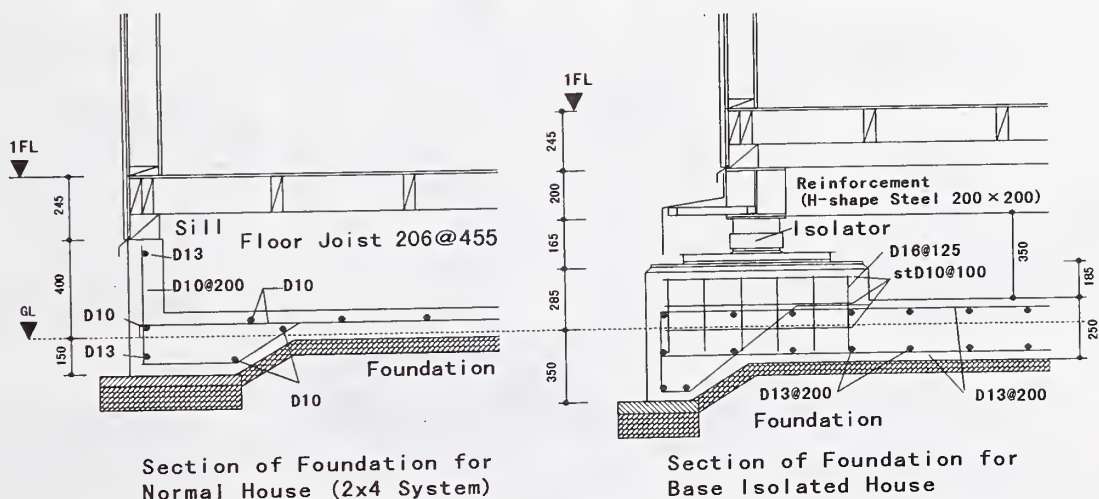


Fig. 3 Section of Isolated Story and Foundation

girders are large with increasing distance between concentrated load acts on the foundation, use of isolators. The weight of building is transferred to the foundation through the isolators. Since the individual and mat foundations, or reinforcement of continuous foundation shall be considered.

Figure 3 illustrates a section of 1st floor and foundation for ordinary and base isolated houses.

4) Cost performance is important.

Cost for isolation is considerably large. The effort shall be made to reduce the cost for isolation. Standardization of isolator devices and simplification of building confirmation system are necessary.

In Article 38 of the Building Standard Law of Japan, there is a description of special material or methods of construction as follows; the provisions of this chapter of those of order or ordinances based thereon shall not apply to building using special building materials and methods of construction unanticipated thereunder, in cases where the Minister of Construction determines that the said building materials or methods of construction are equivalent or superior to the specified in the said provision⁵⁾. As it is judged that the building with base isolation have special materials, the permission of the Minister of Construction is necessary for structural

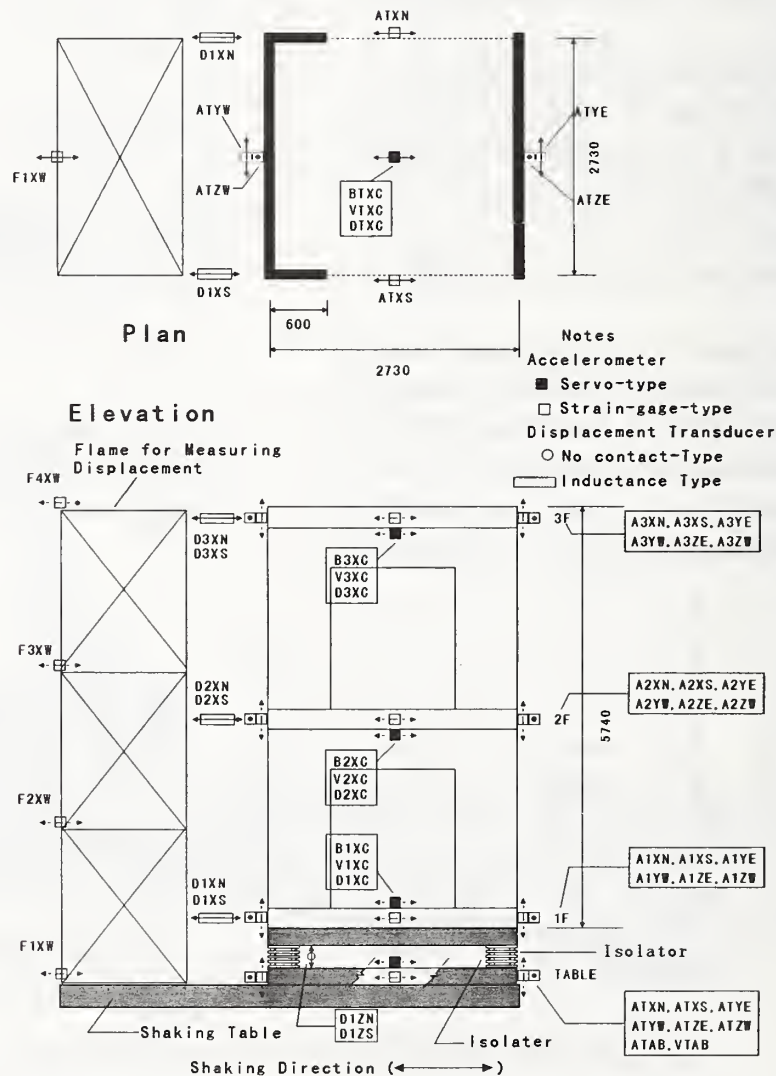


Fig.4 Test Specimen and Arrangement of Transducers

safety of the buildings.

4. SHAKING TABLE TEST ON BASE ISOLATED HOUSE MODELS

4.1 Test Specimens

To solve the issue that houses are relatively light, the shaking table test on base isolated model with isolators of different mechanical properties was carried out. Effects of isolation on response of houses will be discussed.

A specimen for house model is a wood frame(2 x 4 inches structure) with 2 stories (story height 2.7m and 2.73 x 2.73m in plan), as shown in Fig. 4. The house model has two plywood plates with 60cm in width and 9mm in thickness to keep stiffness in the vibrating direction. The natural period and damping ratio of the house model with fixed base are 4.2 Hz and about 3%, respectively.

The experiment was conducted on the base isolated specimens with various kinds of isolators. Typical isolators used in the test are shown in Fig. 5. One is the rubber bearing device with multi layers(Device A). The second is the sliding bearing device which is called the Friction Pendulum System(Device E). The third is the rolling bearing devices (Device G).

The isolators were installed at each corner of the house and between two steel frames. In the case of the

rubber bearing isolators, an additional weight (about 8 tons) was attached in the steel frame to elongate a natural period of isolated models. In order to measure relative displacement of the specimens, there was a tall frame in neighborhood of the specimen.

4.2 Excitation and Measurement

Methods of excitation to the specimen are as follows.

1)Free vibration

Characteristics of the model (natural frequency and damping ratio) will be obtained by free vibration with initial displacement at roof floor.

2)Shaking table excitation

a) White noise random vibration

To clarify fundamental characteristics of the model (resonant property), the wave form with white noise in frequency domain were used as input motion.

b)Earthquake excitation

To evaluate seismic behavior of the base isolated models and situation in the house, several earthquake motions were used. As earthquake motion records, such as, El Centro(1940, NS component), Taft (1952,EW), Hachinohe Harbor(1968,NS) and Meteorological Marine Observatory at Kobe(1995, NS, JMA Kobe), were selected. Maximum amplitude of the earthquake excitation was adjusted by maximum velocity of

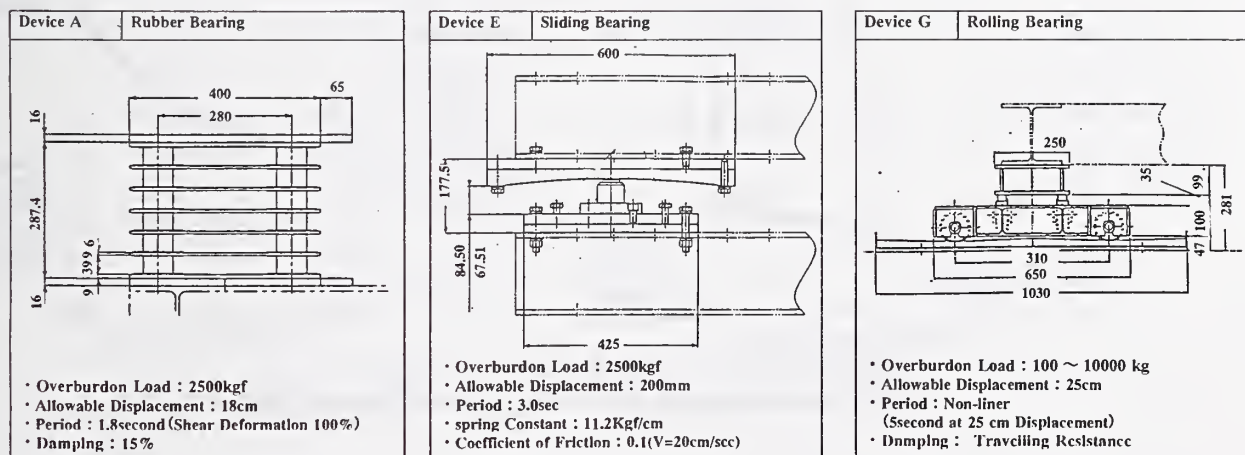


Fig. 5 Representatives for each kind of Isolators

displacement of isolated layer with sliding system(E) is smaller than those with another systems(A and G). The sliding system is effective to reduce the displacement of isolator.

Inter-story drifts of superstructure are shown in Fig. 11. The story drifts of 1st and 2nd story without base isolation subject to the Kobe Earthquake of 50cm/s are 1/128 and 1/196, respectively. In case of isolated houses with devices A, E and G, they are 1/410 and 1/443, 1/385 and 1/500, and 1/1220 and 1/1282, respectively. As the inter-story drifts of isolated house are 0.1 to 0.4 times of those of non-isolated house, the base isolation will be sure to protect from not only severe damage on structural elements but that on non-structural elements.

5. CONCLUSIONS

Required performance for base isolated house are discussed in the research activities in collaboration with house builders and isolator companies. There are a lot of issues to be solved to spread base isolation of houses, compared with those of low-and medium-rise buildings.

To solve the issue that houses are relatively light, the shaking table test on base isolated model with isolators of different mechanical properties was carried out. The effect of these isolators on the response of superstructure during earthquakes has been demonstrated. It is shown that the response of houses is remarkably dependent on characteristics of isolators.

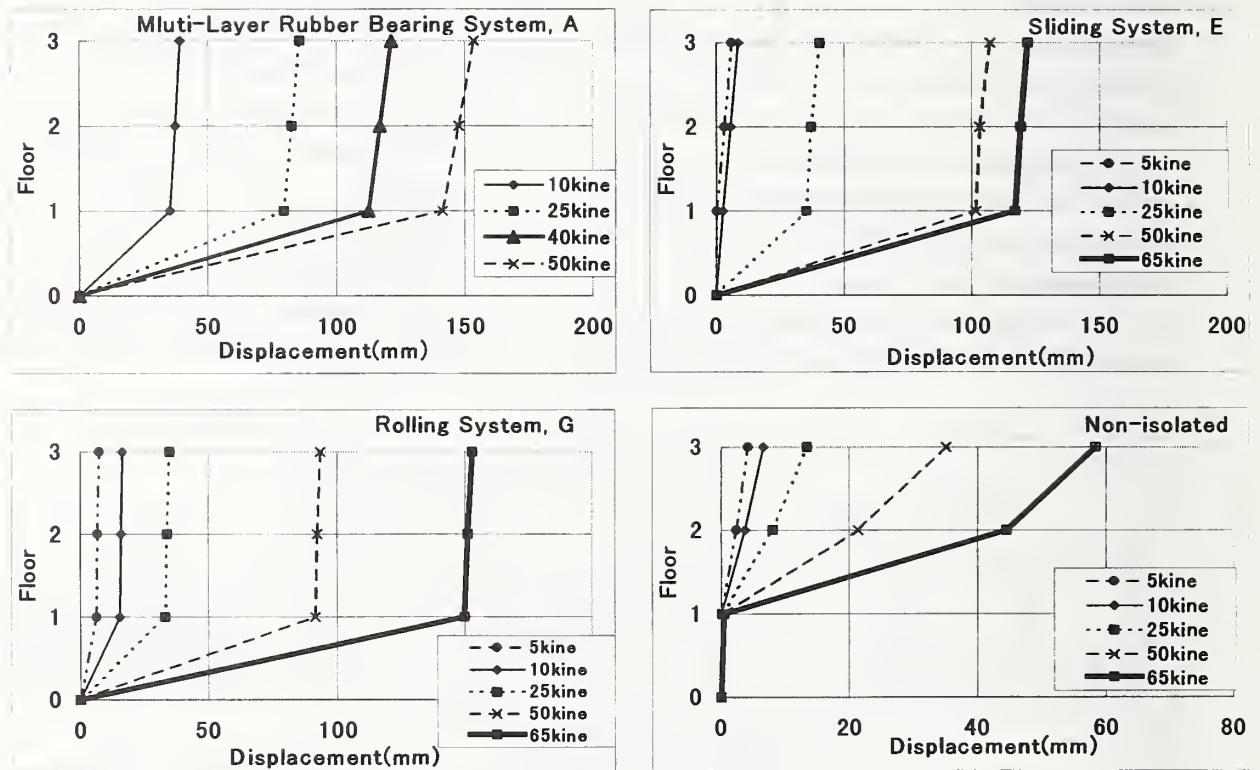


Fig. 10 Distribution of Maximum Displacement Response(JMA Kobe NS)

ACKNOWLEDGEMENT

The shaking table test and data analysis were conducted under the committee on cooperative research "Development of seismic isolated house(chaired by Mr. Shoichi Yamaguchi, president of Tokyo-Kenchiku structural Engineers). The authors express our sincere thanks to the members of the committee.

REFERENCES

1. Building Research Institute : A Survey Report for Building Damages due to the 1995 Hyogo-ken Nanbu Earthquake, 1996 March
2. The Building Center of Japan : Base isolated Buildings -Technical development and Earthquake Motion Observation Records Part 2-, 1995 June (in Japanese)
3. Yamanouchi H., M. Midorikawa and M. Iiba (Editor) : Research and Development on Base Isolation Technology for House -Survey of Knowledge and Shaking Table Test on House Model, for Evaluation of Performance on Base isolated House-, Kenchiku Kenkyu Siryo No. 89, 1997 March (in Japanese)
4. Date by the courtesy of Building Center of Japan
5. Building Guidance Division & Urban Building Division , Housing Bureau, The Ministry of Construction(Editor) : The Building Standard Law of Japan, The Building Center of Japan , 1990 Sep.

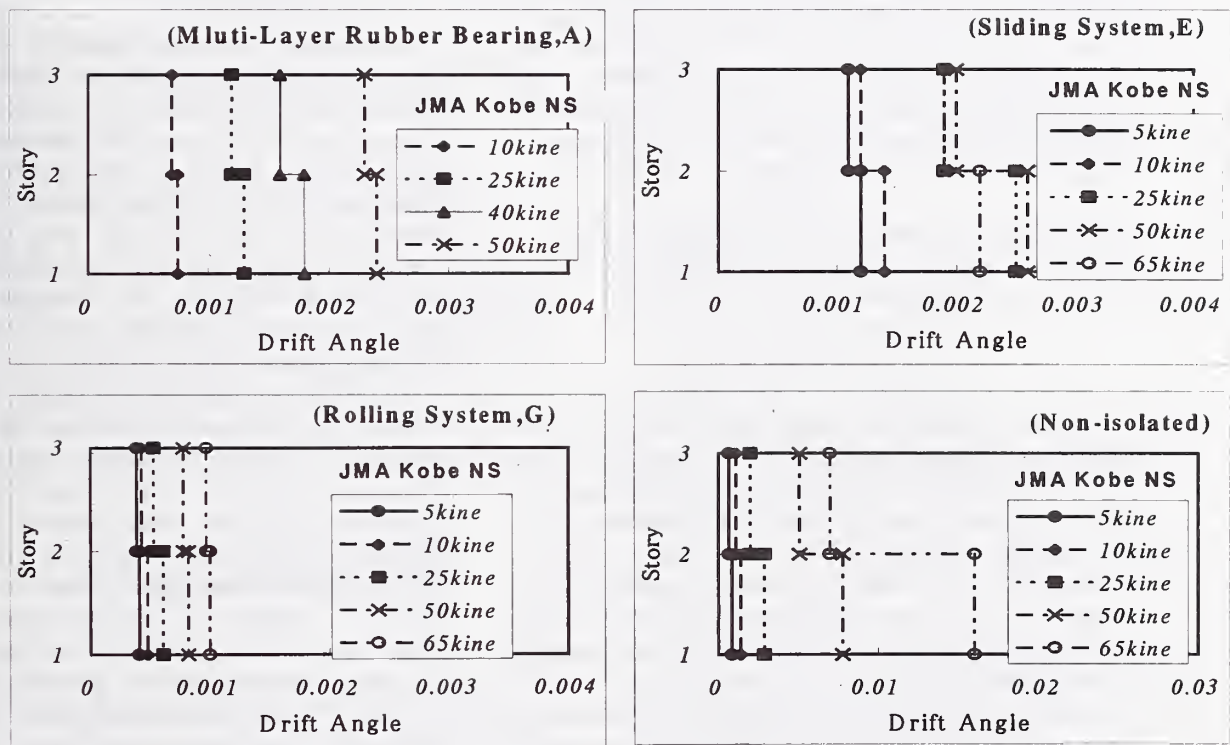


Fig. 11 Inter-story Drifts of House (JMA Kobe NS)

Dense Strong Motion Instrument Array in Sendai

by

Izuru Okawa¹⁾, Toshihide Kashima²⁾ and Shin Koyama²⁾

ABSTRACT

This paper describes an on-going earthquake observation project in Sendai, Japan. The observation system includes 11 observation sites and a control center. A number of records with intermediate amplitudes have been obtained to this date.

In this report, the earthquake observation system is introduced at first. The description includes the outline of the geological condition of the Sendai area, the objective area of the observation, the surface geology of the 11 observation sites from the investigation in sites, and the recorded data until the project started. During the period, the seismic activity of the area was not so high. Therefore, the amplitudes of acceleration records are not large enough to be called "strong motion". However, these data are essential for the purpose to examine the dynamic amplification property of the surface soils.

Key words: Instrument Array, Local Site Effect, Strong Earthquake Motion, Surface Geology

1. INTRODUCTION

It has often been said that the damage to structures during earthquake is more or less associated with the subsoil conditions on which they stood. It means that characteristics of earthquake ground motions at ground surface greatly reflect the dynamic properties of underlying soils. However, the dynamic property varies with surficial geology such as irregularity and inhomogeneity of soil deposits.

The Building Research Institute (BRI) started the earthquake observation program 40 years ago, when the development of the recording system and analysis programs was underway.

In 1983, BRI started to install instruments in Sendai City area to accumulate earthquake records focusing on the effect of surface geology on seismic motion with a long-term vision of re-establishing the methodology to specify design

input motions for buildings¹⁾. Private companies (16 general contractors and a group of design firms) cooperatively merged this project from 1987. At the end of the fiscal year of 1989, the recording system was completed, consisting of 11 sites including outcrop rock, reclaimed land, soft soil ground around which considerable damage was found during the 1978 Miyagi-ken-oki earthquake²⁾.

This report introduces the earthquake recording system and results of analyses of the recorded motions. In addition, other observation projects operated by BRI are introduced.

2. ARRAY CONFIGURATION

The Sendai area is assigned as one of sites with the highest priority in Japan for the deployment of strong motion instrument arrays. The array system of our project consists of eleven sites as shown in Fig. 1, with spacing of 3 to 4 kilometers on the E-W line passing through the center of the city, and the N-S line passing through Nigatake and Oroshimachi. These areas, i.e., around Nigatake and Oroshimachi, also suffered severe structural damage during the 1978 Miyagi-ken-oki earthquake.

Four of the sites, SHIR, OKIN, TRMA and NAKA, are located where the thickness of alluvium is 60 to 80 meters. A fault, Rifu-Nagamachi tectonic line, is also the line of separation of the two zones. Most of the damage occurred on the eastern side during the 1978 Miyagi-ken-oki earthquake. Table 1 shows the installation depths of accelerometers, and the shear wave velocity of the layer in which the lowermost accelerometer is placed. Also shown in Table 1 is the soil classification, specified in the Building Standard Law of Japan, for each of the observation sites.

1) Head, International Institute of Seismology and Earthquake Engineering (IISEE), Building Research Institute (BRI), Ministry of Construction, Tsukuba Science City, 305-0802, Japan

2) Senior Research Engineer, ditto

3. OBSERVATION SYSTEM

Each site has three accelerometers arranged vertically. One on the surface, one at 20 to 30 m underground with a shear wave velocity of 300 to 400 m/s, and one on the base layer having a shear wave velocity of 700 to 800 m/s and underlying at depth of 50 to 80m in the area. A controlling and monitoring center is located at BRI in Tsukuba and is connected to a sub-controlling-center in Sendai via public telephone line. The sub-controlling-center is facilitated in the building of the Local Headquarters of Ministry of Construction for the Tohoku (northeastern) district of Japan in Sendai. The sub-controlling-center is further connected to all observation sites via exclusive telephone lines. Figure 2 shows a block diagram of the entire system.

The array observation system consists essentially of three accelerometers, an amplifier, an A-D converter, a pre-event memory, a digital magnetic tape recorder, and a clock. In order to obtain both a large dynamic range and a high resolution in recording, a digital system is used. Specifications of the array observation system are shown in Table 2.

4. OBSERVED EARTHQUAKES

Table 3 lists acceleration records are used in this report. The JMA (Japan Meteorological Agency) Seismic Intensities for those earthquakes were 3 or above at Sendai. The JMA magnitudes of earthquakes ranged from 4.1 to 8.1 and epicentral distances extended to 800 km. The maximum acceleration was 106 cm/s^2 on the ground surface at NAGA site.

5. CHARACTERISTICS OF EARTHQUAKE MOTIONS

In this chapter, the geological condition and configuration of accelerometers are outlined for each site. And then amplification effect of subsoil is discussed through the comparison of spectral ratios between observational results and analytical ones. Fourier spectral ratios in the E-W direction and theoretical transfer functions of SH-wave with damping ratios of 5 % and 10 % for each site is shown in Figs. 3 to 13. All Fourier spectra are smoothed using the Parzen window with a width of 0.2 Hz. Fourier spectral ratio is obtained from a spectrum of the record on the

ground divided by one at the lowermost point.

(1) MIYA site (Miyagino)

This site is classified as lowland, close to the border between the hill. The Tertiary Pliocene layer is found at 26 meters below the surface. The degree of compaction of the Tertiary layer is lower at the upper layer, which changes to sand. The compaction for the lower layers is high. The sand-gravel layer, found at the upper part of the Tertiary, contains clay, and is firm.

Fourier spectral ratios in the E-W direction are shown in Fig. 3. The broken line and the dotted line indicate transfer functions of SH-wave with damping ratios of 5 % and 10 %, respectively. Large amplification can be observed in the frequency range near 2.4 Hz on both of observed and theoretical results.

(2) NAKA site (Nakano)

This site lies on the basin of Nanakita-gawa River. The Tertiary layer is found approximately 58 meters below the surface. Thick alluvia layer lies above the layer. This site belongs to the soft soil category. The Tertiary pelite or tuff deposit is fairly firm but fragile against a light hammer blow. The upper layer is rather loose, but the lower is fairly firm.

Fourier spectral ratios of observed records and theoretical transfer function are drawn in Fig. 4. Shapes of both results are in full accord with each other and peak at a frequency of 1.3 Hz.

(3) TAMA site (Tamagawa)

This site is on the Tertiary rock formation except for the thin fill layer on the surface. The rock consists mainly of tuff and sand. The upper portion of the rock is loose, the lower is extremely firm. TAMA site can be the reference site to discuss amplification effect of surface geology at other sites.

Figure 5 shows spectral ratios and theoretical transfer functions. Peaks of spectral ratios appear at a frequency of 7.5 Hz. However, these are not so high as theoretical peaks.

(4) ORID site (Oridate)

This site consists mainly of relatively soft pelite or tuff. The lower part of the layer is andesite with upper part of andesite being weathered and fragile. The layer at more than 70 meters below the surface is fairly firm.

Through the comparison between observed

and theoretical results in Fig. 6, good agreement can be recognized

(5) TSUT site (Tsutsujigaoka)

Up to 5 meters below the surface is a loose layer consisting of diluvial sand-gravel, clay, and fill. The Tertiary deposits are below the layer. The upper part of the layer consists of a firm sandstone layer, and a mostly firm sand-gravel-like layer. The deeper we go, the firmer the soil becomes, but it is very fragile.

Figure 7 points out remarkable amplification at the higher frequency range of 5 to 7 Hz. The agreement between Fourier spectral ratios and transfer functions is also good.

(6) TRMA site (Tsurumaki)

This site is on the basin of Nanakita-gawa River. Due to the erosion of the riverbed, the Tertiary layer lies at the depth of valley-shaped soil structure. Consequently, the depth of the Tertiary layer extends as much as 80 meters. The layer is sandstone. The consolidation is low and the layer is fragile. The alluvial deposit contains surface layers, partly thin sand or clay layers. Most of the layers of the deposit are sand gravel, which are fairly firm.

The first predominant frequency of the transfer function is 1.26 Hz, but peaks of Fourier spectral ratios appear at the higher frequencies and are lower than the peaks of transfer functions, as shown in Fig. 8.

(7) OKIN site (Okino)

This site is on the basin of Natori-gawa River. The Tertiary layer is found at approximately 50 meters below the surface. It consists mainly of sandstone, relatively firm but fragile. The upper alluvial part has layers of clay and sand at the uppermost, the remaining part is mostly sand gravel. The sand gravel layer contains clay and is fairly firm.

Figure 9 indicates theoretical transfer function and Fourier spectral ratios of observed acceleration records. The spectral ratios generally accord with the theoretical results, although vary widely.

(8) SHIR site (Shiromaru)

This site, along with Okino site, is on the basin of Natori-gawa River. The Tertiary layer is found at approximately 50 meters below the surface. The upper part of the layer is getting

weathered, and has a non-consolidated portion. On the other hand, the lower part is fairly firm and a sand-gravel layer is found as well. The alluvial layers consist mostly of sand-gravel layers, except for the surface layer of approximately a 3-meter thickness, which also contains clay fines, and is a fairly consolidated layer. The diameters of some of the gravels are large.

Spectral ratios and transfer functions in Fig. 10 show similar trend to results of OKIN site. The deviation of spectral ratios is relatively large.

(9) TRGA site (Tsurugaya)

A Tertiary layer is found below the surface fill. The layer contains sand and tuff sandstone. The consolidation is fairly high near the surface.

Figure 11 shows quite low agreement between Fourier spectral ratios and theoretical transfer functions. Physical parameters of soil layers must be reevaluated.

(10) NAGA site (Nagamachi)

This site is on the basin of Natori-gawa River, and also close to the Rifu-Nagamachi tectonic line. The Tertiary layer is found at the depth of approximately 57 meters below the surface. The layer consists mainly of sandstone. The consolidation of the upper part of the layer is low. The upper part of the alluvial deposit contains loose composite layers of clay, sand, and gravel, up to the depth of approximately 30 meters from the surface. The lower part of the deposit consists of sand gravel containing clay and is fairly firm.

Transfer functions of SH-wave, in Fig. 12, have agreement with observed spectral ratios up to the second predominant period. In the higher frequency range, differences of both become larger.

(11) ARAH site (Arahama)

This site is between Nanakita-gawa and Natori-gawa Rivers. Although this site is classified as a hill, the Tertiary layer is found at a relatively shallow depth. The depth of the layer is approximately 35 meters below the surface, and consists of sandstone and pelite. The consolidation is relatively low. The upper alluvial deposit consists of layers of sand and silt, and makes a formation of a loose soil deposit. A sand gravel layer is found, with a thickness of 4 meters, at the interface above the Tertiary layer.

The first predominant period of transfer

functions is 1.22 Hz as shown in Fig. 13. This is the softest ground condition in our observation sites. Although number of records is few, a degree of accordance is satisfactory.

6. OTHER PROJECTS OF BRI

BRI is carrying out earthquake motion observation projects not only in Sendai but also all over Japan. We are briefly introducing other project in this chapter.

(1) Nationwide Strong Motion Observation

BRI has installed strong-motion instruments in major cities throughout Japan. There are now 47 observation sites in operation using the digital strong-motion instrument. The objects of observation are mainly buildings, and the measuring point is usually placed both on the top and in the foundations of the building. Every observation site is connected to BRI via telephone line in order to mitigate maintenance work and to collect data immediately.

The observation network has obtained many noteworthy records. For example, in the 1993 Kushiro-oki (Off Kushiro) Earthquake, 711 gal was recorded as the peak acceleration on the ground surface at Kushiro Local Meteorological Observatory. Also, in the 1994 Sanriku-haruka-oki (Far off Sanriku) Earthquake, an enormous acceleration record was obtained in the building next to the severely damaged old Hachinohe municipal office building.

(2) Strong-Motion Instrument Network in the Metropolitan Area

The 1995 Hyogo-ken-nanbu Earthquake (Kobe Earthquake) awakened us again to the importance of disaster prevention measures for large-scale urban areas. It is important to predict the probability of a future earthquake and its impact, and make as many preparations as possible in anticipation of such an event. It is also very essential to grasp the damage situation immediately to put in effect the necessary countermeasures. BRI has established twenty new observation sites placed radially in the Tokyo metropolitan area. This project aims to investigate the characteristics of the seismic motion affecting the whole Kanto Plain through observation records. The system immediately collects information on the seismic intensity at the time of an earthquake occurrence.

(3) Strong-motion observation at Annex, BRI

The project to observe the complicated behavior of the building and the effect of the soil-structure interaction during earthquakes has been started with the construction of the Urban Disaster Mitigation Research Center (Annex) building in BRI recently. The amplification process by the ground surface layers and the three-dimensional behavior of the buildings are recorded using twenty-two accelerometers placed in and around the annex and main buildings.

7. CONCLUSIONS

The earthquake observation project with dense accelerometer array configuration is now under way. High quality records are being accumulated year by year. We are ready to make these data open to the public via the Internet, hoping the research of ground motion prediction becomes more active and the seismic design methodology for buildings is more upgraded in the future.

The earthquake records used in this study have been obtained in the Dense Strong Motion Earthquake Seismometer Array Observation Project which has been implemented as a cooperative research project between Building Research Institute (BRI), Ministry of Construction and the Association for Promotion of Building Research (KSKS). For the implementation of the project, the steering committee for Dense Strong Motion Earthquake Seismometer Array Observation, which consists of 18 organizations (i.e., BRI, 16 general contractors and a union of design office firms), is organized by KSKS.

REFERENCES

- 1) Kitagawa Y., et al., "Dense Array Observation and Analysis of Strong Ground Motions at Sites with Different Geological Conditions in Sendai", BRI Research Paper No.139, Building Research Institute, July 1994
- 2) Building Research Institute, "Report on the Damage by 1978 Off-Miyagi Prefecture Earthquake" (in Japanese), Research Report of BRI, No.86, pp.75-81, 1978.

Table 1 Location and geology of observation sites and depths of accelerometers

Site name	Abr.	Latitude	Longitude	Soil type*	f_1 (Hz)	Year	V_s (m/s)	Depth (m)		
Miyagino	MIYA	38°15'24"N	140°55'16"E	2	2.40	1984	680	1	22	54
Nakano	NAKA	38°15'14"N	141°00'26"E	3	1.28	1985	720	1	30	61
Tamagawa	TAMA	38°19'03"N	141°00'34"E	1	7.50	1986	1400	2	11	33
Oridate	ORID	38°15'26"N	140°48'39"E	1**	2.06	1987	1050	1	57	76
Tsutsujigaoka	TSUT	38°15'30"N	140°53'36"E	2	2.08	1988	950	1	36	59
Tsurumaki	TRMA	38°15'38"N	140°58'15"E	3	1.26	1988	660	1	25	79
Okino	OKIN	38°13'26"N	140°55'05"E	3	2.14	1988	820	1	17	62
Shiromaru	SHIR	38°11'29"N	140°54'53"E	2	2.70	1988	830	1	20	76
Tsurugaya	TRGA	38°17'16"N	140°54'53"E	2	1.78	1988	1000	2	37	62
Nagamachi	NAGA	38°13'45"N	140°53'01"E	2	1.44	1989	700	1	29	81
Arahama	ARAH	38°13'11"N	140°59'00"E	3	1.22	1989	750	1	31	76

f_1 : Theoretical first predominant frequency, V_s : Shear wave velocity of lowermost layer.

* Soil types according to Japan Building Standard. 1: hard, 2: medium, 3: soft.

** Although the soil condition for ORID site was presumed hard soil, it was confirmed by the soil survey that the surface soils were so heavily weathered that the soil condition type might be assigned to be the second classification.

Table 2 Specifications of the array observation system

Instrument	Specification
Accelerometer	Type: Tri-axial velocity-feedback type
	Frequency range: 0.05 to 30 Hz for 1G
Amplifier and AD Converter	Resolution: 16 bit
	Dynamic range: 96dB
	Sampling rate: 1/100 or 1/200 sec.
Pre-event Memory	Delay device: IC memory
	Delay time: 5 sec.
Clock	Oscillator: Quartz with accuracy of 10^{-7} , 10^{-8}
	Precision: ± 0.01 sec.
	Calibration by: NHK(JBC)
Digital Data Recorder	Medium: Digital magnetic tape with 9 track, half-inch in width and 1600 BPI in recording density

Table 3 List of observed earthquakes

#	Date	Time	M	h (km)	Δ (km)	Max. Acc.	I
8608	1986/10/14	06:11	5.0	53	135	26.2 (NAKA)	3
8615	1986/12/01	5:15	6.0	51	108	29.6 (TAMA)	3
8701	1987/1/9	15:14	6.6	72	191	43.5 (NAKA)	4
8702	1987/1/14	20:04	7.0	119	505	11.1 (NAKA)	3
8704	1987/1/21	8:36	5.5	50	112	48.8 (NAKA)	3
8708	1987/2/06	21:24	6.4	30	178	47.4 (NAKA)	3
8709	1987/2/6	22:16	6.7	35	167	94.1 (NAKA)	4
8717	1987/3/10	12:24	5.6	29	166	15.7 (NAKA)	3
8719	1987/4/7	9:41	6.6	37	136	74.5 (NAKA)	4
8721	1987/4/17	4:23	6.1	45	151	45.3 (NAKA)	3
8724	1987/4/23	5:13	6.5	49	145	75.0 (NAKA)	3
8739	1987/9/4	13:55	5.8	42	185	25.4 (NAKA)	3
8740	1987/10/4	19:27	5.8	51	125	60.1 (NAKA)	3
8911	1989/4/28	0:27	4.9	53	98	29.0 (OKIN)	3
8915	1989/6/24	4:59	4.1	14	11	35.0 (TRMA)	3
8926	1989/11/02	3:26	7.1	0	256	22.8 (TRMA)	3
9217	1992/7/18	17:37	6.9	0	269	11.2 (TRMA)	3
9234	1992/12/18	1:21	5.9	34	160	41.0 (TRMA)	3
9305	1993/1/15	20:07	7.8	101	594	36.3 (TRMA)	3
9325	1993/11/11	9:06	5.5	36	154	18.5 (TRMA)	3
9327	1993/11/27	15:11	5.9	112	51	104.2 (NAKA)	4
9409	1994/8/14	18:06	6.0	42	136	45.3 (NAKA)	3
9410	1994/8/16	19:09	6.0	22	154	22.0 (ARAH)	3
9413	1994/10/4	22:24	8.1	23	806	59.7 (OKIN)	3
9414	1994/12/10	18:26	5.1	51	111	28.4 (NAKA)	3
9417	1994/12/28	21:20	7.5	0	343	35.3 (NAGA)	3
9502	1995/1/7	7:37	6.9	30	261	28.0 (OKIN)	3
9602	1996/2/17	0:23	6.5	6	178	106.4 (NAGA)	4
9604	1996/4/23	13:08	5.2	76	117	75.0 (OKIN)	3
9701	1997/2/20	5:22	5.3	88	99	46.7 (SHIR)	3

M : JMA (Japan Meteorological Agency) magnitude, h : focal depth, Δ : averaged epicentral distance, I : JMA seismic intensity at Sendai

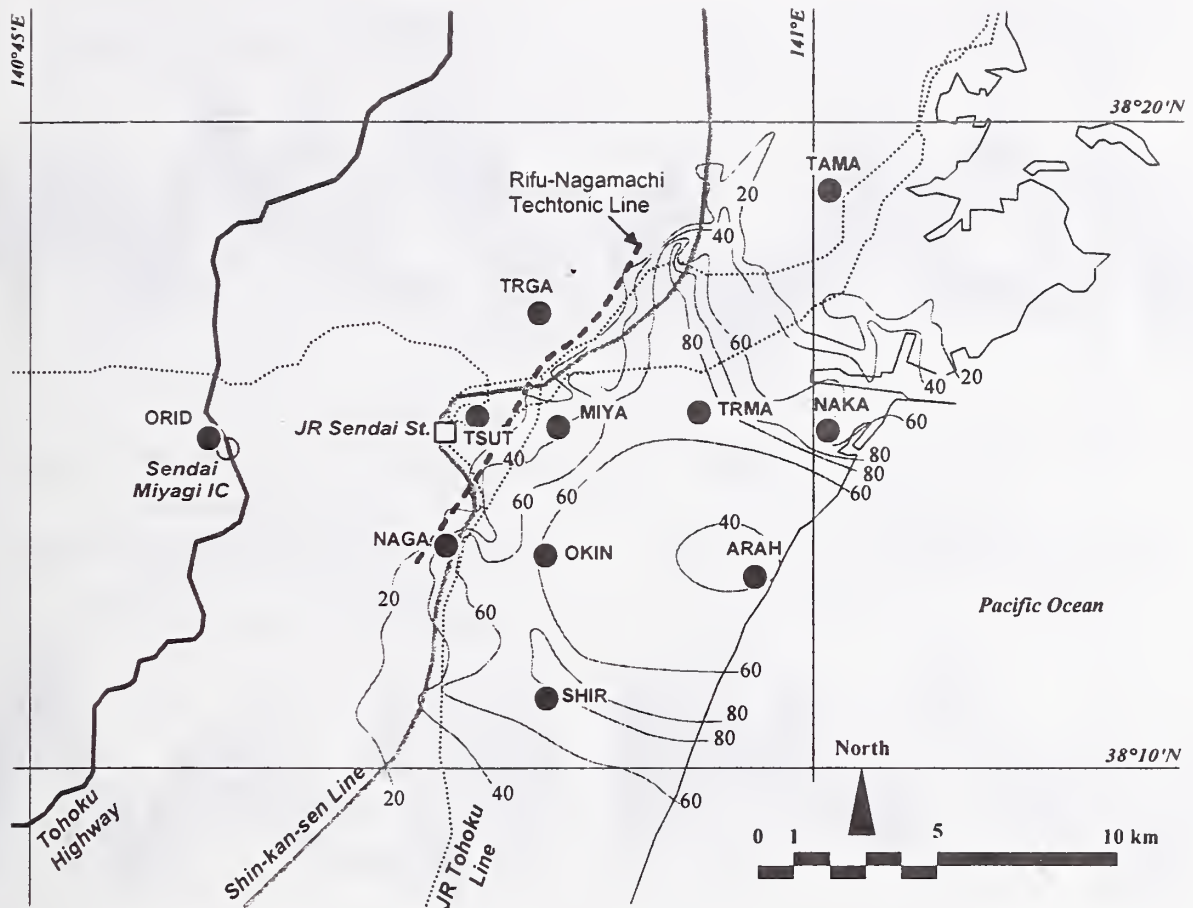


Fig. 1 Location of observation sites in Sendai. Contour lines indicate thickness of alluvium.

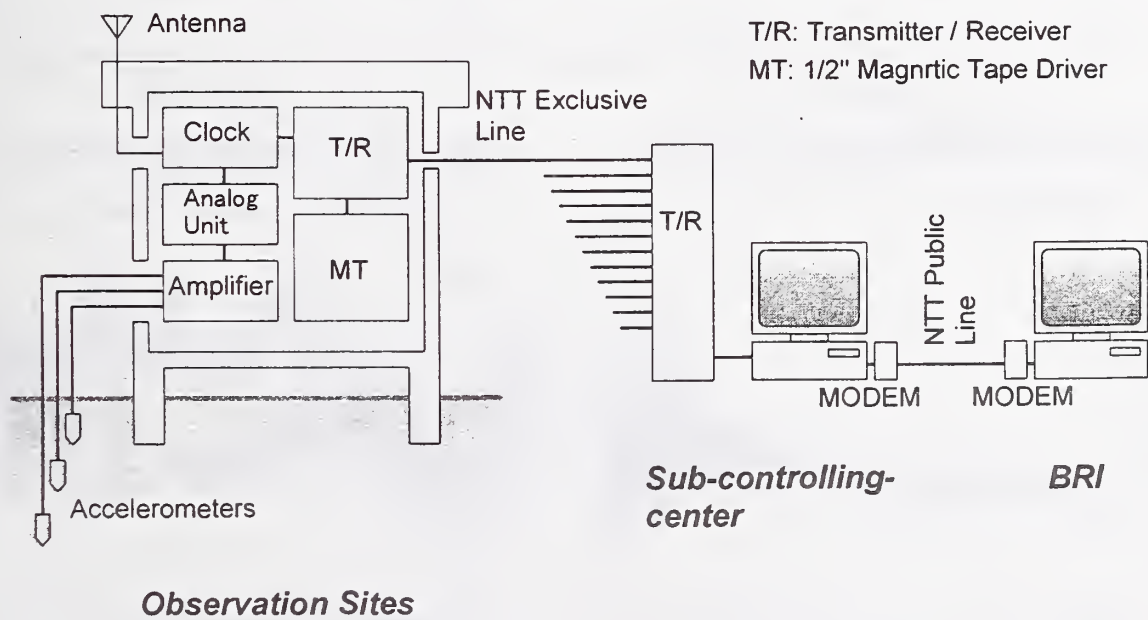


Fig. 2 Block diagram of observation system. Observation sites and the sub-controlling-center are located in Sendai.

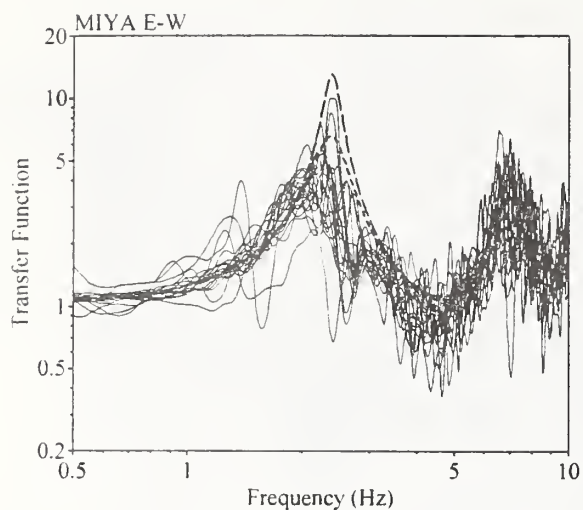


Fig. 3 Fourier spectral ratio at MIYA site

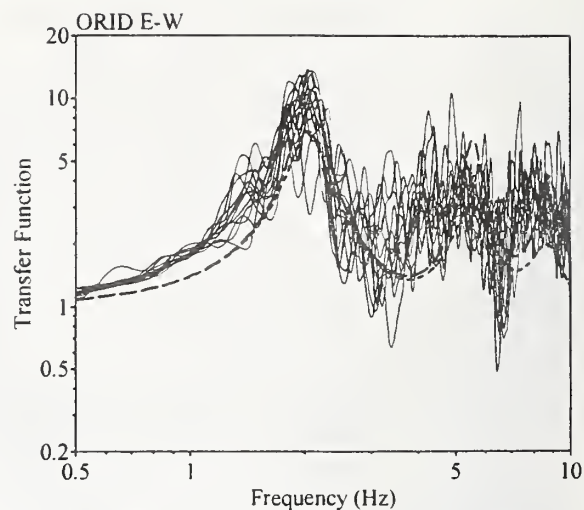


Fig. 6 Fourier spectral ratio at ORID site

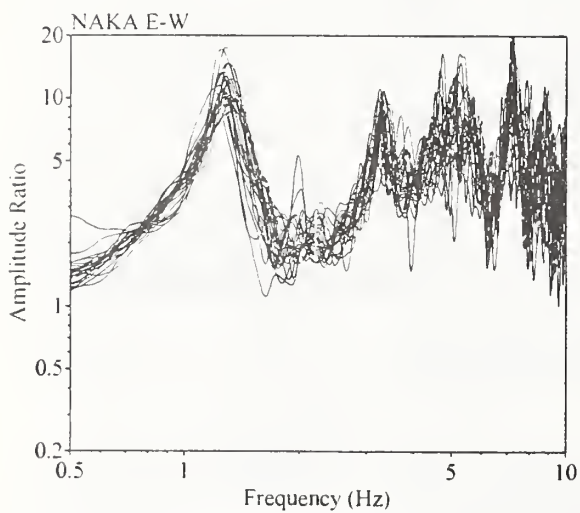


Fig. 4 Fourier spectral ratio at NAKA site

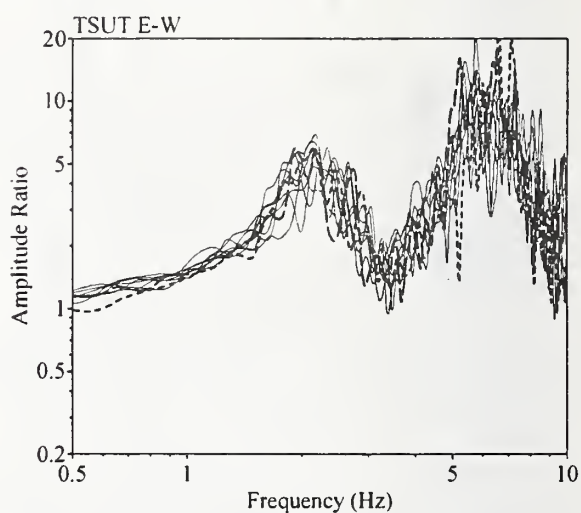


Fig. 7 Fourier spectral ratio at TSUT site

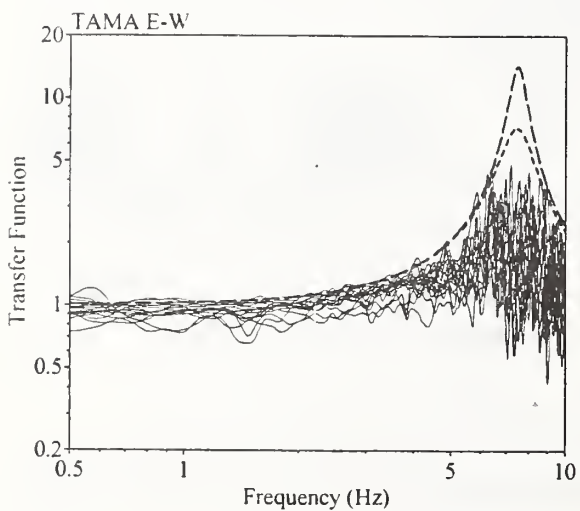


Fig. 5 Fourier spectral ratio at TAMA site

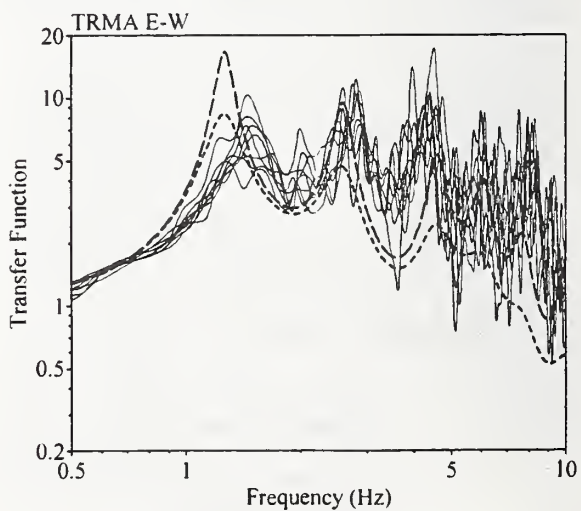


Fig. 8 Fourier spectral ratio at TRMA site

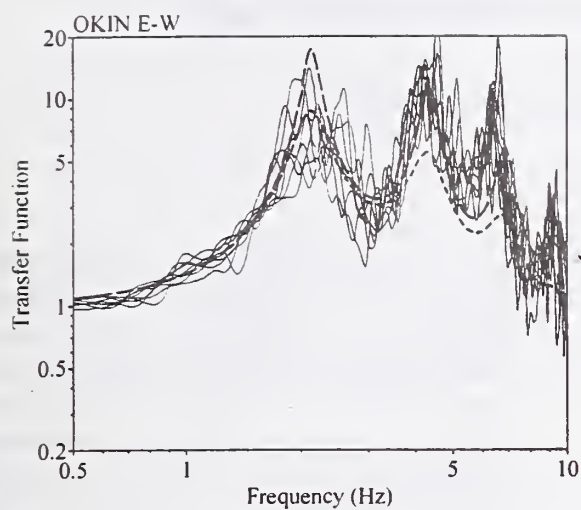


Fig. 9 Fourier spectral ratio at OKIN site

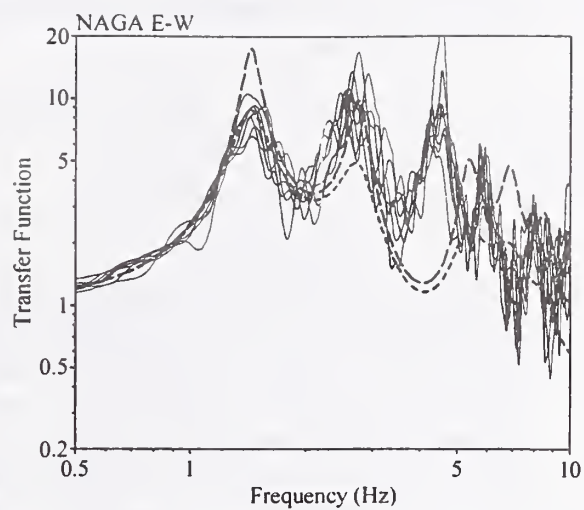


Fig. 12 Fourier spectral ratio at NAGA site

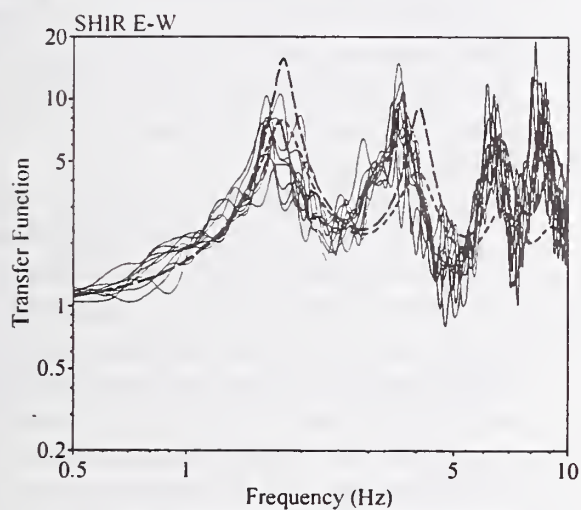


Fig. 10 Fourier spectral ratio at SHIR site

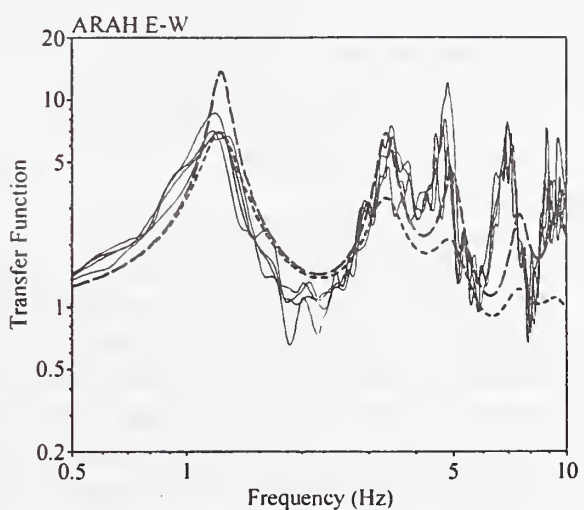


Fig. 13 Fourier spectral ratio at ARAH site

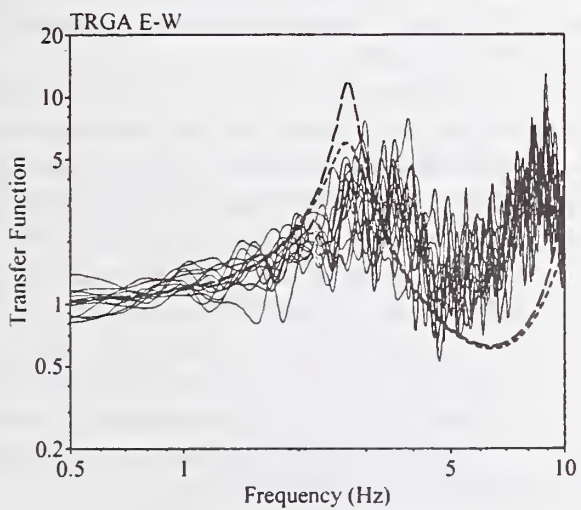


Fig. 11 Fourier spectral ratio at TRGA site

Deposition of Oil spilled from A Russian Tanker on Coasts

by

Fuminori Kato¹⁾ and Shinji Sato²⁾

ABSTRACT

Heavy oil spilled from a Russian tanker deposited on coasts facing the Japan Sea in January 1997. Especially, coasts in Fukui Prefecture and Ishikawa Prefecture were attacked by disastrous oil deposition. On the basis of detailed field reconnaissance, the behavior of deposited oil was described for sandy beaches, pebble beaches and rocky coasts. Impacts of oil deposition on coastal environment were also estimated.

Key Words :Coastal Environment,
Oil Deposition, Oil Spill,
Winter Storm

1. INTRODUCTION

The Russian tanker "Nakhodka" sank in the Japan Sea off Oki Islands on January 2, 1997. Huge amount of 6,240 kl heavy oil was spilled from the tanker. The amount ranks with the worst oil spill accident in Japan, that is, the accident at Mizushima oil plant of Mitsubishi Petroleum Corporation in 1971 in which 7,500 - 9,500 kl of C heavy oil was spilled. The spilled oil from the Russian tanker polluted the coasts facing the Japan Sea from Yamagata Prefecture to Shimane Prefecture. Deposited oil on coasts was removed with the help of many volunteers. Oil removal activities were performed under severe weather conditions and greatly influenced by winter storms. Since the long-term impacts of oil deposition on coastal environments were anticipated, field observation was conducted on the behavior of the deposited oil on coasts and its impact on coastal environments.

2. MOVEMENT OF SPILLED OIL AND EFFORTS FOR RECOVERY

The oil spill accident occurred when the Russian tanker "Nakhodka" was traveling in the Japan Sea from Shanghai to Petropavlovsk in the Kamchatka Peninsula, Russia. The tanker was carrying 19,000 kl of C heavy oil. On January 2, 1997, the tanker was accidentally broken into two pieces by storm off Oki Islands. The bow drifted in Japan Sea and the rest of the body sank onto the sea bottom of 2,500 m depth. A total amount of 6,240 kl of oil was spilled from the two pieces of the tanker. Part of the oil deposited the coasts facing the Japan Sea from Yamagata Prefecture to Shimane Prefecture.

After drifting on the sea surface, the bow stranded on the coast of Mikuni Town, Ishikawa Prefecture, on January 7. Photo 1 illustrates the stranded bow and deposited sludge-like oil on the coast. In the town, oil deposited on the beach intermittently for about two months from the accident. Sludge-like oil drifted toward the coast in the beginning of the time. About one month after the first oil deposition, only oil grain deposited on the beach. Oil in the stranded bow was completely removed on February 25, but oil grain occasionally deposited on the coast even after that.

Figure 1 shows the date of the first oil arrival on the coast and the total amount of removed oil. From Kaga Coast in Ishikawa Prefecture to Tottori Coast, the first arrival date was January 7-9. As the spilled oil was transported by the strong Tsushima currents and wind-driven currents, the arrival of oil delayed

1) Research Engineer, Coast Division, River Department, Public Works Research Institute,

Ministry of Construction, Tsukuba, 305-0804 Japan

2) Head, Coast Division, ditto

on the northern coasts.

The amount of oil deposited on the coasts was not estimated, however, it can be inferred from the amount of oil removed by March 28 which includes not only oil but also sand, gravel and sea water. The total amount of removed oil was 38,000 kl. The removed oil in Fukui Prefecture was about 18,000 kl, and that in Ishikawa Prefecture was about 13,000 kl. The total amount of oil removal was especially large in the area around Mikuni Town, eastern part of Wakasa Bay, and northern part of outer side of Noto Peninsula.

Figure 2 shows the temporal variation of significant wave height and average wind velocity recorded at Tokumitsu oceanographic observation station in Mattou City, Ishikawa Prefecture (see Fig.1). A ultrasonic-type wave gage is fixed on the sea bottom at the point of 15 m depth, 1,500 m off the coast. A wind meter is installed at about 15 m above the ground. Significant wave height in January and February 1997 was mostly over 1 m, sometimes exceeded the highest significant wave height 4.93 m between 1988 and 1996. Wind speed in the period was frequently over 10 m/s. Prevailing wind direction was from northwest. Such winter storm made oil removal quite difficult.

Oil removal works on the beach was started immediately after the first oil arrival. The total amount of oil removal in Mikuni Town reached 2,170 kl by January 20 and 2,520 kl by March 28. It included sand, gravel and sea water which were collected with oil. At a gravel beach in Mikuni Town, pebbles were wiped out with a piece of cloth steeped by kerosene in March. In Hamaji Coast, a sandy beach in the town, thorough oil removal was conducted even after oil removal on the surface. The removal of oil from the sand layer was conducted by two ways; one was sand sieving by hand and the other was pushing out oil-mixed sand into the sea expecting for the stir by waves.

3. FIELD RECONNAISSANCE ON REMAINED OIL

Field reconnaissances on remained oil

were conducted several times on coasts in Fukui, Ishikawa and Kyoto Prefectures. The result shows sediments in the coast influenced oil deposition.

On sandy beach, Sand accretion after the oil deposition resulted in the confinement of oil in sand. Photo 2 illustrates typical oil deposition on sandy beach. Lumps of oil were scattered on the surface. In order to investigate the presence of oil underground, sand in an area of 12 m by 1.5 m was excavated to the depth of 1.5 m. Figure 3 and Photo 3 illustrate an oil layer in the ground of Hamaji Coast, Mikuni Town, Fukui Prefecture, observed on February 6, 1997. Depth of the layer was over 1 m. Oil concentration in the layer was 20,000 mg/kg (oil weight per 1 kg of sand). Since there were no traces of oil penetration above the underground oil layer, it was considered that the oil was remained underground owing to the rapid accretion of sand.

On gravel beach, oil penetrated into the void space among the gravels. Photo 4 shows oil in the space among gravels near the stranded bow. The gravels were coated thickly by oil. Photo 5 illustrates a gravel beach adjacent to Hamaji Coast on the other side of Imazu River, observed on June 11, 1997. There were gravels covered with oil on the surface. Figure 4 shows oil concentration in sediments was 72.7-415 mg/kg in 50-70 cm depth, 15 mg/kg in 90-100 cm, 0 mg/kg in 130-150cm on March 6. The thickness of the gravel layer was up to 1m. The deeper part is consisted of only sand. This means that oil has penetrated into the border of the sand layer.

On rocky coast, oil has filled rock cracks. Photo 5 and 6 illustrates oil deposition on rocky coast in Shiga Town, Ishikawa Prefecture. Deposited oil was seen in rock cracks even in splash zone.

4. IMPACT OF REMAINED OIL ON COASTAL ENVIRONMENTS

(1) Remained Oil on Coasts

Oil deposition on coasts have a serious impact on coastal environments. Field

observation of the impact was conducted in Mikuni Town.

Figure 5 shows oil concentration in seawater taken at Hamaji Coast. Line 1 is across the zone in which detached breakwaters is built. Line 2 is out of the zone. Onshore point is 50 m off the coastal line. Offshore point is 150 m off the coastal line. Oil was detected on February 2, February 25, June 11 and November 21, 1997. It shows oil was detected intermittently. Leveling on the beach for sea bathing may push sand into sea on June 11. Oil in sand on the beach can be washed away by big waves.

Figure 6 shows oil concentration in sand on the beach of Hamaji Coast. Although sand on the surface has contained oil by March, it has rarely contained oil since May. On the other hand, oil was detected in the ground even in November. It indicates that oil is scattered in the ground of the sandy beach although oil on the surface has been removed by removal activities.

Figure 7 shows oil concentration in marine sediments on Hamaji Coast. Oil in marine sediments was detected only on February 25. It indicates oil-mixed sand may deposit on the sea bottom.

(2) Impact on Coastal Organisms

Observation of macrobenthos on the beach was conducted at Hamaji Coast. Species and number of macrobenthos in 30 cm square, 30cm in depth, was measured. Table 1 shows the result. Macrobenthos were found to be rare before the end of February. Species and the number of macrobenthos increased after March. It is considered that macrobenthos will not be present in surface sediments during winter since vigorous sediment movement will occur under winter storms. It is still uncertain whether the variation of macrobenthos was due to seasonal change or due to the impact of oil deposition.

Observation of macrobenthos in marine sediments was conducted at Hamaji Coast. Table 2 shows species and number of the macrobenthos. There were few macrobenthos on the sea bottom in the beginning of February as well as on the beach. The same reason can

be considered. Impact of oil deposition is also unknown.

Observation of sessile creatures was conducted on a gravel coast and a rocky coast in Mikuni Town. Species and number of sessile creatures in 30 cm square was measured. Table 3 shows the result. No significant changes in their species and number are recognized. Creatures of low activity have never been observed between 1 month and 11 months after the first oil arrival. To conclude, impact of oil deposition on sessile creatures was not recognized.

Observation of seaweeds was conducted on the same coasts as sessile creatures observation. Species and weight of seaweeds in 30 cm square was measured. Table 4 shows the result. Extreme changes in their species is not recognized. It indicates seaweeds was not influenced by oil deposition so much.

Totally speaking, impacts of oil deposition on coastal environments have not been clearly detected yet. Further monitoring survey will be necessary for a few years.

(3) Impact on Beach Utilization

Inquiry from the sea bathing people on the beaches in Fukui Prefecture and Ishikawa Prefecture was conducted on August 8-9. The result shows that they had no reluctance for past oil deposition.

Laboratory experiments on remained oil recognition were conducted. The result suggests the guideline for recreational beaches, that is, there should be no visible oil on the surface and oil concentration in sand should be less than 20 mg/kg.

5. Conclusion

Field surveys were conducted in order to understand the effects of vast deposition of spilled oil on coastal environments. Main conclusions are summarized as follows:

(1) The behavior of deposited oil on coasts varied among sandy beach, pebble beach and rocky coast.

(2) Further long-time monitoring will be necessary to understand the impacts on ecological system.

Table 1 Species and number of macrobenthos on Hamaji Coast

Unit: /0.09m²

Line	Distance from the coastal Line	January 28		February 25		March 18		June 11		November 6	
		Species	Number	Species	Number	Species	Number	Species	Number	Species	Number
1	35m	0	0	1	1	3	49	—	—	—	—
	20m	0	0	1	1	3	13	5	27	6	421
2	25m	0	0	0	0	3	5	—	—	—	—
	20m	0	0	0	0	1	2	6	89	2	11

Table 2 Species and number of macrobenthos in marine sediments of Hamaji Coast

Unit: /0.1m²

Line	Distance off the Coastal Line	February 6		February 25		March 18		June 11		November 21	
		Species	Number	Species	Number	Species	Number	Species	Number	Species	Number
1	50m	2	4	4	48	6	48	7	185	8	118
	150m	0	0	6	124	4	22	6	173	13	29
2	50m	2	10	5	69	7	50	7	46	13	347
	150m	2	9	6	34	11	127	9	179	15	167

Table 3 Species, number and weight of sessile creatures on the coasts in Mikuni Town

Unit: /0.09m²

Point	Item	Jan.28, Feb.5	Feb.25	Mar. 18	Jun.11	Dec.6
Gravel Coast	Species	22	37	40	64	63
	Number	61	101	287	368	346
	Weight(g)	3.29	9.6	9.26	56.01	16.5
Rocky Coast	Species	61	74	44	61	30
	Number	247	299	125	206	242
	Weight(g)	27.41	28.61	8.61	40.62	18.7

Table 4 Species and weight of seaweeds on the coasts in Mikuni Town

Unit: /0.09m²

Point	Item	Jan.28, Feb.5	Feb.25	Mar.18	Jun.11	Dec.6
Gravel Coast	Species	32	24	36	20	25
	Weight(g)	43.51	214.66	133.31	398.36	221
Rocky Coast	Species	34	31	29	22	26
	Weight(g)	82	92.01	165.09	86	198

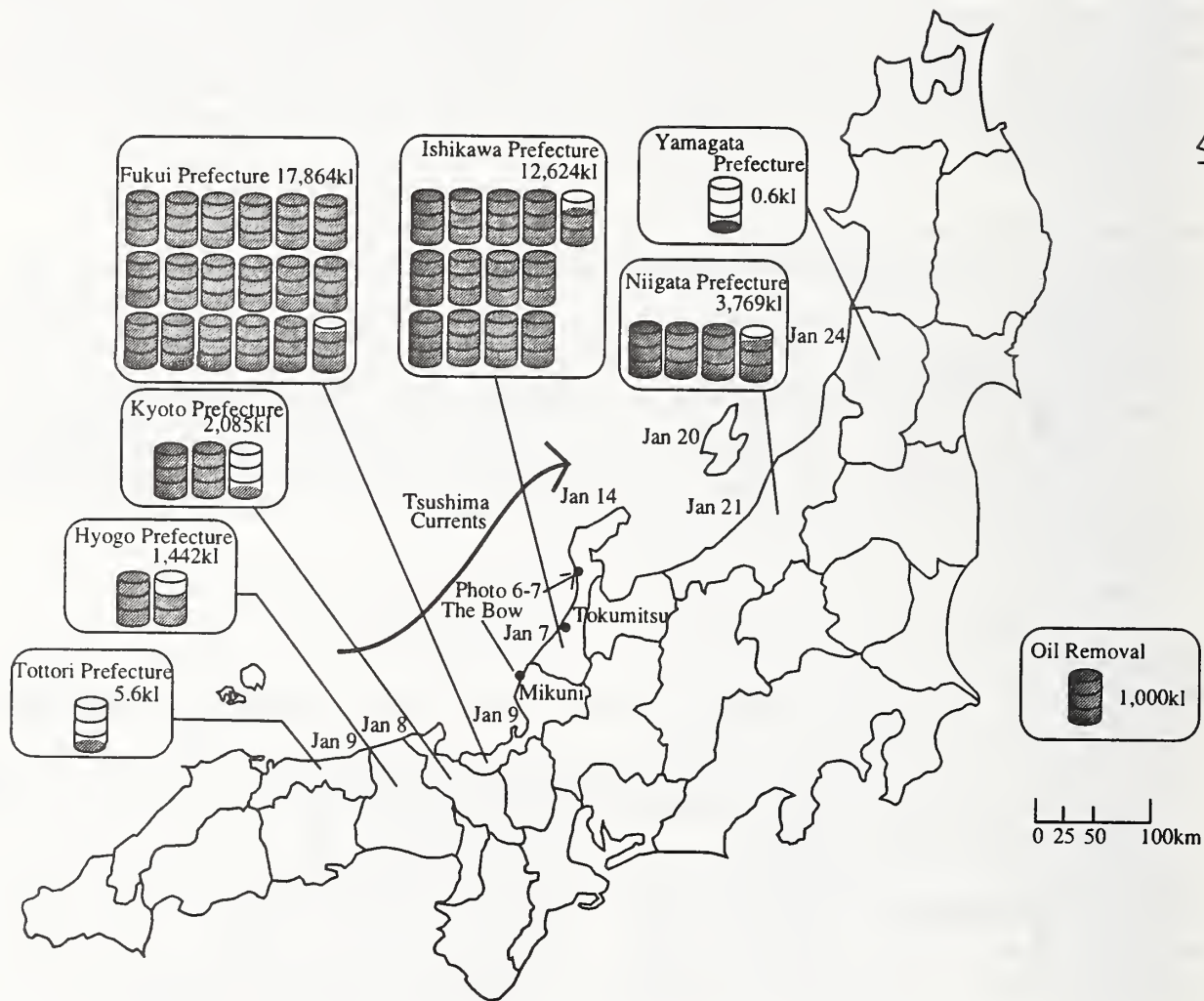


Fig.1 The first oil arrival date and the total amount of removed oil by March 28, 1997.

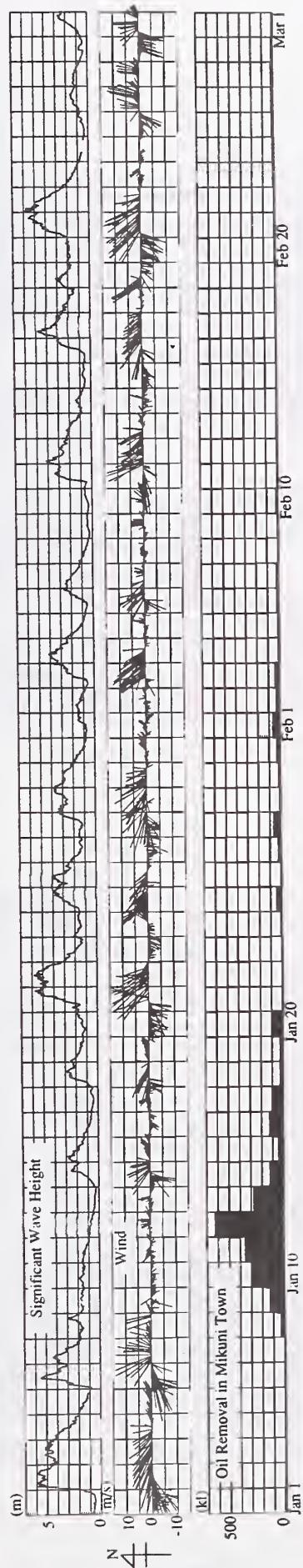


Fig.2 Significant wave height and wind speed at Tokumitsu oceanographic observation station, and the amount of oil removal in Mikuni Town

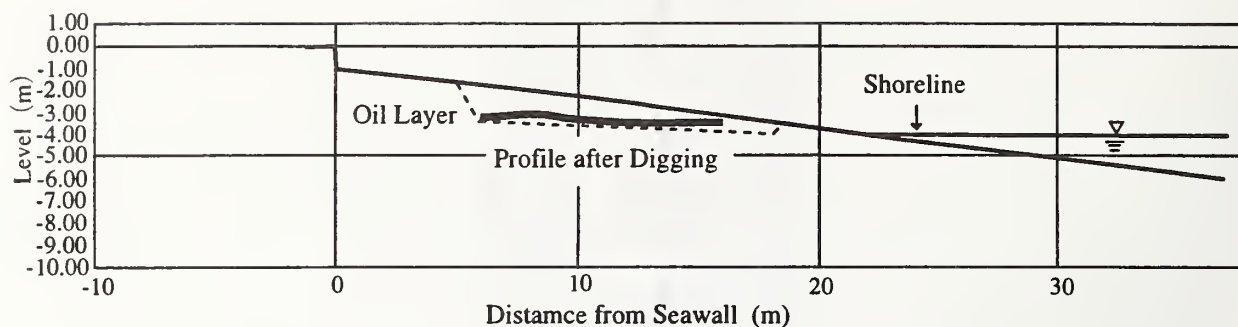


Fig.3 Oil layer in the ground of Hamaji Coast

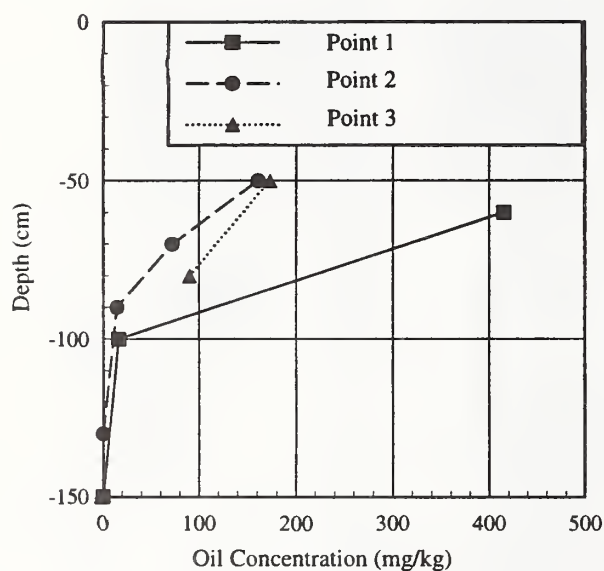


Fig.4 Oil concentration in gravels

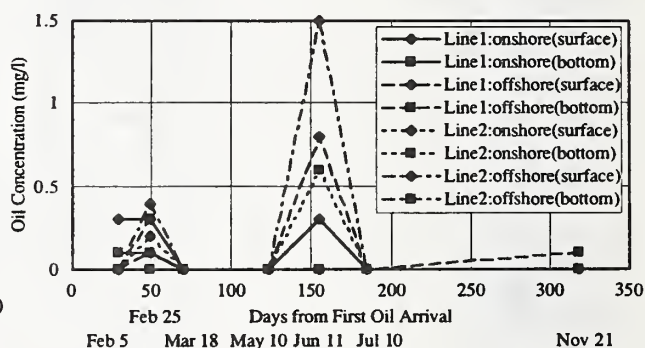


Fig.5 Oil concentration in seawater of Hamaji Coast

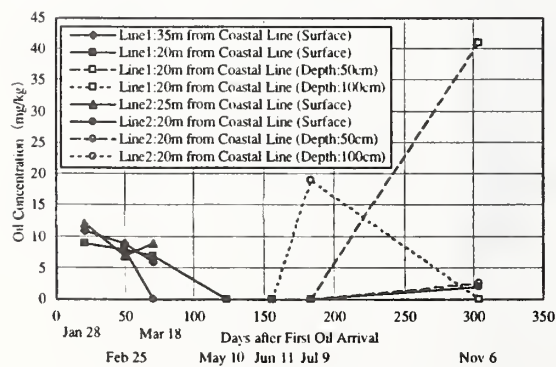


Fig.6 Oil concentration in sand on the beach of Hamaji Coast

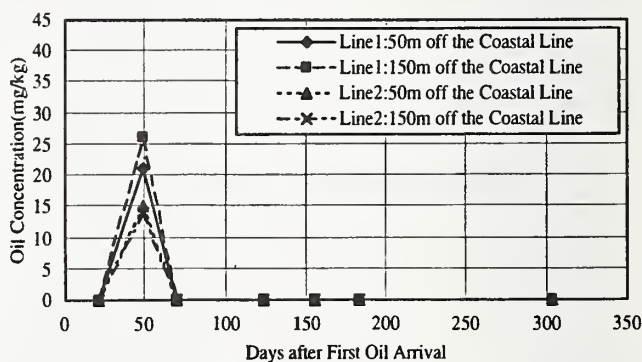


Fig.7 Oil concentration in marine sediments on Hamaji Coast

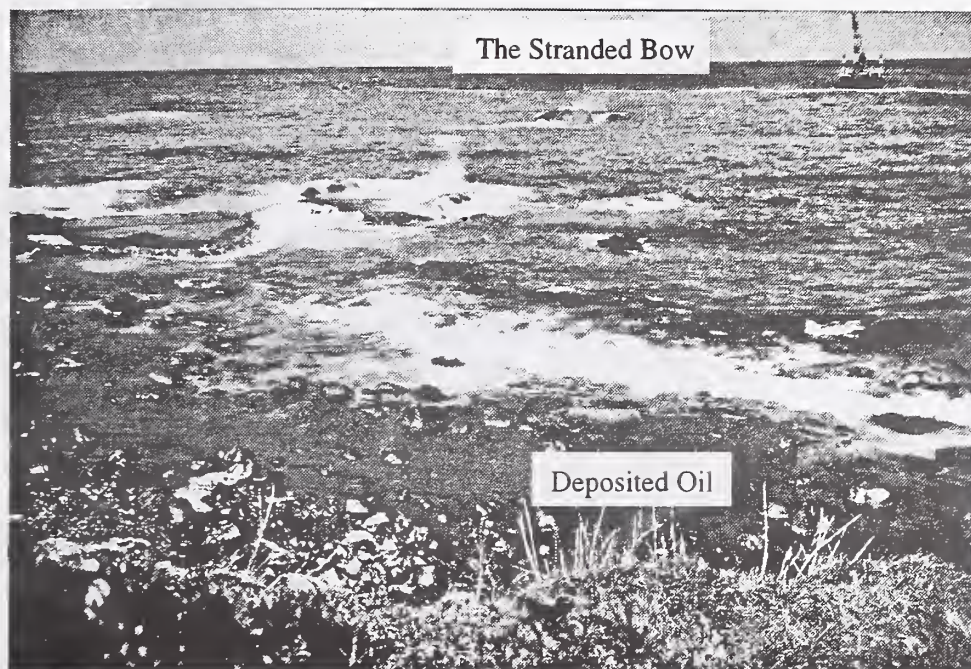


Photo 1 The stranded bow near the coast (January 11, 1997)



Photo 2 Oil deposition on sandy beach (Sunset Beach in Mikuni Town, January 11, 1997)



Photo 3 Oil layer in the ground of Hamaji Coast, Mikuni Town (February 6, 1997)

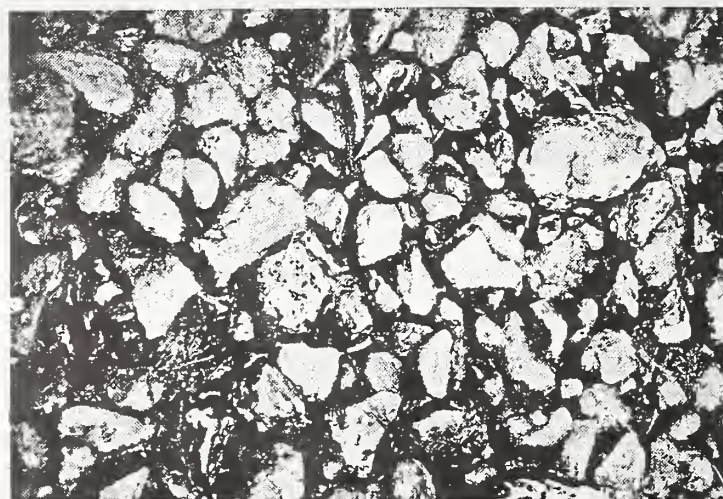


Photo 4 Deposited oil in the space among gravels near the stranded bow (February 6, 1997)



Photo 5 Gravel beach adjacent to Hamaji Coast, Mikuni Town (June 11, 1997)

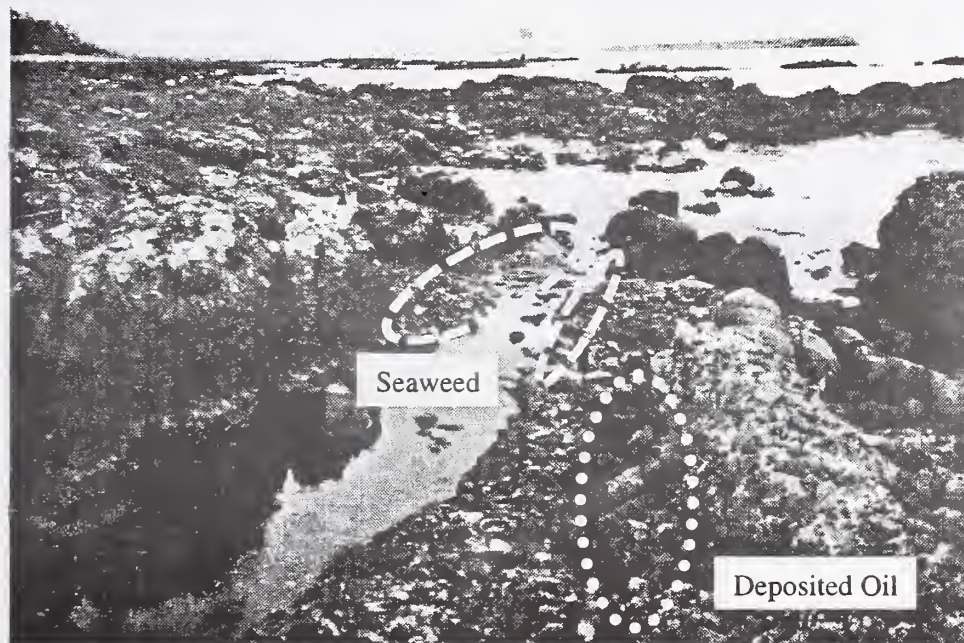


Photo 6 Rocky coast in Shiga Town, Ishikawa Prefecture (February 10, 1997)

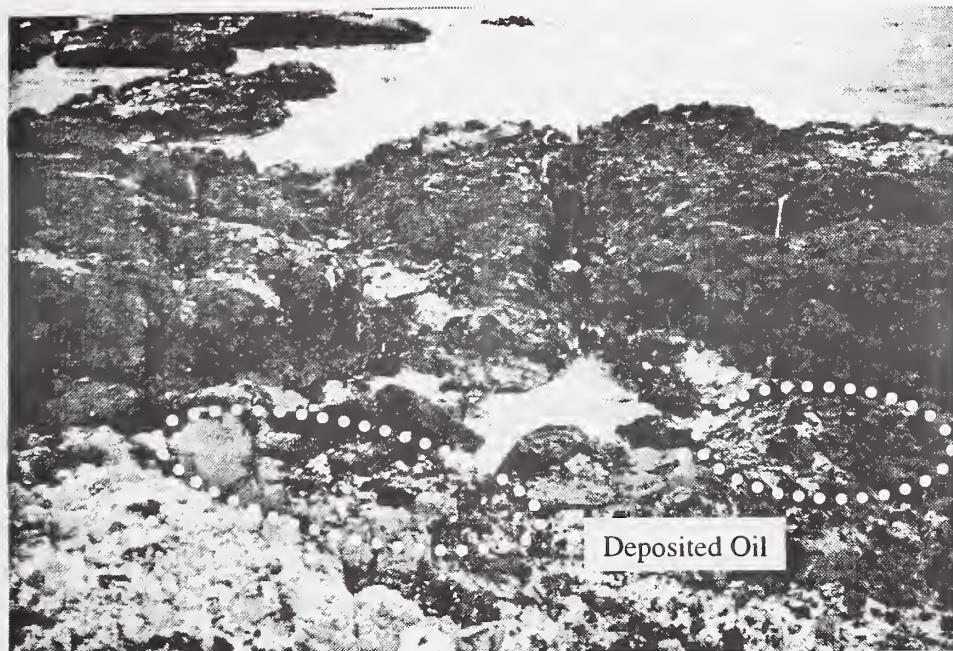
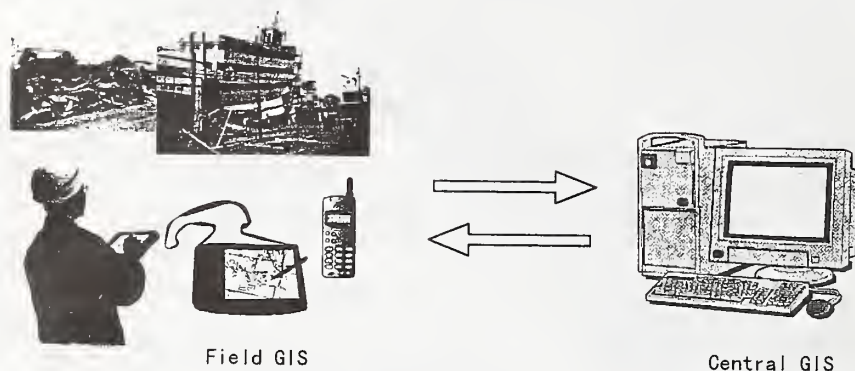


Photo 7 Oil deposition around a tide pool (February 10, 1997)

GIS With Mobile Communication For Countermeasure against Natural Disaster

by

Naoki TAKAYAMA ¹⁾



ABSTRACT

The Geographical Survey Institute(GSI), Ministry of Construction has made effort to fully produce of the Digital Maps on Japan and to enforce utilization of the Geographical Information System (GIS). It was recognized again that importance of utilizing the GIS through experiences with the Hyogo-ken-nanbu Earthquake.

This paper reports the mobile communication GIS developed for rescue operation and reconstructing activity by transmitting real-time information obtained on field investigations. On the field, this system can be easily operated to input obtained data by adopting menu-oriented interface. In the headquarters, this system can display same information as on the field, so that it is possible to carry out countermeasures certainly against with linking the other related information.

1. Introduction

The Hyogo-ken-nanbu Earthquake which occurred at 5:46 AM on 17 January 1995, was a

terribly large epicentral earthquake which magnitude of 7.2. The earthquake killed more than 5,500 people and destroyed housings over 100,000, and it seemed that sufferers were over 320,000. Thus it was the worst miserable disaster in recent Japan

In respect to the information systems for social works and private enterprises activities, a lot of computers and telecommunication systems were destructed exhaustively. Also the region's economic infrastructures, including water and gas networks, telephone lines, power cables were crippled. Such destruction paralyzed business and social operations in Japan. As a result, it was recognized that importance for risk management, so that the Government, the local municipalities and researchers started to reexamine plans for countermeasures against natural disasters such as rescue operation and repair of social infrastructures.

Especially it is indispensable to realize the measures for obtaining and transmitting information, just after the outbreak of disaster.

1) Photo and Map Information Division, Geographical Survey Institute, Ministry of Construction

2. The outline of the study

For rescue operations and reconstructing activities just after the disaster, it was recognized that GIS played key roles in assembling information on real time, in linking the information with other related information such as public facilities, equipment for anti-disaster, geographic characteristics, social conditions, and realizing enforcement for prompt anti-disaster actions.

In this study, GSI developed the mobile GIS for smooth rescue and repair activities. Also GSI investigated the methods for efficient assembling and communicating information of damage, and providing information through computer networks such as Internet.

3. The outline of the system

3.1. Functions of the system

This system was integrated by customizing GIS software on the market. Main functions are as follows.

- Basic functions
 - Call out a map
 - Magnification, Reduction, Scroll
 - Display each layer, overlay of layers
 - Overlay raster image data and vector data
- Input
 - Input figures according to damage item (i.e. housing, public civil facility)
 - Input attributes according to damage item
 - Update damage information
 - Input by pen-operation
 - Measure (Distance between two points, Area of a polygon)
- Communication
 - Data transmission by portable phone (TCP/IP)
 - Auto dial

- Image management
 - Capture photo data, image data, Correction, Management
 - Retrieve and display

3.2 Damage Items

The damage items and their attributes which are able to assemble in this system are housing, public civil facility for road, river, railway and so on, and extent of liquefaction. Also figures such as point, line, polygon, which express location of damaged position, can be registered on the map viewed on the display, according to the damage item.

Table 1 shows the list of damage items.

3.3 Communication method

For rescue operation and reconstructing activity, it is necessary to grasp real and accurate situation in the damaged area. In this sense, we have to input the real-time information obtained by the field investigation, and put the information into the GIS in the headquarters by using mobile telecommunication media such as the portable phone.

However the telecommunication media or the public telephone lines may lose their function by the disaster, for example, overflow of the capacity or destruction of the local telephone exchange system.

There are some communications media, such as the public telephone, the portable phone, the personal handy-phone system, the satellite telephone system and the wireless phone system for anti-disaster, it is hardly to look out the system which is completely able to overcome the troubles stated above.

In this study, we adopted the digital portable phone as communication media because of its stability for data transmitting.

3.4 System components

- Headquarters
 - Desktop PC

- Modem
- Software
 - WindowsNT
 - GIS software
- Field system
 - Pen computer
 - Portable phone
 - Digital Camera
 - Modem
 - Software
 - Windows for PenComputing
 - FieldNotes

3.5 Effect for systematization

Thus far, when a disaster occurred, officials in charge of anti-disaster assembled information on the damaged area, and they brought it to the headquarters themselves, or reported it by using the public telephone or the wireless phone system for anti-disaster. In this case, so that the subjectivity of the officials could influence the quality of information, the reliability of information might be sometimes doubtful slightly.

If the mobile communication GIS for rescue operation and reconstructing activity is used, it is possible to transmit pictures of the damaged situation from the field promptly. The facts such as pictures are effective to grasp the damaged situation and to take countermeasures against the disaster.

On the other hand, to be shared common information by the headquarters and the field, is also effective for managing real time information and providing information to the related organizations.

3.6 Applicable fields of this system

In this study, it is considered the feasibility of the mobile communication GIS with a portable phone. As an application for the other field, it seems to be used for the support system on the field research.

The major applicable businesses are as follows.

- Update topographic map data
- Basic investigation for the City Planning (land use survey, research of housings)
- Confirmation of building houses (Field investigation for comparison)
- Investigation of fixed property, building site
- Investigation of possessions on the roads
- Welfare
- Marketing

4. Conclusion

In this study, the mobile communication GIS was developed in order to enforce smooth rescue operation and reconstructing activity at the disaster, through the experience from the Hyogo-ken-nanbu earthquake. This system was just developed as a prototype system, improvement of the functions will be needed for practical use. Also it is necessary to establish organizations and liaisons for utilizing the system.

On the other hand, it is prerequisite to settle the main computer at the headquarters. Hence it is also needed the risk management such as aseismatic structuring of the building of the headquarters, countermeasures for fire, prevention for falling down of the computers, and backup of the data.

Concerning to the risk management for computer systems, there are some manuals, for example, the security management guideline for the computer system, or the guideline for system inspection, and based on such guidelines many kinds of countermeasures have been taken. In spite of these measures, the unexpected damages of the computer system were recognized at the Hyogo-ken-nanbu earthquake. Thus the reexamine of the risk management is quite necessary. To avoid functional disorder of the computer aided anti-disaster system by hazardous earthquake, it is strongly expected that further strengthen the countermeasure for security, through researching, analyzing and investigating of the computer system in damaged situation.












ITEM	Symbol			CONTENT OF ATTRIBUTES (selecting on menu window)
	type	image	color	
House	point		red	Situation : completely destroyed, partial destroyed, slightly destroyed, burned down, other
	polygon			Restoring condition : pulled down, rebuilding, repairing, other
				Comment
Road	point		gray	Place : roadway, sidewalk, median, slope, side ditch, bridge, tunnel, other institutions, other
	line			Situation : depression, upheaval, clack, collapse, other
	polygon			Quantities : meter, square meters
				Comment
River	point		blue	Place : levee, river course, water gate, barrage, pond, other
	line			Damage : collapse, flooding, ravage of institution, other
	polygon			Quantities : meter, square meters
				Comment
Railroad	point		olive-green	Place : rail. overhead wire, station building, garage, railroad bridge, other
	line			Situation : depression, upheaval, collapse, cut off, other
				Quantities : meter, square meters
				Comment
Water pipe	point		light blue	Comment
	line			
Sewer	point		brown	Comment
	line			
Gas pipe	point		purple	Comment
	line			
Electric power	point		green	Place : electric light pole, overhead wire, underground interconnection system, other
	line			Comment
Telephone	point		yellow	Damage : telephone pole, overhead wire, underground, other
	line			Comment
Liquefaction	polygon		navy-blue	Comment
Other	point line polygon		black	Comment
Place of photography	point		pink	Number of photograph (input by 10key)
	line image			Comment
Note	image		black	

Table 1 The Item List of Collecting Damage Information

Aerodynamic databases and electronic standards for wind loads: A pilot application

by

Timothy Whalen^{1,2}, Emil Simiu¹, Gilliam Harris³, Jason Lin⁴, and David Surry⁴

ABSTRACT

As part of ongoing National Institute of Standards and Technology research on the development of a new generation of standard provisions for wind loads, we present results of a pilot project on the use of large aerodynamic databases for the improved estimation of wind-induced bending moments and shear forces in low-rise building frames. We use records of wind pressure time histories measured at a large number of taps on the building surface in the Boundary Layer Wind Tunnel of the University of Western Ontario. Time histories of moments and shear forces in a frame are obtained by adding pressures at all taps tributary to that frame multiplied by the respective tributary areas and influence coefficients. The latter were obtained from frame designs provided by CECO Building Systems. We compare results obtained by using the pressure time history records with results based on ASCE 7 standard provisions. The comparison shows clearly that provisions which use aerodynamic databases containing the type of data described in this work can result in designs that are significantly more risk-consistent as well as both safer and more economical than designs based on conventional standard provisions. We outline future research on improved design methodologies made possible by our proposed approach to wind loading standardization. Finally, the proposed methodologies may be used for damage assessment for insurance purposes.

KEYWORDS: Building technology; aerodynamics; codes and standards; databases; risk; structural engineering; wind engineering.

1. INTRODUCTION

Conventional standard provisions for wind loads

reflect two conflicting needs: (1) to assure that they are risk-consistent, the provisions should reflect the information on which they are based as completely and realistically as possible; and (2) conventional standards have limitations that impose reductive formats and simplifications, with consequent loss of information and risk-consistency.

Owing to current information storage and computational capabilities standard provisions need no longer be based on reductive -- and distorting -- tables and plots. It is now practical to develop user-friendly standard provisions that incorporate large amounts of useful information [1,2]. In this paper we present results that illustrate aspects of the development and advantages of such provisions in the specific case of low-rise building frames.

In Section 2 we describe (1) the geometry of the buildings chosen as our test cases, (2) the design criteria for the frames, and (3) basic information on the frames, which were designed by CECO Building Systems. In Section 3 we briefly describe the wind tunnel tests performed at the Boundary Layer Wind Tunnel Laboratory of the University of Western Ontario (BLWTL) [3]. In Section 4 we describe the procedure used to calculate wind-induced internal forces (i.e., bending moments, shear forces and axial forces),

¹Building and Fire Research Laboratory, National Institute of Standards and Technology, Gaithersburg, MD 20899

²Present address: School of Civil Engineering, Purdue University, West Lafayette, IN 47907

³CECO Building Systems, Columbus, MS 39703

⁴Boundary Layer Wind Tunnel Laboratory, University of Western Ontario, London, Ont., Canada N6A 5B9

using: (1) the ASCE 7-93 Standard provisions on wind loads [4], and (2) time-dependent loads based on the wind tunnel measurements. In Section 5 we present and discuss our results. In Section 6 we discuss the vast potential for improving both the safety and economy of structural designs offered by the approach described in this paper, and future research aimed at realizing that potential.

2. BUILDING GEOMETRIES, DESIGN CRITERIA, AND FRAMES

The buildings studied in this pilot project are rectangular in plan with dimensions 61 m (200 ft) \times 30.5 m (100 ft), and have gable roofs with 1/24 slopes and ridge parallel to the long dimension. For the first set the eave height is $H=6.1$ m (20 ft); for the second set it is $H=9.75$ m (32 ft). Each set consists of four buildings with identical geometry. Two of the four buildings are located near Miami, Florida. The other two are located near Charleston, S.C. For each of these locations one building is in open terrain and one is in suburban terrain. All buildings are located at 13 km (8 miles) inland from the coastline and are assumed to be Category 1 [4].

The frames were designed by CECO Building Systems in accordance with Metal Buildings Manufacturers Association (MBMA) current practices, which are based on the the ASCE 7-93 Standard and the 1989 AISC Design Manual (Allowable Stress Design). The configuration of the frames is shown in Fig. 1. For the direction normal to the ridge, the main wind load resisting systems consist of 2 end frames and 7 interior frames. The distance between interior frames is 7.62 m (25 ft) center to center. The end frames are equally spaced from the respective neighboring interior frame. The frame dimensions and the cross-sectional dimensions of the webs and flanges are identical for all frames of a given building. We refer to the Miami (M) building with $H=6.1$ m (20 ft) in suburban (S) terrain as MS20. The other buildings are designated MS32, CS20, CS32, and MO20, MO32, CO20, CO32 (C designates Charleston;

O designates open terrain).

3. WIND TUNNEL TESTS

Building models were tested at 1:200 and 1:100 scales for suburban terrain and 1:200 scale for open terrain. Pressure taps were installed at about 500 locations for the buildings with $H=9.75$ m and 440 locations for the buildings with $H=6.1$ m. The tap locations are shown in Fig. 2. Pressure time histories were measured for each of 37 wind directions between 0° and 180° at 5° intervals. Pressure coefficients C_p obtained from the pressure measurements were referenced to the experimental dynamic pressures at the eave height H . The approximate wind tunnel mean flow speeds $V_h(H)$ at the model eave height H correspond to the full-scale hourly speeds listed in Table 1.

In this paper we consider only the 1:200 model tests. The characteristics of the wind tunnel flows conform to standard representations of atmospheric boundary-layer flows over open and suburban terrain -- see [3] for details.

The time series were sampled at 400 Hz for 60 s. The processed time series were corrected for residual non-simultaneity, and digitally low-pass filtered at 150 Hz. The resolution for the pressure coefficients is about 0.01. The data were archived onto 8 mm cassette tapes. Each tape contains two directories. Each directory contains all the data for one building with specified eave height in one type of terrain. The size of a directory is about 2 GigaBytes when uncompressed and about 600 MegaBytes when compressed. For details on the data file structure and on restoring data from tapes see [3].

4. WIND-INDUCED INTERNAL FORCES

Wind-induced internal forces were obtained for two types of wind loadings: (1) the wind loading specified by the ASCE 7-93 Standard and (2) the wind loading obtained from the wind tunnel data. The ASCE loading is based on wind speeds estimated without regard for direction. For

consistency our estimates of the wind loading obtained from wind tunnel tests are based on similar estimates of the wind speeds. The pressures are

$$p(t) = 0.613 C_p(t) V_h^2(H) \quad (\text{N/m}^2) \quad (1)$$

$$V_h(H) = 1.046 (K_z)^{1/2} V c, \quad (2)$$

where C_p is the pressure coefficient as determined from the wind tunnel tests, 1.046 is the importance factor for Category 1 buildings located at 13 km (8 miles) from the coastline (Table 5 of [4]), H is the eave height in meters, $V_h(H)$ is the mean hourly speed at elevation H , V is the basic wind speed in m/s ($V=42.5$ m/s (95 mph) for Charleston and 49.6 m/s (111 mph) for Miami -- see Fig. 1 of [4]), K_z is an exposure coefficient whose square root transforms the fastest-mile wind speed at 10 m elevation over open terrain into the fastest-mile wind speed at elevation H over the specified type of terrain (for $H=6.1$ m (20 ft), $K_z=0.87$ for open terrain and $K_z=0.42$ for suburban terrain; for $H=9.75$ m (32 ft), $K_z=0.996$ for open terrain and $K_z=0.514$ for suburban terrain -- see Table 6 of [4]), and c is a coefficient that transforms fastest-mile wind speeds to mean hourly speeds ($c \approx 1/1.30$ for Charleston and $c \approx 1/1.31$ for Miami -- see Sect. 6.5.2.2 and Fig. C5 of the Commentary in [4]).

The internal forces were obtained by summing up the pressures at all taps contributing to the loading of a frame times the respective tributary area and influence coefficient. The influence coefficients were calculated using standard linear analysis techniques, and accounted for the position of the tap with respect to the frame. It was assumed that the load associated with any given tap is transmitted to the frame by simply supported girts or purlins, and that there is no load redistribution among the frames. For the loading based on wind-tunnel results this procedure yielded time histories of the internal forces being sought, from which r.m.s. values of the internal forces were obtained. The internal force corresponding to a nominal one-hour loading is defined as the mean value plus the

r.m.s. value times the peak factor

$$k_{pk} = (2 \ln 3600 v_p)^{1/2} + 0.577 / (2 \ln 3600 v_p)^{1/2} \quad (3)$$

[5], where v_p is the mean zero upcrossing rate of the fluctuating part (excluding the mean) of the internal force for the prototype. The rate v_p is obtained from its model counterpart by equating reduced frequencies for the model and prototype. This yields $v_m/v_p = \{[V_h(H)]_m/[V_h(H)]_p\} (D_p/D_m)$, where the subscripts p and m indicate model and prototype, respectively, and D_p/D_m is the reciprocal of the model scale. The speed $V_h(H)$ for the model is taken from Table 1. It is assumed that the wind speed specified by the ASCE 7-93 Standard can blow from any direction.

5. RESULTS

For 6 cross-sections shown in Fig. 1, Table 2 lists the ratio between the worst case bending moments induced by the time-dependent load modeled on the basis of the wind tunnel tests (for brevity, we will refer to this load as the actual loading) and their counterpart worst case bending moments induced by ASCE Standard 7-93 loads. In both cases the respective most unfavorable wind loading conditions were assumed. If the loading specified by the Standard were "on target", i.e., if it reflected consistently the actual loading, then all entries in Table 2 would be unity. Such consistency is impossible owing to the constraints imposed on the volume of information that can be conveyed in conventional standard provisions. Given those constraints the ASCE 7-93 Standard writers attempted to specify information as consistently as possible. However, we note that for any given frame the ratios of Table 2, instead of being unity, differ significantly and nonuniformly from unity in most cases. For example, for the frames of building CS20, the ratios vary from a minimum of 0.5 to a maximum of 0.82. This means that some cross-sections will be more over-designed than others. The sections that are the most over-designed contribute little to the overall safety of the frame. The statement can

therefore be made -- conditional on the strength having a given value -- that the least over-designed cross-section would fail if a sufficiently powerful storm occurred, with the additional strength reserve of the more over-designed cross-sections being wasted. The ratio between the maximum and the minimum entry for a given type of frame is denoted by r_f , and is a measure of the inconsistency of the design over the cross-sections listed in Table 2 for that type of frame. We also list in Table 2 the ratio, denoted by r_{inf} , between the maximum to the minimum entry across types of frames for cross-sections #2, #4, and #6 (these sections are the section at the frame knee, girder pinch, and ridge line, where comparisons between frame types are meaningful). The ratio r_{inf} is a measure of the extent to which the influence lines of the frames affect the capability of the conventional standard provisions to reflect the actual moments occurring in the frames. This capability is affected by the fact that the standard provisions were based on one specific type of influence lines. Inconsistencies between effects of loads in conventional standard provisions and effects of actual loads inevitably arise should the design of the frames deviate from the design assumed in development of the conventional standard provisions. It can be seen in Table 2 that r_{inf} can be as large as 1.52. (We also note that the ASCE standard does not differentiate between loads on two-hinged and three-hinged frames, even though the respective influence lines are significantly different. Nor does the ASCE 7 standard make allowance for the distance between frames, even though owing to the fluctuating nature of the loads this distance can affect significantly the magnitude of the internal forces.)

The adoption of standard provisions that use large aerodynamic databases would result in moment and shear diagrams allowing the designs would be risk-consistent both within a frame and across different frames. The waste inherent in non-uniformities within a frame would therefore be eliminated. For example, for frame CS32, the design would be safer if instead of the ratio 1.00 (for cross-section #6), the ratio 0.9 were used,

and it would also be more economical if the ratios 0.65, 0.67, 0.74, 0.58, and 0.87 were to be changed to the ratio 0.9.

Design technology has progressed to the point where designers can achieve designs with stresses that are within a few percentage points of the stresses induced by the standard loads. However, this close match provides only the illusion of good design, since the designer is deprived by conventional standard provisions of the knowledge of the actual loads and the associated actual stresses. A standard using large aerodynamic databases would allow the designer to design for the best available loading information that can be produced in the present state of the art, without the significant artificial distortions due to the conventional standards' antiquated way of conveying loading information.

Since the present investigation is exploratory, we considered only wind directions 0° , 30° , 60° , 90° , and 120° . In a forthcoming report all 37 wind directions will be considered. Preliminary searches have indicated that consideration of the results for all 37 directions will leave Table 2 essentially unchanged.

6. FUTURE RESEARCH

As already indicated, the aim of this paper is to present a pilot study. An exhaustive investigation along the lines presented in this paper is planned, however, which will include consideration of all wind directions. It will also consider the effects of wind directionality, which we assumed here to be characterized by a circular extreme wind rosette. This assumption is used in the ASCE 7-93 Standard, but it is fact not necessarily warranted, as shown by the example of the wind rosette of Fig. 3 (milepost 1950, near Charleston, see [6]). We plan to investigate the effect of modeling scale using the results obtained in the wind tunnel for 1:100 models. Instead of estimating moments for a few selected sections, we plan to produce full moment and shear force diagrams for the entire frames. It is conceivable that automated production will render desirable in

the future designs that may be somewhat different for the various frames of a given building. Moment and shear force diagrams corresponding to various mean recurrence intervals can be produced for each of those individual frames, giving the designer the option of considering the possibility of reducing the amount of material for some frames, if this is warranted by the moment and shear force diagrams.

We also plan to study the possibility of automated iterative designs, starting with a design based, for example, on conventional standard provisions, refining the design on the basis of moment and shear diagrams based on actual wind loads, recalculating the moments and shears based on the influence lines of the new frame, until a satisfactory convergence is achieved. Only then will designs accommodating calculated stresses to within a few percentage points make sense, that is, offer the substance rather than the illusion of good engineering design. We note that anticipated progress in Computational Fluid Dynamics might allow the entire load definition process to be computerized in the future, at least for certain applications. Finally, we note that the power of the computer and the availability of databases for time histories of wind pressures make it possible for researchers and designers to study the plastic behavior of frames in the time domain on the basis of realistic fluctuating wind loads. Plastic designs are currently viewed by the industry as uneconomical, and allowable stress designs are used instead, but further research made possible by the availability of appropriate databases containing aerodynamic pressure time histories will enable research to be conducted that might lead to a change of current design philosophy.

7. REFERENCES

1. Simiu, E. and Stathopoulos, T. (1997), "Codification of wind loads on buildings using bluff body aerodynamics and climatological data bases," *J. Wind Eng. Ind. Aerodyn.* (in press).
2. Simiu, E., Garrett, J.H., and Reed, K.A. (1993), "Development of Computer-based Models of Standards and Attendant Knowledge-base and Procedural Systems," in *Struct. Eng. In Natural Hazards Mitigation, Structures Congress*, Irvine, Calif., American Society of Civil Engineers, New York.
3. Lin, J. and Surry, D. (1997), *Simultaneous Time Series of Pressures on the Envelope of Two Large Low-rise Buildings*, BLWT-SS7-1997, Boundary-Layer Wind Tunnel Laboratory, The Univ. of Western Ontario, London, Ontario, Canada.
4. *ASCE Standard 7-93* (1993), American Society of Civil Engineers, New York.
5. Davenport, A.G. (1964), "Note on the Distribution of the Largest Values of a Random Function with Application to Gust Loading," *J. Inst. Civ. Eng.* **24**, 187-196.
6. Simiu, E. and Scanlan, R.H. (1996), *Wind Effects on Structures: Fundamentals and Applications to Design*, 3rd Ed., Wiley-Interscience, New York.

Table 1. Wind tunnel mean flow speeds $V_h(H)$

1:200 model, open terrain, $H=6.10$ m:	10.15 m/s
1:200 model, open terrain, $H=9.75$ m:	10.95 m/s
1:200 model, suburban terrain, $H=6.10$ m:	8.30 m/s
1:200 model, suburban terrain, $H=9.75$ m:	8.95 m/s
1:100 model, suburban terrain, $H=6.10$ m:	9.35 m/s
1:100 model, suburban terrain, $H=9.75$ m:	10.05 m/s

Table 2. Ratios of maximum moments due to loads modeled by wind tunnel data to moments induced by ASCE 7-93 Standard provisions, for six frame cross-sections

Frame for building type	CS20	CO20	CS32	CO32	MS20	MO20	MS32	MO32	r_{inf}
Cross-section (see Fig. 1)									
#1	0.60	0.61	0.75	0.65	0.60	0.61	0.74	0.62	
#2	0.66	0.66	0.78	0.66	0.65	0.66	0.78	0.67	1.20
#3	0.75	0.76	0.89	0.74	0.75	0.75	0.87	0.73	
#4	0.50	0.46	0.68	0.58	0.51	0.52	0.70	0.67	1.52
#5	0.79	0.76	0.90	0.87	0.78	0.75	0.89	0.86	
#6	0.82	0.79	1.00	0.96	0.81	0.78	0.98	0.85	1.28
$r_f = r_{max}/r_{min}$	1.64	1.72	1.47	1.66	1.59	1.50	1.40	1.39	

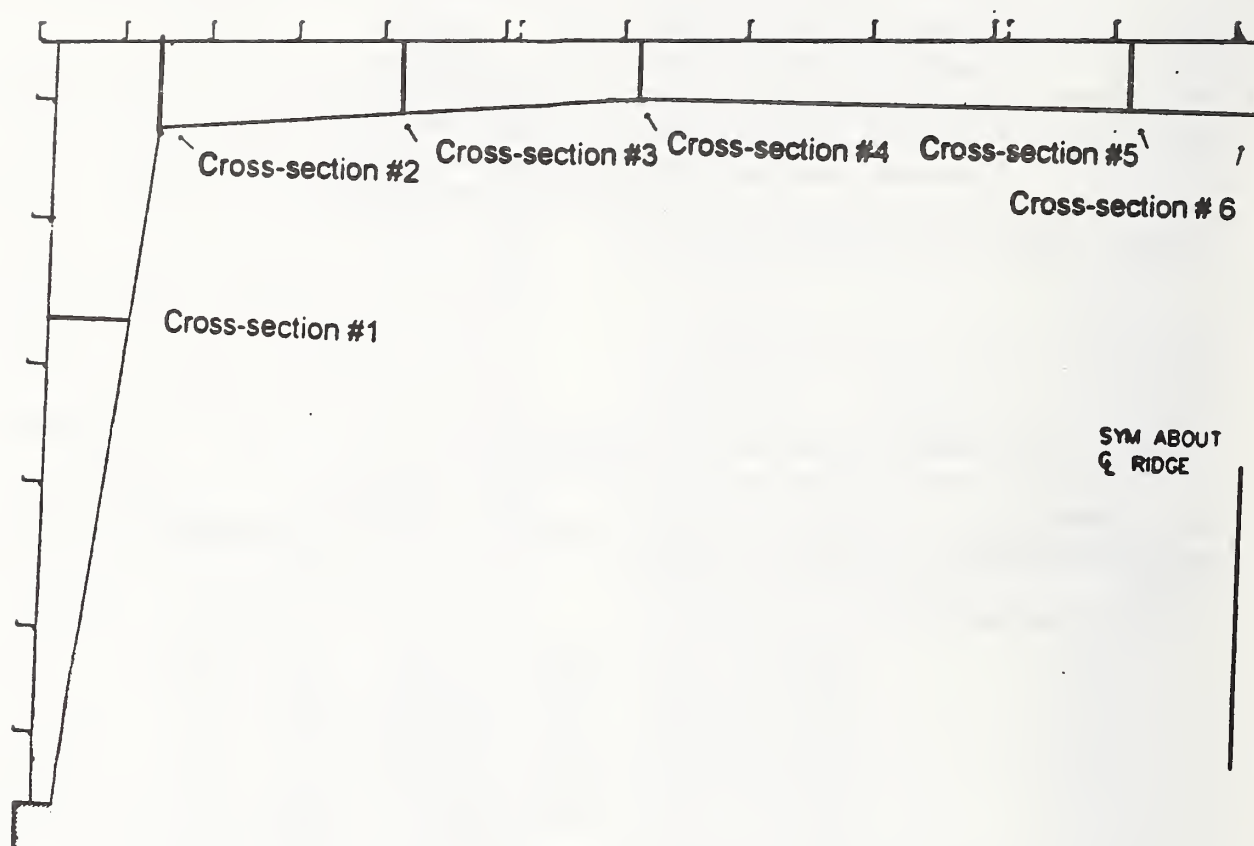


Fig. 1. Schematic of typical frame taken from construction drawing.

1803 1802	1709	1708	1615	1614	1605	1604	1510	1509	1416	1415	1406	1405
1804 1801	1710	1707	1616	1613	1606	1603	1511	1508	1414	1414	1407	1404
1805 1716	1711	1706	1612	1607	1602	1512	1507	1502	1413	1413	1408	1403
1806 1715	1712	1705	1611	1608	1516	1513	1506	1503	1412	1412	1409	1402
1807 1714	1713	1704	1610	1609	1515	1514	1505	1504	1411	1411	1410	1401



TOTAL 500													
NUMBER OF TAPS													
ROOF 14x15 = 210													
SIDE WALLS 14x15x2 = 140													
END WALLS 15x5x2 = 150													
1901	2001	2100	2200	2300	2400	2500	2600	2700	2800	2900	3000	3100	3200
1902	2002	2102	2202	2302	2402	2502	2602	2702	2802	2902	3002	3102	3202
1903	2003	2103	2203	2303	2403	2503	2603	2703	2803	2903	3003	3103	3203
1904	2004	2104	2204	2304	2404	2504	2604	2704	2804	2904	3004	3104	3204
1905	2005	2105	2205	2305	2405	2505	2605	2705	2805	2905	3005	3105	3205
1906	2006	2106	2206	2306	2406	2506	2606	2706	2806	2906	3006	3106	3206
1907	2007	2107	2207	2307	2407	2507	2607	2707	2807	2907	3007	3107	3207
1908	2008	2108	2208	2308	2408	2508	2608	2708	2808	2908	3008	3108	3208
1909	2009	2109	2209	2309	2409	2509	2609	2709	2809	2909	3009	3109	3209
1910	2010	2110	2210	2310	2410	2510	2610	2710	2810	2910	3010	3110	3210
1911	2011	2111	2211	2311	2411	2511	2611	2711	2811	2911	3011	3111	3211
1912	2012	2112	2212	2312	2412	2512	2612	2712	2812	2912	3012	3112	3212
1913	2013	2113	2213	2313	2413	2513	2613	2713	2813	2913	3013	3113	3213
1914	2014	2114	2214	2314	2414	2514	2614	2714	2814	2914	3014	3114	3214
1915	2015	2115	2215	2315	2415	2515	2615	2715	2815	2915	3015	3115	3215

195	194	193	192	191
196	195	194	193	192
197	196	195	194	193
198	197	196	195	194
199	198	197	196	195
200	199	198	197	196
201	200	199	198	197
202	201	200	199	198
203	202	201	200	199
204	203	202	201	200
205	204	203	202	201
206	205	204	203	202
207	206	205	204	203
208	207	206	205	204
209	208	207	206	205
210	209	208	207	206
211	210	209	208	207
212	211	210	209	208
213	212	211	210	209
214	213	212	211	210
215	214	213	212	211
216	215	214	213	212
217	216	215	214	213
218	217	216	215	214
219	218	217	216	215
220	219	218	217	216
221	220	219	218	217
222	221	220	219	218
223	222	221	220	219
224	223	222	221	220
225	224	223	222	221
226	225	224	223	222
227	226	225	224	223
228	227	226	225	224
229	228	227	226	225
230	229	228	227	226
231	230	229	228	227
232	231	230	229	228
233	232	231	230	229
234	233	232	231	230
235	234	233	232	231
236	235	234	233	232
237	236	235	234	233
238	237	236	235	234
239	238	237	236	235
240	239	238	237	236
241	240	239	238	237
242	241	240	239	238
243	242	241	240	239
244	243	242	241	240
245	244	243	242	241
246	245	244	243	242
247	246	245	244	243
248	247	246	245	244
249	248	247	246	245
250	249	248	247	246
251	250	249	248	247
252	251	250	249	248
253	252	251	250	249
254	253	252	251	250
255	254	253	252	251
256	255	254	253	252
257	256	255	254	253
258	257	256	255	254
259	258	257	256	255
260	259	258	257	256
261	260	259	258	257
262	261	260	259	258
263	262	261	260	259
264	263	262	261	260
265	264	263	262	261
266	265	264	263	262
267	266	265	264	263
268	267	266	265	264
269	268	267	266	265
270	269	268	267	266
271	270	269	268	267
272	271	270	269	268
273	272	271	270	269
274	273	272	271	270
275	274	273	272	271
276	275	274	273	272
277	276	275	274	273
278	277	276	275	274
279	278	277	276	275
280	279	278	277	276
281	280	279	278	277
282	281	280	279	278
283	282	281	280	279
284	283	282	281	280
285	284	283	282	281
286	285	284	283	282
287	286	285	284	283
288	287	286	285	284
289	288	287	286	285
290	289	288	287	286
291	290	289	288	287
292	291	290	289	288
293	292	291	290	289
294	293	292	291	290
295	294	293	292	291
296	295	294	293	292
297	296	295	294	293
298	297	296	295	294
299	298	297	296	295
300	299	298	297	296

1901 2001	2100	2200	2300	2400	2500	2600	2700	2800	2900	3000	3100	3200
1902 2002	2102	2202	2302	2402	2502	2602	2702	2802	2902	3002	3102	3202
1903 2003	2103	2203	2303	2403	2503	2603	2703	2803	2903	3003	3103	3203
1904 2004	2104	2204	2304	2404	2504	2604	2704	2804	2904	3004	3104	3204
1905 2005	2105	2205	2305	2405	2505	2605	2705	2805	2905	3005	3105	3205
1906 2006	2106	2206	2306	2406	2506	2606	2706	2806	2906	3006	3106	3206
1907 2007	2107	2207	2307	2407	2507	2607	2707	2807	2907	3007	3107	3207
1908 2008	2108	2208	2308	2408	2508	2608	2708	2808	2908	3008	3108	3208
1909 2009	2109	2209	2309	2409	2509	2609	2709	2809	2909	3009	3109	3209
1910 2010	2110	2210	2310	2410	2510	2610	2710	2810	2910	3010	3110	3210
1911 2011	2111	2211	2311	2411	2511	2611	2711	2811	2911	3011	3111	3211
1912 2012	2112	2212	2312	2412	2512	2612	2712	2812	2912	3012	3112	3212
1913 2013	2113	2213	2313	2413	2513	2613	2713	2813	2913	3013	3113	3213
1914 2014	2114	2214	2314	2414	2514	2614	2714	2814	2914	3014	3114	3214
1915 2015	2115	2215	2315	2415	2515	2615	2715	2815	2915	3015	3115	3215

Fig. 2. Schematic showing arrangement of pressure taps.

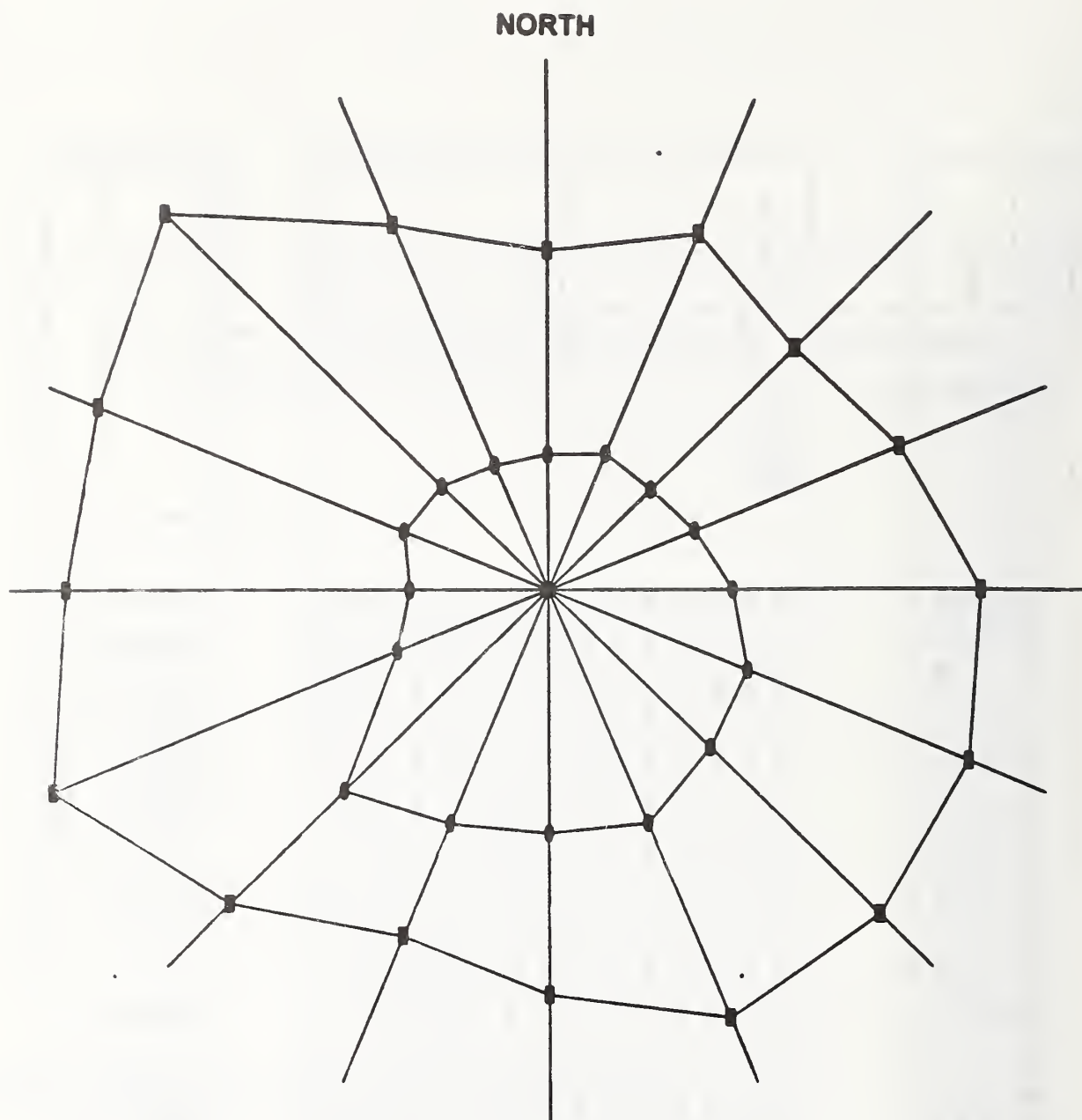


Fig. 3. Maximum and mean hurricane winds for 16 azimuths near Charleston, S.C. Largest directional speeds are 50 m/s (WSW and NW directions.)

GPS MONITORING OF STRUCTURES: RECENT ADVANCES

by

Mehmet Çelebi¹, Will Prescott¹, Ross Stein¹, Ken Hudnut², Jeff Behr³ and Steve Wilson⁴

ABSTRACT

Relative displacements used to assess stress and drift conditions of structures are difficult to measure directly. Accelerometers are the most common instruments used to monitor structural systems during earthquakes or strong winds, but to arrive at displacements requires processing including double integration. In most cases, such processing does not take place in real-time or near real-time because of requisite steps including choice of filters for signal processing. These choices could introduce errors at periods relevant to structural response. However, recent advances in Global Positioning System (GPS) technology recording at 10 samples per second (sps) allows reliable monitoring of long-period structures such as suspension or cable-stayed bridges and tall buildings. GPS units with a capability of resolving motion at the centimeter level (± 1 cm for horizontal, ± 2 cm for vertical accuracy) with sampling rates of 10 sps are now available from several manufacturers. The majority of tall buildings (20-40 stories or more) are flexible steel framed structures whose fundamental period (T , in seconds) can be estimated with the empirical formula $T = 0.1 N$, where N is the number of stories of a building. Thus, the frequencies corresponding to the fundamental periods of most buildings over 20 stories are 10-20 times the Nyquist frequency of the sampling, which is sufficient to assess accurately its

average drift ratio⁵. With this method, displacement is measured directly in real-time.

In this paper, we discuss the scientific justification and feasibility of using GPS technology to monitor long-period structures. We describe an experiment simulating the response of a tall building. The results indicate that sampling at 10 sps provides a clear and accurate response history from which drift ratios and dynamic characteristics of the specimen can be derived. The paper discusses in detail how data recorded from tall buildings monitored with GPS units can be used by engineers and building owners or managers to assess the building performance during extreme

¹ U.S. Geological Survey, MS977, 345 Middlefield Rd., Menlo Park, Ca. 94025

² U.S. Geological Survey, 525 S. Wilson Ave., Pasadena, CA 91106

³ SCIGN, 525 S. Wilson Ave., Pasadena, Ca. 91106

⁴ Leica GPS, 23868 Hawthorne Blvd., Torrance, CA., 90505

⁵ Drift ratio is the relative displacement of two consecutive floors divided by the height of the floor. In this case, we are defining average drift ratio between the roof level and the ground level as the relative displacement between those two levels divided by the height between the two levels.

motions caused by earthquakes and strong winds, by establishing threshold displacements or drift ratios and identifying changing dynamic characteristics. Such information can then be used to secure public safety and/or take steps to improve the performance of the building.

KEYWORDS: global positioning system, building, bridge, monitoring, long-period, structural response, frequency

1. INTRODUCTION

Seismic monitoring of structural systems constitutes an integral part of National Earthquake Hazard Reduction Program. In general, until recently, monitoring the response of structural systems for the purpose of assessment and mitigation of earthquakes (and also severe winds) has relied on measuring shaking response by deploying accelerometers throughout a particular structure of interest to the scientific and engineering community. In contrast, there are no efficient or feasible methods to measure displacements during an earthquake or severe wind. Recordings of the acceleration response of structures have served us well. Studies conducted on such records have been useful in assessing design/analyses procedures, improving code provisions and in correlating the response with damage.

Since the $M_s=6.7$ Northridge (17 January 1994) and $M_s=6.8$ Kobe (17 January 1995) earthquakes, drift studies and assessment of susceptibility to damage of tall buildings have become important issues – particularly because so many steel framed buildings were damaged, some severely and some lightly. In the Los Angeles area, for example, following the Northridge event, several hundred steel-

framed buildings had to be examined, assessed, repaired and/or retrofitted. Only three of these buildings were instrumented prior to the event, providing some limited acceleration response data to be used for interpretation of the widespread damage. Additional data, if available in real-time or near real-time could have been very useful for studies and design of repair and retrofitting projects that followed. Therefore there is a great need for better monitoring of tall buildings.

Relative displacements, which are key to assessing drift and stress conditions of structures, are difficult to measure directly. On the other hand, measuring acceleration response requires a double integration process to arrive at displacements. The integration process is not readily automated because of the nature of signal processing -- which (a) requires selection of filters and baseline correction (the constants of integration), and (b) often requires substantial judgement when anomalies exist in the records. Consequently, this process can lead to errors in the calculation of velocities and displacements. This problem is more acute for permanent displacements. Accelerometer measurements cannot be used to recover the permanent displacements at the centimeter level; and even if they were, it is questionable if it can be done so in real-time. To the authors' best knowledge, such comparisons have not been made. That is, the level of accuracy of displacements calculated from accelerations has not been widely verified by observations (e.g. some shake table tests performed to compare the performances of accelerometers and accelerographs have not been directed to check displacements).

As an alternative method of measuring relative displacements while monitoring structural systems, we introduce GPS technology. In general, GPS monitoring systems are used for other purposes because of the sampling rates used (e.g., 1 sample per hour, day etc). A few such applications including those for structural systems are summarized in Appendix A. However, the technology has advanced to such a stage that it is now possible to record at 10 sps. This provides a great opportunity to monitor long-period structures reliably (e.g. tall buildings that are 20-40 stories or more). The majority of the tall buildings are flexible steel framed structures. The fundamental period of such a flexible framed building can be estimated with the empirical formula⁶: $T = 0.1 N$, where N is the number of stories of the building. This means that at least 20 - 40 data points will be recorded for one cycle of motion of a 20 - 40 story building vibrating at the fundamental period. This provides sufficient accuracy to assess the average drift ratio of a building. Such information can be very useful in assessing the damage to a building. In addition, the main value in using GPS technology to assess the condition of a building is that the displacement measurements can be made directly in real-time and with sufficient precision. As discussed later, we have made preliminary tests to prove the technical feasibility of the application of GPS to monitoring structures.

There is great potential for the development of the application of GPS technology to

⁶ For most flexible buildings, the fundamental period (T) is approximated by $0.1N$, where N is the number of floors of a building (even though the fundamental period can vary between $[0.05-0.15]N$ depending on the flexibility of the building). Therefore, to simulate a 40-story building, we set the period (frequency) equal to 4 s (0.25 Hz) and proportioned the length, width and thickness of the cantilever.

monitor long-period structures during earthquakes. The application can also be extended to monitoring wind-induced deformation of tall buildings, long-span suspension and cable-stayed bridges and tall chimneys. Furthermore, with future advances in GPS technology and improvements in sampling capability (e.g. higher than 10 sps), it will be possible to monitor short-period structures as well. The current technologies do not readily lend themselves to automated, real-time applications. Additionally, direct measurements of displacements will enable us to reliably detect structural movement caused by failure of the ground under the structure (e.g. liquefaction).

2. TECHNICAL JUSTIFICATION

2.1 Model Tests Simulating A Tall Building

To investigate the feasibility of using GPS technology to monitor tall buildings (and other long-period structures), we conducted 2 experiments. Figure 1 depicts a photo and the overall set-up for a simple experiment designed by selecting a standard stock steel bar to simulate a 30-40 story flexible building. We selected the length, thickness and width of the two bar specimens to yield a fundamental period of approximately 4 seconds in the weak direction. To make things simple, we purposefully selected the width and thickness of each of two bars with an extremely weaker axis in one direction. The width was varied to show the sensitivity of measurements during vibration and at 10 Hz sampling rate. Each bar was fixed at the base and the GPS unit was attached at its tip. By providing an initial displacement, each bar was set into free vibration and its motion was recorded. Results are summarized in Table 1. Figure 2 shows the particle motion and time-history

of one of the tests performed. The axes of the bar were at an angle to the NS (and EW) direction. Therefore, the NS and EW components of displacements are identical in phase and proportional in amplitude. Also, since the GPS unit is not symmetrically and concentrically mounted in the weak direction (Photo in Figure 1), the amplitudes of positive and negative displacements measured are not the same. The detection of the effect of the eccentric mass adds to the assurance that the measurements are accurate and sensitive.

Figure 3 is a plot of NS components of measured relative displacements and corresponding amplitude spectra of Bars A and B. The figure shows the accuracy and sensitivity of the GPS monitoring technology at 10 samples/second. The measurements differentiate between the frequency of the free-vibration response of the two bars with different dynamic characteristics. From the data, the fundamental frequency (period) of the two bars are identified to be 0.245 Hz (4.08 s) and 0.296 Hz (3.38 s) respectively. Also, a damping percentage of approximately 2% is extracted. This simple test shows that sampling at 10 Hz with GPS units provides a clear and accurate displacement response history from which drift ratios and dynamic characteristics of the specimen can be derived (Çelebi *et al*, 1997a). The implications of this go beyond just the measurements. It can be shown that identification of variation of dynamic characteristics can be used to identify not only different structural systems, but also the possible non-linearities that occurs during vibration (e.g. due to damage and plastic behavior of the structural members, components and/or joints or soil-structure

interaction under varying amplitudes of input motions).

2.2 GPS Ambient Test of a 44-story Building and Strong-motion Acceleration Records

In a second test, we measured ambient vibration (due to winds and traffic noise) of a 44-story building with a GPS unit temporarily deployed on its roof. A reference GPS unit was located within 500 m of the building. The signals were very noisy and amplitudes very small; therefore, most common methods to identify structural characteristics did not work. Only the cross-spectrum of the two orthogonal, horizontal, low-amplitude ambient displacement recordings (when the signals are coherent and approximately 180° degree out of phase) was used to identify the fundamental frequency of the building at 0.23 Hz (Figure 4), with another frequency at ~ 0.3 Hz. Despite the very small signal, these frequencies appear to be reliable when compared with the 0.23 Hz frequency calculated from accelerations recorded with a triaxial accelerograph on the 38 th floor (accepted here as the roof response) during a small earthquake (Figure 5). A comparison of these frequencies is provided in Figure 6.

Despite the small displacements (<1 cm) and large noise to signal ratio of this experiment, the fact that dynamic frequencies could be identified indicates that during larger displacements, better identification of the dynamic characteristics as well as drift ratios can be made with higher confidence.

3. LOOKING TO THE FUTURE: REAL TIME MONITORING

We are developing a real-time structural monitoring technique using GPS. Our approach in developing this application is as follows:

- We are planning to deploy GPS units on one or more tall buildings that are already instrumented with accelerometers. This will facilitate comparison of absolute and relative displacements. The GPS units will be configured to provide data to indicate the real-time average drift ratio and changes in the dynamic characteristics of the tall building. This information can be made available to building managers (or interested parties) in real-time or whenever a predetermined displacement threshold is reached. The building managers can assess the response of the buildings according to (a) different threshold displacements (*e.g.* A, B and C as shown in Figure 7), (b) drift ratios, or (c) changing dynamic characteristics. If a situation is serious, the management can make decisions to evacuate the building for additional inspection. Therefore, one by-product of the effort would be to secure the safety of the occupants and significant contents of the building. Thus, a real-time structural health monitoring environment will be created. At least 3 GPS units per building are required to monitor a tall building. Two of the units should be deployed on the roof to detect translational and torsional response of the building. The third unit will serve as a reference ground station to evaluate relative displacement. This also needs a site with excellent sky visibility.
- Similar deployments are being planned for other types of long-period structures. One project in development at this time is for deploying GPS units on one of the long-period suspension bridges such as the Golden Gate Bridge and Bay Bridge (San Francisco) or Vincent-Thomas Bridge (Los Angeles). As in the case of tall buildings, changes in dynamic characteristics after the displacements at critical locations of a bridge have exceeded predetermined thresholds can be calculated in near real-time (Figure 8). When warranted, the management can make decisions to inspect the bridge (*e.g.* decisions can be made to stop the traffic, thus securing the bridge safety, which is one of the objectives of lifeline earthquake engineering). With the GPS technology, we can furnish time-dependent displacements for the relative movements of critical locations of structures. For example, for the bridges, GPS units placed at pre-selected locations of bridge elements can indicate, in real-time, the amplitude of the displacements of the decks and towers, as well as movements of key bridge elements relative to local bedrock reference points. Thus, movements of the piers relative to the abutments, the top of a tower with respect to its base, or the span with respect to the ground, can be made at a centimeter-level of precision, in real-time. We will recover both the dynamic motions that accompany the earthquake, as well as the static or permanent displacements experienced by the bridge once the shaking has stopped. Such permanent displacements affect the state of stress of a bridge, and provide evidence for distortion or failure of bridge elements or subsidence of piers

due to ground compaction induced by earthquake shaking.

- Requisite software is being developed to assess and mitigate the two natural hazards (earthquake and severe wind) affecting the structures by using the displacements measured by the GPS units.
- The collected information on the response of the structure during strong motion events (or strong winds) can be used to make decisions for further evaluation of the susceptibility to damage of the structure and future repair/retrofit schemes may be developed.
- The recorded data can be used to analyze the performance of the structure and such results can be used to improve future analyses/design procedures.
- The data collected will also be used to assess long-term displacements of critical locations of structural systems (e.g. permanent displacements, settlement of foundations, long-term deformations due to change of temperature and the plate tectonic deformation spanning the San Francisco Bay and parts of the Los Angeles Basin) and to develop methodologies on how the findings can be incorporated into useful practical design procedures.

4. CONCLUSIONS:

It is shown in this paper that recent advances in sampling rates of GPS technology allows real-time monitoring of long-period structures such as tall buildings and long-span bridges. The advantage is that relative

displacements can be measured in real-time and with sufficient accuracy. The technical feasibility is illustrated through two tests conducted on two vertically cantilevered bars that simulated tall buildings and ambient test of a 44-story building. Both approaches show that GPS monitoring of long-period structures provide sufficiently accurate measurements of relative displacements and that dynamic characteristics of the vibrating systems can be accurately identified. This capability can be very useful to be used for structural health monitoring purposes. Procedures and software are being developed to permanently deploy GPS units on tall buildings and suspension bridges.

5. REFERENCES:

- Celebi, M., Presscott, W., Stein, R., Hudnut, K., and Wilson, S., 1997, Application of GPS in Monitoring Tall Buildings in Seismic Areas, Abstract, AGU Meeting, San Francisco, Ca. Dec. 1997
- Celebi, M., 1998, GPS and/or strong and weak motion structural response measurements – Case studies, Structural Engineers World Congress (SEWC), San Francisco, Ca., July 1998 (paper submitted).
- Hodgkinson, K. M., R. S. Stein, K. W. Hudnut, J. Satalich, and J. H. Richards, Damage and restoration of geodetic infrastructure caused by the 1994 Northridge, California, earthquake, U.S. Geol. Surv. Open File Rep., 96-517, 1-70, 1996.
- Hudnut, K. W., Z. Shen, M. Murray, S. McClusky, R. King, T. Herring, B. Hager, Y. Feng, P. Fang, A. Donnellan, and Y. Bock, Coseismic displacements of the 1994

Northridge, California, earthquake, Bull. Seis. Soc. Amer., 86, S19-S36, 1996.

Hudnut, K., 1996, Continuous GPS monitoring of dam deformation, EOS, no. 46, pp. F139 (abstract).

Hudnut, K.W., and Behr, J., 1998, Continuous GPS monitoring of deformation of Pacoima Dam, Ca., (paper in preparation).

King, N. E., H. Johnson, W. H. Prescott, M. H. Murray, J. L. Svarc, R. Clymer, and B. Romanowicz, 1996, Estimates of GPS and monument noise from the Bay Area Regional Deformation (BARD) permanent array: EOS, Transactions, American Geophysical Union, v. 77, p. 153.

King, N. E., M. H. Murray, and W. H. Prescott, 1994, The Bay Area Regional Deformation (BARD) permanent GPS array (Abs.): EOS, Transactions, American Geophysical Union, v. 75, p. 470.

King, N. E., J. L. Svarc, E. B. Fogelman, W. K. Gross, K. W. Clark, G. D. Hamilton, C. H. Stiffler, and J. M. Sutton, 1995, Continuous GPS observations across the Hayward fault, California, 1991-1994: J. Geophys. Res., v. 100, p. 20,271-20,284.

Prescott, W. H., 1996, Will a continuous GPS array for L.A. help earthquake hazard assessment?: EOS, Transactions, American Geophysical Union, v. 77, p. 417.

Stein, R. S., K. W. Hudnut, J. Satalich, and K. M. Hodgkinson, Monitoring seismic damage to bridges and highways with GPS: Insights from the 1994 Northridge earthquake, in Natl. Seismic Confr. on Bridges and Highways, (pp. 347-360),

Sacramento, Fed. Highway Admin. and Calif. Dept. of Transportation, 1997.

Stein, R. S., G. A. Marshall, and M. H. Murray, Permanent ground movement associated with the 1992 M=7 Cape Mendocino, California, earthquake: Implications for damage to infrastructure and hazards to navigation, U.S. Geol. Surv. Open-File Rep., 93-383, 36 p., 1993.

APPENDIX A: OTHER APPLICATIONS

A.1. Post-Earthquake GPS surveys on Bridges

The Federal Emergency Management Agency funded two USGS studies, in consort with the National Geodetic Survey and Caltrans, in which the permanent (or static) displacements of bridges and other engineered structures were measured following large earthquakes. These studies revealed that large permanent displacements of bridge abutments are easily measured from GPS and leveling surveys. After the M=7.0 Cape Mendocino, California, earthquake, displacement of geodetic monuments on bridge abutments relative to the ground revealed damage to a major bridge crossing the Eel River, as well as road and rail embankment failures caused by landslides and liquefaction. One abutment settled 70 mm, and the abutment on the opposite bank settled 130 mm [Stein, et al., 1993]. After the 1994 M=6.7 Northridge earthquake, the USGS resurveyed the 1045 leveling and GPS monuments, and added 128 new GPS monuments spaced 5 km apart along the I-405 Freeway for rapid damage assessment after future earthquakes. The Northridge analysis revealed four monuments in bridge abutments with subsidence of up to 116 mm, and uplift of up to 58 mm [Hodgkinson, et al., 1996, Hudnut, et al., 1996]. Because few bridge or other highway structures were assessed for earthquake effects except by visual inspection, subtle or hidden damage suggested by the settlement or uplift of the structures merits re-inspection. This study is accessible via www-socal.wr.usgs.gov/fema.

A.2. Pacoima Dam Pilot Project

An experimental pilot project with Los Angeles County to monitor Pacoima Dam (Figure A1) has demonstrated the feasibility of a precise telemetered GPS monitoring system. The USGS began monitoring the double-arch dam wall in 1995, and initiated near real-time production of results in January 1996 [Hudnut, 1996, Stein, et al., 1997]. Daily plots are posted on the internet (www-socal.wr.usgs.gov/hudnut/hudnut/dam.html). Horizontal repeatability of the data between daily estimates is <4 mm, and vertical repeatability is <12 mm. The experiment demonstrates the field reliability of continuous GPS units on an engineered structure, and the results (Figure 4) reveal heretofore-unmeasured thermal expansion and contraction of 20 mm seasonally (Hudnut and Behr, 1998).

A.3. Bay Area Regional Deformation (BARD) and Southern California Integrated GPS Network (SCIGN)

Continuous GPS nets in Southern and Northern California, SCIGN (50 stations growing to 250 within two years) and BARD (20 stations within the San Francisco Bay Area), provide continuously updated information about the regional strain pattern to which the bridges are subjected. The bridge and building monitoring stations discussed herein will be located within a few kilometers of existing BARD or SCIGN sites. Long-term deformation associated with plate tectonics for the SCIGN and BARD sites is well established, thus, there will be a good background against which to examine both the static and dynamic deformation indicated by the bridge units.

Table 1. Results of Tests with GPS Unit

Specimen	Length [H] ft (m)	Width [B] in.(cm)	Thickness [t] in. (cm)	Measured Frequency [f](Hz)	Measured Period [T](s)	Damping [ξ](%)
BAR A	6 (1.82)	1.5(3.8)	1/8 (0.32)	0.245	4.08	~ 2.0
BAR B	6	2.0(5.0)	1/8	0.296	3.38	~ 2.0

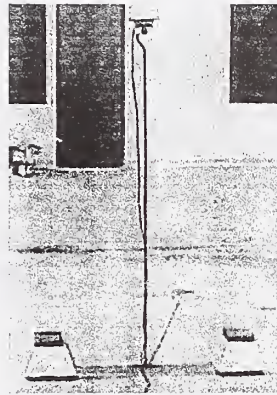


Figure 1a. Photo of Test Set-up for using GPS for monitoring tall buildings

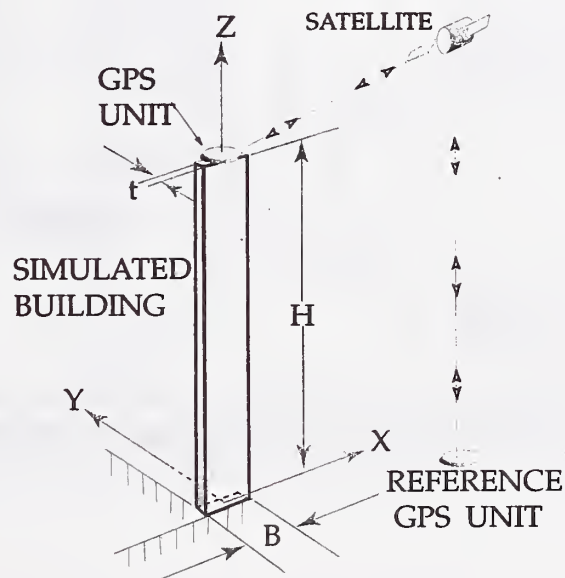


Figure 1b. Schematic of Test Set-up for using GPS for monitoring tall buildings

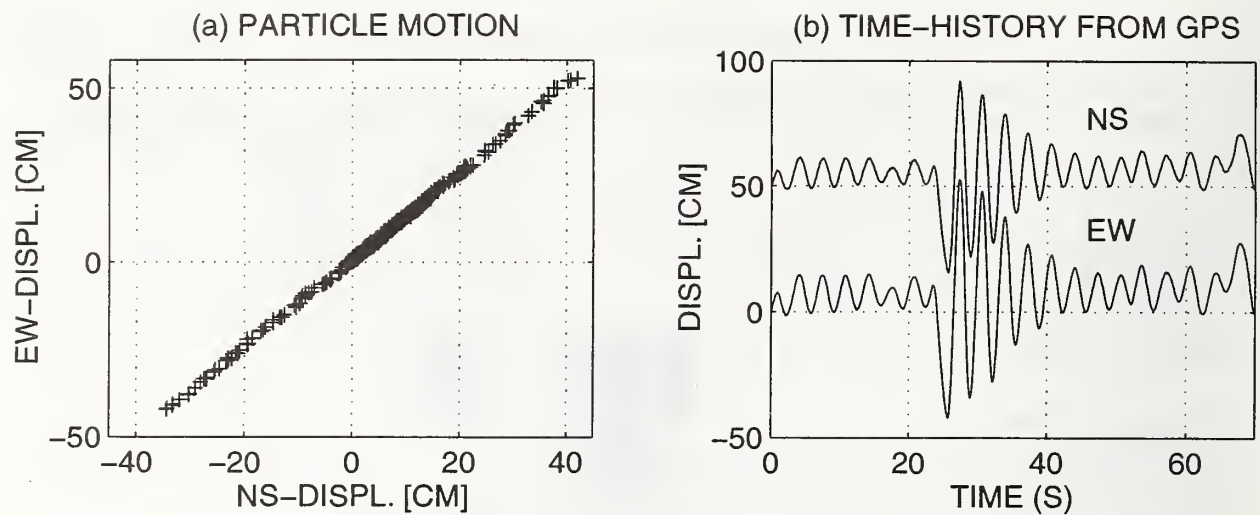


Figure 2. Particle motion and time-history of relative displacements (NS and EW components) of simulated test specimen.

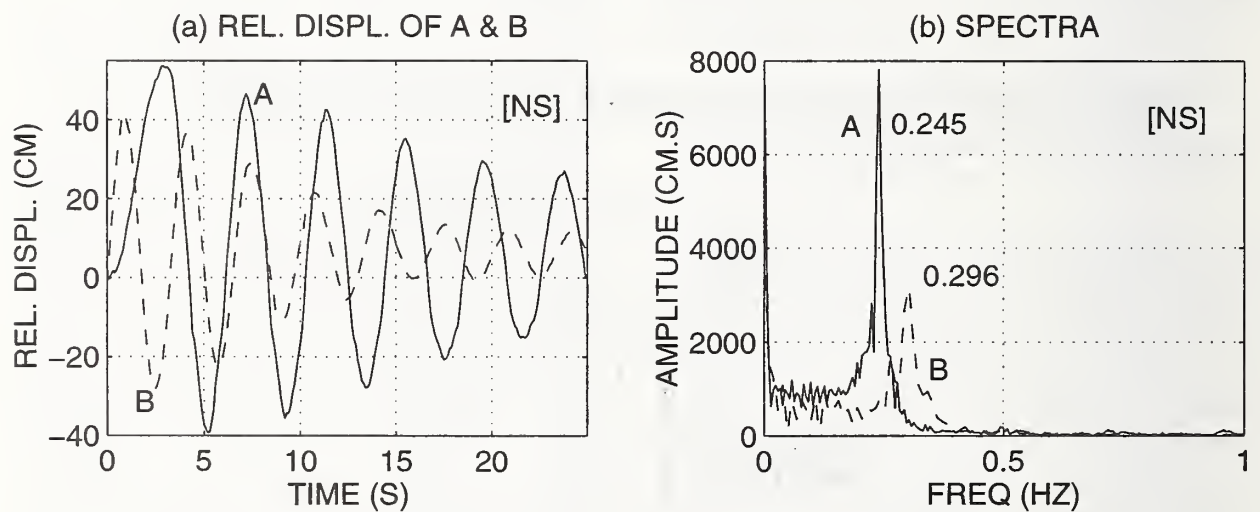


Figure 3. Relative displacements of two test specimens (NS components only) in free-vibration and corresponding amplitude spectra identifying the fundamental frequencies of the test specimens

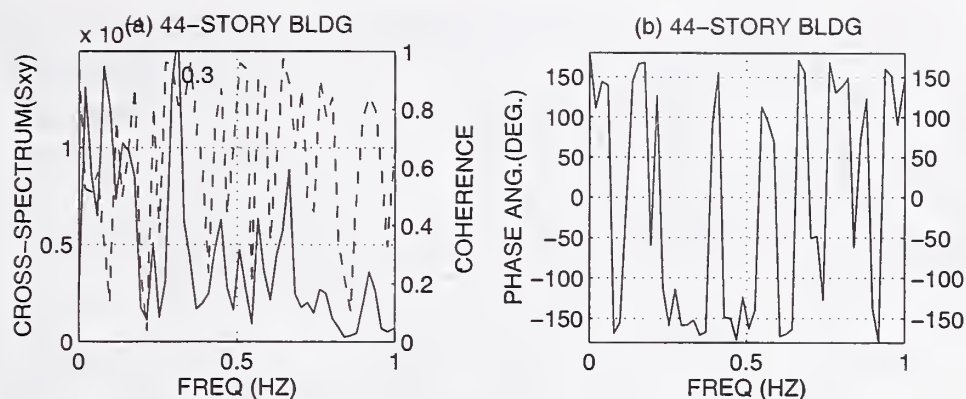


Figure 4. Ambient test of a 44-story building with GPS technology: Cross-spectrum (left-solid), coherence (left-dashed) and phase-angle (right) of two orthogonal horizontal motions.

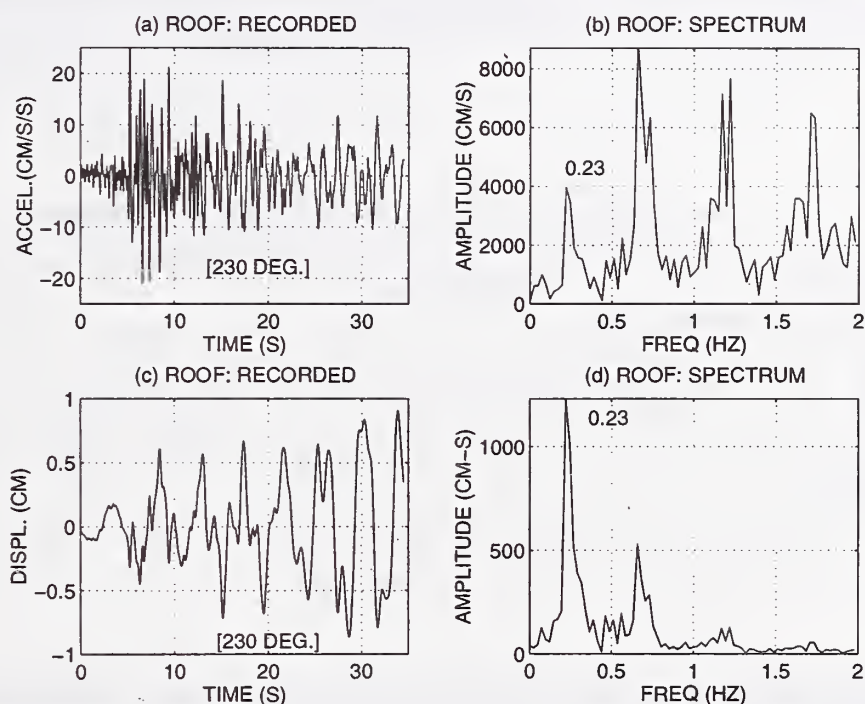


Figure 5. Recorded roof (38th floor accepted in lieu of roof) accelerations of a 44-story building and displacements (derived by double integration) and amplitude spectrum.

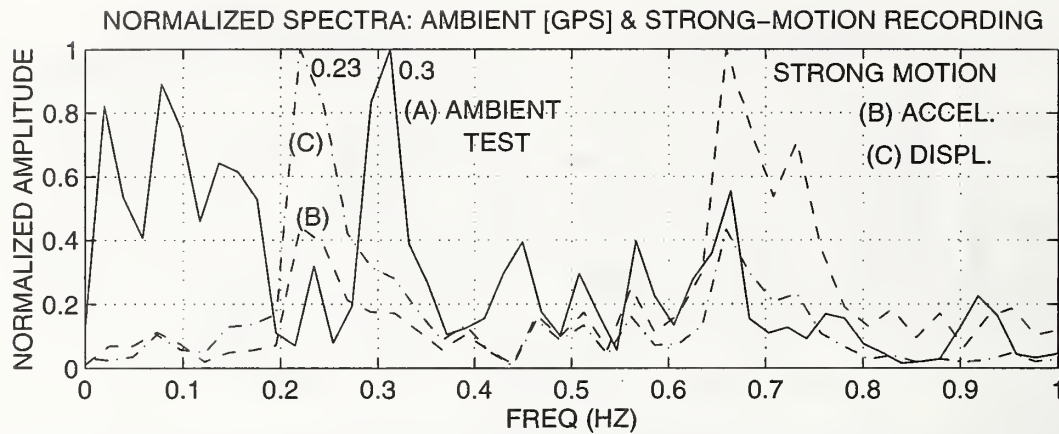


Figure 6. Comparison of normalized frequencies for ambient GPS recording (from cross-spectrum) and strong-motion recording (from amplitude spectrum).

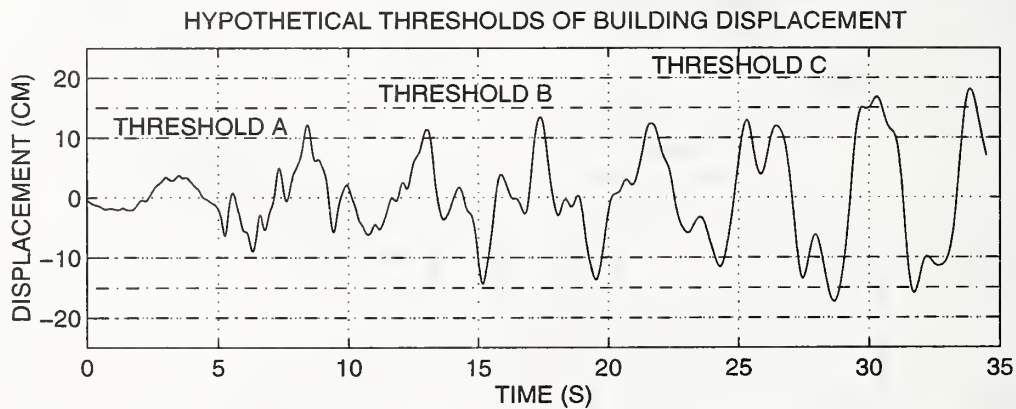


Figure 7. Hypothetical thresholds of displacements. The time-history of displacements shown is actually integrated from accelerations recorded at the 38th floor (accepted in lieu of roof) of a 44-story building. The actual record (in Figure 5) is amplified by 20 times for illustration purposes.

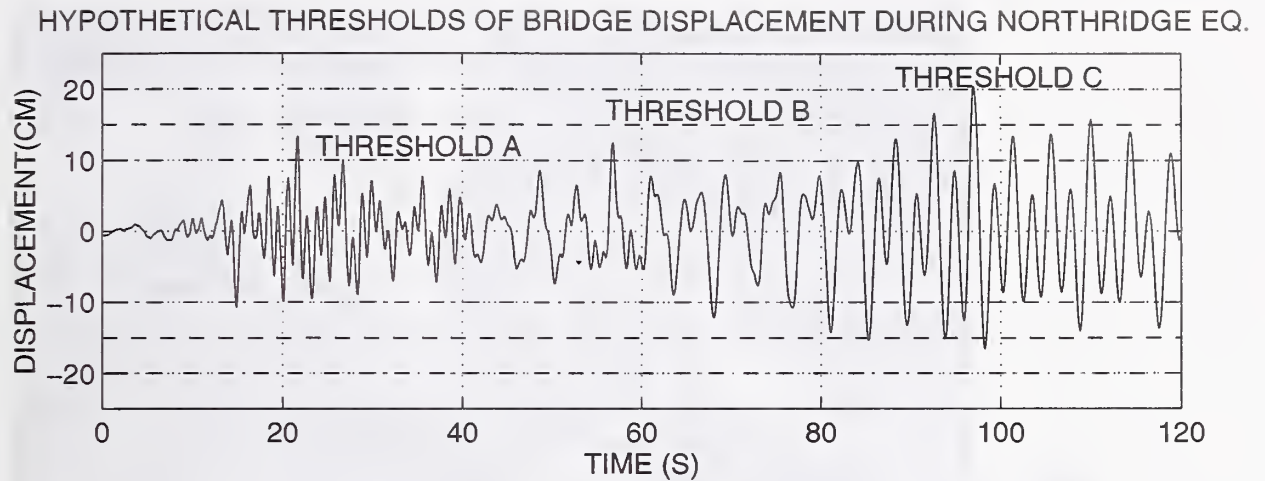


Figure 8. Hypothetical thresholds for displacement (from double-integration of recorded acceleration) of channel 21 (vertical at mid side-span) of Vincent Thomas Bridge (1994 [M=6.7] Northridge earthquake).

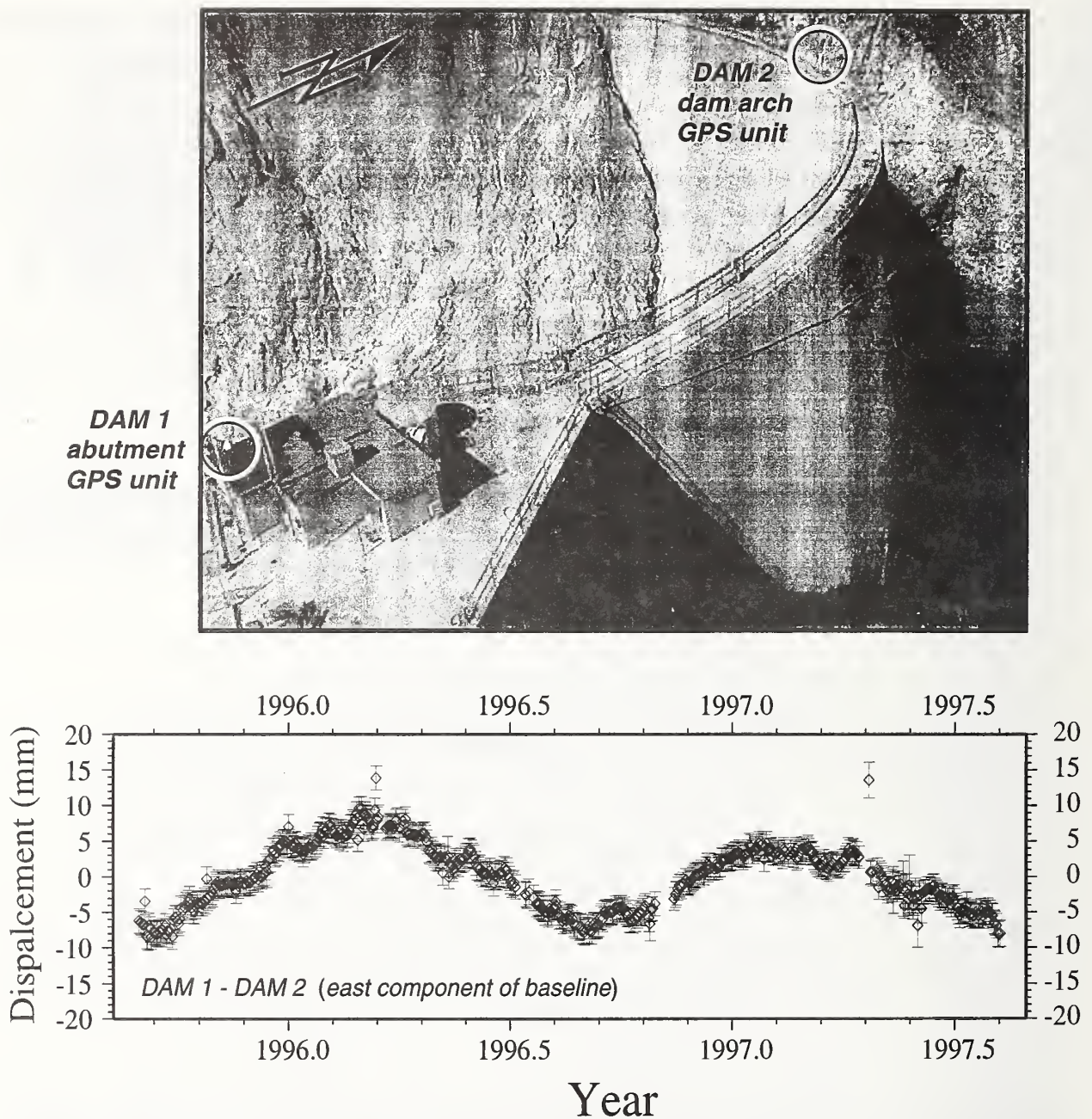


Figure A1. Structural displacement history of Pacoima Dam, Los Angeles, from continuous GPS measurements of a remotely operated, telemetered 3-station network run by Kenneth Hudnut (USGS) since 1995. Pacoima Dam was damaged by $\sim 1g$ accelerations during both the 1971 San Fernando and 1994 Northridge earthquakes. Two GPS stations are visible in the photograph; a third station is located several km away on bedrock. Thermal contraction of the 120 m high double-arch structure is evident, as well as an apparent long-term expansion of the arch of several millimeters per year. Note that horizontal precision is ± 2 mm. The experiment demonstrates field reliability of telemetered, autonomous GPS installations on large engineered structures; the results reveal previously unmeasured thermal processes (adopted from Hudnut & Behr, 1998).

APPENDIX

TASK COMMITTEE A-K REPORTS AND NEW T/C ON SEISMIC INFORMATION SYSTEMS



Figure 1. A line graph showing the relationship between two variables over time.



REPORT OF TASK COMMITTEE A STRONG MOTION DATA AND APPLICATIONS

Date: 12 May 1998

Place: National Institute of Standards and Technology, Gaithersburg, Maryland

Attendees:	Japan side --	Susumu Iai (Chairman)	PHRI
		Kazushige Endo	PWRI
	U. S. side --	Roger D. Borchardt (Chairman)	USGS
		Jon Ake	USBR
		Michael Blackford	NOAA
		William B. Joyner	USGS

1. Objective and Scope of Work

To coordinate and promote sharing of strong motion earthquake data among researchers and practicing engineers, and to develop techniques and exchange information for evaluating the destructive effects of earthquake motion.

The scope of work includes:

1. instrumentation,
2. recording, processing, and analyzing strong motion data,
3. engineering characterization of ground motion,
4. design applications, and
5. seismic zonation.

The activities of the Task Committee include:

1. regular exchange of data and publications,
2. creating procedures for disseminating significant strong motion digital data with regard for the rights and expectations of (a) owner(s), (b) data users and (c) the earthquake engineering community,
3. planning and conducting T/C workshops and meetings, and
4. coordinating relevant research activities.

2. Accomplishments

The 1994 Northridge and the 1995 Hanshin-Awaji earthquakes had a tremendous impact on various aspects of strong motion studies, including characterization of near field motion and site response. Research developments since these earthquakes have been very rapid, including proposals for new seismic guidelines, recommendations and codes in both the U.S. and Japan as well as a new proposal of a worldwide seismic hazard map for use in specifying seismic guidelines for offshore structures by the International Standards Organization (ISO). All these developments happened since 1995 and more are coming in 1998. In view of these developments, Task Committee A accomplished:

1. Closely monitored and contributed to seismic guidelines and codes in both countries, including UBC97 and NEHRP97 in the U.S. and ISO/WG67 in Japan,
2. At the suggestion of the Task Committee A members, a call for cooperation between U. S. and Japan in strong motion studies was included in the Earthquake Policy Symposium of the Common Agenda,
3. K-Net was completed with the effort of Task Committee A members. Rapidly accessible data standards established by K-Net are a model that should be followed by other U. S. and Japan strong motion programs during future development. Recently, the second CD-ROM with K-Net strong-motion data has been released in both Japanese and English,
4. Chairmen and members of Task Committee A contributed in January 1998 to a widely attended workshop sponsored by the Southern California Earthquake Center on the important subject of "Nonlinear Soil Response".

Tragic losses from the 1994 Northridge earthquake and the 1995 Hanshin-Awaji earthquake have emphasized the urgent need to mitigate the effects of future earthquakes during the next millennium. Recent efforts in the United States emphasize that inadequate sets of strong-motion recordings are presently a major obstacle to earthquake hazard mitigation. Towards developing a vision for strong-motion recording in the next millennium, Task Committee A members have contributed to several recent accomplishments. These include:

1. Participating on the Committee for the Advancement of Strong Motion Programs (CASMP) by US members,
2. Contributing to the organization and proceedings of the international workshop entitled "Vision 2005: An Action Plan for Strong-Motion Programs to Mitigate Earthquake Losses in Urbanized Areas", Monterey, CA, April 1997,
3. Contributing to the development and organization of the Consortium of Organizations for Strong-Motion Observation Systems (COSMOS),
4. Developing an initiative in the U.S. to instrument Federally owned and leased buildings with endorsement provided by CASMP and appropriate committees of the Interagency Committee for Seismic Safety in Construction (ICSSC).

3. Future Plans

Future plans include:

1. Planning a Task Committee workshop on Soil-structure Interaction (Chairmen: Celebi and Okawa, September 1998 in U. S.).
2. Hosting a new workshop in December 1998 on strong motion studies, which could be held in conjunction with ESG 98 (Effect of Surface Geology), to review and integrate, where possible, the most recent developments since the 1996 workshop.
3. Coordinating, where appropriate, ongoing U.S. and Japan developments in strong-motion-recording and data-dissemination programs, in conjunction with activities of recently established committees such as CASMP and organizations such as COSMOS.
4. Develop recommendations for Common Agenda, possibly in a workshop, regarding U.S. and Japan needs for strong-motion measurement in densely urbanized areas to significantly improve public earthquake safety.
5. Coordinating, where appropriate, ongoing developments in seismic hazard mapping and seismic codes for generalization and worldwide use.
6. Recognizing the developing emphasis in the engineering and emergency response communities on near-real time data availability, TC/A will continue to promote and exchange new developments in real-time data acquisition, processing, and notification. This activity will be in conjunction with the proposed TC on Seismic Information Systems.
7. Pursuing the idea of establishing a WWW page, which provides links to home pages of participating strong-motion organizations in conjunction with other UJNR WWW activities.

REPORT OF TASK COMMITTEE B
TESTING AND EVALUATION PROCEDURES FOR BUILDING SYSTEMS

Date: 12 May 1998

Place: National Institute of Standards and Technology, Gaithersburg, MD, U.S.A

Attendees: U. S. Side -- H. S. Lew (Chairman) NIST
Daniel Abrams MAE Center

Japan Side -- Keiichi Ohtani (Chairman) NIED
Makoto Watabe Keio University

1. Objective and Scope of Work

The objective of the Task Committee is to develop and recommend rational test procedures and to collect performance data of dynamic response of structures through both laboratory testing of prototype structures and field testing of structures in-situ.

The scope of work includes:

1. Plans and conducts workshops and joint meetings to identify research topics and develops joint research programs.
2. Coordinates research projects carried out by various laboratories in the U. S. and Japan. Facilitates publication of research results and implementation of findings in codes and standards.
3. Facilitates exchange of research personnel, technical information and available testing facilities.
4. Develops uniform testing procedures including test loading history for case of comparison of results of tests carried out by various researchers, and for establishment of data base.
5. Develops guidelines for interpretation of test results in consideration for design of structures.
6. Develops methodology for evaluation and interpretation of physical test results.

2. Accomplishments

1. The third phase of the U. S. Precast Seismic Structural Systems Program (PRESSSS) was initiated in 1995. Studies, including the testing of a full scale, five story frame

structure are in progress. Large-scale frame testing will be carried out at the University of California – San Diego.

2. In Japan, a 3-year program on the development of design guidelines for precast/prestressed buildings has been underway for the past two years and will be completed in 1998.
3. The research program on Composite and Hybrid Structures (CHS) in Japan was completed in early 1998. Experimental and analytical work was carried out jointly. The Building Research Institute, several universities and construction companies, and the Japan Structural Consultant Association undertook an applications study for implementing research results into practice.
4. The research program on CHS in the U.S. was initiated in 1995 under the sponsorship of the National Science Foundation. Over 16 research projects are in progress. Additional projects on composite wall systems are being initiated.
5. The Fourth U.S.-Japan Joint Technical Coordinating Committee (JTCC) meeting on CHS was held in October 1997 in Monterey, CA. Both sides agreed to continue to coordinate efforts in the development of design guidelines and to transfer technology to the design profession.
6. The 6th U.S.-Japan Cooperative Research on "Smart Structural Systems" (Auto-Adaptive Media) was initiated in 1998.

3. Future Plans

1. The Fifth U.S.-Japan Joint Technical Coordinating Committee Meeting on CHS will be held in October 1998 in Japan, in conjunction with an International Symposium to commemorate the 20th Anniversary of U.S.-Japan Cooperative Research.
2. Several TCC meetings will be scheduled in respective countries in the coming year.
3. In support of the International Decade for Natural Disaster Reduction (IDNDR) Program, techniques will be explored to disseminate findings of completed joint research projects to countries with high seismic risks.
4. A joint workshop on Test Procedure, Documentation, Retrieval of Test Data, and Experimental Facilities will be held to maximize the usefulness of research data. The date and location will be established prior to the 31st Joint Panel Meeting.
5. Future plans for U.S.-Japan cooperative programs shall consider existing and planned experimental research programs of the three new NSF earthquake engineering research centers.

REPORT OF TASK COMMITTEE C
DESIGN, EVALUATION AND IMPROVEMENT OF STRUCTURES

Date: 12 May 1998

Place: National Institute of Standards and Technology, Gaithersburg, MD, USA

Attendees:	U.S.-side--	Shi-Chi Liu (Acting Chairman)	NSF
		Noel Raufaste	NIST
		Lawrence Hultengren	DOS
	Japan-side--	Hisahiro Hiraishi (Chairman)	BRI
		Jun-ichi Hoshikuma	PWRI
		Michio Okahara	PWRI
		Takao Masui	NLA
		Akiyoshi Mukai	BRI

1. Objective and Scope of Work

The objective of Task Committee (C) is to develop disaster mitigation guidelines and programs that will improve the performance of new structures and the capacity of existing structures in resisting wind and seismic forces. To establish adequate evaluation of performance, each country will coordinate the development of condition assessment, screening, structural analysis, and design methodologies. Enhance performance can be obtained by the intelligent renewal, repair, and retrofit of existing buildings and other structures. Certain structures will be analyzed and instrumented and then evaluated after disasters. Also, effective use of new advanced materials, smart materials, and structural systems associated with appropriate design methods, will provide structural performance in the life cycle.

The scope of work includes:

1. Exchanging information, planning and hosting workshops on new design technologies, evaluation technologies, and repair and retrofit techniques.
2. Studying new materials and methods for repairing and retrofitting existing structures and for new construction.
3. Developing a uniform system for screening and analyzing wind and seismic resistance capacity of structures in each country.
4. Evaluating, composite/hybrid building structures and smart structural systems and providing documentation for post-disaster evaluation of performance.
5. Developing reliable condition assessment systems for new and existing structures.

6. Coordinating research projects in the U.S. and Japan to minimize duplication and maximize benefits.

2. Accomplishments

1. Conducted the fourth U.S.-Japan Technical Coordinating Committee Meeting on Composite and Hybrid Structural Systems, Monterey, CA, USA, during 12-14 October 1997.
2. In the field of hybrid structural systems, Dr. H. Kuramoto, BRI, completed a one-year (October 1996-September 1997) research assignment at Cornell University, and Prof. R. Frosh, Purdue University, visited BRI in March 1998 to discuss the 6th U.S.-Japan Cooperative Research Program on Smart Structural Systems.
3. Initiated Phase 6 of the U.S.-Japan Cooperative Research Program on "Auto-Adaptive Media (Smart Structural Systems).

3. Future Plans

The following activities are planned for T/C (C):

1. Conduct the 5th U.S.-Japan Technical Coordinating Committee Meeting on Composite and Hybrid Structural Systems, October 1998, Japan.
2. Conduct Workshops on Auto-Adaptive Media (Smart Structural Systems), in May at Sonoma, CA, and Fall (to be determined), USA, 1998.
3. Conduct a 20-year commemoration symposium on Cooperative Earthquake Engineering Research, October 1998, Tokyo.
4. Continue the 6th U.S.-Japan Cooperative Research Project on Auto-Adaptive Media (Smart Structural Systems).
5. Develop a reliable methodology for screening and analyzing wind and seismic resistant capacity, and advanced instrumentation technology and expert systems to provide condition assessment of existing structures.
6. Compile a database of advance materials/systems that have potential for improving structural performance of new construction, and for use in rehabilitating and strengthening existing buildings.
7. Investigate new design methodologies based on required structural performance using advanced materials and systems.

8. Continue to encourage participants by private industry, consulting engineers, universities, national and local government agencies involved in instrumentation, evaluation, condition assessment, and retrofit and strengthening of existing buildings, for seismic and wind resistance.

4. Other Activities

The following activities support the work of T/C (C):

1. U.S. research sponsored by NSF, Corps of Engineers, NIST and FWHHA have developed reports on seismic rehabilitation and retrofit strategies, including innovative techniques for strengthening existing buildings and bridges.
2. Continue development of NSF's Civil Infrastructure Systems Research Program, including strong emphasis on evaluation and improvement of structures.
3. Continue to encourage conduct of research in the area of retrofit and repair of buildings and structures.

5. Develop and Harmonize T/Cs C & G

The consolidation of the T/Cs (C&G) was proposed at the U.S.-side Domestic Panel Meeting of September 1997 and was approved by both sides at their respective Domestic Panel Meetings, December 1997. T/C (C) requests approval from the full Panel at the 30th Joint Panel Meeting of May 1998 to consolidate T/Cs (C&G) into a new T/C (C). The revised name and proposed mission will be proposed by the respective T/C Chairs at both sides Fall 1998 Domestic Meetings. Suggested new T/C titles were:

1. High Performance Structural Systems and Auto-Adaptive Media.
2. High Performance Systems: Design, Repair, Evaluation, and Auto-Adaptive Media.

Suggested objective and scope of work and the future plans of the renewal Task Committee (C) are as follows:

1. Exchange information, and plan and conduct workshops on new design technologies, evaluation technologies, repair and retrofit techniques.
2. Study advanced materials and methods for new construction and for repairing and retrofitting existing structures.
3. Develop reliable condition assessment systems for new, existing and damaged structures.
4. Develop and Harmonize performance based structural design developed in each country.

5. Coordinate research projects on design, evaluation and improvement of structures in the U.S. and Japan to minimize duplication and maximize benefits.

REPORT OF TASK COMMITTEE D

EARTHQUAKE ENGINEERING FOR DAMS

Date: 12 May 1998

Place: National Institute of Standards and Technology, Gaithersburg, MD, USA

Attendees:	U.S.-side--	Robert Hall (Chairman)	USAE
		Joseph Koester	USAE
		William Roper	USAE
		Larry Nuss	USBR
		Frank McLean	USBR
	Japan-side--	Takashi Sasaki (Acting-Chairman)	PWRI
		Mitsu Okamura	PWRI
		Hideki Sugita	PWRI

1. Objective and Scope of Work

To develop technical insights into better understanding of the response of dams to seismic effects, the T/C will plan, promote, and develop research initiatives to assist in assuring seismic safety and economical protective countermeasure against earthquake loading for these structures.

The scope of work includes:

1. Methods of analysis for seismic design of dams including outlet works. Comparison of design methods and criteria between U.S. and Japan. Development of "Design Earthquake Ground Motions" for analysis and evaluation of dams. Assessment of investigation and dynamic analysis methods as tools (modeling, calculation codes).
2. Dynamic characteristics of dam construction materials and site conditions. Strength and deformation characteristics during earthquakes (concrete, soil and rock).
3. Analysis of observed behavior of dams and outlet works during earthquakes. Investigation of the mechanism of damages due to earthquake loading. Application of the analysis of the observed behavior during earthquake to the earthquake-resistant design.

2. Accomplishments

1. T/C (D) conducted the First U.S.-Japan Workshop on Advanced Research on Earthquake Engineering for Dams at the Waterways Experiment Station in Vicksburg, Mississippi, USA, on 12-14 November, 1996.
2. Articles related to the first Workshop were printed in the Panel's Technical Bulletin *Winds and Seismic Effects*, Issue 4, and in the PWRI Newsletter, No. 68.
3. In the field of seismic design for concrete dams, Mr. Takashi Sasaki, PWRI, started a one-year (December 1997-December 1998) research at University of California, Berkeley.
4. Some members of T/C (D) of U.S. and Japan sides participated in the 4th International Conference on Case Histories in Geomechanical Engineering in St. Louis, Missouri, USA on 9-12 March 1998, and exchanged the latest results of research/investigation and the newest technical information about dam earthquake engineering.

3. Future Plans

1. Exchange of the results of research/investigation and technical information about dam earthquake engineering is encouraged, and feasibility of joint research and investigation is in continuous consideration.
2. Exchange visits to the institutes concerned, of scientists and engineers between U.S. and Japan, is to be extended for the effective communications.
3. The proceedings of the first Workshop will be published and distributed to the T/C members and Panel Secretariats.
4. In the field of seismic design for embankment dams, Mr. Tomoya Iwashita, PWRI, will start a one-year (August 1998-August 1999) research at University of California, Berkeley.
5. T/C (D) will hold the Second Workshop at the Public Works Research Institute, Tsukuba, Japan, or at another location in Japan that would enhance field observation opportunities in conjunction with the 31st Joint Panel Meeting in 1999.
6. Update the Task Committee membership.

REPORT OF TASK COMMITTEE E
DESIGN FOR WIND AND WIND HAZARD MITIGATION

Date: 12 May 1998

Place: National Institute of Standards and Technology, Gaithersburg, MD, USA

Attendees:	U.S.-side --	Joseph Golden (Chairman)	NOAA
		Bogusz Bienkiewicz	CSU/FHWA
		Art Chiu	University of Hawaii at Manoa
		Harold Bosch	FHWA
	Japan-side --	Hiroshi Sato (Co-Chairman)	PWRI
		Shigetoshi Kobayashi	PWRC

1. Objective and Scope of Work

To exchange technical information and to jointly plan, promote and foster research and dissemination, to improve understanding of wind and its effects on structures, establish more rational wind resistant design methods for structures, and to contribute to wind hazard mitigation.

The scope of work includes:

1. Characterization of strong wind, especially boundary layer extreme winds.
2. Wind effects (wind loading on and wind-induced response of structures).
3. Experimental and analytical methods to predict wind and its effects.
4. Damage and risk assessment.
5. Wind hazard assessments and wind hazard mitigation.

2. Accomplishments

Held the first joint Workshop on Design for Wind and Wind hazard Mitigation at the East-West Center at the University of Hawaii on October 7-9, 1997. Seven Japan-side members and ten U.S.-side members participated in the Workshop. After presenting recent research results, the participants discussed potential research topics that could be pursued in a collaborative program. Many of the participants visited the NOAA Tsunami Warning Center and the National Weather Service Office on Oahu; and some also visited the NOAA Mauna Loa Observatory on Hawaii following the Workshop. The proceedings of the Workshop will be published by the U.S.-side, and distributed to all the Task Committee members.

3. Future Plans

1. Hold the second joint workshop in Japan in the autumn of 1998, possibly November.
2. Pursue the possibility of collaborative research on the topics recommended at the first workshop. PWRI and the University of Washington are discussing possible collaborative research on "Development of Prediction Methods for Wind Response of Long Span Bridges."
3. Exchange technical information on the following subjects:
 - a) Topographical effects on wind and the use of field measurements, numerical models and geographic information systems (GIS) to study these effects.
 - b) Control of wind-induced response of structures.
 - c) Computational fluid dynamics and wind tunnel tests.
 - d) Prediction of wind-induced response of full-scale structures.
 - e) Investigation of wind hazards, including post-storm damage assessment methodologies.
 - f) Wind resistant design codes, standards and recommendations.

REPORT OF TASK COMMITTEE F DISASTER PREVENTION METHODS FOR LIFELINE SYSTEMS

Date : 12 May 1998

Place : National Institute of Standards and Technology, Gaithersburg, MD, USA

Attendees :	U.S.-side –	Riley Chung (Chairman)	NIST
		Ronald Andrus	NIST
		Josephine Malilay	CDC
		Phillip Yen	FHWA
	Japan-side –	Keiichi Tamura (Acting-Chairman)	PWRI
		Takaharu Kiriyaama	NLA
		Keiko Ogawa	Tohoku University

1. Objectives and Scope of Work

To improve the performance of lifeline systems during earthquakes and extreme winds, and to promote the development and implementation of technical and non-technical countermeasures, including the capability in damage estimation techniques and inspection procedures, through:

1. Planning and conducting workshops.
2. Facilitating exchange of technical information and personnel.
3. Promoting development of design guidelines and standards.

2. Accomplishments

1. Members of this T/C participated in the planning of the second earthquake policy symposium held in Kobe, Japan in September 1997. The symposium was led by the U.S. Federal Emergency Management Agency and the National Land Agency of Japan, under the U.S.-Japan Natural Disaster Reduction Initiative of the U.S.-Japan Framework for New Economic Partnership (Common Agenda).
2. Task Committee (F) held the Seventh Joint Workshop on Disaster Prevention for Lifeline Systems on November 4 through 7, 1997, in Seattle, Washington. The workshop was co-sponsored by the Public Works Research Institute of Japan and the National Science Foundation and the National Institute of Standards and Technology of the United States. Forty-five experts, representing government, academia, industry and private practice, participated in the workshop. Thirty papers were presented, many of them focused on the results of the studies of the two most recent devastating earthquakes; the 1994 Northridge earthquake in California and the 1995 Kobe earthquake in Japan.
3. Under the auspices of Task Committees (F&H), Dr. Ronald D. Andrus, an NIST researcher in geotechnical earthquake engineering, had a successful visit in December 1997 to PWRI, PHRI, and other

universities and private companies. The purpose of his visit was to collect additional information on shear wave velocities at sites where liquefaction has happened or not happened during past earthquakes in Japan and to explore the use of shear wave velocities for evaluating liquefaction potential for lifeline systems.

3. Future Plans

1. Encourage collaborative research and development in areas such as: performance prediction and post-earthquake damage assessment of lifeline systems; systems approach to lifeline performance; soil-structure interaction; and cost-effective ground improvement techniques and other countermeasures for lifeline facilities.
2. Encourage and strengthen current efforts in both countries for developing seismic design guidelines and standards for lifeline systems. Existing UJNR channels should be fully utilized to facilitate the exchange of relevant information concerning the development of guidelines and standards. Possible collaboration of developing guidelines and standards for lifeline systems should be pursued.
3. Initiate cooperative efforts, including development of a database, between lifeline engineering and public health to assess consequences due to the disruption of lifeline systems.
4. Hold the Eighth Joint Workshop on Disaster Prevention for Lifeline Systems in the Fall of 1999 in Japan. Specific location, time, and theme of the workshop will be determined through correspondence between the co-chairs of this task committee.

REPORT OF TASK COMMITTEE G
STRUCTURAL CONTROL AND INTELLIGENT MATERIAL SYSTEMS

Date: 12 May 1998

Place: National Institute of Standards and Technology, Gaithersburg, MD, USA

Attendees:	U.S.-side –	Shi-Chi Liu (Chairman)	NSF
		Noel Raufaste	NIST
		Lawrence Hultengren	DOS
	Japan-side –	Jun-ichi Hoshikuma (Acting-Chairman)	PWRI
		Hisahiro Hiraishi	BRI
		Michio Okahara	PWRI
		Takao Masui	NLA
		Akiyoshi Mukai	BRI

1. Objective and Scope of Work

1. Develop research plans in control of equipment and structures and in high performance structural and material systems;
2. Implement control techniques for motion reduction and modification;
3. Implement use of advanced materials in actual design and construction of buildings and other infrastructure systems under seismic or wind environments;
4. Promote U.S.-Japan cooperation in structural control and intelligent material systems research;
5. Bring together governmental, academic, and industrial participants in joint pursuit of these efforts; and
6. Contribute to IDNDR by organizing joint research and other technical activities in structural and intelligent material systems research based on international cooperation.

T/C (G) works closely with other organizations to provide the leadership in this emerging research by facilitating the exchange of data and information through UJNR mechanisms. The scope of work includes:

1. Providing technical assistance, consultation and coordination of UJNR affiliated research organization in the initiation, development, and execute their programs in research areas.
2. Promoting joint government-university-industry collaborative efforts to facilitate technology transfer and practical implementation.

3. Sponsoring and conducting interdisciplinary workshops and meetings to identify key area of research and opportunities for cooperation, and to stimulate public awareness and interest in this field of research.
4. Developing promotional and demonstrative activities to stimulate public awareness and interest in this field of research.
5. Providing information useful for the establishment of performance standards, design and also retrofit/rehabilitation of existing structures.
6. Promoting research in intelligent material systems, sensors, actuators, optional control system design, and encourage laboratory and field experiments of prototype and full-scale structures.

2. Accomplishments

1. In 1998, a five-year U.S.-Japan Cooperative Research Program on Urban Earthquake Disaster Mitigation between NSF and Monbusho (Ministry of Education) was initiated under U.S.-Japan Common Agenda.
2. Phase 6 of the U.S.-Japan Cooperative Research Program on "Auto-Adaptive Media" (Smart Structural Systems) was initiated in 1998.

3. Future Plans

1. To implement Phase 6 of the above U.S.-Japan Cooperative Research Program on Auto-Adaptive Media.
2. Task Committee (G) confirmed its agreement to consolidate with T/C (C) into a new T/C (C). The activities of T/C (G) will be continued in the new T/C (C) and in T/C (J).

4. Develop and Harmonize T/Cs C&G

The consolidation of the T/Cs (C&G) was proposed at the U.S.-side Domestic Panel Meeting of September 1997, and was approved by both sides at their respective Domestic Panel Meetings, December 1997. T/C (G) requests approval, from the full Panel at the 30th Joint Panel Meeting of May 1998, to consolidate T/Cs (C&G) into a new T/C (C). The revised name and proposed mission will be proposed by the respective T/C Chairs at both sides' Fall 1998 Domestic Meetings. Suggested new T/C titles were:

1. High Performance Structural Systems and Auto-Adaptive Media
2. High Performance Systems: Design, Repair, Evaluation, and Adaptive Media.

Suggested objective and scope of work and the future plans of the consolidated T/C (C) are as follows:

1. Exchange information, and plan and conduct workshops on new design technologies, evaluation technologies, repair and retrofit techniques.

2. Study advanced materials and methods for new construction and for repairing and retrofitting existing structures.
3. Develop reliable condition assessment systems for new, existing and damaged structures.
4. Develop and Harmonize performance based structural design developed in each country.
5. Coordinate research projects on design, evaluation, and improvement of structures in the U.S. and Japan to minimize duplication and maximize benefits.

REPORT OF TASK COMMITTEE H
SOIL BEHAVIOR AND STABILITY DURING EARTHQUAKES

Date: 13 May 1998

Place: National Institute of Standards and Technology, Gaithersburg, MD, USA

Attendees: U.S.-side – Joseph P. Koester (Acting-Chairman) WES
Jon Ake USBR
Larry Nuss USBR
Ronald Andrus NIST
Frank McLean USBR
William Joyner USGS

Japan-side – Mitsu Okamura (Acting-Chairman) PWRI
Takashi Sasaki PWRI

1. Objective and Scope of Work

Government agencies responsible for public works must assure seismic safety and provide economical protection against earthquake hazards.

The objective of the Task Committee (H) is to assist in meeting these needs by enhancing the availability of technology for predicting the dynamic behavior of soils, foundations and earth structures, and analyzing dynamic soil/structure interaction to assure their safe performance during earthquakes.

In accordance with the objective, the scope of work includes:

1. Exchange information on technological developments, state-of-the-art and practice related to soil behavior and stability during earthquakes.
2. Exchange information and technical data relating to field performance, research, and methods of practice.
3. Plan and conduct programs of cooperative research and/or workshops in coordination with the proposed or on-going programs.
4. Make other efforts needed including exchange of researchers between U.S. and Japanese research institutions, and publication of research results and recommended practice.

2. Accomplishments

1. The National Research Institute for Earth Science and Disaster Prevention (NIED), the Building Research Institute (BRI), and Wayne State University (WSU), have continued to work in their cooperative research program "Physical and Numerical Simulation of Structural Damages Due to Liquefaction and Development of Countermeasure Techniques," 1994-1998.
2. Port and Harbor Research Institute (PHRI), Colorado School of Mines and the Lovelace Institutes (Albuquerque, NM) have continued joint research on application of the Nuclear Magnetic Resonance Imaging (NMRI) method to the study of soil behavior and stability during earthquakes.
3. Under the auspices of Task Committees (F&H), Dr. Ronald R. Andrus, a NIST researcher in geotechnical engineering, had a successful visit to PWRI, PHRI, several universities, and private companies in December 1997. The purpose of his visit was to collect data on shear wave velocities at sites where liquefaction was observed and not observed, and to explore the use of shear wave velocities at sites for use in evaluating liquefaction potential for lifeline systems.

3. Future Plans

1. Task Committee (H) plans to hold a workshop on the Use of Centrifuge Modeling for Research into Soil Behavior and Stability During Earthquakes 28-29 September 1998, Tsukuba, Japan. It will be held just after the International Conference CENTRIFUGE '98 in Tokyo, organized by Japanese Geotechnical Society and International Society for Soil Mechanics and Geotechnical Engineering (ISSMGE).
2. Continue collaborations on liquefaction prediction based on field performance data and shear wave velocity measurements.

4. Other Activities

The Japanese Geotechnical Society has published a Handbook on Liquefaction remediation. English translation and editing of the draft was completed with the assistance of Panel members.

REPORT OF TASK COMMITTEE I

STORM SURGE AND TSUNAMIS

Date: 13 May 1998

Place: National Institute of Standards and Technology, Gaithersburg, MD, USA

Attendees: U.S.-side – Michael Blackford (Chairman) NOAA
Japan-side – Shigetoshi Kobayashi (Acting-Chairman) PWRC
Keiichi Tamura PWRI

1. Objective and Scope of Work

The objective of this Task Committee is to mitigate damage from storm surge and tsunami through cooperative research and shared technology and information. The primary cause of storm surge is considered to be tropical cyclones (hurricane, typhoons). The primary cause of tsunamis is considered to be sudden sea floor deformation due to earthquakes, volcanic activity and landslides. Both hazards may cause disasters along coastal regions.

The scope of this T/C is as follows:

1. Exchange results of research on storm surge and tsunami occurrence, generation, propagation, and coastal effects. This includes observations on historical, current, and theoretical tsunamis. Of particular interest is the effort by U.S. and Japan to acquire deep ocean tsunami measurements.
2. Exchange results and status of storm surge and tsunami mitigation activities including analysis of the problem, planning, warning and engineering approaches.
3. Exchange information on development of technologies such as computer programs to predict travel times, land-fall locations, inundation and run-up heights, and wave characteristics, improved instrumentation, and use of satellite communication for detection and warning.
4. Facilitate dissemination through exchanges of literature, technical reports at joint meetings, special workshops, joint projects, and direct interaction among participants. The storm surge research community which functions through many related societies and international organizations, defines and stimulates work in the field. The Task Committee, through its meetings and workshops, encourages exchanges of ideas and joint study by U.S. and Japanese investigators of tsunami events throughout the world.

2. Accomplishments

1. The Task Committee agreed to support the improvement of the gridded bathymetry and coastal-topography data initiated by International Tsunami Commission.
2. The Task Committee exchanged ideas on large-scale laboratory experiments on tsunami run-up.
3. Deep ocean tsunami detection systems were deployed off the coasts of Alaska and Washington by the U.S. NOAA's Pacific Marine Environmental Laboratory (PMEL) during the summer of 1997. These instruments initially functioned well, however winter storms proved it will be necessary to modify the communication system.

3. Future Plans

1. The 5th Storm Surge and Tsunami Workshop will be held in Sapporo, Japan, in July 1998.
2. Modified deep ocean detection systems will be redeployed during the summer of 1998 by PMEL.

REPORT OF TASK COMMITTEE J
WIND AND EARTHQUAKE ENGINEERING
FOR TRANSPORTATION SYSTEMS

Date: 13 May 1998

Place: National Institute of Standards and Technology, Gaithersburg, MD, USA

Attendees:	U.S.-side --	Dr. Phillip Yen (Acting-Chair)	FHWA
		Dr. Daniel Abrams	MAEC
		Dr. Bogusz Bienkiewicz	CSU
		Dr. Arthur Chiu	University of Hawaii at Manoa
		Dr. Joseph Golden	NOAA
	Japan-side --	Dr. Michio Okahara (Acting-Chair)	PWRI
		Dr. Hiroshi Sato	PWRI
		Dr. Jun-ichi Hoshikuma	PWRI
		Dr. Hisahiro Hiraishi	BRI

1. Objectives and Scope of Work

1. Plan, promote, and foster research on the behavior of highway bridges when subjected to wind and seismic forces, and
2. Disseminate research results and provide specifications and guidelines based on the Task Committee's findings. Surface transportation systems play a vital role in the movement of goods and people. Highway bridges are especially influenced by the forces of wind and earthquakes because of their open exposure to those forces.

The scope of work includes:

1. Researches on highway bridges without limitation on their size and function.
2. Investigations existing and new bridge designs.
3. The behavior of whole bridge systems and/or single components of a bridge.

2. Accomplishments

The 13th U.S.-Japan Bridge Engineering Workshop was held during 2-3 October 1997, in Tsukuba, Japan. The workshop was attended by 19 U.S. and 58 Japanese participants. The proceedings of the workshop has been published and will be distributed.

3. Future Plans

1. The 14th U.S.-Japan Bridge Engineering Workshop will be held during the Fall of 1998, in Pittsburgh, Pennsylvania, USA.
2. Continue to investigate and exchange technical information on improved seismic retrofit and strengthening procedures for highway bridges based on experimental, analytical, and field studies. This exchange should include information on maintenance of existing bridges.
3. Continue to conduct cooperative research on the seismic performance of bridge piers and columns experimentally and analytically, and encourage research on seismic isolation and hybrid control of bridges.
4. Continue the coordinated research study to compare the seismic design criteria for bridges in Japan and the U. S. and discuss the method and analysis procedures for bridge column design. Continue to exchange information on the application of the limit state design method.
5. Encourage a research study on seismic, aeroelastic, and aerodynamic response of long span bridges such as cable-supported bridges with emphasis on behavior of composite materials, cable inspection, vibration control, and corrosion protection.
6. Encourage a coordinated research study on seismic response and control, system identification techniques, nondestructive evaluation of bridge structures, use and performance of structural materials including new materials, and performance of jointless bridges.
7. Dr. Jun-ichi Hoshikuma, Research Engineer of Earthquake Engineering Division, PWRI started his one-year guest research assignment on seismic design of bridges at UCSD from March, 1998.

REPORT OF TASK COMMITTEE K
WIND AND EARTHQUAKE ENGINEERING FOR OFFSHORE
AND COASTAL FACILITIES

Date: 13 May 1998

Place: National Institute of Standards and Technology, Gaithersburg, MD, USA

Attendees:	U.S.-side –	Charles Smith (Chairman)	MMS
		Martin Eskijian	CSLC
	Japan-side –	Susumu Iai (Acting-Chairman)	PHRI
		Akiyoshi Mukai	BRI

1. Objective and Scope of Work

To develop technical insights necessary to mitigate damage to offshore and coastal facilities due to extreme wind and seismic effects. The Task Committee will plan, promote and develop research initiatives to meet this objective and will disseminate the results of their research for incorporation into future specification or design guidelines. Criteria for the design of offshore and coastal facilities may differ greatly from their onshore counterparts. These differences can arise due to their unique design or mass distribution, to the fluid/structure or wind/structure interaction, to the placement of foundation elements in or on soft, fully saturated soils that can be subject to large hydrodynamic pressures, and to the lack of specific environmental data or engineering experience that has been developed for most onshore sites.

The scope of work includes:

1. Sponsoring and conducting workshops and meetings to identify key areas of research, opportunities for cooperation, and the exchange of knowledge.
2. Predicting strong ground motions for offshore and coastal sites including assessing the effects of basin geometry, linear, and nonlinear local geological effects using actual seafloor response measurements.
3. Determining the dynamic response and the interaction of structure/foundation/soil systems to seabed motions and/or extreme wind forces.
4. Assessing the dynamic response and behavior of various operational facilities mounted on offshore and coastal structures.
5. Developing assessment methodologies for earthquakes and other characteristics of potential seismic sources (e.g. faults) for offshore and coastal sites in regards to how these conditions relate to structural design criteria.

6. Promoting the implementation of new research results into current design and construction processes.
7. Developing research efforts to include laboratory and field programs to obtain data on the response of offshore and coastal facilities to extreme wind and seismic forces.
8. Creating performance standards, design specifications, guidelines, and code recommendations for applications to new construction as well as remedial action for existing facilities.

2. Accomplishments

1. Members of Task Committee (K) helped to organize and participated in the workshop, "Earthquake Criteria Workshop- Recent Development in Seismic Hazard and Risk Assessment for Port, Harbor, and Offshore Structures," held concurrently with the International Offshore Mechanics and Arctic Engineering (OMAE 1997) Conference in Yokohama, Japan on April 17, 1997.
2. Task Committee (K) held initial planning phase to conduct a third international workshop. The theme of this workshop will focus on seismic, wind, and hazard mitigation techniques for offshore and coastal facilities. It is to be held in Japan in late 1999 or early 2000.

3. Future Plans

1. Develop workshop agenda of the third U.S.-Japan Workshop on Wind and Earthquake Engineering for Offshore and Coastal Facilities.
2. Coordinate, where possible, on-going research on wind and earthquake engineering for offshore and coastal facilities of interest to the members of the Task Committee. This includes sharing of research reports and publications where possible.
3. Since tsunamis have been less severe in the U.S. than in Japan, the U.S. has fewer researchers in this specialty. The Task Committee, through its meetings and workshops, encourages exchanges of ideas and joint study by U.S. and Japanese investigators of tsunami events throughout the world.
4. Task Committee (K) will work within the framework of the U.S.-Japan Common Agenda Program focusing on the issue of acceptable seismic risk guidelines for ports and harbors.
5. Task Committee (K) will coordinate activities with the Pacific Earthquake Engineering Research (PEER) Program on ports and harbors centered at the University of Southern California.

REPORT OF NEW TASK COMMITTEE SEISMIC INFORMATION SYSTEMS

Date: 13 May 1998

Place: National Institute of Standards and Technology, Gaithersburg, MD, USA

Attendees: U.S.-side --	Dr. Stuart Nishenkō (Co-chairman)	FEMA
	Dr. William Roper (Co-chairman)	USACE
	Dr. Roger Borchardt	USGS
	Dr. Mehmet Celebi	USGS
	Dr. Josephine Malilay	CDC
	Mr. Noel Raufaste	NIST
Japan-side --	Mr. Takaharu Kiriya (Co-chairman)	NLA
	Dr. Hideki Sugita (Co-chairman)	PWRI
	Mr. Takao Masui	NLA
	Dr. Makoto Watabe	Keio University
	Mr. Keiichi Ohtani	NIED
	Dr. Keiko Ogawa	Tohoku University

1. Objective and Scope of Work

The objective of this Task Committee is to improve understanding of earthquakes and their societal impacts using seismic information systems (SIS), loss estimation methodologies and computational models that describe the effects of seismic loading on the built environment. The Task Committee will foster cooperation between the US and Japan policy and research community. It will be a principal Panel technical resource to the Earthquake Policy Cooperation under the US-Japan Common Agenda.

The Task Committee will serve as a forum for exchanging information between the two nations on identifying, developing, and reviewing data, systems, and methodologies involved in SIS, earthquake loss estimation, geospatial and topographic information systems, real-time seismic warning systems, and their application to earthquake disaster mitigation, preparedness, emergency response, and recovery. The Task Committee also will review various disaster information networks like the Global Disaster Information Network (GDIN) and assess their applicability.

The scope of work for this Task Committee is as follows:

- A. Plan and conduct T/C workshops and joint meetings to identify research topics and develop joint research programs.
- B. Review the principles, objectives, structure and uses of existing SIS systems, loss estimation methodologies and real-time earthquake warning systems.

- C. Review existing Geographic Information Systems (GIS), identify data structures and operations required for successful integration into SIS. Results of this review may identify applications to other natural disaster phenomena such as wind, storm surge, tsunami, and flooding. If applicable, additional modules will be addressed in the future to be incorporated into the system.
- D. Facilitate the exchange of policy and research personnel, technical information, and data.
- E. Assist in the coordination of policy initiatives and research projects in the US and Japan to minimize duplication and maximize the benefits of bringing together government, academic, and private sector participants in these efforts.
- F. Facilitate the publication and distribution of earthquake policy and research results related to SIS and the implementation of these findings in guidelines, codes, and standards
- G. Provide technical assistance, consultation, and coordination of the Panel's affiliated research organizations to support related work identified by the Common Agenda's Earthquake Policy High Level Forum.
- H. Facilitate the exchange of information between U S and Japan policy makers to promote the application of SIS.
- I. Develop promotional and demonstrative activities to stimulate public awareness and interest in these emerging technologies.
- J. Disseminate the knowledge gained from this US-Japan cooperation to other nations.
- K. This Task Committee will cooperate with the UJNR Panels on Earthquake Research and on Fire Research and Safety to identify specific tasks of mutual interest.
- L. L. This Task Committee will promote and exchange new developments in real-time data acquisition, processing, and notification in conjunction with T/C (A).

2. Meeting Accomplishments

- A. Tasks concerned with the establishment of this Task Committee have been completed, including definition of the committee objectives and scope of work, establishment of the initial membership, and development of future plans.
- B. Committee Membership is proposed for government participants and candidate non-government participants are indicated.

Government Membership

U.S.-side --	Dr. Stuart Nishenko (Co-chairman)	FEMA
	Dr. William Roper (Co-chairman)	CORPS
	Dr. Harley Benz	USGS
	Dr. Roger Borchardt	USGS

	Dr. Mehmet Celebi	USGS
	Dr. William Ellsworth	USGS
	Mr. Richard Eisner	State of California, OES
	Dr. Walter Hays	USGS
	Dr. H. S. Lew	NIST
	Dr. Peter Ward	USGS
Japan-side --	Mr. Kazuo Okayama (Co-chairman)	NLA
	Dr. Hideki Sugita (Co-chairman)	PWRI
	Mr. Akira Kinoshita	GSI
	Mr. Hiroshi Masaharu	GSI
	Mr. Akira Nagai	JMA
	Mr. A. Ito	MRI
	Dr. Hiroyuki Yamanouchi	BRI
	Mr. Tomofumi Nozaki	PWRI
	Mr. Toshiaki Yokoi	BRI
	Dr. Izuru Okawa	BRI
	Mr. Atsushi Nozu	PHRI
	Dr. Keiichi Ohtani	NIED

Proposed Non-Government Membership

U.S.-side --	Dr. Scott Lawson	RMS
	Dr. James Goltz	Caltech
	Mr. Ron Eguchi	EQE
	Dr. David Simpson	IRIS
	Dr. Tim Ahern	IRIS
Japan-side --	Mr. Yoshiyuki Murayama	Tohoku University
	Dr. Keiko Ogawa	Tohoku University

3. Future Plans

Plan and hold a joint workshop. The proposed time of the workshop is summer to autumn of 1999. Further discussions on the time, theme, location of the workshop will take place over the next several months. This workshop would review national policies and programs on earthquakes, use of real-time warning and notification systems, use of remote sensing and geospatial sensors and analysis technology applications, use of real-time and near-real time strong motion measurement, damage assessment and emergency response systems, use of earthquake loss-estimation methodologies and emergency response models.

- A. Review current real-time and near real-time earthquake warning/notification systems in the US and Japan, e.g.
 - CUBE/TriNet in Southern California (USGS, CDMG, Caltech)

- REDI in Northern California (UC, Berkeley)
 - SCIGN (USGS, SCEC)
 - GDIN (US govt.)
 - MOC-Net (MOC)
 - JMA net (JMA)
- B. Review real time and near real-time earthquake strong motion measurement, damage assessment and emergency response systems in the US and Japan, e.g.
- Health Impact Surveillance System for Natural Disasters (ARC-CDC)
 - California Strong Motion Instrumentation Program (CDMG)
 - US National Strong Motion Program (USGS)
 - GPS-LPS (USGS)
 - Kyoshin net (NIED)
 - SIGNAL (Tokyo Gas)
 - SATURN (PWRI)
 - UrEDAS (JR)
- C. Review earthquake loss estimation methodologies and emergency response models, e.g.
- HAZUS (FEMA)
 - EPEDAT (EQE)
 - Early Estimation System (NLA)
 - Loss Estimation Model
 - Fire and Disaster Management Agency model (FDMA)
 - Local government models

NIST Technical Publications

Periodical

Journal of Research of the National Institute of Standards and Technology—Reports NIST research and development in those disciplines of the physical and engineering sciences in which the Institute is active. These include physics, chemistry, engineering, mathematics, and computer sciences. Papers cover a broad range of subjects, with major emphasis on measurement methodology and the basic technology underlying standardization. Also included from time to time are survey articles on topics closely related to the Institute's technical and scientific programs. Issued six times a year.

Nonperiodicals

Monographs—Major contributions to the technical literature on various subjects related to the Institute's scientific and technical activities.

Handbooks—Recommended codes of engineering and industrial practice (including safety codes) developed in cooperation with interested industries, professional organizations, and regulatory bodies.

Special Publications—Include proceedings of conferences sponsored by NIST, NIST annual reports, and other special publications appropriate to this grouping such as wall charts, pocket cards, and bibliographies.

National Standard Reference Data Series—Provides quantitative data on the physical and chemical properties of materials, compiled from the world's literature and critically evaluated. Developed under a worldwide program coordinated by NIST under the authority of the National Standard Data Act (Public Law 90-396). NOTE: The Journal of Physical and Chemical Reference Data (JPCRD) is published bimonthly for NIST by the American Chemical Society (ACS) and the American Institute of Physics (AIP). Subscriptions, reprints, and supplements are available from ACS, 1155 Sixteenth St., NW, Washington, DC 20056.

Building Science Series—Disseminates technical information developed at the Institute on building materials, components, systems, and whole structures. The series presents research results, test methods, and performance criteria related to the structural and environmental functions and the durability and safety characteristics of building elements and systems.

Technical Notes—Studies or reports which are complete in themselves but restrictive in their treatment of a subject. Analogous to monographs but not so comprehensive in scope or definitive in treatment of the subject area. Often serve as a vehicle for final reports of work performed at NIST under the sponsorship of other government agencies.

Voluntary Product Standards—Developed under procedures published by the Department of Commerce in Part 10, Title 15, of the Code of Federal Regulations. The standards establish nationally recognized requirements for products, and provide all concerned interests with a basis for common understanding of the characteristics of the products. NIST administers this program in support of the efforts of private-sector standardizing organizations.

Order the following NIST publications—FIPS and NISTIRs—from the National Technical Information Service, Springfield, VA 22161.

Federal Information Processing Standards Publications (FIPS PUB)—Publications in this series collectively constitute the Federal Information Processing Standards Register. The Register serves as the official source of information in the Federal Government regarding standards issued by NIST pursuant to the Federal Property and Administrative Services Act of 1949 as amended, Public Law 89-306 (79 Stat. 1127), and as implemented by Executive Order 11717 (38 FR 12315, dated May 11, 1973) and Part 6 of Title 15 CFR (Code of Federal Regulations).

NIST Interagency or Internal Reports (NISTIR)—The series includes interim or final reports on work performed by NIST for outside sponsors (both government and nongovernment). In general, initial distribution is handled by the sponsor; public distribution is handled by sales through the National Technical Information Service, Springfield, VA 22161, in hard copy, electronic media, or microfiche form. NISTIR's may also report results of NIST projects of transitory or limited interest, including those that will be published subsequently in more comprehensive form.

U.S. Department of Commerce
National Institute of Standards
and Technology
Gaithersburg, MD 20899-0001

Official Business
Penalty for Private Use \$300